Master Thesis, Department of Geosciences

Contemporary Geochemical characterization methods for reservoir core bitumen and oil – Application to samples from Mid-Norway and the Norwegian Barents Sea – Source Rock Facies and Maturity Assessment & Biodegradation effects as measured on Inclusion gas and Reservoir Oil samples

Muhammad Jamil

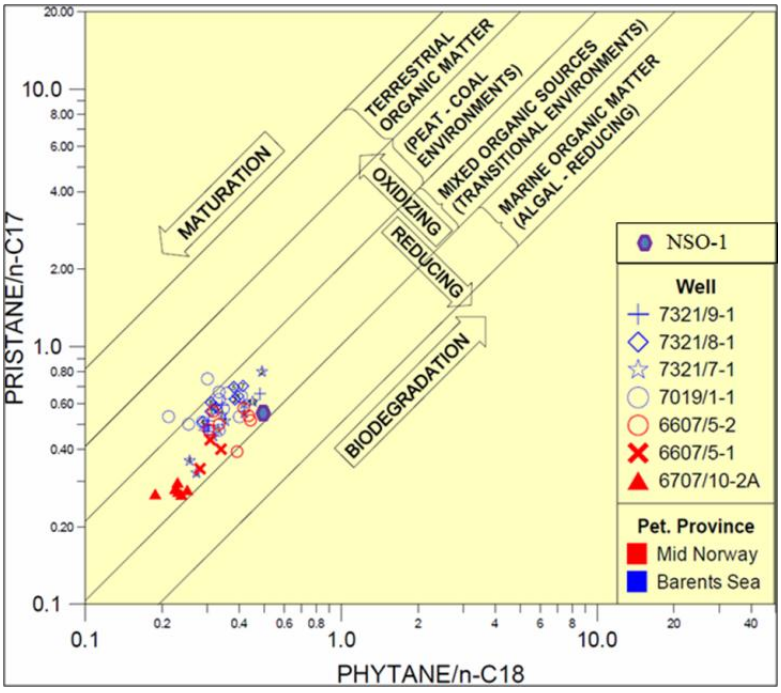

UNIVERSITY OF OSLO

FACULTY OF MATHEMATICS AND NATURAL SCIENCES

Contemporary Geochemical characterization methods for reservoir core bitumen and oil – Application to samples from Mid-Norway and the Norwegian Barents Sea – Source Rock Facies and Maturity Assessment & Biodegradation effects as measured on Inclusion gas and Reservoir Oil samples

Muhammad Jamil

Master Thesis in Geosciences
Discipline: Geology
Department of Geosciences
Faculty of Mathematics and Natural Sciences

University of Oslo
03.12.2012

Tutor(s): **Professor Dag A. Karlsen**

This work is published digitally through DUO – Digitale Utgivelser ved UiO

http://www.duo.uio.no

It is also catalogued in BIBSYS (http://www.bibsys.no/english)

Abstract

A total of seventy reservoir core samples from nine wells of the Mid-Norway and the Barents Shelf were geochemically analyzed to compare the composition, alteration effects, maturation and organic facies. The analytical techniques, like gas analysis from inclusions and TLC-FID of bitumen samples not only disclose the wet components of hydrocarbons in each well but also mention the parts of reservoir affected by biodegradation from relative fraction of each type of hydrocarbon compounds. The geochemical methods GC-FID, GC-MS reveal the organic facies for the selected wells along with their level of maturation.

Gases from inclusions of wells from the Mid-Norway suggested the condensate phase of petroleum at the time of generation shown by relatively dry gases from inclusions while higher wet gases in the Barents Sea indicate the oil system at the time of generation. Higher butane isomers ($i\text{-}C_4/n\text{-}C_4$) from gas inclusions and Iatroscan results discover palaeo-petroleum in the Utgard High owing to high polar fraction, whereas oil phase shown by dominance of saturated compounds in the Barents Sea samples except the well 7321/7-1 showing the alteration effects. The relatively more anoxic conditions prevailed in the samples from the Mid-Norway and lower maturity of the Barents Sea samples inferred from isoprenoids to normal alkane ratios. Mostly the samples from the Mid-Norway and the Barents Sea are labeled as typical Spekk (Hekkingen) marine facies noticed from concentration of steranes and aromatic hydrocarbons. The medium range parameters from GC-MS results define the maturation of samples commonly lie in medium oil window.

In addition, selected oil samples from the Norwegian Continental Shelf were studied to apply Thompson and Halpern parameters for light hydrocarbons to characterize the degree of transformation in various oils and correlation of source rock facies that generated the petroleum in these fields. Biodegradation is pronounced in the Heidrun, Gulfaks Sør and Goliat fields while evaporative fractionation predominates in Snøhvit and Midgard fields. Water washing effect can be observed in the Smørbukk and Ula fields. Most of the oils represent to be derived from the same organo facies (Draupne/Spekk/Hekkingen formations).

Acknowledgements

It is the mark of honour for me to pay faithful expression of thanks to ALLAH, whose generous benediction qualified me to accomplish my ambitions and exceptional tribute to Prophet Muhammad (PBUH), who is blessing for whole humanity.

I convey the expression of gratitude to my supervisor Professor Dag Arild Karlsen whose promising guidance and encouragement has been thought provoking during the present study. His immense counseling facilitates me to maintain the project on right track and enabled to complete the thesis in time. Through the entire thesis work, he has been very kind and was available for discussions all the time.

I am grateful to Tesfamariam Berhane Abay for introducing the lab work, managing the results and making the better look of manuscript with his constructive input. Thanks to Kristian Backer-Owe to allow independent lab work along with understanding the lab instruments and Kristin Dale for data on light hydrocarbons. I extend my acknowledgement to Norwegian Petroleum Directorate (NPD) for availability of core samples included in the present study.

The prayers, patience and great support of family especially my parents is indeed a vital factor for accomplishment of thesis. Their appreciation and guidance always act as momentum for the study. The essential role of Zafar Abbas and his family made me proficient for higher education. Thanks to Amdad Ali for support in crushing the core samples, Attiq Ur Rehman for reviews, Azeem Hussain for comments, Zeeshan Mohabbat & Arif Butt for suggestions. Opinions from Waqas Javed and Salman were useful in writing the document. Finally, I would like to acknowledge all the staff of Department of Geosciences to provide the opportunity of studying in world class research institute.

Muhammad Jamil.

Table of Contents

List of Figures

List of Tables

1. Introduction

Petroleum geochemistry incorporates both source rock geochemistry, oil and gas geochemistry and maturation of source rocks, also the timing of migration, the understanding of primary and secondary migration processes of oils, and processes associated with reservoir filling and production. These are all important elements and key factors for the exploration of oil and gas and to the development of reservoirs.

The petroleum geochemistry is of great importance when applied in combination with other methodologies like reservoir characterization and seismic stratigraphy (Peters and Fowler, 2002). The forecasting accuracy and efficiency of exploration based on geophysical and structural data increases significantly when prospects are evaluated by taking into account the geochemical parameters (Peters and Fowler, 2002). In the study of petroleum systems, the basinal distribution of petroleum is widely affected by episodes of migration in the past both concerning migration effectiveness and reservoir filling (Karlsen and Skeie 2006).

Petroleum geochemistry not only identifies the petroleum systems of the basin and helps in overall exploration risks but will also help to define the fluid flow and thermal maturity parameters for modeling determined by the secondary processes occurred during migration and entrapment of reservoirs. Hunt (1996) described petroleum geochemistry as the application of chemical principles in order to study the origin, migration, accumulation and alteration of petroleum and implementation of concepts for petroleum exploration and development.

The molecules or organic compounds produced by living organisms can be deposited in reducing sediments with insignificant or no alterations, (in general only removal of functional groups) and these are termed as biomarkers. Although they have very low concentration in the oils and condensates, these compounds deposited in specific environments and form specific precursor organisms, will be found in migrated petroleum and holds clues for understanding of the origin and migration of oil and condensates (Tissot and Welte, 1984).

The chemical properties of the biomarkers, which occur mostly in C_{26} to C_{35} region, with higher molecular weight have been applied in reservoir geochemistry to infer the maturation and migration routes of petroleum. The key components of a petroleum system can be

explained by geochemistry by estimating the generation and migration timing, extension and quality of reservoir and changes within the reservoir during production of hydrocarbons.

This is all based on good and thorough knowledge of geochemical techniques and methods. Today petroleum geochemistry is applying methodology from chemistry and the interpretation scheme are largely from organic geochemistry. It is necessary for a geologist to have a good knowledge of the methods applied to oil, condensates and source rocks to be able to interpret the results properly. For this reason, the target of this thesis was to learn several of contemporary analytical methods and to apply these methods to a suite of samples from the offshore Norwegian Continental Shelf. This is not a thesis to solve a specific geological problem in a region or in a field but the aim of the thesis is to focus on the study for several geochemical methods and interpretation schemes which are beneficial to petroleum geochemistry of oil, gas or reservoir rocks.

Reservoir core samples and oils from the wells at various localities from offshore Mid-Norway and from the Norwegian Barents Shelf were used to perform the geochemical analysis which today form the back-bone of modern petroleum system understanding in oil companies and service laboratories. The results of analytical work are displayed as chromatograms and in tables and commonly used interpretation diagrams using several geochemical parameters to infer the properties of the investigated petroleum phases, this could be gases in the inclusions, or field or reservoir bitumen samples from oil and sometimes dry wells.

This is all done to demonstrate applications of modern petroleum geochemical methodology in determination of the maturity and source rock facies of migrated petroleum (oil and gas) with also identification of alteration processes such as phase fractionation during migration and intra-reservoir biodegradation.

In this study, there is also an expression of the application of light hydrocarbons in oils and condensates which is an often neglected methodology compared to application of biomarkers and it is hoped that this work will display the application of Thompson and Halpern parameters, and how evaporative fractionation, biodegradation and water washing has affected the samples from the Norwegian Continental Shelf.

The comparative study of core samples including some oil samples from the Norwegian Continental Shelf emphasize on the following motives:

- To learn and apply geochemical methods to typical reservoir rock samples including whole oil samples using GC-FID and GC-MS methodologies.
- To determine commonly used organic facies and maturity parameters in C_{15}+ fractions of reservoir core samples from dry wells of the Mid-Norway and from the Barents Sea.
- To measure typical light hydrocarbon parameters on a suite of oil samples from the Norwegian Continental Shelf.
- To provide interpretation of datasets of reservoir core samples and oils concerning GC-FID and GC-MS methods with focus on source rock maturity and source rock organic facies for migrated bitumen.
- It is also a point of focus to look at evidences for biodegradation and water washing in the migrated petroleum as this phenomenon points to important geological processes which has affected the petroleum reservoir.

1.1 Dataset

A brief description of nine exploratory wells from the offshore Mid-Norway and the Norwegian Barents Sea are shown in Fig. 1.1. The core samples of all these wells were obtained from the Norwegian Petroleum Directorate (NPD). The Mid-Norway wells were selected from the Nyk High (6707/10-1, 6707/10-2A & 6707/10-2S) and the Utgard High (6607/5-1, 6607/5-2) as stated in factpages (NPD). All the studied wells from the offshore Mid-Norwegian Shelf were drilled in the Vøring Basin. The most of the Barents Sea wells were chosen from the Bjørnøya Basin. The other Barents Sea well 7019/1-1, selected for study, was drilled at the eastern margin of the Tromsø Basin (Seldal, 2005).

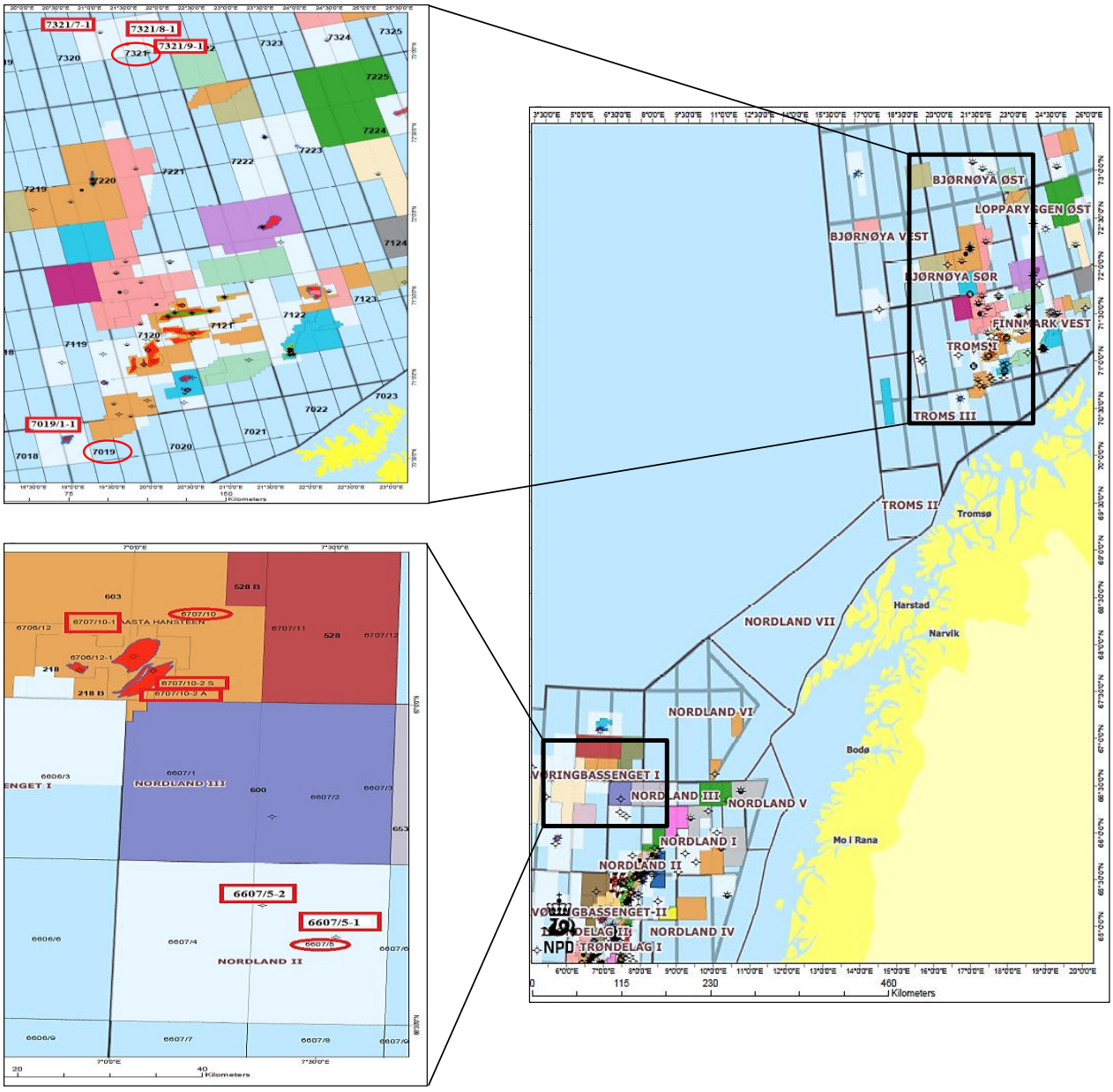

Figure 1.1 The Map of the study area of the Mid-Norway and the Barents Sea with regional overview of area. The wells are indicated by red rectangles and blocks numbers labeled with red ovals. Note that the scale for each map is different due to variation of zoom in level of the maps (modified from npdmap1, NPD).

The information related to each exploratory well from Mid-Norway which is included in the present study is mentioned in Tab. 1.1 whereas the description of studied wells from the Barents Sea is discussed in Tab. 1.2. In both tables, the geothermal gradient was also calculated to show the relative difference of temperature profiles between the two regions.

Table 1.1 The description of various wells from offshore Mid-Norway selected for present study. Note that these exploratory wells were drilled upto Creatceous resevoirs with relatively low geothermal gradients but with greater water depths than the Barents Sea wells (factpages, NPD).

Well Name	Drilling Operator	NS UTM	EW UTM	Entry Date	Completion Date	Oldest age penetrated	Oldest formation penetrated	Content	Water Depth	Total Depth	Final V. Depth	B.H. Temp.	Geo. Grad.
		(m)	(m)						(m)	(m)	(m)	(°C)	(°C/km)
6707/10-1	BP Norway limited U.A	7440629.70	413490.42	19.04.1997	23.07.1997	Late Cretaceous	Kvitnos Formation	Gas	1274	5039	5026.5	114	22.68
6707/10-2A	StatoilHydro ASA	4738113.36	415608.90	14.10.2008	01.12.2008	Late Cretaceous	Kvitnos Formation	Gas	1248	4850	4325	109	25.20
6707/10-2S	StatoilHydro ASA	7438113.36	415608.90	31.08.2008	13.10.2008	Late Cretaceous	Nise Formation	Gas	1248	3365	3356	86	25.55
6607/5-1	Esso EandP Norway A/S	7391750.71	435359.29	09.06.1987	11.09.1987	Late Cretaceous	Lange Formation	Dry	368	3817	3805	112	29.43
6607/5-2	Esso EandP Norway A/S	7397329.73	427403.49	07.08.1991	17.11.1991	Late Cretaceous	Kvitnos Formation	Dry	523	4684	4666	140	30.00

Table 1.2 The list of selected wells from the Norwegian Barents Shelf included in the study which were penetrating mostly into Mesozoic strata having some hydrocarbon shows. The geothermal gradient is relatively higher but drilled at shallower water levels than the studies wells from offshore Mid-Norway (factpages, NPD).

Well Name	Drilling Operator	NS UTM	EW UTM	Entry Date	Completion Date	Oldest age penetrated	Oldest formation penetrated	Content	Water Depth	Total Depth	Final V. Depth	B.H. Temp.	Geo. Grad.
		(m)	(m)						(m)	(m)	(m)	(°C)	(°C/km)
7019/1-1	Norsk Agip As	7869589.80	429692.26	06.10.2000	03.12.2000	Early Jurassic	Tubåen Formation	Gas	190	3003	2998	108	36.02
7321/7-1	Mobil Exploration Norway Inc.	8158249.22	311704.77	26.06.1988	22.10.1988	Middle Triassic	Snadd Formation	Gas shows	475	3550	3545	121	33.00
7321/8-1	Norsk Hydro Produksjon As	8146601.96	321501.02	23.06.1987	03.09.1987	Late Permian	Røye Formation	Shows	468	3482	3470	108	31.12
7321/9-1	Norsk Hydro Produksjon As	8138267.66	329361.05	25.10.1988	28.11.1988	Late Triassic	Snadd Formation	Shows	459	1800	1799	44	24.46

The core samples selected at various depths in each well have been studied to analyze the properties of bitumen extracts from core samples. The core samples were selected based on the criterian to have good quality sandstone samples available for analysis of migrated bitumen. Samples with some visible potential staining had already been selected and were available for this project.

Table 1.3 The core samples obtained at various depths from the Mid-Norwegian wells. The samples mostly consist of siliciclastic sandstone sediments representing the Late Cretaceous reservoir units and an attempt was made to select samples with visible bitumen staining. (factpages,NPD).

No.	Well	Depth	Description of core samples			Rock Formation	Formation Age
		(m)	colour	grain size	lithology		(Period)
1	6707/10-1	3023.65	Light grey	Fine to medium	Sandstone	Delfin Formation (Informal)	Late Cretaceous
2	6707/10-1	3035.50	Grey	Fine to medium	Sandstone	Delfin Formation (Informal)	Late Cretaceous
3	6707/10-1	3059.00	Grey	Fine to medium	Sandstone	Delfin Formation (Informal)	Late Cretaceous
4	6707/10-1	3082.70	Brownish grey	Fine to medium	Sandstone	Delfin Formation (Informal)	Late Cretaceous
5	6707/10-1	3112.25	Light grey	Fine to medium	Sandstone	Delfin Formation (Informal)	Late Cretaceous
6	6707/10-1	3114.00	Light grey	Fine to medium	Sandstone	Delfin Formation (Informal)	Late Cretaceous
7	6707/10-1	3125.00	Light grey	Fine to medium	Sandstone	Delfin Formation (Informal)	Late Cretaceous
8	6707/10-1	3140.65	Grey	Fine to medium	Sandstone	Delfin Formation (Informal)	Late Cretaceous
9	6707/10-1	3143.10	Grey	Fine to medium	Sandstone	Delfin Formation (Informal)	Late Cretaceous
10	6707/10-1	4122.25	Brownish grey	Fine to medium	Sandstone	Nise Formation	Late Cretaceous
11	6707/10-1	4131.35	Grey	Fine to medium	Sandstone	Nise Formation	Late Cretaceous
12	6707/10-2A	4460.25	Grey	Fine to medium	Sandstone	Kvitnos Formation	Late Cretaceous
13	6707/10-2A	4472.15	Light grey	Fine to medium	Sandstone	Kvitnos Formation	Late Cretaceous
14	6707/10-2A	4475.50	Grey	Fine to medium	Sandstone	Kvitnos Formation	Late Cretaceous
15	6707/10-2A	4482.60	Grey	Medium	Sandstone	Kvitnos Formation	Late Cretaceous
16	6707/10-2A	4485.45	Grey	Fine to medium	Sandstone	Kvitnos Formation	Late Cretaceous
17	6707/10-2A	4486.30	Grey	Medium	Sandstone	Kvitnos Formation	Late Cretaceous
18	6707/10-2S	3166.75	Grey	Fine to medium	Sandstone	Nise Formation	Late Cretaceous
19	6707/10-2S	3186.50	Grey	Fine	Sandstone	Nise Formation	Late Cretaceous
20	6707/10-2S	3202.45	Grey	Fine to medium	Sandstone	Nise Formation	Late Cretaceous
21	6707/10-2S	3206.00	Brownish grey	Fine to medium	Sandstone	Nise Formation	Late Cretaceous
22	6707/10-2S	3218.85	Grey	Fine to medium	Sandstone	Nise Formation	Late Cretaceous
23	6707/10-2S	3263.00	Dark grey	Fine to medium	Sandstone	Nise Formation	Late Cretaceous
24	6707/10-2S	3281.00	Grey	Fine to medium	Sandstone	Nise Formation	Late Cretaceous
25	6707/10-2S	3294.00	Grey	Fine to medium	Sandstone	Nise Formation	Late Cretaceous
26	6607/5-1	2979.00	Dark grey	Very fine to fine	Silty mudstone	Lysing Formation	Late Cretaceous
27	6607/5-1	2980.00	Dark grey	Very fine to fine	Silty mudstone	Lysing Formation	Late Cretaceous
28	6607/5-1	2982.00	Blackish Grey	Very fine to fine	Silty mudstone	Lysing Formation	Late Cretaceous
29	6607/5-2	4163.00	Brownish grey	Fine to medium	Sandstone	Delfin Formation (Informal)	Late Cretaceous
30	6607/5-2	4163.80	Light grey	Fine to medium	Sandstone	Delfin Formation (Informal)	Late Cretaceous
31	6607/5-2	4168.00	Grey	Medium	Sandstone	Delfin Formation (Informal)	Late Cretaceous
32	6607/5-2	4170.80	Light grey	Fine to medium	Sandstone	Delfin Formation (Informal)	Late Cretaceous
33	6607/5-2	4171.80	Light grey	Fine to medium	Sandstone	Delfin Formation (Informal)	Late Cretaceous
34	6607/5-2	4183.15	Grey	Fine to medium	Sandstone	Delfin Formation (Informal)	Late Cretaceous
35	6607/5-2	4187.60	Grey	Fine to medium	Sandstone	Delfin Formation (Informal)	Late Cretaceous

A sample from Oseberg (NSO-1) was included in dataset as reference. The information regarding each sample from the Mid-Norway is summarized in the Tab. 1.3.

Table 1.4 The representation of the core samples taken from Mesozoic units in vaious exploratory wells in the Barents Sea. Note that most of samples have good quality sandstone which seemed to have staining of bitumen in composition from Triassic, Jurassic and Cretaceous age of rock formations (factpages, NPD).

No.	Well	Depth	Description of core samples			Rock Formation	Formation Age
		(m)	Colour	Grain size	Lithology		(Period)
1	7019/1-1	2224.90	Brownish grey	Fine to medium	Sandstone	Knurr Formation	Early Cretaceous
2	7019/1-1	2225.40	Greyish Brown	Fine to medium	Sandstone	Knurr Formation	Early Cretaceous
3	7019/1-1	2226.65	Greyish Brown	Fine to medium	Sandstone	Knurr Formation	Early Cretaceous
4	7019/1-1	2227.65	Greyish Brown	Fine to medium	Sandstone	Knurr Formation	Early Cretaceous
5	7019/1-1	2457.00	Light grey	Fine to medium	Sandstone	Stø Formation	Middle Jurassic
6	7019/1-1	2459.0 A	Light grey	Fine to medium	Sandstone	Stø Formation	Middle Jurassic
7	7019/1-1	2459.0 B	Brownish grey	Medium	Sandstone	Stø Formation	Middle Jurassic
8	7019/1-1	2463.35	Light grey	Fine to medium	Sandstone	Stø Formation	Middle Jurassic
9	7019/1-1	2565.35	Light grey	Fine to medium	Sandstone	Stø Formation	Middle Jurassic
10	7019/1-1	2567.45	Light grey	Fine to medium	Sandstone	Stø Formation	Middle Jurassic
11	7321/7-1	1907.85	Greyish black	Very fine to fine	Silty sandstone	Knurr Formation	Early Cretaceous
12	7321/7-1	2003.20	Dark grey	Fine to medium	Silty sandstone	Stø Formation	Middle Jurassic
13	7321/7-1	2003.90	Grey	Fine to medium	Sandstone	Stø Formation	Middle Jurassic
14	7321/7-1	2005.85	Grey to dark grey	Fine to medium	Sandstone	Stø Formation	Middle Jurassic
15	7321/7-1	2006.40	Dark grey	Fine to medium	Sandstone	Stø Formation	Middle Jurassic
16	7321/7-1	2006.60	Brownish grey	Fine to medium	Sandstone	Stø Formation	Middle Jurassic
17	7321/7-1	2386.80	Light grey	Fine to medium	Sandstone	Snadd Formation	Middle Triassic
18	7321/7-1	2388.40	Light grey	Fine to medium	Sandstone	Snadd Formation	Middle Triassic
19	7321/7-1	2391.35	Light grey	Fine to medium	Sandstone	Snadd Formation	Middle Triassic
20	7321/7-1	2393.40	Light grey	Fine to medium	Sandstone	Snadd Formation	Middle Triassic
21	7321/8-1	1482.50	Light grey	Fine to medium	Sandstone	Fruholmen Formation	Late Triassic
22	7321/8-1	1490.00	Grey	Fine to medium	Sandstone	Fruholmen Formation	Late Triassic
23	7321/8-1	1497.20	Grey	Fine to medium	Sandstone	Fruholmen Formation	Late Triassic
24	7321/8-1	1501.00	Grey	Fine to medium	Sandstone	Fruholmen Formation	Late Triassic
25	7321/8-1	1501.30	Grey	Medium	Sandstone	Fruholmen Formation	Late Triassic
26	7321/8-1	1503.85	Light grey	Fine to medium	Sandstone	Fruholmen Formation	Late Triassic
27	7321/8-1	1505.00	Grey	Medium	Sandstone	Fruholmen Formation	Late Triassic
28	7321/8-1	1507.65	Light grey	Fine to medium	Sandstone	Fruholmen Formation	Late Triassic
29	7321/9-1	1376.50	Dark grey	Fine	Silty sandstone	Fuglen Formation	Late Jurassic
30	7321/9-1	1381.35	Grey	Fine to medium	Silty sandstone	Stø Formation	Middle Jurassic
31	7321/9-1	1382.00	Brownish grey	Fine	Silty sandstone	Stø Formation	Middle Jurassic
32	7321/9-1	1383.25	Light grey	Fine to medium	Sandstone	Stø Formation	Middle Jurassic
33	7321/9-1	1390.75	Grey to dark grey	Fine	Sandstone	Stø Formation	Middle Jurassic
34	7321/9-1	1393.70	Grey to dark grey	Fine	Sandstone	Stø Formation	Middle Jurassic
35	7321/9-1	1589.00	Brownish grey	Fine to medium	Sandstone	Snadd Formation	Middle Triassic

Samples from the Barents Sea were also collected to study potential genetic relationship and application of geochemical parameters to understand the maturity and facies relationship in that region. The reservoir core samples are from the Mesozoic sandstone sediments listed in Tab. 1.4 which also includes the rock formations for the samples.

In addition to core samples, some oil samples with chromatograms from the Haltenbanken area were selected from previous project (Dale, 1997) for the work on the light hydrocarbon parameters (Tab. 1.5). The light hydrocarbons are well suited for the study of biodegradation water washing and evaporative fractionation.

Table 1.5 Selected oil samples with chromatograms from the Norwegian Continental Shelf used for the light hydrocarbons work in this thesis. Sample no. 1 to 5 are from the North Sea, samples 6 to 18 represent the Haltenbanken region and 19-20 samples are from the Barents Sea (chromatograms from Dale, 1997).

No.	Field	Test	Well	Code
1	NSO-1	-	-	43978.00
2	Gyda	DST2	2/1-3	43980.00
3	Ula	DST2	7/12-6	43981.00
4	Hild	DST3	29/6-1	43982.00
5	Gulfaks Sør	DST2	34/10-16	43984.00
6	Tyrihans Sør	DST1	6407/1-2	43986.00
7	Midgard	DST1	6407/2-2	43990.00
8	Mikkel-1	DST1	6407/6-3	43993.00
9	Mikkel-2	DST3	6407/6-3	43995.00
10	Draugen-1	DST2	6407/9-2	43400.00
11	Draugen-2	DST1	6407/9-5	44001.00
12	Smørbukk-1	DST4	6506/11-2	44004.00
13	Smørbukk-2	DST5	6506/11-2	44005.00
14	Smørbukk-3	DST6	6506/11-2	44006.00
15	Smørbukk Sør-1	DST3	6506/12-3	44018.00
16	Smørbukk Sør-2	DST5	6506/12-3	44020.00
17	Smørbukk Sør-3	DST6	6506/12-3	44021.00
18	Heidrun	DST2	6507/7-3	44043.00
19	Goliat	-	-	Goliat
20	Snøhvit	-	-	Snøhvit

2. Geological Settings

The core samples from Nyk and Utgrad off Mid-Norway and the samples from the Norwegian Barents Sea regions were selected to study the geochemical properties of bitumen from reservoir units. The geological settings of both these regions are discussed separately as follows:

2.1 The Mid-Norway

2.1.1 Introduction

The passive continental margin of the Mid-Norway extends from 62° to 69°30'. The structural style of the Mid-Norway was developed as a result of tectonic activity which influenced since Permo-Carboniferous times (Bukovics and Ziegler, 1985). The formation of supercontinent occurred by the collision of the Baltican and Laurentian plates in Silurian-Devonian of Paleozoic era. Thus, the basement underneath the current Mesozoic sedimentary strata was produced during Caledonian orogeny. The breakup of Pangaea during Late Paleozoic to Early Triassic resulted in the rifting of continents and extension of crust, while the second phase of extension happened in Late Jurassic to Early Cretaceous when the Norwegian Continental Shelf was filled by marine sediments containing source and reservoir units. The final rifting event cause the formation of oceanic crust by sea floor spreading and opening of the Norwegian Greenland Sea in Early Cenozoic time (Faleide et al., 2008).

The portion of the Norwegian Continental Shelf represented in this study, which is 250 km offshore Mid-Norway (Knaust, 2009) includes the Nyk High (well 6707/10-1, 6707/10-2A, 6707/10-2S) and two wells from the Utgard High (6607/5-1 and 6607/5-2). Both highs are the part of the Vøring Basin as presented in Fig. 2.1 and wells from the Utgard High are dry while the well 6707/10-1 contains gas and called as Nyk discovery well.

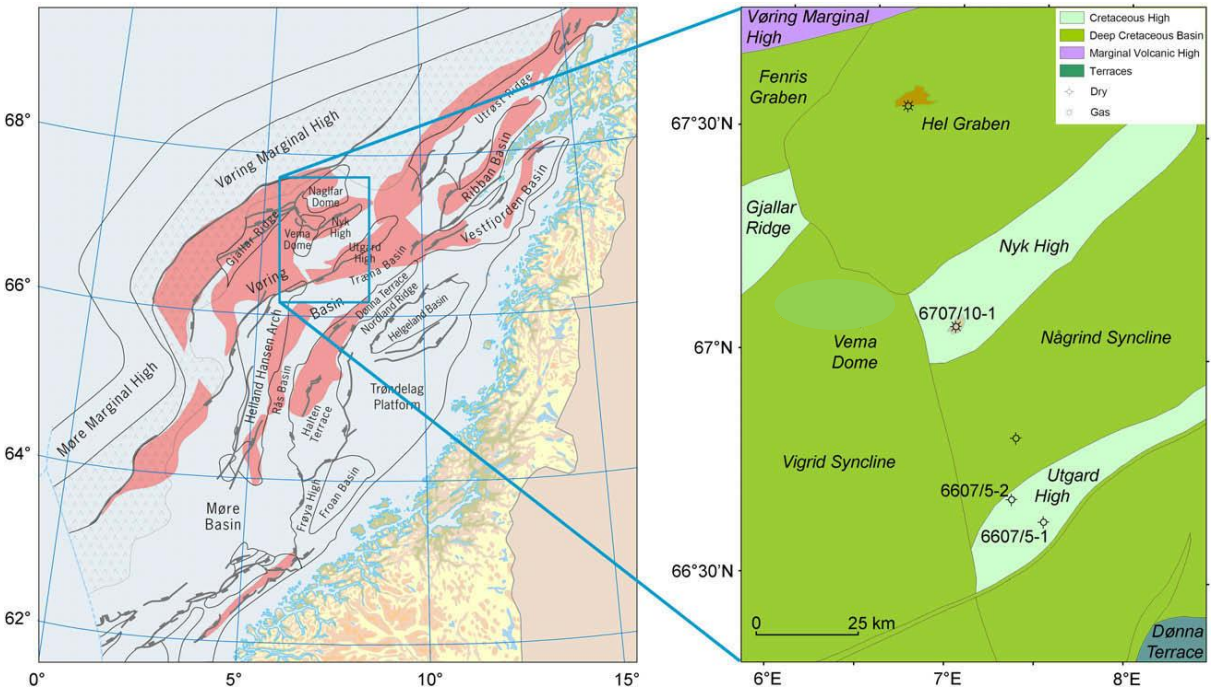

Figure 2.1 Regional map of a part of the offshore Mid-Norway region including the Vøring Basin with reservoir units of Upper Cretaceous rocks and also the studied wells (6707/10-1, 6607/5-1 and 6607/5-2) located in the Vøring Basin (Knaust, 2009). The Dønna Terrace is located in the East of Vøring Basin while Vøring Marginal High marks the western limit.

2.1.2 Structural and tectonic settings

The two significant tectonic activities including Carboniferous to Permian rifting and Caledonian orogeny which account for major development of the Mid-Norway in the Paleozoic time. After the closure of Iapetus and collision of two plates (Laurentia and Baltica) in Ordovician-Early Devonian period, the mountain chain was formed which later collapsed in Middle Devonian (Blystad et al., 1995). A palaeozoic Devonian based source rock system may exist from this period in the Hegeland Basin (Karlsen et al., 1995). In the Norwegian Sea, the extensional phase over-ruled in Late Permian to Early Triassic period that is intimated by the breakup of supercontinent. During Triassic period, the continental and marine environments simultaneously prevailed over the lowland area of the Norwegian-Greenland Sea and the basins received clastic input from Scandinavian Caledonites (Smelror et al., 2007).

The thick successions of alluvial conglomerates, sandstones and fine grained clastics were deposited in Middle Triassic to Early Jurassic rifting resulting from uplift and erosion

(Smelror et al., 2007; Gabrielsen et al., 2010). The second extension regime initiated in Late Jurassic period resulted in formation of horst and graben province in the North Sea and the Mid-Norwegian Shelf. The Vøring and Møre basins were developed in the region that was proceedingly influenced by erosion and exhumation (Smelror et al., 2007). The faulting continued in earliest Cretaceous followed by subsidence of crust and deposition of thick successions of deep marine sandstone turbidites in various places of the Mid-Norway. Major uplifting occurred in Late Cretaceous-Early Paleocene that resulted in erosion of the basin margins and platform regions (Blystad et al., 1995; Smelror et al., 2007).

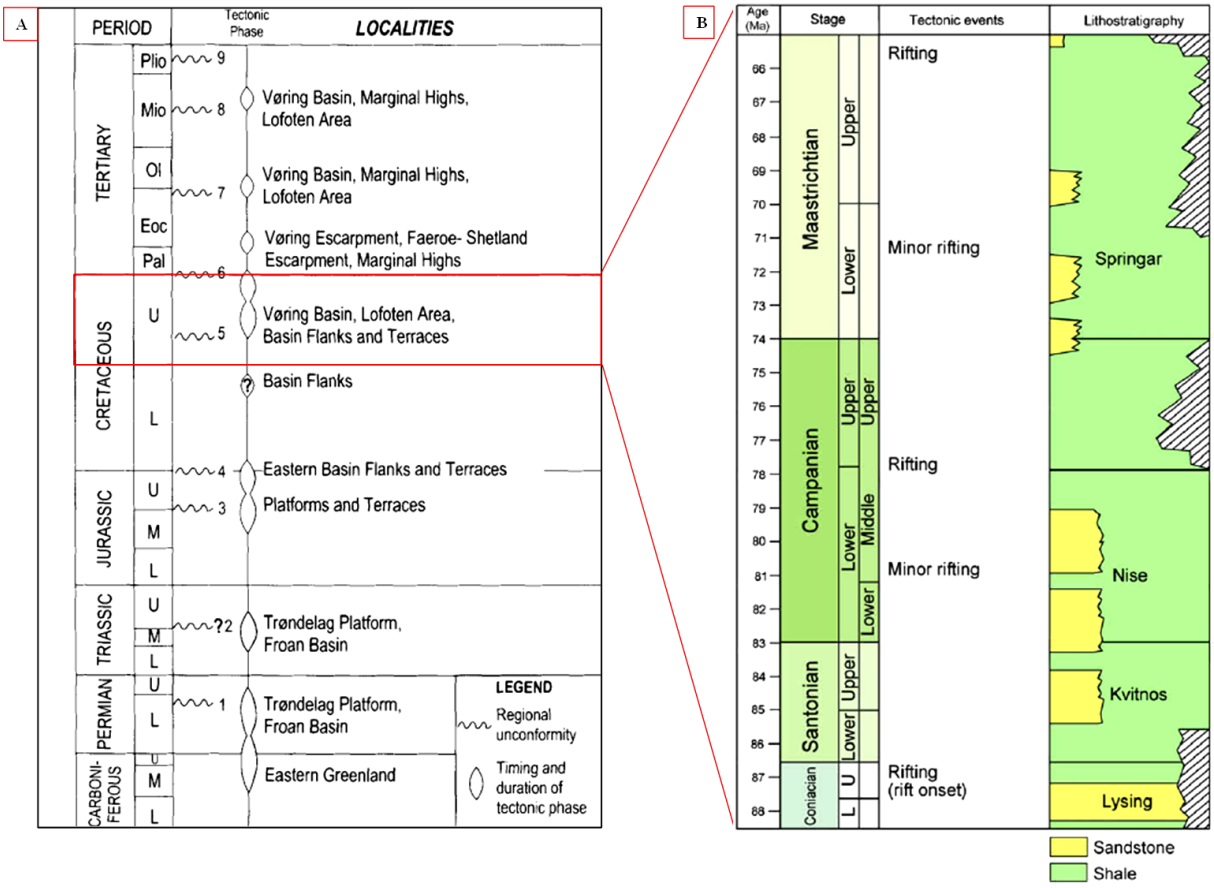

Figure 2.2 Tectonic development of the Norwegian Continental Shelf (A) and tectonic events emphasizing the Upper Cretaceous (B). The duration of each tectonic event and unconformable surfaces are mentioned with respect to age in this diagram (Brekke, 2000) whereas lithology (sandstone and shale) and stratigraphy (Lysing, Nise and Kvitnos formations) are also illustrated in (B) part of the figure (from Knaust, 2009).

The Vøring Basin was tectonically dynamic in Late Cretaceous and act as rift basin alongwith widespread rifting of the Norwegian-Greenland Sea (Ren et al., 2003). Major uncertainities exist as to the existence in this region of Cretaceous source rock of the type known from Greenland. The rifting of Vøring Basin is described in Fig. 2.2 which points the onset of rifting in start of Late Cretaceous along with minor rifting events and major rifting phases.

In Early Paleocene, the extension of crust proceeded and attained its peak in Early Eocene with breakup of continent and opening of the Norwegian Greenland Sea. The present continental margin is the resultant of outbuilding of large sediment deposition from mainland Norway (Faleide et al., 2010). The development of sill intrusive bodies, lava deposits and associated magmatism in the Vøring Basin, was at the highest level prior to and during the splitting of the Norway-Greenland continents (Henriksen et al., 2005). The first phase of compression initiated at eastern margin basins of the Norwegian Sea while a second compression was evident in Middle Miocene (Doré and Lundin, 1996; Smelror et al., 2007). The deposition of fine grained sediments in the Vøring Basin prevalent after second stage of compression with filling of sediments at the end of Miocene. Finally, glacial activity in Pleistocene eroded and deposited the sediments in the Norwegian Shelf (Brekke et al., 2001; Smelror et al, 2007).

2.1.3 Stratigraphy of the Mid-Norway

The exploration history of the offshore Mid-Norway was reaching a high point in 1981 with the discovery of the Midgard Field and drilling produced data of tertiary and Mesozoic strata including Triassic deposits; however, the information regarding pre-Triassic strata was limited at this point (Dalland et al., 1988). Whereas, the deposition of continental sediments in Middle Triassic to Early Jurassic times was evident form the Trøndelag Platform and the Halten Terrace. The Åre Formation contains evaporite succession, red beds which were overlain by clastic deposits of coal bearing delta plain facies (Whitley, 1992). The Jurassic strata of the Båt Group comprise sandstones with siltstone and shale alternated units in the Trøndelag Platform and the Halten Terrace (Dalland et al., 1988).

Shallow marine environments prevailed during the deposition of the Åre, Tilje, Ror and Tofte formations which together made the Båt Group (Dalland et al., 1988). Mainly sandstone and clay with interbedding of coaly claystone (having great source potential) and coal formed the

Åre Formation (Heum et al., 1986; Forbes et al., 1991). The sand content greatly increases in the Tilje Formation consisting of only fine to coarse grained sandstone with shale and siltstone interbedding (Dalland et al., 1988) whereas, coarse grained sandstone of the Tofte Formation has been deposited only in the western part of the Halten Terrace. Grey to dark grey mudstone along with interbedding of sand and silt formed the Ror Formation where coarsening upward sequence is present in sand and silt units (Dalland et al., 1988).

Table 2.1 Major source and reservoir units of the offshore Mid-Norway (Patience, 2003). The table not only explains the stratigraphical division of several rock formations in their groups with respect to age but also mentions the petroleum potential of each formation.

Age	Group	Formation	Pet. Potential
TERTIARY	Nordland	Naust	
		Kai	
	Hordland	Brygge	
	Rogaland	Tare	
		Tang	
CRETACEOUS	Shetland	Springer	
		Nise	
		Kvitnos	
	Cromer Knoll	Lysing	Reservoir
		Lange	Reservoir
		Lyr	
JURASSIC	Viking	Spekk	Source
		Rogn	Reservoir
		Melke	Source
	Fangst	Garn	Reservoir
		Not	
		Ile	Reservoir
	Båt	Ror	
		Tofte	Reservoir
		Tilje	Reservoir
		Åre	Source/ Reservoir

Middle Jurassic sedimentary deposits of the Fangst Group are commonly correlated with the Brent Group of the North Sea. As a result of regression, the Ile Formation,the Not Formation

and the Garn Formation, constituting the Fangst Group, were deposited (Ehrenberg et al., 1992). Fine to medium grained sandstone laminated with siltstone and shale of the Ile Formation, having good reservoir properties (as shown in Tab. 2.1), deposited over the entire Haltenbanken region while normally towards East the units thins out on the Trøndelag Platform (Dalland et al., 1988).

The bioturbated mica rich, carbonate cemented sandstones units along with claystone define the Not Formation that has no correlative unit in the North Sea. Most parts of the Haltenbanken region contains good to excellent reservoir (Heum et al., 1986) that is well sorted, medium to coarse grained sandstone of Garn Formation that may only be absent from structural highs because of erosion (Dalland et al., 1988).

The Viking Group was deposited under marine conditions and contains three formations namely the Melke, the Spekk and the Rogn Formations where the moderately organic rich (TOC upto 4%) Melke Formation (Ehrenberg et al., 1992) of open marine environment is mainly comprised grey to dark brown calystones with interbedding of limestone and siltstone but the formation is not a proven source rock in the Haltenbanken area (Heum et al., 1986). With high organic type II kerogen, the dark brown to grey shale of the Spekk Formation was deposited over the entire Haltenbanken region but may absent from structural highs. It formed under anoxic bottom water conditions and is equivalent to the Draupne Formation in the Norwegian North Sea (Dalland et al., 1988). The shallow marine sand bar deposits of the Rogn Formation comprised siltstone and coarsening upward sequences from shale to sandstone with upward decrease in clay content and makes a good reservoir (Dalland et al., 1988; Patience, 2003). The Comer Knoll and the Shetland Groups containing shale with few turbiditic sandstone deposits were preserved in shallow to deep marine environments during the Cretaceous period (Ehrenberg et al., 1992). The Tertiary claystone deposits form the Rogaland and Hordaland Groups in the Haltenbanken region while the Kai formation of the Nordland Group marks an unconformable contact with underlying Paleogene sedimentary strata. During Late Pliocene times, the Naust Formation containing alternate shale and poorly sorted sandstone was deposited over the Haltenbanken region (Ehrenberg et al., 1992).

The Vøring Basin

The Vøring Basin is an essential part of the Norwegian passive margin (Bjørnseth et al., 1997) and constitutes a large sedimentary basin located from 64° to 68°N and 2° to 10°E containing

structural highs, grabens and sub-basins. The Vøring escarpment along the Vøring Marginal High marks the western boundary of the Vøring Basin (Fig. 2.3), whereas the eastern boundary is defined by the Trøndelag Platform. The Bivorst lineament in the North and the Jan Mayen lineament in the South identify the boundary of the basin while in Paleocene-Eocene; the mafic sills intruded the Vøring basin (Bukovics and Ziegler, 1985; Blystad et al., 1995; Brekke, 2000).

Many sub-basin and structural highs form the Vøring Basin of which most distinguish is the Helland Hansen Arch developed during Cenozoic compressional tectonics, present in the central southern part of the basin. On the western side of the Nordland ridge, there lies the important petroleum province of the Dønna Terrace which is also part of the Vøring Basin. Many lineaments and faults cut the Vøring Basin (Blystad et al., 1995).

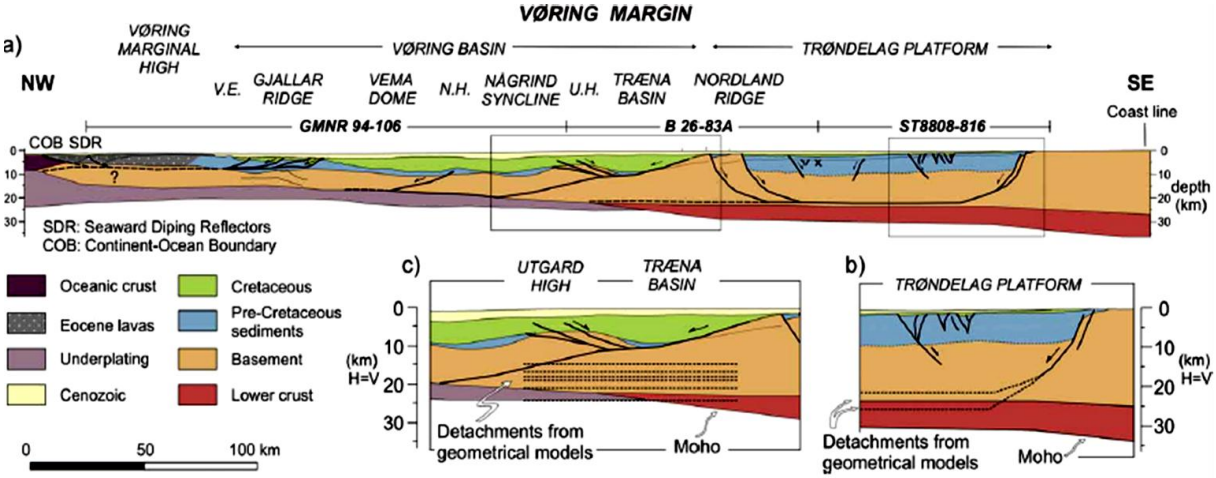

Figure 2.3 Recent geological section of the Vøring Margin (Gomez et al., 2004). The Utgard High (U.H) and Nyk High (N.H.) are separated by Någrind Syncline while the Vøring Escarpment (V.E.) and Trøndelag Platform mark the boundaries of the Vøring Basin. The structural elements of Vøring Margin are explained in part "a" of the figure whereas the stratigraphic deposition and structures of Trøndelag Platform is marked in part "b" of the figure. The strucutures present in the Cretaceous sediments and basement in the Utgard High is described in part "c" of the figure.

2.1.4 Petroleum system of the Mid-Norway

Source rocks

In the Mid-Norway region, three major rock units of Jurassic age have been identified as organic rich source rocks (Tab. 2.1) namely the Spekk, the Melke and the Åre formations (Karlsen et al., 2004; Karlsen and Skeie, 2006). The maturity of Lower Jurassic Åre Formation increases as we move from the East towards the West in the Vøring Basin. In Early Triassic period, the Åre formation achieved the oil generation window in region of the Halten Terrace (Campbell and Ormamassen, 1987; Karlsen et al., 1995). According to Karlsen et al., (1995), the Åre formation in the Midgard and the Draugen fields has been contemplated as immature.

The shale units with silt and clay intercalations represent the organic rich Melke formation (having 1 to 4 % TOC), but the Melke Formation has unsubstantial oil potential than Spekk and Åre formations (Heum et al., 1986; Cohen et al., 1987). The Spekk formation of Late Jurassic age is considered to be thick and relatively mature in the region except the eastern area of the Trøndelag Platform while it becomes over mature towards the West in the Vøring Basin (Karlsen et al., 1995).

Reservoir rocks

Faleide et al., (2010) stated the sand units with alternate shale layers of Early and Middle Jurassic age named as Åre, Tilje, Tofte, Ile and Garn formations are believed to be reservoir rocks in the offshore Mid-Norway region (Tab. 2.1). These formations constitute the Jurassic Fangst Group in the Smørbukk and Heidrun fileds as reservoir whereas; the reservoirs in the Njord Field appertained to the Båt Group. Karlsen et al., (1995) suggested that only one formation (Rogn Formation) of Late Jurassic age has been considered to be reservoir in Darugen Field.

Traps

According to Faleide et al., (2010), the rotated fault blocks in horst and graben system of Jurassic age acted as trap in the Halten region, where these structures were conceived by extensional tectonics but the upwelling of salt in Triassic period resulted in some salt induced structures that formed the Smørbukk Sør and Tyrihans South Field (Jackson and Hastings, 1986; Karlsen et al., 1995) whilst towards the East (Trøndelag Platform) the mechanism of

trapping had failed to occur and in the Draugen Field and hydrocarbons were trapped in the gentle anticlinal structures (Provan et al., 1992; Karlsen et al., 1995).

2.2 The Barents Sea

2.2.1 Introduction

The Barents Sea has considerably large area (245,000 sq. km) than the Norwegian North Sea which has surface area of 130,000 sq. km. Furthermore, the rate of success is one in three wells in the Norwegian Barents Sea which is higher than for the Norwegian North Sea with reference to the number of dry wells before the first commercial recovery (Ohm et al., 2008). Moreover, the multiple source rock intervals at various stratigraphic levels underline the multi-source rock aspect of the Barents Sea in contrast to the North Sea having only one Kimmeridge Shale source rock that is equivalent to the Hekkingen Formation. The less commercial status was attributed to the Barents Sea which results in expansion of gas, forcing oil out of traps. Nevertheless, the oil discoveries in the Goliat and the Skrugard suggested the need for refined exploration models for the Barents Sea.

The Barents Sea covers the northwestern part of the Eurasian Continental Shelf which was formed by collision of two continents, followed by younger continental separations. The northern and western margin of the Barents Sea is relatively younger and passive which were formed by the opening of the Norwegian-Greenland Sea and Eurasian Basin while the northern part of mainland Norway delineates the Barents Sea to the South and Novaya Zemlya to the East (Faleide et al., 1993).

2.2.2 Structural and tectonic settings

Fault complexes, mosaic of basins and intra-basinal highs structurally composed the Barents Sea. The shaping of main structural trends took place in the Devonian while Caledonian orogeny itself must be linked by some significant features (Gabrielsen et al., 1990). In Late Silurian- Early Devonian times, the thick continental clastic succession is the result of erosion followed the Caledonian orogeny deposited the Old Red Sandstone (Dengo and Røssland, 1992). Towards the southeast of Bjørnøya, there could be post-Caledonian extensional collapse field analogue of collapse that might have taken place in Devonian Graben of the

Spitsbergen (Gudlaugsson et al., 1998). Nevertheless, such types of grabens are not present in the SW Barents Shelf (Johansen et al., 1994).

According to Faleide et al., (2010), three rifting periods (which encompass several short-lived tectonic events) were identified in Late Devonian-Carboniferous, Middle Jurassic-Early Cretaceous and finally in the Early Tertiary which operated the geological evolution of the western Barents Sea. Steel and Worsely (1984) suggested the formation of half graben structures which accommodate the depocentres for the floodplain and alluvial fan along with the carbonates. The Hammerfest, Tromsø, Bjørnøya, and Nordkapp basins were formed by half graben structures (Dengo and Røssland, 1992). The movement along sinistral strike-slip fault in the western Barents Sea and a conjugate dextral strike slip fault in the central Barents Sea evolve the first rifting phase in the western Barents Sea (Faleide et al., 1984). Whereas, the Barents Sea has relatively less active tectonics in northeastern and eastern part while in the Mesozoic and Cenozoic period, there is throughout deformation phase in the western part of the Barents Sea as stated by Gabrielsen et al., (1990).

The major structural architecture of the Barents Sea could be the result of structural features developed in Late Paleozoic time whereas the period of Triassic to Early Jurassic was marked as calmness of tectonics while subsidence was continued in the eastern Barents Shelf during this time (Gabrielsen et al., 1990). However, during Late Jurassic-Early Cretaceous time, the initiation of rifting took place between the Greenland and the Norway where the Loppa High is dominated by major zone of deformation (Dengo and Røssland, 1992). A high rate of tectonic subsidence, in Early Cretaceous period, is evident from the Tromsø Basin and western portion of the Bjørnøya Basin (Gabrielsen et al., 1990).

The opening of Arctic and North Atlantic Ocean related with the deformation that happened to be in Tertiary period at the Paleocene-Eocene changeover, the breakup of continents transpired (Faleide et al., 1993). A regional uplift was experienced by the western Barents Shelf since Mid-Miocene (Dengo and Røssland, 1992).

2.2.3 Stratigraphic succession

Gudlaugsson et al., (1998) stated that relatively thick and considerably complete strata from Late Paleozoic to Quaternary time constitute the stratigraphy of the Barents Sea but the

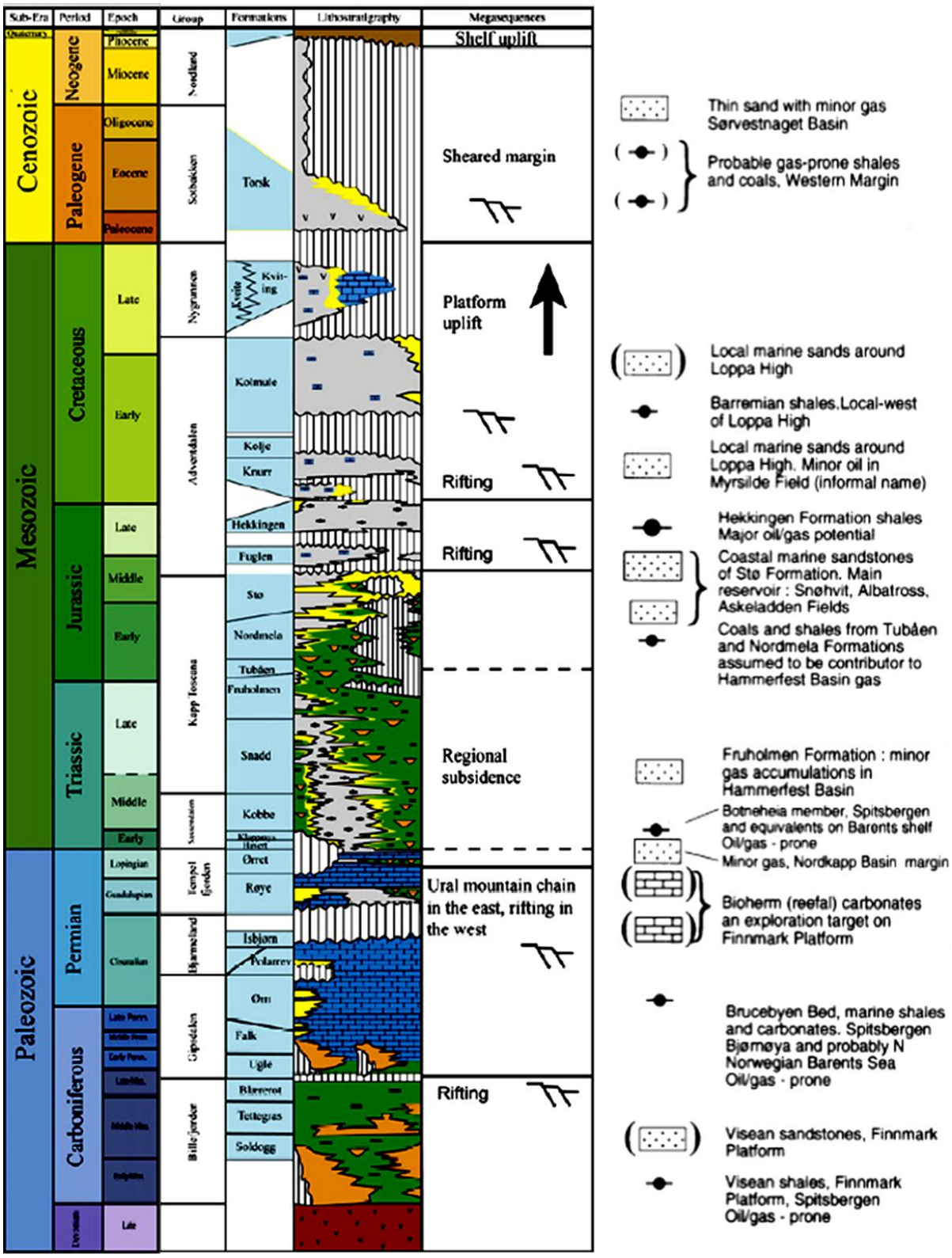

Figure 2.4 Stratigraphy (Glorstad-Clark et al., 2010) and petroleum potential of the Norwegian Barents Sea (Dore, 1995). The source units are symbolized by the lines in the filled circles where the size of black circles define the source potential and boxes filled with dots represent sandstone reservoir while bricks in the boxes point out the carbonate reservoirs.

thickness and facies vary laterally and vertically (Fig. 2.4). The stratigraphic succession is comprised mixed clastics, carbonates as well as the evaporites of the Late Paleozoic era covered by clastic sedimentary rocks of the Mesozoic and Cenozoic era (Faleide et al., 2010). The Permo-Carboniferous rocks in the Barents Sea extend throughout in the Bjørnøya, NE Greenland and Svalbard where the wellbore drilled had penetrated up to Permian deposits. Deposition of considerable transgressive-regressive successions of Triassic rocks is present throughout the Barents Sea while Lower-Middle Jurassic sandstones are existent along the Hammerfest Basin while thickness of the sandstones extends towards the Tromsø Basin (Faleide et al., 1993).

The sedimentation during Middle to Late Jurassic was much related to rift settings where deposition of shales and clays was preponderant while marly limestone subordinated along with rare deposition of sandstone and siltstone which depicted the environment of basin was deep at that time (Faleide et al., 1993). During Cretaceous period, there was open marine deep shelf environment which is represented by deposition of only shales and claystone in the Tromsø Basin whereas it alters to calcareous dominated in the Hammerfest Basin, indicating shelf environment with starvation of detrital material (Faleide et al., 1993; Worsley, 2008). Thin interbedded siltstone, carbonates and tuff mark the open to deep marine shelf environment in Paleogene time. Although the lower Paleogene deposits have great lateral variation, the unit extends throughout the southwestern Barents Sea. The strata younger than Plaeogene is only present in the Tromsø and Harstad Basins (Faleide et al., 1993).

The Tromsø Basin

In the North of town of Tromsø, there lies the Tromsø Basin that extends from 71° to 72°15’N and 17°30’ to 19°50’E where the Senja Ridge lies towards West while eastern boundary is marked by the Ringvassøy-Loppa Fault complex and Troms-Finnmark Fault Complex defines the southeastern boundary but southwestern limit is less understood. Inter-basinal high separates the Tromsø Basin from the Bjørnøya Basin in the North (Gabrielsen et al., 1990). The structural feature of the Tromsø Basin trends NNE-SSW that accommodate variety of salt diapirs linked by smooth flexure (Fig. 2.5) and arrangement of detachment fault relates them (Gabrielsen et al., 1990).

In Late Triassic to Early Jurassic period, the Tromsø, Bjørnøya and Hammerfest basins constitute an entire basin while the Tromsø Basin separated from the Hammerfest in Early

Cretaceous time (Gabrielsen et al., 1990). But in the North there is indication of a separate Tromsø Basin, coupled with the Bjørnøya Basin in Paleozoic time and separated by horizontal movement along the Bjørnøyrenna Fault Complex in the Early Cretaceous period. The activity of faulting is limited only in Eocene, and at later time there is in the form of halokinesis (Gabrielsen et al., 1990) which played a considerable role in developing the structures in the Tromsø Basin. Nonetheless, the evolution of the Tromsø Basin in the Mesozoic and Cenozoic era can be account for large-scale extension (Hanisch, 1984) or shear movements (Gabrielsen et al., 1990) that suggested the break up position of the crust.

The Bjørnøya Basin

The location of the Bjørnøya Basin is more or less from 32°30'N to 74°N (NS direction) and 18°E to 22°E (WE direction). The depth of basin generally increases towards the West as shown in Fig. 2.5 (Faliede et al., 1984; Gabrielsen et al., 1990; Faleide et al., 2010). In the Late Jurassic – Early Cretaceous period, the Bjørnøya Basin originated due to the rifting that generates NE-SW trending structures. The rifting was followed by subsidence and resulted in the development of the space for the deposition of sediments (Gabrielsen et al., 1990). Deep Cretaceous and Cenozoic sediments filled the basin (Faleide et al., 1993) like other basins of the Harstad, Tromsø and Sørvestsnaget, while at different rates for all these basins. The depth of the crystalline basement is suggested at be about 18 to 20km which is quite similar to adjoining the Tromsø Basin (Gabrielsen et al., 1997).

The Fingerdjupet Sub-basin in the Bjørnøya area

The shallow Fingerdjupt sub-basin constitutes the northeastern part of the Bjørnøya Basin (Fig. 2.5) which was formed in the Bjørnøya Basin in Early Cretaceous period by tectonic events of extension. The sub-basin is bounded to the East by the Loppa High and Bjarmeland Platform while western part is limited by the Leirdjupt Fault Complex (Gabreilsen et al., 1990). The history of the Fingerdjupt Sub-basin is quite similar to that of the Loppa High and Stappen High except for the thick Permian deposits exist in Fingerdjupt sub-basin, while in Late Tertiary, owing to erosion, at least 2000m strata was removes that made it hard to know about the Tertiary deposits (Gabreilsen et al., 1990).

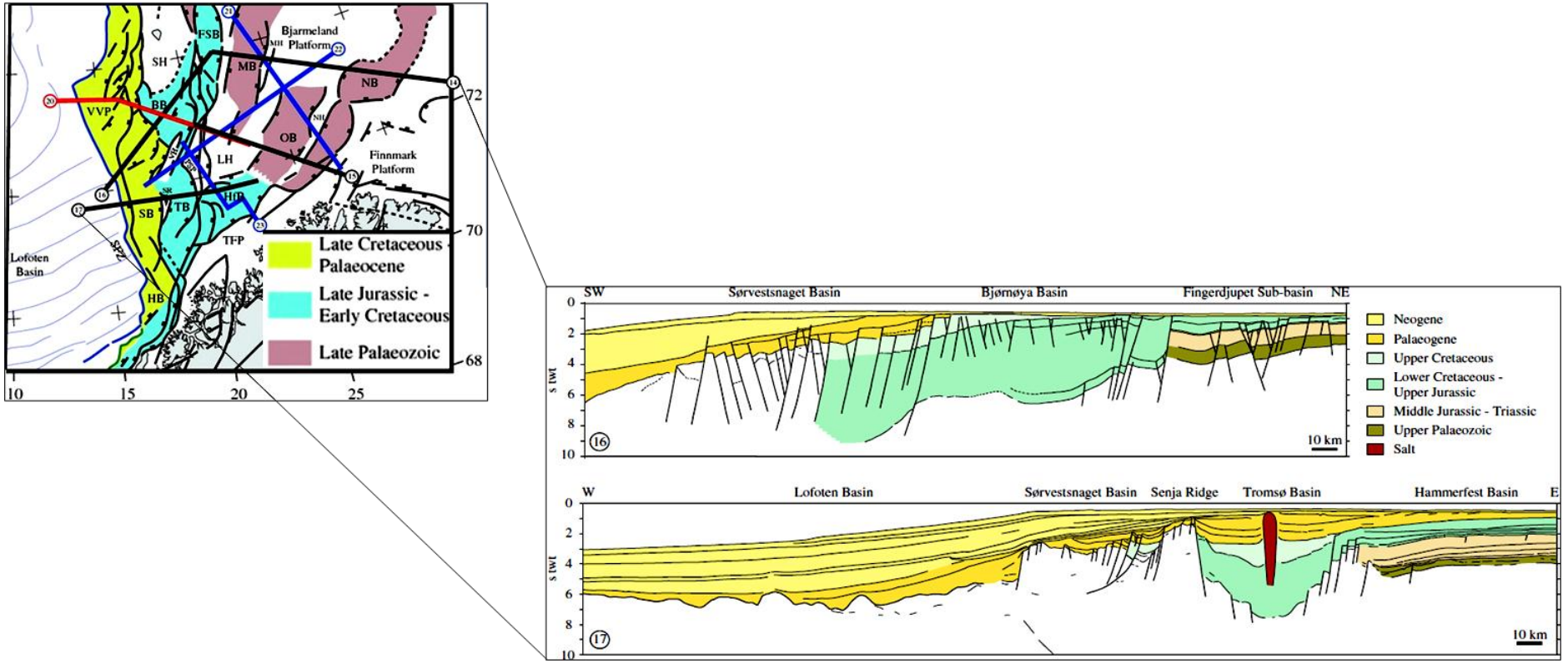

Figure 2.5 Stratigraphy and structural elements of Fingerdjupet Sub-basin and Tromsø basin in Norwegian Barents Sea (modified from Faleide et al., 2010).

2.2.4 Petroleum system of the Barents Sea

An active source rock and genetically related oil or gas accumulation constitutes the petroleum system which incorporates all the geological processes and elements imperative for hydrocarbons accumulation for instance source, reservoir and cap rock along with overburden and trap formation, generation and migration and finally accumulation of hydrocarbons. Timing and space for all these events play a fundamental role to the formation of petroleum system. Tertiary migration of hydrocarbons from the traps was provoked by different events of erosion and uplift in Cenozoic era, consequently affecting the petroleum system of the Barents Sea making less production potential for hydrocarbons by displacing the hydrocarbon kitchen to the shallower level. Several source and reservoir intervals are recapitulated by Dore (1995) as shown in Fig. 2.4.

Source rock

The kerogen (organic matter) rich rock unit, capable of producing hydrocarbons (oil or gas or both) when adequate burial temperature in a sedimentary basin is encountered is termed as source rock. In the Barents Sea, the most widely distributed source rock is the dark organic rich shale of the Hekkingen Formation (equivalent to the Kimmeridge Shale of the North Sea), belonging to the Adventalen Group and deposited in deep marine anoxic settings (Dalland et al., 1988). The hydrocarbon potential and total organic carbon (TOC) are very high in the Hekkingen Formation (Fig. 2.4) than the deeper marine Fuglen Formation. The rock units present in the Nordmela, Snadd, Kobbe and Tubåen formations may indicate some potential of acting as source in Permian period (Ohm et al., 2008).

The maturity of the Hekkingen Formation in the Nordkapp Basin is influenced by the high thermal conductivity of salt in the region. The generation of Hydrocarbons is negatively influenced by the exhumation and erosion. Nevertheless, the aspect of live petroleum systems is enhanced by the clue of cogenetic gas in the Barents Sea. The cooling of source rock as a result of uplift, impact severly on the generation of oil and gas in the central parts of the Barents Sea, but uplift could conceivably result in re-migration of oil and gas up-dip (Ohm et al., 2008).

Reservoir units

The Klappmyss, Kobbe, Snadd, Fruholmen and Tubåen Formations are major reservoir rocks in the Barents Sea region (Fig. 2.4). The lithostratigraphy of the Tubåen formation was described by Dalland et al., (1988) as resulting from high energy marginal marine sandstone dominated with shale and minor amounts of coal that could represent tide-dominated barrier complexes or estaurine environments. The Fruholmen Formation of the Kap Toscana Group represents rather open marine shale with fluvial or coastal sandstone.

In addition, the Kap Toscana Group also contain the reservoir unit of the Snadd Formation comprising shales and some interbeds of sandstone and siltstone while limestone and calcareous only interbed in middle and lower part representing distal marine facies. Basal shaley strata of the Kobbe Formation are mainly interbedded with siltstones and carbonate sandstones while open marine dark grey shales of coarsening upward successions commonly occur interbedded with siltstone, sandstone and shale have some coastal progradation towards the North.

Trap

The uplift and erosion initiated tertiary migration of hydrocarbons and drastically affected the sealing capacity of cap rocks in the region. Major cap rocks situated near the flanks of the basin are generally faulted and thinner (reducing the sealing potential) than the same rock units acting as cap in the centre of the basin (Ohm et al., 2008). The base of the Snadd Formation proves to be poor cap rock as Snadd Formation is relatively coarser than cap rock unit of the Fuglen Formation whereas the strata of the Fuglen Formation found to bear good sealing capability.

3. Analytical Methods and Parameters

3.1 Introduction

The geochemical properties of samples, either rock or oil, can be analyzed by using diagnostic geochemical parameters which can be divided into two major groups. The first group is associated with the molecular parameters which are specified to the chemistry of only a

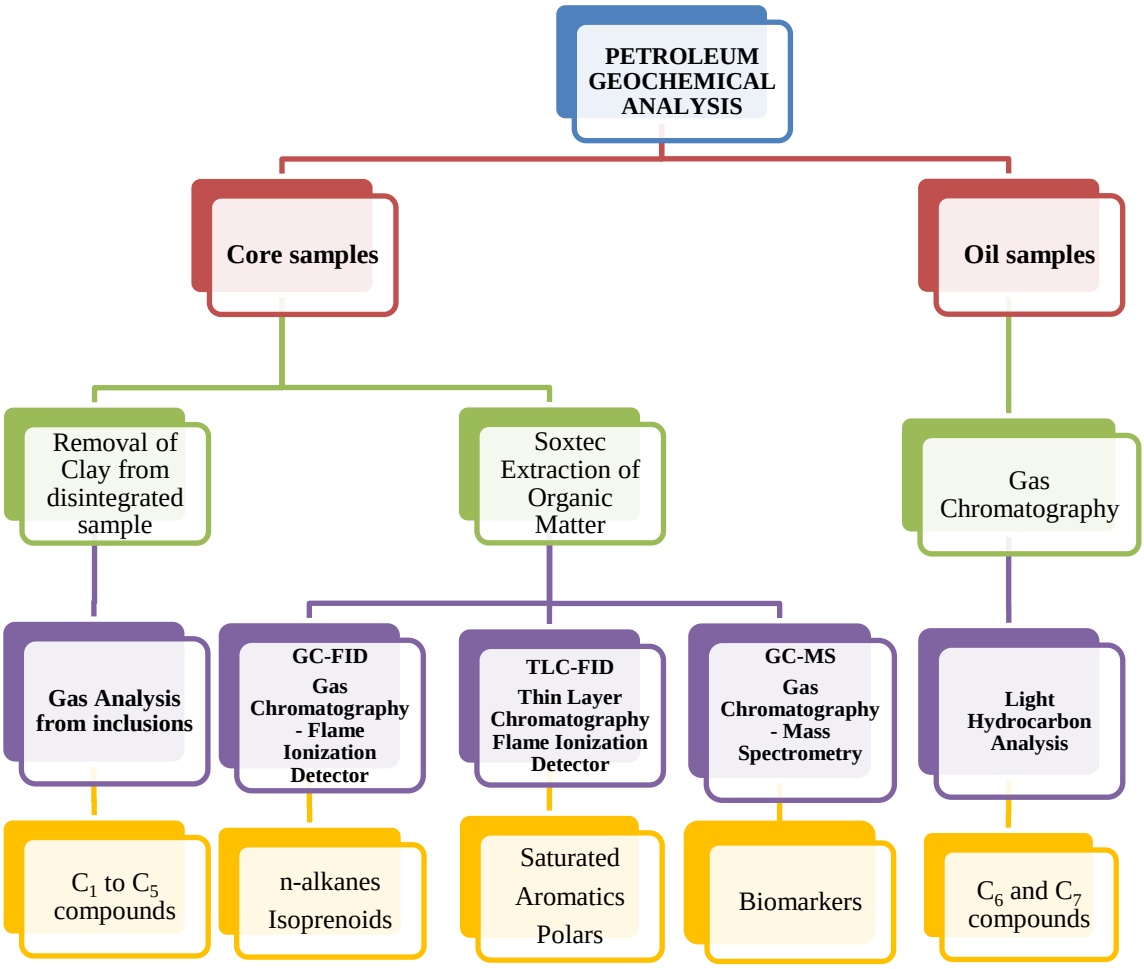

Figure 3.1 The work scheme to obtain the results from various hydrocarbon samples. Two types of samples are shown in the red boxes while analytical methods are mentioned in the purple boxes.

fraction of a sample or the whole sample for instance, Gas Chromatography - Flame Ionization Detector (GC-FID). The detector shows the distribution of normal alkanes, isoprenoids and aromatic hydrocarbons while Gas Chromatography - Mass Spectrometry (GC-MS) is normally used as mass sensitive detector to monitor molecular fragments representing the specific biomarker compounds.

The second group of geochemical properties is connected with the bulk parameters which are illustrative of whole oil or extract sample composition and separate oil or a bitumen sample into saturated hydrocarbons, aromatic hydrocarbons and polar compounds. Thin Layer Chromatography - Flame Ionization Detector (TLC-FID) as represented by the Iatroscan method (Karlsen and Larter, 1991) in which the chromatographic separations will give the compound classes, while the FID will do the quantification.

Light hydrocarbons are present in all migrated oil, condensate and gas samples and also in source rocks, albeit these compounds are normally lost from the rock samples under normal extraction procedures. These C_4-C_8 hydrocarbons represent a rather large proportion of oils and condensates and various methods have been developed for their analysis in the rock samples (Schaefer et al., 1978) whereas these compounds in oil can be analyzed directly by normal GC-FID applications (Peters et al., 2005). In this project, light hydrocarbons present in a suite of oils have been investigated to shed some light on thermal maturity, provenance, and expulsion history along with potential biodegradation of oils investigated.

The present study also includes the gases (C_1-C_4) compounds liberated from inclusions (Fig. 3.1) measured using preparation techniques and GC-FID methods (Karlsen et al., 1993). This allows a view of the gases present in a trap at a previous time. The methods for chromatographic separation are the same as for production gases and parameters can therefore be directly compared.

3.2 Preparation and extraction of samples

A total of 70 core samples from different wells of the Mid-Norway and the Barents Sea were studied in addition to oil samples for light hydrocarbons studies. The crushing of core samples into powder form is essential for geochemical analysis before extraction. The extraction unit Soxtec system HT-1043 was used to derive the bitumen from the crushed sample. About 3g of

powdered sample is used in pre-extracted cellulose cartridges and glass wool is used to cover the sample. In order to extract the sample, 50ml of mixture of dichloromethane (93%) and methanol (7%) solvent was utilized which is then heated so that the boiling and evaporated solvent will condensate and percolated through the sample in a reflux fashion. Six samples can be boiled in the solvent at the same time using individual extraction cells, and after boiling for two hours and rinsing for one hour to effectively extract all bitumen from the rock samples. The back flux of solvent into the cartridges is controlled by the valve, which is closed for the concentration of the extract. Glass vials of 15ml volume are used for transferring the concentrated extract which is then sealed with Teflon lined plastic corks. These extracts are used for geochemical analysis by GC-FID, GC-MS and TLC-FID and are further concentrated, sieved or treated with other solvents before usage depending on the type of analytical method. The following analytical methods were used for examination of rock samples, their extracts and the oils from the Norwegian Continental Shelf:

1. Gas Chromatography – Flame Ionization Detector (GC-FID)

2. Gas Chromatography – Mass Spectrometry (GC-MS)

3. Thin Layer Chromatography – Flame Ionization Detector (TLC-FID) or Iatroscan

4. Light hydrocarbons analysis from GC FID

During all the analytical methods, the North Sea Oil (NSO-1) is repeatedly used as a reference oil sample from the Norwegian Petroleum Directorate (NPD) and the oil sample represents the Oseberg Field, for which the source rock is the Draupne Formation of Upper Jurassic age and this formation is equivalent to the Kimmeridge Formation (Dahl and Speers, 1985).

3.3 GC-FID of Gases from inclusions

The preliminary method to determine the hydrocarbon composition is gas chromatography that is used to separate the organic compounds from complex mixture into individual molecular groups (idealy just one isomer type) where each peak is representative of the fraction quantitative fraction of each organic compound. The method is based on the principle of boiling point chromatography in which the system has a stationary phase, in which

substances are somewhat retarded from further migration, and a mobile phase which is in GC a gaseous phase. Compounds elute from the column according to molecular boiling points.

The carrier gas drives the soluble substances through the column in the chromatograph, in which the temperature was programmed. In order to avoid the interaction of carrier gas with the analyzed sample, helium, hydrogen and nitrogen are generally utilized as these carrier gases are inert and therefore well suited as carrier gases. The selection of carrier gas depends mainly on the movement of substance from the column and how fast the chromatography should take place, so the carrier gas affects the efficiency of column and the time of analysis. Helium and hydrogen are allowing faster chromatography than more viscous nitogen. However, helium is very expensive and hydrogen is explosive resulting in nitrogen being commonly selected as carrier gas. The other thing which plays a vital role for movement of gas from the cylinder to the column is the pressure which is kept in between 2-3kg/cm^2 (bar) and flow of gas is kept constant by the pressure valve.

The unit where sample is inserted into the column in gas chromatography is termed as the injector. The sample is vaporized in the injector and split and then moved through the column. The column is made of quartz and the shape of column is coiled up into spiral to fit inside the GC oven. The coating on the inner tube wall of small diameter of column acts as stationary phase where in the center of column the flow of substance takes place. The adjustment of temperature of the GC oven i.e. the temperature program is essential for moving compounds with higher boiling points through the column and for resolving peaks with optimum peak shape.

In the column, the sample is separated into various components which can be measured by the detector. The detection of components can be done either by mass-flow-dependent detectors or by concentration-dependent detectors. Usually detectors are flame ionization detector (FID) or thermal conductivity detector (TCD) where former destroys the sample by burning the organic compounds and has more linear range and more accurate measurements while the later dont destroy the organic compound in the process of detection, but only determines the heat change in the detector when the substance passes through it, but the magnitude of linear range is not large in the TCD and overall sensitivity is far lower than of a modern FID.

3.3.1 GC-FID parameters for gases from inclusions

The geochemical parameters applied to gas chromatograms of gases can be described as:

1. The wetness parameters i.e. percentage of C_2+ hydrocarbons.
2. The ratio of i-C_4/n-C_4 to distinguish the thermogenic gases from oil and gas zone.

1. Percentage of C_2+ hydrocarbons

The presence of oil in the sample can be determined by the percentage of C_2+ hydrocarbons that includes the sum of percentages of ethane, propane, butane and pentane hydrocarbons. If the percentage of C_2+ compounds is more than 15% than the gas sample is so-called oil associated i.e. generated together with oil. Wetness down towards 5% represents condensate associated gas. This parameter is commonly termed as the wetness parameter (Schoell, 1983) and biogenic gases are basically always a C_2+ value of less than 1%.

2. Ratio of butane isomers i-C_4/n-C_4

The relation between the concentration of iso-butane and normal-butane is determined by the thermodynamic conditions in the source rock and also by later secondary processes such as biodegradation (Schoell 1983; Whiticar 1994). For unaltered (fresh) hydrocarbons which have not undergone any secondary effect or degradation by bacterial activity, the ratio of i-C_4/n-C_4 will be close to 0.5. If the amount of n-butane exceed significantly than this value, it represents the degree of biodegradation in the given sample.

3.4 GC-FID of oil / bitumen from rock samples

The column is programmed from 40°C to 325°C for a total time of 95 minutes. Initial temperature was 40^{o}C with an increament of 4°C/min up to 325°C with final holding time of 20 minutes, so that the molecules having low vapor pressure at ambient temperature can be mobilized, hence, one run for analysis of a sample can be completed in 95 minutes. After the molecules passed through the column they entered into flame ionization detector and the signal from the detector is recorded (Fig. 3.2) that gives the chromatogram where intensity is plotted along Y-axis and time is representing along X-axis.

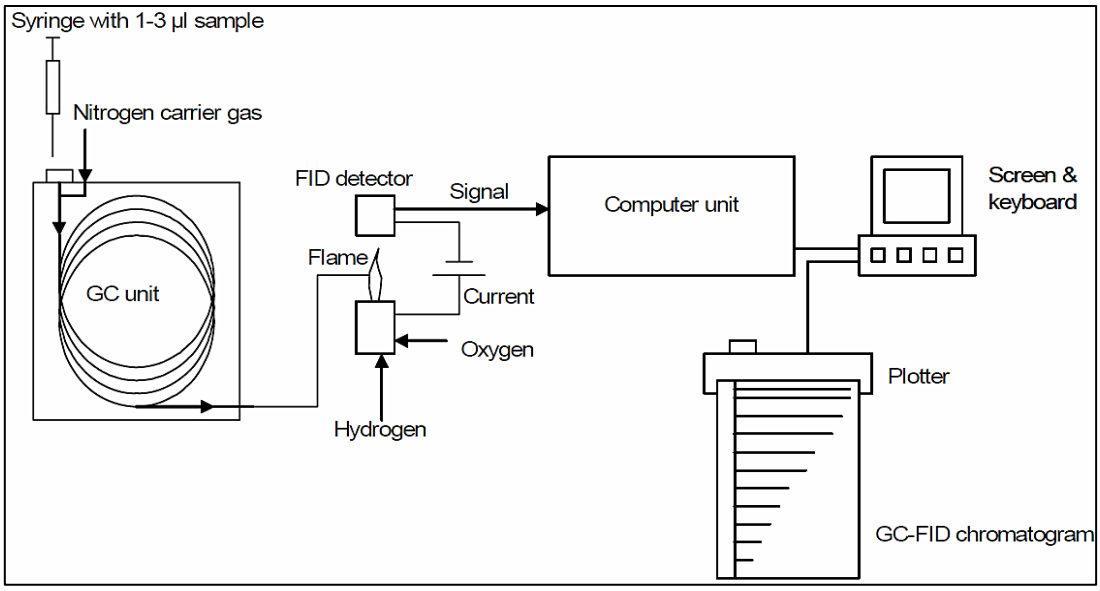

Figure 3.2 A schematic diagram of a GC-FID instrument by Pedersen (2002). The sample is injected into the GC unit and move through the column to reach the flame ionization chamber. Thereby give rise to signal to the computer unit that generates chromatogram with peaks for individual molecular groups.

In this way, the height of peaks in the chromatogram indicate greater intensity while increase in time is directly related with temperature and compounds with low vapor pressure appeared in the later part of chromatogram. In order to perform GC-FID analysis, a Varian Capillary Gas Chromatography Model 3800 was used with the 25m long and diameter of 0.2mm of Hewlett Packard Ultra II cross-linked Methyl Silicon Gum Column and the thickness of film is about 0.33µm. Nitrogen was used as carrier gas with initial temperature of 40ºC and increasing rate of 4ºC/min. along with holding time of 2ºC/min. that took 75min. to reach the maximum temperature level of 330ºC, finally holding the maximum temperature for 20min. making total run time of 95min.

3.4.1 GC-FID parameters for oil and bitumen from rocks

The geochemical parameters used in GC-FID chromatograms to evaluate the maturation and facies of respective samples are:

1. Pristane/n-C_{17} and Phytane/n-C_{18}
2. Pristane/phytane
3. CPI and the pattern of n-alkanes peaks

1. Pristane/n-C_{17} and Phytane/n-C_{18}

Pristane and phytane are isoprenoids which are principally acquired from the side chain of the chlorophyll molecule phytol where oxidation and decarboxylation of phytol results in pristane while phytane is formed due to reduction and dehydration and both can easily be identified in GC-FID analysis. The level of biodegradation, facies and maturation can be determined by these ratios together with other parameters as bacteria assimilate n-alkanes (Peters and Moldowan, 1993). The maturity of source rock during expulsion is directly measureable as isoprenoids as far less thermally stable compared to the n-alkanes. Therefore, more mature samples have much lower ratios of pristane/n-C_{17} and phytane/n-C_{18}. On the other hand, great care must be taken into account as organic input may also influence the ratios (Peters and Moldowan, 1993).

2. Pristane/Phytane ratio

The oxic and anoxic conditions in the palaeo-depositional environment of the source rock samples and hence oil or bitumen samples can be inferred by the value of pristane to phytane (Pr/Ph) ratio. A ratio less than unity represents highly anoxic and possibly carbonate depositional marine settings, while the normal marine good anoxia of siliciclastic source rocks is indicated by Pr/Ph values in the range of 1.0 to 1.5 and even 1.8. The ratios of Pr/Ph higher than 3.0 is generally ascribed to coals. Ratios between 1.8 and 3.0 would often represent marine source rock with a lot of vitrinite in the kerogen. However, enhanced values can also result from extensive phase fractionation, and can therefore be found in condensates from normal marine settings (Karlsen et al., 1995; 2004). The stability of pristane is higher than phytane which also concludes that Pr/Ph ratio keeps on increasing with increase in maturity (Alexander et al., 1981).

3. CPI and Pattern of n-alkanes peaks

The carbon preference index (CPI) is applied on selected chromatograms with a visible Zig-Zag or up-and-down shift of n-alkane peak heights i.e. in which the relative amount of normal alkanes in which the odd number n-alkanes vary form that of those with even numbers. Two CPI values were calculated on the basis of C_{20} to C_{30} alkanes modified from Philippi (1977), where,

$$CPI\text{-}1 = (2\times C_{23})/ (C_{22}+C_{24})$$

$$CPI\text{-}2 = (2\times C_{29})/ (C_{28}+C_{30})$$

Peters and Moldowan (1993) suggested the classification of chromatograms on the basis of n-alkanes peaks in order to determine the sample facies and maturity. In normal oils of the North Sea there is decrease in height of peaks asymptotical with increase in carbon number which imparts the concave-shaped curve on the chromatogram. The effects of biodegradation can be inferred from a rise of unresolved complex mixture (UCM) of compounds, and also from missing n-alkanes in the chromatograms, typically in the C_{10} to C_{15} region in case of incipient biodegradation (Karlsen et al., 1995).

3.5 GC-MS of oils and bitumen from rock samples

The gas chromatography (GC) for compound separation, and mass spectrometer (MS) using ionization, combine to form GC-MS analysis for detection and identification of separated compounds with their respective masses. GC-MS is quite important in identifying and quantifying the biomarkers which play a vital role in geochemical interpretation of oil and reservoir core samples, but straight chains hydrocarbons like n-alkanes found in oils and extracts adversely affect the signals of biomarkers. Therefore, the enhanced signals of biomarkers are primarily achieved by removing the n-alkanes from the samples. For this purpose, the molecular sieving is done to limit the unnecessary interference peaks formed due to normal alkanes in the analyte.

The process of removal of asphaltenes and resins is executed by the molecular sieving of the samples. In the method of sieving, the long chained hydrocarbon structures are trapped in the sieve which has channels like pores which allow n-alkanes to enter but branched alkanes and cyclohexanes may not. Thus, normal alkanes are removed, and the surface of molecular sieve will also remove resins and asphaltenes from the samples. So, the molecular sieving enriched the biomarkers and aromatics while n-alkanes are depleted in the solution.

In a 15ml glass vial, about 0.20g of molecular sieve (5Å UOP MHS2-4120LC silica) is introduced with 3 drops of sample to mix with powder-like sieve using a pipette. Cyclohexane is used as a solvent to dilute the sample by mixing the cyclohexane and the analyte and by

vigorously stirring it thoroughly. Centrifugation of the glass vial in a Heraeus Septech Labofuge H at 2000rpm for 3 minutes allows the settling of sieve. The liquid sample was poured with the help of pipette into a new 15ml glass vial, 75% of the liquid is then evaporated by blowing with nitrogen over it to concentrate the sample and then to seal it all with Teflon-lined caps for GC-MS analysis.

The molecules present in the mixture are separated according to their chemical properties when the sample moves through the column. The retention time in the column varies for each compound in gas chromatograph which makes it possible for the mass spectrometer to capture and ionize the molecules into fragments and specific mass to charge ratios is then detected by the mass spectrometer.

The mass to electronic charge ratio (m/z) is specific for several molecules of interest like hopanes and triterpanes biomarkers have m/z= 191. The relative abundance of ions is registered by the detector where data is recorded and managed by the PC program which plot the retention time along the X-axis while the m/z ratio representing the relative abundance of molecules is shown along the Y-axis.

The bulk composition of the samples is analyzed by a Fisons Instrument MD800 GC-MS system in SIM-mode (ion-monitoring) having a Chromopak CP-SIL 5CB-MS FS 50X.32 (40) WCOT 50m long column of fused silica-type with 0.32mm of inner diameter that is comprising a CP-SIL5CB low bleed/MS stationary phase. The column has an initial temperature of 80ºC, with heating with 10ºC/min up to 180ºC and further 1.7 ºC/min up to 310ºC, and finally the temperature 310ºC is kept constant for 30 minutes.

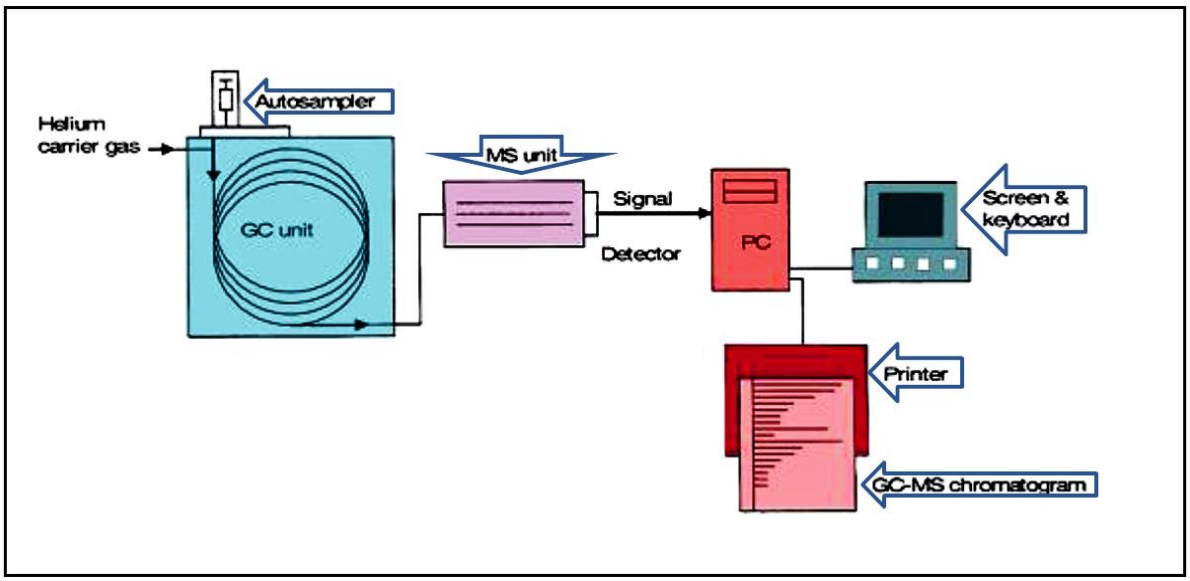

Figure 3.3 An overview of a GC-MS instrument according to Pedersen (2002). The sample is injected in GC unit and moved to MS unit. The signals generated from MS unit are presented by a computer in form of chromatograms.

3.5.1 Geochemical parameters for GC-MS analysis

In the present study, m/z ratios of 191, 217, 218, 231, 251, 178,192 and 198 were used to establish the source, maturity and facies of the samples from the different regions.

Table 3.1 The various ratios of m/z in chromatographs used in GC-MS analysis.

No.	Mass/ion (m/z) Ratio	Type	Compound class
1	191	Terpane	Saturated hydrocarbons
2	217	Steranes	Saturated hydrocarbons
3	218	Steranes	Saturated hydrocarbons
4	231	Triaromatic Steroids	Aromatic hydrocarbons
5	253	Monoaromatic steroids	Aromatic hydrocarbons
6	178	Phenanthrene	Aromatic hydrocarbons
7	192	Methylphenanthrene	Aromatic hydrocarbons
8	198	Methyldibenzothiphenes	Aromatic hydrocarbons

Most of the peaks in the chromatograms of different m/z ratios are calculated for evaluation of facies and maturity parameters which are documented in Tab. 3.1.

Terpanes

Terpanes are the group of saturated hydrocarbons that can be identified in m/z=191 (Fig. 3.4), and some of the most important to our work are those shown in Tab. 3.2.

Table 3.2 Chromatogram peaks of triterpanes at m/z=191 (Fig. 3.4).

No.	Peak	Stereochemistry	Composition	Compound Name
1	P		$C_{23}H_{42}$	Tricyclic terpane
2	Q		$C_{24}H_{44}$	Tricyclic terpane
3	R	17R+17S	$C_{25}H_{46}$	Tricyclic terpane
4	S		$C_{24}H_{42}$	Tetracyclic terpane
5	U		$C_{28}H_{48}$	Tricylclic terpane
6	V		$C_{29}H_{50}$	Tricyclic terpane
7	A		C_{27}	18α(H)-trisnorneohopane
8	B		C_{27}	17α(H)-trisnorneohopane
9	Z		$C_{28}H_{48}$	17α(H), 21β(H)-bisnorhopane
10	C		$C_{29}H_{50}$	17α(H), 21β(H)-norhopane
11	29Ts		C_{29}	18α(H)- 30-norhopane
12	X		$C_{30}H_{52}$	15α-methyl-17α(H)-27-diahopane
13	D		$C_{29}H_{50}$	17β(H), 21α(H)-30-normoretane
14	E		$C_{30}H_{52}$	17α(H), 21α(H)-hopane
15	F		$C_{30}H_{52}$	17β(H), 21α(H)-moretane
16	G	22S	$C_{31}H_{54}$	17α(H), 21β(H)-22-homohopane
17	H	22R	$C_{31}H_{54}$	17α(H), 21β(H)-22-homohopane

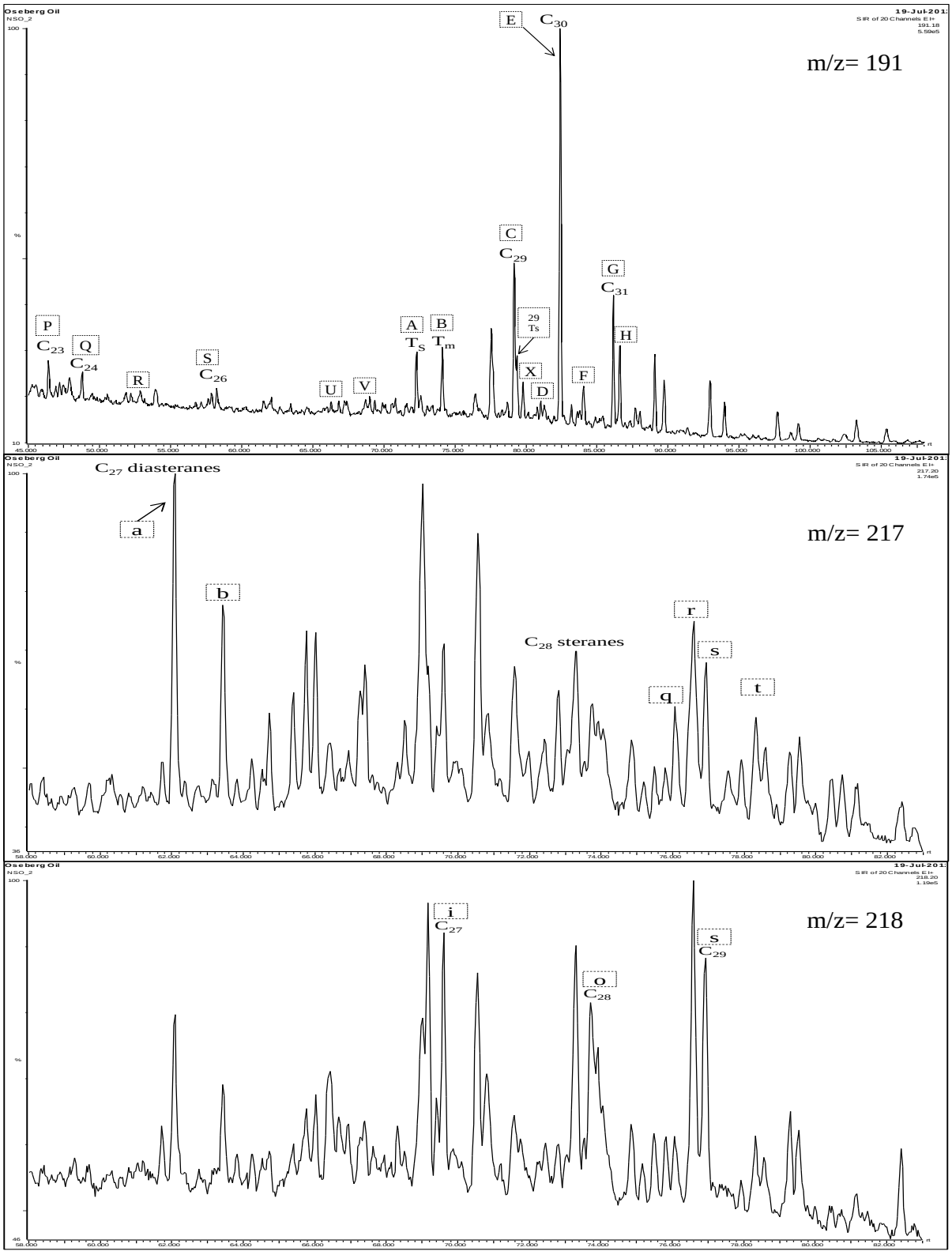

Figure 3.4 GC-MS chromatogram for m/z = 191, 217 and 218.

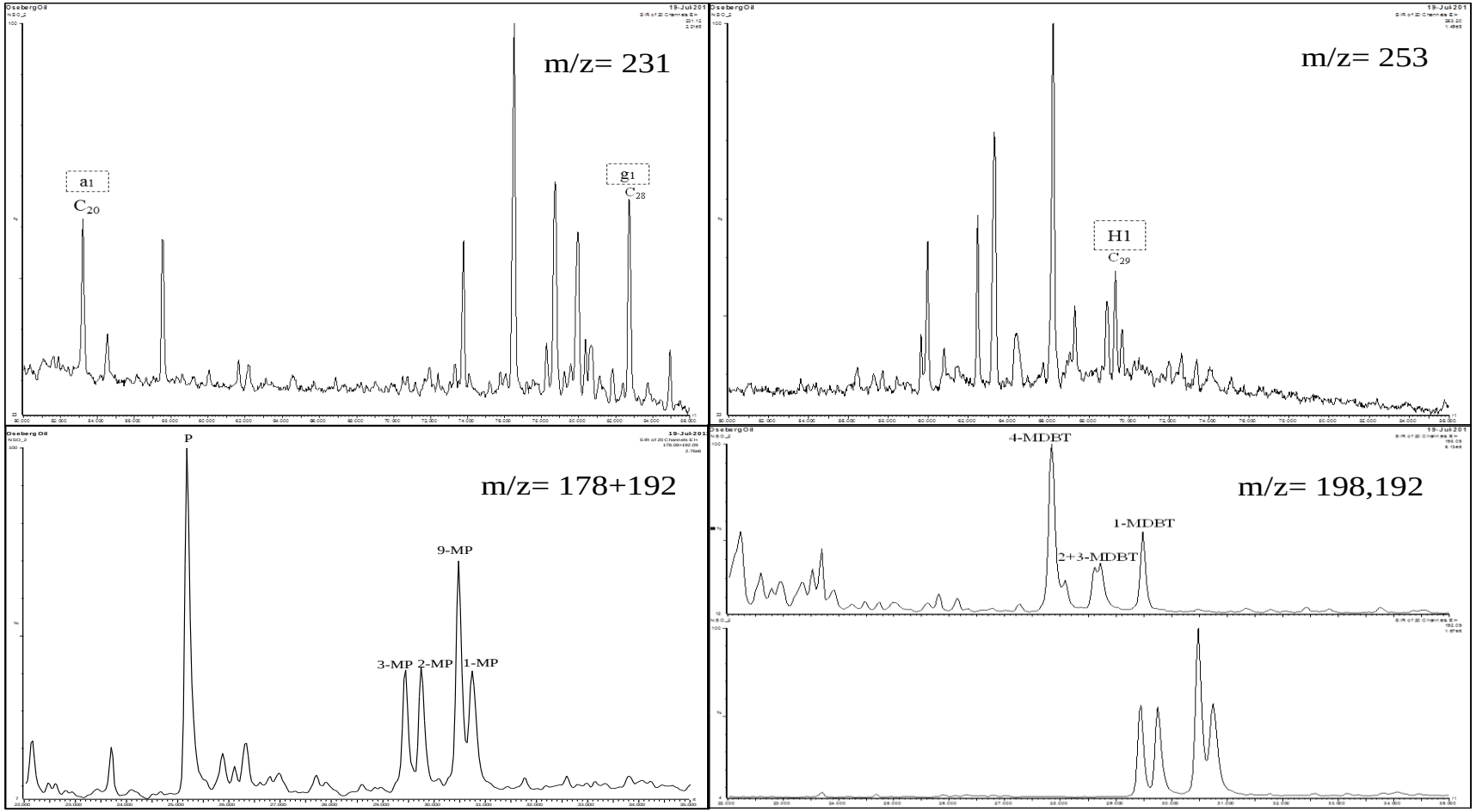

Figure 3.5 GC-MS chromatograms for m/z = 231, 253, 178+192, and 198,192.

Steranes

The group of tetracyclic saturated hydrocarbons which are identified on m/z=217, i.e. steranes (Fig. 3.4) are given in Tab. 3.3.

Table 3.3 Chromatogram with m/z=217 showing identified steranes (Weiss et al., 2000).

No.	Peak	Stereochem.	Compound name	Composition
1	a	20S	13β(H), 17α(H), 20(S)-cholestane (diasterane)	$C_{27}H_{12}$
2	b	20R	13β(H), 17α(H), 20(R)-cholestane (diasterane)	$C_{27}H_{48}$
3	q	20S	24-ethyl-5α(H), 14α(H), 17α(H), 20(S)-cholestane	$C_{29}H_{52}$
4	r	20R	24-ethyl-5α(H), 14β(H), 17β(H), 20(R)-cholestane	$C_{29}H_{52}$
5	s	20S	24-ethyl-5α(H), 14β(H), 17β(H), 20(S)-cholestane	$C_{29}H_{52}$
6	t	20R	24-ethyl-5α(H), 14α(H), 17α(H), 20(R)-cholestane	$C_{29}H_{52}$

However, Tab. 3.4 enlists the steranes which can be identified on m/z=218 (Fig. 3.4).

Table 3.4 The peaks identified on chromatogram with m/z=218 (Fig. 3.4) showing steranes (Weiss et al., 2000).

No.	Peak	Name
1	i	C_{27} regular sterane (5α(H), 14β(H), 17β(H), 20(S)-cholestane
2	o	C_{28} regular sterane (24-methyl-5α(H), 14β(H), 17β(H), 20(S)-cholestane
3	s	C_{29} regular sterane (24-ethyl-5α(H), 14β(H), 17β(H), 20(S)-cholestane

Triaromatic steroids

Aromatic hydrocarbons identified on m/z=231 are termed triaromatic steroids (Fig. 3.5) which are helpful in evaluating the maturity of samples, and two important steroids were identified in Tab. 3.5.

Table 3.5 Triaromatics steroid peaks on m/z=231 (Fig. 3.5).

No.	Peak	Name
1	a1	C_{20} triaromatic steroid
2	g1	C_{28} triaromatic steroid

Monoaromatic steroids

The predecessor of triaromatic steroids are monoaromatic steroids that can be detected on m/z=253 (Fig. 3.5) and these are together with the triaromatic steroid, worthwhile both for maturity assessment and correlation. The relevant monoaromatic is presented in Tab. 3.6.

Table 3.6 Peak identified as monoaromatic steroids on m/z = 253 (Fig. 3.5).

No.	Peak	Name
1	H1	C_{29} monoaromatic steroid

Phenanthrene and methylphenanthrene

Medium range maturity indicating aromatic hydrocarbons are phenanthrene and methylphenanthrene which are C_{14} and C_{15} aromatic hydrocarbons and they appear in the form of peaks in chromatogram with m/z is 178 and 192 (Fig. 3.5), and these are listed in Tab. 3.7. These are useful for estimating the maturity of condensates and also the medium range fraction of oils which have a mixed origin with biomarkers signifying the C_{27}+ range.

Table 3.7 Phenanthrene and methylphenanthrene identified on chromatograms with m/z=178 and 192. (Fig. 3.5).

No.	Peak	Name
1	P	Phenanthrene
2	3-MP	3-methylphenanthrene
3	2-MP	2-methylphenanthrene
4	9-MP	9-methylphenanthrene
5	1-MP	1-methylphenanthrene

Methyldibenzothiophene

These are C_{13} aromatic hydrocarbons containing sulphur and are therefore belonging to the medium range hydrocarbons and are present in chromatogram of m/z=198 (Fig. 3.5), where they are mainly used for estimation of maturity. Greater difference in height of 4-MBDT and 1-MBDT represents increasing maturity (Peters et al., 2005). These aromatic hydrocarbons are presented in Tab. 3.8.

Table 3.8 Represents the methyldibenzothiophene aromatic hydrocarbons (peaks of aromatic hydrocarbons are identified in Fig. 3.5).

No.	Peak	Name
1	4-MDBT	4-methyldibenzothiophene
2	1-MBDT	1-methyldibenzothiophene
3	2+3MDBT	2+3-methyldibenzothiophene

3.5.2 Description of parameters

Various peaks representing the complex hydrocarbon compounds are used for measurement of parameters. These parameters are applied for the purpose of interpreting the depositional

environment and maturity of samples from the Barents Sea and the Mid-Norway region. These parameters are presented in Tab. 3.9.

Parameters from m/z=191

The following parameters can be computed from the chromatogram with m/z=191 which identify triterpanes and terpanes:

Parameter 1: (peaks A and B)

The parameter is applied for maturity indication of samples where maturation increases the amount of Ts (C_{27}18α(H) - trisnorneohopane) as compared to Tm (C_{27}17α(H)- trisnorhopane). The maximum ratio of Ts/ (Ts+Tm) is allotted as 1.0 for the samples and is best fit for immature, mature and over-matures oil (Peters and Moldowan, 1993).

Parameter 2: (peaks X and D)

Peters and Moldowan (1993) suggested the ratio of diahopane/ (diahopane + normorentane) as a good maturity parameter, where higher values are indicative of high maturity.

Parameter 3: (peaks G and H)

The S and R isomers of the C_{31}17α(H), 21β(H)-hopanes behave in a different manner with maturation. The isomer 22S is relatively higher in stability than 22R which imparts increase in the ratio of 22S. As a consequence, the parameter is designed as 22S/ (22S+22R) of C_{31}17α(H), 21β(H)-hopanes and has been found to have a maximum value of about 0.6 (Peters and Moldowan, 1993).

Parameter 4: (peaks E and F)

The stability of the C_{30}-hopane is relatively higher than that of the C_{30}-moretane with increase in temperature and maturity. The usefulness of this parameter is limited to the early part of the oil window due to low thermal stability of the C_{30}-moretane so the ratio will only be applicable for the early part of the oil window.

Parameter 5: (peaks 29Ts and C)

Moldowan et al., (1991) described this parameter as a result of better chromatography which allowed the C_{29}Ts to show up as a shoulder on the C_{29} peak. The stability of the C_{29}Ts is significantly higher than that of the norhopane resulting in the most useful parameter. The

ratio of 29Ts/29Ts+norhopane is directly related with increase in the maturation (Hughes et al., 1995).

Table 3.9 Description of parameters for GC-MS chromatograms.

Parameter	Description
1	Ts/(Ts+Tm) from Seifert and Moldwan, (1978).
2	Diahopane/(diahopane+normoretane), (Conford et al., 1986).
3	22S/22S+22R of C_{31}17α(H), 21β(H)-hopane (Mackenzie et al., 1985).
4	C_{30}-hopane/(C_{30}-hopane+C_{30}-moretane), (Mackenzie et al., 1985).
5	29Ts/(29Ts + norhopane) after Moldowan et al., (1991).
6	bisnorhopane/(bisnorhopane+norhopane), (Wilhelms and Larter, 1994).
7	C_{23}-C_{29}tricyclic terpanes/C_{30} aß-hopane (modified from Mello et al., 1988).
8	C_{24}tetracyclic terpane/C_{30} aß-hopane (Mello et al., 1988).
9	Hopane/Sterane (Mackenzie et al., 1984).
10	ßß/(ßß+αα) of C_{29} (20R+20S) sterane isomers (Mackenzie et al., 1980).
11	20S/(20S+20R) of C_{29} 5a(H),14a(H),17a(H) sterane isomers (Mackenzie, 1984).
12	diasteranes/(diasteranes+regular steranes), (Mackenzie et al., 1985).
13	% C_{27} of C_{27}+C_{28}+C_{29} ßß-steranes (Mackenzie et al., 1985).
14	% C_{28} of C_{27}+C_{28}+C_{29} ßß-steranes (Mackenzie et al., 1985).
15	% C_{29} of C_{27}+C_{28}+C_{29} ßß-steranes (Mackenzie et al., 1985).
16	C_{20}/ (C_{20}+C_{28}) triaromatic steroides (TA) (Mackenzie et al., 1985).
17	C_{28} TA/(C_{28} TA+C_{29} MA) (Peters and Moldowan., 1993).
18	Methylphenanthrene ratio, MPR (Radke et al., 1982b).
19	Methylphenanthrene index 1, MPI1 (Radke et al., 1982a).
20	Methylphenanthrene distribution fraction1, MPDF (F1) (Kvalheim et al., 1987).
21	Methyldibenzothiophene ratio, MDR (Radke, 1988).
22	Calculated vitrinite reflectivity, Rm = 1.1log10 MPR+0.95 (Radke, 1988).
23	Calculated vitrinite reflectivity, %Rc = 0.60×MPI1+0.40 (Radke, 1988).
24	Calculated vitrinite reflectivity, % Ro = 2.242×F1-0.166 (Kvalheim et al., 1987).
25	Calculated vitrinite reflectivity, Rm = 0.073×MDR+0.51 (Radke, 1988).
26	3-methylphenanthrene/4-methyldibenzothiophene (Radke et al., 2001).
27	Methyldibenzothiophenes/methylphenanthrenes (Radke et al., 2001).

Parameter 6: (peaks Z and C)

Peters and Moldowan (1993) considered bisnorhopane as representative of very anoxic environments. However, the bisnorhopane is not very stable at higher maturities and therefore is relative proportion of bisnorhopane reduced throughout the oil window. On the other hand,

the norhopane is direct representative of maturation as it increases with increase in maturity. Therefore, the ratio of bisnorhopane/(bisnorhopane+norhopane) decreases with increase in maturity.

Parameter 7: (peaks P, Q, R, T, U, V and E)

The fraction of C_{23}-C_{29} tricyclic terpanes relative to C_{30} αβ-hopane is indicative of increase in maturity but Karlsen et al., (1995) stated that the evaporative fractionation and phase fractionation adversely affect the parameter so that it will always be high in condensates, and lower in oils.

Parameter 8: (peaks S and E)

The maturation of sample can also be determined by the amount of C_{24} tricyclic terpanes compared to C_{30} αβ-hopane as proposed by Peters and Moldowan (1993).

Parameters from m/z=217

Parameter 9: (peaks q, r, s, t and E)

The hopanes are indicative of bacteria while steranes are representative of higher plants and algae. Therefore, Peters and Moldowan (1993) introduced the ratio of hopane to sterane as a guide for recognizing organic facies. In addition, the steranes have higher stablility at higher temperatures.

Parameter 10: (peaks q, r, s and t)

The ββ-isomers of steranes respond in the sense of having higher stability with increasing temperarture as compared to the αα-isomers with increase in maturation. The maximum equilibrium ratio is 0.7 reached representing about 0.9%Rc, while mineralogy affects the parameter to some degree (Peters and Moldowan, 1993).

Parameter 11: (peaks q, r, s and t)

Seifert and Moldowan (1986) suggested the conversion of 20R isomer to 20S during maturation and equilibrium is reached at the middle of oil window. The parameter has the maximum ratio is 0.55 representing about 0.8%Rc, but it can be affected by biodegradation (Peters and Moldowan, 1993).

Parameter 12: (peaks a, b, q, r, s and t)

The ratio of diasternes/ (diasteranes + regular steranes) increases with thermal maturity in contrast to regular steranes. Peters and Moldowan (1993) suggested that this is an effective parameter for the whole oil window.

Parameters from m/z=218

Parameter 13, 14 and 15: (peaks i, o and s)

The percentages of C_{27}, C_{28}, C_{29} ββ-steranes displayed by peak i, o, and s, respectively. The plotting of fraction of the peaks in ternary diagram is representative of the organic facies of the palaeo-depositional environment (Huang and Meinschein, 1979; Moldowan et al., 1985).

Parameters from m/z=231 and 253

Parameter 16: (peaks a1 and g1)

The triaromatic steroid cracking parameters (TA) parameter is quite valid for the whole oil window, but phase fractionation limits this parameter when comparing oils to condensates as it will always be artificially high in condensates (Karlsen et al., 1995). The maturation increases the amount of C_{20} comparative to C_{28}. The ratio of C_{20}/ (C_{20} + C_{28}) is used to determine the maturation level where unity would correspond to a maturity in the range of 1.3 to 1.4%Rc (Peters et al., 2005).

Parameter 17: (peaks g1 and H1)

The maturity is indicated by monoaromatics (MA) which rearrange themselves to triaromatics (TA). Thus this is an aromatization parameter and Peters and Moldowan (1993) suggested that the ratio will reach its maximum value of unity at a maturity of about 0.8%Rc which correspond well to the experience of Karlsen et al., (1995) concerning Haltenbanken oils and condensates.

Parameters from m/z=198 and 192

In chromatograms of m/z=198+192, the tricyclic aromatic hydrocarbons are identified while methylphenanthrene compounds can also be utilized in which 3-MP and 2-MP are the most stable isomers of methyl group while 9-MP and 1-MP represents much less stable isomer which are reduced at higher maturities.

Parameter 18, 19 and 20 (peaks P, 1, 2, 3and 9)

The parameter 18 represents maturity and defined by the ratio of two compounds of methylphenanthrene (MPR=2-MP/1-MP). The methylphenanthrene index 1 (MPI-1) is equated as 1.5(3-MP + 2-MP) / (P + 9-MP + 1-MP) and represent the parameter 19. The maturity parameter 20 is the methylphenanthrene distribution factor (MPDF) and is explained by the following equation MPDF = (3-MP + 2-MP)/ (3-MP + 2-MP + 1-MP + 9-MP).

Parameter 21: (peaks 4 and 1)

The methyldibenzothiophene ratio (MDR) is expressed by parameter 21 and is a pure maturity parameter which responds better than the methylphenanthrenes at lower maturities (Karlsen et al., 1995; 2004). Radke et al., (1988) expressed the ratio as MDR = 4-MDBT / 1-MDBT. The quantity of MDBT in oils reflects the sulphur content which is present in the thiophene structure and the amount of methyldibenzothiophenes relative to the methylphenanthrenes is a measure of the palaeo-depositional environment.

Parameter 22, 23, 24 and 25: (measure of vitrinite reflectivity)

The parameters were designed to calculate the vitrinite reflectivity (equations below) from the parameters listed above:

Parameter 22 (from parameter 18): $R_{m(1)} = 1.1 \times \log 10MPR + 0.95$

Parameter 23 (from parameter 19): $\%R_c = 0.6 \times MPI\ 1 + 0.4$

Parameter 24 (from parameter 20): $\%R_o = 2.242 \times MPDF - 0.166$

Parameter 25 (from parameter 21): $R_{m\,(2)} = 0.073 \times MDR + 0.51$

Parameter 26: (peaks 3 and 4)

Various types of organic facies can be identified by using the ratio of 3-methylphenanthrene/4-methyl dibenzothiophene in combination with the ratio of Pr/Ph. In particular, this ratio is relevant for identifying carbonate environments as opposed to siliciclastic source rock environments. The relative quantity of sulphur can also be inferred from this parameter (Radke, 1988).

Parameter 27: (peaks 1, 2+3 and 4)

The parameter is measured from chromatogram m/z = 178+92 where the peaks 1, 2, 3, 4 and 9 are identified and peaks 1, 2+3 and 4 from chromatogram with m/z = 192. The value of this parmeter indicating the facies as carbonate facies corresponds to a value of more than unity, while shale facies is represented by values less than one.

3.6 Thin Layer Chromatography-Flame Ionization Detection (TLC-FID)

The TLC-FID analysis of a series of reservoir core samples can be used to depict the heterogeneities in the petroleum column by determining the vertical and horizontal distribution of composition of petroleum by separating the percentages of asphaltenes plus resins (polars), aromatics and saturated hydrocarbons (Karlsen and Larter, 1991). In fact, the extracted sample not only contains hydrocarbons (compounds consisting soley hydrogen and carbons) but it also contains some non-hydrocarbons like asphaltenes and resins. The instrument for the analysis is actually a silica rod for sample application and liquid chromatography, and FID scanning and quantification of extract is an electronically integrated process in which the flame ionizes the sample into different components.

The TLC-FID of solvent extracts not only a rapid method as it take less time for analysis as compared to MPLC (Medium Pressure Liquid Chromatography), but it is also accurate since it uses a FID for quantification and gives the percentages of each compound type in the extract. The characterization of petroleum population can be observed by the variation between these compounds (Bhullar et al., 2000). TLC-FID makes it possible to distinguish between in-situ hydrocarbons and migrated hydrocarbons which are present in reservoir core samples (Karlsen and Larter, 1991; Abay, 2010). Thus, the analysis is appropriate for sorting out trends in the composition of oil reservoirs, but also for general characterization of quantification of reservoir or source rock extracts.

Reservoir samples were analyzed on a MK-05 model Iatroscan instrument which has a flame ionization detector (FID) to an electronic integrator (Perkin-Elmer LCI-100) which serves for quantification and scanning of the rod (Fig. 3.6). The separated fractions of the extracts were calculated by the electronic integrator. The silica rods of type Chromarods-SIII, with pore

diameter 60Å and particle size of 5µm, separate the components present in the extracts. In order to activate the rods before chromatography, and to remove any possible contaminants on the rods, the chromarods were passed through the FID. The two out of ten chromarods have been used for test runs (one NSO-1 and one blank) while samples are placed on the eight others chromarods.

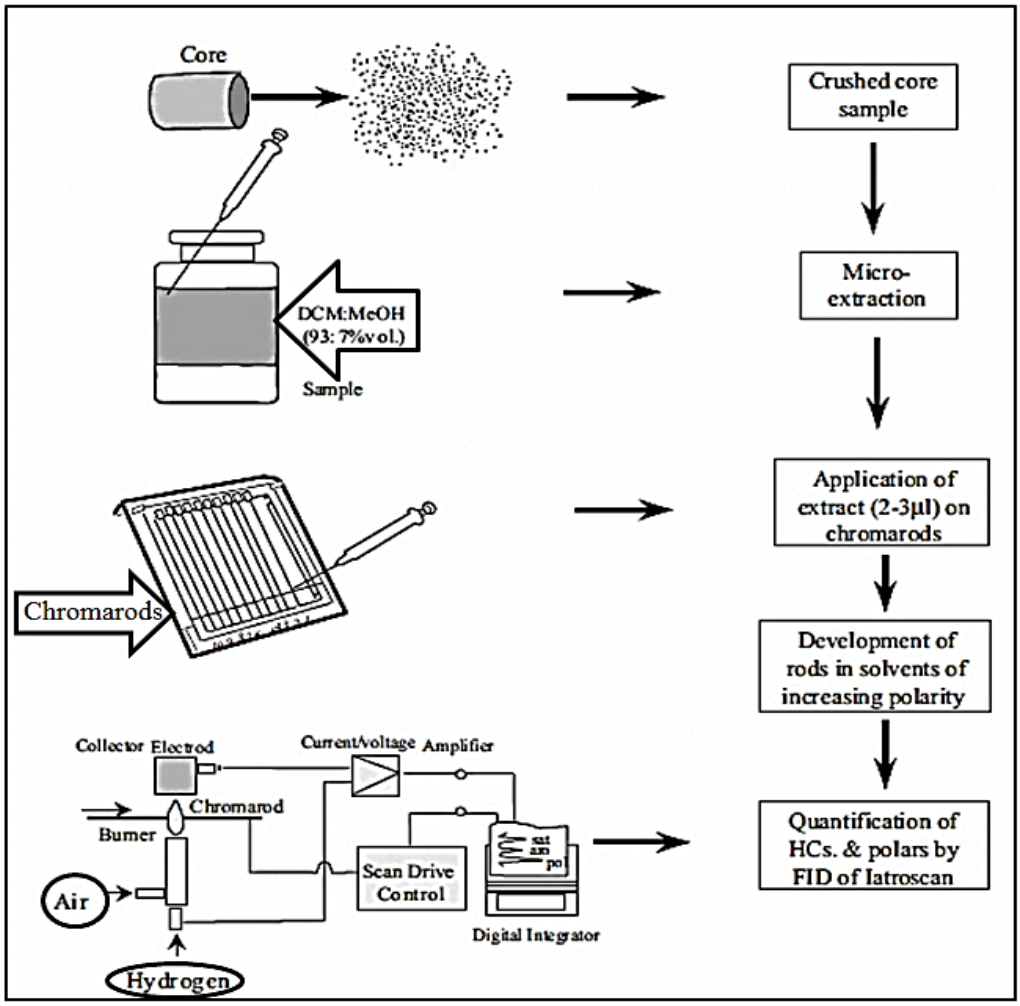

Figure 3.6 The schematic representation of the TLC-FID procedure (Bhullar et al., 2000). The crushed sample is extracted and applied on chromarods which are analyzed using FID to get separate peaks for each type of compounds (Karlsen and Larter, 1991).

The separation of hydrocarbons into saturated hydrocarbons, aromatic hydrocarbons and resins plus asphaltenes i.e. polars was completed using solvents of different polarity. The rise

of saturated hydrocarbons up to the uppermost part of the rods occurred by putting the rods in a solvent of normal hexane for 36 minutes. The aromatic hydrocarbons move to the middle of the rod when placed in toluene for 8min, following drying of the rod in air. The rods were dried at 60ºC after each development, while third type of compounds called polar compounds (i.e. resins plus asphaltenes) are immobile in these solvents and hence remain static at the lowermost part of the rods i.e. at the point of application. Finally, the chromarods were placed in the Iatroscan, where pure grade hydrogen of about 180ml/min and air of 2.1l/min were provided and the instrument scans the compounds at the speed of 30sec/scan and quantitates these fractions as saturated hydrocarbons, aromatic hydrocarbons and polar compounds.

3.6.1 Geochemical parameters for TLC-FID

The Iatroscan results for sample extracts gives the composition of the oil, condensate or bitumen in terms of distinct fractions called saturated hydrocarbons, aromatic hydrocarbons and polar compounds and this enable quatification of these components in a very accurate way.

The maturity or API is to some degree reflected by the ratio of saturated hydrocarbons/ aromatic hydrocarbons (SAT/ARO) as suggested by Clayton and Bostick (1986). The increase in this ratio not only depicts the higher maturity level but it could also give an indication of the GOR of the petroleum as PVT changes during migration will affect such fractionation (Karlsen et al., 1995; Østensen, 2005). Furthermore, with extensive biodegradation, the opposite change will occur i.e. enrichment of the polar fraction and the aromatic fraction and with a reduced saturated. Still, the Iatroscan method is mainly a method for quantification of the amount of extracts and also a help to discern diesel contaminated core sample.

3.7 Light hydrocarbons from oil samples

The geochemistry of light hydrocarbons is mainly a result of the thermal maturity of the source rock, but organic facies will also result in different oils having somewhat different compositions of specific light hydrocarbons. A key element is that light hydrocarbons make up several percentages of the total oil readily up to 10-15% while biomarkers occur only in

ppb concentrations. Hence correlation based on light hydrocarbons is of some interest in particular for condensates which are notoriously low in biomarkers, and for mixed system. Several processes greatly affect the amount of light hydrocarbons. Evaporation from oils, biodegradation of oils or condensates inside the reservoir and water washing may affect several of the light hydrocarbon compounds and water soluble compounds benzene and toluene are readily removed by water washing. Thus, monitoring parameters specifically constructed to respond to biodegradation, water washing or maturity is a great help in the study of natural oils and condensates (Thompson, 1987; Halpern, 1995). In this thesis, light hydrocarbon data were found from previous work done by Dale (1997). The objective of this section was mainly to compare the different organo-facies parameters of samples from the Norwegian Continental Shelf with the light hydrocarbon perspective, which could give an alternative way of dealing the petroleum geochemistry of the regions.

3.7.1 Light Hydrocarbon Parameters

Several light hydrocarbon parameters are designed to moniter the maturity, biodegradation and phase fractionation. Halpern (1995) defined parameters that affect biodegradation, maturation and evaporation with the help of “Star diagrams” of which there are two principle types i.e. “Correlation diagrams” used for comparison of organic source facies and “Transformation diagrams” which measures the response to maturity, biodegradation and water washing. Thompson (1987) based on paraffinicity and aromaticity, described the water washing, maturity and source origin of hydrocarbons by graphical comparison in cross-plots. Both methods are complimentary for understanding the different processes affecting the light hydrocarbons.

Halpern Parameters

The differences in composition of oils and condensates can be displayed by geochemical star diagrams, which can also be used for oil-condensate and oil-oil correlation These star diagrams are not only fast and cost-efficient in application, but they are also relatively easy to use and visually informative and are used for both exploration and production (Wever, 2000). Chemical compositions of hydrocarbons can be represented by star diagrams that are multivariate plots in polar coordinates.

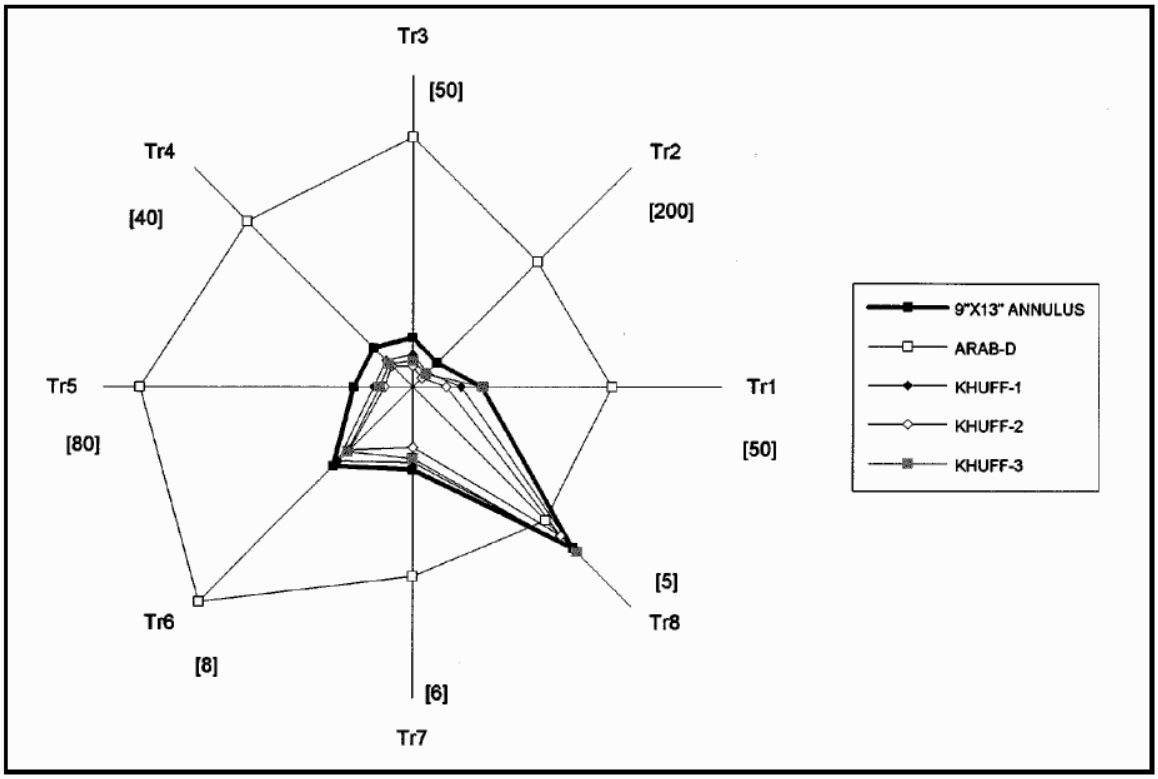

Figure 3.7 Halpern star diagram of C_7 oil transformation parameters where the samples referred to as KHUFF 1-3 are producing condensates. Ratios from Tr1 to Tr8 are plotted and the endpoints values are shown in brackets (from Halpern, 1995).

According to Halpern (1995), C_7 compounds are more feasible from other lighter hydrocarbons because:

- Higher boiling point and low rate of evaporation than other lighter hydrocarbons.
- Seventeen isomers of C_7 compounds allow us to construct large number of ratios plotted as variables in different experiments.
- Water washing and biodegradation varies in different C_7 compounds that help us to measure the amount of transformation of hydrocarbons.

As mentioned above many condensates of higher maturity not contain enough biomarkers for normal analytical approaches, thus making it difficult to correlate them with less mature oils. Such correlation is generally possible using light hydrocarbons, and with the help of C_7 based star diagrams using components, which are present in both oil and condensates. The changes in chemical composition can be indicated by light hydrocarbon correlation, which shows

small changes among the oils of same reservoir. In production, these star diagrams define the connectivity, fractions, and boundaries of the reservoir while these star diagrams also express different processes in reservoir and quality of pay zones that are important for exploration (Halpern, 1995).

Halpern (1995) proposed that in order to study alteration processes in oils present in the reservoir, star diagrams are applied with eight C_7 ratios (Fig. 3.7). These are C_7 hydrocarbons which show more resistant to biodegradation and include 1,1-dimethylcyclopentane (1,1-DMCP). For this reason, it is used as denominator in seven of the eight ratios (Tr1 to Tr8), where Tr6 is the most resistant to alteration processes than other compound ratio. In this way Tr6 reflects the evaporation or fractionation effect. The description of the ratios is presented in Tab. 3.10.

Table 3.10 Halpern parameters that are applied in star diagrams for understanding of alteration processes and correlation of oils (Halpern, 1995). Where, X= 1,1-Dimethylcyclopentane (B.P = 87.8°C and solubility 24ppm), P2 = 2-methylhexane+3-methylhexane with B.P = 91°C and solubility 2.6ppm, P3 = 2,2-dimethylpentane+ 2,3-dimethylpentane+ 2,4-dimethylpentane+3,3-dimethylpentane+3-ethylpentane with boiling point (B.P) = 85°C and solubility 5ppm.

No.	Ratio	Name	Purpose	Boiling Point (°C)	Solubility (ppm)
1	Toluene/X	TR1	Water washing	22.8	496
2	n-C_7 /X	TR2	Biodegradation	10.6	-21.8
3	3-Methylhexane/X	TR3	Biodegradation	4	-21.4
4	2-methylhexane/X	TR4	Biodegradation	2.2	-21.5
5	P2/X	TR5	Biodegradation	3.2	-21.4
6	1-cis-2-Dimethylcyclopentane/X	TR6	Evapo. Frac. and Biodegradation	11.7	-11
7	1-trans-3-dimetylcyclopentane/X	TR7	Biodegradation	3	-4
8	P2/P3	TR8	Biodegradation	6	-2.4
9	2,2-Dimetylpentane/P3	C1	Correlation	-5.8	-0.6
10	2,3-Dimetylpentane/P3	C2	Correlation	4.8	0.3
11	2,4-Dimetylpentane/P3	C3	Correlation	-4.5	-0.6
12	3,3-Dimetylpentane/P3	C4	Correlation	1.1	0.9
13	3-Ethylpentane/P3	C5	Correlation	8.5	-2

The parameter including the water soluble toluene is parameter Tr1 ratio while other ratios (Tr2 to Tr5) determine the rate of biodegradation. Normal alkanes are more susceptible to biodegradation than iso- or cyclo- alkanes. Light hydrocarbons useful in understanding the various secondary processes and compartments within the reservoir and also for correlation purposes with the help of these star diagrams.

Thompson Parameters

The amount of light hydrocarbons in source rocks will exponentially increase with depth and increase in temperature meaning that kerogen will form hydrocarbons at exponential rate with respect to temperature (Thompson, 1979). The source rock kerogen will breakdown to crude oil with increase in temperature and then condensate and gas may be formed at even high temperature. We can observe the changes in oil with varying temperature by monitoring the light hydrocarbon parameters and thus can be able to decipher the thermal history and alterations. Several alteration processes can be monitored by the aromaticity ratio (B= toluene/n-heptane) and the paraffinicity ratio (F= n-heptane/methylcyclohexane), where different compounds have different solubility and volatility values. In case of evaporative fractionation, F decreases and B increases T, as represented in B-F diagram (Fig. 3.8).

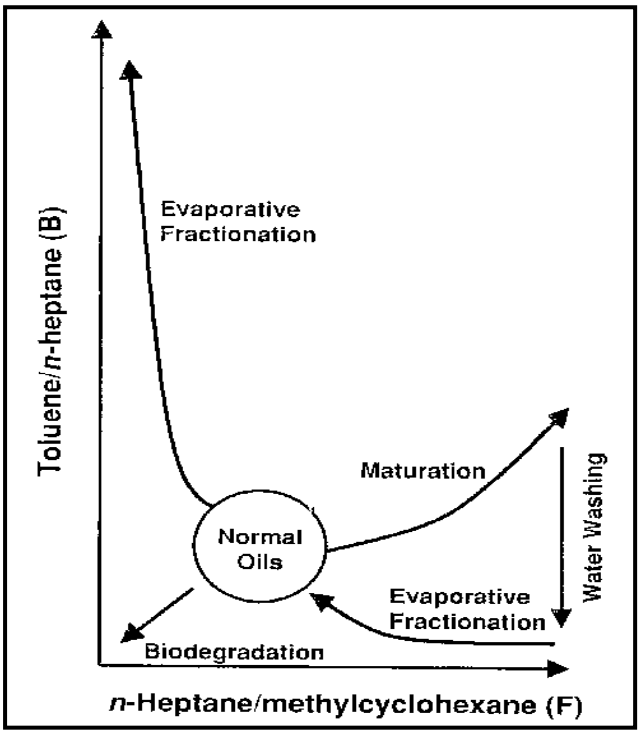

Figure 3-8 The cross-plot by Thompson that incorportes the effects of maturity, biodegradation and evaporative fractionation as monitored by the parameters in the cross-plot and it is the most useful diagram to the study of oils and condensates (Thompson, 1987). The circular region marked as 'normal oils' represents oils which are not affected by post-depositional processes.

Table 3.11 Light hydrocarbon parameters of Thompson explaining the alteration processes and level of maturation (Thompson,1987; Peters et al., 2005). Where, DMCP = Dimethylcyclopentane, H= Heptane Ratio, Heptane ratio: ratio of n-heptane and sum of cyclohexane+2-methylhexane+1,1-DMCP+3-methylhexane+1-cis-3-DMCP+1-trans-3-DMCP+1-trans-2-DMCP+n-heptane+ methylcyclohexane.

No.	Name	Ratio	Purpose	Property
1	A	Benzene/n-hexane	Fractionation, TSR and Water washing	Aromaticity
2	B	Toluene/n-heptane	Fractionation, TSR and Water washing	Aromaticity
3	C	(n-hexane+n-heptane)/ (cyclohexane+methylcyclohexane)	Biodegradation and Maturity	Paraffinicity
4	F	n-heptane/methylcyclohexane	Biodegradation and Maturity	Paraffinicity
5	G	n-heptane/sum of compounds eluting from cyclohexane to methylcyclohexane	Maturity	Paraffinicity
6	H	(100× n-heptane)/ ∑ cyclohexane + C_7 HCs	Biodegradation, Maturity and source	Paraffinicity
7	J	1,1-DMCYP+2-Mhex+3-hexane/1-cis-3DMCYP +1-trans-3-DMCYP+3ethylP+1-trans-2-DMCYP	Maturity	Paraffinicity
8	R	n-hexane/2-methylhexane	Biodegradation, Maturity and source	Parffin branching
9	R2	2-methylhexane/3-methylhexane	Maturity	Paraffinicity
10	S	n-hexane/2,2-dimethylbutane	Biodegradation, Maturity and source	Parffin branching
11	U	Cyclohexane/methylcyclohexane	Maturity and source	Nephtane branching
12	W	Benzene/methylcyclohexane	Mautrity	Paraffinicity

The degree of maturation is directly related with ratio of n-hexane to methylcyclopentane (Jonathan et al. 1975; Thompson, 1979). If the heptane ratio is 18 to 22 then it is normal, 22 to 30 shows more mature hydrocarbons while more than 30 value of this ratio represents super mature hydrocarbons. In order to determine the maturity, the extent of degrading by microbial activity and the source of hydrocarbons for oils and condensates, an evaluation of the light hydrocarbons may prove helpful (Thompson, 1983). The significant increase in the heptane-isoheptane ratio indicates the process of breaking of complex hydrocarbons i.e. thermal cracking. Oils from different sources may also show the variation in the ratio normal heptane to iso-heptane. The ratios developed by Thompson not only used to correlate the maturation of the samples but also account for the changes that occured due to migration of hydrocarbons.

4. Description of Geochemical Results

The description of results from different geochemical techniques applied to the sample sets of this thesis is presented in this chapter. The discussion of the findings will be represented in the following chapter with the use of classification diagrams and with references made to literature. The intension of this chapter is to furnish a best possible presentation of results of the methods applied to the data.

4.1 Gas analysis results from inclusions

The core samples from several wells from offshore Mid-Norway and from the Barents Sea were examined for inclusion gases using gas chromatography. The major hydrocarbons for this study were methane to pentane (C_1 to C_5). In order to avoid contaminants of drilling mud, the samples were cleaned and washed prior to analysis. The ratios of methane to pentane compounds were calculated from chromatograms presented in Appendix A.

4.1.1 Wells from the Mid-Norway

Well 6707/10-1

This well is the discovery well on the Nyk High and is located in the Vøring Basin of the Mid-Norway region. It is claimed that water based mud was used for drilling from depth 3023.65m to 4131.35m of given samples with addition of sodium chloride (NaCl), potassium chloride and glycol (factpages, NPD). The various salts and other compounds make any core extracts from this well totally contaminated, but the inclusions are hermetically sealed against the contaminants from the drilling of the well. The percentages of C_2+ vary at different depths, where the lowest value of C_2+ is 4.5% for the sample at depth of 3143.10m (Tab. 4.1). The highest percentage of C_2+ is found in the deepest sample 4131.35m which is 7.2%. Hence, the average value of C_2+ is 5.85%. The ratios of iso-butane and normal-butane deviate significantly with increase in depth as it is more than unity from depth 3023.65m to 3114.0m but less than unity from 3125.0m to 3140.65m and deeper samples of 4122.25m to 4131.35m. The ratios of pentane isomers mostly show values greater than unity.

Table 4.1 The composition of gases from inclusions for samples of the Mid-Norway.

No.	Well	Depth (m)	Weight (g)	C_1%	i-C_4/n-C_4	i-C_5/n-C_5	C_2+	$C_1/(C_2+C_3)$	C_1 ppm	C_1 ppm/ g rock
1	6707/10-1	3023.65	5.01	94.75	2.00	1.33	5.25	21.04	739.13	147.53
2	6707/10-1	3035.50	5.04	93.27	1.67	1.43	6.73	19.33	456.56	90.59
3	6707/10-1	3059.00	5.01	94.41	2.00	1.50	5.59	20.99	500.68	99.94
4	6707/10-1	3082.70	5.03	94.40	1.60	1.20	5.60	20.11	470.99	93.64
5	6707/10-1	3112.25	5.02	93.17	1.29	0.94	6.83	19.79	313.82	62.51
6	6707/10-1	3114.00	5.01	94.64	1.50	1.31	5.36	22.10	378.89	75.63
7	6707/10-1	3125.00	5.02	94.57	0.78	1.11	5.43	25.31	144.02	28.69
8	6707/10-1	3140.65	5.01	94.53	0.67	1.13	5.47	25.23	114.45	22.84
9	6707/10-1	3143.10	5.00	95.46	1.17	0.75	4.54	33.64	87.14	17.43
10	6707/10-1	4122.25	5.01	94.91	0.80	1.13	5.09	27.43	114.21	22.80
11	6707/10-1	4131.35	5.01	92.80	0.90	1.12	7.20	23.03	127.12	25.37
12	6707/10-2A	4460.25	5.00	92.62	0.65	1.35	7.38	16.60	385.40	77.08
13	6707/10-2A	4472.15	5.00	91.84	0.46	0.73	8.16	15.63	394.65	78.93
14	6707/10-2A	4475.50	5.01	90.74	0.33	0.71	9.26	14.63	256.52	51.20
15	6707/10-2A	4482.60	5.01	82.36	0.31	0.65	17.64	10.17	240.20	47.94
16	6707/10-2A	4485.45	5.01	90.21	0.53	0.65	9.79	14.61	222.96	44.50
17	6707/10-2A	4486.30	5.02	89.26	0.40	0.58	10.74	16.07	183.41	36.54
18	6707/10-2S	3166.75	5.00	88.94	0.61	0.97	11.06	11.62	416.01	83.20
19	6707/10-2S	3186.50	5.01	88.65	0.60	0.95	11.35	11.18	186.85	37.30
20	6707/10-2S	3202.45	5.00	89.79	0.64	0.93	10.21	12.77	362.01	72.40
21	6707/10-2S	3206.00	5.02	90.00	0.59	0.97	10.00	12.22	337.99	67.33
22	6707/10-2S	3218.85	5.01	87.44	0.45	0.68	12.56	12.22	154.24	30.79
23	6707/10-2S	3263.00	5.01	88.49	0.66	0.64	11.51	13.92	89.86	17.94
24	6707/10-2S	3281.00	5.02	90.48	0.57	0.70	9.52	20.27	77.34	15.41
25	6707/10-2S	3294.00	5.00	90.23	0.66	0.83	9.77	17.27	83.85	16.77
26	6607/5-1	2979.00	5.00	90.07	1.50	0.80	9.93	19.74	51.28	10.26
27	6607/5-1	2980.00	5.01	90.82	1.33	0.82	9.18	20.55	57.24	11.43
28	6607/5-1	2982.00	5.00	87.75	0.88	1.24	12.25	16.28	45.49	9.10
29	6607/5-2	4163.00	5.02	90.79	1.04	1.50	9.21	19.18	119.25	23.76
30	6607/5-2	4163.80	5.01	91.67	1.31	1.76	8.33	19.06	96.42	19.25
31	6607/5-2	4168.00	5.01	88.97	1.13	1.25	11.03	18.10	159.71	31.88
32	6607/5-2	4170.80	5.02	91.96	0.83	1.29	8.04	17.37	119.25	23.76
33	6607/5-2	4171.80	5.02	88.36	0.71	1.12	11.64	13.59	165.25	32.92
34	6607/5-2	4183.15	5.00	83.36	0.84	4.16	16.64	10.95	155.98	31.20
35	6607/5-2	4187.60	5.03	89.85	0.76	1.07	10.15	14.34	169.01	33.60

Well 6707/10-2A

In the Mid-Norway region, the well is located on the Nyk High a bit further down the flank of the structure, and it was drilled with oil-based mud for the range of depths from 4460.25m to 4486.30m as mentioned in the (factpages, NPD). The value of C_2+ is the highest at depth 4482.60m (Tab. 4.1) where it exceeds more than 15% while shallow sample at 4460.25m shows the lowest C_2+ value (7.4%) in the sample set of this well. In general, most of the samples from this well were found to contain C_2+ values of less than 10%. The iso-butane to

n-butane ratios of of all samples were calculated to be less than unity with values ranging from 0.3 to 0.6. The ratios of iso-pentane to n-pentane in the samples decrease with increasing depth. The ratios of i-C_4 to n-C_4 are bit higher than 0.5 which denotes virgin gases, but the ratios are greater depths are lower than in the apex well 6707/10-1.

Well 6707/10-2S

The water based drilling mud was used for the exploration well 6707/10-2S located at the Nyk High off Mid-Norway (factpages, NPD). The percentages of C_2+ compounds are generally higher than 10% (Tab. 4.1). The ratios of i-C_4 to n-C_4 vary from 0.45 to 0.66 which are a bit higher than 0.5 but closer to this equilibrium value than the ratio calculated from other Nyk High wells.

Well 6607/5-1

The well was drilled at the Utgard High with water based KCl mud (factpages, NPD) and the gas analysis show greater percentages of C_2+ compounds. The maximum value of C_2+ compounds is at 2982.0m where it is 12.24% while other samples have nearly 10% C_2+ compounds (Tab. 4.1). The ratio of butane isomers (i-C_4/n-C_4) is nearly unity for the more shallow samples. All the samples have ratio more than unity for pentane isomers. The wet compounds (C_2+) of this well are comparable to well 6707/10-2S while ratios of pentane and butane isomers (i-C_4/n-C_4 and i-C_5/n-C_5) are generally higher than well 6707/10-2S.

Well 6607/5-2

The well also from the Utgard High was drilled by using KCl in water based mud at the Utgard High (factpages, NPD). The percentages of C_2+ compounds generally show an increasing trend with the depth range from 8.3 to 16.6 % (Tab. 4.1). The ratios of iso-butane to n-butane become higher than unity in the samples from shallow depths but lower with increase in depth. The concentration of iso-pentane is greater than unity in all samples while the sample at depth 4183.15m it show anomalous ratio of 4.15.

4.1.2 Wells from the Norwegian Barents Shelf

Well 7019/1-1

This well was drilled in the western part of the Barents Sea with pre-hydrated bentonite mud (factpages, NPD). The gas from the inclusion is characterized by wet gas with of C_2+

compound generally more than 15% (Tab. 4.2), while these compounds show maximum percentages at shallower samples (30.9% at 2224.90m) and at greater depth is the percentage value decreasing but still near to 15%. The sample at depth of 2457.0m have exceptionally high ratios for both butane and pentane isomers. Generally, the ratio of iso-butane to normal-butane varies from 0.52 to 0.61 and 0.8 to 1.27 for pentane isomers.

Table 4.2 The composition of gases from inclusions from wells of the Barents Sea. The ratios of butane and pentane isomers were also incorporated with the percentage of methane and C_2+ compounds.

No.	Well	Depth (m)	Weight (g)	C_1 %	i-C_4/n-C_4	i-C_5/n-C_5	C_2+	C_1/(C_2+C_3)	C_1 ppm	C_1 ppm/ g rock
1	7019/1-1	2224.90	5.01	69.07	0.61	0.90	30.93	4.24	398.45	79.53
2	7019/1-1	2225.40	5.02	67.55	0.57	0.87	32.45	4.27	319.93	63.73
3	7019/1-1	2226.65	5.01	74.15	0.61	0.93	25.85	4.88	387.22	77.29
4	7019/1-1	2227.65	5.01	74.12	0.61	0.90	25.88	4.91	388.59	77.56
5	7019/1-1	2457.00	5.02	89.00	2.06	7.09	11.00	15.59	1000.05	199.21
6	7019/1-1	2459.0 A	5.01	78.67	0.53	0.85	21.33	6.96	706.87	141.09
7	7019/1-1	2459.0 B	5.00	80.85	0.50	0.85	19.15	7.13	816.18	163.24
8	7019/1-1	2463.35	5.02	83.27	0.56	0.80	16.73	7.46	541.74	107.92
9	7019/1-1	2565.35	5.01	81.44	0.55	0.88	18.56	7.18	701.19	139.96
10	7019/1-1	2567.45	5.00	85.81	0.52	1.27	14.19	8.69	538.33	107.67
11	7321/7-1	1907.85	5.01	61.78	0.72	1.41	38.22	2.95	97.27	19.42
12	7321/7-1	2003.20	5.03	83.30	0.66	0.93	16.70	7.57	303.24	60.29
13	7321/7-1	2003.90	5.02	81.74	0.74	0.89	18.26	7.79	225.72	44.96
14	7321/7-1	2005.85	5.01	85.47	0.69	0.83	14.53	8.21	350.94	70.05
15	7321/7-1	2006.40	5.01	81.26	0.66	0.83	18.74	7.78	429.30	85.69
16	7321/7-1	2006.60	5.03	84.46	0.88	0.91	15.54	8.19	236.80	47.08
17	7321/7-1	2386.80	5.01	95.16	1.38	1.86	4.84	25.93	1192.50	238.02
18	7321/7-1	2388.40	5.02	95.00	1.33	2.31	5.00	24.49	1041.06	207.38
19	7321/7-1	2391.35	5.00	94.76	1.89	3.26	5.24	28.27	347.70	69.54
20	7321/7-1	2393.40	5.02	95.97	1.29	1.67	4.03	28.71	528.79	105.34
21	7321/8-1	1482.50	5.01	78.24	0.68	1.45	21.76	6.09	347.53	69.37
22	7321/8-1	1490.00	5.02	83.12	0.56	1.04	16.88	6.95	366.10	72.93
23	7321/8-1	1497.20	5.03	80.46	0.56	0.92	19.54	6.16	226.58	45.04
24	7321/8-1	1501.00	5.00	78.84	0.79	2.24	21.16	6.57	424.19	84.84
25	7321/8-1	1501.30	5.01	78.88	0.55	0.98	21.12	6.02	474.79	94.77
26	7321/8-1	1503.85	5.01	81.27	0.52	0.98	18.73	6.33	519.59	103.71
27	7321/8-1	1505.00	5.03	78.41	0.56	0.96	21.59	6.33	528.11	104.99
28	7321/8-1	1507.65	5.01	81.18	0.65	1.03	18.82	6.54	96.93	19.35
29	7321/9-1	1376.50	5.02	84.85	0.64	1.33	15.15	8.18	107.33	21.38
30	7321/9-1	1381.35	5.03	83.98	0.58	1.17	16.02	7.76	200.00	39.76
31	7321/9-1	1382.00	5.01	82.31	0.64	0.92	17.69	5.98	2768.31	552.56
32	7321/9-1	1383.25	5.03	85.78	0.50	0.91	14.22	7.69	967.39	192.32
33	7321/9-1	1390.75	5.01	86.22	0.66	1.00	13.78	8.45	159.63	31.86
34	7321/9-1	1393.70	5.04	81.29	0.66	1.11	18.71	6.96	262.01	51.99
35	7321/9-1	1589.00	5.03	85.90	0.54	0.90	14.10	8.19	434.07	86.30
36	STD			36.32			63.68	0.30	500.00	

Well 7321/7-1

This well is located in the Fingerdjupet Sub-Basin of Bjørnøya area and water-based mud was used for the drilling of the well (factpages, NPD). The percentage of C_2+ compounds is greater (14% to 38%) in shallower samples from 1907.85m to 2006.60m (Tab. 4.2) while the C_2+ compounds have very less values 4.0% to 5.24% in deeper samples 2386.80m to 2393.40m. The ratio between butane isomers (i-C_4/n-C_4) is close to the universal value of 0.5 for virgin gases, and lower in the shallower samples while the values increases for the deeper samples. The pentane isomers ratio follow a variable trend as its 1.4 in the sample 1907.85m but it decreases up to 2006.60m and then increases even more than 3.0 in the deeper samples.

Well 7321/8-1

Water based mud was applied to drill this well 7321/8-1 in the Bjørnøya East area of the Norwegian Barents Sea (factpages, NPD) where all the core samples have more than 15% values for C_2+ compounds (Tab. 4.2) while the ratio of i-C_4/n-C_4 varies from 0.52 to 0.78. The corresponding ratio of pentane isomers ranges from 0.91 to 1.45 where most of samples have greater than unity ratio for pentane isomers.

Well 7321/9-1

At southern margin of Fingerdjupet Sub-Basin of Bjørnøya region was drilled by water based mud (factpages, NPD) where all the samples available for study have C_2+ compounds greater than 10% (Tab. 4.2) and the values lie in between 13.7% to 18.7%. The ratio of iso-butane to n-butane ranges from 0.5 to 0.66 while pentane isomers have greater values (up to 1.3) at shallower level of 1381.35m while in deeper samples (1382.0m to 1589.0m) the values approaching to unity.

4.2 GC-FID results from bitumen samples

In order to perform more analytical work on core samples, the extracts for each sample was prepared to study n-alkanes, pristane to phytane ratios. The type of oil profile developed and North Sea Standard Oil (NSO-1) was used as reference sample to ensure the accuracy and measure of response factor of n-alkanes. All the results from GC-FID is available in Appendix B.

4.2.1 Wells from the Mid-Norway Region

Well 6707/10-1

Due to excessive contaminants in the core samples from 3023.65m to 4131.35m of the well 6707/10-1, the pristane peak is masked by a huge peak of contaminant (ethylene glycol, an addtitive in drilling mud). Therefore, it is hard to determine the pristane to phytane ratio, while the ratio of n-C_{18} and phytane ranges from 0.27 to 0.43 (Tab. 4.3). Most of the samples have very few peaks representing C_{16} to C_{32} compounds.

Well 6707/10-2A

The samples from depths 4460.25m to 4486.30m representing well 6707/10-2A from the Mid-Norway have pristane to phytane ratio between 3.3 and 1.6 where the ratios decrease with depth (Tab. 4.3). Pristane to n-C_{17} ratios have a much more limited range of 0.27 to 0.30 and the ratio of phytane to n-C_{18} lie in between 0.19 to 0.25. The peaks of lighter compounds (less than C_{16} compounds) have much higher peaks but compounds ranging from C_{16} to C_{32} have no significant peaks.

Well 6707/10-2S

The samples from depth 3166.75m to 3294.0m were available for GC-FID analysis where the peaks of pristane are concealed by the contaminant while other measurements were possible. The ratio of phytane to n-C_{18} ranges from 0.15 to 0.55 (Tab. 4.3) while other ratios could not be determined due to a lack of identification of pristane. The C_{16}+ compounds have considerably visible and expressive peaks in the chromatogram.

Well 6607/5-1

The chromatograms for the samples 2979.0m to 2982.0m describe the pristane to phytane ratios from 1.21 to 2.94, while pristane to n-C_{17} ratios range from 0.34 to 0.66 (Tab. 4.3). The proportion between phytane to n-C_{18} confined from 0.31 to 0.48. Some peaks for lighter compounds shows much higher concentrations while minor peaks for C_{16}+ compounds occurred.

Table 4.3 GC-FID results indicating the isoprenoids and n-alkanes ratios for the Mid-Norway samples. Some samples from well 6707/10-1 and 6707/10-2S have contaminant making it hard to identify the isoprenoids in the chromatograms. Where, ND= Not Determined (due to contaminant).

No.	Well	Depth (m)	Pr/Ph	Pr/n-C_{17}	Ph/n-C_{18}
1	6707/10-1	3023.65	ND	ND	ND
2	6707/10-1	3035.50	ND	ND	0.43
3	6707/10-1	3059.00	ND	ND	0.37
4	6707/10-1	3082.70	ND	ND	ND
5	6707/10-1	3112.25	ND	ND	0.35
6	6707/10-1	3114.00	ND	ND	0.33
7	6707/10-1	3125.00	ND	ND	0.38
8	6707/10-1	3140.65	ND	ND	0.34
9	6707/10-1	3143.10	ND	ND	0.27
10	6707/10-1	4122.25	ND	ND	0.27
11	6707/10-1	4131.35	ND	ND	0.29
12	6707/10-2A	4460.25	3.33	0.27	0.19
13	6707/10-2A	4472.15	2.73	0.30	0.23
14	6707/10-2A	4475.50	2.29	0.27	0.24
15	6707/10-2A	4482.60	2.91	0.28	0.22
16	6707/10-2A	4485.45	2.56	0.27	0.23
17	6707/10-2A	4486.30	1.67	0.28	0.25
18	6707/10-2S	3166.75	ND	ND	0.16
19	6707/10-2S	3186.50	ND	ND	0.15
20	6707/10-2S	3202.45	ND	ND	0.23
21	6707/10-2S	3206.00	ND	ND	0.55
22	6707/10-2S	3218.85	ND	ND	0.26
23	6707/10-2S	3263.00	ND	ND	0.15
24	6707/10-2S	3281.00	ND	ND	0.12
25	6707/10-2S	3294.00	ND	ND	0.51
26	6607/5-1	2979.00	2.94	0.44	0.31
27	6607/5-1	2980.00	2.38	0.40	0.34
28	6607/5-1	2982.00	2.88	0.34	0.28
29	6607/5-2	4163.00	1.60	0.58	0.42
30	6607/5-2	4163.80	1.53	0.52	0.44
31	6607/5-2	4168.00	1.55	0.54	0.43
32	6607/5-2	4170.80	1.42	0.39	0.39
33	6607/5-2	4171.80	1.21	0.48	0.30
34	6607/5-2	4183.15	2.46	0.56	0.32
35	6607/5-2	4187.60	1.78	0.50	0.33

Well 6607/5-2

The GC-FID results for the well 6607/5-2 demonstrate low concentration peaks up to C_{10} compounds while peaks are importantly higher for C_{12}+ compounds whereas C_{20}+ compounds are explained by small peaks at shallower level while some peaks showing C_{20}+ compounds are quite visible for deeper samples. The pristane to phytane ratio varies from 1.21 to 2.46

(Tab. 4.3). The pristane to n-C_{17} fraction varies from 0.39 to 0.66 while the values for phytane to n-C_{18} show limit from 0.30 to 0.48.

4.2.2 Wells from the Barents Sea

Well 7019/1-1

The samples from 2224.90m to 2567.45m depth show great variance in pristane to phytane ratios from 0.67 to 2.25 (Tab. 4.4). The pristane to phytane ratio values varies from 0.47 and reach up to a maximum value of 0.75, while the ratio of phytane to n-C_{18} have a limited range of 0.21 to 0.41. The shallower samples (from 2224.90m to 2227.65m) have asymmetric bell-shaped pattern of peaks for C_{20}+ compounds indicating oil profile of n-alkanes. The chromatograms representing the deeper samples have low concentration of normal alkanes not only the lighter fraction but also the heavy hydrocarbons.

Well 7321/7-1

This well have samples available for the project from depths of 1907.85m to 2393.40m and the ratio of pristane to phytane ranges from 0.6 to 1.4 while the ratio of pristane to n-C_{17} ranges from 0.32 to 0.80 (Tab. 4.4). The values of phytane to n-C_{18} change from 0.26 to 0.49. Most of the samples at shallow depths have significantly higher peaks for C_{15} to C_{30} compounds, while these compounds are represented by lower peaks due to camouflage caused by few high peaks which could be contaminant in the extracts of the samples. The samples from shallow depths have higher distribution of n-alkanes while the deeper samples (2386.80m to 2393.40m) much less pronounced peaks for n-alkanes.

Well 7321/8-1

All the chromatographs from the samples of well 7321/8-1 show good and well developed peaks for the compounds between C_{15} to C_{30} compounds but the pattern varies significantly and most of samples have less concentration of lighter compounds demonstrated by minor peaks of for the compounds lighter than C_{15} which is typical for core extracts. The values of pristane to phytane fraction show a maximum value of 2.1 and a minimum value of 1.5 while the ratios of pristane to n-C_{17} ranges from 0.51 to 0.7. The ratios of phytane to n-C_{18} vary from 0.29 to 0.41 (Tab. 4.4).

Table 4.4 Isoprenoids to n-alkanes ratios obtained from GC-FID results of the Barents Sea samples. The sample NSO-1 was added in dataset as a reference.

No.	Well	Depth (m)	Pr/Ph	Pr/n-C_{17}	Ph/n-C_{18}
1	7019/1-1	2224.90	0.86	0.51	0.29
2	7019/1-1	2225.40	0.77	0.57	0.35
3	7019/1-1	2226.65	1.00	0.50	0.25
4	7019/1-1	2227.65	1.05	0.53	0.21
5	7019/1-1	2457.00	0.83	0.63	0.33
6	7019/1-1	2459.0 A	1.00	0.75	0.30
7	7019/1-1	2459.0 B	0.67	0.67	0.33
8	7019/1-1	2463.35	1.23	0.47	0.33
9	7019/1-1	2565.35	2.25	0.53	0.40
10	7019/1-1	2567.45	1.32	0.66	0.36
11	7321/7-1	1907.85	1.32	0.52	0.35
12	7321/7-1	2003.20	0.64	0.80	0.49
13	7321/7-1	2003.90	1.52	0.48	0.33
14	7321/7-1	2005.85	1.13	0.36	0.26
15	7321/7-1	2006.40	0.88	0.32	0.27
16	7321/7-1	2006.60	1.40	0.45	0.32
17	7321/7-1	2386.80	1.41	0.54	0.34
18	7321/7-1	2388.40	0.91	0.55	0.42
19	7321/7-1	2391.35	0.96	0.60	0.42
20	7321/7-1	2393.40	0.80	0.61	0.45
21	7321/8-1	1482.50	1.71	0.64	0.40
22	7321/8-1	1490.00	2.10	0.62	0.38
23	7321/8-1	1497.20	1.87	0.56	0.31
24	7321/8-1	1501.00	1.89	0.51	0.29
25	7321/8-1	1501.30	1.73	0.70	0.38
26	7321/8-1	1503.85	1.52	0.58	0.32
27	7321/8-1	1505.00	1.69	0.70	0.41
28	7321/8-1	1507.65	2.03	0.61	0.31
29	7321/9-1	1376.50	1.76	0.59	0.34
30	7321/9-1	1381.35	1.67	0.48	0.29
31	7321/9-1	1382.00	1.55	0.52	0.30
32	7321/9-1	1383.25	1.93	0.47	0.30
33	7321/9-1	1390.75	1.58	0.49	0.30
34	7321/9-1	1393.70	1.61	0.50	0.30
35	7321/9-1	1589.00	1.53	0.66	0.48
36	NSO-1		1.53	0.66	0.48

Well 7321/9-1

The sample from depth 1376.50m to 1589.0m were selected from well 7321/9-1. The ratios of pristane to phytane vary from 1.53 to 1.93 while the fraction of pristane to n-C_{17} varies from 0.47 to 0.66 (Tab. 4.4). The values of phytane to n-C_{18} are varying from 0.29 to 0.48. The peak prfiles from C_{15} to C_{30} changes significantly with depth and chromatograms display higher concentration of compounds at shallow depth while smaller peaks represented in the deeper samples.

Carbon preference index

Selected chromatograms from the Barents Sea wells, having developed peak of normal alkanes, can be utilized for carbon preference index (CPI) in order to study odd-carbon number predominance. Two values of CPI were selected to infer the maturation of samples (see Sec. 3.4.1 for CPI equations). All the samples show a close range of values from 0.94 to 1.13 (Tab. 4.5). Philippi (1977) described the samples with CPI value approaching to 1.0 was termed as waxy crude oils. In addition the values close to unity propose thermally mature samples (Peters et al., 2005).

Table 4.5 Carbon preference index values for selected samples of the Barents Sea.

No.	Well	Depth (m)	CPI-1	CPI-2
1	7019/1-1	2224.90	1.08	1.01
2	7019/1-1	2225.40	1.07	1.00
3	7019/1-1	2226.65	1.05	1.10
4	7019/1-1	2227.65	1.04	1.05
7	7321/7-1	1907.00	1.06	0.94
8	7321/7-1	2003.90	1.01	1.06
9	7321/7-1	2005.85	1.02	1.09
10	7321/7-1	2006.40	1.03	1.11
11	7321/7-1	2006.60	1.02	1.10
12	7321/8-1	1482.50	1.02	1.05
13	7321/8-1	1490.00	1.03	1.04
14	7321/8-1	1497.20	1.07	1.13
15	7321/8-1	1501.00	1.03	1.13
16	7321/8-1	1501.30	0.98	1.03
17	7321/8-1	1503.85	1.07	1.09
18	7321/8-1	1505.00	1.05	1.10
19	7321/8-1	1507.65	1.04	1.08
20	7321/9-1	1376.50	1.05	1.04
21	7321/9-1	1381.35	1.07	1.07
22	7321/9-1	1390.75	1.03	1.00
23	7321/9-1	1393.70	1.05	1.04

4.3 GC-MS results from bitumen samples

Biomarkers are the compounds having higher molecular weight and can be examined by using GC-MS instrument. It can be workable to study even if the compounds have small concentration in the complex matrix of petroleum. In addition to biomarkers, some other compounds like methyldibenzothiophenes and phenanthrene compounds were also identified in GC-MS analysis. Peaks in the GC-MS chromatogram help to determine the facies and maturity parameters in Appendix C. All the explanation of parameters is discussed in previous chapter of methods and parameters in Tab. 3.9.

4.3.1 Wells from the Mid-Norway

Well 6707/10-1

Samples from well 6707/10-1 were analyzed to calculate the various parameters of GC-MS in which the ratios of Ts/ (Ts+Tm) range from 0.49 in sample 3140.65m to 0.66 at greater depth of 4122.25m that is maximum in all samples from the Mid-Norway (Tab. 4.6). The diahopane to norhopane ratio and 29Ts to norhopane ratios are minimum (0.29 and 0.17 respectively) and follow the same trend. Hopanes are much dominant than steranes and regular steranes have higher concentrations than diasteranes. The values of maturity parameter C_{20}/ (C_{20}+C_{28}) triaromatic steroides (TA) (Mackenzie et al., 1985) range from 0.42 to 0.61. The average values for calculated vitrinite reflectivity remain higher than unity in the samples of well 6707/10-1.

Well 6707/10-2A

Samples from the well 6707/10-2A represent an increase in the values for Ts/ (Ts+Tm) with the depth and range from 0.33 to 0.53 but the ratios of diahopane to normorentane indicate minor variation from 0.56 to 0.57 (Tab. 4.6). The hopane compounds are significantly higher than steranes while regular sterane dominate the diasterane compounds. Maturity parameter C_{20}/ (C_{20}+C_{28}) triaromatic steroides (TA) (Mackenzie et al., 1985) represents higher values at shallower depth and considerably decreases with the depth. The paramters describing the vitrinite reflectance remain similar (1.07) to the well 6707/10-1.

Well 6707/10-2S

Striking chromatograms from the samples of well 6707/10-2S indicate large range of Ts/ (Ts+Tm) ratio from 0.33 to 0.51 whereas diahopane to normorentane shows same minimum value of 0.33 but it reaches up to 0.61 in the sample depth of 3218.85m (Tab. 4.6). There is great variation of hopane to sterane ratio but the value remain higher than 2.0 in all samples and ranges between 2.34 to 5.46 which is highest in all samples of the Mid-Norway. Diasteranes to regular steranes ratio vary from 0.35 to 0.64 while the maturity parameter (triaromatic steroid) depicts the range of values from 0.38 to 0.64 that is maximum value in all the Mid-Norway samples. The average values for all the parameters describing the vitrinite reflectance are slightly higher (1.10) in well 6707/10-2S than the two other wells from the Nyk High.

Well 6607/5-1

The values for dihopane to normorentane limit from 0.22 to 0.28 while the ratio of bisnorhopane to norhopane represent a significant decrease with increase in depth and ranges from 0.34 to 0.75 which is maximum value in all samples from Mid-Norway. Hopane to sterane ratio ranges from 1.53 to 1.30 while diasterane to regular sterane ratio vary from 0.39 to 0.47. The maturity parameter (triaromatic steroid) values lie from 0.23 to 0.48. The well shows lower values for calculated vitrinite reflectance (0.89) than all the wells from the Nyk High.

Well 6607/5-2

The ratio of Ts/(Ts+Tm) denote the values from 0.46 to 0.64 in samples of well 6607/5-2 while diahopane to normorentane ratios range from 0.33 to 0.50 while least values represent the ratio between bisnorhopane to norhopane from all other Mid-Norway samples. There exist great variations in hopane to sterane ratio from 0.5 to 2.06 while diasterane to regular sterane ratio have slight variation from 0.52 to 0.75. The maturity parameter has maximum value of 0.69 which is the highest in all Mid-Norway wells while its decreases to 0.45 in other samples of same well whereas the average values for calculated vitrinite reflectance (0.97) is higher than the samples from well 6607/5-1 but lower than all the wells from the Nyk High.

Table 4.6 Biomarker parameters (see Tab. 3.9 for description of parameters) used in GC-MS analysis results of both the Mid-Norway and the Barents Sea samples.

No.	Well	Depth (m)	1	2	3	4	5	6	7	8	9	10	11	12	13	14	15	16	17	18	19	20	21	22	23	24	25	26	27
1	6707/10-1	3035.50	0.54	0.56	0.59	0.89	0.35	0.52	1.59	0.08	3.44	0.44	0.32	0.68	40.40	33.77	25.83	0.42	0.17	2.34	0.93	0.62	4.56	1.36	0.96	1.23	0.84	8.49	0.13
2	6707/10-1	3082.70	0.55	0.52	0.62	0.86	0.33	0.53	1.30	0.08	3.98	0.41	0.29	0.69	37.58	33.56	28.86	0.43	0.23	2.38	0.69	0.66	5.13	1.36	0.81	1.31	0.88	9.16	0.14
3	6707/10-1	3140.65	0.49	0.58	0.58	0.86	0.32	0.47	0.77	0.05	3.69	0.43	0.29	0.56	35.35	30.70	33.95	0.61	0.34	1.61	0.65	0.57	6.17	1.18	0.79	1.11	0.96	5.08	0.21
4	6707/10-1	4122.25	0.66	0.29	0.59	0.93	0.17	0.06	2.67	0.12	4.07	0.53	0.51	0.62	43.48	22.28	34.24	0.55	0.60	2.54	0.63	0.63	4.23	1.40	0.78	1.26	0.82	11.51	0.11
5	6707/10-2A	4475.50	0.33	0.57	0.55	0.83	0.24	0.23	0.18	0.03	6.14	0.37	0.19	0.33	36.73	30.61	32.65	0.54	0.54	2.33	0.73	0.66	5.00	1.35	0.84	1.31	0.88	17.10	0.07
6	6707/10-2A	4482.60	0.53	0.56	0.56	0.85	0.17	0.10	0.89	0.11	3.44	0.53	0.39	0.53	43.40	26.42	30.19	0.38	0.45	1.77	0.78	0.61	5.46	1.22	0.87	1.20	0.91	20.37	0.05
7	6707/10-2S	3166.75	0.39	0.58	0.56	0.86	0.22	0.21	0.58	0.02	5.46	0.36	0.19	0.52	37.12	28.03	34.85	0.38	0.36	2.03	0.94	0.60	4.69	1.29	0.96	1.19	0.85	12.83	0.08
8	6707/10-2S	3202.45	0.51	0.38	0.59	0.88	0.20	0.13	1.41	0.06	2.57	0.46	0.33	0.51	38.08	25.10	36.82	0.64	0.17	2.24	0.75	0.61	5.46	1.34	0.85	1.20	0.91	14.45	0.07
9	6707/10-2S	3218.85	0.37	0.61	0.56	0.84	0.25	0.22	0.27	0.03	4.23	0.33	0.20	0.37	34.27	30.07	35.66	0.54	0.55	3.00	0.31	0.73	4.88	1.47	0.59	1.47	0.87	23.70	0.06
10	6707/10-2S	3263.00	0.42	0.48	0.57	0.86	0.23	0.21	0.63	0.04	2.43	0.41	0.23	0.47	38.51	29.31	32.18	0.63	0.62	3.00	0.45	0.70	5.57	1.47	0.67	1.40	0.92	19.53	0.07
11	6707/10-2S	3281.00	0.33	0.46	0.53	0.84	0.23	0.21	0.31	0.03	3.30	0.35	0.23	0.35	36.99	24.66	38.36	0.50	0.65	3.00	0.36	0.71	5.30	1.47	0.61	1.43	0.90	21.60	0.06
12	6707/10-2S	3294.00	0.53	0.33	0.60	0.92	0.19	0.11	3.91	0.14	2.34	0.54	0.37	0.64	42.62	27.43	29.96	0.60	0.27	3.25	0.46	0.70	5.33	1.51	0.68	1.41	0.90	17.69	0.08
13	6607/5-1	2979.00	0.53	0.24	0.25	0.73	0.24	0.75	1.99	0.07	1.51	0.35	0.14	0.39	32.23	32.23	35.55	0.48	0.29	1.73	0.27	0.53	3.53	1.21	0.56	1.02	0.77	6.05	0.14
14	6607/5-1	2980.00	0.46	0.22	0.32	0.88	0.22	0.58	2.69	0.13	1.53	0.39	0.14	0.47	32.19	35.96	31.85	0.23	0.30	1.00	0.14	0.64	4.33	0.95	0.48	1.27	0.83	2.37	0.69
15	6607/5-1	2982.00	0.38	0.28	0.54	0.89	0.21	0.34	2.47	0.16	1.30	0.51	0.31	0.43	39.93	28.73	31.34	0.48	0.41	1.45	0.26	0.54	4.60	1.13	0.55	1.05	0.85	4.47	0.19
16	6607/5-2	4163.00	0.64	0.40	0.58	0.91	0.21	0.12	4.44	0.30	2.06	0.56	0.41	0.75	46.12	27.85	26.03	0.45	0.13	2.15	0.58	0.58	10.00	1.32	0.75	1.13	1.24	3.49	0.24
17	6607/5-2	4163.80	0.46	0.50	0.53	0.92	0.16	0.19	10.05	0.41	0.50	0.38	0.17	0.52	48.74	23.53	27.73	0.69	0.59	1.56	0.50	0.53	4.41	1.16	0.70	1.03	0.83	11.07	0.08
18	6607/5-2	4170.80	0.53	0.33	0.65	0.94	0.18	0.13	3.60	0.20	1.25	0.53	0.33	0.68	40.07	31.56	28.37	0.46	0.46	2.00	0.05	0.60	0.56	1.28	0.43	1.18	0.55	2.81	3.44
19	7019/1-1	2225.40	0.47	0.68	0.63	0.90	0.23	0.23	0.76	0.07	4.28	0.59	0.48	0.40	36.11	27.38	36.51	0.80	0.31	1.10	0.64	0.45	1.03	1.00	0.78	0.84	0.59	28.03	0.05
20	7019/1-1	2226.65	0.47	0.71	0.63	0.91	0.24	0.25	0.96	0.07	2.41	0.55	0.78	0.31	36.98	29.17	33.85	0.55	0.49	0.62	0.34	0.34	3.00	0.72	0.60	0.60	0.73	14.06	0.05
21	7019/1-1	2457.00	0.39	0.71	0.64	0.89	0.37	0.16	1.88	0.12	1.94	0.54	0.48	0.49	40.24	21.95	37.80	0.63	0.58	1.00	0.19	0.36	6.67	0.95	0.52	0.65	1.00	3.74	0.16
22	7019/1-1	2459.00	0.46	0.50	0.60	0.86	0.30	0.13	9.63	0.32	2.18	0.40	0.17	0.65	23.08	28.85	48.08	0.54	1.00	14.25	4.30	0.85	6.36	2.22	2.98	1.75	0.97	6.47	0.04
23	7321/7-1	2003.90	0.45	0.40	0.57	0.83	0.16	0.19	5.42	0.50	1.55	0.50	0.45	0.21	42.11	31.58	26.32	0.63	0.40	2.08	0.87	0.60	8.75	1.30	0.92	1.19	1.15	10.02	0.08
24	7321/7-1	2005.85	0.50	0.57	0.60	0.77	0.37	0.29	3.80	0.35	1.81	0.48	0.38	0.75	41.67	20.83	37.50	0.79	0.31	3.39	1.21	0.69	12.67	1.53	1.12	1.38	1.43	8.92	0.11
25	7321/7-1	2006.60	0.29	0.50	0.60	0.89	0.15	0.15	4.41	1.29	1.66	0.41	0.28	0.28	23.81	28.57	47.62	0.75	0.38	2.69	0.50	0.65	9.17	1.42	0.70	1.29	1.18	7.67	0.11
26	7321/7-1	2386.80	0.64	0.40	0.59	0.92	0.83	0.83	2.08	0.08	0.65	0.45	0.33	0.50	50.00	26.92	23.08	0.55	0.61	1.79	0.92	0.59	6.45	1.23	0.95	1.16	0.98	5.17	0.15
27	7321/8-1	1501.00	0.64	0.50	0.40	0.83	0.30	0.59	13.80	0.40	0.69	0.40	0.33	0.39	41.67	25.00	33.33	0.71	0.51	1.82	0.41	0.57	4.93	1.24	0.65	1.11	0.87	12.12	0.07
28	7321/8-1	1503.85	0.56	0.40	0.44	0.68	0.57	0.25	5.95	0.11	0.78	0.56	0.33	0.75	52.17	8.70	39.13	0.69	0.27	1.20	0.51	0.50	4.75	1.04	0.70	0.95	0.86	7.41	0.11
29	7321/9-1	1376.50	0.58	0.50	0.56	0.86	0.47	0.20	3.17	0.11	1.24	0.59	0.40	0.63	40.54	18.02	41.44	0.92	0.18	1.23	0.44	0.48	5.92	1.05	0.67	0.90	0.94	9.98	0.07
30	NSO-1		0.51	0.63	0.59	0.92	0.31	0.41	0.25	0.04	3.24	0.57	0.43	0.51	38.28	28.52	33.20	0.45	1.00	0.91	0.61	0.41	2.38	0.90	0.77	0.76	0.68	4.16	0.19

4.3.2 Wells from the Barents Shelf

Well 7019/1-1

The samples from the well 7019/1-1 reflect slight variance for Ts/ (Ts+Tm) ratio from 0.39 for sample 2457.0m to 0.47 for the sample 2226.65m but greater difference in ratio between diahopane to normorentane from 0.50 for sample 2459.0m to 0.71 for the sample 2226.65m. The ratio of bisnorhopane to norhopane decreases with the depth and varies from 0.25 for shallow sample to 0.13 for deeper sample which is least in all samples of the Barents Sea. The ratios of hopanes to steranes decreases significantly with increase in depth and attain maximum value of 4.28 in shallow sample of the well which is the highest value in the wells of the Barents Sea. The diasteranes to regular sterane ratio ranges from 0.31 to 0.65 while the maturity parameter (TA steroides) ranges from 0.53 to 0.80. Excluding the abnormal value of calculated vitrinite reflectivity (more than 2.0) for sample at depth of 2459.0m, most of the shallow samples have average value of vitrinite relectance (0.75) which is less than all the samples in the dataset.

Well 7321/7-1

The ratio of Ts/ (Ts+Tm) extends from 0.29 to 0.64 while diahopane to normorentane ratio varies from 0.40 to 0.57 (Tab. 4.6). The fraction explaining the relation of bisnorhopane to norhopane differ from 0.15 to 0.83 while hopane to sterane concentration is expressed by the range from 0.65 to 0.84. The values of diasterane to regular sterane range from 0.21 to 0.75. The maturity parameter (TA steroides) for samples has minimum 0.55 to the maximum value of 0.79 whereas the methylphenanthrene index changes from 0.50 to 1.21. Higher average of value for the parameters explaining the vitrinite reflectance is higher (1.18) than all the samples from the Mid-Norway.

Well 7321/8-1

The samples from the well 7321/8-1 has Ts/ (Ts+Tm) ratio from 0.56 to 0.64 whereas diahopane to normorentane ranges from 0.40 to 0.50 (Tab. 4.6). The relative concentration of bisnorhopane to norhopane varies from 0.25 to 0.59. The ratio of hopane to sterane limits from 0.69 to 0.78 whereas diasterane to regular sterane fraction 0.39 to 0.75. The values for maturity parameter (TA steroides) lie in between 0.69 to 0.71 while methylphenanthrene index ranges from 0.41 to 0.51. The average value for parameters of vitrinite reflectance (0.93) is higher than well 7019/1-1 but lower than the samples from the well 7321/7-1.

Well 7321/9-1

The samples from well 7321/9-1 depict the ratio of Ts/ (Ts+Tm) as 0.58 while diahopane to normorentane ratio lies close to 0.50 (Tab. 4.6). The relative fraction of bisnorhopane to norhopane limits from 0.20. The hopane to sterane ratio is more than one that narrates to higher peaks of hopanes than the steranes whereas the concentration of diasteranes is higher than regular steranes. The maturity parameter (TA steroides) reaches the maximum value of 0.92 which is greater than other wells of the Barents Sea while 0.44 is designated value for methylphenanthrene index. The average caluculated vitrinite reflectance (0.89) is equal to the well 6607/5-1 which is higher than well 7019/1-1 but lower than samples fom two other samples from the Barents Sea.

4.4 Iatroscan (TLC-FID) results of bitumen samples

The gross composition of and the relative percentages of saturated, polars and aromatic compounds can be analyzed by using Iatroscan in Appendix D which identifies that concentration of each component, display peaks which areas encountered with the response factor measures the percentage of type of organic compound in the hydrocarbons.

4.4.1 Wells from the Mid-Norwegian Shelf

Well 6607/5-1

The samples from the well 6607/5-1 represent higher percentages of polar compounds that remain more than 60% in the samples (Tab. 4.7) while the percentage of saturated compounds vary from 29 to 36.6%. The aromatic compounds are least and have less than 5% in the sample results in high SAT/ARO and range from 11.7 to 28.2.

Well 6607/5-2

The percentage of saturated hydrocarbons in the samples from well 6607/5-2 depicts great variation with depth. In shallow samples the percentage of saturated hydrocarbons is more than 50% at depth of 4163.80m while commonly it decreases with depth up to 11.2% (Tab. 4.7). The percentage of aromatic hydrocarbons remain less than 1% in all samples of the well which higher the ratio of SAT/ARO, while polar compounds show an increase in value with depth from 40.5 to 88.7%.

Table 4.7 Iatroscan resluts for various wells from the Mid-Norway and the Barents Sea samples which not only shows the relative fraction of compounds but also shows the content of hydrocarbons in mg/g of rock.

No.	Well	Sample ID	Weight (g)	Total vol. (ml)	vol. used (ul)	Area			Extract concentration (mg/ml)				Extract Concentration (%)				Extract yield (mg/g rock)				
						SAT	ARO	POL	SAT	ARO	POL	TOTAL	SAT	ARO	POL	TOTAL	SAT	ARO	POL	TOTAL	SAT/ARO
1	6607/5-1	2979.00	10.16	0.080	3	12540	1156	52726	4.14	0.35	9.44	13.94	29.71	2.53	67.76	100	0.0326	0.0028	0.0744	0.11	11.72
2	6607/5-1	2980.00	10.12	0.045	3	32885	1256	102488	10.86	0.38	18.36	29.60	36.68	1.30	62.02	100	0.0483	0.0017	0.0816	0.13	28.29
3	6607/5-2	4163.00	10.16	0.050	3	14316	50	37807	4.73	0.02	6.77	11.51	41.05	0.13	58.81	100	0.0233	0.0001	0.0333	0.06	309.39
4	6607/5-2	4163.80	10.11	0.040	3	19128	175	24221	6.32	0.05	4.34	10.71	58.98	0.50	40.52	100	0.0250	0.0002	0.0172	0.04	118.11
5	6607/5-2	4168.00	10.06	0.045	3	3540	538	34922	1.17	0.16	6.26	7.59	15.40	2.17	82.43	100	0.0052	0.0007	0.0280	0.03	7.11
6	6607/5-2	4170.80	10.12	0.035	3	1975	68	13418	0.65	0.02	2.40	3.08	21.20	0.68	78.13	100	0.0023	0.0001	0.0083	0.01	31.38
7	6607/5-2	4171.80	10.20	0.070	3	1445	0	20345	0.48	0.00	3.64	4.12	11.58	0.00	88.42	100	0.0033	0.0000	0.0250	0.03	-
8	6607/5-2	4183.15	10.08	0.035	3	1765	0	25710	0.58	0.00	4.61	5.19	11.23	0.00	88.77	100	0.0020	0.0000	0.0160	0.02	-
9	6607/5-2	1487.6.	10.18	0.075	3	1957	29	17184	0.65	0.01	3.08	3.73	17.31	0.24	82.45	100	0.0048	0.0001	0.0227	0.03	72.92
10	7019/1-1	2224.90	10.13	0.035	3	7546	34	21258	2.49	0.01	3.81	6.31	39.49	0.16	60.35	100	0.0086	0.0000	0.0132	0.02	239.83
11	7019/1-1	2225.40	10.14	0.060	3	874	336	44091	0.29	0.10	7.90	8.29	3.48	1.24	95.28	100	0.0017	0.0006	0.0467	0.05	2.81
12	7019/1-1	2459.00	10.12	0.050	3	3946	8	20453	1.30	0.00	3.66	4.97	26.22	0.05	73.73	100	0.0064	0.0000	0.0181	0.02	533.00
13	7019/1-1	2463.35	10.18	0.060	3	2200	785	15037	0.73	0.24	2.69	3.66	19.85	6.55	73.60	100	0.0043	0.0014	0.0159	0.02	3.03
14	7019/1-1	2565.35	10.08	0.085	3	3593	151	19857	1.19	0.05	3.56	4.79	24.77	0.96	74.26	100	0.0100	0.0004	0.0300	0.04	25.71
15	7321/7-1	2003.90	10.19	0.070	3	73375	105	52100	24.23	0.03	9.33	33.59	72.12	0.10	27.78	100	0.1664	0.0002	0.0641	0.23	755.13
16	7321/7-1	2005.85	10.12	0.065	3	37070	62	33912	12.24	0.02	6.07	18.33	66.76	0.10	33.13	100	0.0786	0.0001	0.0390	0.12	646.09
17	7321/7-1	2006.40	10.04	0.075	3	18535	28	109132	6.12	0.01	19.55	25.68	23.84	0.03	76.13	100	0.0457	0.0001	0.1460	0.19	715.31
18	7321/7-1	2006.60	10.07	0.075	3	21879	151	9048	7.22	0.05	1.62	8.89	81.25	0.52	18.23	100	0.0538	0.0003	0.0121	0.07	156.57
19	7321/7-1	2386.80	10.11	0.035	3	16152	448	9049	5.33	0.14	1.62	7.09	75.21	1.93	22.86	100	0.0185	0.0005	0.0056	0.02	38.96
20	7321/7-1	2391.35	10.19	0.030	3	8304	95	41880	2.74	0.03	7.50	10.27	26.69	0.28	73.03	100	0.0081	0.0001	0.0221	0.03	94.45
21	7321/7-1	2393.40	10.12	0.035	3	14472	214	115715	4.78	0.07	20.73	25.57	18.69	0.26	81.06	100	0.0165	0.0002	0.0717	0.09	73.08
22	7321/8-1	1482.50	10.20	0.085	3	4146	19	31654	1.37	0.01	5.67	7.04	19.43	0.08	80.48	100	0.0114	0.0000	0.0472	0.06	235.80
23	7321/8-1	1490.00	10.13	0.110	3	11461	67	103403	3.78	0.02	18.52	22.33	16.95	0.09	82.96	100	0.0411	0.0002	0.2011	0.24	184.85
24	7321/8-1	1497.20	10.17	0.085	3	9064	85	6491	2.99	0.03	1.16	4.18	71.57	0.62	27.80	100	0.0250	0.0002	0.0097	0.03	115.23
25	7321/8-1	1501.30	10.18	0.075	3	40010	789	27277	13.21	0.24	4.89	18.34	72.04	1.31	26.64	100	0.0973	0.0018	0.0360	0.14	54.80
26	7321/8-1	1503.85	10.11	0.065	3	17494	147	18301	5.78	0.04	3.28	9.10	63.48	0.49	36.02	100	0.0371	0.0003	0.0211	0.06	128.60
27	7321/8-1	1505.00	10.08	0.060	3	48097	1352	34881	15.88	0.41	6.25	22.54	70.45	1.83	27.72	100	0.0945	0.0025	0.0372	0.13	38.44
28	7321/8-1	1507.65	10.19	0.080	3	44018	3020	30164	14.53	0.92	5.40	20.86	69.68	4.42	25.90	100	0.1141	0.0072	0.0424	0.16	15.75
29	7321/9-1	1381.35	10.18	0.045	3	49926	11164	42995	16.48	3.41	7.70	27.60	59.73	12.36	27.91	100	0.0729	0.0151	0.0340	0.12	4.83
30	7321/9-1	1383.25	10.12	0.055	3	7967	716	21776	2.63	0.22	3.90	6.75	38.97	3.24	57.79	100	0.0143	0.0012	0.0212	0.04	12.02
31	7321/9-1	1390.75	10.11	0.060	3	10495	1140	18028	3.47	0.35	3.23	7.04	49.20	4.95	45.85	100	0.0206	0.0021	0.0192	0.04	9.95
32	7321/9-1	1393.70	10.16	0.075	3	19616	2545	26724	6.48	0.78	4.79	12.04	53.79	6.46	39.75	100	0.0478	0.0057	0.0353	0.09	8.33
33	7321/9-1	1589.00	10.20	0.045	3	18541	1314	33244	6.12	0.40	5.95	12.48	49.06	3.22	47.72	100	0.0270	0.0018	0.0263	0.06	15.25
34	NSO	-	-	-	3	30588	21668	22724	10.10	6.62	4.07	20.79	48.58	31.85	19.58	100	-	-	-	-	1.53

4.4.2 Wells from the Barents Sea

Well 7019/1-1

The polar compounds dominate the composition of samples from the well 7019/1-1 and fraction of polars ranges from 60.3 to 95.3% while the saturated compounds vary from 3.5 to 39.5% (Tab. 4.7) but the average values for saturated exceed than 20% whereas the aromatic compounds have least fraction in the extract and contribute only 0.05 to 6.5%. Therefore, the SAT/ARO ratio varies significantly from 3 to more than 100.

Well 7321/7-1

The ratios of SAT/ARO remain higher from 40 to more than 100 due to minor fraction of aromatic compounds in the samples (Tab. 4.7). Where in shallow samples have greater percentage of saturated compounds from 72 to 81 percent while at depth the percentage of polar compounds increases from 27 to 81%. In the deep samples of the well 7321/7-1, the fraction of saturated compound considerably decreases from 81% to most deep sample having least value of 18%.

Well 7321/8-1

In the samples from well 7321/8-1, the fraction of saturated compounds is relatively less in shallow samples (16 to 19%) but from depth of 1497m the percentage increases abruptly to more than 70 percent (Tab. 4.7) while lower aromatic component make it possible for SAT/ARO ratio to vary from 38 to more than 100. The percentages of polar compounds remain higher in shallow samples up to the depth of 1490m but it remains 29 to 36% in deep samples.

Well 7321/9-1

The aromatic fraction in the samples is the highest than all dataset of the Barents Sea samples and ranges from 3.2 to 12.3% (Tab. 4.7). The higher percentages of aromatic essentially lessen the SAT/ARO ratio from 4.8 to 15. The fractions of saturated compounds vary from 38.9% to 59.7% while the amount of polar compounds varies from 27.9 to 57.78 % in the samples. Generally, the fraction of saturated components remains more than 40 % in all samples.

4.5 Light hydrocarbons results

Several samples from the Norwegian Continental Shelf have been included in the study (Appendix E) to overlook the light hydrocarbon parameters defined by Halpern (1995) and Thompson (1987). The parameters not only describe the transformation of hydrocarbons but also correlate the various oils in the region. It is also important to note that the results generated from Thompson transformation diagram depict the similarity with the star diagrams proposed by Halpern.

4.5.1 Light hydrocarbons from the North Sea

The samples from the Ula, Gyda, Hild and Gulfaks Sør fields were included from the North Sea in which the Tr1 and Tr2 ratios are the highest in the Hild Field illustrating the transformation of hydrocarbons by considering the Halpern parameters. Tr3 ratio is the highest in the Ula while Tr4, Tr5 and Tr8 ratios are the highest in the Gulfaks Sør Field. The Gyda filed shows higher ratios of Tr6 and Tr7 while Tr1 is least in the Ula Field. The correlation parameters (C1 to C5) show close values of the North Sea fields. By applying the Thompson parameters, it is obvious that the A, B, R and S ratios are the highest in the Hild Field while C, F, G and J ratios are higher in the Ula Field. The Ula Field contains least value of A and B while the Gulfaks Sør Field contains least ratio of C and F parameters of Thompson.

4.5.2 Light hydrocarbons from the Haltenbanken

The fields available for study in Haltenbanken area includes one well from the Tyrihans Sør and Midgard where A, B and W ratios of Thompson parameter are higher in the Midgard sample while three samples from the Smørbukk Field indicate least ratio in A and B but greater ratios of C, G, J and R parameters while F ratio is the highest in Draugen-2 sample. The S parameter has highest value in Smørbukk-1 sample which also has maximum values for Tr1 to Tr5 ratios of Halpern parameters. The Mikkel-1 sample has higher value of Tr6 and Tr7 while Tr8 ratio is the highest in the Smørbukk-3 sample of the Haltenbanken area. The correlation parameters for the Haltenbanken area show slight variation from 0.18 to 0.24.

Table 4.8 Results of light hydrocarbon analysis of samples form the Norwegian Continental Shelf applied in different pramaeters designed by Thompson (A to S) and Halpern (Tr1 to Tr8 transforation ratios, C1 to C5 correlation ratios and H is the heptane ratio)

No.	FIELD	TEST	WELL	Code	A	B	C	F	G	J	R	U	W	R2	S	Tr1	Tr2	Tr3	Tr4	Tr5	Tr6	Tr7	Tr8	C1	C2	C3	C4	C5	H Ratio
1	NSO			43978	0.27	0.60	1.93	1.02	15.18	1.20	1.44	0.81	6.94	1.06	7.75	1.42	2.36	1.55	1.64	3.18	1.14	1.11	0.61	0.19	0.21	0.21	0.21	0.18	16.17
2	Gyda	DST2	2/1-3	43980	0.20	0.51	1.94	0.93	15.10	1.26	1.44	0.79	5.52	1.04	10.00	1.32	2.60	1.73	1.81	3.54	1.15	1.13	0.74	0.19	0.23	0.22	0.17	0.18	16.00
3	Ula	DST2	7/12-6	43981	0.18	0.41	2.40	1.18	17.36	1.39	1.54	0.91	6.15	1.01	10.00	1.18	2.84	1.82	1.84	3.66	1.08	1.08	0.76	0.19	0.23	0.22	0.18	0.19	18.48
4	Hild	DST3	29/6-1	43982	0.34	0.79	1.51	0.79	14.42	1.31	1.68	0.84	6.65	1.03	12.31	2.42	3.08	1.77	1.83	3.60	1.13	1.10	0.77	0.19	0.23	0.20	0.19	0.19	15.09
5	Gulfaks Sør	DST2	34/10-16	43984	0.29	0.63	1.11	0.69	13.85	1.34	1.52	0.65	4.19	1.04	5.30	1.79	2.81	1.79	1.86	3.64	1.11	1.07	0.80	0.19	0.25	0.21	0.18	0.17	14.60
6	Tyrihans Sør	DST1	6407/1-2	43986	0.48	0.83	1.37	1.03	12.58	1.02	1.20	0.45	7.88	0.99	2.59	1.09	1.32	1.11	1.10	2.20	1.04	1.03	0.44	0.20	0.20	0.20	0.20	0.20	13.88
7	Midgard	DST1	6407/2-2	43990	0.86	0.96	0.90	0.86	12.35	1.03	1.16	0.33	8.21	1.00	1.22	1.22	1.26	1.09	1.09	2.18	1.02	1.02	0.44	0.20	0.20	0.20	0.20	0.20	13.66
8	Mikkel-1	DST1	6407/6-3	43993	0.17	0.50	1.45	0.75	13.66	1.22	1.52	0.70	3.27	1.00	10.13	1.46	2.96	1.95	1.94	3.89	1.27	1.20	0.84	0.17	0.24	0.19	0.21	0.18	14.22
9	Mikkel-2	DST3	6407/6-3	43995	0.38	0.79	1.30	0.91	12.09	1.08	1.14	0.47	6.13	1.00	3.17	1.11	1.40	1.23	1.23	2.46	1.06	1.05	0.48	0.20	0.21	0.20	0.20	0.19	13.23
10	Draugen-1	DST2	6407/9-2	43400	0.38	0.84	1.33	0.91	11.46	1.05	1.05	0.45	6.47	1.01	2.41	0.99	1.17	1.11	1.12	2.22	1.02	1.01	0.45	0.20	0.20	0.20	0.20	0.20	12.69
11	Draugen-2	DST1	6407/9-5	44001	0.39	0.81	1.50	1.22	12.27	1.05	1.10	0.42	6.56	1.01	2.37	1.00	1.23	1.11	1.12	2.23	1.02	1.01	0.45	0.20	0.20	0.21	0.20	0.20	13.61
12	Smørbukk-1	DST4	6506/11-2	44004	0.28	0.57	1.93	0.99	15.54	1.85	1.00	0.91	7.11	1.64	12.67	2.02	3.52	2.14	3.52	5.66	1.14	1.11	1.20	0.18	0.24	0.23	0.18	0.17	16.25
13	Smørbukk-2	DST5	6506/11-2	44005	0.24	0.46	2.22	1.18	17.20	1.56	1.46	1.01	7.04	1.08	10.62	1.40	3.04	1.92	2.08	4.00	1.04	1.04	0.79	0.19	0.23	0.23	0.19	0.17	18.34
14	Smørbukk-3	DST6	6506/11-2	44006	0.11	0.39	2.21	1.10	17.03	1.58	1.41	0.99	3.26	1.08	7.25	1.24	3.16	2.08	2.24	4.32	1.08	1.04	0.87	0.19	0.23	0.22	0.19	0.18	18.04
15	Smørbukk Sør-1	DST3	6506/12-3	44018	0.25	0.57	1.89	0.97	16.06	1.42	1.60	0.94	6.35	0.99	14.33	1.88	3.27	2.06	2.04	4.10	1.12	1.10	0.86	0.18	0.24	0.21	0.19	0.18	16.90
16	Smørbukk Sør-2	DST5	6506/12-3	44020	0.21	0.55	1.76	1.03	15.68	1.27	1.62	0.78	4.78	0.99	11.32	1.55	2.82	1.76	1.75	3.51	1.18	1.07	0.74	0.19	0.24	0.21	0.18	0.17	16.58
17	Smørbukk Sør-3	DST6	6506/12-3	44021	0.53	0.79	0.93	0.78	12.00	1.05	1.22	0.40	5.57	0.98	2.07	1.10	1.39	1.17	1.14	2.31	1.06	1.04	0.46	0.20	0.21	0.21	0.20	0.19	13.12
18	Heidrun	DST2	6507/7-3	44043	0.35	0.64	0.72	0.55	13.86	0.67	1.53	0.58	3.18	0.96	3.68	1.26	1.99	0.00	1.30	1.30	1.31	1.08	0.31	0.18	0.25	0.21	0.18	0.18	14.60
19	Goliat			Goliat	1.00	7.65	0.11	0.08	3.32	0.52	0.88	0.37	1.40	1.12	ND	5.50	0.72	0.73	0.81	1.54	1.50	1.38	0.32	0.14	0.24	0.18	0.14	0.29	3.42
20	Snøhvit			Snøhvit	1.18	1.08	0.83	0.84	11.85	1.02	1.11	0.31	9.55	1.00	ND	1.29	1.19	1.07	1.07	2.14	1.02	1.01	0.43	0.20	0.20	0.20	0.20	0.20	13.15

4.5.3 Light hydrocarbons from the Barents Sea

The samples from the Barents Sea include each sample from the Goliat and Snøhvit fields. The application of Thompson parameters shows higher values of B, U and R2 for the Goliat filed while A, C, F, G, J, R and W ratios represented in the Snøhvit Field. The Halpern parameters only have higher values of Tr1 and Tr6 while Tr2 to Tr5, Tr7 and Tr8 are higher in the Snøhvit filed. The C1 to C5 parameters of correlation depict similar values in the Snøhvit (0.20) while all the ratios applied for correlation vary in case of the Goliat sample.

5. Discussions

The analytical results of the samples were presented in preceding chapter and are here interpreted within the context of existing methodology and articles related to petroleum geochemistry. The focus of this discussion is on application of maturity and organic facies concepts and to argue the samples within a framework of maturity and organic source rock facies.

Thus, the aim is to look at the evidences allowing the source rock facies of the Barents Sea samples to be compared with that of the Mid-Norway (Vøring Basin and Utgard High). In addition to medium range hydrocarbon parameters, some maturity parameters from the biomarkers were also included in the study.

5.1 Composition of hydrocarbons

The gross composition of hydrocarbons in each well is demonstrated by various geochemical results and in terms of e.g. gases is the gross composition represented by the molecular expression composition, while for core extracts is the gross composition referring to the percentage amount of saturated hydrocarbons, aromatic hydrocarbons and polar compounds (resins+asphaltenes). Whiticar (1994) stated that the percentage composition of gases is strongly influenced by the type of kerogen and maturity. The percentage of C_2+ compounds define the origin of the hydrocarbon gases as biogenic or thermogenic where C_2+ gases are generally considered to be result of thermal cracking of heavy or complex hydrocarbons while less than 1% of C_2+ gases along with most of methane is generated by biological activities (biogenic gas). Methanogenic bacteria are responsible for generating biogenic gases at temperature less than 50°C. Higher C_2+ compositions reflect oil associated gases i.e. gases generated together with oils in the “oil-window” and the demarcation line between drier condensate associated gas and oil associated gas is placed at between 12-15% on a sliding scale (Schoell, 1983).

The increase in maturation significantly raises the percentage of higher boiling hydrocarbons (Whiticar, 1994) from biogenic to thermogenic gases, and it reaches a maximum of about 20-25% in the oil-window before it falls back towards 5% for condensates. It is for this reason

that examination of the C_2+ content informs about the origin of the petroleum phase entrapped in inclusions (Karlsen et al., 1993; Nedkvitne et al., 1993). It follows the composition of gases in each well is discussed separately, see below:

5.1.1 Wells from the Mid-Norway region

The gas analysis results indicate the percentage of C_2+ compounds which is representative of wet gas existence. In the sample of the well 6707/10-1 the percentage of C_2+ compounds is more than 5% which reflect thermogenic generation of hydrocarbons but this value is also less than 10% in all samples of this well. According to Schoell (1983), this gas is therefore representing condensate associated gas. The ratio of iso-butane to normal butane is higher than unity in all the samples while the ratio of butane isomers ranges from 0.3 to 0.5 in North Sea gases. The increase in the butane isomers ratio reveals the alteration processes including biodegradation or gas fractionation (Horstad and Larter, 1997). The well 6707/10-2A shows quite distinct characteristics although its much near to the well 10-1 as the percentage of C_2+ compounds normally ranges up to 10% but in one case its even advances up to 17.64% making it quite favourable for wet gases and higher hydrocarbons. The ratio of butane isomers (i-C_4/n-C_4) varies to a limited range from 0.31 to 0.64 placing the samples of well 6707/10-2A in category of non-altered and non-biodegraded gases. The relative amount of lighter components of hydrocarbons in the core samples of 6707/10-2S are determined by gas analysis from inclusion in which the percentage of C_2+ compounds slightly varies with the depth but the values remain higher than 10% in all samples like the wells from the Utgard High (6607/5-1 and 6607/5-2).

The drilling wells in deep water area to the West of the Haltenbanken region was assigned as dry biodegraded gas in the Nyk High where over-pressured areas are dry until the traps are adequately deep to abstain from fracture gradient while, the dry gas contained in the Nyk High could have Jurassic source rock origin mainly with some possibility of Cretaceous origin (Karlsen et al., 2004).

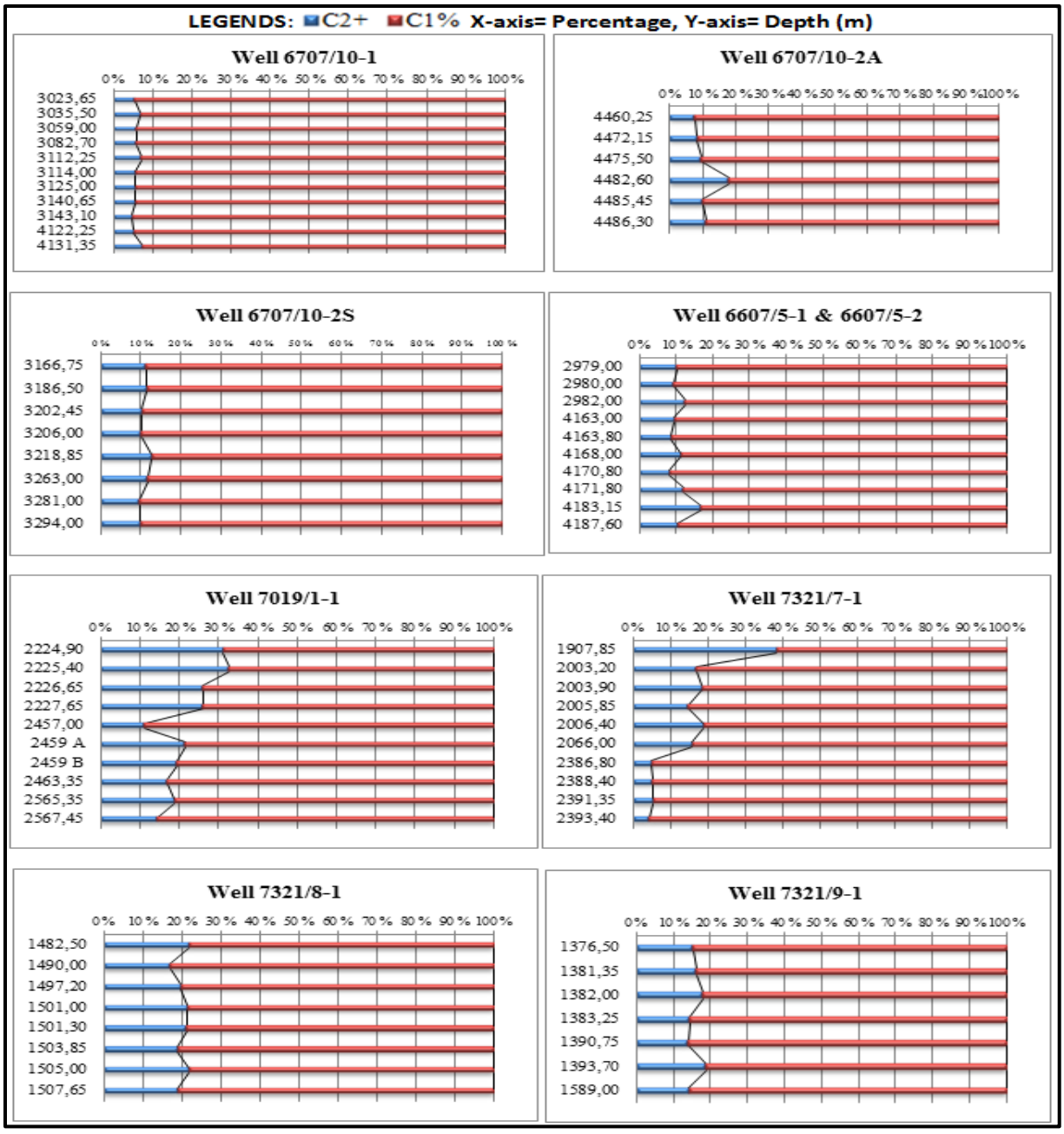

Figure 5.1 The percentage of methane (C_1%) compared to wet components of hydrocarbons (C_2+%) in all the samples from the Mid-Norway and the Barents Sea. Note the high C_2+ gas wetness in the Barents Sea wells and the generally drier gas in the Vøring Basin and Utgard wells. The separation between "condensate associated" gases and "oil associated" gases is normal place at between 12-15% (Schoell, 1983) on a sliding scale as this would also depend on PVT conditions at the time of formation of the inclusions (Karlsen et al., 1993; Nedkvitne et al., 1993). It is safe to conclude that the inclusion samples from the Barents Sea samples represent general oil systems. Thus oil was present in these traps at the time for the formation of the inclusions. At Nyk/AAsta Hansteen can we conclude that wet thermogenic gas existed in the traps system at the time of inclusion formation and that the petroleum phase was most likely condensates to light oil.

The results from Iatroscan signifies the amount of polar compounds contain more than 50% in both wells of 6607/5-1 and 6607/5-2 from the Mid-Norway while saturated component is the second in abundance while aromatic compounds only limited up to 3% in the samples of the Mid-Norway wells (6607/5-1 and 6607/5-2). The high polar content could be the result of leakage in the Cretaceous strata due to over-pressure in the western part of the Haltenbanken area which propagate the fractures within the reservoir (Karlsen et al., 2004). In Iatroscan results, due to less effect transformation processes, the polar and aromatic hydrocarbons retain the original facies signature than the saturated compounds but due to low mobility aromatic and polar compounds can conveniently mixed with subsequent entrance of petroleum (Karlsen et al., 1995).

5.1.2 Wells from the Norwegian Barents Sea

The fraction of C_2+ compounds from the well 7019/1-1 ranges from more than 30% at shallower level but decrease to 15% in deep samples. In the samples of well 7321/7-1, the percentage of C_2+ compounds remains greater than 15 % in shallow samples but from depth 2386.80m to 2393.40m the fraction of C_2+ compounds fall up to 5% indicating two different situations in the same well. The well 7321/8-1 contain C_2+ compounds that remain near to 20% in all samples unlike 7321/7-1 where the percentage significantly decreases to 5% whereas, the fraction of C_2+ compound remain 15 to 20 % in all samples of the well 7321/9-1 (Fig. 5.1). On the whole, the Barents Sea is have values of C_2+ at shallower levels where it exceed 30% in some cases placing in oil associated gases while it limits to less than 10 % in few cases categorizing in condensate associated gas to dry gas (Schoell, 1983) but the percentage of C_2+ compounds commonly greater in the Barents sea sample than the samples from the Mid-Norway.

The Iatroscan results for the samples of the Barents Sea describe the variable signatures of quantity of hydrocarbons from various wells (Fig. 5.2) where the samples from 7019/1-1 well comprise more than 60% polar fraction while saturated compounds ranges from 5 to 40% but aromatics remain limited from 0 to 5%. The zone rich in polar compounds both in well 7019/1-1 represents the migration channels or precipitation occurred during petroleum migration (Bhullar et al., 2000).

The shallower part of the Barents Sea well 7321/7-1 have greater fraction of saturated compounds while the polar fraction dominated in the deeper samples that may reflects the different population of petroleum in the deeper part of well (Karlsen and Larter 1991). The relative concentration of polar compounds reversed in the well 7321/8-1 where shallower part

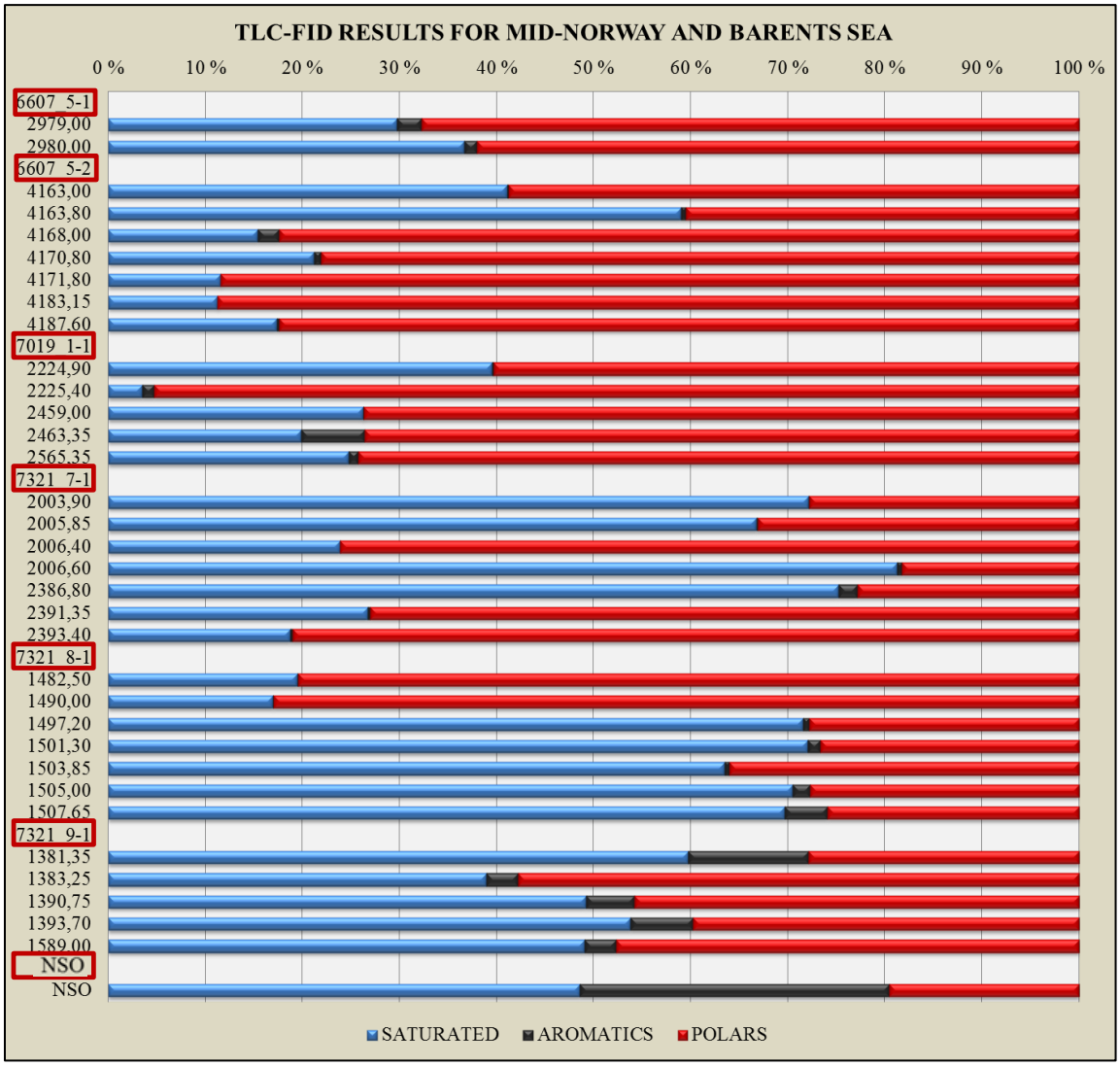

Figure 5.2 Bar chart depicting the percentage composition of saturated, aromatics and polar compounds from TLC-FID results. The relative proportion of saturated compounds is generally higher in the samples from the Barents Sea. Note that core extracts are normally higher in polar compounds than produced oil like the North Sea Oil standard NSO-1 (Karlsen and Larter, 1989; 1991; Karlsen et al., 1995; 2004, Bhullar et al., 2000). The comparatively high amounts of polar compounds in the Utgard system i.e. 6607/5-1 and 6607/5-2 suggest the palaeo-petroleum. The Barents Sea wells show variably the same signatures of palaeo-oils and condensates, with condensates typically representing systems with very low amounts of aromatic hydrocarbons.

has more polar fraction and deeper samples are composed of saturated compounds and slight increase in aromatic components. Like the well 7321/8-1, the samples from well 7321/9-1 have less aromatic compounds while the saturated fraction has slightly greater part than the polar constituents in the composition of hydrocarbons from the well 7321/9-1.

5.2 Transformation processes

The alteration of reservoirs by various transformation processes like biodegradation is vital in order to understand the quality of hydrocarbons that not only affect the API gravity but also vary the composition of oil columns and oil fields (Larter et al., 2012). Microbial degradation of oil preferably removes the saturated hydrocarbons which in result increase the percentage of polar compounds in the residual oil. The removal of wet components (C_2+) of gases in reservoirs is favoured in the progress in biodegradation that amplify the percentage of (C_1) methane (Wenger et al., 2002). Sufficient porosity and permeability, temperature less than 80°C, micro-organisms efficient for degradation of hydrocarbons and salinity less than 100 to 150 parts per thousand controls the biodegradation of petroleum (Peters et al., 2005).

In the present study, the alteration of petroleum is suggested by relative quantity of butane isomers (i-C_4/n-C_4), removal of normal alkanes (Peters et al., 2005) from GC-FID chromatograms, removal of wet part of gases (C_2+) evident from gas analysis from inclusions and increase the polar fraction in the hydrocarbons presented in Iatroscan results.

5.2.1 Altered Mid-Norway samples

Gases from inclusions of core samples from Well 6707/10-1 (Nyk High) contain iso-butane to n-butane ratio (i-C_4/n-C_4) greater than 1.5 from depth 3023.65m to 3114.0m corresponding to higher methane percentage (94% average) while GC-FID chromatograms reveal lower concentration of normal alkanes hydrocarbons indicating the phenomenon of transformation.

The shallower samples of well 6607/5-2 from the Utgard High have i-C_4 to n-C_4 ratios greater than unity from depth 4163.80m to 4168.0m (Fig. 5.3) directing towards the bacterial degradation which is also observable from relatively smaller peaks of normal alkanes in GC-FID chromatogram of 4168.0m. The other clue appeared from relative increase in the

percentage of polar compounds with the depth, unlike the unaltered oil where saturated compound generally increases with the depth (see Iatroscan bar chart, Fig. 5.2).

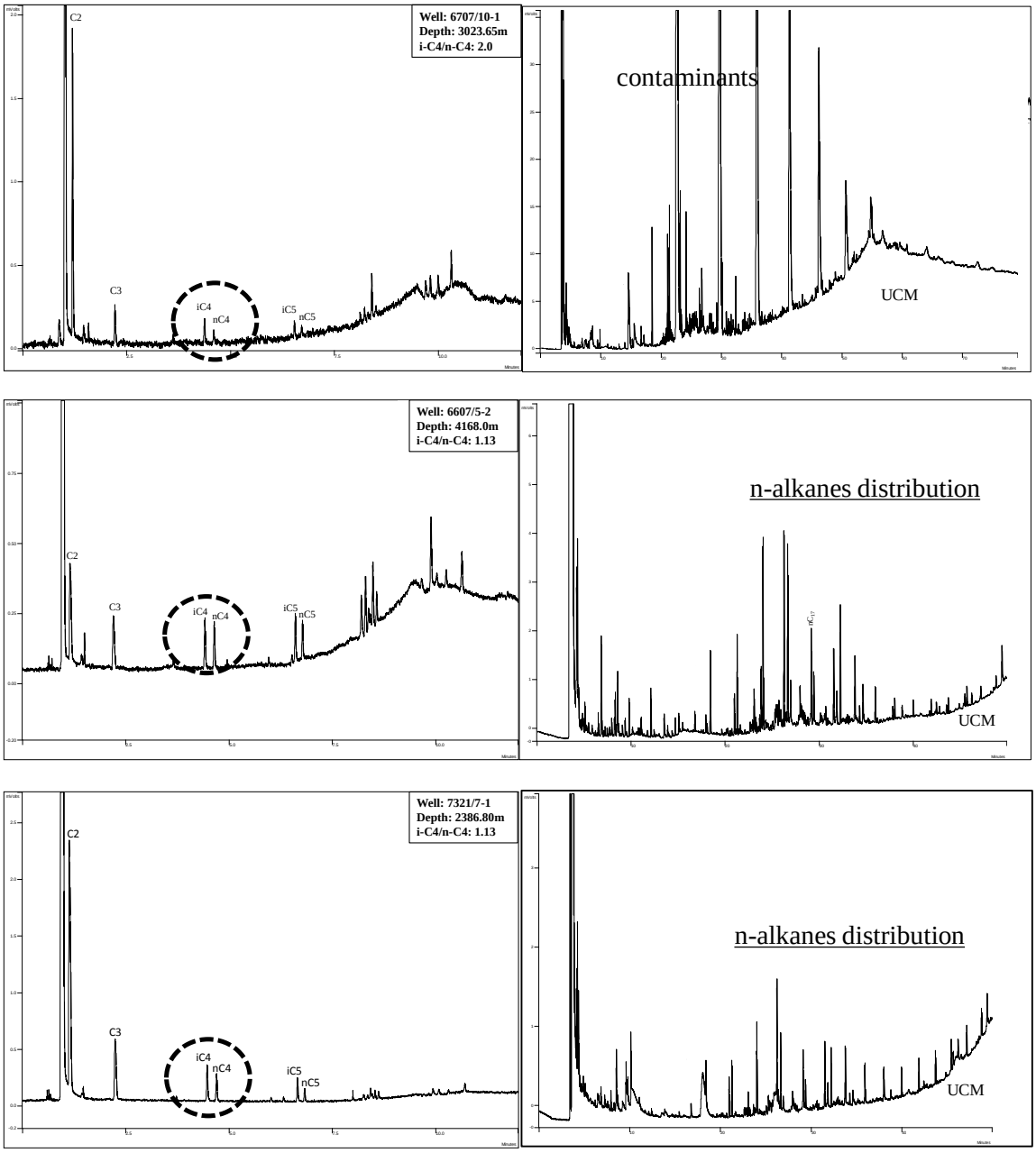

Figure 5.3 The evidences of altered petroleum in shallower portion of well 6707/10-1 (Nyk High), shallower hydrocarbons from the Utgard High (6607/5-2) and deeper reservoir part of well 7321/7-1 (SW Barents Sea). The chromatograms represent the gases from inclusions with higher ratios of butane isomers (i-C_4/n-C_4) marked by dashed circles while GC-FID traces of respective samples show incomplete distribution of n-alkanes.

5.2.2 Degraded Barents Sea samples

The transformation of hydrocarbons from the Barents Sea is discernible in relatively deeper portion of well 7321/7-1 where the samples from depth 2386.80m to 2393.40m has significant increase in butane isomers ratio ($i\text{-}C_4/n\text{-}C_4$) from 1.3 to 1.89 (Fig. 5.3) that is much higher than the ratio in shallower samples (0.66 to 0.88). The percentage of methane is higher (95% average) in deeper samples also depicting the removal of wet components by microbial action. The considerable loss of n-alkanes in GC-FID chromatograms from depth 2386.80m to 2391.35m is also an expression of degraded hydrocarbons. The abnormal increase in fraction of polar compounds with depth in the samples at depth 2391.35m and 2393.40m also intimates the alteration of oils (Fig. 5.2).

5.3 Organic facies

5.3.1 Facies defined by isoprenoids and n-alkanes

The environment of deposition can be explained by facies parameters which include the ratios of isoprenoids (Pr and Ph) to n-alkanes. Fig. 5.4 is a cross-plot of $Pr/n\text{-}C_{17}$ versus $Ph/n\text{-}C_{18}$ which not only determines the oxic/anoxic conditions and depositional environment but also accounts for the maturation and transformation processes.

Generally, the reducing conditions endured in the Mid-Norway samples while the Barents Sea samples have slightly oxidizing environment (Fig. 5.4). Most of samples both from the Mid-Norway and the Barents Shelf depict marine conditions while variations of samples in the plot within the same well point towards biodegradation like some samples from well 6607/5-2 from the Mid-Norway and 7321/7-1 from the Norwegian Barents Sea.

The maturation level varies from less mature at the Utgard High to more mature area of the Nyk High in case of the Mid-Norway samples but there exists slight variation of maturation for the Barents Sea samples where 7321/8-1 and 7321/9-1wells have less maturity than samples from the Mid-Norway. One sample from 7321/7-1 is seen to be an outlier that may be due to the effect of biodegradation (Fig. 5.4).

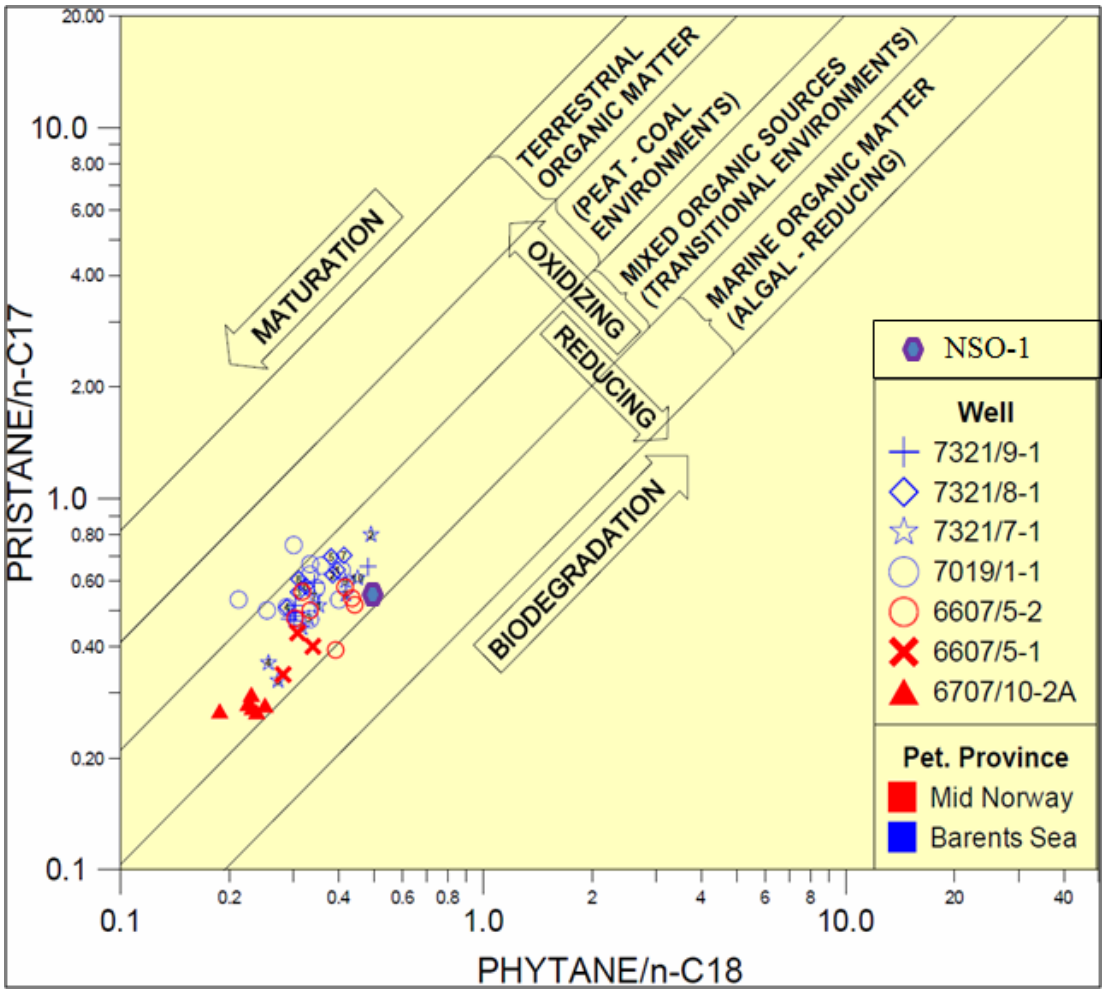

Figure 5.4 Facies diagram proposed by Shanmugam (1985) to describe the relative changes in facies for vaious samples.This facies and maturity diagram suggests slightly higher maturities for some of the Mid-Norway samples e.g. well 6707/10-2A (Nyk/AAsta Hansten) as compared to the situation for the Utgard well wells 6607/5-1 and 6607/5-2 which has close maturation level as that of the Barents Sea samples. The organic facies is also in this case normal marine and typical for samples from the Spekk/Hekkingen/Draupne/Kimmeridge system, with possibly a slightly less anoxic source facies for the Barents Sea samples.

5.3.2 Facies estimation from steranes isomers

The environment of deposition can also be explained with the help of facies parameters from biomakers. One such parameter is the percentages of C_{27}, C_{28} and C_{29}-steranes which are plotted in ternary diagram as presented in Fig. 5.5. The divisions of the triangle represent the type of depositional environment or source of hydrocarbons. The abundance of C_{29} steranes refers to higher plants acted as source of organic matter while lacustrine environment is depicted by high concentration of C_{28} steranes. (Shanmugam, 1985). The dependance on the concentration of steranes limits the authorization of ternary diagram (Moldowan et al., 1985)

but still it is widely used for environmental interpretation. The variation of sterane concentration is slightly more in case of the Barents Sea samples than samples for the Mid-Norwegian Shelf. The well 7321/7-1 lie from open marine to estaurine conditions while well 7019/1-1 from the Barents Sea also indicate the effect of estaurine deposition as seen in Fig. 5.5.

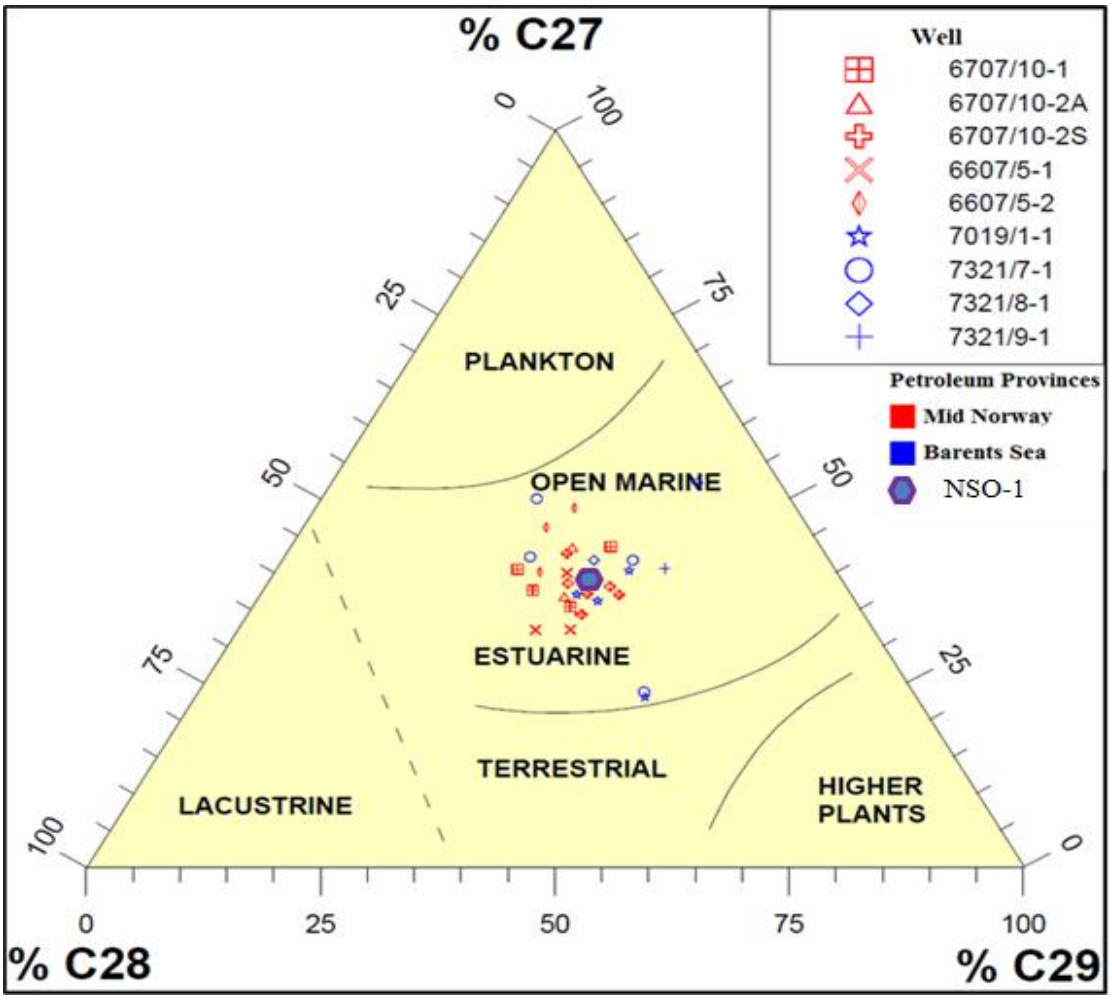

Figure 5.5 The distribution of steranes (C_{27}, C_{28} and C_{29}) for prediction of organic facies for studied samples. All the samples from the Mid-Norway and the Barents Sea well plotted within the centre portion of this sterane diagram, a situation typical for petroleums sourced from Spekk/ Hekkingen/Draupne/Kimmeridge derived petroleums (Shanmugam, 1985). The samples from the Mid-Norway and the Barents Sea lie in marine environment. However, few samples from well 7019/1-1 and 73217/7-1 are influenced by estaurine conditions. The overall variation in environmental conditions is more in the Barents Sea samples than the Mid-Norway but all the samples from the Nowegian Shelf lie in marine window indicating same source rock facies for generation of petroleum in the region.

5.3.3 Facies identified from isoprenoids and aromatic hydrocarbons

The distribution of source rock facies representing the crude oil can be illustrated by the ratios of isoprenoids and methylphenanthrene rations as shown in Fig. 5.6 (modified from Hughes et al., 1995) where most of the samples both from the Mid-Norway and the Barents Shelf were deposited in marine and lacustrine environment (Zone 3). The dispersion of samples from the Mid-Norwegian Shelf and the Barents Sea reveal the wider range of Barents Sea samples from marine (Zone 3) to sulphate poor lacustrine environment (Zone 2) whereas all of Mid-

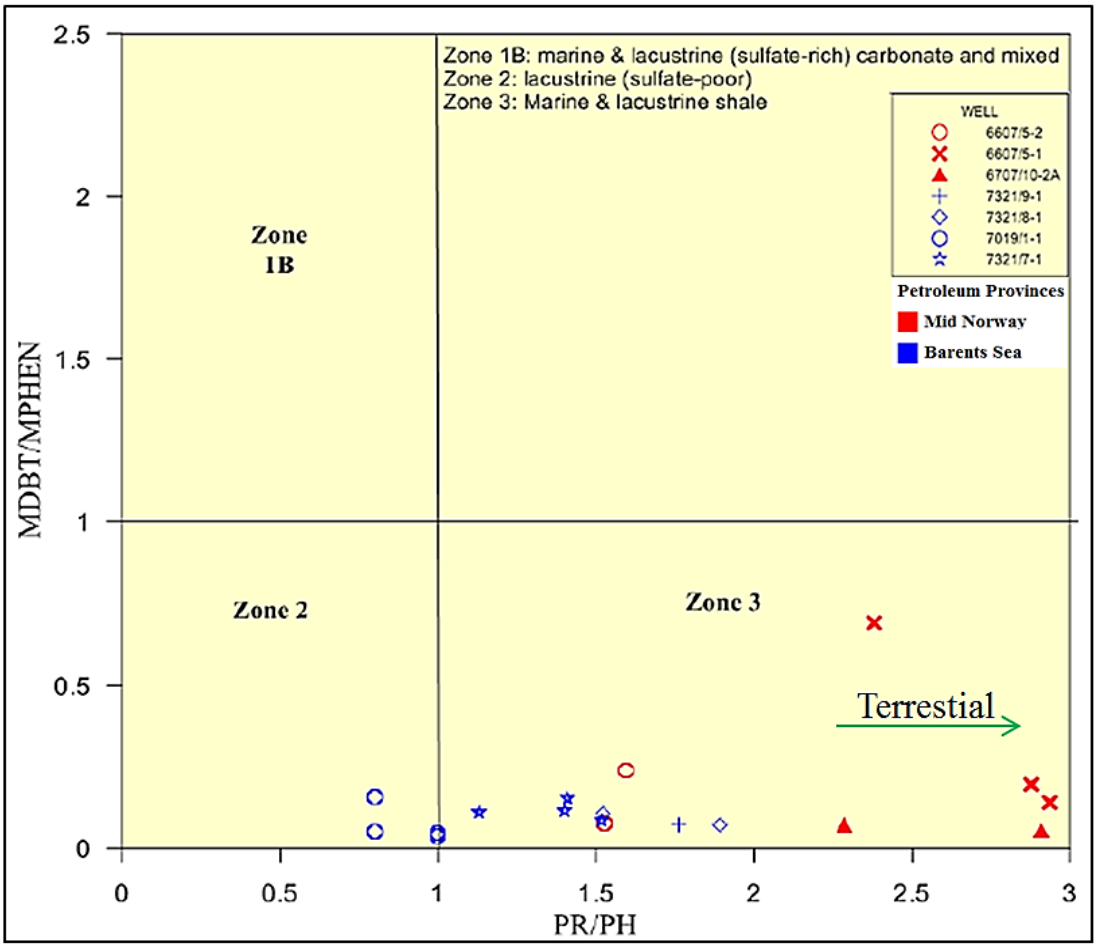

Figure 5.6 The samples of this study plot mostly in "Zone 3" representing marine and lacustrine shales which is typical for Spekk/Hekkingen/Draupne/Kimmeridge derived oils and condensates. The main reason that two of the 7019/1-1 samples plot within "Zone 2" is related to high evaporative losses of pristane (Pr) relative to phythane (Ph) from the cores of this deep and hot well with its light condensate (modified from Hughes et al., 1995).

Norway samples fall in zone 3 of marine and lacustrine shale environment except few samples of the Mid-Norway (well 6607/5-1) are influenced by terrestrial input. The relative change of depositional environment from marine to terrestrial is an indicator of variation in petroleum potential as proposed for Cretaceous reservoirs of the Noth Sea (Justwan and Dahl, 2005). Both ratios mentioned in the plot are influenced by the maturation in a complex manner (Radke et al., 2001). The wells from the Utgard High suggest the decrease in terrestrial input from the East (well 6607/5-1) to the West (well 6607/5-2) stated by Karlsen et al., (2004). In addition to this, the oil and condensate present in the Cretaceous sediments are affected by fractionation that is evident from vertical migration through open fractures as mentioned in Karlsen et al., (1995) where fractionation process can also be a good description for the samples from well 7019/1-1 (Barents Sea).

5.4 Maturity

5.4.1 Maturity concluded from non-biomarkers

In this section, the demonstration of the maturity of the samples based parameters such as isoprenoids to n-alkanes ratio, CPI vales, aromatic hydrocarbons and their associated calculated vitrinite reflectances will be discussed.

Isoprenoids to n-alkanes ratio (pristane to n-C_{17} and phytane to n-C_{18}) have inverse relation with the degree of maturation since the cracking increases the amount of normal alkanes in petroleum (Tissot et al., 1971). The relation of maturation with the aid of these parameters can be observed in Fig. 5.4 which also demonstrates that these ratios are also affected by secondary processes like biodegrardation. In case of the Mid-Norway, the ratios explained very well the variation of maturity for various wells as well 6607/5-1 has lower value of maturation than well 6707/10-2A but biodegradation masked the maturity of the Barents Sea samples lower than the Mid-Norway. Several other parameters determine the level of maturation for each sample which assigned the position of samples in the stages of hydrocarbons generation. The second indication of maturity can be evident from the carbon preference index (CPI) where significant higher or lower value than unity for CPI indicate lower maturity (Peters et al., 2005) but in the given dataset, the selected samples form the Barents sea show values of CPI near to unity which provide clue towards mature samples

(Fig. 5.7). The values of CPI for limited dataset of the Barents Sea samples represent very close CPI values ranging from 0.95 to 1.10, which indicates less variation in maturation of the samples from siliciclastic provenance. It is important to note that the values of CPI-2 are slightly ahead than CPI-1 which depict that heavy saturated alkanes show resistance to secondary alteration processes.

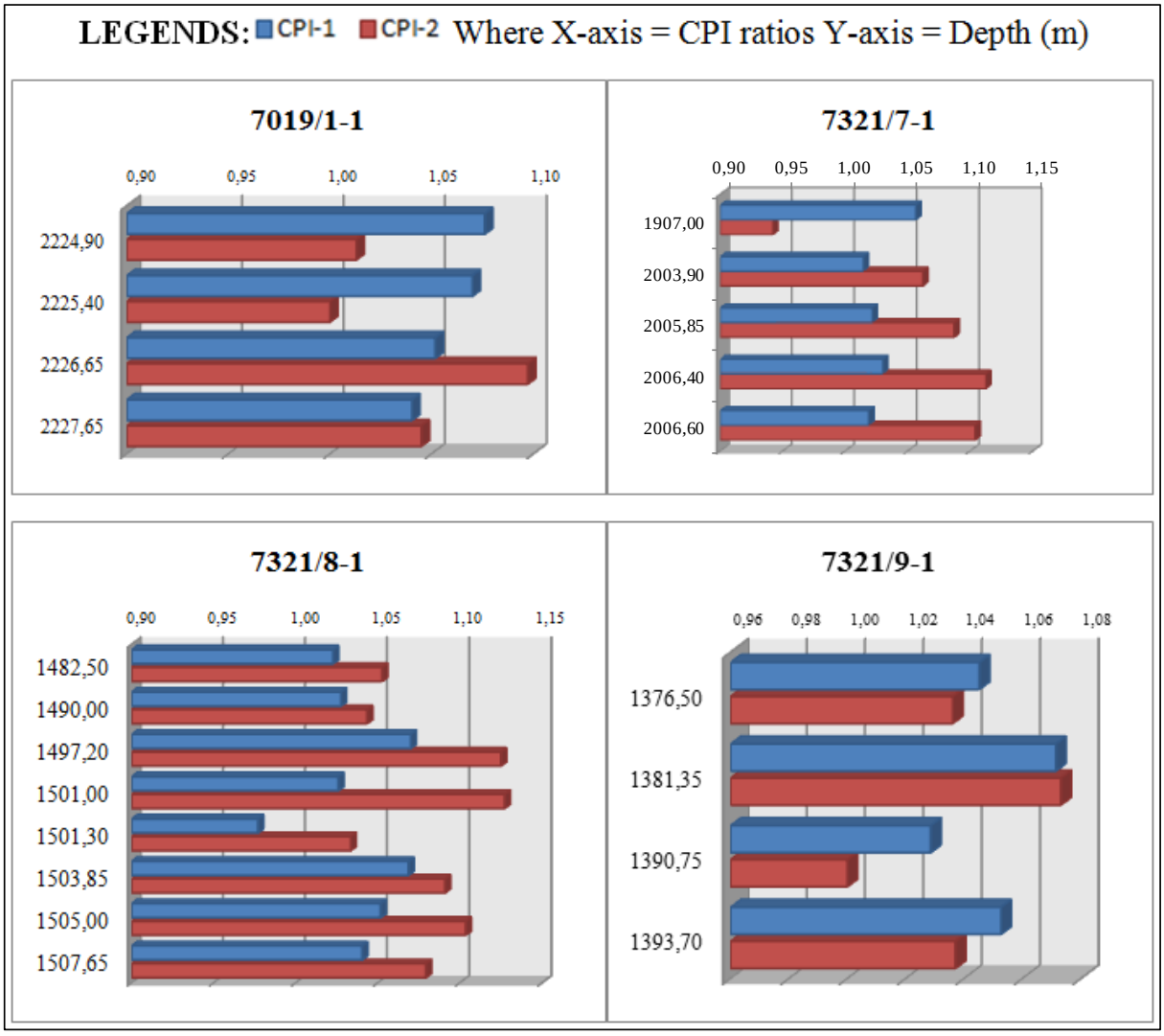

Figure 5.7 The samples selected from various wells of the Barents Sea region show CPI value in the range of 0.95 to 1.13 which represent mature samples and sourced from silisiclastic source rocks. The higher value for the CPI-2 which represents n-alkanes in the range of C_{28} to C_{30} is reflecting that these longer chain alkanes are less transformed than the shorter chain alkanes of the CPI-1.

Values for Vitrinite reflectance have been calculated from the aromatic maturity indicators such as methylphenanthrene and methyldibenzothiophenes. Karlsen and Skeie (2006) suggested that both of these compounds depict the level of maturation but in variable range as methylphenanthrene generally represent the higher end of oil window while methyldibenzothiophene is limited to lower half of oil window. In addition, the parameter (MPI) is influenced by evaporative fractionation (Karlsen et al., 1995). The calculated results are presented in charts showing these values (Fig. 5.8).

All the samples from well 6707/10-1 (Mid-Norway) have higher maturation values which donot vary with the depth like the well 6707/10-2A. While there exists a slight increase in the maturity of samples from well 6707/10-2S as the depth increases (sample at 3166.75m has relatively lower maturation than the sample taken from the depth of 3294.0m). Samples form well 6607/5-1 has lower values of vitrinite reflectance than all the wells of the Mid-Norway while the normal trend of increase in maturity is not obvious in the well 6607/5-2 which can also indicate the transformation effect at 4163.80m as the maturation value is inversely affected by the biodegradation (Fig.5.4).

In case of the Barents Sea, shallow sample of well 7321/9-1 and shallower portion of well 7019/1-1 has lower maturation but at depth (2459.0m in well 7019/1-1) there is significant increase in maturation which can also be obsereved in Fig. 5.11 where only one sample have considerably higher maturity than all the dataset. The effect of biodegradation can also be explained in well 7321/7-1 where the sample at the depth of 2386.80m (also see section 5.2.2) where the relative maturation level from all maturity parameters is lower at depth while normally the maturity increases with depth due to increase in temperature but relative lower maturity at depth is an evidence of tramformation process. The average values for offshore Mid-Norway generally greater than the samples from the Barents Sea and the petroleum in the Mid-Norway was expelled at maturity of about 0.7 to 0.9 value of vitrinite reflectance (Karlsen et al., 1995). Secondly, the solid bars in Fig. 5.8, representing each parameter show a slight variation in vitrinite reflectance value owing to difference in isomers and loss of lighter fraction of hydrocarbons in the extracts.

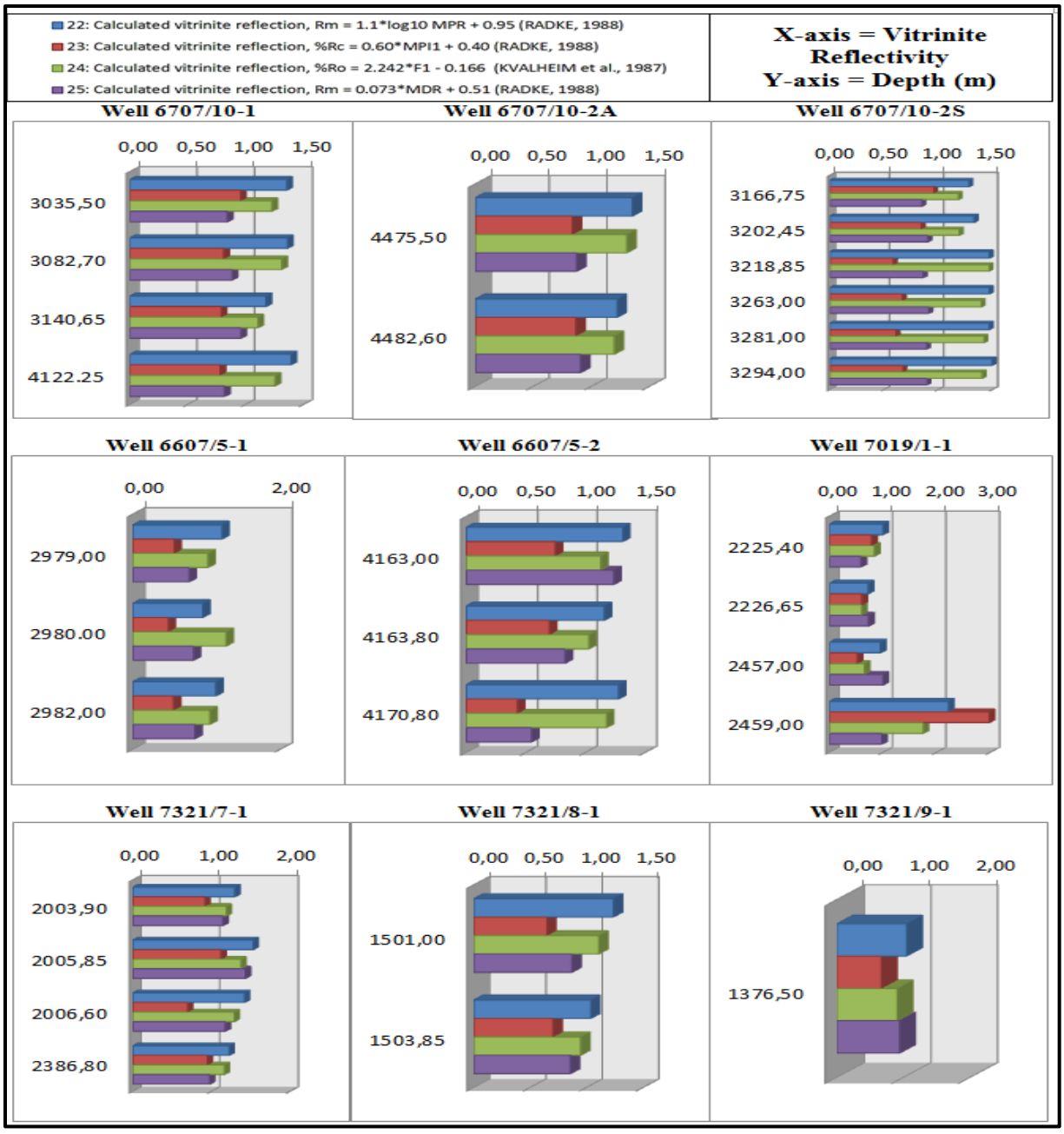

Figure 5.8 Represention of values of calculated vitrinite reflectivity by various medium range parameters which show general mid-oil window maturities for the samples in the dataset. Note that maturities calculated based on the MDR ratio i.e. methyldibenzothiophenes is normally more responsive in the early part of the "oil window" compared to the methylphenathrenes which often respond better towards the later part of the "oil window" (Karlsen and Skeie, 2006). It is, however, not often one observes as systematic differences between the methyldibenzothiophenes and the methylphenthrenes as seen here for the Mid-Norway system. The similarity between parameter 22 and 24 is due to application of similar isomer pairs. While parameter 23 includes the non-isomer phenanthrene and could be high in this dataset as we here work with residual bituem samples which have lost light ends i.e. more loss of phenthrene than of methylphenthrenes. We note that no system seems to indicate expulsion of petroleum at lower than c 0.8%Rc as observed also by Karlsen et al., (1995) for the Haltenbanken samples.

5.4.2 Maturity assessment from biomarkers

The heavier portion of petroleum contains long chain biomarkers that represent maturation which may vary from the maturity determined by medium range parameters. In general, the maturity or phase fractionation decreases the concentration of biomarkers (Mackenzie et al., 1985; Karlsen and Skeie 2006). The range for each biomarker parameter for demonstration of maturation varies in accordance to the ratio of organic compounds. The relation of these parameters with the stages of generation of oil and value of vitrinite reflectivity can be illustrated in Fig. 5.9.

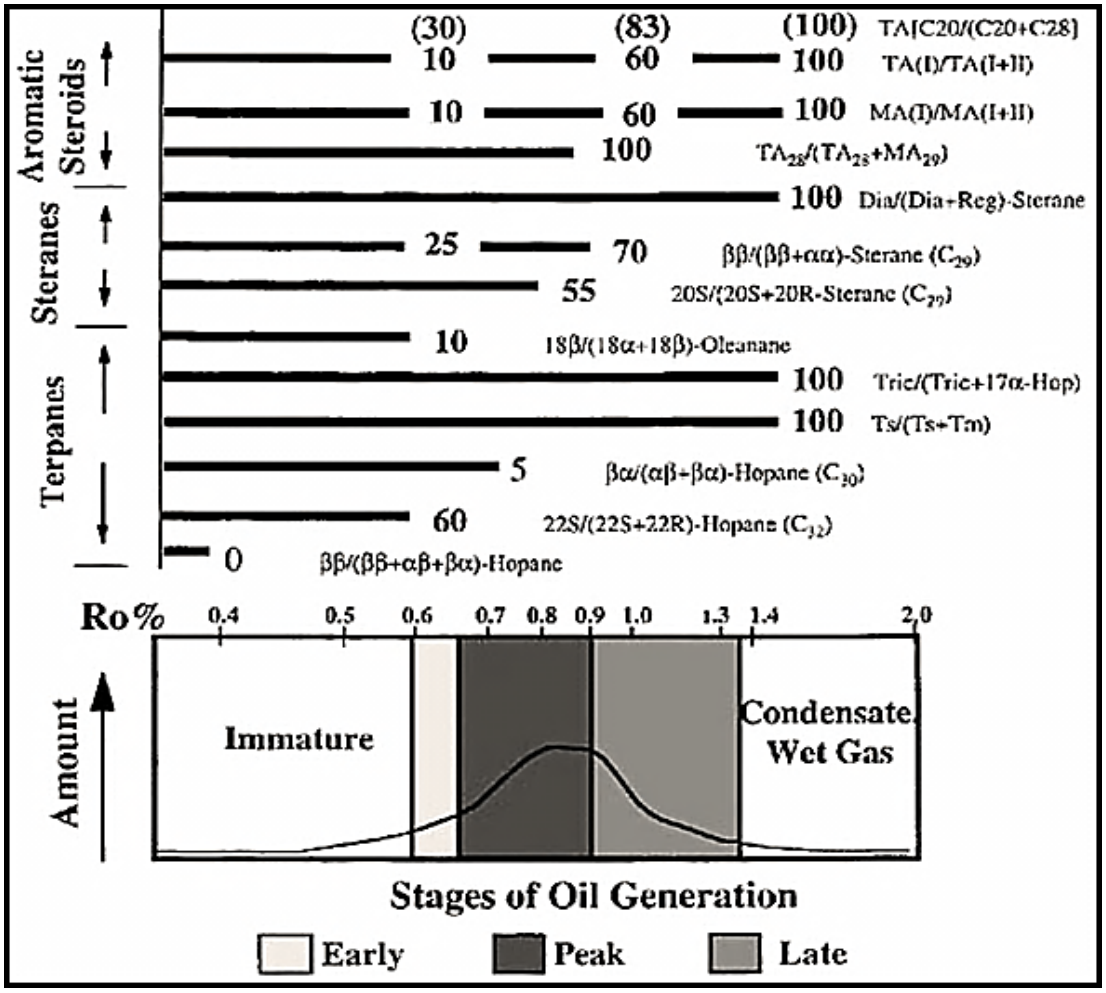

Figure 5.9 Biomarker maturation parameters corresponding to range of maturation to estimate the maturity of extract. The solid bars represent the range of each ratio of compounds with respect to the stages of generation of oil that may vary with heating rate, lithofacies and organic facies of source rock modified from Peters et al., (2005).

The relationship between two maturity parameters such 20S/ (20S+20R) against ββ/ (ββ+αα) is expressed in Fig. 5.10. The steranes are specified only for immature to mature range and measured by using m/z=217, where 20S/(20S+20R) has maximum value of 0.55 corresponding to vitrinite reflectivity value of 0.9 while ββ/(ββ+αα) sterane of C_{29} has peak value of 0.70 with respect to R_c value of 0.9 as presented in Fig. 5.9. The ratios between isomers of steranes in general show linear maturity relationship between the samples representing the Mid-Norway and the Barents Shelf where higher ratios depict the higher degree of maturation.

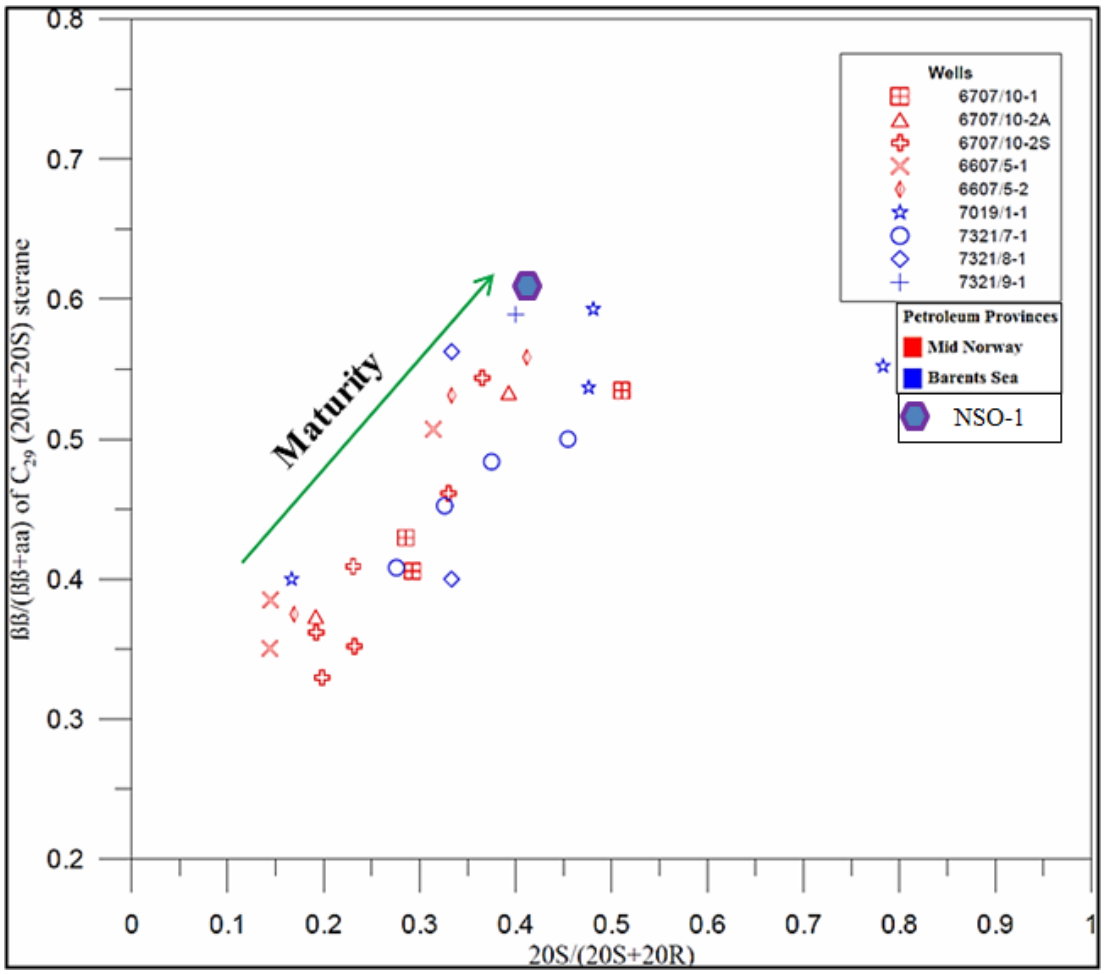

Figure 5.10 As shown there is a nice linear relationship of maturaion between the two different types of sterane isomerization parameters. According to the literature (Peters et al., 2005), the equilibrium values of these parameters are about 0.55 for the S/R parameter and about 0.70 for the ββ/αα steranes and we conclude that the source rocks for these petroleum had a normal type of burial history and increasing temperature with the only difference being slightly lower isomerization ratios off Mid-Norway.

The high sterane ratios of these samples points towards higher degree of maturation. The maturity of the organic matter representing the Mid-Norway samples varies significantly. Based on these two parameters, the samples representing well 6607/5-1 and 6707/10-2S show the lowest maturity level of the samples set (Fig. 5.10). It is important to note that the applicability of these parameters is limited for certain range of maturity level. The four isomers of methylphenanthrene (3-, 2-, 9- and 1-MP) determine the aromatic maturity of the extracts of both regions.

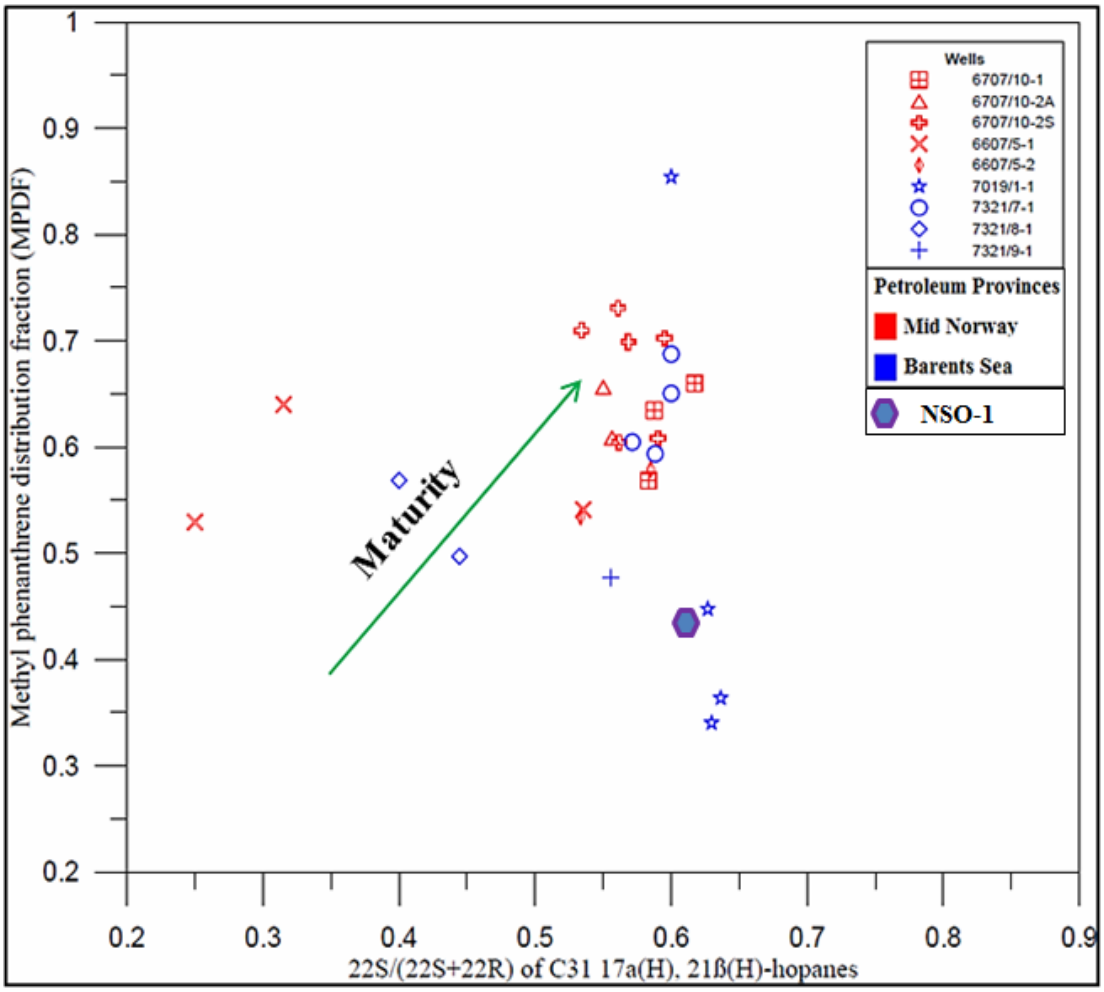

Figure 5.11 Using cross-plots of medium range HC parameters like methylphenanthrenes (C_{15}) plotted against biomarker range parameters (C_{31}) is a way to evaluate mixing of two different petroleum systems (Karlsen et al., 1995; 2004). In this case, we note that there is possibly a slight effect for the Mid-Norway samples suggesting mixing of a low to medium mature black-oil with a high maturity condensate as this will result in "higher than normal" methylphenanthrene maturities for a given biomarker maturity.

parameter termed as methylphenanthrene distribution factor (MPDF) is incorporated with 22S/ (22S+22R) biomarker parameter to define the maturation of available samples. As shown in Fig. 5.11, most of the samples have value of 22S/ (22S+22R) from 0.57 to 0.63 that indicate the span of main phase of oil generation (Peters et al., 2005). This relatively higher maturity level of the Mid-Norway samples could be due to the mixing of two oil populations with variable maturation that gives an overall higher maturity. Karlsen et al., (1995) recommended the mixed petroleum refers to possibly different source rock. According to these maturity parameters, the samples representing the Mid-Norway wells are seen to have similar maturity levels, except two samples from well 6607/5-1, which are plotted to represent lower degree of maturation.

Looking at the maturity levels of the samples from the Barents Shelf, one can note the great variation of maturation degrees from one well to the other. Samples from well 7321/8-1 and 7019/1-1 are shown to be experienced lower maturity than those samples from well 7321/7-1. In contrast, the samples from well 7019/1-1 have less value for methylphenanthrene isomer than the samples from other wells (e.g. 7321/7-1) of the Barents Shelf.

The degree of isomerization for hopanes and steranes are displayed in a cross-plot (Fig. 5.12) where the extent of maturation is directly related to increase in ratios for both compounds. There exists a similar grade of isomerization for samples from the Mid-Norway and the Barents Sea as most of samples are placed in between 0.5 to 0.65 showing medium oil window whereas, few samples from the Mid-Norway (6607/5-1) and the Barents Sea (7321/8-1) and place below 0.5 value of both ratios of isomers. This lower values show the stage of early oil window having relatively lower maturity. All the samples from well 6707/10-1 show relatively higher maturation than the samples from well 6707/10-2A and few samples from well 6707/10-2S higher quite similar maturation level to well 6707/10-1 but some samples of well 6707/10-2S show comparable maturation to well 6707/10-2A. Therefore it is possible to place the well 6707/10-2S in between wells 6707/10-1 and 6707/10-2A. The lower value for Mid-Norway may also be correlated with DST sample expressing the Cretaceous source rock from well 6507/2-2 (Karlsen pers. com, 2012). The relative degree of maturation in the Barents Sea samples shows that well 7321/9-1 has lower than well 7321/7-1. The rank of maturation in well 7321/8-1 is lower in the plot (Fig. 5.12) which is quite similar pattern to the previous plot between hopanes and methylphenanthrene distribution factor (Fig. 5.11).

The other similar maturity indication can also be seen in case of samples from well 6607/5-1 of the Mid-Norway which has lower maturity in both plots (Fig. 5.11 and 5.12). Although there is no ample contrast in the maturation of both plots yet a feeble amplification of maturity for the samples of well 6707/10-2S than 6707/10-1 is present in cross-plot (Fig. 5.11) which is not higher in the Fig. 5.12. In addition to this minor contrariety, the rate of maturation is almost the same for the sample of well 7321/7-1 in the both plots (Fig. 5.11 & 5.12). The most of the samples in the dataset lie in the early to medium oil window.

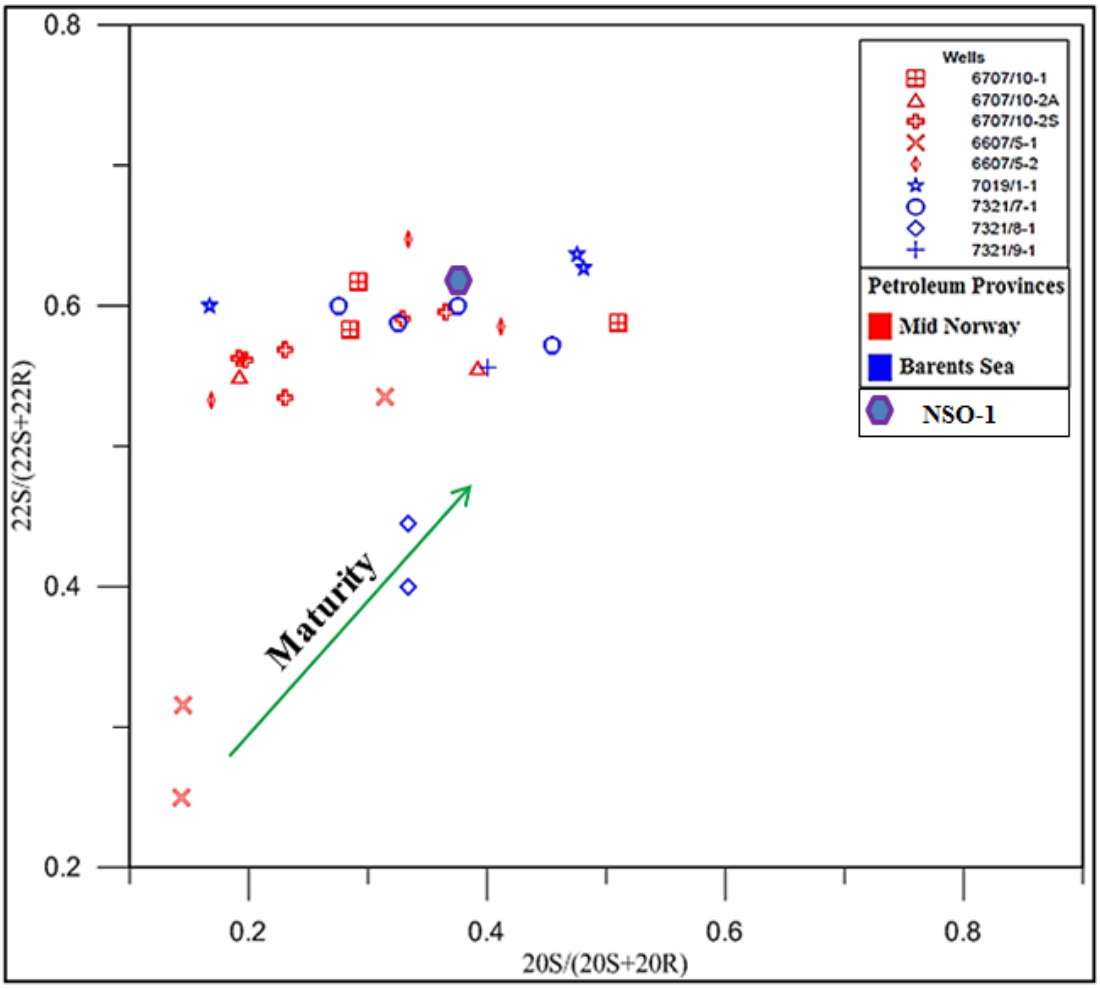

Figure 5.12 Demonstrating the maturation level of the Mid-Norway and the Barents Sea samples based on hopane and sterane isomerization parameters. Note that these are normally fully isomerized and earlier so far the hopane 22S/R parameter than for the sterane 20S/R parameter. It is clear that most of the samples are basically fully isomerized, irrespective of basin, and of "Early Oil Window" to "Medium Oil Window" maturity. However, the strikingly low isomerization ratio in some of the 6607/5-1 samples – a feature noted also in 6507/2-2 DST 2 which is expected to be derived from Cretaceous source rocks (Karlsen pers com 2012). Low values are also observed for the 7321/8-1 sample.

There exists a direct relation of maturation with the ratio of C_{24} tetracyclic terpanes with C_{30} hopane and C_{23}-C_{29} tricyclic terpanes with C_{30} hopane combinations (Fig. 5.13) but these ratios may affected by phase fractionation. The plot show less concentration of C_{24} tetracyclic terpanes for most of the samples as compared to tricyclic terpanes which narrow the plot area of the samples. The variation in composition of petroleum such as enrichment of tricyclic terpanes is caused by vertical migration of petroleum which resulted in phase separation (Karlsen and Skeie, 2006). The plot shows higher maturaion of well 6607/5-2 than the well 6707/10-1 of the Mid-Norway that point towards the influence of transformation process in well 6707/10-1.

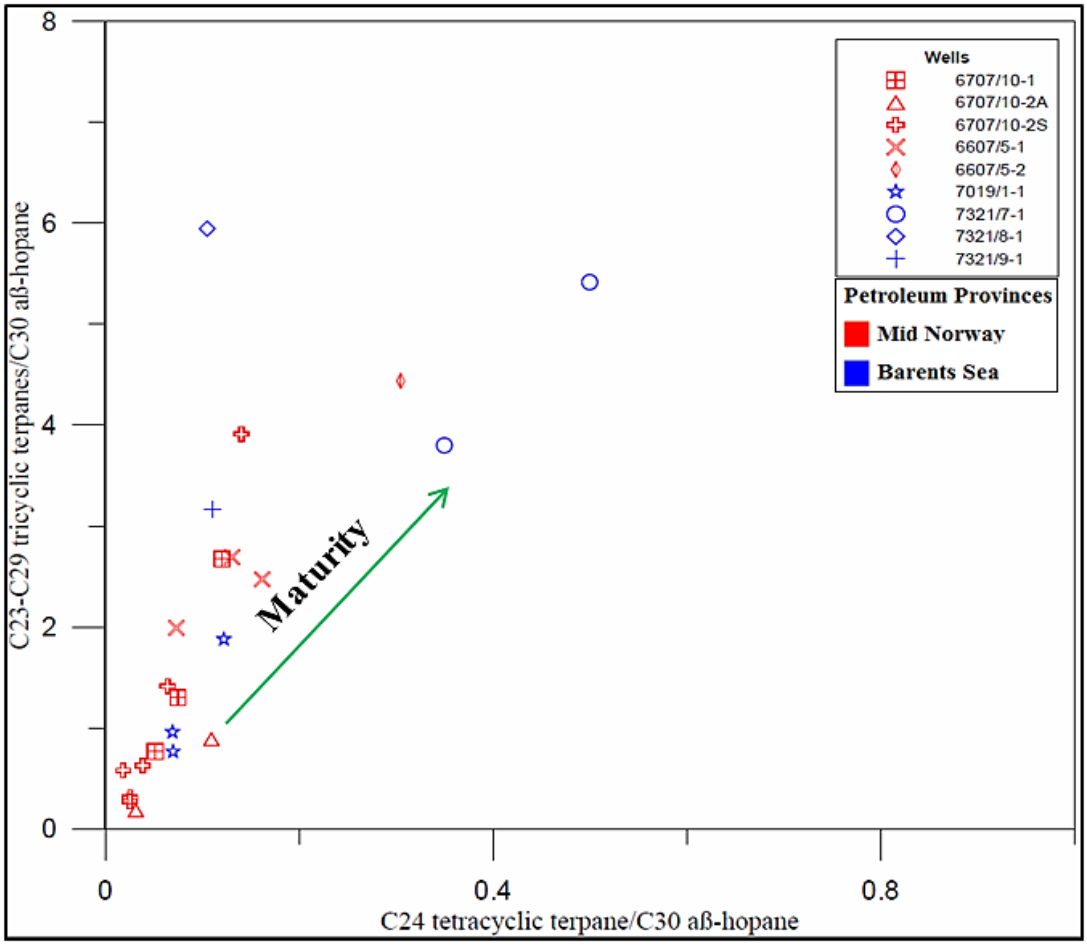

Figure 5.13 The relation between these two biomarker maturity parameters including tetracyclic and tricyclic terpanes and hopanes. The cross-plot suggests that most samples are uniformly representing just one oil migration event as the samples fall close to a general linear trend, albeit these parameters are also influenced by phase fractionation during migration and also loss of light ends from the core during storage (Karlsen et al., 2004; Karlsen and Skeie, 2006).

The maturation can also be portrayed using the ratio of diasteranes and regular steranes against Ts and Tm ratio (Fig. 5.14) which revealed a linear pettern for the Mid-Norway and the Barents Sea region while the parameter Ts/Tm is sensitive to organic facies. Therefore these ratio may indicate the various depositional environments unlike the present study in which linear pattern of cross-plot (Fig. 5.14) reflects same organic facies. All the samples from well 6607/5-1 of the Mid-Norway demonstrate the values lower than 0.5 for both parameters and most of the samples from well 7019/1-1 stated lower range from 0.3 to 0.5 illustrating lower degree of maturation. Both ratios are effective for the samples that have higher degree of maturation i.e. 1.0%Rc (Peters et al., 2005).

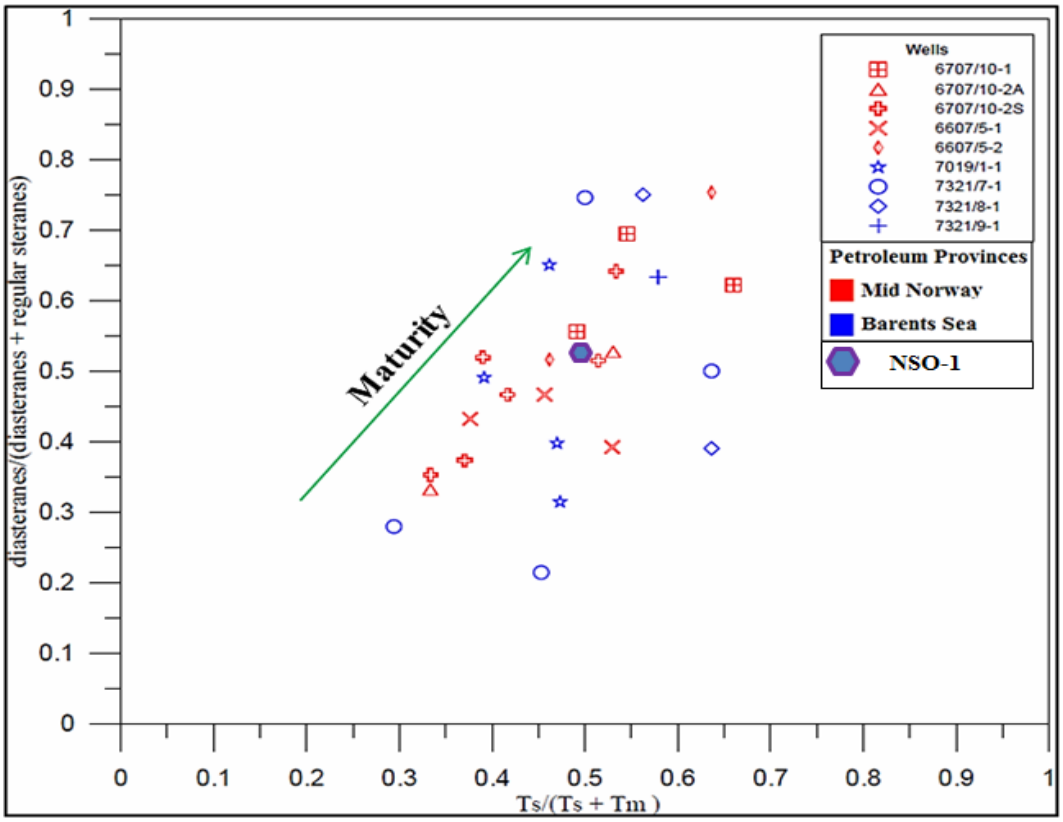

Figure 5.14 The maturity cross-plot of studied samples on the basis of Ts and Tm along X-axis and diasteranes and regular sterane on Y-axis. Compared to the preceding diagram with components in each parameter being influenced by phase fractionation, in this diagram we have components in each parameters which are less influenced by phase fractionation as these are in case of Ts/Tm molecules of the same carbon number, and in case of the steranes, components which at the most differ two carbon number. The diasterane ratio is a facies and maturity parameters and the Ts/Tm ratio is a maturity parameter with some sensitivity to organic facies. The sample distribution is also in this diagram, as in the preceding, basically a broad 45 degree sloping trend indicating that the sample set is for each well representing one oil phase and one migration event and most likely form the same type of anoxic source rock facies.

The influence of organic facies on the ratio of Ts/Tm can also be found in the cross-plot where norhopane was also considered as stable with no influence of phase fractionation (Fig. 5.15) where lack of linear relation for samples from the Mid-Noway could be related to consequence of organic facies on Ts/Tm ratio and indicative of different source facies . While there exists a linear pattern for the Barents Sea samples suggesting relatively same source rock facies. There exists a great variation in maturity of samples from the well 7321/7-1 which mark the boundaries of linear pattern of Barents Sea which could be due to alteration processes affecting the petroleum.

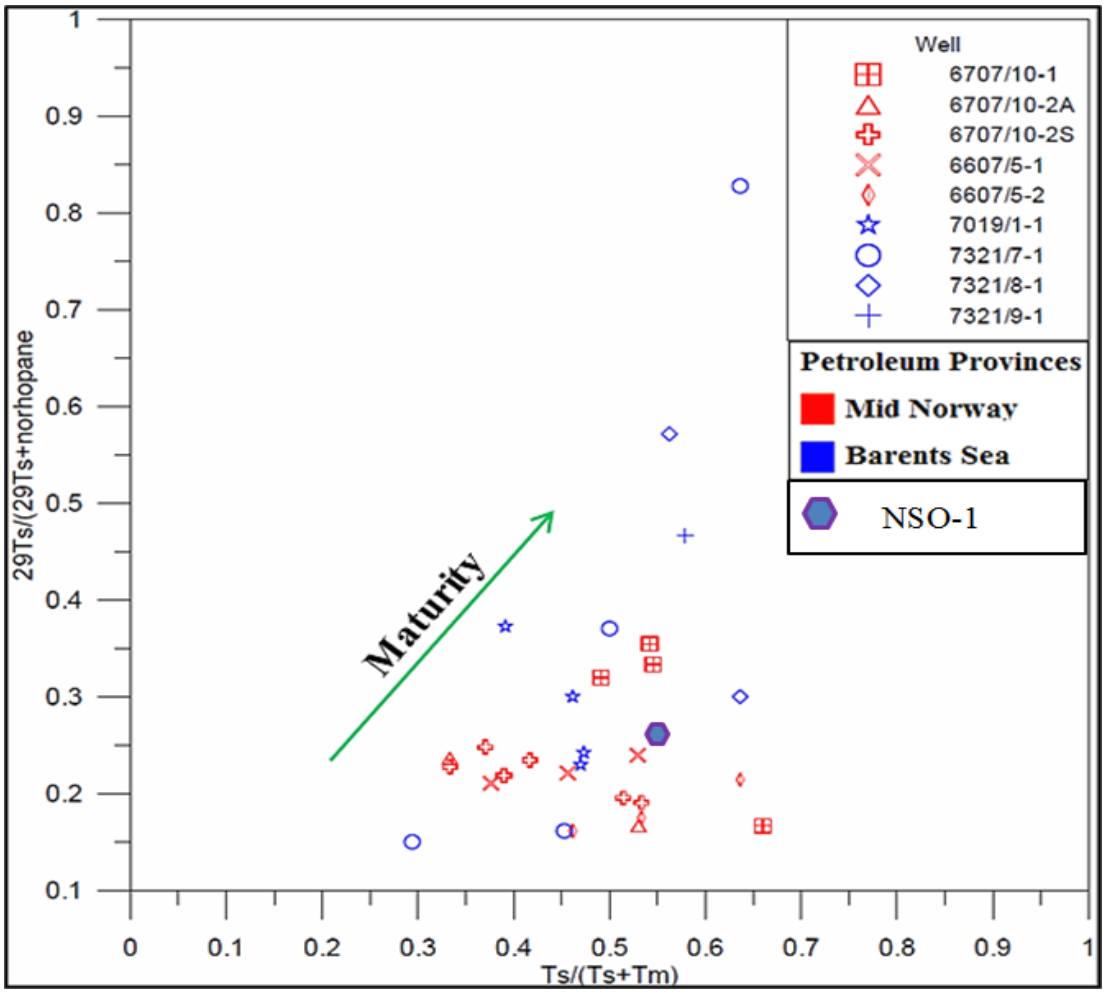

Figure 5.15 Cross-plot of two maturity parameters of which Ts/Tm has potentially some organic facies influence to it while the parameter C_{29}Ts/norhopane is absolutely insensitive to phase fractionation and it is among our best biomarker range maturity paramters overall. The lack of linear relationship for in particular the "red samples" i.e. the Vøring and Utgard samples would suggest that we are dealing with a specific source rock facies other than the Spekk/Draupne/Hekkingen/Kimmeridge, while the more linearity for the "blue samples" could suggest a typical Hekkingen relationship as indeed expected.

5.5 Light hydrocarbons analysis of oil samples

Various structural elements play a significant role in the accumulation and trapping of economically viable petroleum. The petroleum in some of the studied fields such as the Midgard and Heidrun in the Haltenbanken is present on rotated fault blocks formed by extensional faulting whilst the petroleum in the Smørbukk Sør Field is associated with salt induced domal structure. Anticlinal structures with gentle limbs are responsible for the petroleum in the Draugen Field (Karlsen et al., 1995).

The samples from the Smørbukk Field show a differential behaviour with respect to secondary processes because of compartmentalization of field caused by heterogeneity in lithology and secondary diagenesis as described by Karlsen et al. (2004). During uplift the pumping of meteoric water is responsible for penetration of fresh water with bacteria into the reservoir (Karlsen and Skeie, 2006) which happened in case of the Goliat Field in the southern Barents Sea, as indicated by the biodegradation process.

The potential transformation processes are illustrated by the star diagrams (Fig. 5.16) as proposed by Halpern (1995) and B-F diagram (Fig. 5.19) designed by Thompson (1987), that includes the ratio of toluene/ n-heptane (B) on Y-axis and n-heptane/ methylcyclohexane (F) ratio along X-axis, for studying of vaious transformation effects. The Halpern correlation diagram (Fig. 5.18), plotted for various samples from the Norwegian Continental Shelf seems not to demonstrate significant source rock differences for the whole region, which is supported by geochemical study of the Haltenbanken area using GC-MS and GC-FID by Karlsen et al., (1995).

The signatures of transformation can be shown by star diagrams (Fig. 5.16 and 5.17) designed by Halpern where the ratios between light hydrocarbons determine the values from Tr1 to Tr8 and the ratios are representative of different tranformation effects (Tab. 3.10). The samples from the Haltenbanken area (Smørbukk Sør-3) and the Barents Sea (Snøhvit) demonstrate fairly similar patterns to transformation ratios that points to the phenomenon of evaporative fractionation which is also strenghtened by Thompson B-F plot (Fig. 5.19).

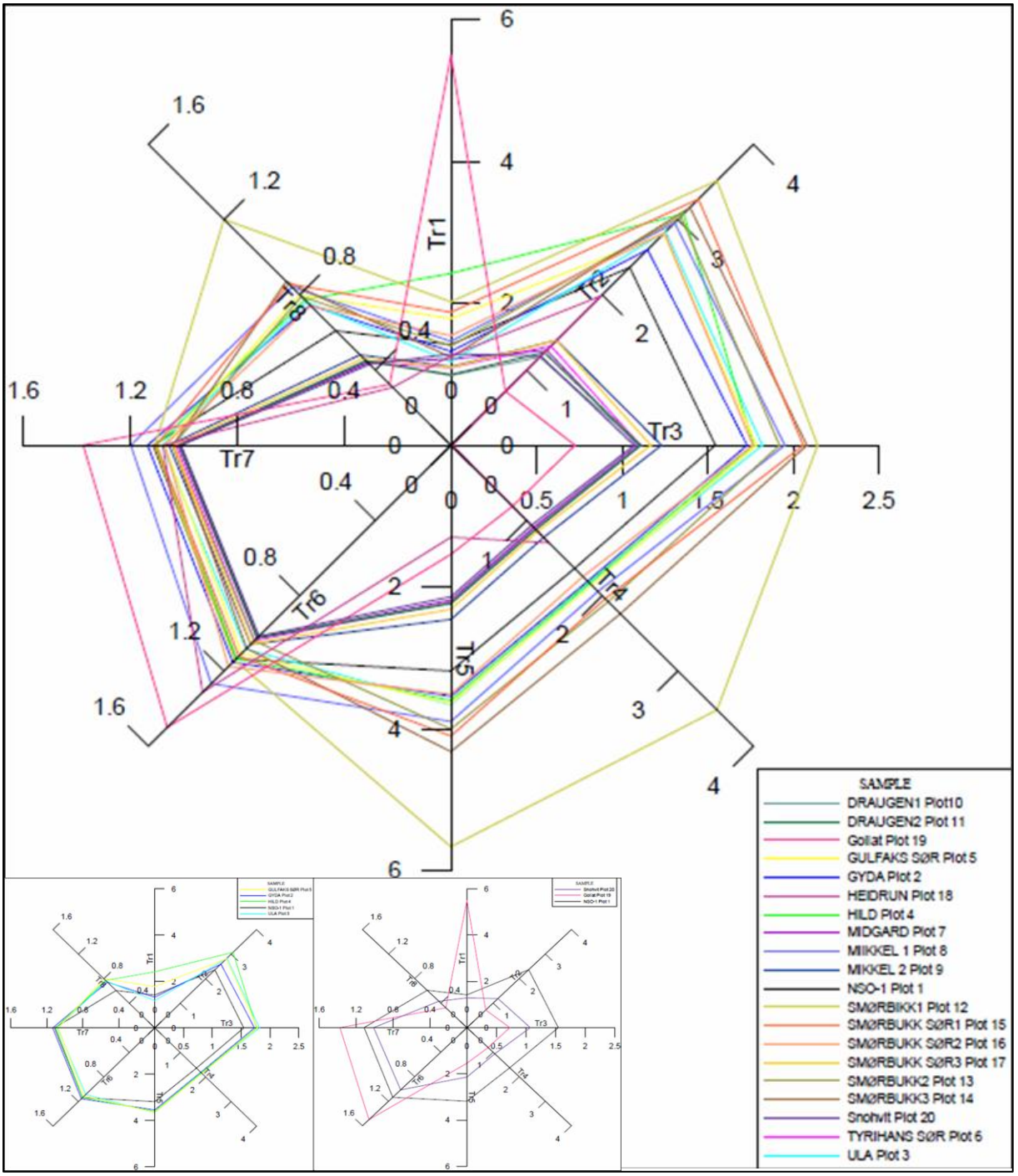

Figure 5.16 The star diagrams (from Halpern, 1995) to highlight the various transformation processes in the samples from the North Sea, the Haltenbanken and the Norwegian Barents Sea. Note in particular the Goliat oil which differs from all other samples and which is biodegraded in C_{15}+ fraction (Ohm et al., 2008). The small plots below the figure shows the transformation processes affecting in the North Sea and the samples from the Barents Sea which seem to really show significantly different signatures of transformation.

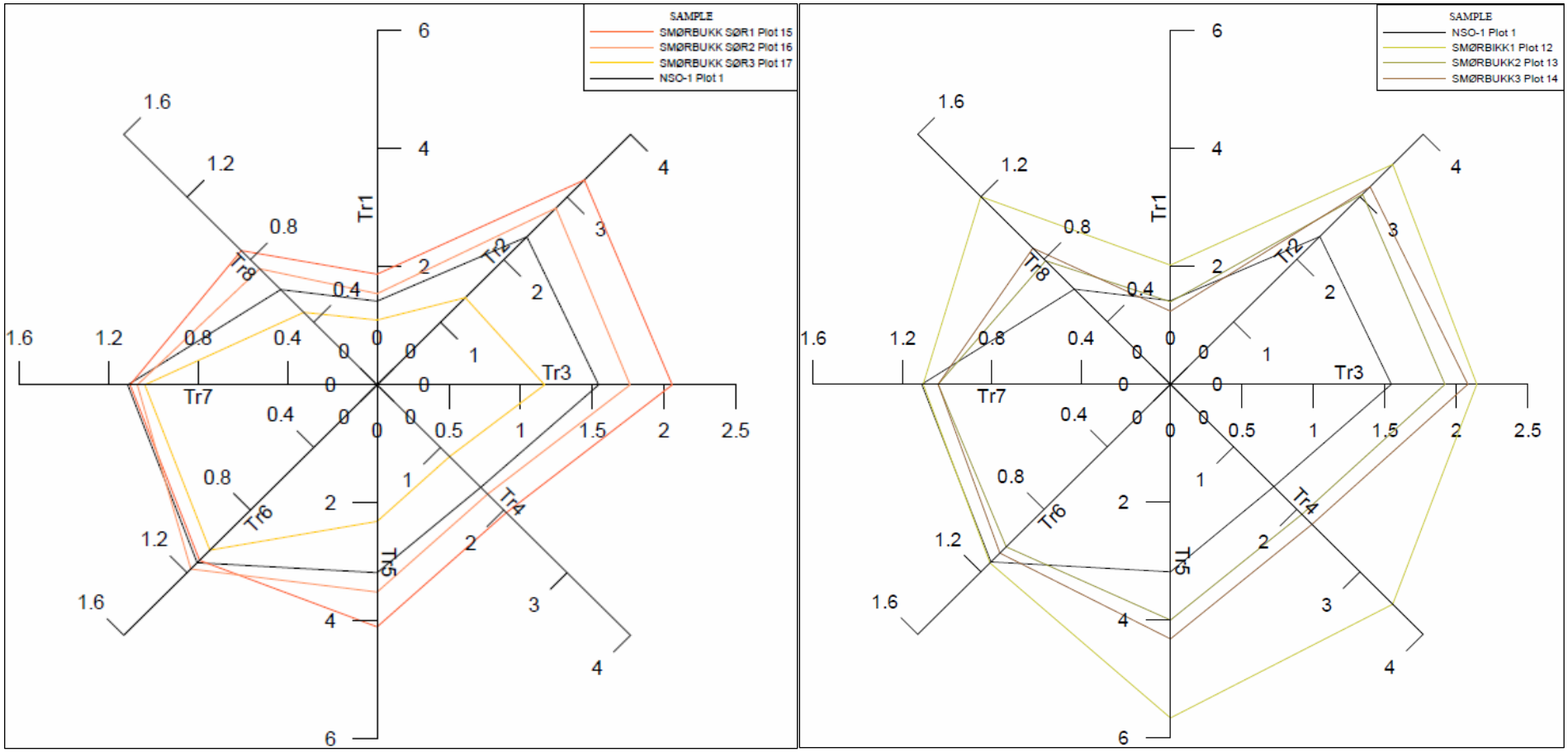

Figure 5.17 The star diagrams (from Halpern, 1995) to highlight the variation in the transformation processes in the Smørbukk Sør and Smørbukk fields. It is obvious from the transformation plot that the effect of the transformation varies within the samples from the Smørbukk and Smørbukk Sør fields. The sample from Smørbukk Sør-3 shows variable signature of transformation from the other two samples of Smørbukk Sør likewise the sample Smørbukk-1 has different values of transformation ratios.

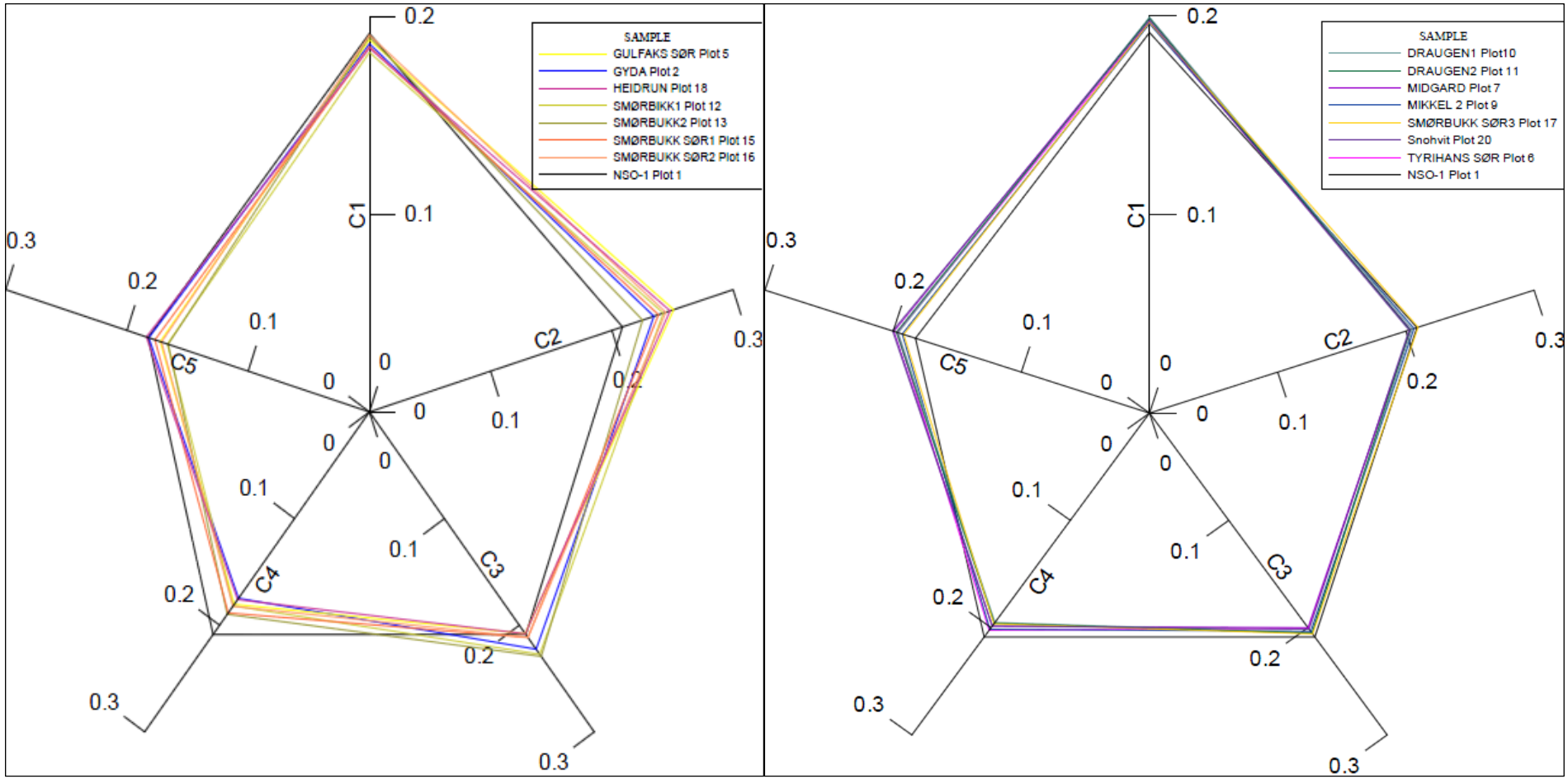

Figure 5.18 Star correlation diagrams of Halpern (1995) plotted for correlation of organic facies. In the left plot, the oil samples from the North Sea and the offshore Mid-Norway region are plotted together and which show considerable similarity suggesting one uniform organo-facies. The Snøhvit sample in the right hand plot, seem also to fal within these boundaries of uniformity and are hard to differentiate from the Tyrihans, Mikkel, and Midgard samples, possibly illustrating again the overall similarity of Upper Jurassic Hekkingen/ Draupne organo-facies.

In addition to this, the tranformation ratios for sample Ula (North Sea) and Smøbukk-2 resemble (Fig. 5.16 & 5.17) which indicate towards same transformation status as explained in Fig. 5.19 i.e. water washing. The relationship of Smørbukk Sør-1 and Smørbukk Sør-2 which have almost similar ratios of transformation (Tr1 to Tr8) for Halpern diagrams (Fig. 5.18) that has also the same result from Thompson diagram (Fig. 5.19). The both samples from Smørbukk Sør Field are placed relatively closer in B-F diagram. Furthermore, the indication of bacterial degradation in the Goliat Field as indicated from transformation plot of Halpern (Fig. 5.16) is strenghtened by the B-F diagram of Thompson (Fig. 5.19) where the toluene to n-heptane ratio is extremely high for the Goliat sample than for any of the samples in the dataset showing the effect of biodegradation as also found by Ohm et al., (2008). The potential difference between the source of the hydrocarbons for available oils is illustrated in Fig. 5.18, where differences in organo-facies between the source rock for various oil would show up with the help of Halpern diagram. However, most samples look very uniform pointing to source rock organo-facies being the same basicllay i.e. versions on the same theme, that is Draupne/ Spekk/ Hekkingen Formation. The uniform source rock facies for the Haltenbanken oils was also suggested by Odden et al., (1998).

The sub-division of samples from the Norwegian Shelf, concerning the secondary alteration effects like biodegradation can be made with the aid of the Thompson diagram where ratio of n-heptane/ methylcyclohexane is denoted as F and taken along X-axis of the plot while the ratio of toluene/ n-heptane is represented by B and plotted along Y-axis. The areas of the plot are classified for various types of transformation processes like water washing, evaporative fractionation and biodegradation while the lower middle part of plot also separates the normal oils from degraded oils. On the basis of ratios along the axes, the cross-plot can also be termed as B-F diagram.

In B-F diagrams all the samples from the Norwegian Continental Shelf are plotted to distinguish between altered and fresh oils (Fig. 5.19). The oil sample from Mikkel-2 is presented in evaporative fractionation window (Fig. 5.20) while the deeper Mikkel-1 close to oil water contact, suggest incipient biodegradation as stated by Karlsen et al., (1995). Karlsen et al., (1995) and Odden (1999) also suggested an affirmed phenomenon of biodegradation in the Heidrun sample that can also be observed in Fig. 5.19. The evaporative fractionation is observed in

Midgard sample due to lateral migration (Karlsen et al., 1995) while both samples from Draugen and Mikkel fields were classified as less mature by Karlsen (1995) on the basis of concentration of monoaromtic steroid hydrocarbons while the current study shows Draugen-2 tend to be in mature window and Mikkel-2 in evaporative fractionation window of Thompson diagram (Fig. 5.19).The placement of Midgrad sample in evaporative fractionation area of B-F plot also confirmed the studies by Odden et al., (1998).

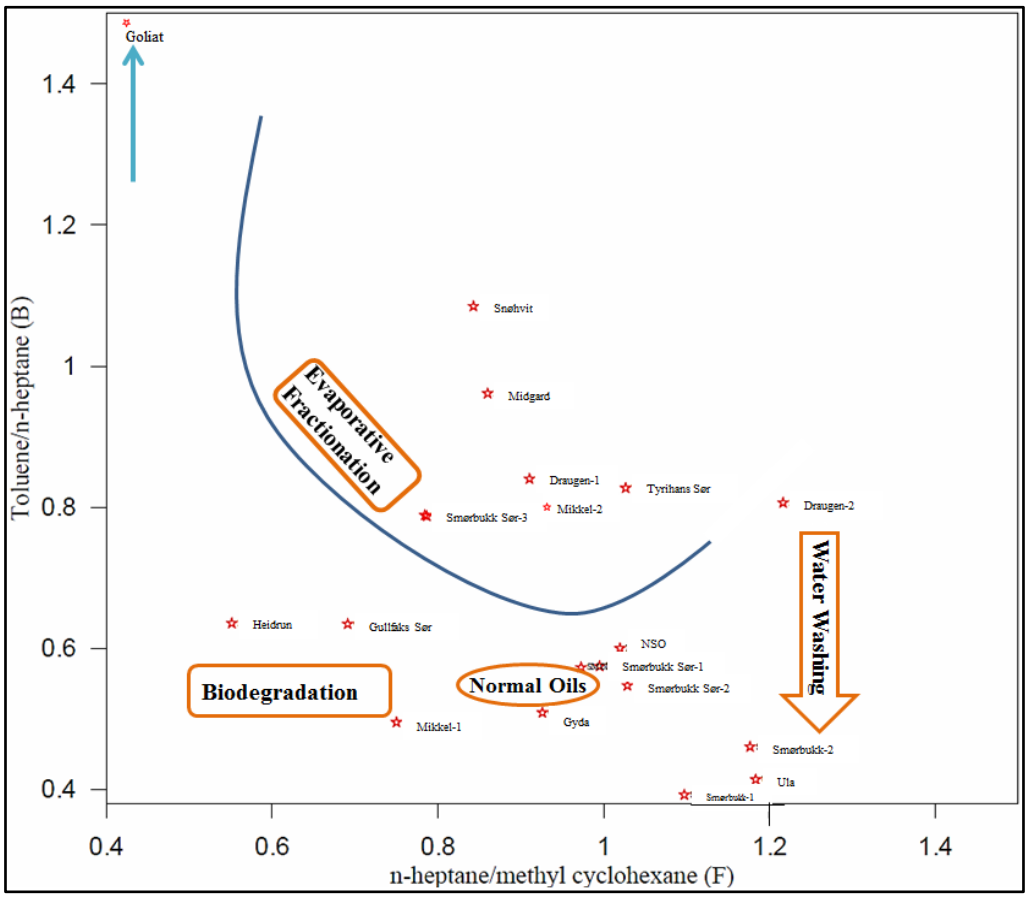

Figure 5.19 Thompson Parameters (1987) for light hydrocarbon samples from the Norwegian Continental shelf point out biodegradation (Heidrun, Gulfaks Sør, and Mikkel-1) and evaporative fractionation for the samples from Snøhvit and Midgrad fields. Note Goliat at the top of diagram as it score high in toluene which is present with almost absence of n-C_7 due to biodegradation. On the other hand benzene is almost depleted in the Goilat sample due to water washing. The tranformation processes can explained effectively utilizing this form of the Thompson diagram where secondary processes affecting the gases can be identified with respect to the various "fields" in the plot. Normal virgin non-altered petroleum samples will plot within the general region of the lower oval and we find in that region, gases from both the North Sea and the Haltenbanken regions. Biodegraded light hydrocarbons are identified by low n-heptane ratios as bacteria will selectively remove n-alkanes compared to branched- and cyclo- alkanes and as biodegradation is associated with water washing which removes toluene. Evaporative fractionation will result in enhanced toluene to n-heptane ratios as this follows the vapor pressures.

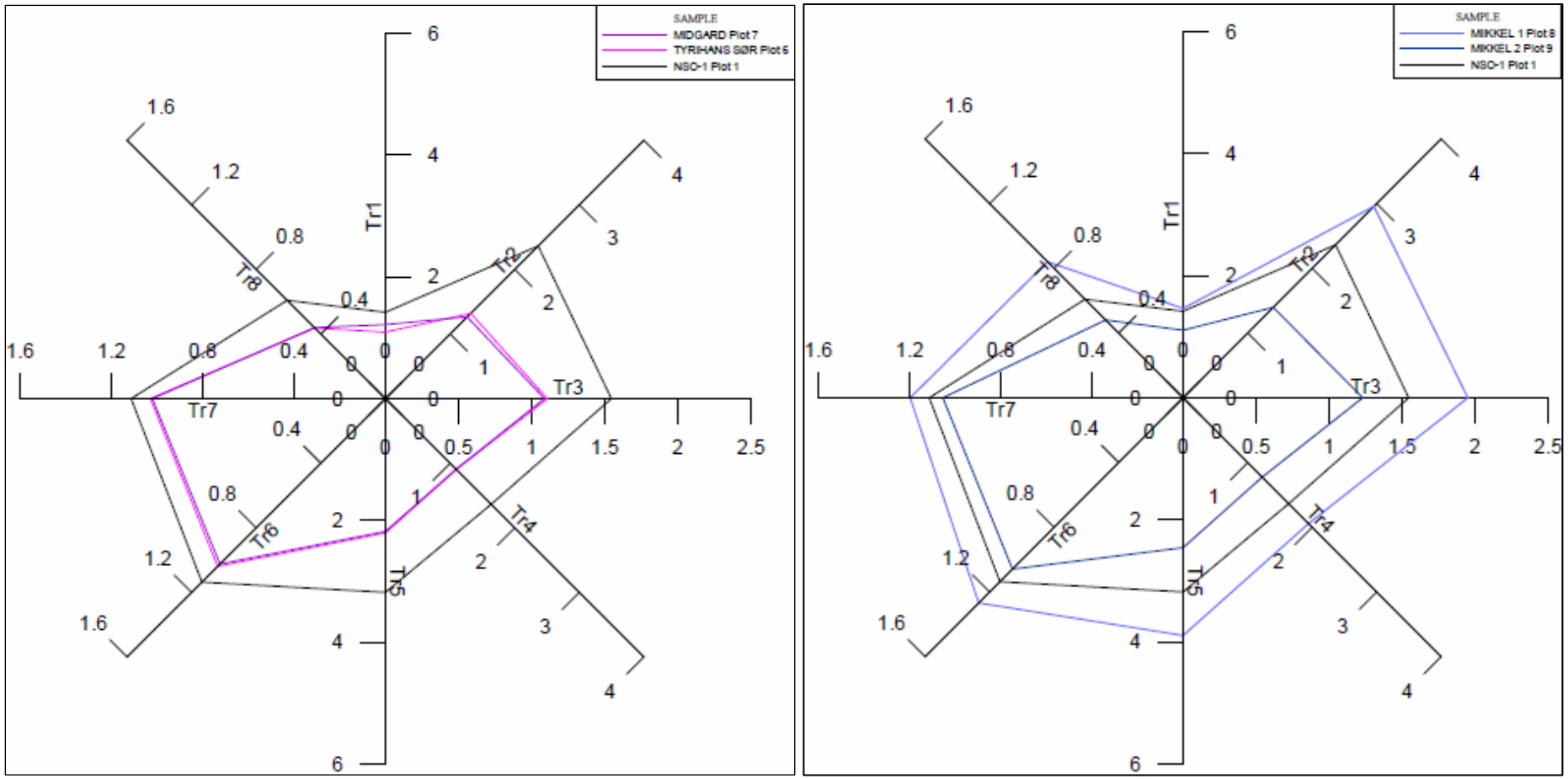

Figure 5.20 Halpern transformation plots where different fields like Midgard and Tyrihans Sør shows the similar ratios indicating the same transformation effect as illustrated by Thompson plot (Fig. 5.19) while in other case different transformation processes is shown within the same field i.e Mikkel Field which has different secondary effect and represent same results by applying Thompson methodology.

6. Highlights of the Study

6.1 Summary

In the present study, two sample types were included for better understanding of application of geochemical techniques and interpretation schemes. The interpretation of results gives information that varies according to the parameters used. Both core samples and oils were included to study the heterogenity of geochemical properties in the Norwegian Continental Shelf. The rock cuttings obtained from core samples were anlyzed and following observations were made:

6.1.1 Core samples

The geochemical study of reservoir samples from the Mid-Norwegian shelf and the Barents Sea describe the composition of residual bitumen in the dry wells, the relation of source rock, maturity at the time of expulsion and possible transformation processes affecting the quality of reservoir. The present study emphasized on all these aspects in a following way:

- Well 6707/10-1, the discovery well at the Nyk High, contains today producible dry gas with a C_2+ conetnts of about 3% yet gas from inclusions show a wetness of about 5% surely pointing towards a time transgressive change from wetter to drier gas in this discovery well at Nyk High. The gas is interpreted as marine in origin (Fig. 5.5) and shallower part of investigated reservoir section is affected by alteration processes indicated by butane isomers (i-C_4/n-C_4) suggesting incipient biodegradation (see Sec. 5.2.1, Fig. 5.3) and the level of maturation is c. 0.8%Rc (Fig. 5.8) thus representing the medium part of the oil window (Fig. 5.12). Thus these results do not support that the source rock for the Nyk gas is super mature and super deep Spekk Formation. Rather a moderate maturity is indicated and the palaeo-gas in the trap was wetter than the current gas.
- Well 6707/10-2A is located farther down the flank of the structure and we note that inclusion gas is even wetter than the gas from well 6707/10-1 reaching about 10% and bitumen is amendable to GC-FID work in this well which is less contaminated compared to the well 6707/10-1 is defined by unaltered oil having slight lower

maturity (Fig. 5.12 & 5.14) but relatively greater component of wet gases than 6707/10-1 (Fig. 5.1) and C_2+ content reach about 10% and only sourced from same Spekk formation (Fig. 5.5) with no mixing of other petroleum population.

- The composition of C_2+ content of inclusion gases in the well 6707/10-2S is even higher than 10%. The core bitumen C_{15}+ core extracts seemingly representing light oil or condensate, showing methylphenanthrene and biomarker and maturity is about 1.10%Rc, where the position of maturity is the highest in the Nyk High system (Fig. 5.8) reaching to oil window (Fig. 5.12) The core extracts depict origin from marine conditions (Fig. 5.5).
- Concerning the Nyk High, it is possible to conclude that the structure has contained condensate or even some light oil in the past and that biodegradation has affected at least the shallower part of the structure. The current dry gas must be a very recent event as inclusion gas is much wetter.
- The samples from the dry Utagrd High wells are of great interest. Well 6607/5-1 conatin wet gases higher than 10% and percentages of polar compounds remain higher than 60% indicative of palaeo-petroleum and possible palaeo-biodegradation in the system (Fig. 5.2). The GC-FID traces show resemblance of condensates or light oils (Appendix B). The maturity based on phenanthrenes and GC-FID traces (Fig. 5.4 & 5.8) it is noticeable that there is less degree of maturation than the Nyk high. Also, the marine source and some terrestrial indication of provenance (Fig. 5.6) differentiate the Utgard system from the Nyk High.
- The second representative well from the Utgard High show bacterial degradation in upper part of reservoir based on gas inclusions (Sec. 5.2.1, Fig. 5.3) which is also supported by anomalous increase of polar fraction in Iatroscan results with depth (Fig. 5.2) which could also a be a sign of palaeo-petroleum and environment of organic facies for well 6607/5-2 tend to be more marine conditions than the well 6607/5-1 (Fig. 5.5 & 5.6). The maturity is based on methylphenanthrenes and methyldibenzothiophene is about 0.97 %Rc which is comparable with the maturity of the well 6607/5-1 which is 0.89%Rc.
- There is some similarity between the palaeo-bitumen from the Utgard and Nyk highs. Although the maturity of Utgard wells are slightly lower than the Nyk well but the maturity of both regions is moderate. It is possible that the bitumen was sourced from

the source rocks which differ from the Spekk Formmation, hence Cretaceous source rocks could be a candidate.

- The hydrocarbons present in the inclusions in the investigated Barents Sea dry well 7019/1-1 are compositionally defined as wet thermogenic gas with C_2+ content of about 30% in shallow wells while it decreases to 18% in deeper samples (Fig. 5.1). The core bitumen C_{15}+ seems to have sourced from the sulphate poor lacustrine conditions (Fig. 5.6). The value of vitrinite reflectance from methylphenanthrenes is lower than the maturation of the offshore Mid-Norway samples (Fig. 5.8).
- The great variation of inclusion gas wetness parameters in well 7321/7-1 (Fig. 5.1) distinguish the reservoir in to two types of petroleum accumulations due to higher ratio of butane isomers i-C_4/n-C_4 (in Fig. 5.3) and is supported by dominance of polar compounds in deeper section (Fig. 5.2) which explain the alteration of petroleum. The deposition of organic matter is dominated by marine conditions (Fig. 5.4 & 5.6) which is inferred from isoprenoids to n-alkanes ratio and distribution of steranes (Fig. 5.5). The level of maturity 1.18%R_C which is estimated from methylphenanthrenes and mthyldibenzothiphenes is greater in well 7321/7-1 than the all other wells from both offshore Mid-Norway and the Barents Sea regions (Fig. 5.8) or comparable with the highest mature well of the Mid-Norway (Fig. 5.11).
- The gas from inclusions of the samples from well 7321/8-1 is represented by percentage of wet hydrocarbons which is c. 20% (Fig. 5.1). The ratios of butane isomers (i-C_4/ n-C_4) indicate the unaltered oils. This evidence is strengthened by the normal increase of saturated compounds with depth in Iatroscan results of bitumen samples (Fig. 5.2). The GC-FID traces show the organic facies of samples from well 7321/8-1 commonly tend to be originated from marine (Fig. 5.4 & 5.6) which is also supported by relative fractions of steranes isomers from GC-MS data. The degree of maturation in well 7321/8-1 is lower than well 7321/7-1 but slightly higher than samples from well 7321/9-1 (Fig. 5.8).
- The wet components of gas (C_2+) from inclusions are slightly lower in well 7321/9-1 from other Barents Sea samples (Fig. 5.1) where isoprenoids to n-alkanes ratios and steranes distribution show marine conditions prevailed at the time of deposition (Fig. 5.5 & 5.6). The level of maturation of the well based on methylphenanthrene and methyldibenzothiophene mark well 7321/9-1 to be in oil window but maturity is

comparable to well 6607/5-1 (Utgard high) and slightly lower than well 7321/8-1 of Vøring Basin (Fig. 5.8).

- Concluding the data on Barents Sea wells, it is possible to say that the dry wells from Barents Sea 7321/9-1 and 7321/7-1 held the same organic facies derived bitumen as found in well 7321/8-1 and inclusions in all wells show wet gas of condensate to oil associatd signatures testifying the fact that the dry wells were at one time contain oil in the reservoir units.
- The comparison of wells from the Vøring Basin and offshore Mid-Norway region it is concluded that gas from inclusions represent the entrapping moment have relatively higher wet components (C_2+) in the Barents sea (Fig. 5.1). Based on isoprenoids to n-alkanes data from GC-FID chromatograms, and distribution of steranes (C_{27}, C_{28} and C_{29}), all the bitumen samples from both regions of the Norwegian continental Shelf were originated from marine environments (Fig. 5.4 & 5.5). The level of maturation based on medium range parameters i.e. show the medium oil window for all the samples of the dataset. Excluding the maturity of well 7321/7-1 the degree of maturation for the Nyk High is higher than Utgard wells but comparable with maturation of wells from the Bjørnøya Basin.

6.1.2 Light hydrocarbons from oil samples

The application of maturity and transformation parameters on oils from the Norwegian Continental Shelf yields the following conclusions:

- Thompson parameters for transformation were applied which separate the unaltered oils (NSO, Gyda, Smørbukk Sør-1 and Smørbukk Sør-2) from biodegraded oils like Heidrun, Gulfaks Sør and Goliat where Mikkel-1, close to oil water contact, is just incipiently biodegraded (Fig. 5.19) which refine the findings of Mikkel samples from Karlsen et al., (1995) which did not find any biodegradation in C_{10}+ fraction.
- Water washing occurred in some portion of the Smørbukk Field (Smørbukk-2) while evaporative fractionation was found in the Snøhvit (Barents Sea), Midgard, a part of Draugen (Draugen-1 sample) and Mikkel (Mikkel-2) fields of Haltenbanken area (Fig. 5.19).

- Halpern star diagrams illustrating secondary processes reveal different signatures of transformation within the Smørbukk and Smørbukk Sør fields while samples from Draugen Field have same effect of transformation. The star plot for the Midgard and Tyrihans Sør slightly vary from each other as indicated in Fig. 5.16.
- The star plots of correlation proposed by Halpern (Fig. 5.18) for samples of the Norwegian Continental Shelf show typical signals for same generation of hydrocarbons from Draupne/ Spekk/ Hekkingen Formation.

6.2 Conclusions

The reservoir core samples from various wells of the Mid-Norway and the Barents Sea were geochemically analysed by various method including gas analysis from inclusions, GC-FID, GC-MS and TLC-FID to determine the organic facies, maturation and transformation processes in the samples. The depositional environment for steranes, isoprenoids and n-alkanes deduce that the organic facies of the studied wells from the Mid-Norway and the Barents Sea derived from open marine with very little terrestrial input. The maturity of samples based on maturity parameters from biomarkers and aromatic hydrocarbons vary in the study but all the maturity indicator reveal that the orgaic matter in the studied samples lie in early to medium oil window. Considering the more reliable aromatic maturity parameters, the Nyk high well have greater maturity than other wells from the Utgard High and Bjørnøya Basin except one well 7321/7-1 drilled in Bjørnøya Basin while the level of maturation is comparable between the Utgard high and the Bjørnøya Basin. Depending on GC-FID data, Iastroscan percentages and gases from inclusions, the shallow samples from well 6707/10-1 and 6607/5-2 of the Mid-Norway region show alteration affects whereas, only deeper samples from well 7321/7-1 of the Norwegian Barents Sea may indicate the transformation process.

The study of light hydrocarbons is done by using Halpern and Thompson parameters. These parameters show evaporative fractionation commonly in the samples from the Haltenbanken area (Draugen, Mikkel, Midgard, one sample from Smørbukk Sør) while the Snøhvit Field of Barents Sea also show evaporative transformation. Water washing is evident from samples of Ula (North Sea), Smørbukk (Haltenbanken) and biodegradation of Gulfaks Sør (North Sea), Heidrun (Haltenbanken), and Goliat (Barents Sea). While sample from Gyda (North Sea), some samples from Smørbukk Sør show no transformation. All the petroleum in the samples

from the Norwegian Continental Shelf derived from same orgaic facies i.e. Kimmeridge/Spekk/ Hekkingen Formation.

References

ABAY, T. B. 2010. Vertical variation in reservoir core geochemistry : bitumen samples from a well in the deep and hot Devonian age Embla oil field, offshore Norway, *Master Thesis, Univeristy of Oslo,* 20-23.

ALEXANDER, R., KAGI, R. I. and WOODHOUSE, G. W. 1981. Geochemical correlation of Windalia oil and extracts of Winning Group (Cretaceous) potential source rocks, Barrow Subbasin, Western Australia. *AAPG Bulletin,* 65**,** 235-250.

BHULLAR, A. G., KARLSEN, D. A., BACKER-OWE, K., TRAN, K. L., SKÅLNES, E., BERCHELMANN, H. H. and KITTELSEN, J. E. 2000. Reservoir characterization by a combined micro-extraction — micro thin-layer chromatography (Iatroscan) method: a calibration study with examples from the Norwegian North Sea. *Journal of Petroleum Geology,* 23**,** 221-244.

BJØRNSETH, H. M., GRANT, S. M., HANSEN, E. K., HOSSACK, J. R., ROBERTS, D. G. and THOMPSON, M. 1997. Structural evolution of the Vøring Basin, Norway, during the Late Cretaceous and Palaeogene. *Journal of the Geological Society,* 154**,** 559-563.

BREKKE, H., SJULSTAD, H. I., MAGNUS, C. and WILLIAMS, R. W. 2001. Sedimentary environments offshore Norway—an overview. *Norwegian Petroleum Society Special Publications,* 10**,** 7-37.

BREKKE, H. 2000. The tectonic evolution of the Norwegian Sea Continental Margin with emphasis on the Vøring and Møre Basins. *Geological Society, London, Special Publications,* 167**,** 327-378.

BLYSTAD, P., BREKKE, H., FÆRSETH, R., LARSEN, B., SKOGSEID, J. and TØRUDBAKKEN, B. 1995. Norwegian Petroleum Directorate Bulletin. *Structural elements of the Norwegian continental shelf. Part II: The Norwegian Sea region,* 8.

BUKOVICS, C. and ZIEGLER, P. A. 1985. Tectonic development of the Mid-Norway continental margin. *Marine and Petroleum Geology,* 2**,** 2-22.

CAMPBELL, C. J. and ORMAASEN, E. 1987. The discovery of oil and gas in Norway: An historical synopsis. *Geology of the Norwegian Oil and Gas Fields***,** 1-37.

CLAYTON, J. L. and BOSTICK, N. H. 1986. Temperature effects on kerogen and on molecular and isotopic composition of organic matter in Pierre Shale near an igneous dike. *Organic Geochemistry,* 10**,** 135-143.

COHEN, M. and DUNN, M. The hydrocarbon habitat of the Haltenbanken–Trænabanken area offshore Mid-Norway. Petroleum Geology of North West Europe. Proceedings of the 3rd Conference, 1987. 1091-1104.

CORNFORD, C., NEEDHAM, C. E. J. and DE WALQUE, L. 1986. Geochemical habitat of North Sea oils and gases. *Habitat of hydrocarbons on the Norwegian continental shelf. Proc. conference, Stavanger, 1985***,** 39-54.

DAHL, B. & SPEERS, G. 1985. Organic geochemistry of the Oseberg Field (I). *Petroleum Geochemistry in Exploration of the Norwegian Shelf. Graham and Trotman, London***,** 185-195.

DALE, K. 1997. Use of light hydrocarbons for classification of oils and condensates in the Haltenbanken area, *Master Thesis, University of Oslo.*

DALLAND, A., WORSLEY, D. and OFSTAD, K. 1988. A lithostratigraphic scheme for the Mesozoic and Cenozoic succes- Sion offshore for the Mesozoic and Cenozoic succession offshore mid- and northern Norway. *Norwegian Petroleum Directorate Bulletin,* 4**,** 65.

DENGO, C. A. and ROSSLAND, K. G. 1992. Extensional tectonic history of the western Barents Sea. *Structural and tectonic modelling and its application to petroleum geology***,** 91-107.

DORE, A. G. 1995. Barents Sea geology, petroleum resources and commercial potential. *Arctic,* 48**,** 207-221.

DORE, A. G. and LUNDIN, E. R. 1996. Cenozoic compressional structures on the NE Atlantic margin; nature, origin and potential significance for hydrocarbon exploration. *Petroleum Geoscience,* 2**,** 299-311.

EHRENBERG, S. N., GJERSTAD, H. M. and HADLER-JACOBSEN, F. 1992. Smorbukk Field: a gas condensate fault trap in the Haltenbanken province, offshore mid-Norway. *Giant oil and gas fields of the decade 1978-1988***,** 323-348.

FALEIDE, J. I., GUDLAUGSSON, S. T. and JACQUART, G. 1984. Evolution of the western Barents Sea. *Marine and Petroleum Geology,* 1**,** 123-150.

FALEIDE, J. I., VÅGNES, E. and GUDLAUGSSON, S. T. 1993. Late Mesozoic-Cenozoic evolution of the south-western Barents Sea in a regional rift-shear tectonic setting. *Marine and Petroleum Geology,* 10**,** 186-214.

FALEIDE, J. I., TSIKALAS, F., BREIVIK, A. J., MJELDE, R., RITZMANN, O., ENGEN, Ø., WILSON, J. and ELDHOLM, O. 2008. Structure and evolution of the continental margin off Norway and the Barents Sea 31, 82-91.

FALEIDE, J. I., BJØRLYKKE, K. and GABRIELSEN, R. H. 2010. Geology of the Norwegian Continental Shelf. *Petroleum Geoscience: From Sedimentary Environments to Rock Physics***,** 467-499.

FORBES, P., UNGERER, P., AB KUHFUSS, F. and EGGEN, S. 1991. Compositional Modeling of Petroleum Generation and Expulsion: Trial Application to a Local Mass

Balance in the Smorbukk Sor Field, Haltenbanken Area, Norway (1). *AAPG Bulletin,* 75**,** 873-893.

GABRIELSEN, R. H., FÆRSETH, R. B., JENSEN, L. N., KALHEIM, J. E. and RIIS, F. 1990. Structural elements of the Norwegian Continental shelf. Part I: The Barents Sea region. *Norwegian Petroleum Directorate Bulletin,* 6**,** 33.

GABRIELSEN, R. H., GRUNNALEITE, I. and RASMUSSEN, E. 1997. Cretaceous and tertiary inversion in the Bjørnøyrenna Fault Complex, south-western Barents Sea. *Marine and Petroleum Geology,* 14**,** 165-178.

GABRIELSEN, R. H., FALEIDE, J. I., PASCAL, C., BRAATHEN, A., NYSTUEN, J. P., ETZELMULLER, B. and O'DONNELL, S. 2010. Latest Caledonian to Present tectonomorphological development of southern Norway. *Marine and Petroleum Geology,* 27**,** 709-723.

GLØRSTAD-CLARK, E., FALEIDE, J. I., LUNDSCHIEN, B. A. and NYSTUEN, J. P. 2010. Triassic seismic sequence stratigraphy and paleogeography of the western Barents Sea area. Marine and Petroleum Geology, 27, 1448-1475.

GUDLAUGSSON, S. T., FALEIDE, J. I., JOHANSEN, S. E. and BREIVIK, A. J. 1998. Late Palaeozoic structural development of the South-western Barents Sea. *Marine and Petroleum Geology,* 15**,** 73-102.

GÓMEZ, M., VERGÉS, J., FERNÀNDEZ, M., TORNE, M., AYALA, C., WHEELER, W. and KARPUZ, R. 2004. Extensional geometry of the Mid Norwegian Margin before Early Tertiary continental breakup. *Marine and Petroleum Geology,* 21**,** 177-194.

HALPERN, H. I. 1995. Development and applications of light-hydrocarbon-based star diagrams. *Journal Name: AAPG Bulletin; Journal Volume: 79; Journal Issue: 6,* 801-815.

HANISCH, J. 1984. THE CRETACEOUS OPENING OF THE NORTHEAST ATLANTIC. *Tectonophysics,* 101**,** 1-23.

HENRIKSEN, S., FICHLER, C., GRØNLIE, A., HENNINGSEN, T., LAURSEN, I., LØSETH, H., OTTESEN, D. and PRINCE, I. 2005. The Norwegian sea during the Cenozoic. *Norwegian Petroleum Society Special Publications,* 12**,** 111-133.

HEUM, O. R., DALLAND, A. and MEISINGSET, K. K. 1986. Habitat of hydrocarbons at Haltenbanken (PVT-modelling as a predictive tool in hydrocarbon exploration, offshore Norway). *Habitat of hydrocarbons on the Norwegian continental shelf. Proc. conference, Stavanger, 1985***,** 259-274.

HORSTAD, I. and LARTER, S. R. 1997. Petroleum migration, alteration, and remigration within Troll Field, Norwegian North Sea. *AAPG Bulletin,* 81**,** 222-248.

HUANG, W.-Y. and MEINSCHEIN, W. G. 1979. Sterols as ecological indicators. *Geochimica et Cosmochimica Acta,* 43**,** 739-745.

HUGHES, W. B., HOLBA, A. G. and DZOU, L. I. P. 1995. The ratios of dibenzothiophene to phenanthrene and pristane to phytane as indicators of depositional environment and lithology of petroleum source rocks. *Geochimica et Cosmochimica Acta,* 59**,** 3581-3598.

HUNT, J. M. 1996. *Petroleum geochemistry and geology,* New York, W. H. Freeman.

JACKSON, J. and HASTINGS, D. 1986. The role of salt movement in the tectonic history of Haltenbanken and Traenabanken and its relationship to structural style. *Habitat of hydrocarbons on the Norwegian continental shelf***,** 241-257.

JOHANSEN, S. E., HENNINGSEN, T., RUNDHOVDE, E., SÆTHER, B. M., FICHLER, C. and RUESLÅTTEN, H. G. 1994. Continuation of the Caledonides north of Norway: seismic reflectors within the basement beneath the southern Barents Sea. *Marine and Petroleum Geology,* 11**,** 190-201.

JONATHAN, D., L'HOTE, G. and DU ROUCHET, J. 1975. Analyse géochimique des hydrocarbures légers par thermovaporisation. *Oil and Gas Science and Technology - Rev. IFP,* 30**,** 65-88.

JUSTWAN, H. & DAHL, B. 2005. Quantitative hydrocarbon potential mapping and organofacies study in the Greater Balder Area, Norwegian North Sea. *Geological Society, London, Petroleum Geology Conference series*. Geological Society of London, 1317-1329.

KARLSEN, D. and LARTER, S. 1989. A rapid correlation method for petroleum population mapping within individual petroleum reservoirs: applications to petroleum reservoir description. *Correlation in hydrocarbon exploration***,** 77-85.

KARLSEN, D. A. and LARTER, S. R. 1991. Analysis of petroleum fractions by TLC-FID: applications to petroleum reservoir description. *Organic Geochemistry,* 17**,** 603-617.

KARLSEN, D. A., NEDKVITNE, T., LARTER, S. R. and BJØRLYKKE, K. 1993. Hydrocarbon composition of authigenic inclusions: Application to elucidation of petroleum reservoir filling history. *Geochimica et Cosmochimica Acta,* 57**,** 3641-3659.

KARLSEN, D. A., NYLAND, B., FLOOD, B., OHM, S. E., BREKKE, T., OLSEN, S. and BACKER-OWE, K. 1995. Petroleum geochemistry of the Haltenbanken, Norwegian continental shelf. *Geological Society, London, Special Publications,* 86**,** 203-256.

KARLSEN, D. A., SKEIE, J. E., BACKER-OWE, K., BJØRLYKKE, K., OLSTAD, R., BERGE, K., CECCHI, M., VIK, E. and SCHAEFER, R. G. 2004. Petroleum migration, faults and overpressure. Part II. Case history: The Haltenbanken Petroleum

Province, offshore Norway. *Geological Society, London, Special Publications,* 237**,** 305-372.

KARLSEN, D. A. and SKEIE, J. E. 2006. Petroleum migration, faults and overpressure, part i: calibrating basin modelling using petroleum in traps — a review. *Journal of Petroleum Geology,* 29**,** 227-256.

KNAUST, D. 2009. Characterisation of a Campanian deep-sea fan system in the Norwegian Sea by means of ichnofabrics. *Marine and Petroleum Geology,* 26**,** 1199-1211.

KVALHEIM, O. M., CHRISTY, A. A., TELNÆS, N. and BJØRSETH, A. 1987. Maturity determination of organic matter in coals using the methylphenanthrene distribution. *Geochimica et cosmochimica acta,* 51**,** 1883-1888.

LARTER, S., HUANG, H., ADAMS, J., BENNETT, B. and SNOWDON, L. R. 2012. A practical biodegradation scale for use in reservoir geochemical studies of biodegraded oils. *Organic Geochemistry,* 45**,** 66-76.

MACKENZIE, A. S., PATIENCE, R. L., MAXWELL, J. R., VANDENBROUCKE, M. and DURAND, B. 1980. Molecular parameters of maturation in the Toarcian shales, Paris Basin, France—I. Changes in the configurations of acyclic isoprenoid alkanes, steranes and triterpanes. *Geochimica et Cosmochimica Acta,* 44**,** 1709-1721.

MACKENZIE, A. S. 1984. Applications of biological markers in petroleum geochemistry. *Advances in petroleum geochemistry,* 1**,** 1-210.

MACKENZIE, A., RULLKÖTTER, J., WELTE, D. and MANKIEWICZ, P. 1985. Reconstruction of oil formation and accumulation in North Slope, Alaska, using quantitative gas chromatography-mass spectrometry. *Alaska North Slope oil/rock correlation study: AAPG Studies in Geology,* 20**,** 319-377.

MELLO, M. R., TELNAES, N., GAGLIANONE, P. C., CHICARELLI, M. I., BRASSELL, S. C. and MAXWELL, J. R. 1988. Organic geochemical characterisation of depositional palaeoenvironments of source rocks and oils in Brazilian marginal basins. *Organic Geochemistry,* 13**,** 31-45.

MOLDOWAN, J. M., SEIFERT, W. K. and GALLEGOS, E. J. 1985. Relationship between petroleum composition and depositional environment of petroleum source rocks. *AAPG Bulletin,* 69**,** 1255-1268.

MOLDOWAN, J. M., FAGO, F. J., CARLSON, R. M. K., YOUNG, D. C., AN DUVNE, G., CLARDY, J., SCHOELL, M., PILLINGER, C. T. and WATT, D. S. 1991. Rearranged hopanes in sediments and petroleum. *Geochimica et Cosmochimica Acta,* 55**,** 3333-3353.

NEDKVITNE, T., KARLSEN, D. A., BJØRLYKKE, K. and LARTER, S. R. 1993. Relationship between reservoir diagenetic evolution and petroleum emplacement in the Ula Field, North Sea. *Marine and Petroleum Geology,* 10**,** 255-270.

ODDEN, W., PATIENCE, R. L. and VAN GRAAS, G. W. 1998. Application of light hydrocarbons (C4–C13) to oil/source rock correlations:: a study of the light hydrocarbon compositions of source rocks and test fluids from offshore Mid-Norway. *Organic Geochemistry,* 28**,** 823-847.

ODDEN, W. 1999. A study of natural and artificially generated light hydrocarbons (C4–C13) in source rocks and petroleum fluids from offshore Mid-Norway and the southernmost Norwegian and Danish sectors. *Marine and Petroleum Geology,* 16**,** 747-770.

OHM, S. E., KARLSEN, D. A. and AUSTIN, T. J. F. 2008. Geochemically driven exploration models in uplifted areas: Examples from the Norwegian Barents Sea. *AAPG Bulletin,* 92**,** 1191-1223.

PATIENCE, R. L. 2003. Where did all the coal gas go? *Organic Geochemistry,* 34**,** 375-387.

PEDERSEN, J. 2002. *A typical oils, unusual condensates and bitumens of the Norwegian Continental Shelf: an organic geochemical study. Cand. Scient.* Thesis in Geology, *University of Oslo.*

PETERS, K. E. and MOLDOWAN, J. M. 1993. *The biomarker guide,* Englewood Cliffs, N.J., Prentice Hall.

PETERS, K. E. and FOWLER, M. G. 2002. Applications of petroleum geochemistry to exploration and reservoir management. *Organic Geochemistry,* 33**,** 5-36.

PETERS, K. E., WALTERS, C. and MOLDOWAN, J. 2005. The Biomarker Guide: Volume 2, Biomarkers and Isotopes in Petroleum Systems and Earth History. *Cambridge University Press, UK.*

PHILIPPI, G. T. 1977. On the depth, time and mechanism of origin of the heavy to medium-gravity naphthenic crude oils. *Geochimica et Cosmochimica Acta,* 41**,** 33-52.

PROVAN, D. M. J. 1992. Draugen Oil Field, Haltenbanken province, offshore Norway. *Giant oil and gas fields of the decade 1978-1988***,** 371-382.

RADKE, M. 1988. Application of aromatic compounds as maturity indicators in source rocks and crude oils. *Marine and Petroleum Geology,* 5**,** 224-236.

RADKE, M., WELTE, D. H. and WILLSCH, H. 1982a. Geochemical study on a well in the Western Canada Basin: relation of the aromatic distribution pattern to maturity of organic matter. *Geochimica et Cosmochimica Acta,* 46**,** 1-10.

RADKE, M., WILLSCH, H., LEYTHAEUSER, D. and TEICHMÜLLER, M. 1982b. Aromatic components of coal: relation of distribution pattern to rank. *Geochimica et Cosmochimica Acta,* 46**,** 1831-1848.

RADKE, M., VRIEND, S. and SCHAEFER, R. 2001. Geochemical characterization of lower Toarcian source rocks from NW Germany: Interpretation of aromatic and saturated hydrocarbons in relation to depositional environment and maturation effects. *Journal of Petroleum Geology,* 24**,** 287-307.

REN, S., FALEIDE, J. I., ELDHOLM, O., SKOGSEID, J. and GRADSTEIN, F. 2003. Late Cretaceous–Paleocene tectonic development of the NW Vøring Basin. *Marine and Petroleum Geology,* 20**,** 177-206.

SCHAEFER, R. G., WEINER, B. and LEYTHAEUSER, D. 1978. Determination of sub-nanogram per gram quantities of light hydrocarbons (C_2-C_9) in rock samples by hydrogen stripping in the flow system of a capillary gas chromatograph. *Analytical Chemistry,* 50**,** 1848-1854.

SCHOELL, M. 1983. Genetic characterization of natural gases. *AAPG Bulletin,* 67**,** 2225-2238.

SEIFERT, W. K. and MICHAEL MOLDOWAN, J. 1978. Applications of steranes, terpanes and monoaromatics to the maturation, migration and source of crude oils. *Geochimica et Cosmochimica Acta,* 42**,** 77-95.

SEIFERT W, K. and MOLDOWAN J, M. 1986. Use of biological markers in petroleum exploration. *Methods in geochemistry and geophysics,* 24**,** 261-290.

SELDAL, J. 2005. Lower Cretaceous: the next target for oil exploration in the Barents Sea? *Geological Society, London, Petroleum Geology Conference,* 6**,** 231-240.

SHANMUGAM, G. 1985. Significance of coniferous rain forests and related organic matter in generating commercial quantities of oil, Gippsland Basin, Australia. *AAPG Bulletin,* 69**,** 1241.

SMELROR, M., DEHLS, J., EBBING, J., LARSEN, E., LUNDIN, E. R., NORDGULEN, Ø., OSMUNDSEN, P. T., OLESEN, O., OTTESEN, D., PASCAL, C., REDFIELD, T. F. and RISE, L. 2007. Towards a 4D topographic view of the Norwegian Sea margin. *Global and Planetary Change,* 58**,** 382-410.

STEEL, R. and WORSLEY, D. 1984. Svalbard's post-Caledonian strata—an atlas of sedimentational patterns and palaeogeographic evolution. *Petroleum geology of the North European margin,* 109-135.

THOMPSON, K. F. M. 1979. Light hydrocarbons in subsurface sediments. *Geochimica et Cosmochimica Acta,* 43**,** 657-672.

THOMPSON, K. F. M. 1983. Classification and thermal history of petroleum based on light hydrocarbons. *Geochimica et Cosmochimica Acta,* 47**,** 303-316.

THOMPSON, K. F. M. 1987. Fractionated aromatic petroleums and the generation of gas-condensates. *Organic Geochemistry,* 11**,** 573-590.

TISSOT, B., CALIFET-DEBYSER, Y., DEROO, G. and OUDIN, J. 1971. Origin and evolution of hydrocarbons in early Toarcian shales, Paris Basin, France. *AAPG Bulletin,* 55**,** 2177-2193.

TISSOT, B. P. and WELTE, D. H. 1984. *Petroleum formation and occurrence*, Berlin, Springer.

WEISS, H., WILHELMS, A., MILLS, N., SCOTCHMER, J., HALL, P., LIND, K. and BREKKE, T. 2000. NIGOGA-The Norwegian Industry Guide to Organic Geochemical Analyses. *Edition four, Published by Norsk Hydro, Statoil, Geolab Nor, SINTEF Petroleum Research and the Norwegian Petroleum Directorate*.

WENGER, L. M., DAVIS, C. L. and ISAKSEN, G. H. 2002. Multiple controls on petroleum biodegradation and impact on oil quality. *SPE Reservoir Evaluation and Engineering,* 5**,** 375-383.

WEVER, H. E. 2000. Petroleum and Source Rock Characterization Based on C_7 Star Plot Results: Examples from Egypt. *AAPG Bulletin,* 84, 1041-1054.

WHITICAR, M. J. 1994. Correlation of natural gases with their sources. *The petroleum system - from source to trap***,** 261-283.

WHITLEY, P. K. 1992. The Geology of Heidrun - a Giant Oil and Gas-Field on the Mid-Norwegian Shelf. *Giant oil and gas fields of the decade 1978-1988,* 54**,** 383-406.

WILHELMS, A. and LARTER, S. R. 1994. Origin of tar mats in petroleum reservoirs. Part II: formation mechanisms for tar mats. *Marine and Petroleum Geology,* 11**,** 442-456.

WORSLEY, D. 2008. The post-Caledonian development of Svalbard and the western Barents Sea. *Polar research,* 27**,** 298-317.

ØSTENSEN, M. 2005. A geochemical assessment of petroleum from underground oil storage caverns in relation to petroleum from natural reservoirs offshore Norway, *Master Thesis, University of Oslo,* 6-8.

http://npdmap1.npd.no/website/npdgis/viewer.htm (Last accessed 30-11-2012)

http://factpages.npd.no/factpages/ (Last accessed 30-11-2012)

Appendix

Appendix A (Gas analysis Results)

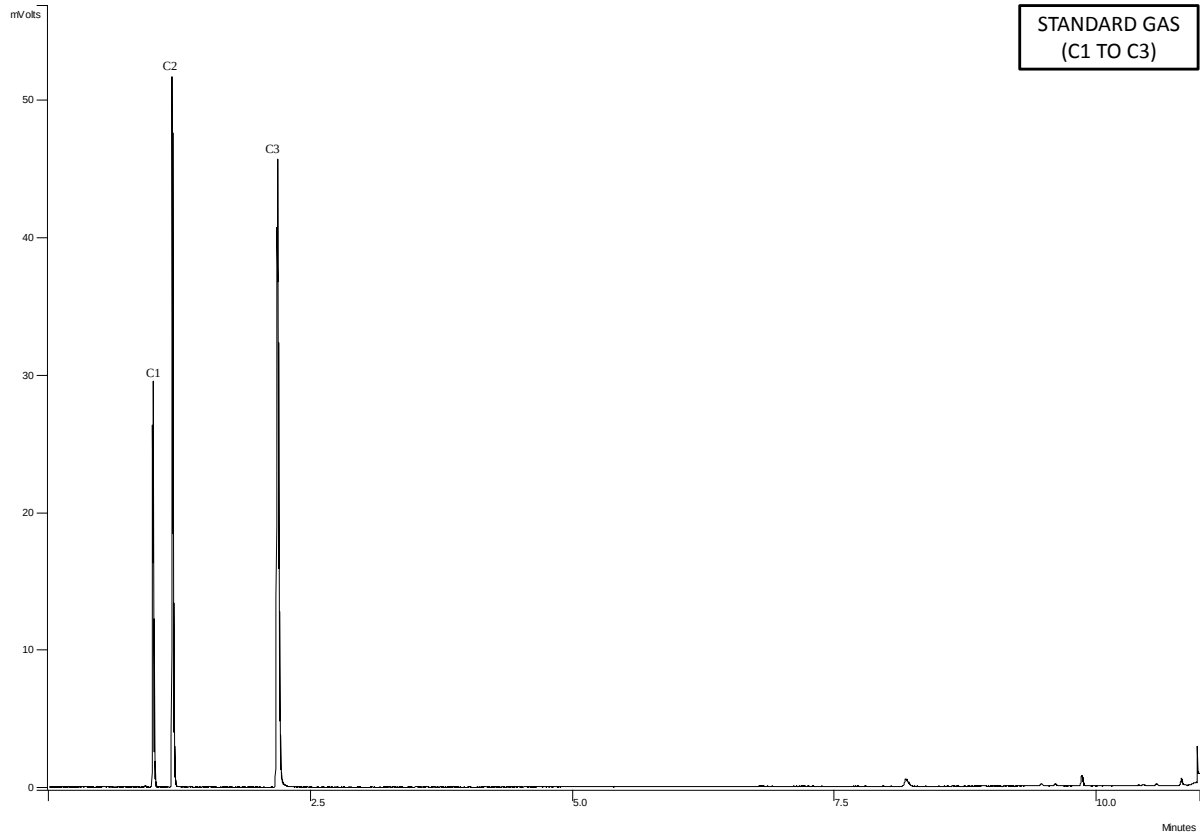
STANDARD GAS
(C1 TO C3)
mVolts
C1
C2
C3
Minutes

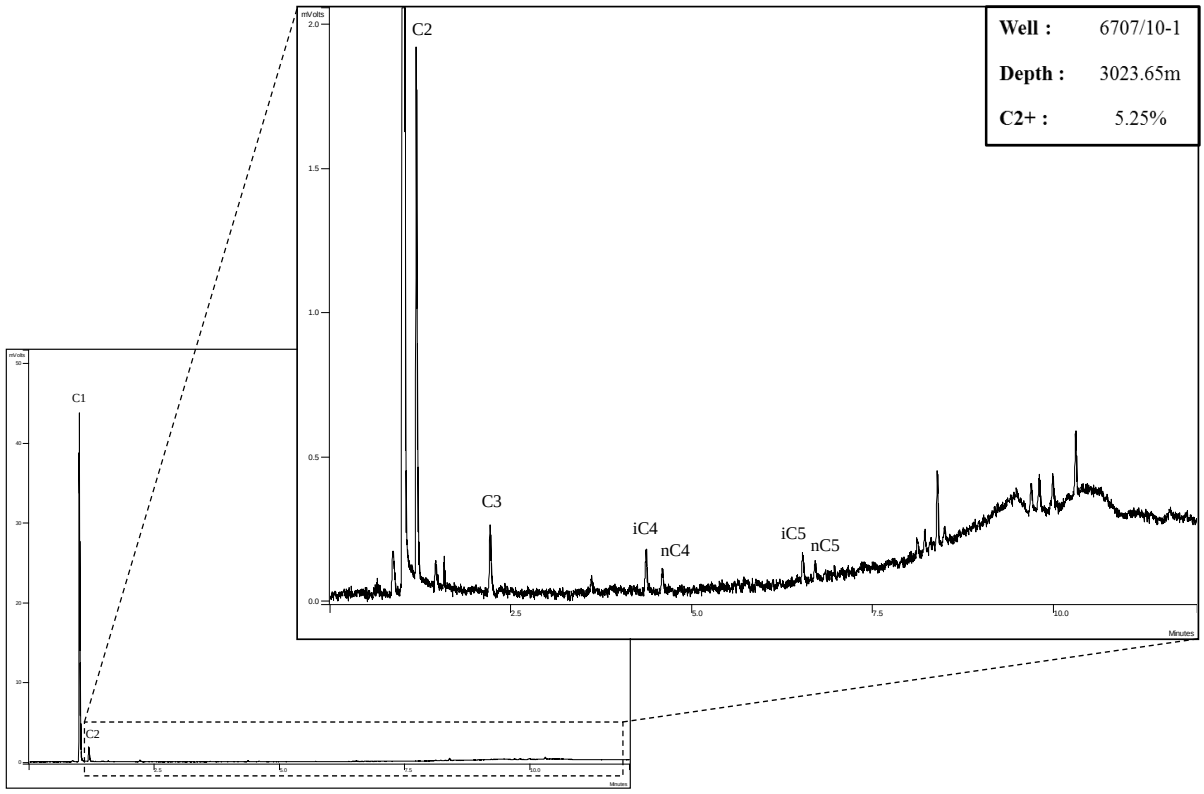
Well : 6707/10-1
Depth : 3023.65m
C2+ : 5.25%
C1
C2
C3
iC4
nC4
iC5
nC5
Minutes

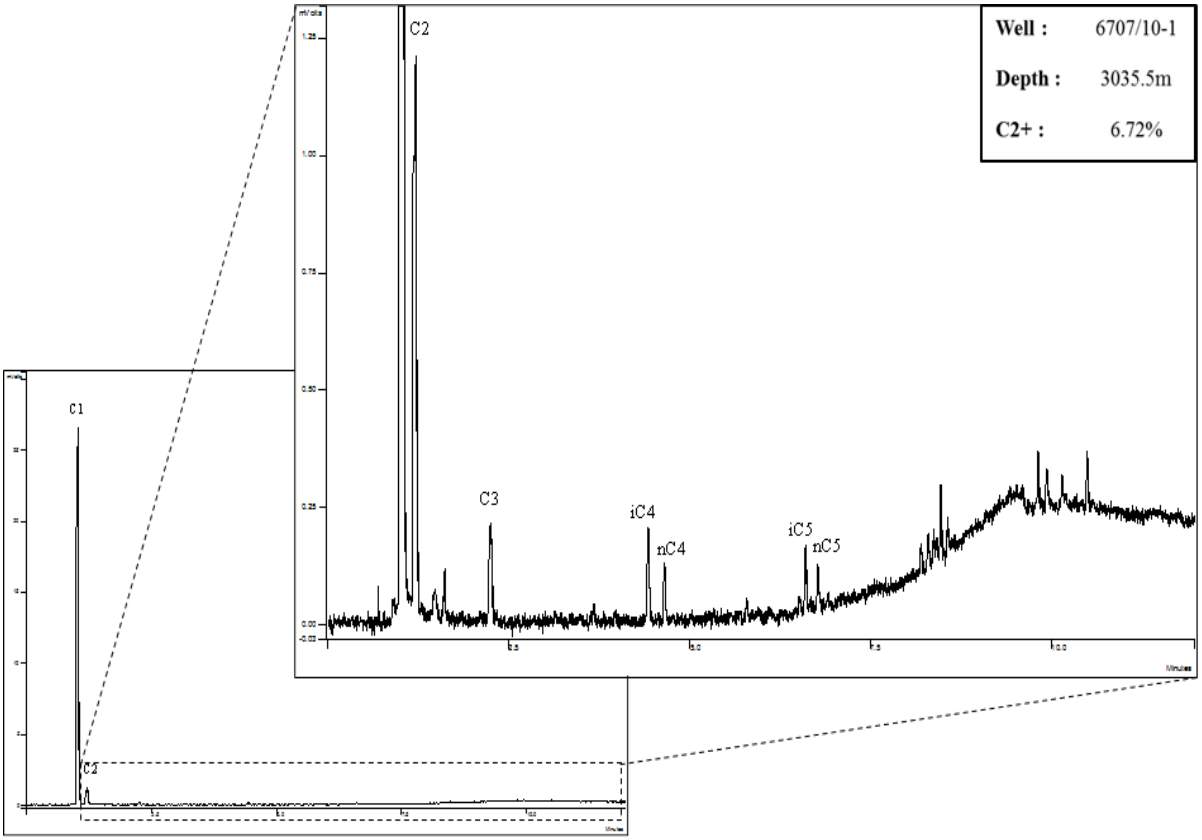
Well : 6707/10-1
Depth : 3035.5m
C2+ : 6.72%
C1
C2
C3
iC4
nC4
iC5
nC5

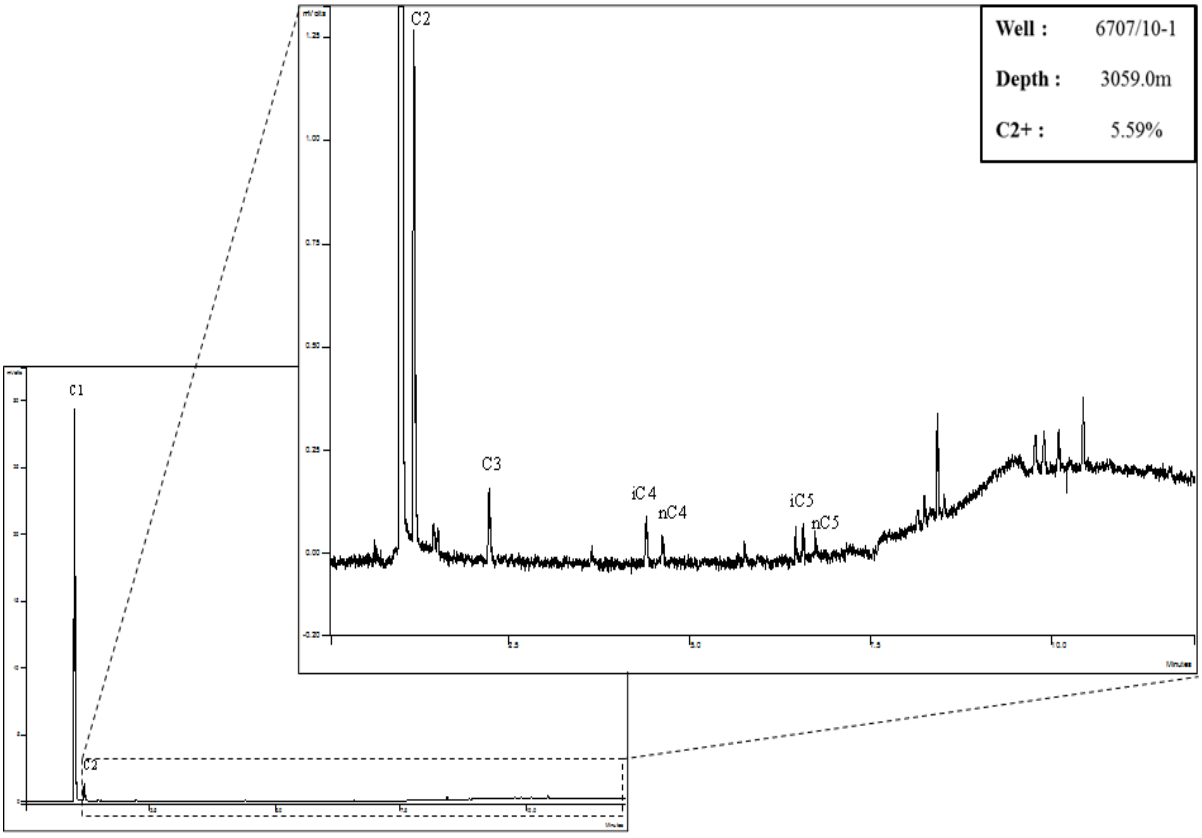
Well : 6707/10-1
Depth : 3059.0m
C2+ : 5.59%
C1
C2
C3
iC4
nC4
iC5
nC5

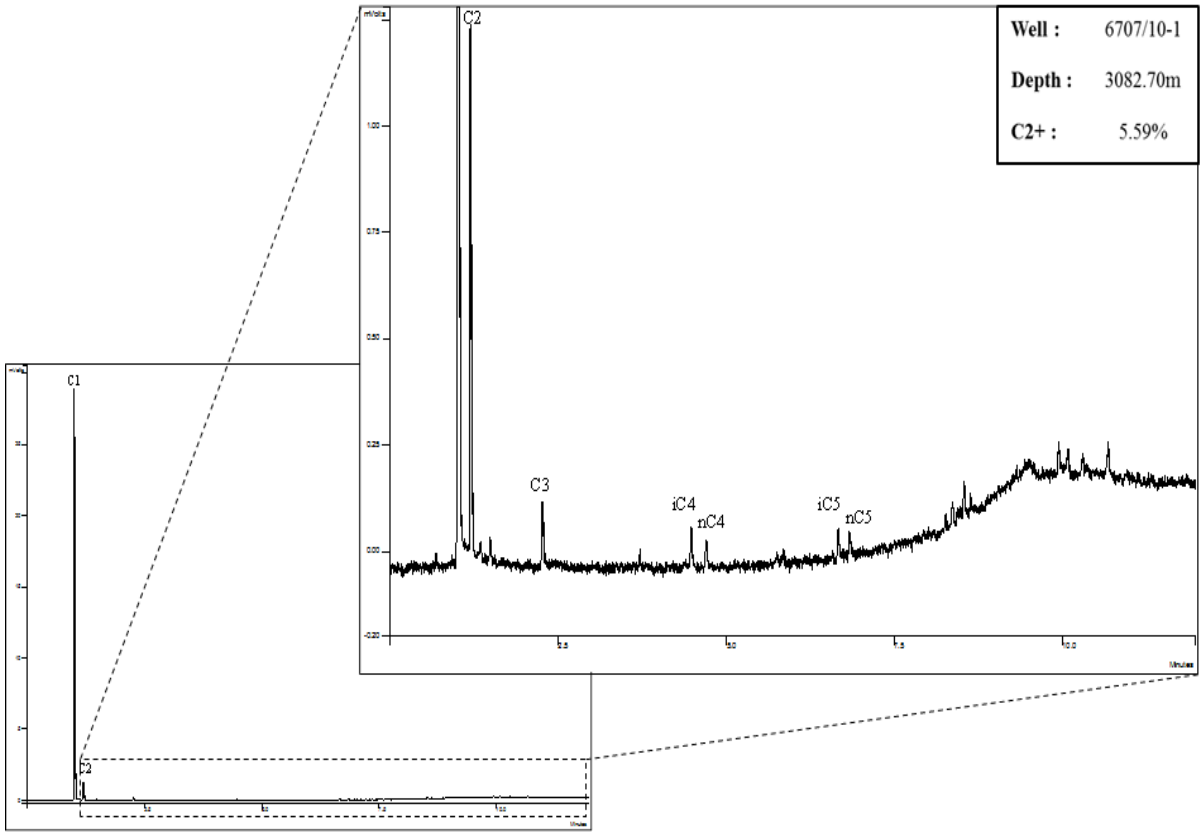
Well : 6707/10-1
Depth : 3082.70m
C2+ : 5.59%
C1
C2
C3
iC4
nC4
iC5
nC5

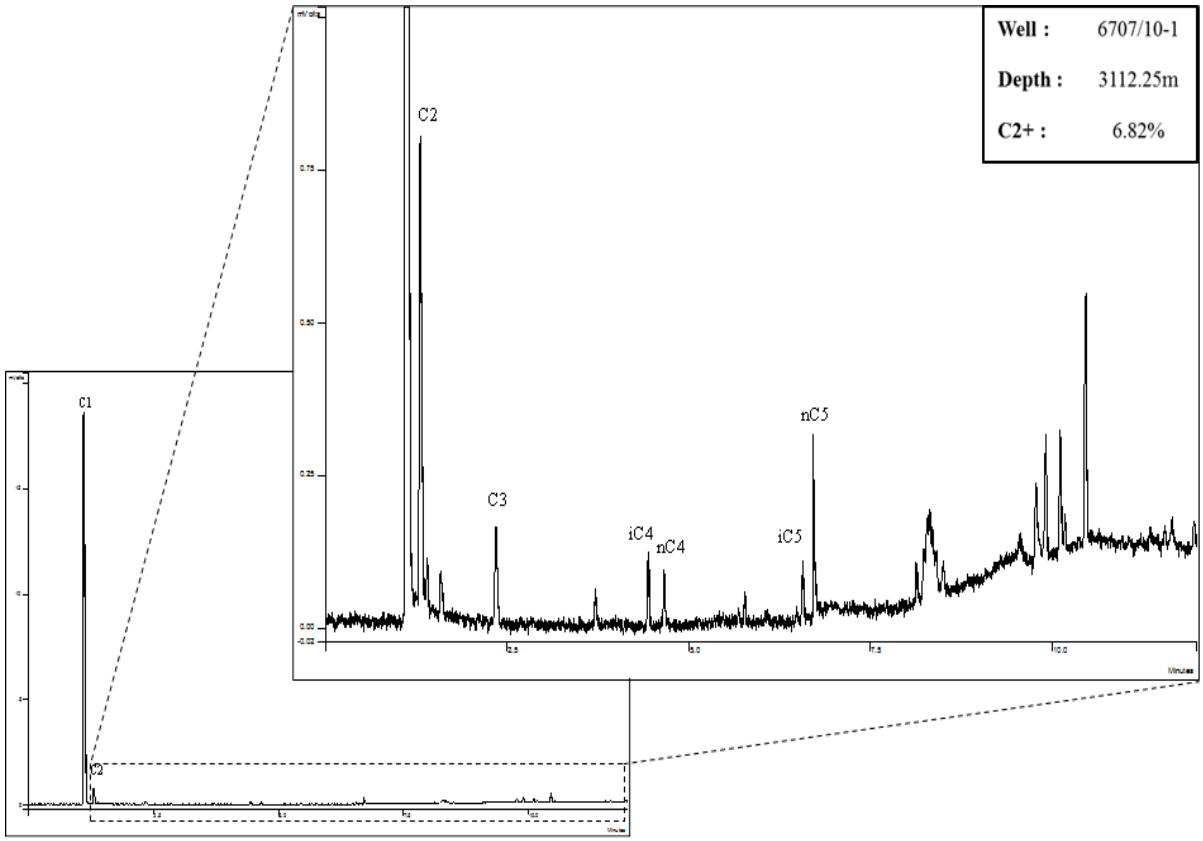
Well : 6707/10-1
Depth : 3112.25m
C2+ : 6.82%
C1
C2
C3
iC4
nC4
iC5
nC5

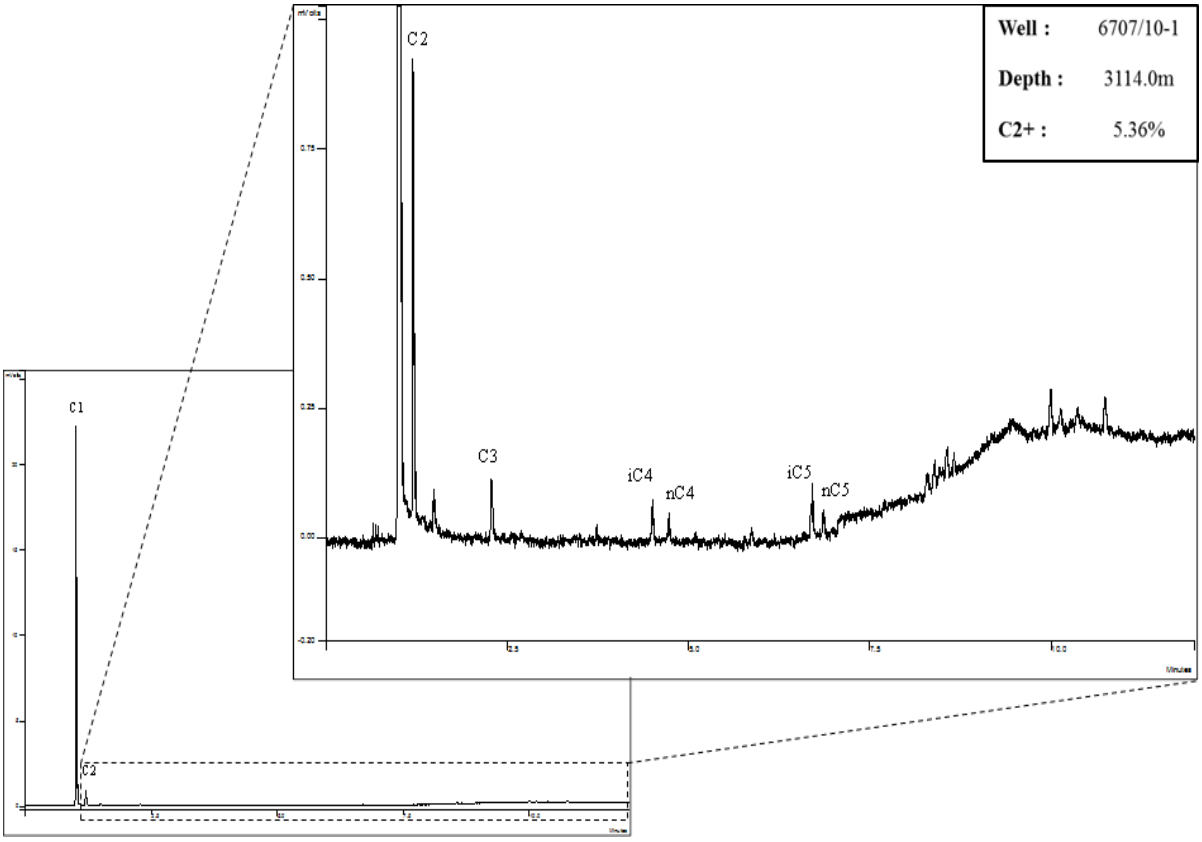
Well : 6707/10-1
Depth : 3114.0m
C2+ : 5.36%
C1
C2
C3
iC4
nC4
iC5
nC5

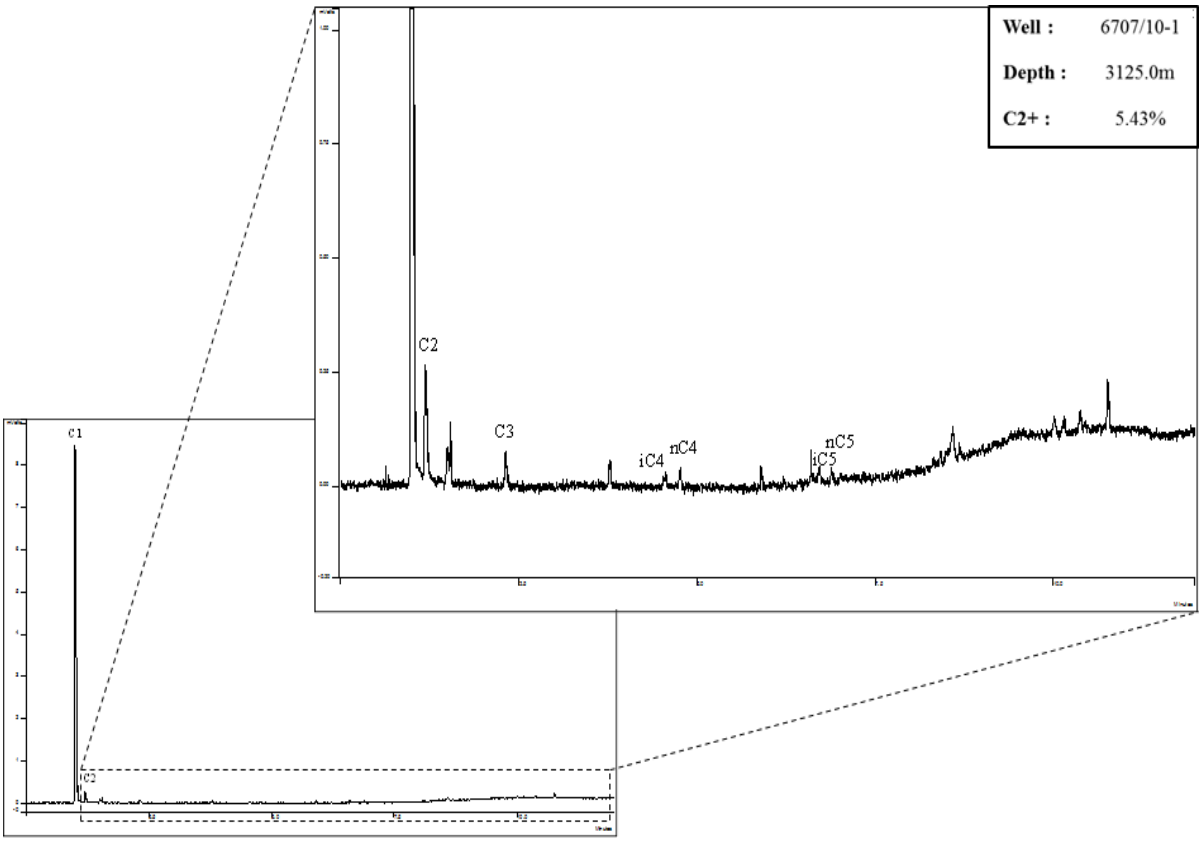
Well : 6707/10-1
Depth : 3125.0m
C2+ : 5.43%
C1
C2
C3
iC4
nC4
iC5
nC5

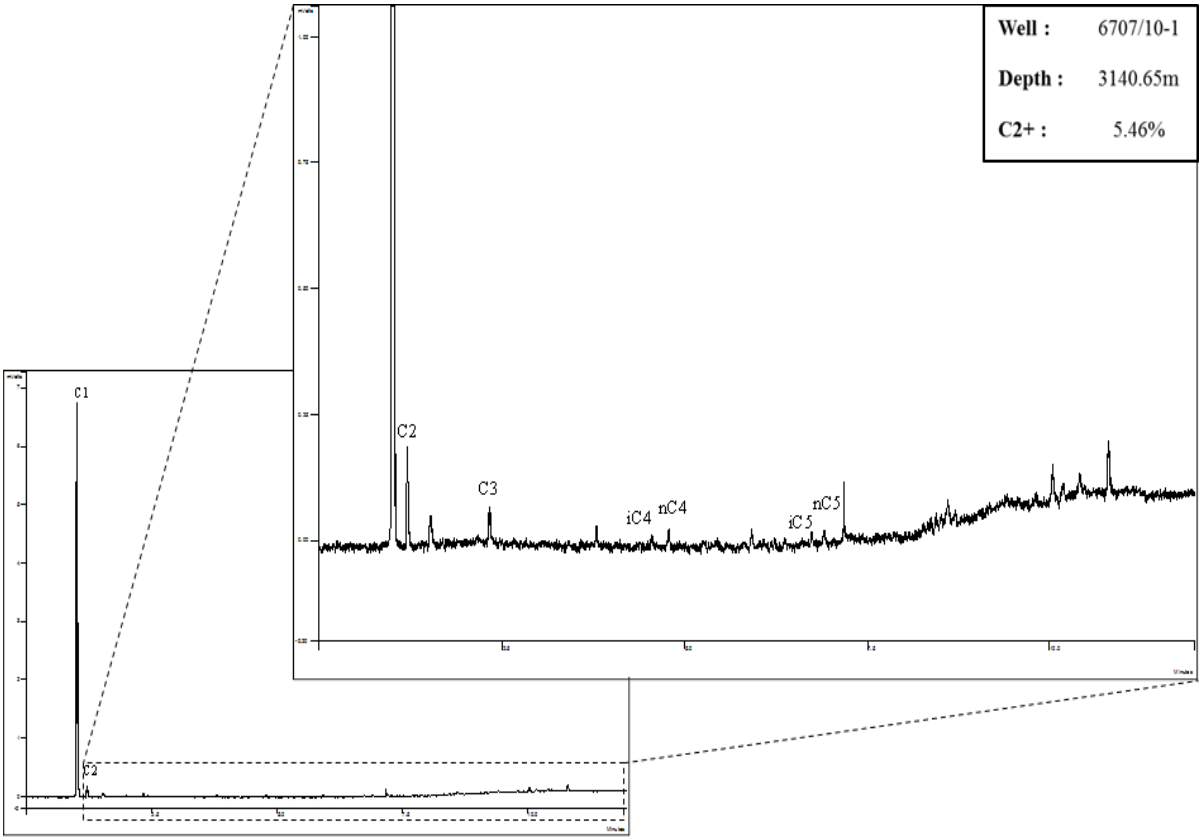
Well : 6707/10-1
Depth : 3140.65m
C2+ : 5.46%
C1
C2
C3
iC4
nC4
iC5
nC5
C2

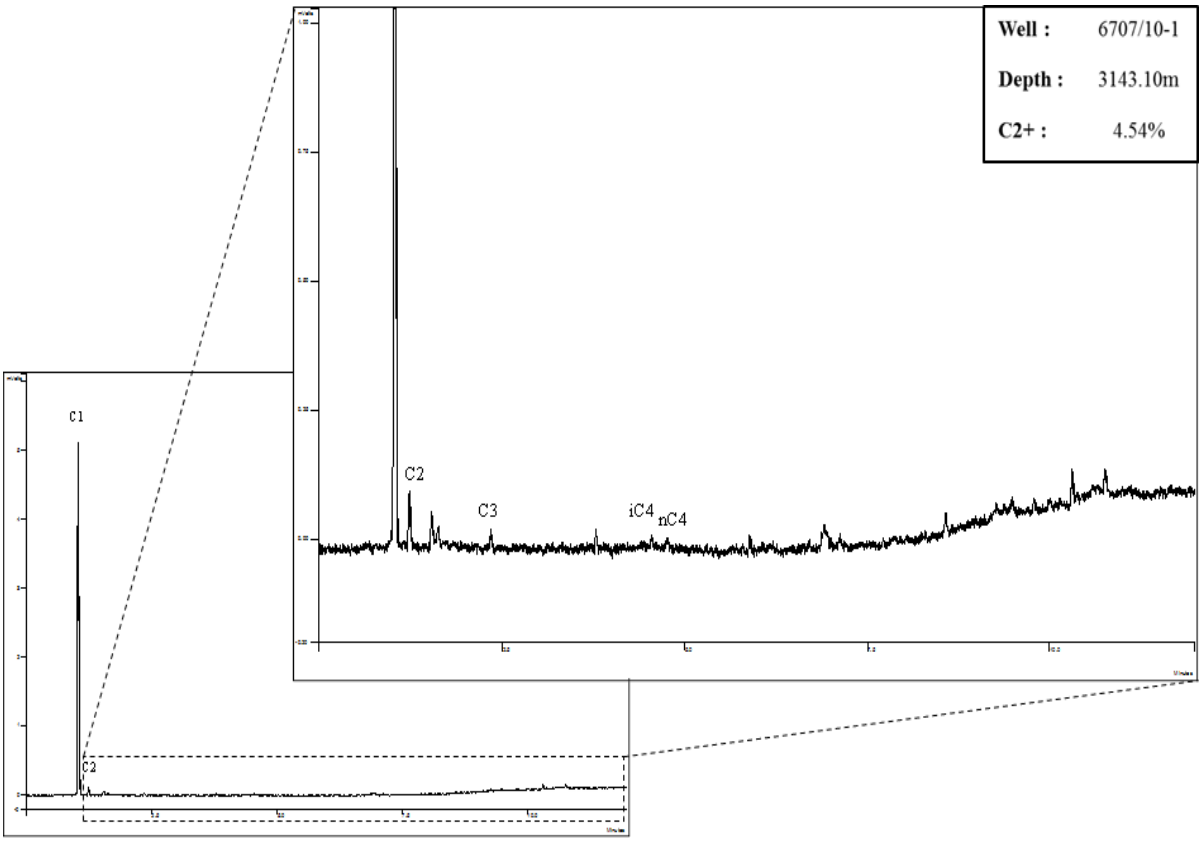
Well : 6707/10-1
Depth : 3143.10m
C2+ : 4.54%
C1
C2
C3
iC4
nC4
C2

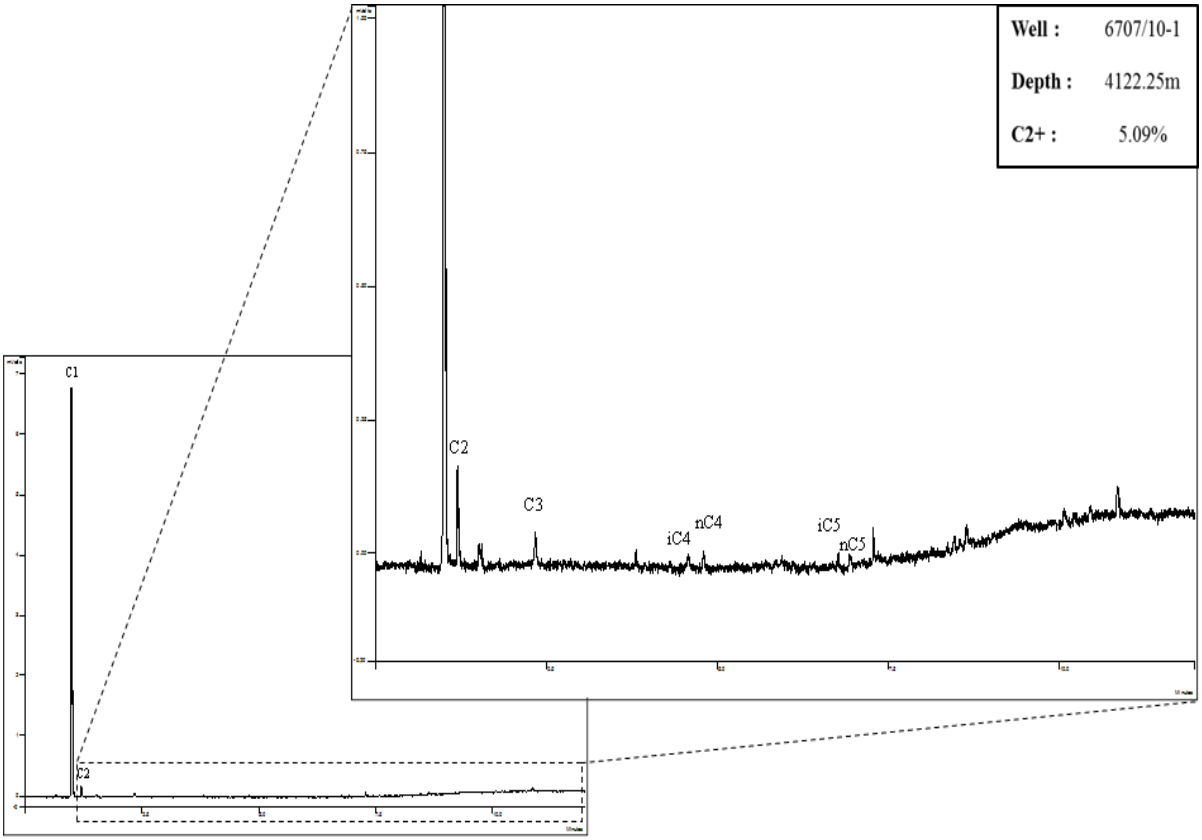
Well : 6707/10-1
Depth : 4122.25m
C2+ : 5.09%
C1
C2
C3
iC4
nC4
iC5
nC5
C2

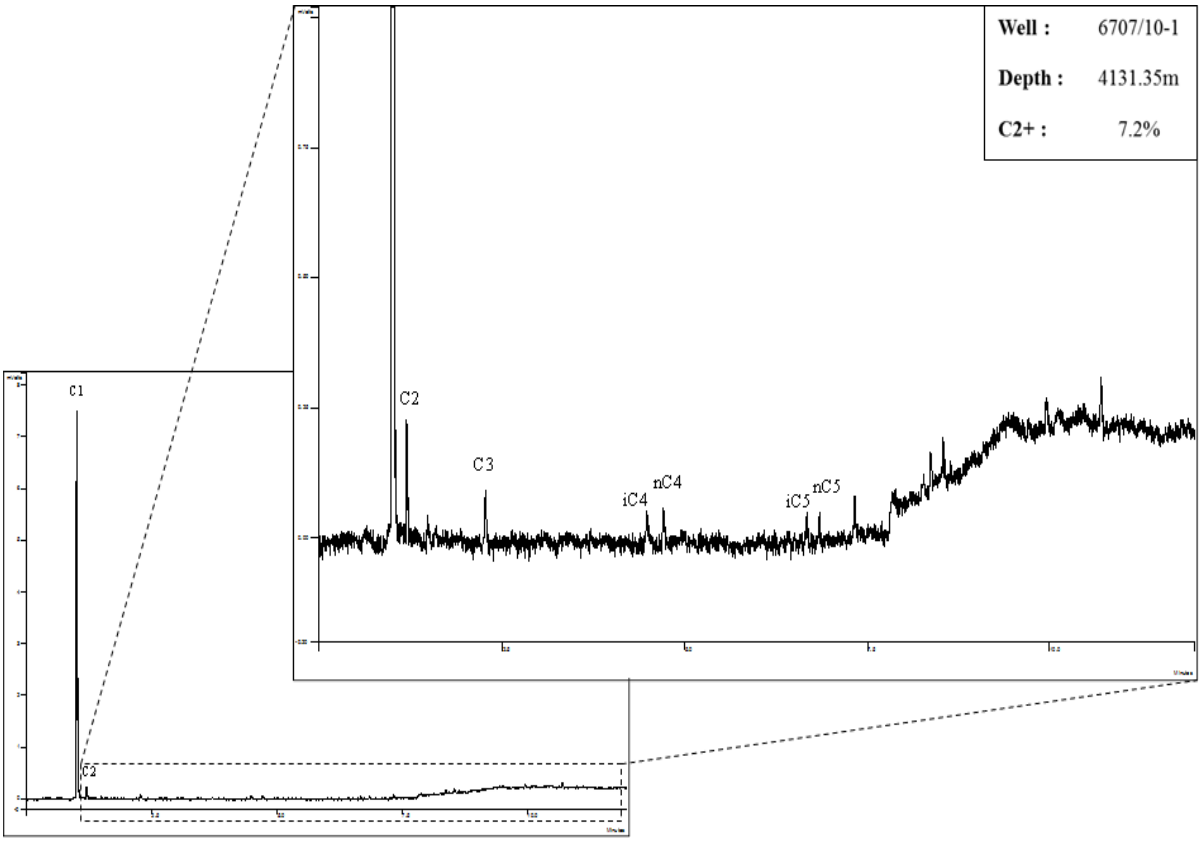
Well : 6707/10-1
Depth : 4131.35m
C2+ : 7.2%
C1
C2
C3
iC4
nC4
iC5
nC5
C2

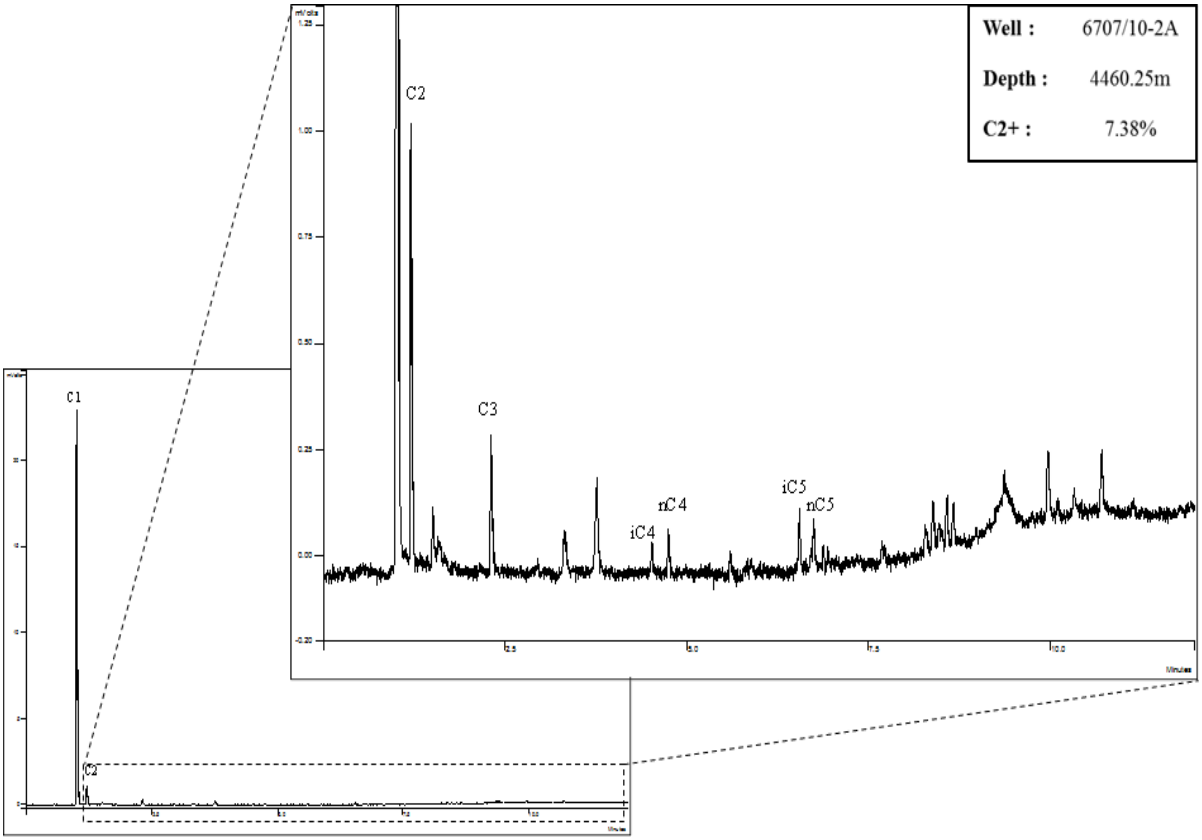
Well : 6707/10-2A
Depth : 4460.25m
C2+ : 7.38%
C1
C2
C3
iC4
nC4
iC5
nC5

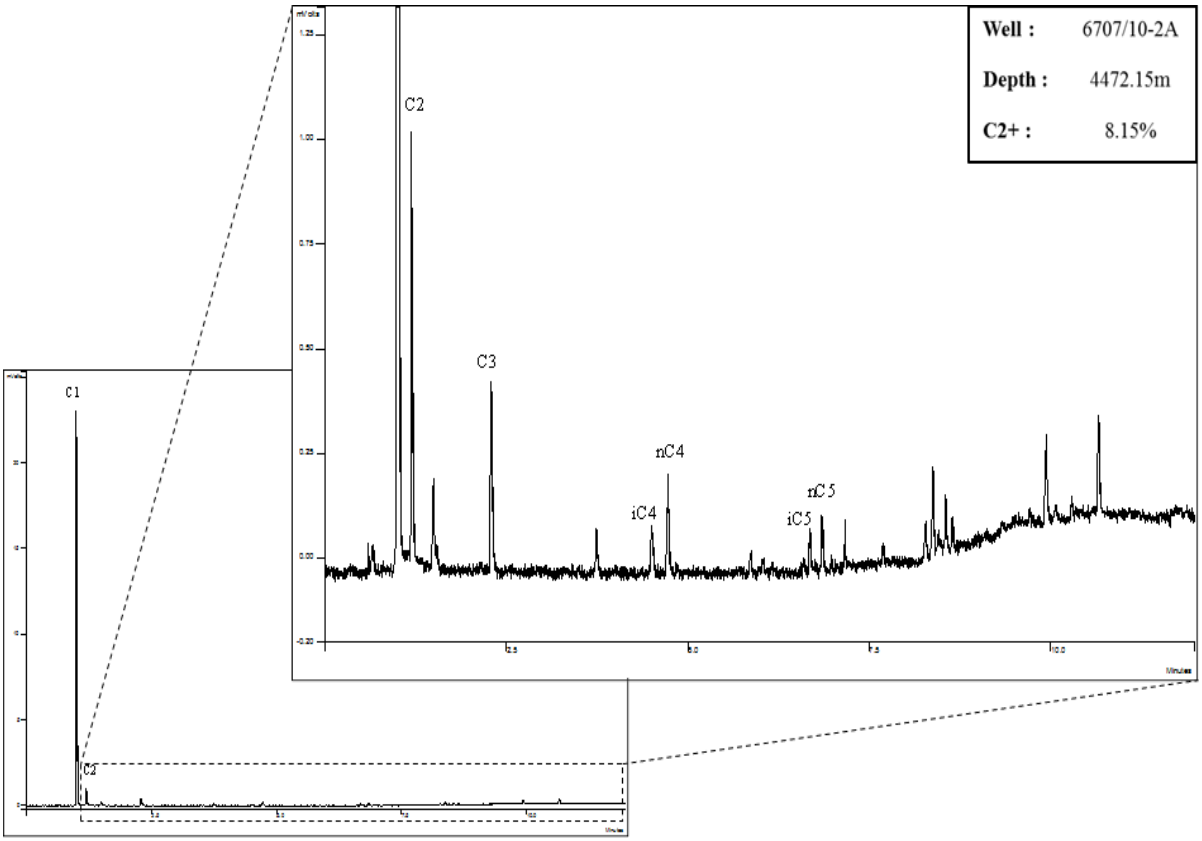
Well : 6707/10-2A
Depth : 4472.15m
C2+ : 8.15%
C1
C2
C3
iC4
nC4
iC5
nC5

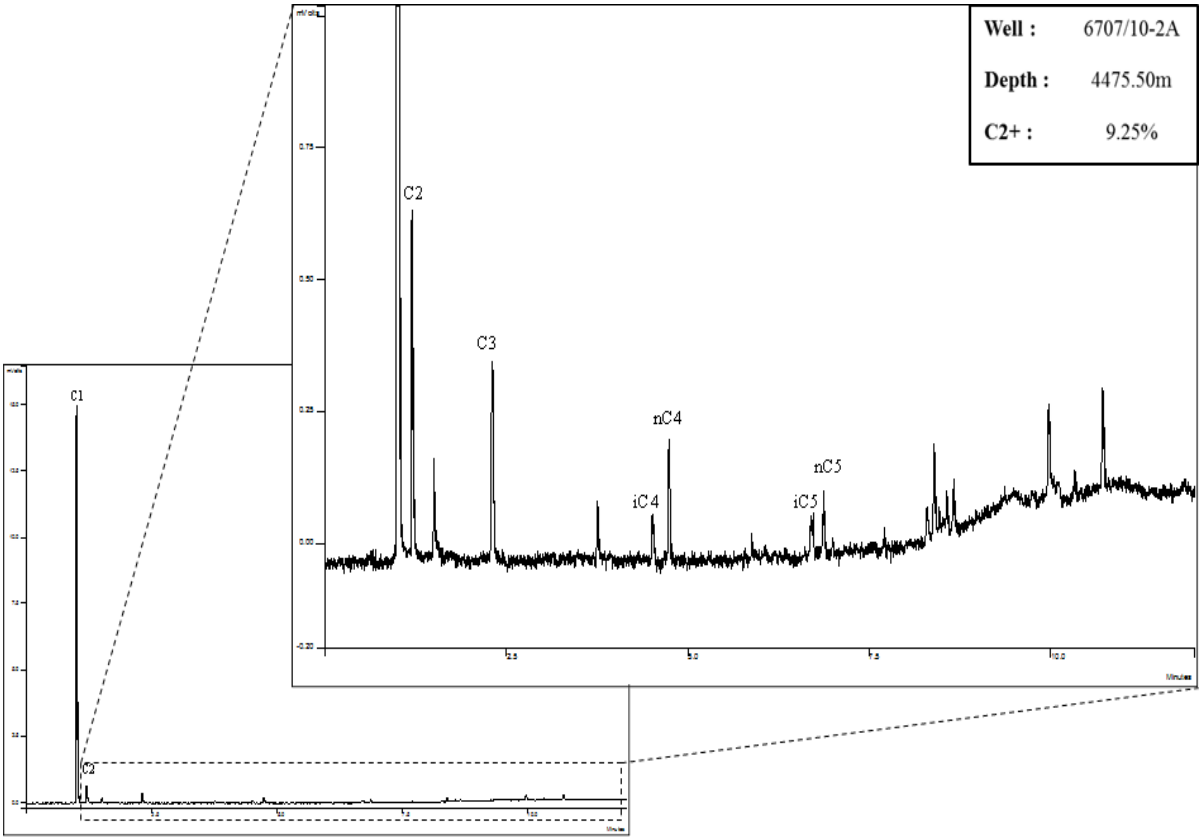
Well : 6707/10-2A
Depth : 4475.50m
C2+ : 9.25%
C1
C2
C3
iC4
nC4
iC5
nC5
Minutes

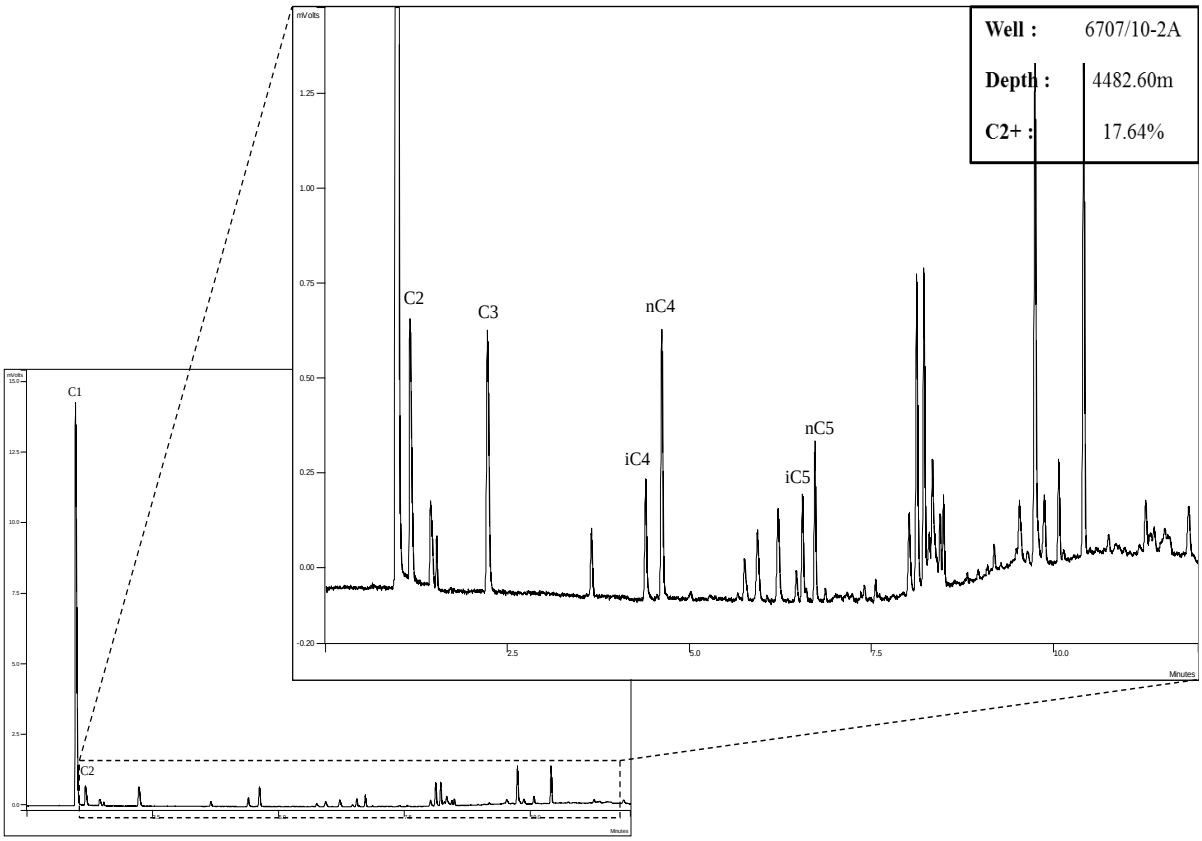
Well : 6707/10-2A
Depth : 4482.60m
C2+ : 17.64%
mVolts
C1
C2
C3
iC4
nC4
iC5
nC5
Minutes

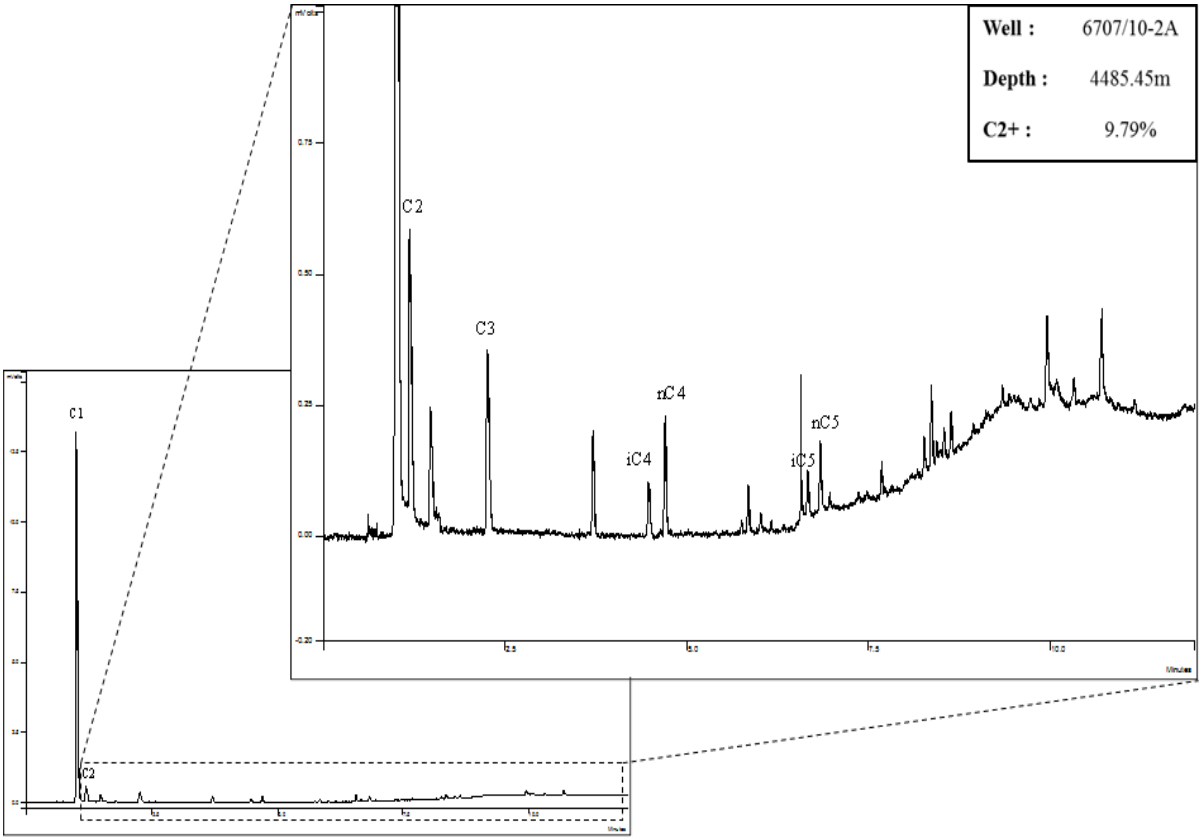
Well : 6707/10-2A
Depth : 4485.45m
C2+ : 9.79%
C1
C2
C3
iC4
nC4
iC5
nC5

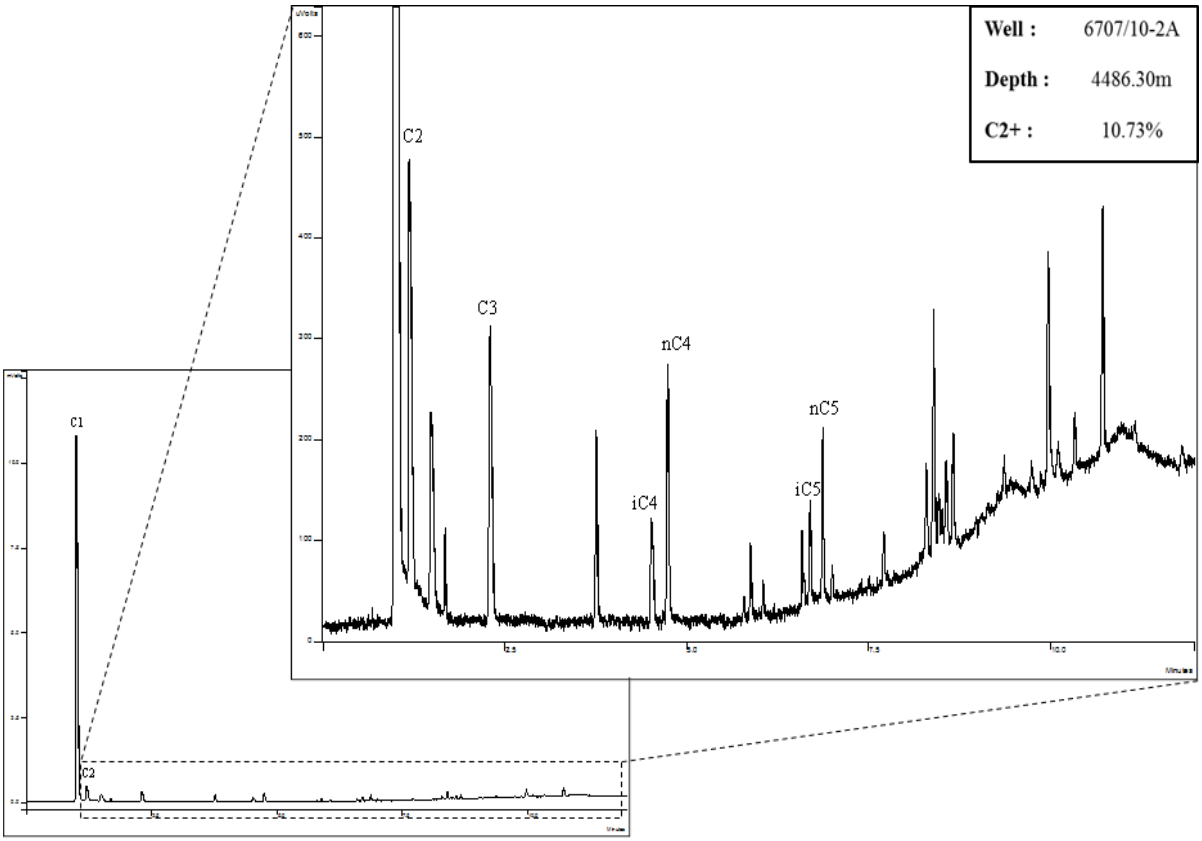
Well : 6707/10-2A
Depth : 4486.30m
C2+ : 10.73%
C1
C2
C3
iC4
nC4
iC5
nC5

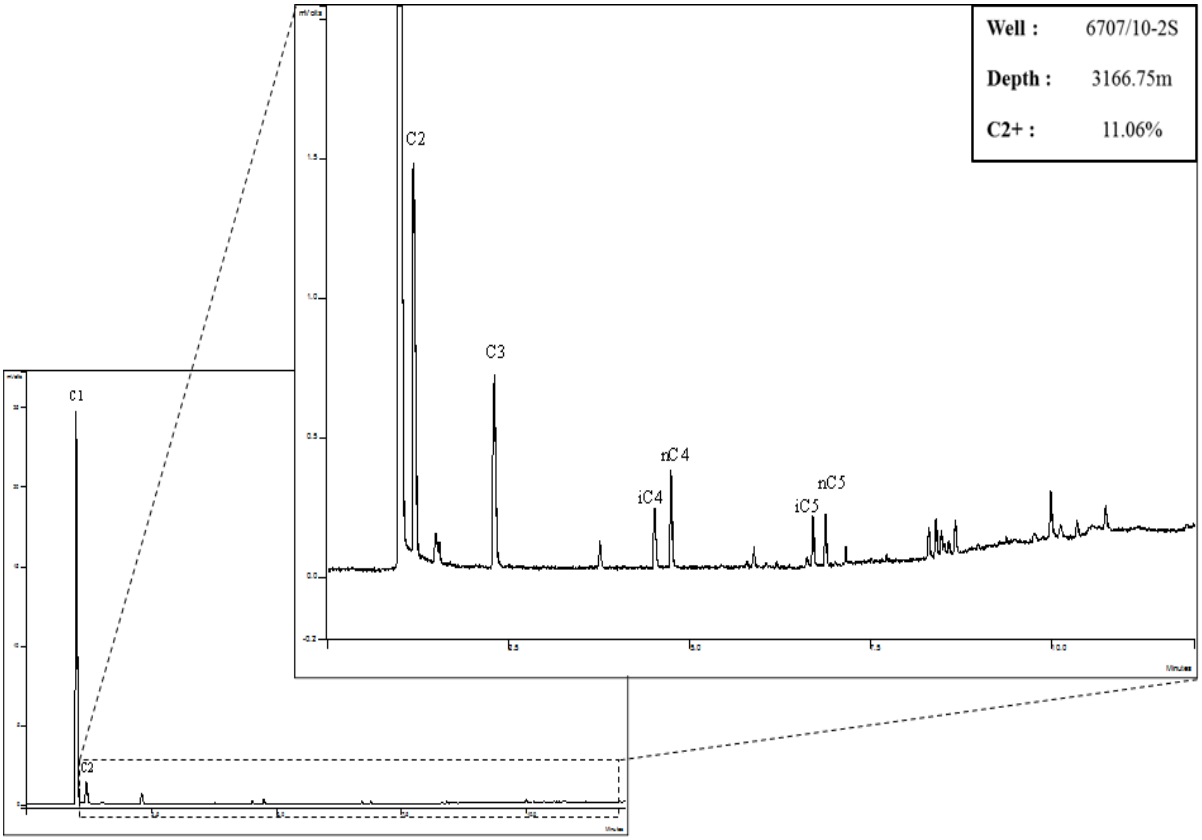
Well : 6707/10-2S
Depth : 3166.75m
C2+ : 11.06%
C1
C2
C3
iC4
nC4
iC5
nC5
Minutes

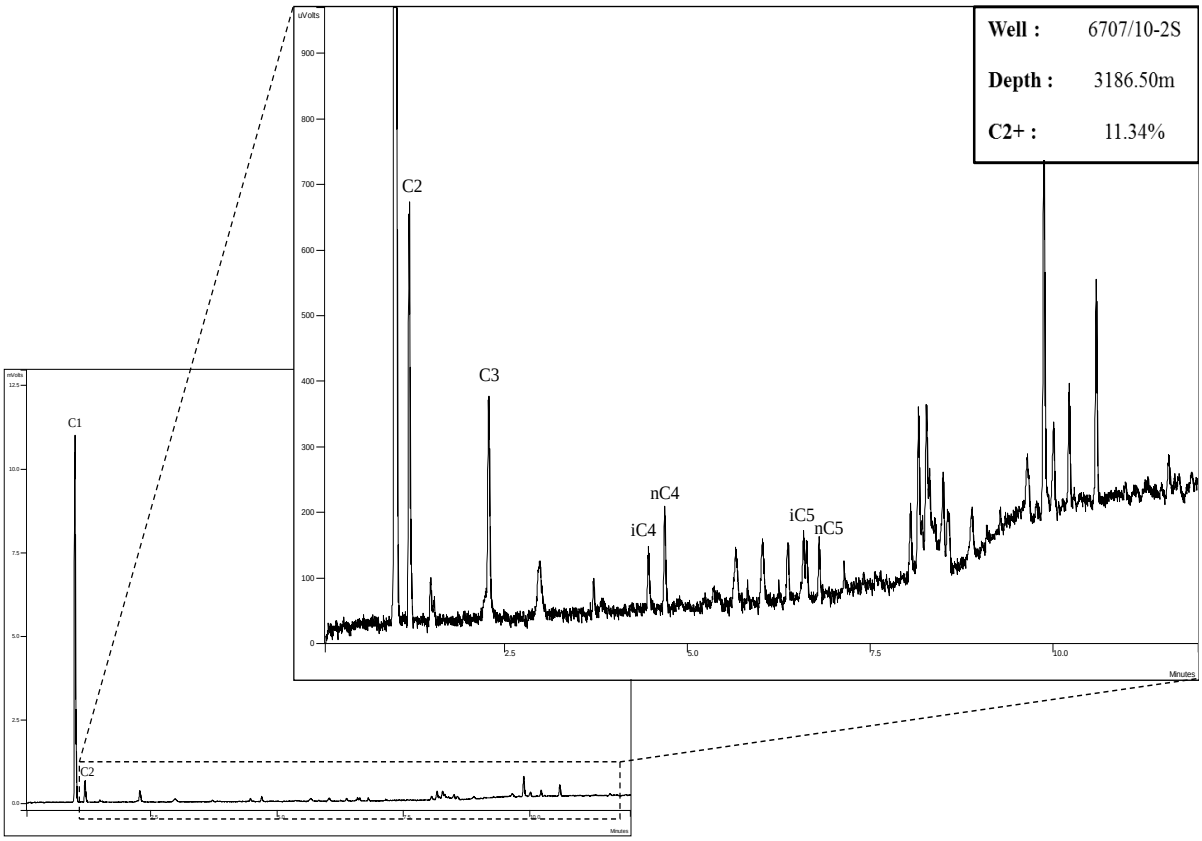
Well : 6707/10-2S
Depth : 3186.50m
C2+ : 11.34%
uVolts
C1
C2
C3
iC4
nC4
iC5
nC5
Minutes

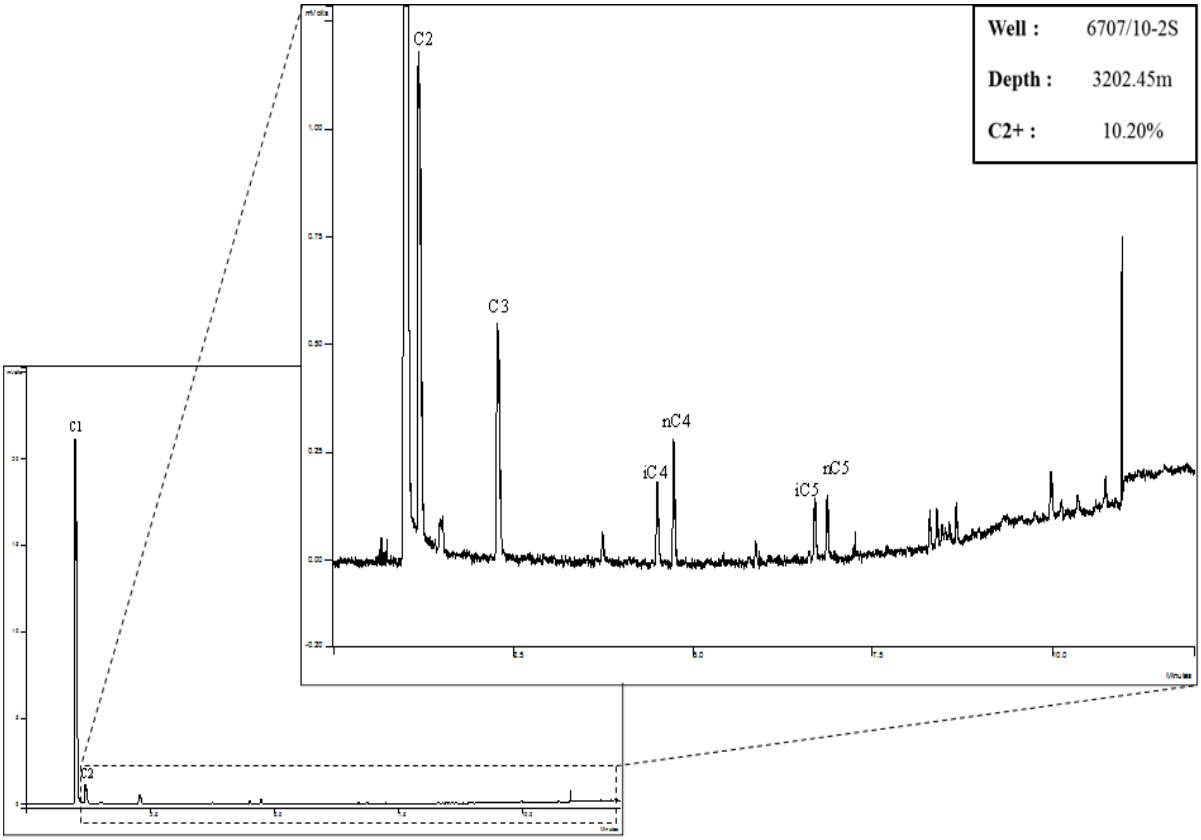
Well : 6707/10-2S
Depth : 3202.45m
C2+ : 10.20%
C1
C2
C3
iC4
nC4
iC5
nC5

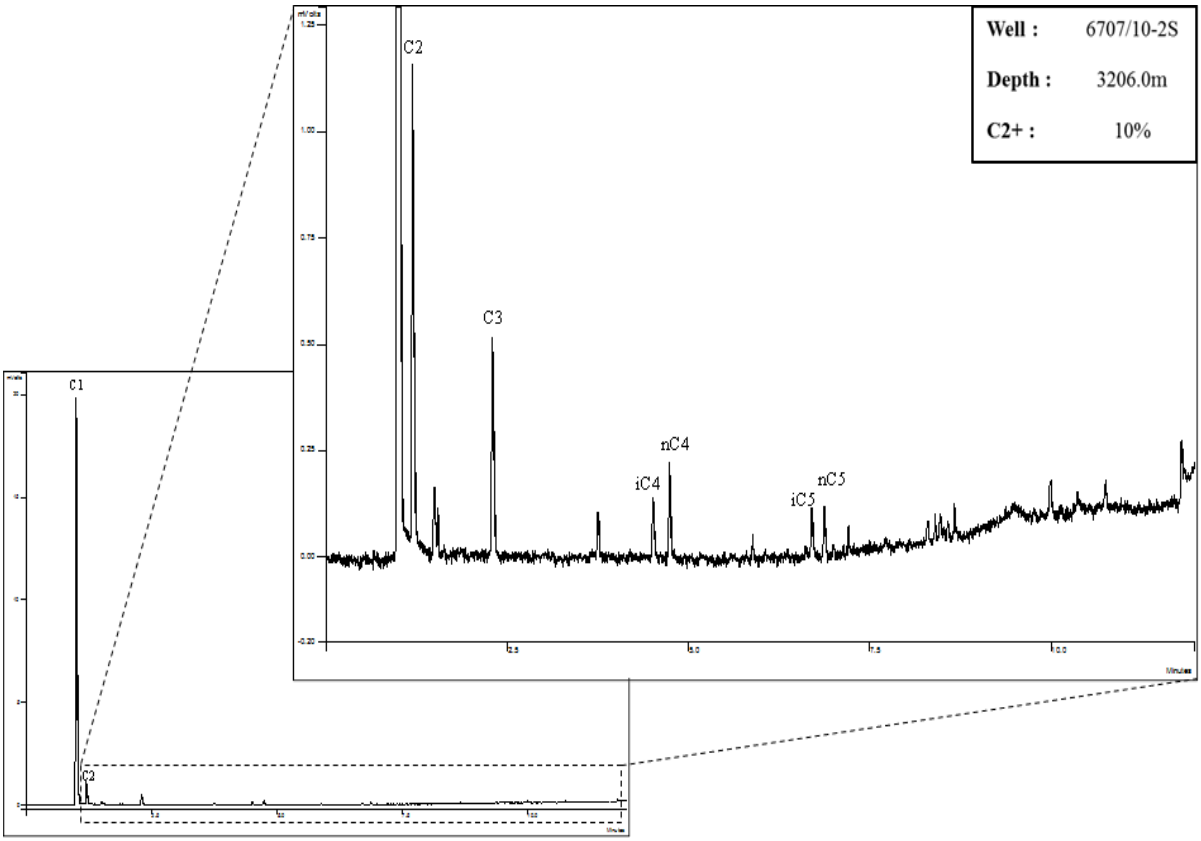
Well : 6707/10-2S
Depth : 3206.0m
C2+ : 10%
C1
C2
C3
iC4
nC4
iC5
nC5

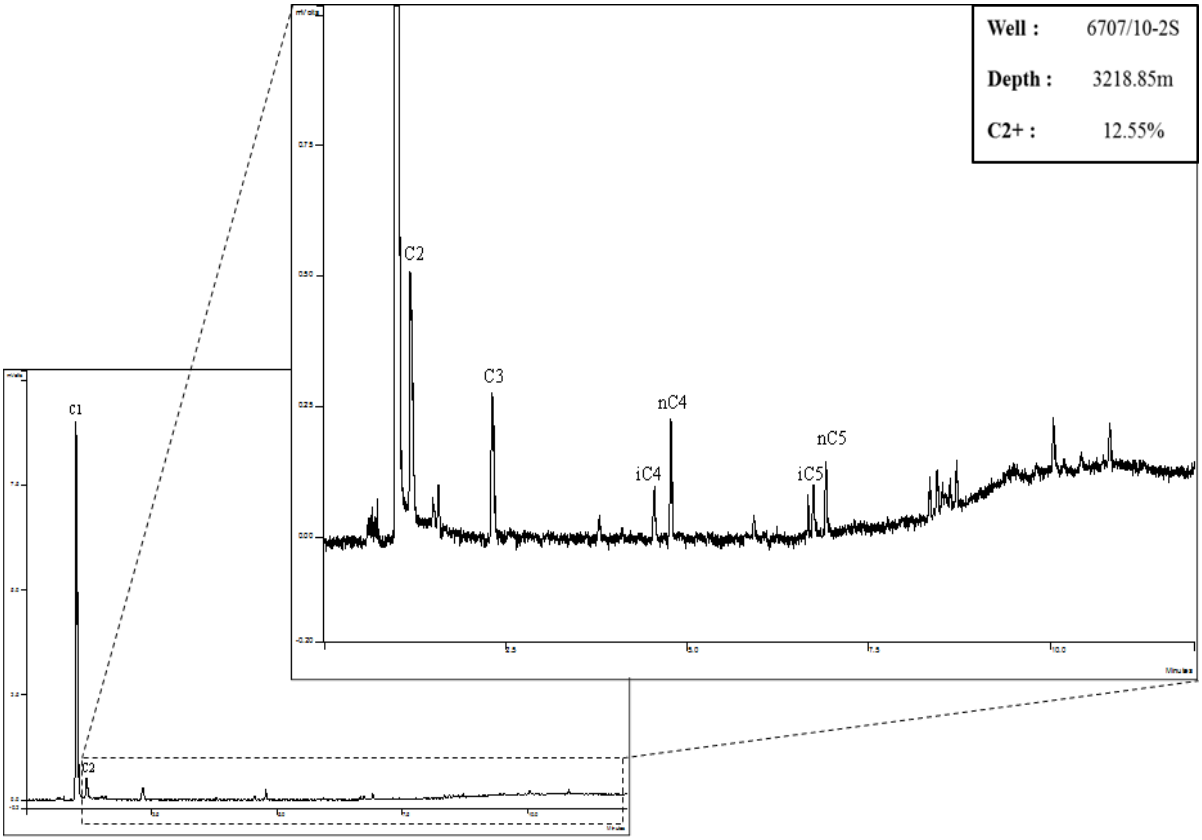
Well : 6707/10-2S
Depth : 3218.85m
C2+ : 12.55%
C1
C2
C3
iC4
nC4
iC5
nC5

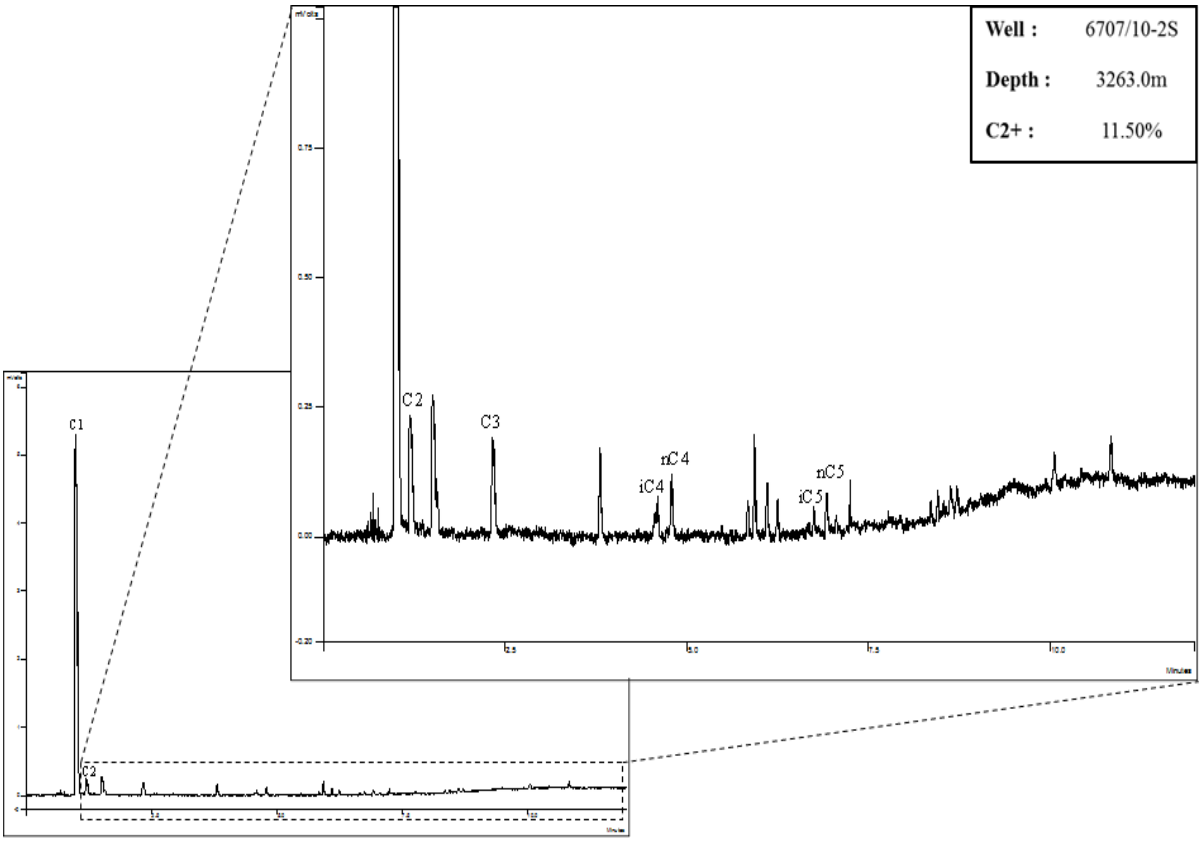
Well : 6707/10-2S
Depth : 3263.0m
C2+ : 11.50%
C1
C2
C3
iC4
nC4
iC5
nC5

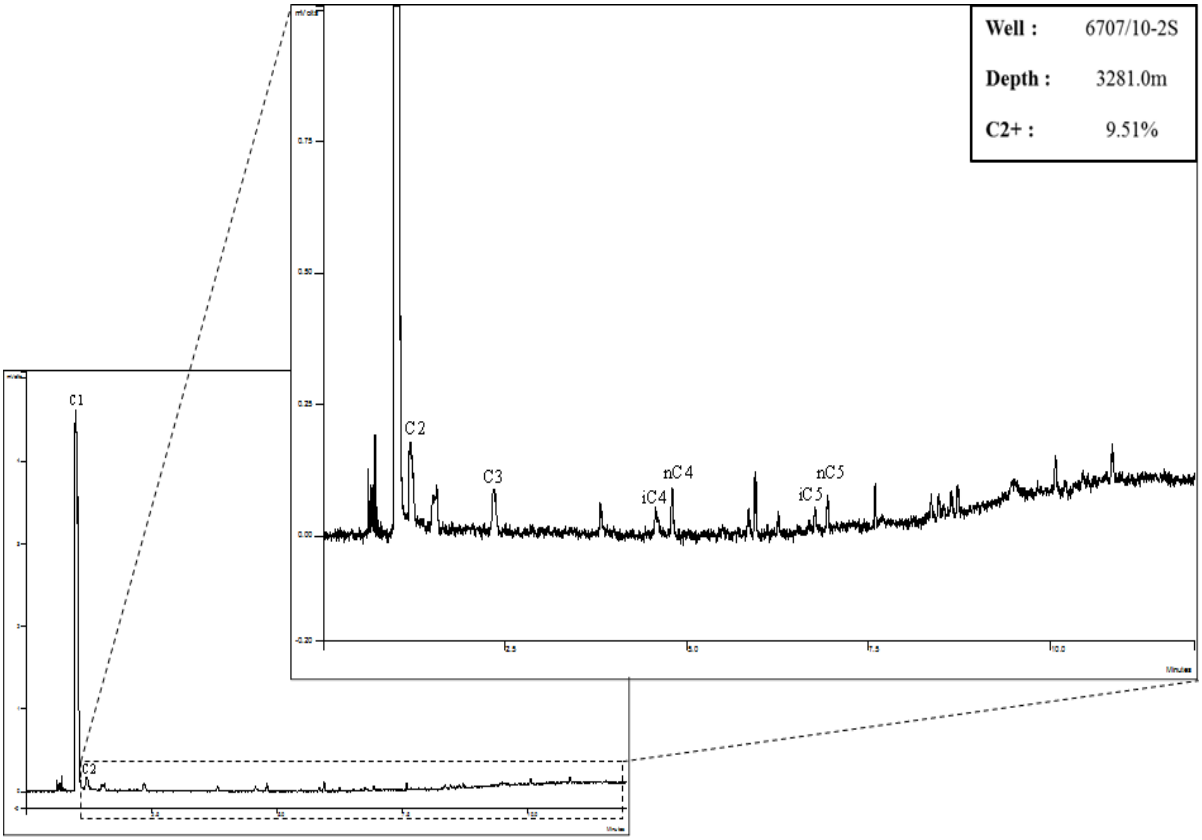
Well : 6707/10-2S
Depth : 3281.0m
C2+ : 9.51%
C1
C2
C3
iC4
nC4
iC5
nC5

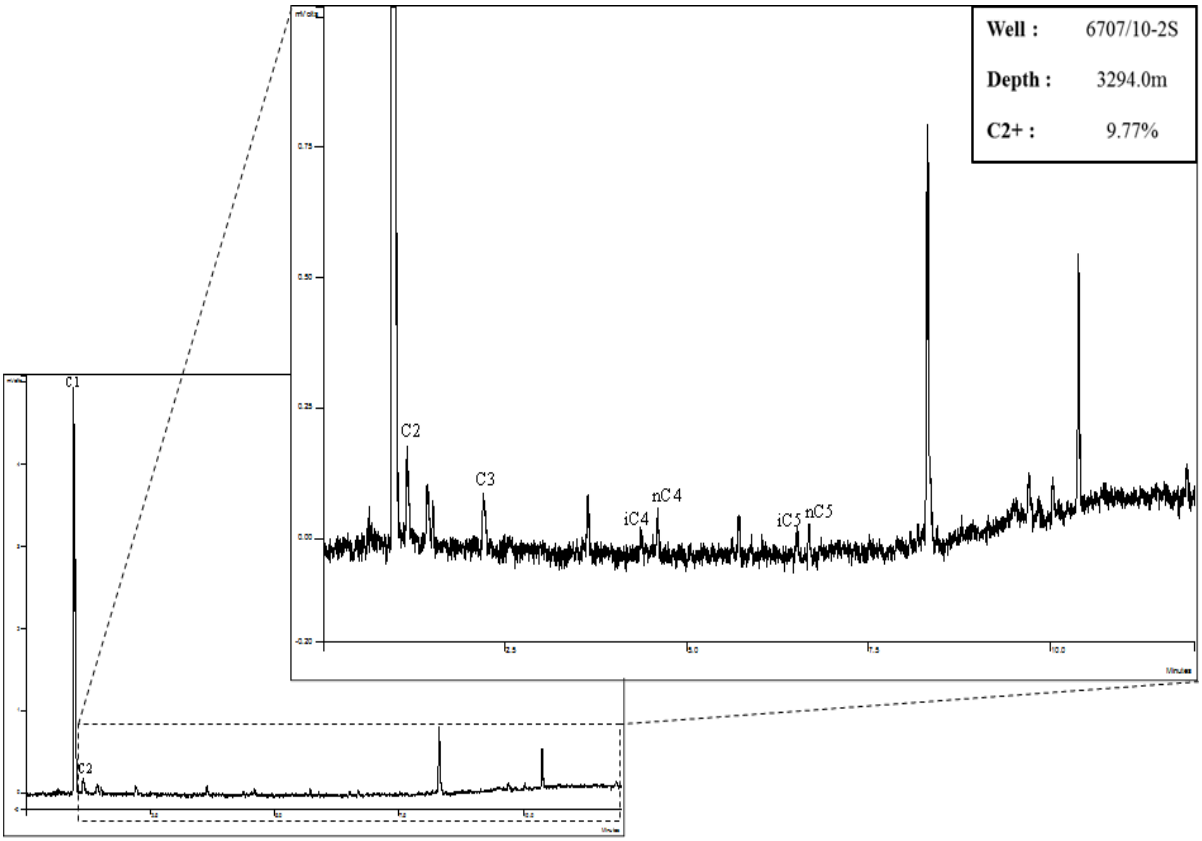
Well : 6707/10-2S
Depth : 3294.0m
C2+ : 9.77%
C1
C2
C3
iC4
nC4
iC5
nC5

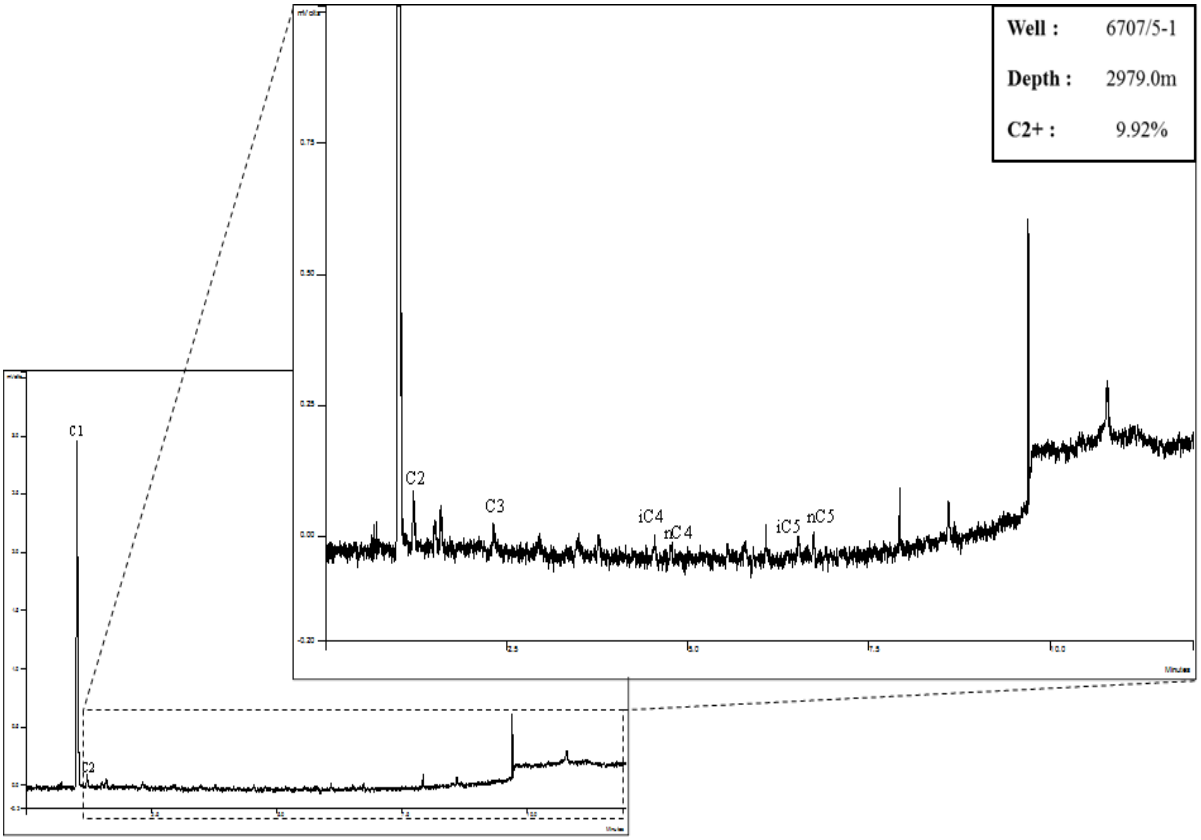
Well : 6707/5-1
Depth : 2979.0m
C2+ : 9.92%
C1
C2
C3
iC4
nC4
iC5
nC5
C2

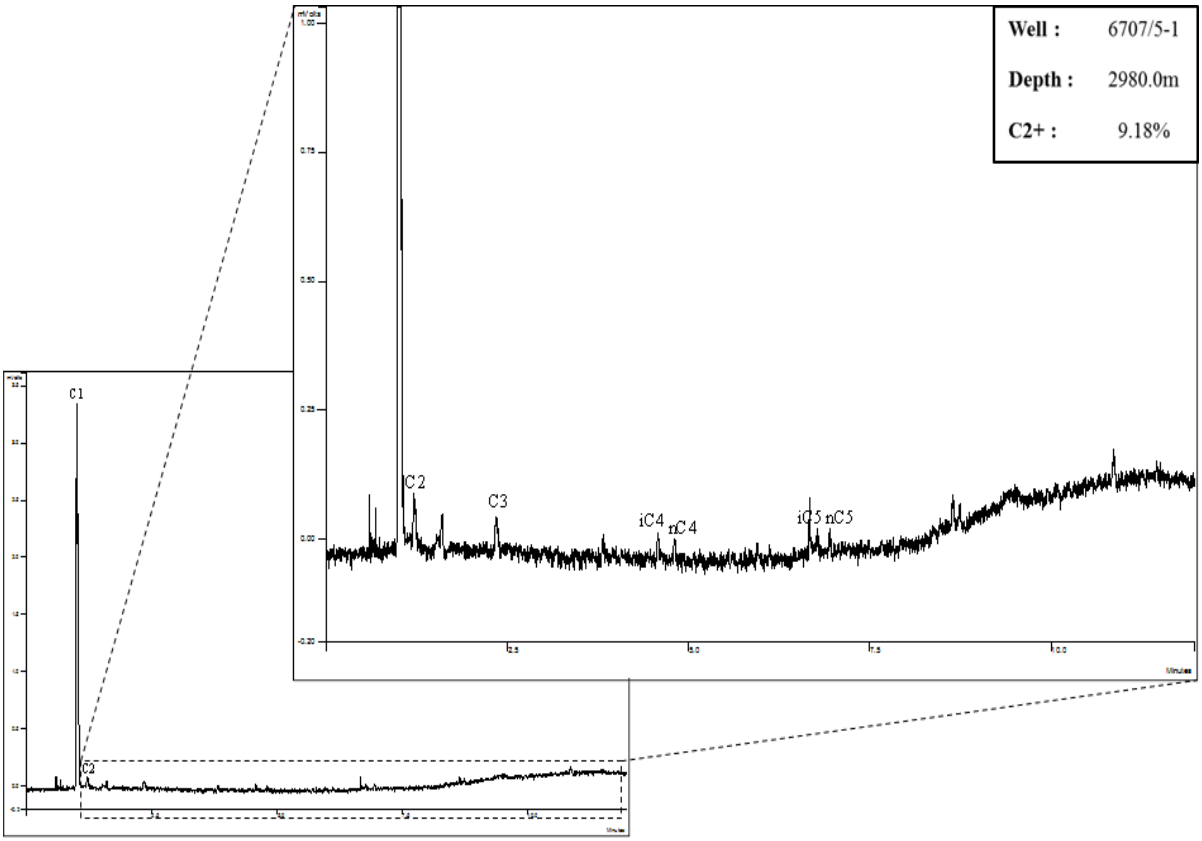
Well : 6707/5-1
Depth : 2980.0m
C2+ : 9.18%
C1
C2
C3
iC4
nC4
iC5
nC5
C2

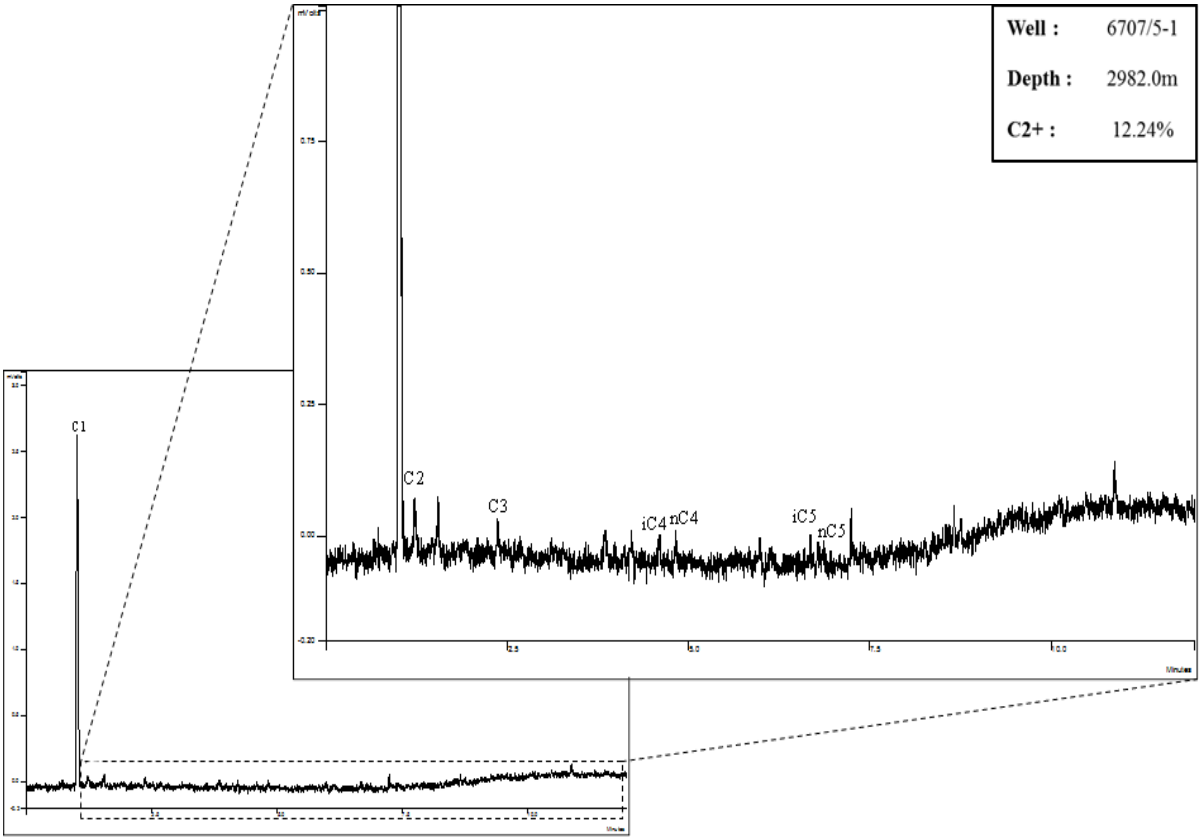
Well : 6707/5-1
Depth : 2982.0m
C2+ : 12.24%
C1
C2
C3
iC4
nC4
iC5
nC5

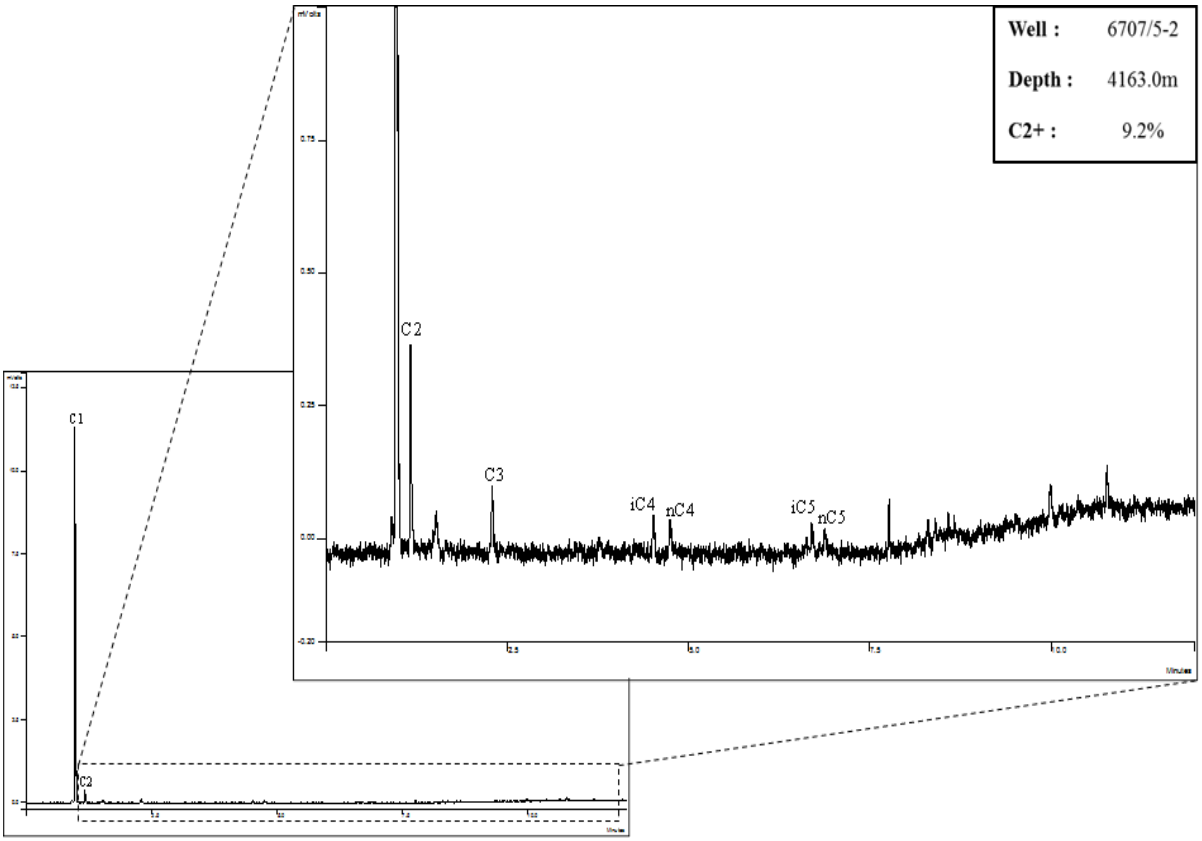
Well : 6707/5-2
Depth : 4163.0m
C2+ : 9.2%
C1
C2
C3
iC4
nC4
iC5
nC5

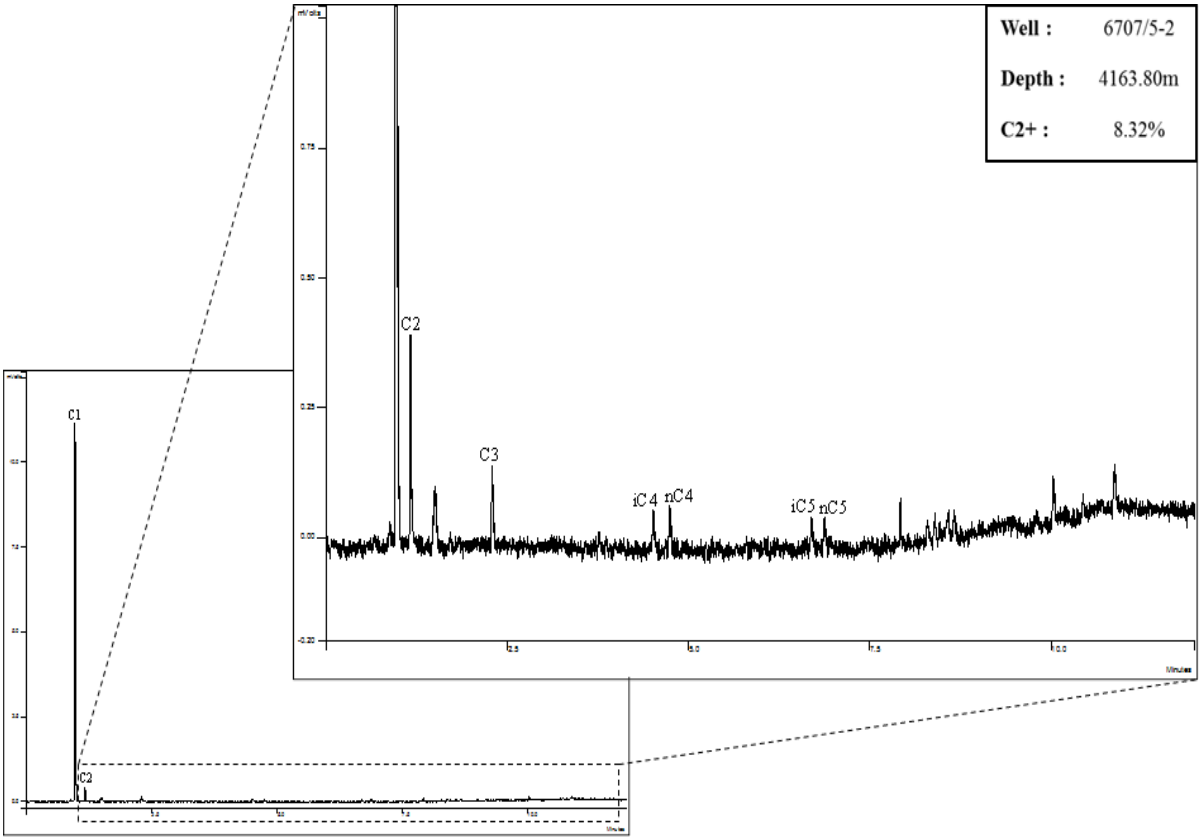
Well : 6707/5-2
Depth : 4163.80m
C2+ : 8.32%
C1
C2
C3
iC4
nC4
iC5
nC5

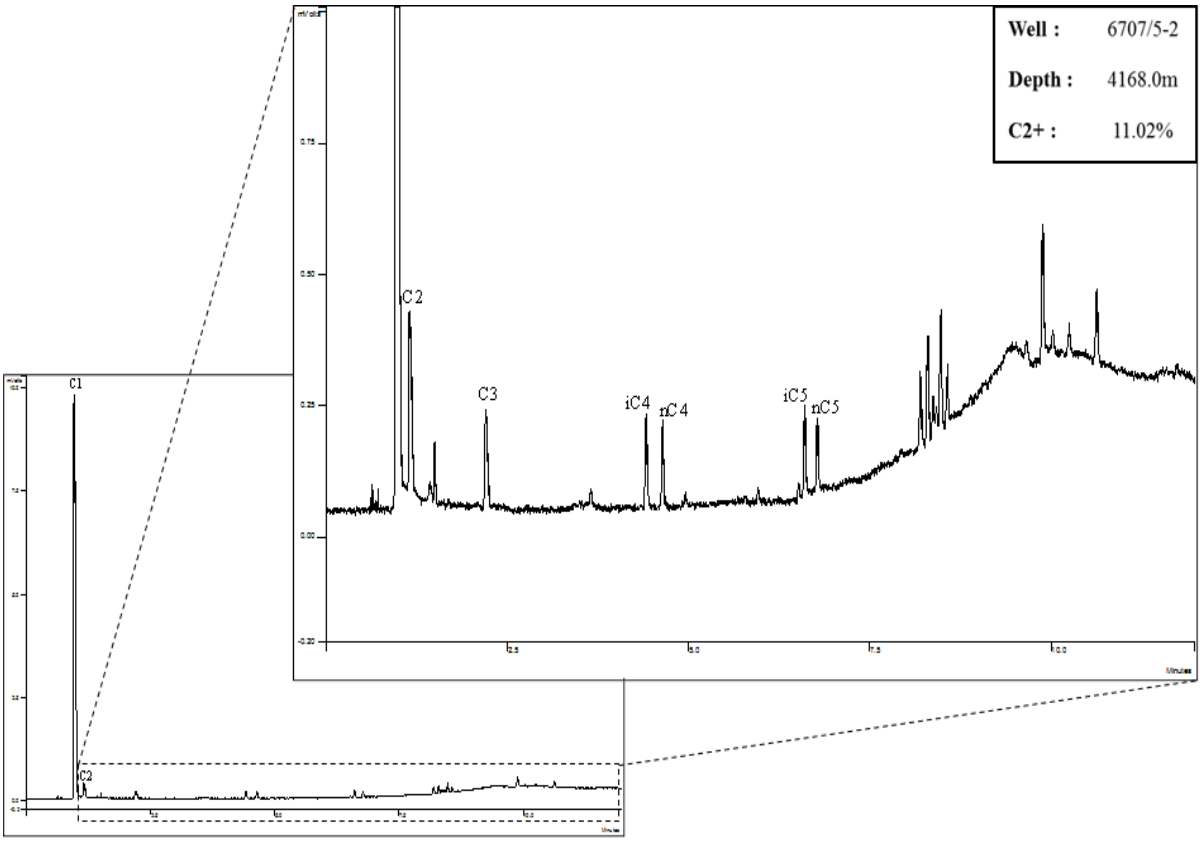
Well : 6707/5-2
Depth : 4168.0m
C2+ : 11.02%
C1
C2
C3
iC4
nC4
iC5
nC5

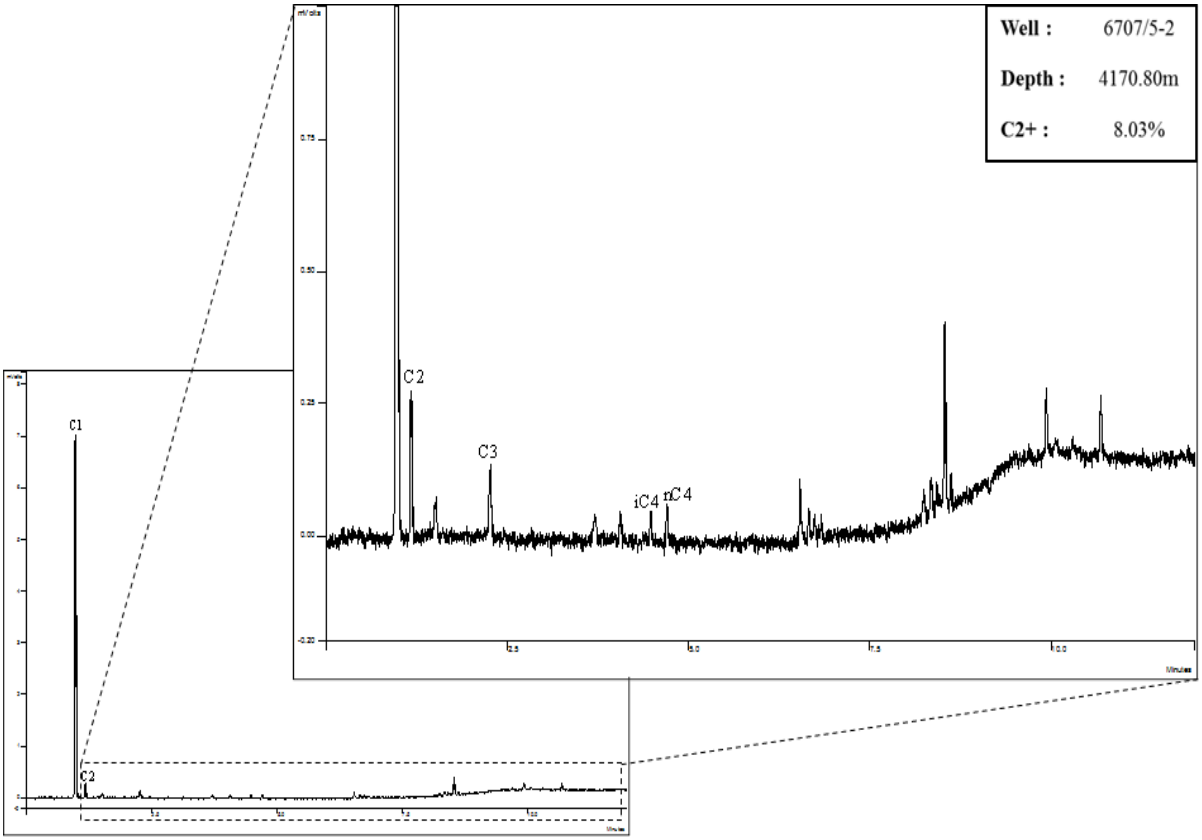
Well : 6707/5-2
Depth : 4170.80m
C2+ : 8.03%
C1
C2
C3
iC4
nC4
C2

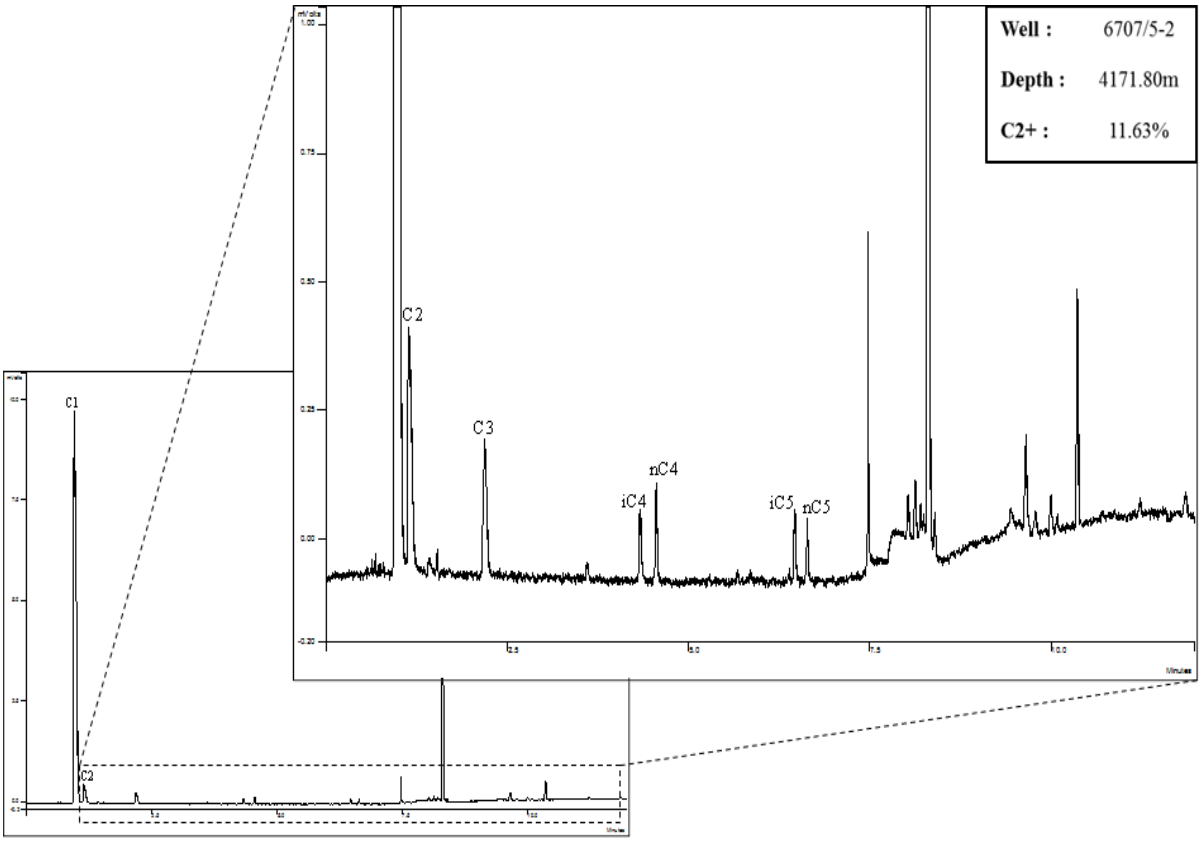
Well : 6707/5-2
Depth : 4171.80m
C2+ : 11.63%
C1
C2
C3
iC4
nC4
iC5
nC5
C2

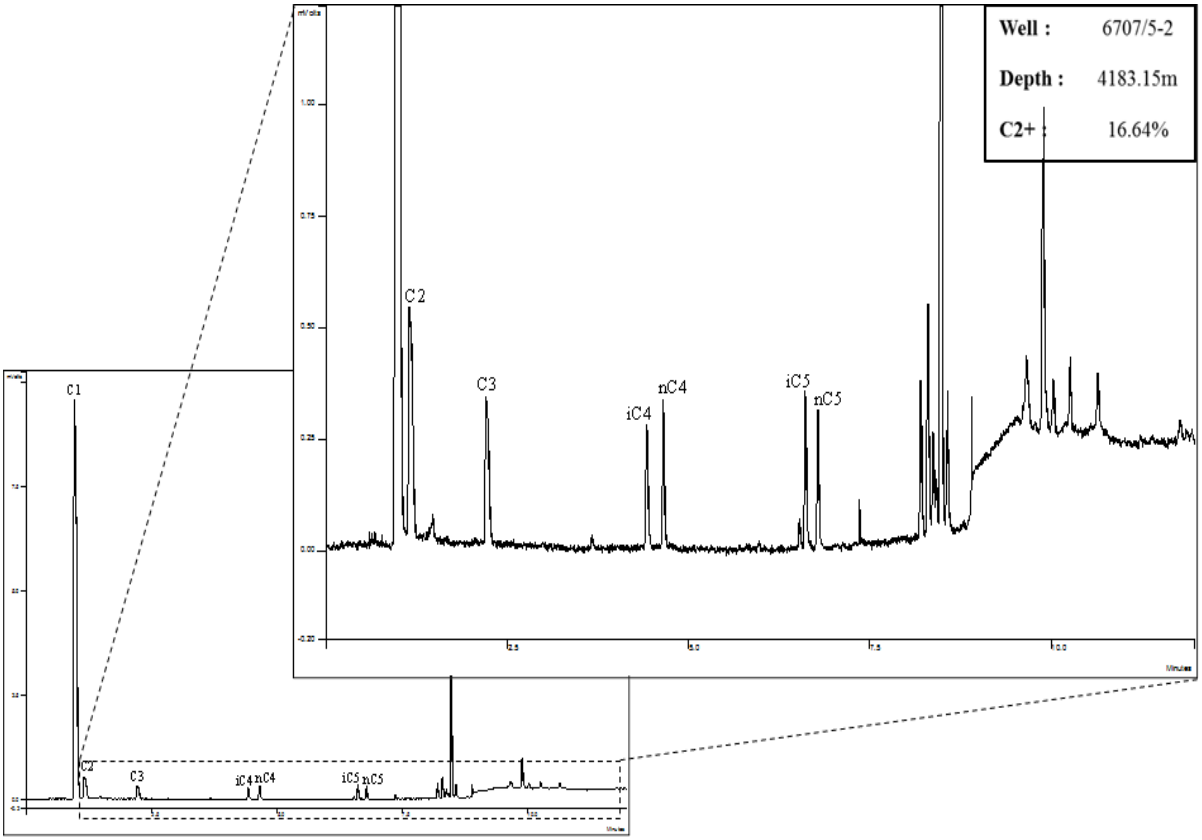
Well : 6707/5-2
Depth : 4183.15m
C2+ : 16.64%
C1
C2
C3
iC4
nC4
iC5
nC5

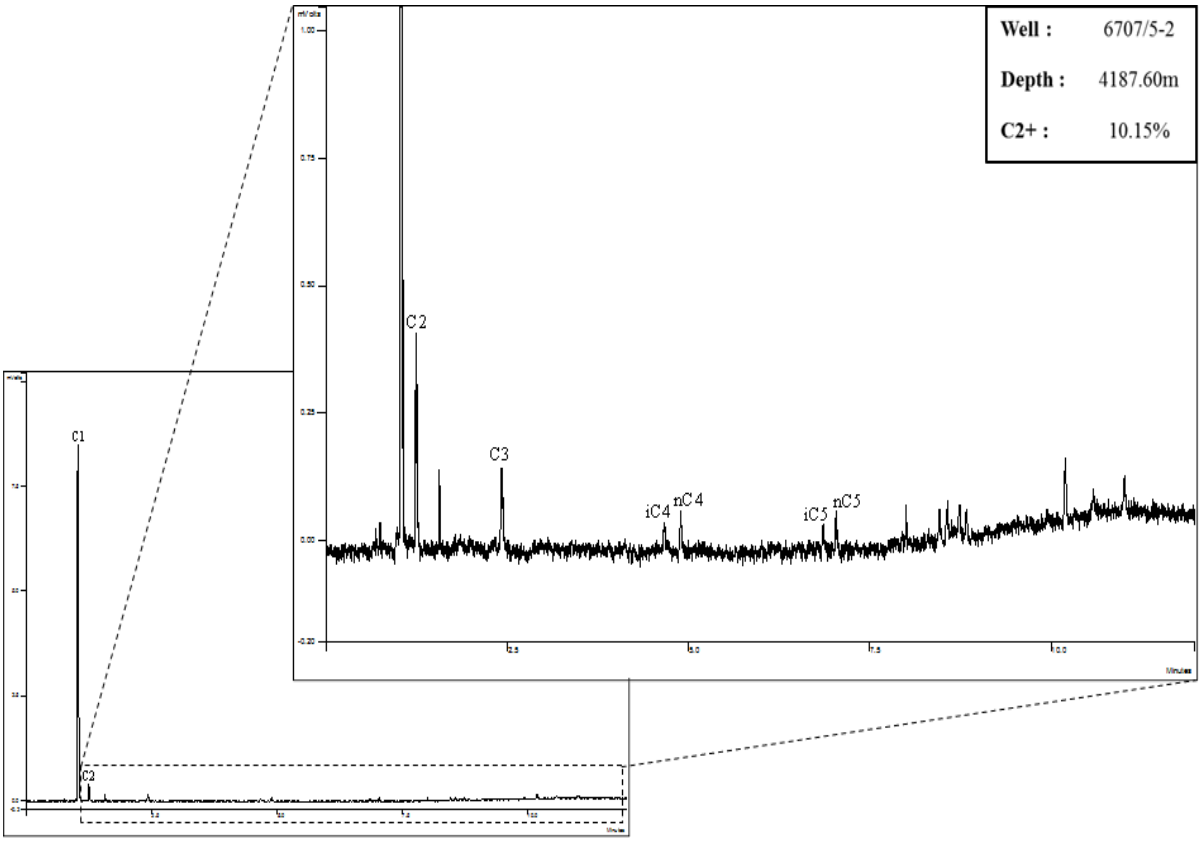
Well : 6707/5-2
Depth : 4187.60m
C2+ : 10.15%
C1
C2
C3
iC4
nC4
iC5
nC5

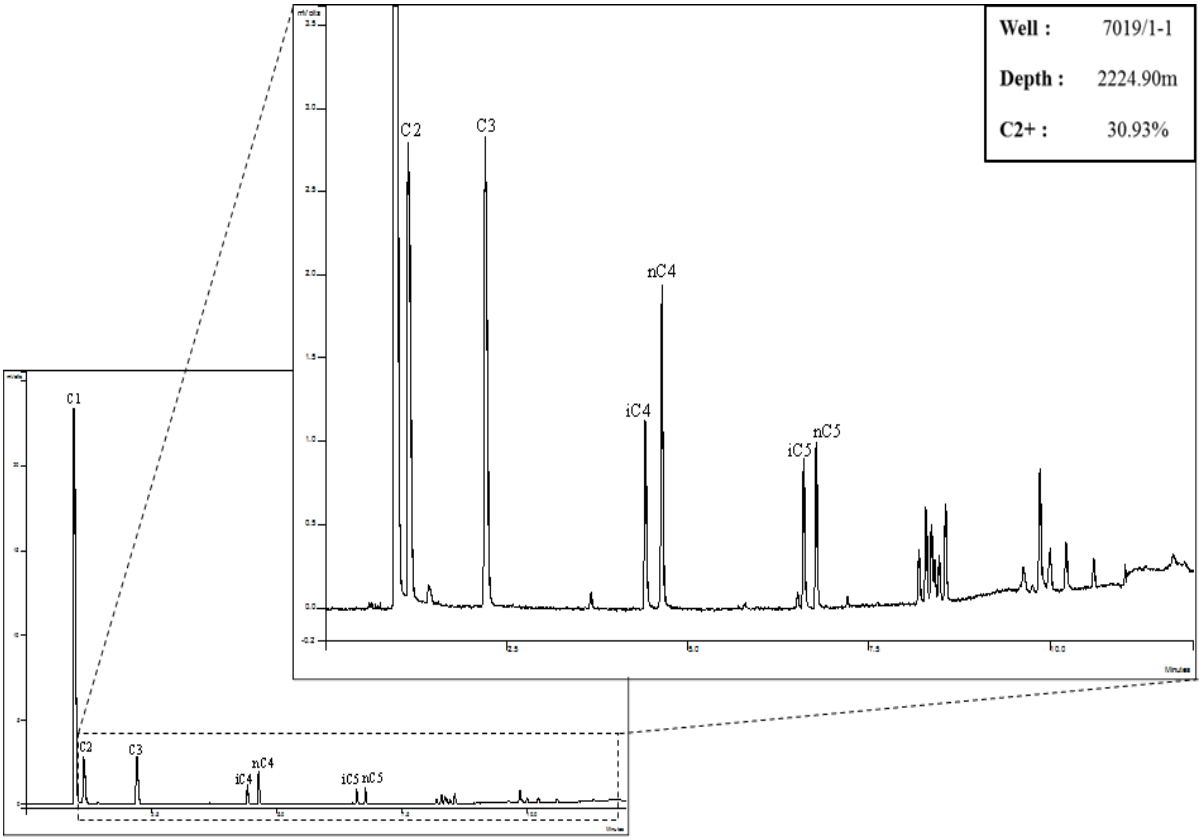
Well : 7019/1-1
Depth : 2224.90m
C2+ : 30.93%
C1
C2
C3
iC4
nC4
iC5
nC5

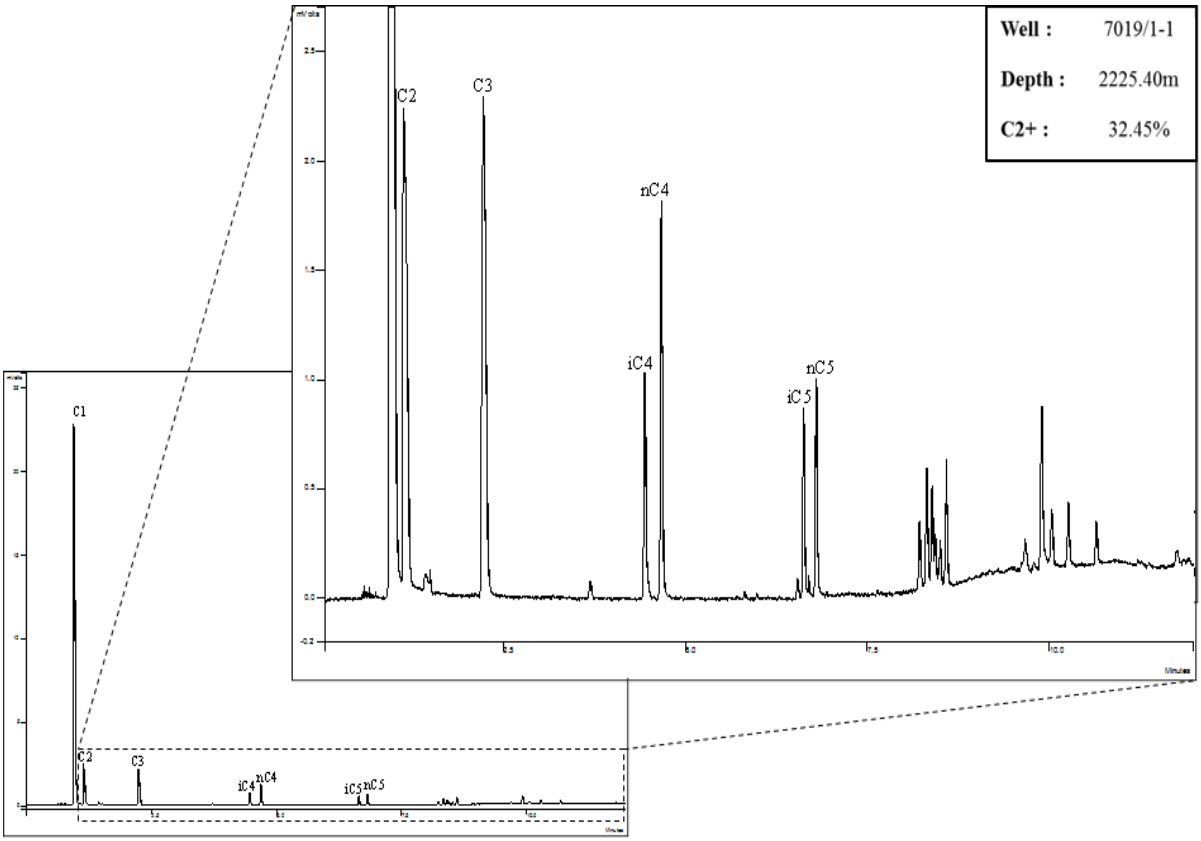
Well : 7019/1-1
Depth : 2225.40m
C2+ : 32.45%
C1
C2
C3
iC4
nC4
iC5
nC5

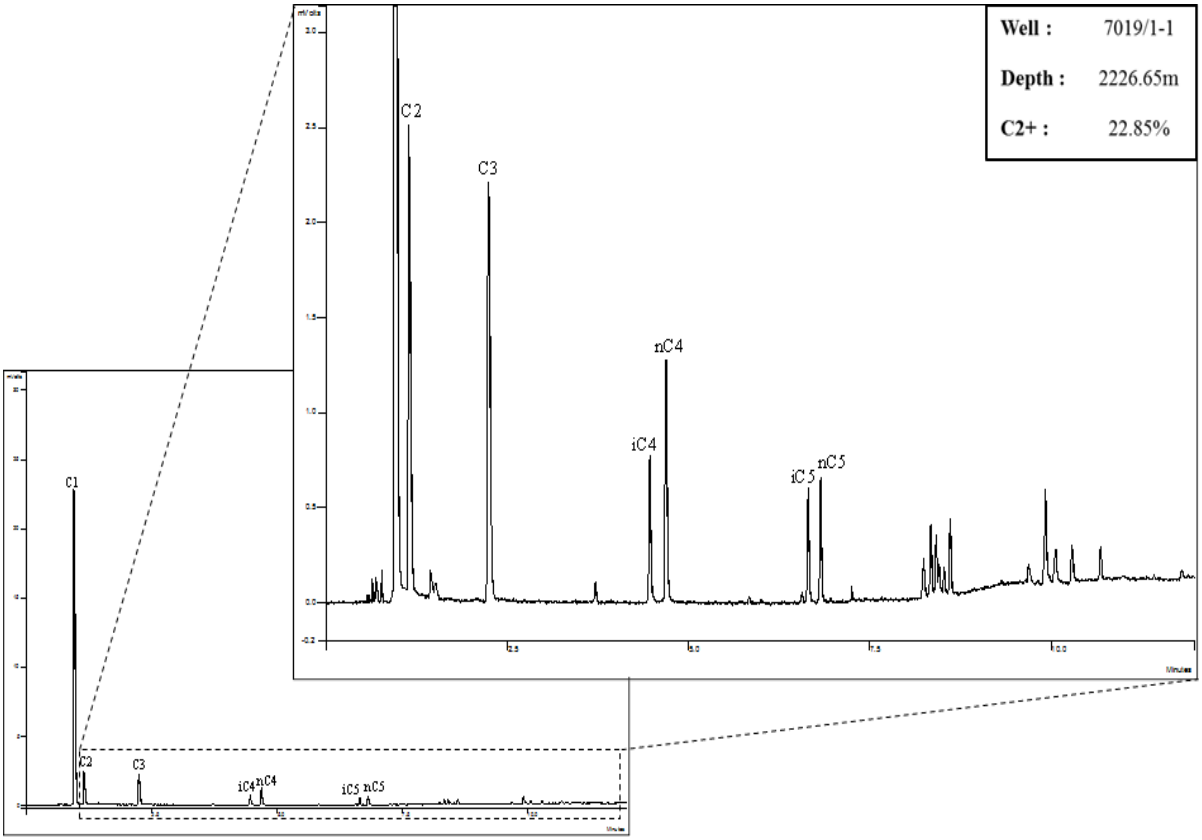
Well : 7019/1-1
Depth : 2226.65m
C2+ : 22.85%
C1
C2
C3
iC4
nC4
iC5
nC5

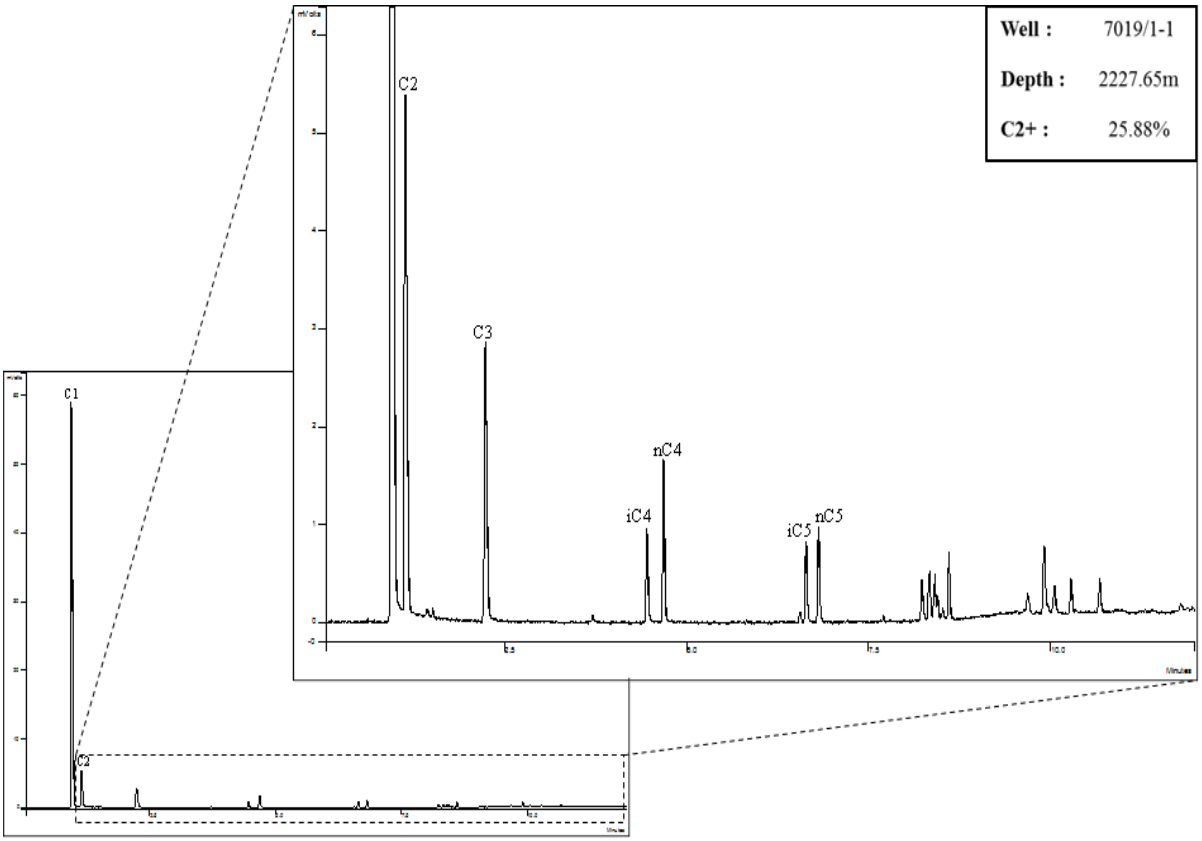
Well : 7019/1-1
Depth : 2227.65m
C2+ : 25.88%
C1
C2
C3
iC4
nC4
iC5
nC5

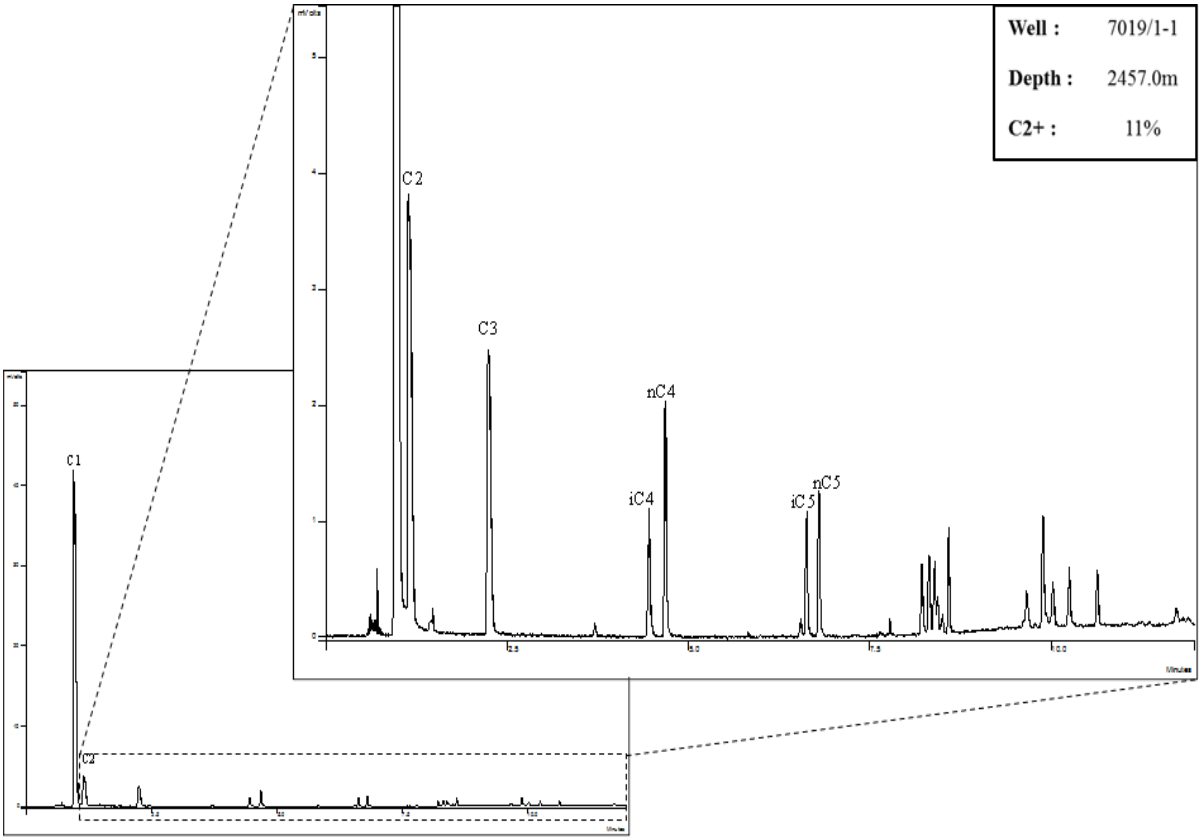
Well : 7019/1-1
Depth : 2457.0m
C2+ : 11%
C1
C2
C3
iC4
nC4
iC5
nC5

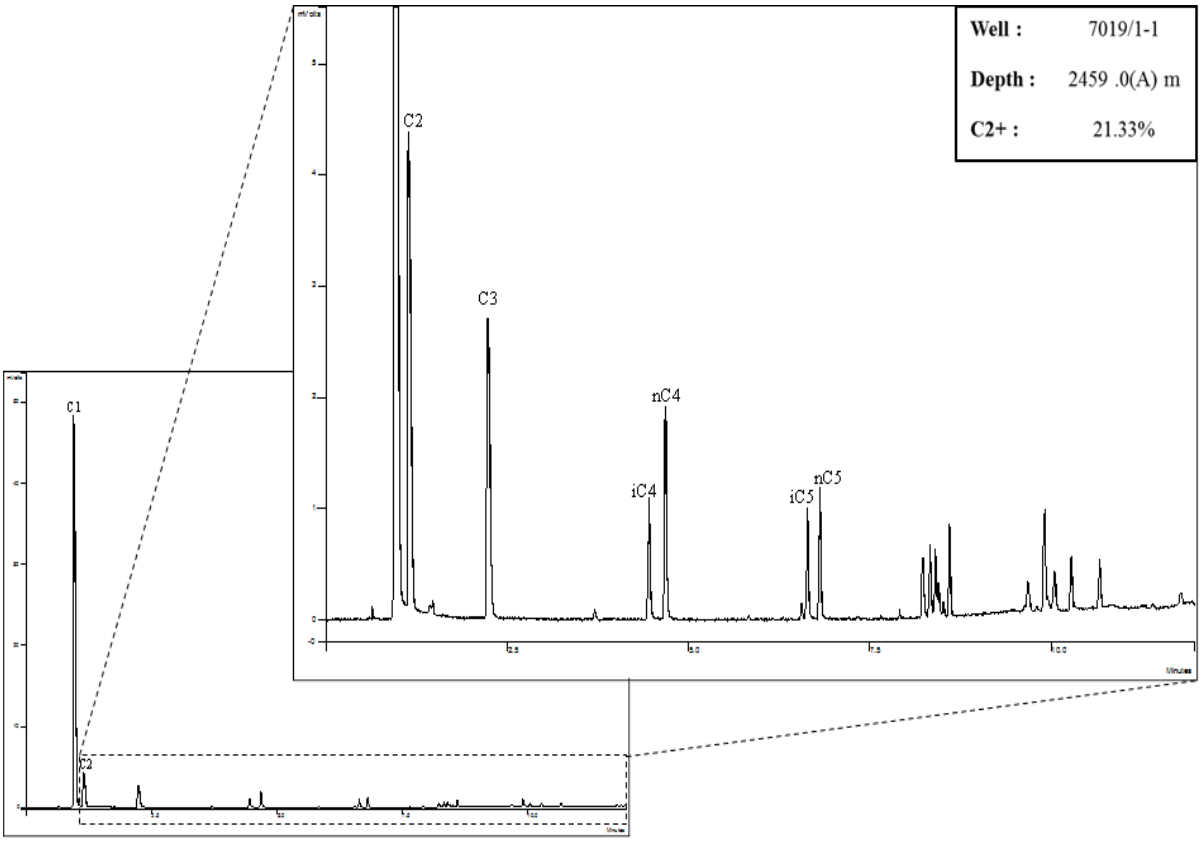
Well : 7019/1-1
Depth : 2459 .0(A) m
C2+ : 21.33%
C1
C2
C3
iC4
nC4
iC5
nC5

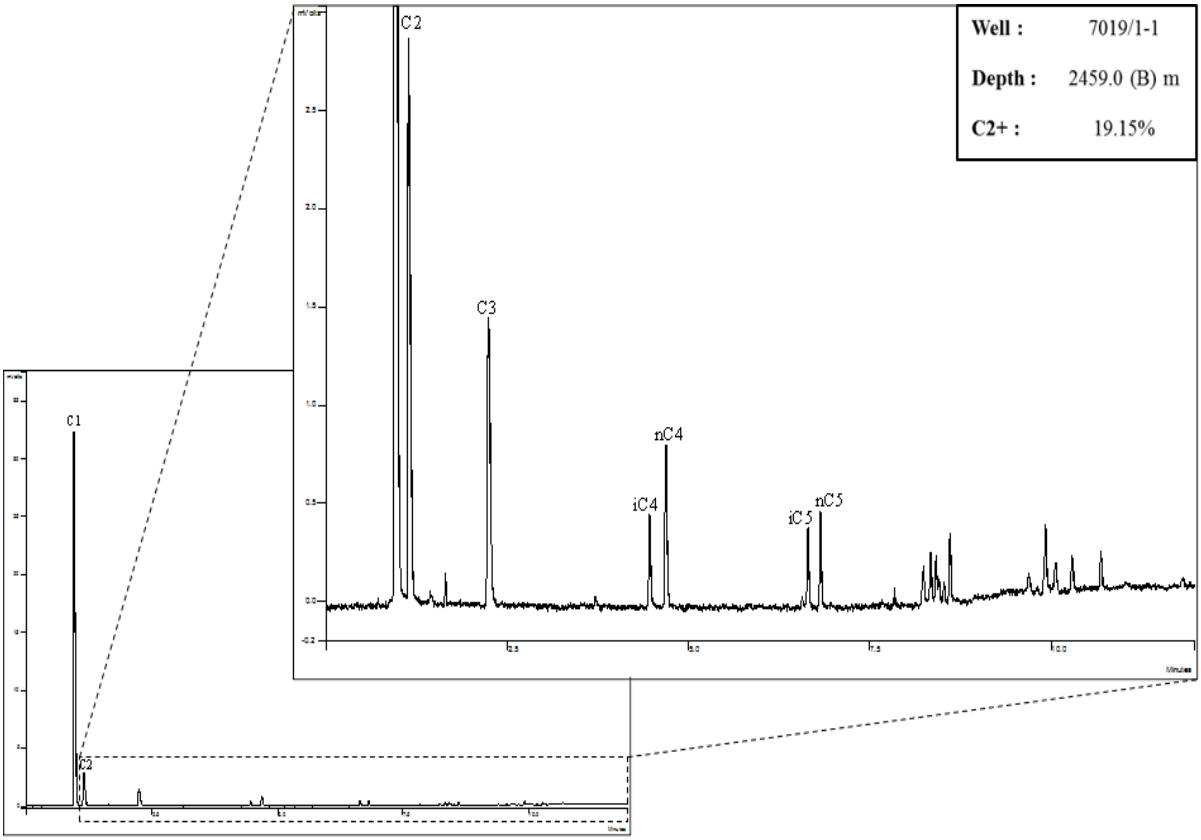
Well : 7019/1-1
Depth : 2459.0 (B) m
C2+ : 19.15%
C1
C2
C3
iC4
nC4
iC5
nC5

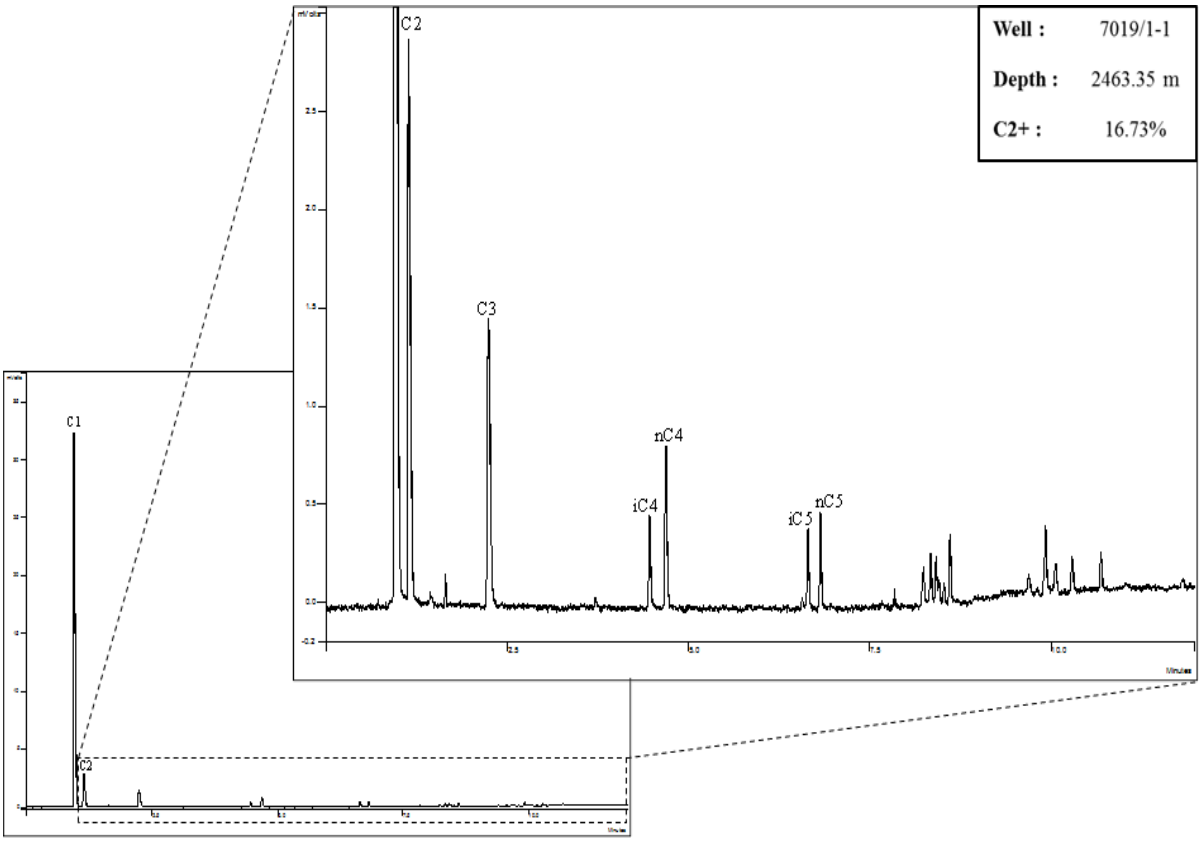
Well : 7019/1-1
Depth : 2463.35 m
C2+ : 16.73%
C1
C2
C3
iC4
nC4
iC5
nC5

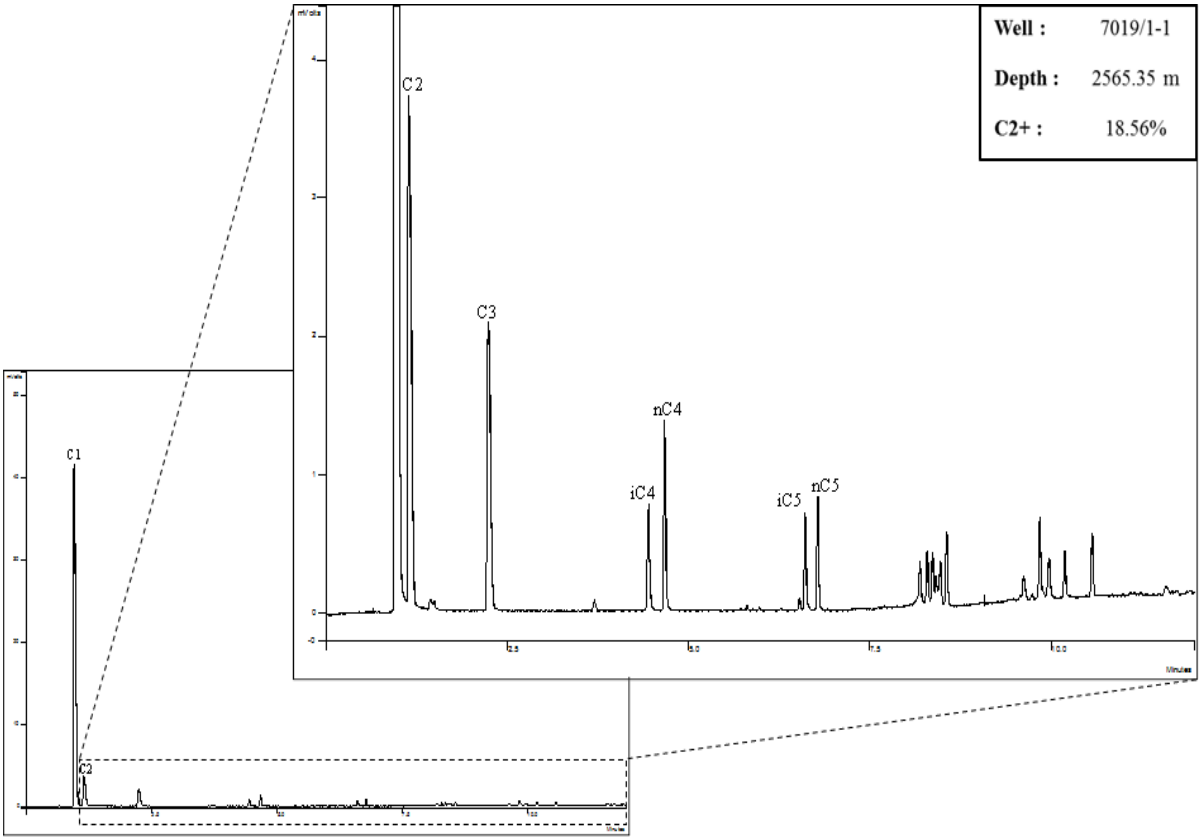
Well : 7019/1-1
Depth : 2565.35 m
C2+ : 18.56%
C1
C2
C3
iC4
nC4
iC5
nC5

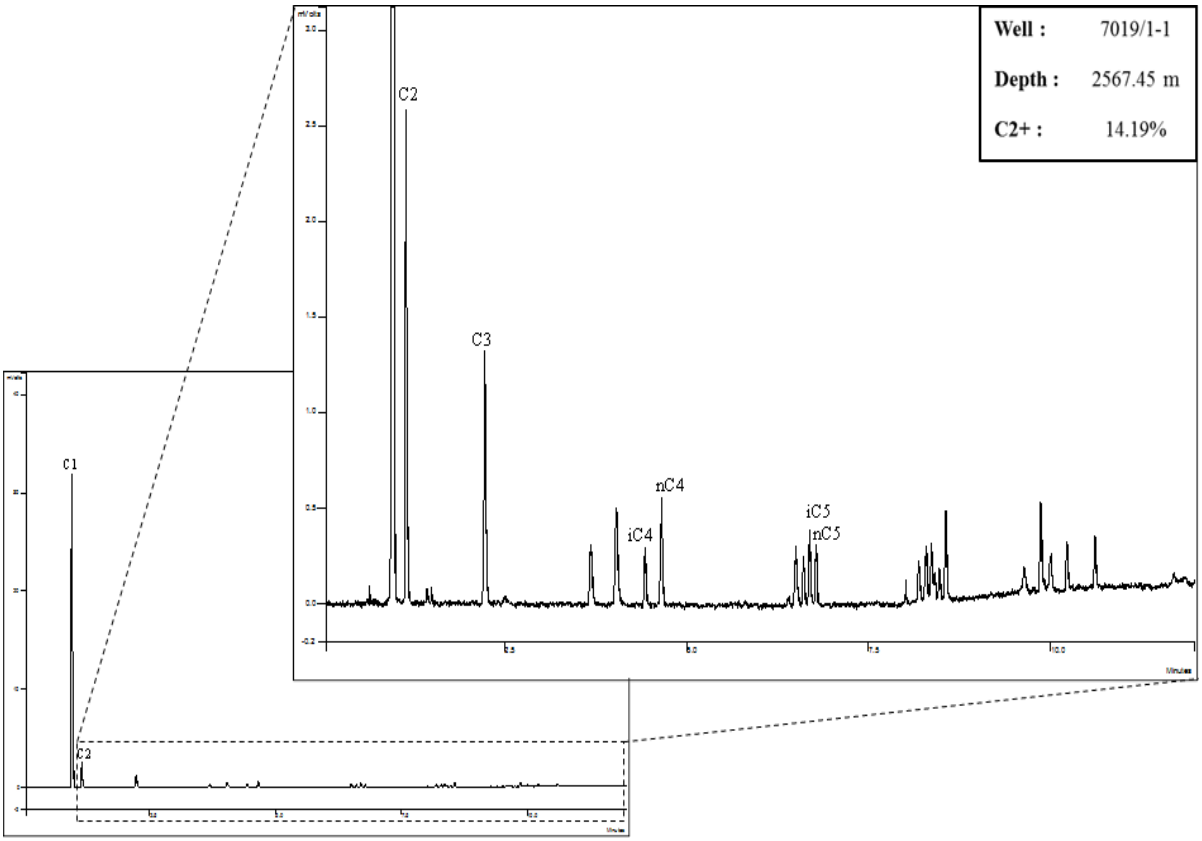
Well : 7019/1-1
Depth : 2567.45 m
C2+ : 14.19%
C1
C2
C3
iC4
nC4
iC5
nC5

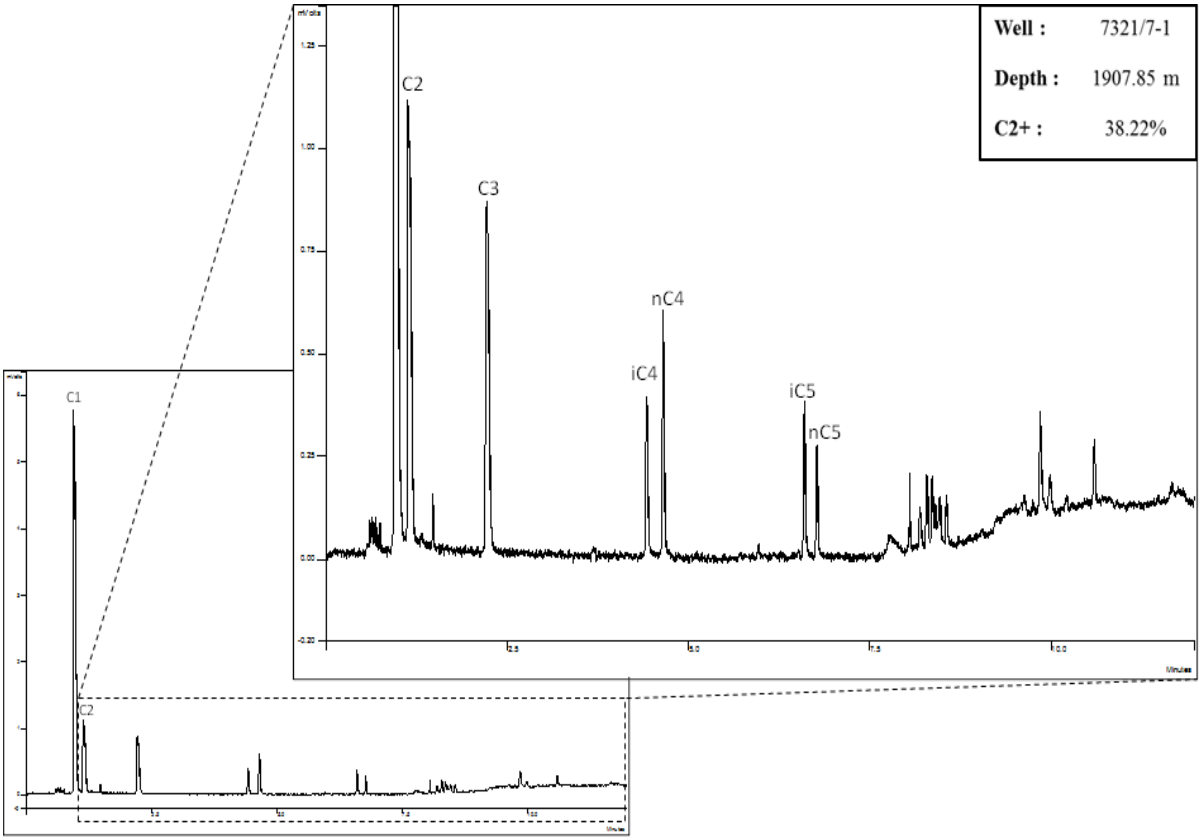
Well : 7321/7-1
Depth : 1907.85 m
C2+ : 38.22%
C1
C2
C3
iC4
nC4
iC5
nC5

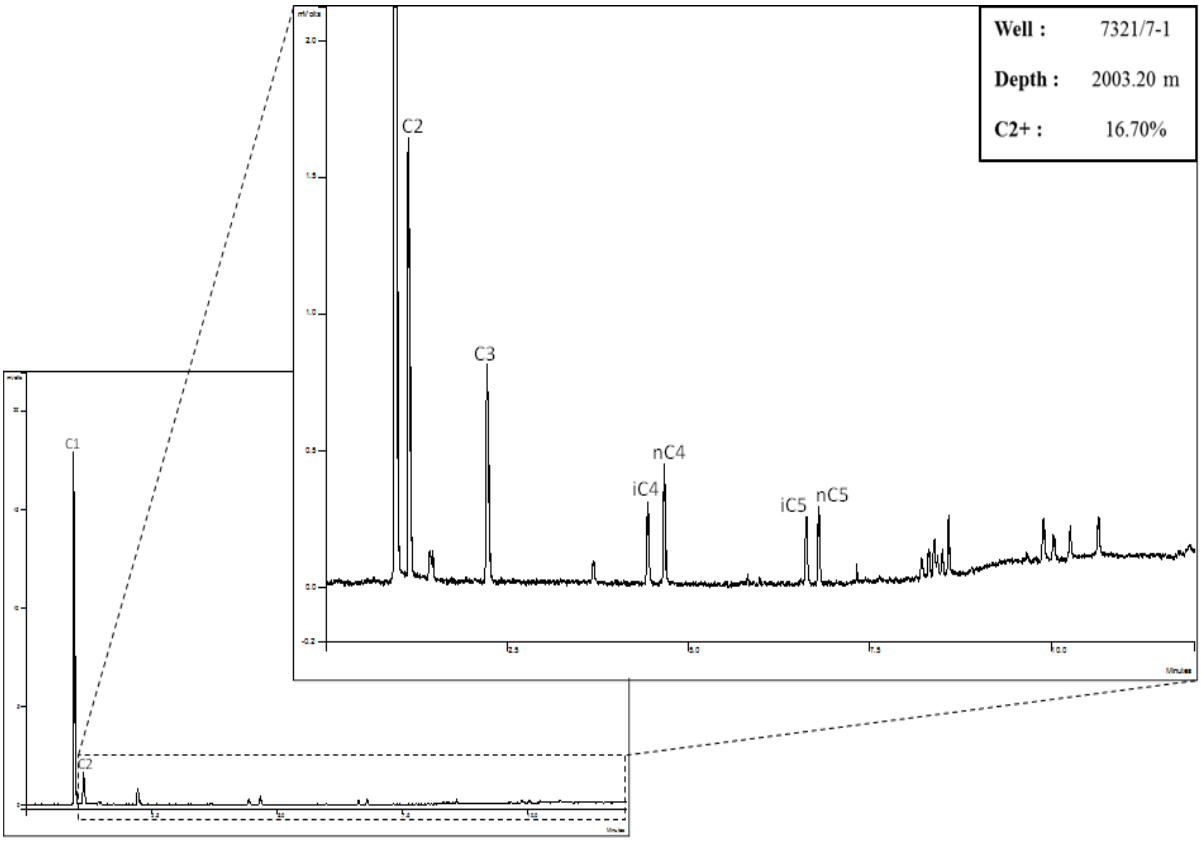
Well : 7321/7-1
Depth : 2003.20 m
C2+ : 16.70%
C1
C2
C3
iC4
nC4
iC5
nC5

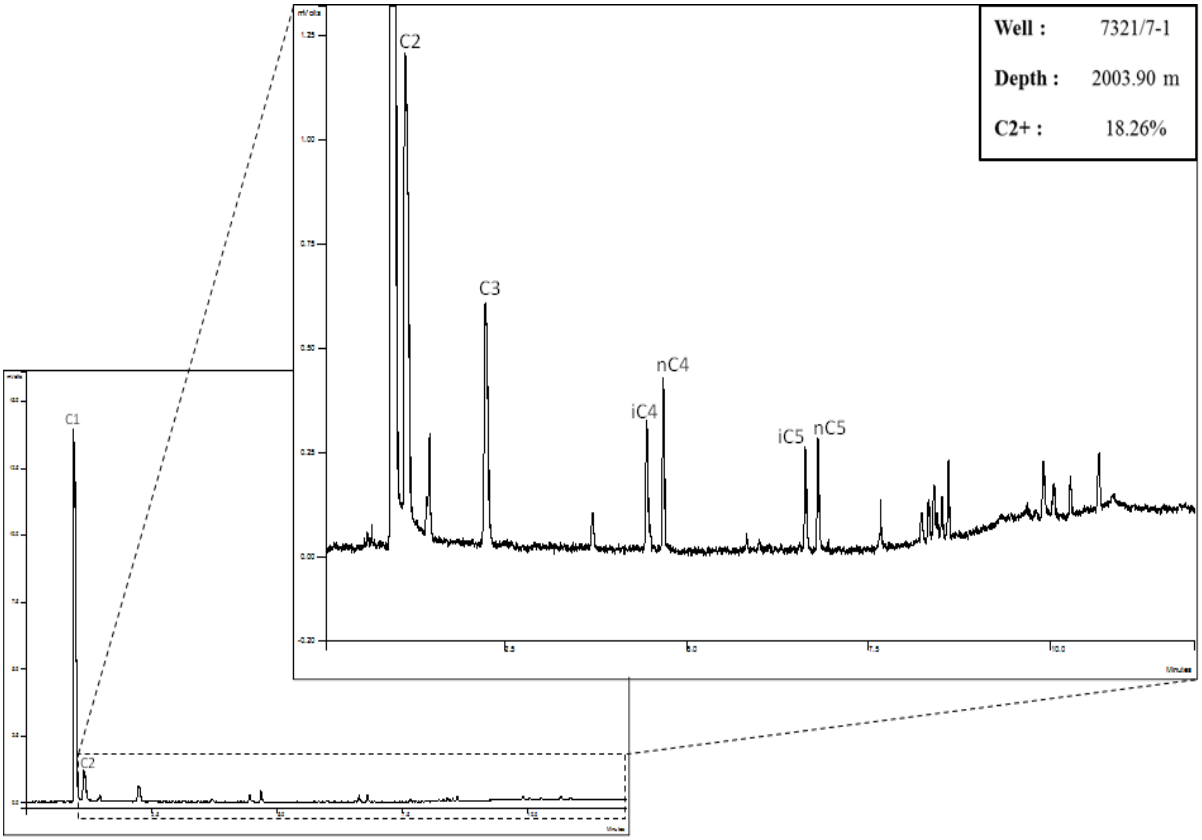
Well : 7321/7-1
Depth : 2003.90 m
C2+ : 18.26%
C1
C2
C3
iC4
nC4
iC5
nC5

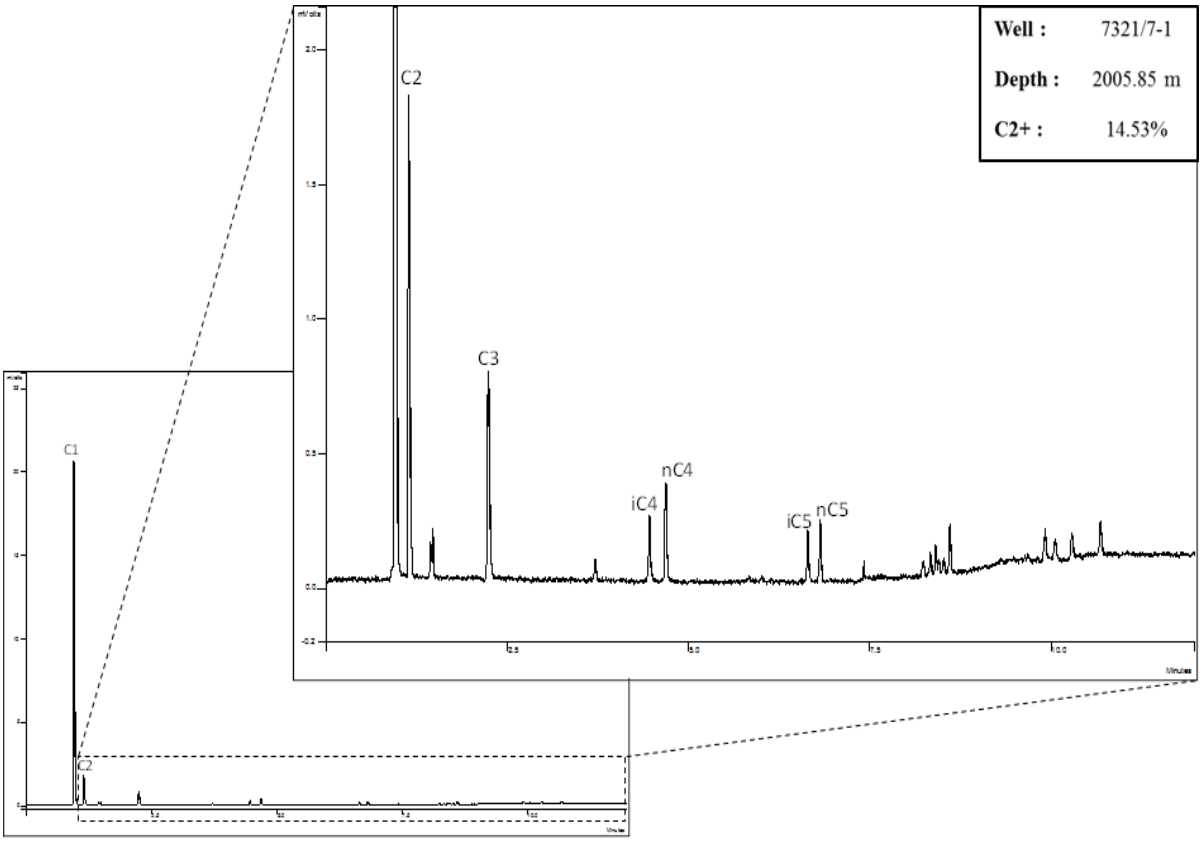
Well : 7321/7-1
Depth : 2005.85 m
C2+ : 14.53%
C1
C2
C3
iC4
nC4
iC5
nC5

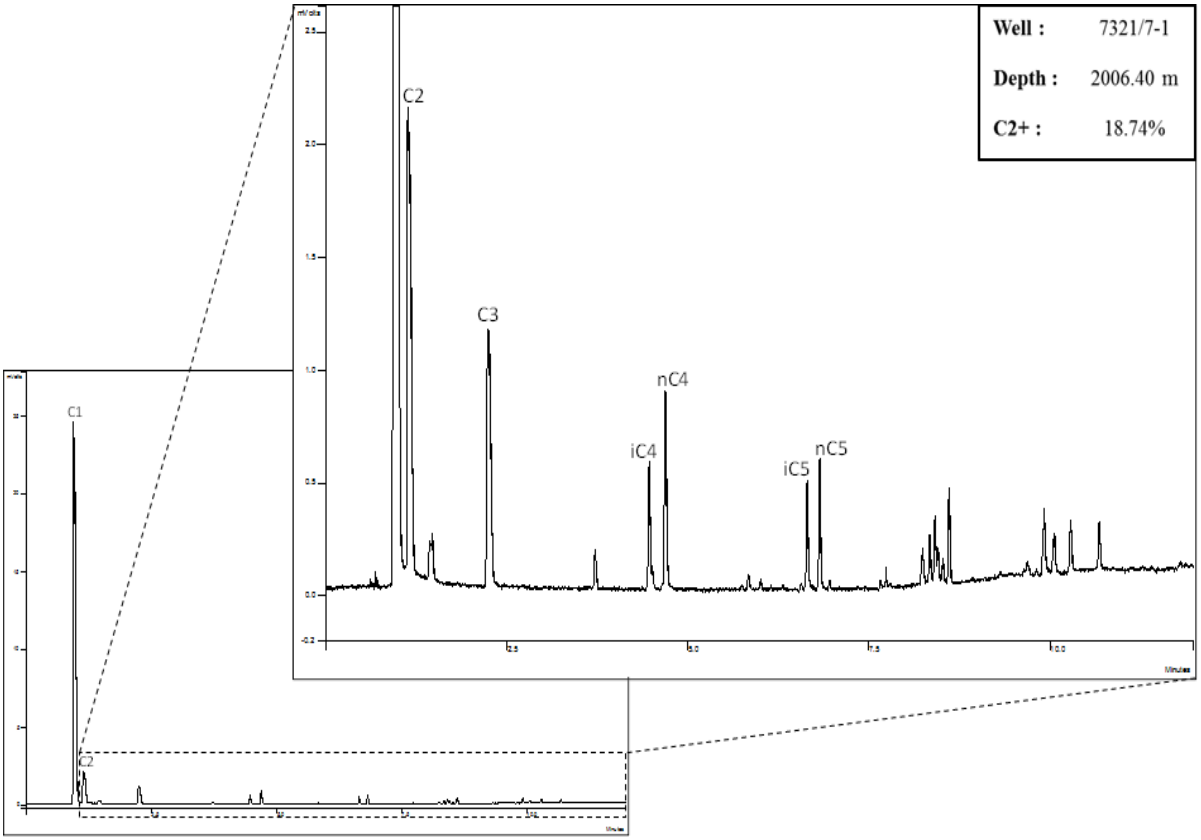
Well : 7321/7-1
Depth : 2006.40 m
C2+ : 18.74%
C1
C2
C3
iC4
nC4
iC5
nC5

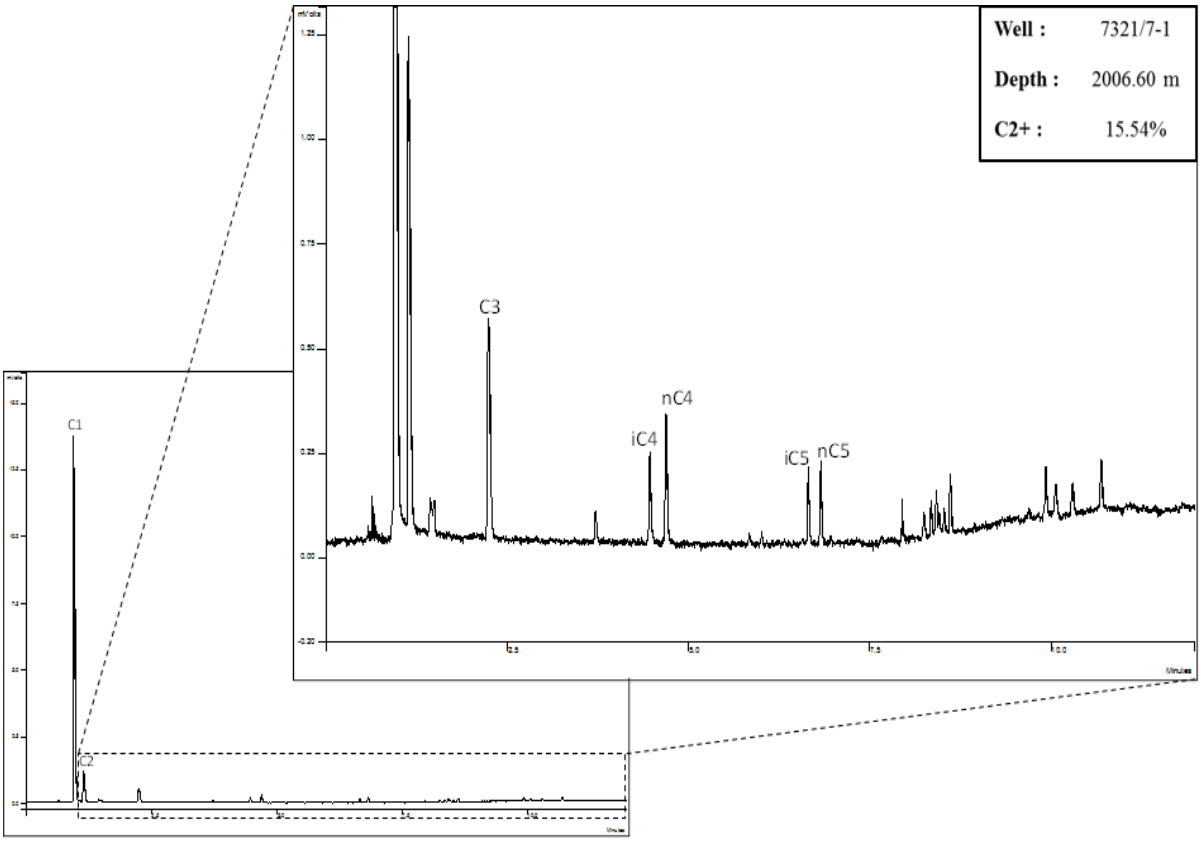
Well : 7321/7-1
Depth : 2006.60 m
C2+ : 15.54%
C1
C2
C3
iC4
nC4
iC5
nC5

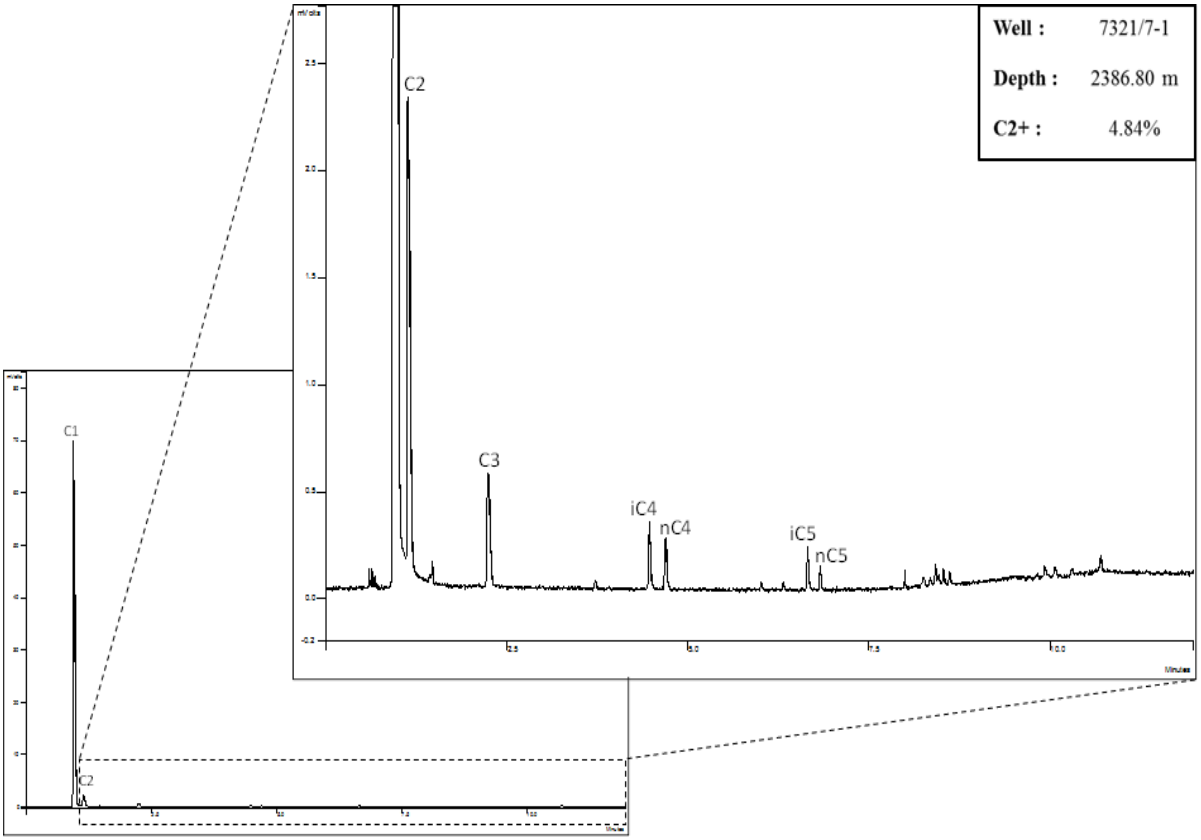
Well : 7321/7-1
Depth : 2386.80 m
C2+ : 4.84%
C1
C2
C3
iC4
nC4
iC5
nC5
Minutes

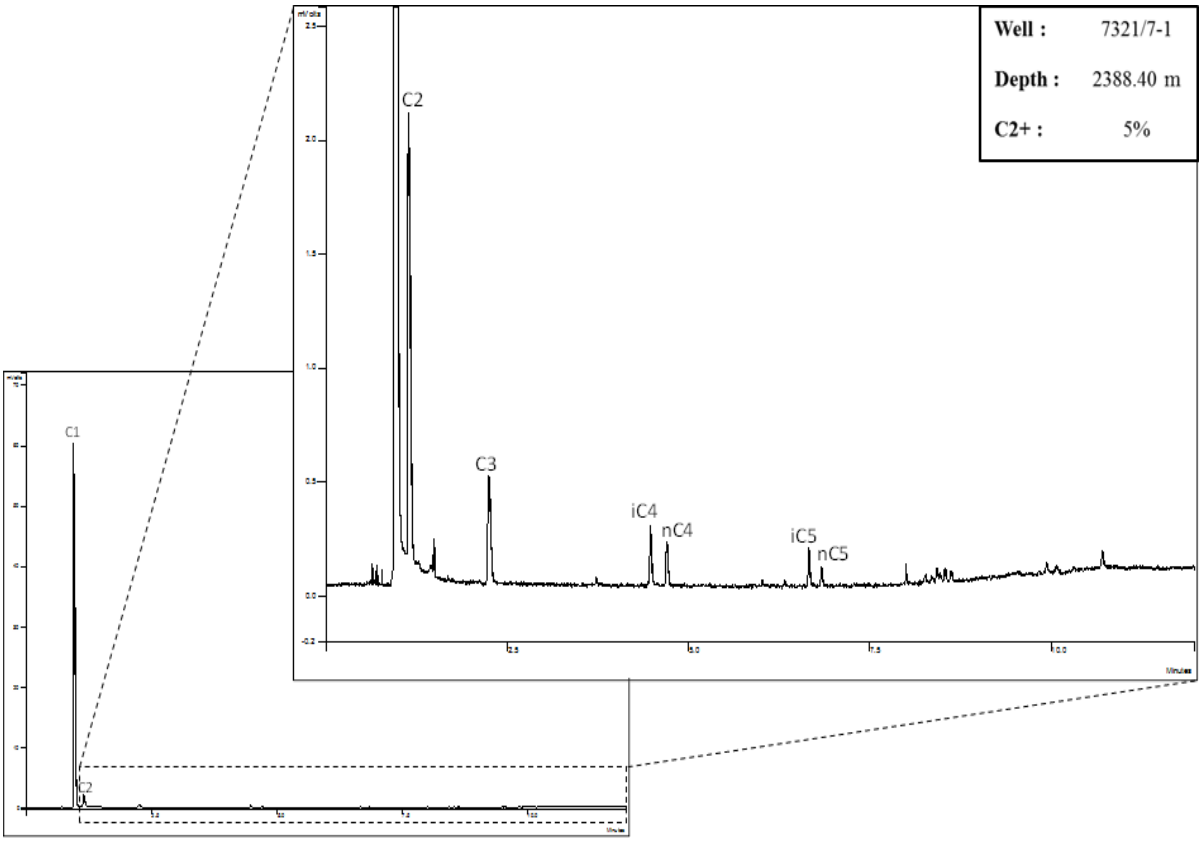
Well : 7321/7-1
Depth : 2388.40 m
C2+ : 5%
C1
C2
C3
iC4
nC4
iC5
nC5
Minutes

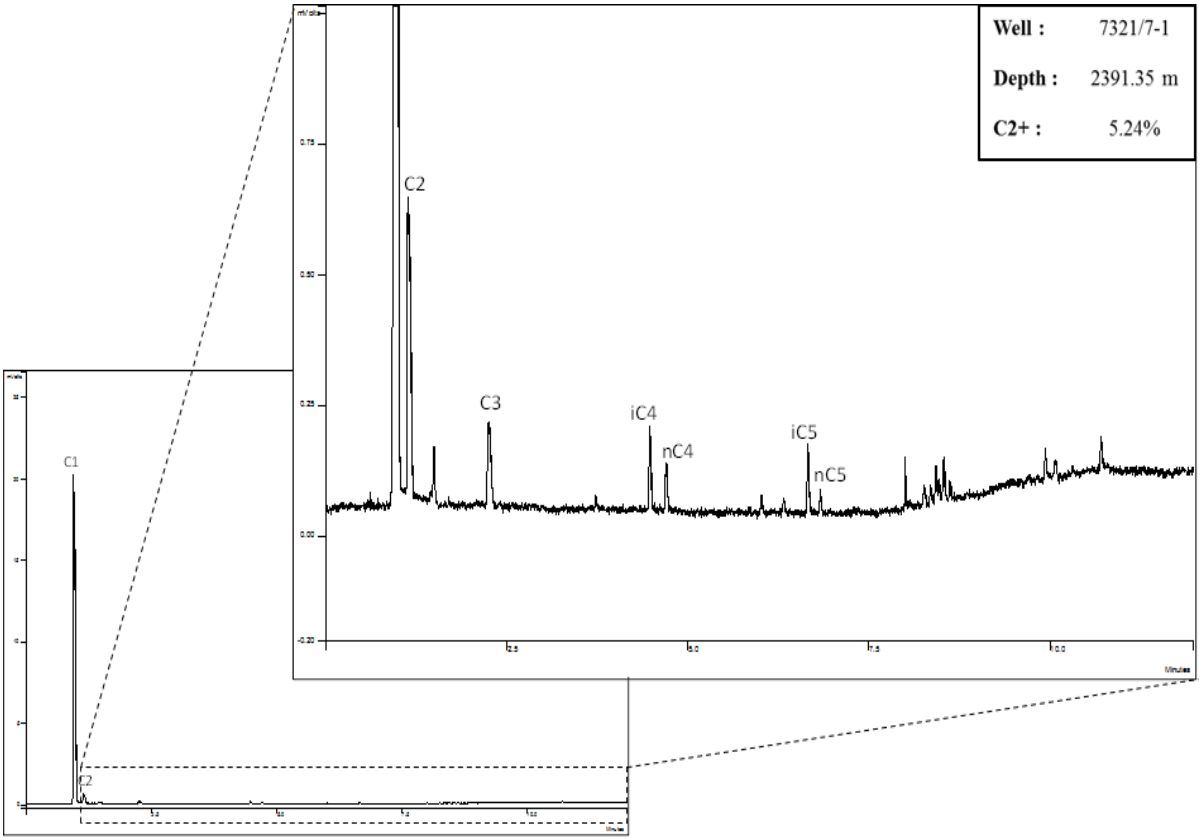
Well : 7321/7-1
Depth : 2391.35 m
C2+ : 5.24%
C1
C2
C3
iC4
nC4
iC5
nC5

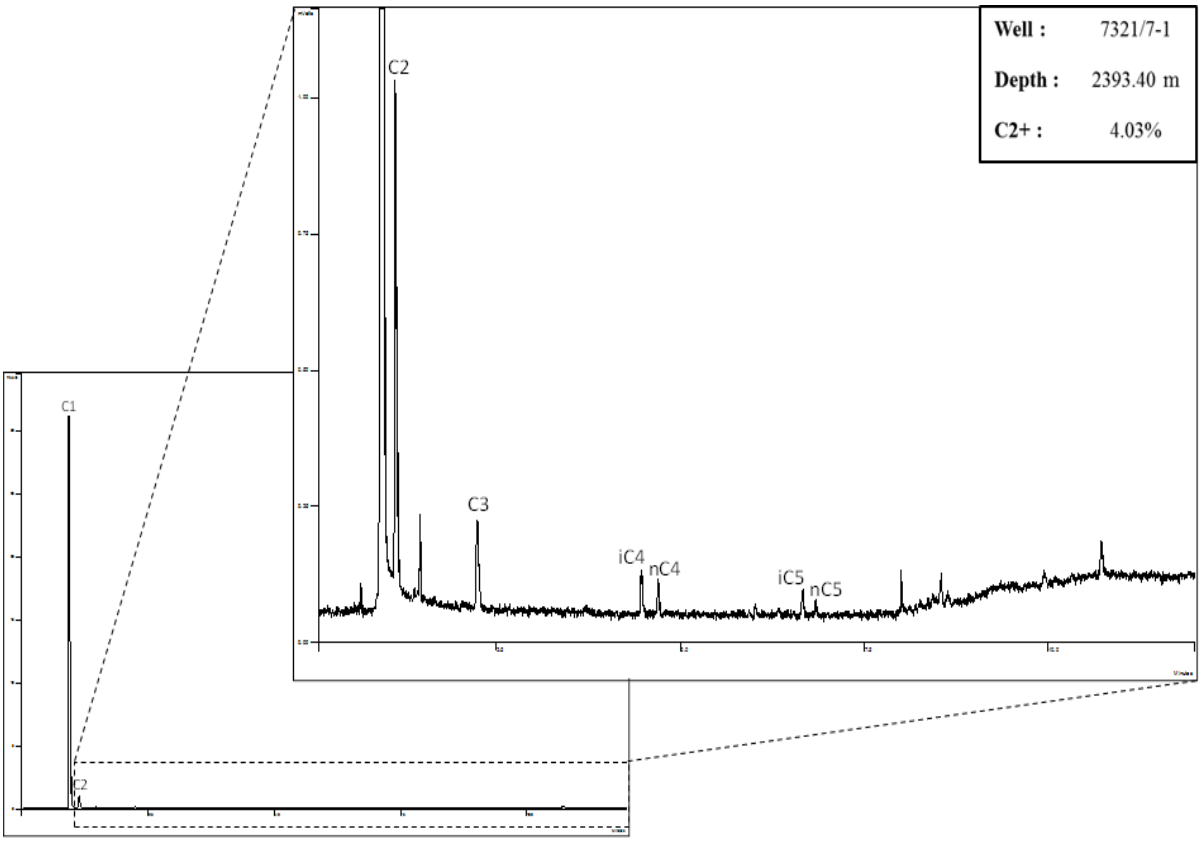
Well : 7321/7-1
Depth : 2393.40 m
C2+ : 4.03%
C1
C2
C3
iC4
nC4
iC5
nC5

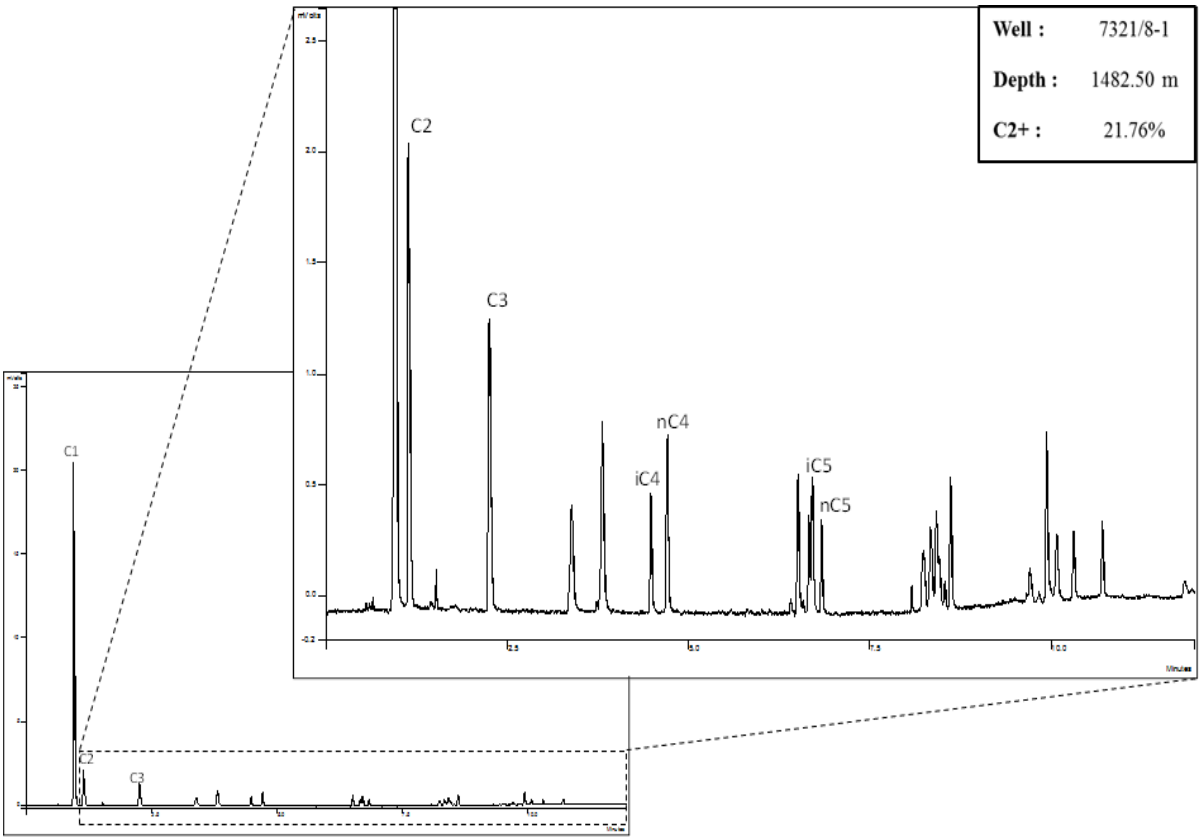
Well : 7321/8-1
Depth : 1482.50 m
C2+ : 21.76%
C1
C2
C3
iC4
nC4
iC5
nC5

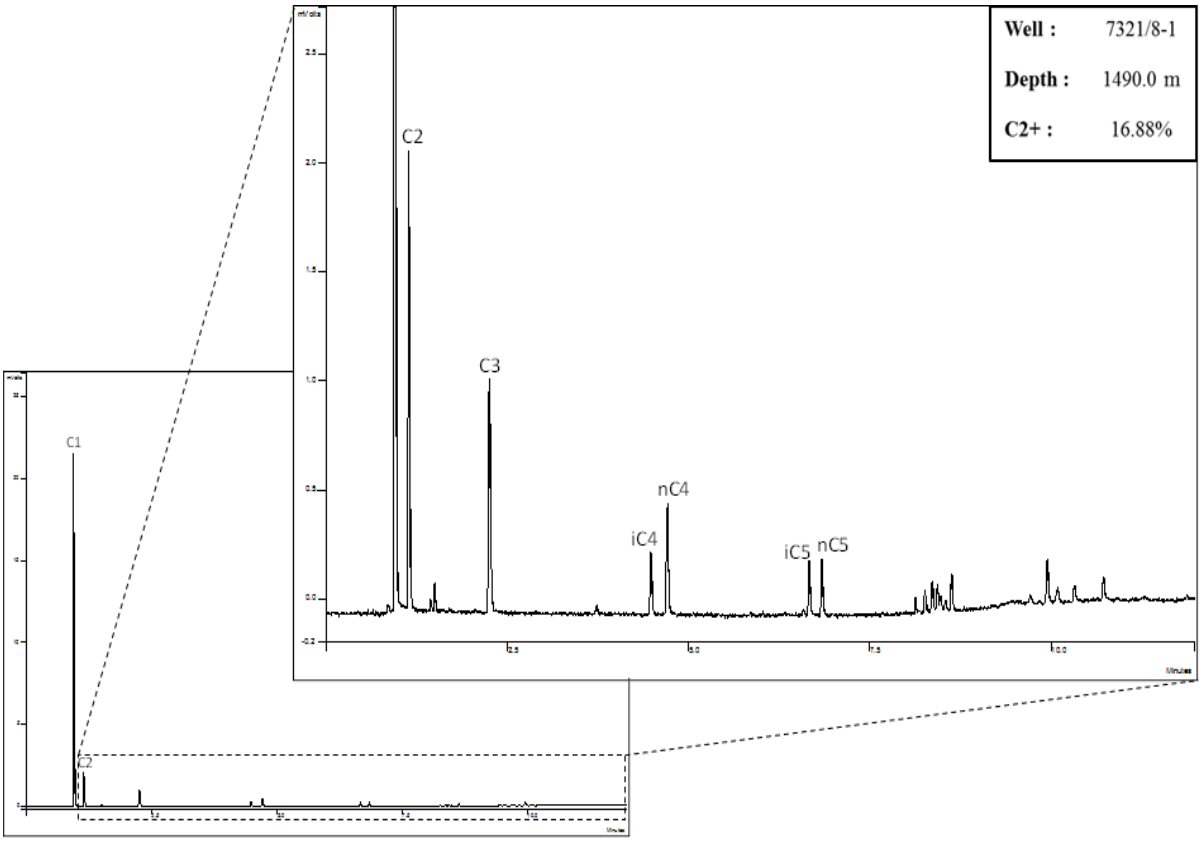
Well : 7321/8-1
Depth : 1490.0 m
C2+ : 16.88%
C1
C2
C3
iC4
nC4
iC5
nC5

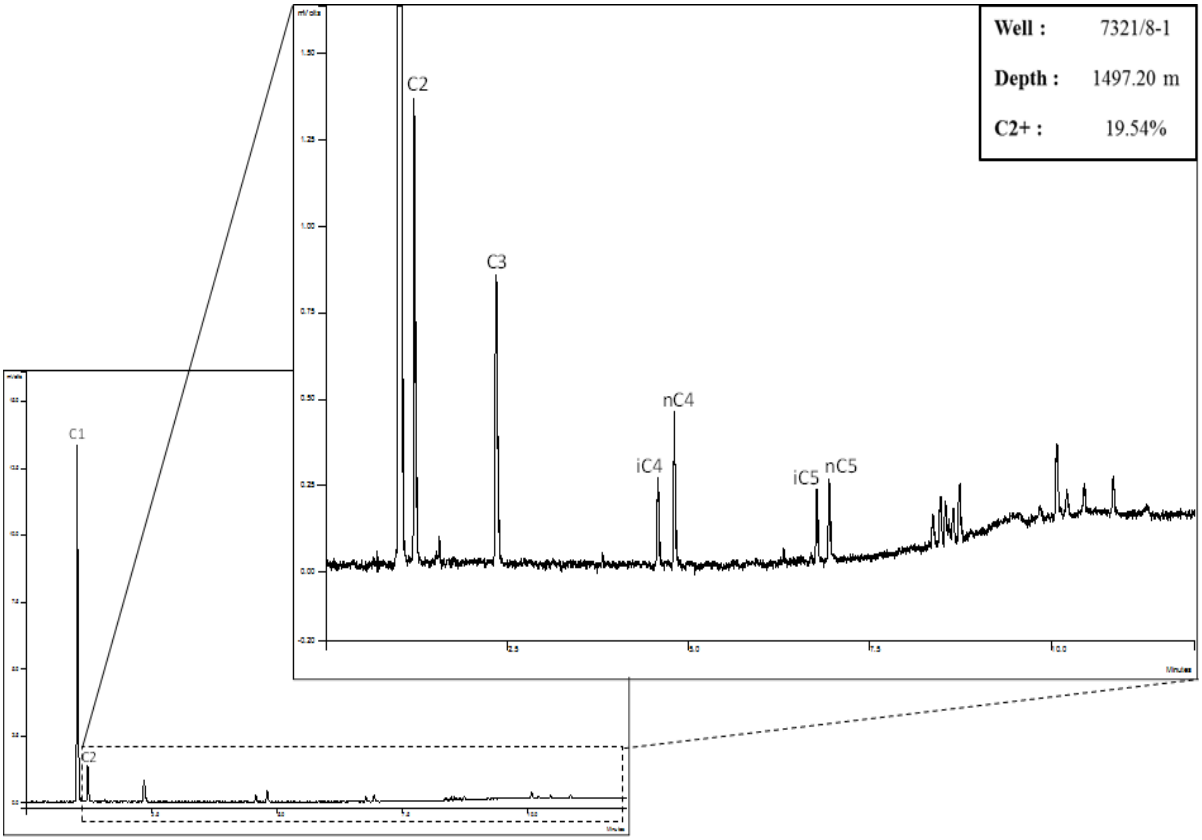
Well : 7321/8-1
Depth : 1497.20 m
C2+ : 19.54%
C1
C2
C3
iC4
nC4
iC5
nC5
Minutes

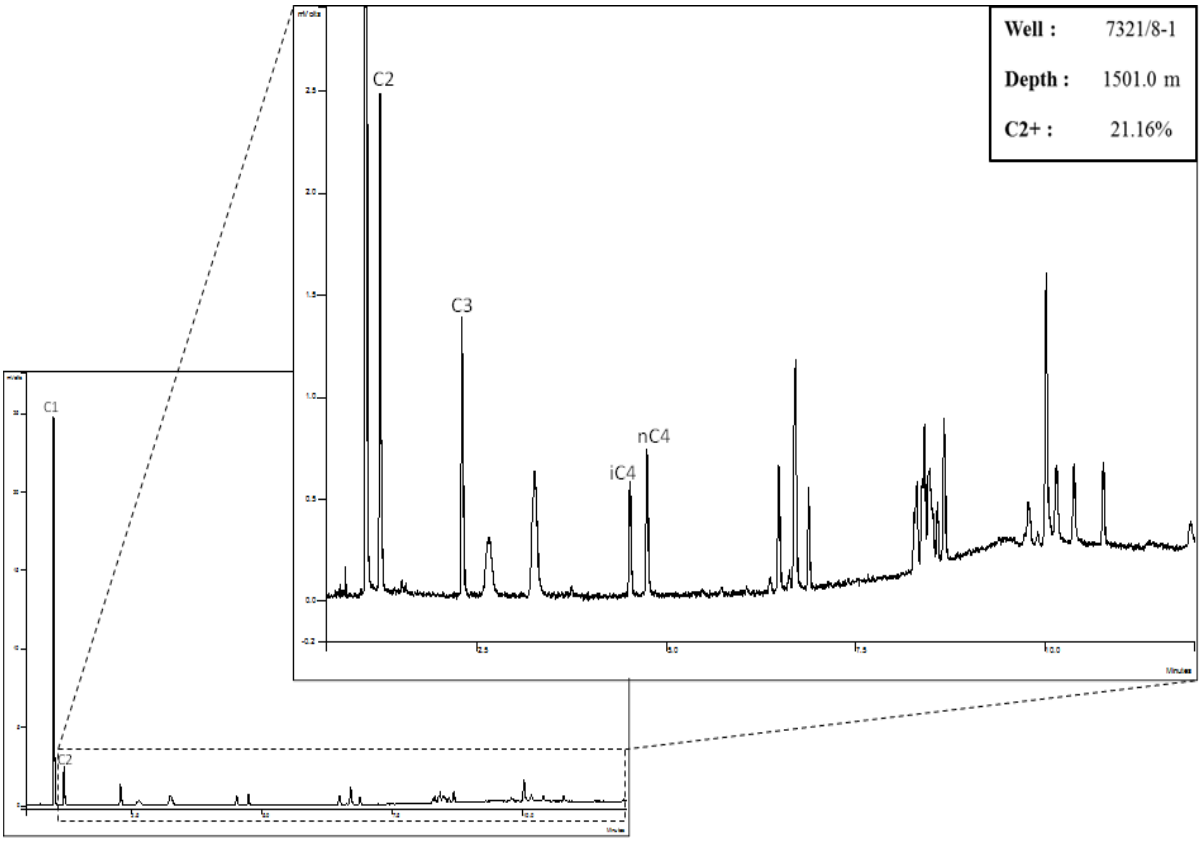
Well : 7321/8-1
Depth : 1501.0 m
C2+ : 21.16%
C1
C2
C3
iC4
nC4
Minutes

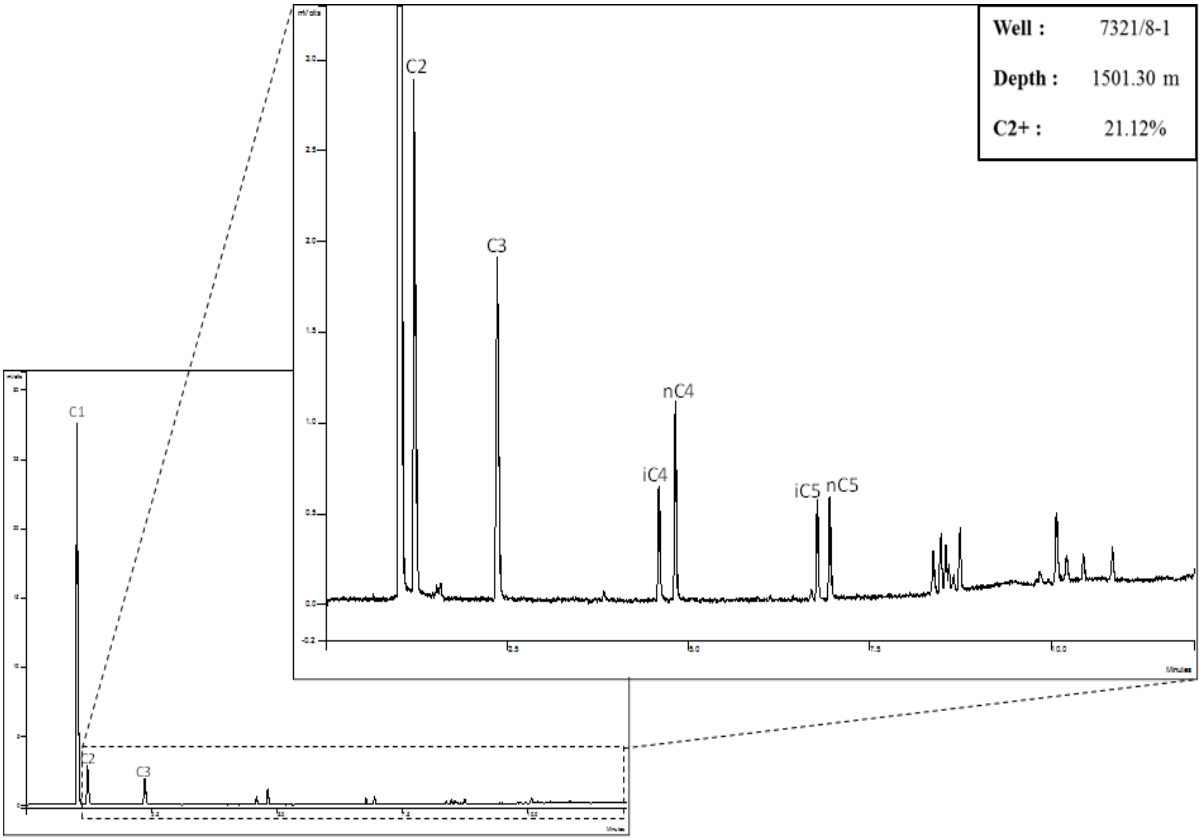
Well : 7321/8-1
Depth : 1501.30 m
C2+ : 21.12%
C1
C2
C3
iC4
nC4
iC5
nC5

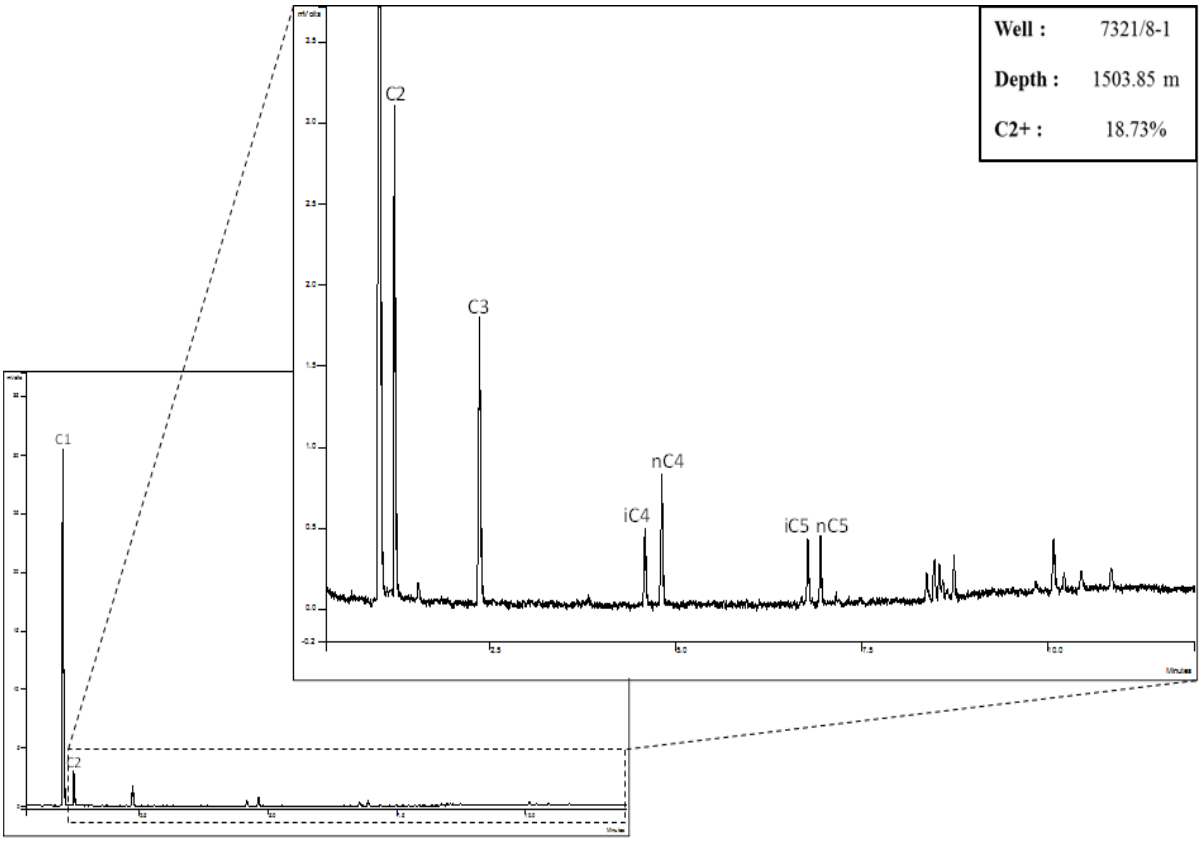
Well : 7321/8-1
Depth : 1503.85 m
C2+ : 18.73%
C1
C2
C3
iC4
nC4
iC5
nC5

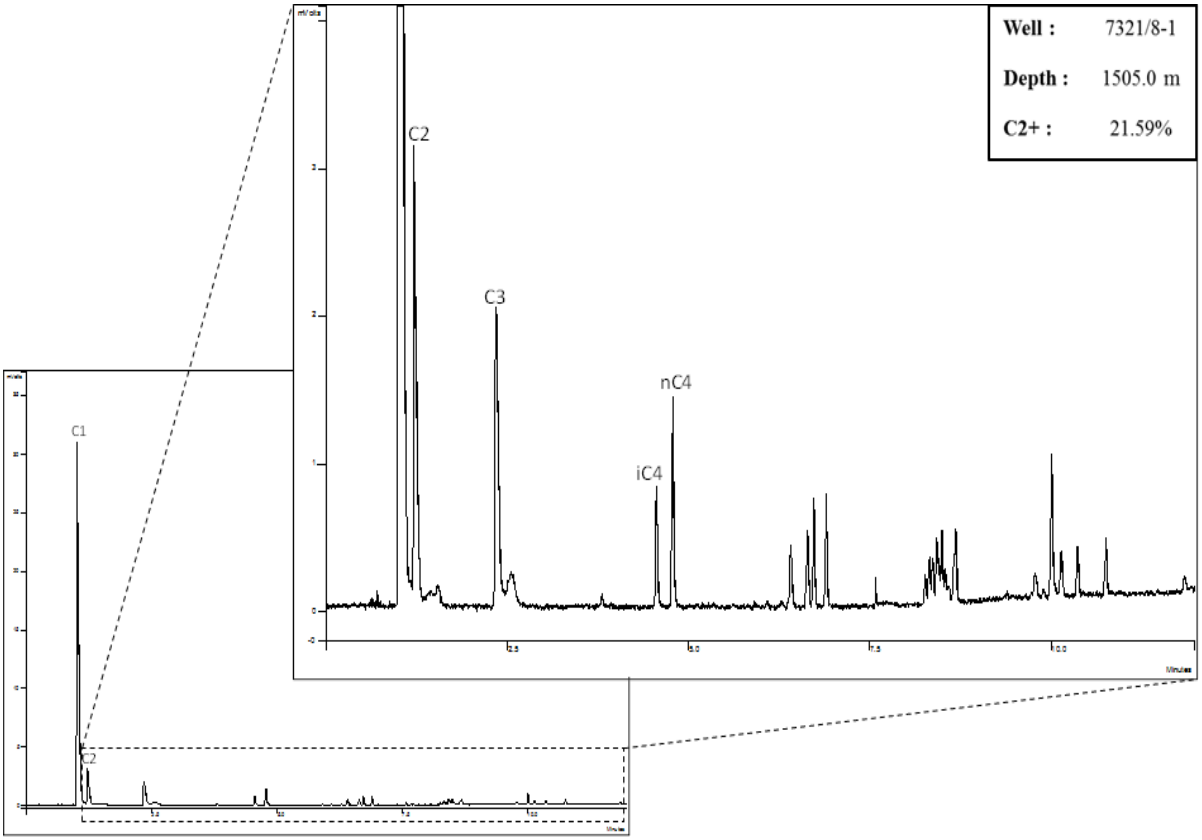
Well : 7321/8-1
Depth : 1505.0 m
C2+ : 21.59%
C1
C2
C3
iC4
nC4

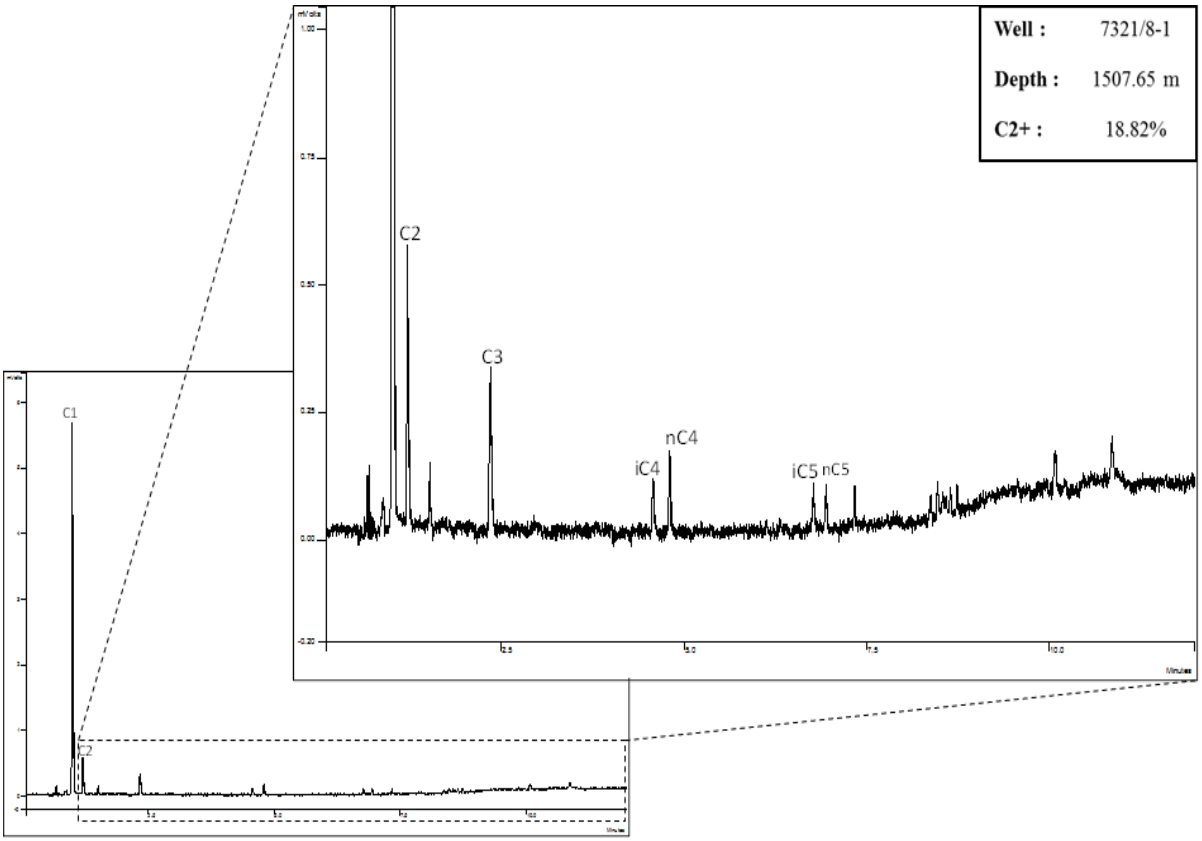
Well : 7321/8-1
Depth : 1507.65 m
C2+ : 18.82%
C1
C2
C3
iC4
nC4
iC5
nC5

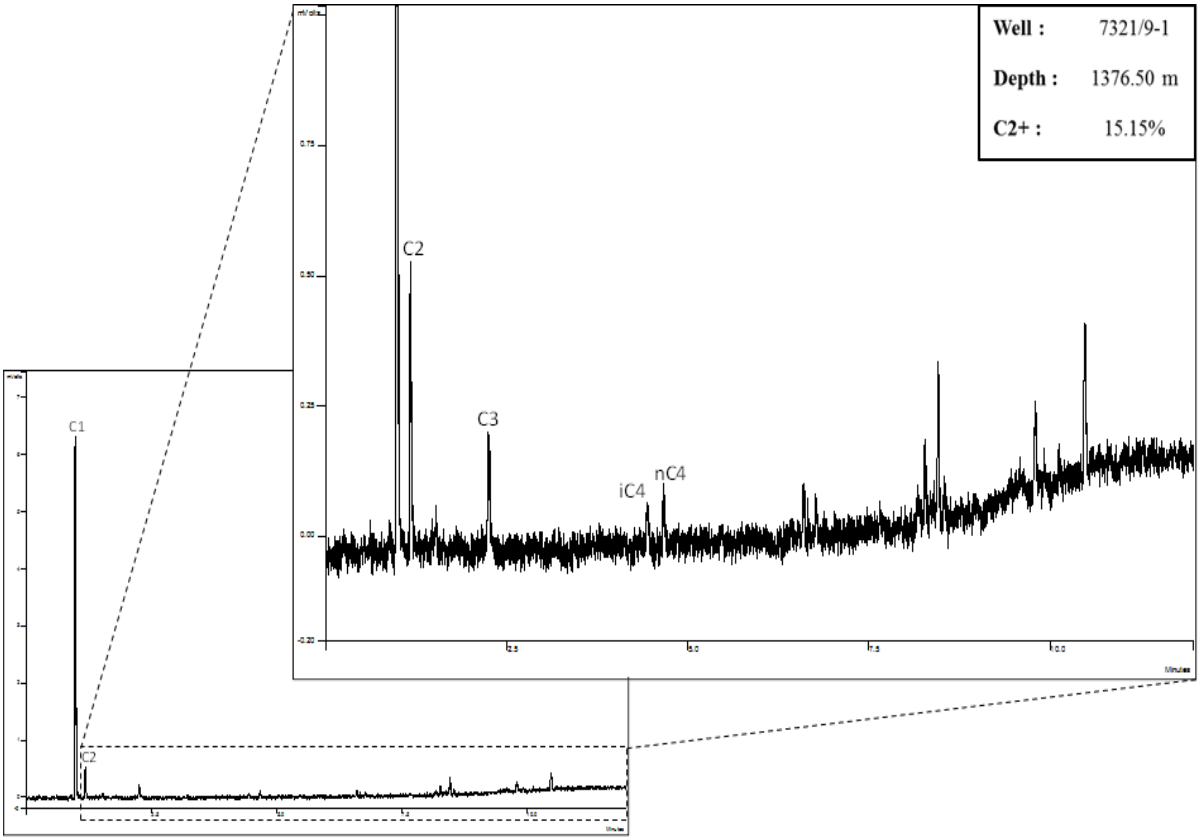
Well : 7321/9-1
Depth : 1376.50 m
C2+ : 15.15%
C1
C2
C3
iC4
nC4
C2

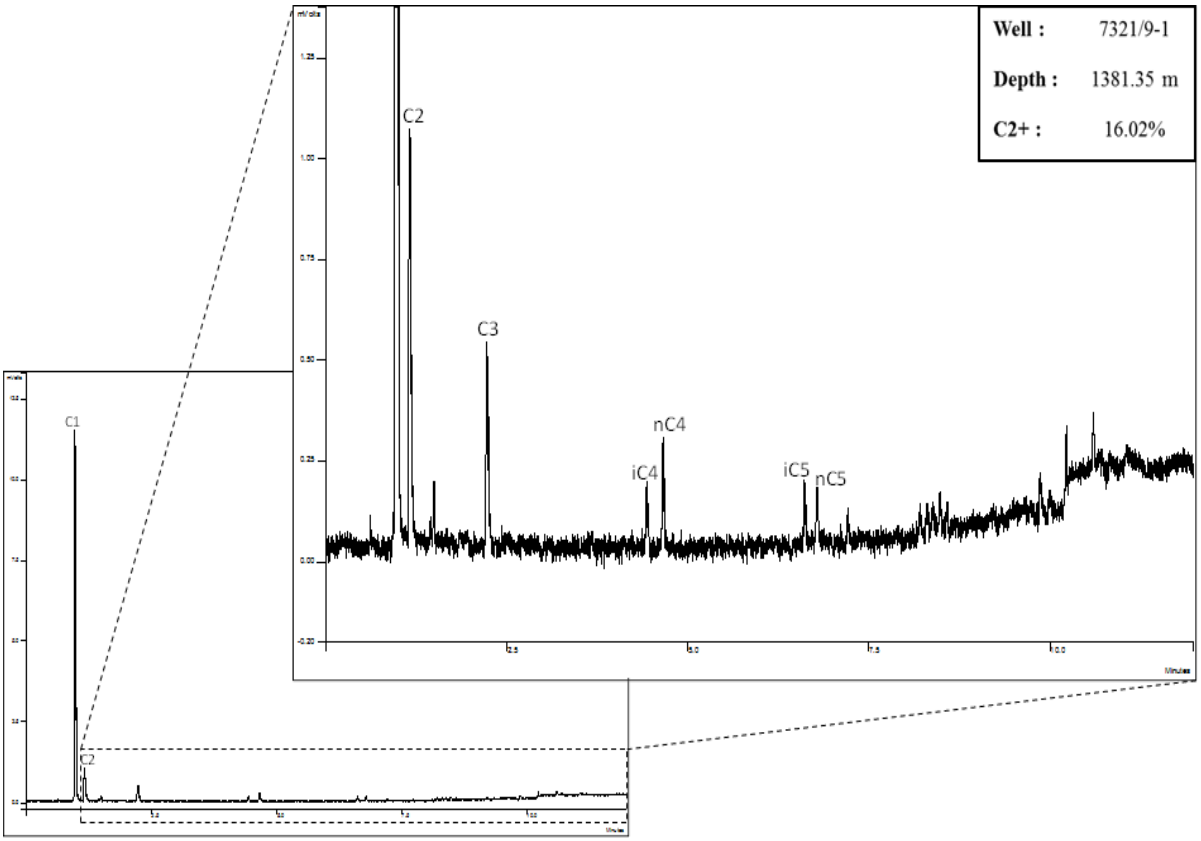
Well : 7321/9-1
Depth : 1381.35 m
C2+ : 16.02%
C1
C2
C3
iC4
nC4
iC5
nC5
C2

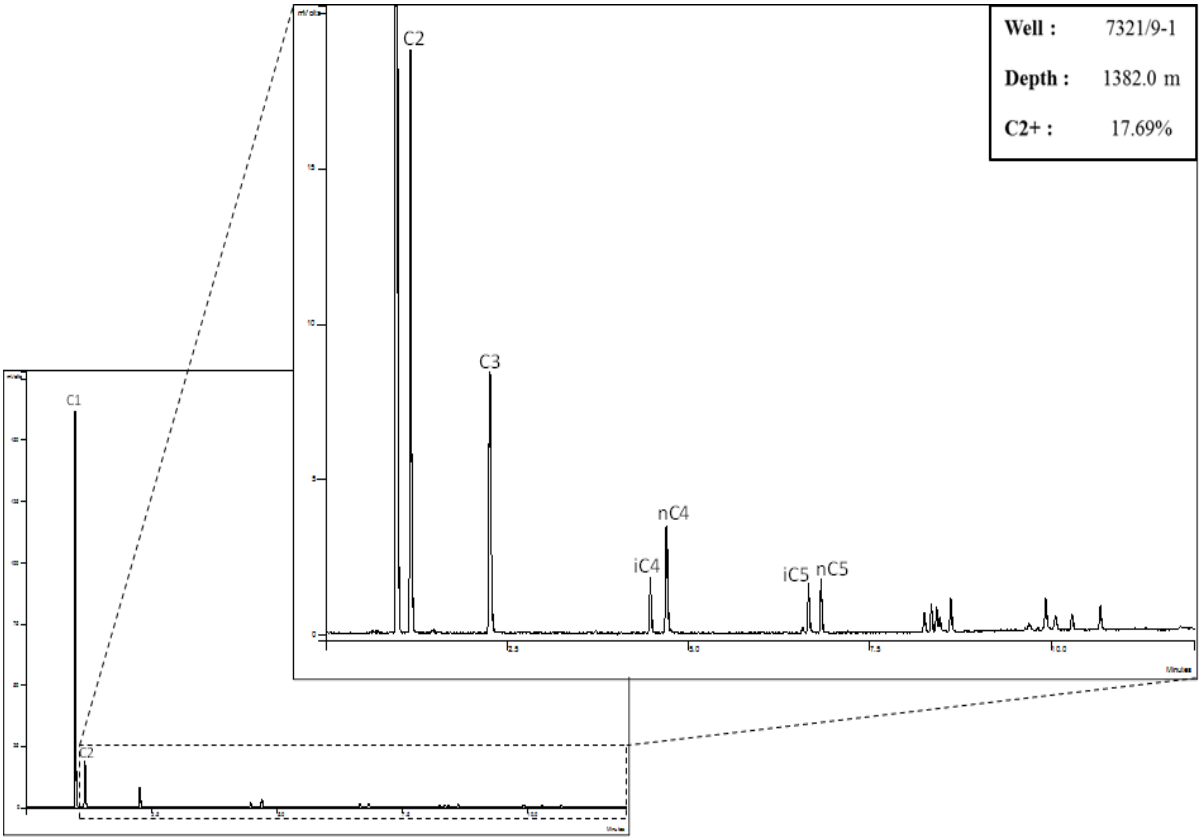
Well : 7321/9-1
Depth : 1382.0 m
C2+ : 17.69%
C1
C2
C3
iC4
nC4
iC5
nC5

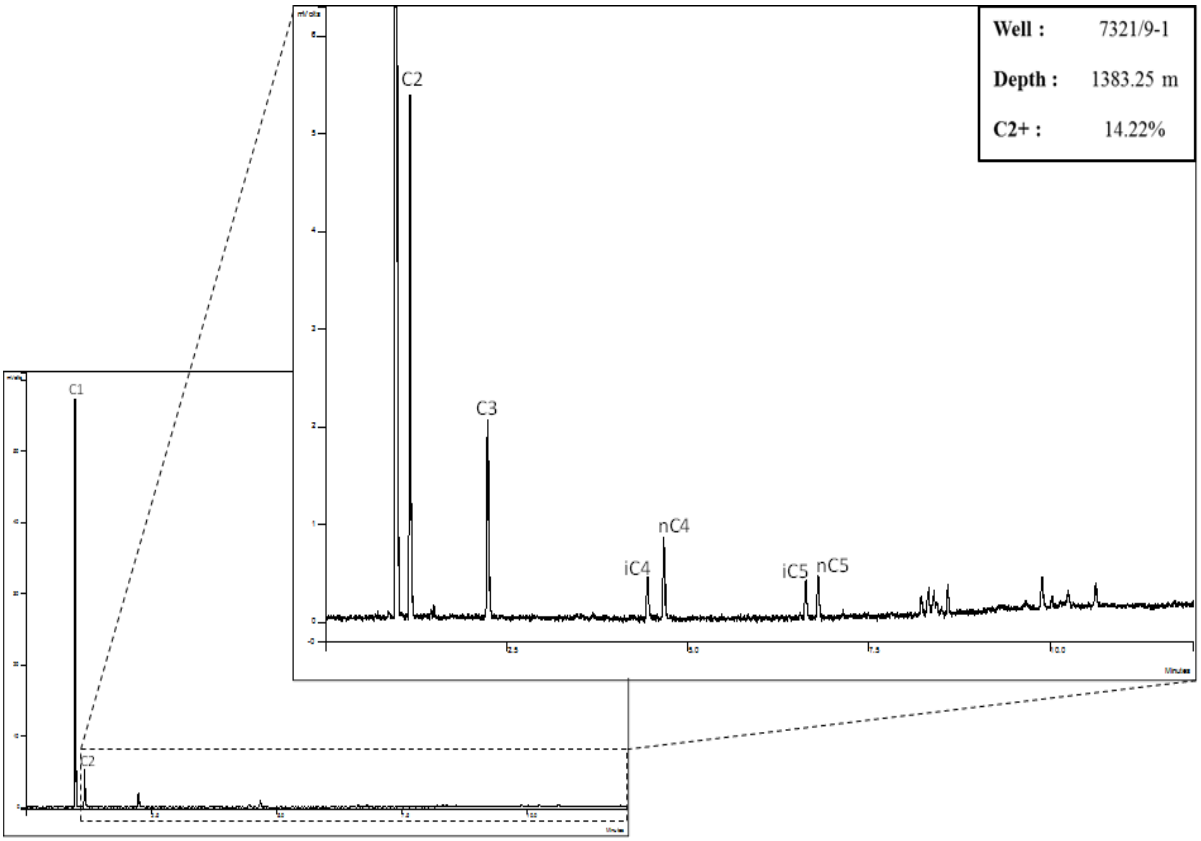
Well : 7321/9-1
Depth : 1383.25 m
C2+ : 14.22%
C1
C2
C3
iC4
nC4
iC5
nC5

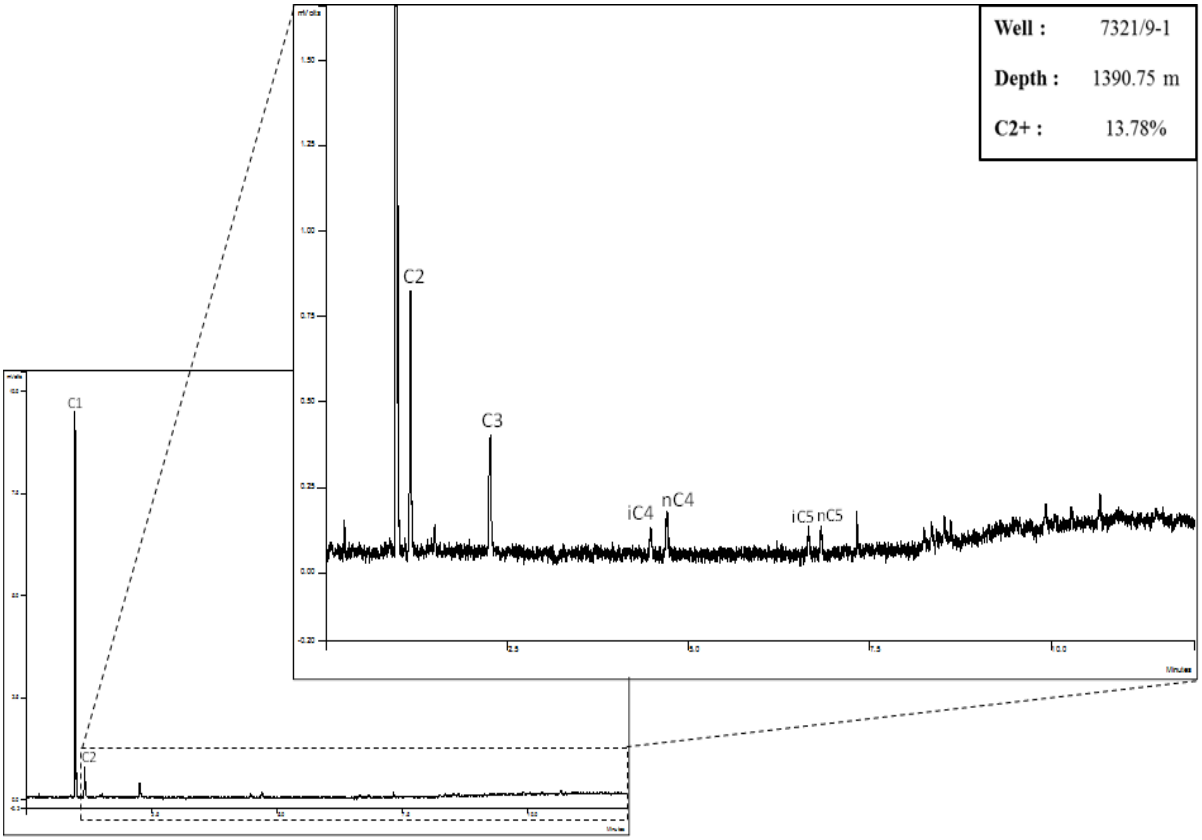
Well : 7321/9-1
Depth : 1390.75 m
C2+ : 13.78%
C1
C2
C3
iC4
nC4
iC5
nC5

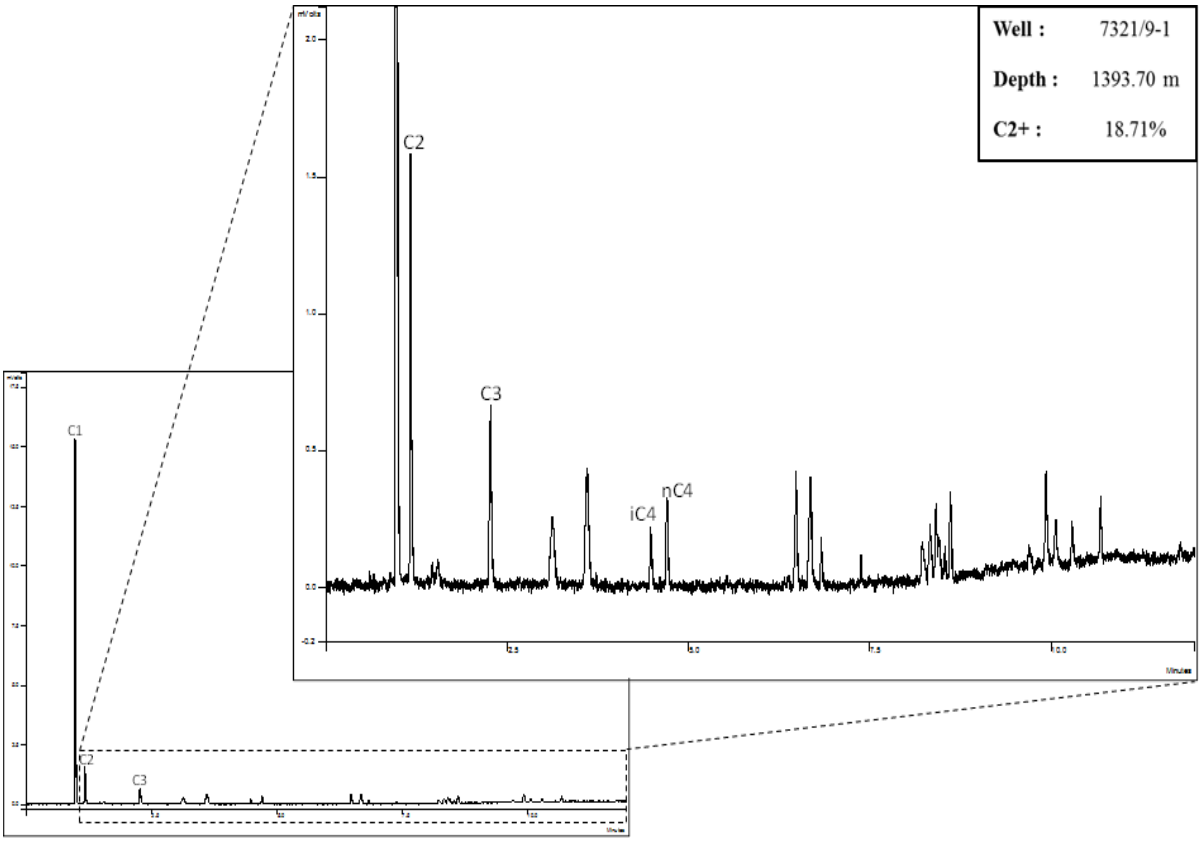
Well : 7321/9-1
Depth : 1393.70 m
C2+ : 18.71%
C1
C2
C3
iC4
nC4

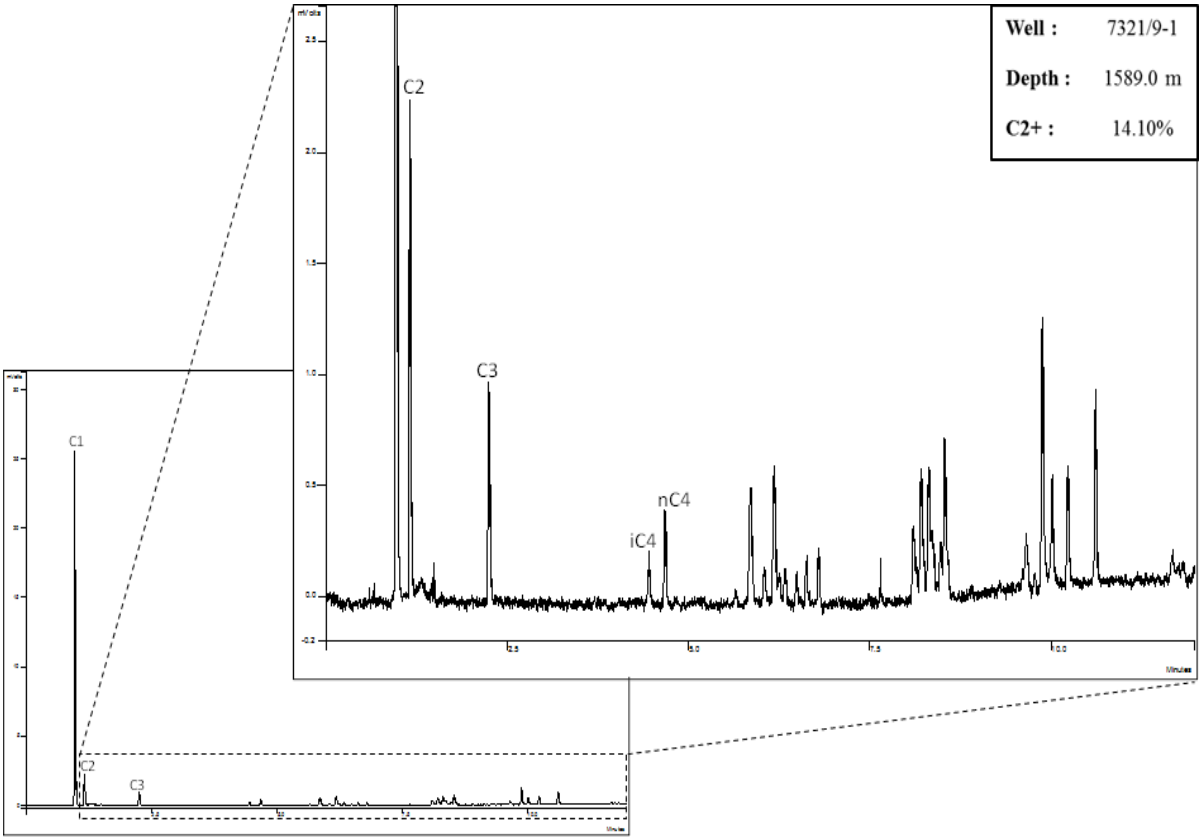
Well : 7321/9-1
Depth : 1589.0 m
C2+ : 14.10%
C1
C2
C3
iC4
nC4

Appendix B (GC-FID Results)

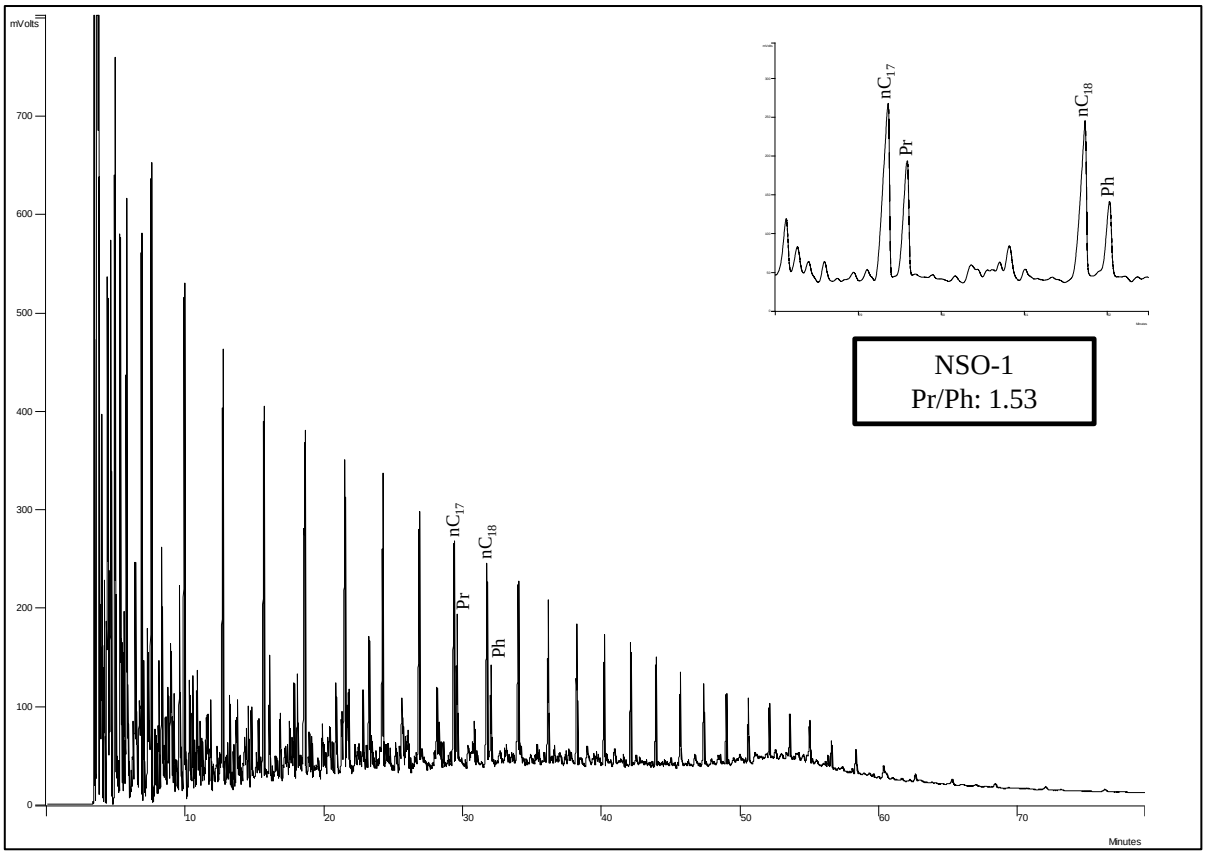
mVolts
700
600
500
400
300
200
100
0
nC17
Pr
nC18
Ph
10
20
30
40
50
60
70
Minutes
nC17
Pr
nC18
Ph
NSO-1
Pr/Ph: 1.53

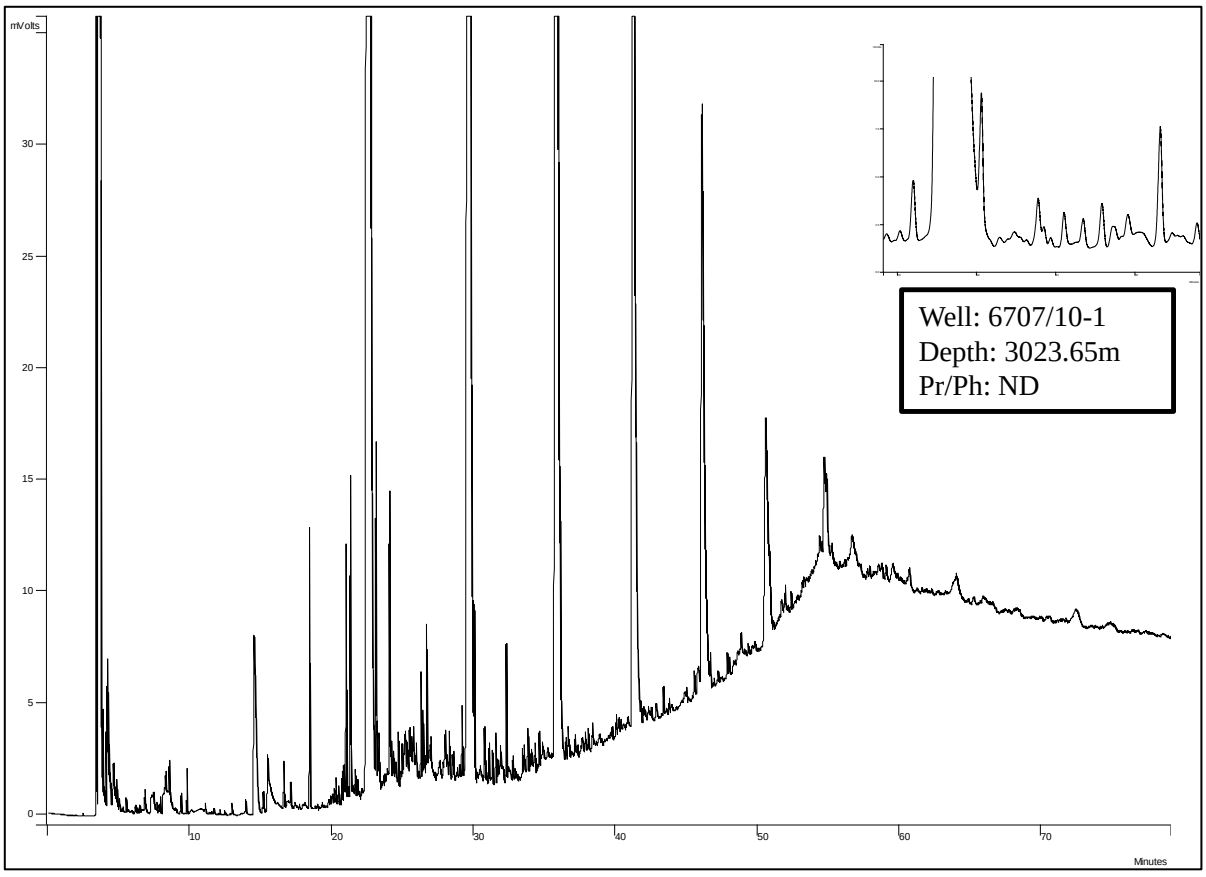
mVolts
30
25
20
15
10
5
0
10
20
30
40
50
60
70
Minutes
Well: 6707/10-1
Depth: 3023.65m
Pr/Ph: ND

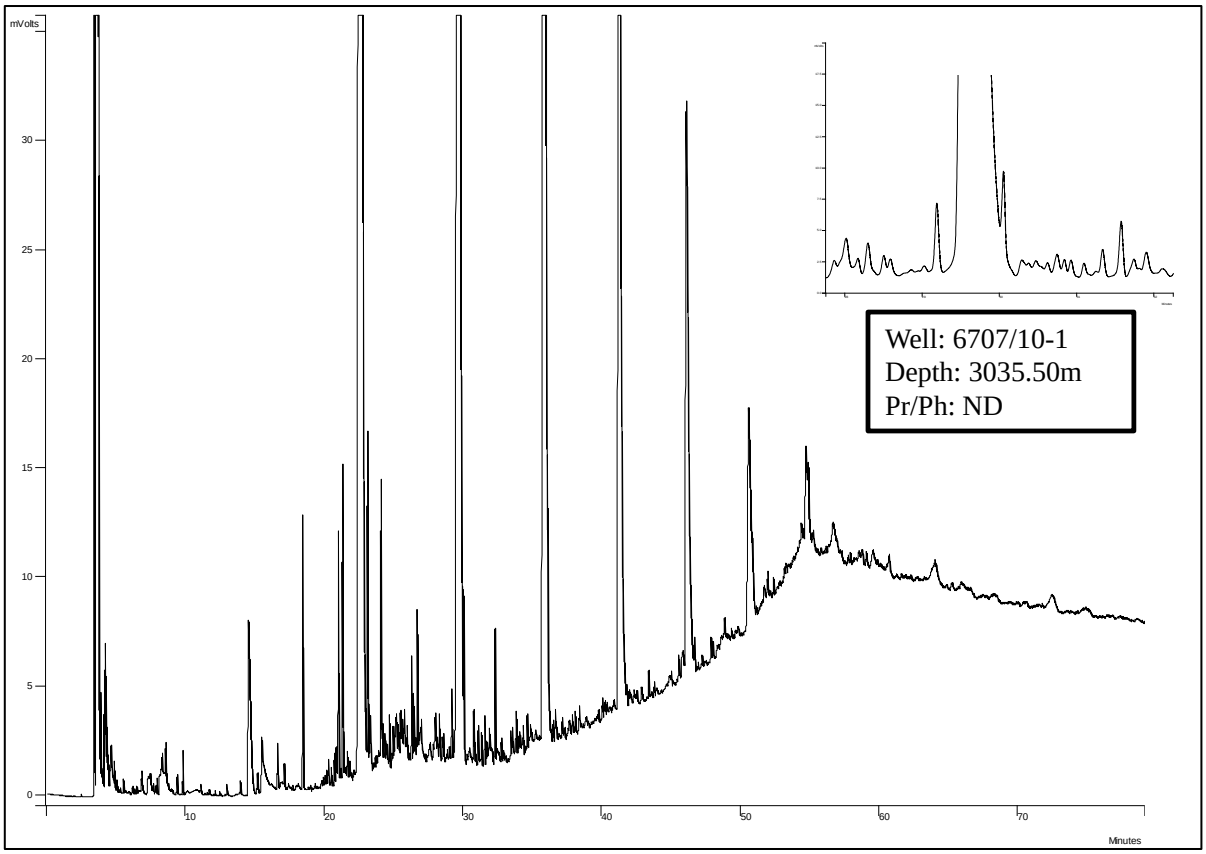
mVolts
30
25
20
15
10
5
0
10
20
30
40
50
60
70
Minutes
Well: 6707/10-1
Depth: 3035.50m
Pr/Ph: ND

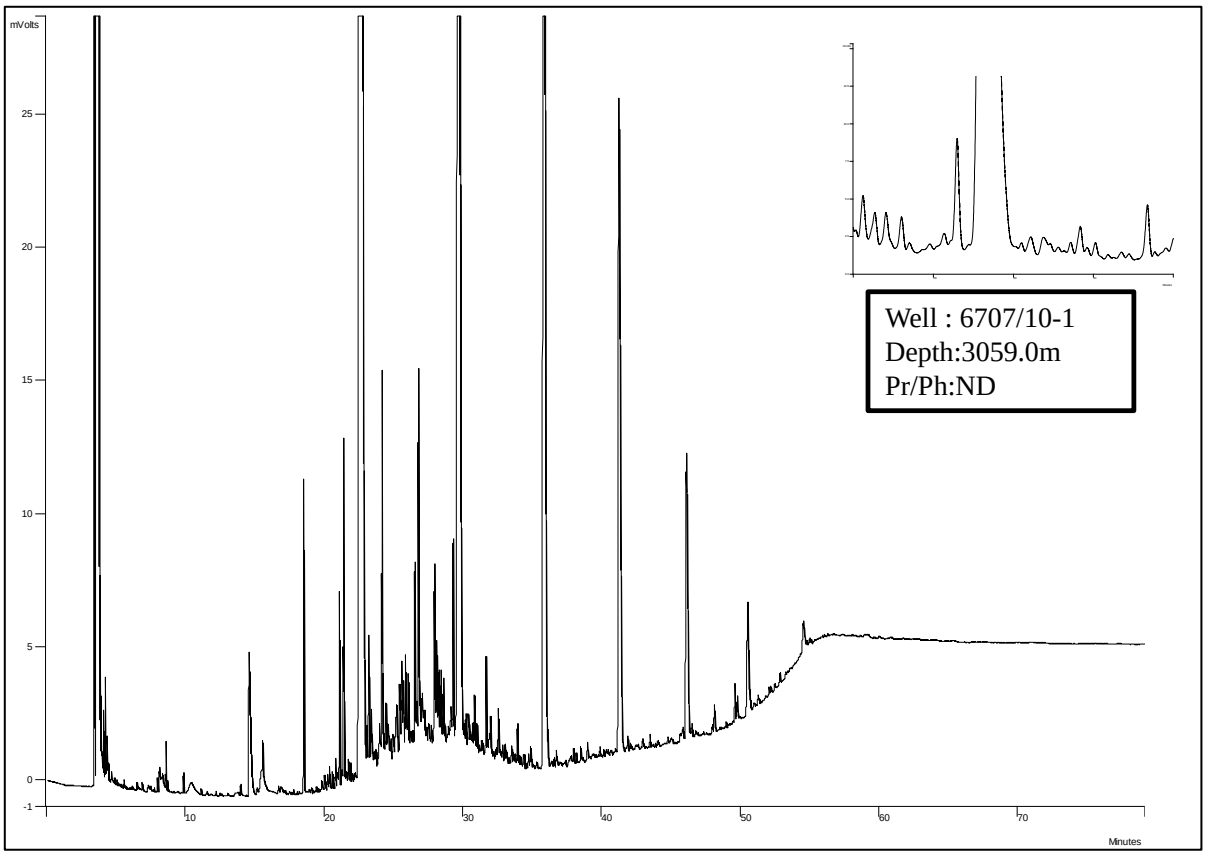
mVolts
25
20
15
10
5
0
-1
10
20
30
40
50
60
70
Minutes
Well : 6707/10-1
Depth:3059.0m
Pr/Ph:ND

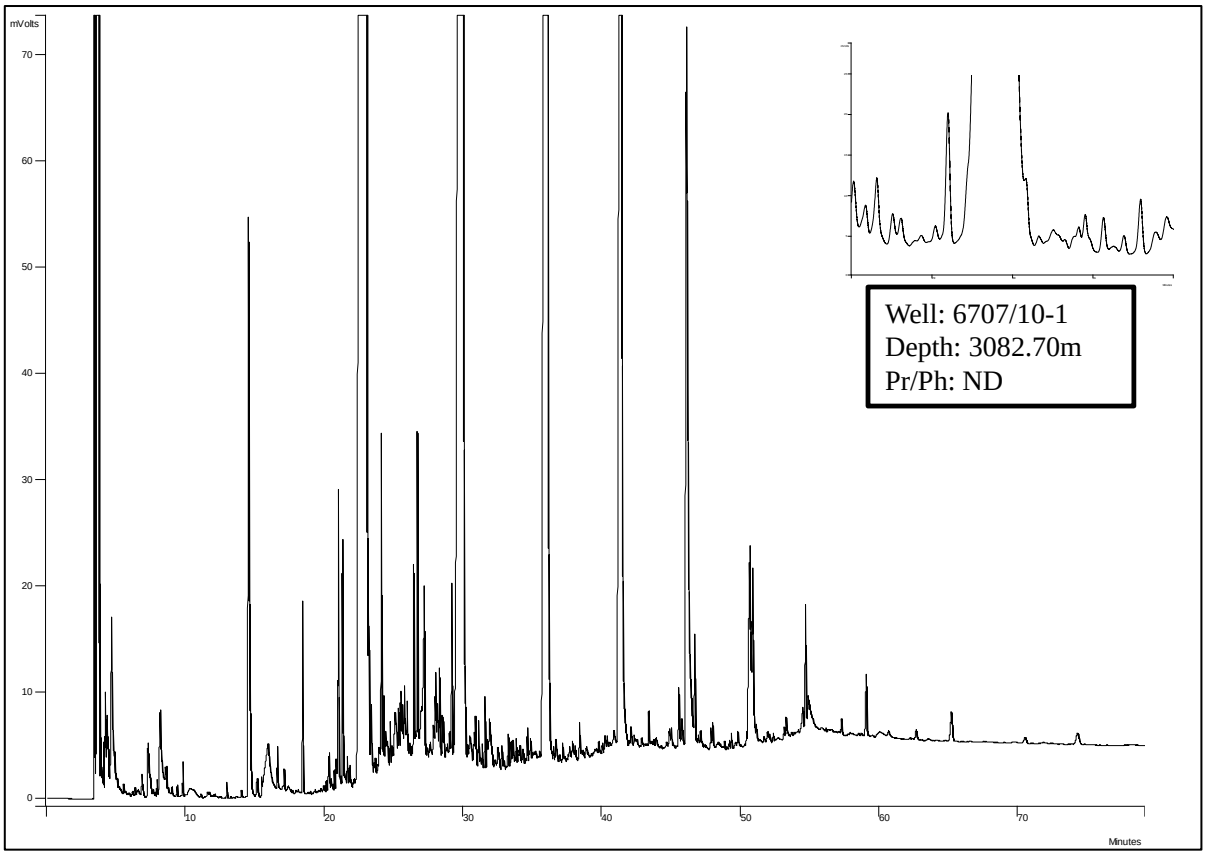
mVolts
70
60
50
40
30
20
10
0
10
20
30
40
50
60
70
Minutes
Well: 6707/10-1
Depth: 3082.70m
Pr/Ph: ND

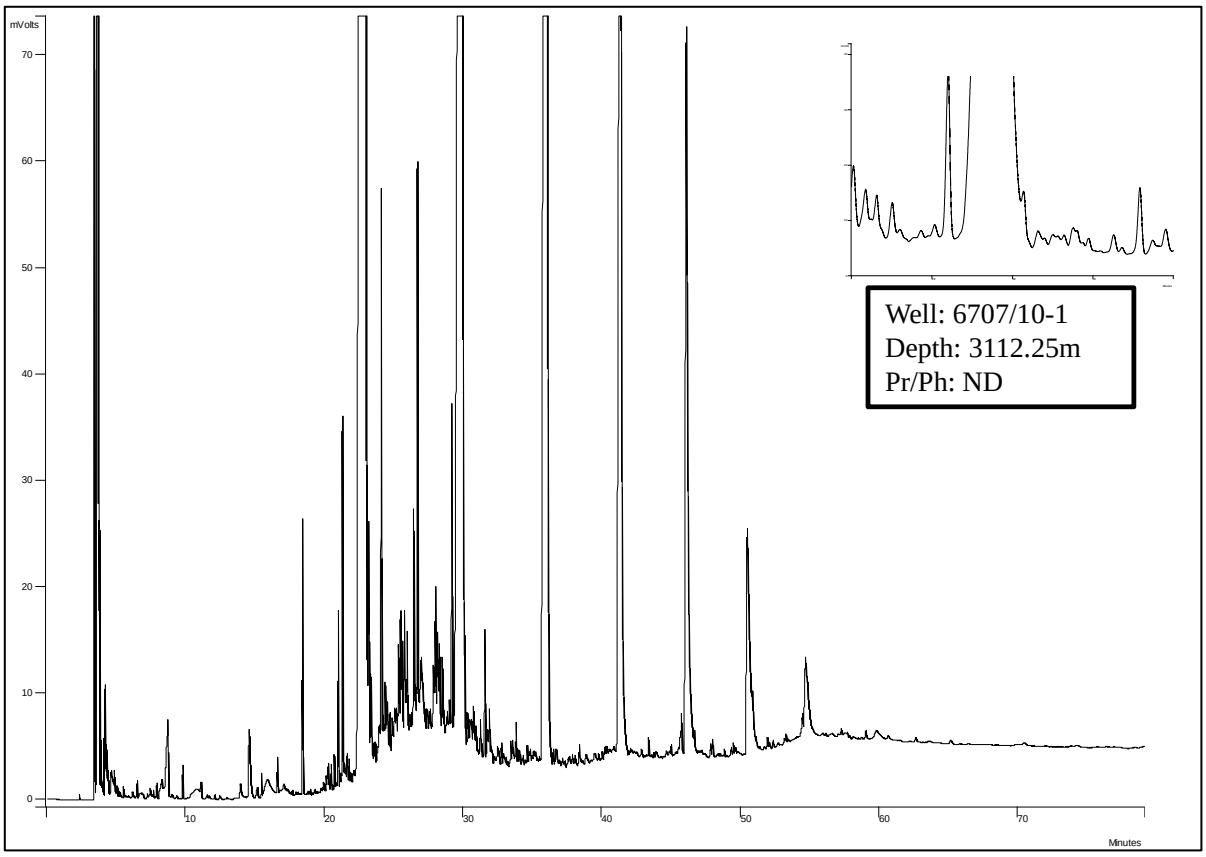
mVolts
70
60
50
40
30
20
10
0
10
20
30
40
50
60
70
Minutes
Well: 6707/10-1
Depth: 3112.25m
Pr/Ph: ND

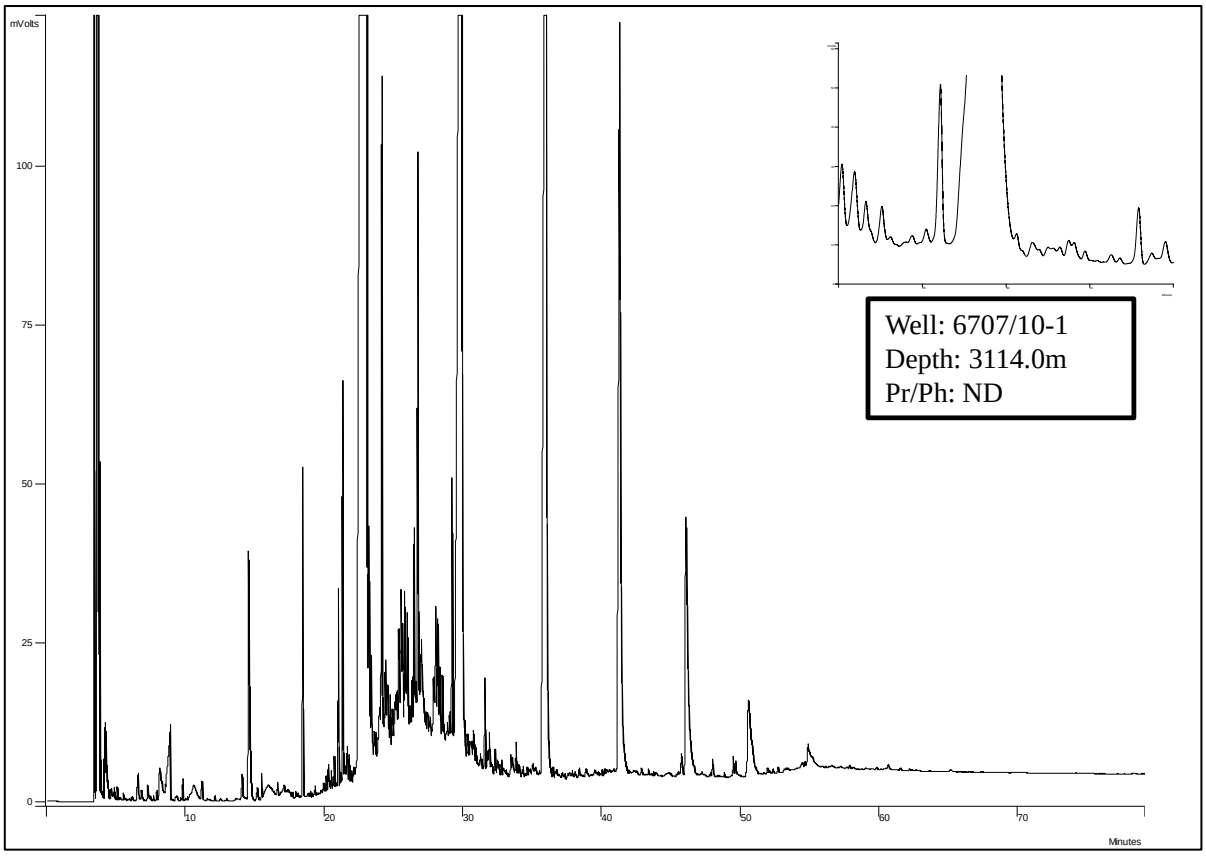
mVolts
100
75
50
25
0
10
20
30
40
50
60
70
Minutes
Well: 6707/10-1
Depth: 3114.0m
Pr/Ph: ND

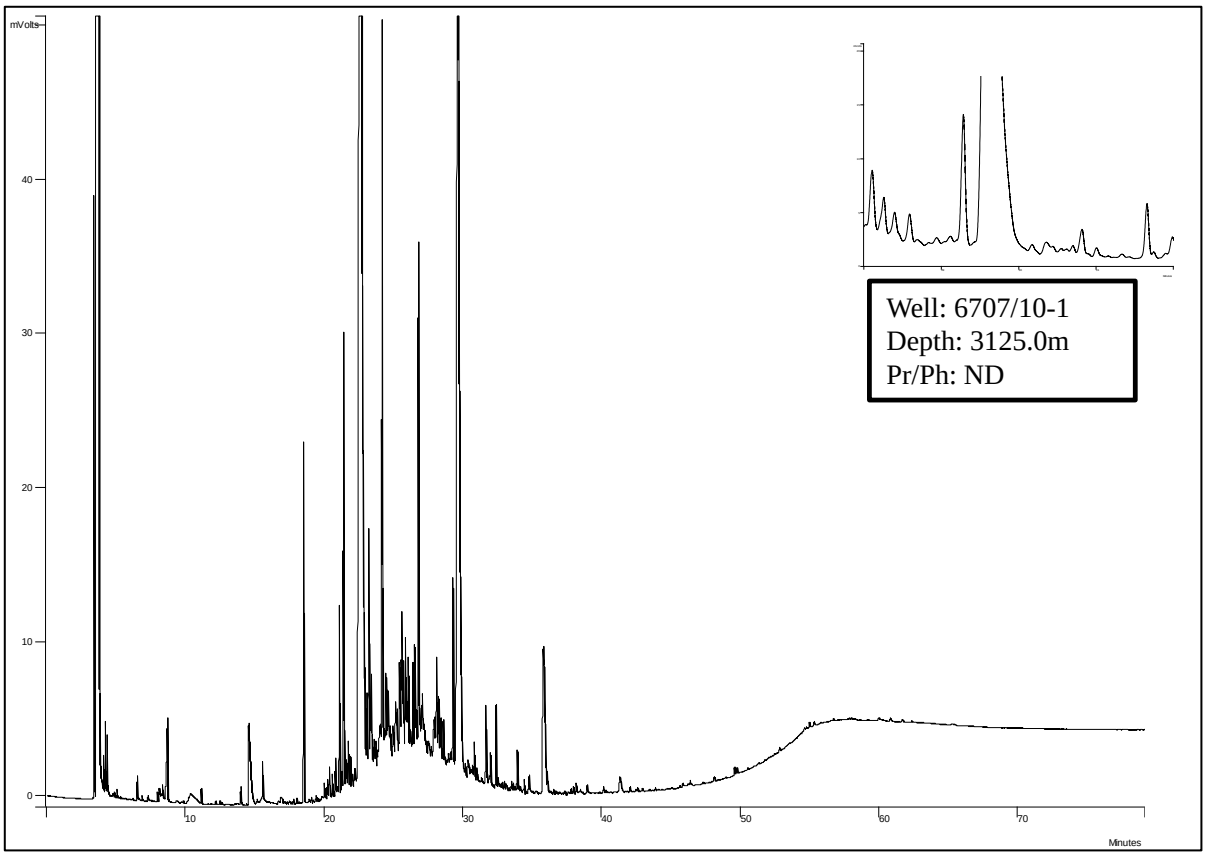
mVolts
40
30
20
10
0
10
20
30
40
50
60
70
Minutes
Well: 6707/10-1
Depth: 3125.0m
Pr/Ph: ND

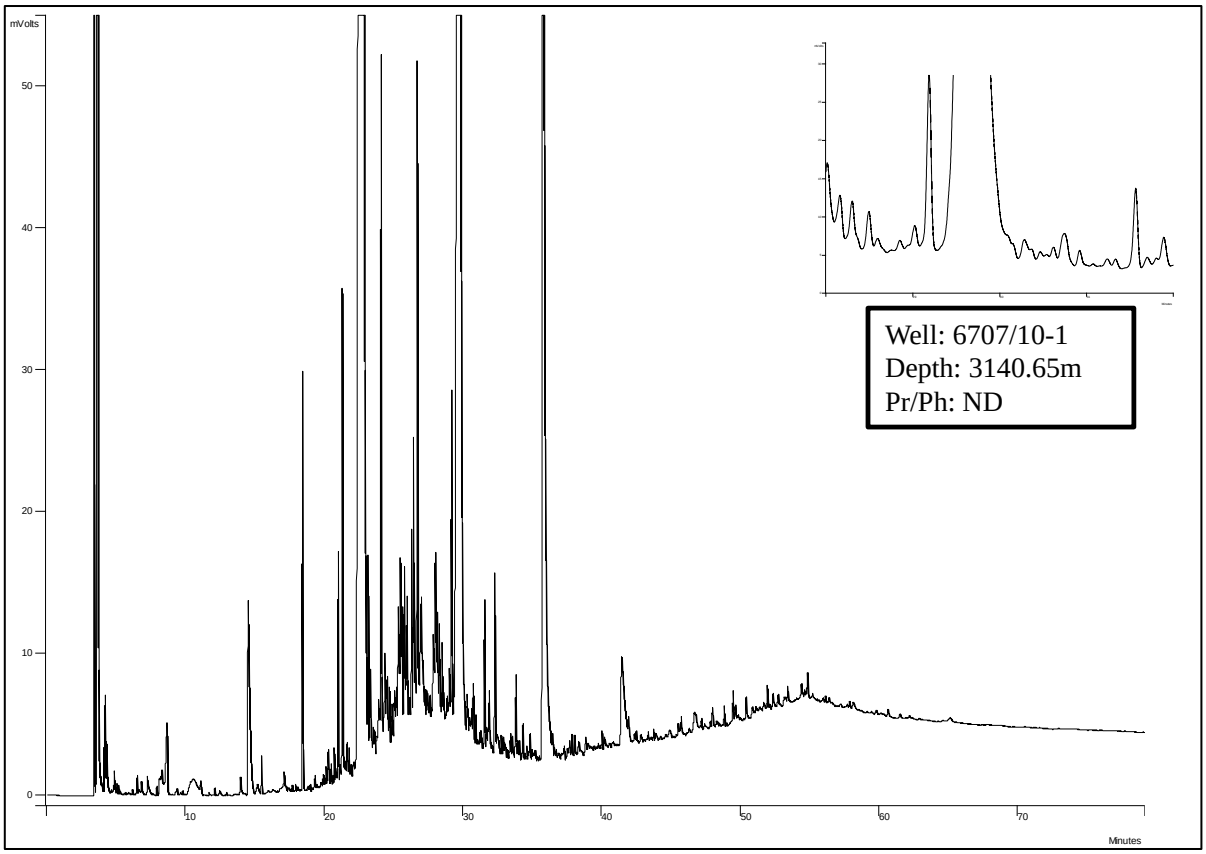
mVolts
50
40
30
20
10
0
10
20
30
40
50
60
70
Minutes
Well: 6707/10-1
Depth: 3140.65m
Pr/Ph: ND

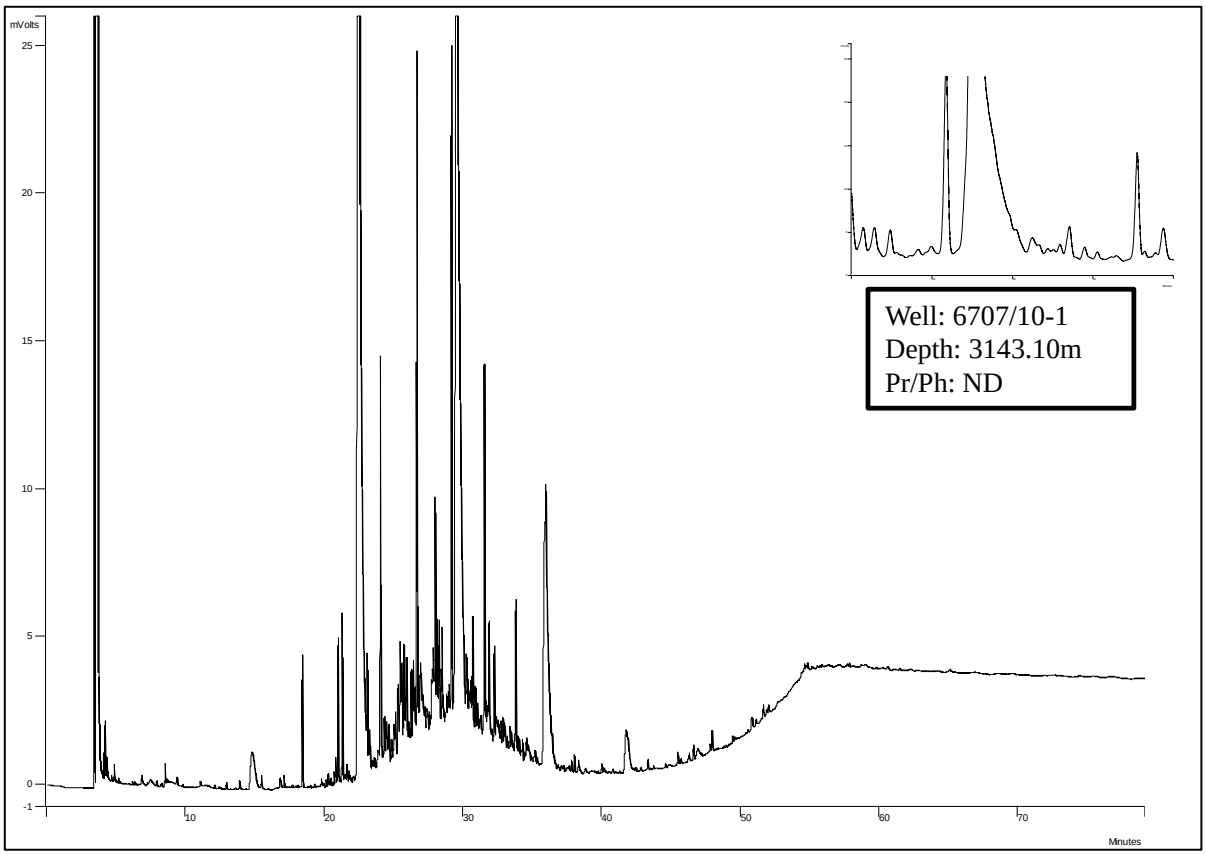
mVolts
25
20
15
10
5
0
-1
10
20
30
40
50
60
70
Minutes
Well: 6707/10-1
Depth: 3143.10m
Pr/Ph: ND

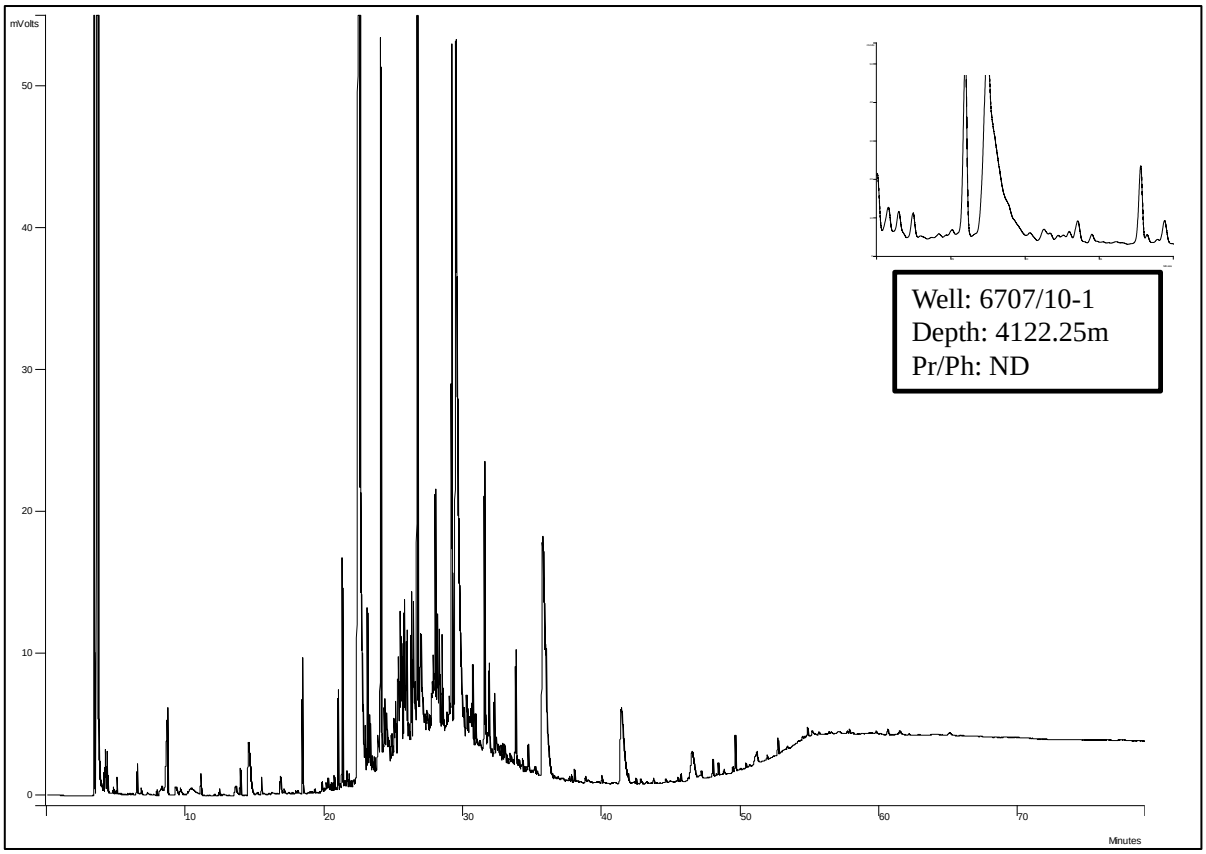
mVolts
50
40
30
20
10
0
10
20
30
40
50
60
70
Minutes
Well: 6707/10-1
Depth: 4122.25m
Pr/Ph: ND

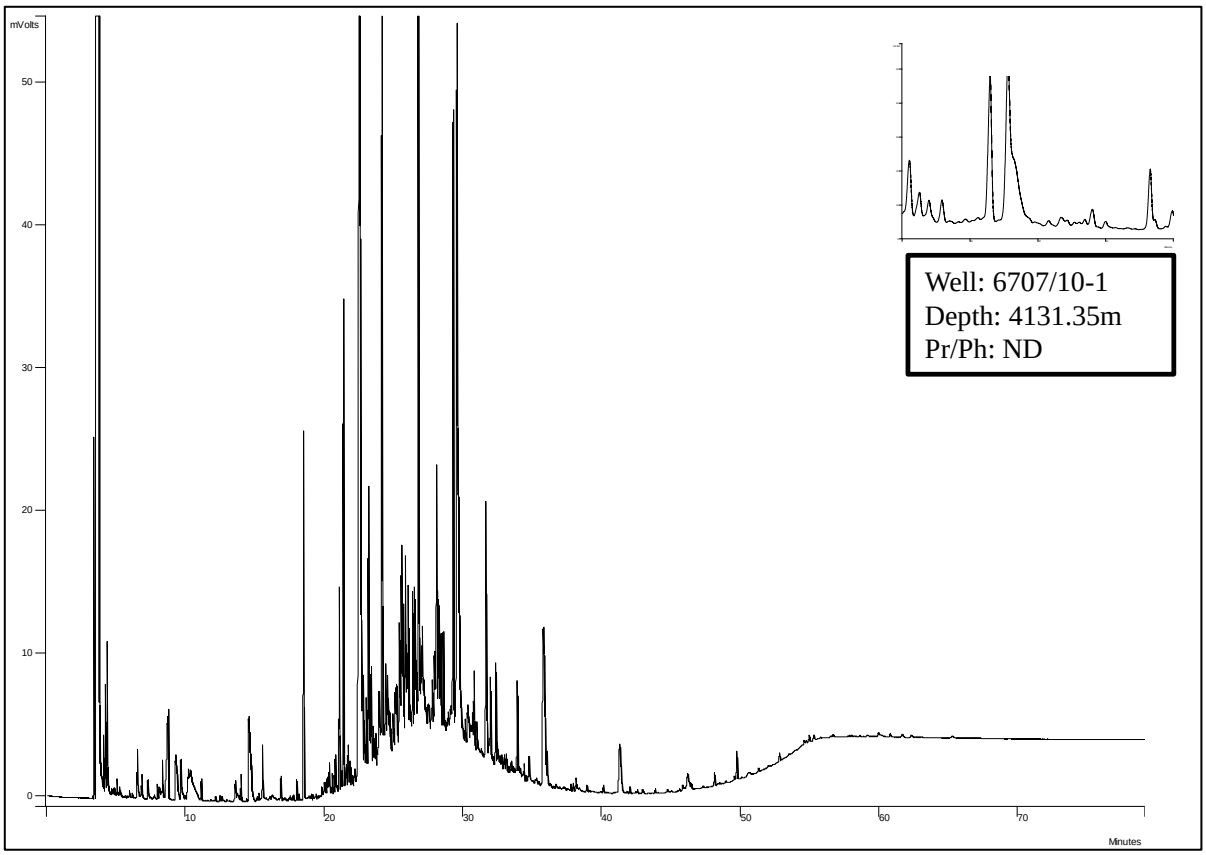
mVolts
50
40
30
20
10
0
10
20
30
40
50
60
70
Minutes
Well: 6707/10-1
Depth: 4131.35m
Pr/Ph: ND

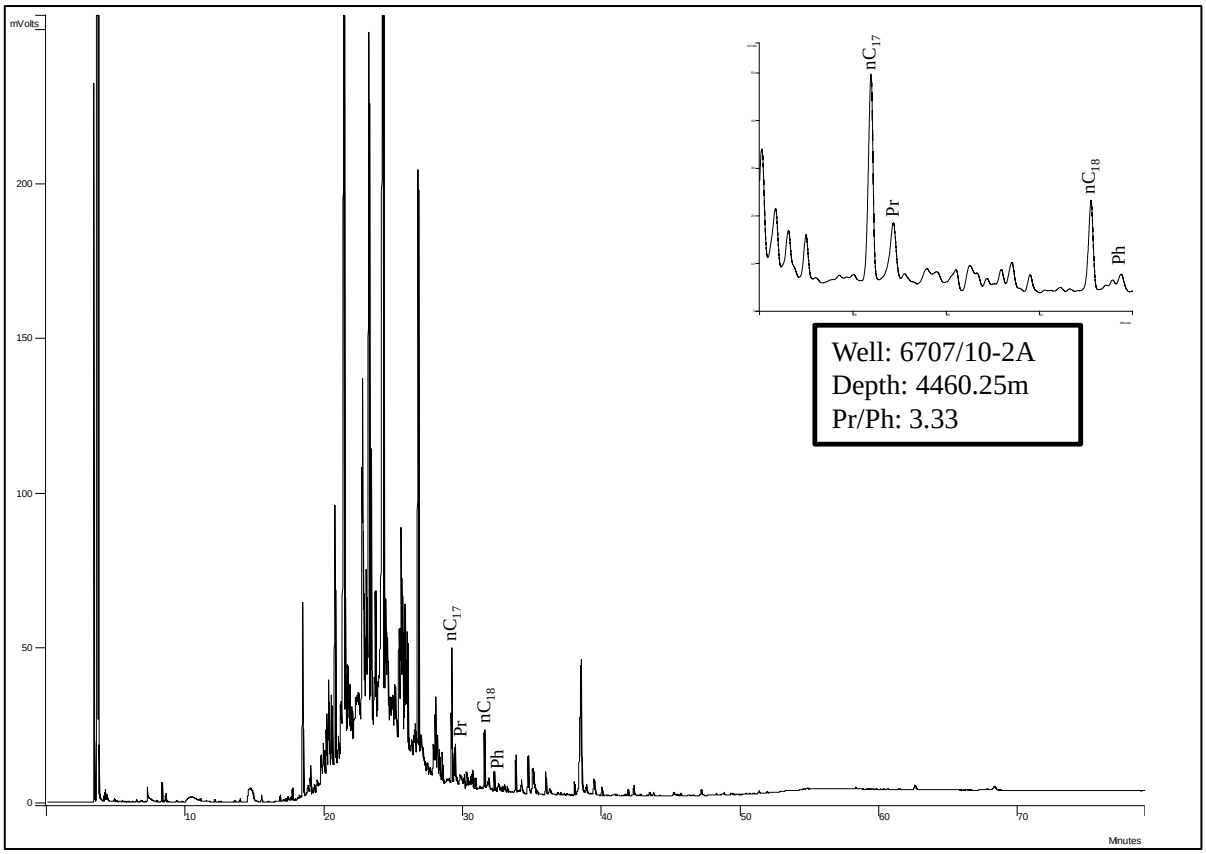
mVolts
200
150
100
50
0
10
20
30
40
50
60
70
Minutes
nC17
Pr
nC18
Ph
nC17
Pr
nC18
Ph
Well: 6707/10-2A
Depth: 4460.25m
Pr/Ph: 3.33

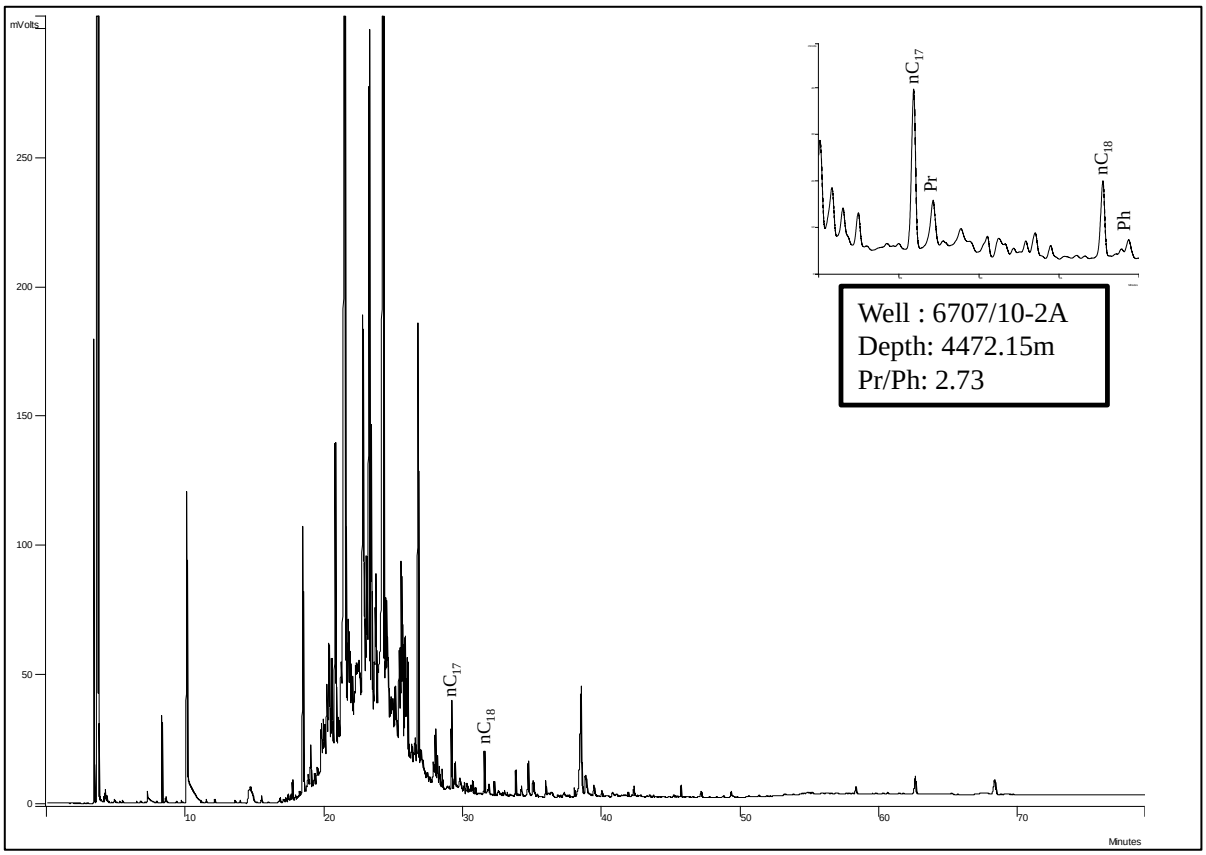
mVolts
250
200
150
100
50
0
10
20
30
40
50
60
70
Minutes
nC17
nC18
nC17
Pr
nC18
Ph
Well : 6707/10-2A
Depth: 4472.15m
Pr/Ph: 2.73

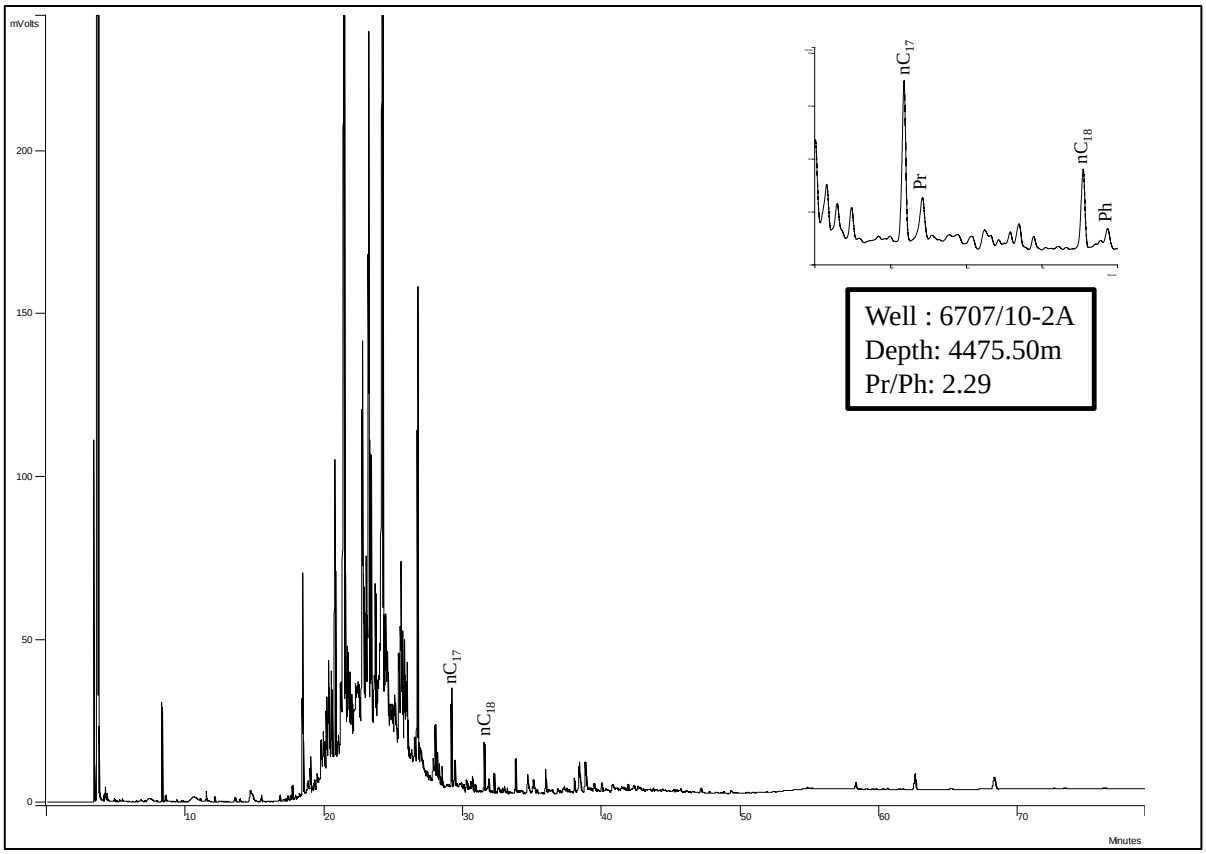
mVolts
200
150
100
50
0
nC17
nC18
10
20
30
40
50
60
70
Minutes
nC17
Pr
nC18
Ph
Well : 6707/10-2A
Depth: 4475.50m
Pr/Ph: 2.29

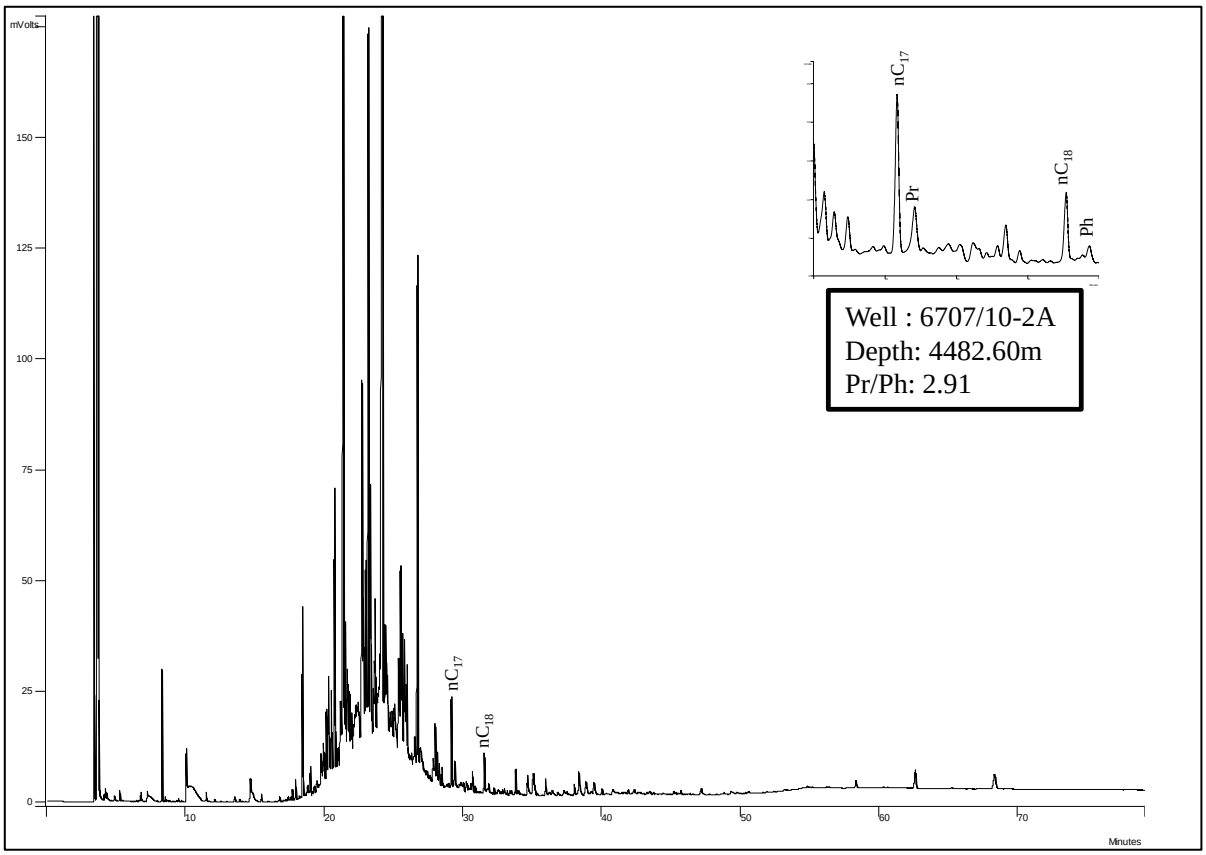
mVolts
150
125
100
75
50
25
0
nC17
nC18
10
20
30
40
50
60
70
Minutes
nC17
Pr
nC18
Ph
Well : 6707/10-2A
Depth: 4482.60m
Pr/Ph: 2.91

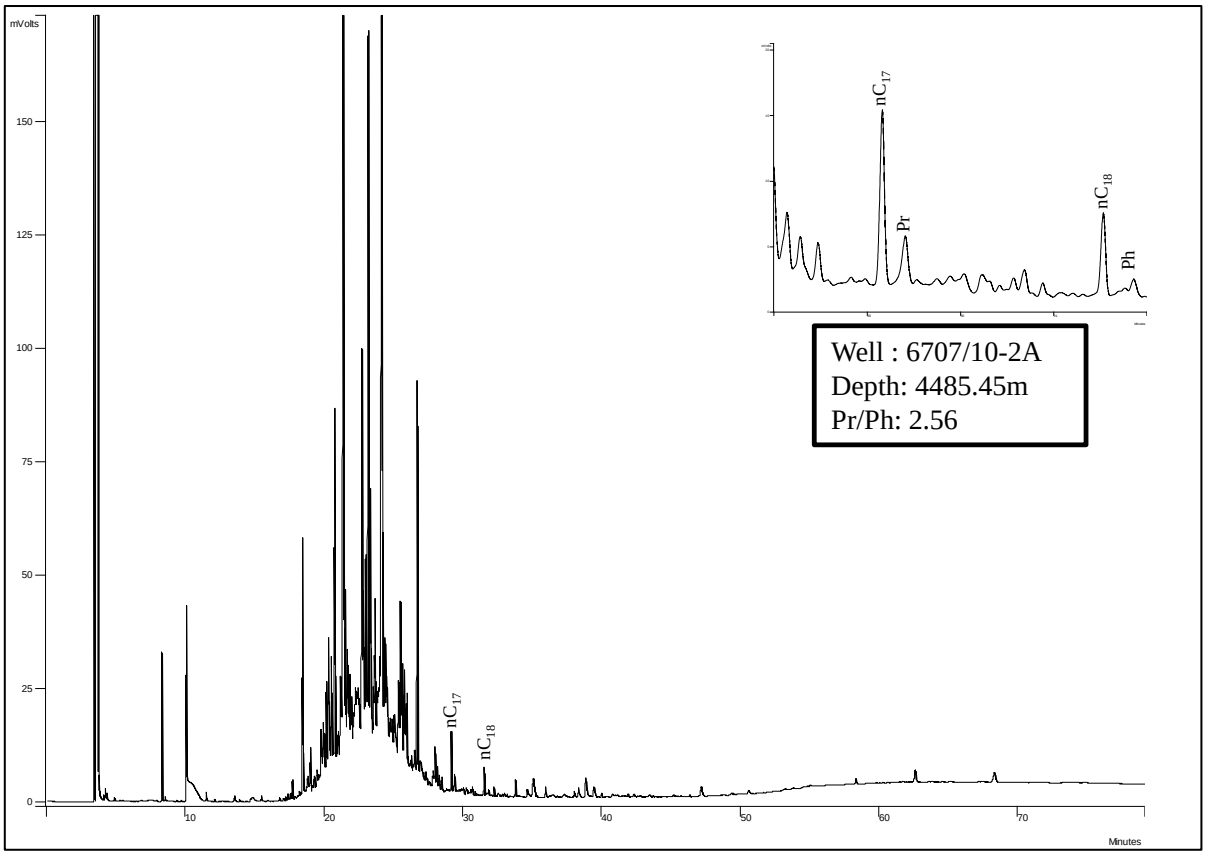
mVolts
150
125
100
75
50
25
0
nC17
nC18
10
20
30
40
50
60
70
Minutes
nC17
Pr
nC18
Ph
Well : 6707/10-2A
Depth: 4485.45m
Pr/Ph: 2.56

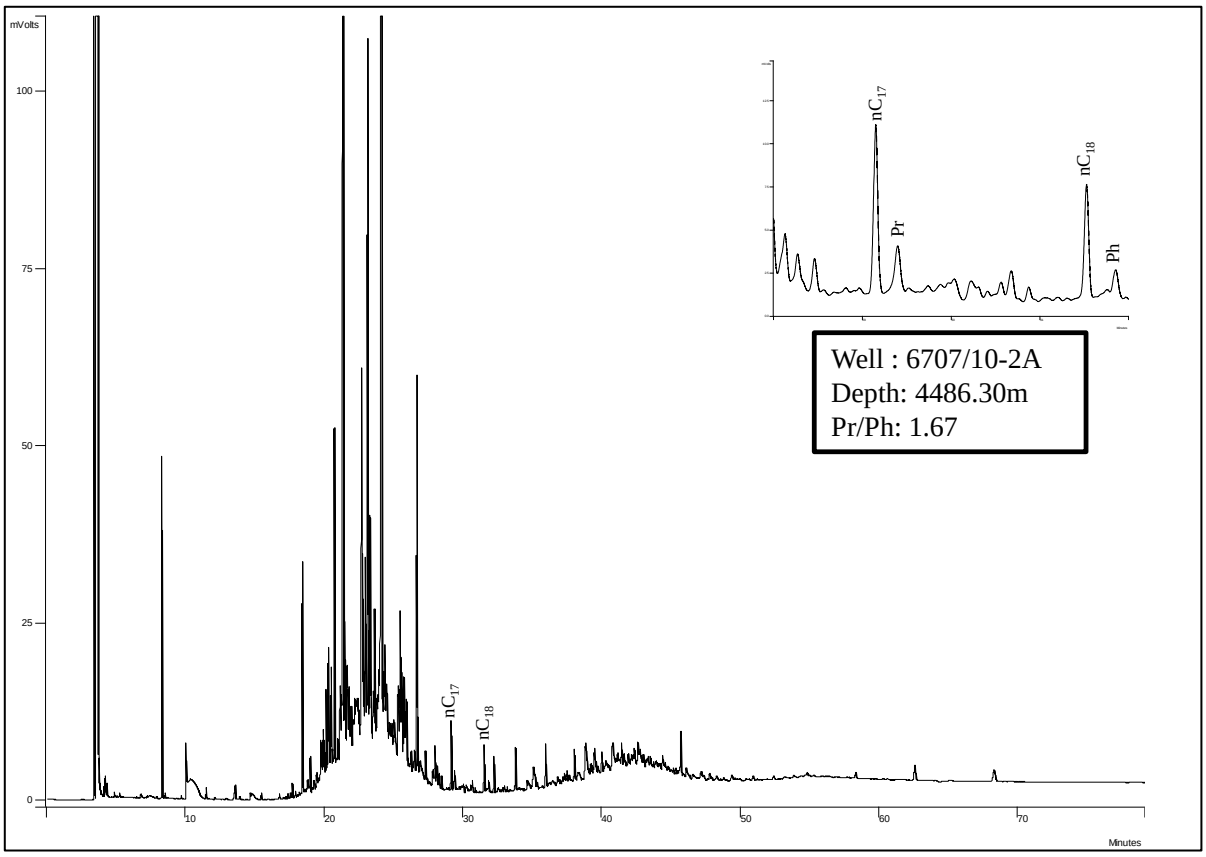
mVolts
100
75
50
25
0
nC17
nC18
10
20
30
40
50
60
70
Minutes
nC17
Pr
nC18
Ph
Well : 6707/10-2A
Depth: 4486.30m
Pr/Ph: 1.67

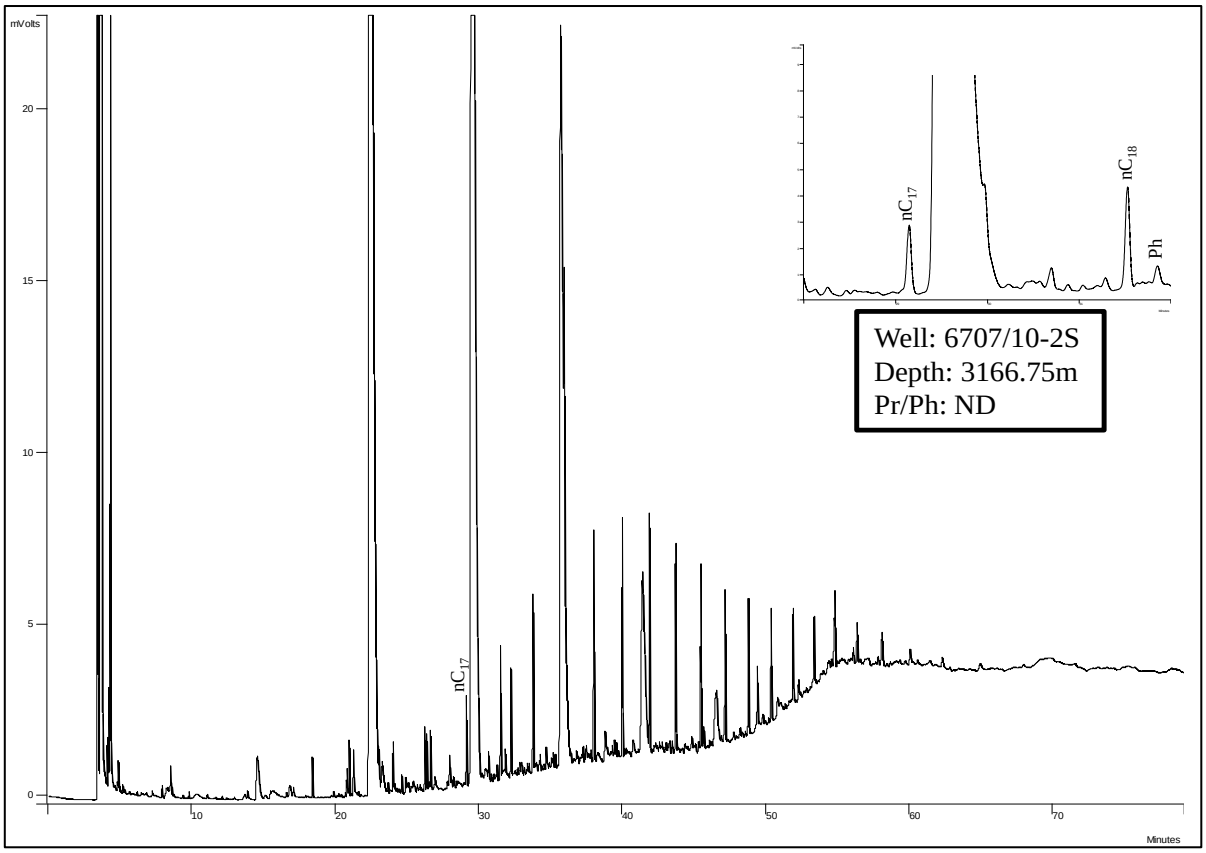
mVolts
20
15
10
5
0
nC17
nC17
nC18
Ph
Well: 6707/10-2S
Depth: 3166.75m
Pr/Ph: ND
10
20
30
40
50
60
70
Minutes

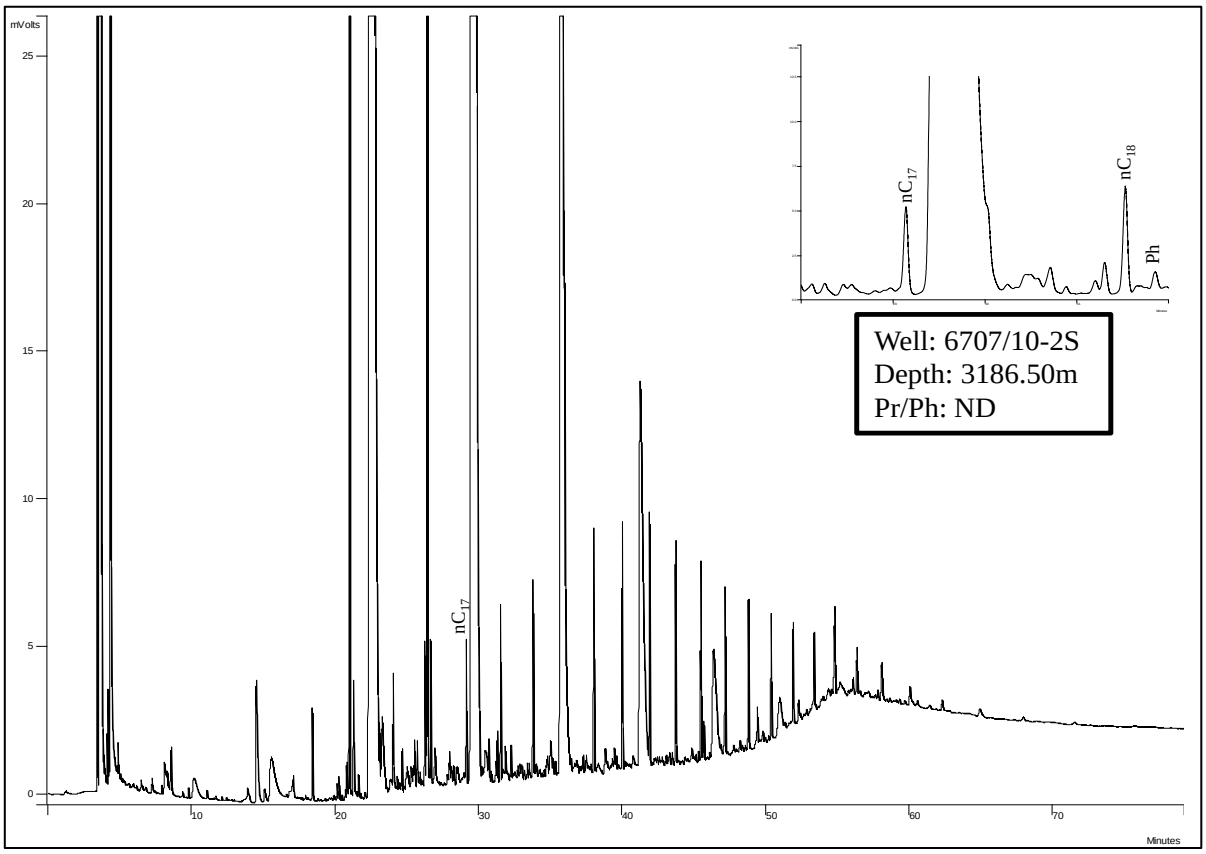
mVolts
25
20
15
10
5
0
nC17
nC17
nC18
Ph
Well: 6707/10-2S
Depth: 3186.50m
Pr/Ph: ND
10
20
30
40
50
60
70
Minutes

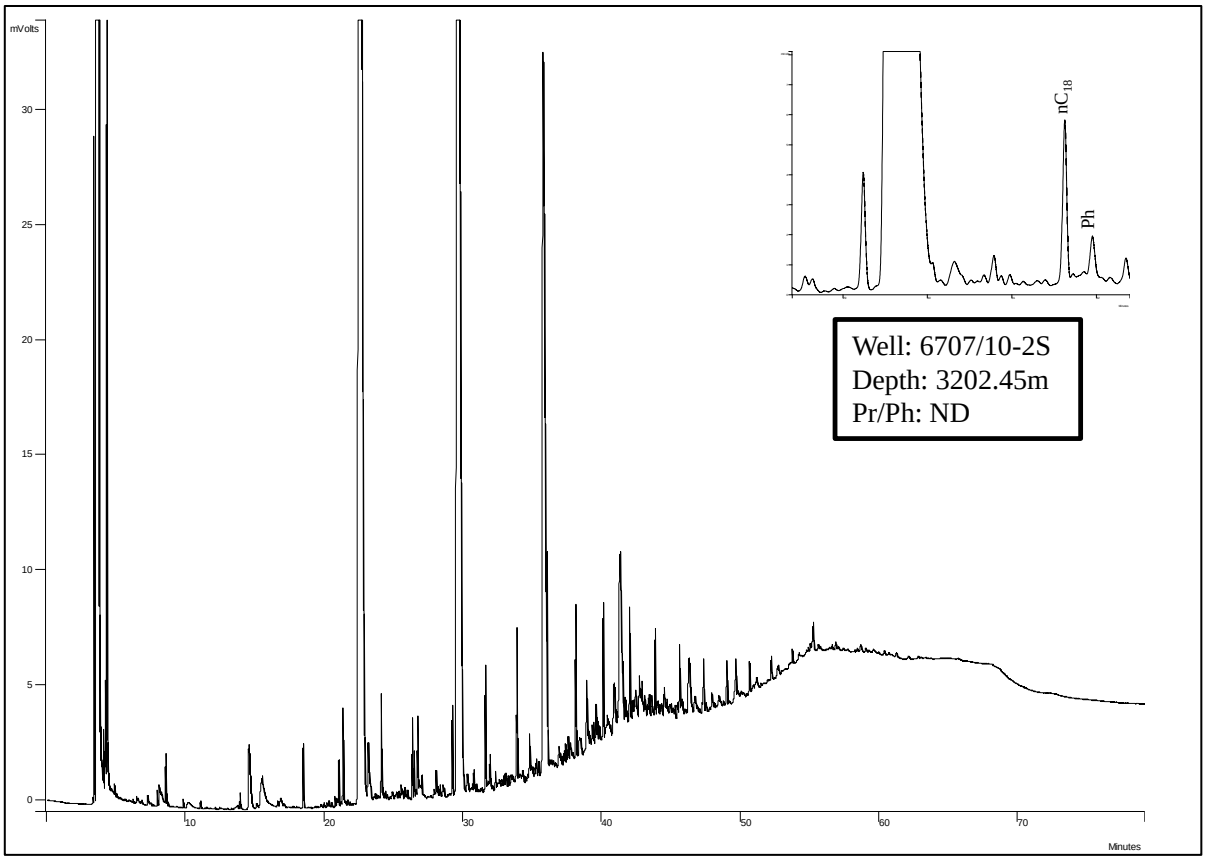
mVolts
30
25
20
15
10
5
0
10
20
30
40
50
60
70
Minutes
nC18
Ph
Well: 6707/10-2S
Depth: 3202.45m
Pr/Ph: ND

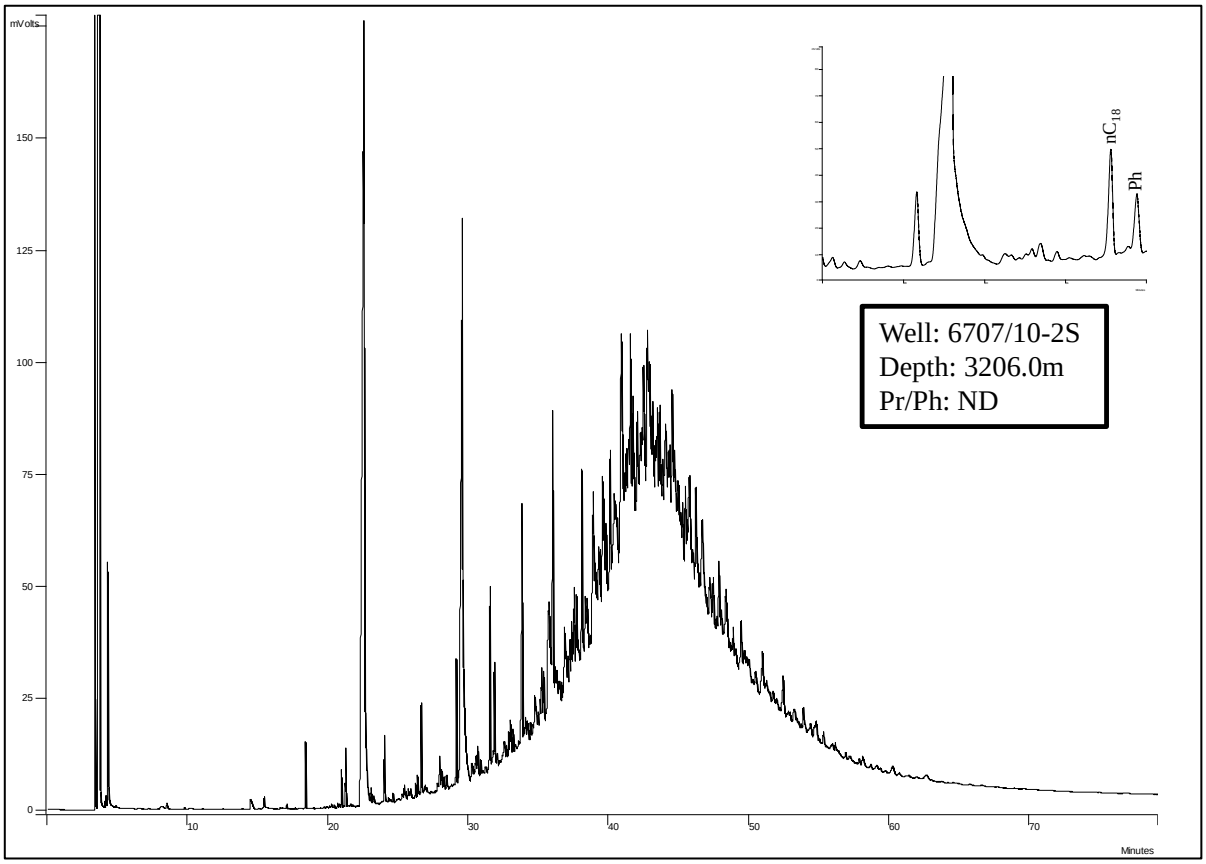
mVolts
150
125
100
75
50
25
0
10
20
30
40
50
60
70
Minutes
nC18
Ph
Well: 6707/10-2S
Depth: 3206.0m
Pr/Ph: ND

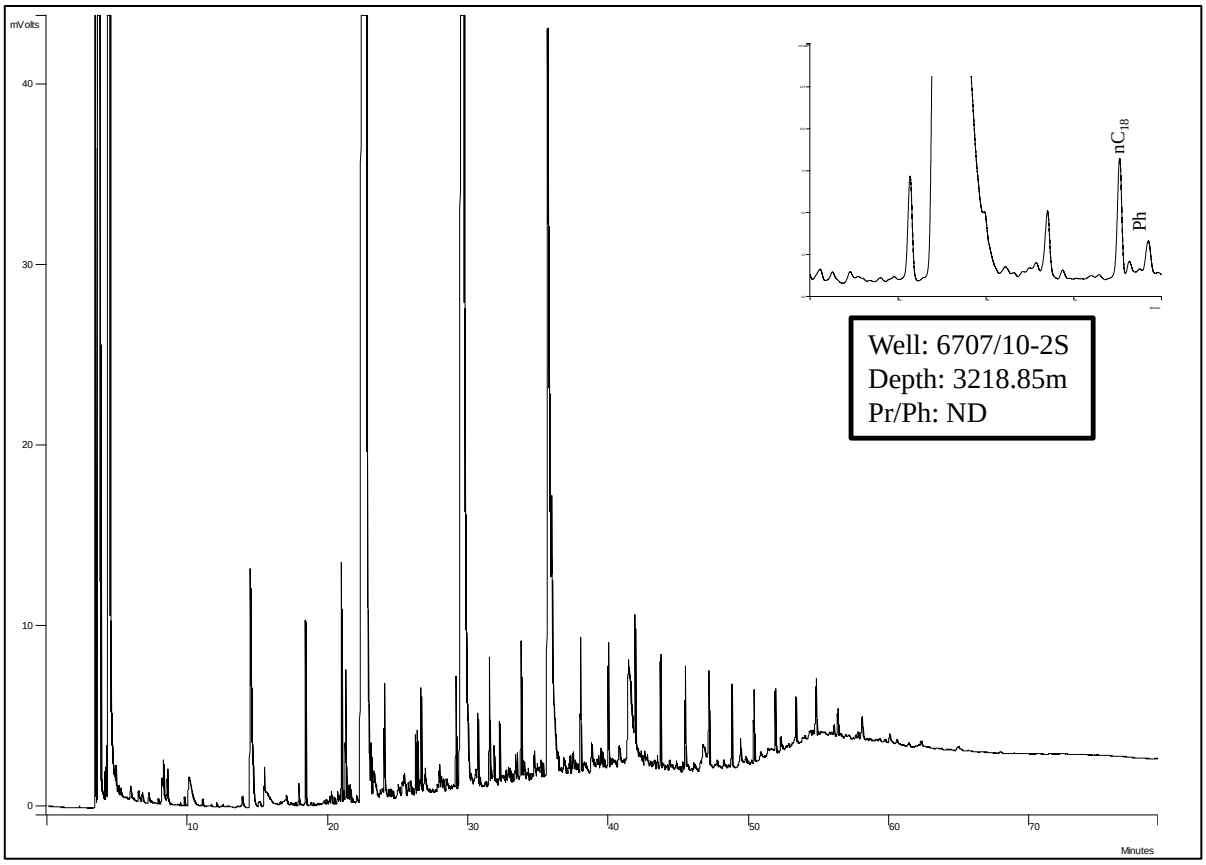
mVolts
40
30
20
10
0
10
20
30
40
50
60
70
Minutes
nC18
Ph
Well: 6707/10-2S
Depth: 3218.85m
Pr/Ph: ND

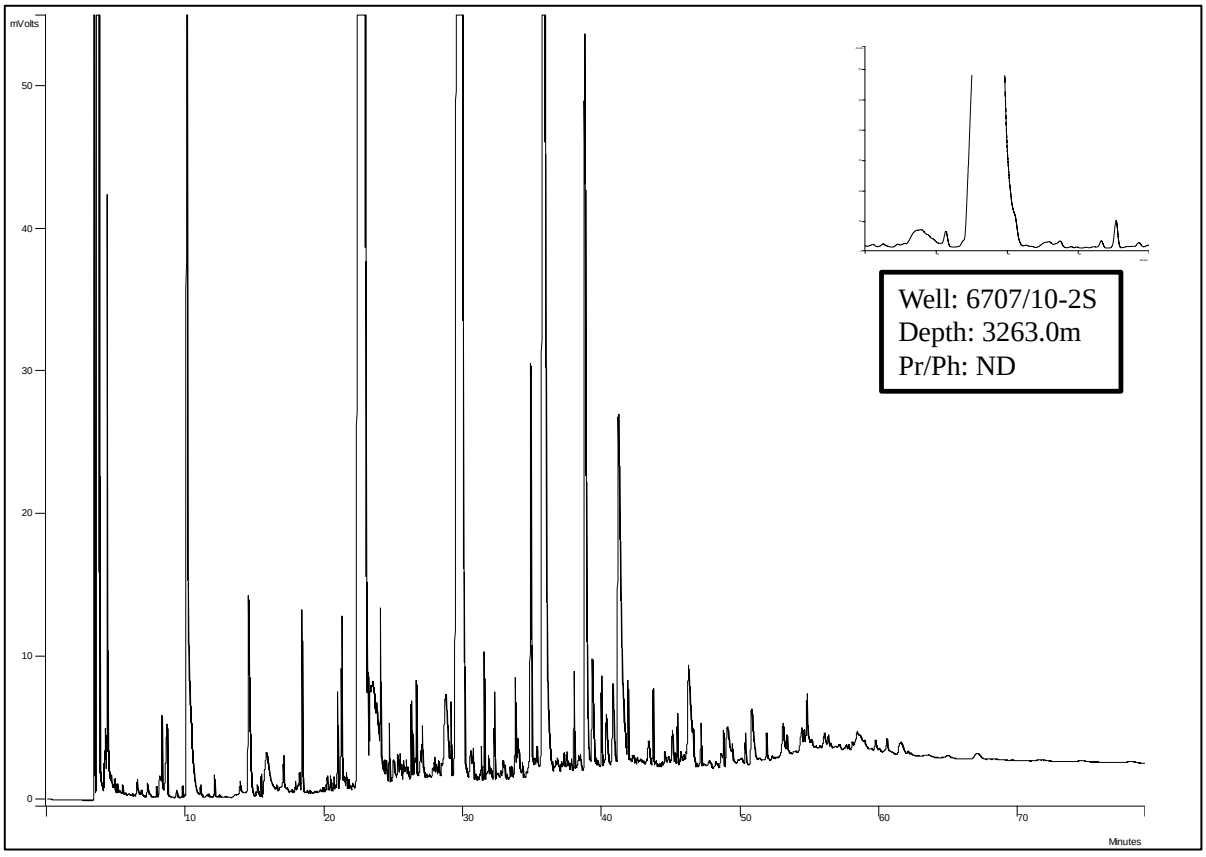
mVolts
50
40
30
20
10
0
10
20
30
40
50
60
70
Minutes
Well: 6707/10-2S
Depth: 3263.0m
Pr/Ph: ND

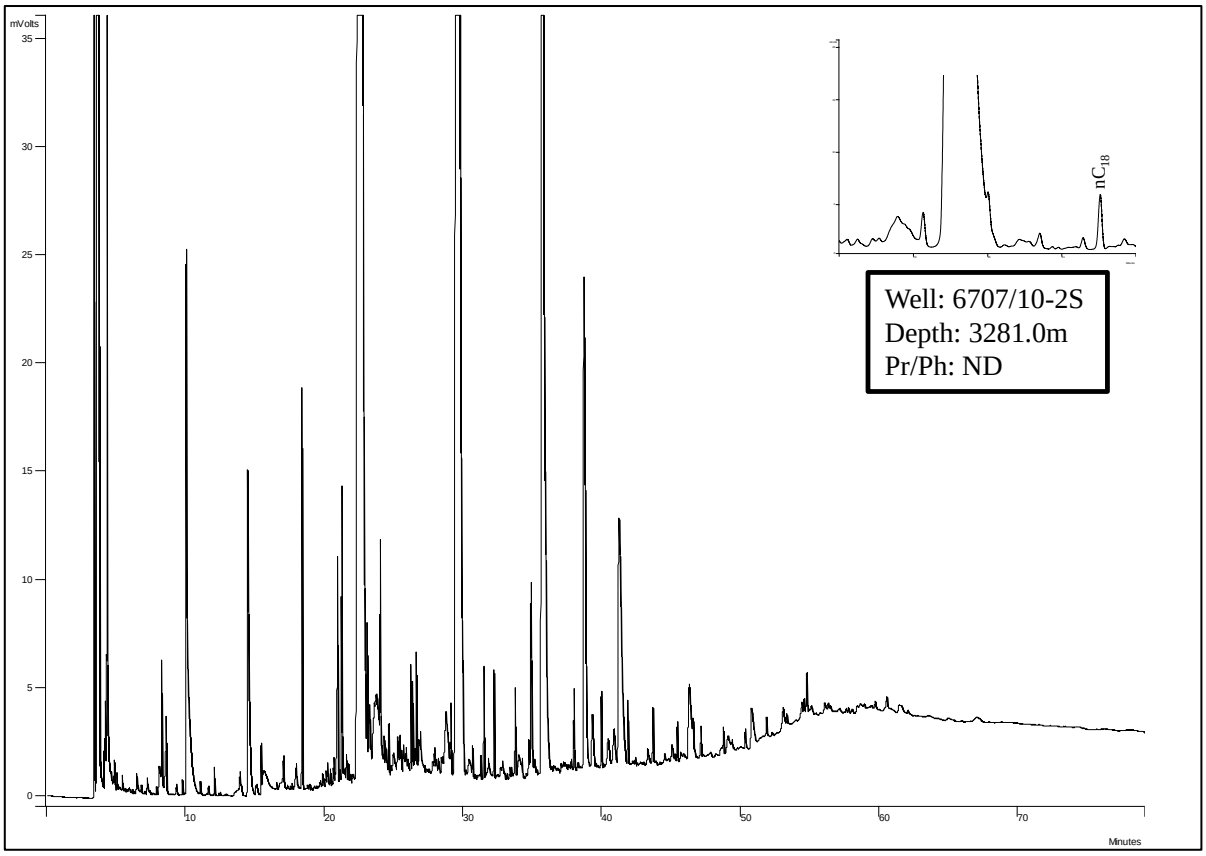
mVolts
35
30
25
20
15
10
5
0
10
20
30
40
50
60
70
Minutes
nC18
Well: 6707/10-2S
Depth: 3281.0m
Pr/Ph: ND

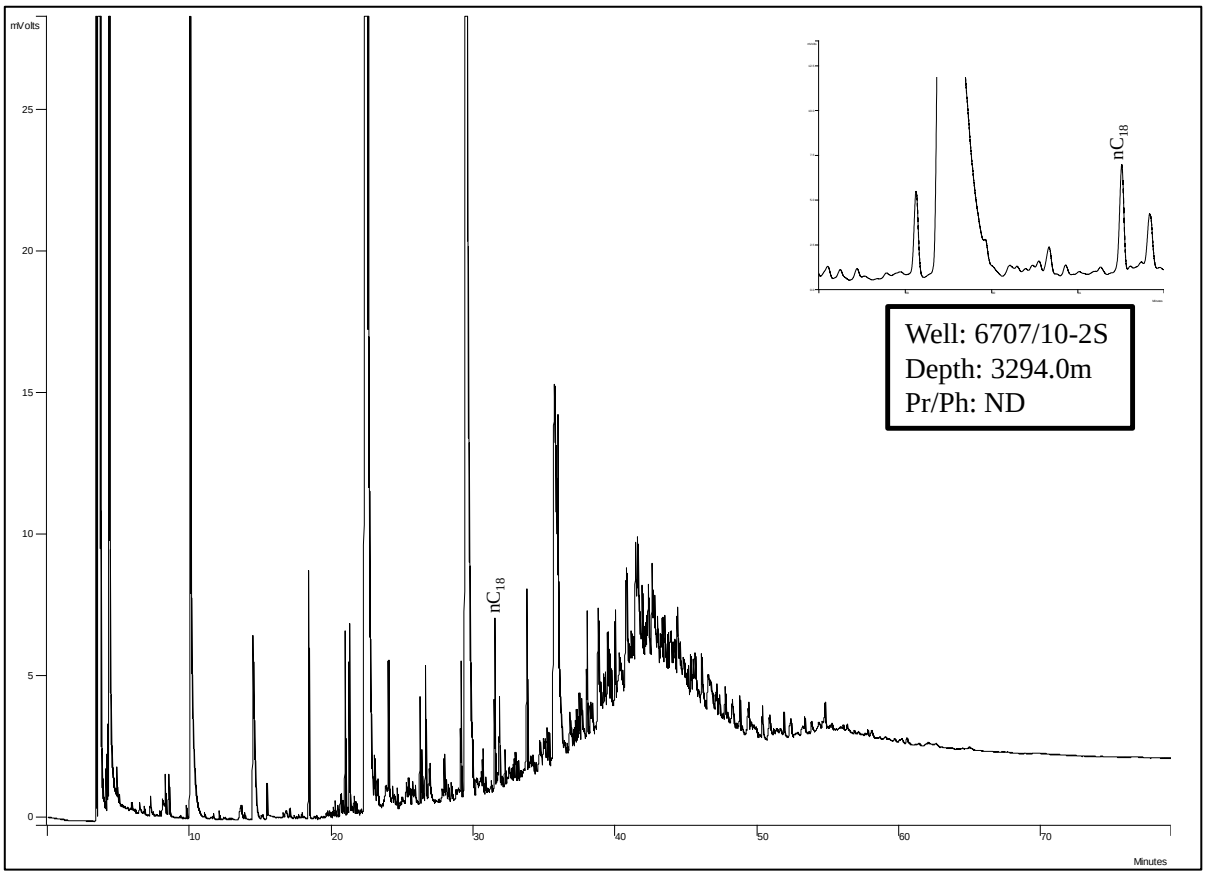
mVolts
25
20
15
10
5
0
10
20
30
40
50
60
70
Minutes
nC18
nC18
Well: 6707/10-2S
Depth: 3294.0m
Pr/Ph: ND

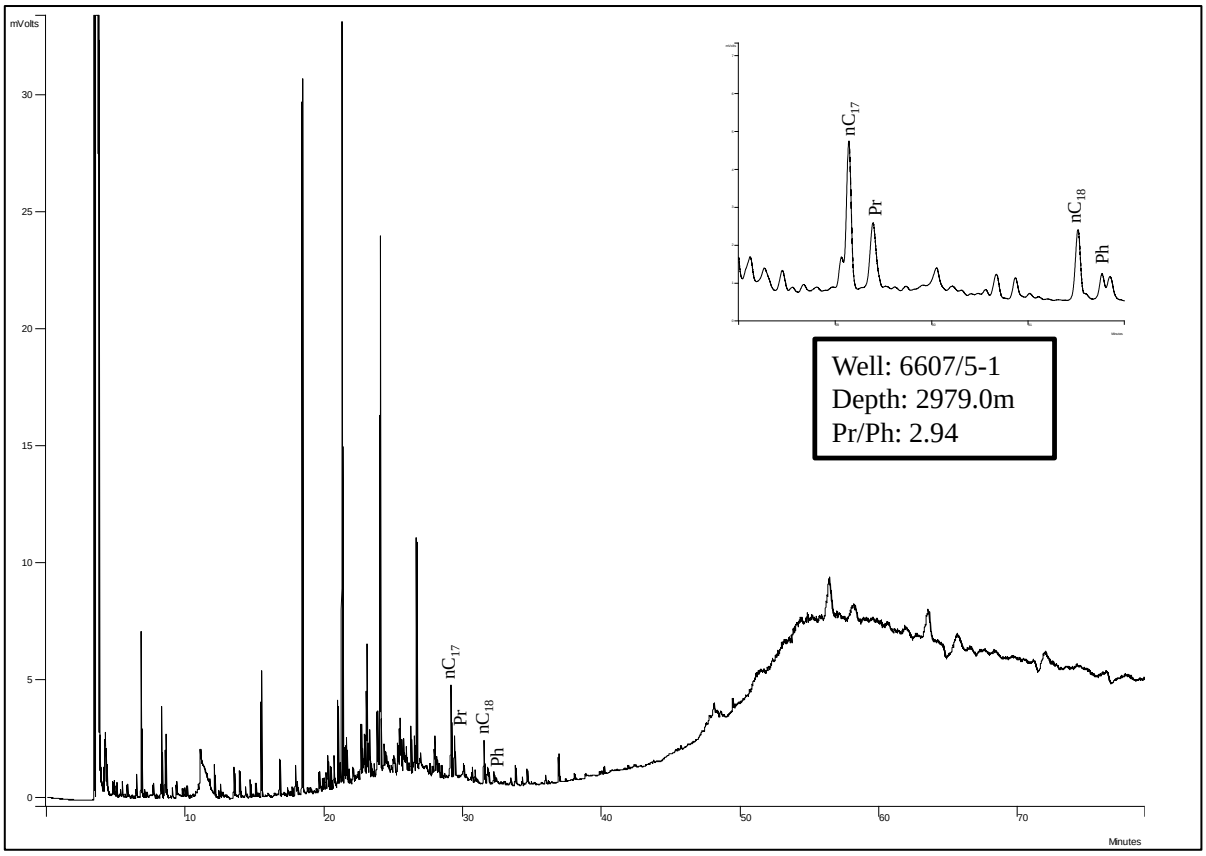
mVolts
30
25
20
15
10
5
0
nC17
Pr
nC18
Ph
10
20
30
40
50
60
70
Minutes
nC17
Pr
nC18
Ph
Well: 6607/5-1
Depth: 2979.0m
Pr/Ph: 2.94

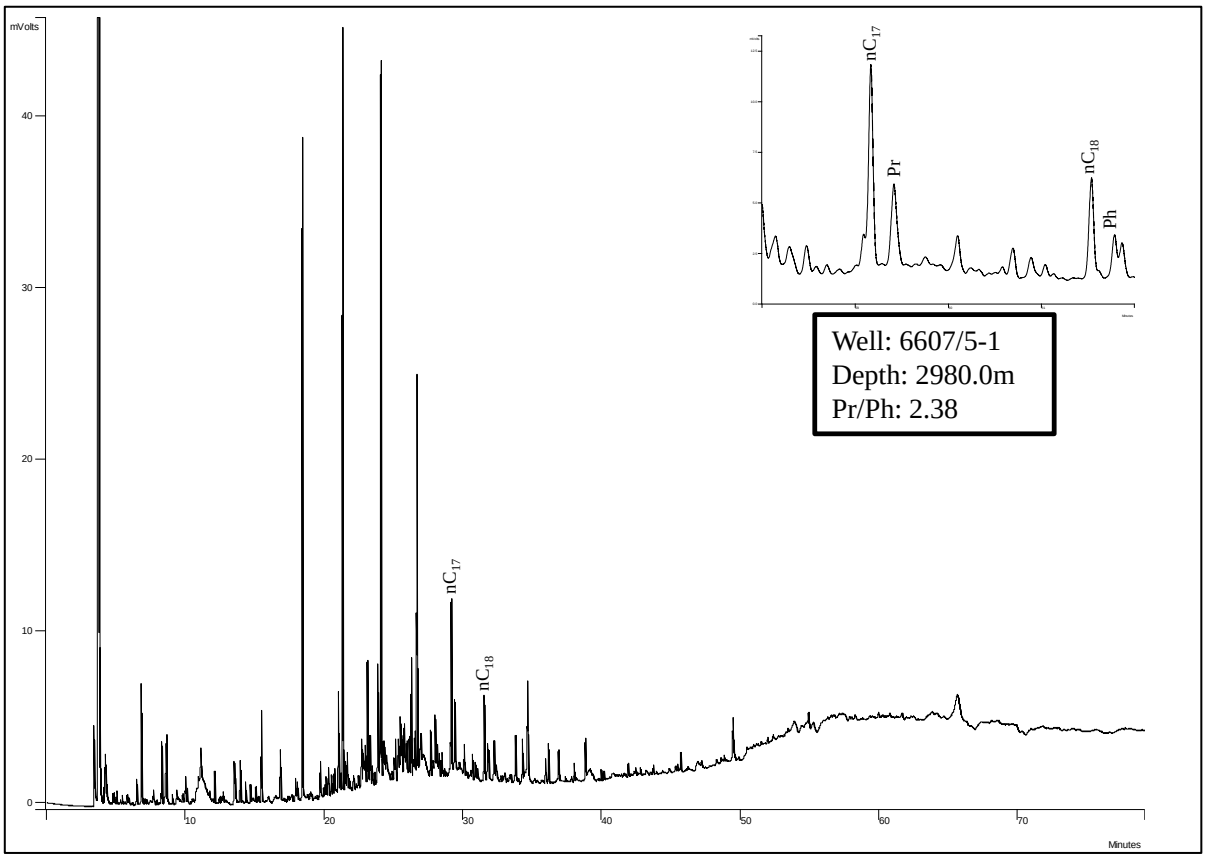
mVolts
40
30
20
10
0
nC17
nC18
10
20
30
40
50
60
70
Minutes
nC17
Pr
nC18
Ph
Well: 6607/5-1
Depth: 2980.0m
Pr/Ph: 2.38

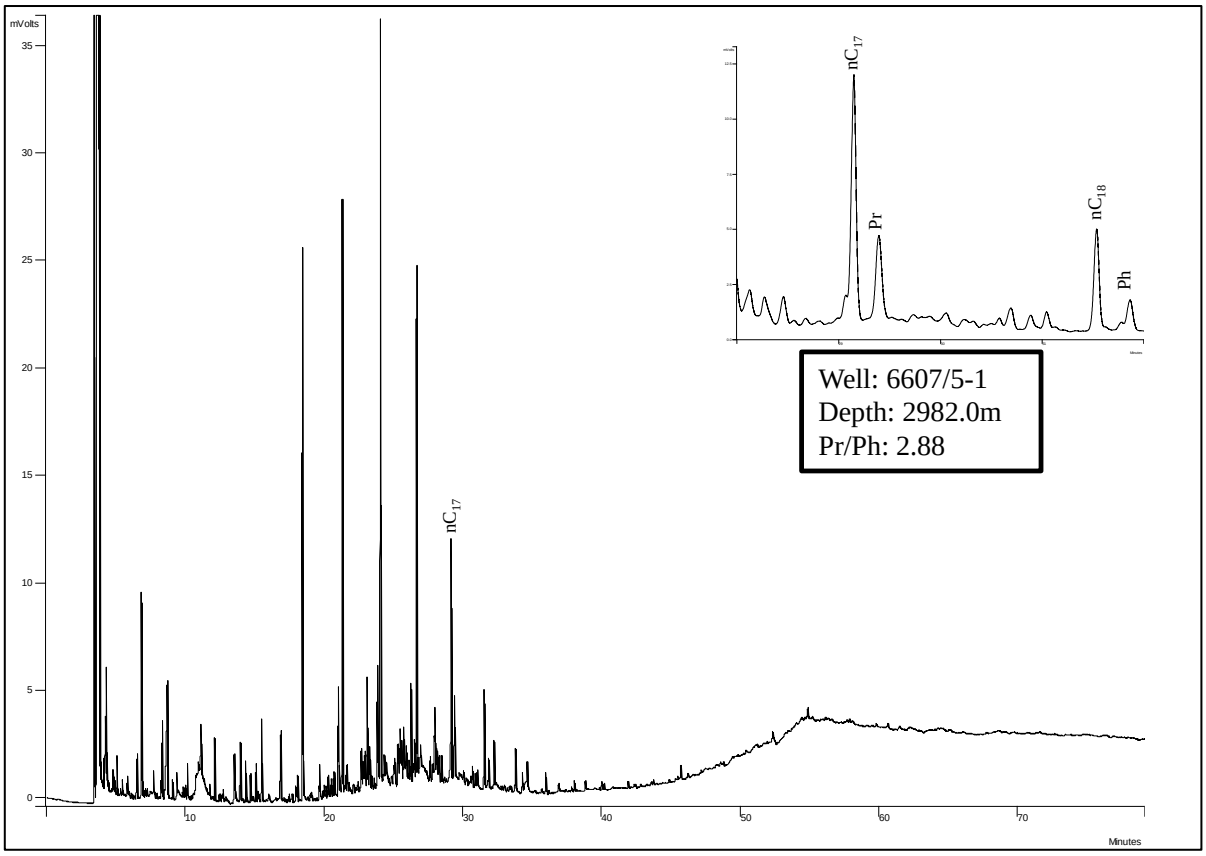
mVolts
35
30
25
20
15
10
5
0
nC17
Pr
nC18
Ph
Well: 6607/5-1
Depth: 2982.0m
Pr/Ph: 2.88
10
20
30
40
50
60
70
Minutes

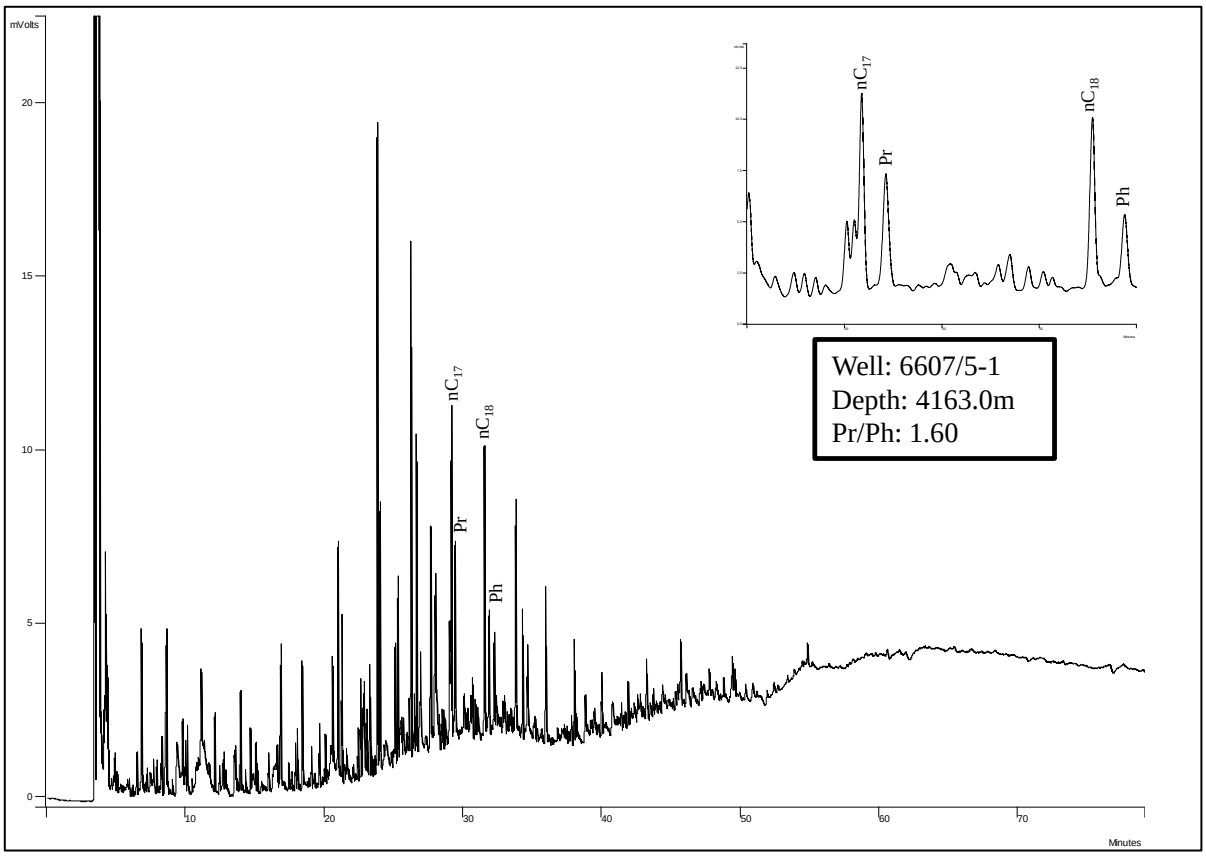
mVolts
20
15
10
5
0
nC17
nC18
Pr
Ph
Well: 6607/5-1
Depth: 4163.0m
Pr/Ph: 1.60
10
20
30
40
50
60
70
Minutes

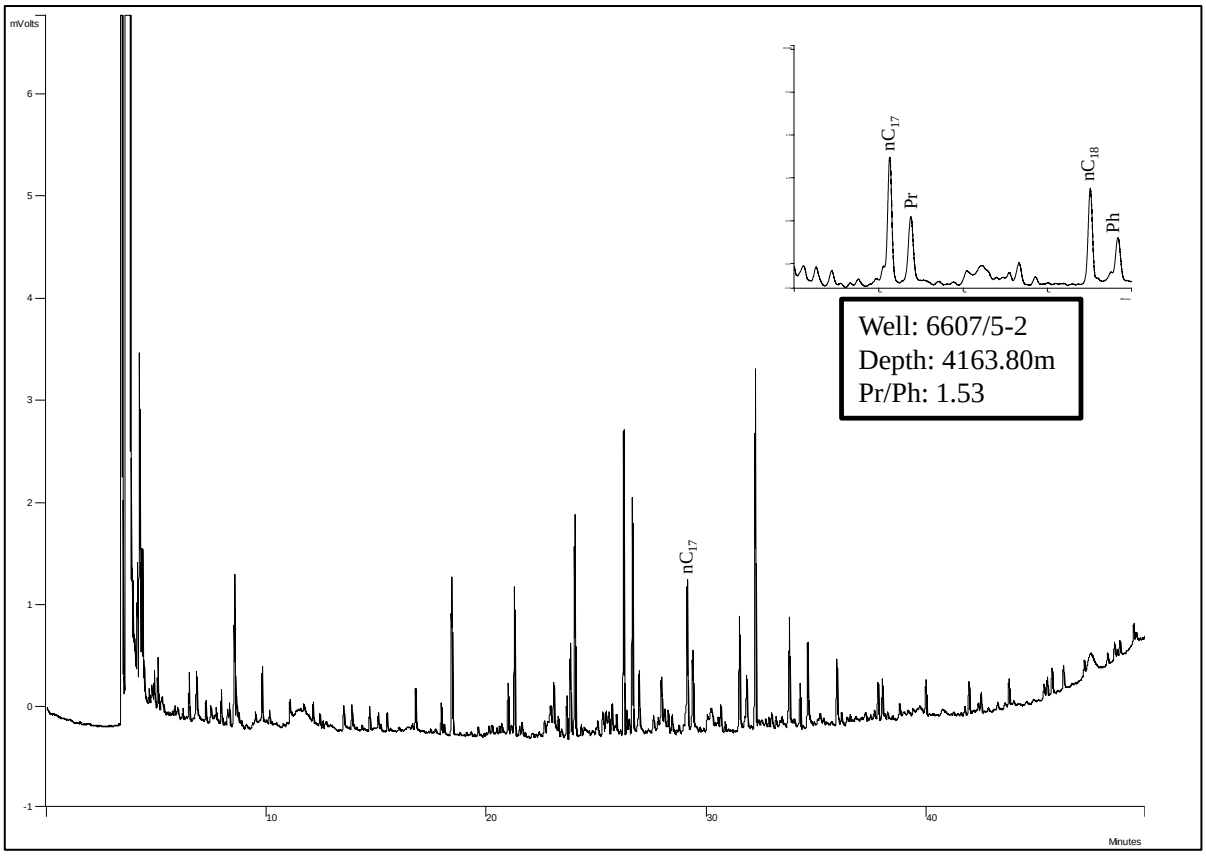
mVolts
6
5
4
3
2
1
0
-1
10
20
30
40
Minutes
nC17
Pr
nC18
Ph
Well: 6607/5-2
Depth: 4163.80m
Pr/Ph: 1.53

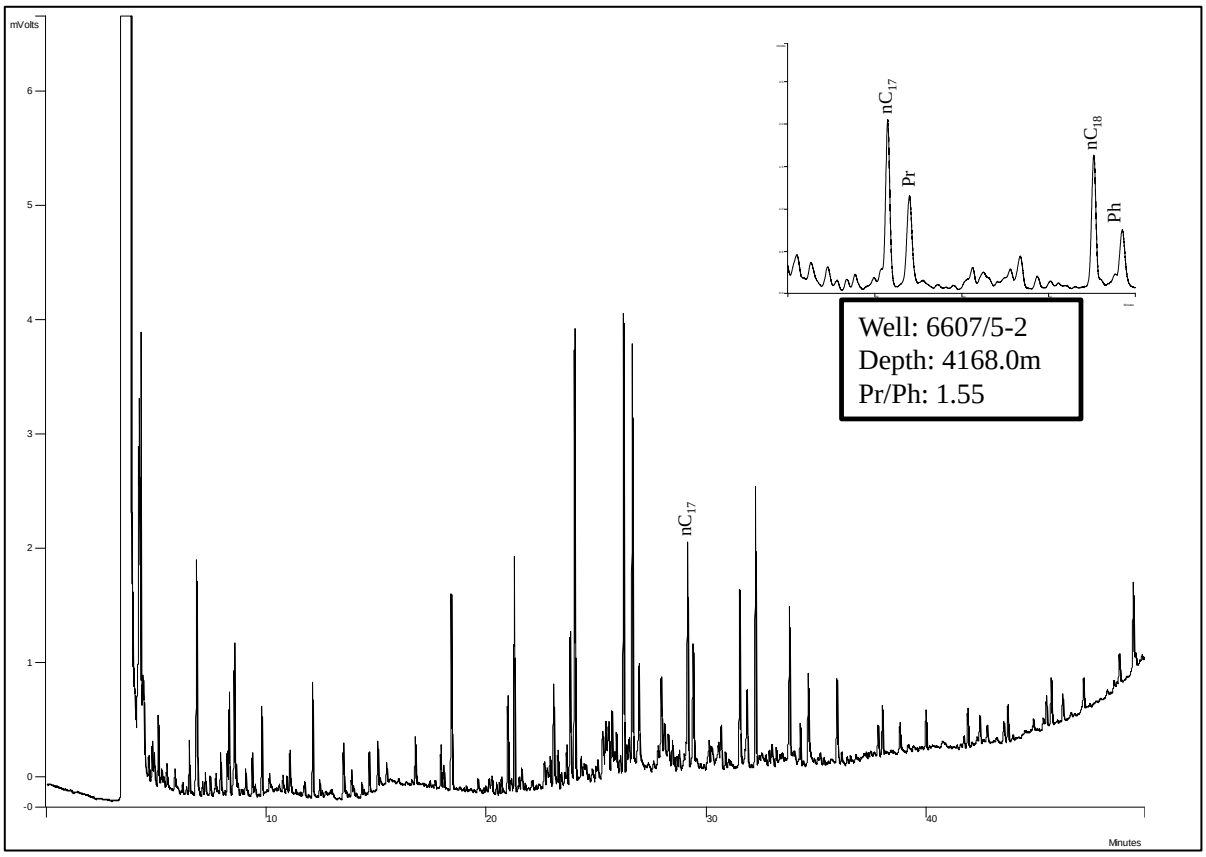
mVolts
6
5
4
3
2
1
0
-0
10
20
30
40
Minutes
nC17
Pr
nC18
Ph
Well: 6607/5-2
Depth: 4168.0m
Pr/Ph: 1.55

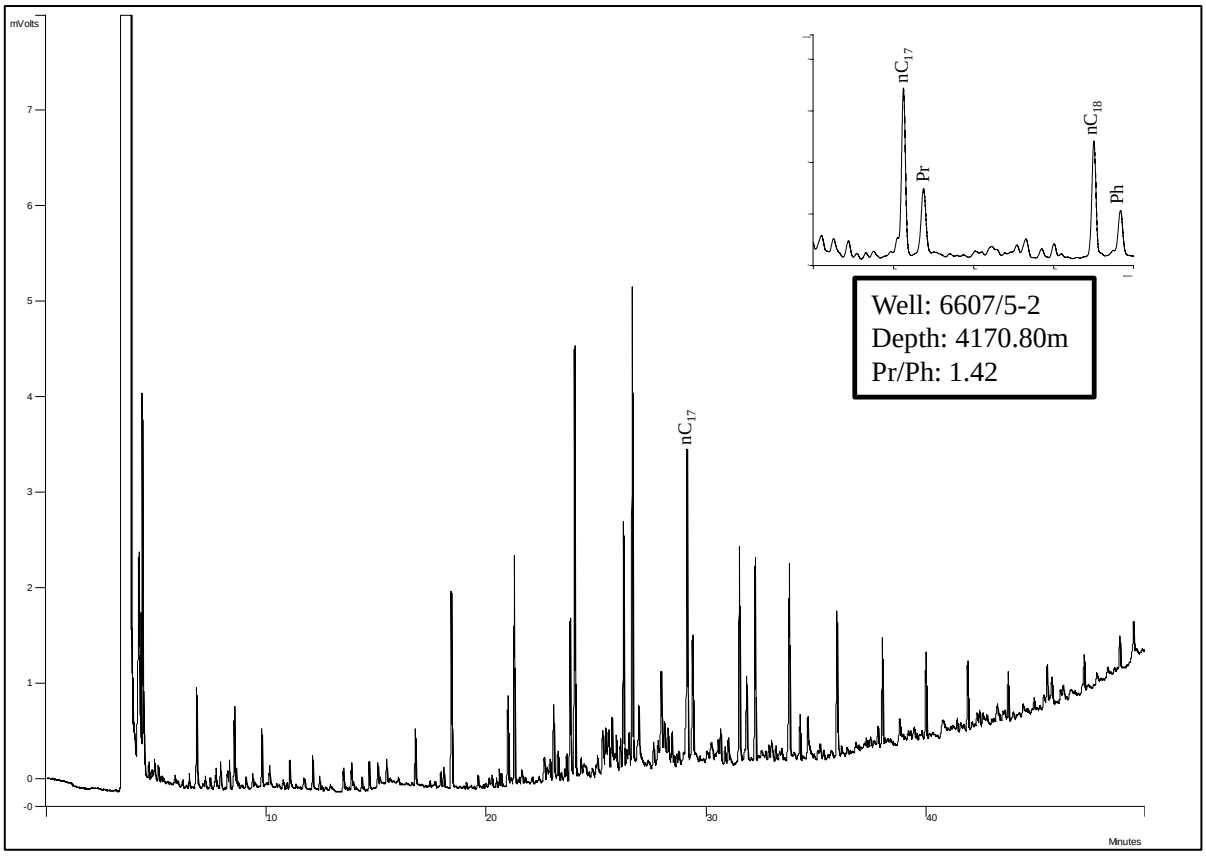
mVolts
7
6
5
4
3
2
1
0
-0
10
20
30
40
Minutes
nC17
nC17
Pr
nC18
Ph
Well: 6607/5-2
Depth: 4170.80m
Pr/Ph: 1.42

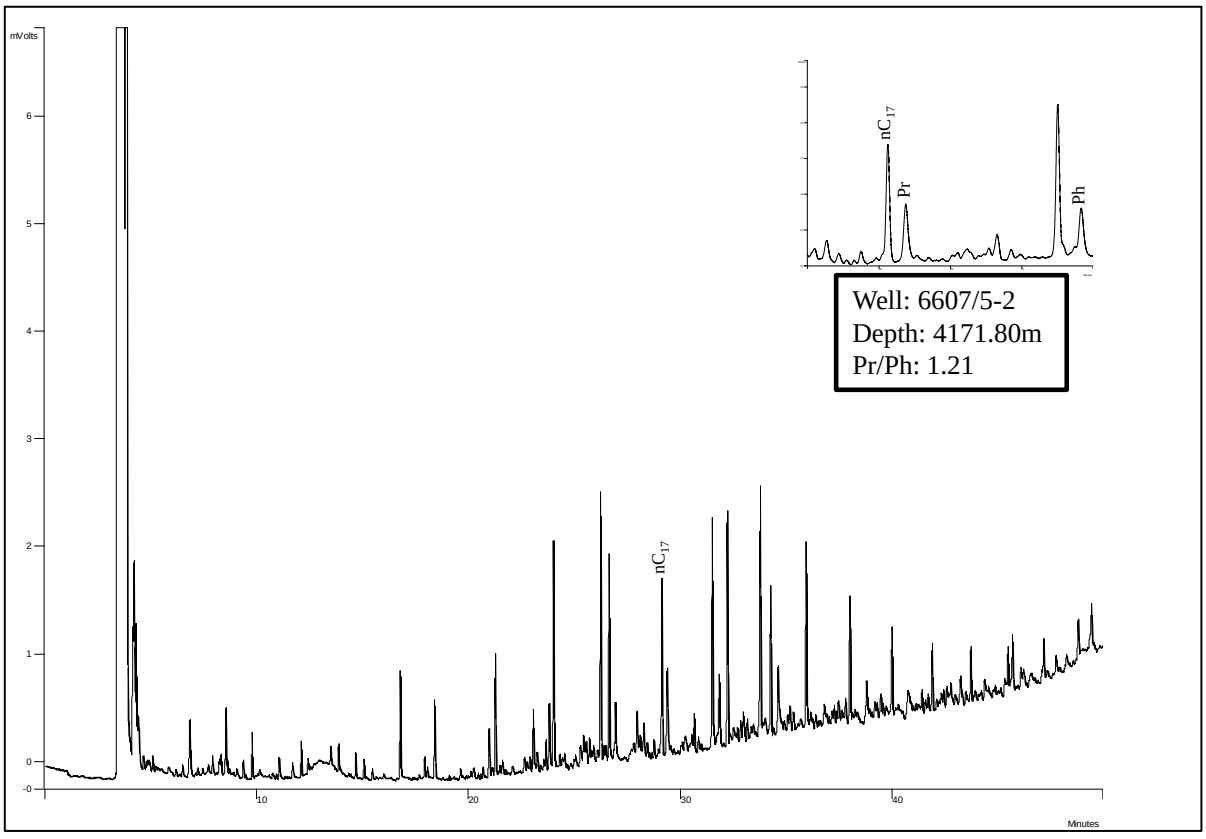
mVolts
6
5
4
3
2
1
0
-0
10
20
30
40
Minutes
nC17
nC17
Pr
Ph
Well: 6607/5-2
Depth: 4171.80m
Pr/Ph: 1.21

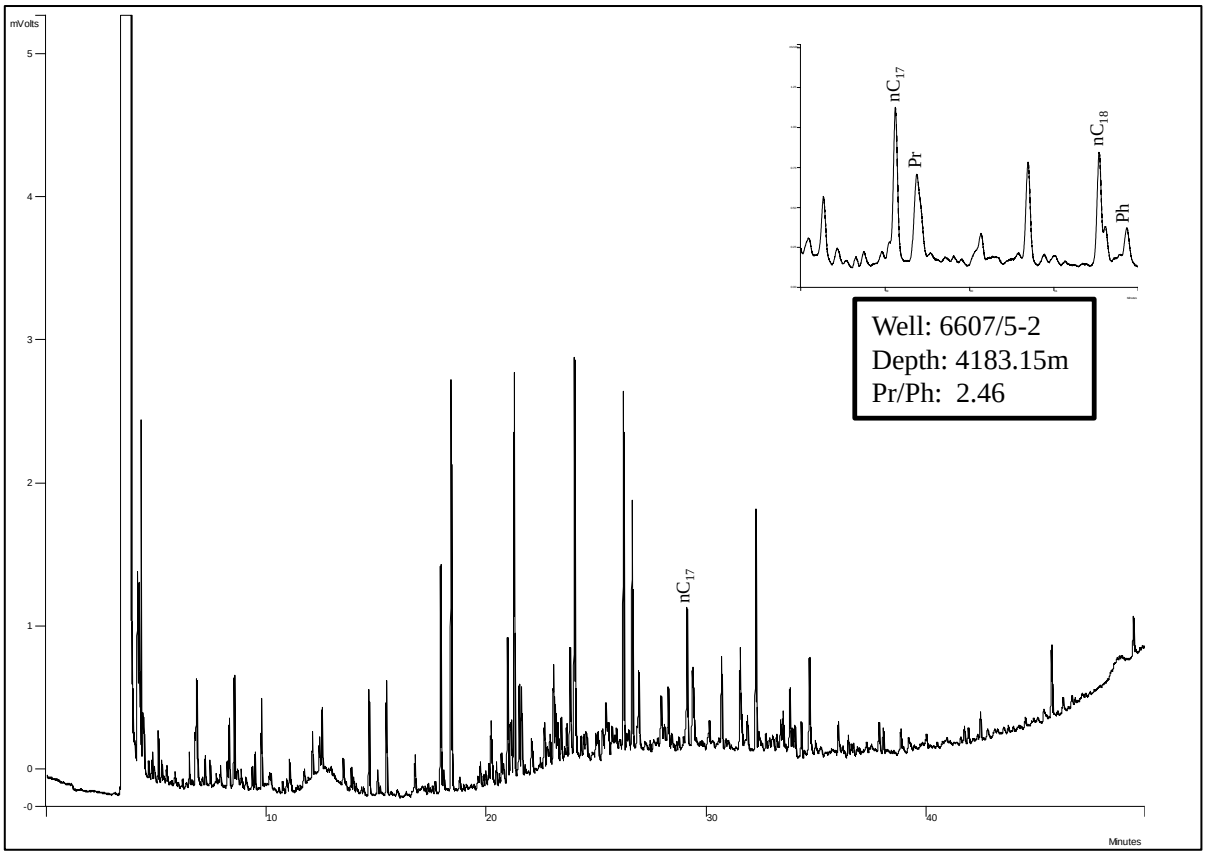
mVolts
5
4
3
2
1
0
-0
10
20
30
40
Minutes
nC17
nC17
Pr
nC18
Ph
Well: 6607/5-2
Depth: 4183.15m
Pr/Ph: 2.46

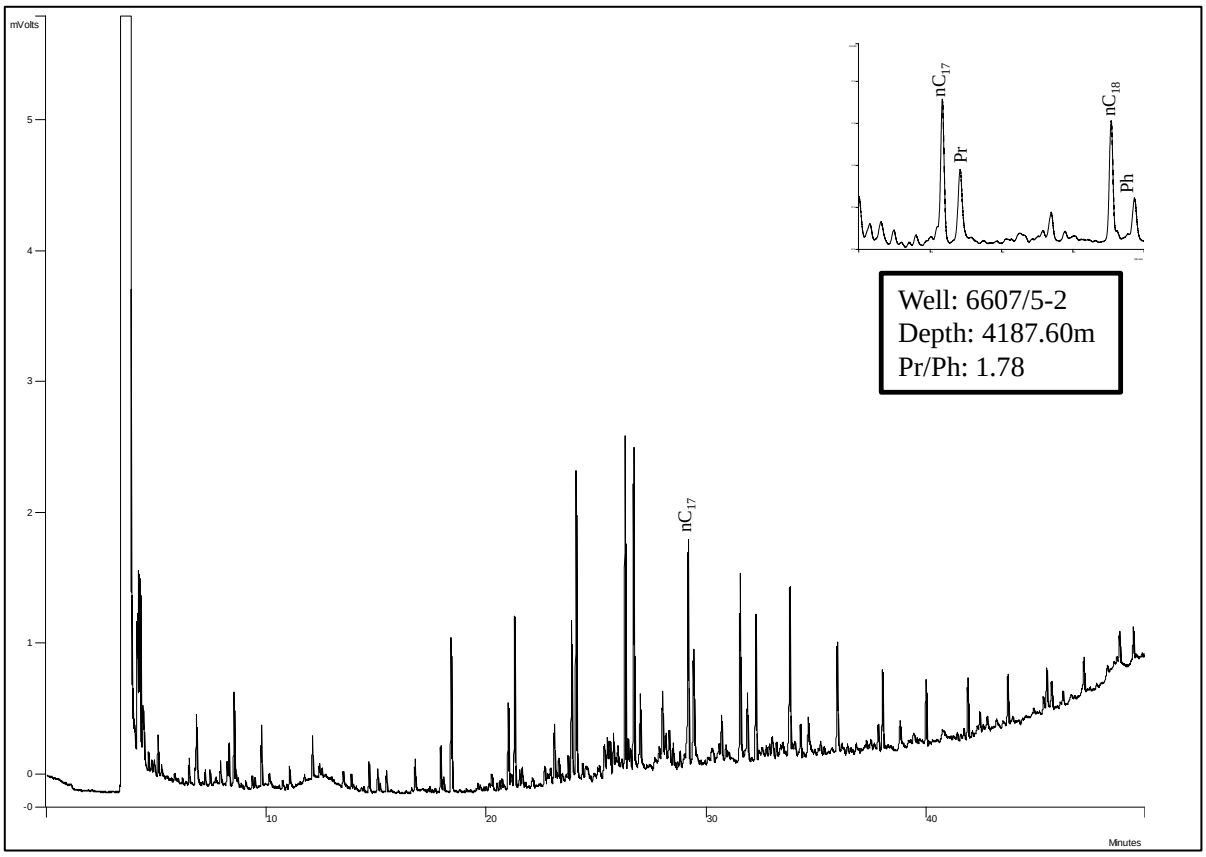
mVolts
5
4
3
2
1
0
-0
10
20
30
40
Minutes
nC17
nC17
Pr
nC18
Ph
Well: 6607/5-2
Depth: 4187.60m
Pr/Ph: 1.78

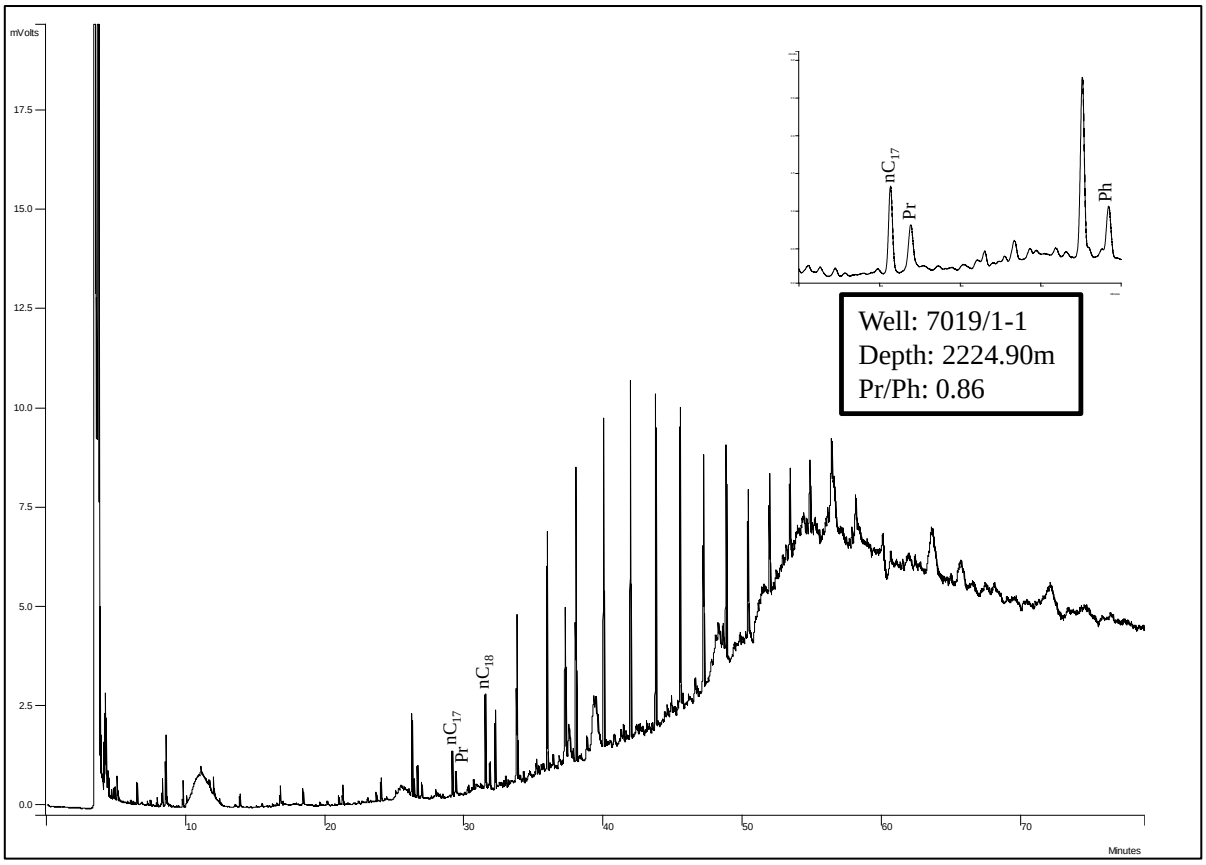
mVolts
17.5
15.0
12.5
10.0
7.5
5.0
2.5
0.0
10
20
30
40
50
60
70
Minutes
nC17
Pr
nC18
nC17
Pr
Ph
Well: 7019/1-1
Depth: 2224.90m
Pr/Ph: 0.86

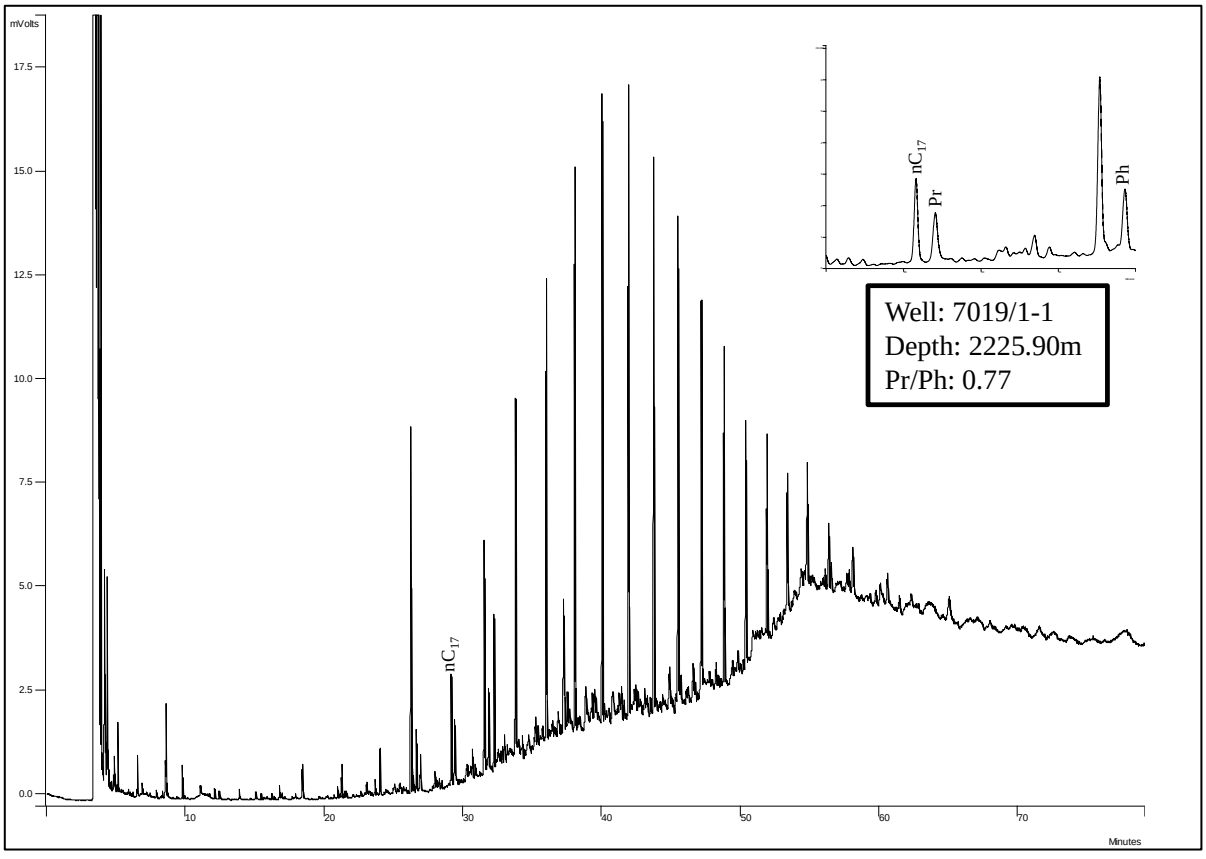
mVolts
17.5
15.0
12.5
10.0
7.5
5.0
2.5
0.0
10
20
30
40
50
60
70
Minutes
nC17
nC17
Pr
Ph
Well: 7019/1-1
Depth: 2225.90m
Pr/Ph: 0.77

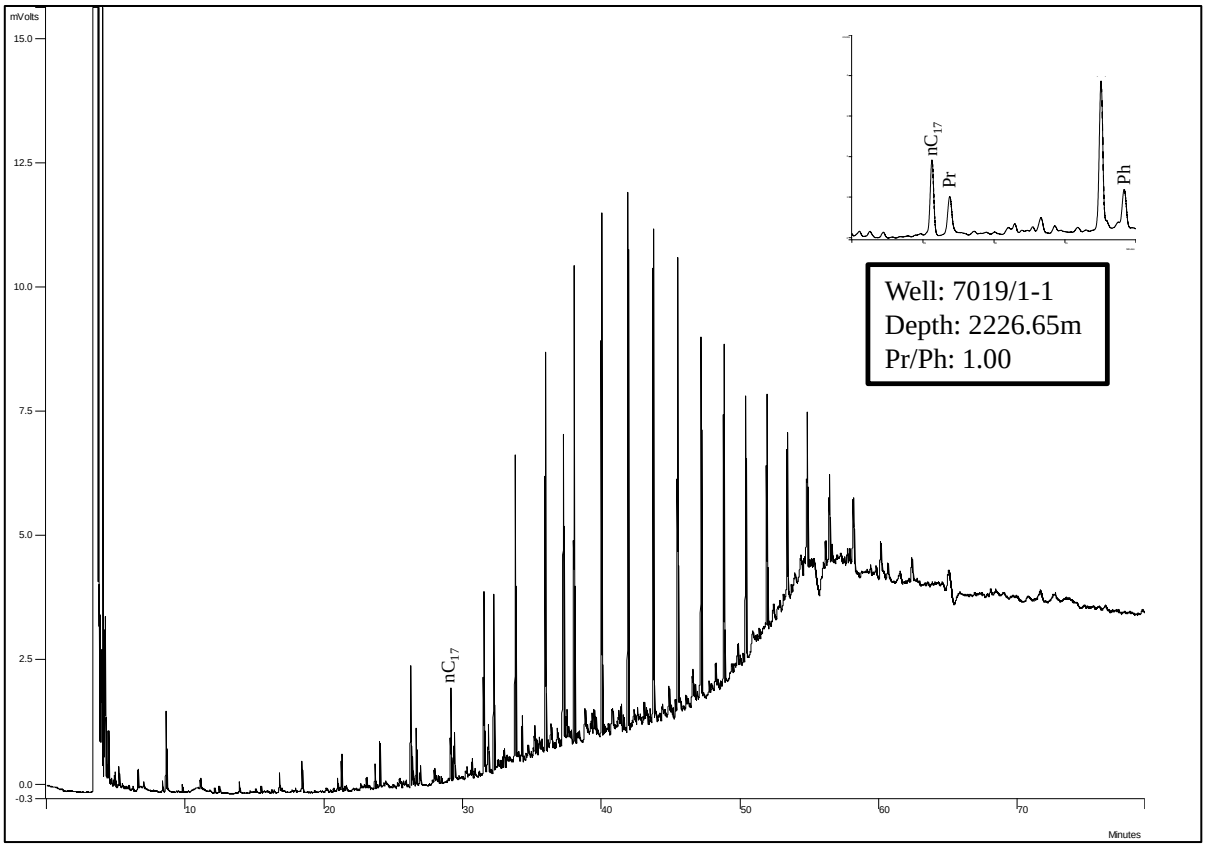
mVolts
15.0
12.5
10.0
7.5
5.0
2.5
0.0
-0.3
10
20
30
40
50
60
70
Minutes
nC17
nC17
Pr
Ph
Well: 7019/1-1
Depth: 2226.65m
Pr/Ph: 1.00

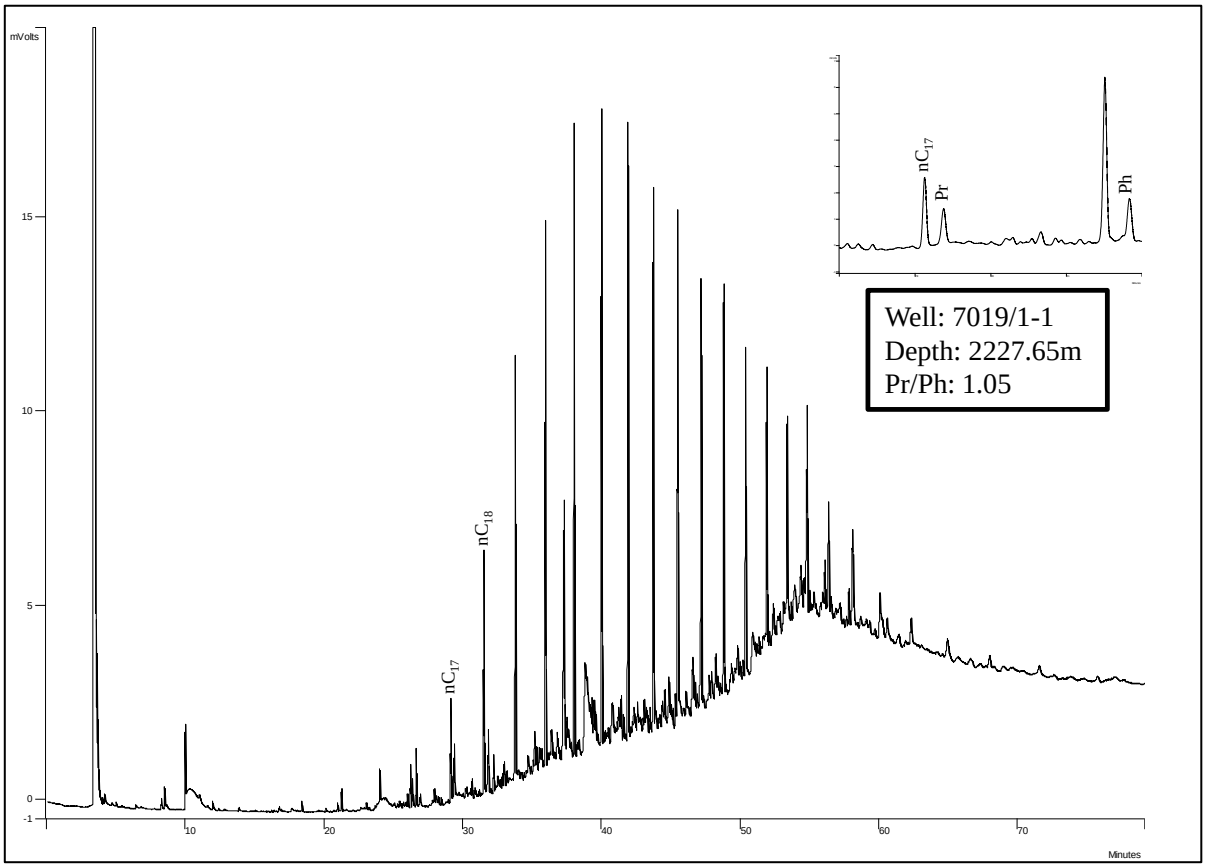
mVolts
15
10
5
0
-1
10
20
30
40
50
60
70
Minutes
nC17
nC18
nC17
Pr
Ph
Well: 7019/1-1
Depth: 2227.65m
Pr/Ph: 1.05

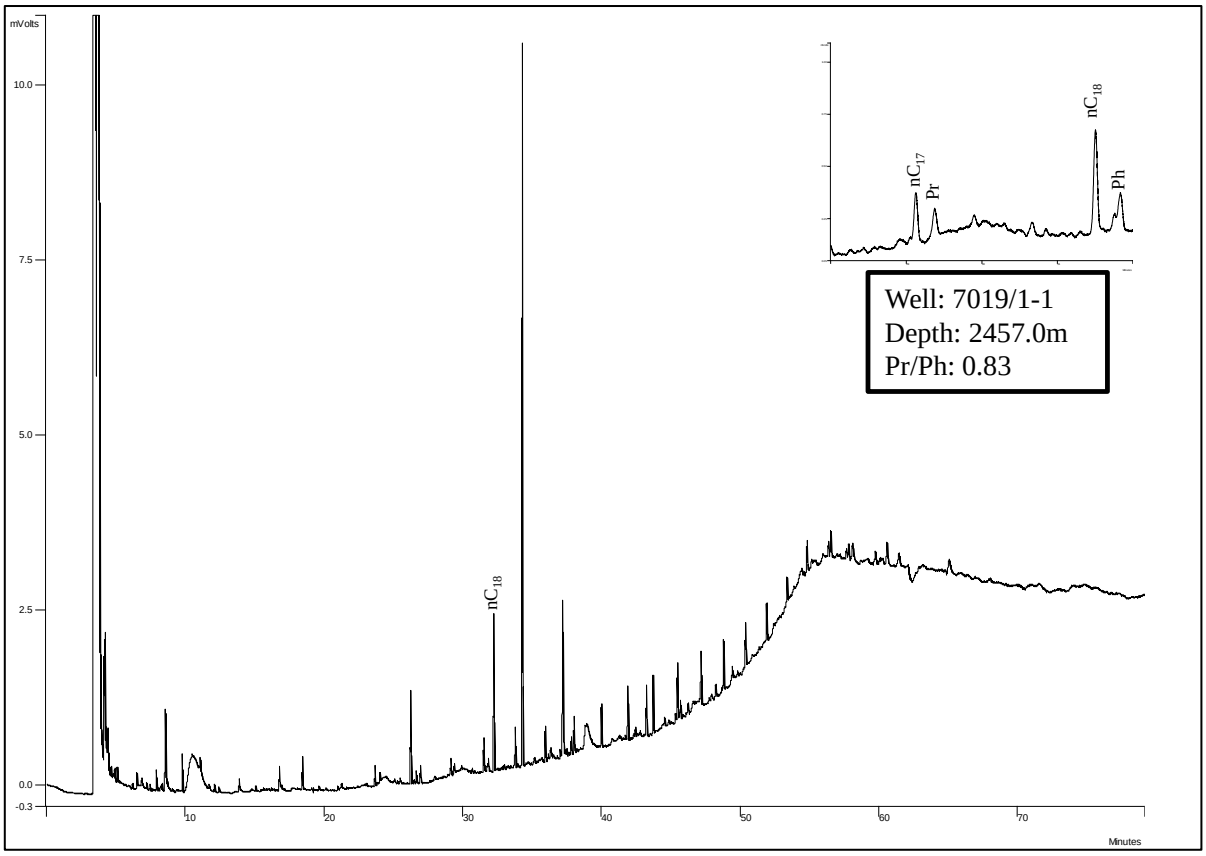
mVolts
10.0
7.5
5.0
2.5
0.0
-0.3
10
20
30
40
50
60
70
Minutes
nC18
nC17
Pr
nC18
Ph
Well: 7019/1-1
Depth: 2457.0m
Pr/Ph: 0.83

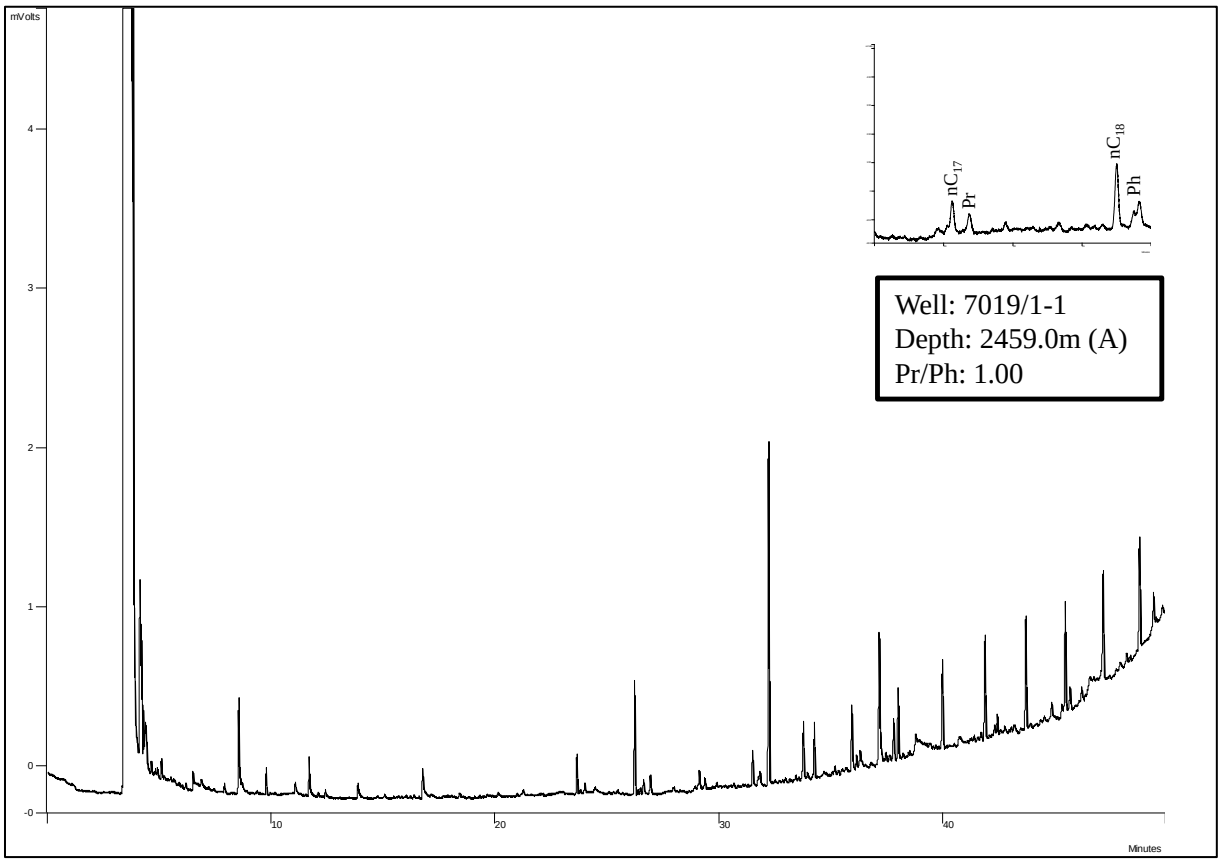
mVolts
4
3
2
1
0
-0
10
20
30
40
Minutes
nC17
Pr
nC18
Ph
Well: 7019/1-1
Depth: 2459.0m (A)
Pr/Ph: 1.00

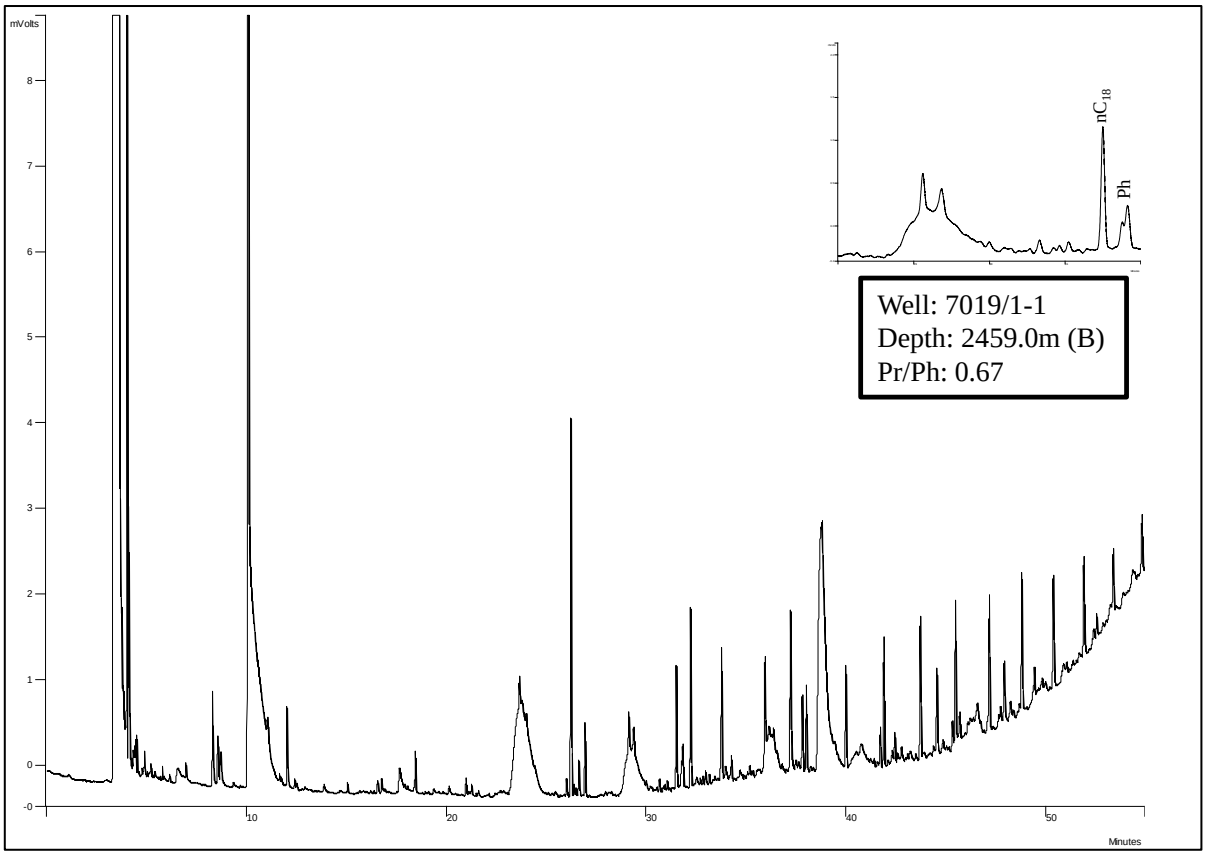
mVolts
8
7
6
5
4
3
2
1
0
-0
10
20
30
40
50
Minutes
nC18
Ph
Well: 7019/1-1
Depth: 2459.0m (B)
Pr/Ph: 0.67

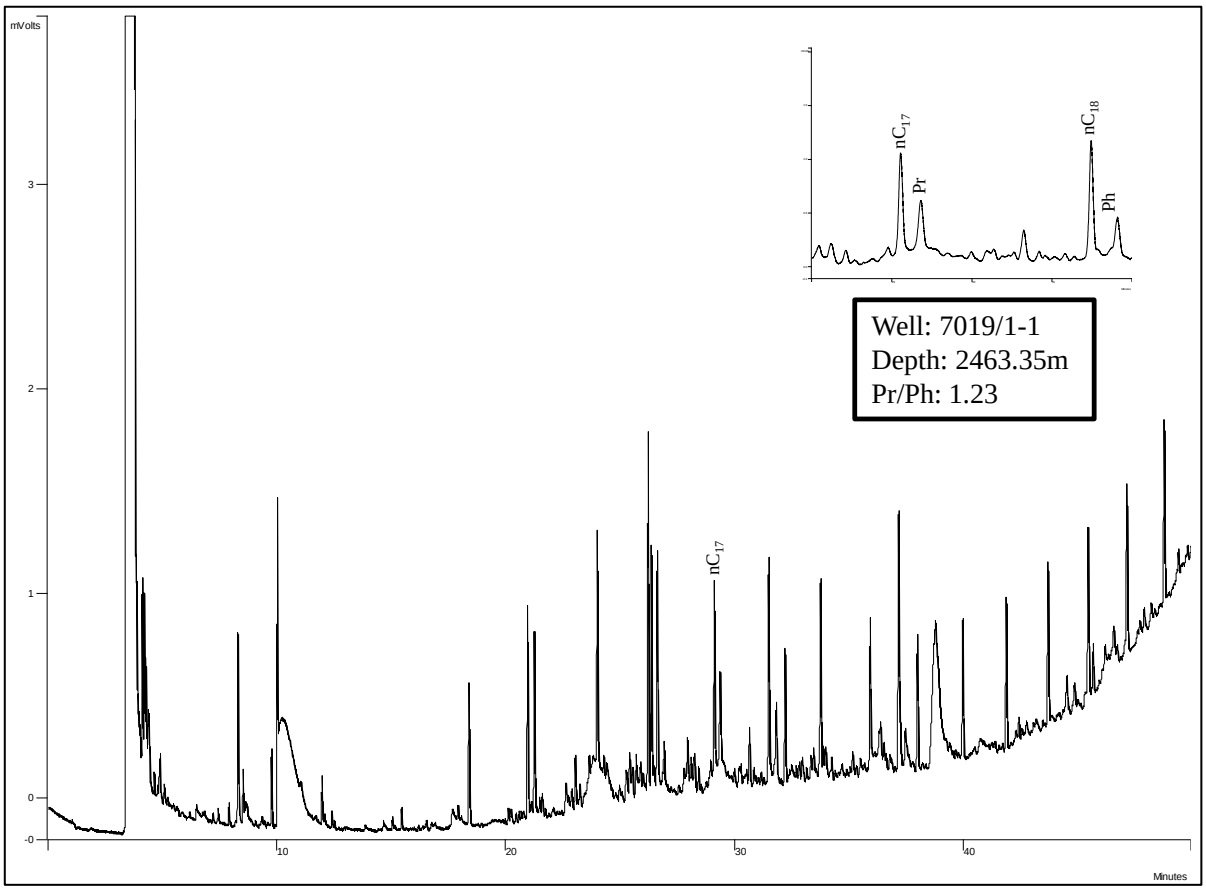
mVolts
3
2
1
0
-0
10
20
30
40
Minutes
nC17
Pr
nC18
Ph
nC17
Well: 7019/1-1
Depth: 2463.35m
Pr/Ph: 1.23

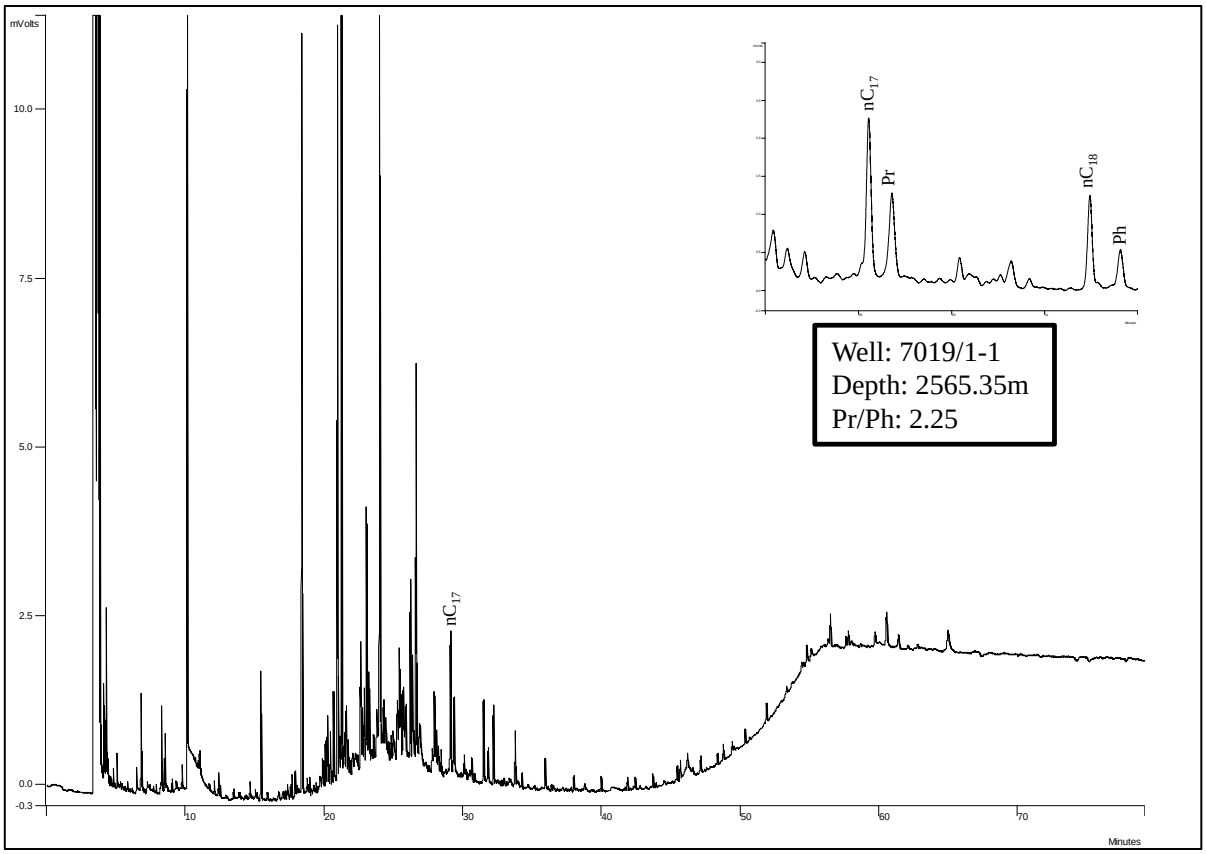
mVolts
10.0
7.5
5.0
2.5
0.0
-0.3
nC17
Pr
nC18
Ph
Well: 7019/1-1
Depth: 2565.35m
Pr/Ph: 2.25
10
20
30
40
50
60
70
Minutes

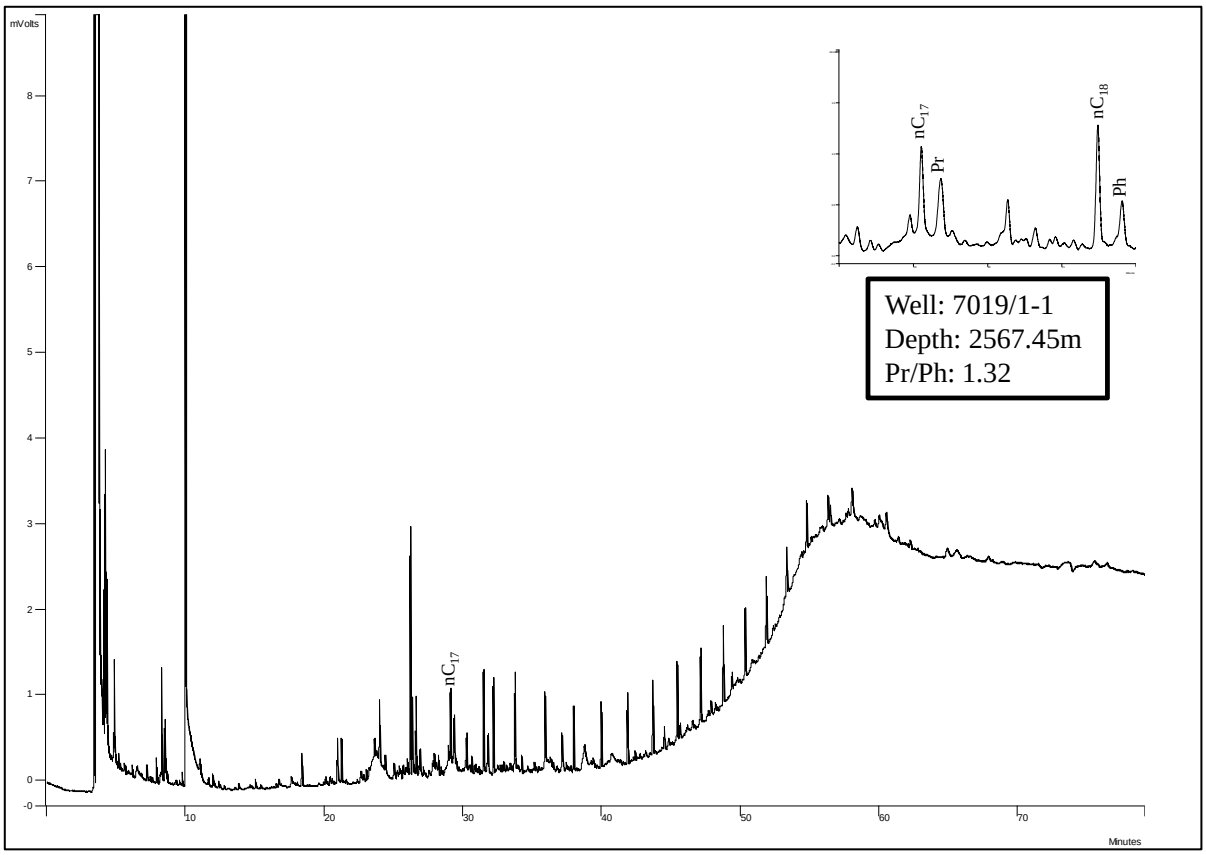
mVolts
8
7
6
5
4
3
2
1
0
-0
nC17
Pr
nC18
Ph
Well: 7019/1-1
Depth: 2567.45m
Pr/Ph: 1.32
10
20
30
40
50
60
70
Minutes

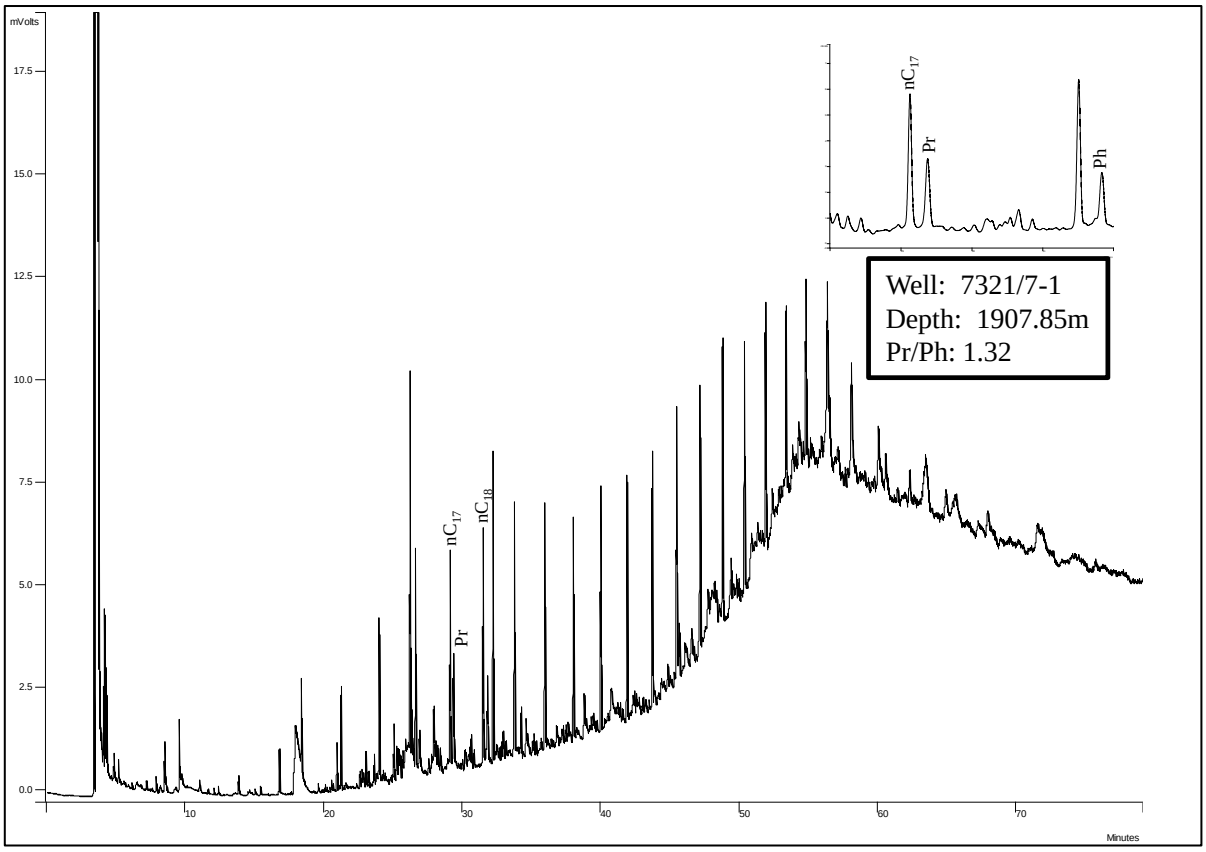
mVolts
17.5
15.0
12.5
10.0
7.5
5.0
2.5
0.0
nC17
Pr
nC18
10
20
30
40
50
60
70
Minutes
nC17
Pr
Ph
Well: 7321/7-1
Depth: 1907.85m
Pr/Ph: 1.32

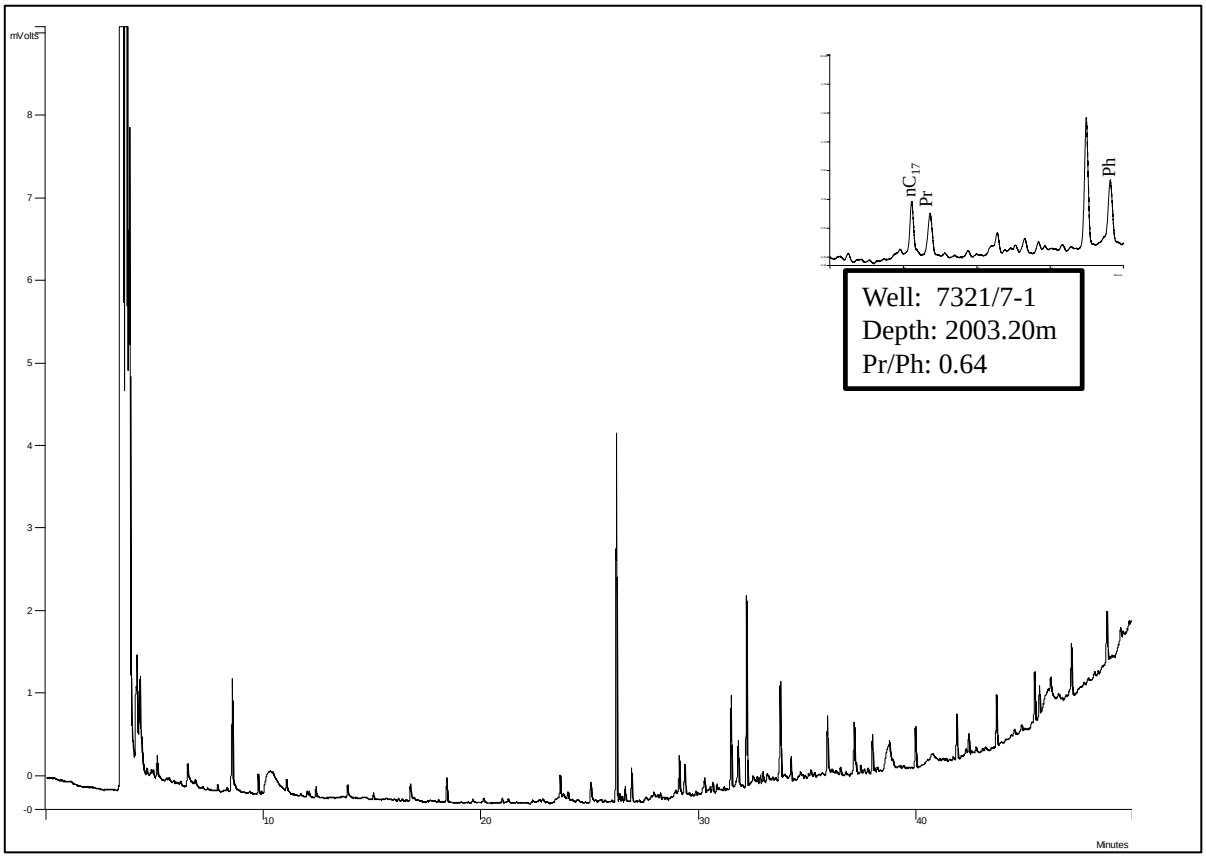
mVolts
8
7
6
5
4
3
2
1
0
-0
nC17
Pr
Ph
10
20
30
40
Minutes
Well: 7321/7-1
Depth: 2003.20m
Pr/Ph: 0.64

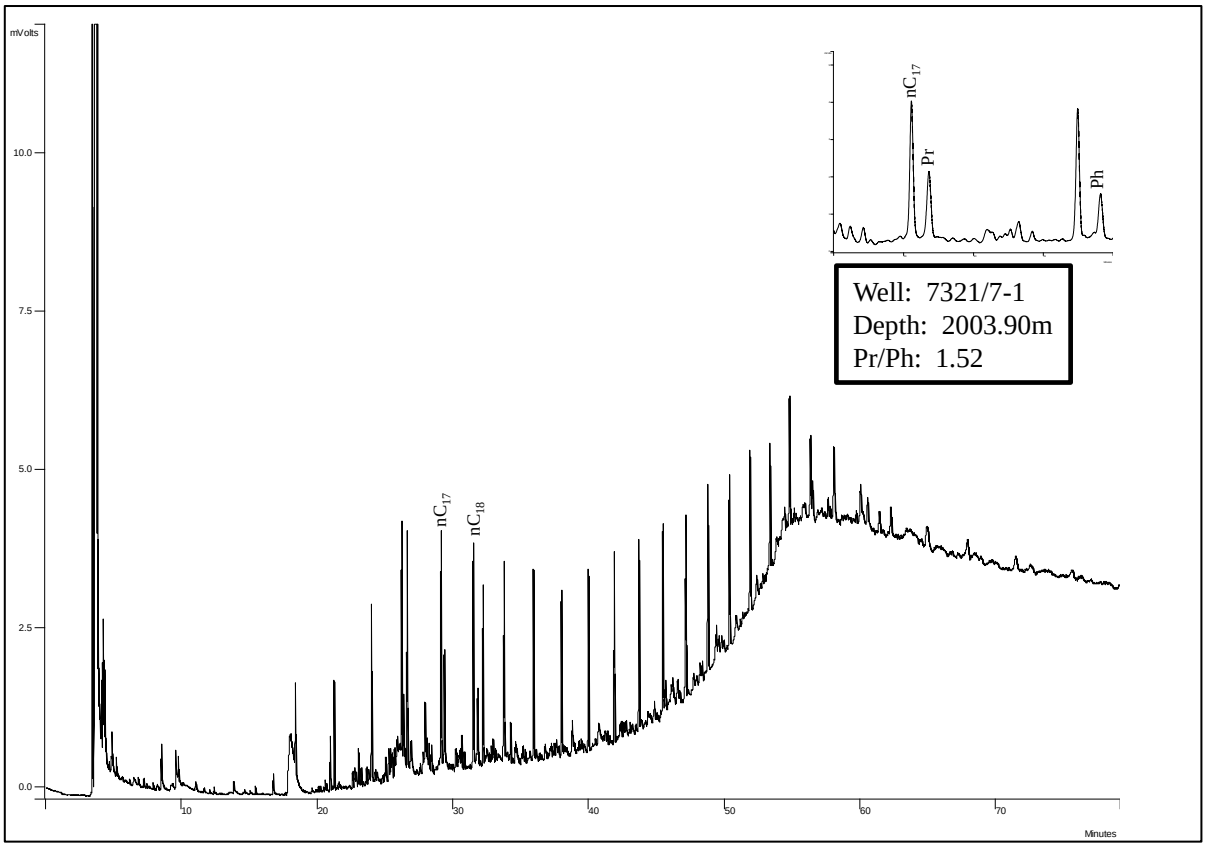
mVolts
10.0
7.5
5.0
2.5
0.0
nC17
nC18
nC17
Pr
Ph
Well: 7321/7-1
Depth: 2003.90m
Pr/Ph: 1.52
10
20
30
40
50
60
70
Minutes

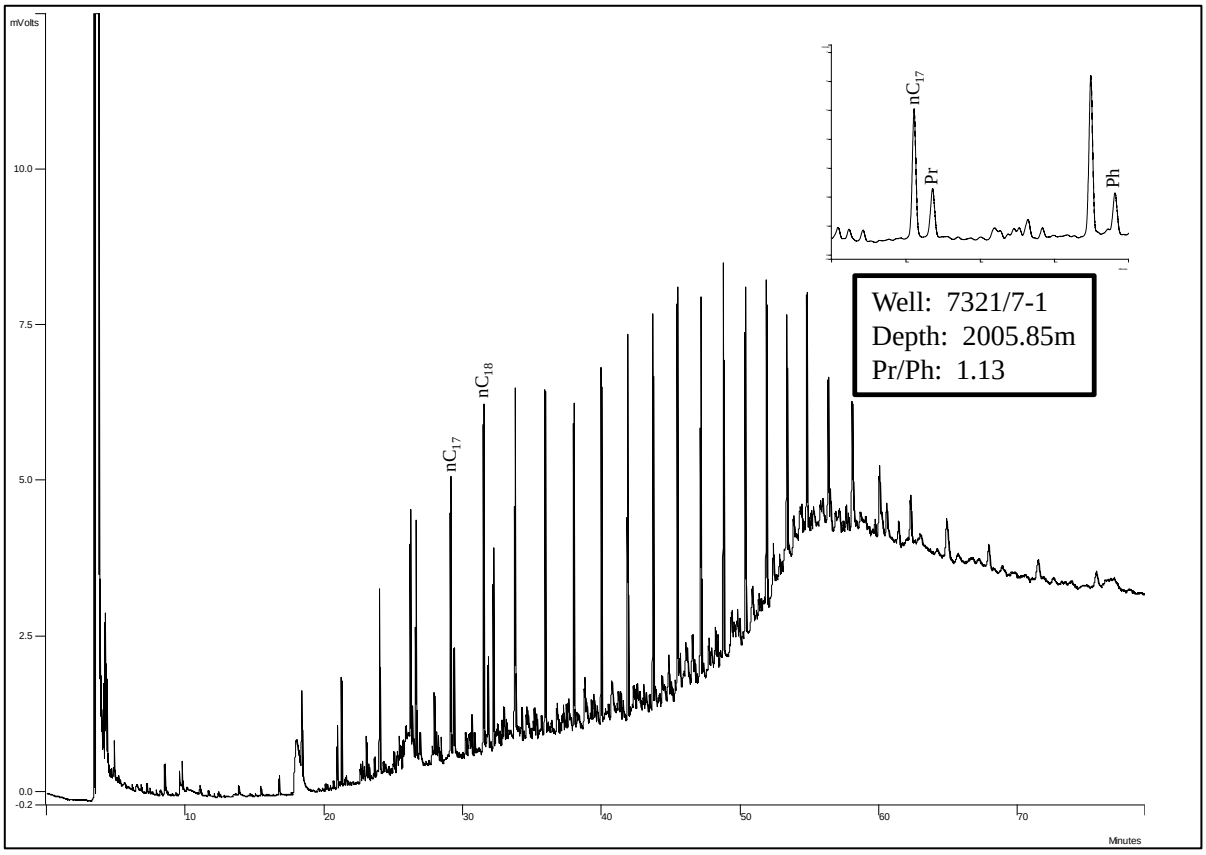
mVolts
10.0
7.5
5.0
2.5
0.0
-0.2
nC17
nC18
nC17
Pr
Ph
Well: 7321/7-1
Depth: 2005.85m
Pr/Ph: 1.13
10
20
30
40
50
60
70
Minutes

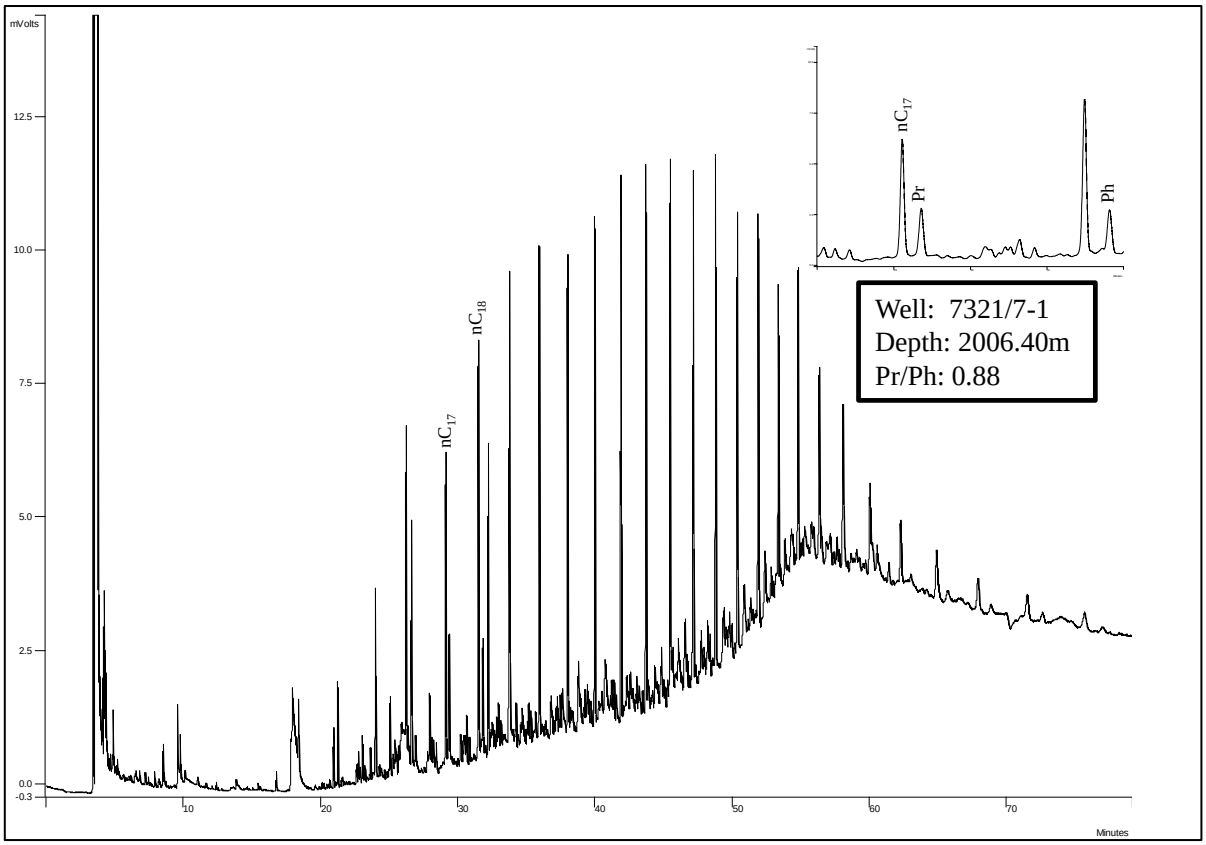
mVolts
12.5
10.0
7.5
5.0
2.5
0.0
-0.3
10
20
30
40
50
60
70
Minutes
nC17
nC18
nC17
Pr
Ph
Well: 7321/7-1
Depth: 2006.40m
Pr/Ph: 0.88

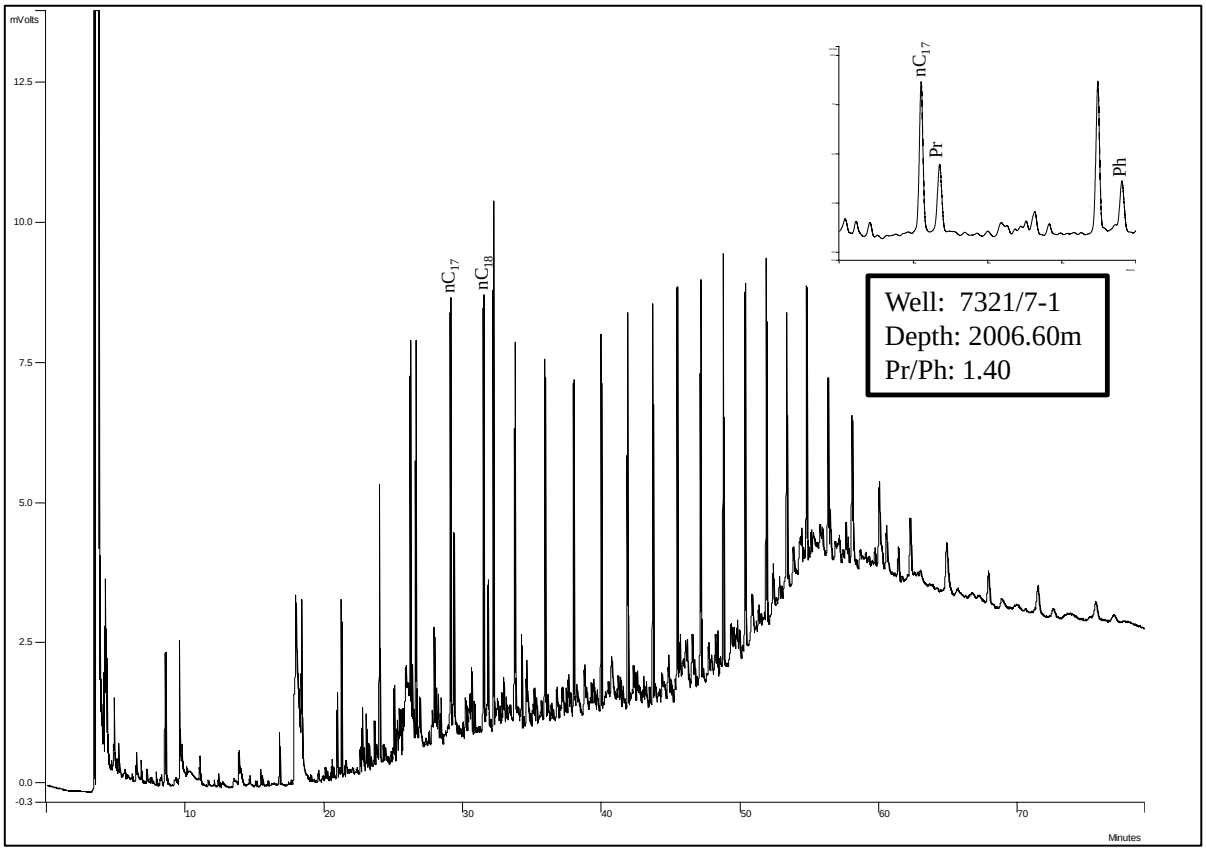
mVolts
12.5
10.0
7.5
5.0
2.5
0.0
-0.3
10
20
30
40
50
60
70
Minutes
nC17
nC18
nC17
Pr
Ph
Well: 7321/7-1
Depth: 2006.60m
Pr/Ph: 1.40

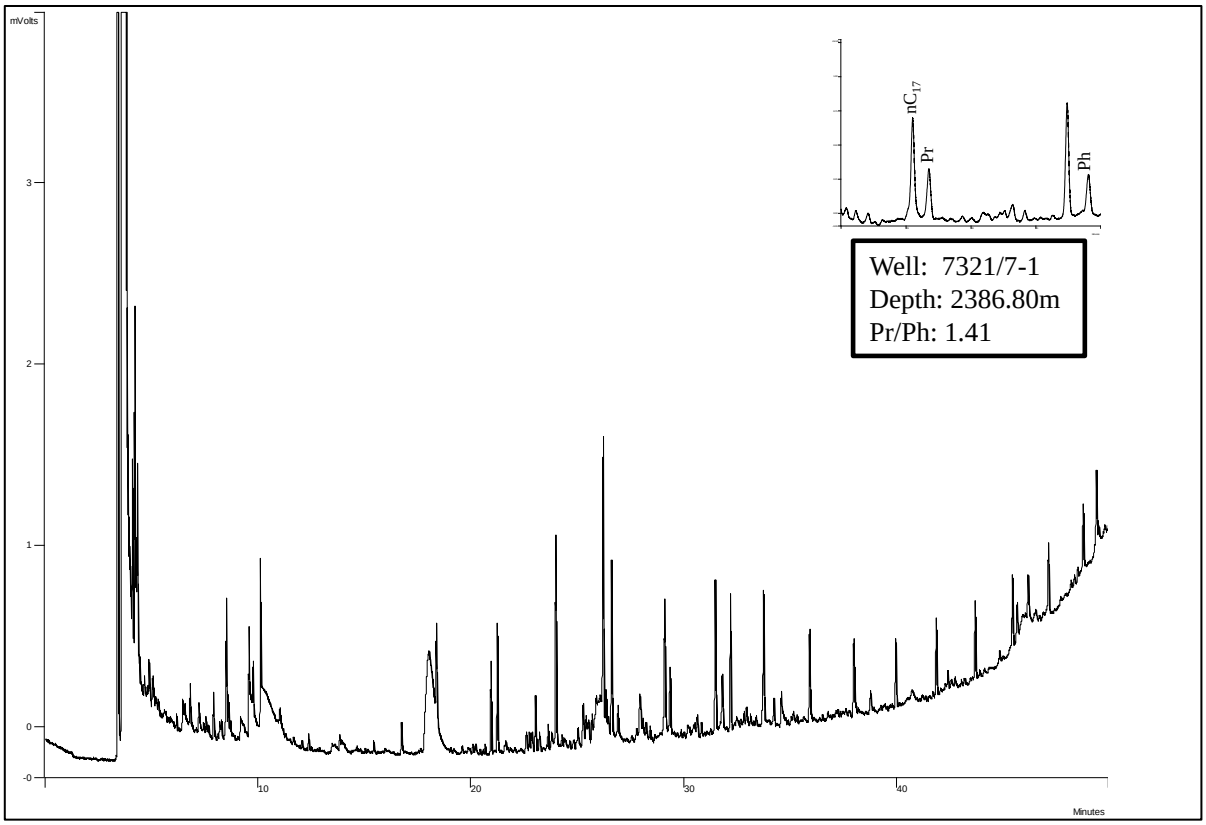
mVolts
3
2
1
0
-0
10
20
30
40
Minutes
nC17
Pr
Ph
Well: 7321/7-1
Depth: 2386.80m
Pr/Ph: 1.41

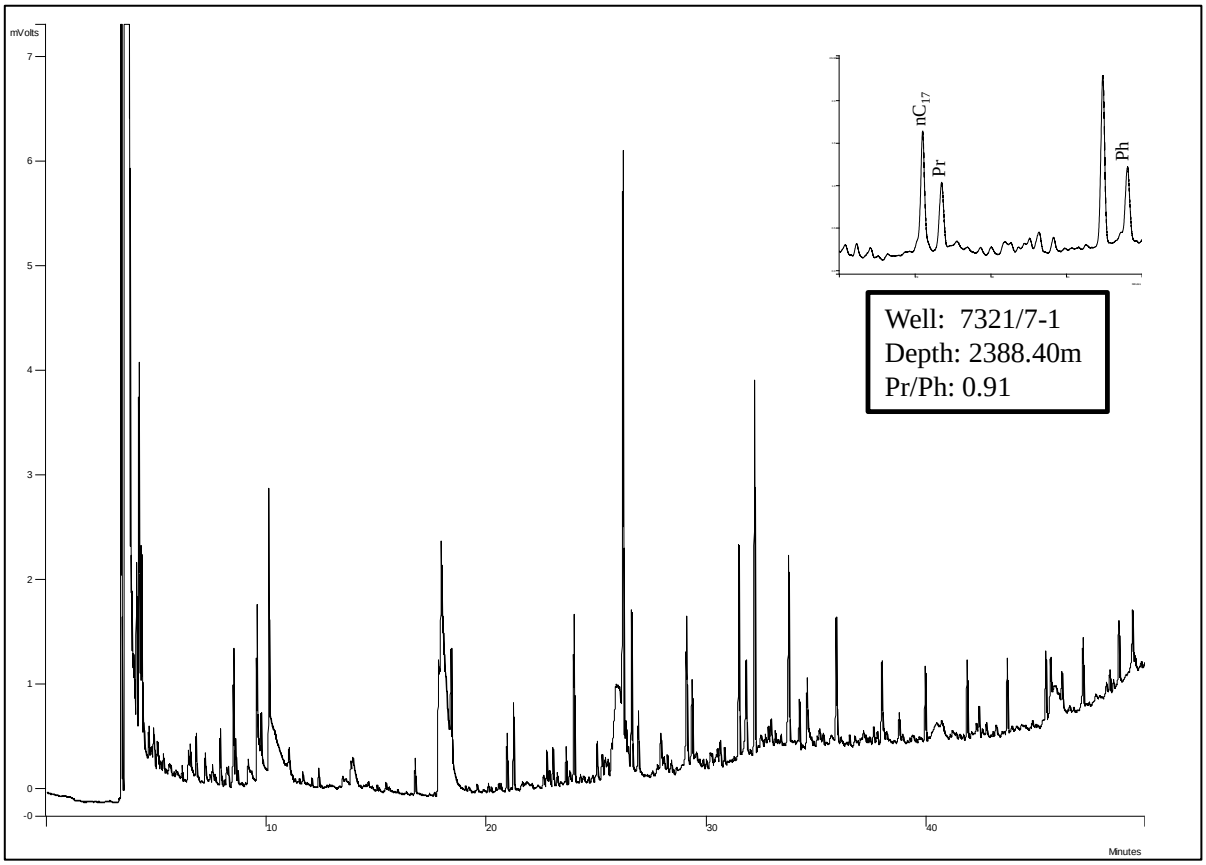
mVolts
7
6
5
4
3
2
1
0
-0
10
20
30
40
Minutes
nC17
Pr
Ph
Well: 7321/7-1
Depth: 2388.40m
Pr/Ph: 0.91

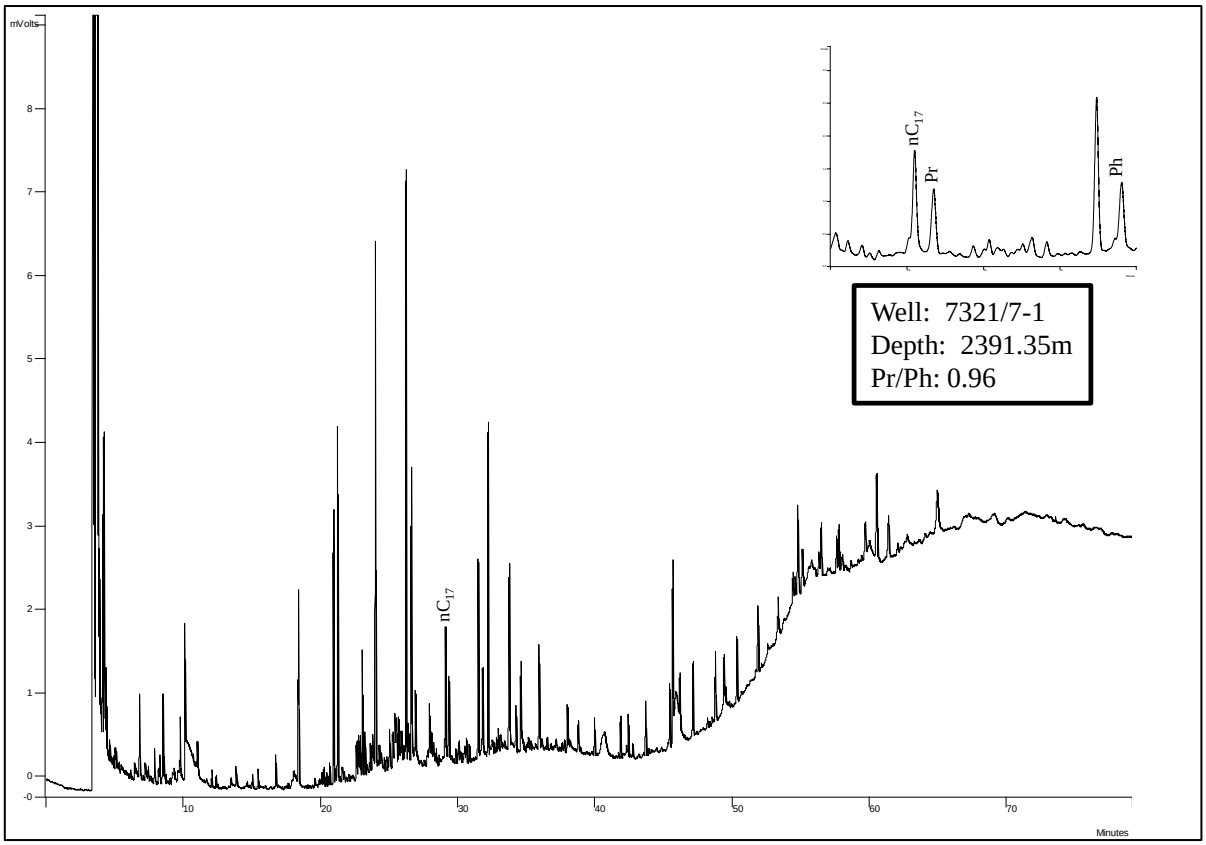
mVolts
8
7
6
5
4
3
2
1
0
-0
nC17
Pr
Ph
Well: 7321/7-1
Depth: 2391.35m
Pr/Ph: 0.96
10
20
30
40
50
60
70
Minutes

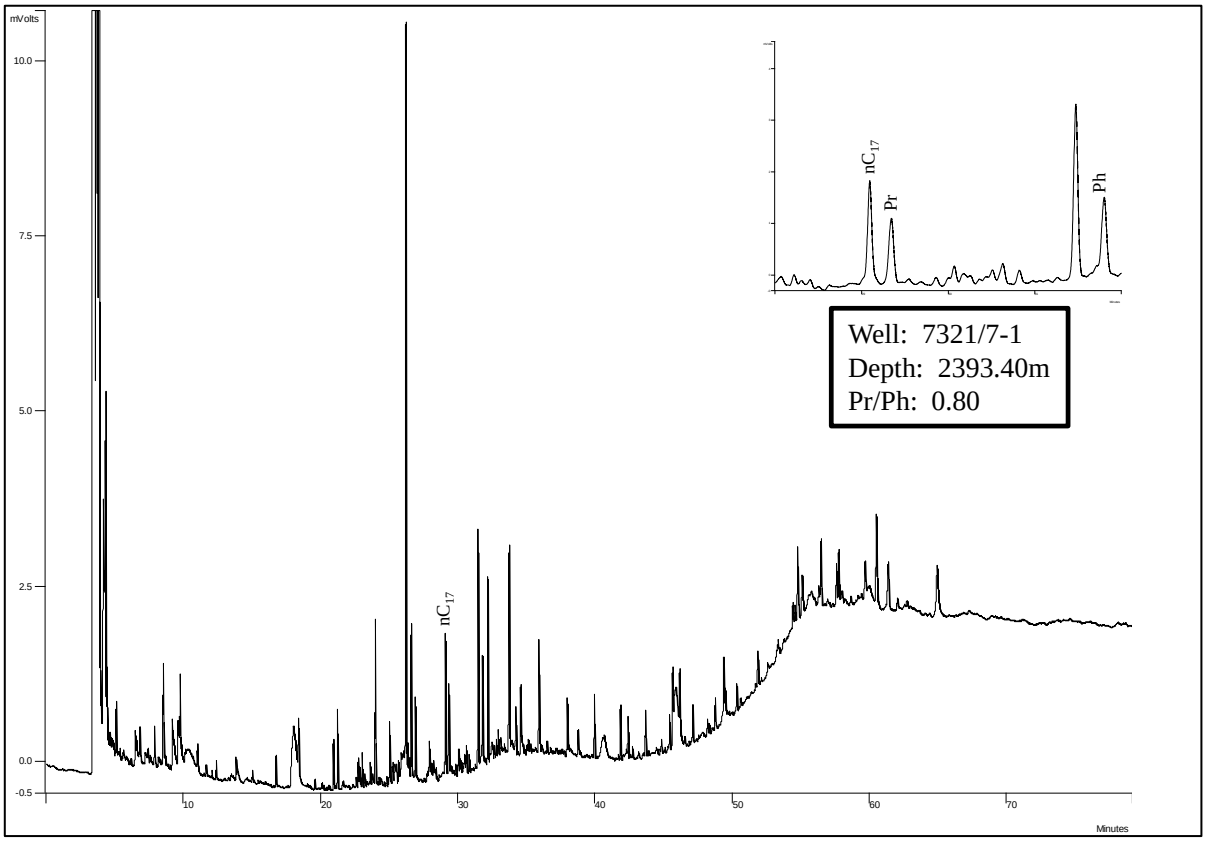
mVolts
10.0
7.5
5.0
2.5
0.0
-0.5
nC17
Pr
Ph
Well: 7321/7-1
Depth: 2393.40m
Pr/Ph: 0.80
10
20
30
40
50
60
70
Minutes

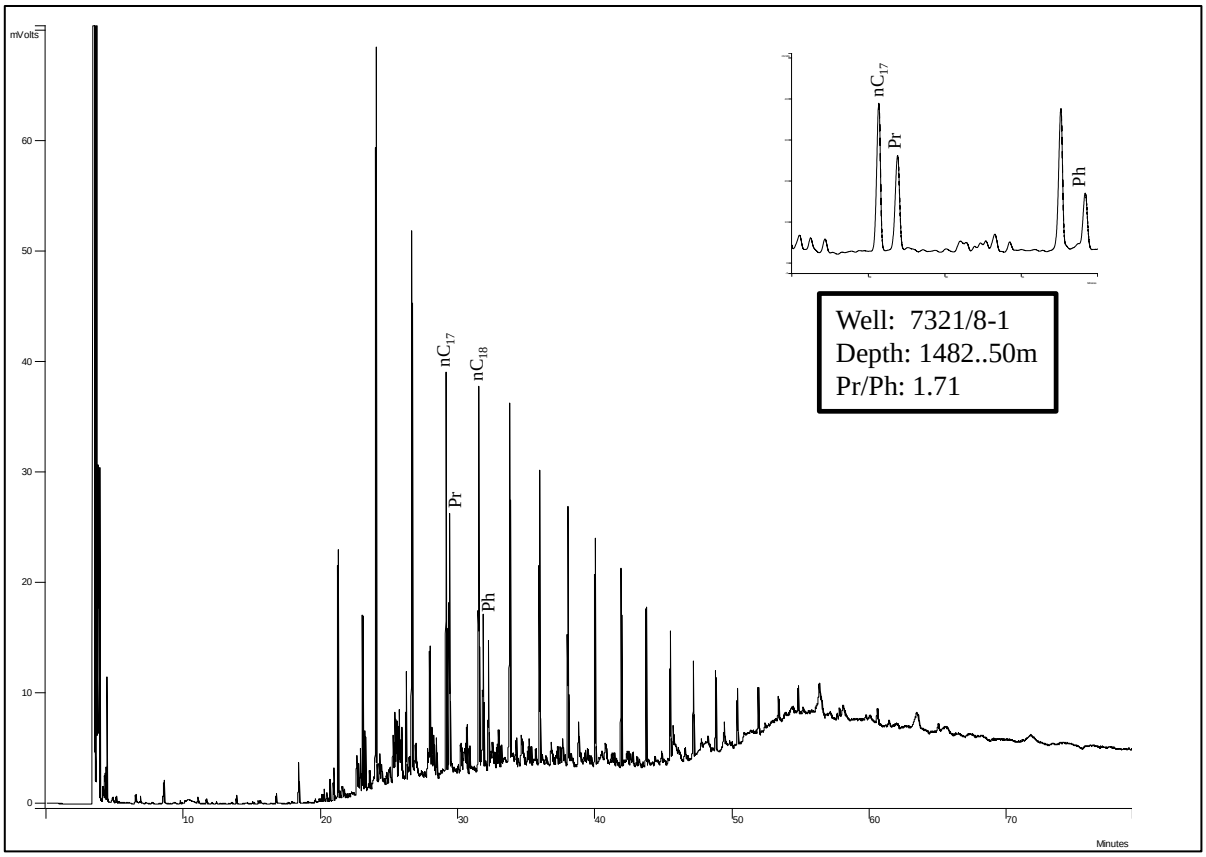
mVolts
nC17
nC18
Pr
Ph
Minutes
Well: 7321/8-1
Depth: 1482..50m
Pr/Ph: 1.71

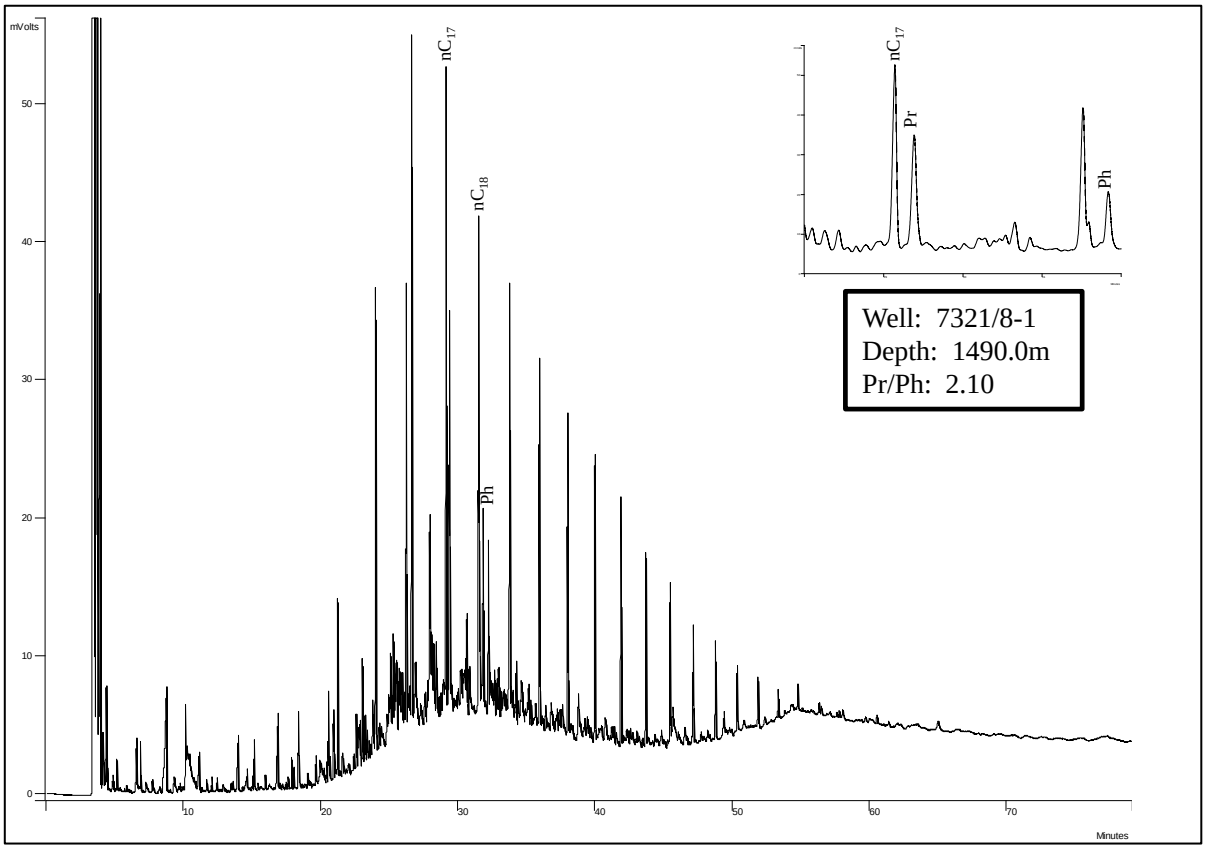
mVolts
nC17
nC18
Pr
Ph
Minutes
Well: 7321/8-1
Depth: 1490.0m
Pr/Ph: 2.10

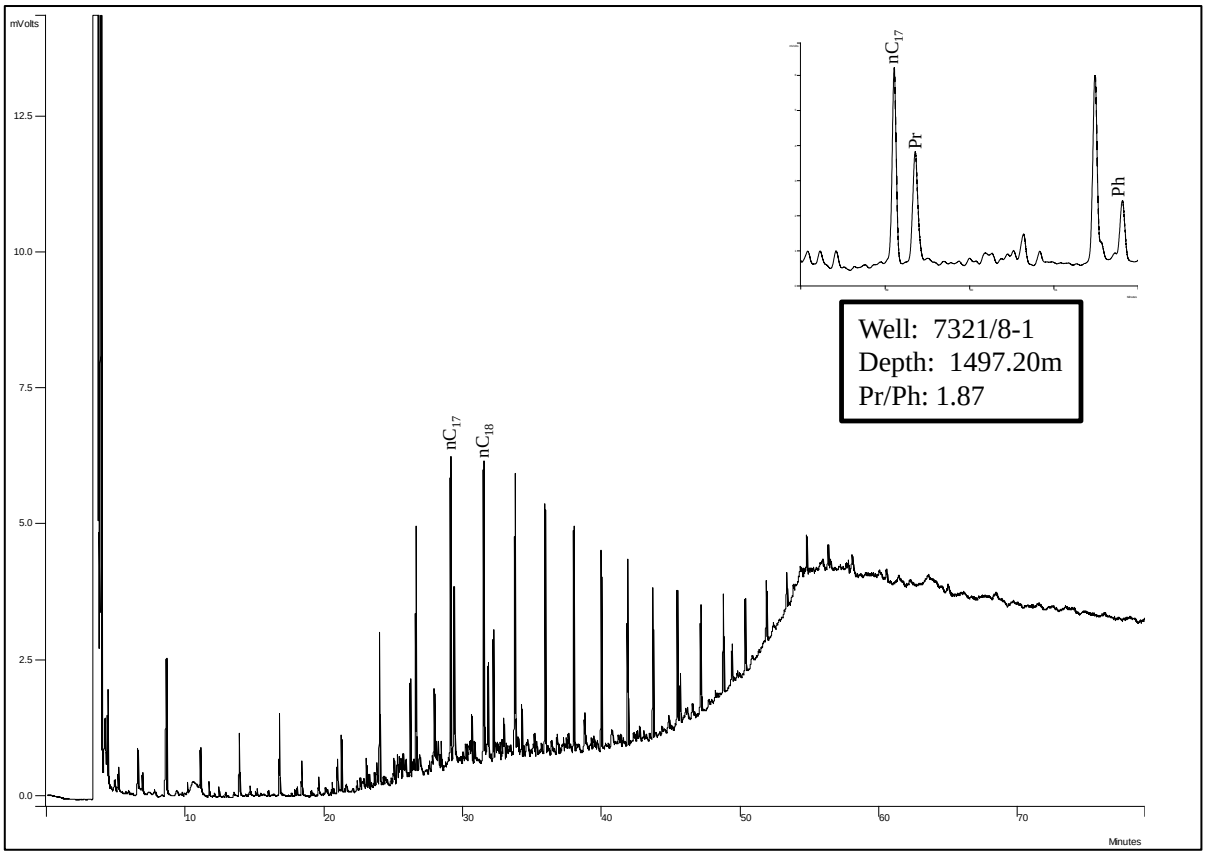
mVolts
12.5
10.0
7.5
5.0
2.5
0.0
nC17
nC18
Pr
Ph
Well: 7321/8-1
Depth: 1497.20m
Pr/Ph: 1.87
10
20
30
40
50
60
70
Minutes

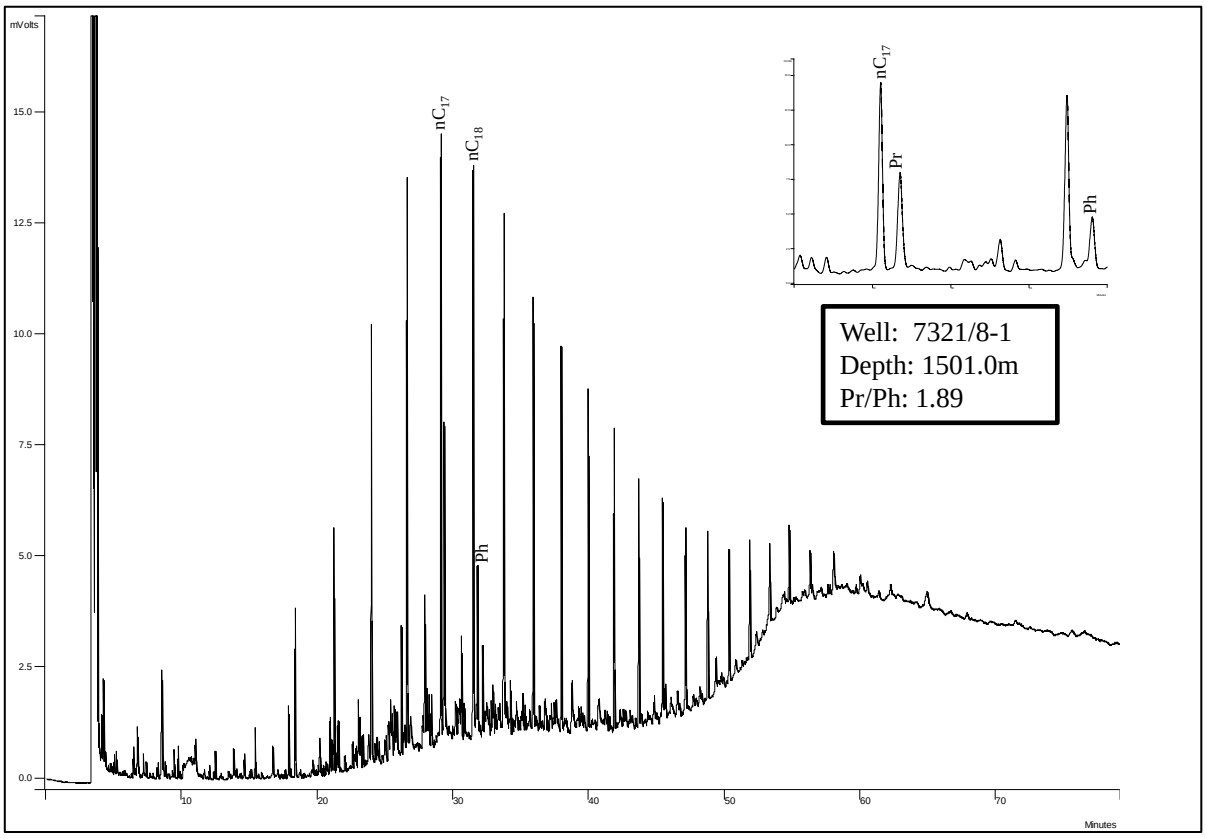
mVolts
15.0
12.5
10.0
7.5
5.0
2.5
0.0
nC17
nC18
Ph
Pr
Ph
Well: 7321/8-1
Depth: 1501.0m
Pr/Ph: 1.89
10
20
30
40
50
60
70
Minutes

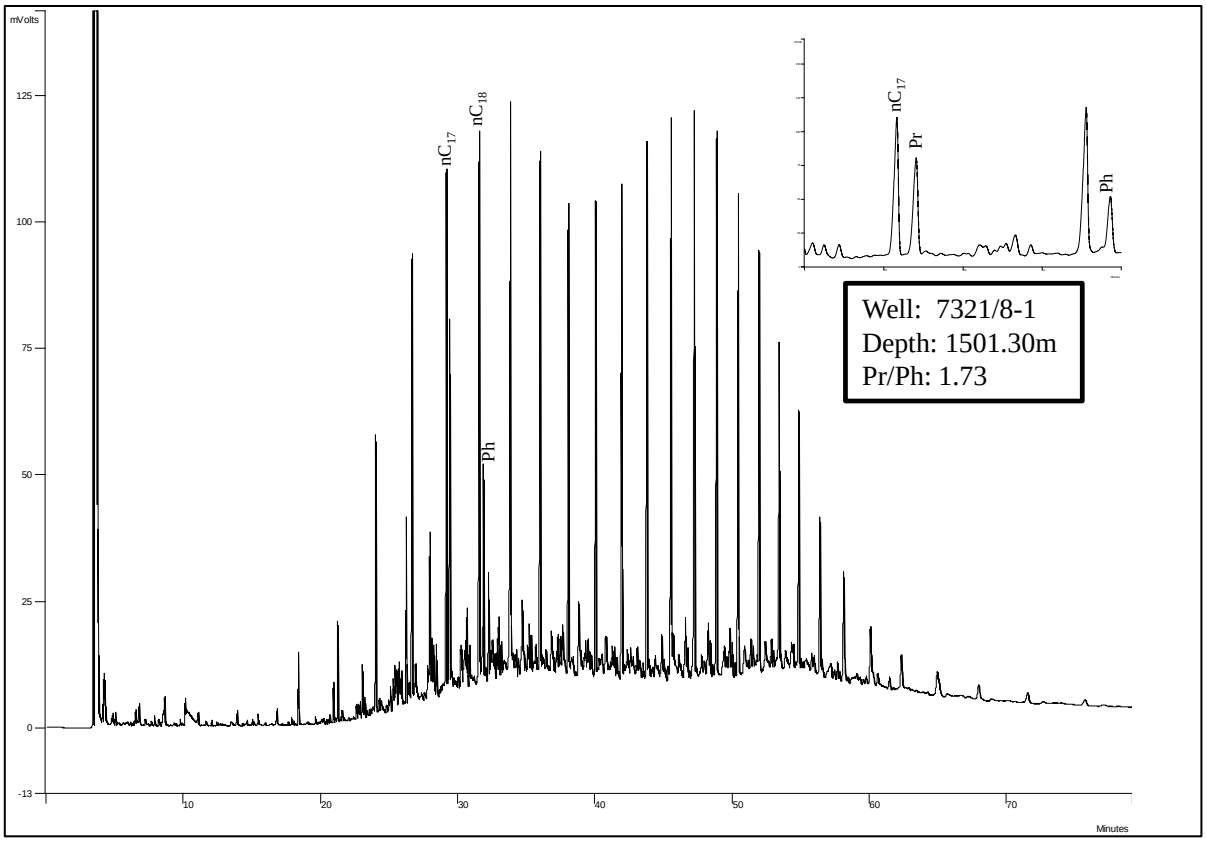
mVolts
125
100
75
50
25
0
-13
10
20
30
40
50
60
70
Minutes
nC17
nC18
Ph
Pr
Well: 7321/8-1
Depth: 1501.30m
Pr/Ph: 1.73

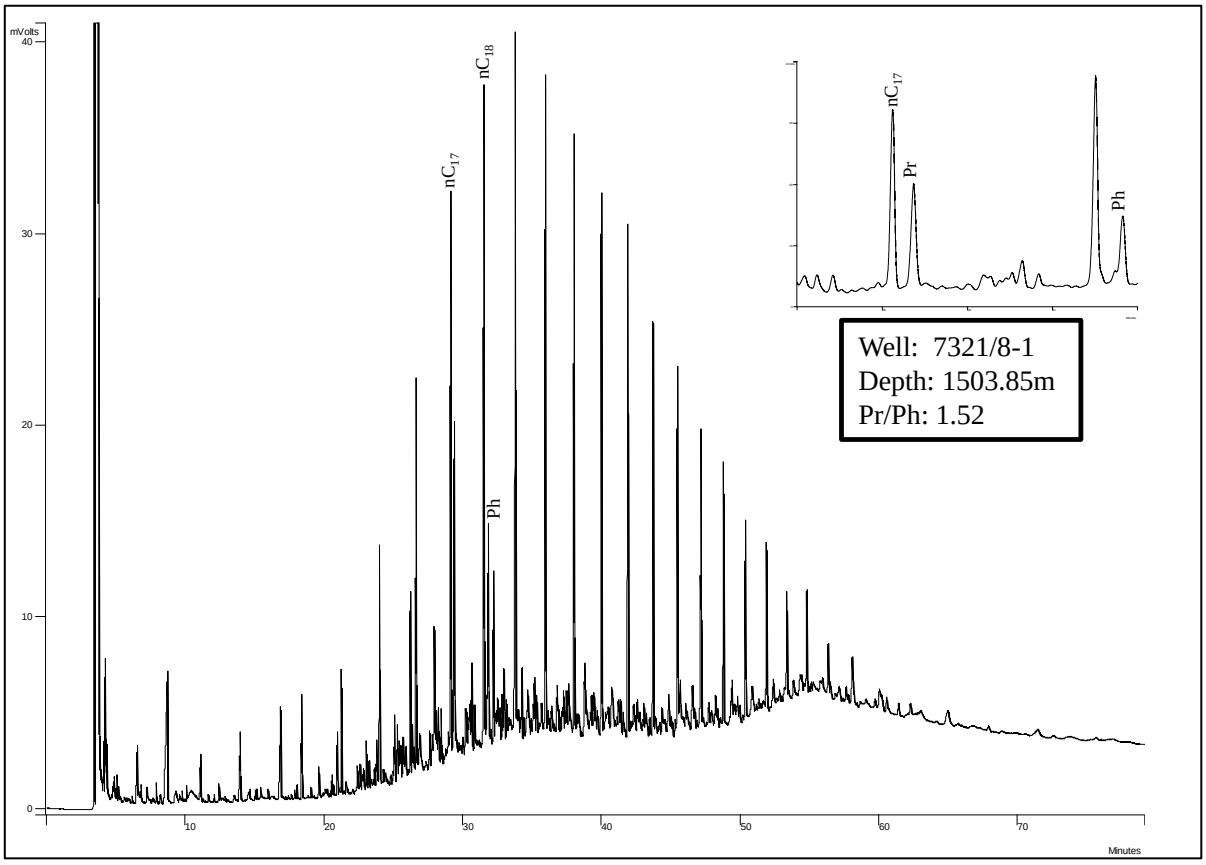
mVolts
40
30
20
10
0
10
20
30
40
50
60
70
Minutes
nC17
nC18
Ph
Pr
Well: 7321/8-1
Depth: 1503.85m
Pr/Ph: 1.52

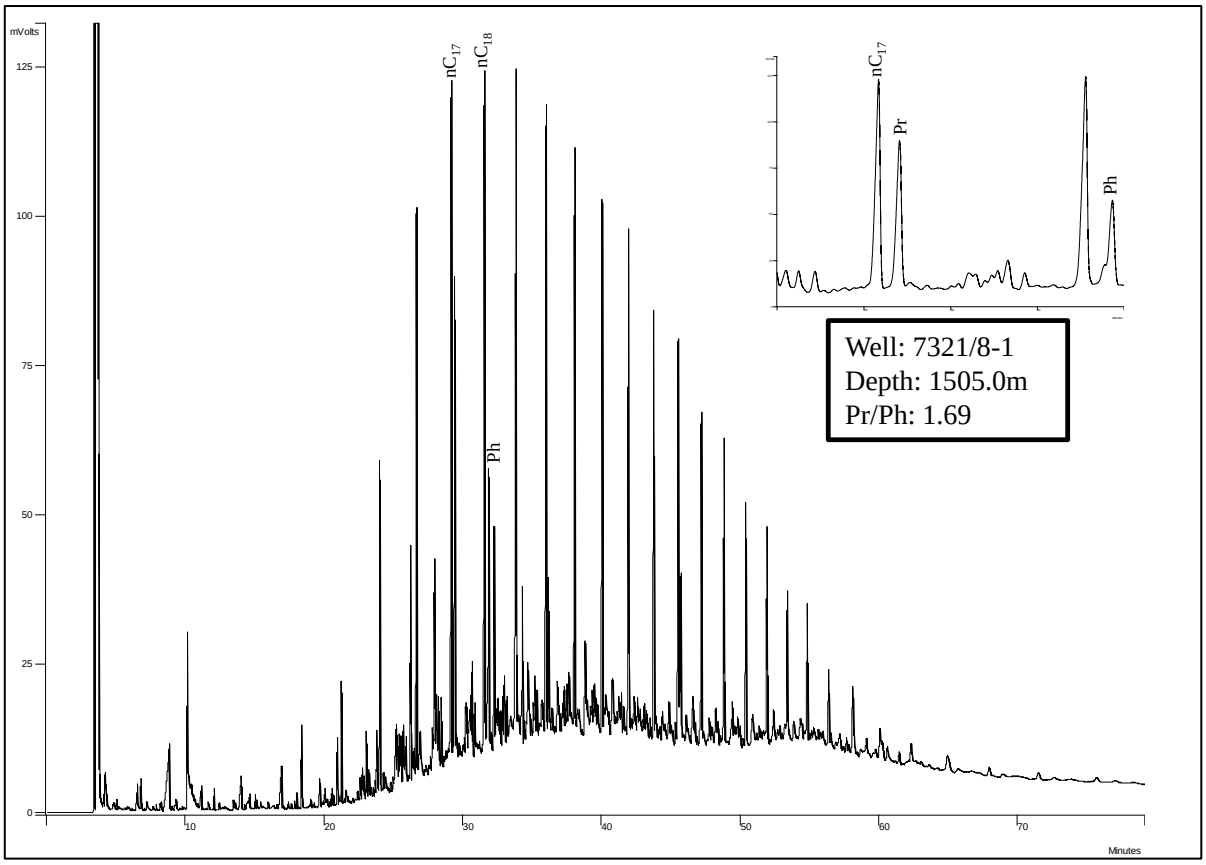
mVolts
125
100
75
50
25
0
nC17
nC18
Ph
nC17
Pr
Ph
Well: 7321/8-1
Depth: 1505.0m
Pr/Ph: 1.69
10
20
30
40
50
60
70
Minutes

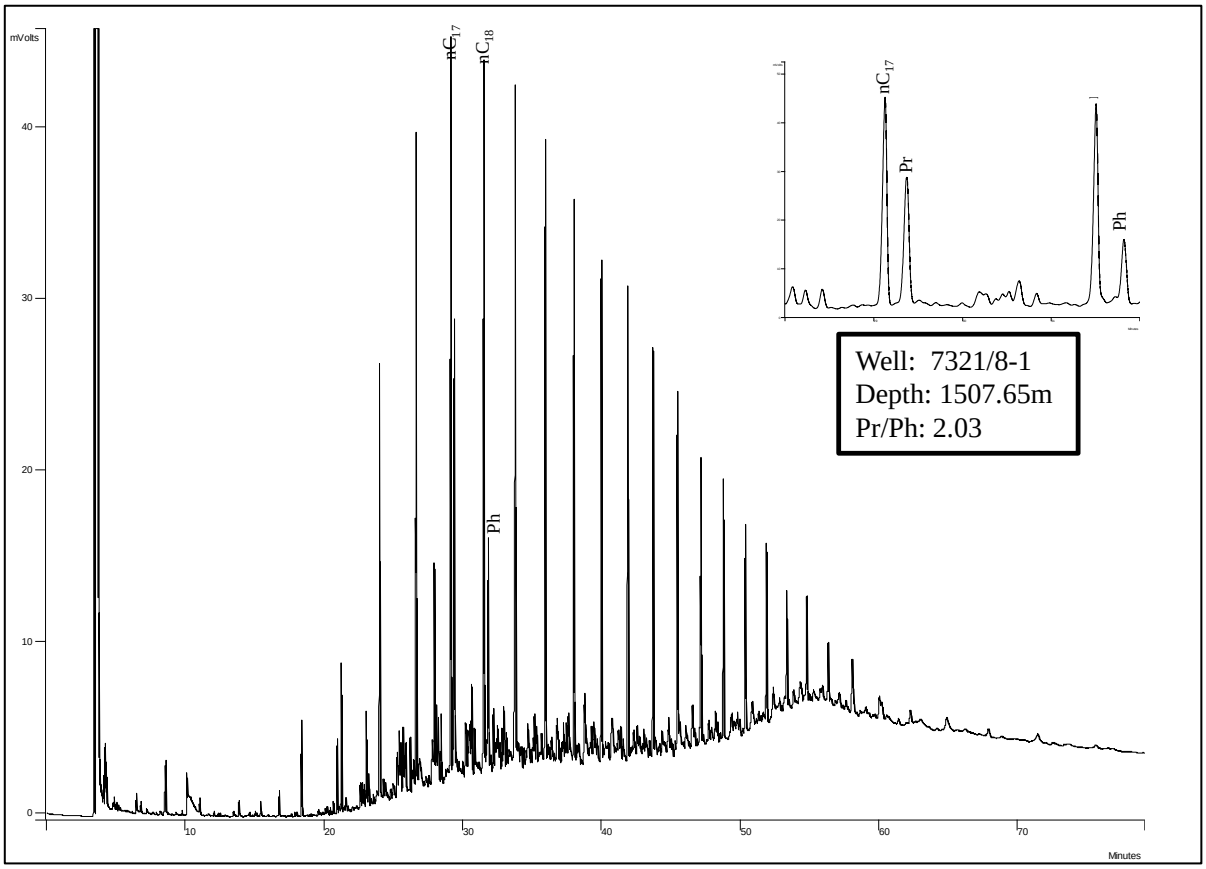
mVolts
40
30
20
10
0
nC17
nC18
Ph
nC17
Pr
Ph
Well: 7321/8-1
Depth: 1507.65m
Pr/Ph: 2.03
10
20
30
40
50
60
70
Minutes

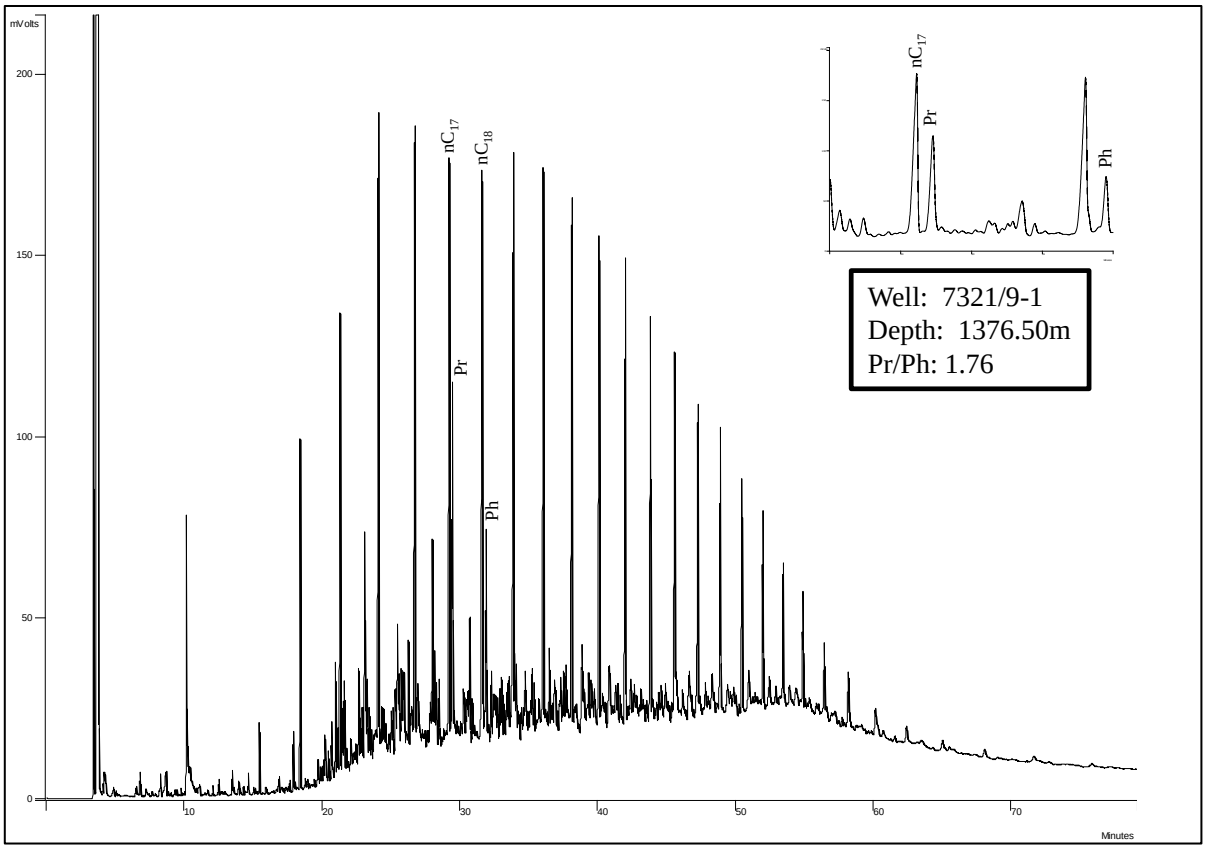
mVolts
200
150
100
50
0
nC17
nC18
Pr
Ph
10
20
30
40
50
60
70
Minutes
Well: 7321/9-1
Depth: 1376.50m
Pr/Ph: 1.76

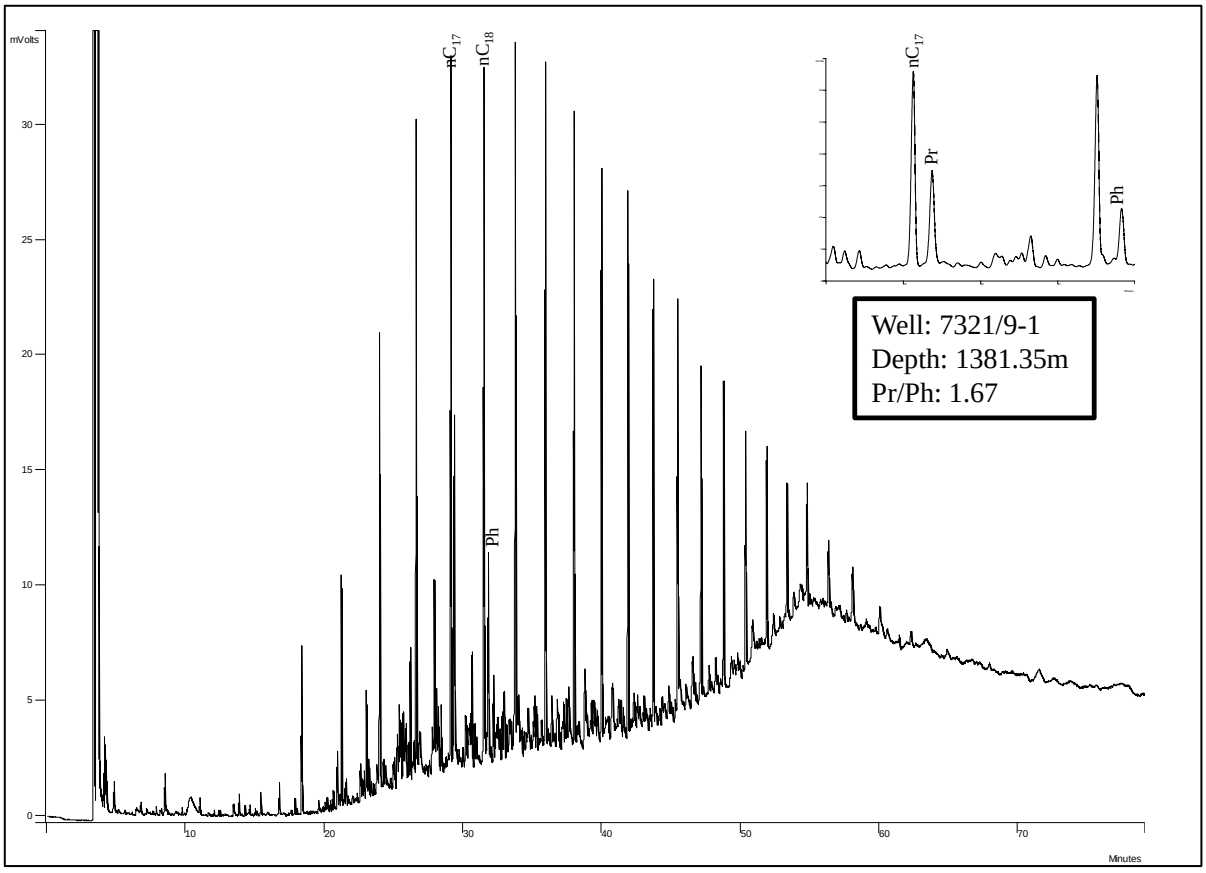
mVolts
30
25
20
15
10
5
0
nC17
nC18
Pr
Ph
10
20
30
40
50
60
70
Minutes
Well: 7321/9-1
Depth: 1381.35m
Pr/Ph: 1.67

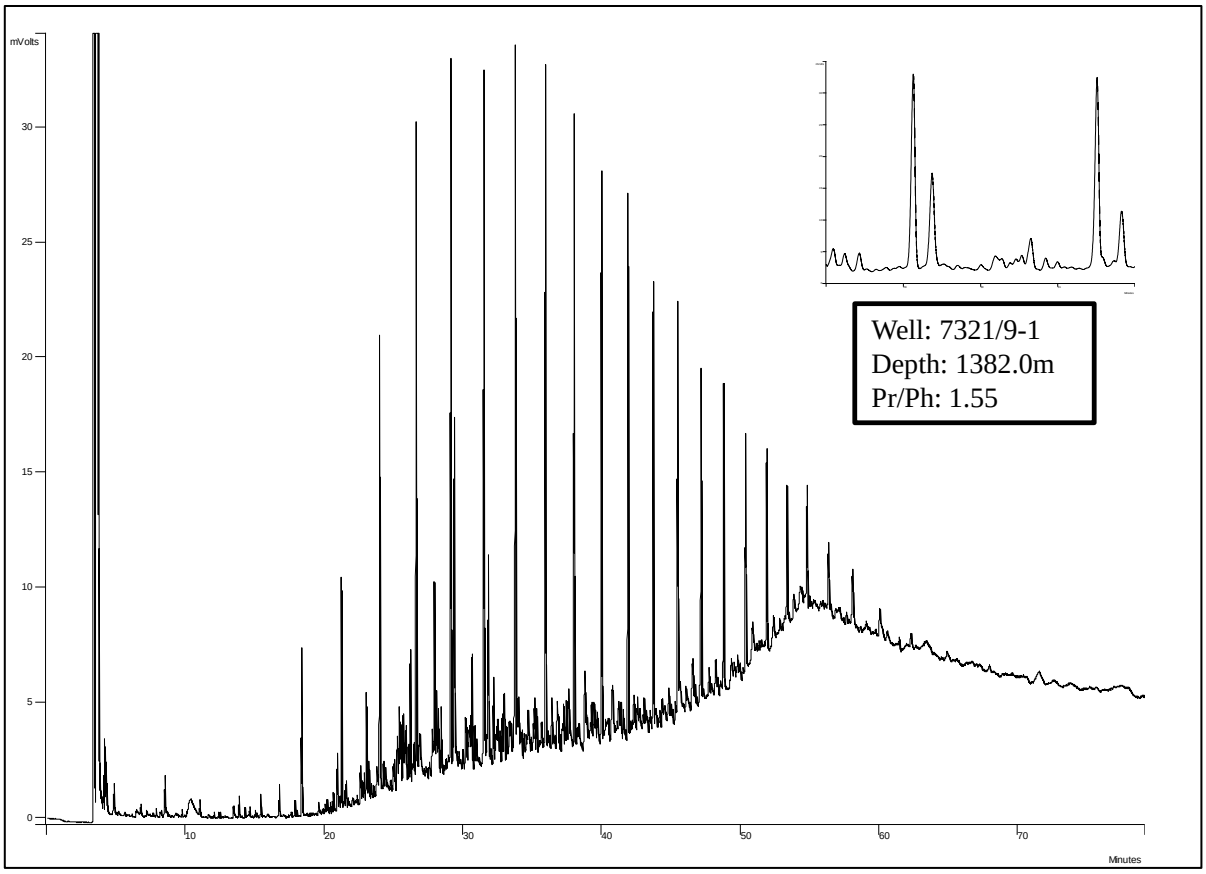
mVolts
30
25
20
15
10
5
0
10
20
30
40
50
60
70
Minutes
Well: 7321/9-1
Depth: 1382.0m
Pr/Ph: 1.55

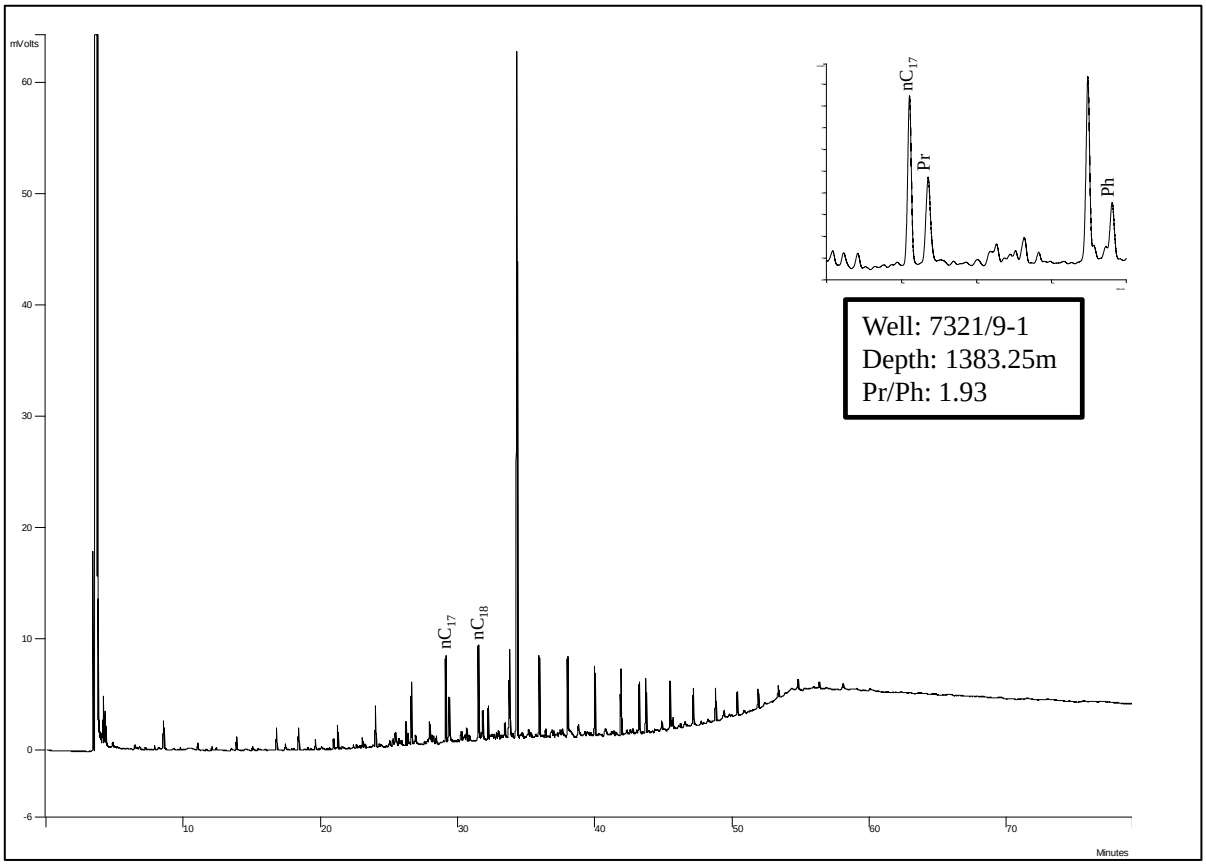
mVolts
60
50
40
30
20
10
0
-6
nC17
nC18
10
20
30
40
50
60
70
Minutes
nC17
Pr
Ph
Well: 7321/9-1
Depth: 1383.25m
Pr/Ph: 1.93

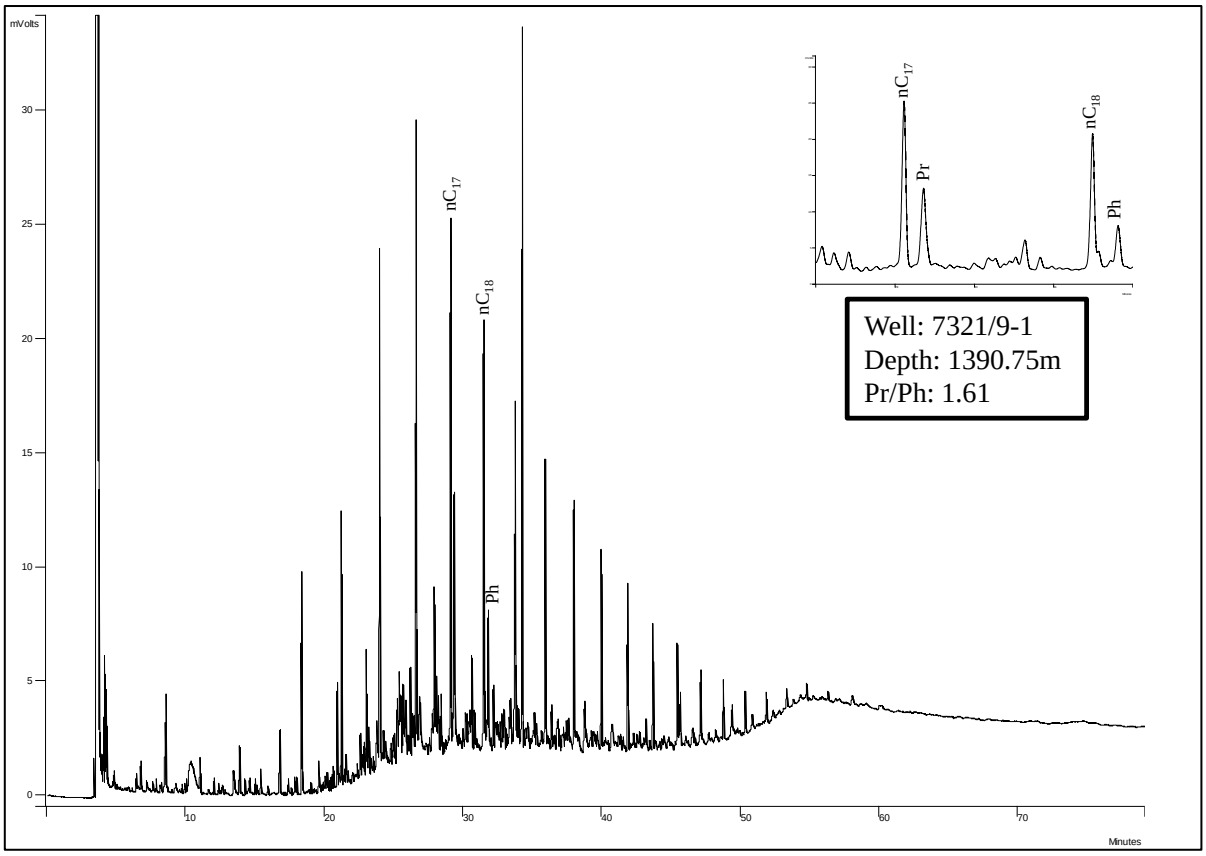
mVolts
30
25
20
15
10
5
0
nC17
nC18
Ph
10
20
30
40
50
60
70
Minutes
nC17
Pr
nC18
Ph
Well: 7321/9-1
Depth: 1390.75m
Pr/Ph: 1.61

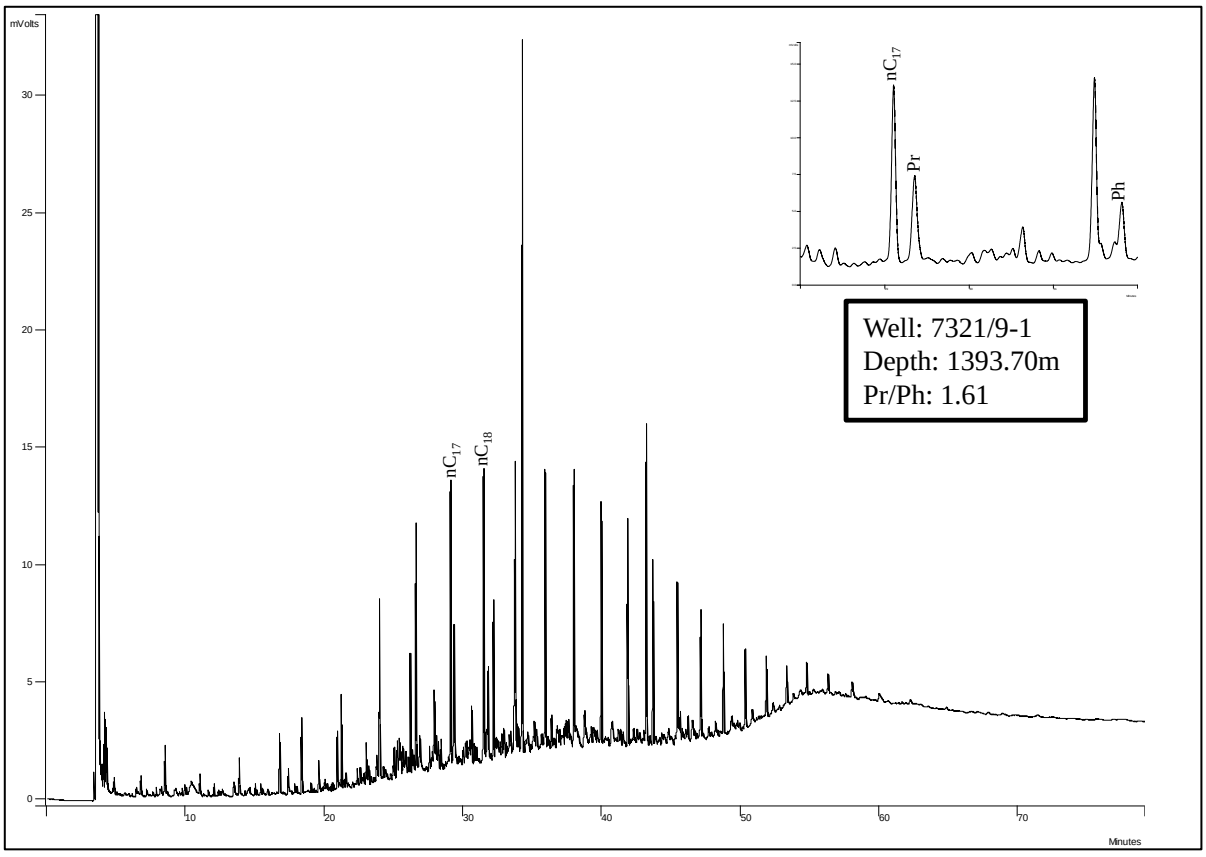
mVolts
30
25
20
15
10
5
0
nC17
nC18
10
20
30
40
50
60
70
Minutes
nC17
Pr
Ph
Well: 7321/9-1
Depth: 1393.70m
Pr/Ph: 1.61

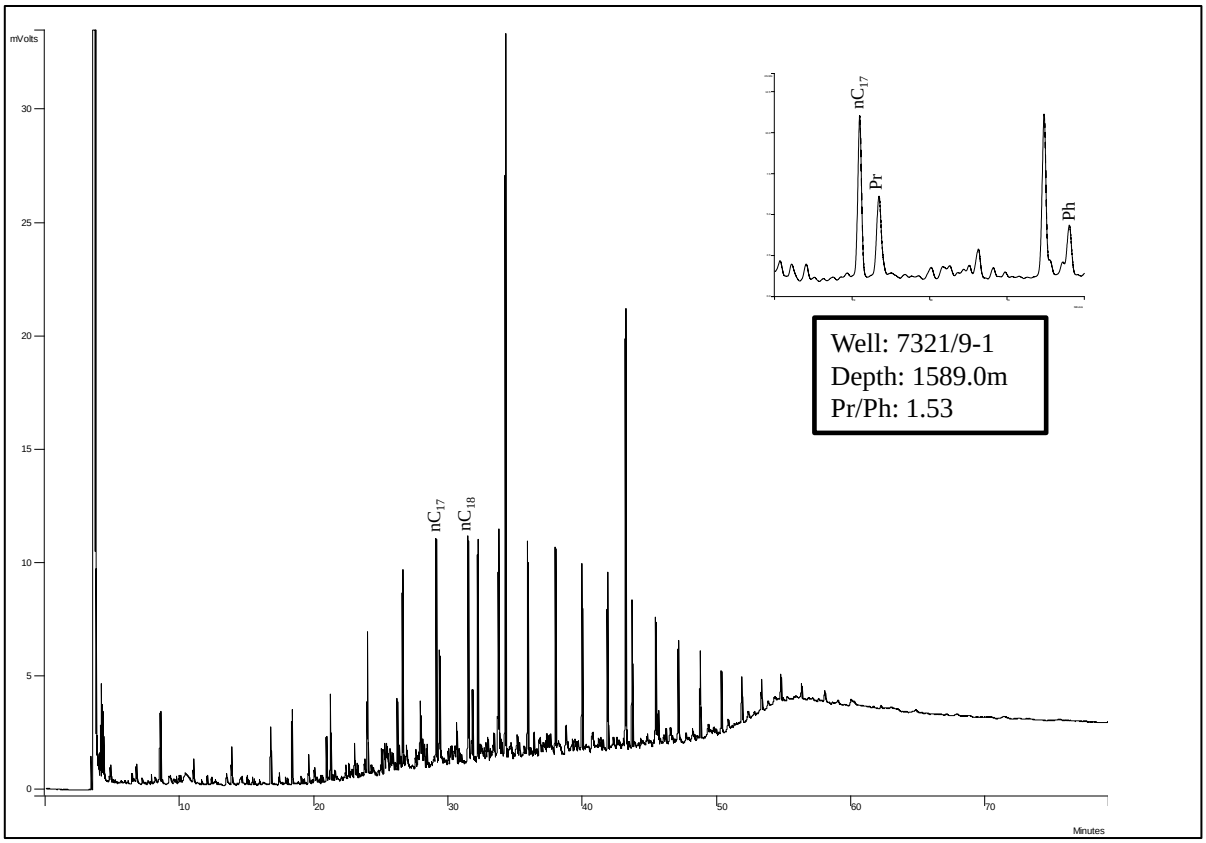
mVolts
30
25
20
15
10
5
0
10
20
30
40
50
60
70
Minutes
nC17
nC18
nC17
Pr
Ph
Well: 7321/9-1
Depth: 1589.0m
Pr/Ph: 1.53

Appendix C (GC-MS Results)

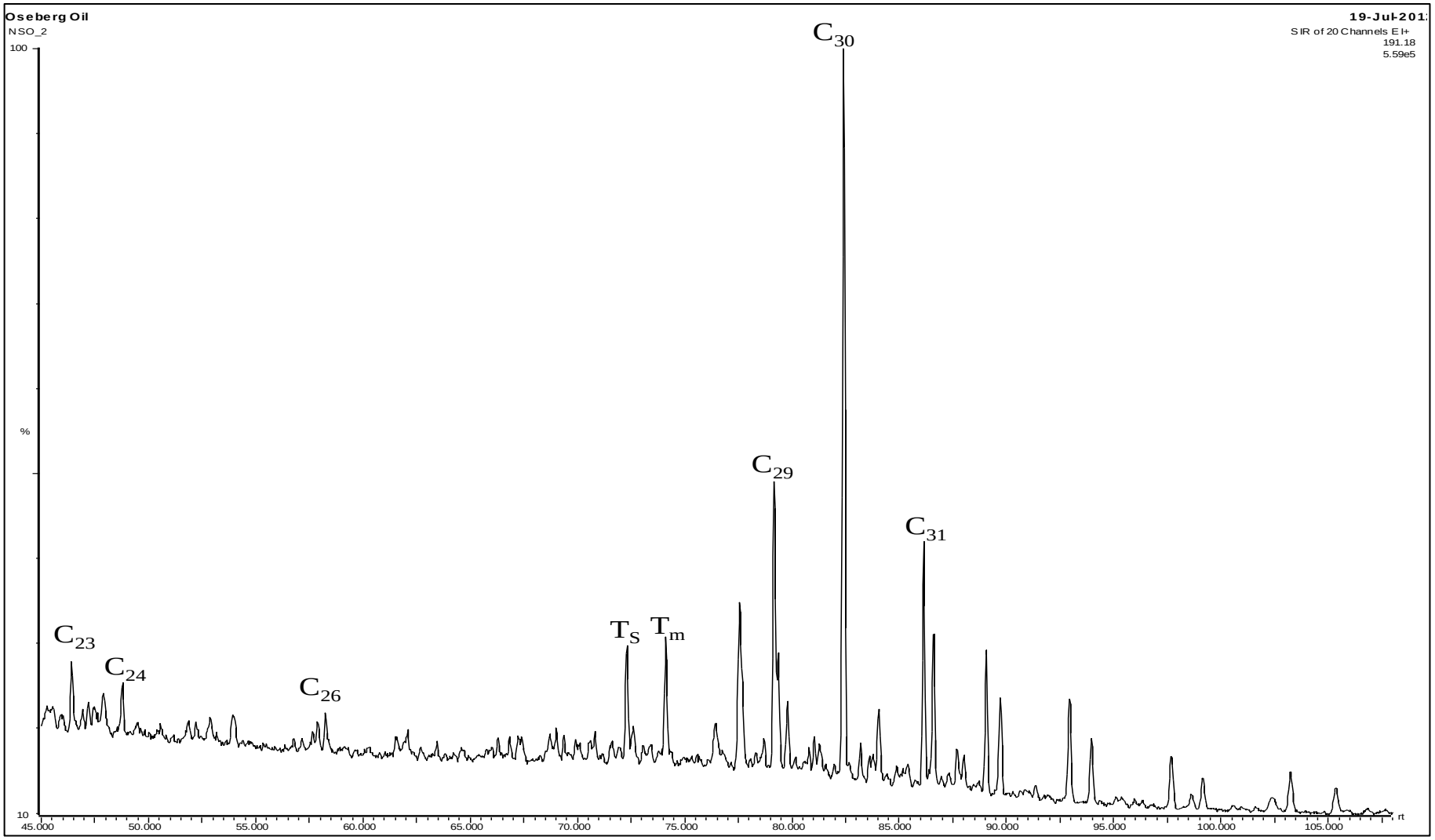
Oseberg Oil
NSO_2
19-Jul-201
SIR of 20 Channels EI+
191.18
5.59e5
100
%
10
C30
C29
C31
C23
C24
C26
TS
Tm
45.000
50.000
55.000
60.000
65.000
70.000
75.000
80.000
85.000
90.000
95.000
100.000
105.000
rt

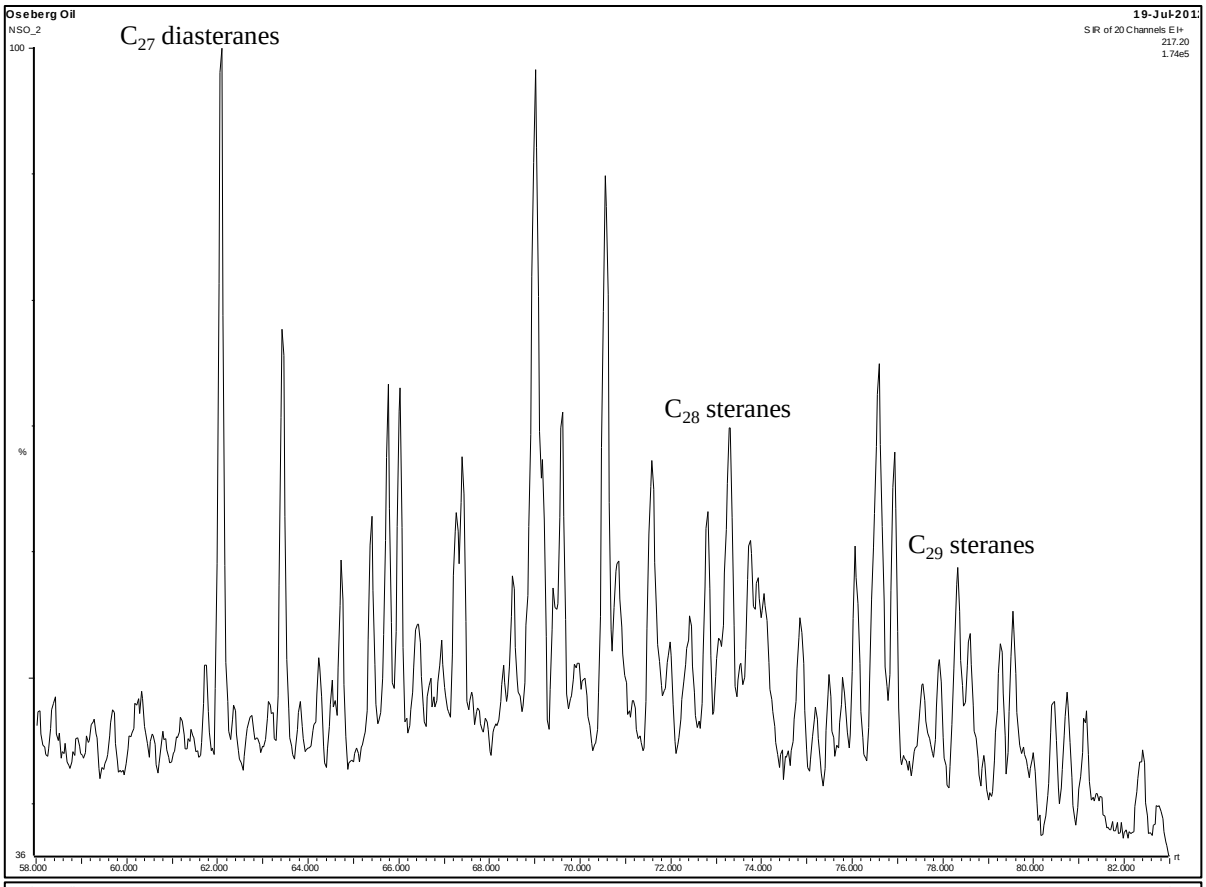
Oseberg Oil
NSO_2
19-Jul-2011
SIR of 20 Channels EI+
217.20
1.74e5
C_{27} diasteranes
C_{28} steranes
C_{29} steranes
100
%
36
58.000
60.000
62.000
64.000
66.000
68.000
70.000
72.000
74.000
76.000
78.000
80.000
82.000
rt

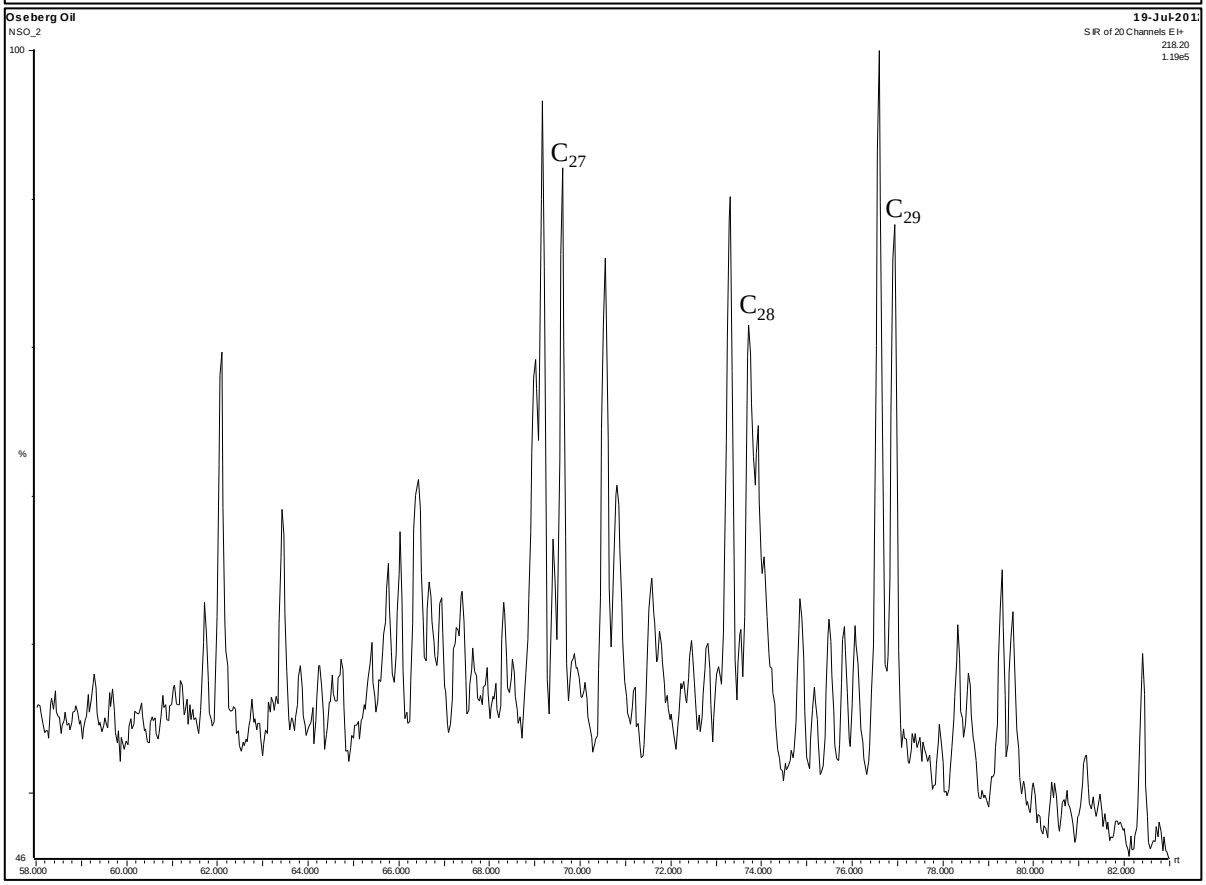
Oseberg Oil
NSO_2
19-Jul-2011
SIR of 20 Channels EI+
218.20
1.19e5
C_{27}
C_{28}
C_{29}
100
%
46
58.000
60.000
62.000
64.000
66.000
68.000
70.000
72.000
74.000
76.000
78.000
80.000
82.000
rt

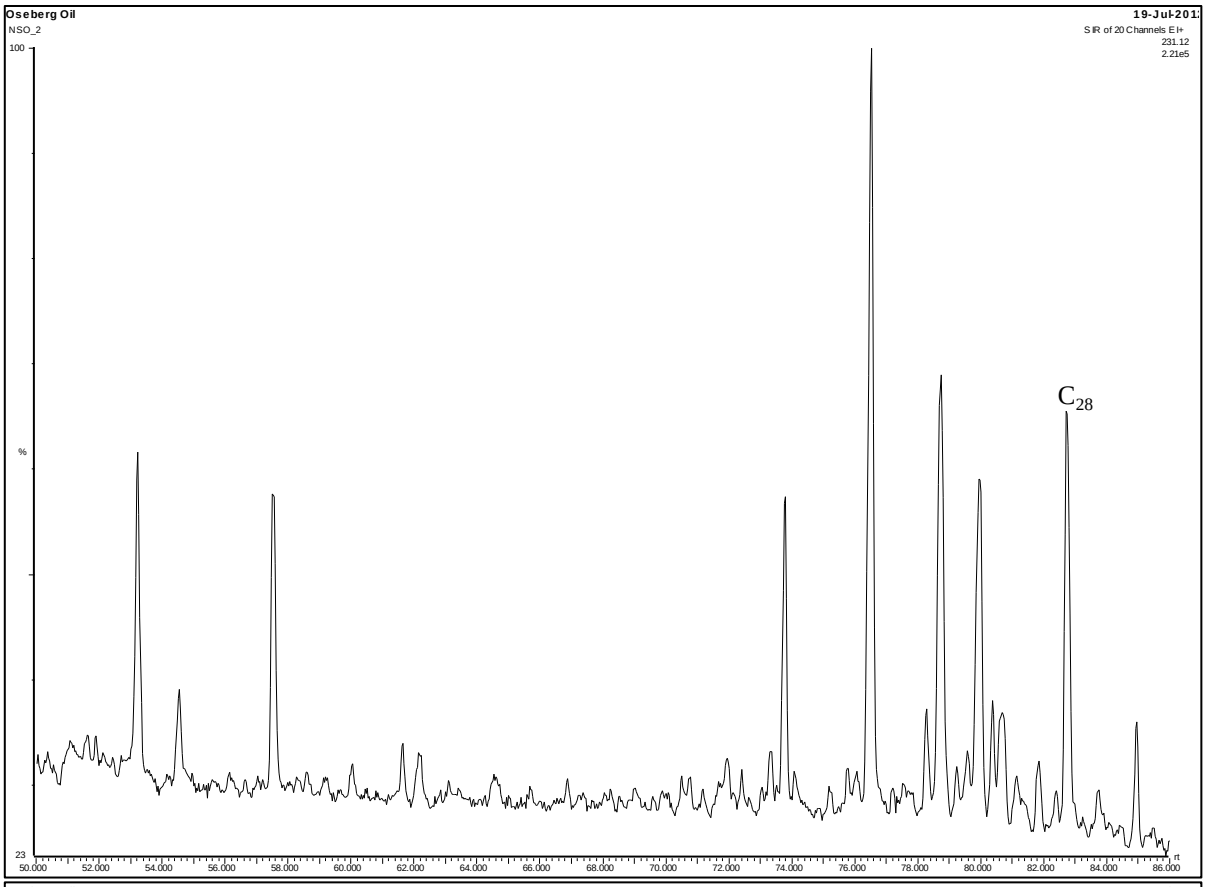
Oseberg Oil
NSO_2
19-Jul-2011
SIR of 20 Channels EI+
231.12
2.21e5
100
%
23
C28
50.000 52.000 54.000 56.000 58.000 60.000 62.000 64.000 66.000 68.000 70.000 72.000 74.000 76.000 78.000 80.000 82.000 84.000 86.000
rt

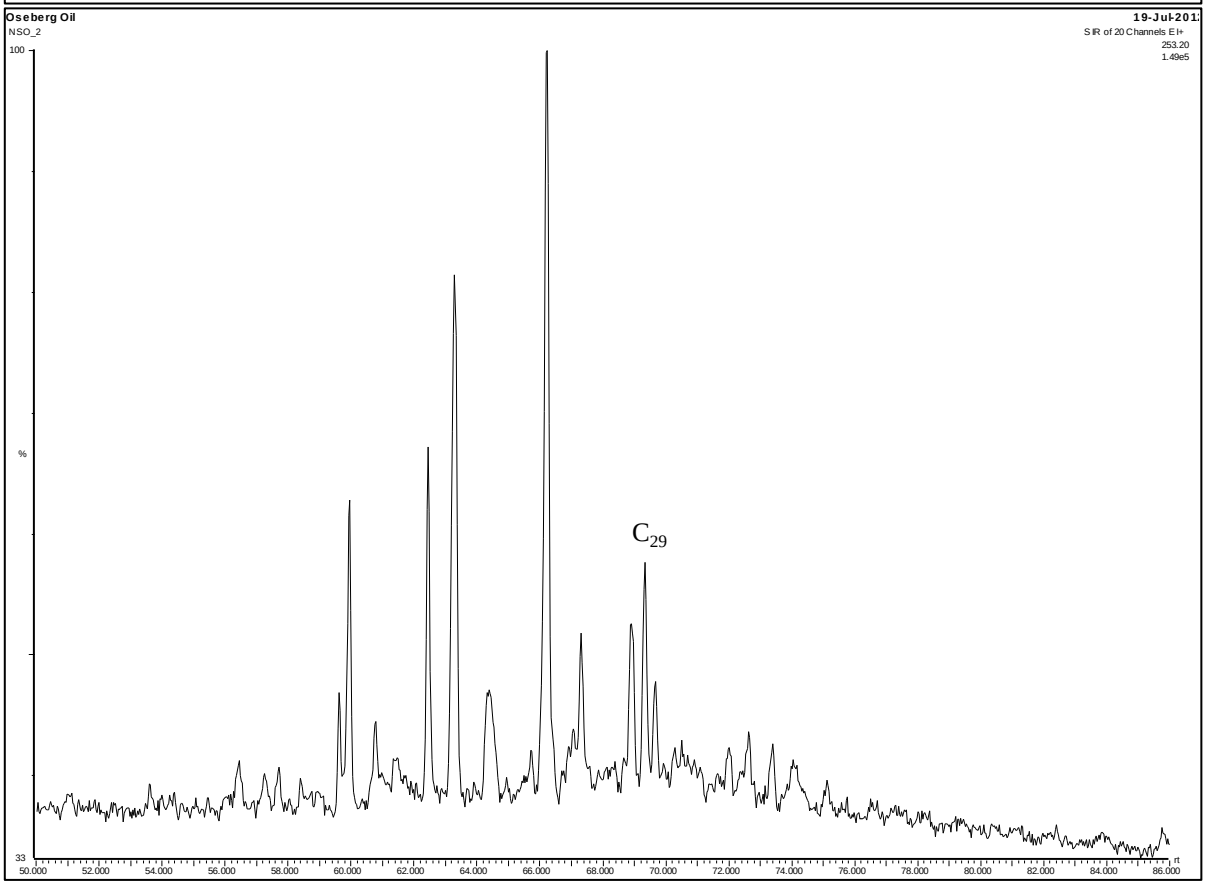
Oseberg Oil
NSO_2
19-Jul-2011
SIR of 20 Channels EI+
253.20
1.49e5
100
%
33
C29
50.000 52.000 54.000 56.000 58.000 60.000 62.000 64.000 66.000 68.000 70.000 72.000 74.000 76.000 78.000 80.000 82.000 84.000 86.000
rt

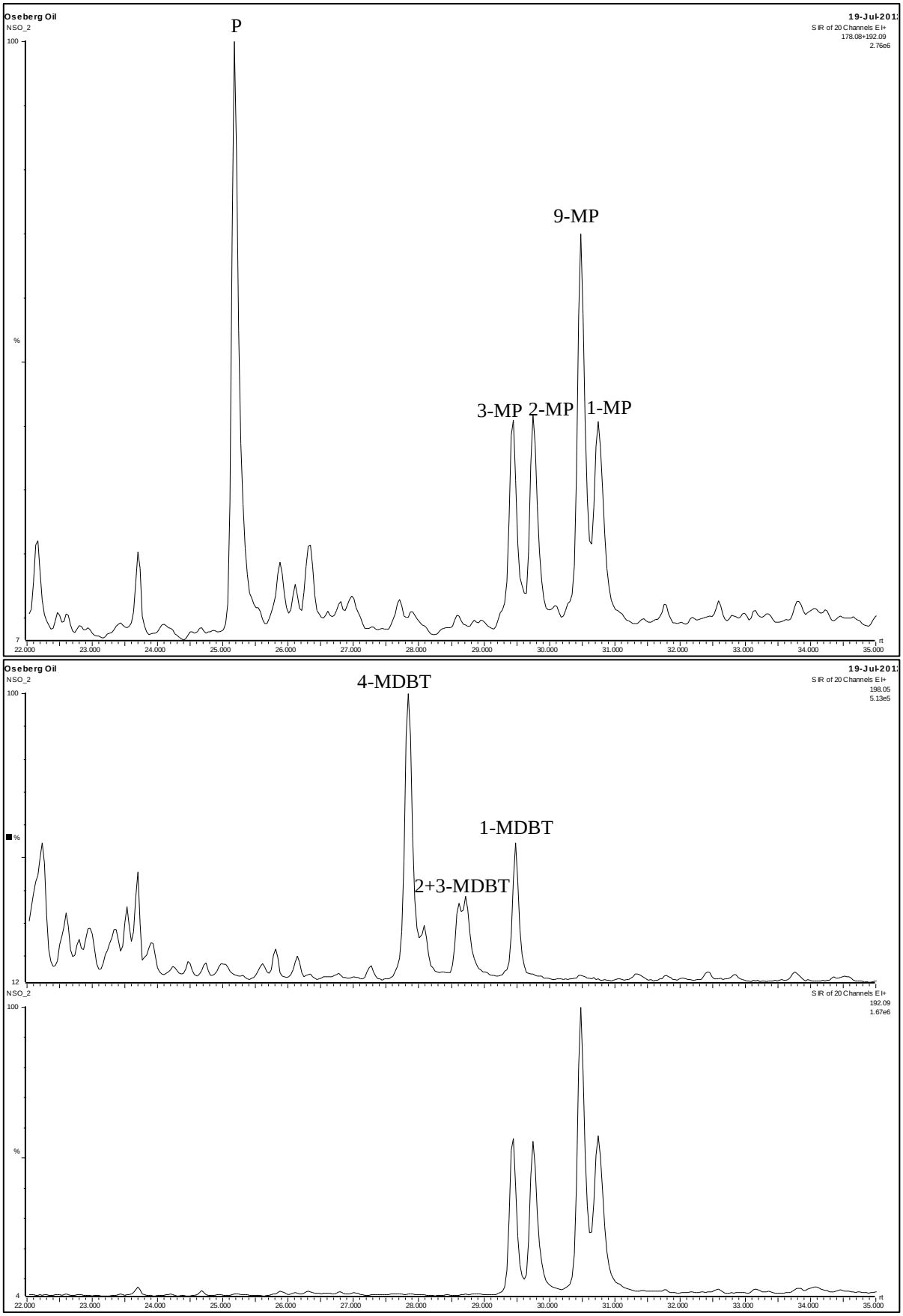
Oseberg Oil
NSO_2
19-Jul-201
SIR of 20 Channels EI+
178.08+192.09
2.76e6
P
9-MP
3-MP
2-MP
1-MP
Oseberg Oil
NSO_2
19-Jul-201
SIR of 20 Channels EI+
198.05
5.13e5
4-MDBT
1-MDBT
2+3-MDBT
NSO_2
SIR of 20 Channels EI+
192.09
1.67e6
22.000
23.000
24.000
25.000
26.000
27.000
28.000
29.000
30.000
31.000
32.000
33.000
34.000
35.000

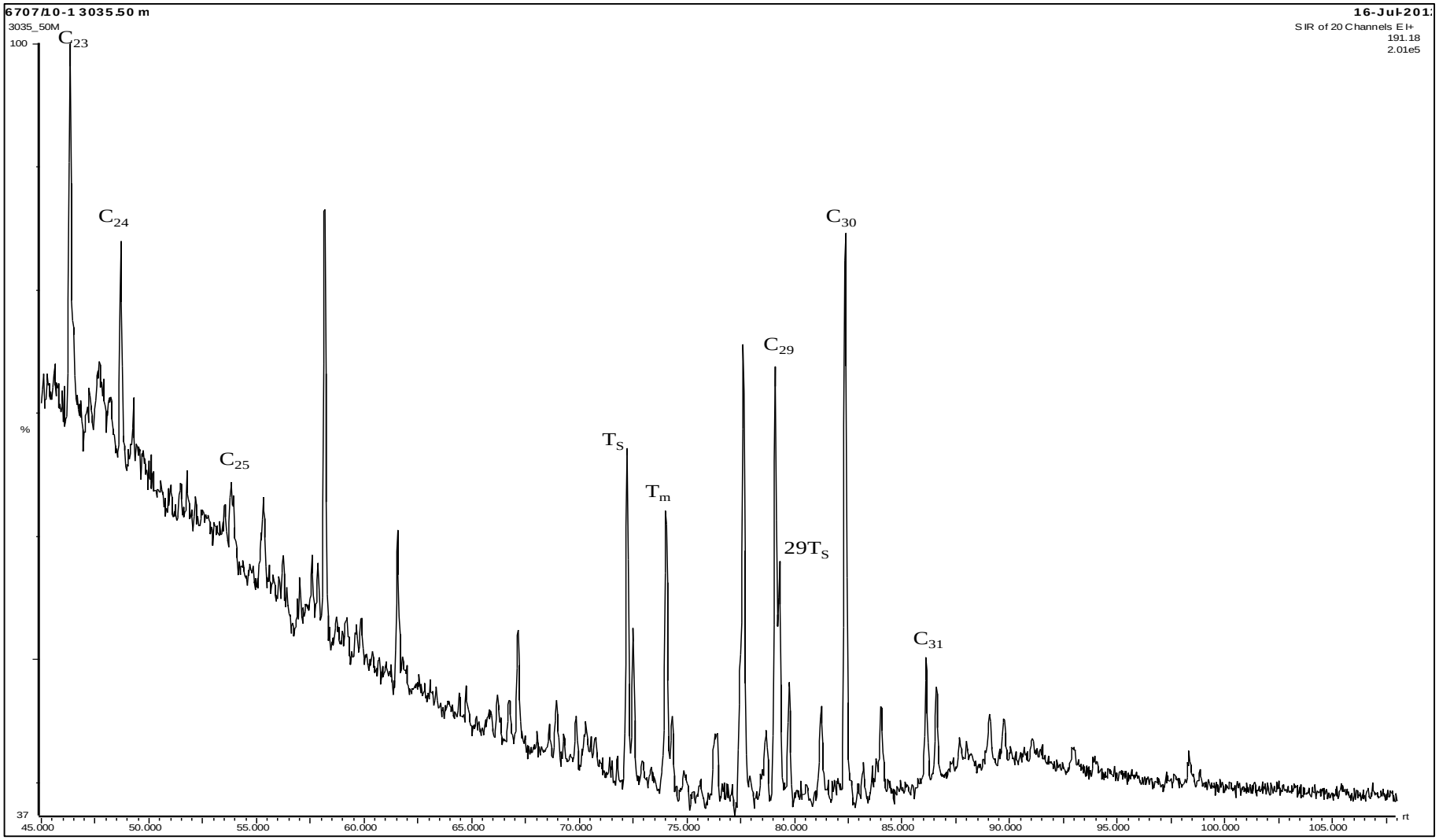
6707/10-1 3035.50 m
3035_50M
16-Jul-201
SIR of 20 Channels EI+
191.18
2.01e5
100
%
37
C23
C24
C25
TS
Tm
C29
29TS
C30
C31
45.000
50.000
55.000
60.000
65.000
70.000
75.000
80.000
85.000
90.000
95.000
100.000
105.000
rt

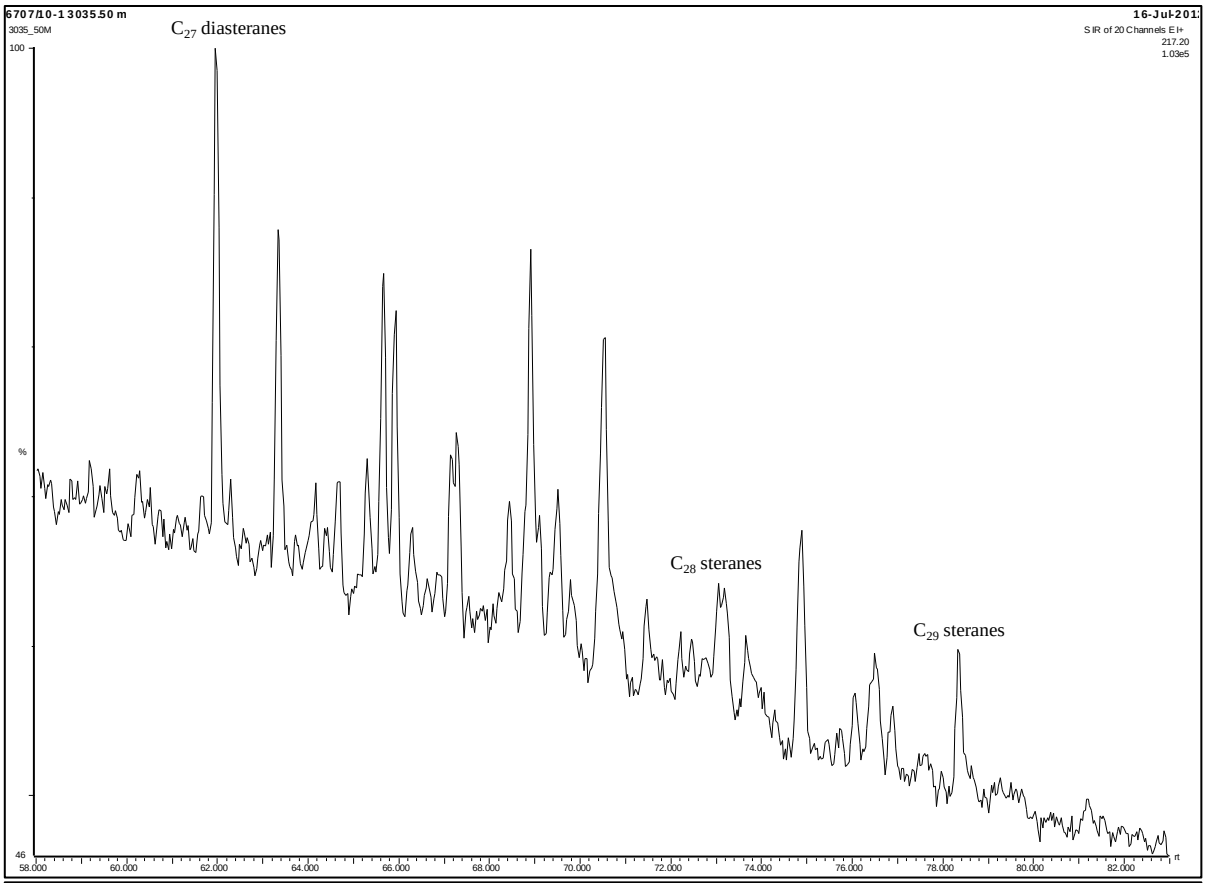
6707/10-1 3035.50 m
3035_50M
16-Jul-201
SIR of 20 Channels EI+
217.20
1.03e5
100
%
46
C27 diasteranes
C28 steranes
C29 steranes
58.000
60.000
62.000
64.000
66.000
68.000
70.000
72.000
74.000
76.000
78.000
80.000
82.000
rt

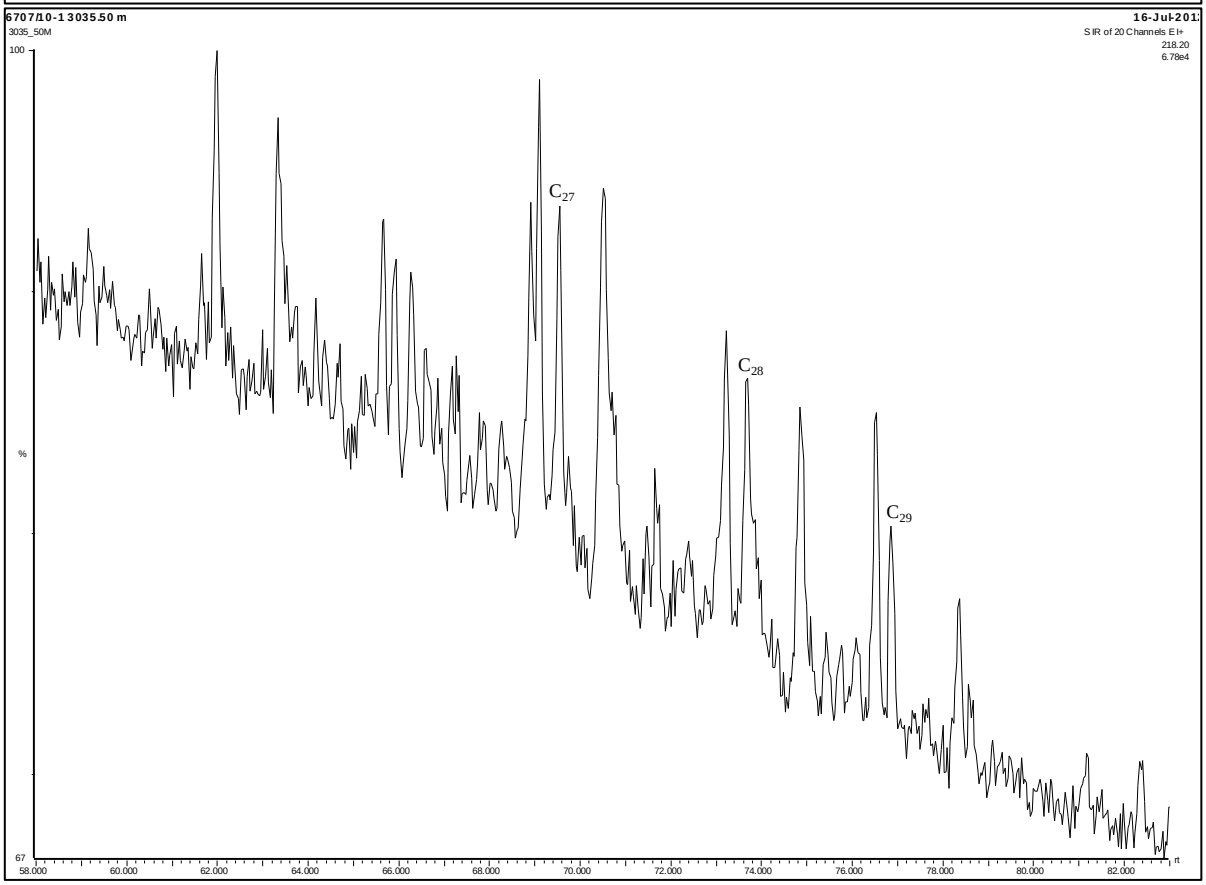
6707/10-1 3035.50 m
3035_50M
16-Jul-201
SIR of 20 Channels EI+
218.20
6.78e4
100
%
67
C27
C28
C29
58.000
60.000
62.000
64.000
66.000
68.000
70.000
72.000
74.000
76.000
78.000
80.000
82.000
rt

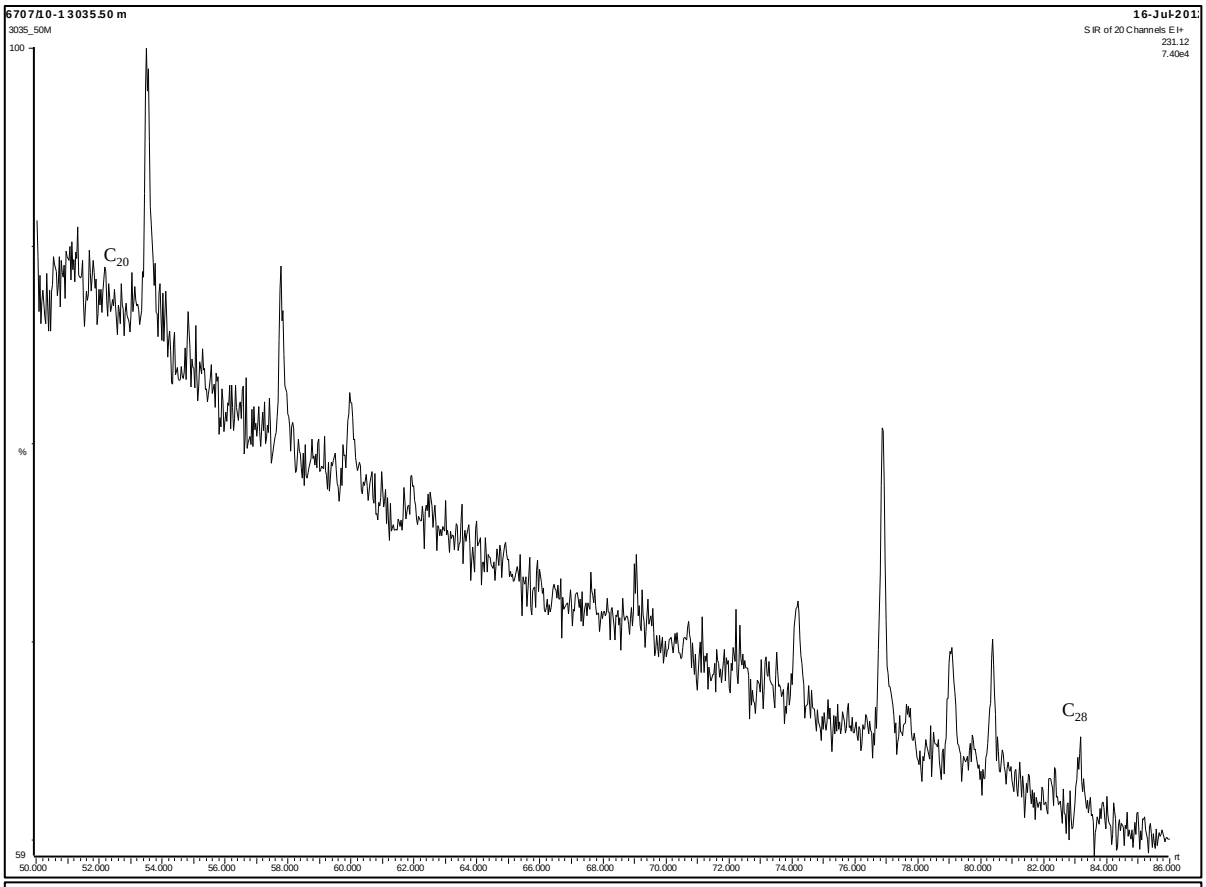
6707/10-1 3035.50 m
16-Jul-201
3035_50M
SIR of 20 Channels EI+
231.12
7.40e4
100
%
59
C20
C28
50.000 52.000 54.000 56.000 58.000 60.000 62.000 64.000 66.000 68.000 70.000 72.000 74.000 76.000 78.000 80.000 82.000 84.000 86.000
rt

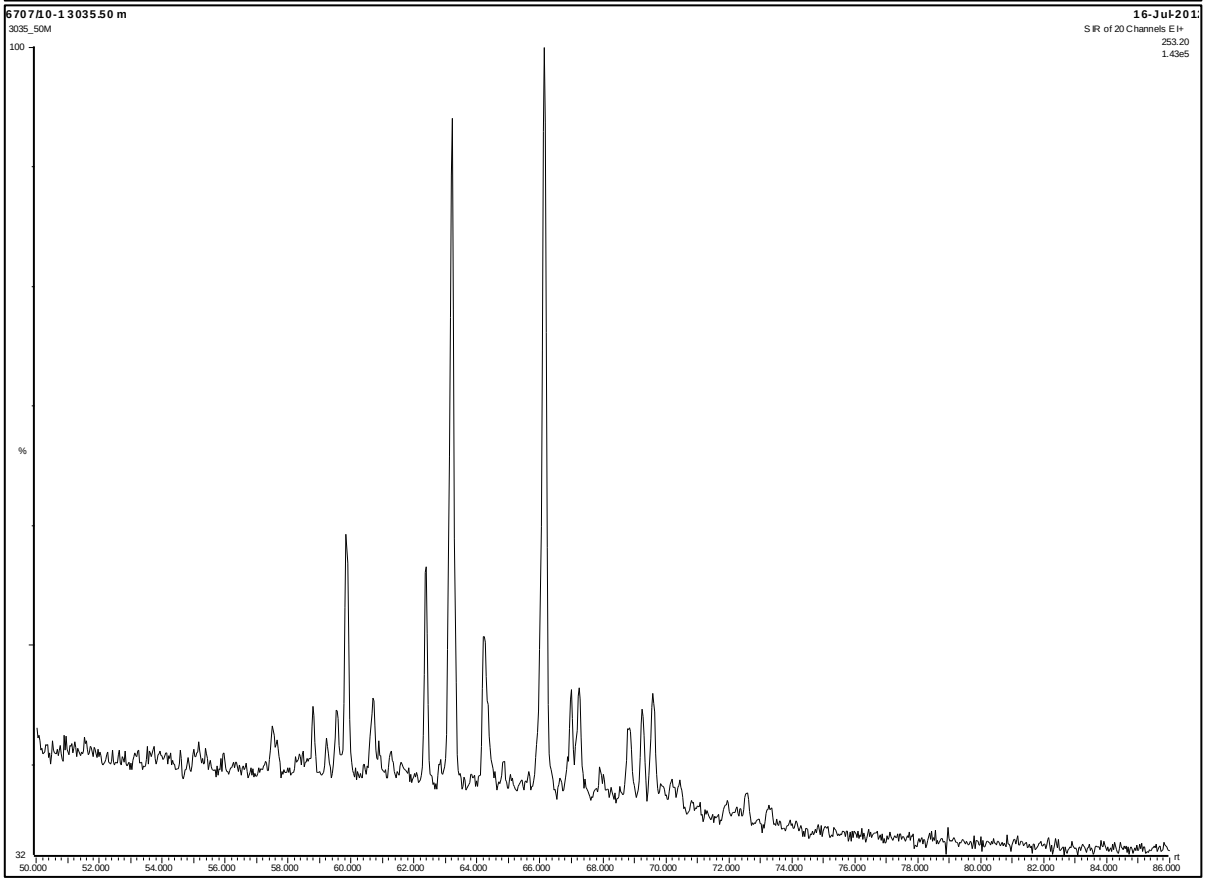
6707/10-1 3035.50 m
16-Jul-201
3035_50M
SIR of 20 Channels EI+
253.20
1.43e5
100
%
32
50.000 52.000 54.000 56.000 58.000 60.000 62.000 64.000 66.000 68.000 70.000 72.000 74.000 76.000 78.000 80.000 82.000 84.000 86.000
rt

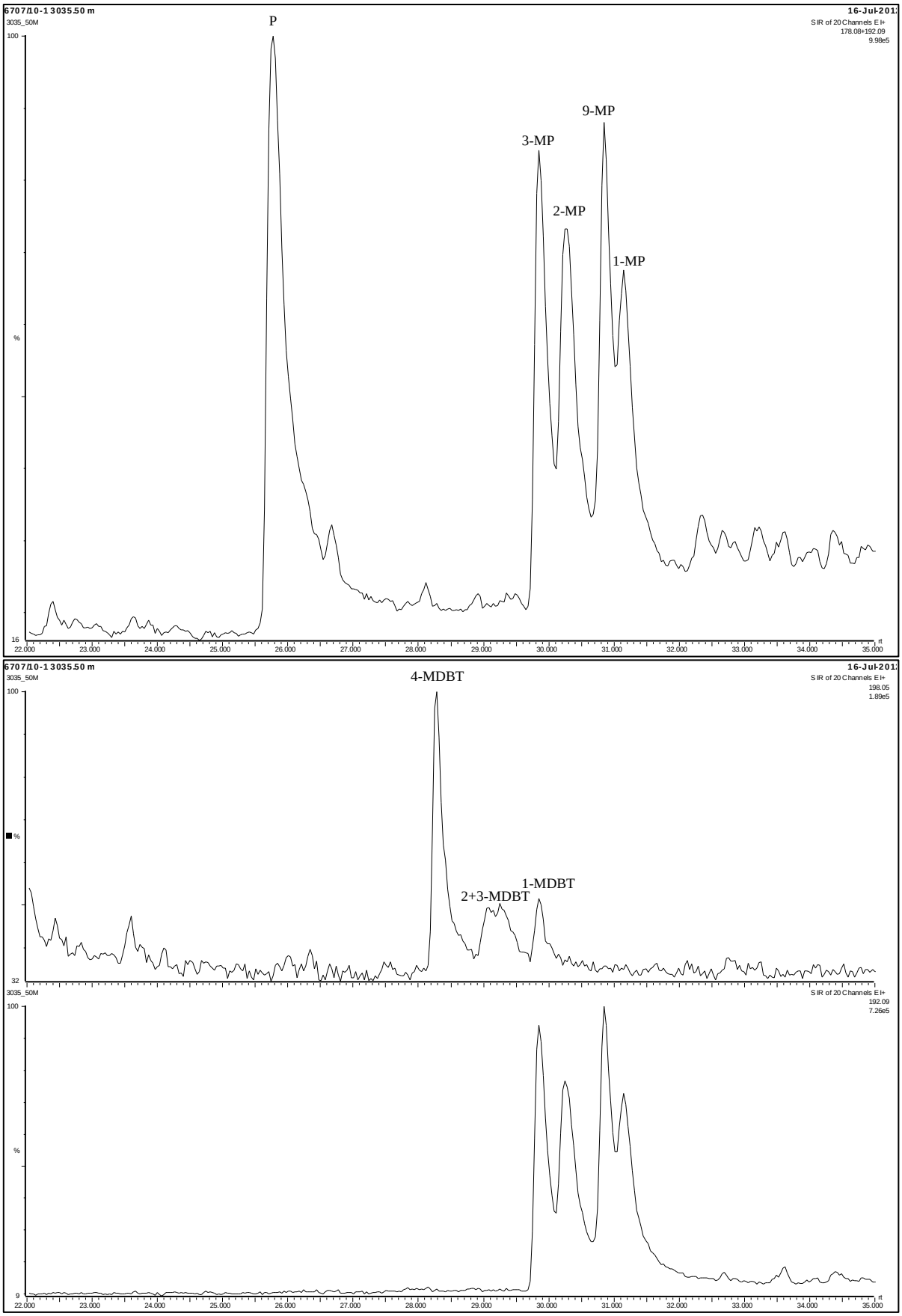
6707/10-1 3035.50 m
3035_50M
16-Jul-201
SIR of 20 Channels EI+
178.08+192.09
9.98e5
P
3-MP
9-MP
2-MP
1-MP
%
rt
22.000
23.000
24.000
25.000
26.000
27.000
28.000
29.000
30.000
31.000
32.000
33.000
34.000
35.000
6707/10-1 3035.50 m
3035_50M
16-Jul-201
SIR of 20 Channels EI+
198.05
1.89e5
4-MDBT
1-MDBT
2+3-MDBT
3035_50M
SIR of 20 Channels EI+
192.09
7.26e5

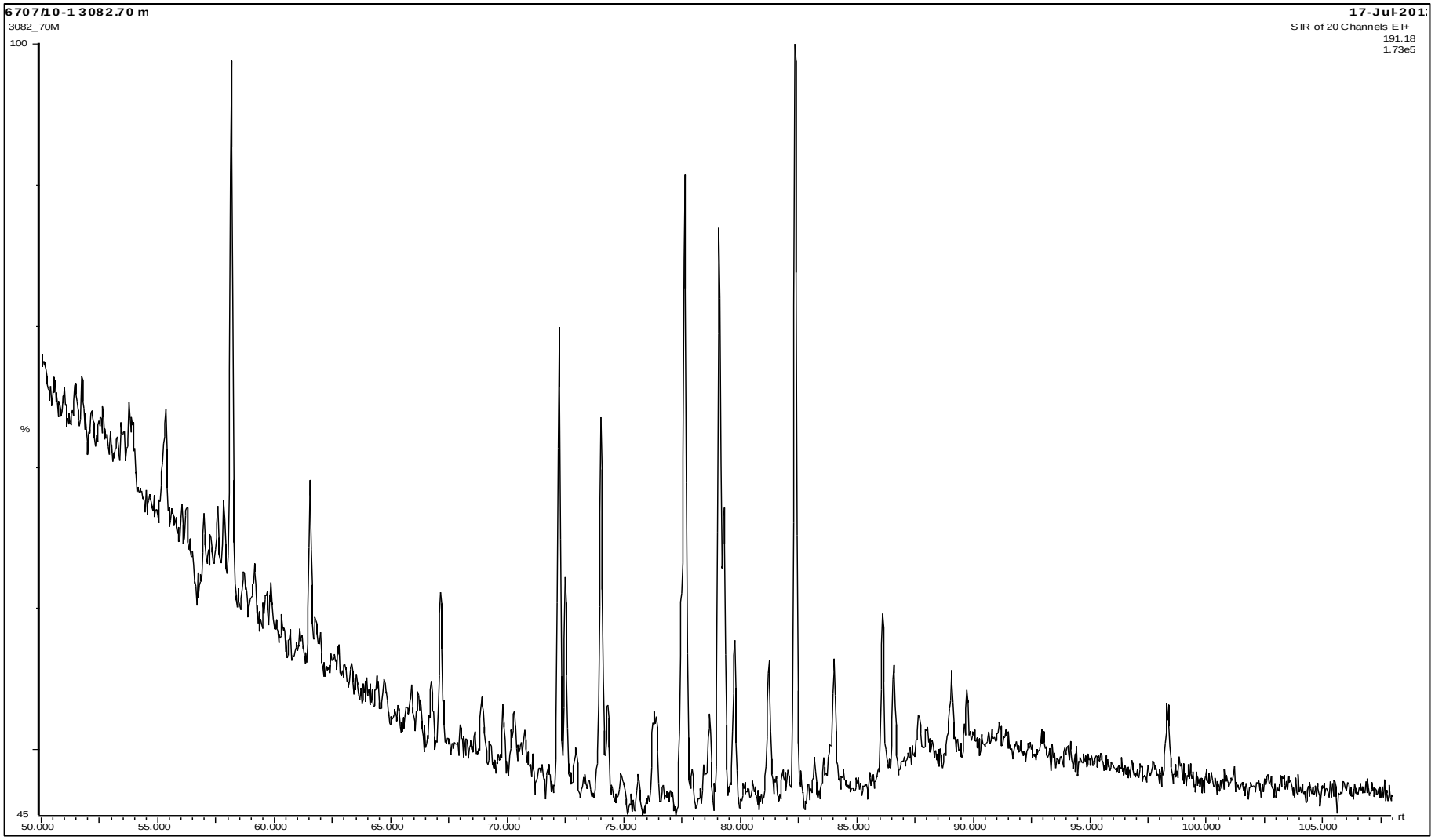
6707A10-1 3082.70 m
17-Jul-201
3082_70M
SIR of 20 Channels EI+
191.18
1.73e5
100
%
45
50.000
55.000
60.000
65.000
70.000
75.000
80.000
85.000
90.000
95.000
100.000
105.000
rt

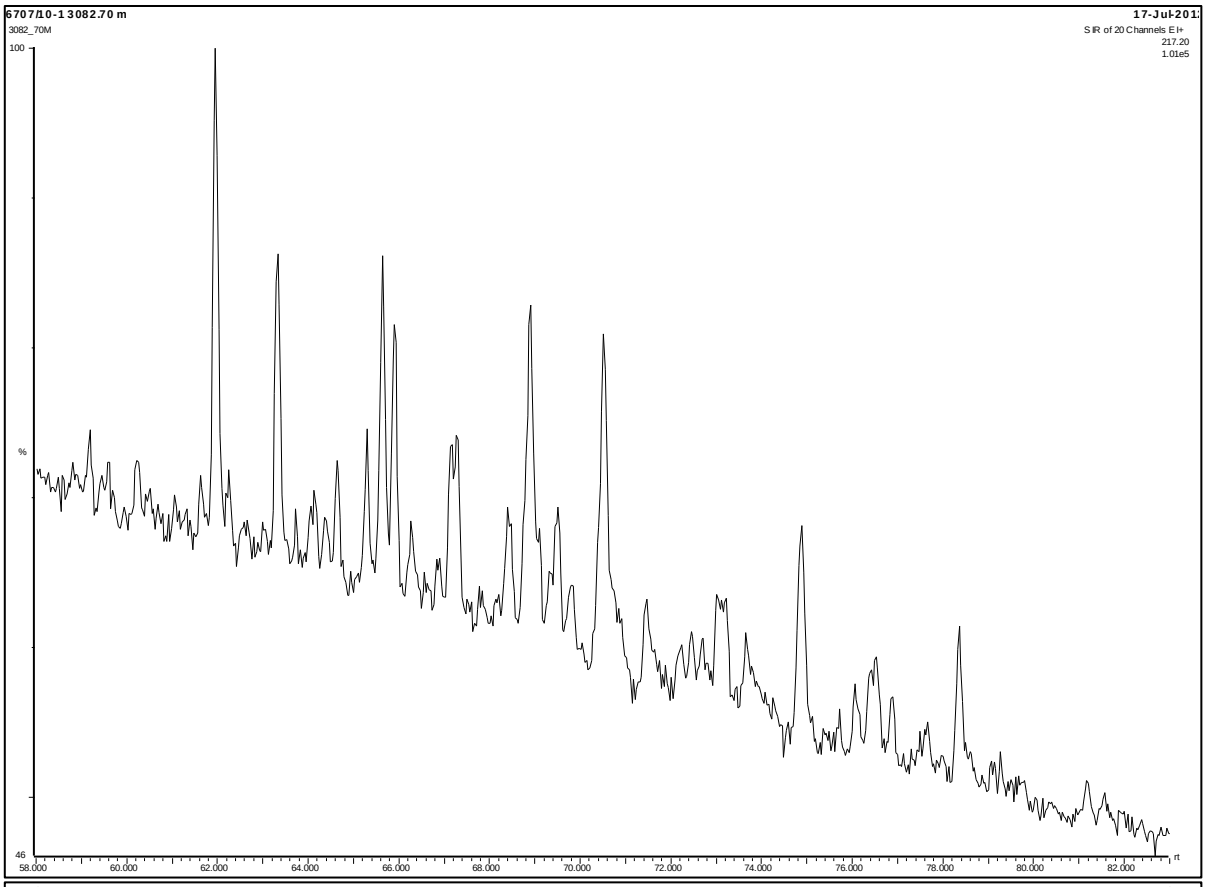
6707/10-1 3082.70 m
3082_70M
17-Jul-201
SIR of 20 Channels EI+
217.20
1.01e5
100
%
46
58.000
60.000
62.000
64.000
66.000
68.000
70.000
72.000
74.000
76.000
78.000
80.000
82.000
rt

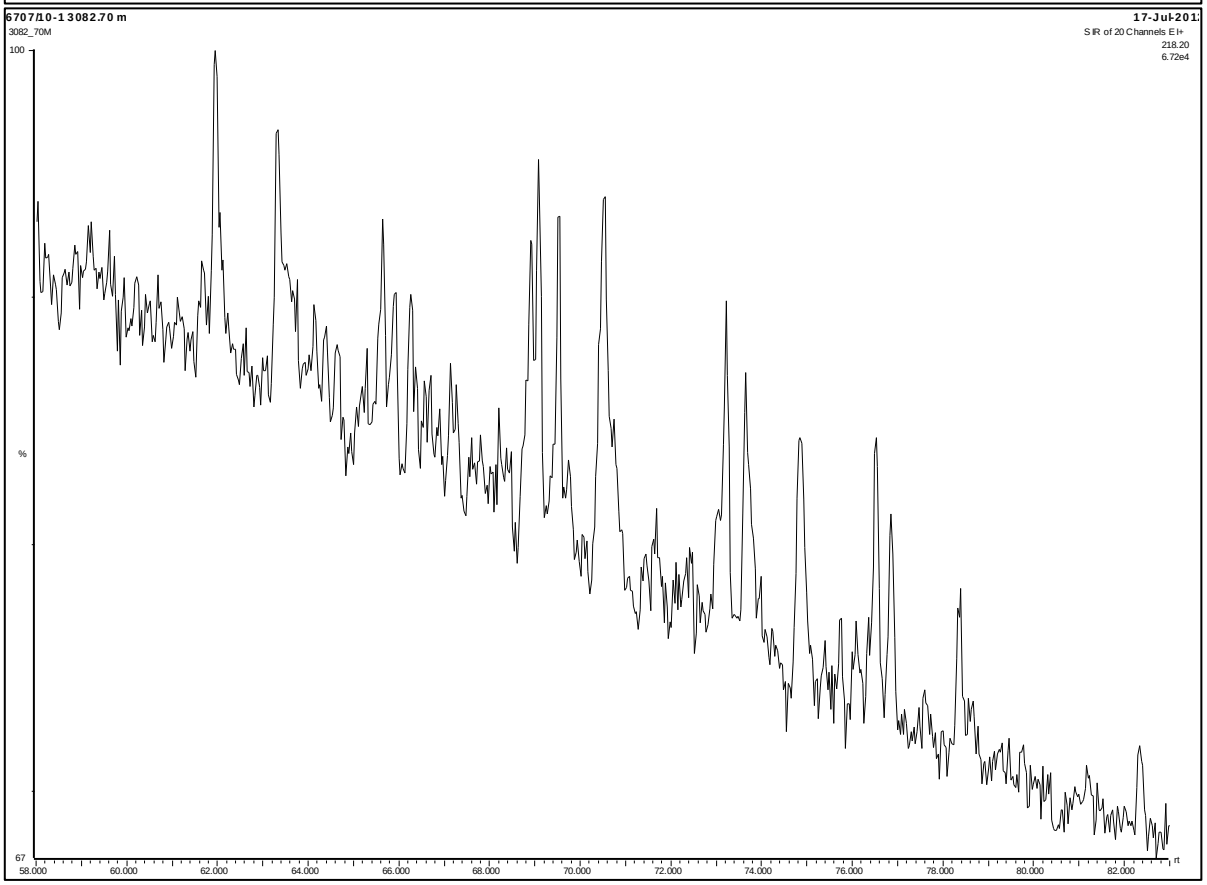
6707/10-1 3082.70 m
3082_70M
17-Jul-201
SIR of 20 Channels EI+
218.20
6.72e4
100
%
67
58.000
60.000
62.000
64.000
66.000
68.000
70.000
72.000
74.000
76.000
78.000
80.000
82.000
rt

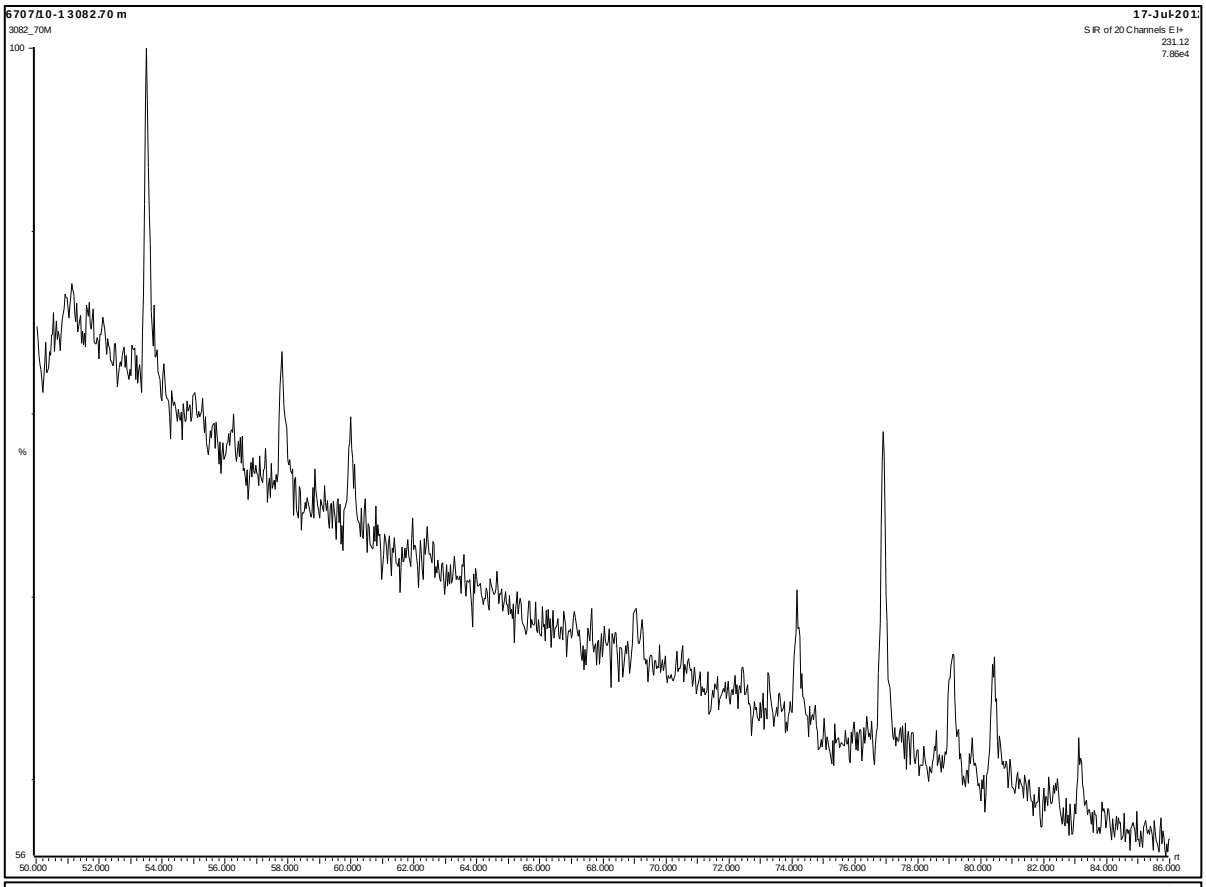
6707/10-1 3082.70 m
17-Jul-201
3082_70M
SIR of 20 Channels EI+
231.12
7.86e4
100
%
56
50.000 52.000 54.000 56.000 58.000 60.000 62.000 64.000 66.000 68.000 70.000 72.000 74.000 76.000 78.000 80.000 82.000 84.000 86.000
rt

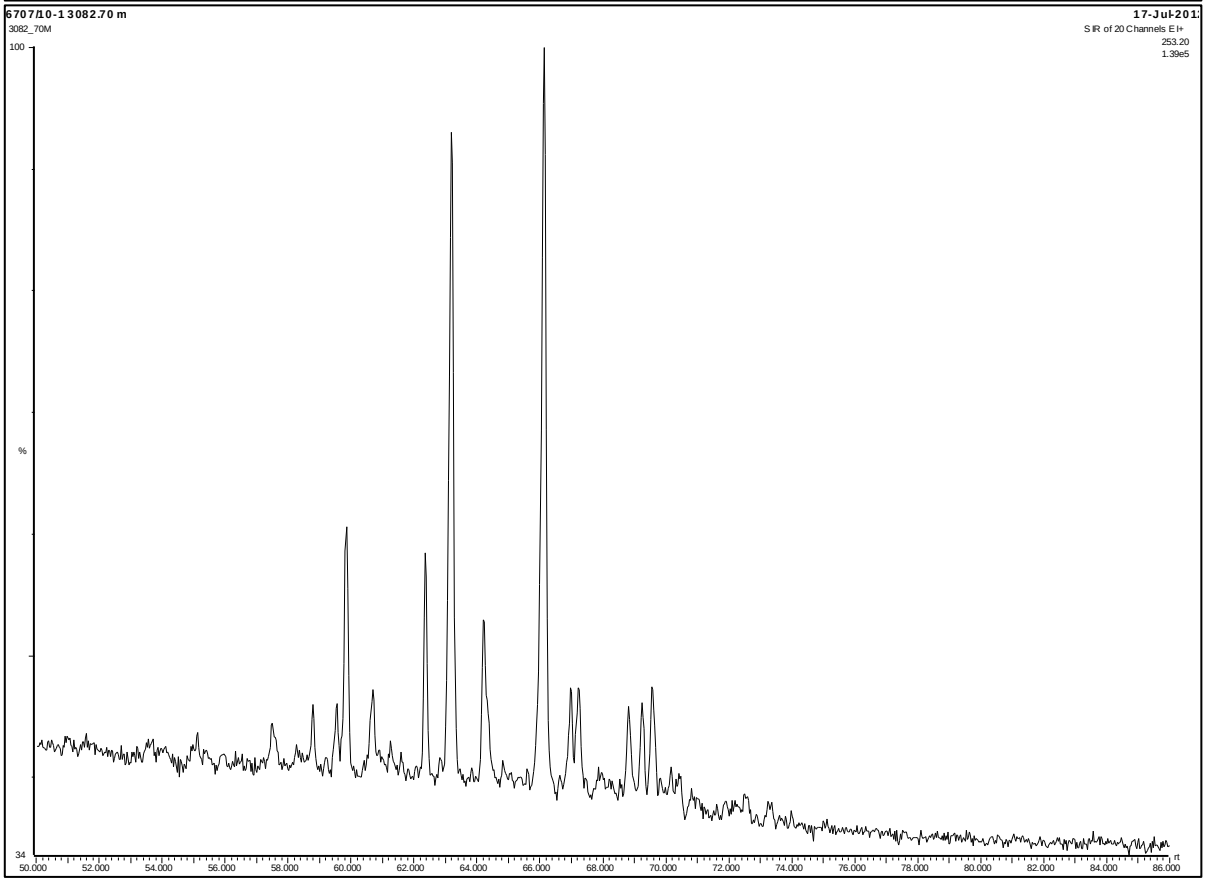
6707/10-1 3082.70 m
17-Jul-201
3082_70M
SIR of 20 Channels EI+
253.20
1.39e5
100
%
34
50.000 52.000 54.000 56.000 58.000 60.000 62.000 64.000 66.000 68.000 70.000 72.000 74.000 76.000 78.000 80.000 82.000 84.000 86.000
rt

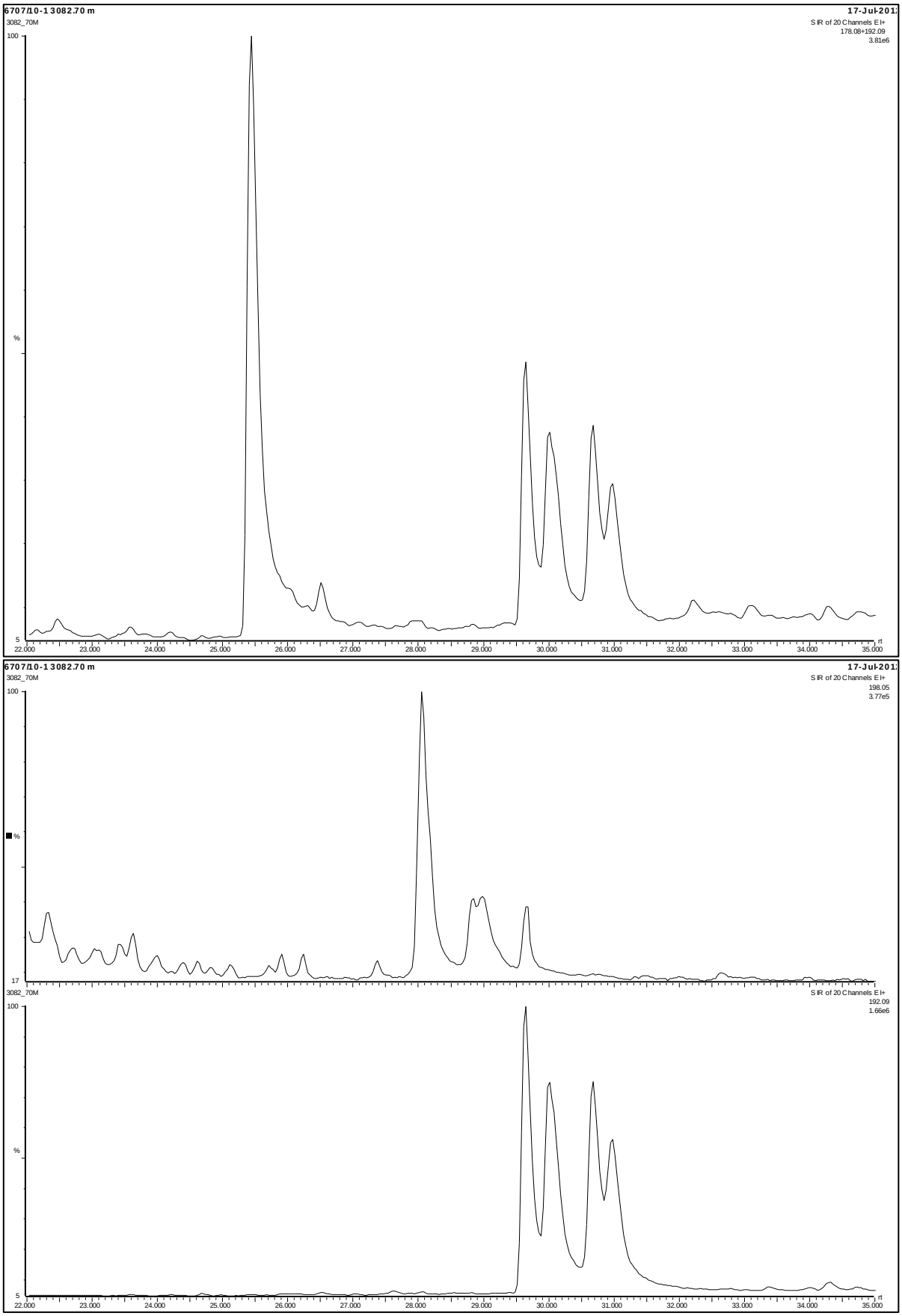
6707/10-1 3082.70 m
17-Jul-201
3082_70M
SIR of 20 Channels EI+
178.08+192.09
3.81e6
100
%
5
22.000
23.000
24.000
25.000
26.000
27.000
28.000
29.000
30.000
31.000
32.000
33.000
34.000
35.000
rt
6707/10-1 3082.70 m
17-Jul-201
3082_70M
SIR of 20 Channels EI+
198.05
3.77e5
100
%
17
3082_70M
SIR of 20 Channels EI+
192.09
1.66e6
100
%
5
22.000
23.000
24.000
25.000
26.000
27.000
28.000
29.000
30.000
31.000
32.000
33.000
34.000
35.000
rt

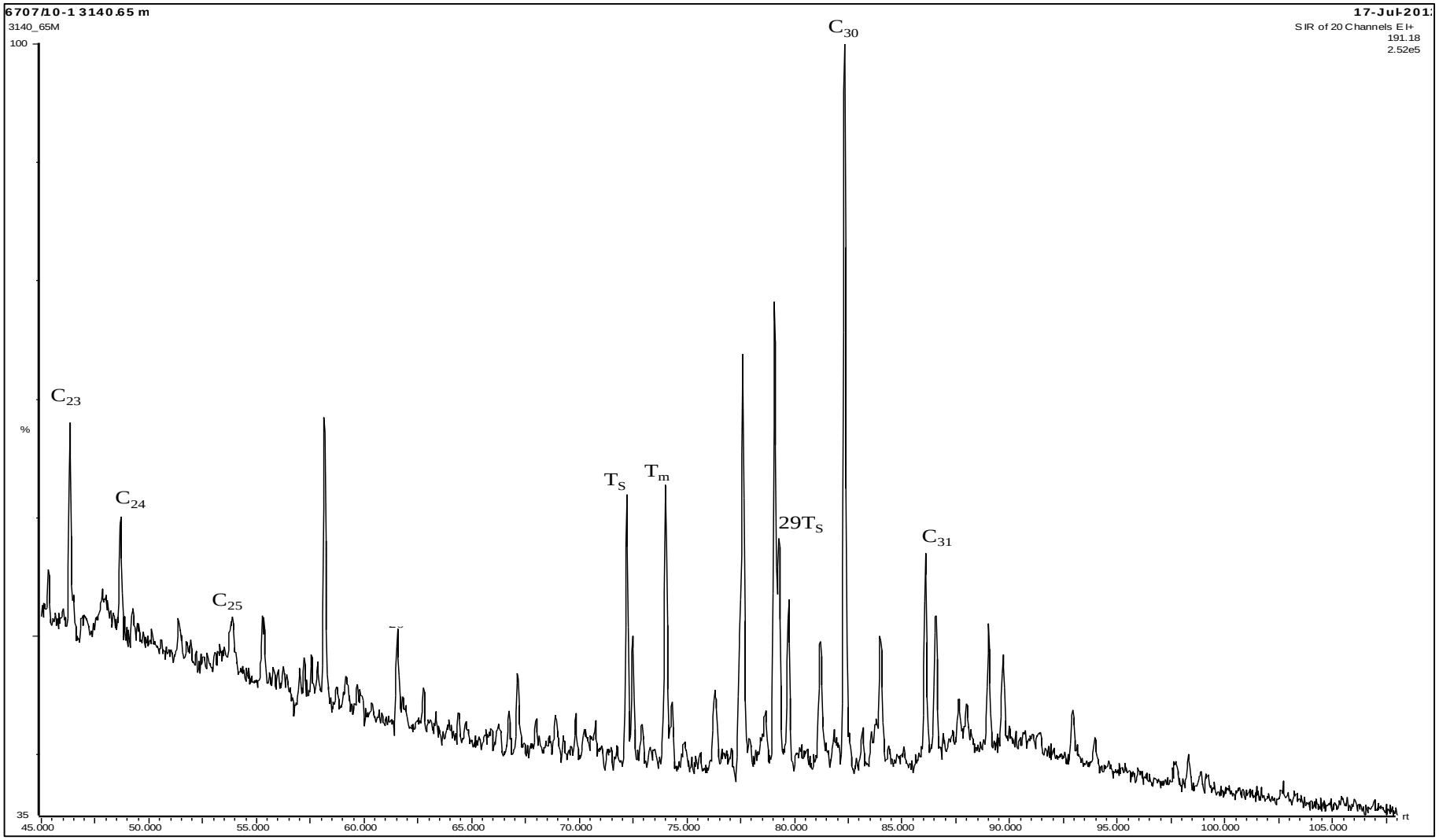
6707/10-1 3140.65 m
3140_65M
17-Jul-201
SIR of 20 Channels EI+
191.18
2.52e5
100
%
35
C23
C24
C25
TS
Tm
29TS
C30
C31
45.000
50.000
55.000
60.000
65.000
70.000
75.000
80.000
85.000
90.000
95.000
100.000
105.000
rt

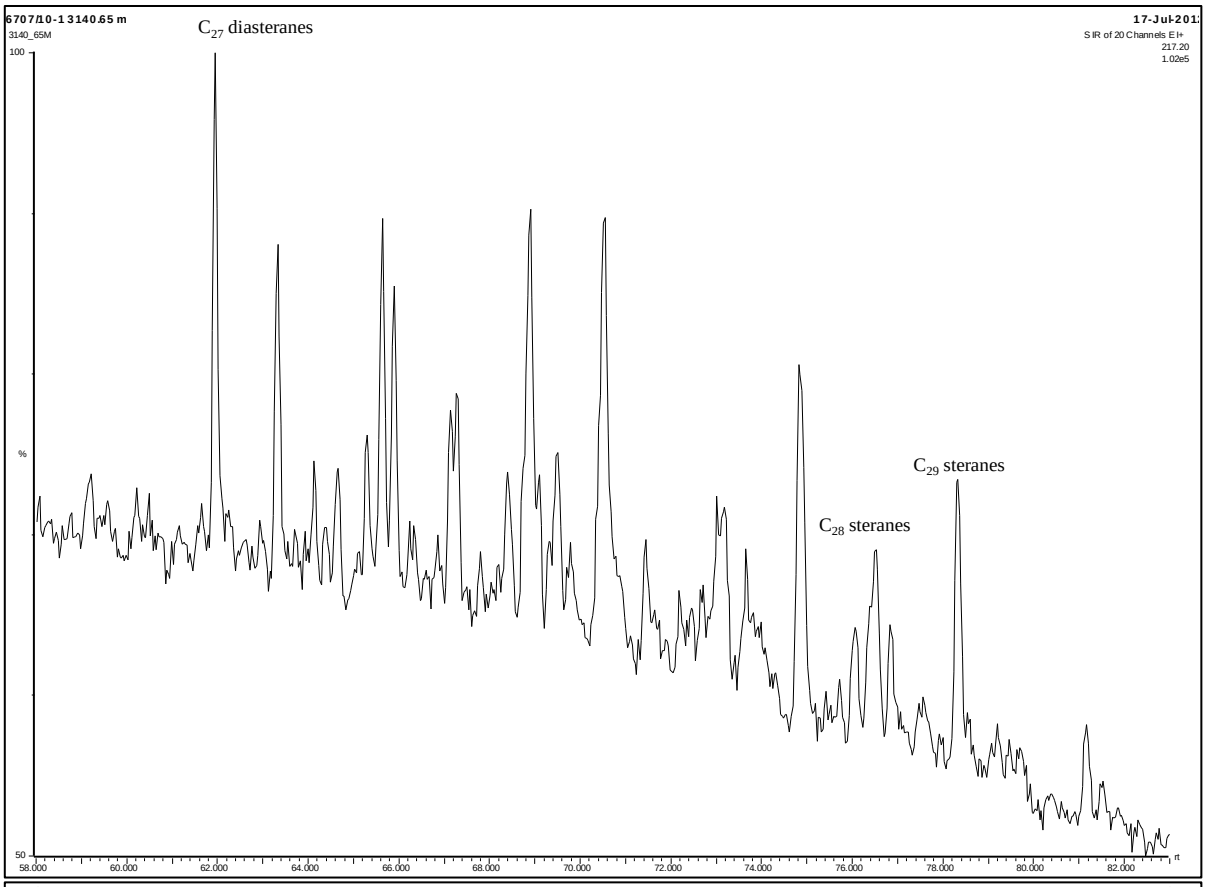
6707/10-1 3140.65 m
3140_65M
17-Jul-201
SIR of 20 Channels EI+
217.20
1.02e5
C27 diasteranes
C29 steranes
C28 steranes
100
%
50
58.000
60.000
62.000
64.000
66.000
68.000
70.000
72.000
74.000
76.000
78.000
80.000
82.000
rt

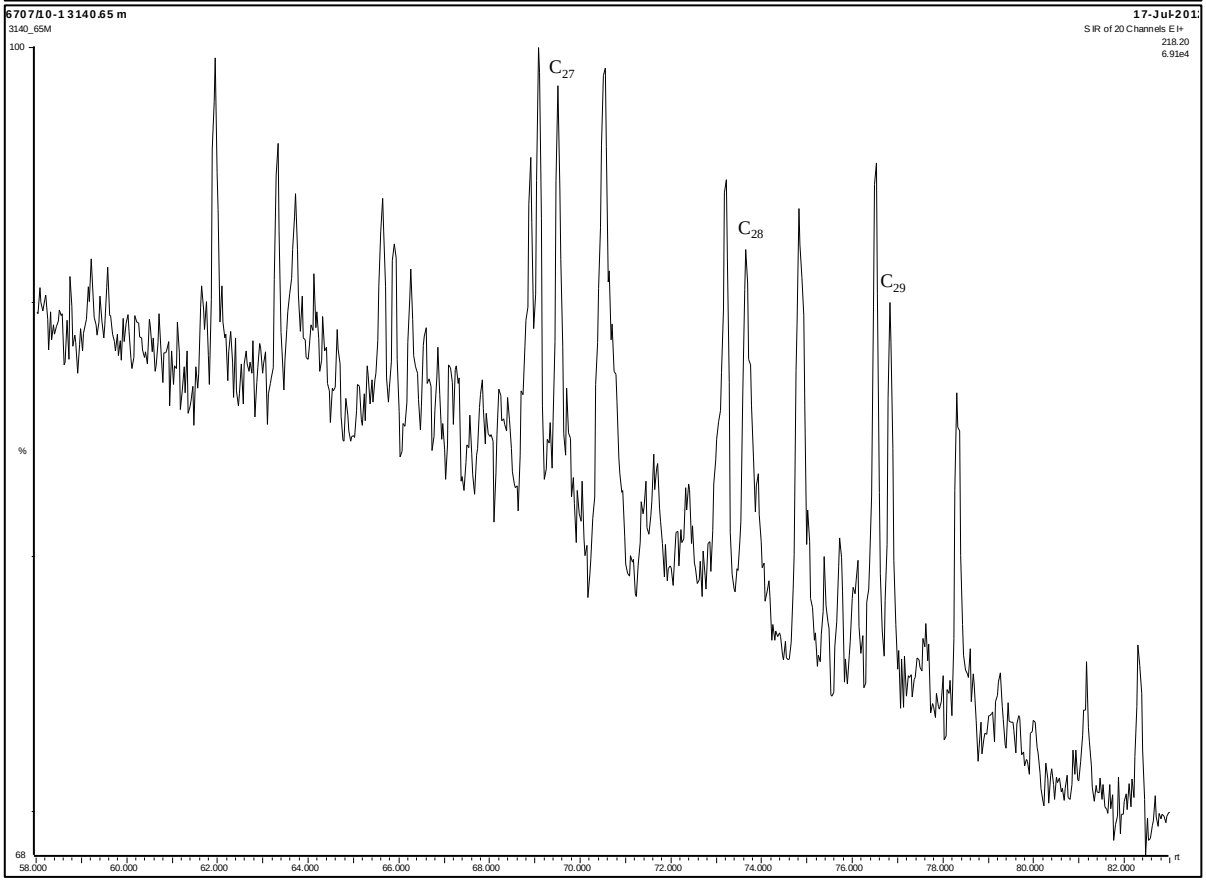
6707/10-1 3140.65 m
3140_65M
17-Jul-201
SIR of 20 Channels EI+
218.20
6.91e4
C27
C28
C29
100
%
68
58.000
60.000
62.000
64.000
66.000
68.000
70.000
72.000
74.000
76.000
78.000
80.000
82.000
rt

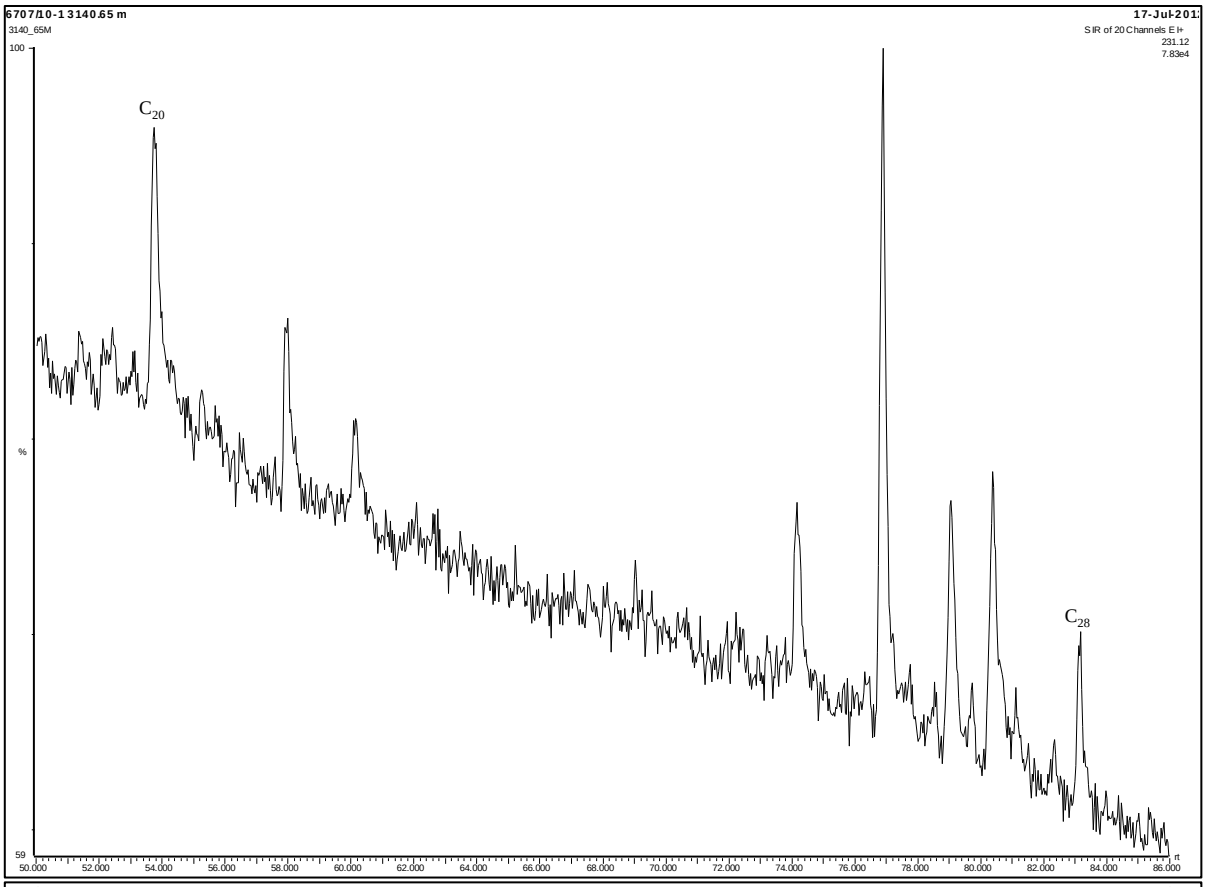
6707/10-1 3140.65 m
3140_65M
17-Jul-201
SIR of 20 Channels EI+
231.12
7.83e4
100
%
59
C20
C28
50.000 52.000 54.000 56.000 58.000 60.000 62.000 64.000 66.000 68.000 70.000 72.000 74.000 76.000 78.000 80.000 82.000 84.000 86.000
rt

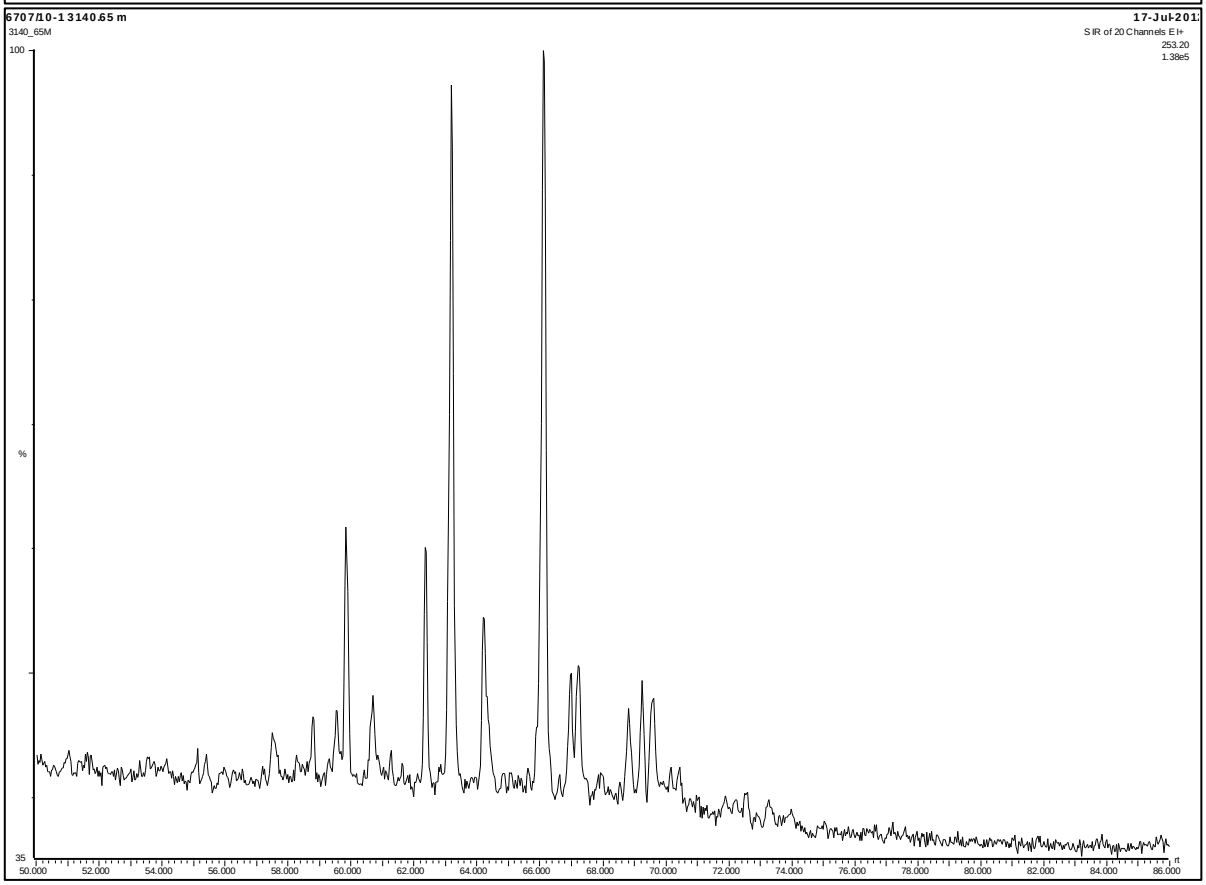
6707/10-1 3140.65 m
3140_65M
17-Jul-201
SIR of 20 Channels EI+
253.20
1.38e5
100
%
35
50.000 52.000 54.000 56.000 58.000 60.000 62.000 64.000 66.000 68.000 70.000 72.000 74.000 76.000 78.000 80.000 82.000 84.000 86.000
rt

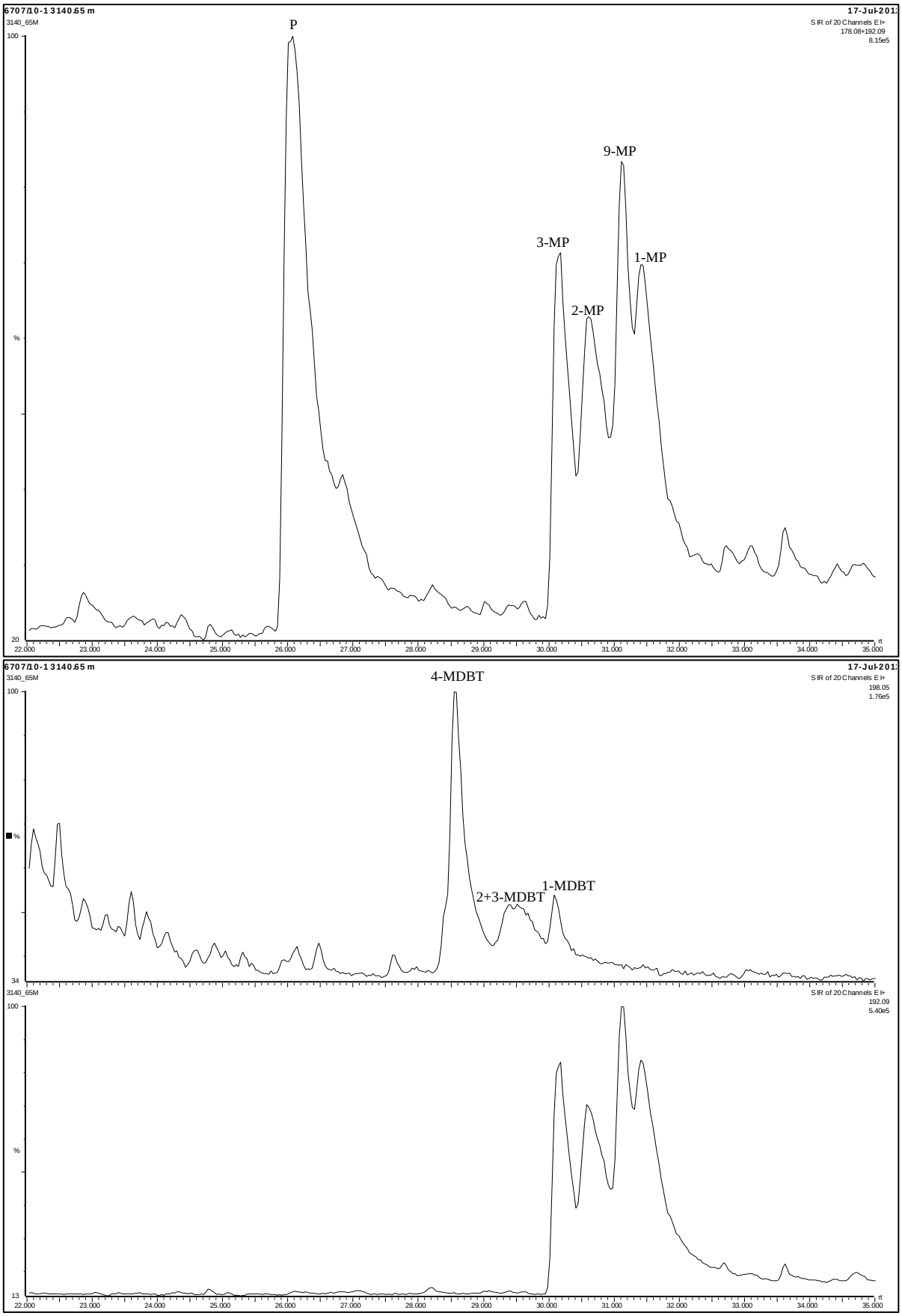
6707/10-1 3140.65 m
3140_65M
17-Jul-201
SIR of 20 Channels EI+
178.08+192.09
8.15e5
P
9-MP
3-MP
1-MP
2-MP
%
100
20
22.000
23.000
24.000
25.000
26.000
27.000
28.000
29.000
30.000
31.000
32.000
33.000
34.000
35.000
rt
6707/10-1 3140.65 m
3140_65M
17-Jul-201
SIR of 20 Channels EI+
198.05
1.76e5
4-MDBT
1-MDBT
2+3-MDBT
100
34
3140_65M
SIR of 20 Channels EI+
192.09
5.40e5
100
13

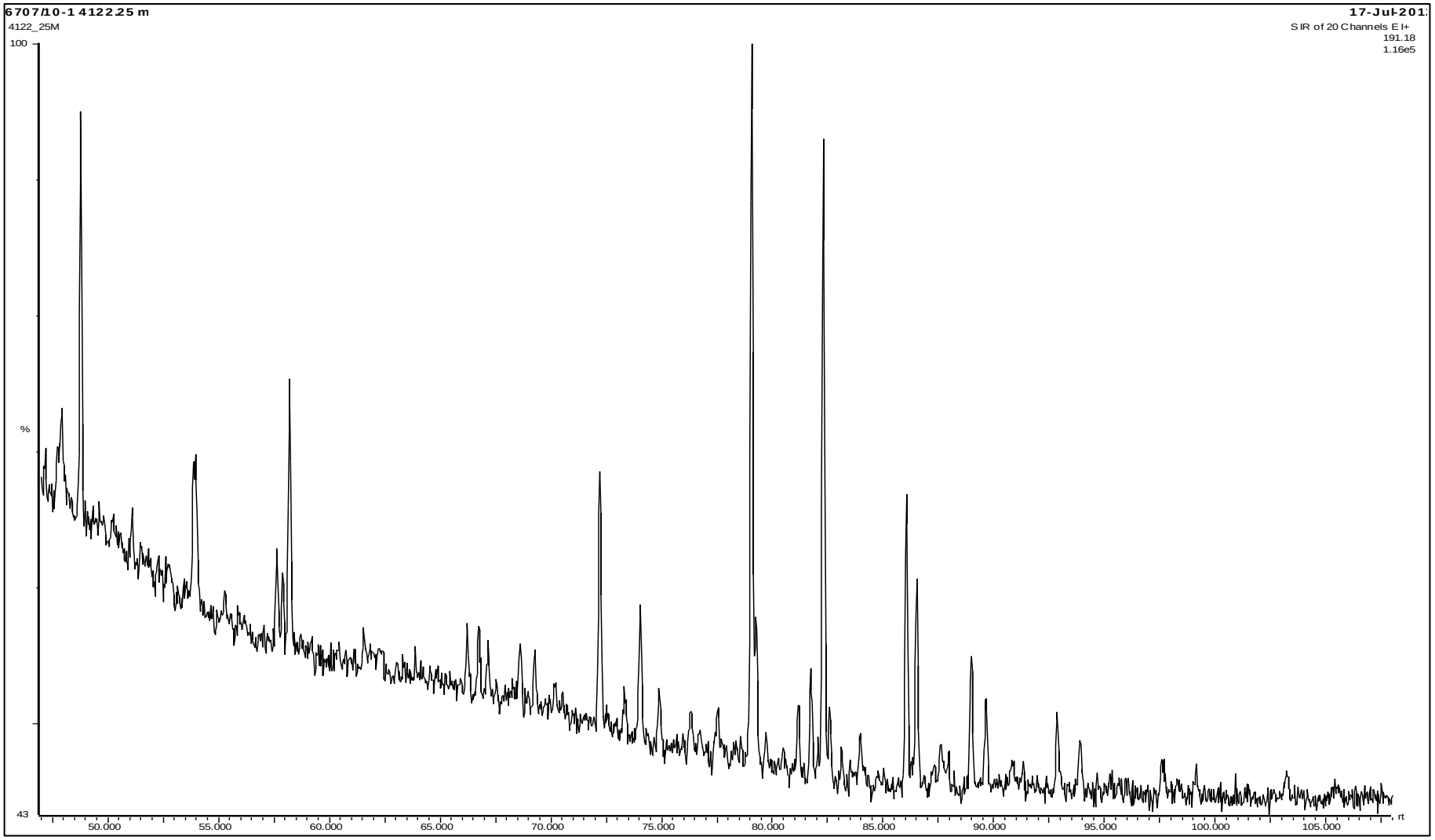
6707/10-1 4122.25 m
4122_25M
17-Jul-201
SIR of 20 Channels EI+
191.18
1.16e5
100
%
43
50.000
55.000
60.000
65.000
70.000
75.000
80.000
85.000
90.000
95.000
100.000
105.000
rt

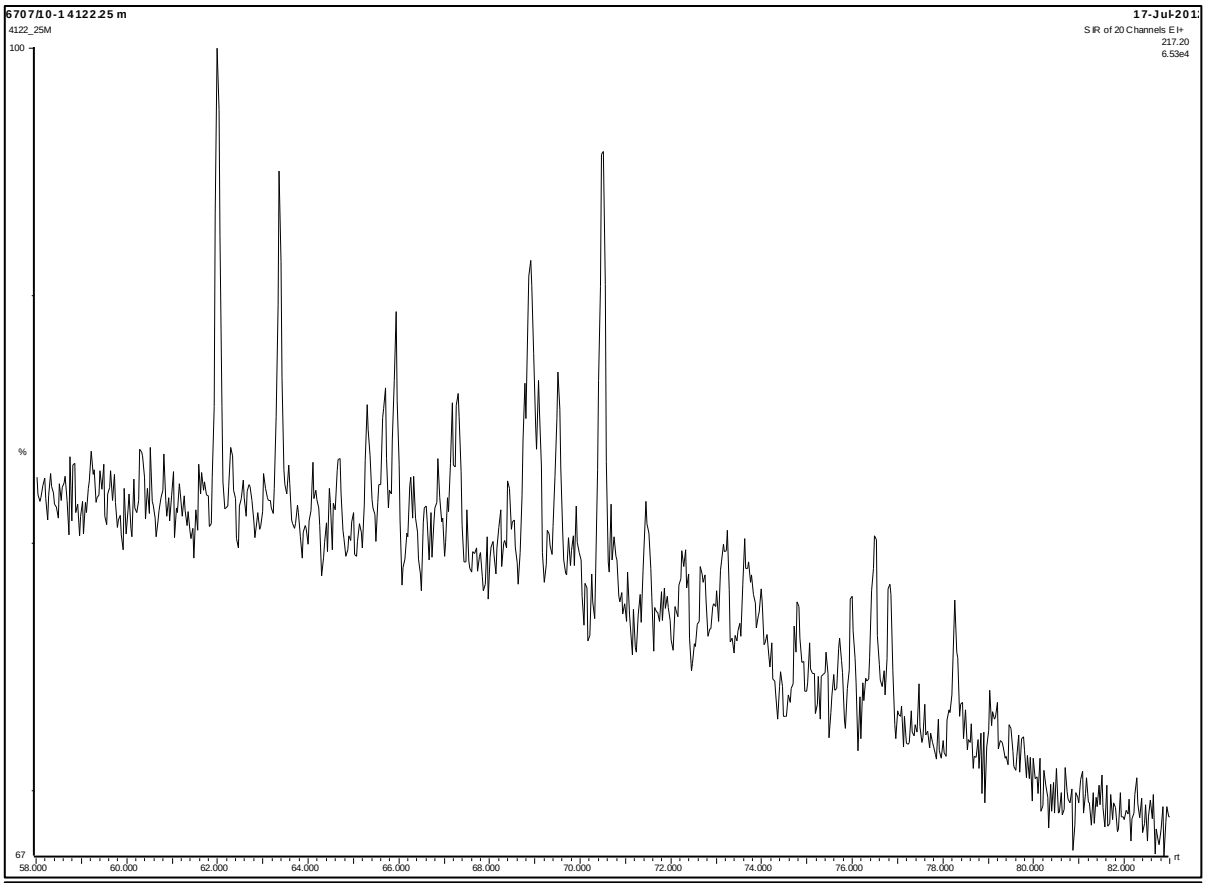
6707/10-1 4122.25 m
4122_25M
17-Jul-201
SIR of 20 Channels EI+
217.20
6.53e4
100
%
67
58.000
60.000
62.000
64.000
66.000
68.000
70.000
72.000
74.000
76.000
78.000
80.000
82.000
rt

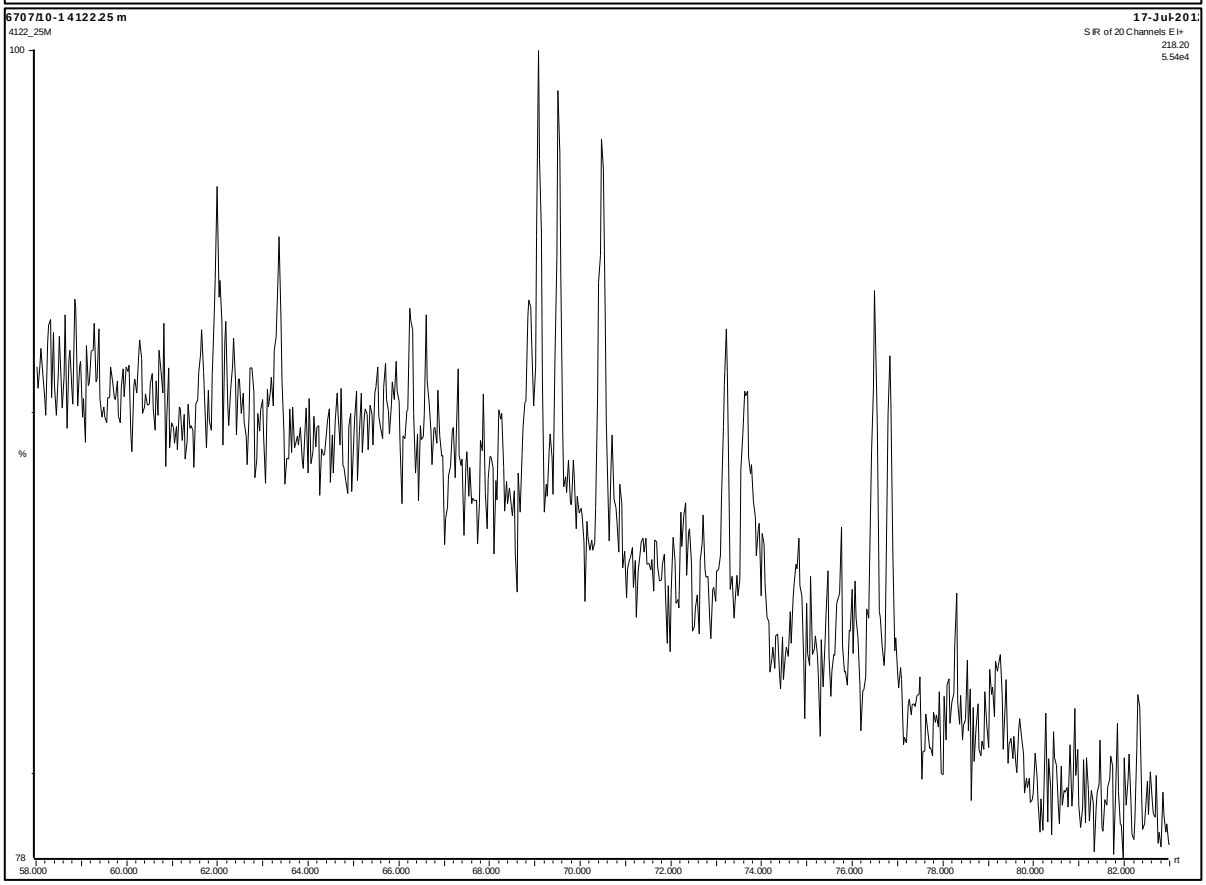
6707/10-1 4122.25 m
4122_25M
17-Jul-201
SIR of 20 Channels EI+
218.20
5.54e4
100
%
78
58.000
60.000
62.000
64.000
66.000
68.000
70.000
72.000
74.000
76.000
78.000
80.000
82.000
rt

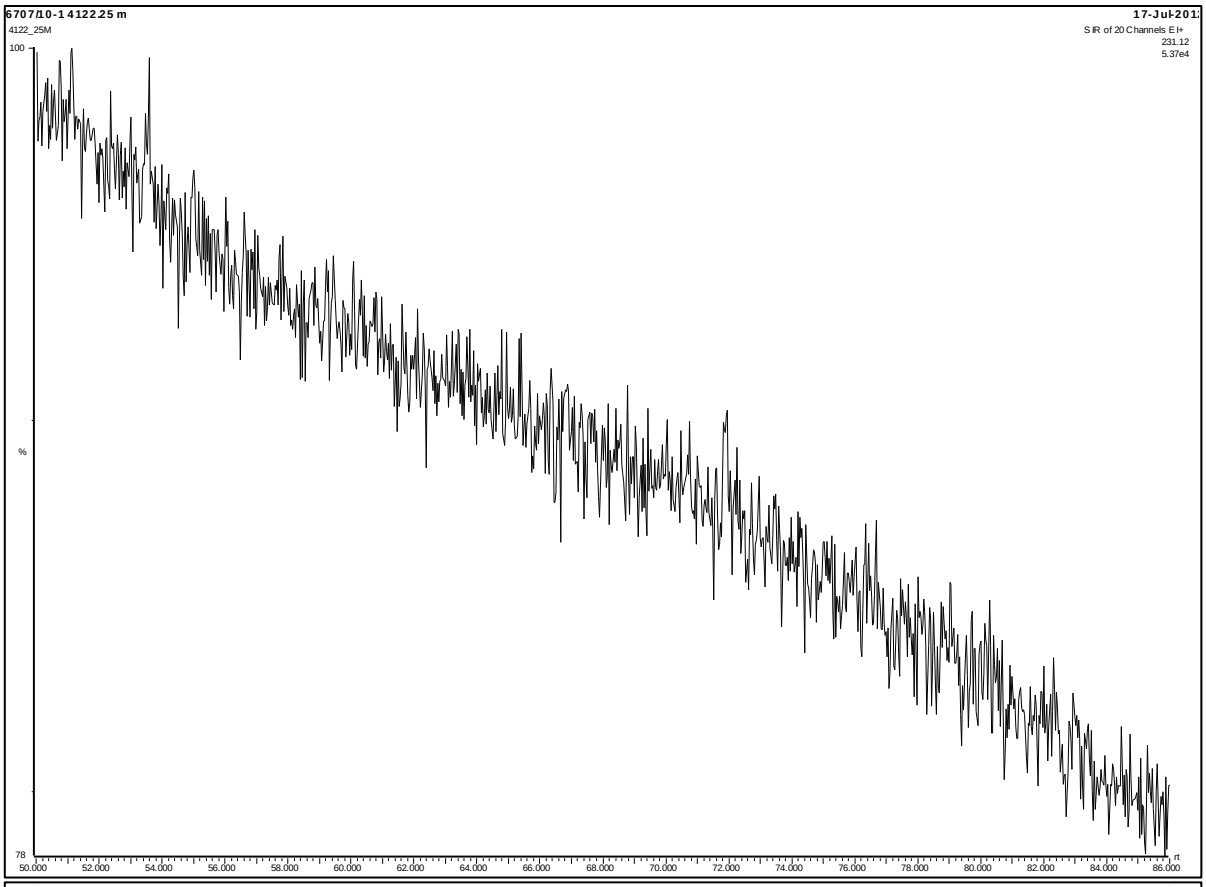
6707/10-1 4122.25 m
17-Jul-201
4122_25M
SIR of 20 Channels EI+
231.12
5.37e4
100
%
78
50.000 52.000 54.000 56.000 58.000 60.000 62.000 64.000 66.000 68.000 70.000 72.000 74.000 76.000 78.000 80.000 82.000 84.000 86.000
rt

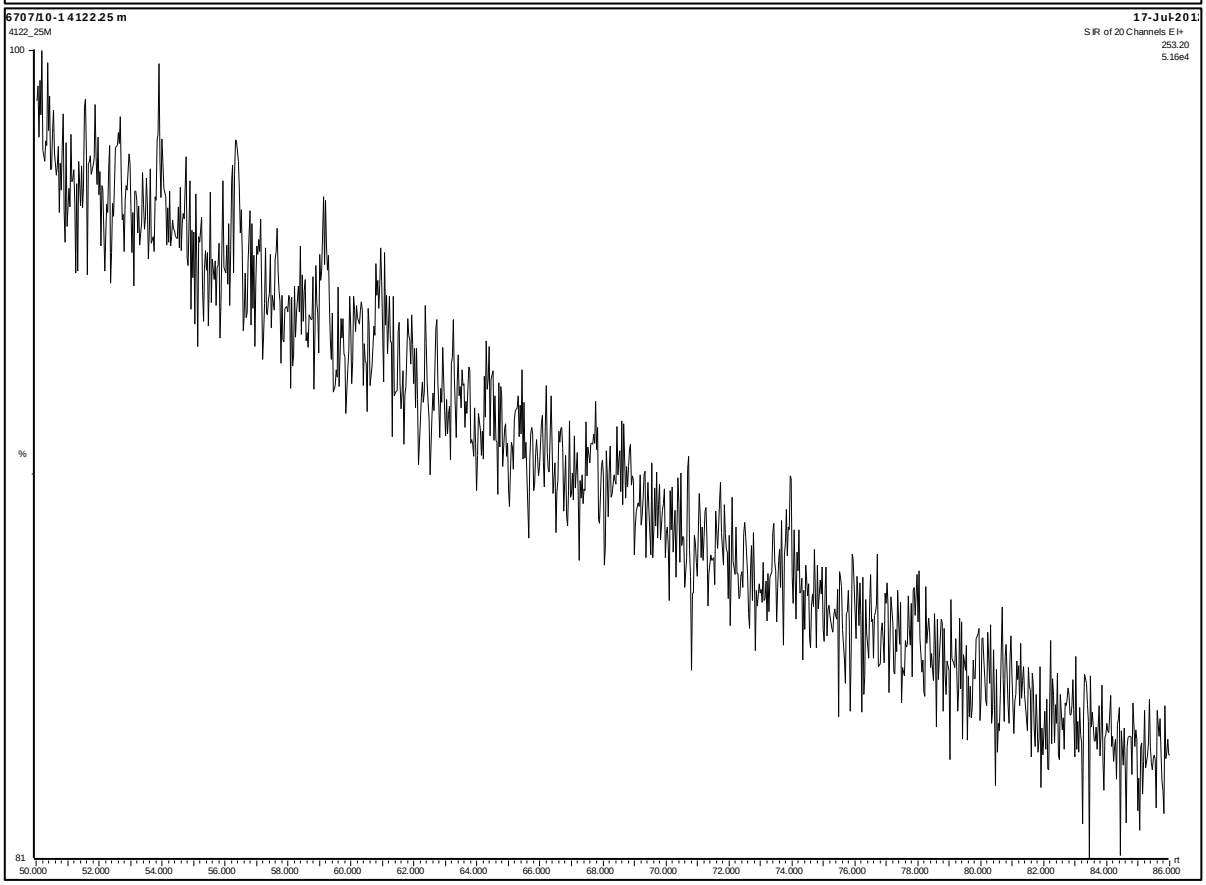
6707/10-1 4122.25 m
17-Jul-201
4122_25M
SIR of 20 Channels EI+
253.20
5.16e4
100
%
81
50.000 52.000 54.000 56.000 58.000 60.000 62.000 64.000 66.000 68.000 70.000 72.000 74.000 76.000 78.000 80.000 82.000 84.000 86.000
rt

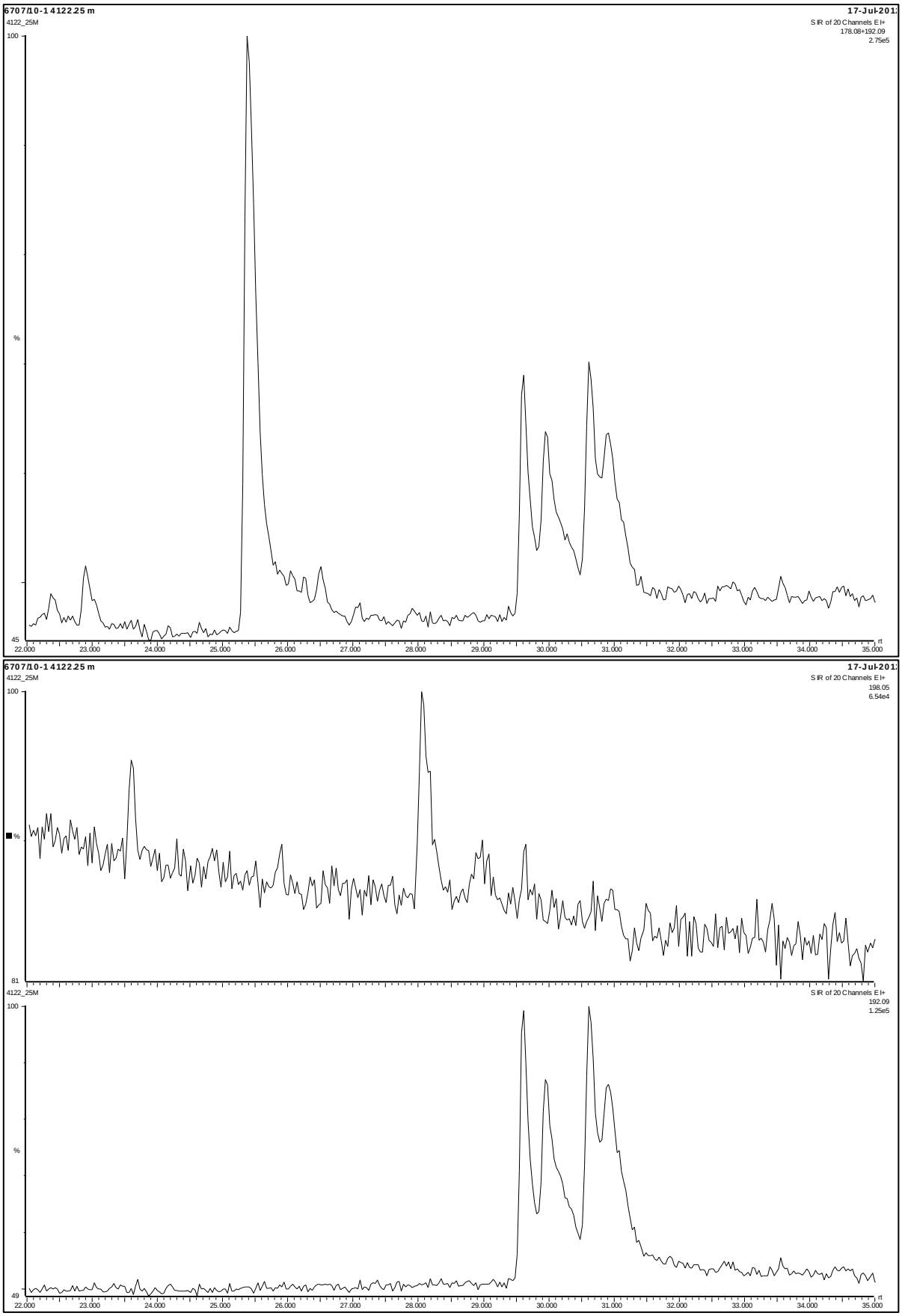
6707/10-1 4122.25 m
17-Jul-201
4122_25M
SIR of 20 Channels EI+
178.08+192.09
2.75e5
100
%
45
22.000
23.000
24.000
25.000
26.000
27.000
28.000
29.000
30.000
31.000
32.000
33.000
34.000
35.000
rt
6707/10-1 4122.25 m
17-Jul-201
4122_25M
SIR of 20 Channels EI+
198.05
6.54e4
100
%
81
4122_25M
SIR of 20 Channels EI+
192.09
1.25e5
100
%
49
22.000
23.000
24.000
25.000
26.000
27.000
28.000
29.000
30.000
31.000
32.000
33.000
34.000
35.000
rt

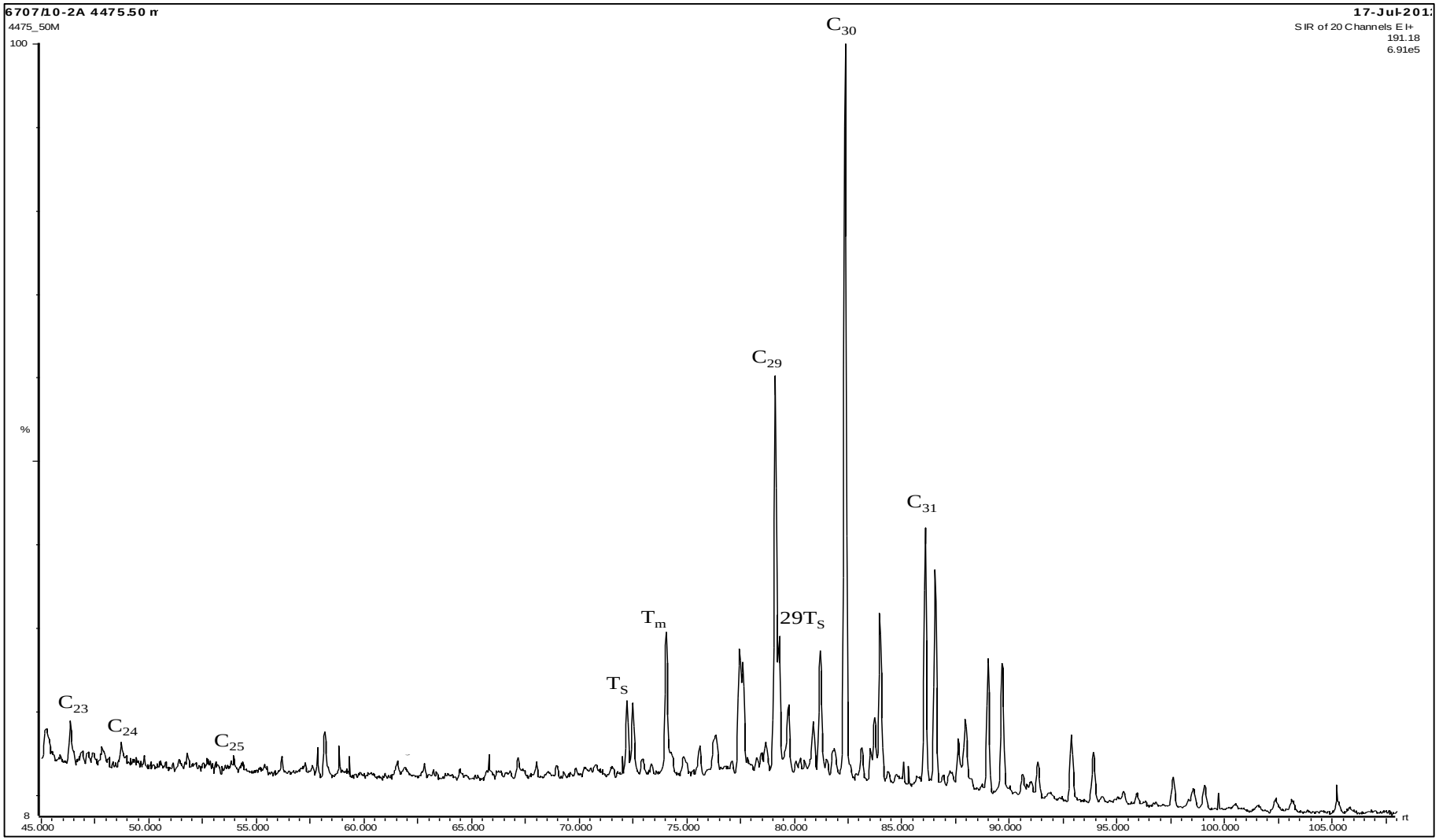
6707/10-2A 4475.50 m
4475_50M
17-Jul-201
SIR of 20 Channels EI+
191.18
6.91e5
100
%
8
C23
C24
C25
TS
Tm
C29
29TS
C30
C31
45.000
50.000
55.000
60.000
65.000
70.000
75.000
80.000
85.000
90.000
95.000
100.000
105.000
rt

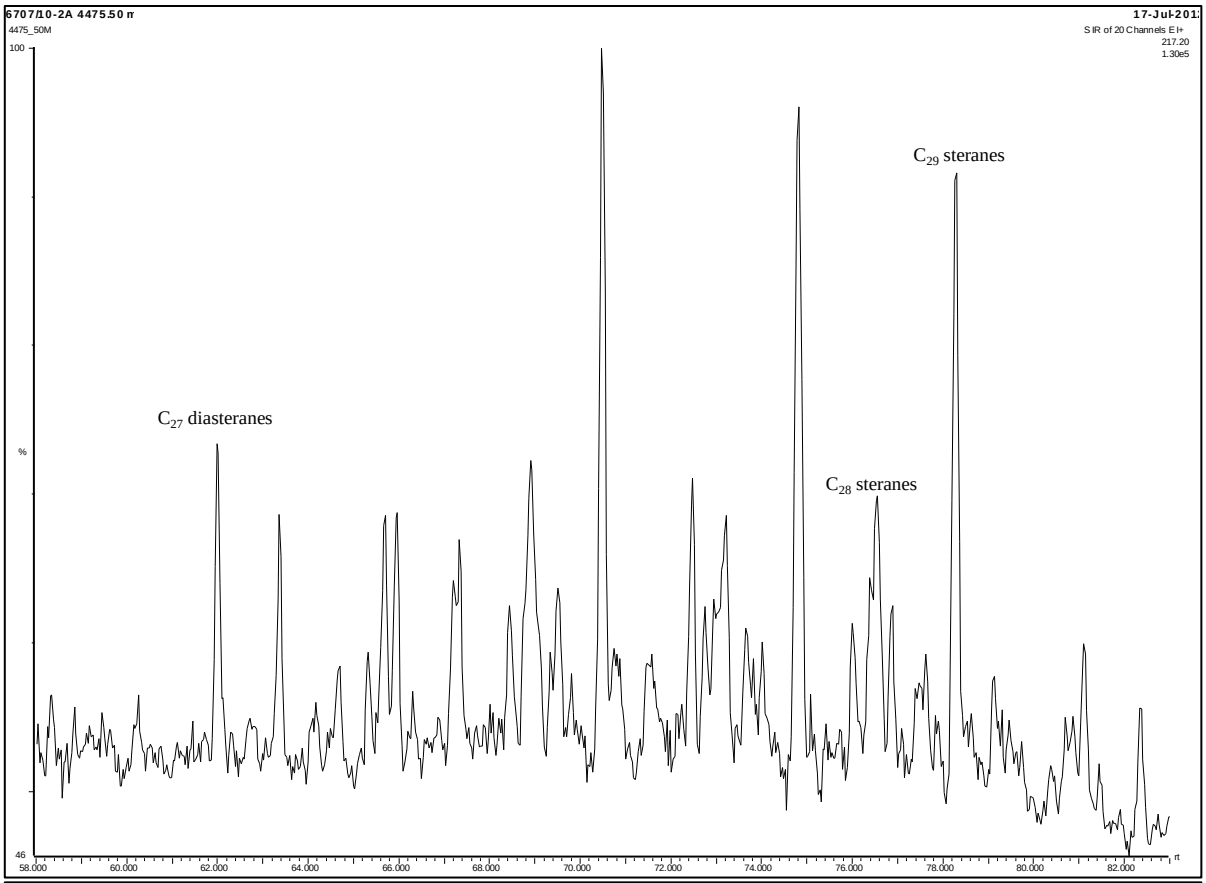
6707/10-2A 4475.50 m
4475_50M
17-Jul-201
SIR of 20 Channels EI+
217.20
1.30e5
100
%
46
C_{27} diasteranes
C_{28} steranes
C_{29} steranes
58.000
60.000
62.000
64.000
66.000
68.000
70.000
72.000
74.000
76.000
78.000
80.000
82.000
rt

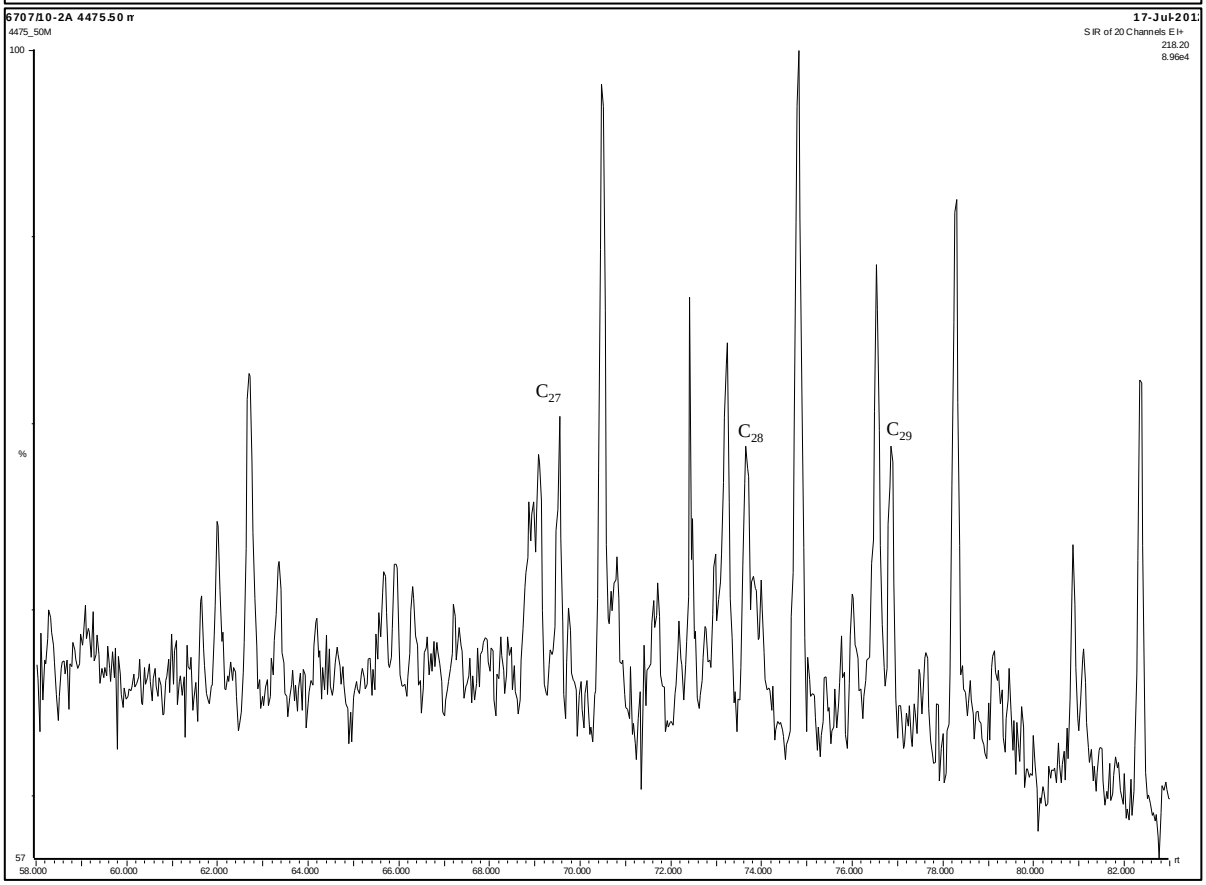
6707/10-2A 4475.50 m
4475_50M
17-Jul-201
SIR of 20 Channels EI+
218.20
8.96e4
100
%
57
C_{27}
C_{28}
C_{29}
58.000
60.000
62.000
64.000
66.000
68.000
70.000
72.000
74.000
76.000
78.000
80.000
82.000
rt

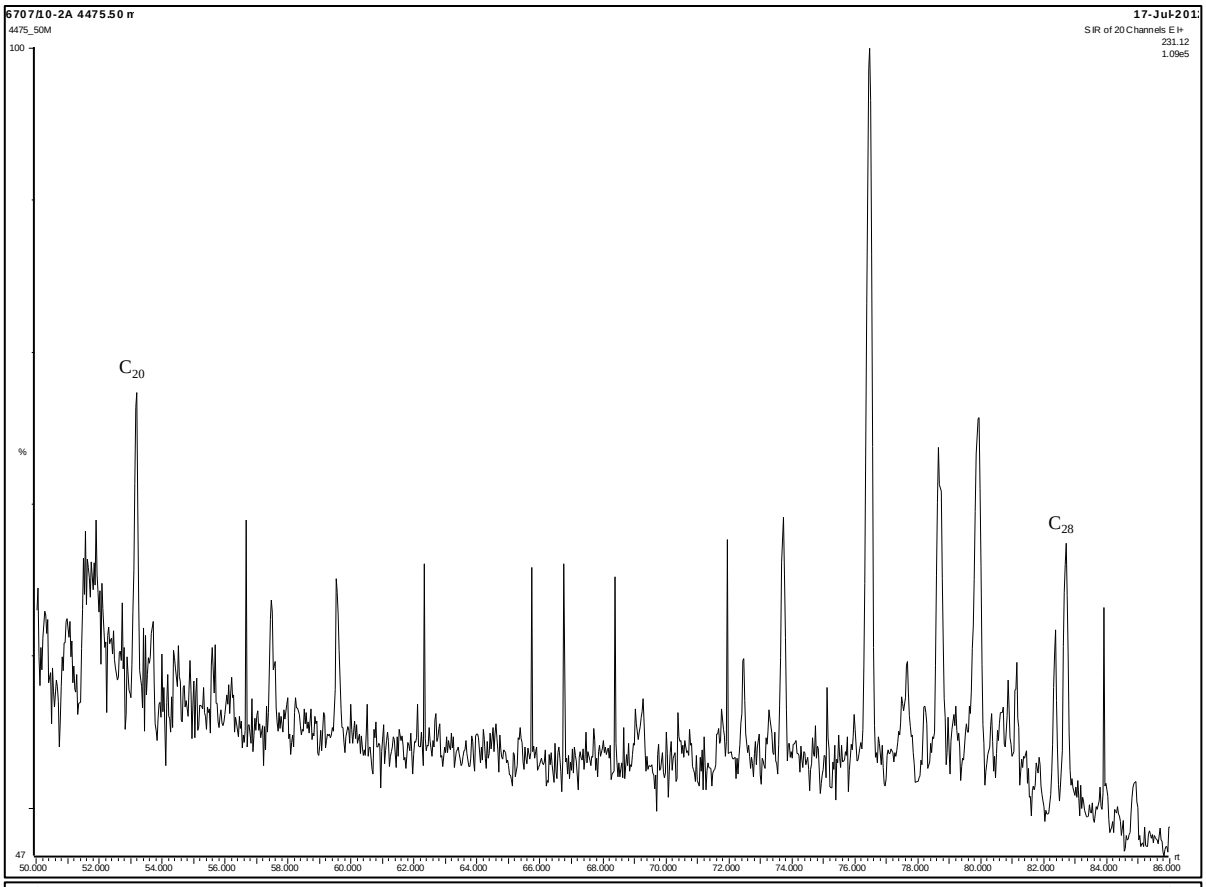
6707/10-2A 4475.50 m
4475_50M
17-Jul-201
SIR of 20 Channels EI+
231.12
1.09e5
100
%
47
C20
C28
50.000 52.000 54.000 56.000 58.000 60.000 62.000 64.000 66.000 68.000 70.000 72.000 74.000 76.000 78.000 80.000 82.000 84.000 86.000
rt

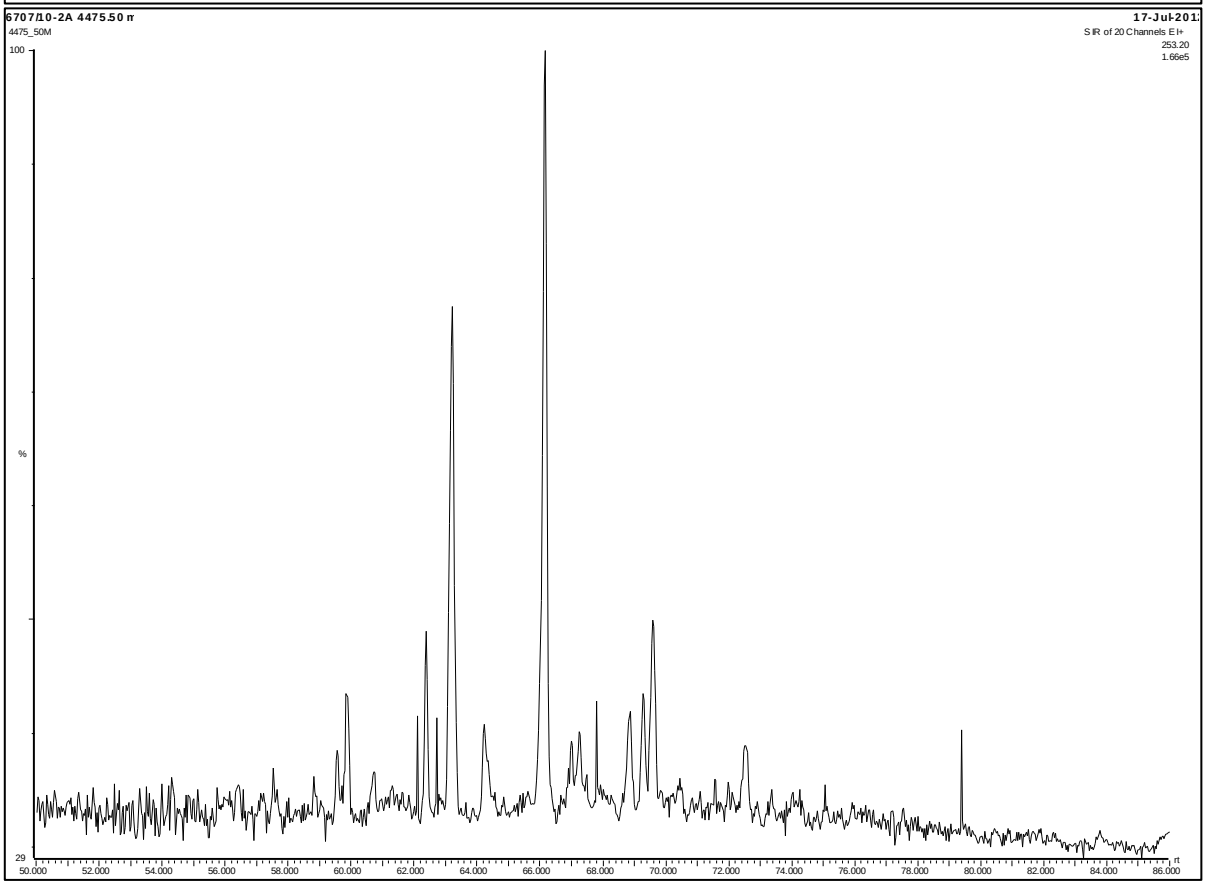
6707/10-2A 4475.50 m
4475_50M
17-Jul-201
SIR of 20 Channels EI+
253.20
1.66e5
100
%
29
50.000 52.000 54.000 56.000 58.000 60.000 62.000 64.000 66.000 68.000 70.000 72.000 74.000 76.000 78.000 80.000 82.000 84.000 86.000
rt

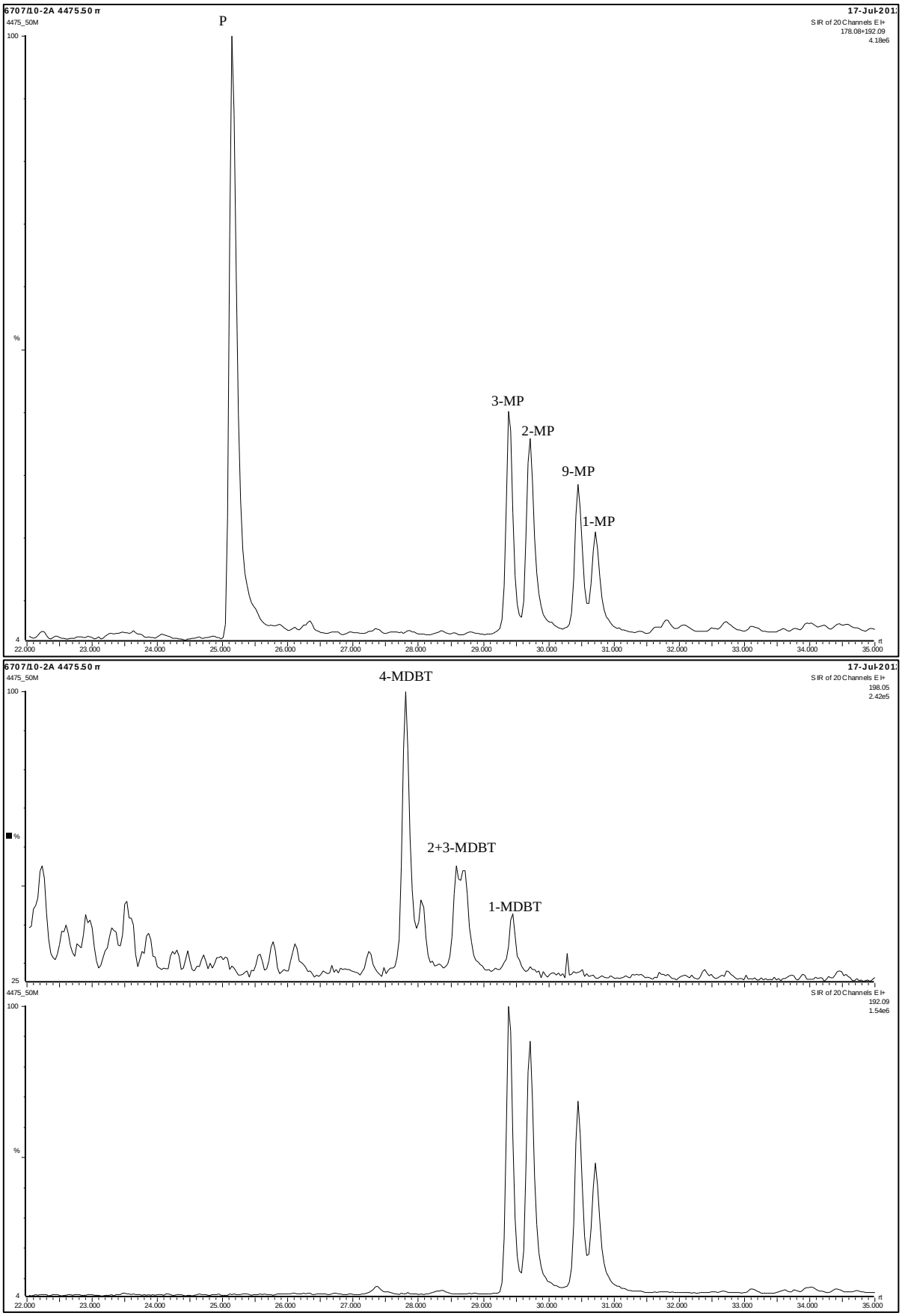
6707L10-2A 4475.50 rr
4475_50M
17-Jul-201
SIR of 20 Channels E I+
178.08+192.09
4.18e6
P
3-MP
2-MP
9-MP
1-MP
%
100
4
22.000
23.000
24.000
25.000
26.000
27.000
28.000
29.000
30.000
31.000
32.000
33.000
34.000
35.000
rt
6707L10-2A 4475.50 rr
4475_50M
17-Jul-201
SIR of 20 Channels E I+
198.05
2.42e5
4-MDBT
2+3-MDBT
1-MDBT
100
%
25
4475_50M
SIR of 20 Channels E I+
192.09
1.54e6
100
%
4
22.000
23.000
24.000
25.000
26.000
27.000
28.000
29.000
30.000
31.000
32.000
33.000
34.000
35.000
rt

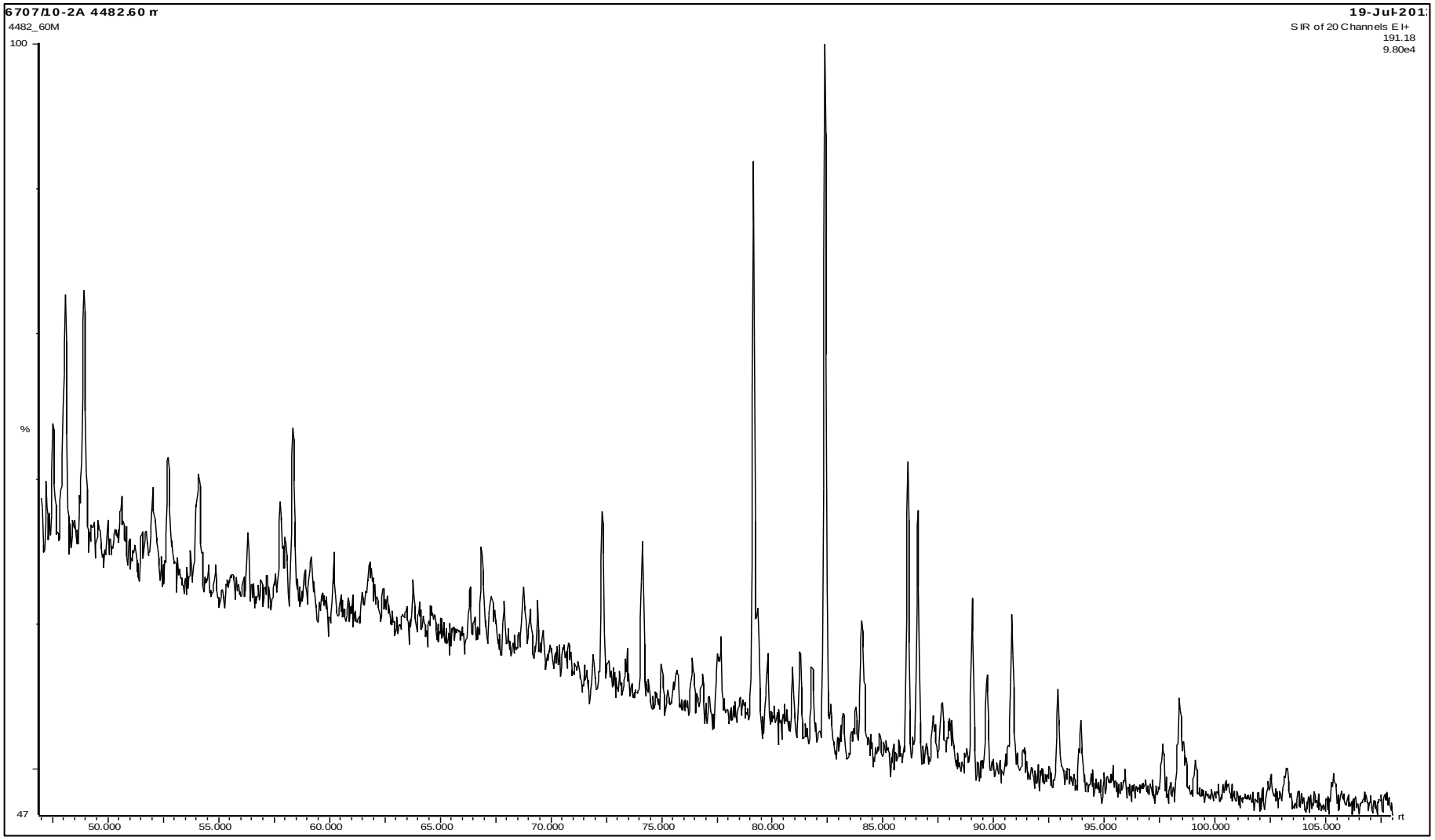
6707l10-2A 4482.60 m
4482_60M
19-Jul-201
SIR of 20 Channels EI+
191.18
9.80e4
100
%
47
50.000
55.000
60.000
65.000
70.000
75.000
80.000
85.000
90.000
95.000
100.000
105.000
rt

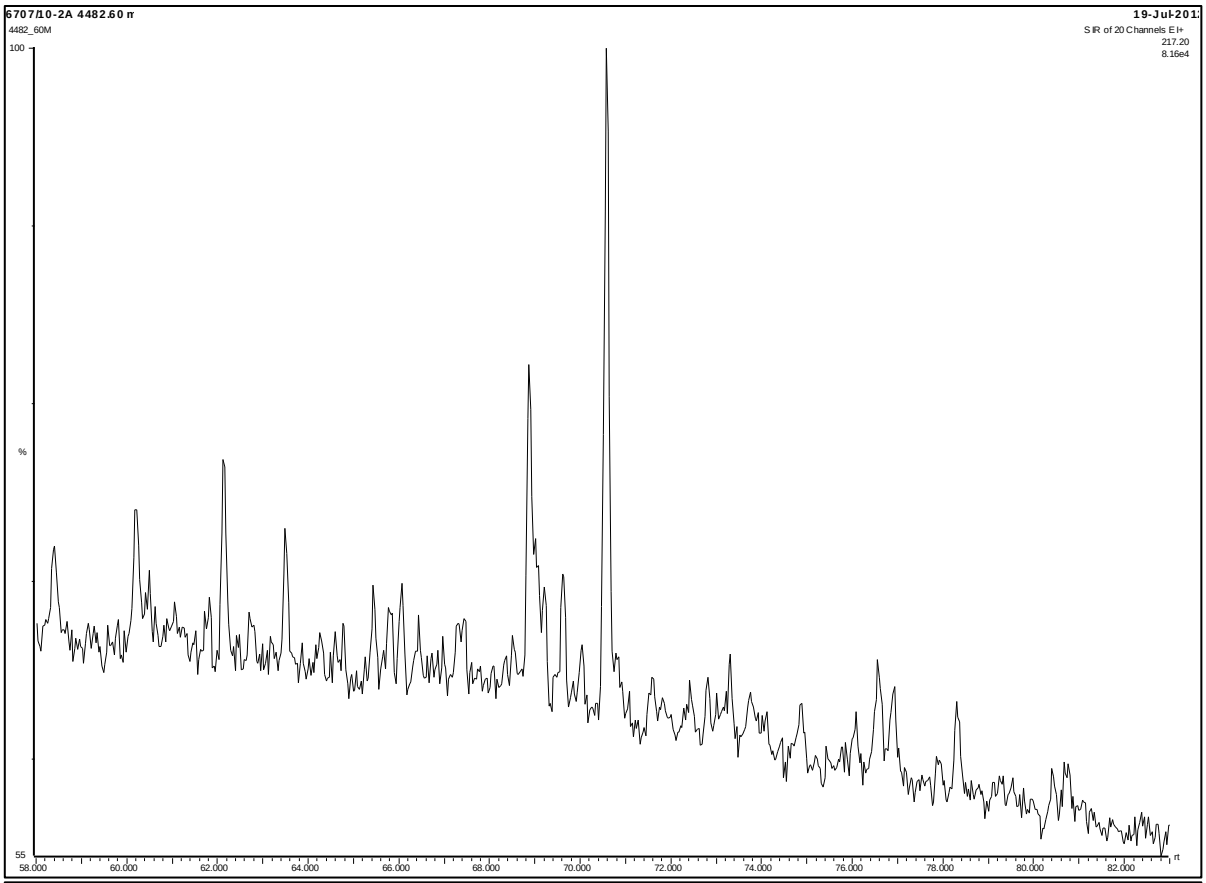
6707/10-2A 4482.60 m
4482_60M
19-Jul-2011
SIR of 20 Channels EI+
217.20
8.16e4
100
%
55
58.000
60.000
62.000
64.000
66.000
68.000
70.000
72.000
74.000
76.000
78.000
80.000
82.000
rt

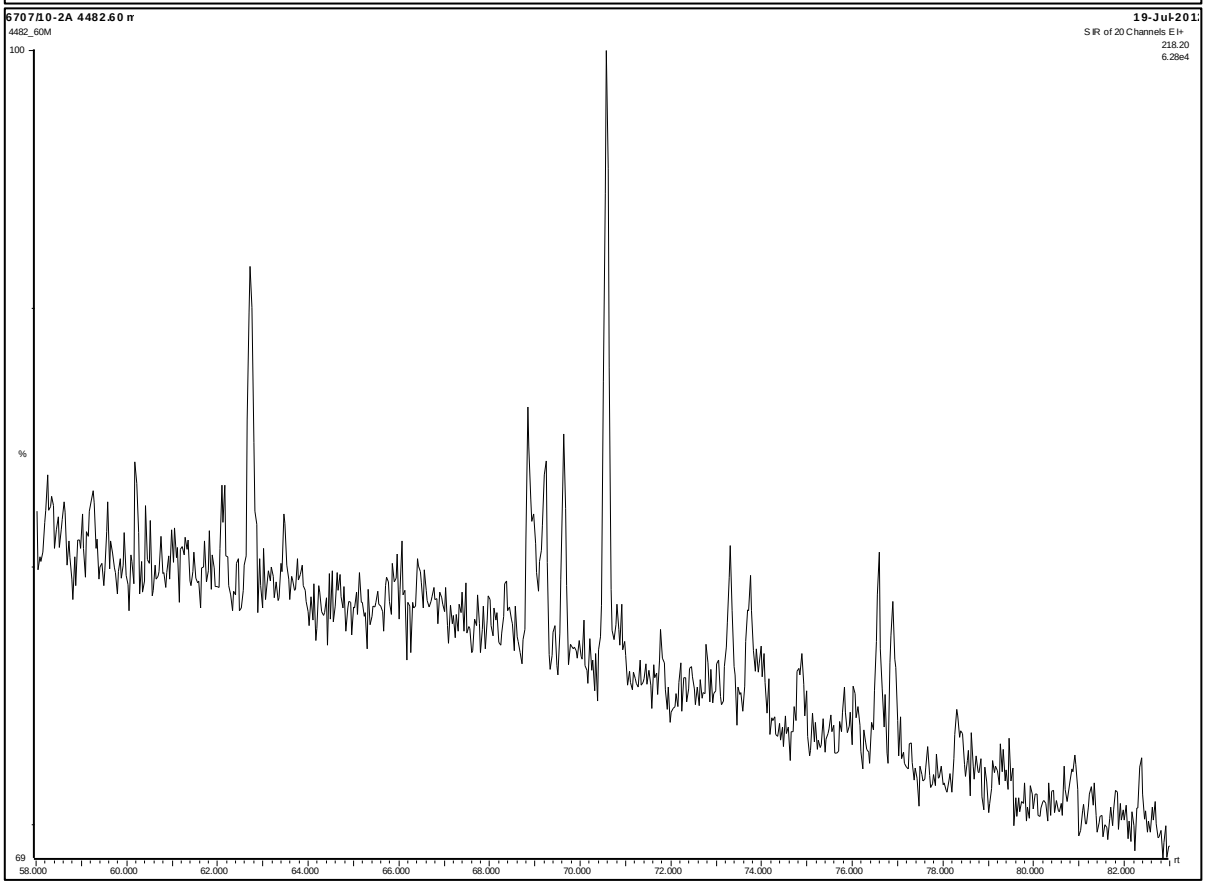
6707/10-2A 4482.60 m
4482_60M
19-Jul-2011
SIR of 20 Channels EI+
218.20
6.28e4
100
%
69
58.000
60.000
62.000
64.000
66.000
68.000
70.000
72.000
74.000
76.000
78.000
80.000
82.000
rt

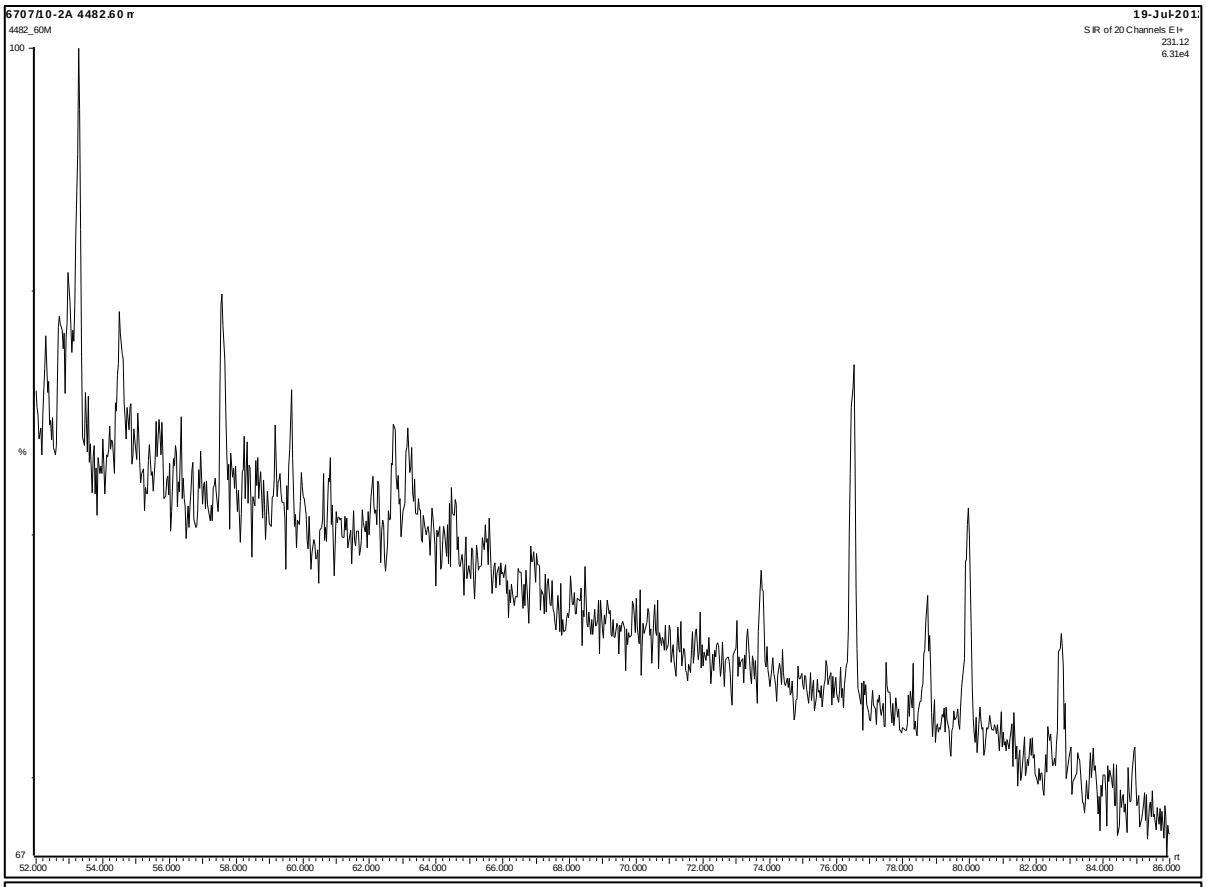
6707/10-2A 4482.60 m
19-Jul-201
4482_60M
SIR of 20 Channels EI+
231.12
6.31e4
100
%
67
52.000 54.000 56.000 58.000 60.000 62.000 64.000 66.000 68.000 70.000 72.000 74.000 76.000 78.000 80.000 82.000 84.000 86.000
rt

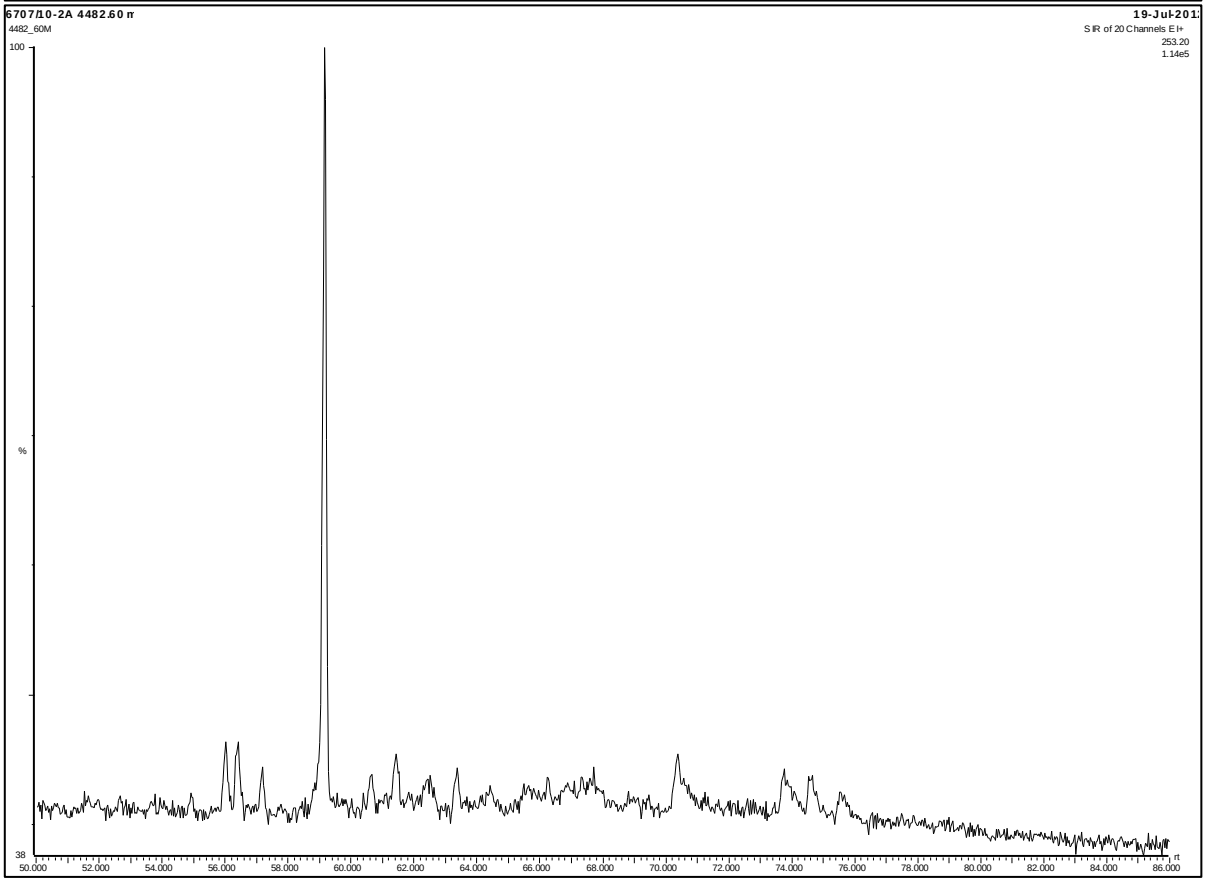
6707/10-2A 4482.60 m
19-Jul-201
4482_60M
SIR of 20 Channels EI+
253.20
1.14e5
100
%
38
50.000 52.000 54.000 56.000 58.000 60.000 62.000 64.000 66.000 68.000 70.000 72.000 74.000 76.000 78.000 80.000 82.000 84.000 86.000
rt

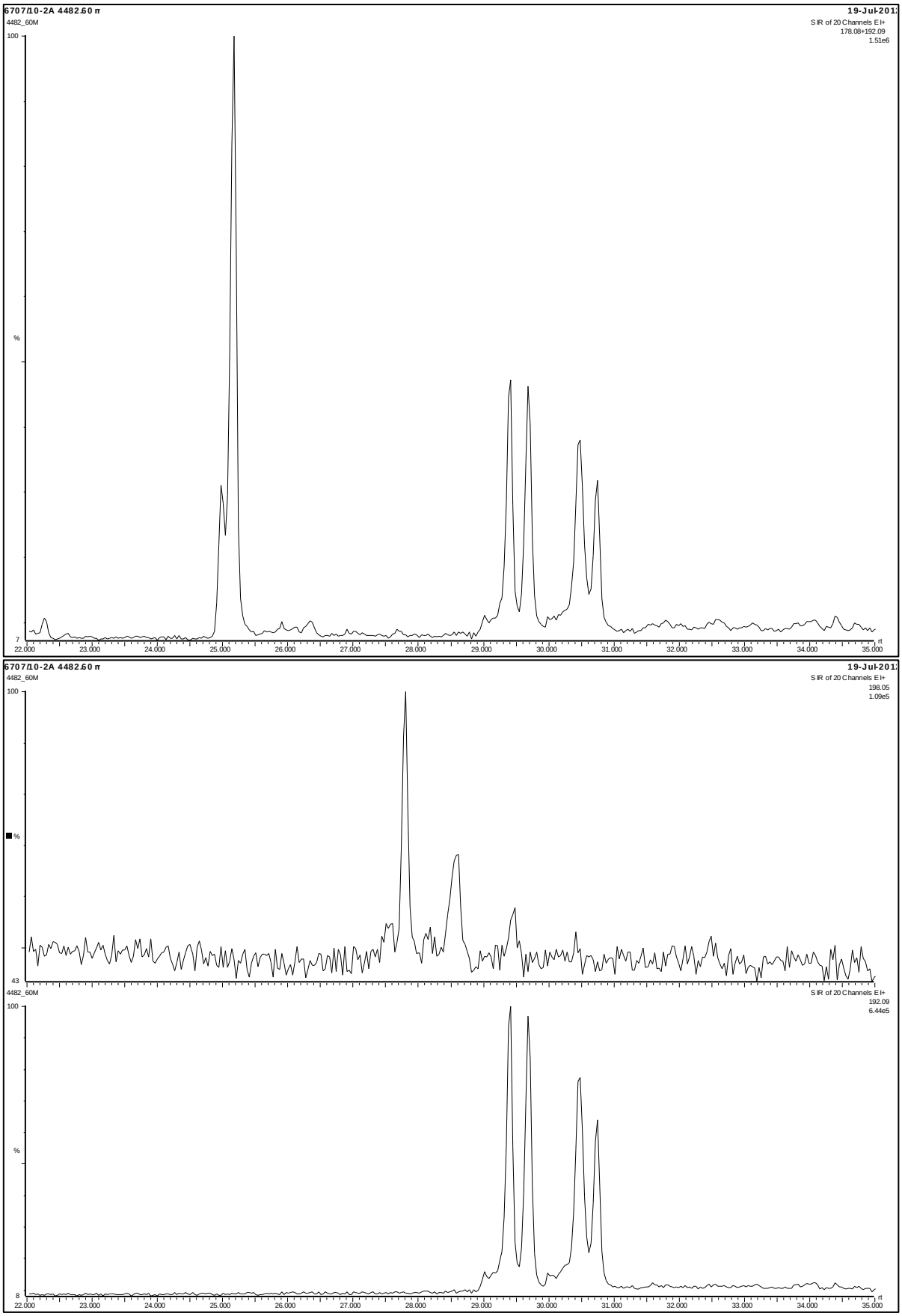
6707/10-2A 4482.60 rr
19-Jul-2011
4482_60M
SIR of 20 Channels EI+
178.08+192.09
1.51e6
100
%
7
22.000
23.000
24.000
25.000
26.000
27.000
28.000
29.000
30.000
31.000
32.000
33.000
34.000
35.000
rt
6707/10-2A 4482.60 rr
19-Jul-2011
4482_60M
SIR of 20 Channels EI+
198.05
1.09e5
100
%
43
4482_60M
SIR of 20 Channels EI+
192.09
6.44e5
100
%
8
22.000
23.000
24.000
25.000
26.000
27.000
28.000
29.000
30.000
31.000
32.000
33.000
34.000
35.000
rt

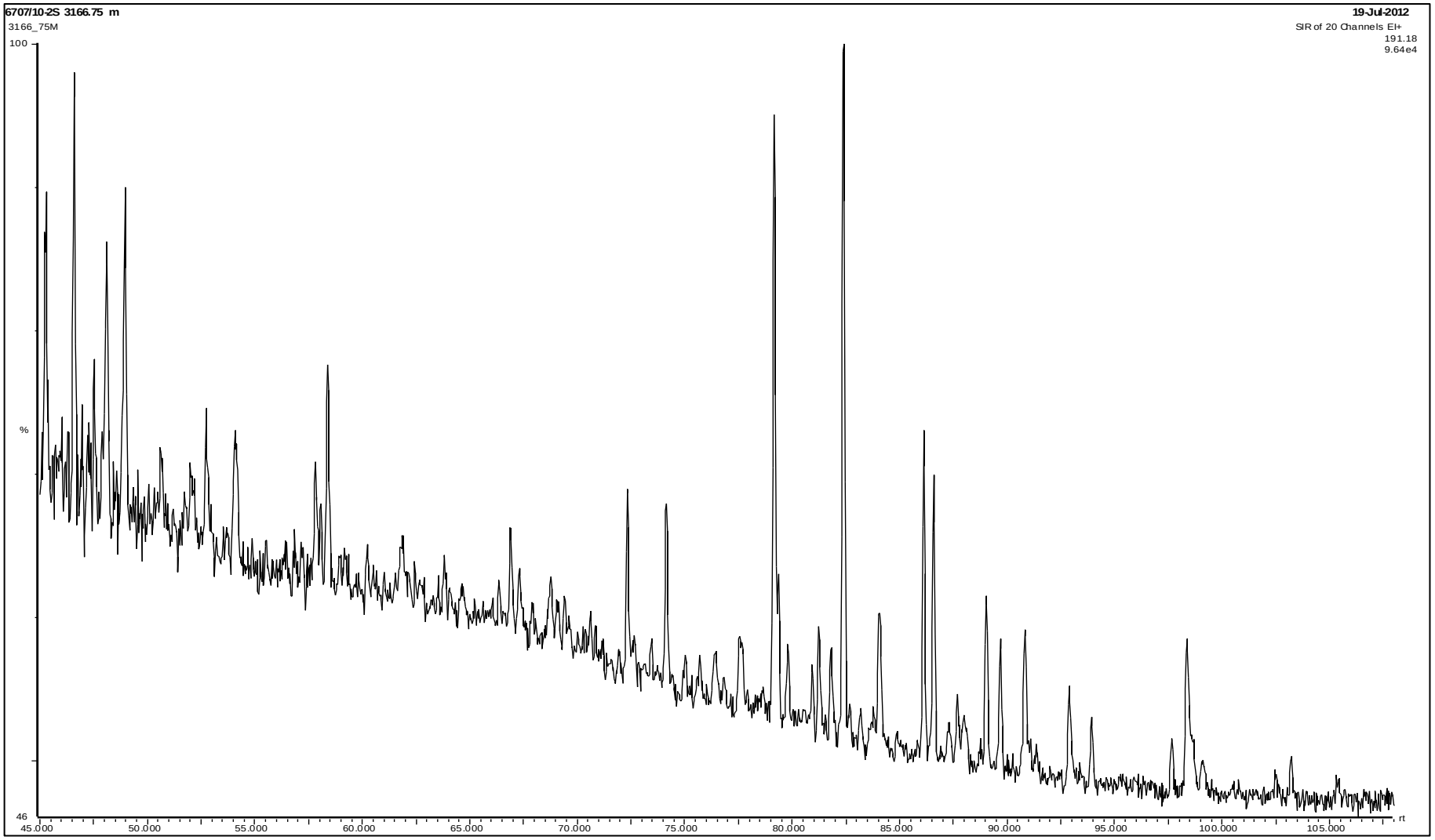
6707/10-2S 3166.75 m
3166_75M
19-Jul-2012
SIR of 20 Channels EI+
191.18
9.64e4
100
%
46
45.000
50.000
55.000
60.000
65.000
70.000
75.000
80.000
85.000
90.000
95.000
100.000
105.000
rt

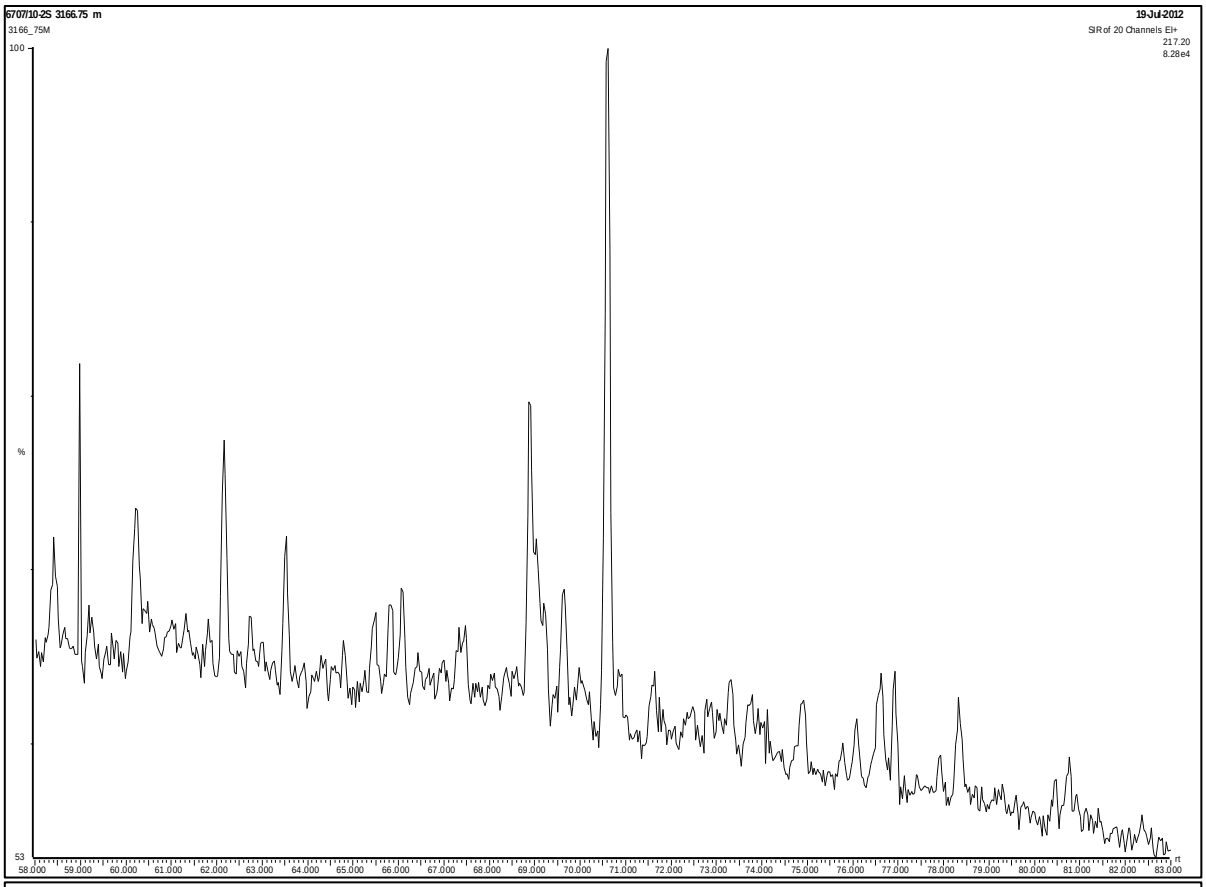
6707/10-2S 3166.75 m
19-Jul-2012
3166_75M
SIR of 20 Channels EI+
217.20
8.28e4
100
%
53
58.000 59.000 60.000 61.000 62.000 63.000 64.000 65.000 66.000 67.000 68.000 69.000 70.000 71.000 72.000 73.000 74.000 75.000 76.000 77.000 78.000 79.000 80.000 81.000 82.000 83.000
rt

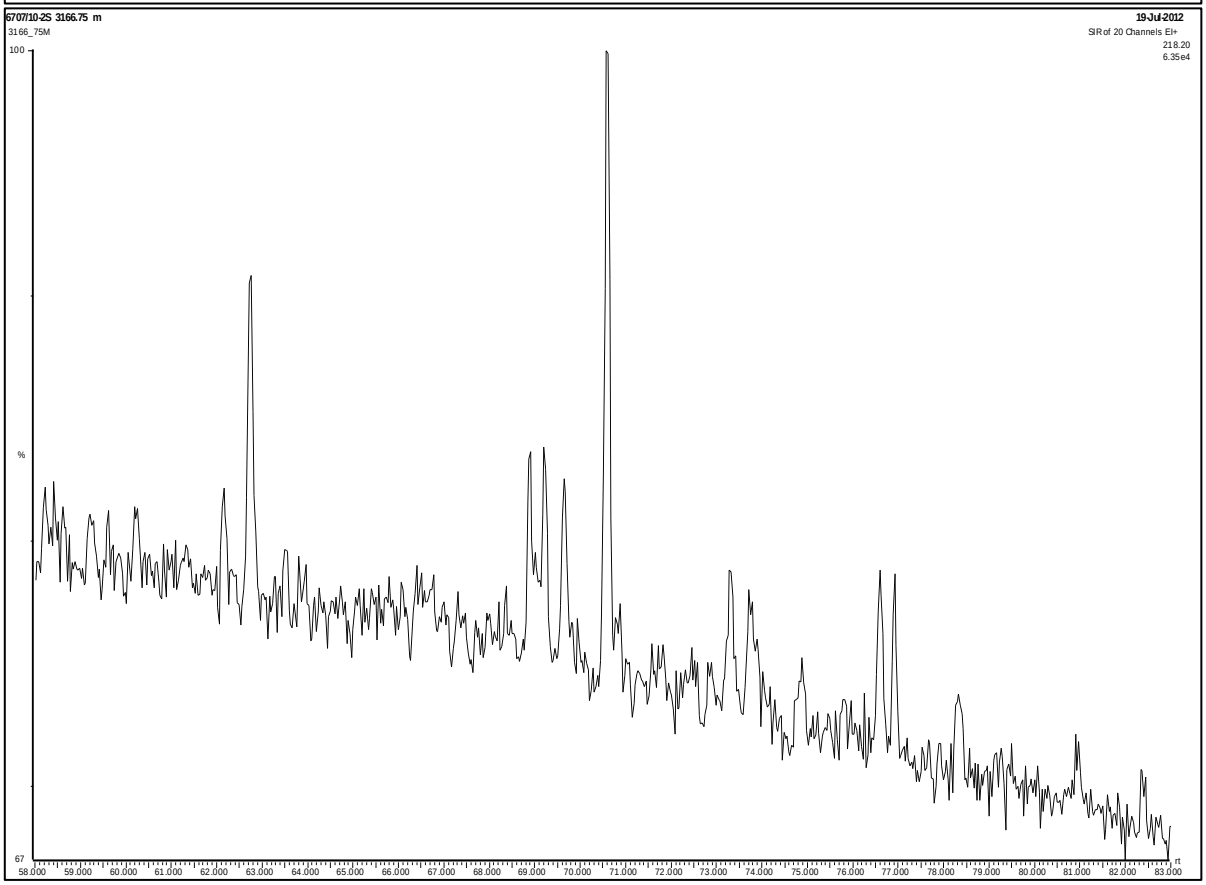
6707/10-2S 3166.75 m
19-Jul-2012
3166_75M
SIR of 20 Channels EI+
218.20
6.35e4
100
%
67
58.000 59.000 60.000 61.000 62.000 63.000 64.000 65.000 66.000 67.000 68.000 69.000 70.000 71.000 72.000 73.000 74.000 75.000 76.000 77.000 78.000 79.000 80.000 81.000 82.000 83.000
rt

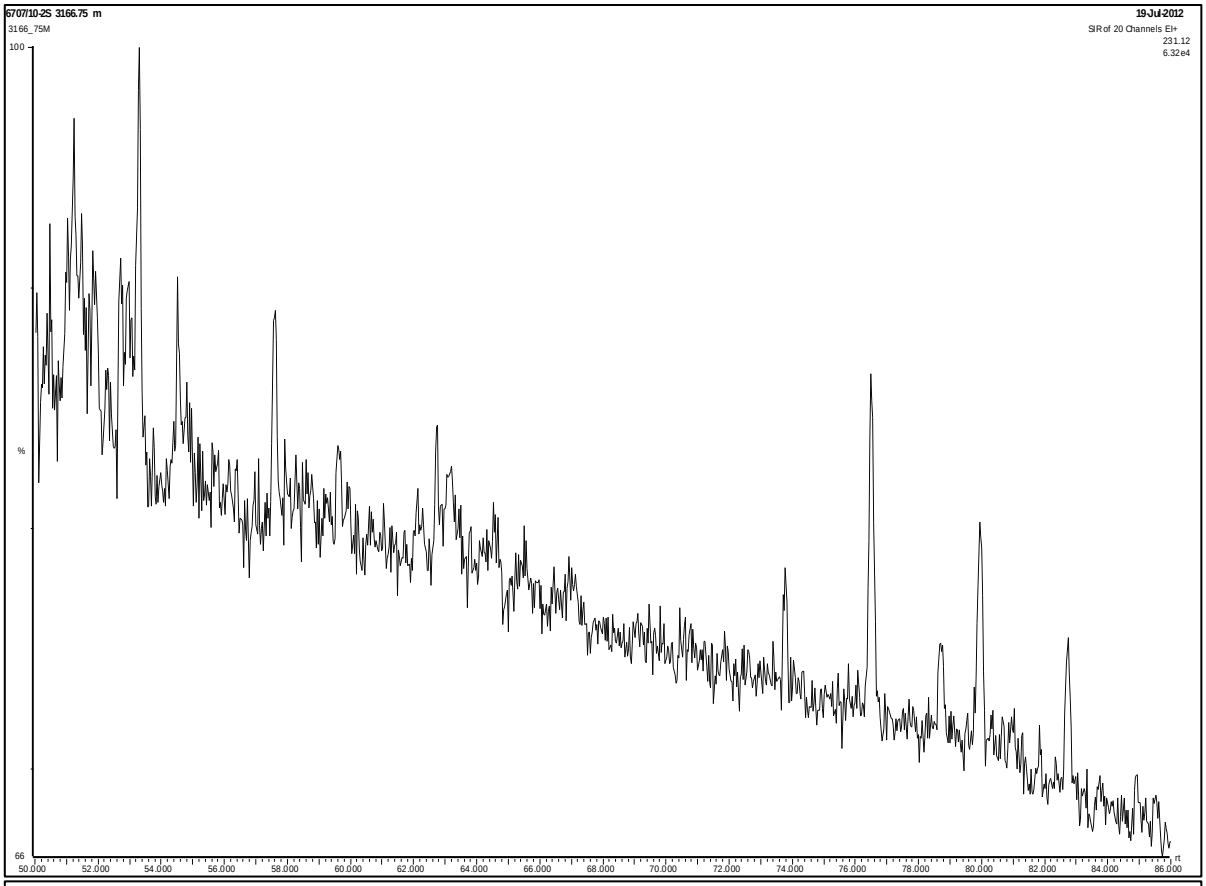
6707/10-2S 3166.75 m
3166_75M
19-Jul-2012
SIR of 20 Channels EI+
231.12
6.32e4
100
%
66
50.000 52.000 54.000 56.000 58.000 60.000 62.000 64.000 66.000 68.000 70.000 72.000 74.000 76.000 78.000 80.000 82.000 84.000 86.000
rt

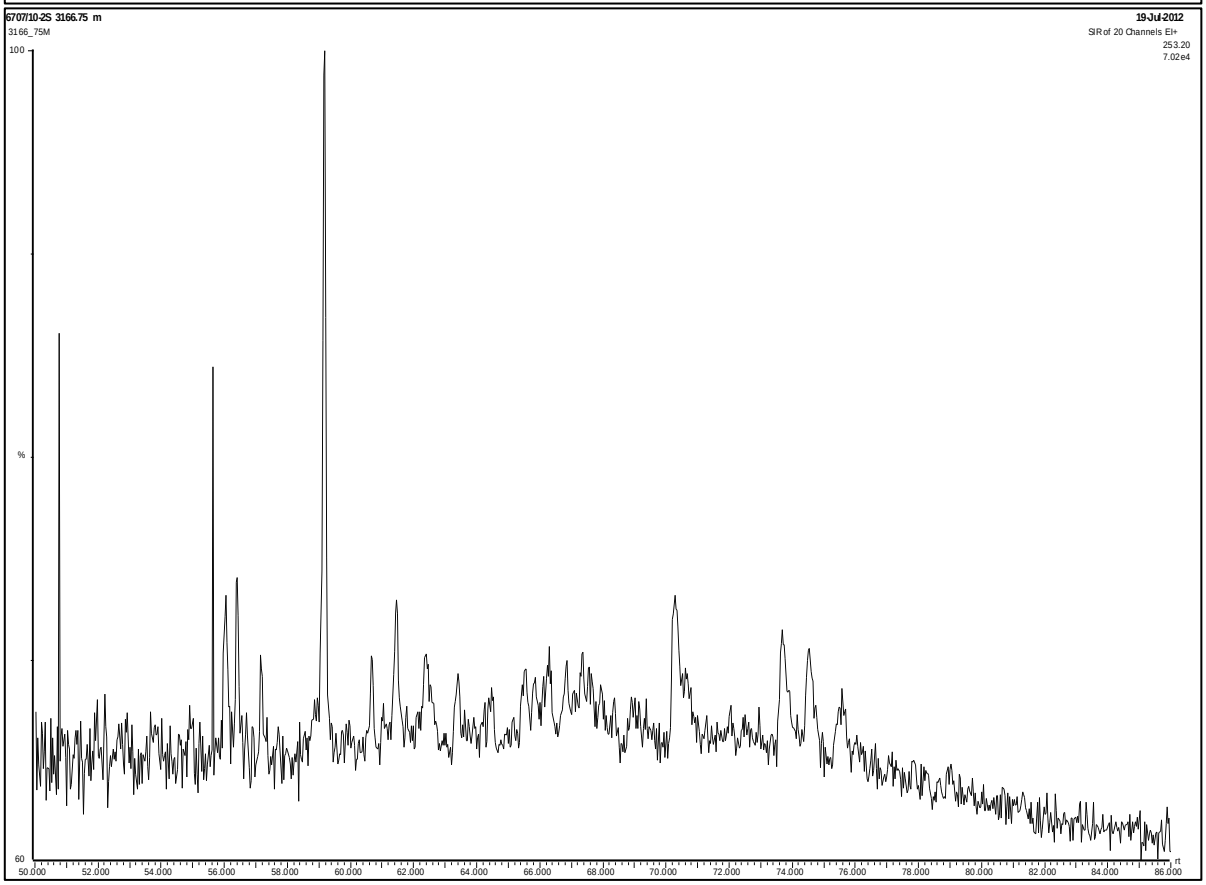
6707/10-2S 3166.75 m
3166_75M
19-Jul-2012
SIR of 20 Channels EI+
253.20
7.02e4
100
%
60
50.000 52.000 54.000 56.000 58.000 60.000 62.000 64.000 66.000 68.000 70.000 72.000 74.000 76.000 78.000 80.000 82.000 84.000 86.000
rt

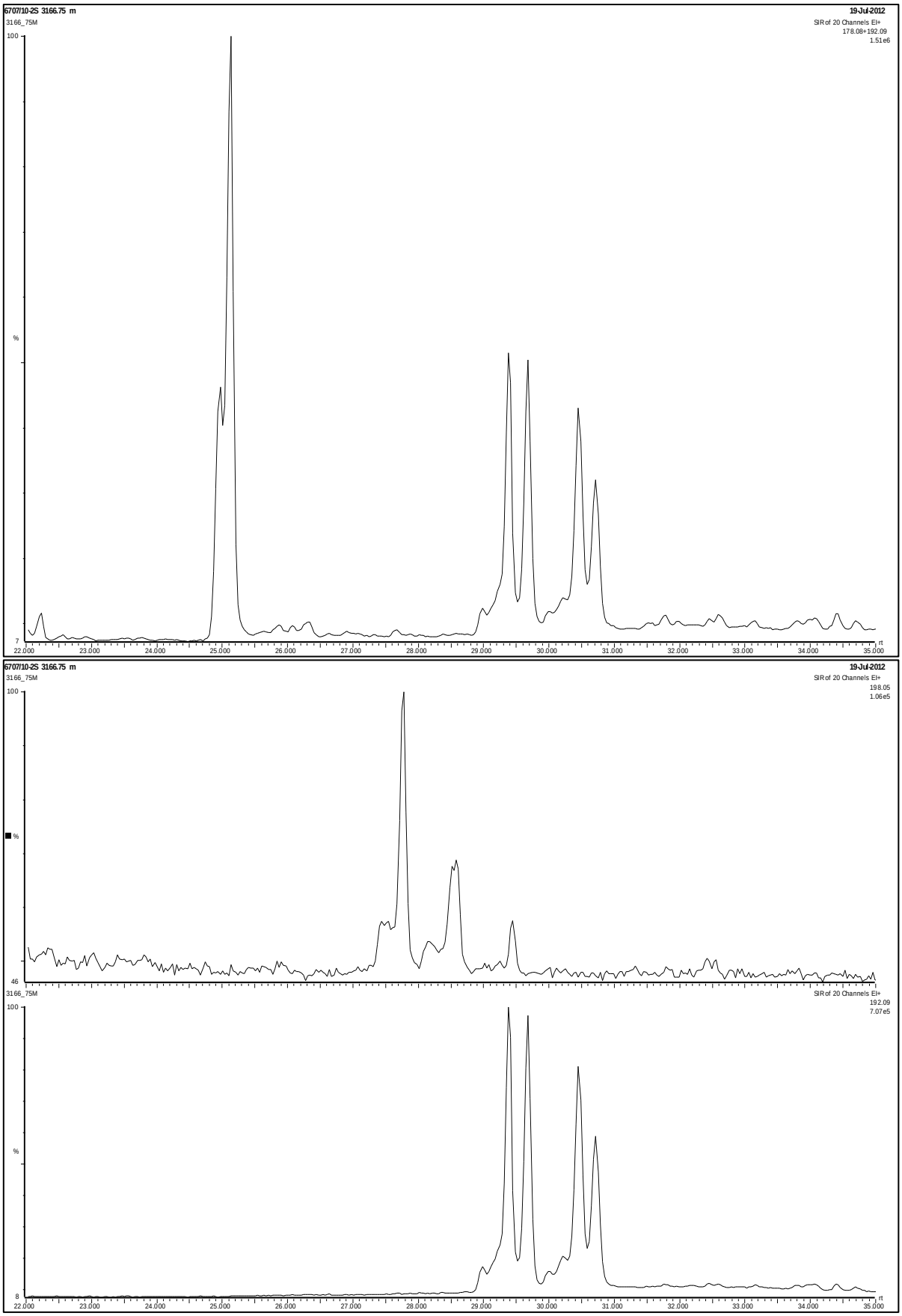
6707/10-2S 3166.75 m
19-Jul-2012
3166_75M
SIR of 20 Channels EI+
178.08+192.09
1.51e6
100
%
7
22.000
23.000
24.000
25.000
26.000
27.000
28.000
29.000
30.000
31.000
32.000
33.000
34.000
35.000
rt
6707/10-2S 3166.75 m
19-Jul-2012
3166_75M
SIR of 20 Channels EI+
198.05
1.06e5
100
%
46
3166_75M
SIR of 20 Channels EI+
192.09
7.07e5
100
%
8
22.000
23.000
24.000
25.000
26.000
27.000
28.000
29.000
30.000
31.000
32.000
33.000
34.000
35.000
rt

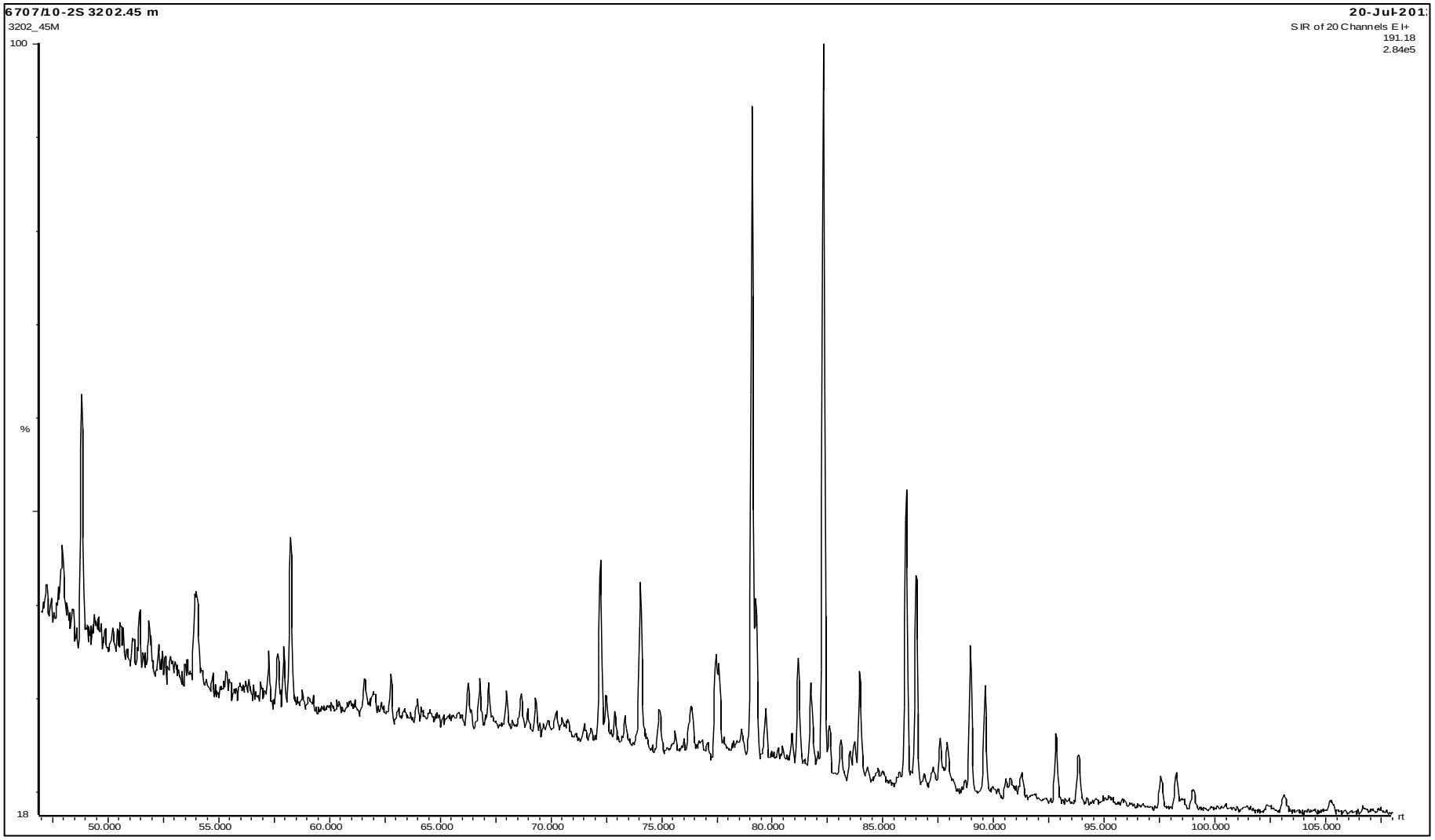
6707A10-2S 3202.45 m
3202_45M
20-Jul-201
SIR of 20 Channels EI+
191.18
2.84e5
100
%
18
50.000
55.000
60.000
65.000
70.000
75.000
80.000
85.000
90.000
95.000
100.000
105.000
rt

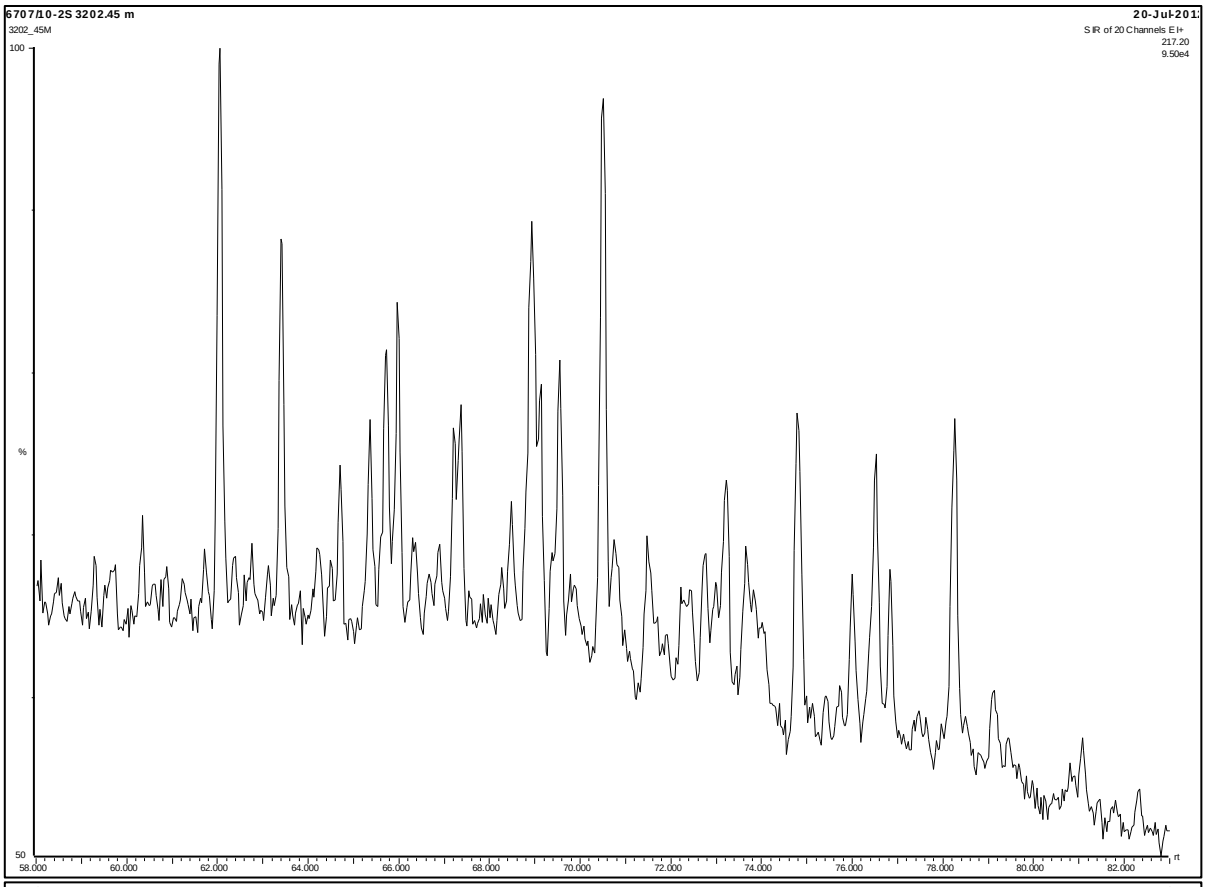
6707/10-2S 3202.45 m
3202_45M
20-Jul-201
SIR of 20 Channels EI+
217.20
9.50e4
100
%
50
58.000
60.000
62.000
64.000
66.000
68.000
70.000
72.000
74.000
76.000
78.000
80.000
82.000
rt

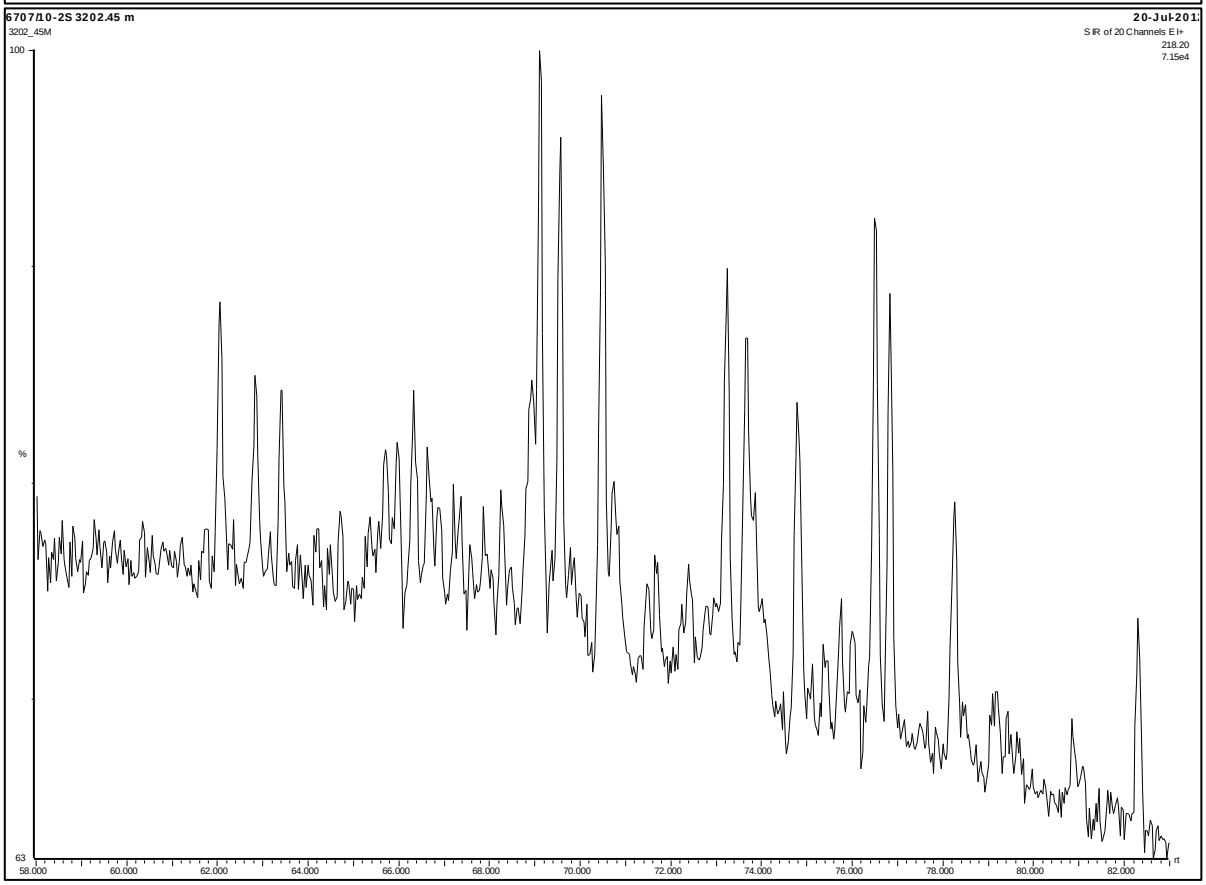
6707/10-2S 3202.45 m
3202_45M
20-Jul-201
SIR of 20 Channels EI+
218.20
7.15e4
100
%
63
58.000
60.000
62.000
64.000
66.000
68.000
70.000
72.000
74.000
76.000
78.000
80.000
82.000
rt

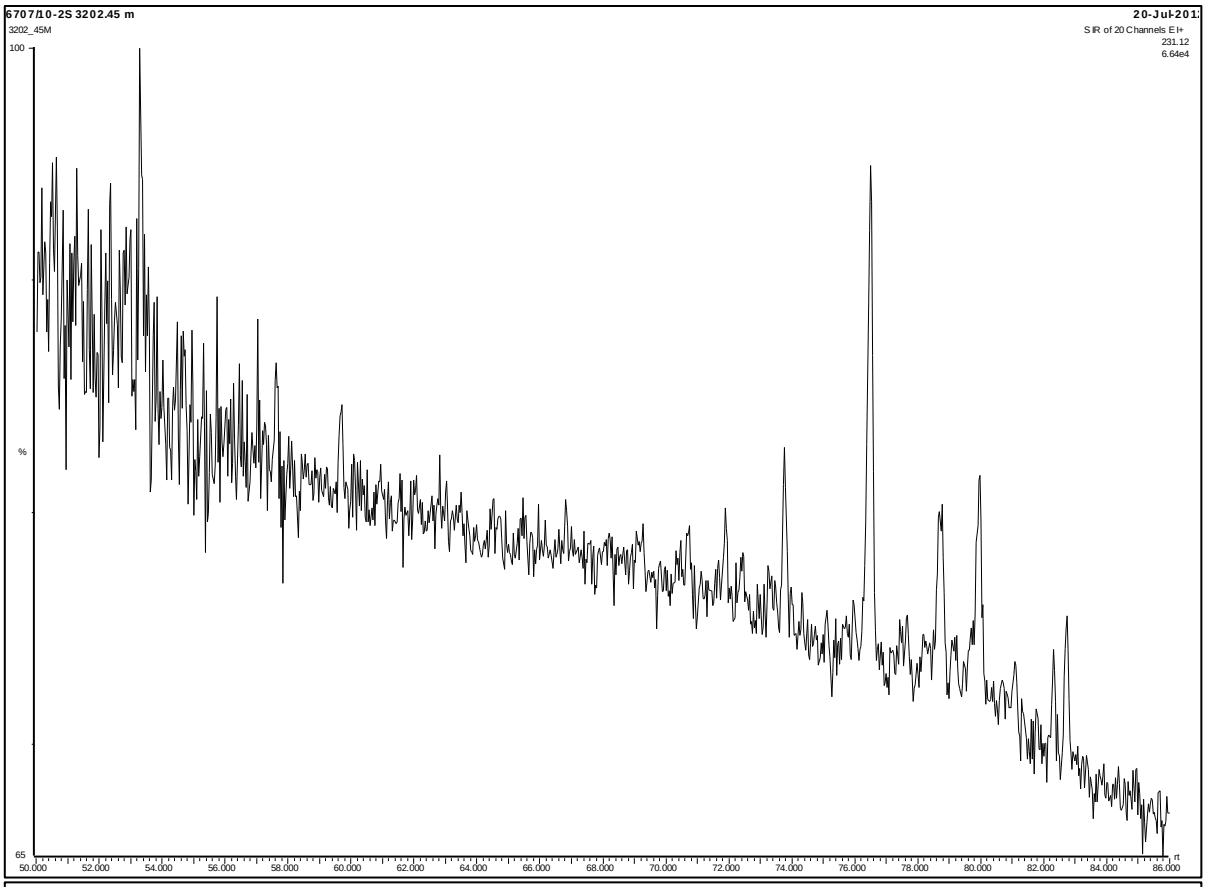
6707/10-2S 3202.45 m
3202_45M
20-Jul-201
SIR of 20 Channels EI+
231.12
6.64e4
100
%
65
50.000 52.000 54.000 56.000 58.000 60.000 62.000 64.000 66.000 68.000 70.000 72.000 74.000 76.000 78.000 80.000 82.000 84.000 86.000
rt

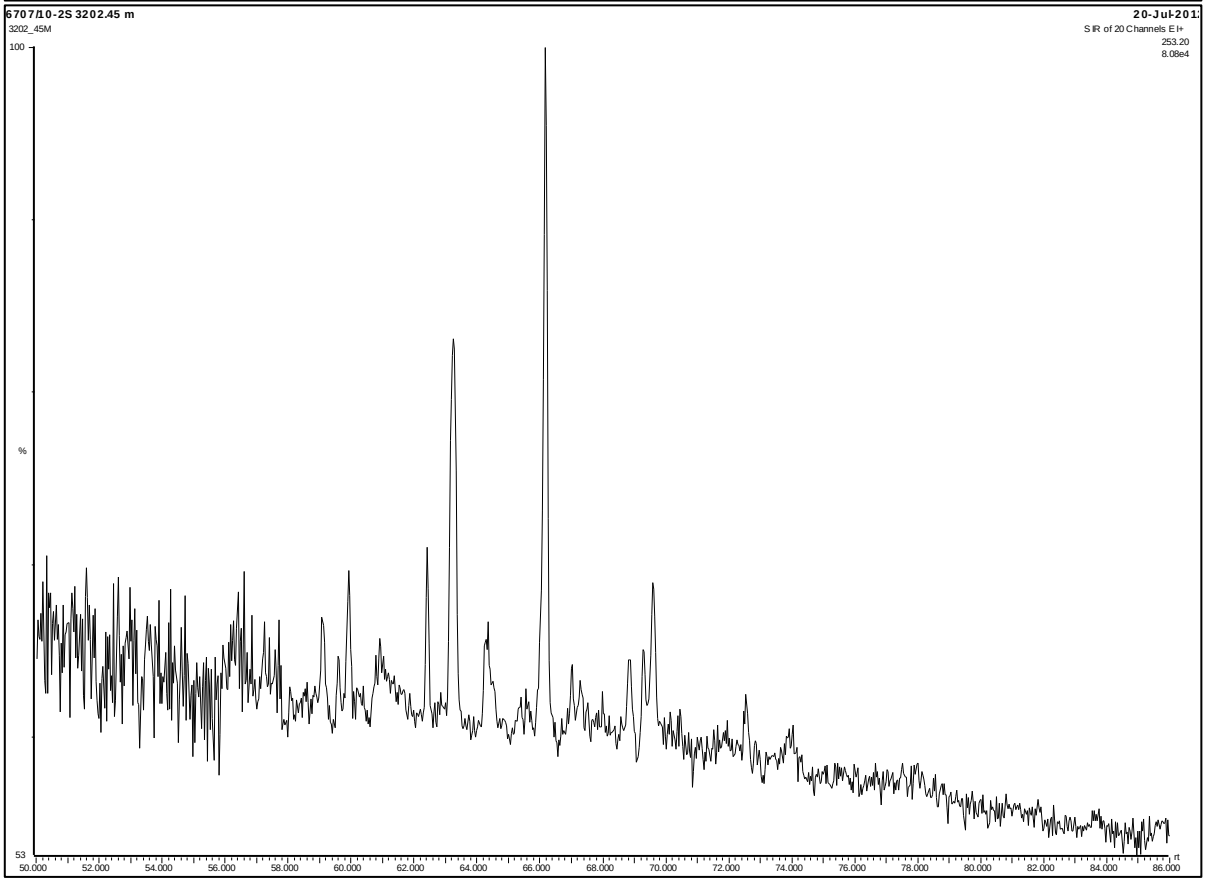
6707/10-2S 3202.45 m
3202_45M
20-Jul-201
SIR of 20 Channels EI+
253.20
8.08e4
100
%
53
50.000 52.000 54.000 56.000 58.000 60.000 62.000 64.000 66.000 68.000 70.000 72.000 74.000 76.000 78.000 80.000 82.000 84.000 86.000
rt

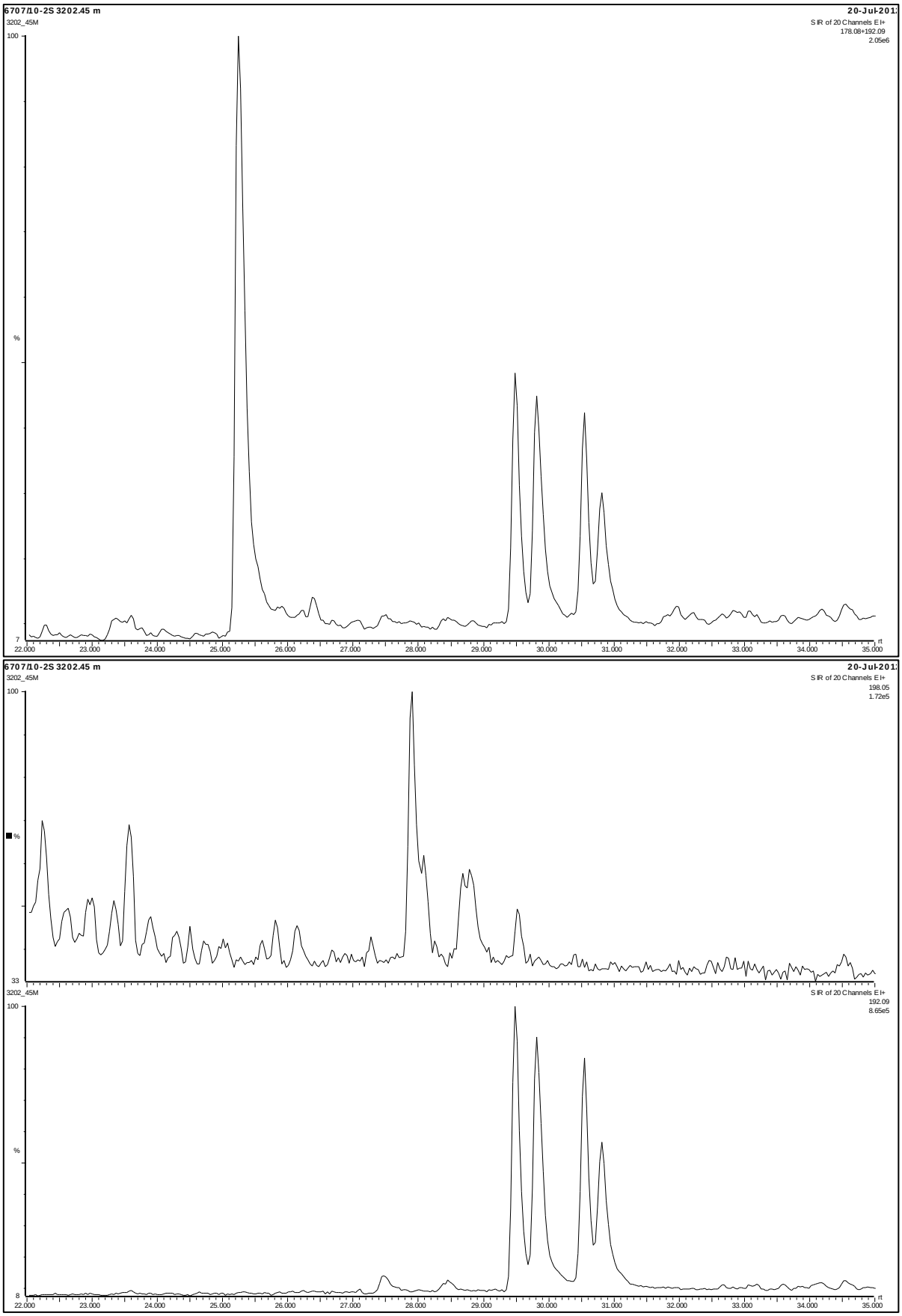
6707/10-2S 3202.45 m
20-Jul-201
3202_45M
SIR of 20 Channels EI+
178.08+192.09
2.05e6
100
%
7
22.000
23.000
24.000
25.000
26.000
27.000
28.000
29.000
30.000
31.000
32.000
33.000
34.000
35.000
rt
6707/10-2S 3202.45 m
20-Jul-201
3202_45M
SIR of 20 Channels EI+
198.05
1.72e5
100
%
33
3202_45M
SIR of 20 Channels EI+
192.09
8.65e5
100
%
8
22.000
23.000
24.000
25.000
26.000
27.000
28.000
29.000
30.000
31.000
32.000
33.000
34.000
35.000
rt

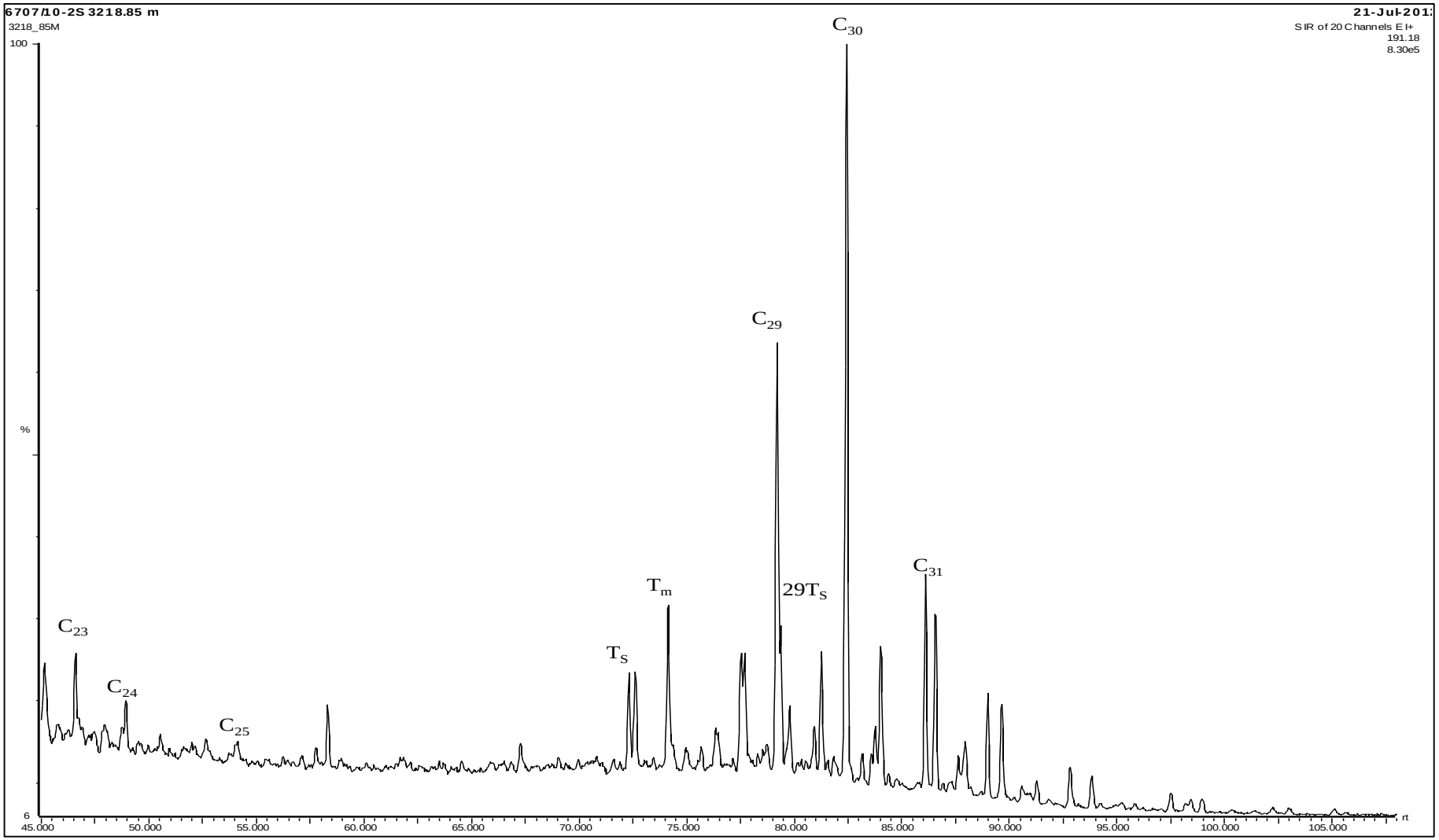
6707/10-2S 3218.85 m
3218_85M
21-Jul-201
SIR of 20 Channels EI+
191.18
8.30e5
100
%
6
C23
C24
C25
TS
Tm
29TS
C29
C30
C31
45.000
50.000
55.000
60.000
65.000
70.000
75.000
80.000
85.000
90.000
95.000
100.000
105.000
rt

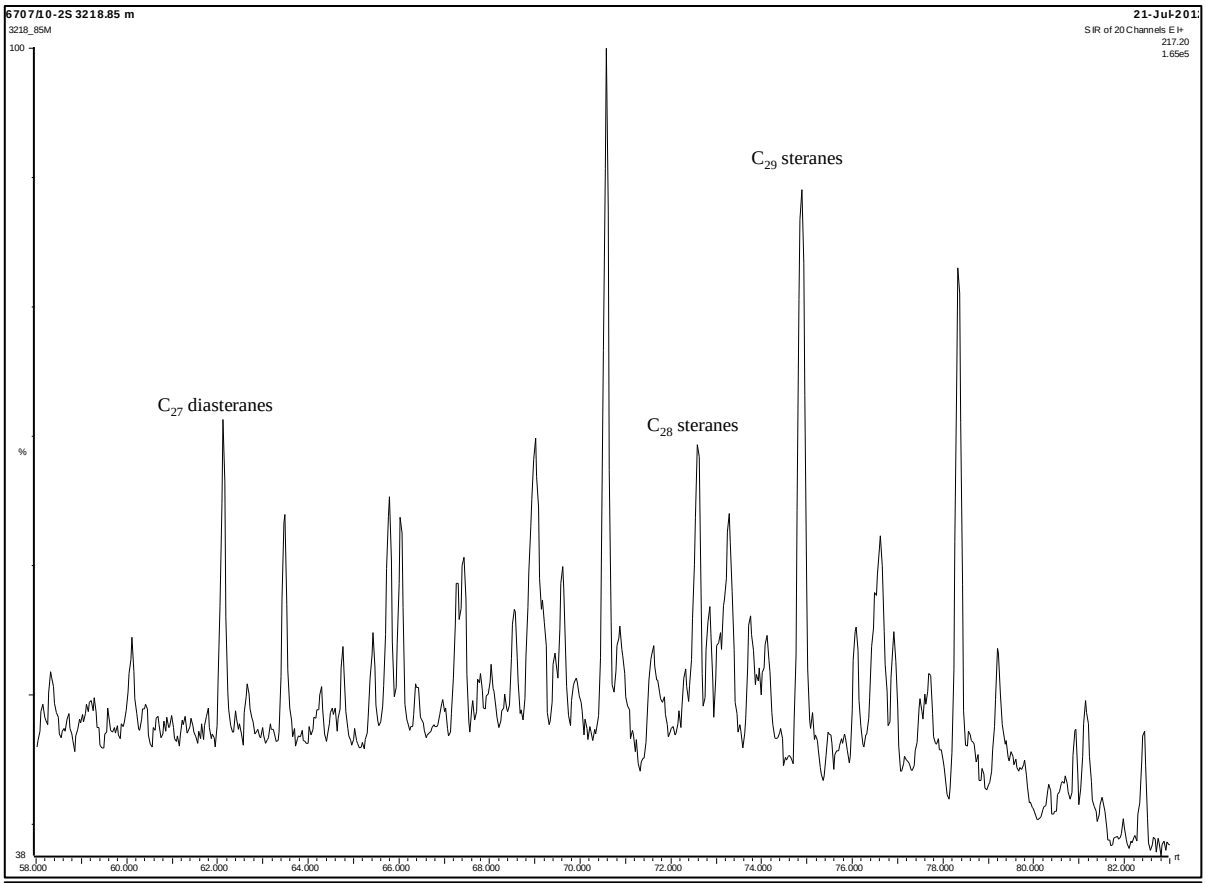
6707/10-2S 3218.85 m
3218_85M
21-Jul-201
SIR of 20 Channels EI+
217.20
1.65e5
100
%
38
C27 diasteranes
C28 steranes
C29 steranes
58.000
60.000
62.000
64.000
66.000
68.000
70.000
72.000
74.000
76.000
78.000
80.000
82.000
rt

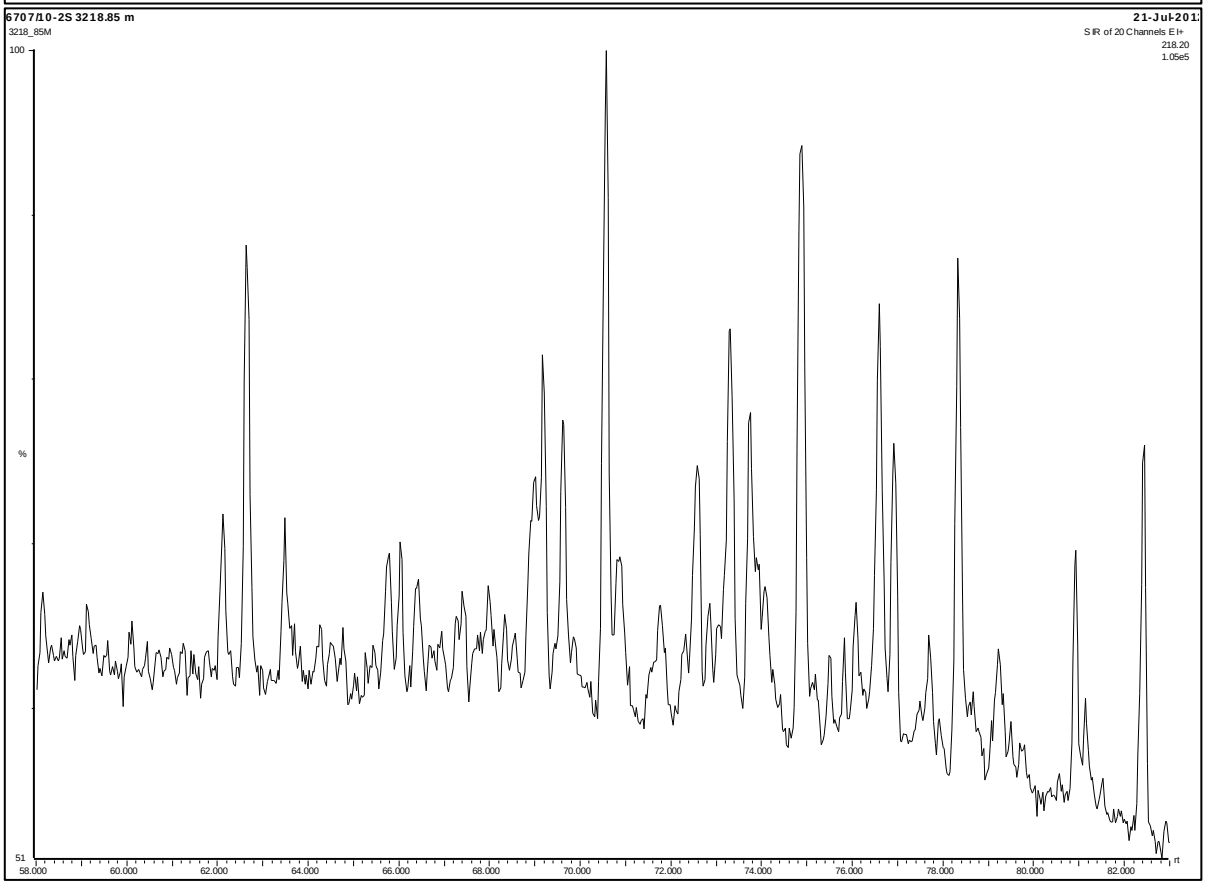
6707/10-2S 3218.85 m
3218_85M
21-Jul-201
SIR of 20 Channels EI+
218.20
1.05e5
100
%
51
58.000
60.000
62.000
64.000
66.000
68.000
70.000
72.000
74.000
76.000
78.000
80.000
82.000
rt

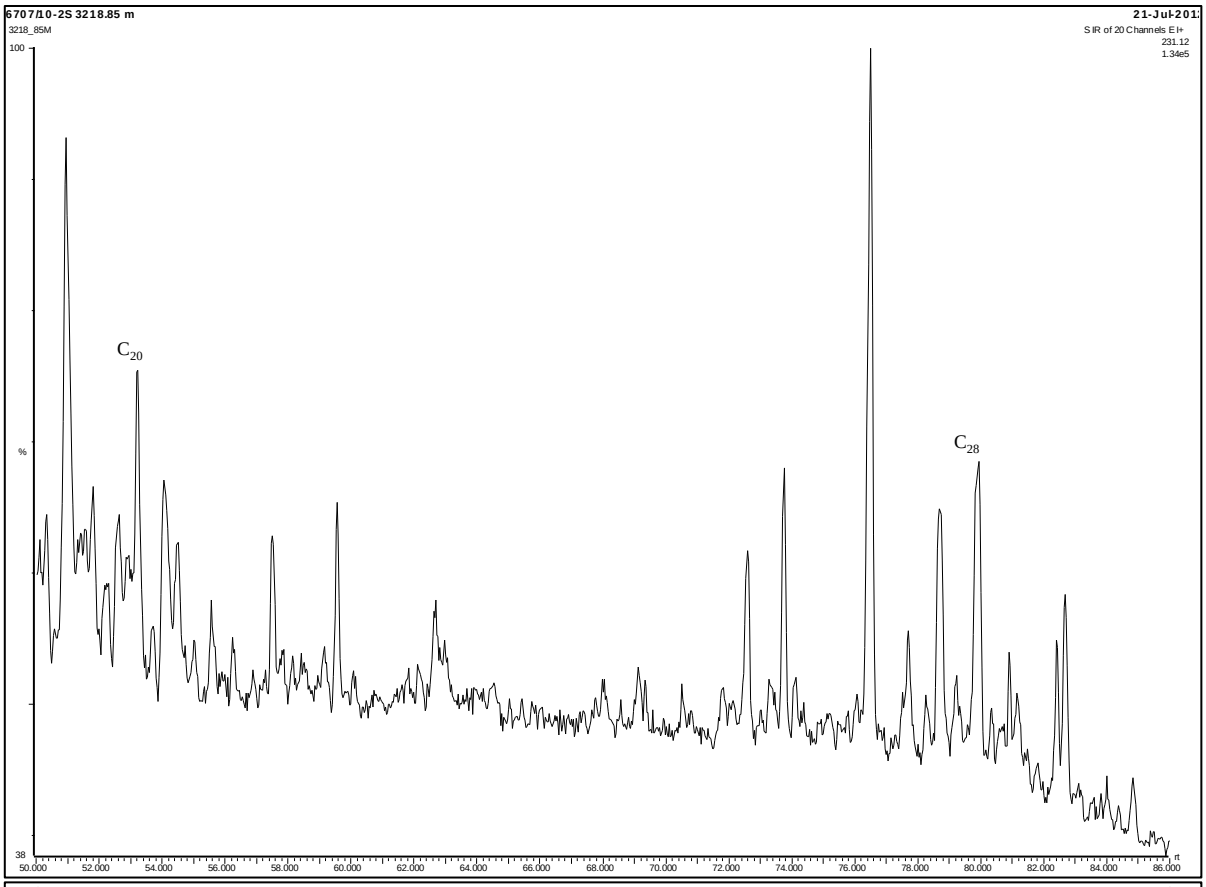
6707/10-2S 3218.85 m
3218_85M
21-Jul-2011
SIR of 20 Channels EI+
231.12
1.34e5
100
%
38
C20
C28
50.000 52.000 54.000 56.000 58.000 60.000 62.000 64.000 66.000 68.000 70.000 72.000 74.000 76.000 78.000 80.000 82.000 84.000 86.000
rt

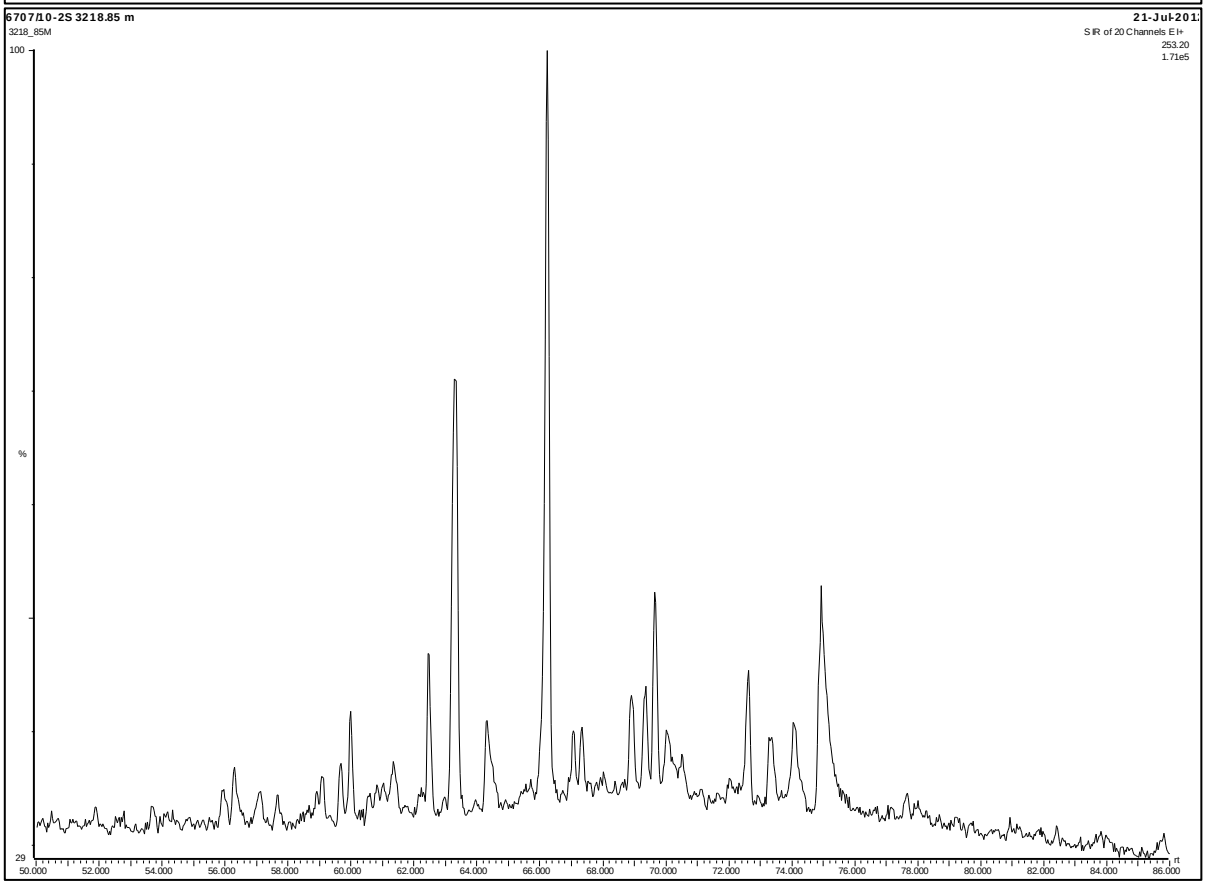
6707/10-2S 3218.85 m
3218_85M
21-Jul-2011
SIR of 20 Channels EI+
253.20
1.71e5
100
%
29
50.000 52.000 54.000 56.000 58.000 60.000 62.000 64.000 66.000 68.000 70.000 72.000 74.000 76.000 78.000 80.000 82.000 84.000 86.000
rt

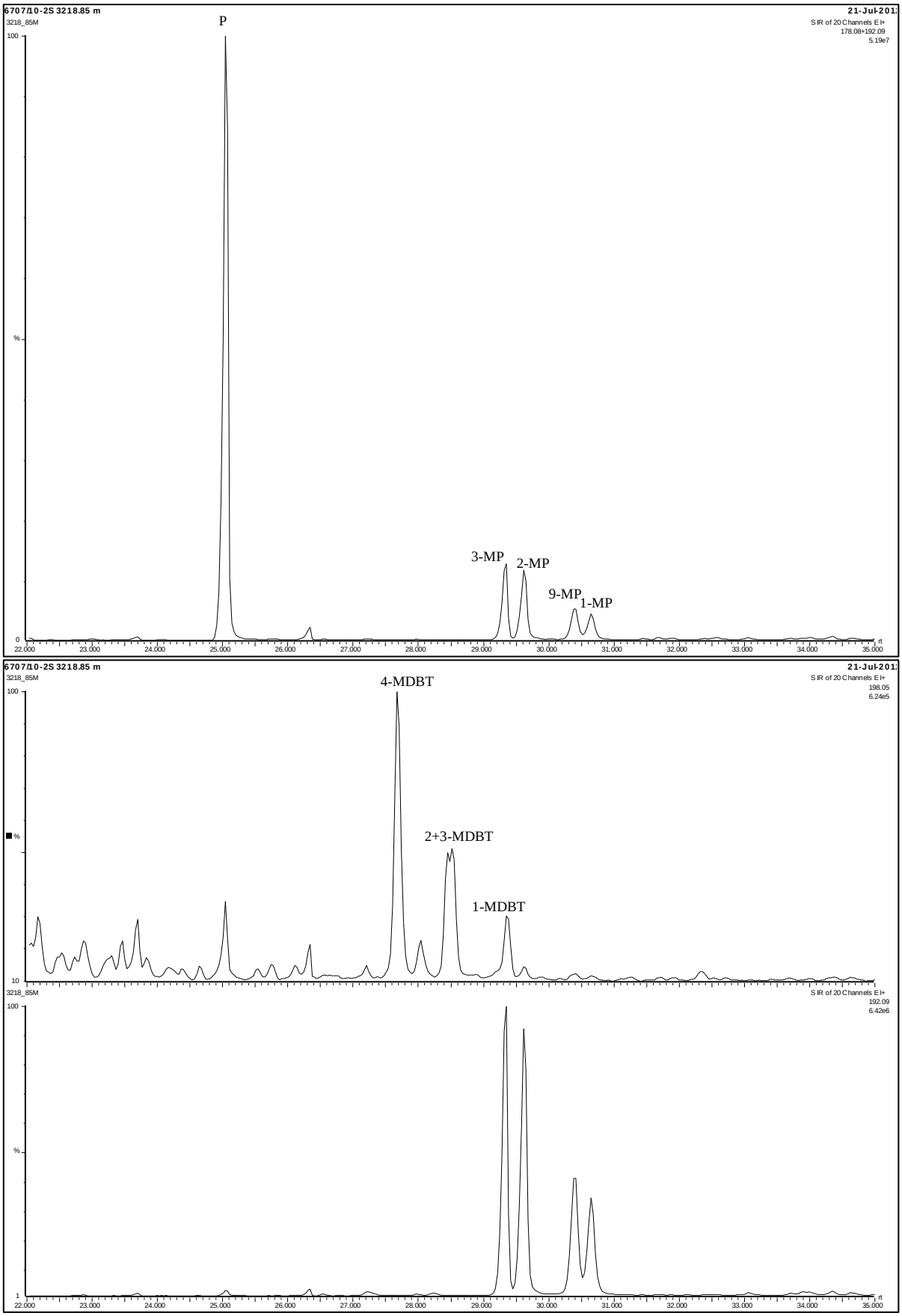
6707/10-2S 3218.85 m
3218_85M
21-Jul-201
SIR of 20 Channels EI+
178.08+192.09
5.19e7
P
3-MP
2-MP
9-MP
1-MP
4-MDBT
2+3-MDBT
1-MDBT
198.05
6.24e5
192.09
6.42e6
%
rt
22.000
23.000
24.000
25.000
26.000
27.000
28.000
29.000
30.000
31.000
32.000
33.000
34.000
35.000

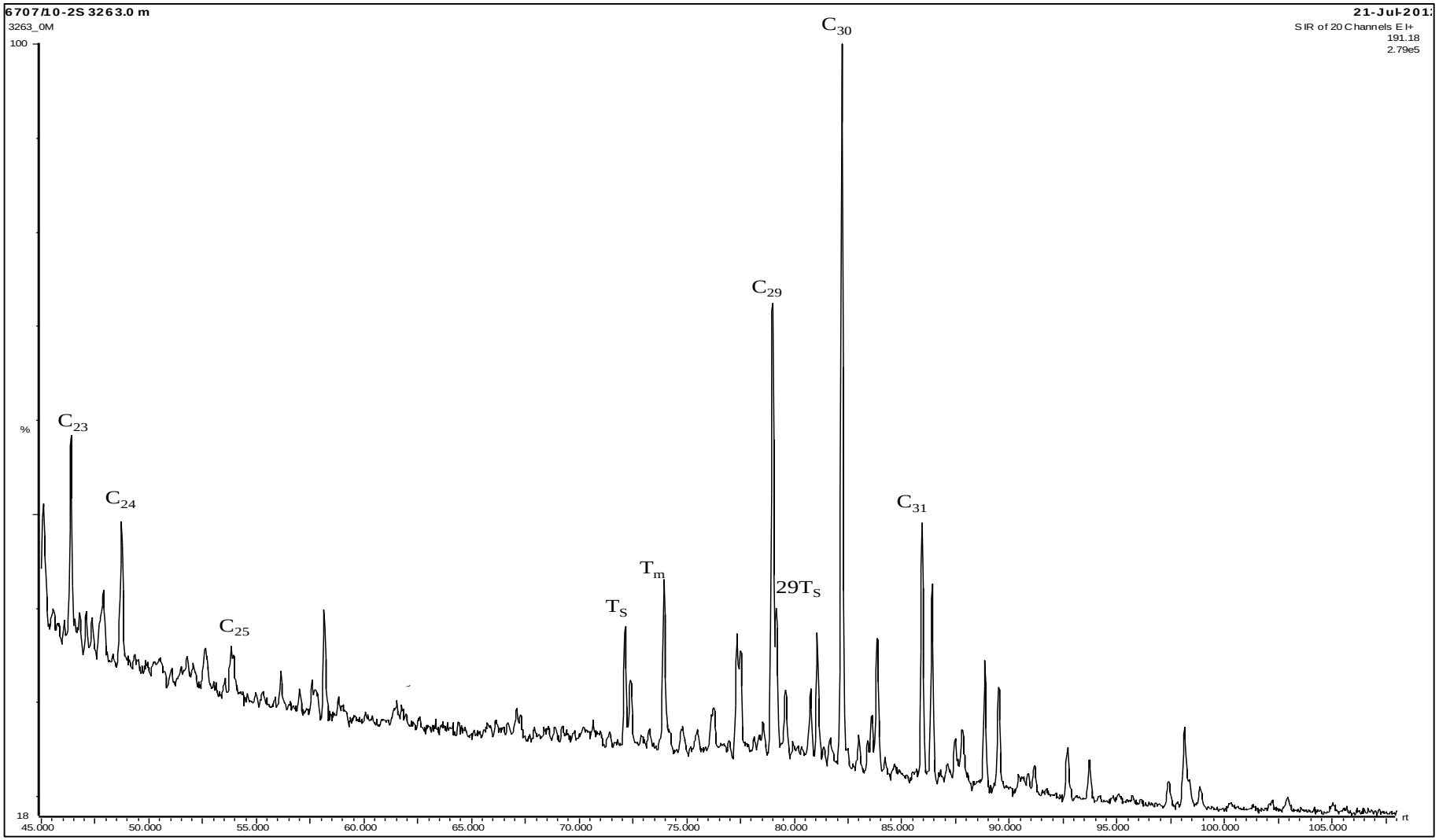
6707/10-2S 3263.0 m
3263_0M
21-Jul-201
SIR of 20 Channels EI+
191.18
2.79e5
100
%
18
C23
C24
C25
TS
Tm
29TS
C29
C30
C31
45.000
50.000
55.000
60.000
65.000
70.000
75.000
80.000
85.000
90.000
95.000
100.000
105.000
rt

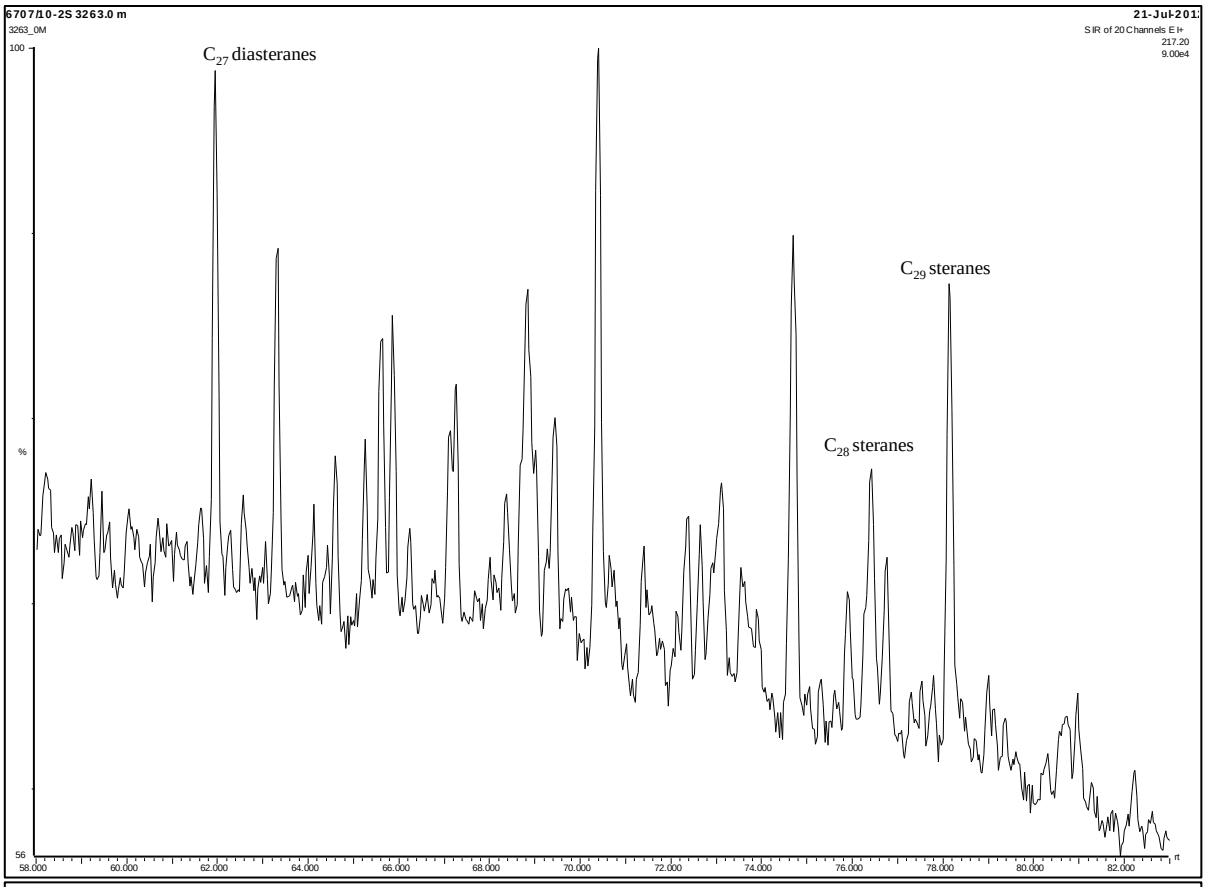
6707/10-2S 3263.0 m
3263_0M
21-Jul-201
SIR of 20 Channels EI+
217.20
9.00e4
100
%
56
C27 diasteranes
C29 steranes
C28 steranes
58.000
60.000
62.000
64.000
66.000
68.000
70.000
72.000
74.000
76.000
78.000
80.000
82.000
rt

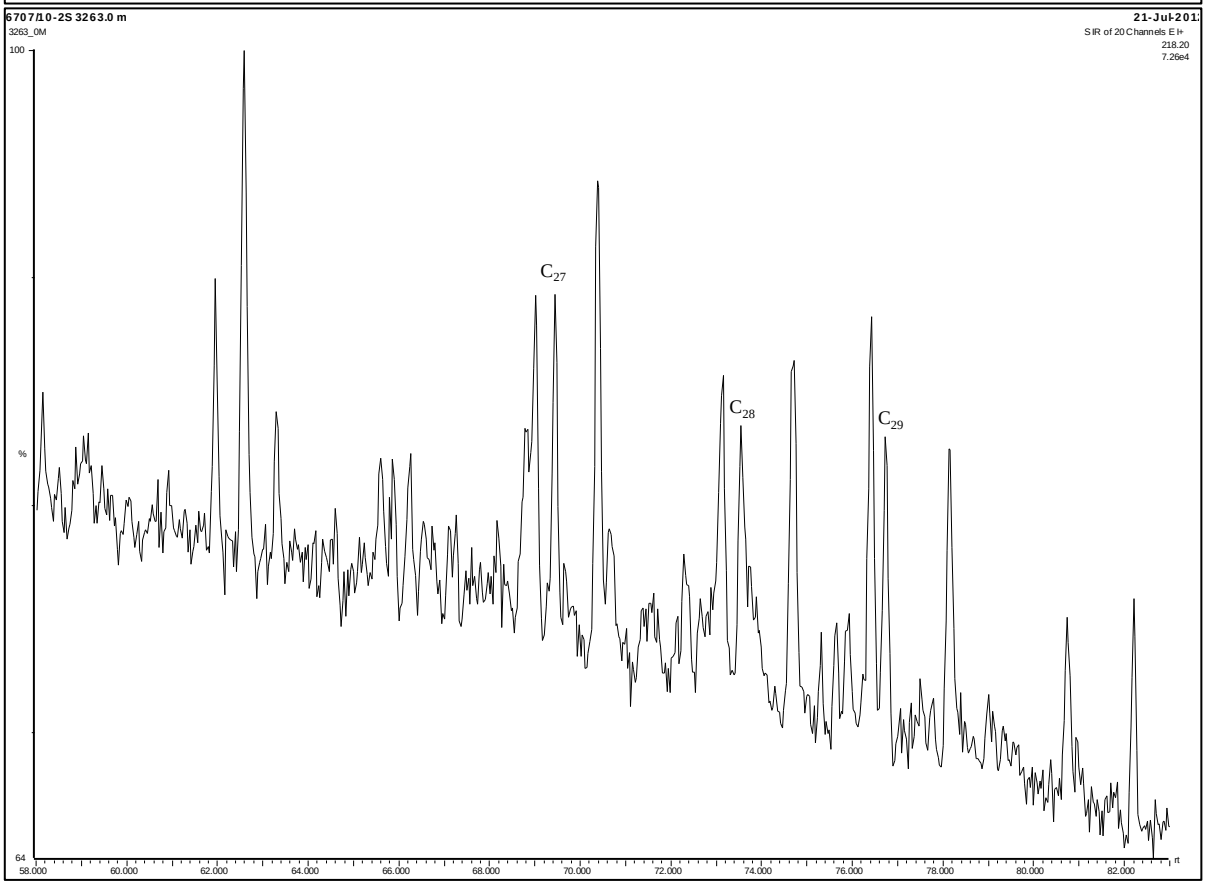
6707/10-2S 3263.0 m
3263_0M
21-Jul-201
SIR of 20 Channels EI+
218.20
7.26e4
100
%
64
C27
C28
C29
58.000
60.000
62.000
64.000
66.000
68.000
70.000
72.000
74.000
76.000
78.000
80.000
82.000
rt

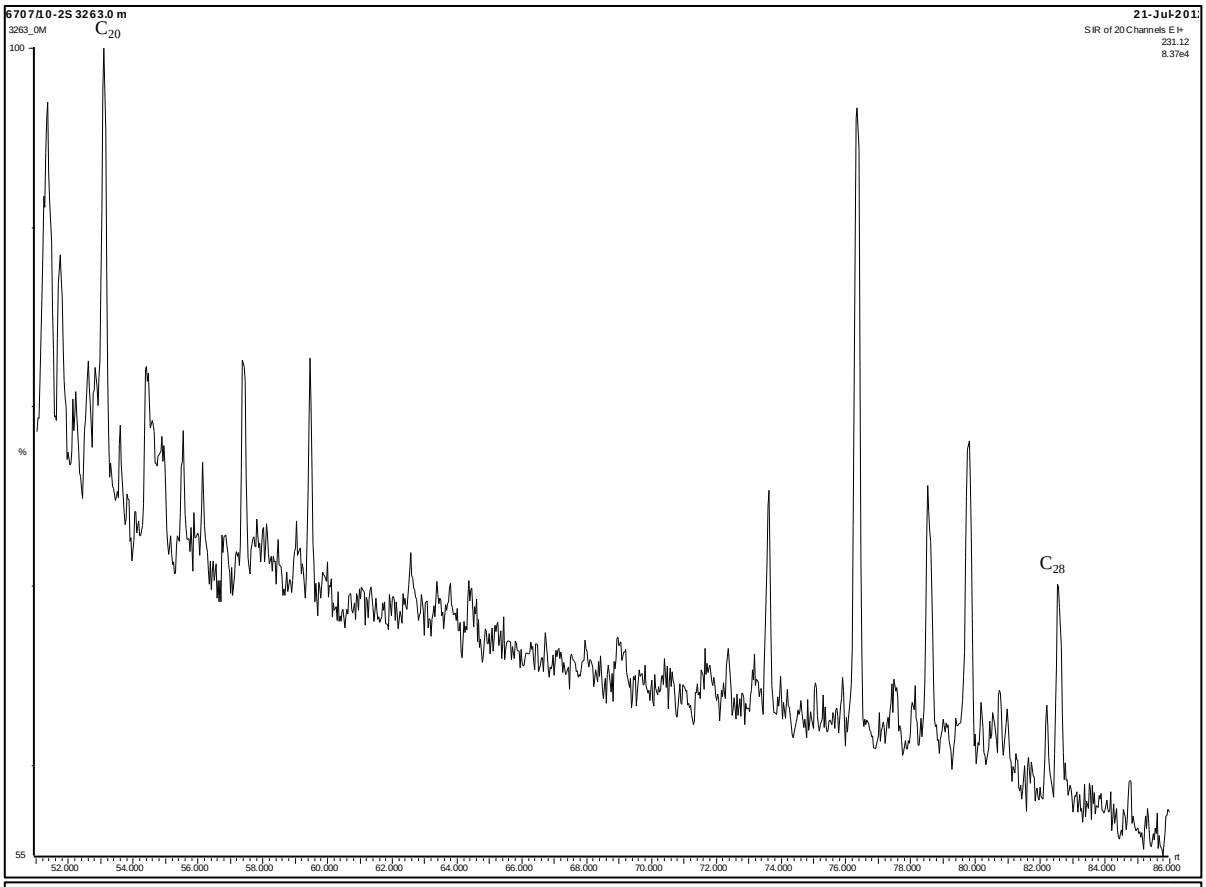
6707/10-2S 3263.0 m
3263_0M
21-Jul-201
SIR of 20 Channels EI+
231.12
8.37e4
C20
C28
100
%
55
52.000 54.000 56.000 58.000 60.000 62.000 64.000 66.000 68.000 70.000 72.000 74.000 76.000 78.000 80.000 82.000 84.000 86.000
rt

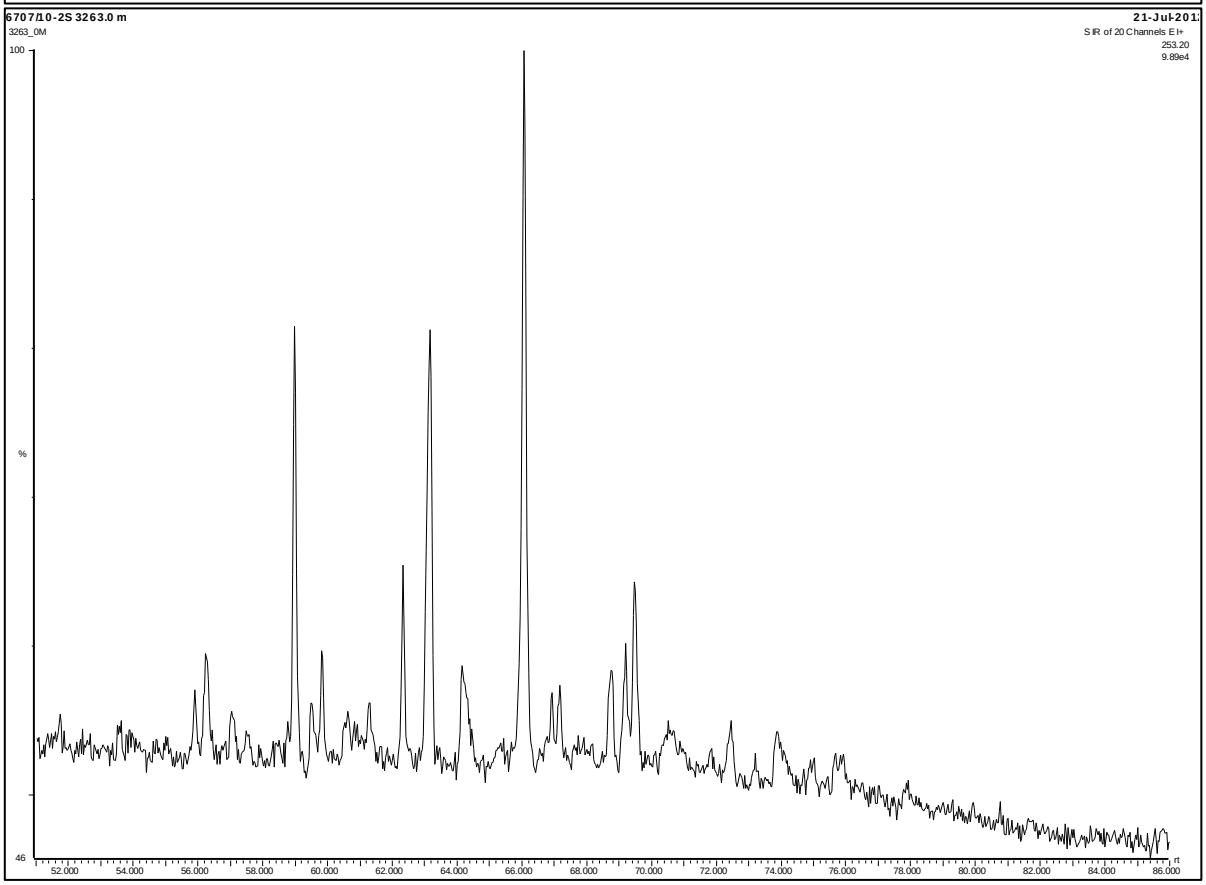
6707/10-2S 3263.0 m
3263_0M
21-Jul-201
SIR of 20 Channels EI+
253.20
9.89e4
100
%
46
52.000 54.000 56.000 58.000 60.000 62.000 64.000 66.000 68.000 70.000 72.000 74.000 76.000 78.000 80.000 82.000 84.000 86.000
rt

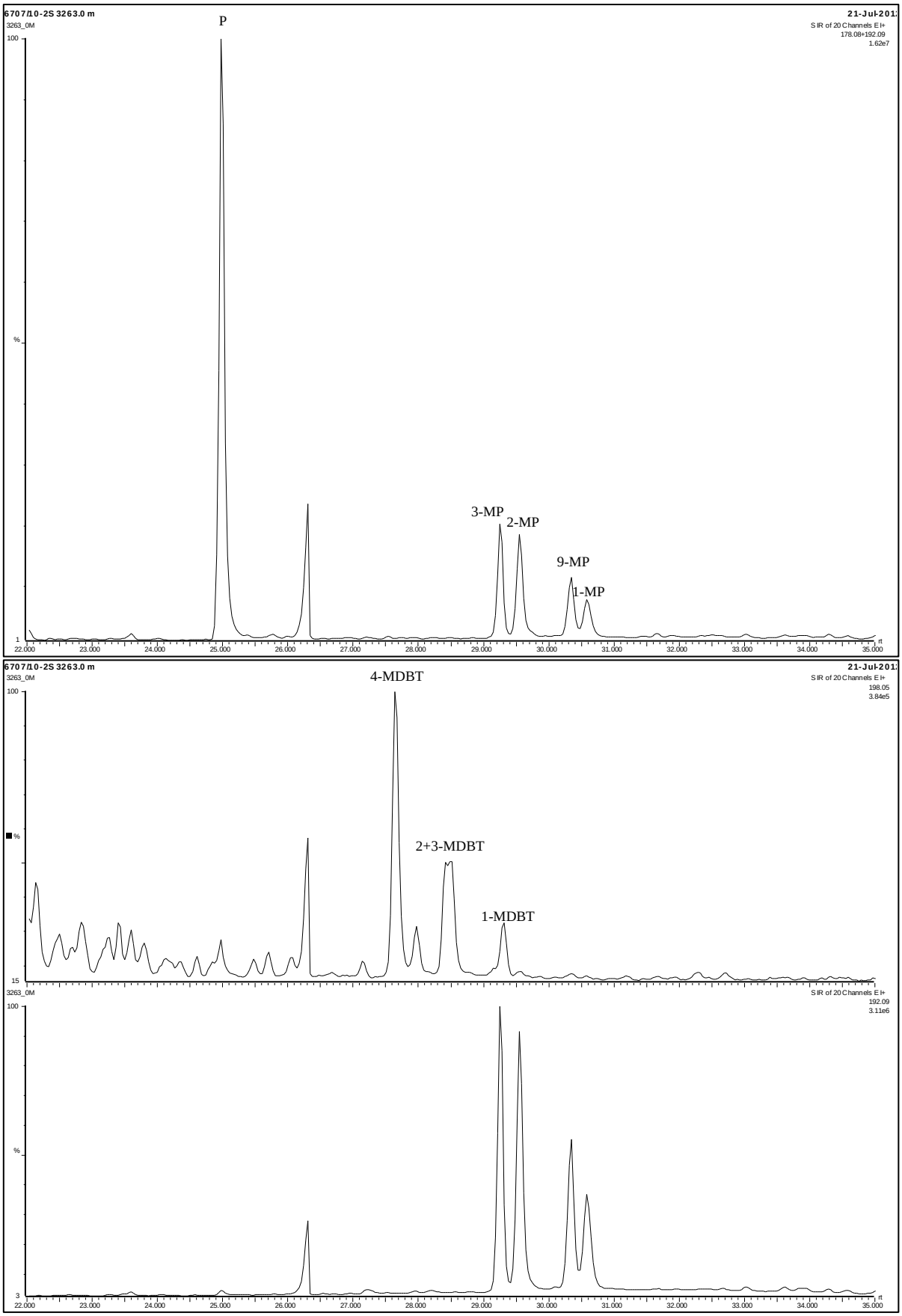
6707/10-2S 3263.0 m
3263_0M
21-Jul-201
SIR of 20 Channels EI+
178.08+192.09
1.62e7
P
3-MP
2-MP
9-MP
1-MP
%
100
1
22.000
23.000
24.000
25.000
26.000
27.000
28.000
29.000
30.000
31.000
32.000
33.000
34.000
35.000
rt
6707/10-2S 3263.0 m
3263_0M
21-Jul-201
SIR of 20 Channels EI+
198.05
3.84e5
4-MDBT
2+3-MDBT
1-MDBT
100
%
15
3263_0M
SIR of 20 Channels EI+
192.09
3.11e6
100
%
3

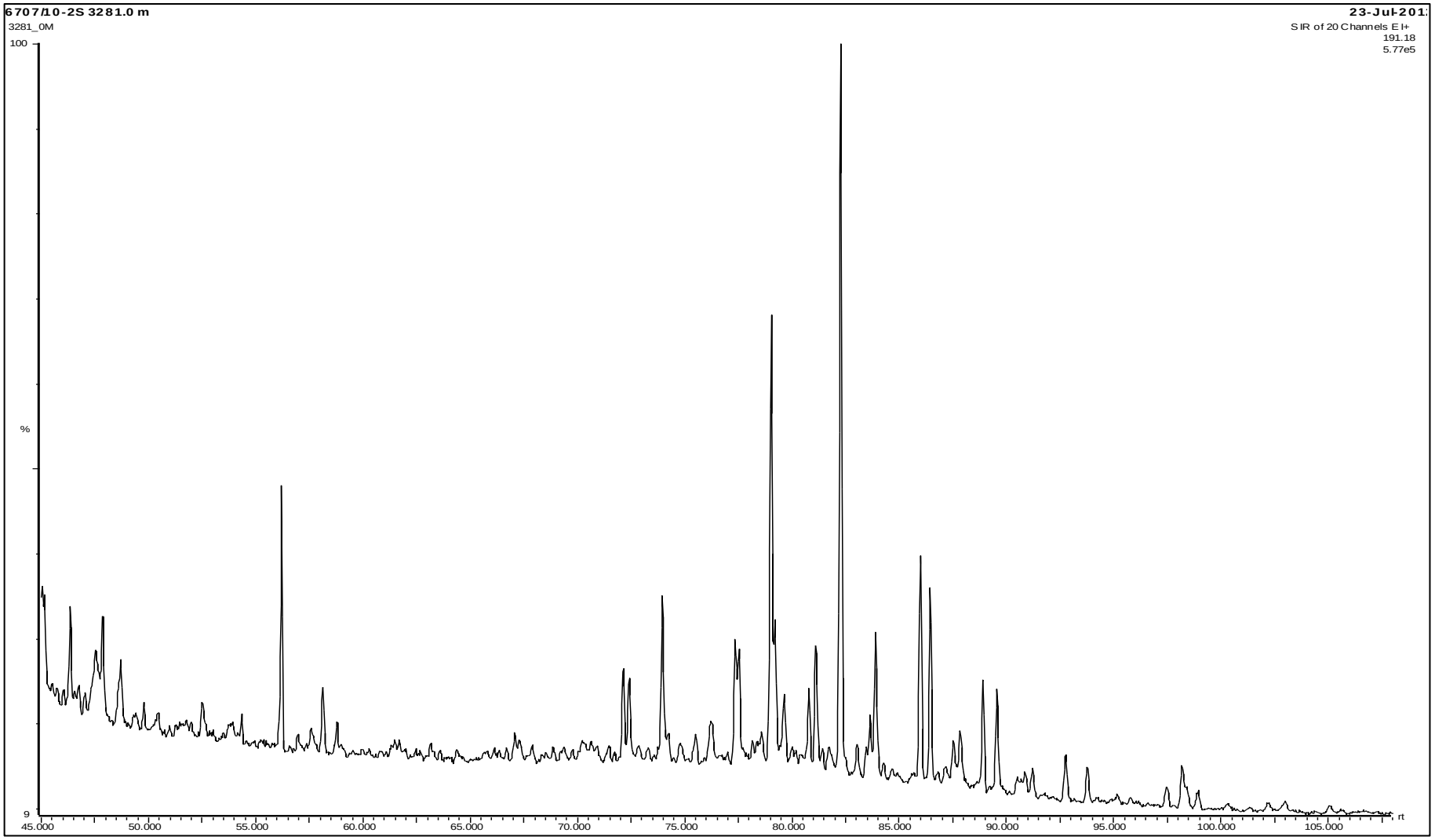
6707A10-2S 3281.0 m
3281_0M
23-Jul-201
SIR of 20 Channels EI+
191.18
5.77e5
100
%
9
45.000
50.000
55.000
60.000
65.000
70.000
75.000
80.000
85.000
90.000
95.000
100.000
105.000
rt

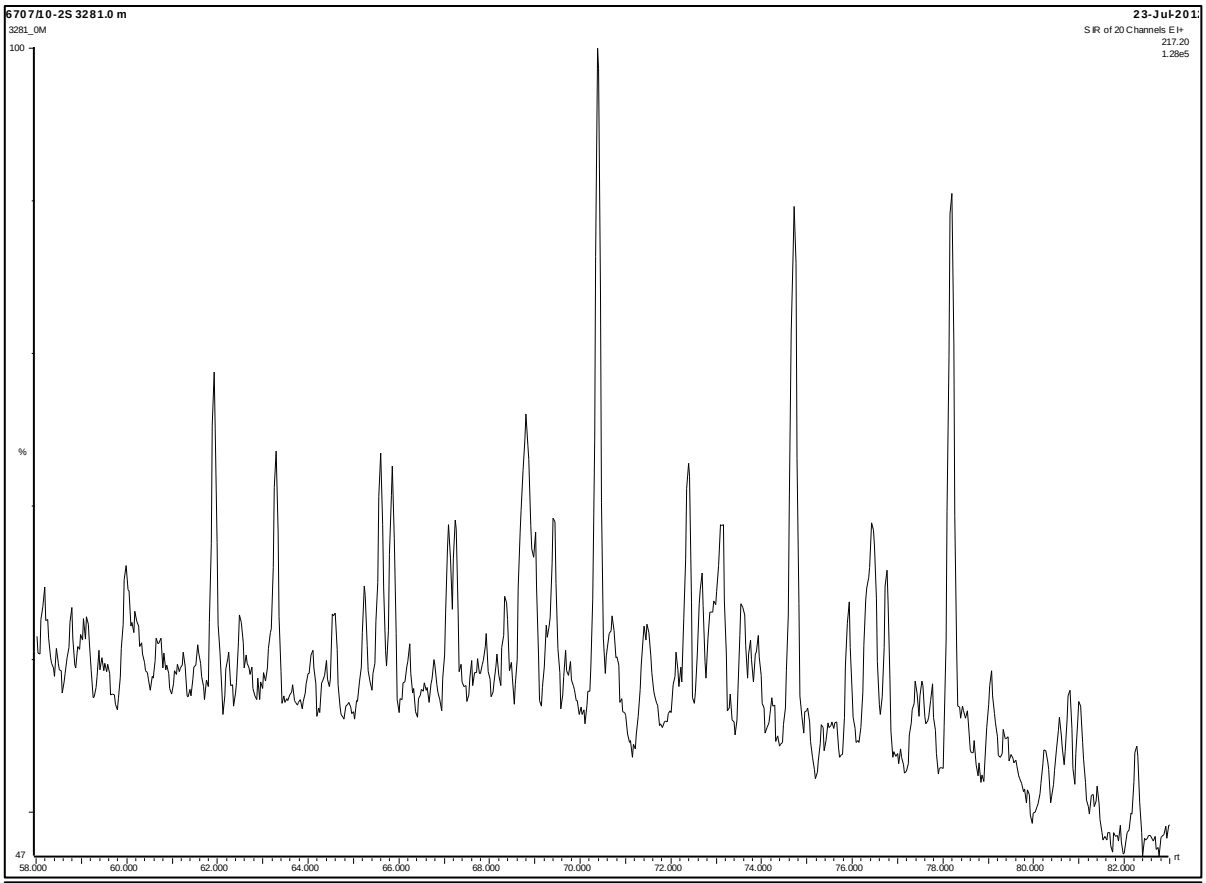
6707/10-2S 3281.0 m
3281_0M
23-Jul-201
SIR of 20 Channels EI+
217.20
1.28e5
100
%
47
58.000
60.000
62.000
64.000
66.000
68.000
70.000
72.000
74.000
76.000
78.000
80.000
82.000
rt

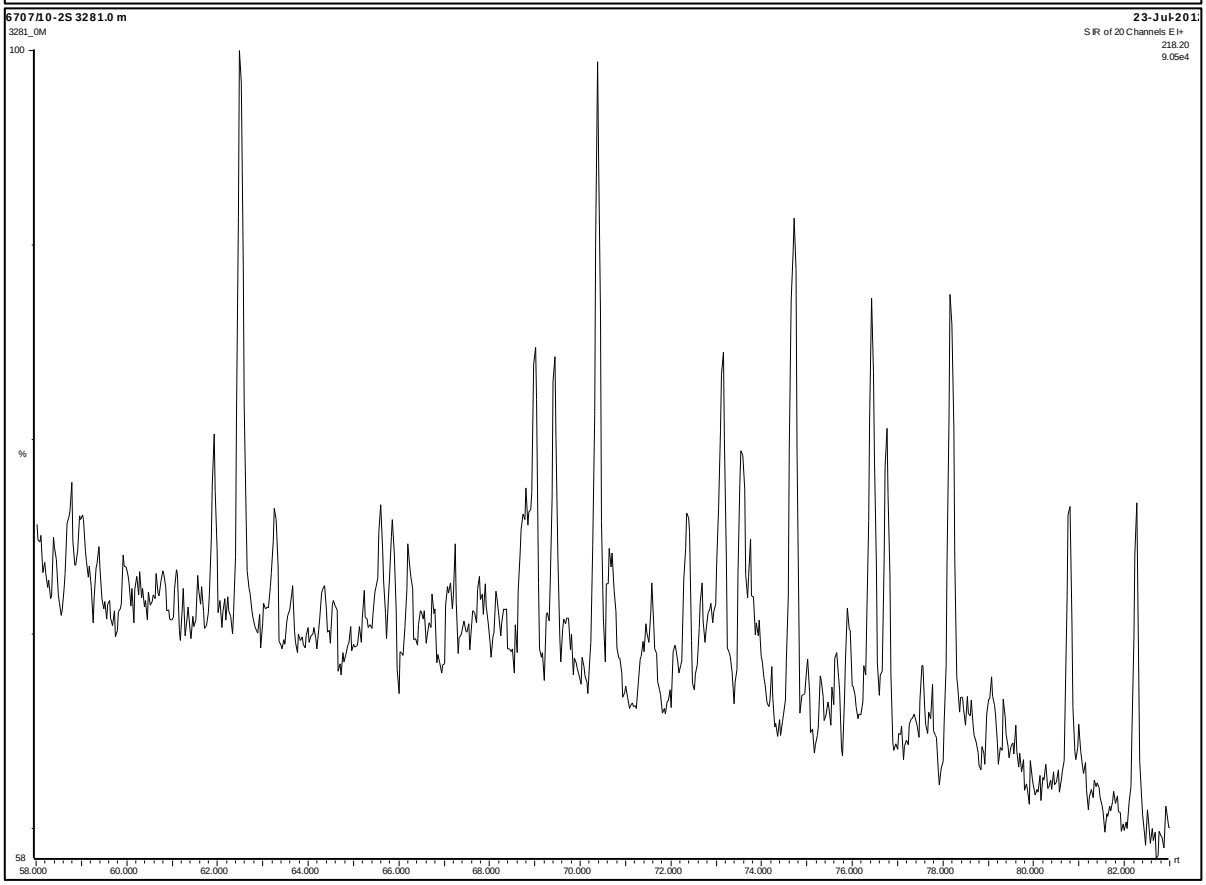
6707/10-2S 3281.0 m
3281_0M
23-Jul-201
SIR of 20 Channels EI+
218.20
9.05e4
100
%
58
58.000
60.000
62.000
64.000
66.000
68.000
70.000
72.000
74.000
76.000
78.000
80.000
82.000
rt

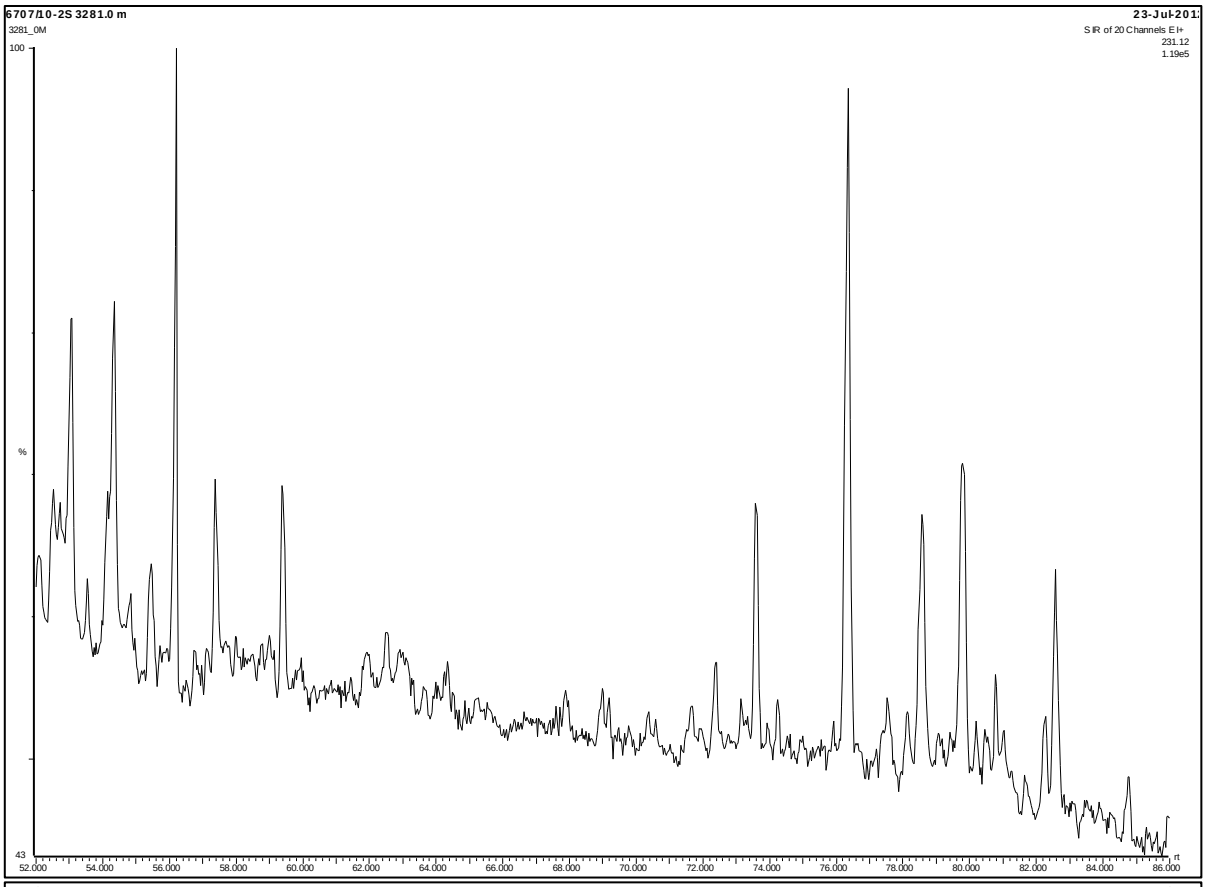
6707/10-2S 3281.0 m
3281_0M
23-Jul-201
SIR of 20 Channels EI+
231.12
1.19e5
100
%
43
52.000 54.000 56.000 58.000 60.000 62.000 64.000 66.000 68.000 70.000 72.000 74.000 76.000 78.000 80.000 82.000 84.000 86.000
rt

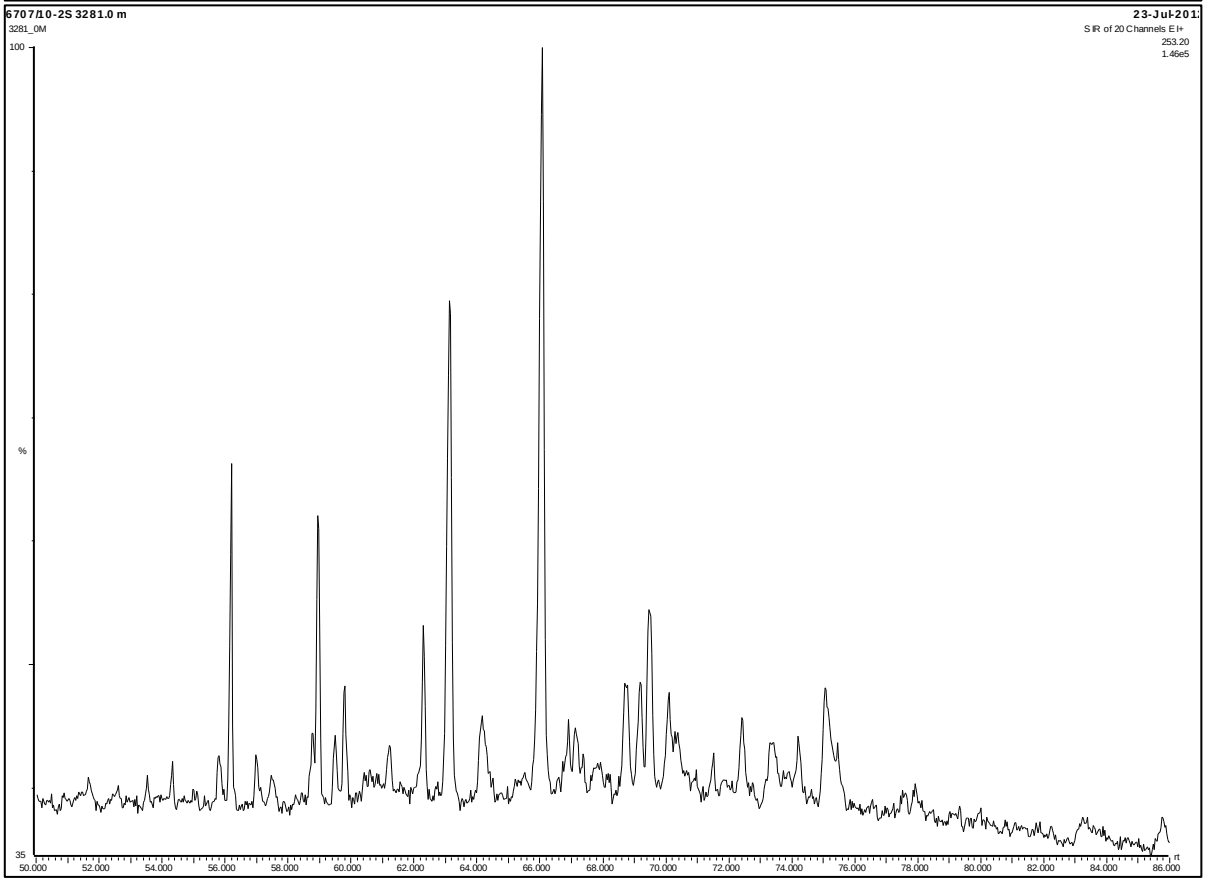
6707/10-2S 3281.0 m
3281_0M
23-Jul-201
SIR of 20 Channels EI+
253.20
1.46e5
100
%
35
50.000 52.000 54.000 56.000 58.000 60.000 62.000 64.000 66.000 68.000 70.000 72.000 74.000 76.000 78.000 80.000 82.000 84.000 86.000
rt

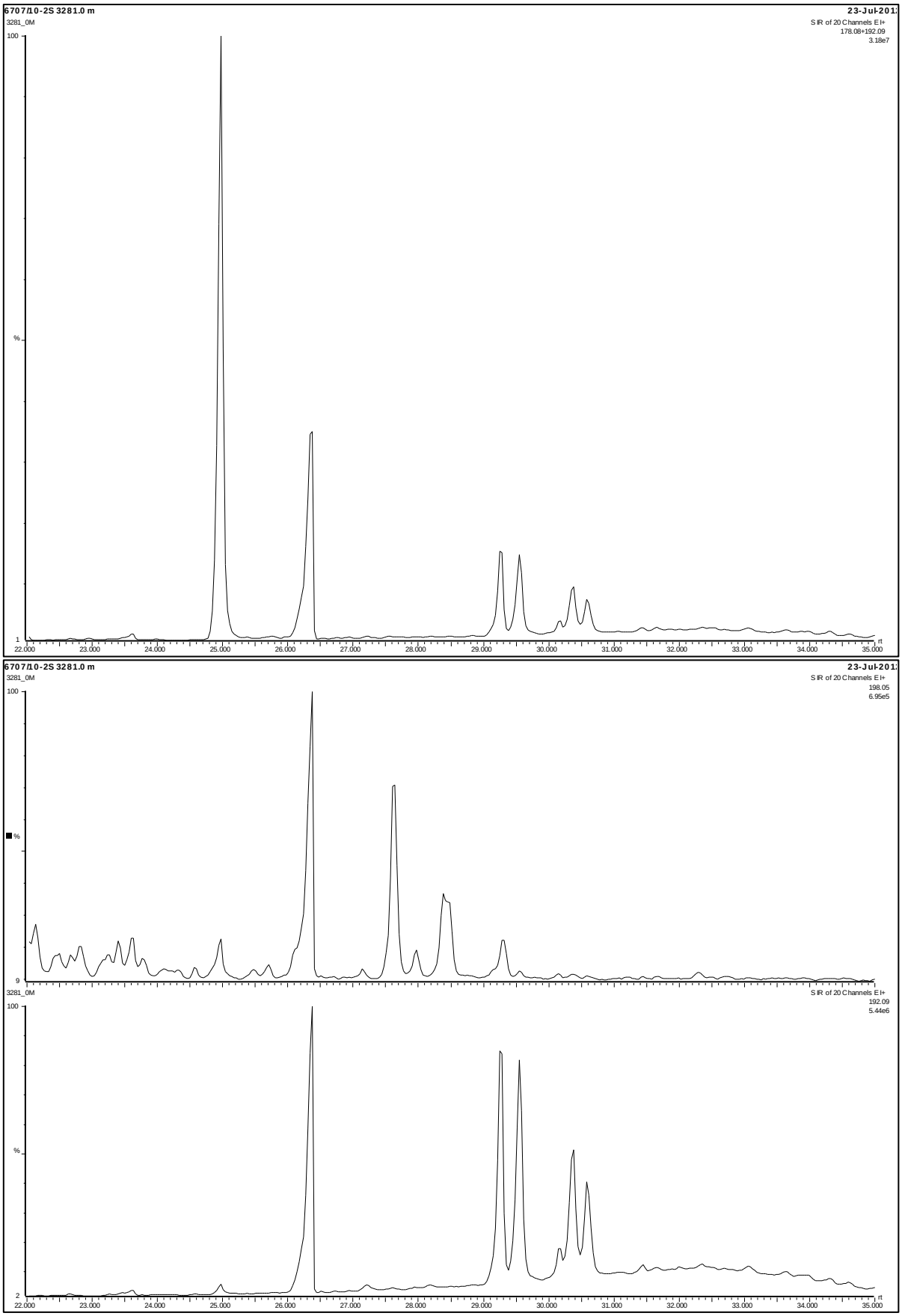
6707/10-2S 3281.0 m
3281_0M
23-Jul-201
SIR of 20 Channels EI+
178.08+192.09
3.18e7
100
%
1
22.000
23.000
24.000
25.000
26.000
27.000
28.000
29.000
30.000
31.000
32.000
33.000
34.000
35.000
rt
6707/10-2S 3281.0 m
3281_0M
23-Jul-201
SIR of 20 Channels EI+
198.05
6.95e5
100
%
9
3281_0M
SIR of 20 Channels EI+
192.09
5.44e6
100
%
2
22.000
23.000
24.000
25.000
26.000
27.000
28.000
29.000
30.000
31.000
32.000
33.000
34.000
35.000
rt

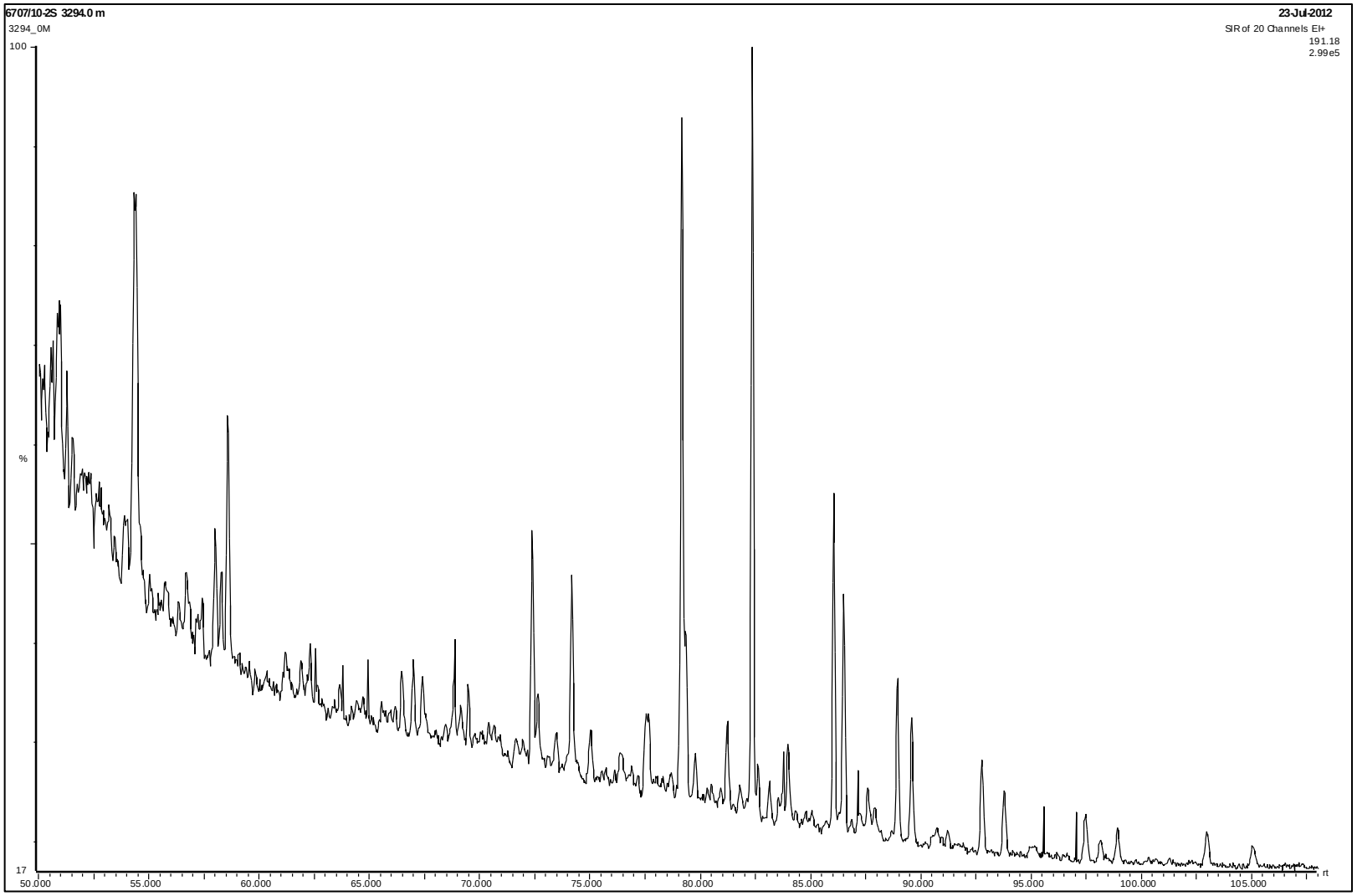
6707/10-2S 3294.0 m
3294_0M
23-Jul-2012
SIR of 20 Channels EI+
191.18
2.99e5
100
%
17
50.000
55.000
60.000
65.000
70.000
75.000
80.000
85.000
90.000
95.000
100.000
105.000
rt

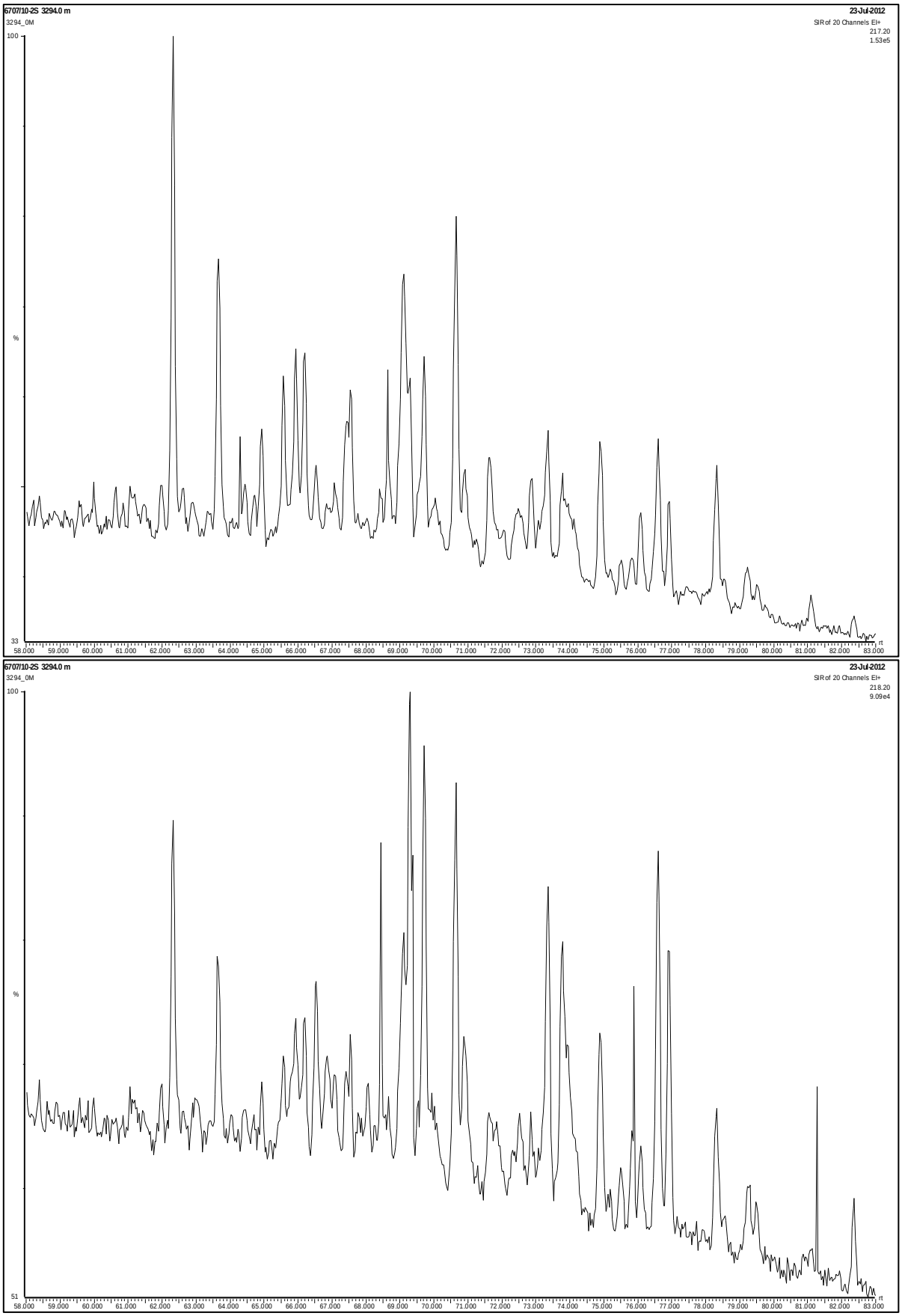
6707/10-2S 3294.0 m
3294_0M
23-Jul-2012
SIR of 20 Channels EI+
217.20
1.53e5
100
%
33
58.000 59.000 60.000 61.000 62.000 63.000 64.000 65.000 66.000 67.000 68.000 69.000 70.000 71.000 72.000 73.000 74.000 75.000 76.000 77.000 78.000 79.000 80.000 81.000 82.000 83.000
rt
6707/10-2S 3294.0 m
3294_0M
23-Jul-2012
SIR of 20 Channels EI+
218.20
9.09e4
100
%
51
58.000 59.000 60.000 61.000 62.000 63.000 64.000 65.000 66.000 67.000 68.000 69.000 70.000 71.000 72.000 73.000 74.000 75.000 76.000 77.000 78.000 79.000 80.000 81.000 82.000 83.000
rt

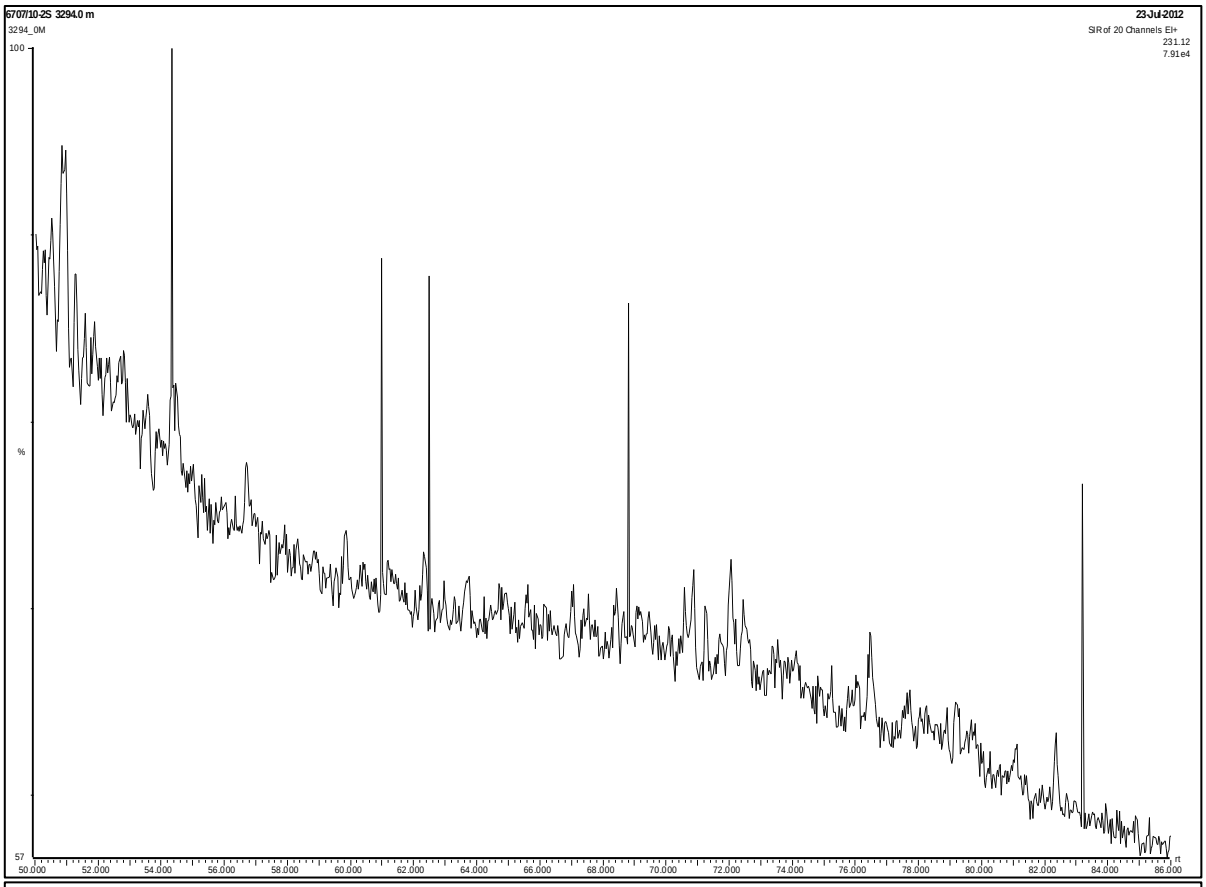
6707/10-2S 3294.0 m
3294_0M
23-Jul-2012
SIR of 20 Channels EI+
231.12
7.91e4
100
%
57
50.000 52.000 54.000 56.000 58.000 60.000 62.000 64.000 66.000 68.000 70.000 72.000 74.000 76.000 78.000 80.000 82.000 84.000 86.000
rt

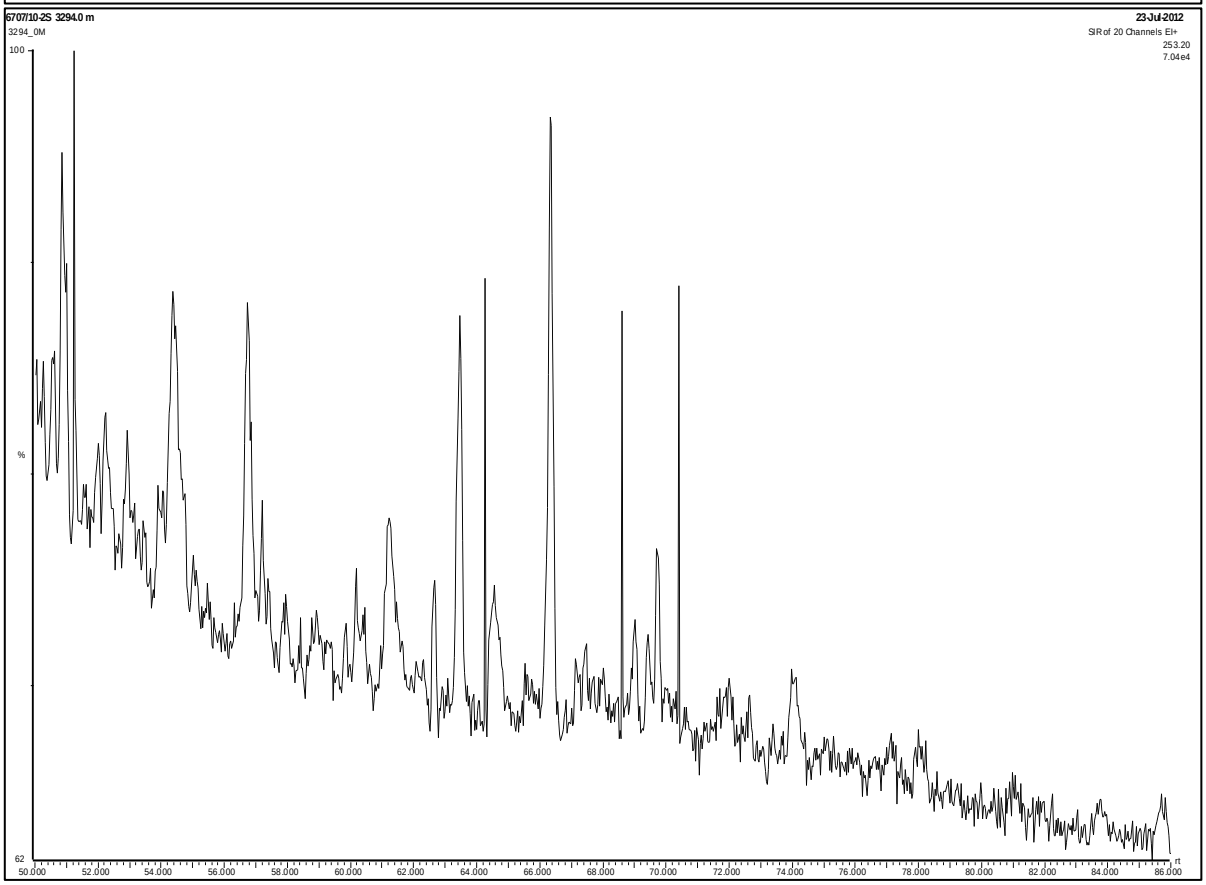
6707/10-2S 3294.0 m
3294_0M
23-Jul-2012
SIR of 20 Channels EI+
253.20
7.04e4
100
%
62
50.000 52.000 54.000 56.000 58.000 60.000 62.000 64.000 66.000 68.000 70.000 72.000 74.000 76.000 78.000 80.000 82.000 84.000 86.000
rt

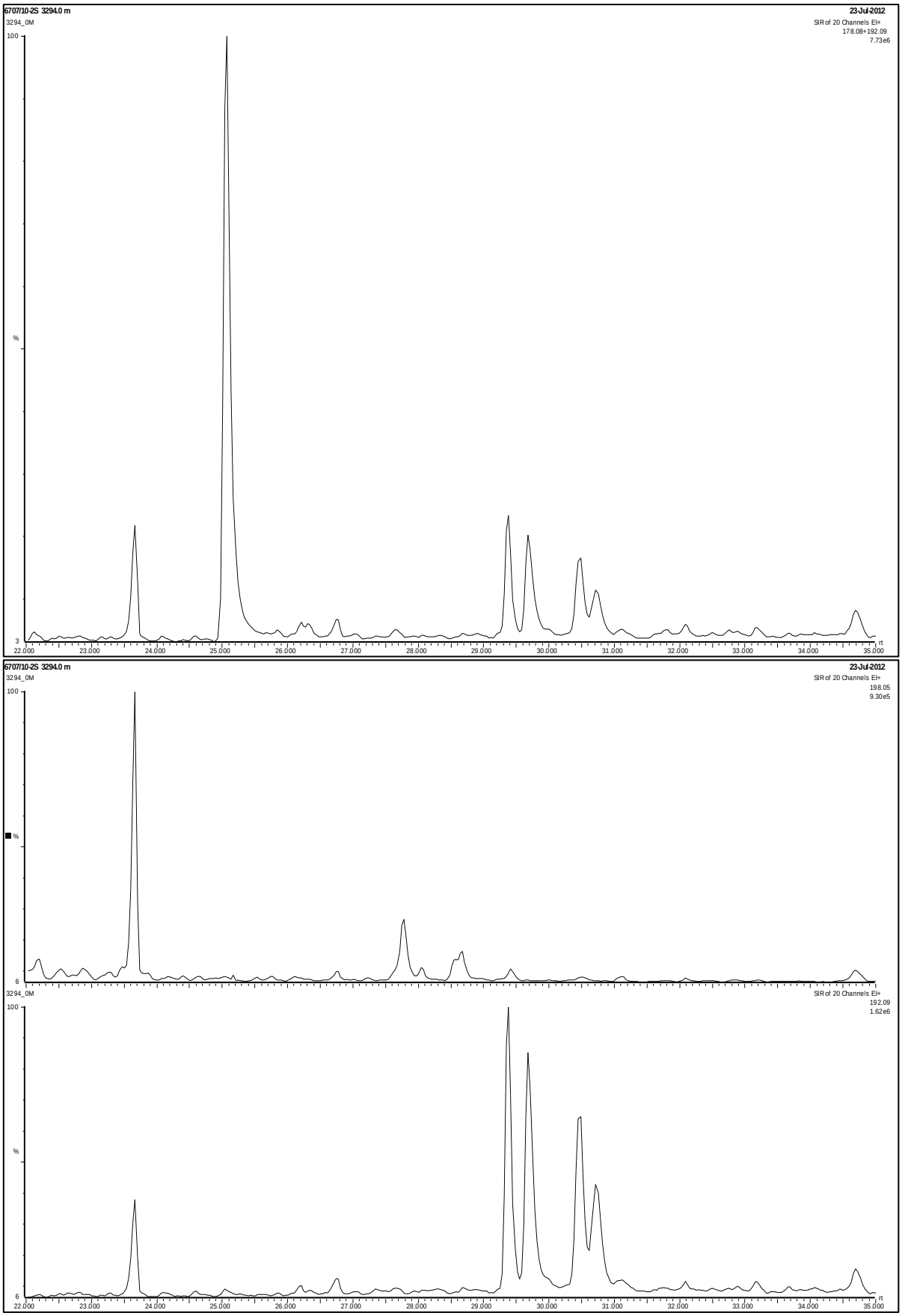
6707/10-2S 3294.0 m
23-Jul-2012
3294_0M
SIR of 20 Channels EI+
178.08+192.09
7.73e6
100
%
3
22.000
23.000
24.000
25.000
26.000
27.000
28.000
29.000
30.000
31.000
32.000
33.000
34.000
35.000
rt
6707/10-2S 3294.0 m
23-Jul-2012
3294_0M
SIR of 20 Channels EI+
198.05
9.30e5
100
%
6
3294_0M
SIR of 20 Channels EI+
192.09
1.62e6
100
%
6
22.000
23.000
24.000
25.000
26.000
27.000
28.000
29.000
30.000
31.000
32.000
33.000
34.000
35.000
rt

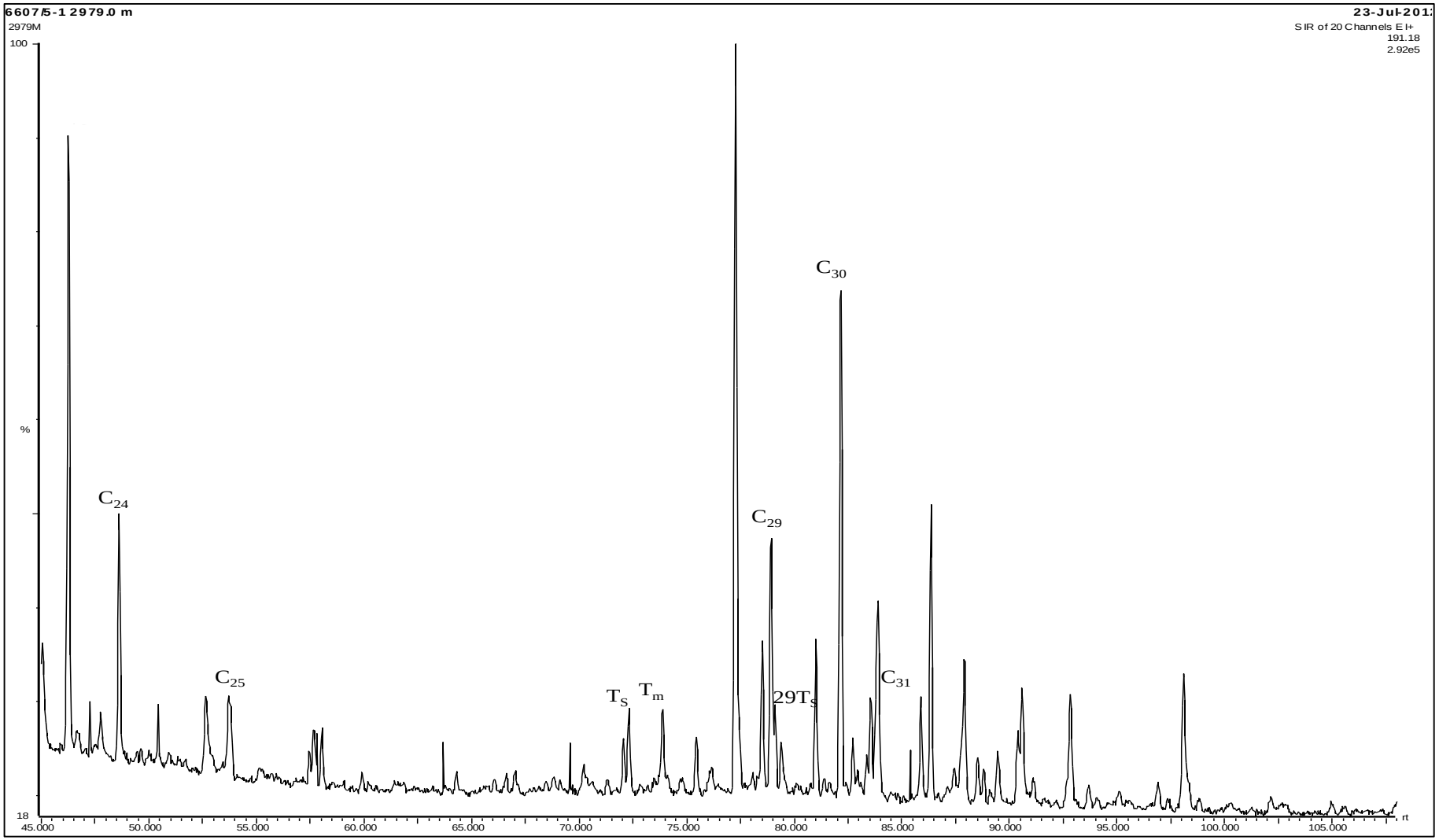
66075-1 2979.0 m
2979M
23-Jul-201
SIR of 20 Channels EI+
191.18
2.92e5
100
%
18
C24
C25
Ts
Tm
C29
29Ts
C30
C31
45.000
50.000
55.000
60.000
65.000
70.000
75.000
80.000
85.000
90.000
95.000
100.000
105.000
rt

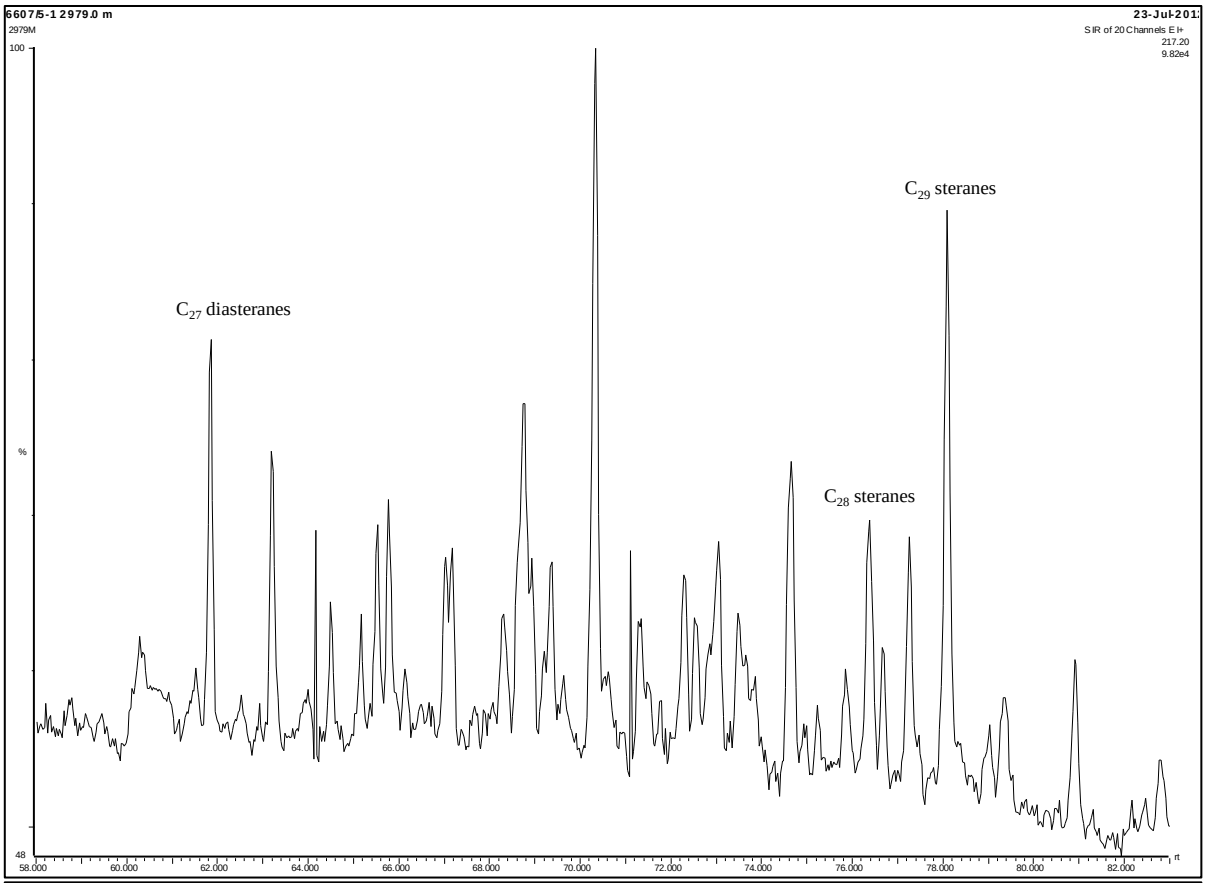
6607/5-1 2979.0 m
2979M
23-Jul-201
SIR of 20 Channels EI+
217.20
9.82e4
100
%
48
C27 diasteranes
C29 steranes
C28 steranes
58.000
60.000
62.000
64.000
66.000
68.000
70.000
72.000
74.000
76.000
78.000
80.000
82.000
rt

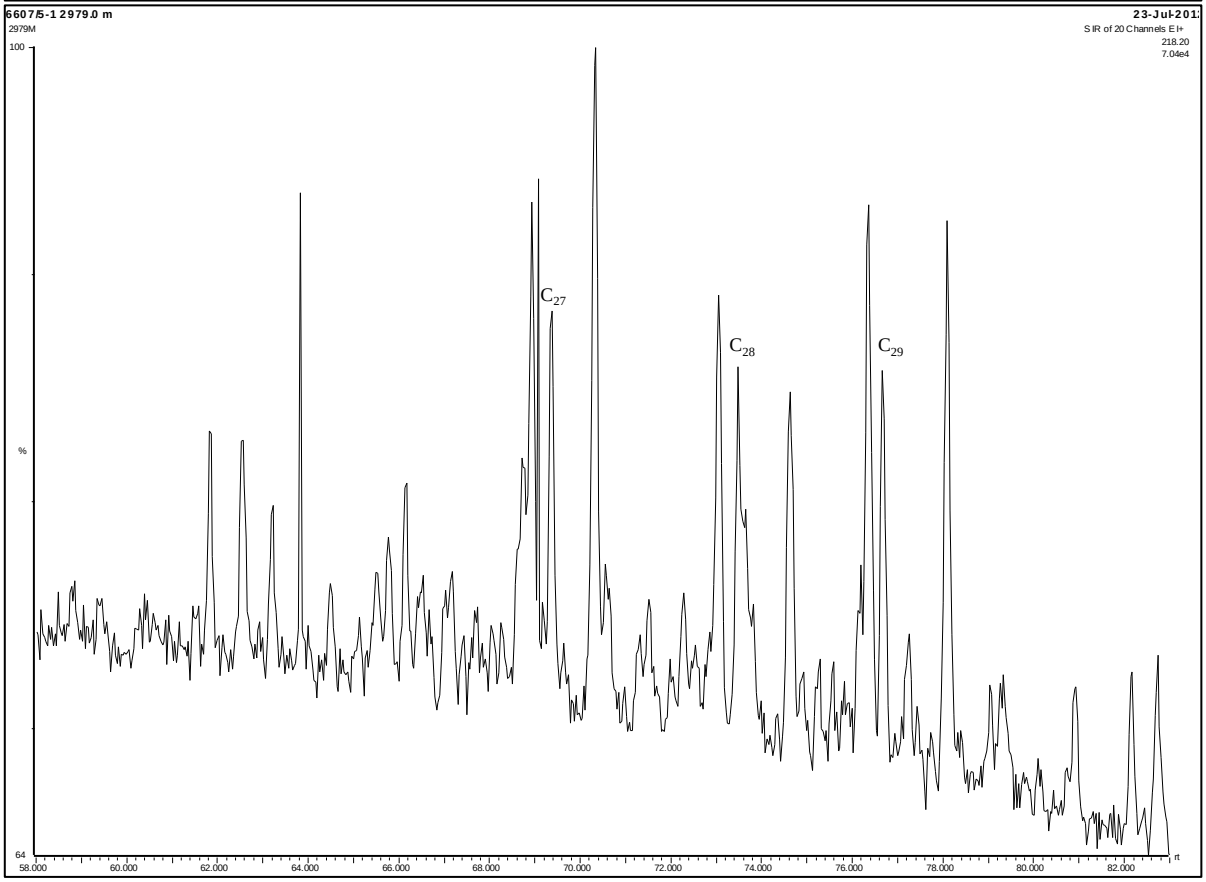
6607/5-1 2979.0 m
2979M
23-Jul-201
SIR of 20 Channels EI+
218.20
7.04e4
100
%
64
C27
C28
C29
58.000
60.000
62.000
64.000
66.000
68.000
70.000
72.000
74.000
76.000
78.000
80.000
82.000
rt

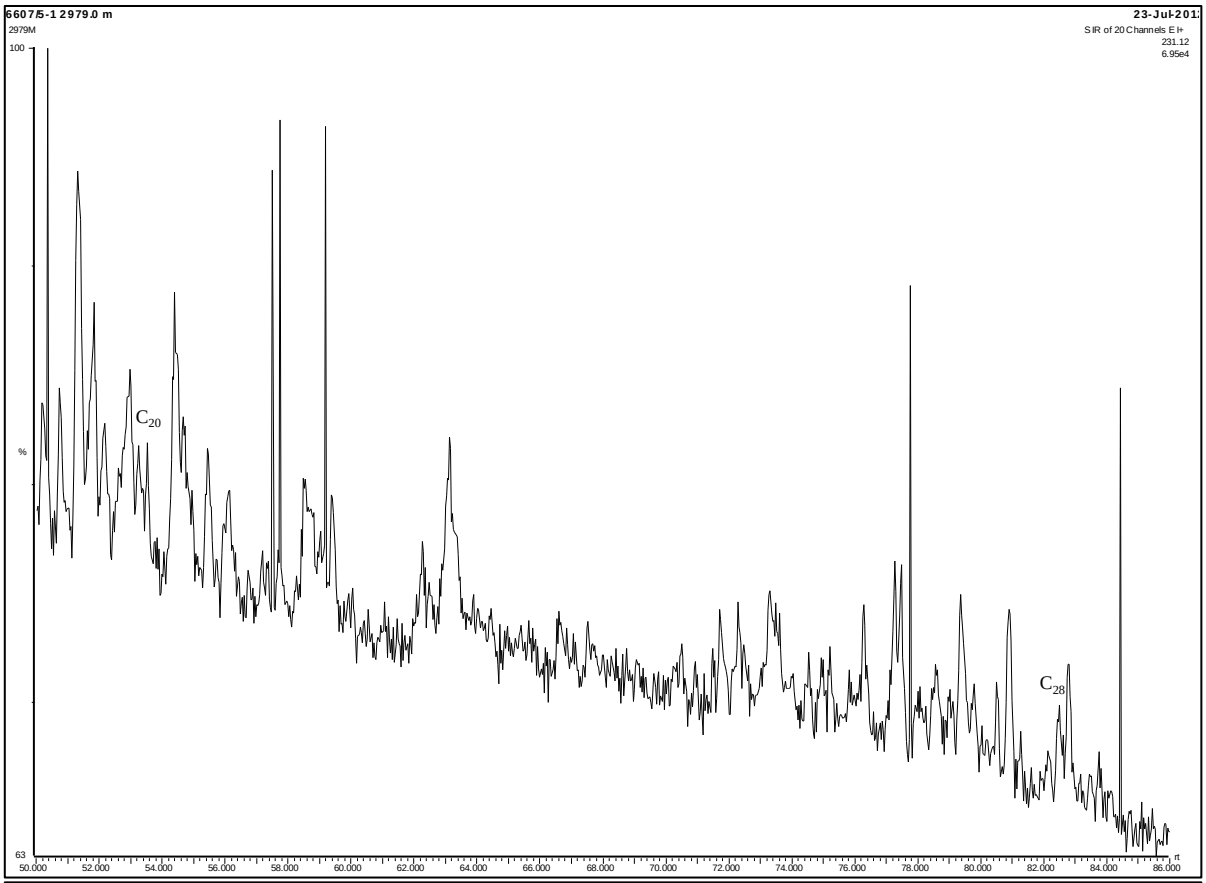
6607/5-1 2979.0 m
2979M
23-Jul-201
SIR of 20 Channels EI+
231.12
6.95e4
100
%
63
C20
C28
50.000 52.000 54.000 56.000 58.000 60.000 62.000 64.000 66.000 68.000 70.000 72.000 74.000 76.000 78.000 80.000 82.000 84.000 86.000
rt

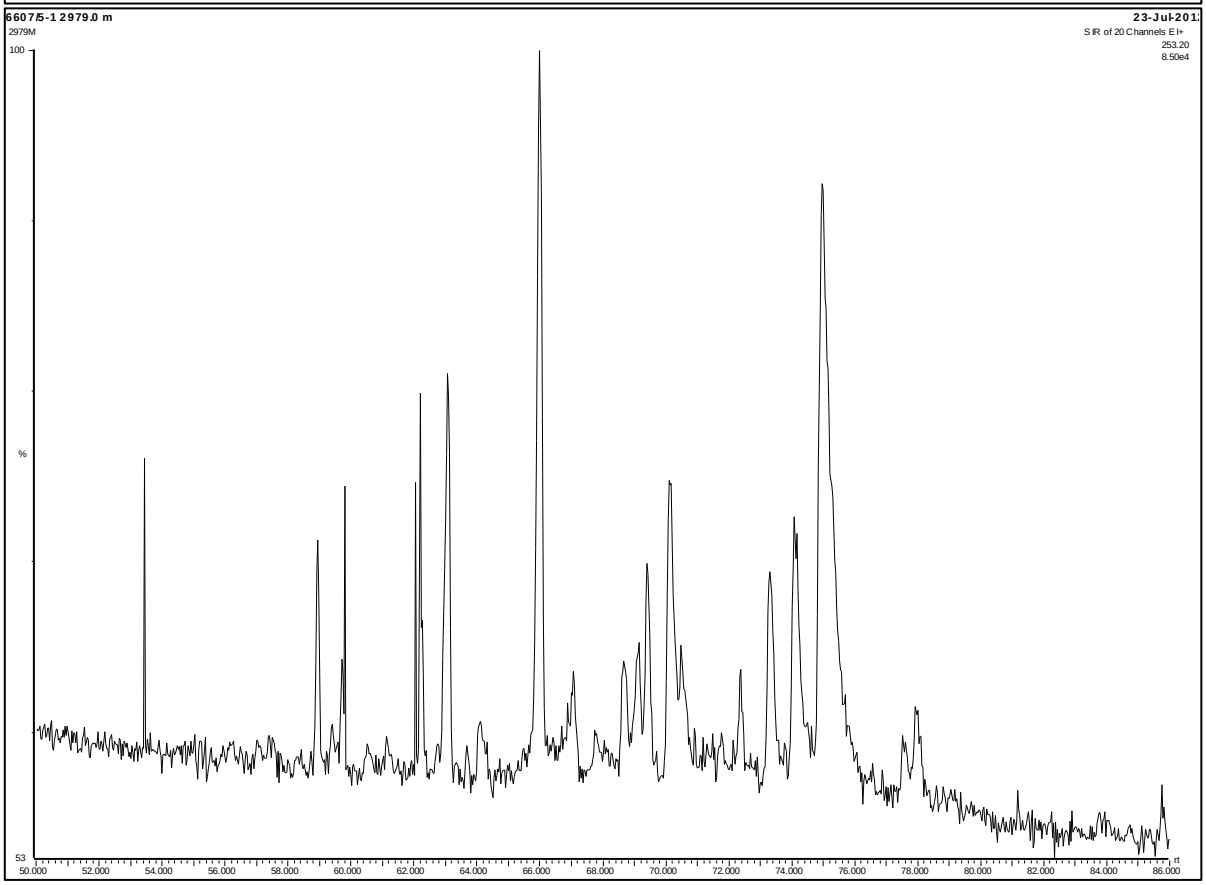
6607/5-1 2979.0 m
2979M
23-Jul-201
SIR of 20 Channels EI+
253.20
8.50e4
100
%
53
50.000 52.000 54.000 56.000 58.000 60.000 62.000 64.000 66.000 68.000 70.000 72.000 74.000 76.000 78.000 80.000 82.000 84.000 86.000
rt

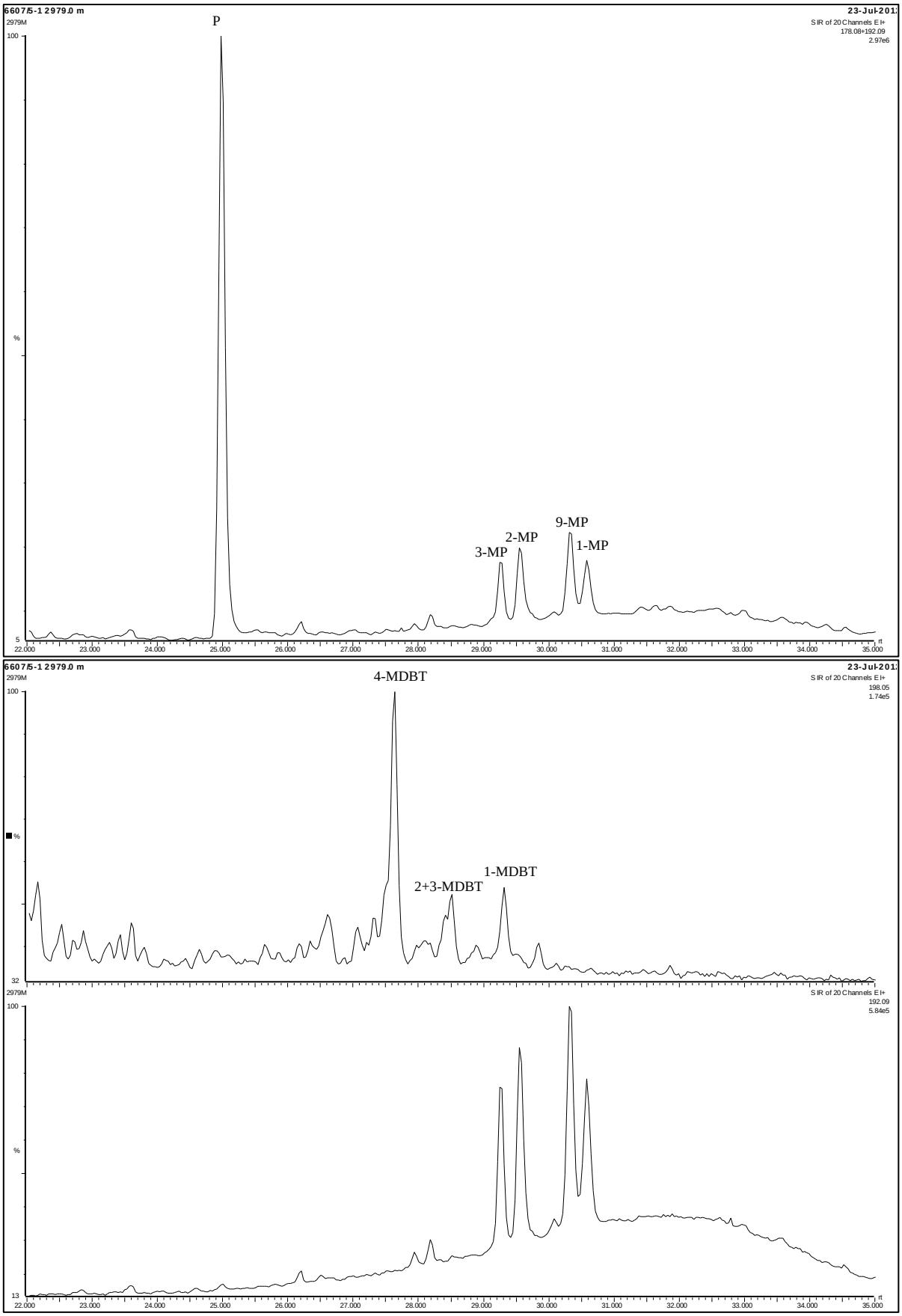
6607/5-1 2979.0 m
2979M
23-Jul-201
SIR of 20 Channels EI+
178.08+192.09
2.97e6
P
3-MP
2-MP
9-MP
1-MP
%
100
5
22.000
23.000
24.000
25.000
26.000
27.000
28.000
29.000
30.000
31.000
32.000
33.000
34.000
35.000
rt
6607/5-1 2979.0 m
2979M
23-Jul-201
SIR of 20 Channels EI+
198.05
1.74e5
4-MDBT
2+3-MDBT
1-MDBT
100
32
2979M
SIR of 20 Channels EI+
192.09
5.84e5
100
13

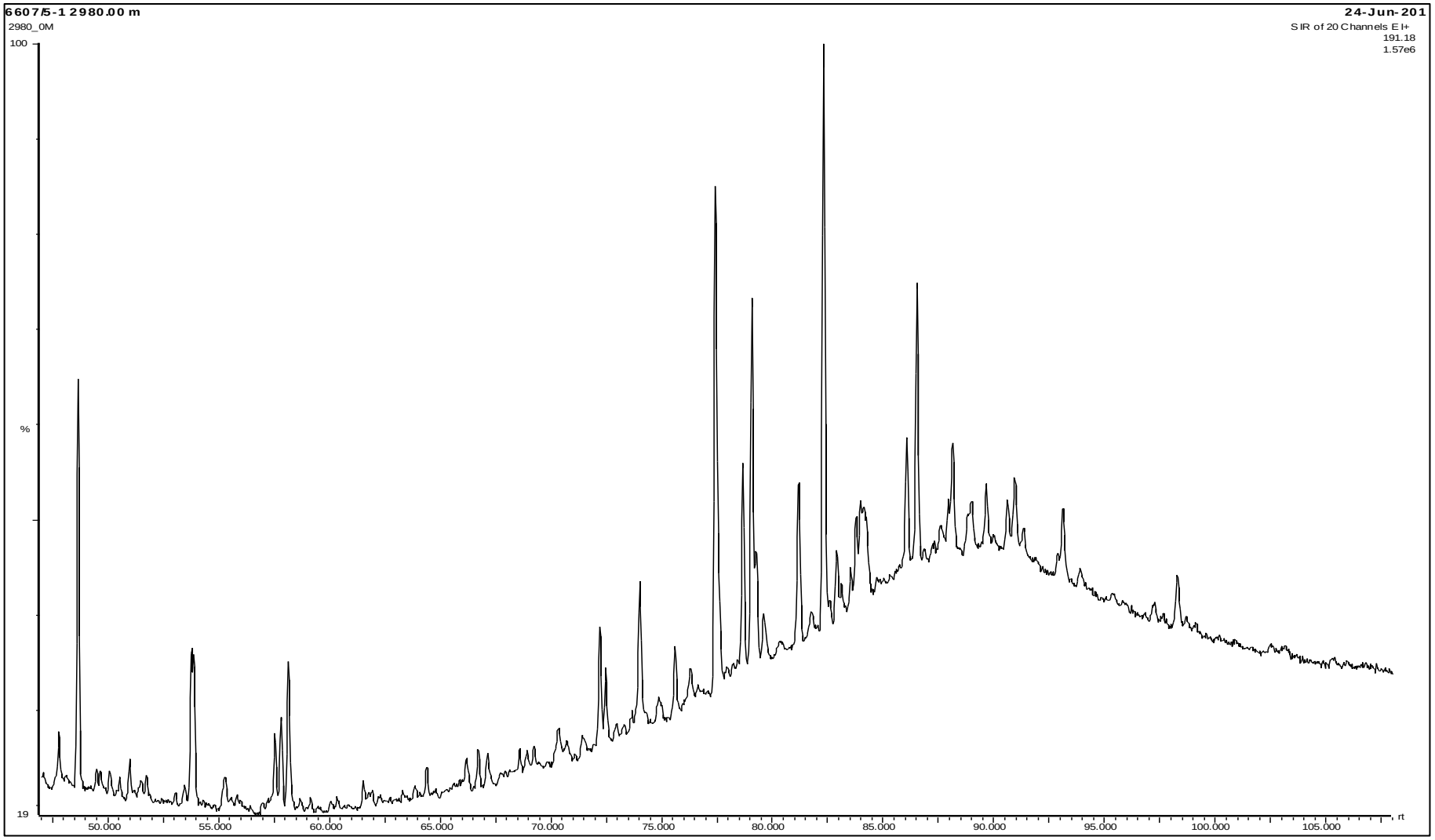
66075-1 2980.00 m
2980_0M
24-Jun-201
SIR of 20 Channels EI+
191.18
1.57e6
100
%
19
50.000
55.000
60.000
65.000
70.000
75.000
80.000
85.000
90.000
95.000
100.000
105.000
rt

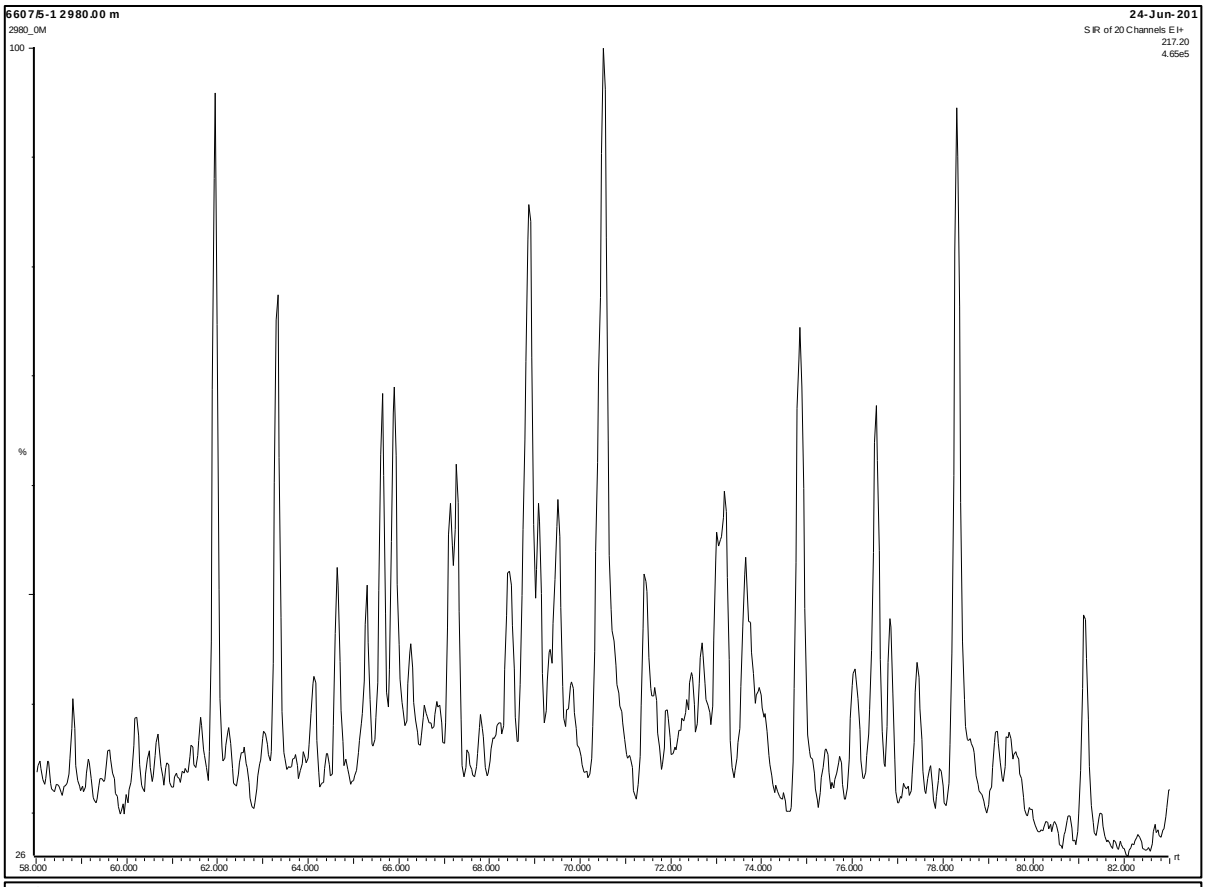
66075-1 2980.00 m
24-Jun-201
2980_0M
SIR of 20 Channels EI+
217.20
4.65e5
100
%
26
58.000
60.000
62.000
64.000
66.000
68.000
70.000
72.000
74.000
76.000
78.000
80.000
82.000
rt

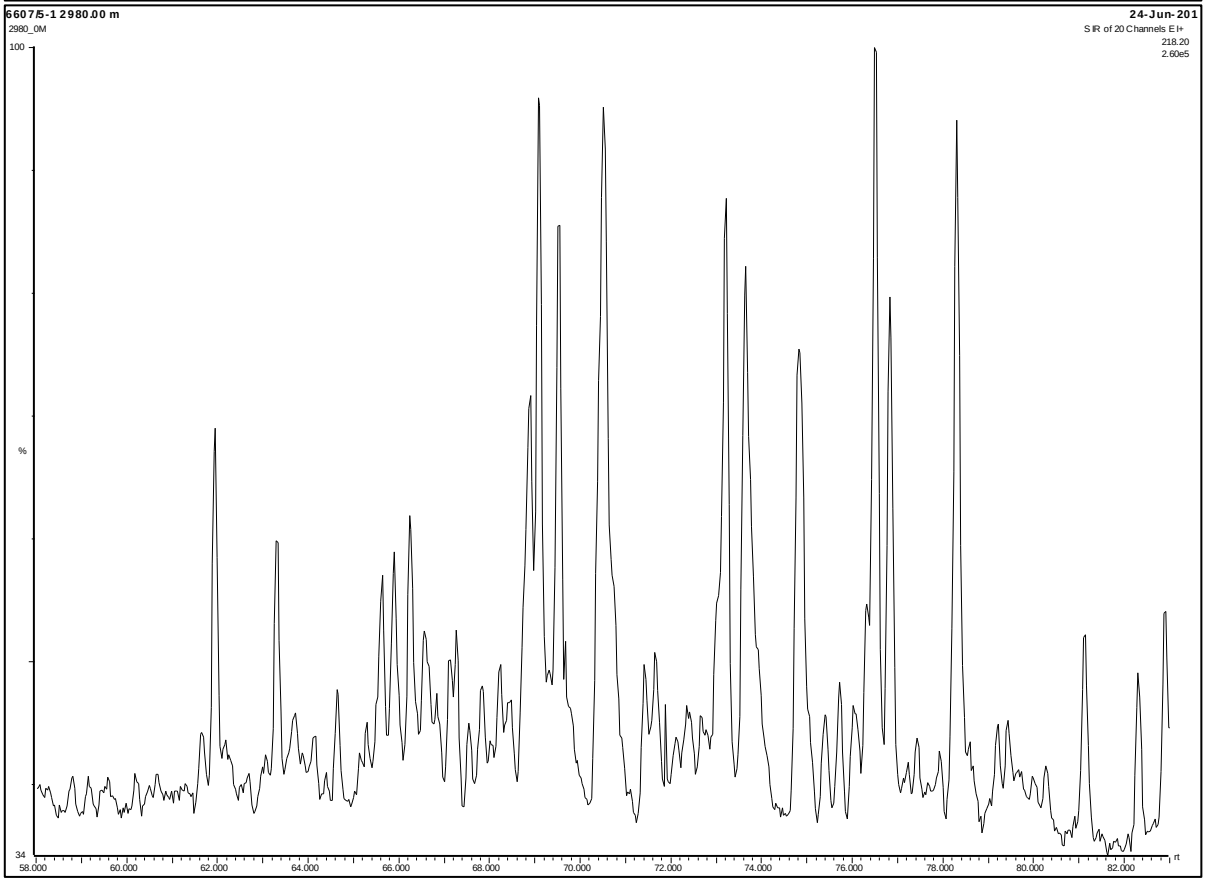
66075-1 2980.00 m
24-Jun-201
2980_0M
SIR of 20 Channels EI+
218.20
2.60e5
100
%
34
58.000
60.000
62.000
64.000
66.000
68.000
70.000
72.000
74.000
76.000
78.000
80.000
82.000
rt

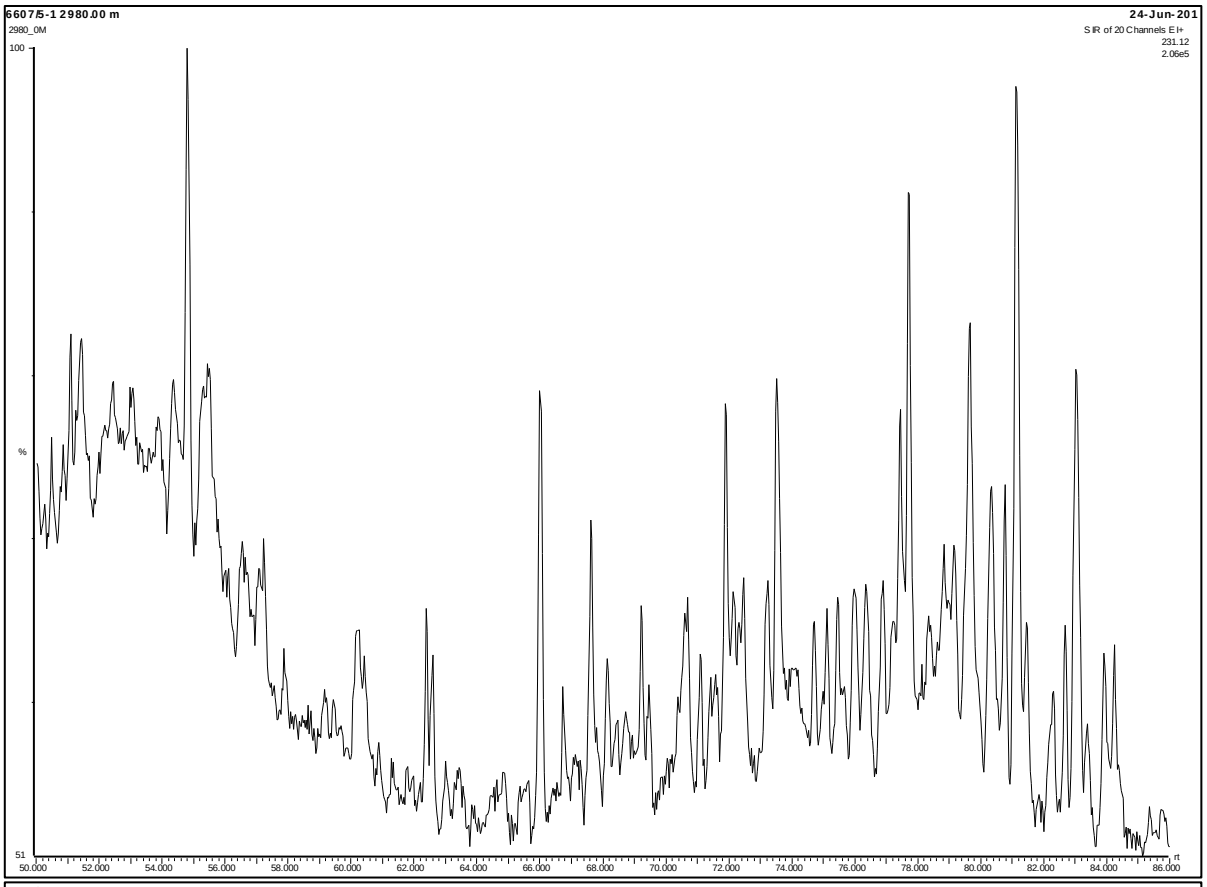
6607/5-1 2980.00 m
24-Jun-201
2980_0M
SIR of 20 Channels EI+
231.12
2.06e5
100
%
51
50.000 52.000 54.000 56.000 58.000 60.000 62.000 64.000 66.000 68.000 70.000 72.000 74.000 76.000 78.000 80.000 82.000 84.000 86.000
rt

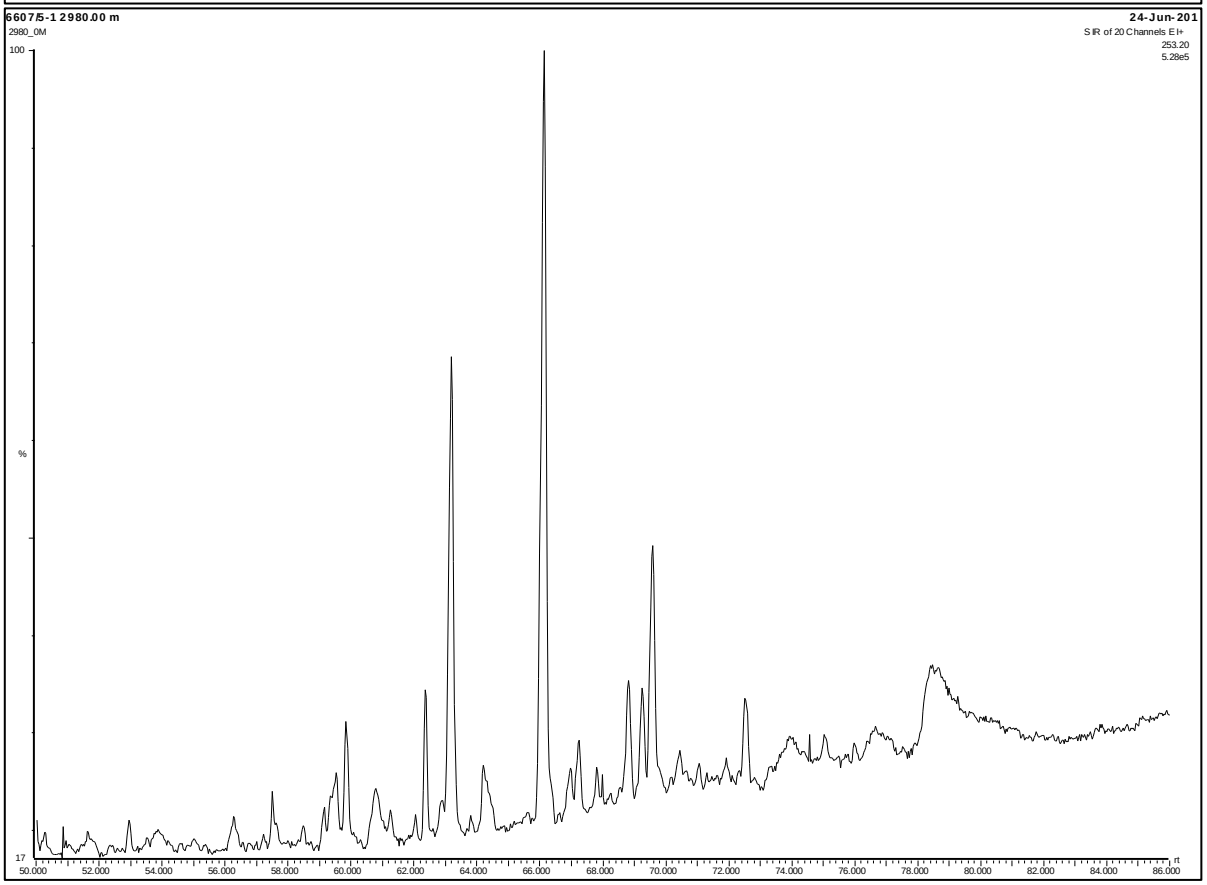
6607/5-1 2980.00 m
24-Jun-201
2980_0M
SIR of 20 Channels EI+
253.20
5.28e5
100
%
17
50.000 52.000 54.000 56.000 58.000 60.000 62.000 64.000 66.000 68.000 70.000 72.000 74.000 76.000 78.000 80.000 82.000 84.000 86.000
rt

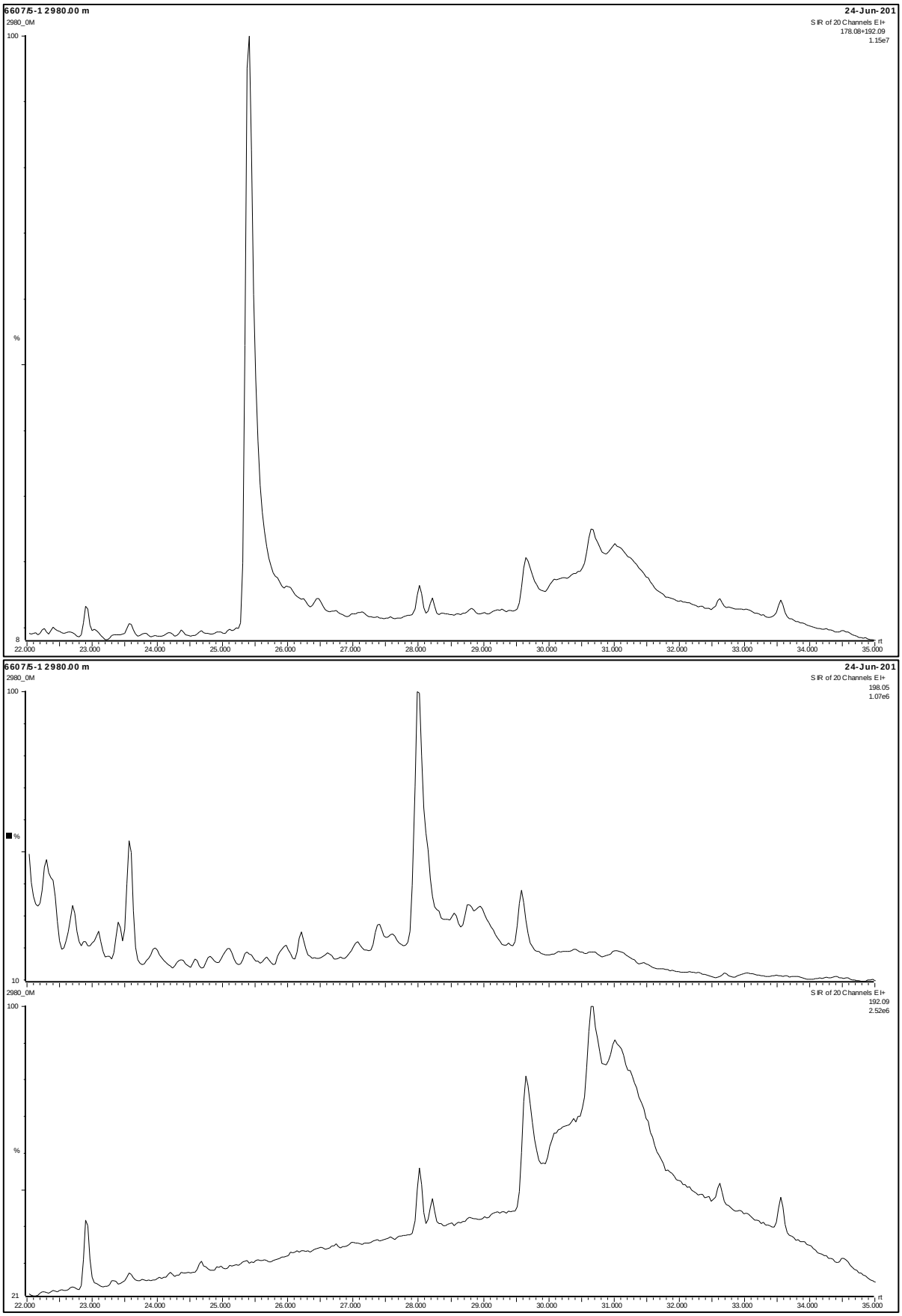
6607/5-1 2980.00 m
24-Jun-201
2980_0M
SIR of 20 Channels EI+
178.08+192.09
1.15e7
100
%
8
22.000
23.000
24.000
25.000
26.000
27.000
28.000
29.000
30.000
31.000
32.000
33.000
34.000
35.000
rt
6607/5-1 2980.00 m
24-Jun-201
2980_0M
SIR of 20 Channels EI+
198.05
1.07e6
100
%
10
2980_0M
SIR of 20 Channels EI+
192.09
2.52e6
100
%
21
22.000
23.000
24.000
25.000
26.000
27.000
28.000
29.000
30.000
31.000
32.000
33.000
34.000
35.000
rt

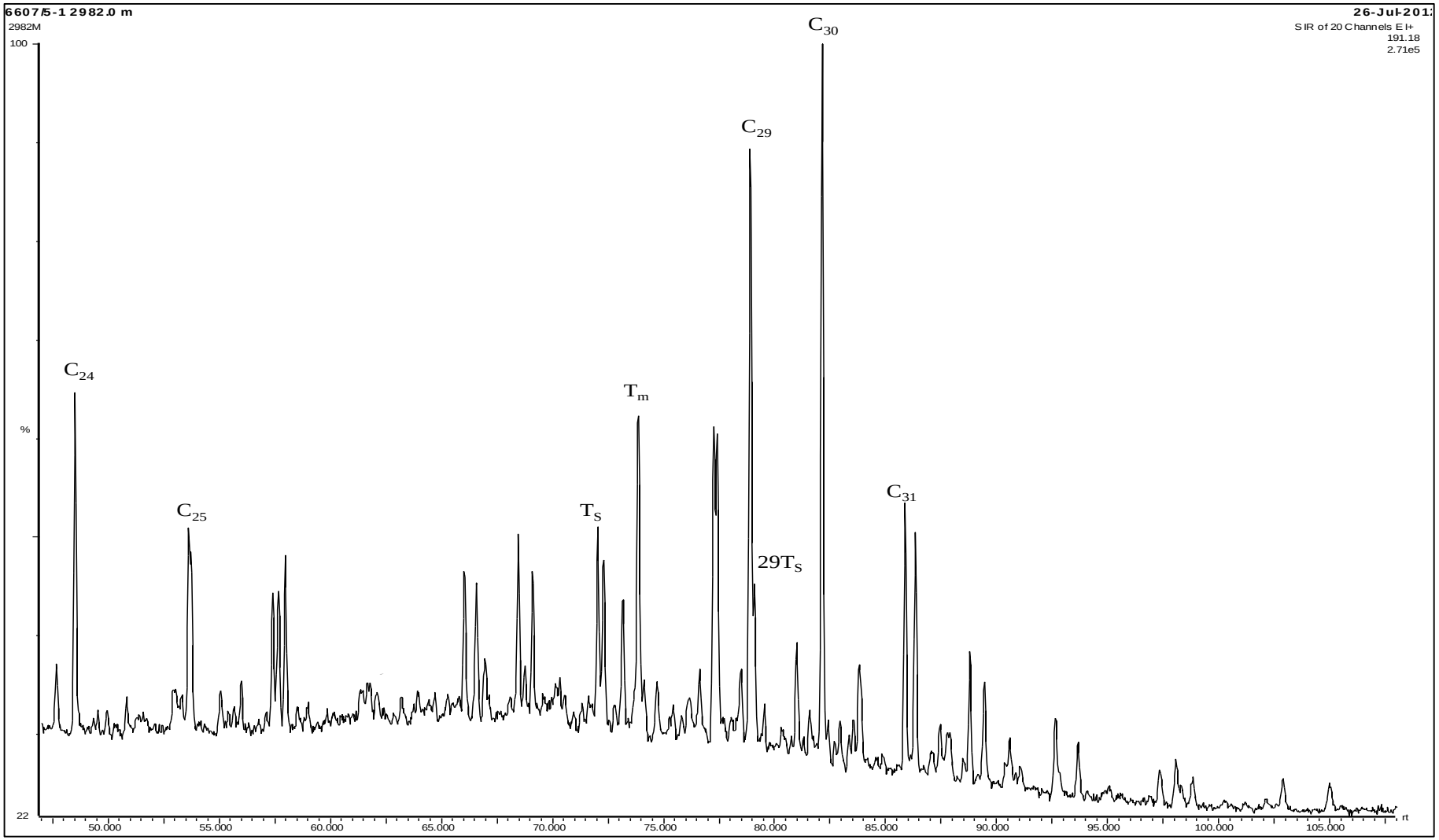
66075-12982.0 m
2982M
26-Jul-201
SIR of 20 Channels EI+
191.18
2.71e5
100
%
22
C24
C25
TS
Tm
C29
29TS
C30
C31
50.000
55.000
60.000
65.000
70.000
75.000
80.000
85.000
90.000
95.000
100.000
105.000
rt

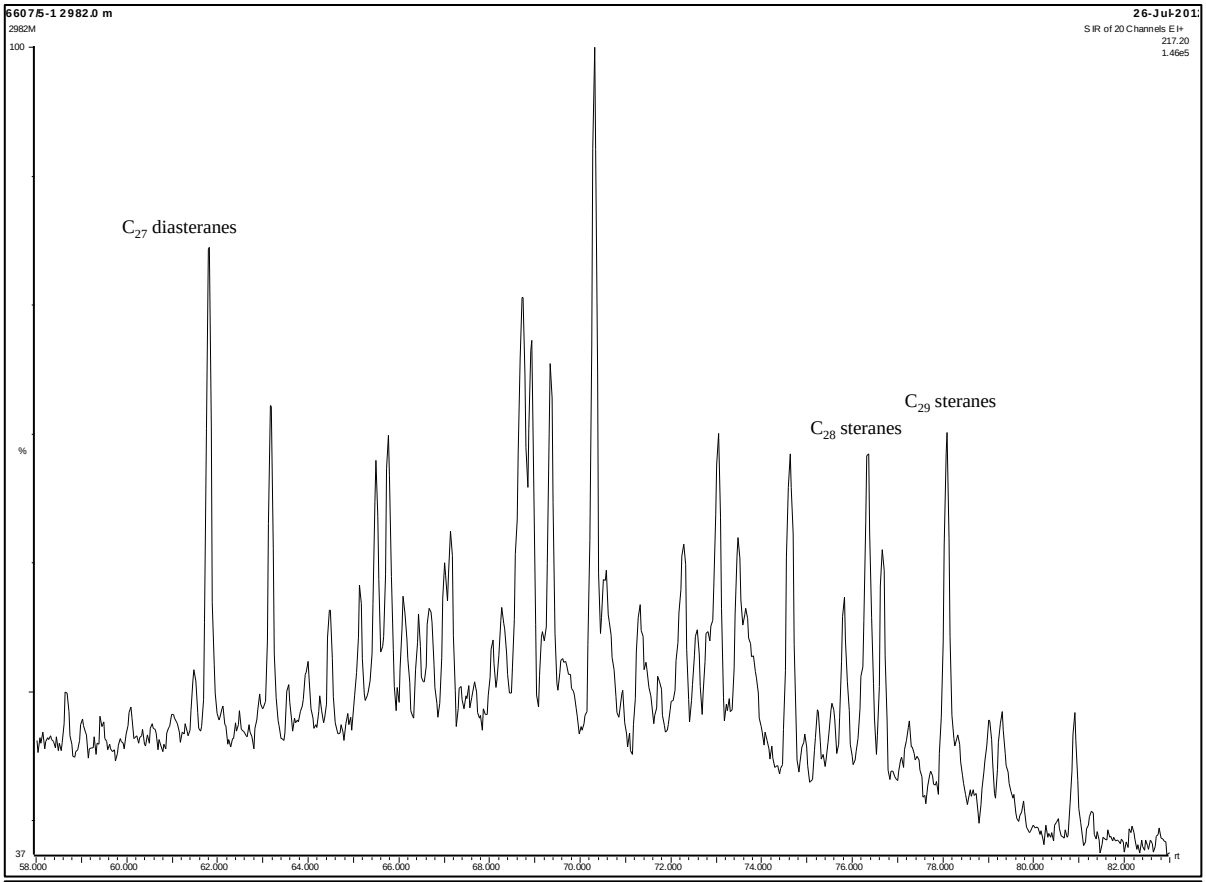
6607/5-1 2982.0 m
26-Jul-201
2982M
SIR of 20 Channels EI+
217.20
1.46e5
100
%
37
C27 diasteranes
C28 steranes
C29 steranes
58.000
60.000
62.000
64.000
66.000
68.000
70.000
72.000
74.000
76.000
78.000
80.000
82.000
rt

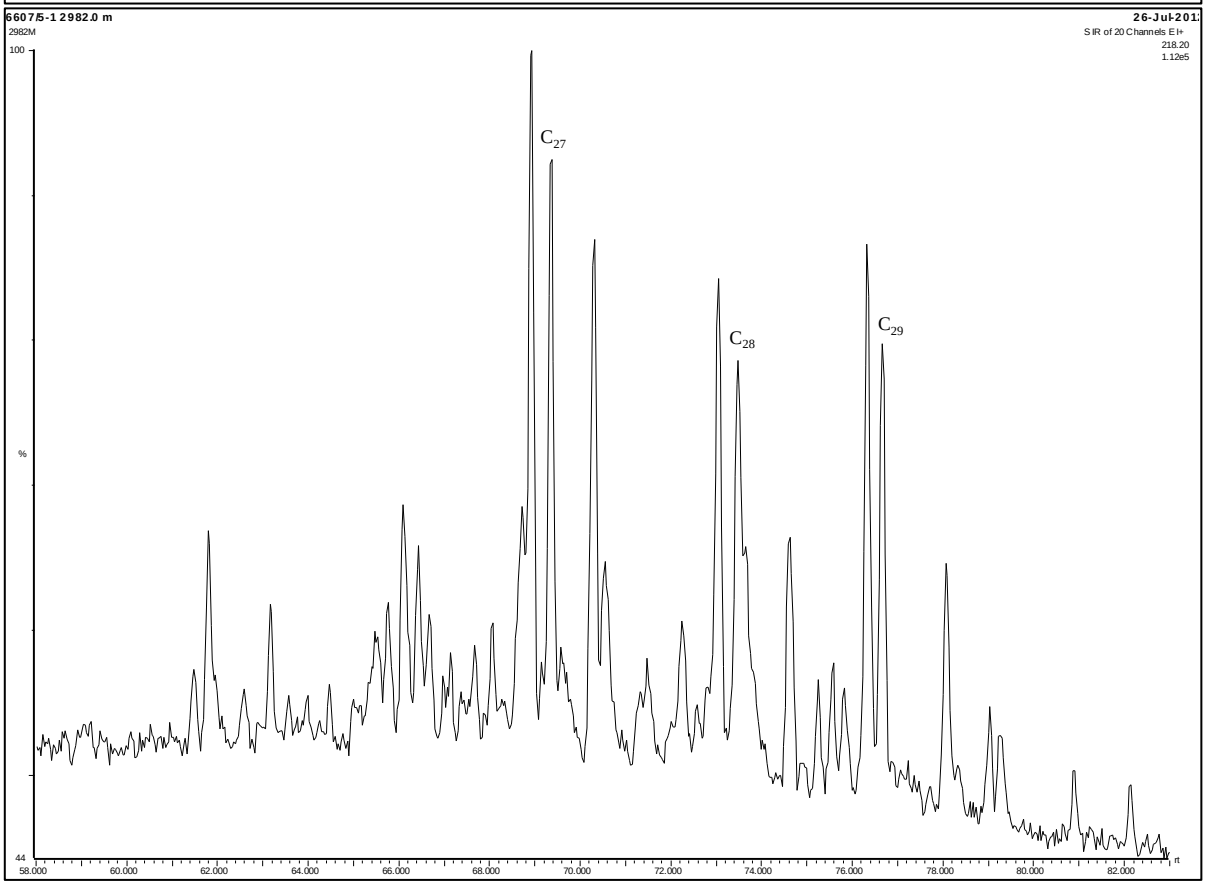
6607/5-1 2982.0 m
26-Jul-201
2982M
SIR of 20 Channels EI+
218.20
1.12e5
100
%
44
C27
C28
C29
58.000
60.000
62.000
64.000
66.000
68.000
70.000
72.000
74.000
76.000
78.000
80.000
82.000
rt

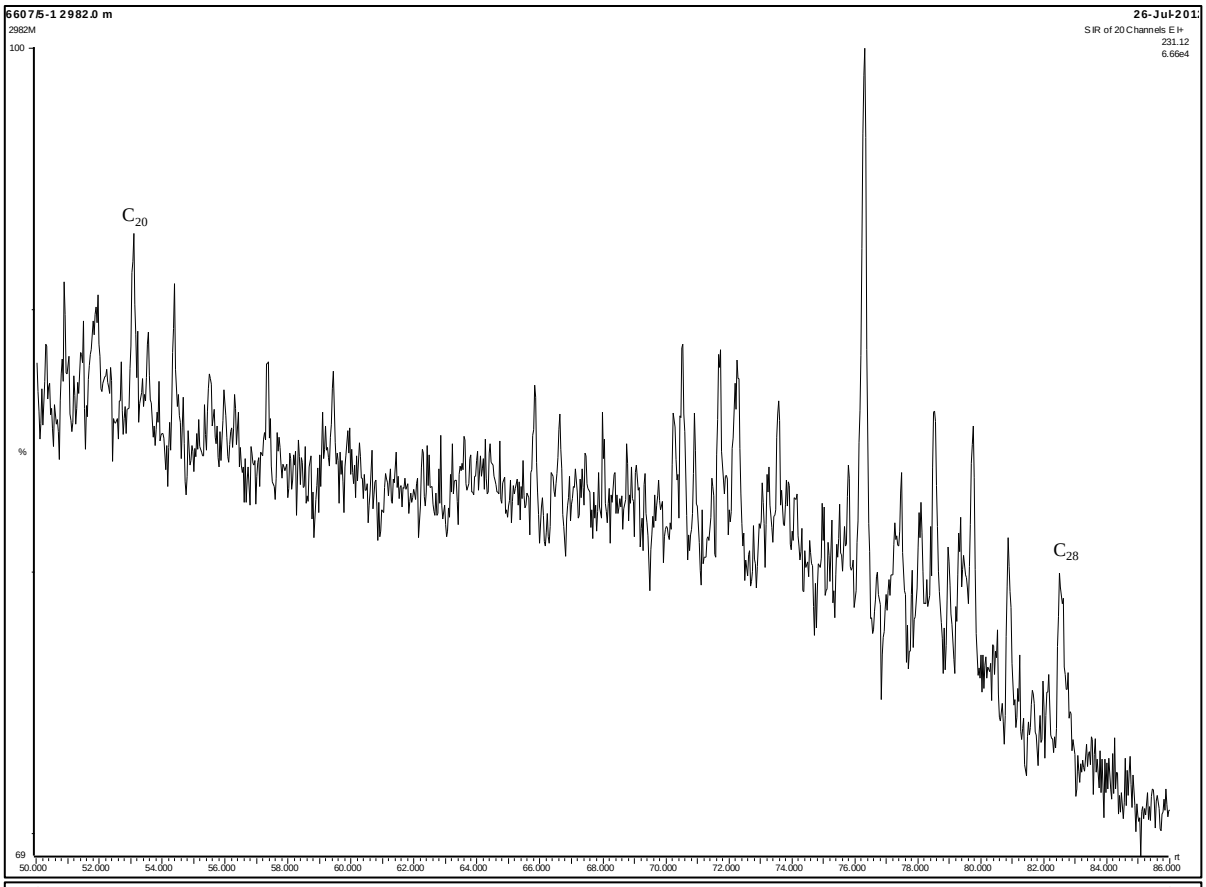
6607/5-1 2982.0 m
26-Jul-201
2982M
SIR of 20 Channels EI+
231.12
6.66e4
100
%
69
C20
C28
50.000 52.000 54.000 56.000 58.000 60.000 62.000 64.000 66.000 68.000 70.000 72.000 74.000 76.000 78.000 80.000 82.000 84.000 86.000
rt

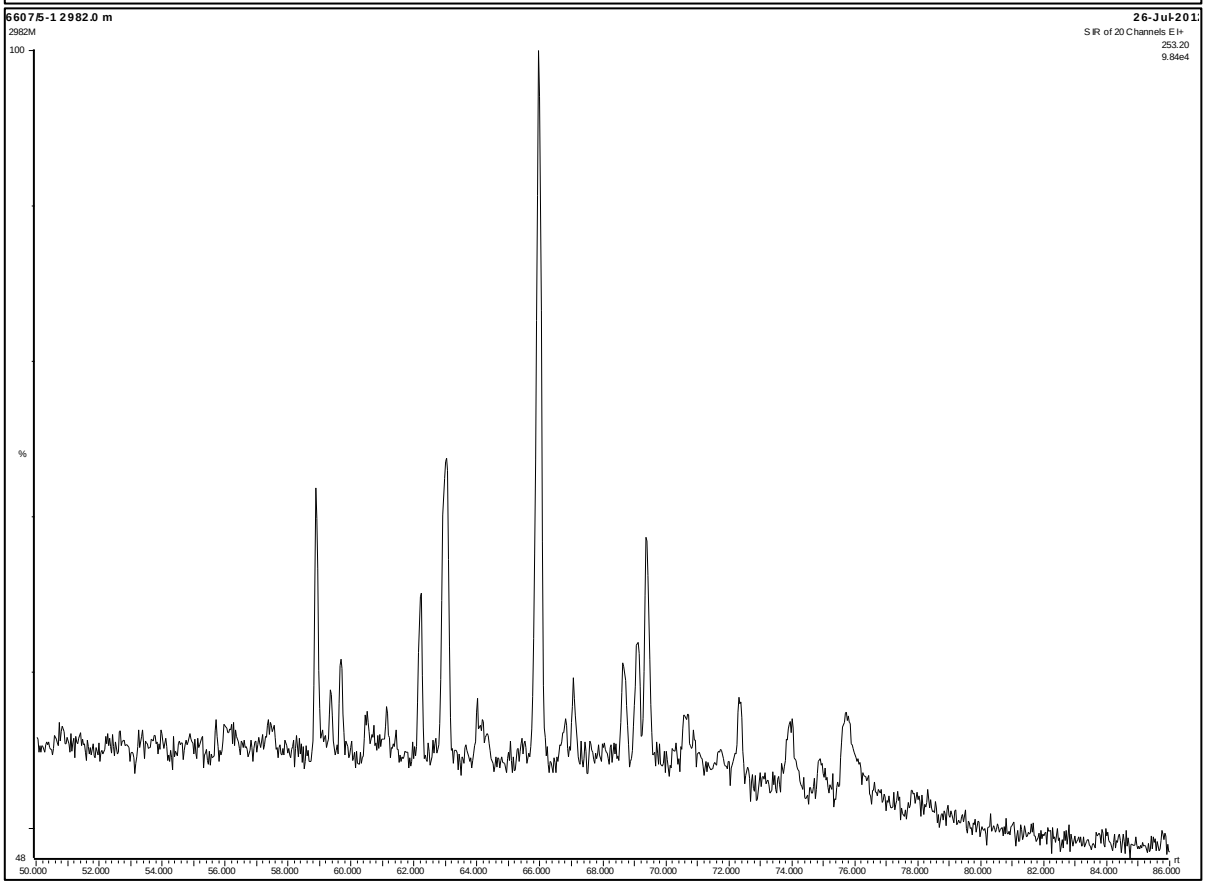
6607/5-1 2982.0 m
26-Jul-201
2982M
SIR of 20 Channels EI+
253.20
9.84e4
100
%
48
50.000 52.000 54.000 56.000 58.000 60.000 62.000 64.000 66.000 68.000 70.000 72.000 74.000 76.000 78.000 80.000 82.000 84.000 86.000
rt

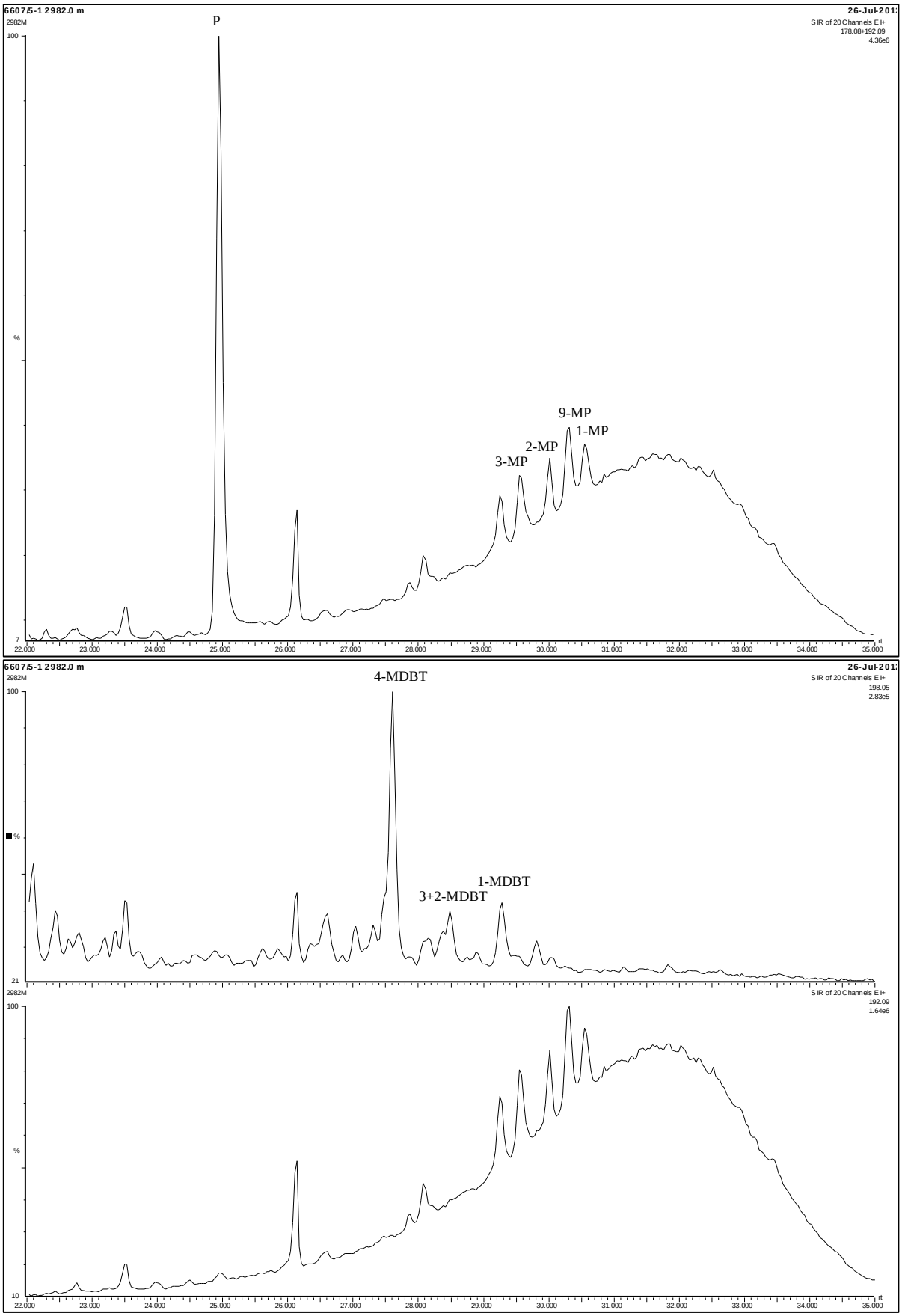
6607/5-1 2982.0 m
26-Jul-201
2982M
SIR of 20 Channels E I+
178.08+192.09
4.36e6
P
9-MP
1-MP
2-MP
3-MP
100
%
7
22.000
23.000
24.000
25.000
26.000
27.000
28.000
29.000
30.000
31.000
32.000
33.000
34.000
35.000
rt
6607/5-1 2982.0 m
26-Jul-201
2982M
SIR of 20 Channels E I+
198.05
2.83e5
4-MDBT
1-MDBT
3+2-MDBT
100
%
21
2982M
SIR of 20 Channels E I+
192.09
1.64e6
100
%
10
22.000
23.000
24.000
25.000
26.000
27.000
28.000
29.000
30.000
31.000
32.000
33.000
34.000
35.000
rt

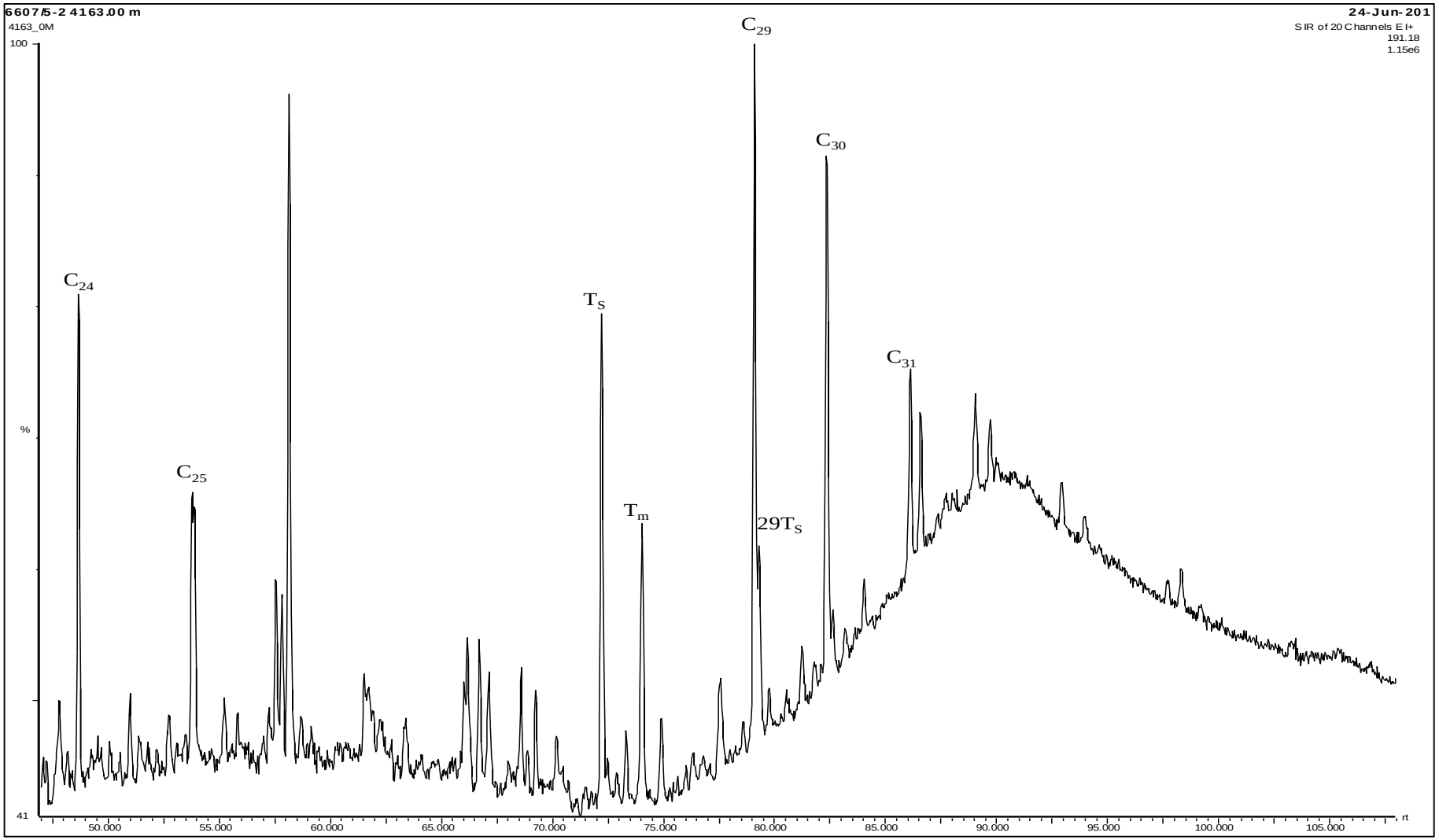
6607/5-2 4163.00 m
4163_0M
24-Jun-201
SIR of 20 Channels EI+
191.18
1.15e6
100
%
41
C24
C25
TS
Tm
29TS
C29
C30
C31
50.000
55.000
60.000
65.000
70.000
75.000
80.000
85.000
90.000
95.000
100.000
105.000
rt

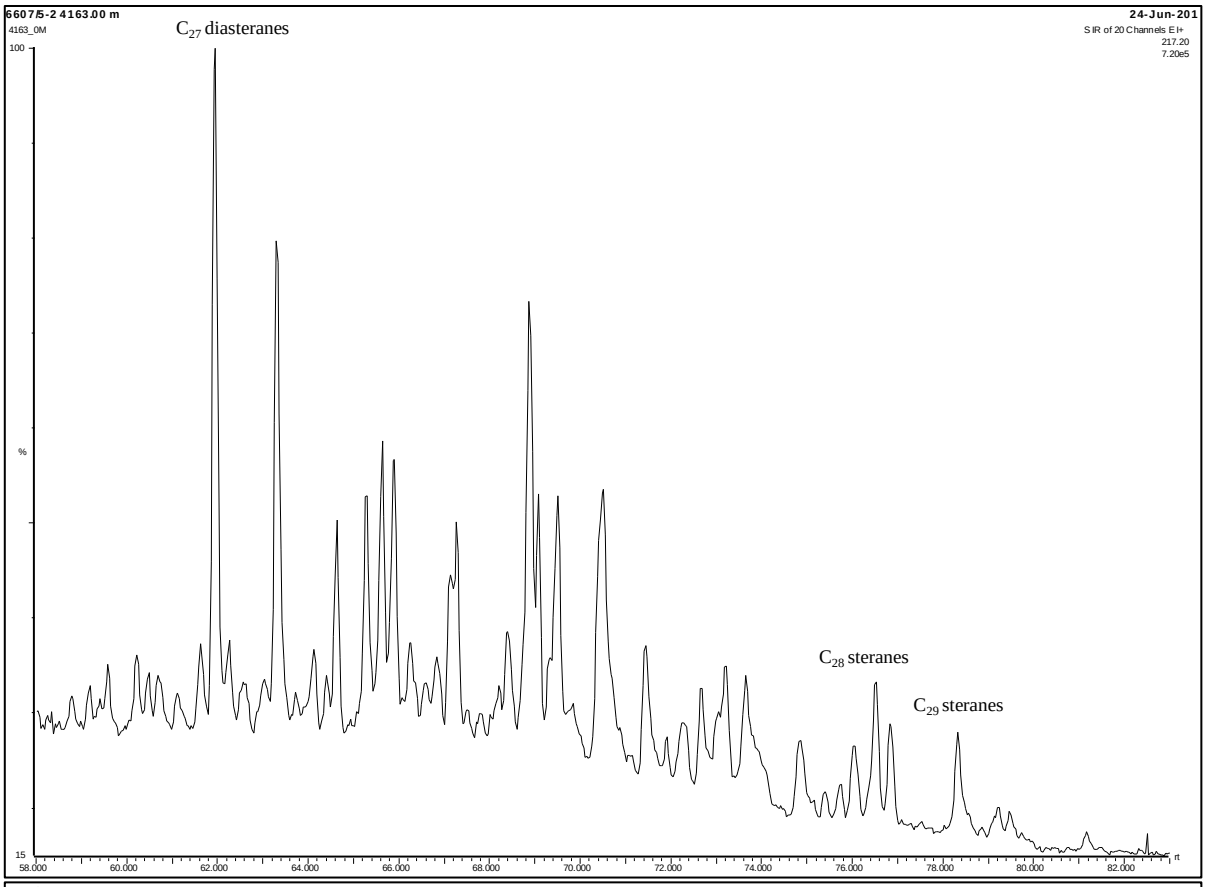
6607/5-2 4163.00 m
4163_0M
24-Jun-201
SIR of 20 Channels EI+
217.20
7.20e5
C27 diasteranes
C28 steranes
C29 steranes
100
%
15
58.000
60.000
62.000
64.000
66.000
68.000
70.000
72.000
74.000
76.000
78.000
80.000
82.000
rt

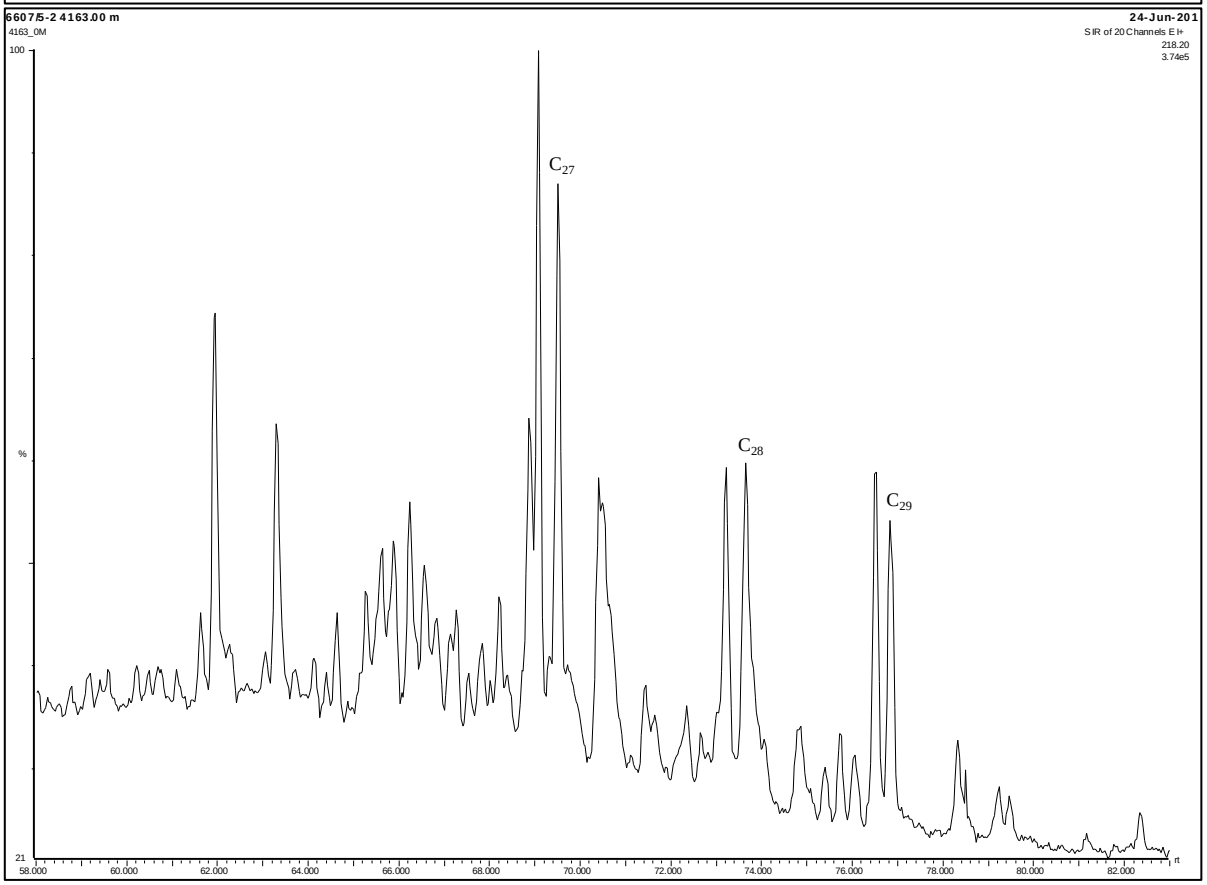
6607/5-2 4163.00 m
4163_0M
24-Jun-201
SIR of 20 Channels EI+
218.20
3.74e5
C27
C28
C29
100
%
21
58.000
60.000
62.000
64.000
66.000
68.000
70.000
72.000
74.000
76.000
78.000
80.000
82.000
rt

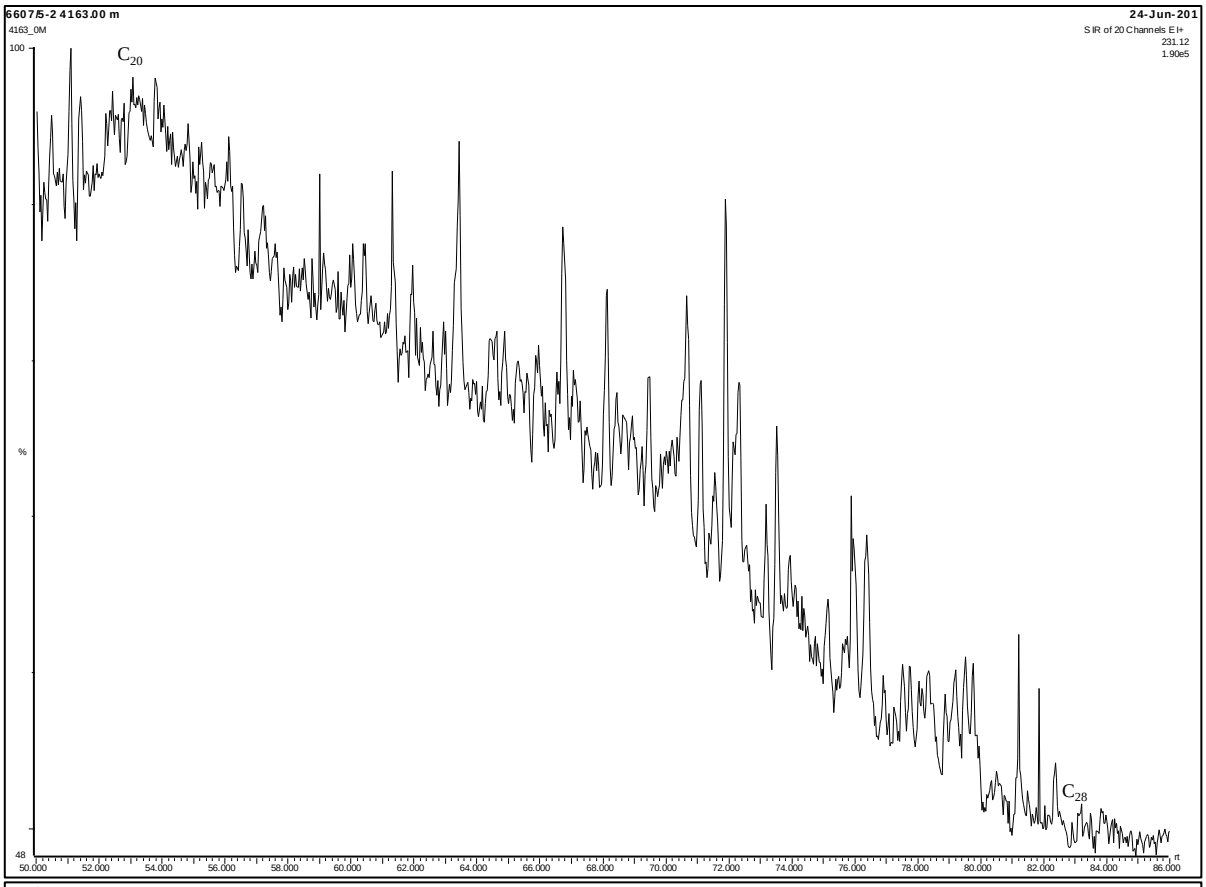
6607/5-2 4163.00 m
4163_0M
24-Jun-201
SIR of 20 Channels EI+
231.12
1.90e5
100
C20
%
C28
48
50.000 52.000 54.000 56.000 58.000 60.000 62.000 64.000 66.000 68.000 70.000 72.000 74.000 76.000 78.000 80.000 82.000 84.000 86.000
rt

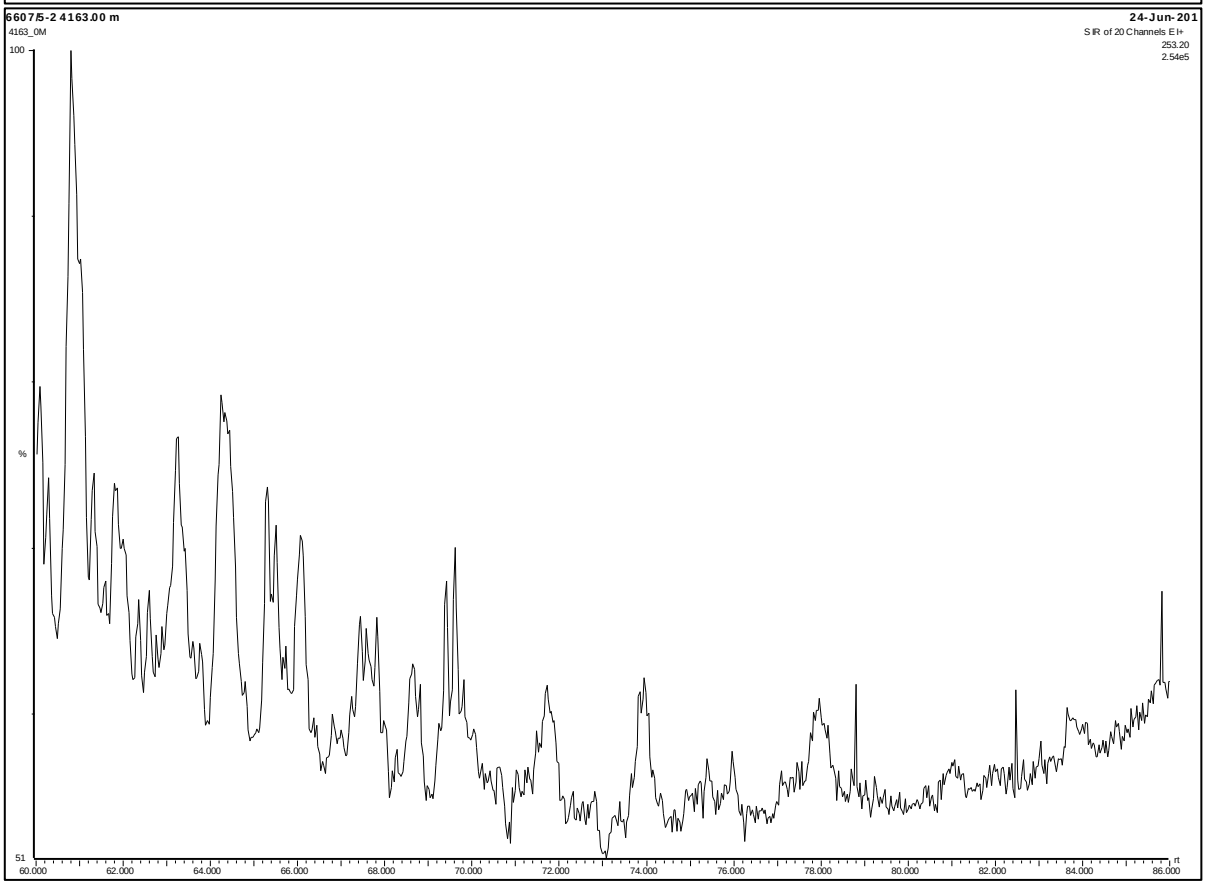
6607/5-2 4163.00 m
4163_0M
24-Jun-201
SIR of 20 Channels EI+
253.20
2.54e5
100
%
51
60.000 62.000 64.000 66.000 68.000 70.000 72.000 74.000 76.000 78.000 80.000 82.000 84.000 86.000
rt

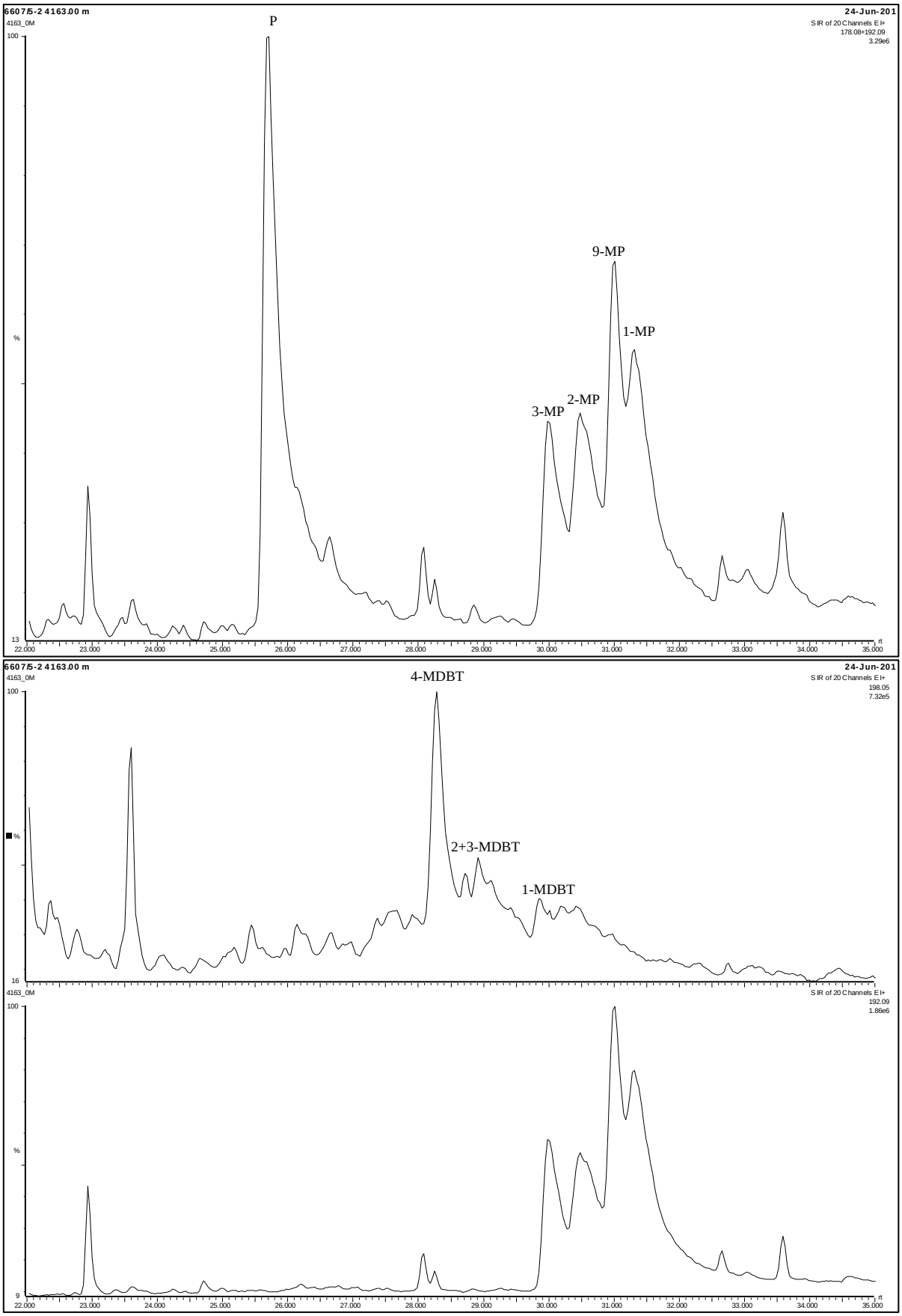
P
9-MP
1-MP
2-MP
3-MP
4-MDBT
2+3-MDBT
1-MDBT

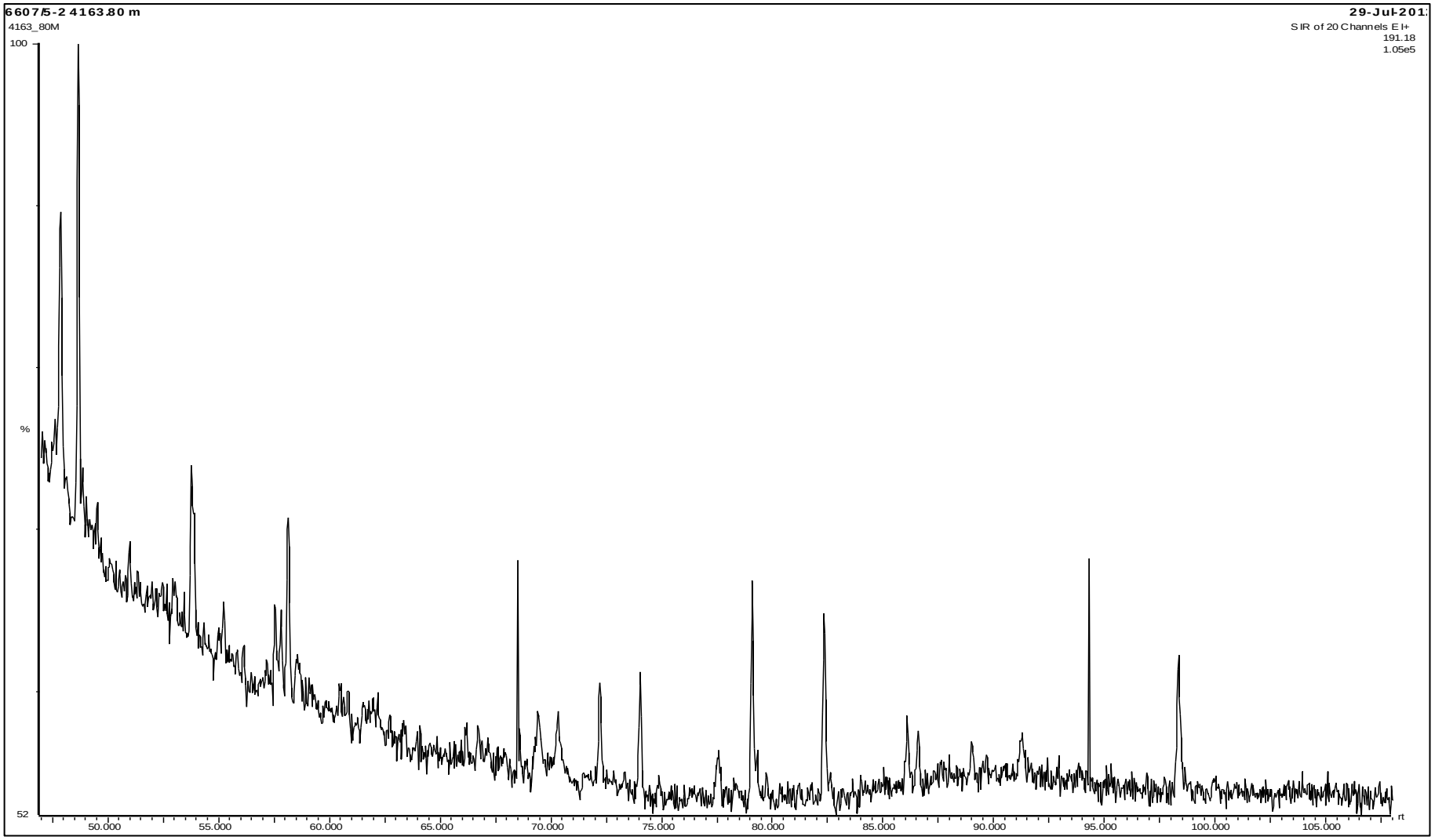
660715-2 4163.80 m
29-Jul-201
4163_80M
SIR of 20 Channels EI+
191.18
1.05e5
100
%
52
50.000
55.000
60.000
65.000
70.000
75.000
80.000
85.000
90.000
95.000
100.000
105.000
rt

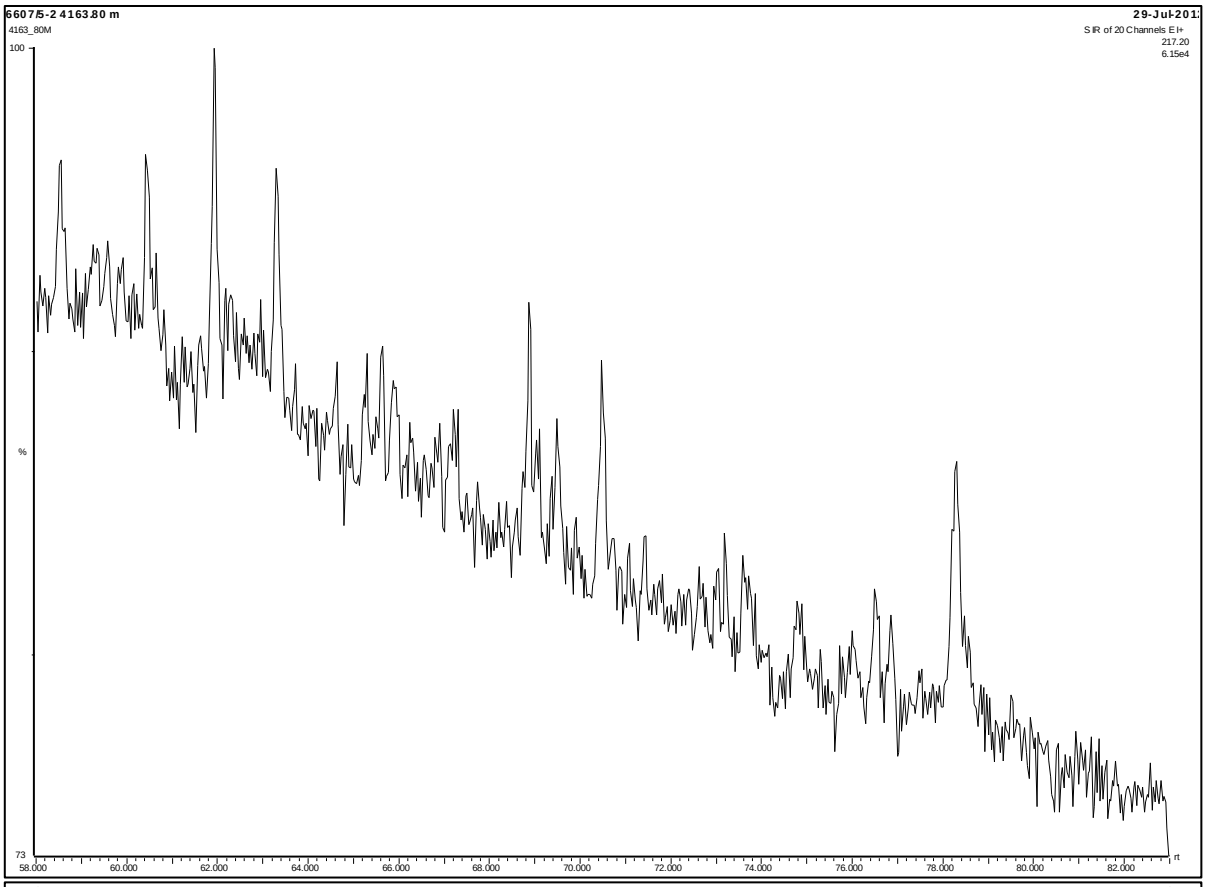
6607/5-2 4163.80 m
4163_80M
29-Jul-201
SIR of 20 Channels EI+
217.20
6.15e4
100
%
73
58.000
60.000
62.000
64.000
66.000
68.000
70.000
72.000
74.000
76.000
78.000
80.000
82.000
rt

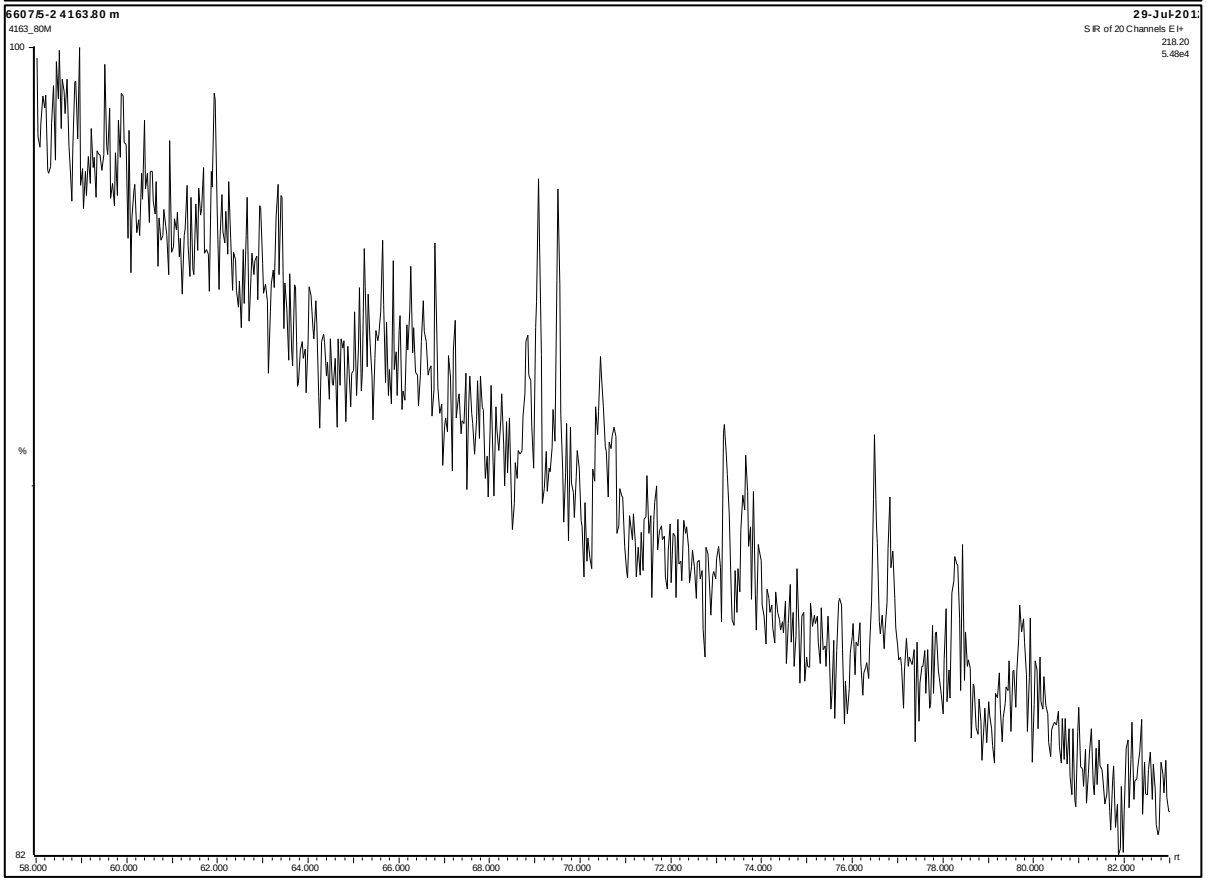
6607/5-2 4163.80 m
4163_80M
29-Jul-201
SIR of 20 Channels EI+
218.20
5.48e4
100
%
82
58.000
60.000
62.000
64.000
66.000
68.000
70.000
72.000
74.000
76.000
78.000
80.000
82.000
rt

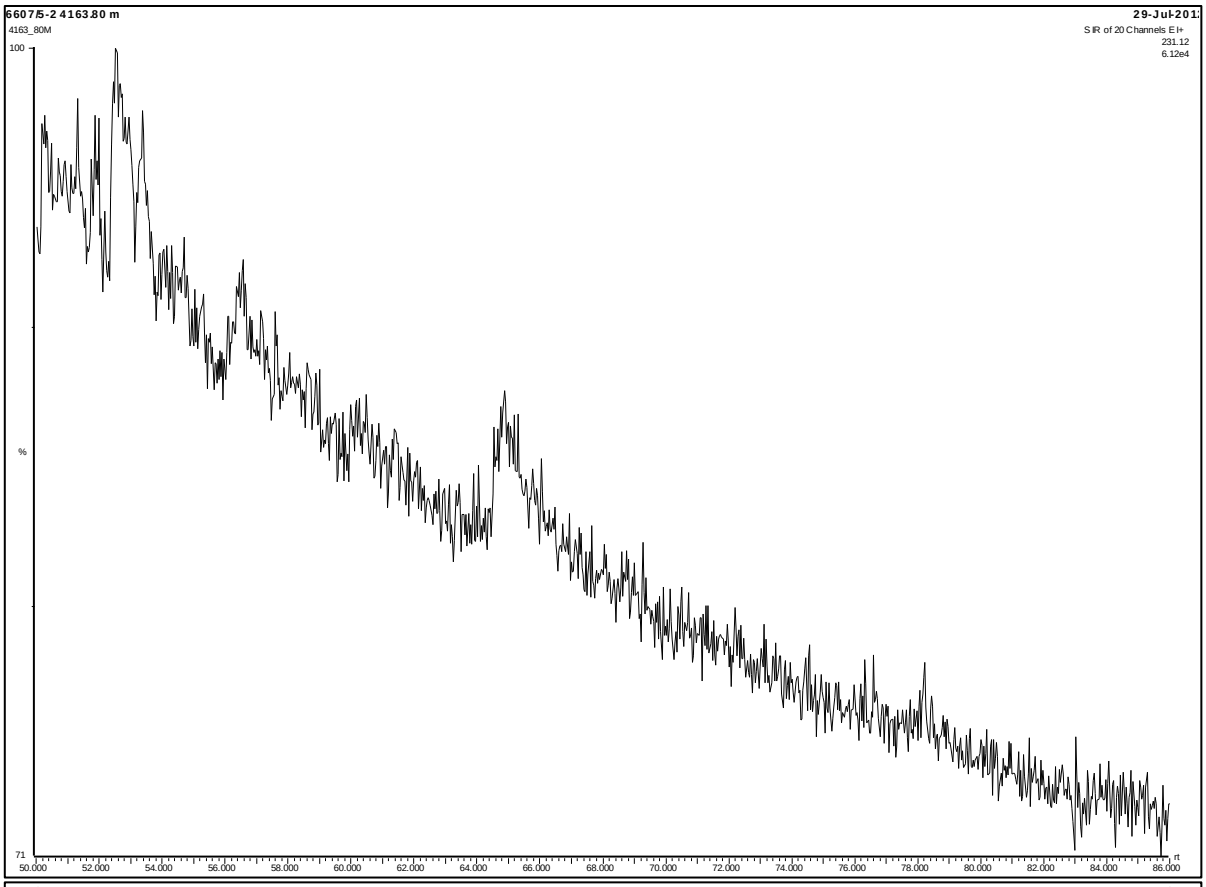
6607/5-2 4163.80 m
29-Jul-201
4163_80M
SIR of 20 Channels EI+
231.12
6.12e4
100
%
71
50.000 52.000 54.000 56.000 58.000 60.000 62.000 64.000 66.000 68.000 70.000 72.000 74.000 76.000 78.000 80.000 82.000 84.000 86.000
rt

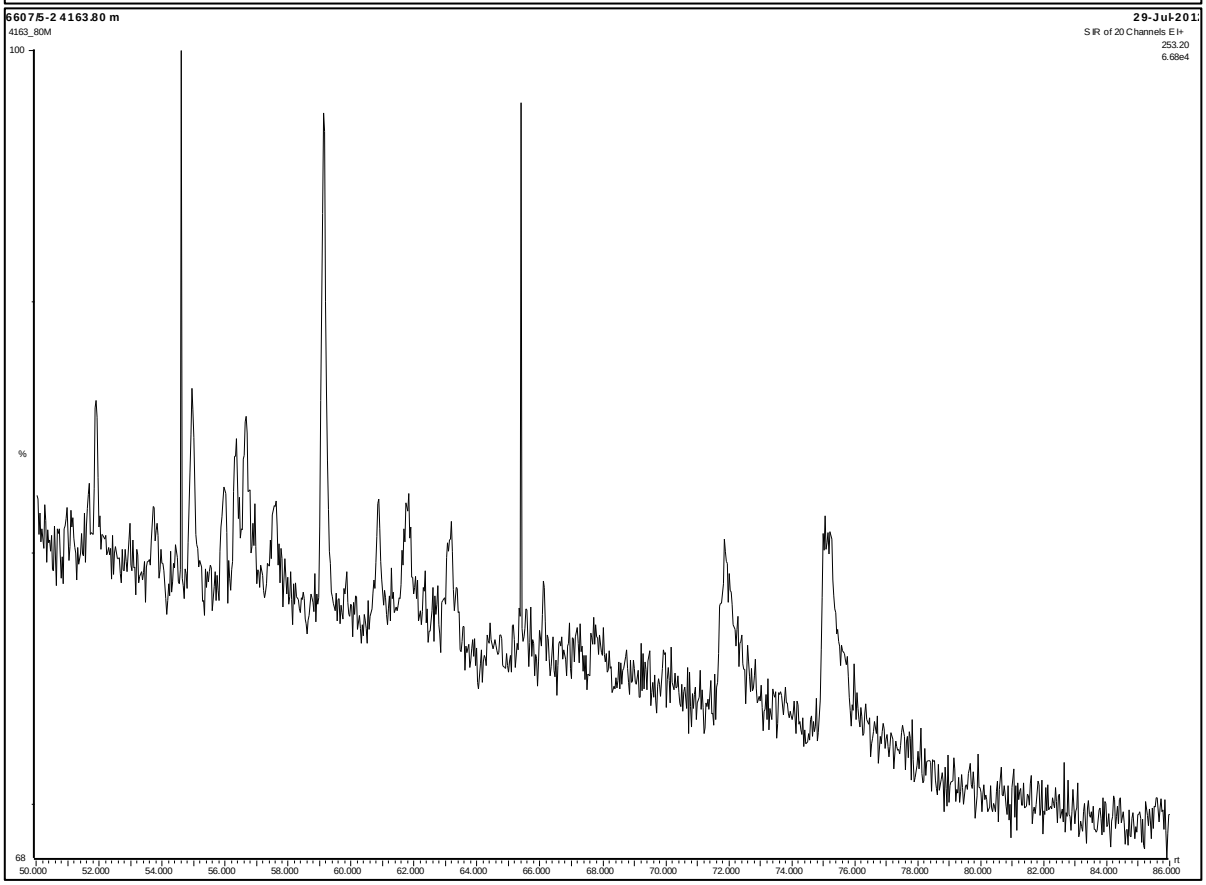
6607/5-2 4163.80 m
29-Jul-201
4163_80M
SIR of 20 Channels EI+
253.20
6.68e4
100
%
68
50.000 52.000 54.000 56.000 58.000 60.000 62.000 64.000 66.000 68.000 70.000 72.000 74.000 76.000 78.000 80.000 82.000 84.000 86.000
rt

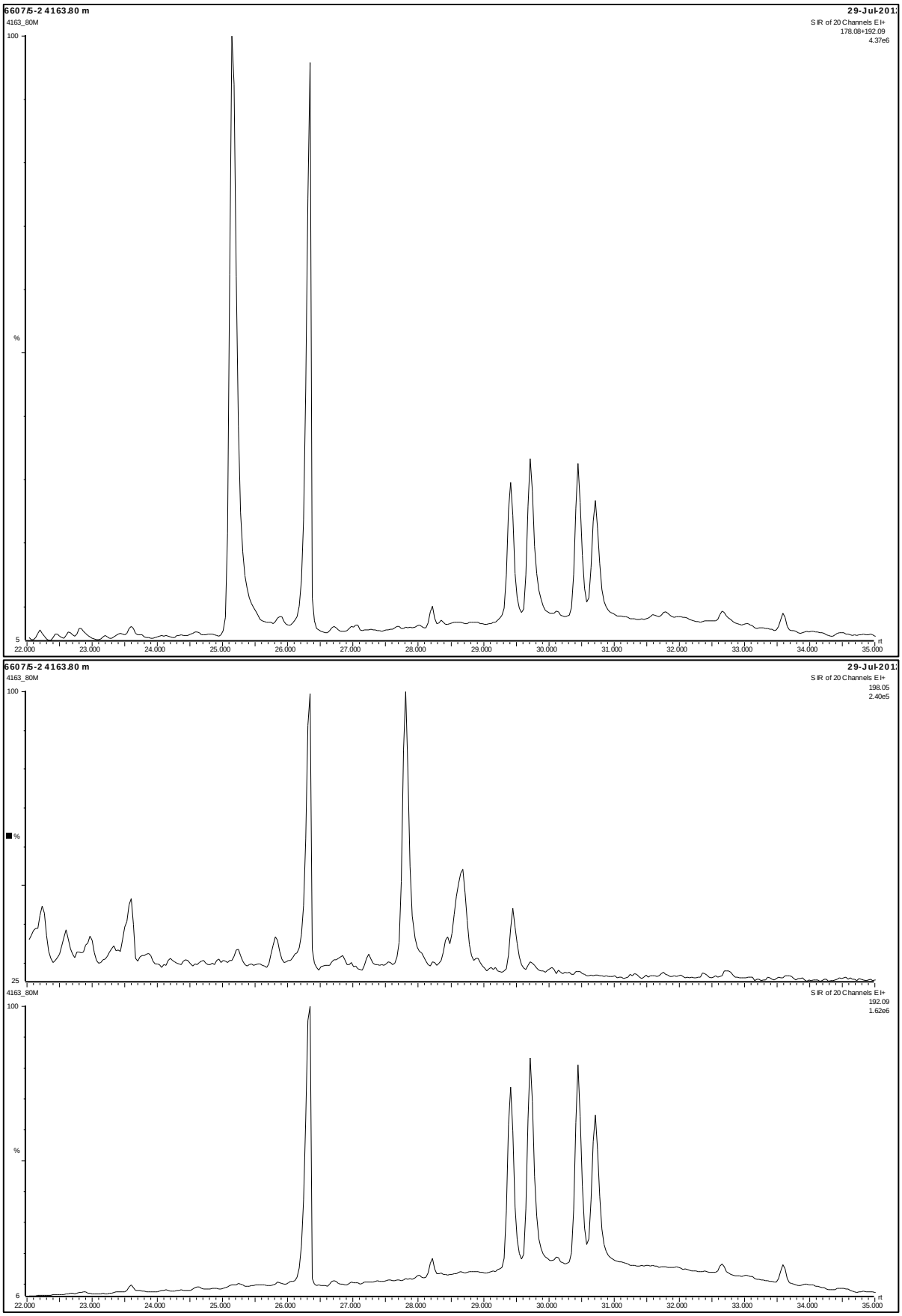
6607/5-2 4163.80 m
29-Jul-201
4163_80M
SIR of 20 Channels EI+
178.08+192.09
4.37e6
100
%
5
22.000
23.000
24.000
25.000
26.000
27.000
28.000
29.000
30.000
31.000
32.000
33.000
34.000
35.000
rt
6607/5-2 4163.80 m
29-Jul-201
4163_80M
SIR of 20 Channels EI+
198.05
2.40e5
100
%
25
4163_80M
SIR of 20 Channels EI+
192.09
1.62e6
100
%
6
22.000
23.000
24.000
25.000
26.000
27.000
28.000
29.000
30.000
31.000
32.000
33.000
34.000
35.000
rt

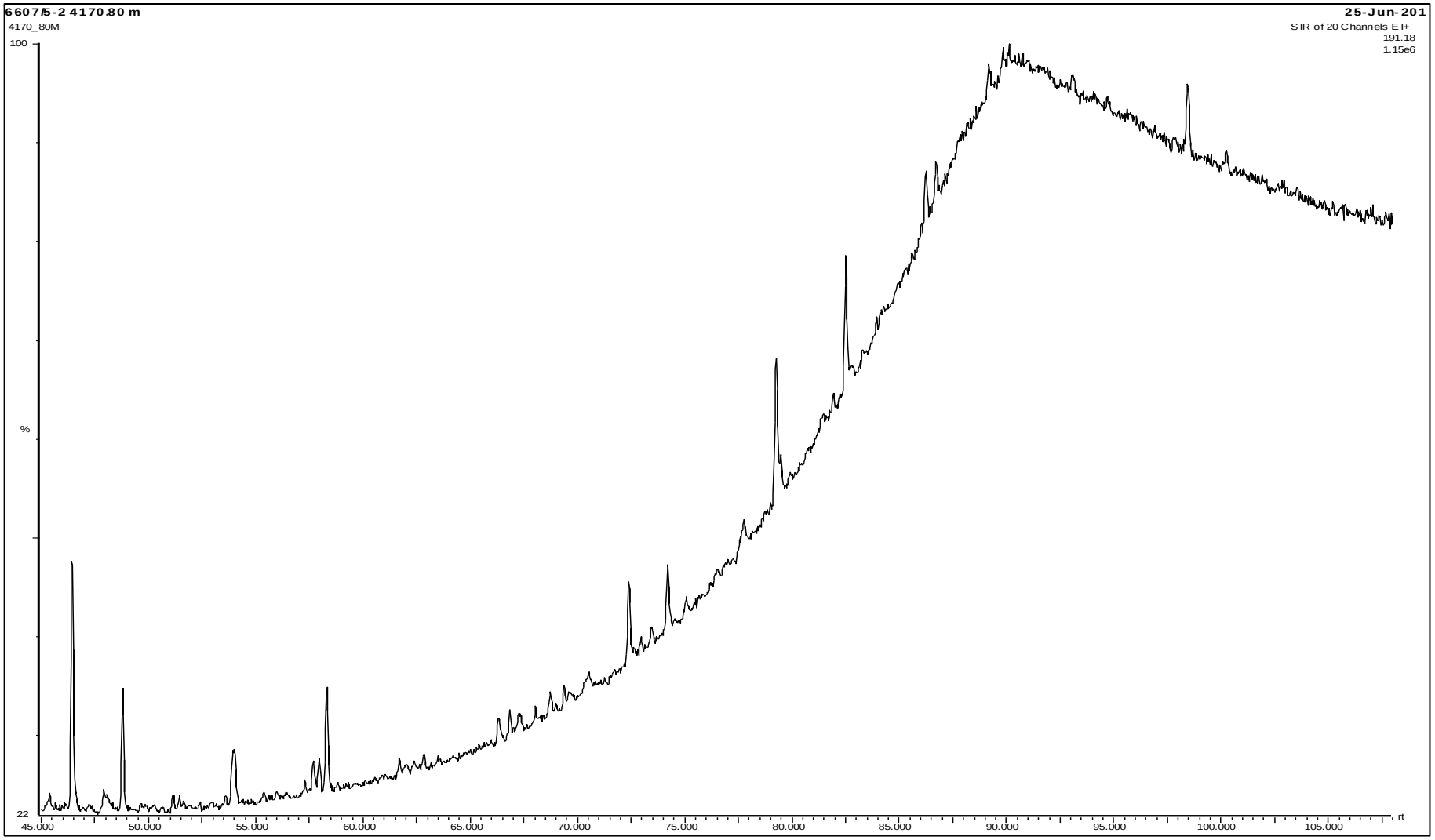
66075-2 4170.80 m
4170_80M
25-Jun-201
SIR of 20 Channels EI+
191.18
1.15e6
100
%
22
45.000
50.000
55.000
60.000
65.000
70.000
75.000
80.000
85.000
90.000
95.000
100.000
105.000
rt

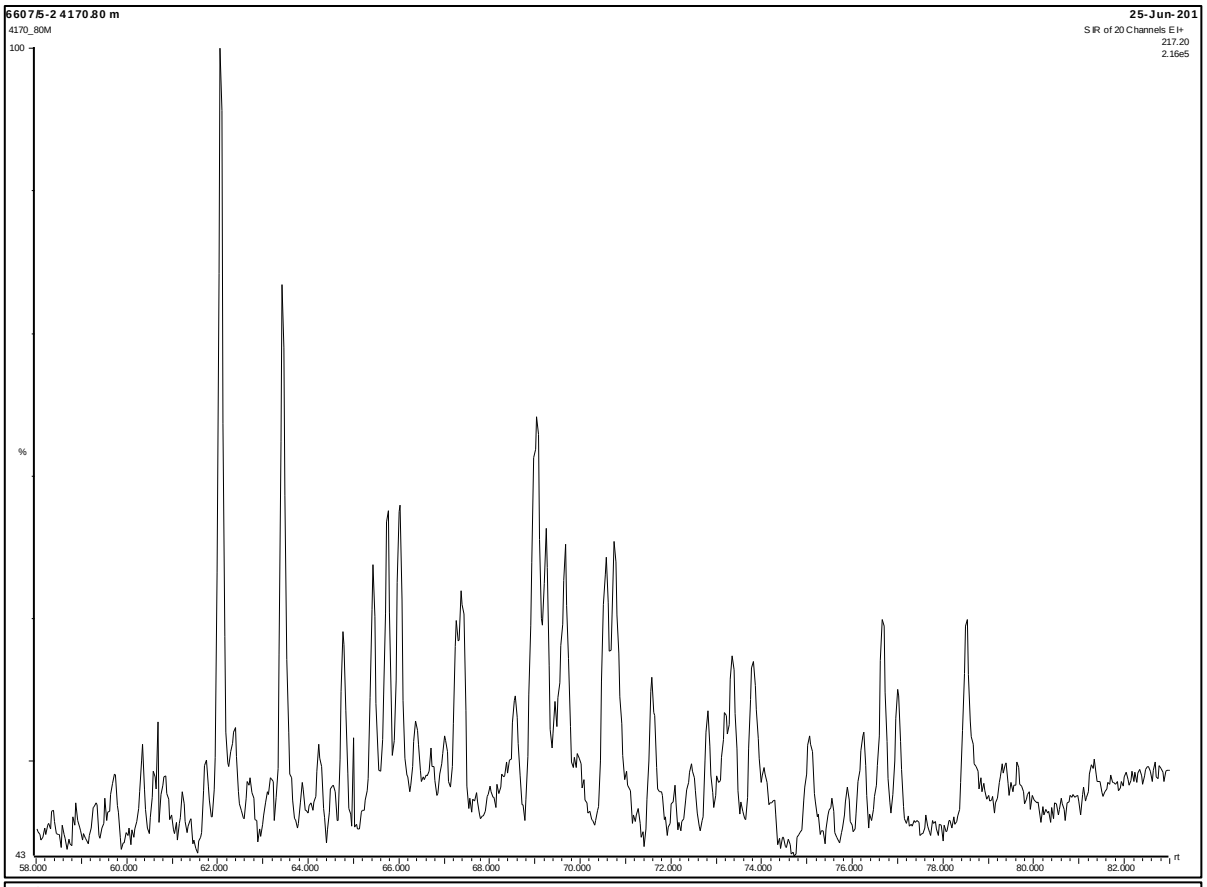
6607/5-2 4170.80 m
4170_80M
25-Jun-201
SIR of 20 Channels EI+
217.20
2.16e5
100
%
43
58.000
60.000
62.000
64.000
66.000
68.000
70.000
72.000
74.000
76.000
78.000
80.000
82.000
rt

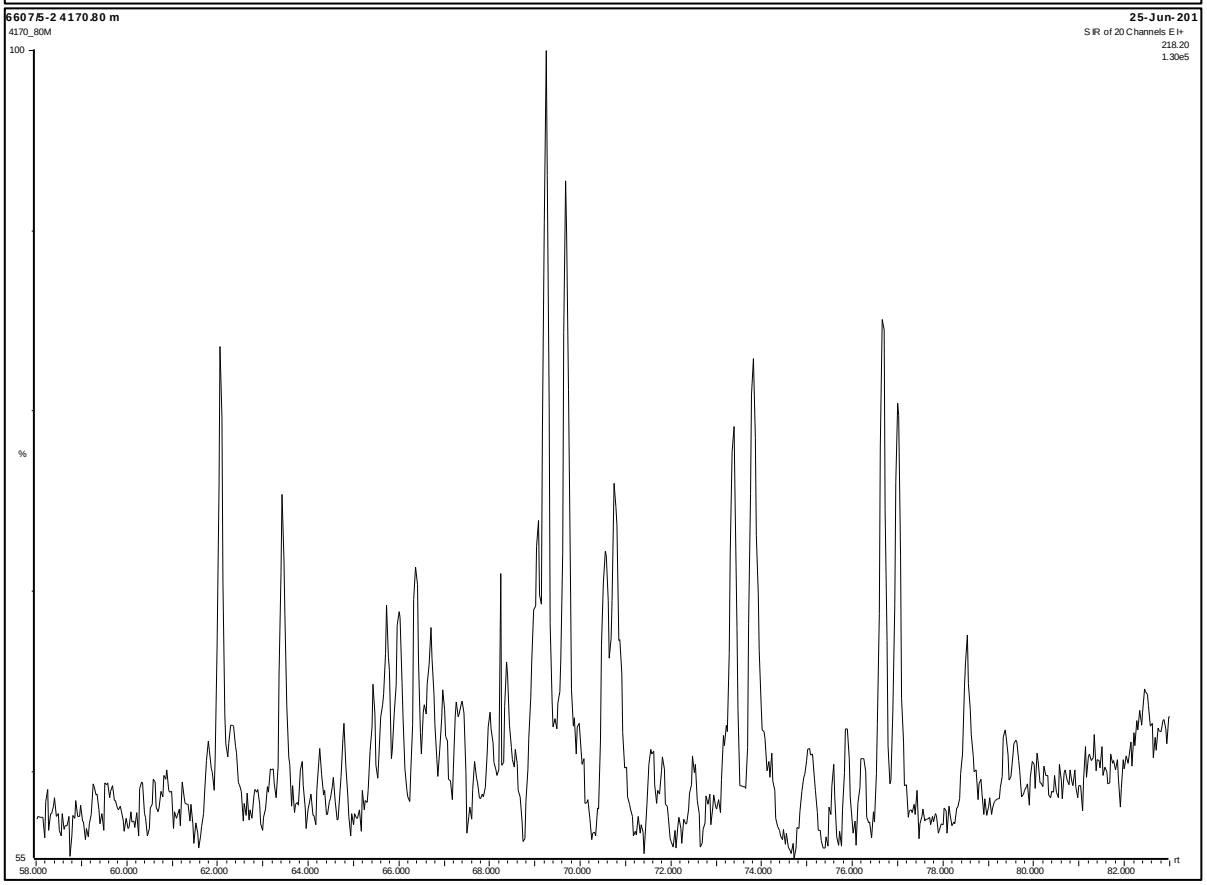
6607/5-2 4170.80 m
4170_80M
25-Jun-201
SIR of 20 Channels EI+
218.20
1.30e5
100
%
55
58.000
60.000
62.000
64.000
66.000
68.000
70.000
72.000
74.000
76.000
78.000
80.000
82.000
rt

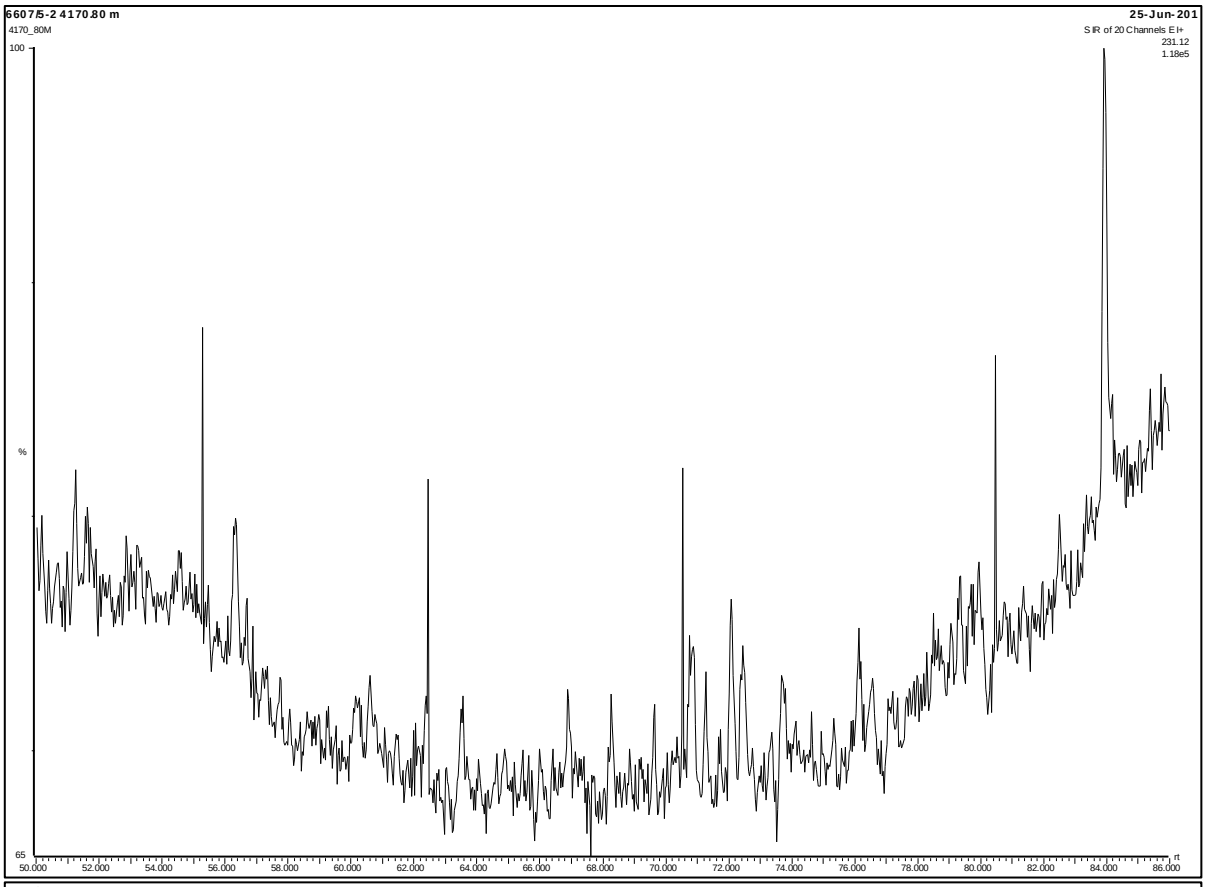
6607/5-2 4170.80 m
25-Jun-201
4170_80M
SIR of 20 Channels EI+
231.12
1.18e5
100
%
65
50.000
52.000
54.000
56.000
58.000
60.000
62.000
64.000
66.000
68.000
70.000
72.000
74.000
76.000
78.000
80.000
82.000
84.000
86.000
rt

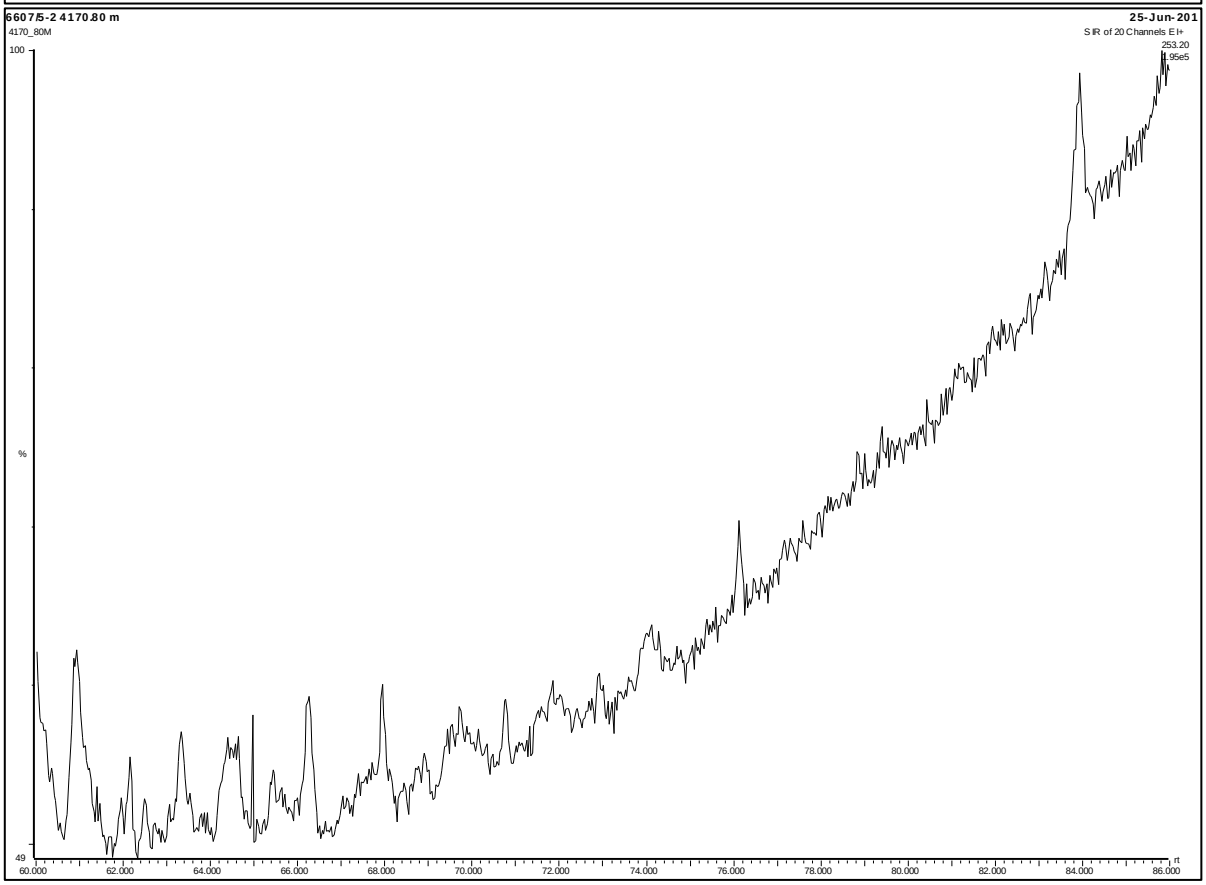
6607/5-2 4170.80 m
25-Jun-201
4170_80M
SIR of 20 Channels EI+
253.20
1.95e5
100
%
49
60.000
62.000
64.000
66.000
68.000
70.000
72.000
74.000
76.000
78.000
80.000
82.000
84.000
86.000
rt

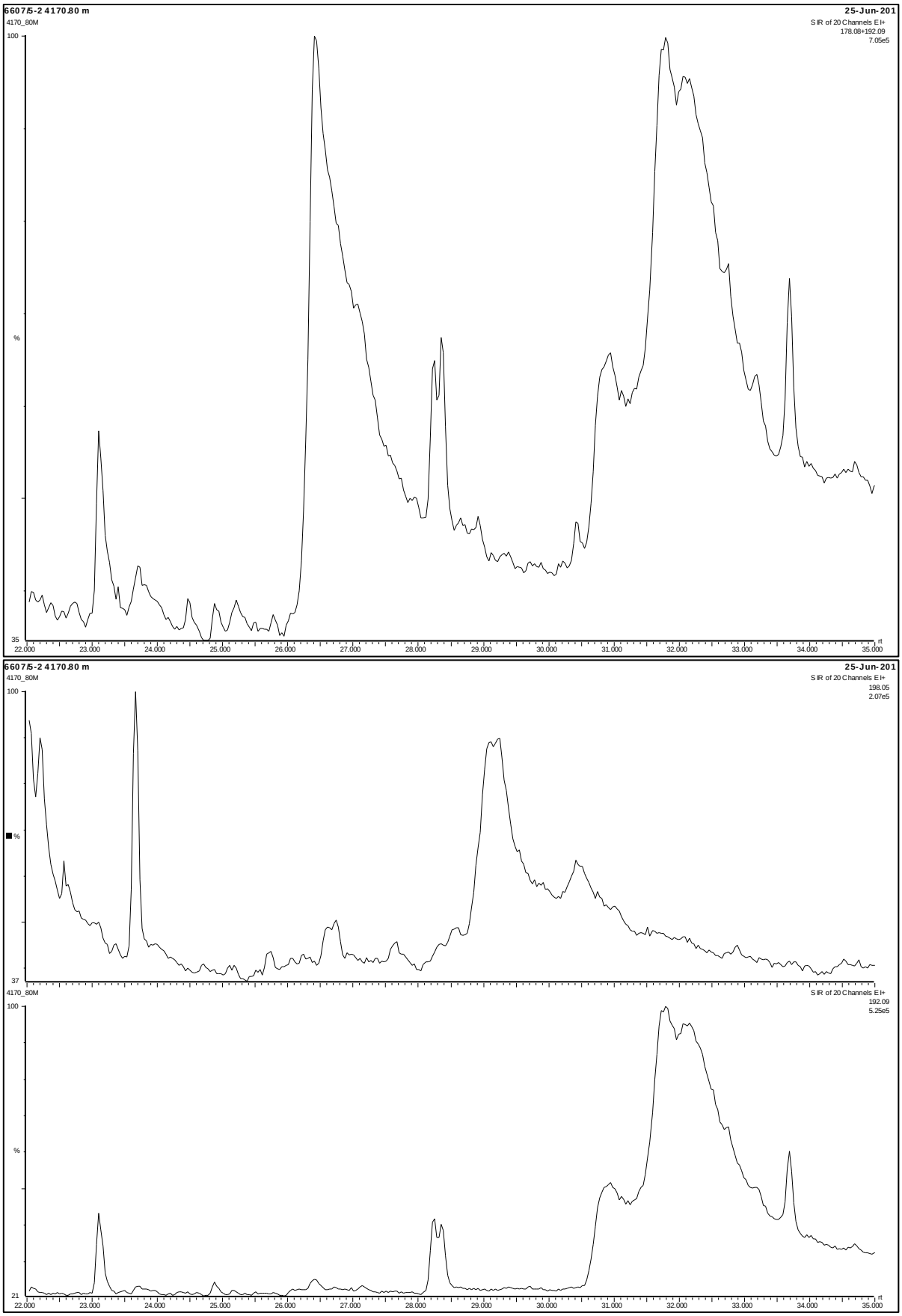
66075-2 4170.80 m
25-Jun-201
4170_80M
SIR of 20 Channels EI+
178.08+192.09
7.05e5
100
%
35
22.000
23.000
24.000
25.000
26.000
27.000
28.000
29.000
30.000
31.000
32.000
33.000
34.000
35.000
rt
66075-2 4170.80 m
25-Jun-201
4170_80M
SIR of 20 Channels EI+
198.05
2.07e5
100
%
37
4170_80M
SIR of 20 Channels EI+
192.09
5.25e5
100
%
21
22.000
23.000
24.000
25.000
26.000
27.000
28.000
29.000
30.000
31.000
32.000
33.000
34.000
35.000
rt

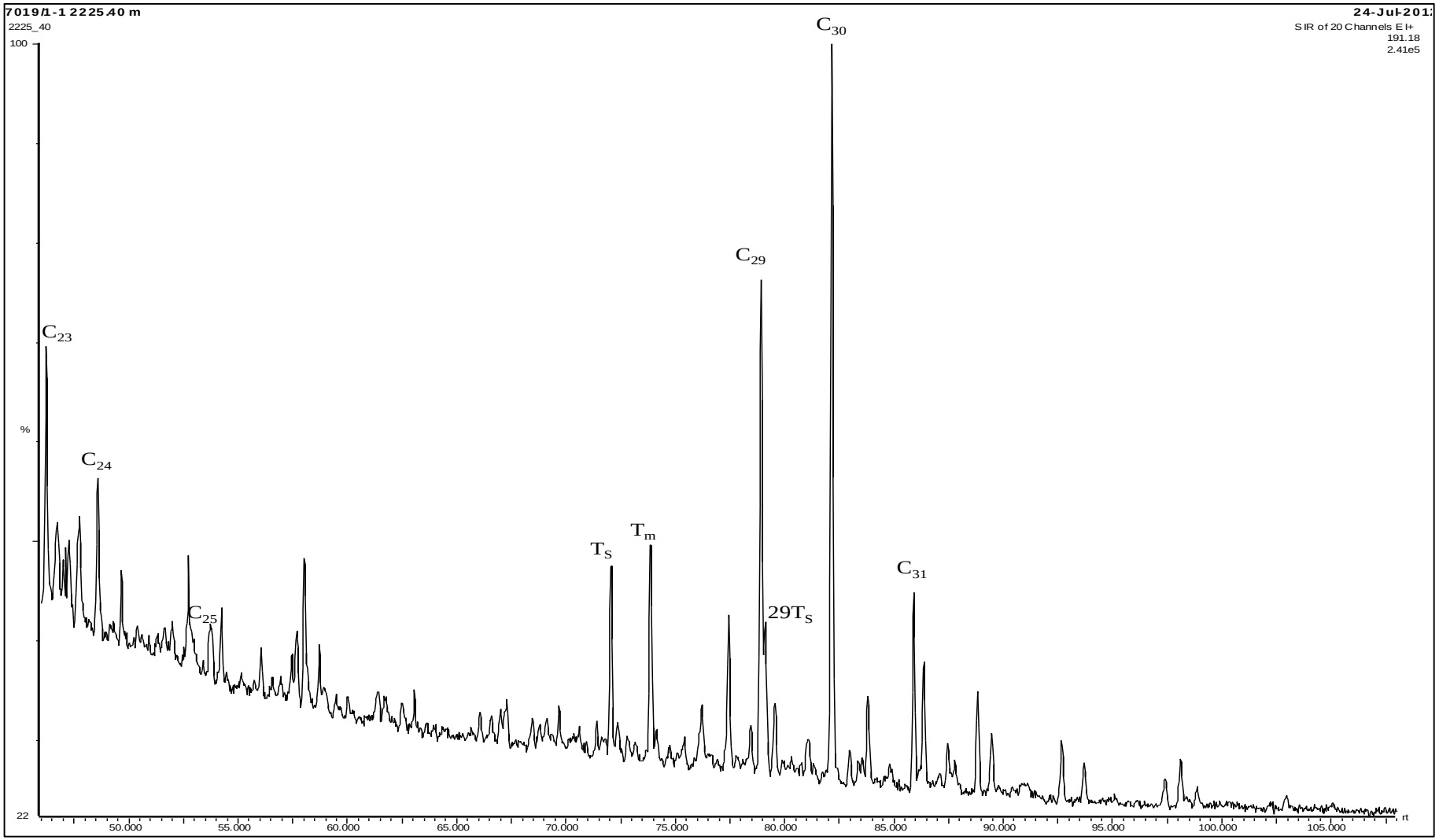
7019A1-1 2225.40 m
2225_40
100
%
22
24-Jul-201
SIR of 20 Channels EI+
191.18
2.41e5
C23
C24
C25
TS
Tm
C29
29TS
C30
C31
50.000
55.000
60.000
65.000
70.000
75.000
80.000
85.000
90.000
95.000
100.000
105.000
rt

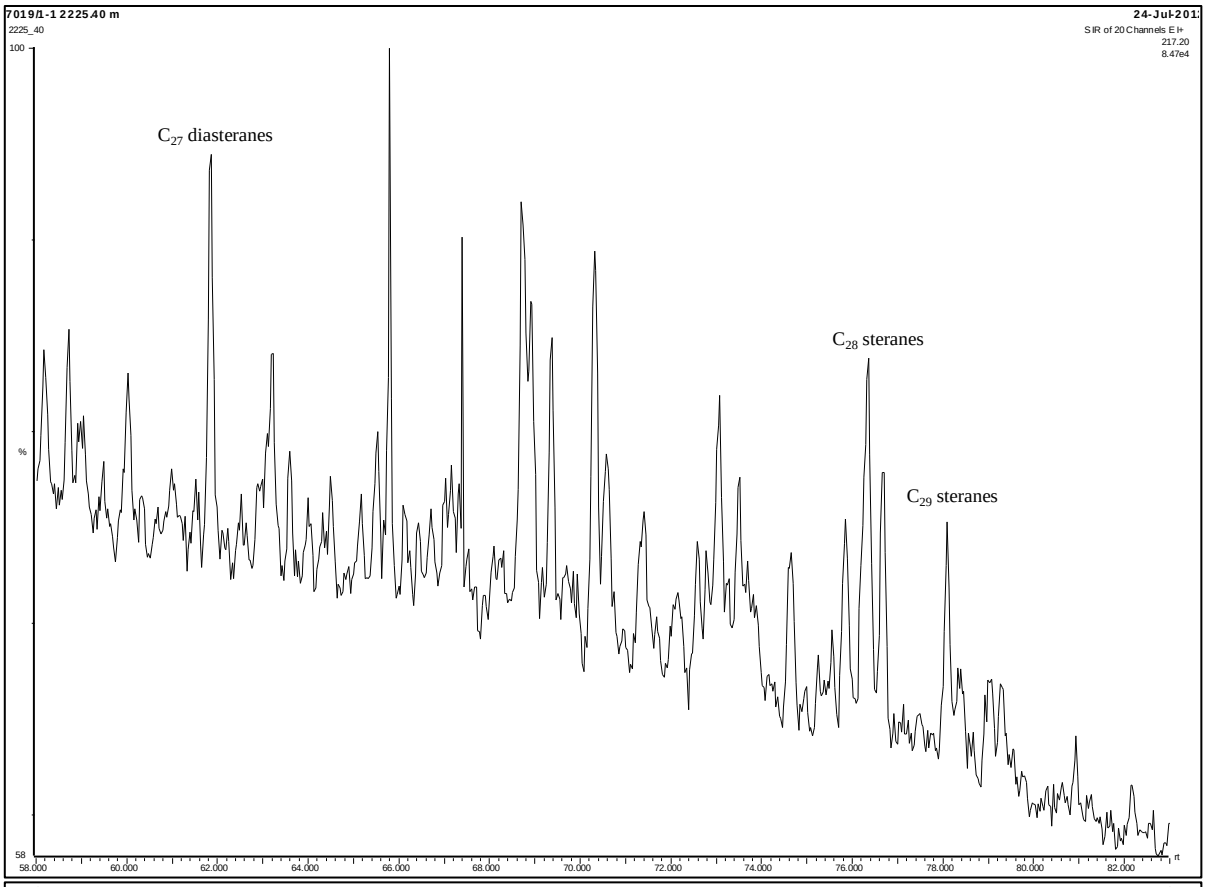
7019/1-1 2225.40 m
24-Jul-201
2225_40
SIR of 20 Channels EI+
217.20
8.47e4
100
%
58
C27 diasteranes
C28 steranes
C29 steranes
58.000
60.000
62.000
64.000
66.000
68.000
70.000
72.000
74.000
76.000
78.000
80.000
82.000
rt

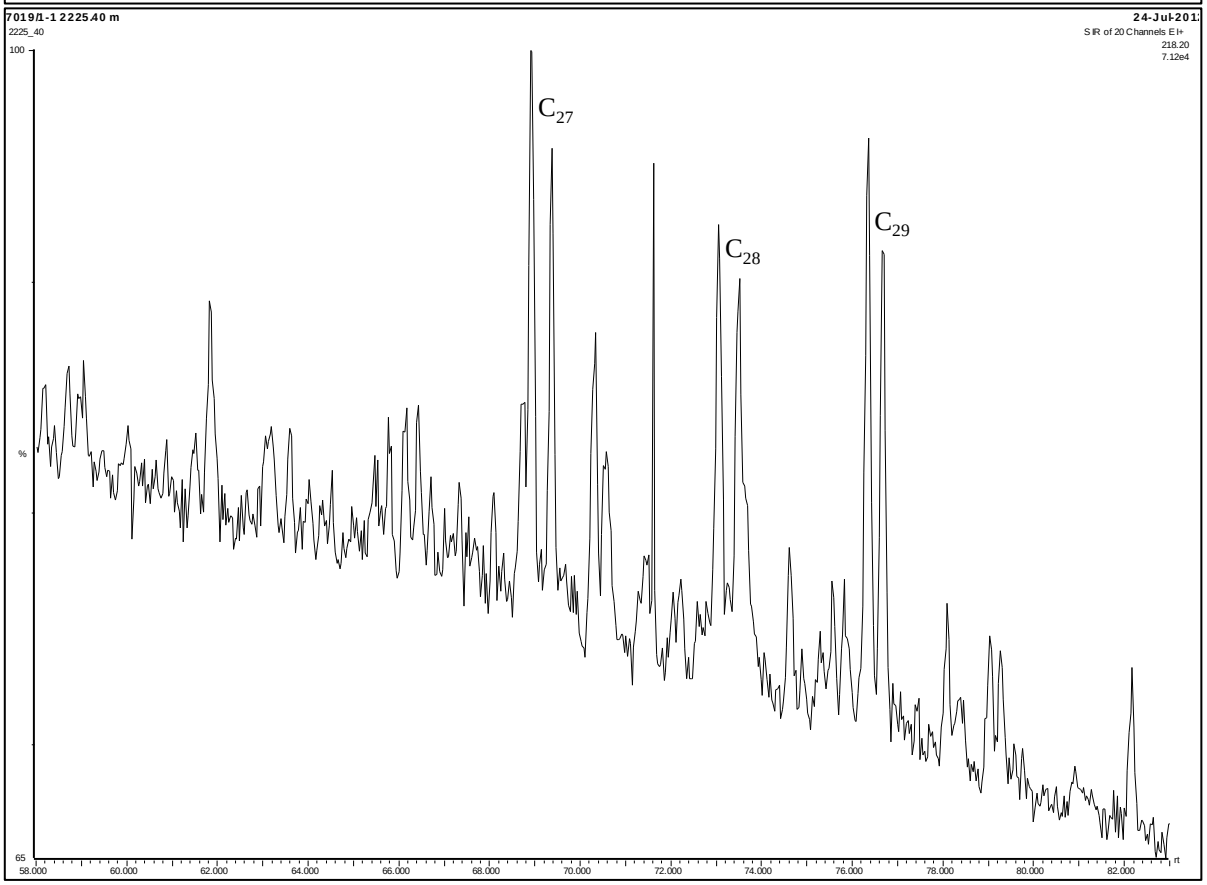
7019/1-1 2225.40 m
24-Jul-201
2225_40
SIR of 20 Channels EI+
218.20
7.12e4
100
%
65
C27
C28
C29
58.000
60.000
62.000
64.000
66.000
68.000
70.000
72.000
74.000
76.000
78.000
80.000
82.000
rt

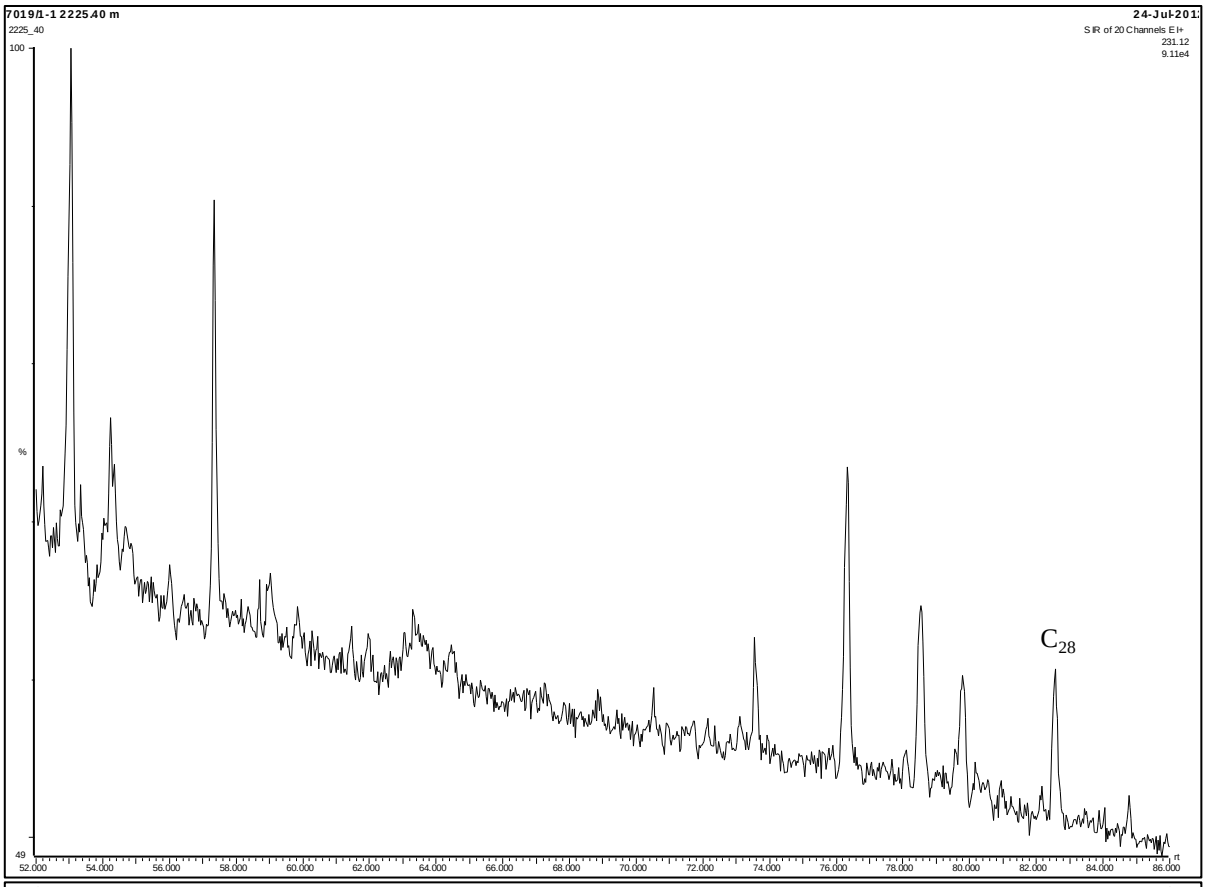
7019/1-1 2225.40 m
24-Jul-201
2225_40
SIR of 20 Channels EI+
231.12
9.11e4
100
%
49
C28
52.000 54.000 56.000 58.000 60.000 62.000 64.000 66.000 68.000 70.000 72.000 74.000 76.000 78.000 80.000 82.000 84.000 86.000
rt

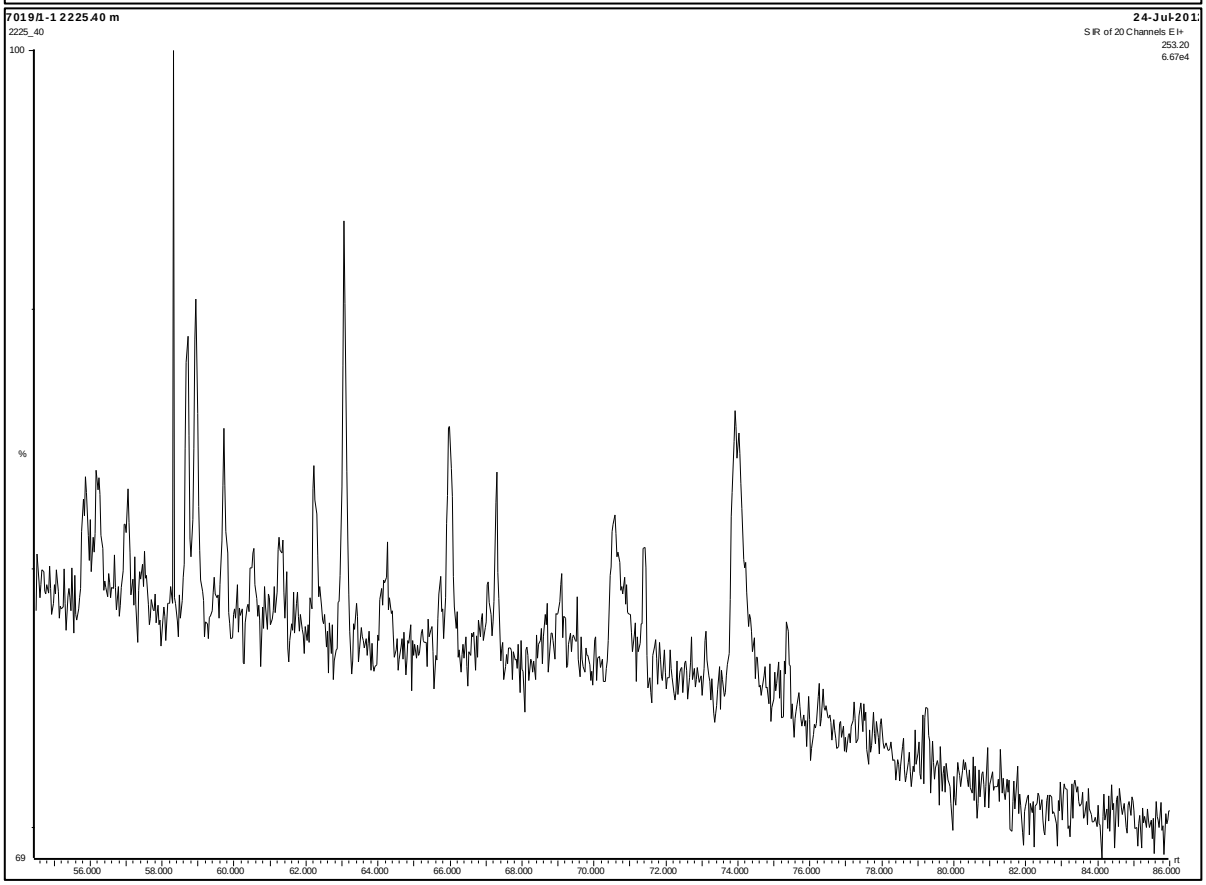
7019/1-1 2225.40 m
24-Jul-201
2225_40
SIR of 20 Channels EI+
253.20
6.67e4
100
%
69
56.000 58.000 60.000 62.000 64.000 66.000 68.000 70.000 72.000 74.000 76.000 78.000 80.000 82.000 84.000 86.000
rt

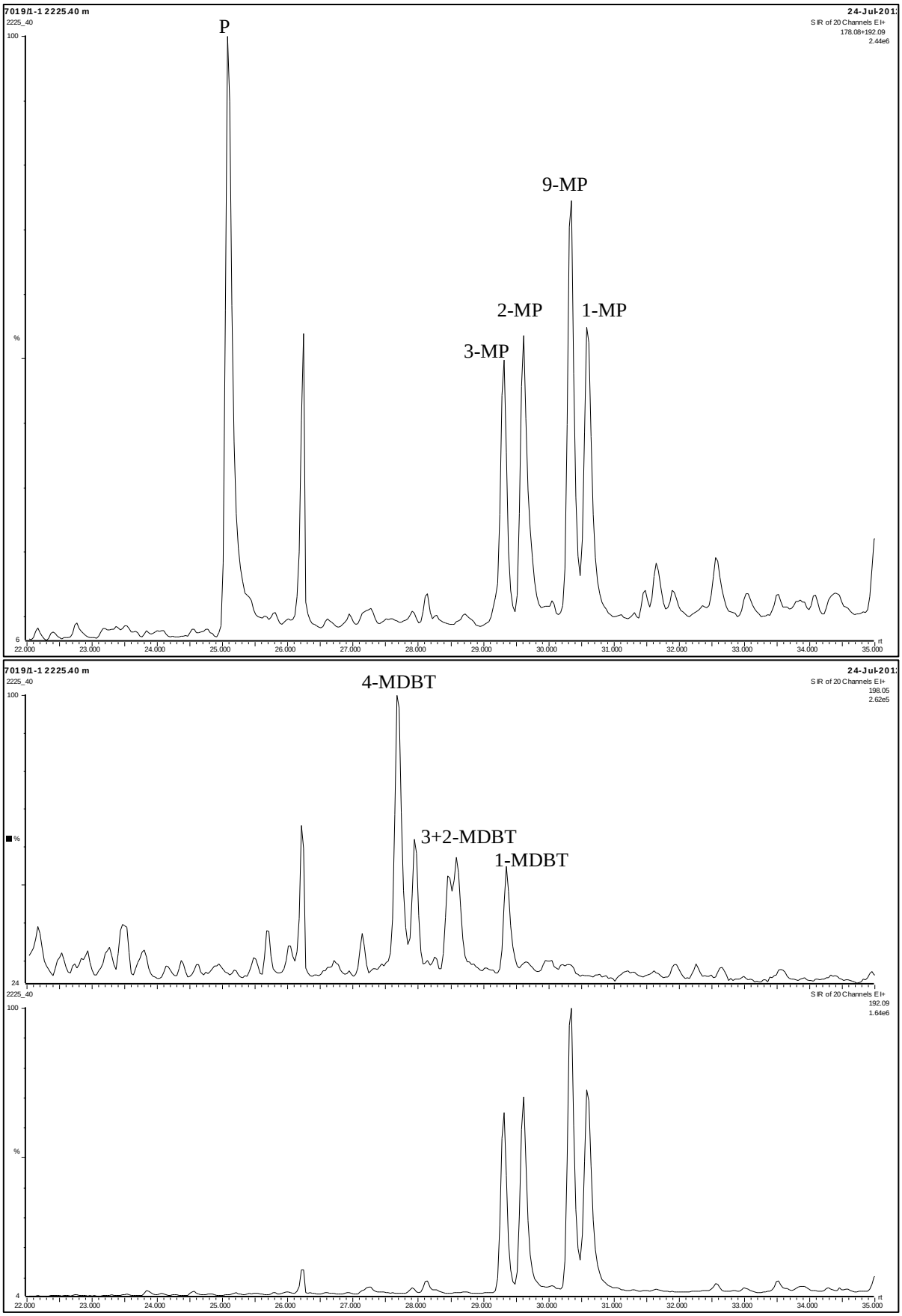
7019Л-1 2225.40 m
2225_40
24-Jul-201
SIR of 20 Channels EI+
178.08+192.09
2.44e6
P
9-MP
2-MP
1-MP
3-MP
%
100
6
22.000
23.000
24.000
25.000
26.000
27.000
28.000
29.000
30.000
31.000
32.000
33.000
34.000
35.000
rt
7019Л-1 2225.40 m
2225_40
24-Jul-201
SIR of 20 Channels EI+
198.05
2.62e5
4-MDBT
3+2-MDBT
1-MDBT
100
%
24
2225_40
SIR of 20 Channels EI+
192.09
1.64e6
100
%
4
22.000
23.000
24.000
25.000
26.000
27.000
28.000
29.000
30.000
31.000
32.000
33.000
34.000
35.000
rt

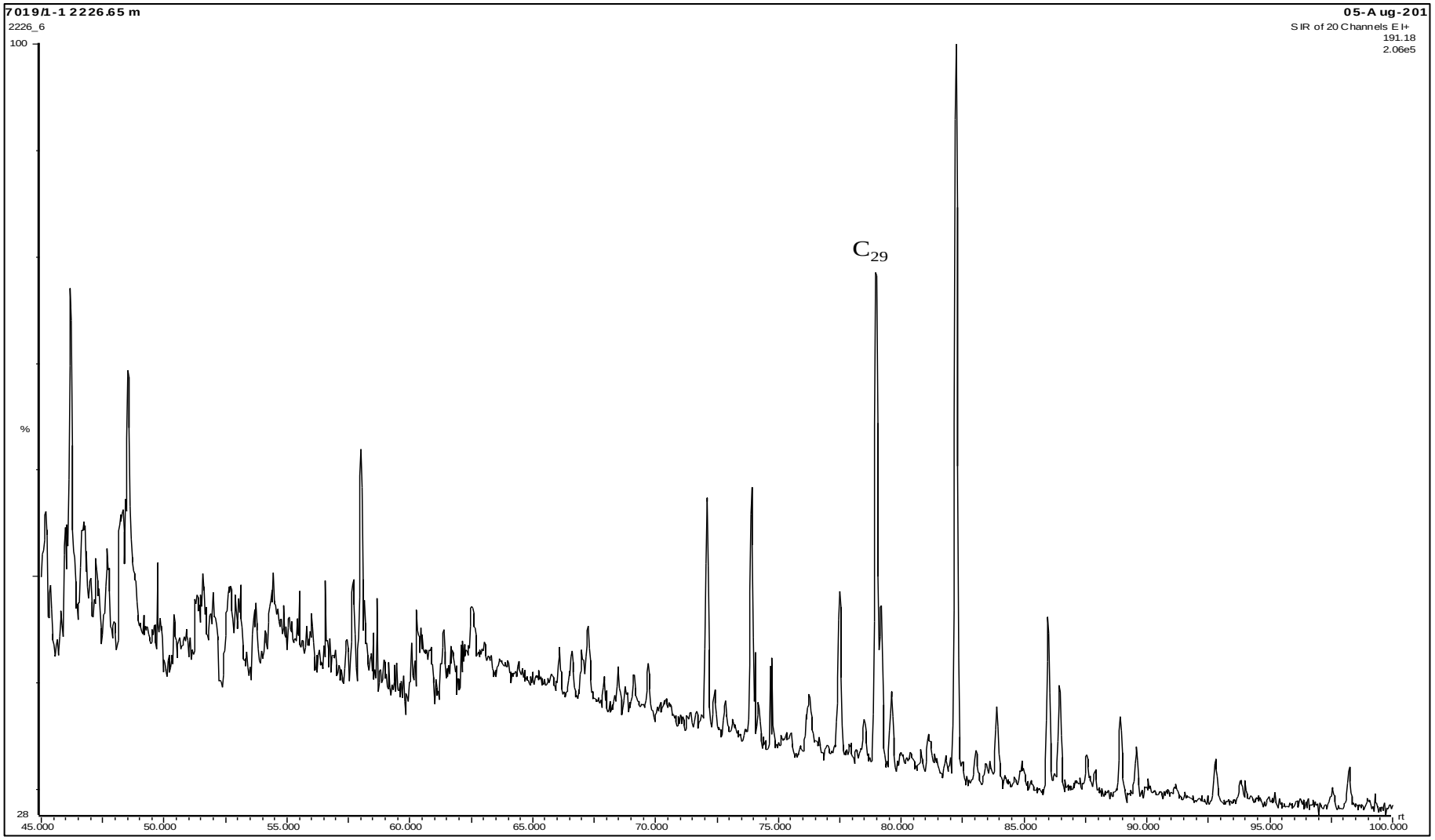
7019/1-1 2226.65 m
2226_6
05-Aug-201
SIR of 20 Channels EI+
191.18
2.06e5
100
%
28
C29
45.000
50.000
55.000
60.000
65.000
70.000
75.000
80.000
85.000
90.000
95.000
100.000
rt

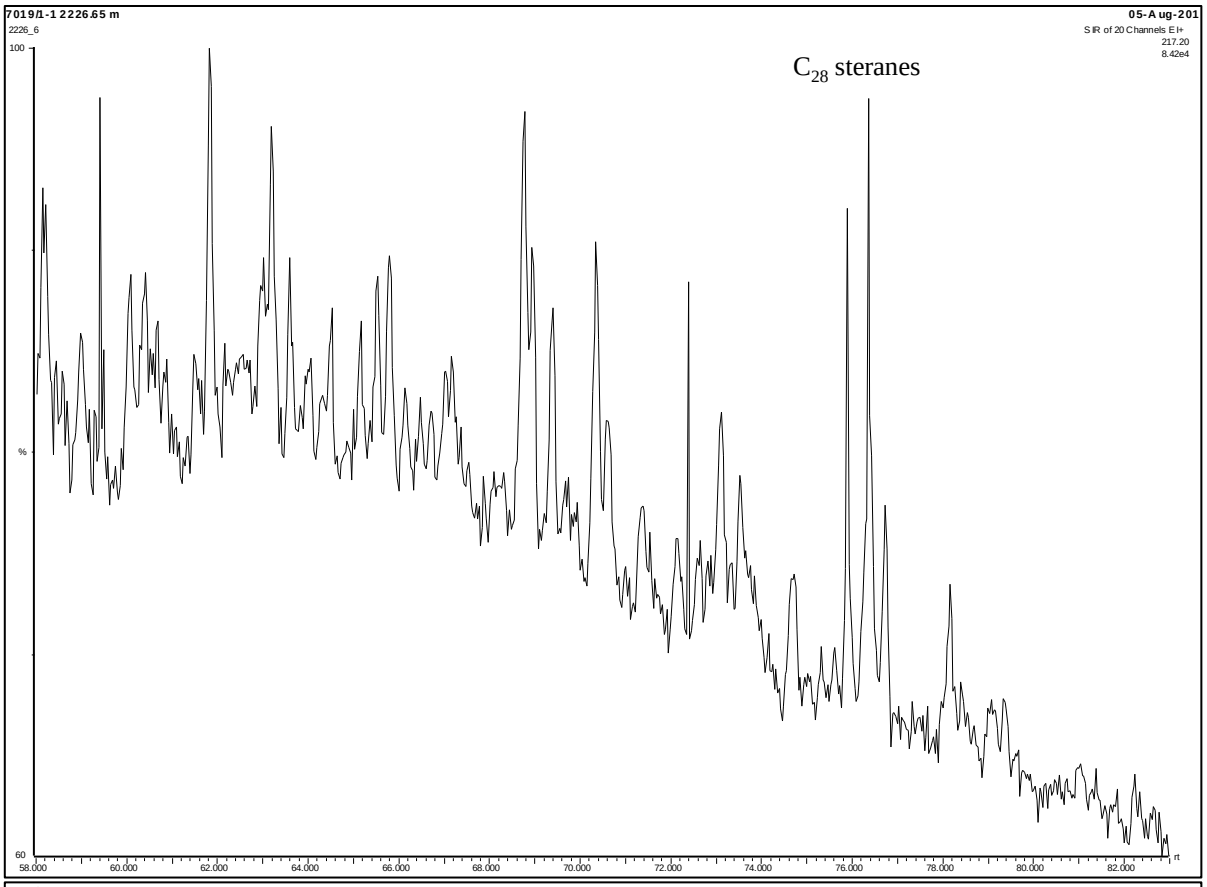
7019/1-1 2226.65 m
2226_6
05-Aug-201
SIR of 20 Channels EI+
217.20
8.42e4
100
%
60
58.000
60.000
62.000
64.000
66.000
68.000
70.000
72.000
74.000
76.000
78.000
80.000
82.000
rt
C28 steranes

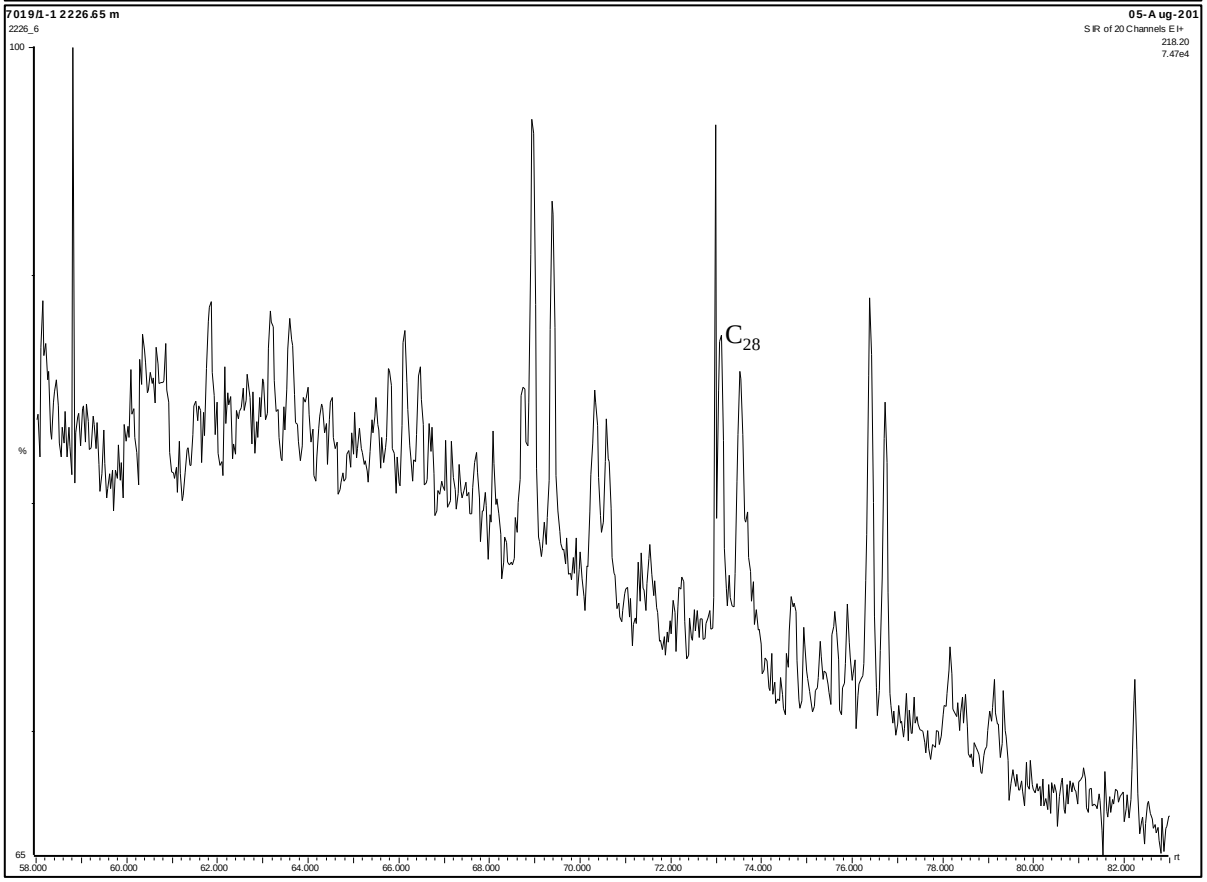
7019/1-1 2226.65 m
2226_6
05-Aug-201
SIR of 20 Channels EI+
218.20
7.47e4
100
%
65
58.000
60.000
62.000
64.000
66.000
68.000
70.000
72.000
74.000
76.000
78.000
80.000
82.000
rt
C28

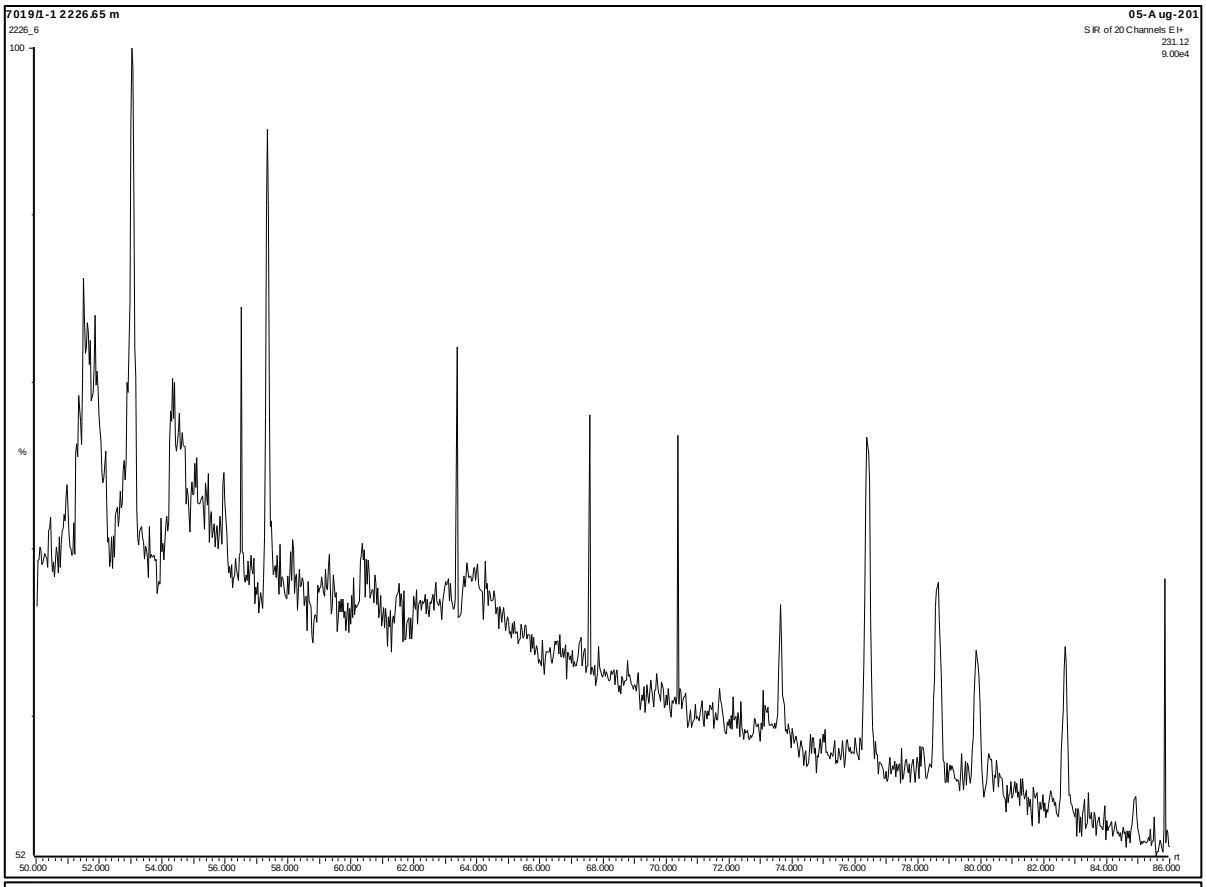
7019/1-1 2226.65 m
2226_6
05-Aug-201
SIR of 20 Channels EI+
231.12
9.00e4
100
%
52
50.000
52.000
54.000
56.000
58.000
60.000
62.000
64.000
66.000
68.000
70.000
72.000
74.000
76.000
78.000
80.000
82.000
84.000
86.000
rt

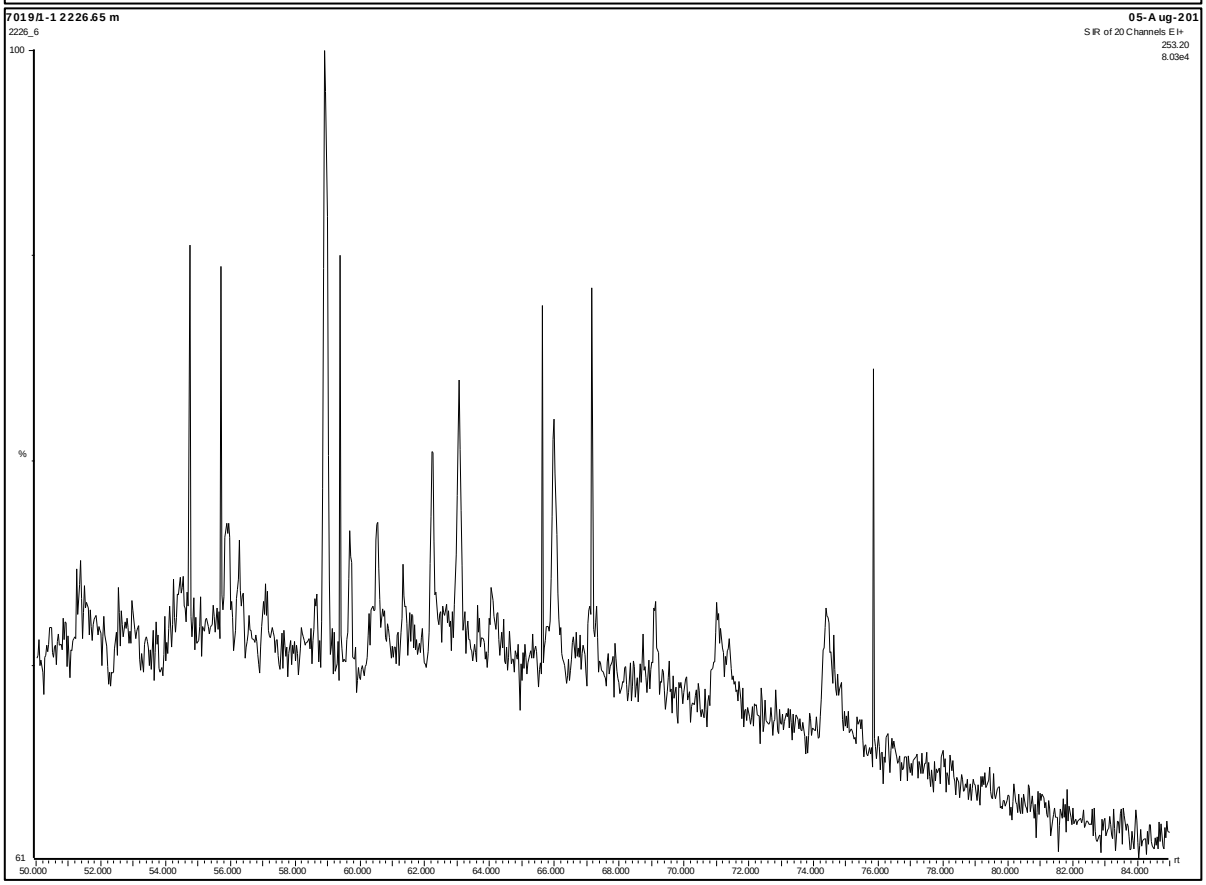
7019/1-1 2226.65 m
2226_6
05-Aug-201
SIR of 20 Channels EI+
253.20
8.03e4
100
%
61
50.000
52.000
54.000
56.000
58.000
60.000
62.000
64.000
66.000
68.000
70.000
72.000
74.000
76.000
78.000
80.000
82.000
84.000
rt

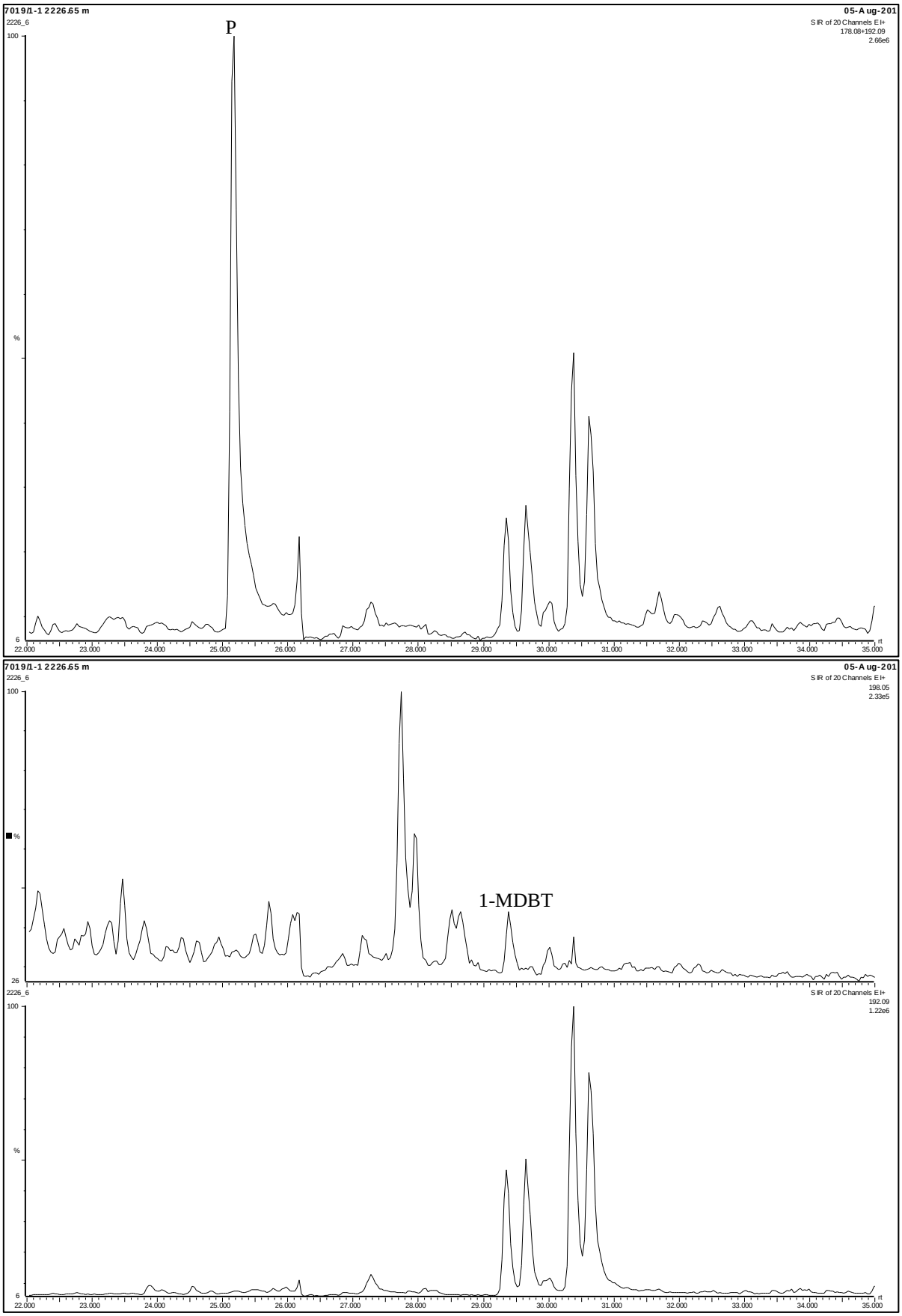
7019/1-1 2226.65 m
05-Aug-201
2226_6
SIR of 20 Channels EI+
178.08+192.09
2.66e6
P
100
%
6
22.000
23.000
24.000
25.000
26.000
27.000
28.000
29.000
30.000
31.000
32.000
33.000
34.000
35.000
rt
7019/1-1 2226.65 m
05-Aug-201
2226_6
SIR of 20 Channels EI+
198.05
2.33e5
100
%
1-MDBT
26
2226_6
SIR of 20 Channels EI+
192.09
1.22e6
100
%
6
22.000
23.000
24.000
25.000
26.000
27.000
28.000
29.000
30.000
31.000
32.000
33.000
34.000
35.000
rt

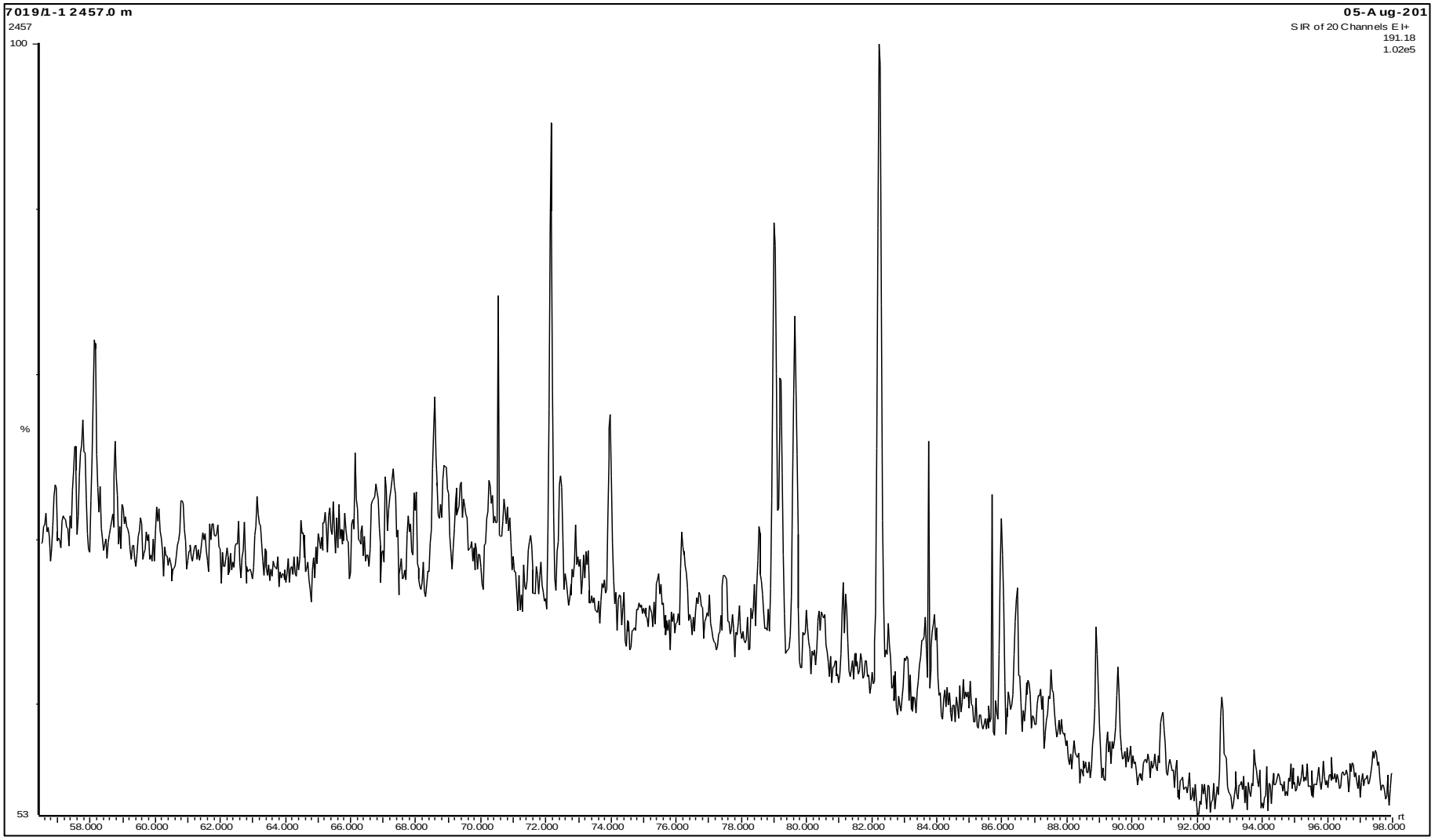
7019/1-1 2457.0 m
05-Aug-201
2457
SIR of 20 Channels EI+
191.18
1.02e5
100
%
53
58.000
60.000
62.000
64.000
66.000
68.000
70.000
72.000
74.000
76.000
78.000
80.000
82.000
84.000
86.000
88.000
90.000
92.000
94.000
96.000
98.000
rt

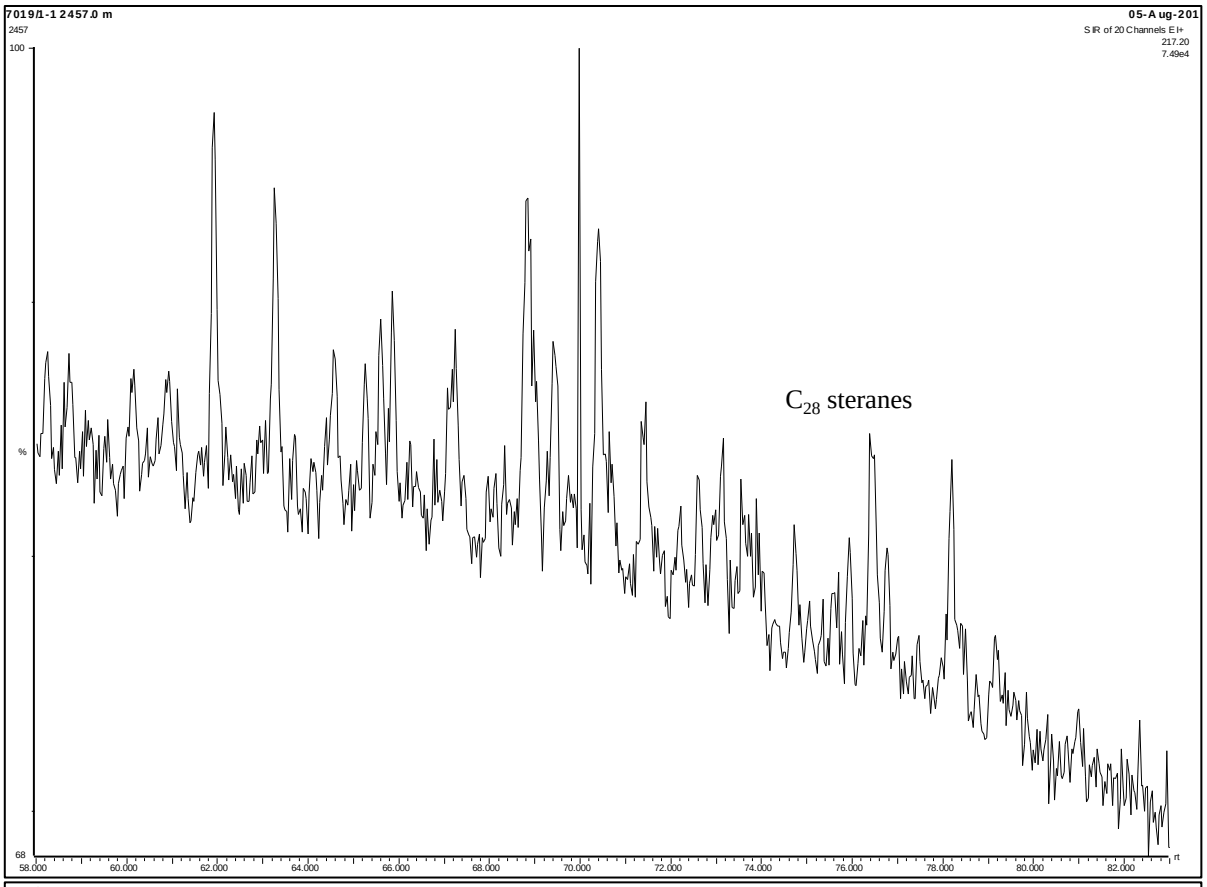
7019/1-1 2457.0 m
05-Aug-201
2457
SIR of 20 Channels EI+
217.20
7.49e4
100
%
68
58.000
60.000
62.000
64.000
66.000
68.000
70.000
72.000
74.000
76.000
78.000
80.000
82.000
rt
C28 steranes

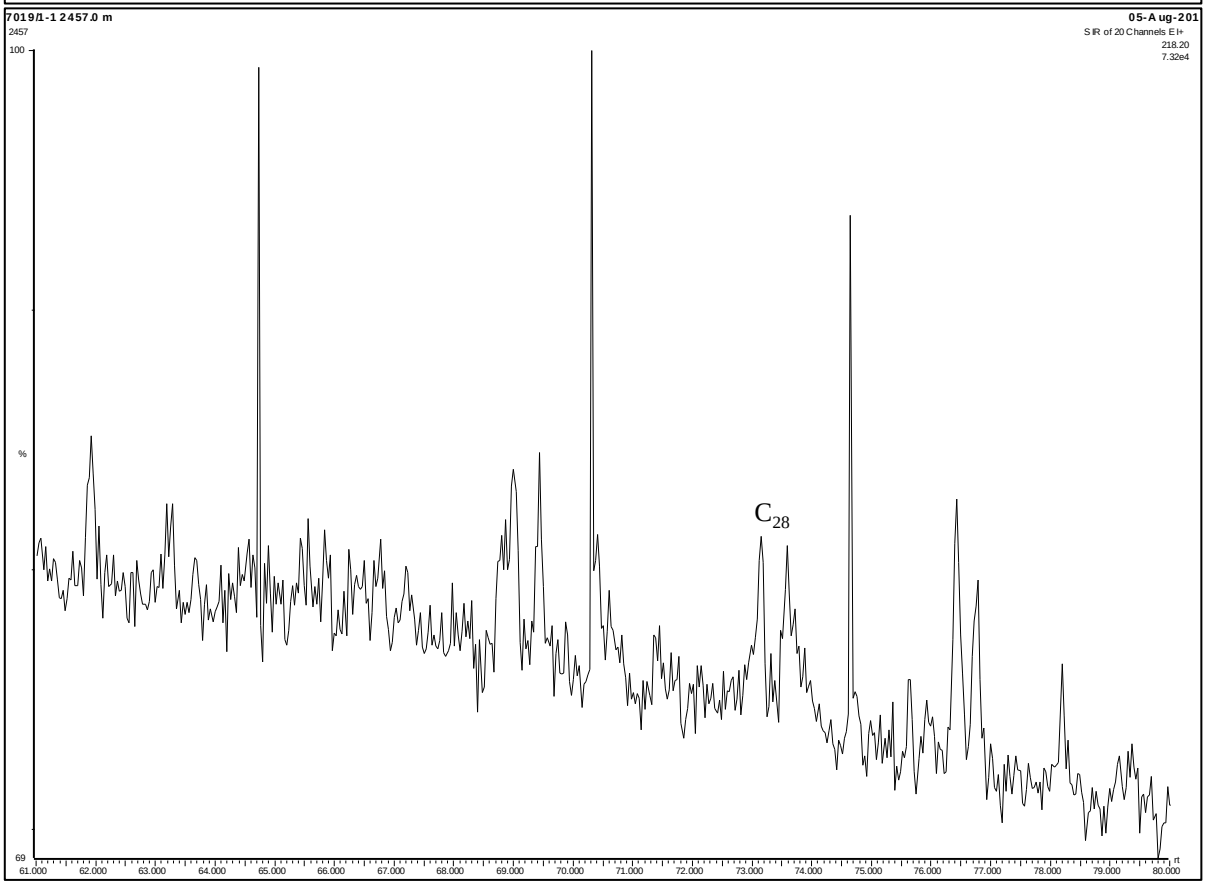
7019/1-1 2457.0 m
05-Aug-201
2457
SIR of 20 Channels EI+
218.20
7.32e4
100
%
69
61.000
62.000
63.000
64.000
65.000
66.000
67.000
68.000
69.000
70.000
71.000
72.000
73.000
74.000
75.000
76.000
77.000
78.000
79.000
80.000
rt
C28

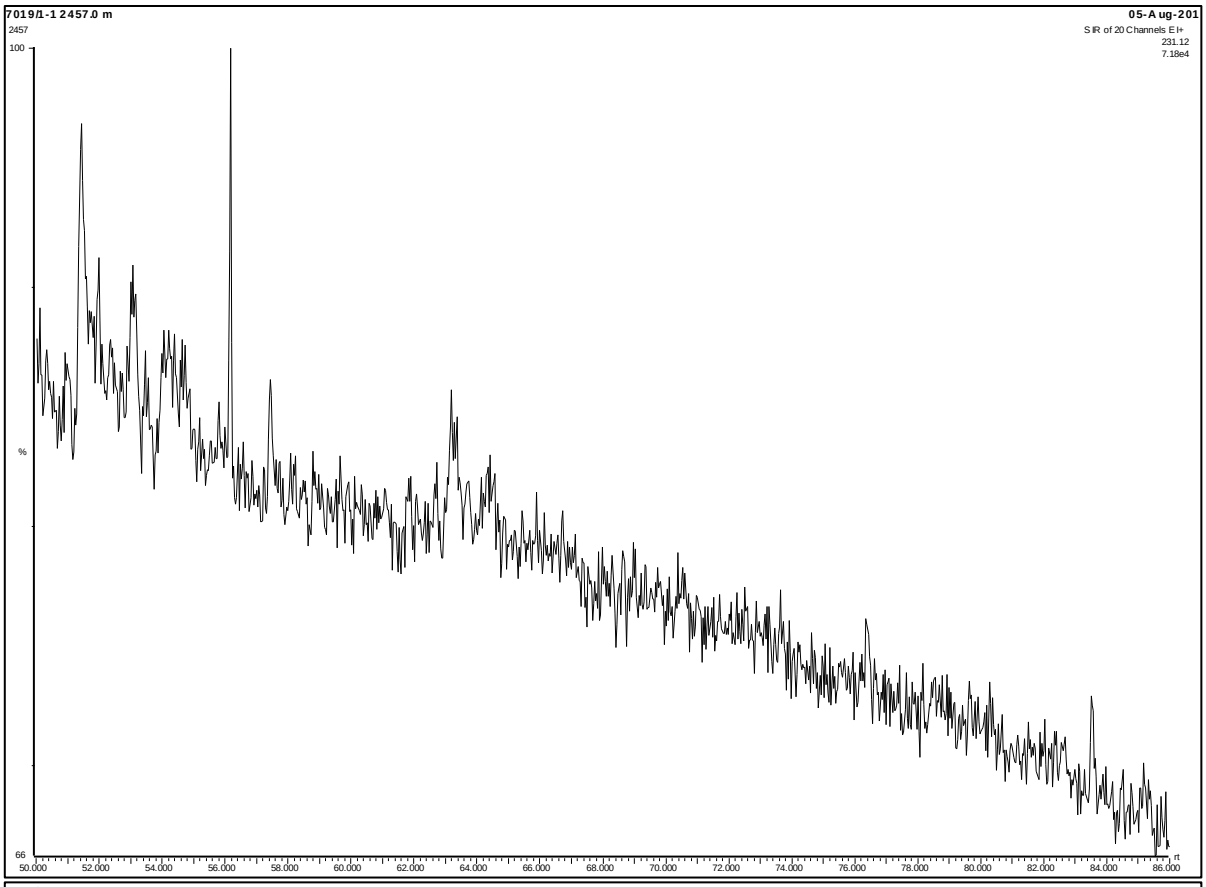
7019/1-1 2457.0 m
05-Aug-201
2457
SIR of 20 Channels EI+
231.12
7.18e4
100
%
66
50.000
52.000
54.000
56.000
58.000
60.000
62.000
64.000
66.000
68.000
70.000
72.000
74.000
76.000
78.000
80.000
82.000
84.000
86.000
rt

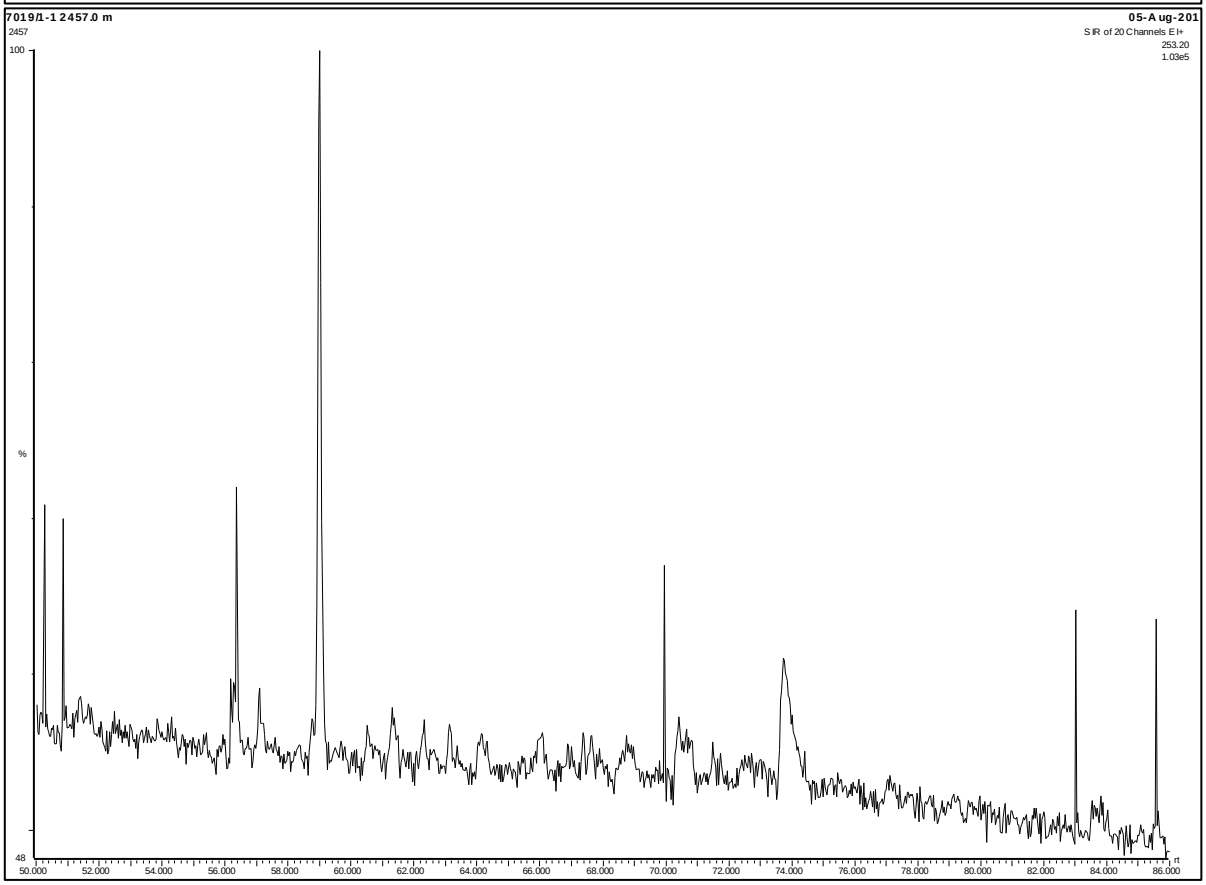
7019/1-1 2457.0 m
05-Aug-201
2457
SIR of 20 Channels EI+
253.20
1.03e5
100
%
48
50.000
52.000
54.000
56.000
58.000
60.000
62.000
64.000
66.000
68.000
70.000
72.000
74.000
76.000
78.000
80.000
82.000
84.000
86.000
rt

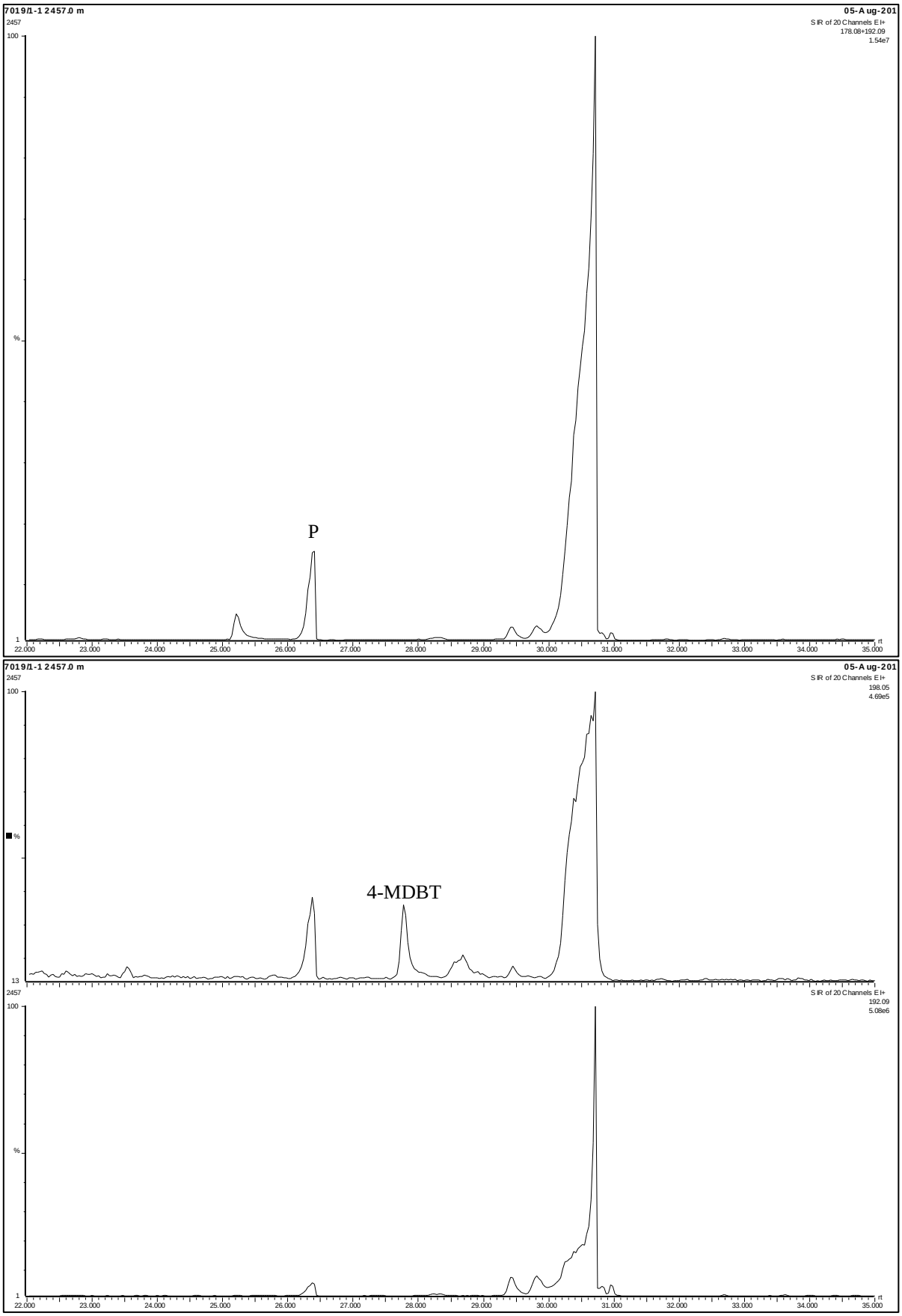
7019/1-1 2457.0 m
05-Aug-201
2457
SIR of 20 Channels EI+
178.08+192.09
1.54e7
100
%
1
P
22.000
23.000
24.000
25.000
26.000
27.000
28.000
29.000
30.000
31.000
32.000
33.000
34.000
35.000
rt
7019/1-1 2457.0 m
05-Aug-201
2457
SIR of 20 Channels EI+
198.05
4.69e5
100
%
13
4-MDBT
2457
SIR of 20 Channels EI+
192.09
5.08e6
100
%
1
22.000
23.000
24.000
25.000
26.000
27.000
28.000
29.000
30.000
31.000
32.000
33.000
34.000
35.000
rt

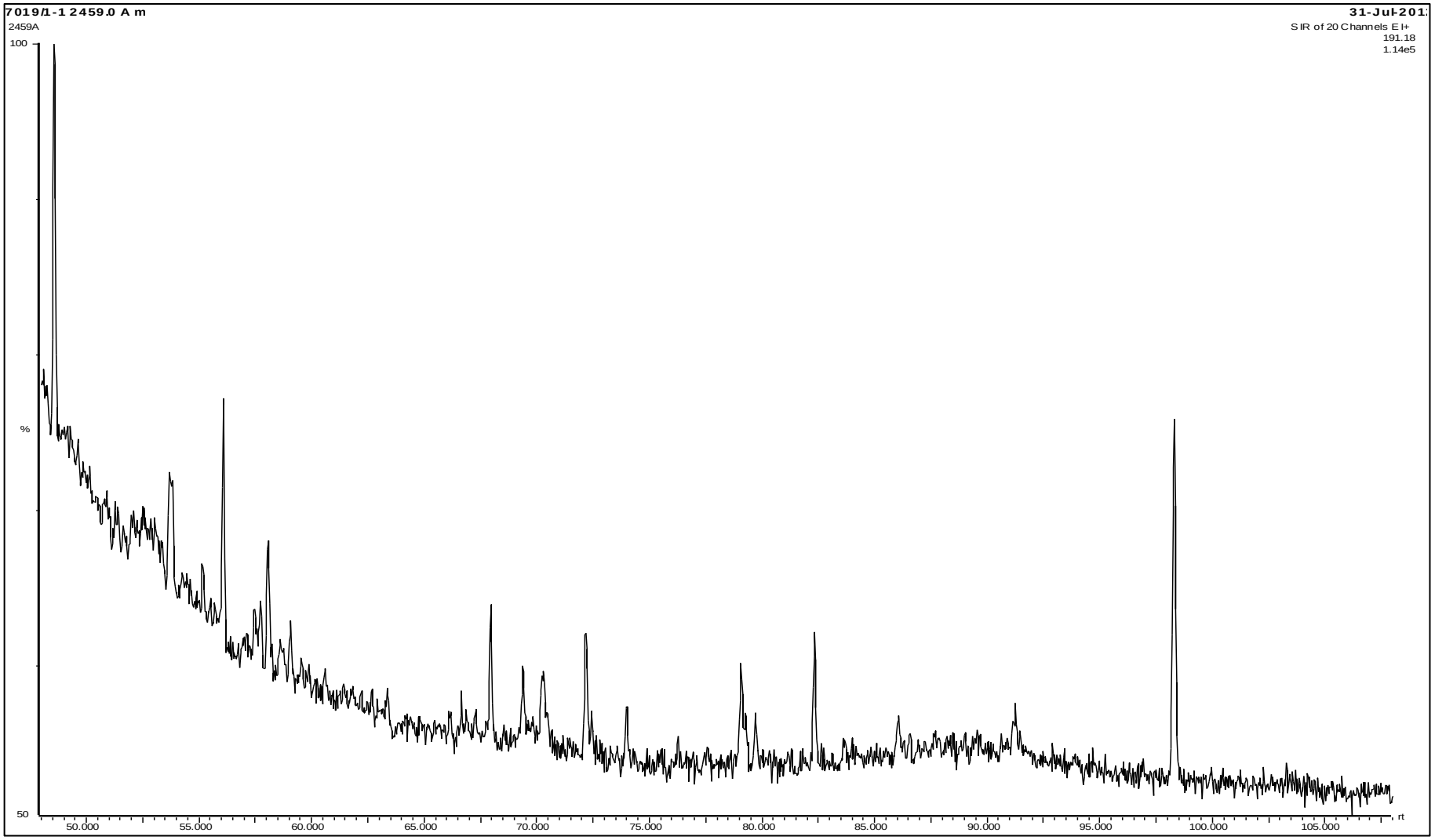
7019/1-1 2459.0 A m
2459A
31-Jul-201
SIR of 20 Channels EI+
191.18
1.14e5
100
%
50
50.000
55.000
60.000
65.000
70.000
75.000
80.000
85.000
90.000
95.000
100.000
105.000
rt

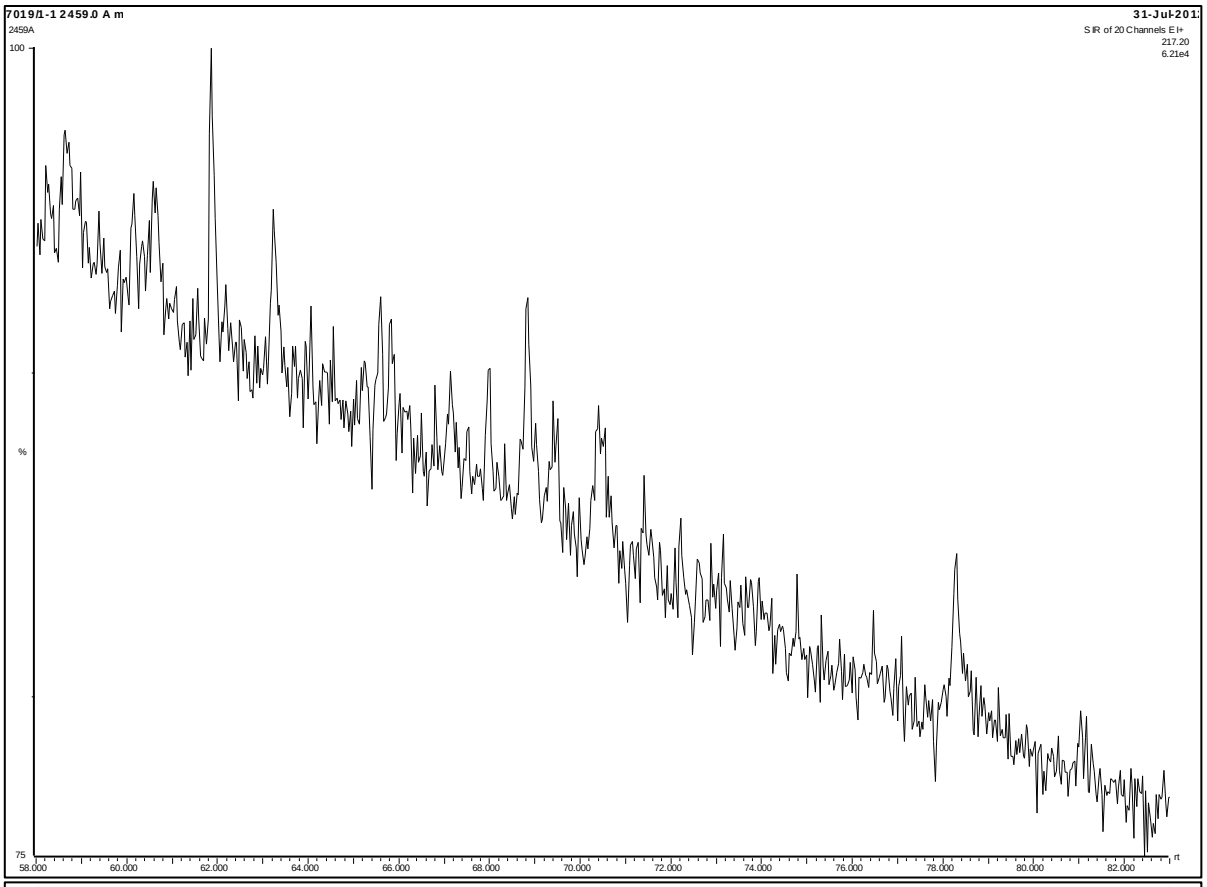
7019/1-1 2459.0 A m
31-Jul-201
2459A
SIR of 20 Channels EI+
217.20
6.21e4
100
%
75
58.000
60.000
62.000
64.000
66.000
68.000
70.000
72.000
74.000
76.000
78.000
80.000
82.000
rt

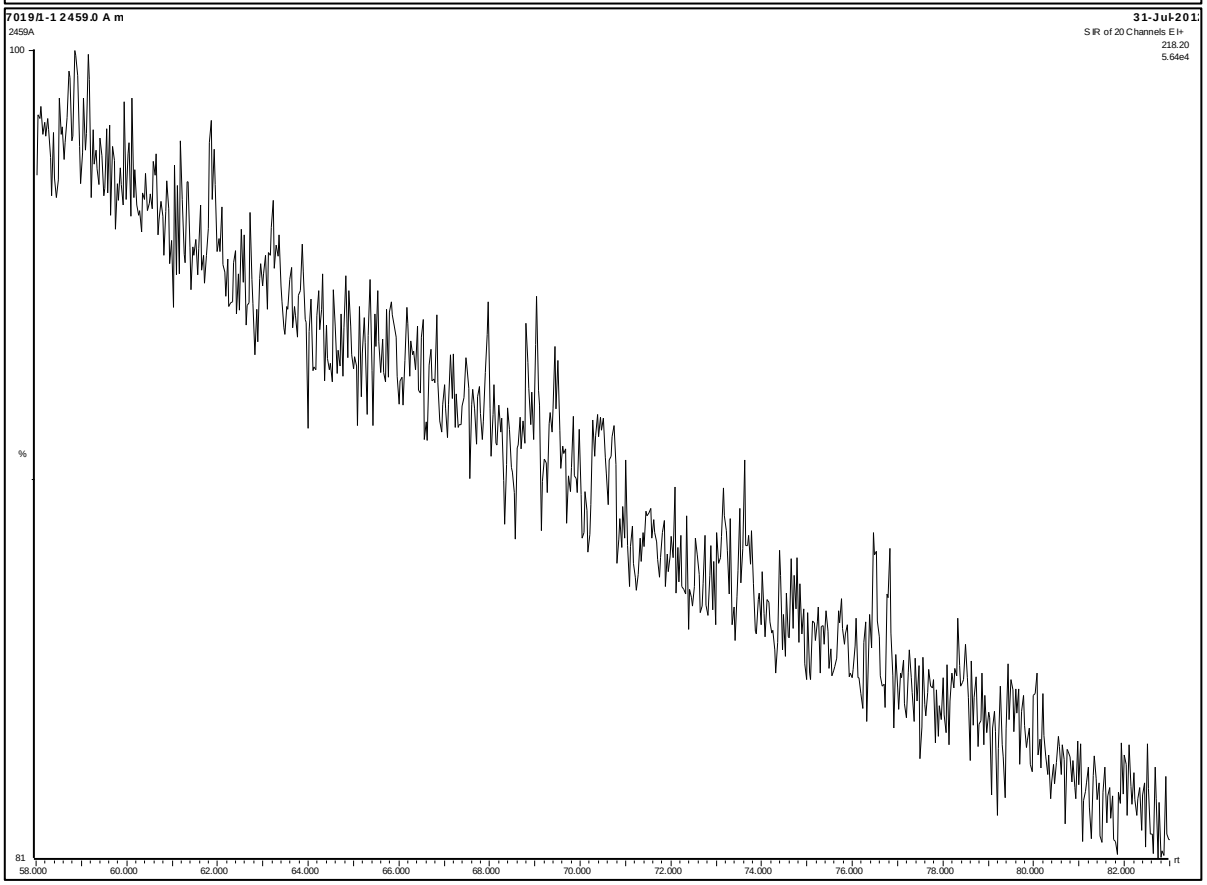
7019/1-1 2459.0 A m
31-Jul-201
2459A
SIR of 20 Channels EI+
218.20
5.64e4
100
%
81
58.000
60.000
62.000
64.000
66.000
68.000
70.000
72.000
74.000
76.000
78.000
80.000
82.000
rt

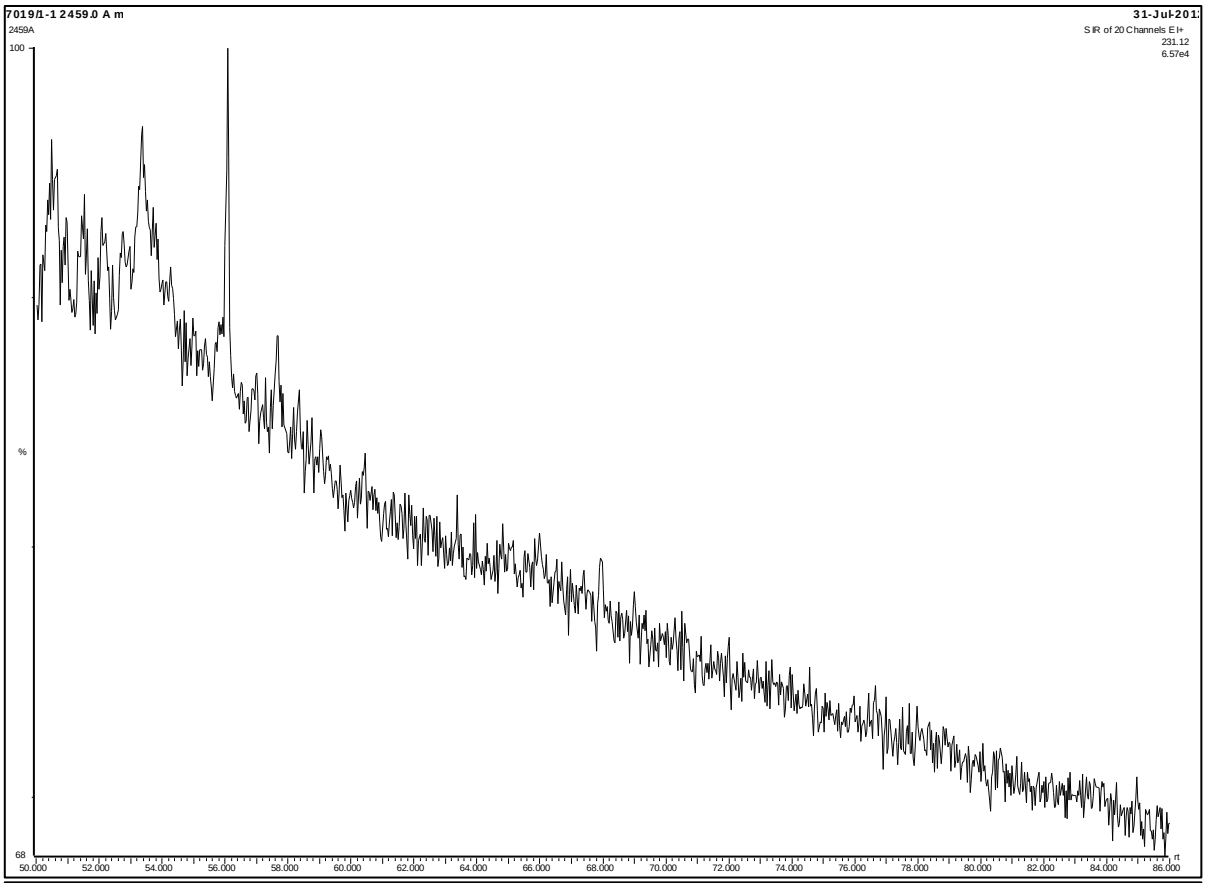
7019/1-1 2459.0 A m
31-Jul-201
2459A
SIR of 20 Channels EI+
231.12
6.57e4
100
%
68
50.000 52.000 54.000 56.000 58.000 60.000 62.000 64.000 66.000 68.000 70.000 72.000 74.000 76.000 78.000 80.000 82.000 84.000 86.000
rt

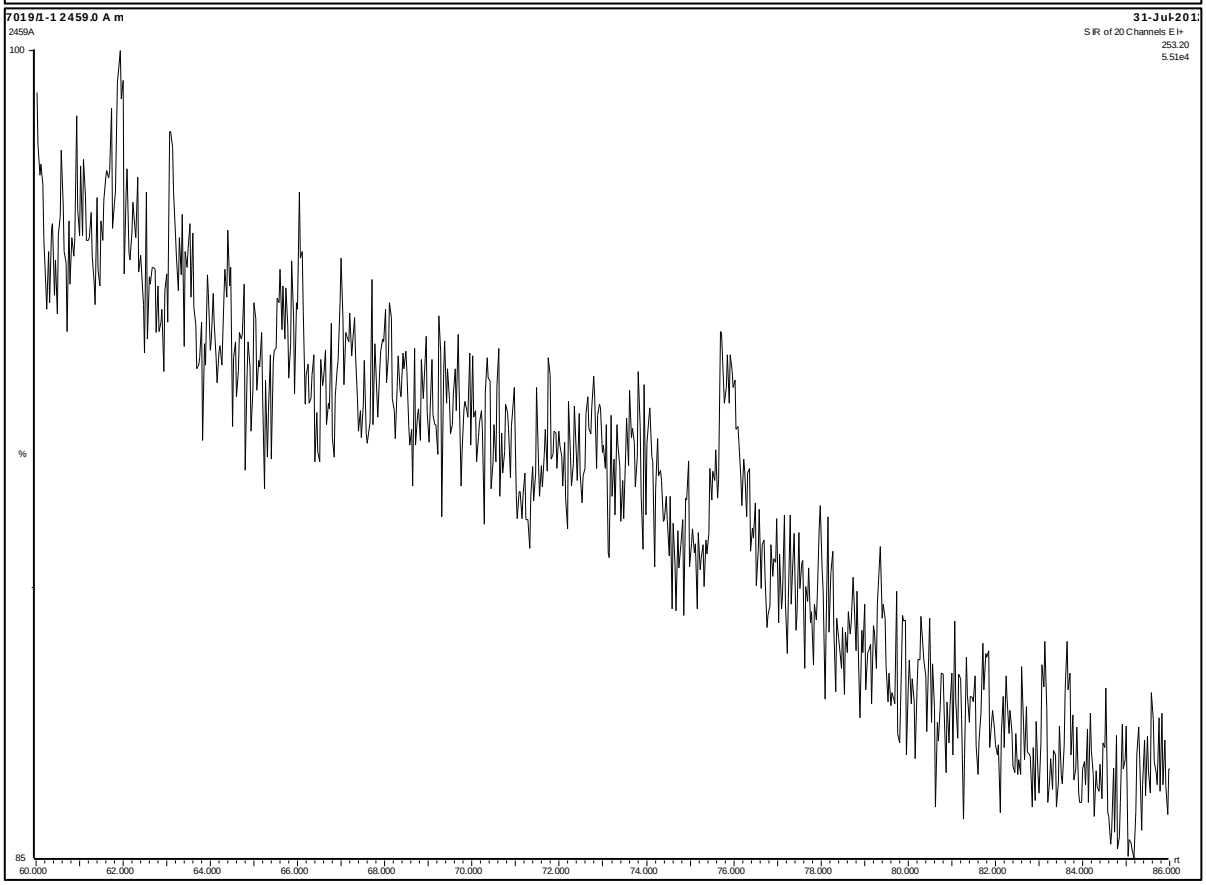
7019/1-1 2459.0 A m
31-Jul-201
2459A
SIR of 20 Channels EI+
253.20
5.51e4
100
%
85
60.000 62.000 64.000 66.000 68.000 70.000 72.000 74.000 76.000 78.000 80.000 82.000 84.000 86.000
rt

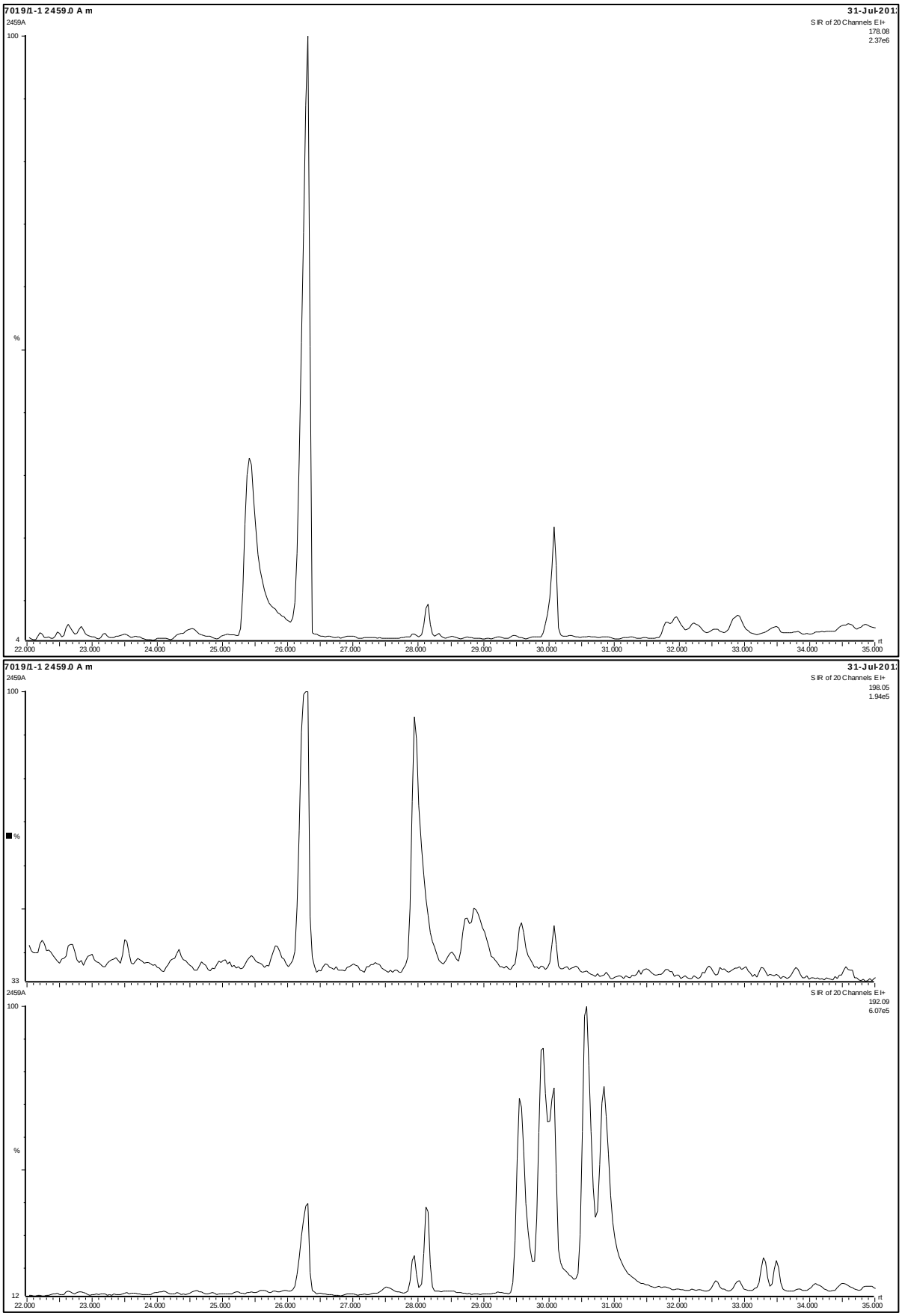
7019/1-1 2459.0 A m
31-Jul-201
2459A
SIR of 20 Channels EI+
178.08
2.37e6
100
%
4
22.000
23.000
24.000
25.000
26.000
27.000
28.000
29.000
30.000
31.000
32.000
33.000
34.000
35.000
rt
7019/1-1 2459.0 A m
31-Jul-201
2459A
SIR of 20 Channels EI+
198.05
1.94e5
100
%
33
2459A
SIR of 20 Channels EI+
192.09
6.07e5
100
%
12
22.000
23.000
24.000
25.000
26.000
27.000
28.000
29.000
30.000
31.000
32.000
33.000
34.000
35.000
rt

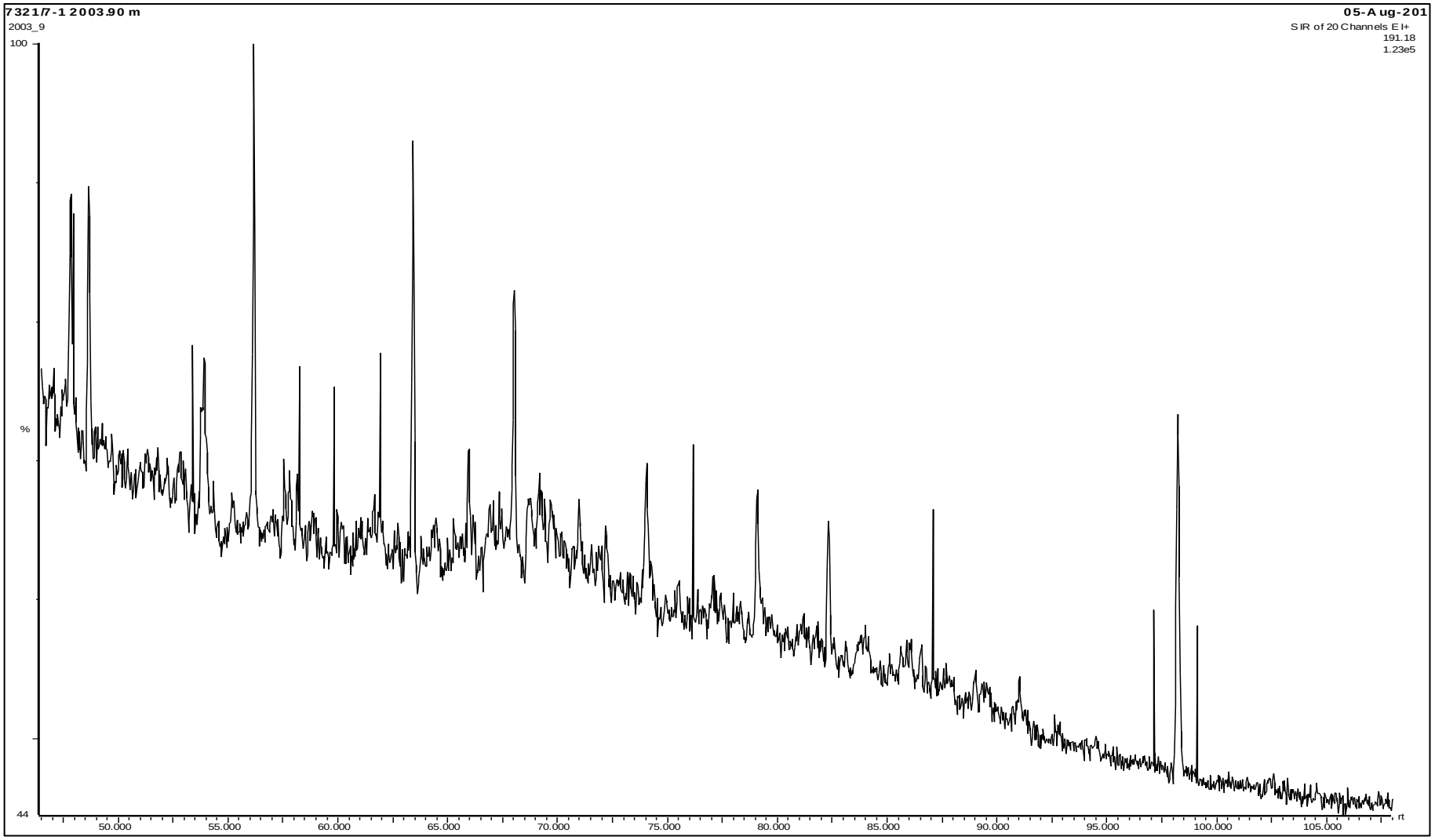
7321/7-1 2003.90 m
2003_9
05-Aug-201
SIR of 20 Channels EI+
191.18
1.23e5
100
%
44
50.000
55.000
60.000
65.000
70.000
75.000
80.000
85.000
90.000
95.000
100.000
105.000
rt

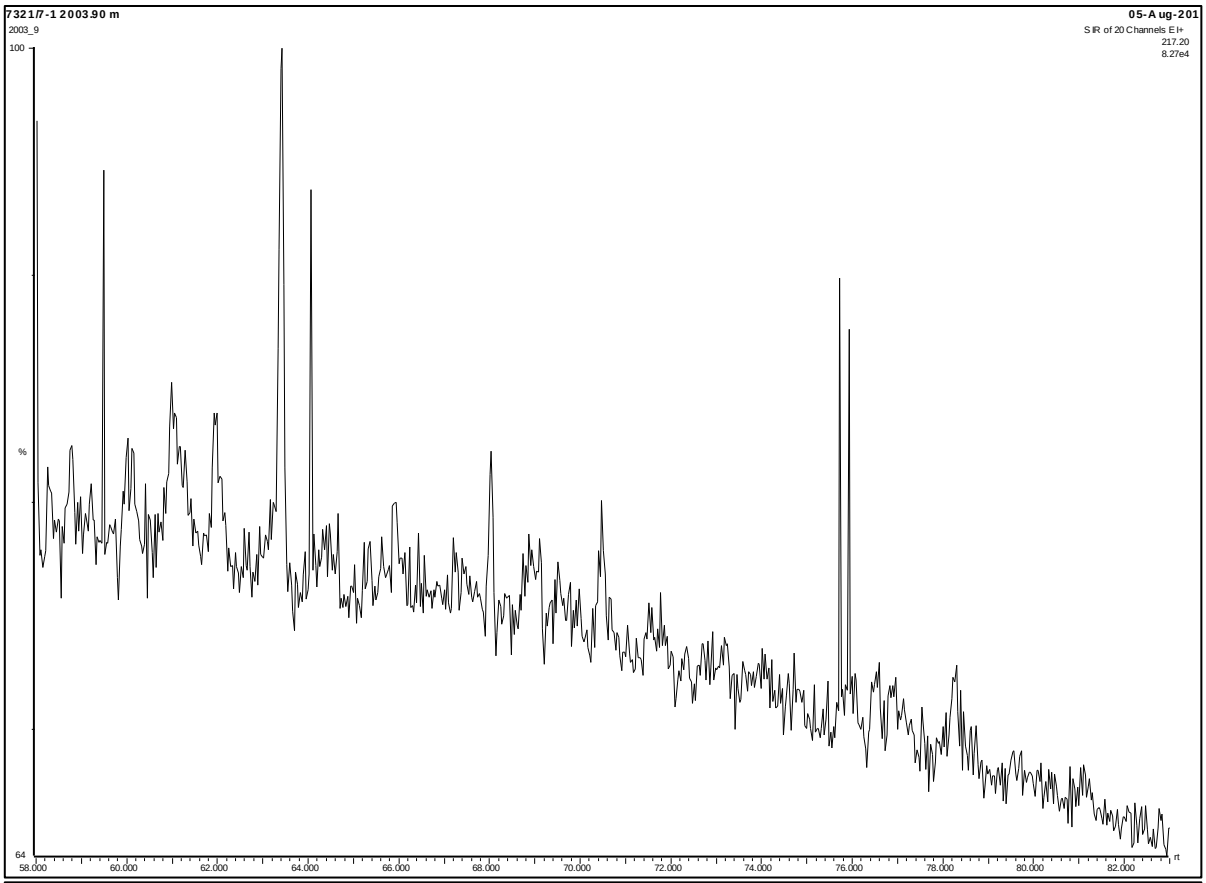
7321/7-1 2003.90 m
05-Aug-201
2003_9
SIR of 20 Channels EI+
217.20
8.27e4
100
%
64
58.000
60.000
62.000
64.000
66.000
68.000
70.000
72.000
74.000
76.000
78.000
80.000
82.000
rt

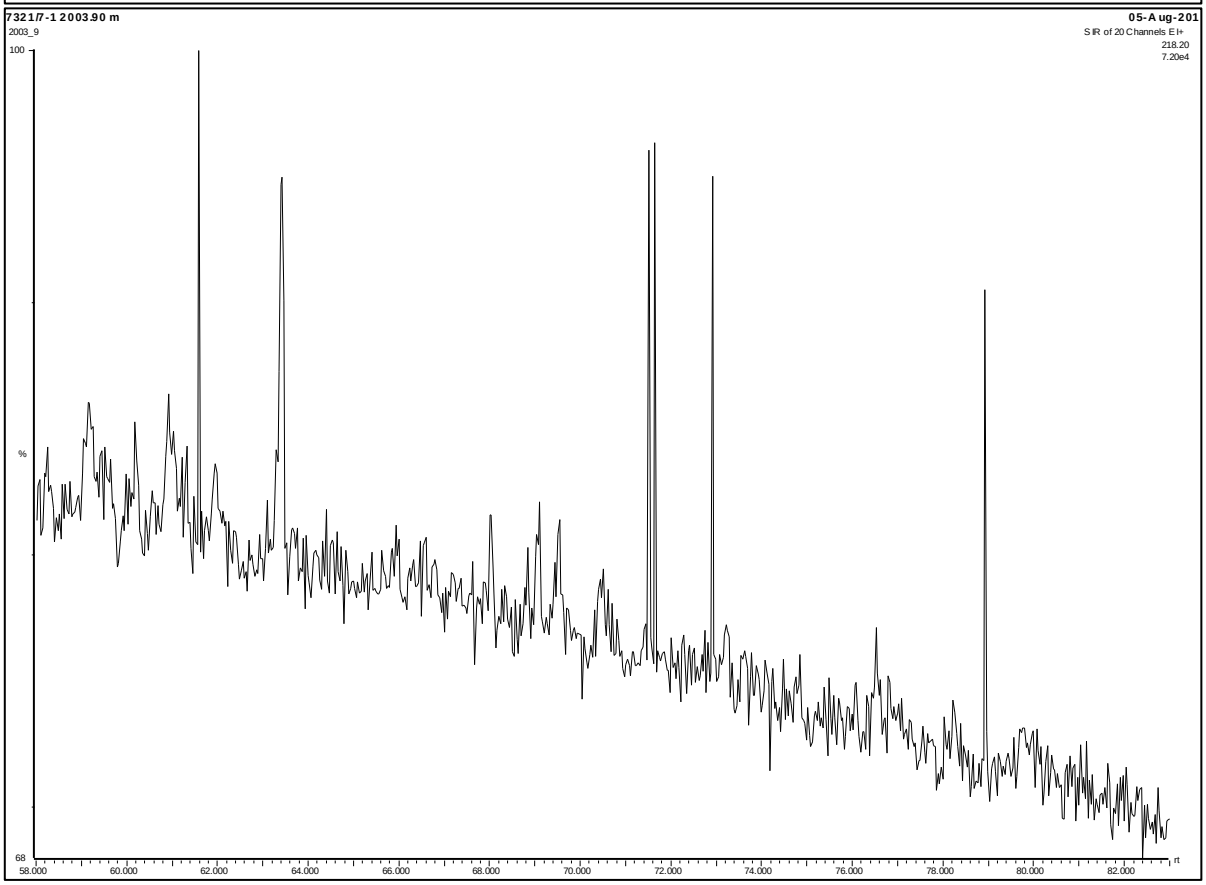
7321/7-1 2003.90 m
05-Aug-201
2003_9
SIR of 20 Channels EI+
218.20
7.20e4
100
%
68
58.000
60.000
62.000
64.000
66.000
68.000
70.000
72.000
74.000
76.000
78.000
80.000
82.000
rt

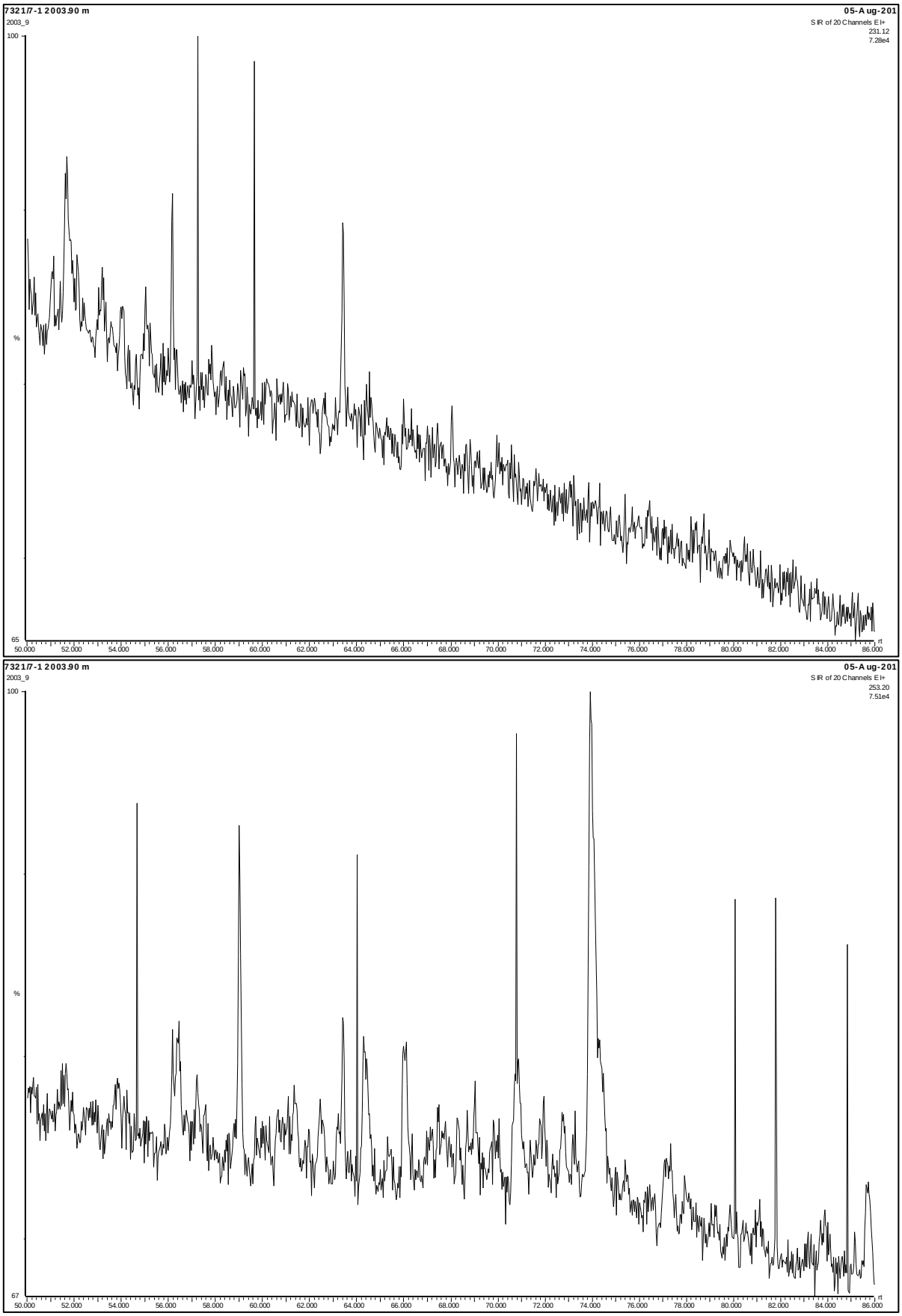
7321/7-1 2003.90 m
2003_9
05-Aug-201
SIR of 20 Channels EI+
231.12
7.28e4
100
%
65
50.000 52.000 54.000 56.000 58.000 60.000 62.000 64.000 66.000 68.000 70.000 72.000 74.000 76.000 78.000 80.000 82.000 84.000 86.000
rt
7321/7-1 2003.90 m
2003_9
05-Aug-201
SIR of 20 Channels EI+
253.20
7.51e4
100
%
67
50.000 52.000 54.000 56.000 58.000 60.000 62.000 64.000 66.000 68.000 70.000 72.000 74.000 76.000 78.000 80.000 82.000 84.000 86.000
rt

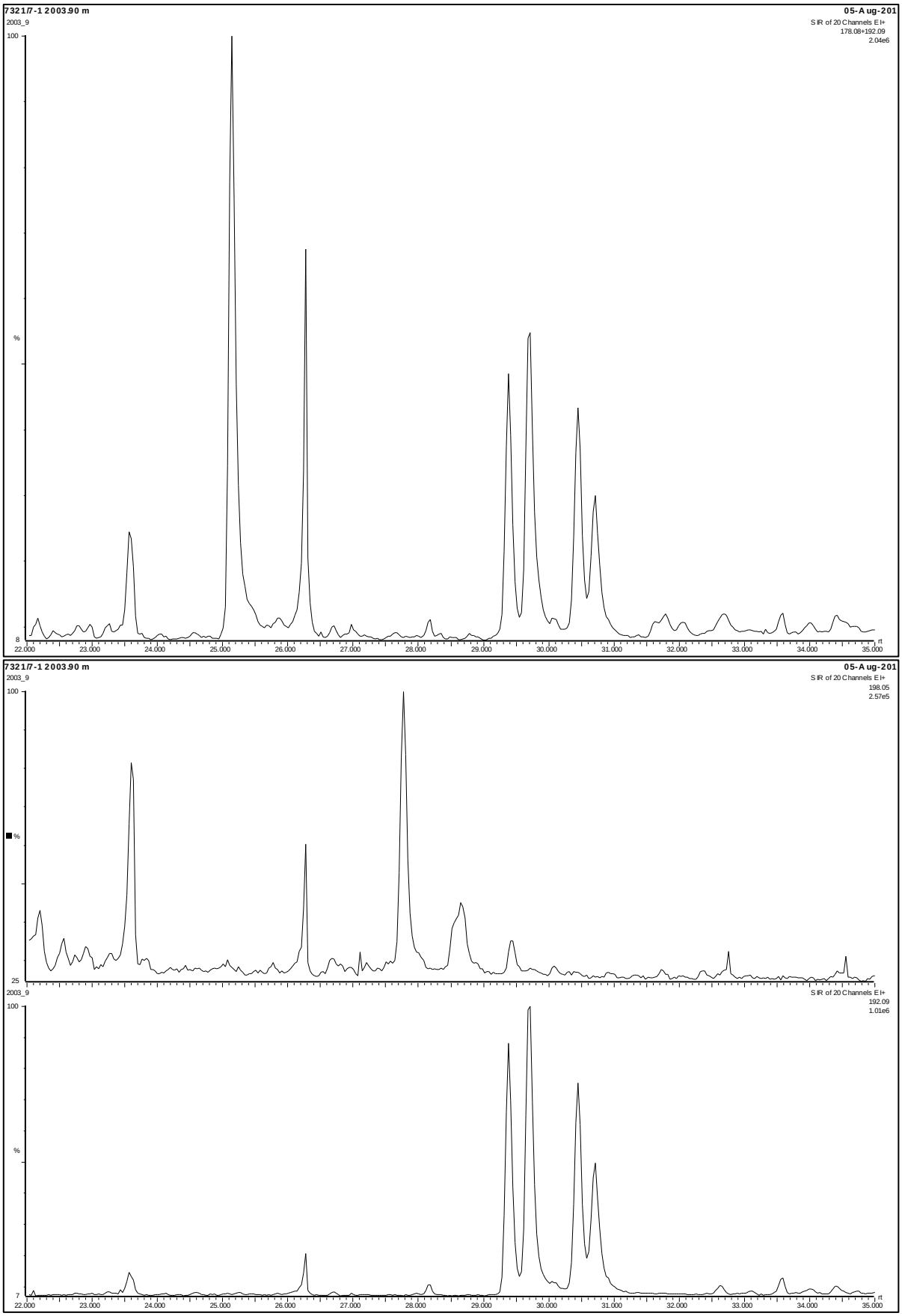
7321/7-1 2003.90 m
05-Aug-201
2003_9
SIR of 20 Channels EI+
178.08+192.09
2.04e6
100
%
8
22.000
23.000
24.000
25.000
26.000
27.000
28.000
29.000
30.000
31.000
32.000
33.000
34.000
35.000
rt
7321/7-1 2003.90 m
05-Aug-201
2003_9
SIR of 20 Channels EI+
198.05
2.57e5
100
%
25
2003_9
SIR of 20 Channels EI+
192.09
1.01e6
100
%
7
22.000
23.000
24.000
25.000
26.000
27.000
28.000
29.000
30.000
31.000
32.000
33.000
34.000
35.000
rt

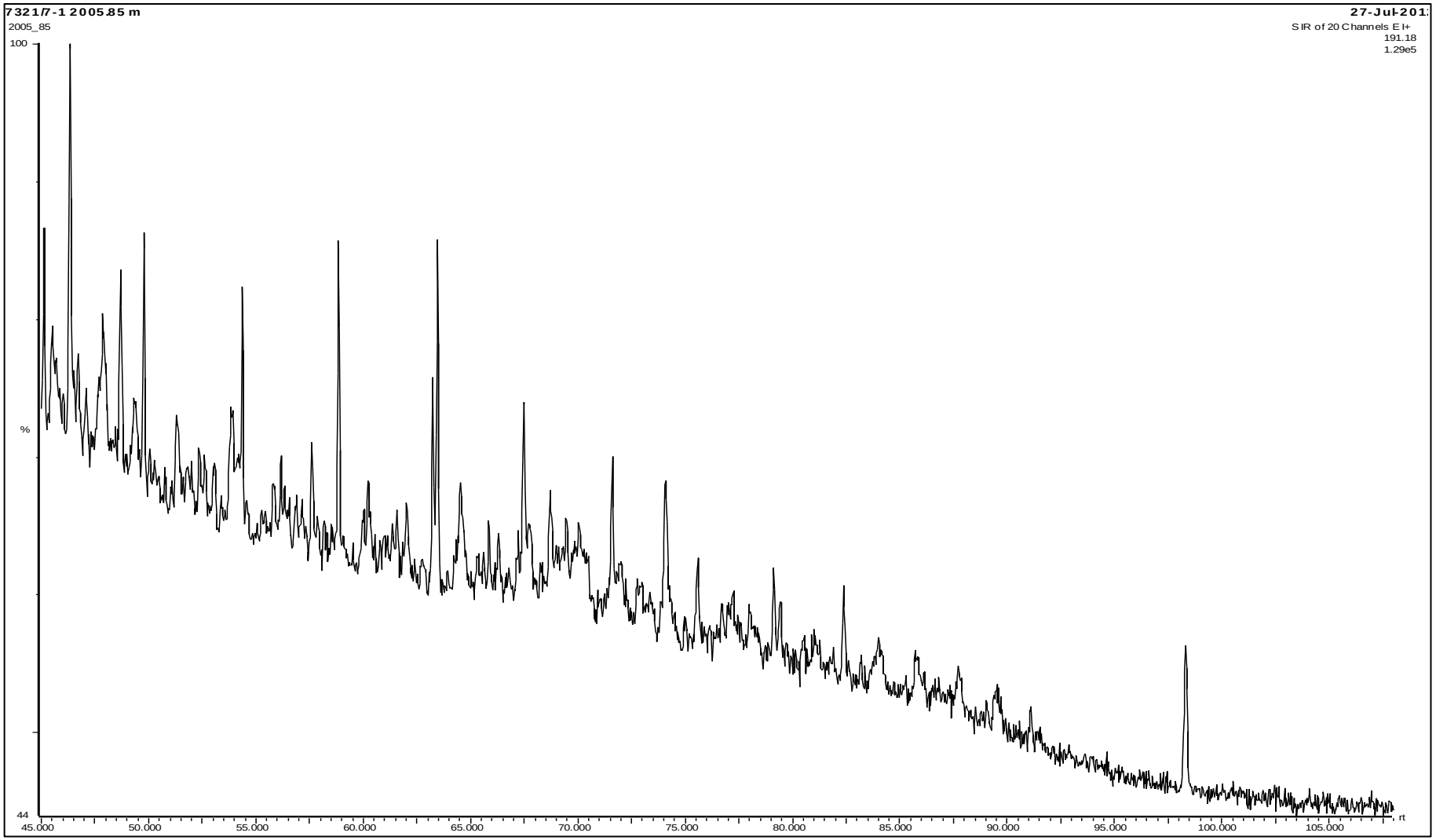
7321/7-1 2005.85 m
2005_85
27-Jul-201
SIR of 20 Channels EI+
191.18
1.29e5
100
%
44
45.000
50.000
55.000
60.000
65.000
70.000
75.000
80.000
85.000
90.000
95.000
100.000
105.000
rt

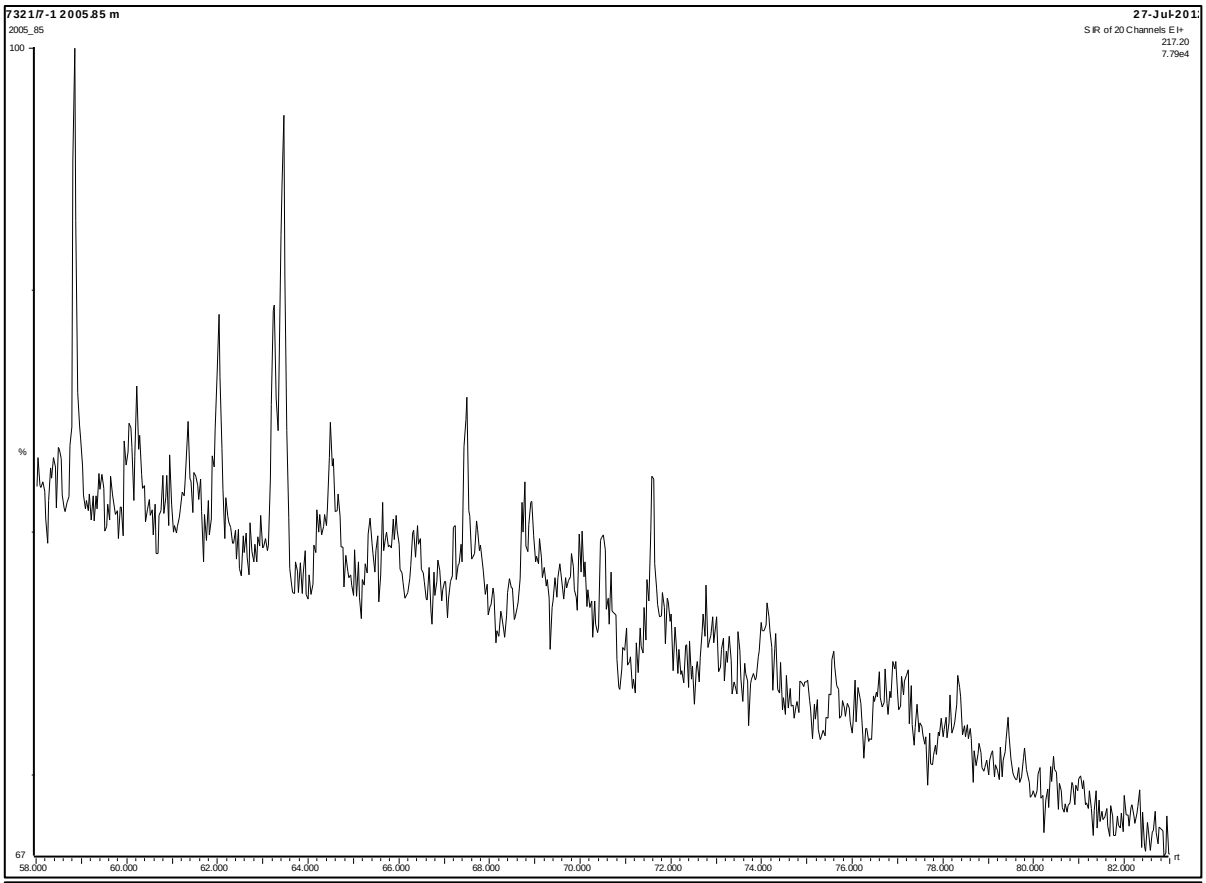
7321/7-1 2005.85 m
2005_85
27-Jul-201
SIR of 20 Channels EI+
217.20
7.79e4
100
%
67
58.000
60.000
62.000
64.000
66.000
68.000
70.000
72.000
74.000
76.000
78.000
80.000
82.000
rt

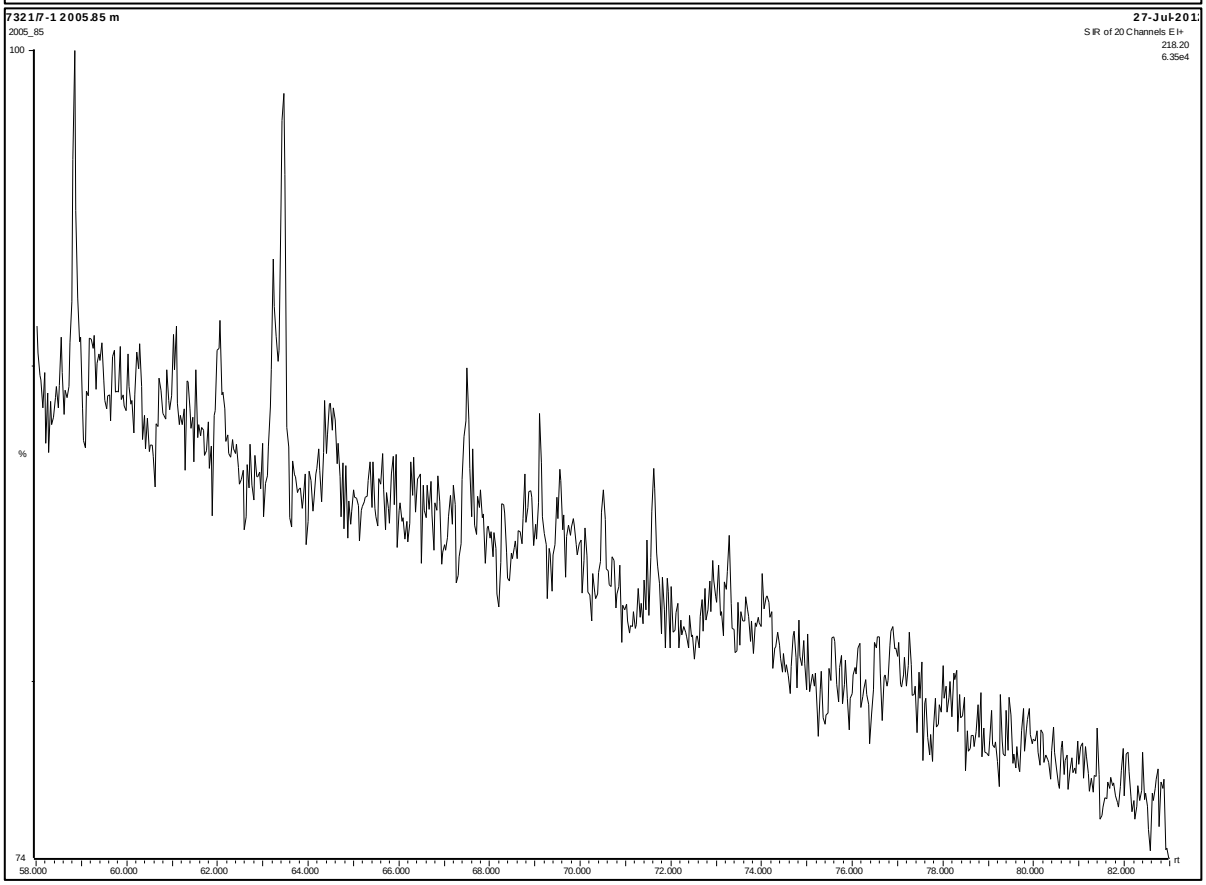
7321/7-1 2005.85 m
2005_85
27-Jul-201
SIR of 20 Channels EI+
218.20
6.35e4
100
%
74
58.000
60.000
62.000
64.000
66.000
68.000
70.000
72.000
74.000
76.000
78.000
80.000
82.000
rt

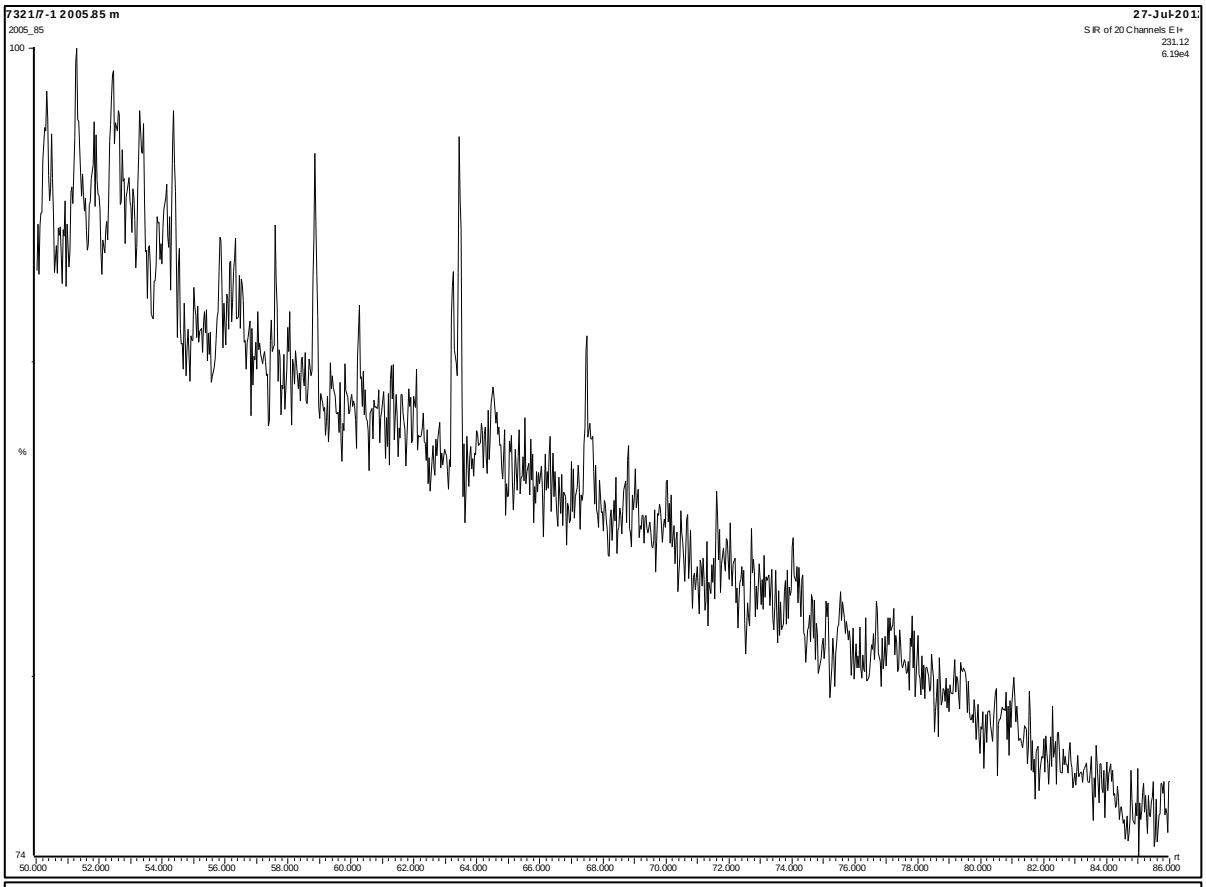
7321/7-1 2005.85 m
2005_85
27-Jul-201
SIR of 20 Channels EI+
231.12
6.19e4
100
%
74
50.000 52.000 54.000 56.000 58.000 60.000 62.000 64.000 66.000 68.000 70.000 72.000 74.000 76.000 78.000 80.000 82.000 84.000 86.000
rt

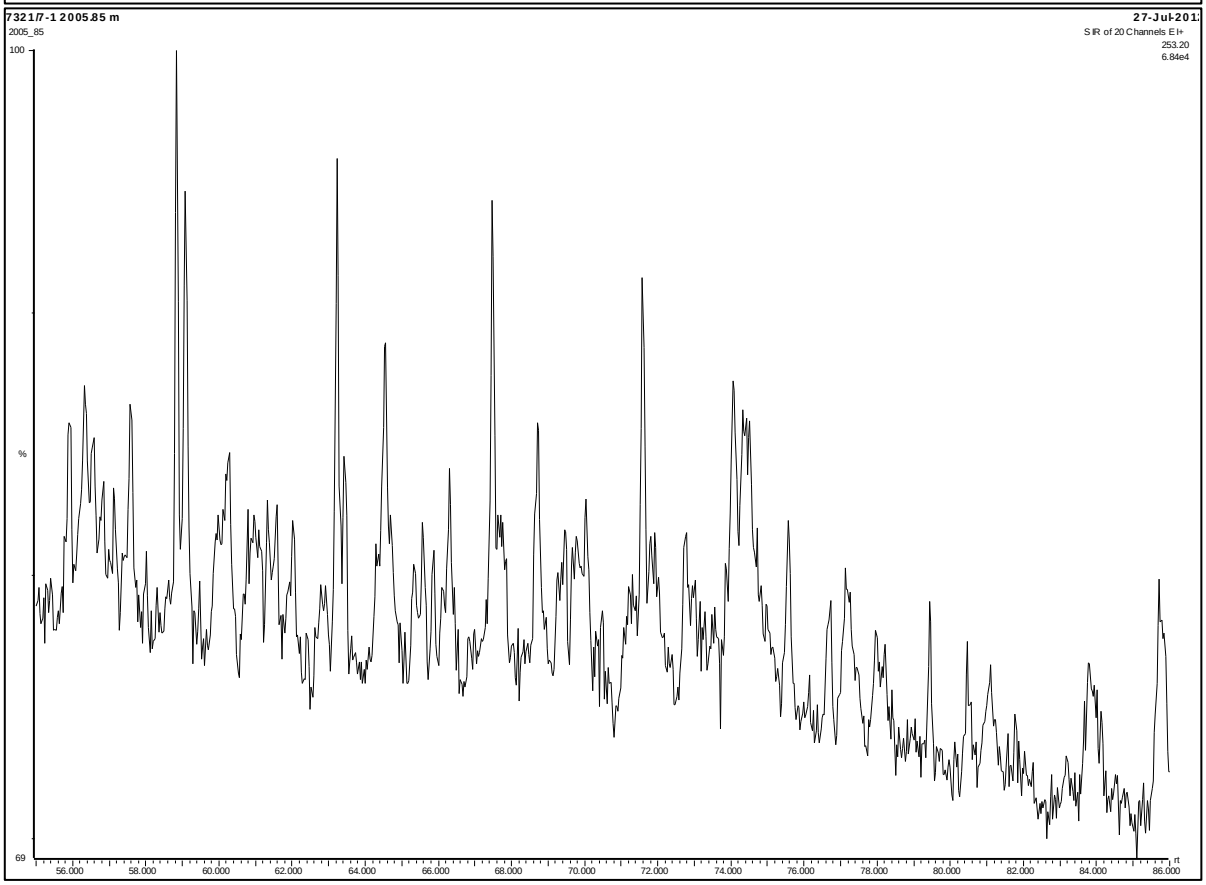
7321/7-1 2005.85 m
2005_85
27-Jul-201
SIR of 20 Channels EI+
253.20
6.84e4
100
%
69
56.000 58.000 60.000 62.000 64.000 66.000 68.000 70.000 72.000 74.000 76.000 78.000 80.000 82.000 84.000 86.000
rt

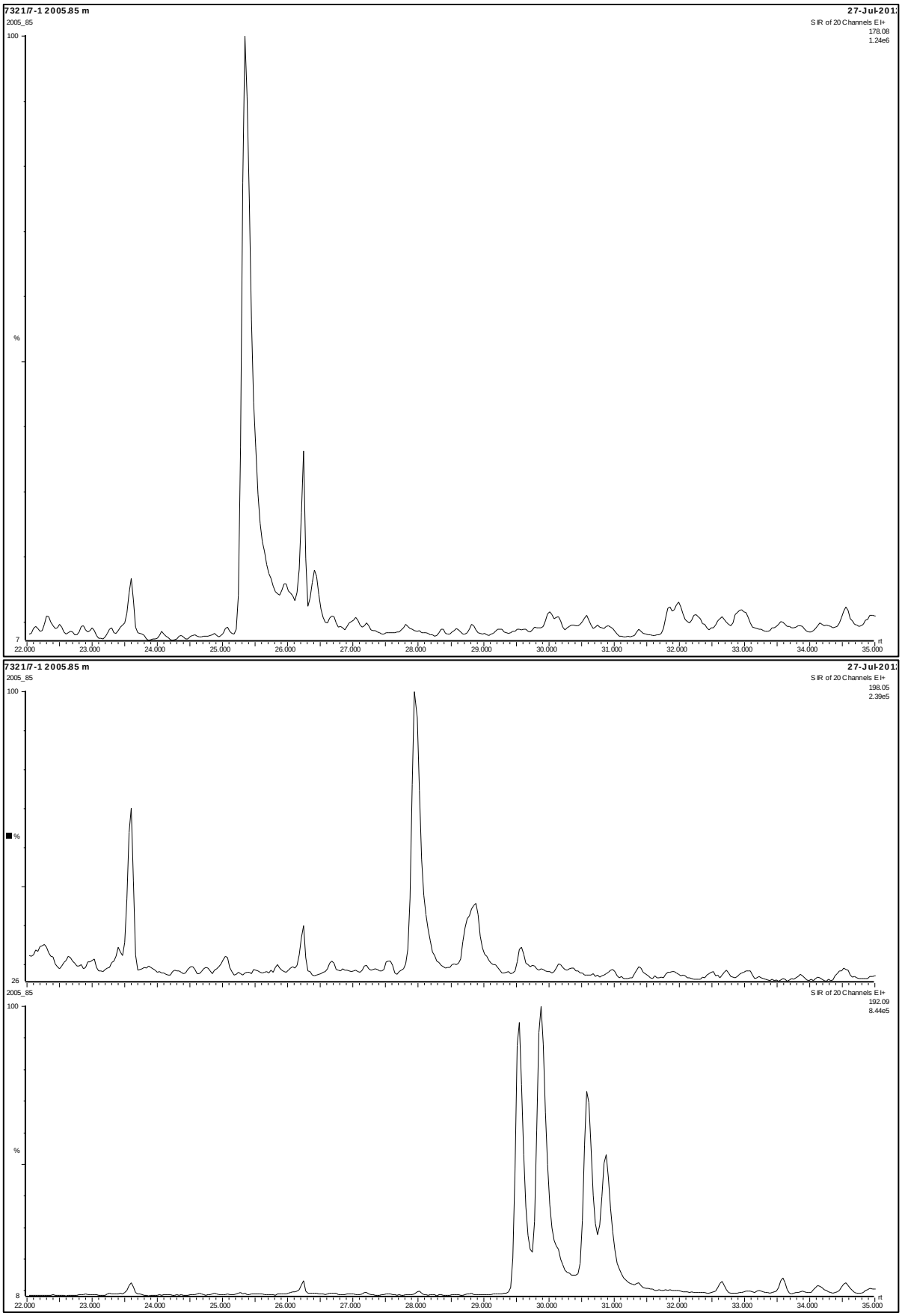
7321/7-1 2005.85 m
27-Jul-201
2005_85
SIR of 20 Channels EI+
178.08
1.24e6
100
%
7
22.000
23.000
24.000
25.000
26.000
27.000
28.000
29.000
30.000
31.000
32.000
33.000
34.000
35.000
rt
7321/7-1 2005.85 m
27-Jul-201
2005_85
SIR of 20 Channels EI+
198.05
2.39e5
100
%
26
2005_85
SIR of 20 Channels EI+
192.09
8.44e5
100
%
8
22.000
23.000
24.000
25.000
26.000
27.000
28.000
29.000
30.000
31.000
32.000
33.000
34.000
35.000
rt

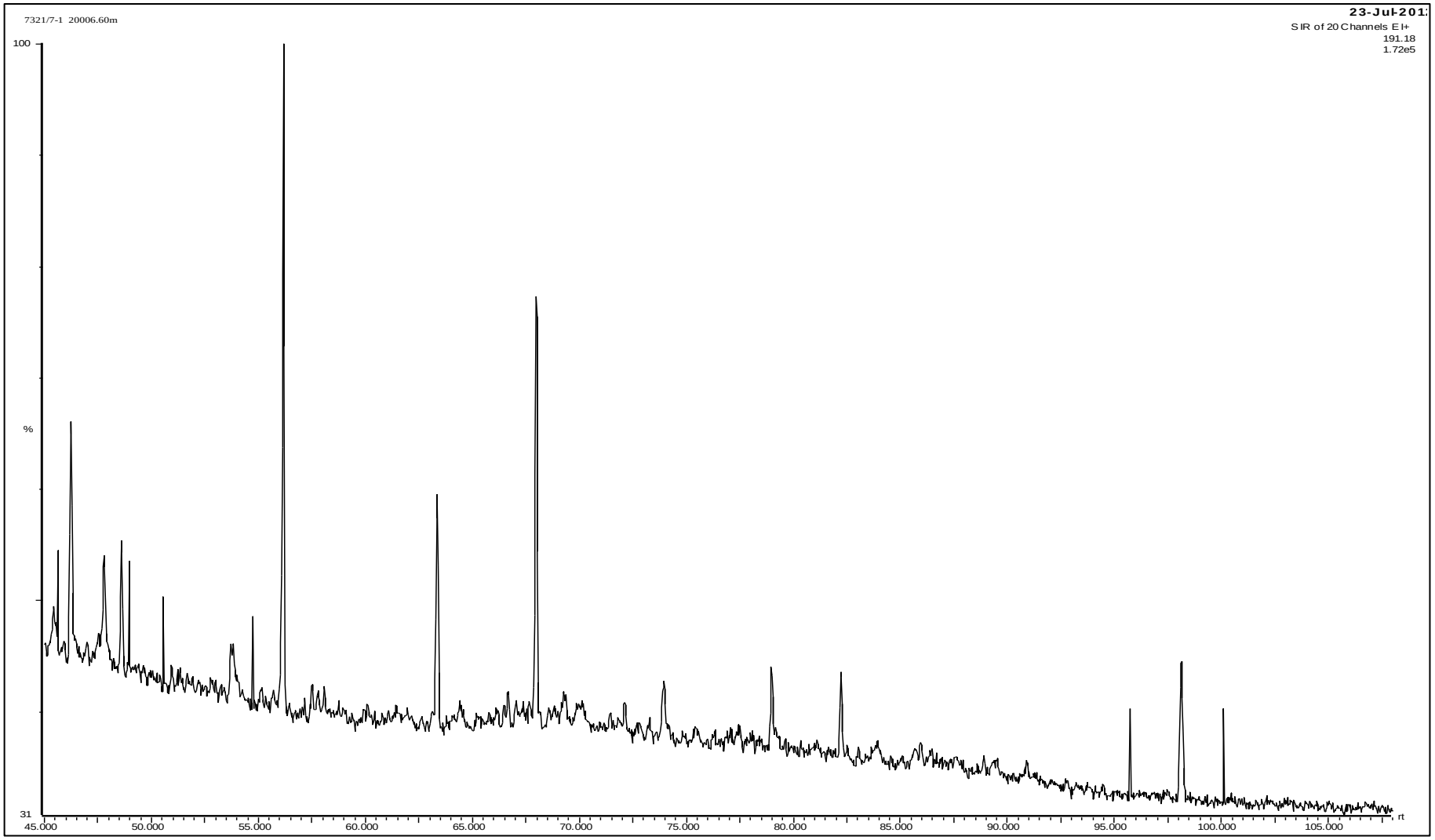
7321/7-1 20006.60m
23-Jul-201
SIR of 20 Channels EI+
191.18
1.72e5
100
%
31
45.000
50.000
55.000
60.000
65.000
70.000
75.000
80.000
85.000
90.000
95.000
100.000
105.000
rt

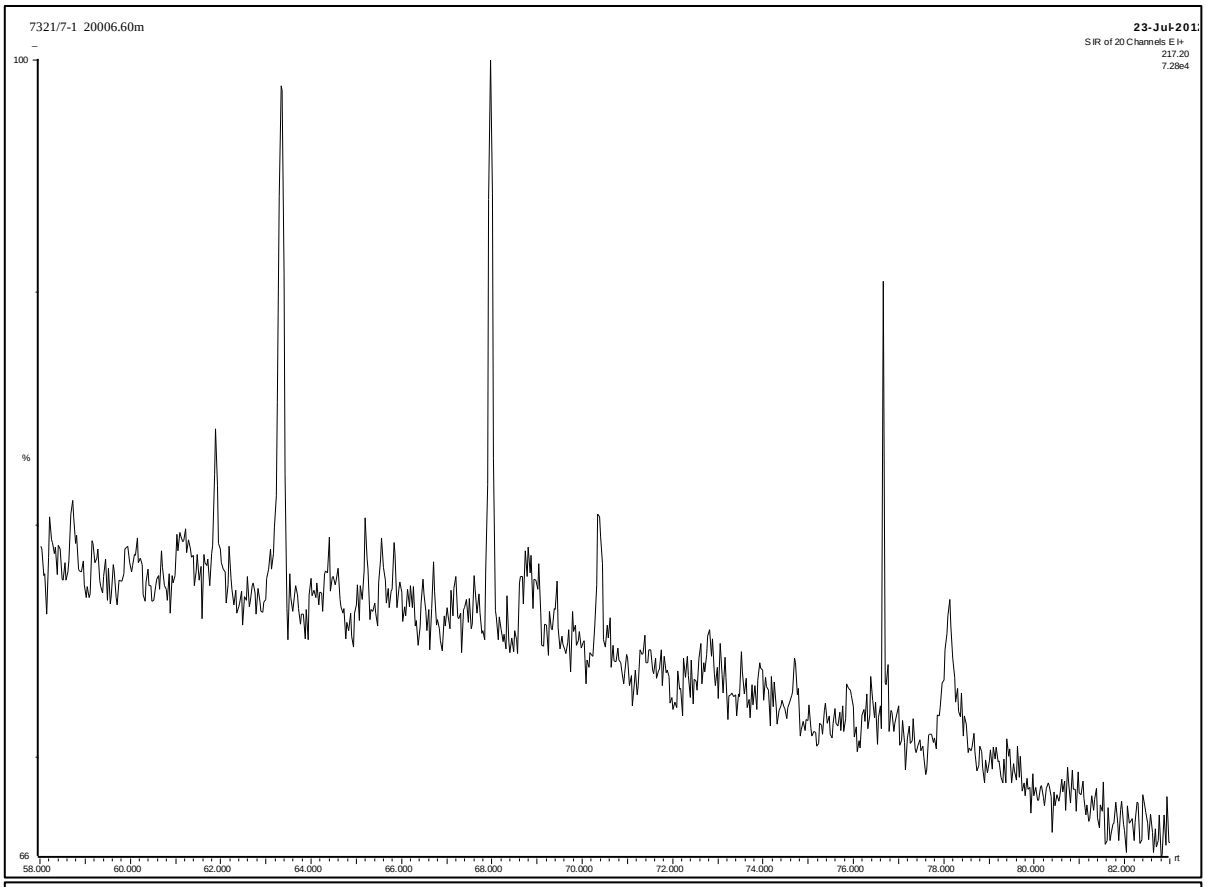
7321/7-1 20006.60m
23-Jul-201
SIR of 20 Channels EI+
217.20
7.28e4
100
%
66
58.000
60.000
62.000
64.000
66.000
68.000
70.000
72.000
74.000
76.000
78.000
80.000
82.000
rt

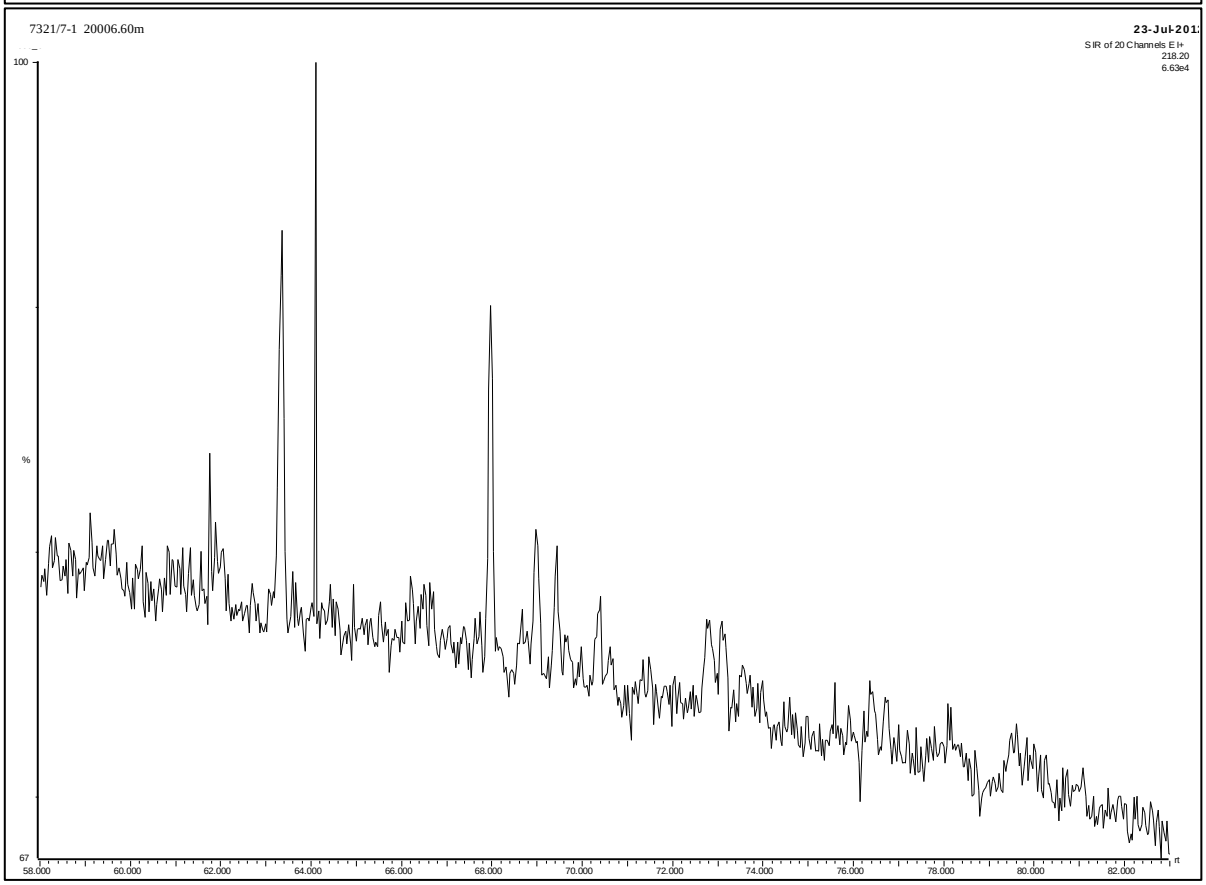
7321/7-1 20006.60m
23-Jul-201
SIR of 20 Channels EI+
218.20
6.63e4
100
%
67
58.000
60.000
62.000
64.000
66.000
68.000
70.000
72.000
74.000
76.000
78.000
80.000
82.000
rt

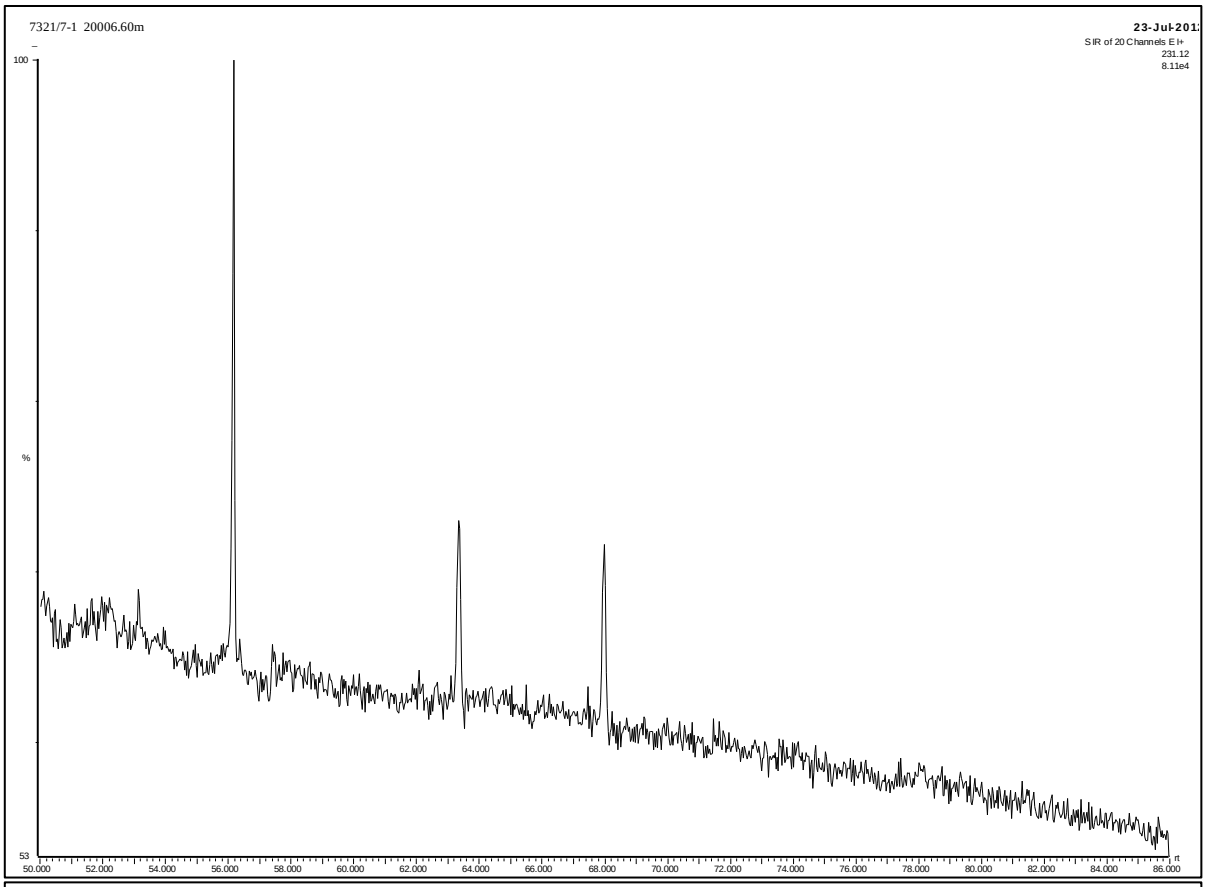
7321/7-1 20006.60m
23-Jul-201
SIR of 20 Channels EI+
231.12
8.11e4
100
%
53
50.000
52.000
54.000
56.000
58.000
60.000
62.000
64.000
66.000
68.000
70.000
72.000
74.000
76.000
78.000
80.000
82.000
84.000
86.000
rt

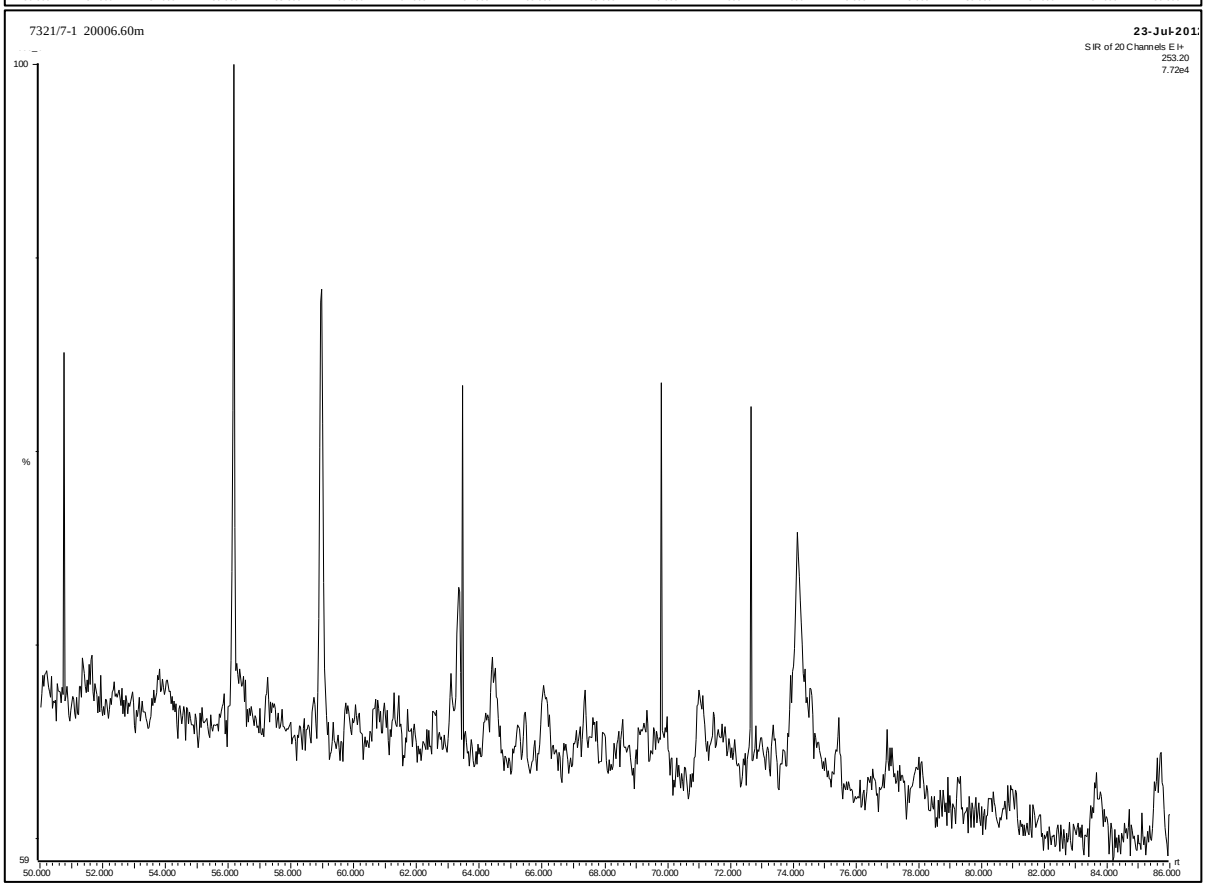
7321/7-1 20006.60m
23-Jul-201
SIR of 20 Channels EI+
253.20
7.72e4
100
%
59
50.000
52.000
54.000
56.000
58.000
60.000
62.000
64.000
66.000
68.000
70.000
72.000
74.000
76.000
78.000
80.000
82.000
84.000
86.000
rt

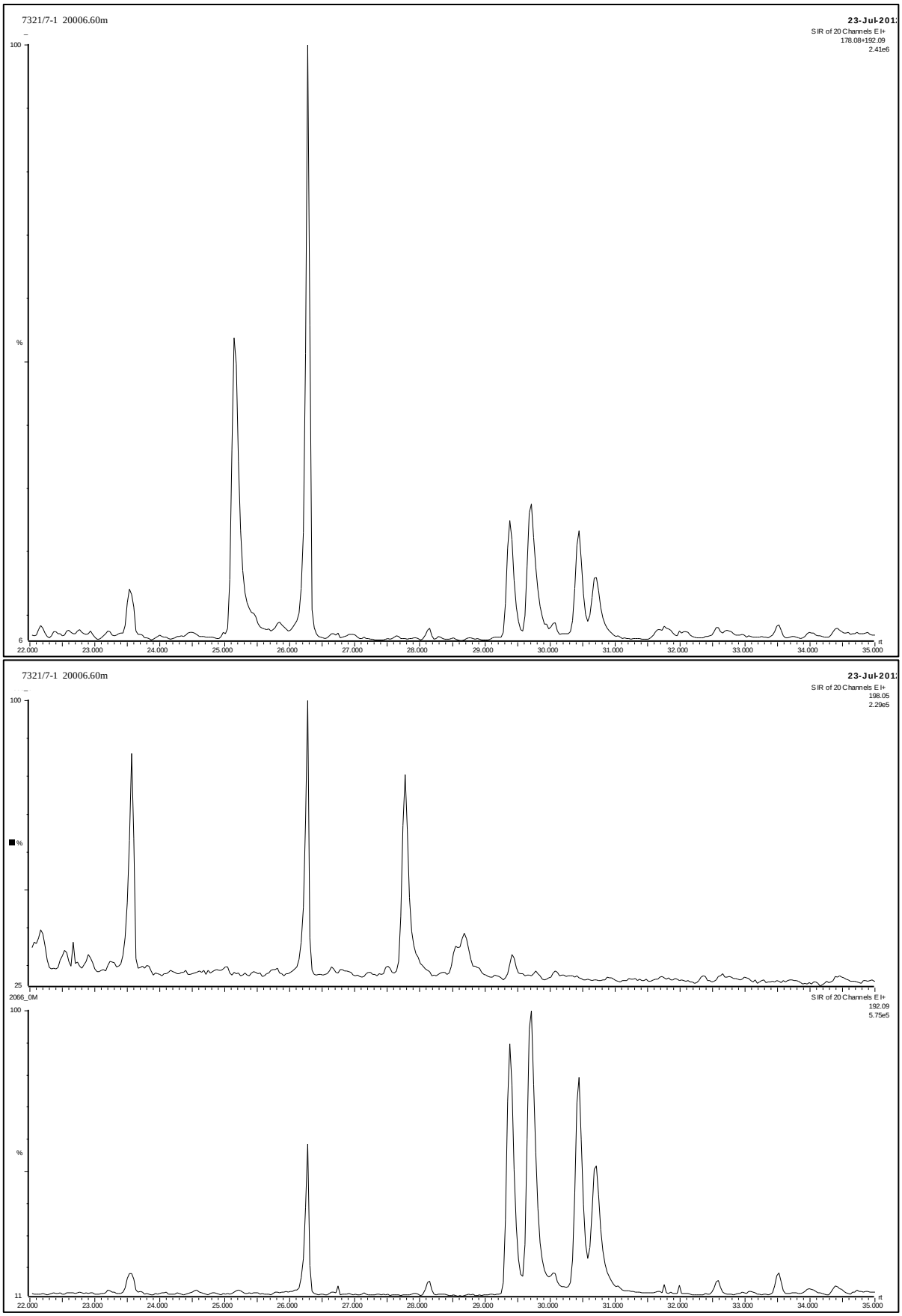
7321/7-1 20006.60m
23-Jul-201
SIR of 20 Channels E I+
178.08+192.09
2.41e6
100
%
6
22.000
23.000
24.000
25.000
26.000
27.000
28.000
29.000
30.000
31.000
32.000
33.000
34.000
35.000
rt
7321/7-1 20006.60m
23-Jul-201
SIR of 20 Channels E I+
198.05
2.29e5
100
%
25
2066_0M
SIR of 20 Channels E I+
192.09
5.75e5
100
%
11
22.000
23.000
24.000
25.000
26.000
27.000
28.000
29.000
30.000
31.000
32.000
33.000
34.000
35.000
rt

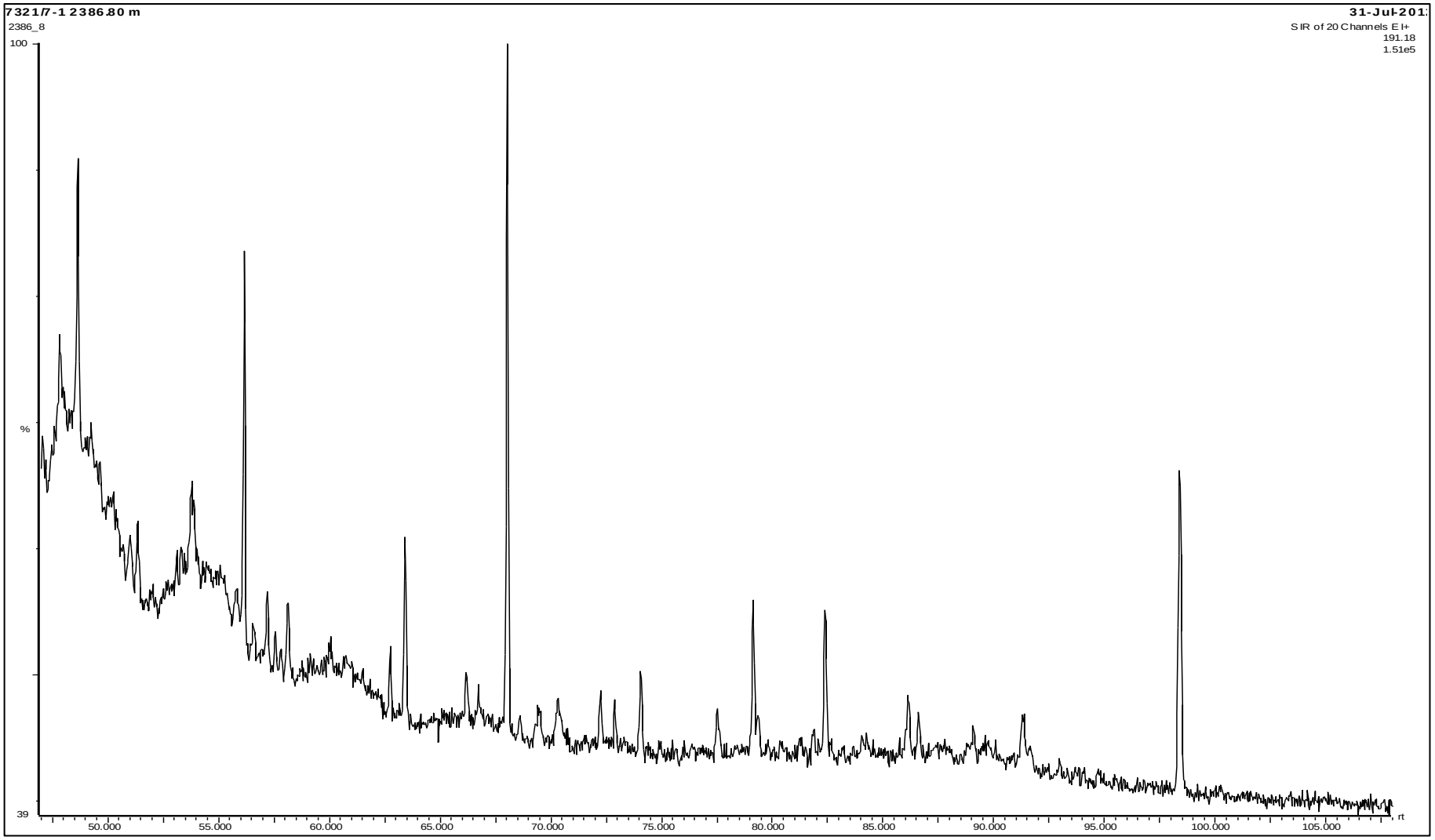
7321/7-1 2386.80 m
2386_8
31-Jul-201
SIR of 20 Channels EI+
191.18
1.51e5
100
%
39
50.000
55.000
60.000
65.000
70.000
75.000
80.000
85.000
90.000
95.000
100.000
105.000
rt

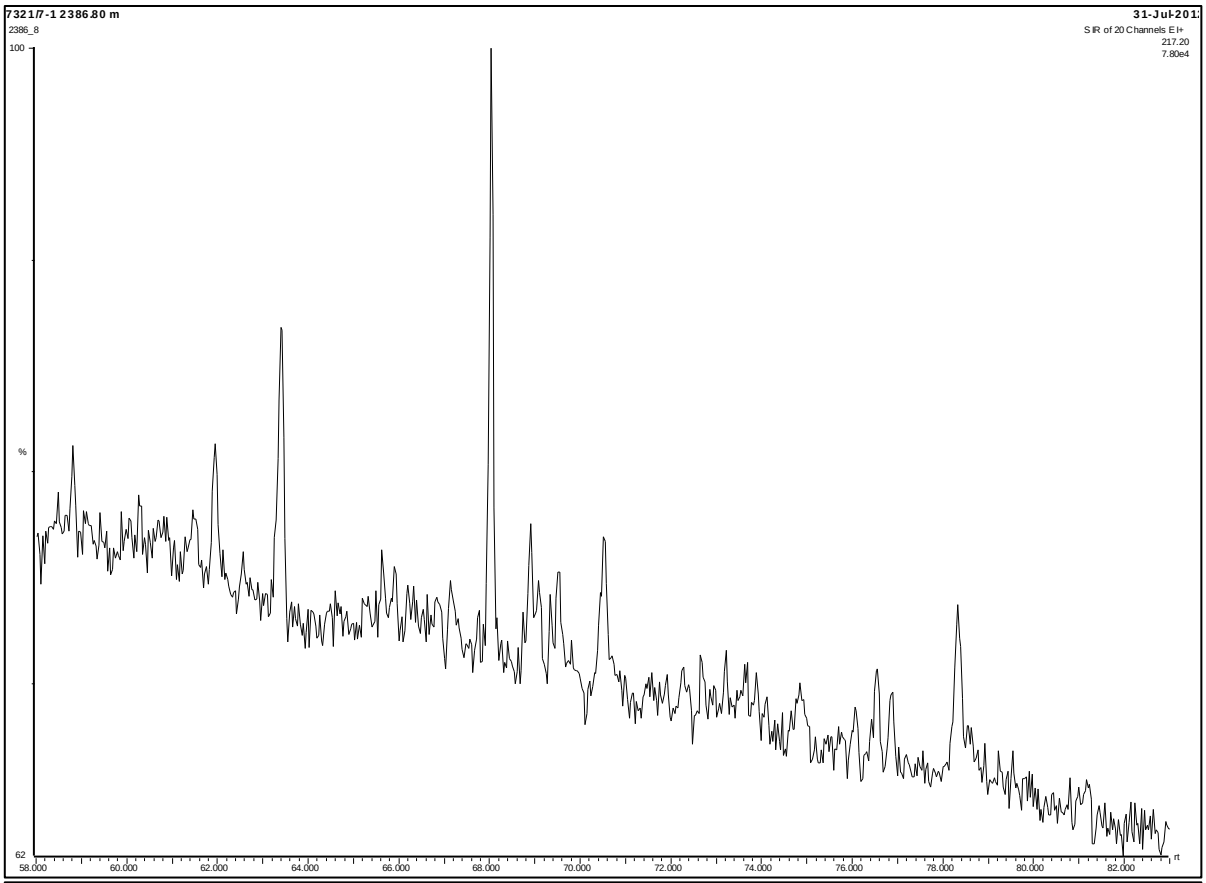
7321/7-1 2386.80 m
2386_8
31-Jul-201
SIR of 20 Channels EI+
217.20
7.80e4
100
%
62
58.000
60.000
62.000
64.000
66.000
68.000
70.000
72.000
74.000
76.000
78.000
80.000
82.000
rt

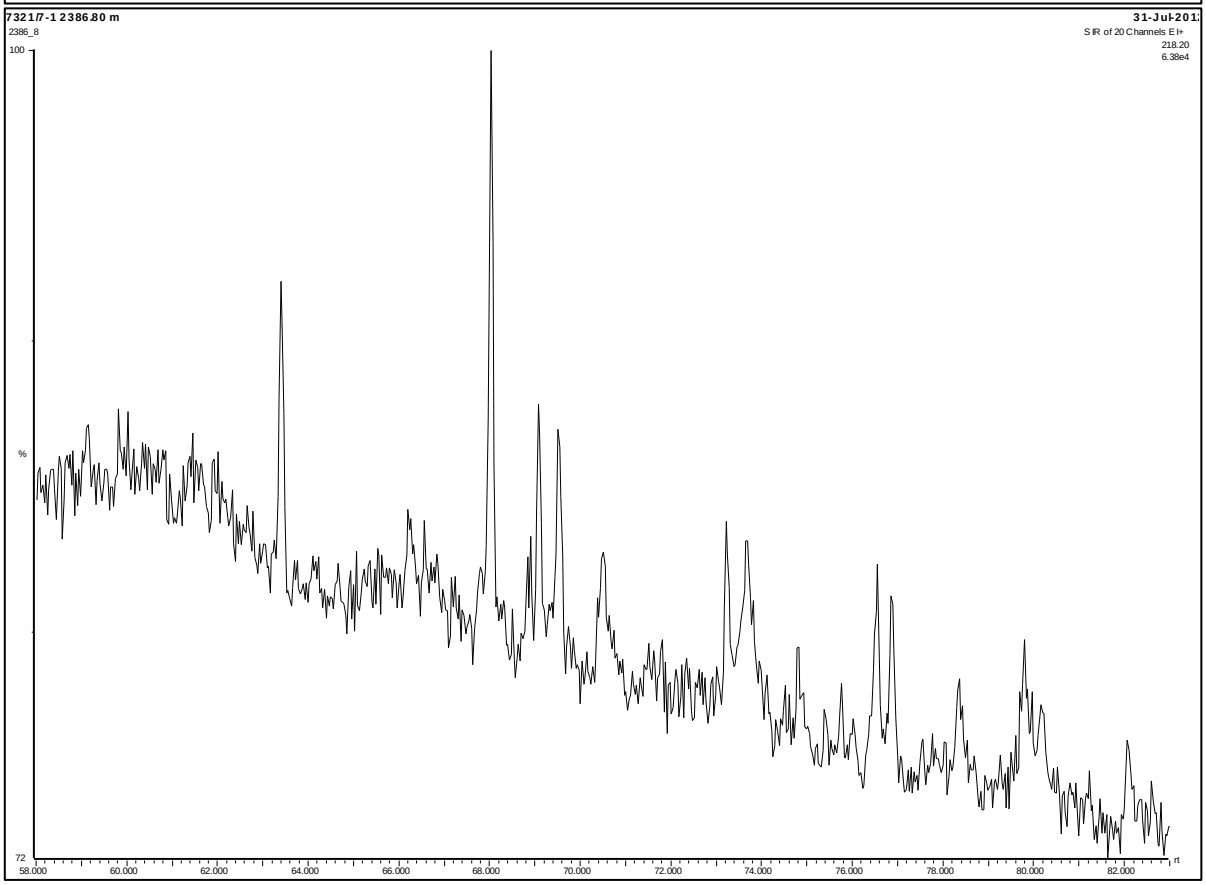
7321/7-1 2386.80 m
2386_8
31-Jul-201
SIR of 20 Channels EI+
218.20
6.38e4
100
%
72
58.000
60.000
62.000
64.000
66.000
68.000
70.000
72.000
74.000
76.000
78.000
80.000
82.000
rt

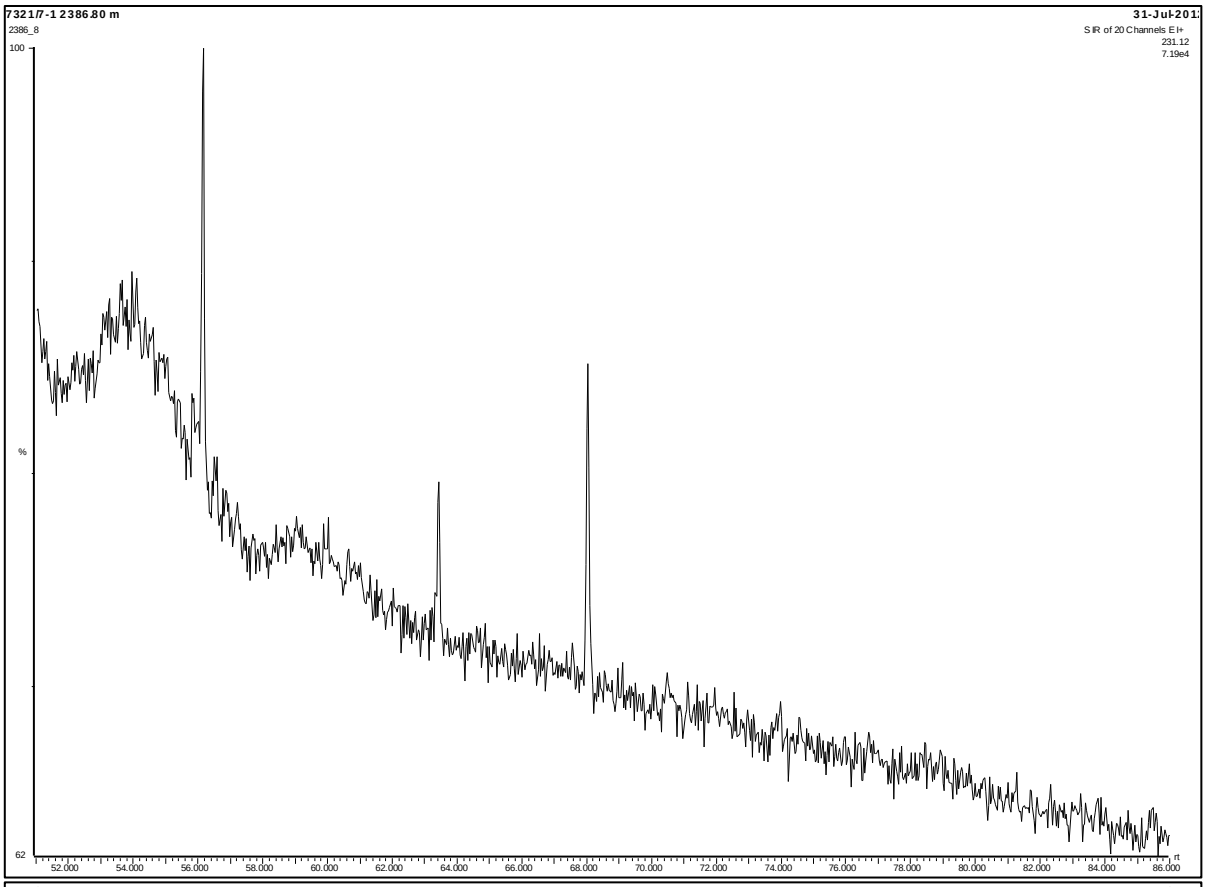
7321/7-1 2386.80 m
2386_8
31-Jul-201
SIR of 20 Channels EI+
231.12
7.19e4
100
%
62
52.000 54.000 56.000 58.000 60.000 62.000 64.000 66.000 68.000 70.000 72.000 74.000 76.000 78.000 80.000 82.000 84.000 86.000
rt

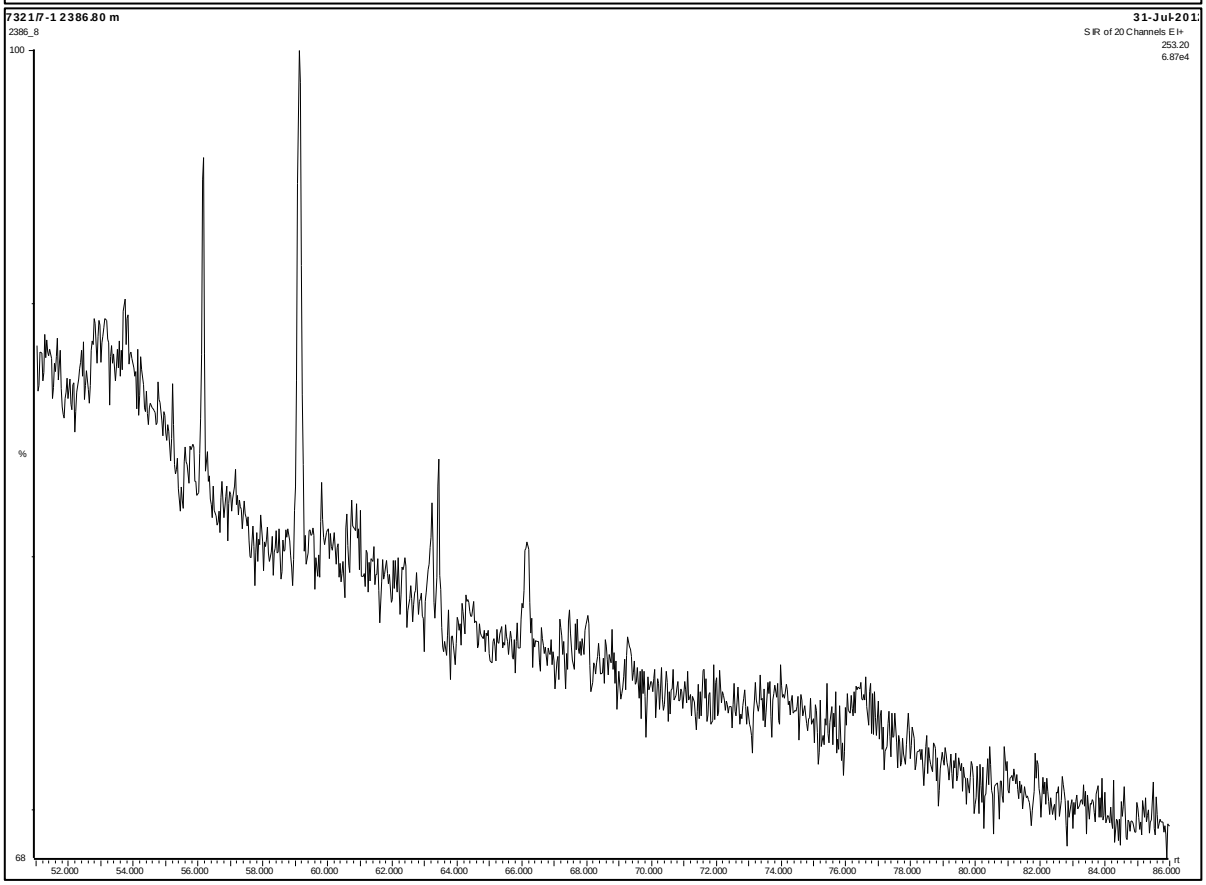
7321/7-1 2386.80 m
2386_8
31-Jul-201
SIR of 20 Channels EI+
253.20
6.87e4
100
%
68
52.000 54.000 56.000 58.000 60.000 62.000 64.000 66.000 68.000 70.000 72.000 74.000 76.000 78.000 80.000 82.000 84.000 86.000
rt

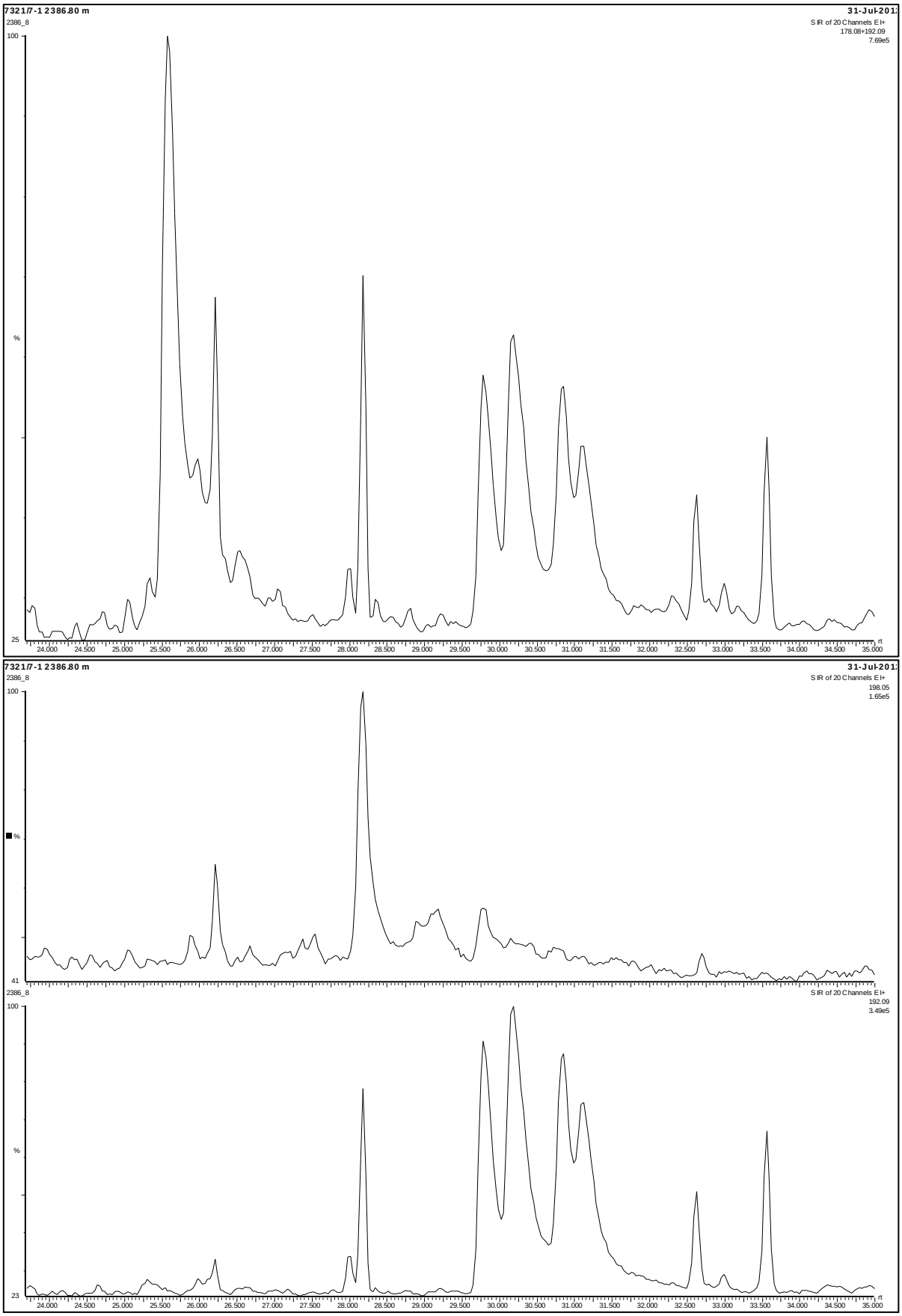
7321/7-1 2386.80 m
31-Jul-201
2386_8
SIR of 20 Channels EI+
178.08+192.09
7.69e5
100
%
25
24.000 24.500 25.000 25.500 26.000 26.500 27.000 27.500 28.000 28.500 29.000 29.500 30.000 30.500 31.000 31.500 32.000 32.500 33.000 33.500 34.000 34.500 35.000
rt
7321/7-1 2386.80 m
31-Jul-201
2386_8
SIR of 20 Channels EI+
198.05
1.65e5
100
%
41
2386_8
SIR of 20 Channels EI+
192.09
3.49e5
100
%
23
24.000 24.500 25.000 25.500 26.000 26.500 27.000 27.500 28.000 28.500 29.000 29.500 30.000 30.500 31.000 31.500 32.000 32.500 33.000 33.500 34.000 34.500 35.000
rt

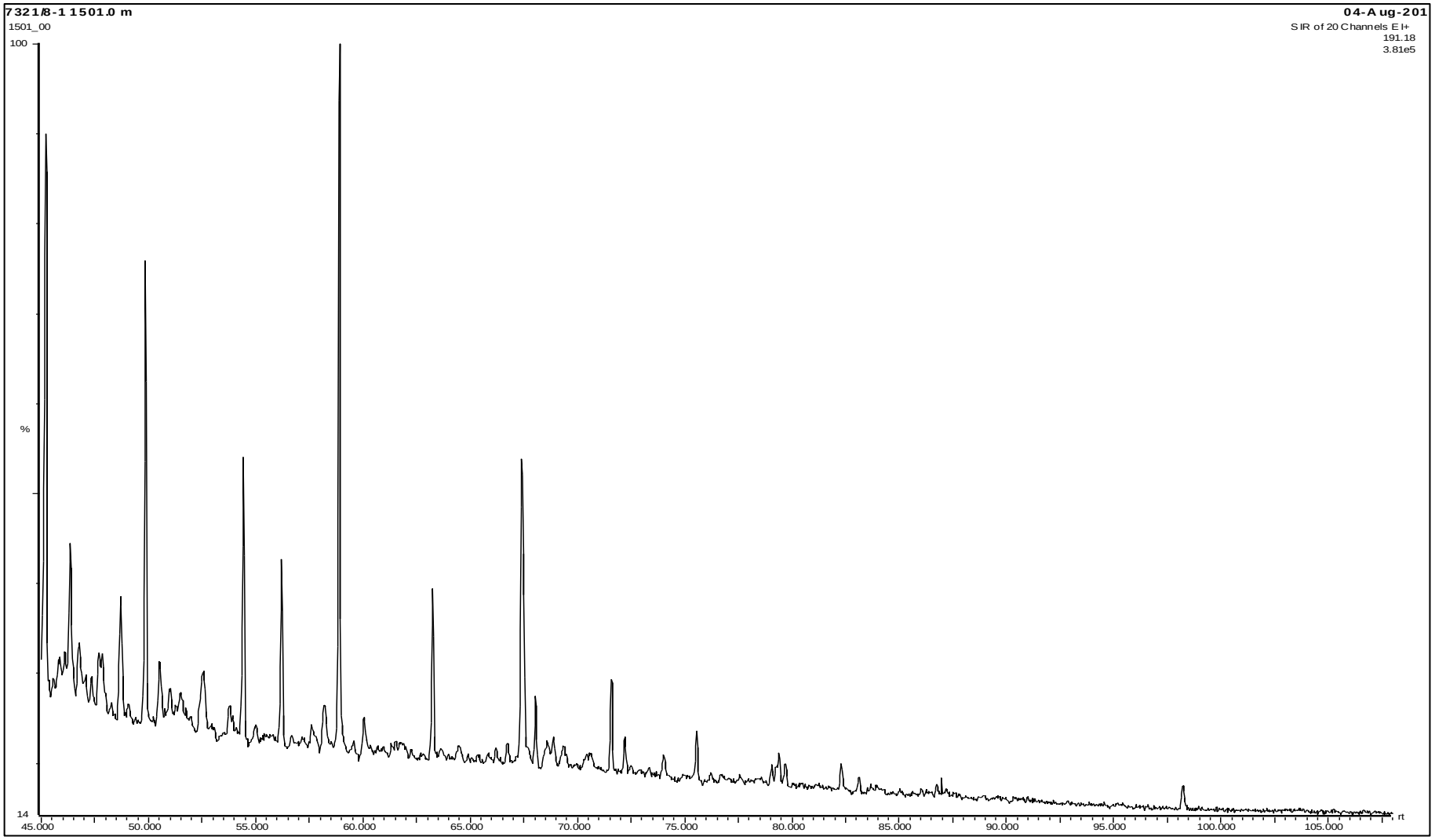
7321/8-1 1501.0 m
1501_00
04-Aug-201
SIR of 20 Channels EI+
191.18
3.81e5
100
%
14
45.000
50.000
55.000
60.000
65.000
70.000
75.000
80.000
85.000
90.000
95.000
100.000
105.000
rt

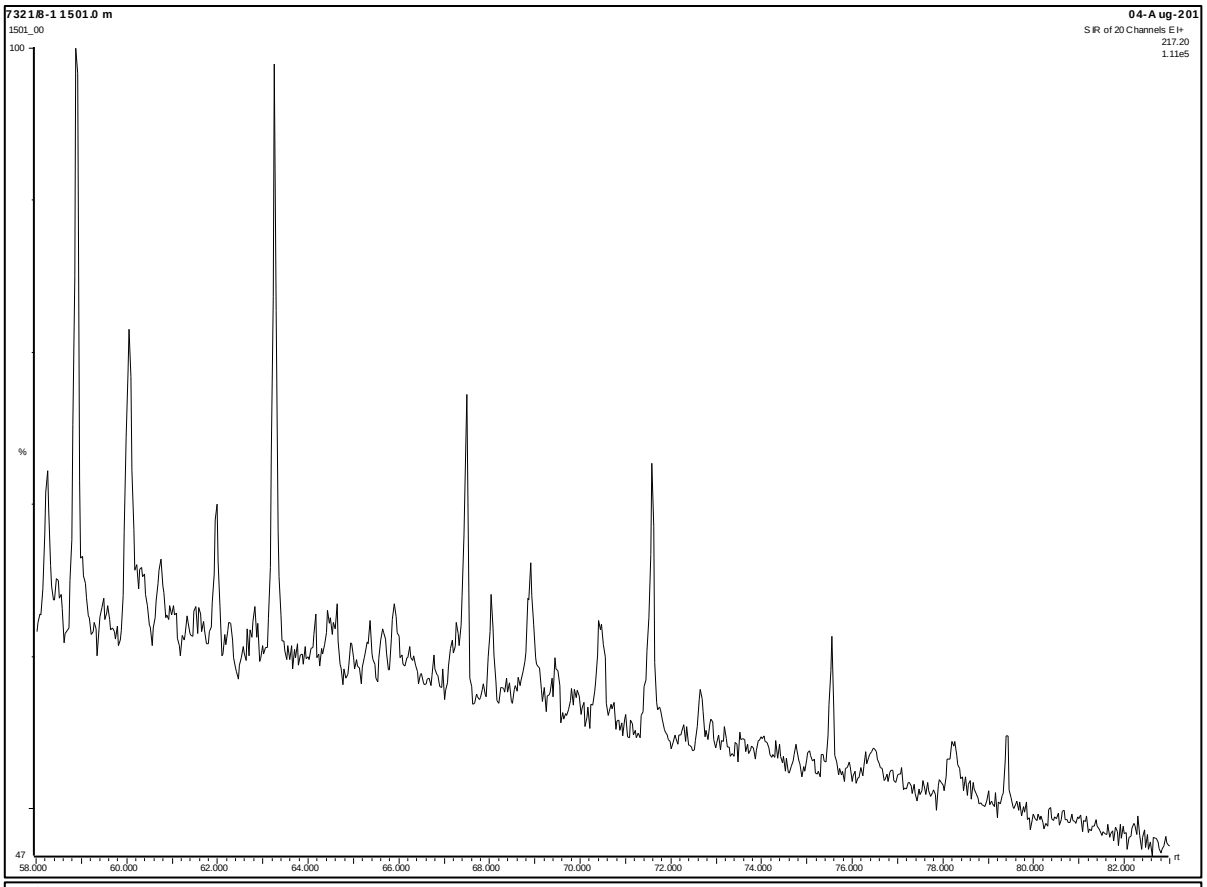
7321/8-1 1501.0 m
1501_00
04-Aug-201
SIR of 20 Channels EI+
217.20
1.11e5
100
%
47
58.000
60.000
62.000
64.000
66.000
68.000
70.000
72.000
74.000
76.000
78.000
80.000
82.000
rt

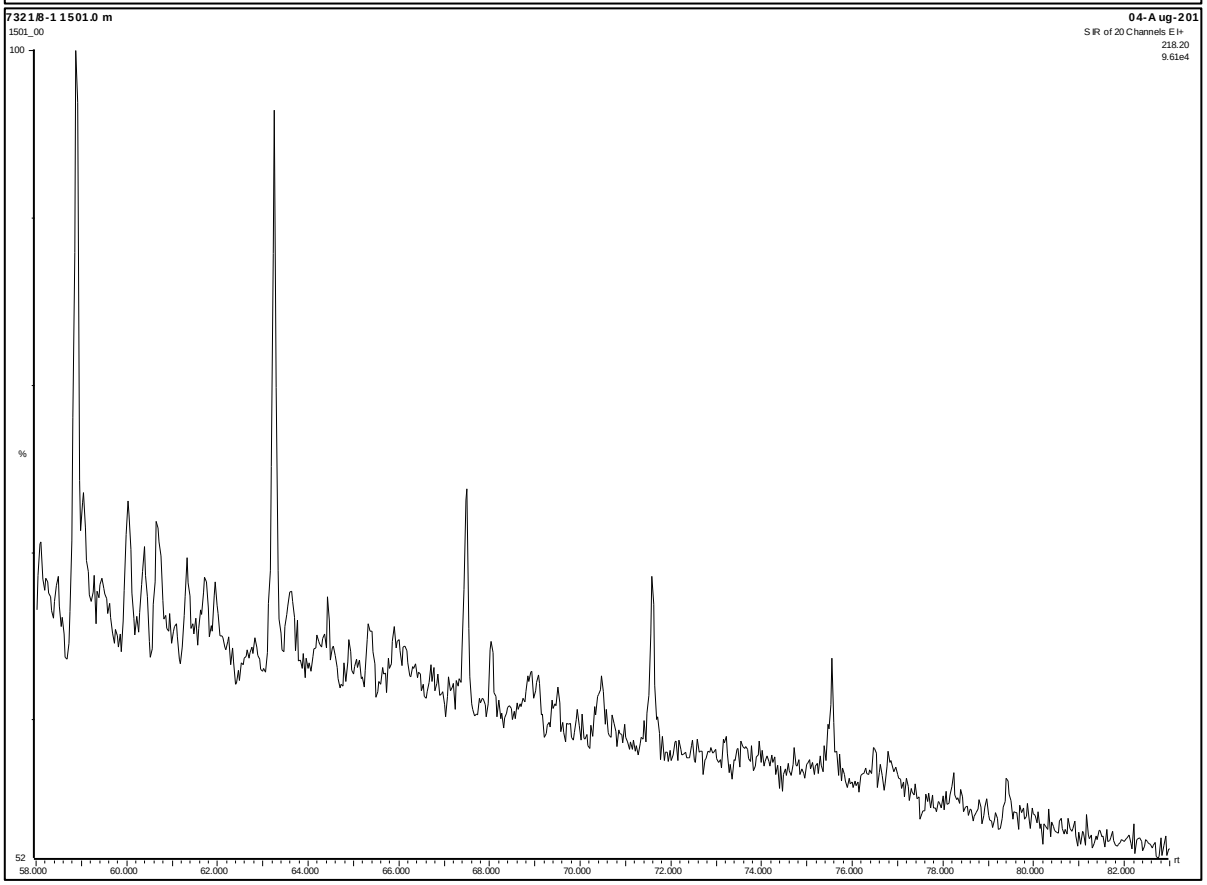
7321/8-1 1501.0 m
1501_00
04-Aug-201
SIR of 20 Channels EI+
218.20
9.61e4
100
%
52
58.000
60.000
62.000
64.000
66.000
68.000
70.000
72.000
74.000
76.000
78.000
80.000
82.000
rt

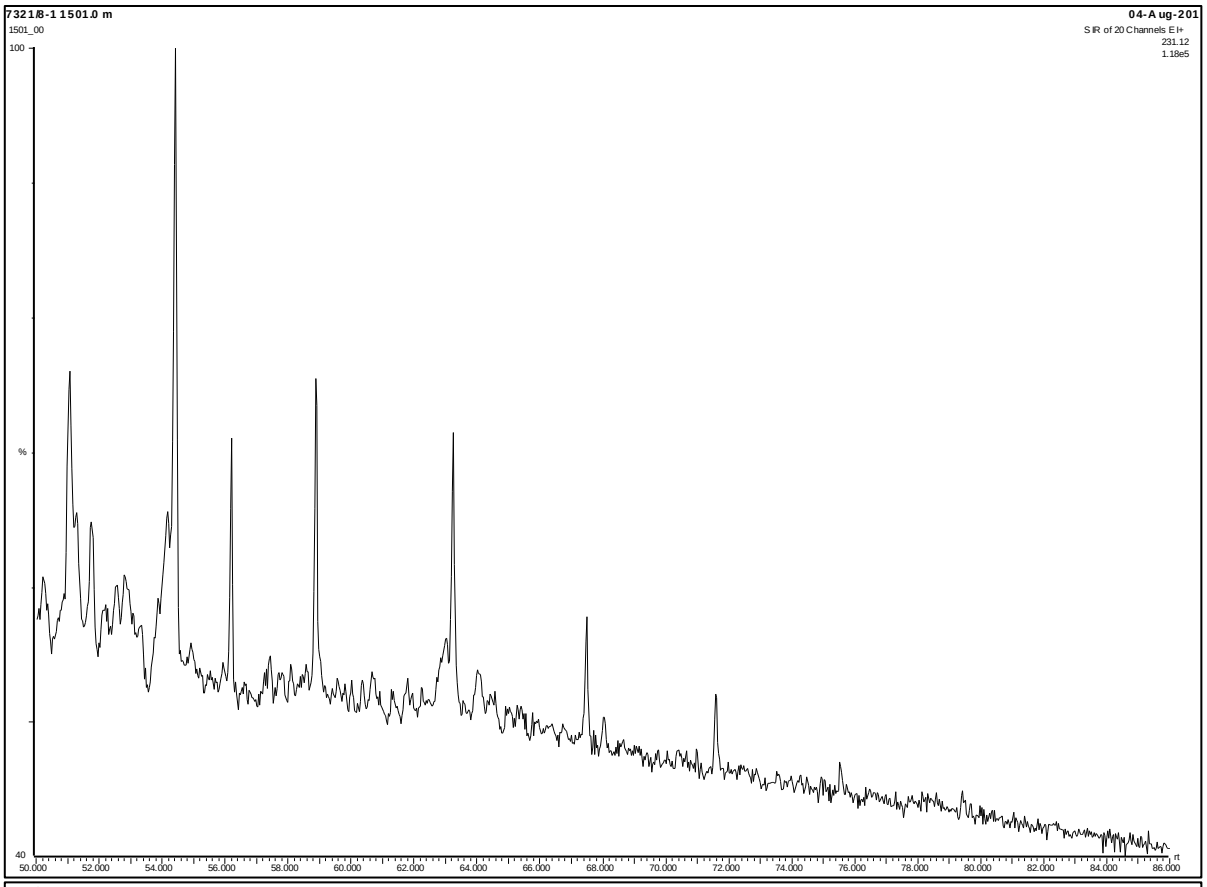
7321/8-1 1501.0 m
1501_00
04-Aug-201
SIR of 20 Channels EI+
231.12
1.18e5
100
%
40
50.000 52.000 54.000 56.000 58.000 60.000 62.000 64.000 66.000 68.000 70.000 72.000 74.000 76.000 78.000 80.000 82.000 84.000 86.000
rt

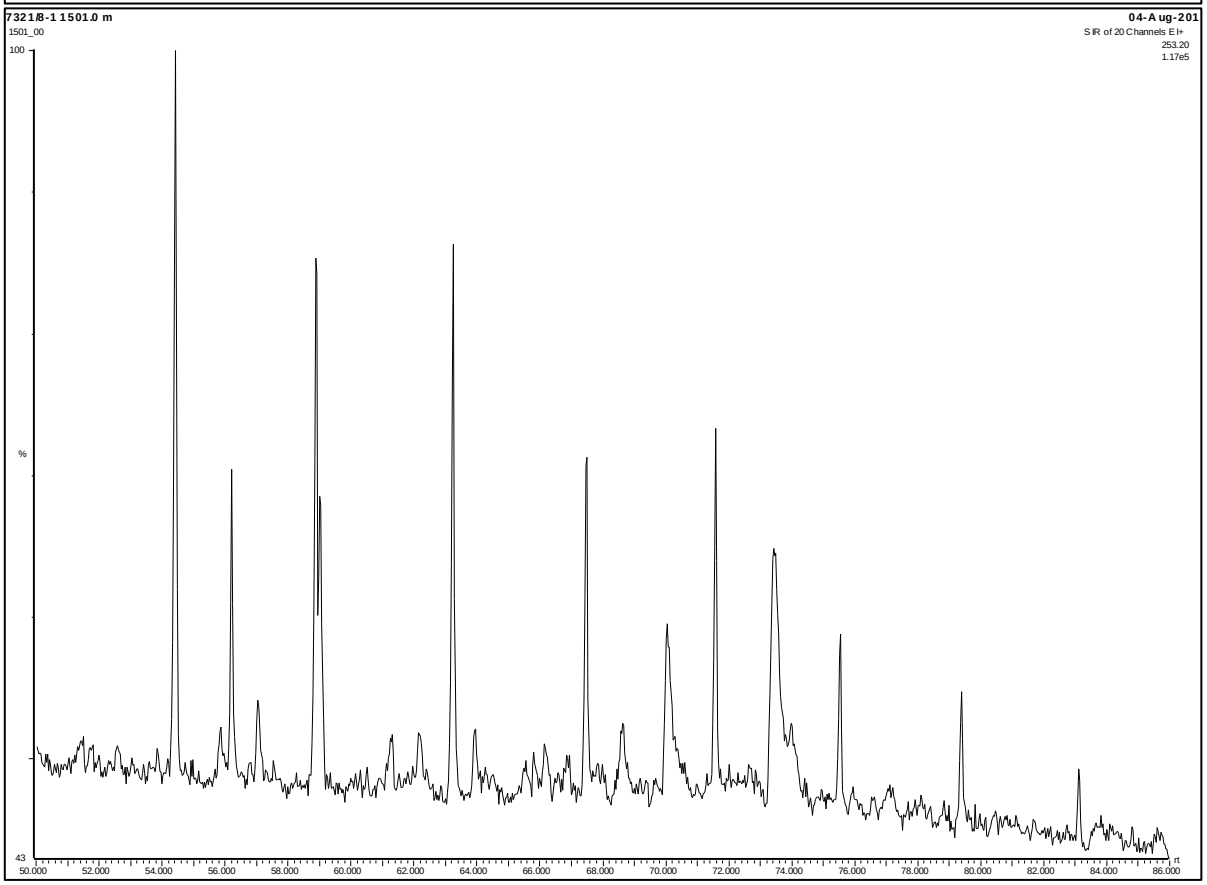
7321/8-1 1501.0 m
1501_00
04-Aug-201
SIR of 20 Channels EI+
253.20
1.17e5
100
%
43
50.000 52.000 54.000 56.000 58.000 60.000 62.000 64.000 66.000 68.000 70.000 72.000 74.000 76.000 78.000 80.000 82.000 84.000 86.000
rt

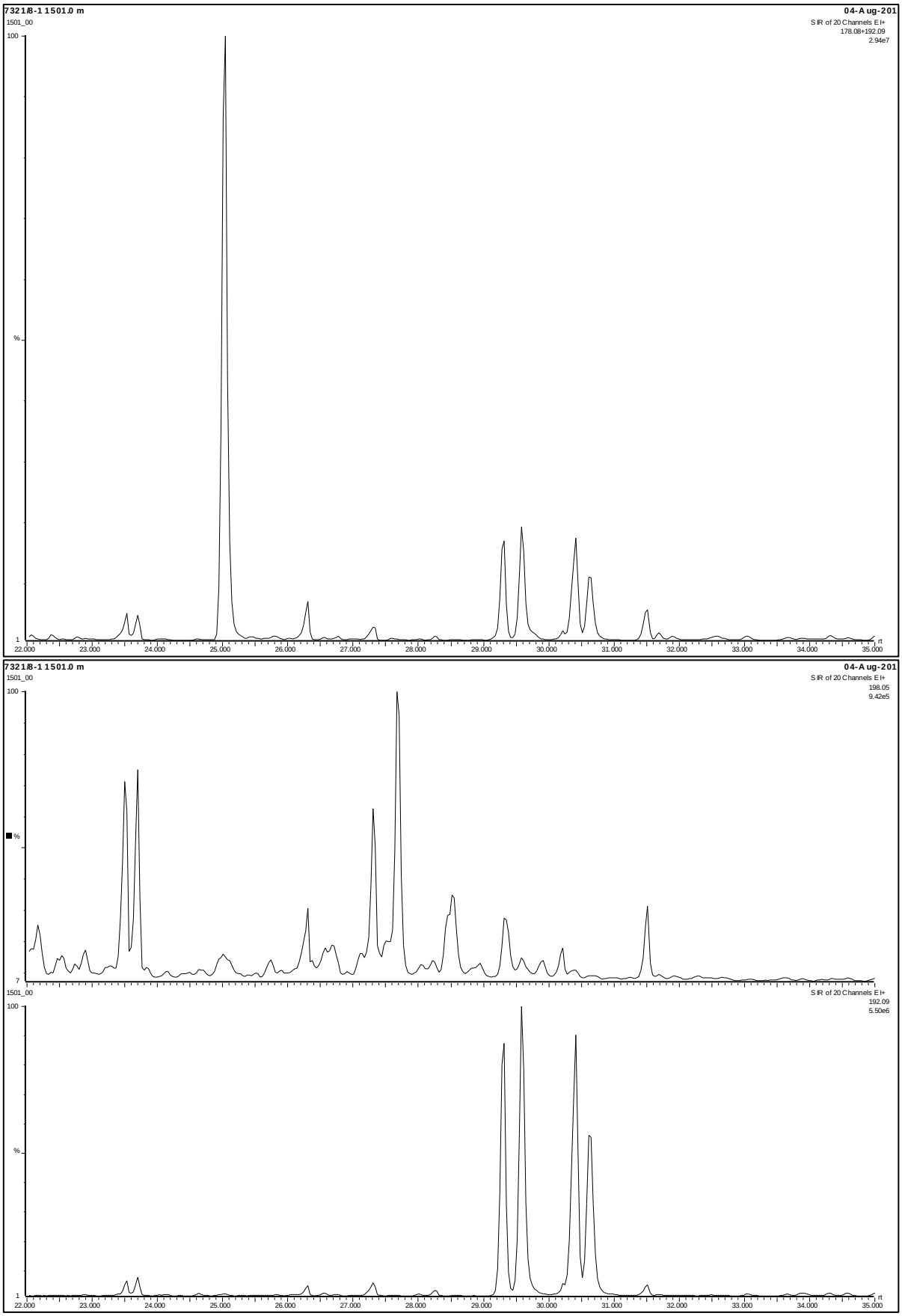
7321/8-1 1501.0 m
04-Aug-201
1501_00
SIR of 20 Channels EI+
178.08+192.09
2.94e7
100
%
1
22.000
23.000
24.000
25.000
26.000
27.000
28.000
29.000
30.000
31.000
32.000
33.000
34.000
35.000
rt
7321/8-1 1501.0 m
04-Aug-201
1501_00
SIR of 20 Channels EI+
198.05
9.42e5
100
%
7
1501_00
SIR of 20 Channels EI+
192.09
5.50e6
100
%
1
22.000
23.000
24.000
25.000
26.000
27.000
28.000
29.000
30.000
31.000
32.000
33.000
34.000
35.000
rt

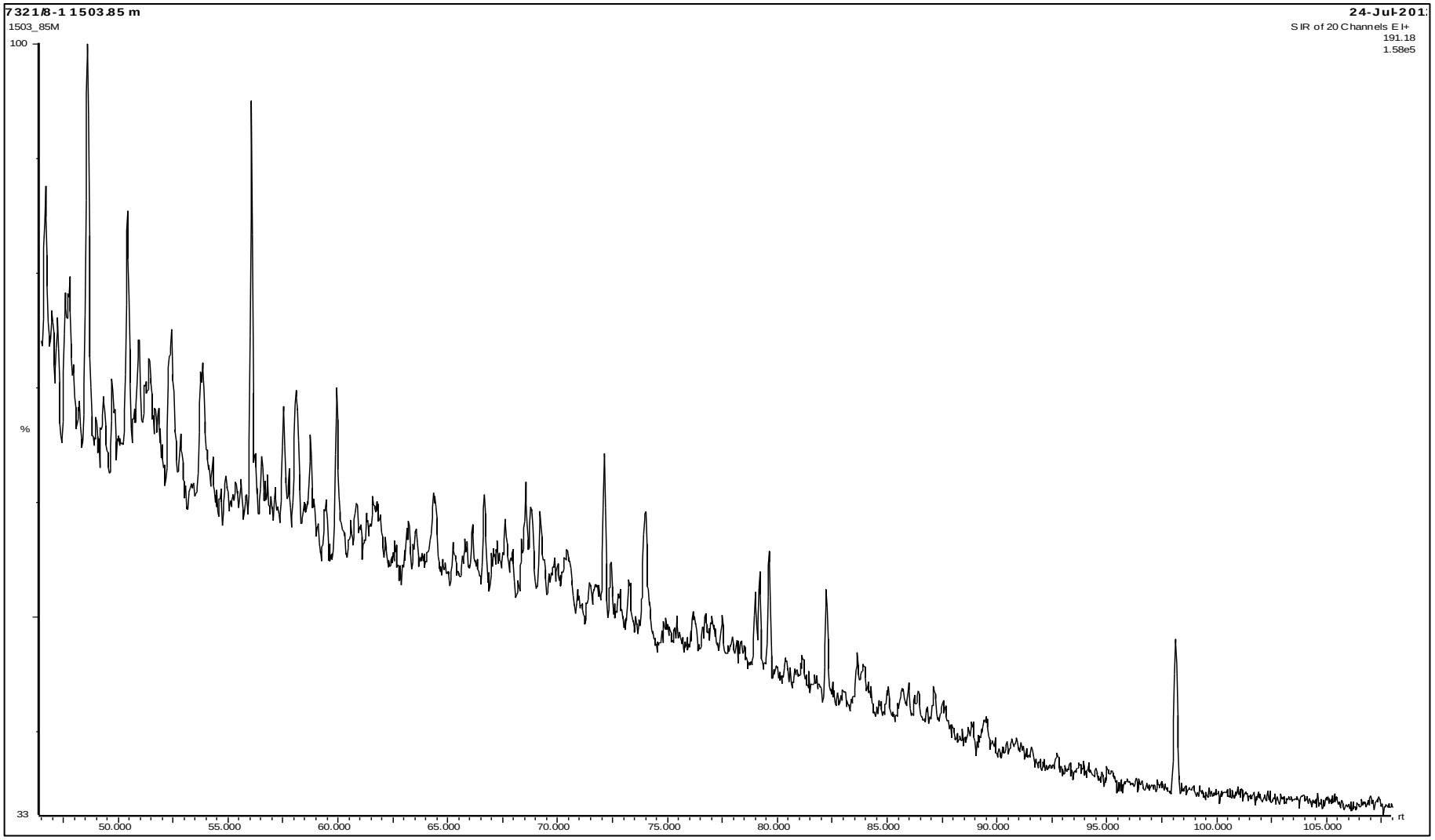
7321/8-1 1503.85 m
1503_85M
24-Jul-201
SIR of 20 Channels EI+
191.18
1.58e5
100
%
33
50.000
55.000
60.000
65.000
70.000
75.000
80.000
85.000
90.000
95.000
100.000
105.000
rt

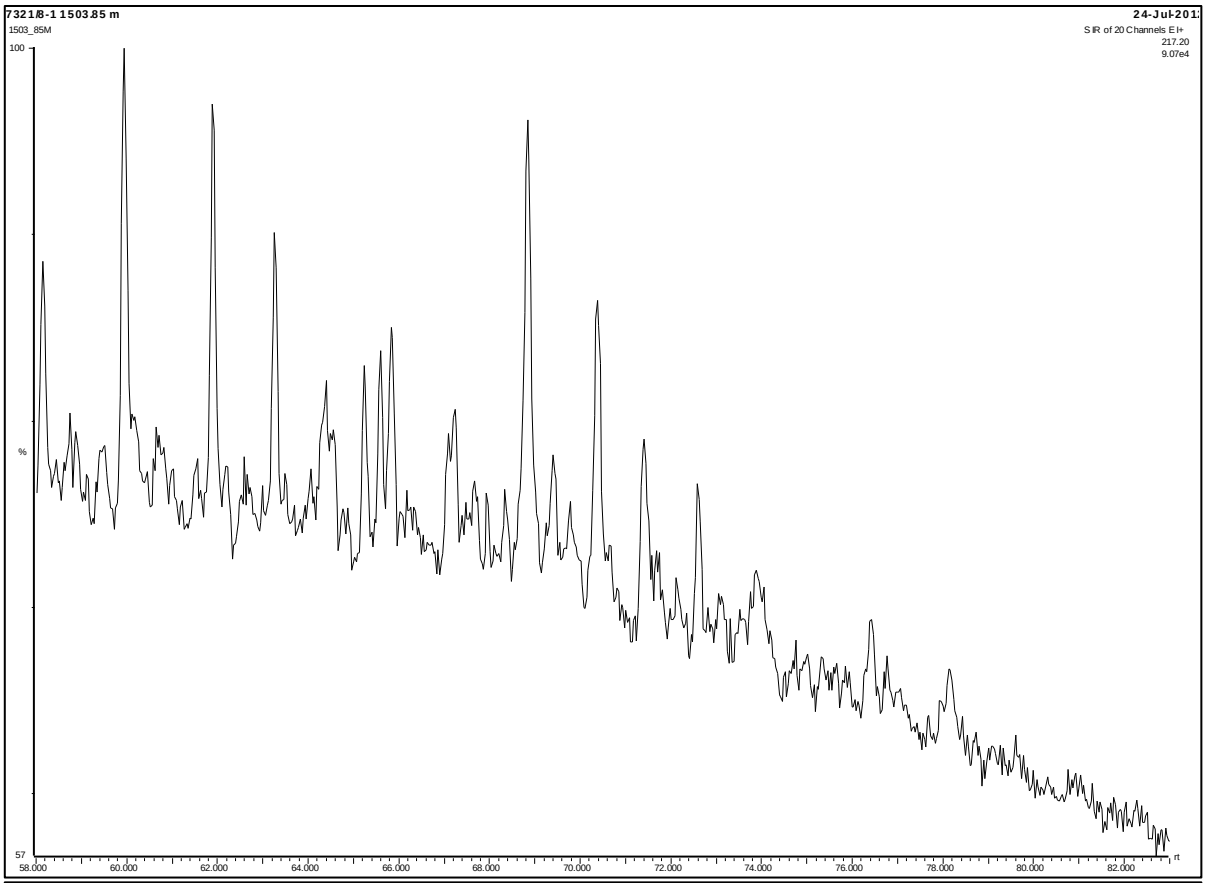
7321/8-1 1503.85 m
1503_85M
24-Jul-201
SIR of 20 Channels EI+
217.20
9.07e4
100
%
57
58.000
60.000
62.000
64.000
66.000
68.000
70.000
72.000
74.000
76.000
78.000
80.000
82.000
rt

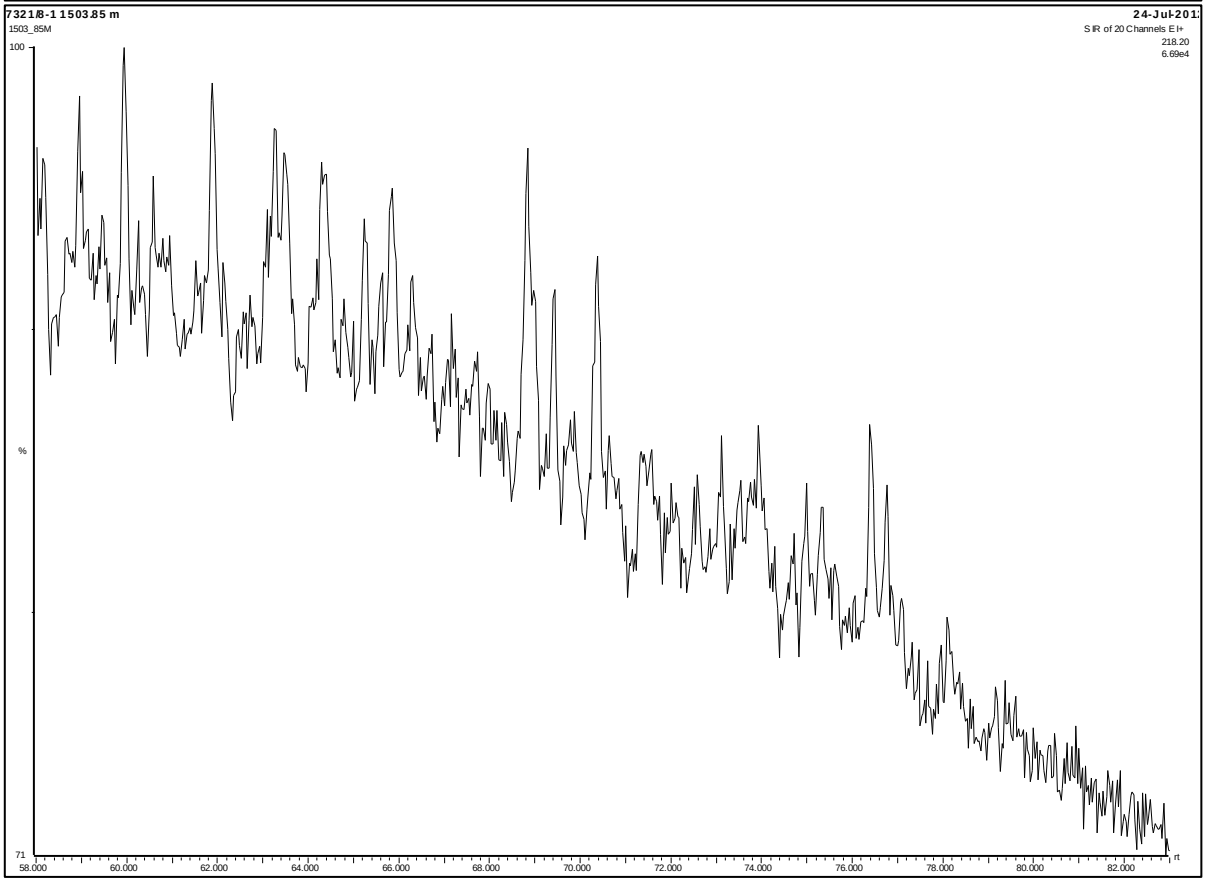
7321/8-1 1503.85 m
1503_85M
24-Jul-201
SIR of 20 Channels EI+
218.20
6.69e4
100
%
71
58.000
60.000
62.000
64.000
66.000
68.000
70.000
72.000
74.000
76.000
78.000
80.000
82.000
rt

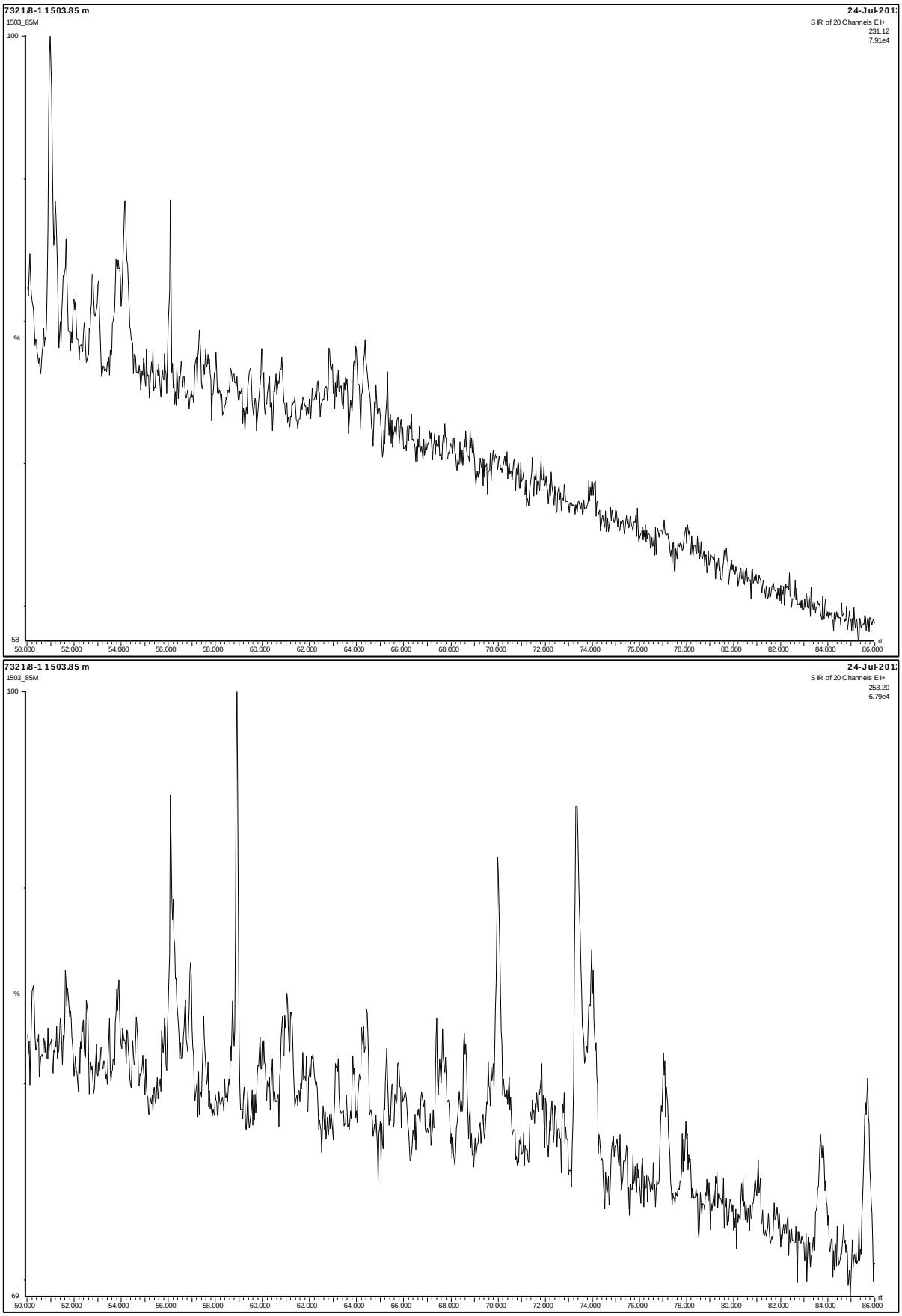
7321/8-1 1503.85 m
1503_85M
24-Jul-201
SIR of 20 Channels EI+
231.12
7.91e4
100
%
58
50.000 52.000 54.000 56.000 58.000 60.000 62.000 64.000 66.000 68.000 70.000 72.000 74.000 76.000 78.000 80.000 82.000 84.000 86.000
rt
7321/8-1 1503.85 m
1503_85M
24-Jul-201
SIR of 20 Channels EI+
253.20
6.79e4
100
%
69
50.000 52.000 54.000 56.000 58.000 60.000 62.000 64.000 66.000 68.000 70.000 72.000 74.000 76.000 78.000 80.000 82.000 84.000 86.000
rt

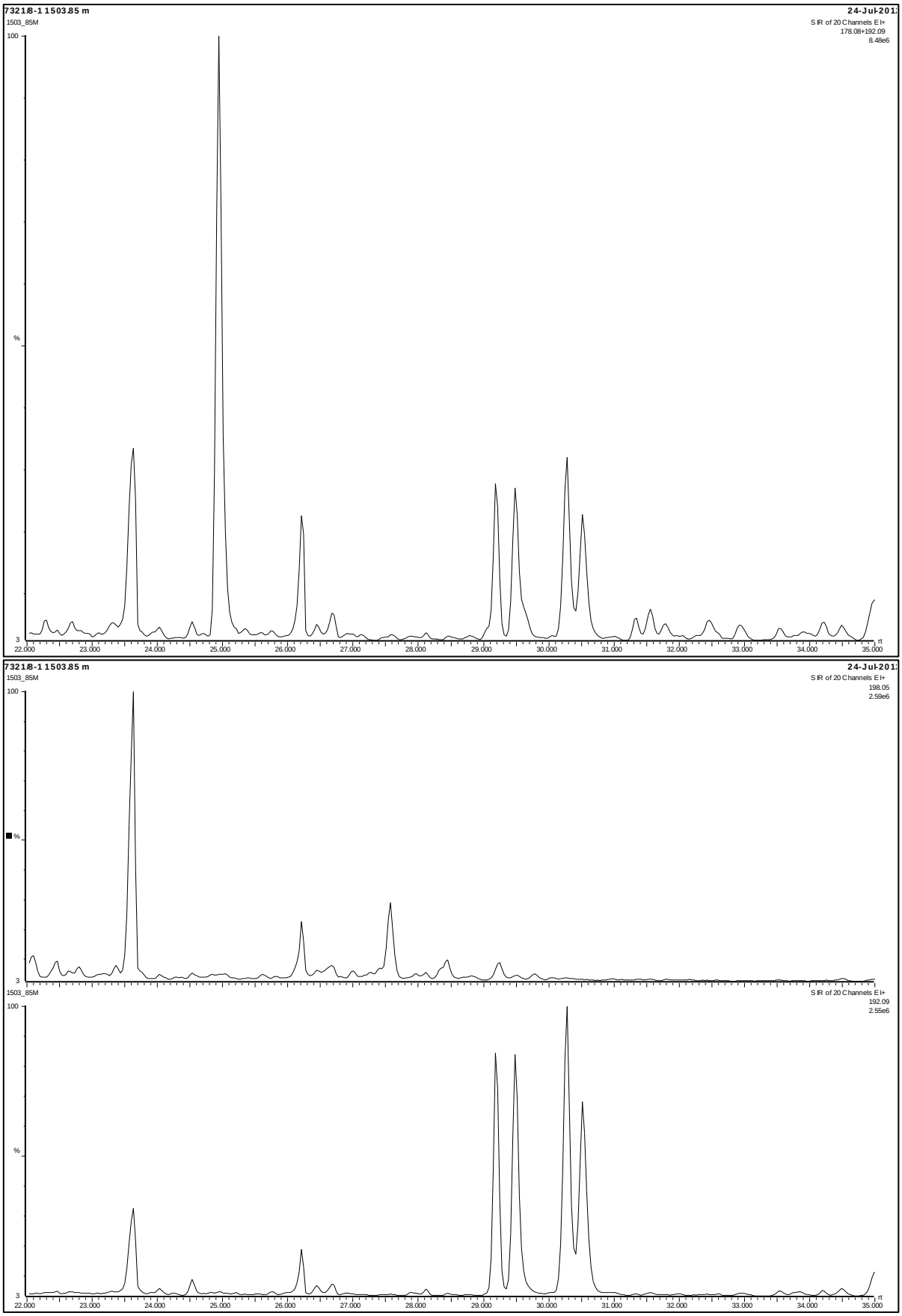
7321/8-1 1503.85 m
24-Jul-201
1503_85M
SIR of 20 Channels EI+
178.08+192.09
8.48e6
100
%
3
22.000
23.000
24.000
25.000
26.000
27.000
28.000
29.000
30.000
31.000
32.000
33.000
34.000
35.000
rt
7321/8-1 1503.85 m
24-Jul-201
1503_85M
SIR of 20 Channels EI+
198.05
2.59e6
100
%
3
1503_85M
SIR of 20 Channels EI+
192.09
2.55e6
100
%
3
22.000
23.000
24.000
25.000
26.000
27.000
28.000
29.000
30.000
31.000
32.000
33.000
34.000
35.000
rt

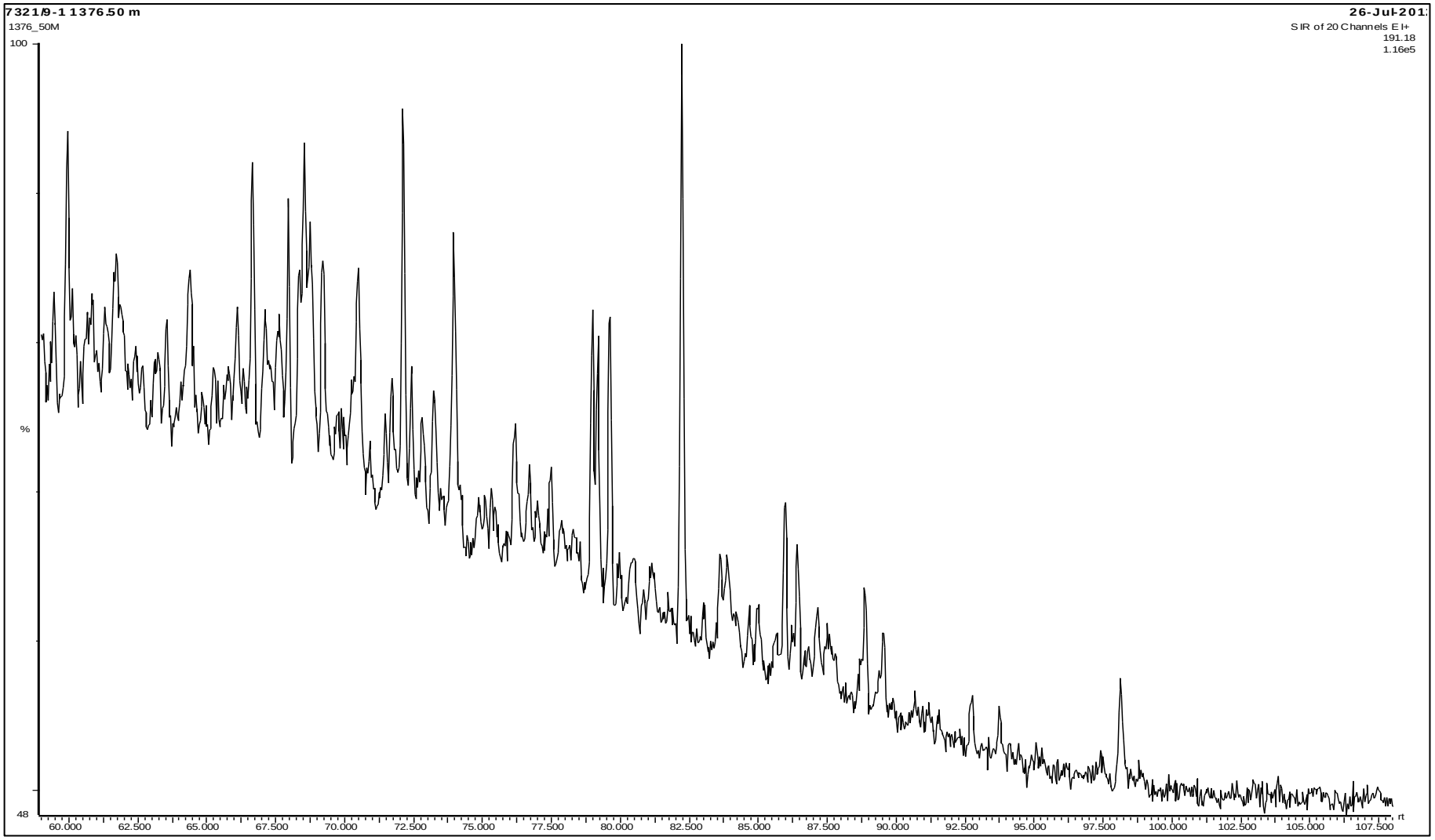
7321/9-1 1376.50 m
1376_50M
26-Jul-201
SIR of 20 Channels EI+
191.18
1.16e5
100
%
48
60.000
62.500
65.000
67.500
70.000
72.500
75.000
77.500
80.000
82.500
85.000
87.500
90.000
92.500
95.000
97.500
100.000
102.500
105.000
107.500
rt

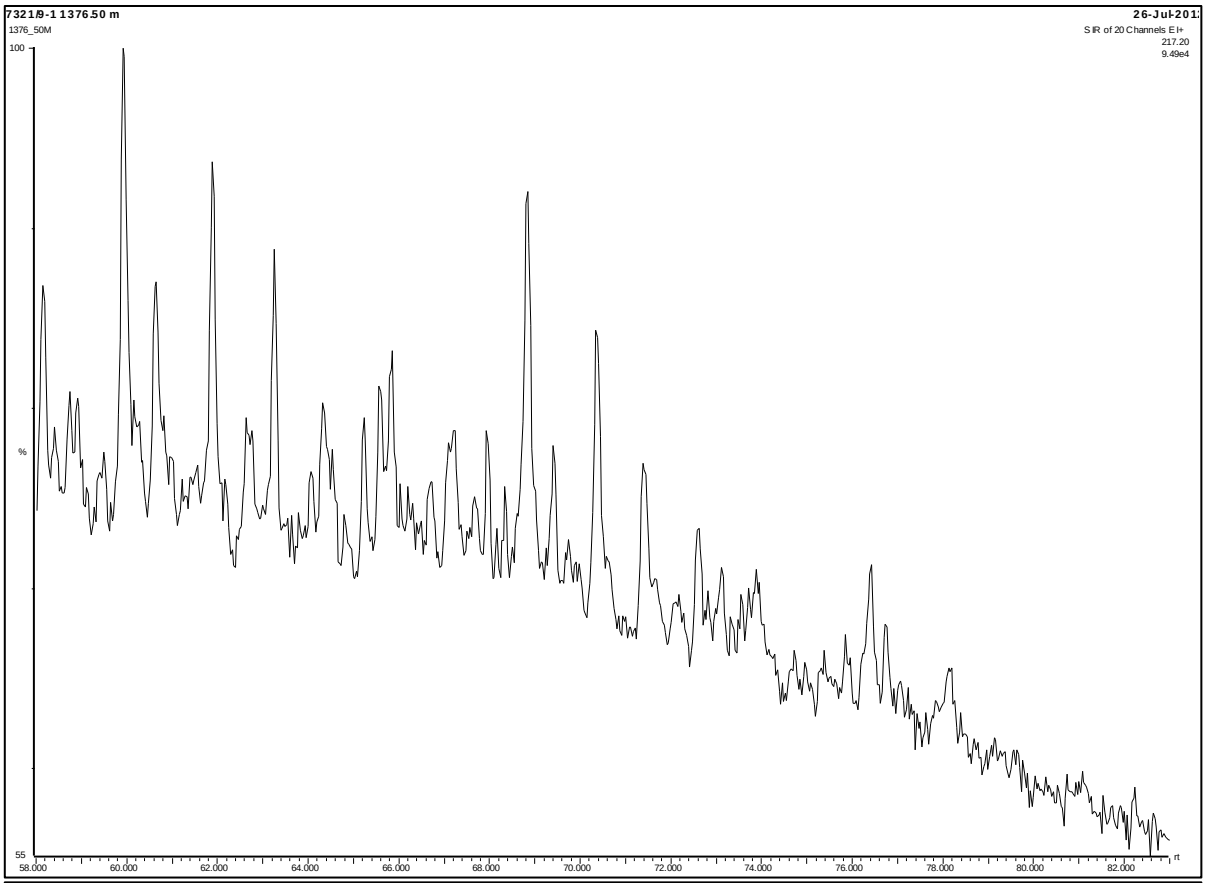
7321/9-1 1376.50 m
1376_50M
26-Jul-201
SIR of 20 Channels EI+
217.20
9.49e4
100
%
55
58.000
60.000
62.000
64.000
66.000
68.000
70.000
72.000
74.000
76.000
78.000
80.000
82.000
rt

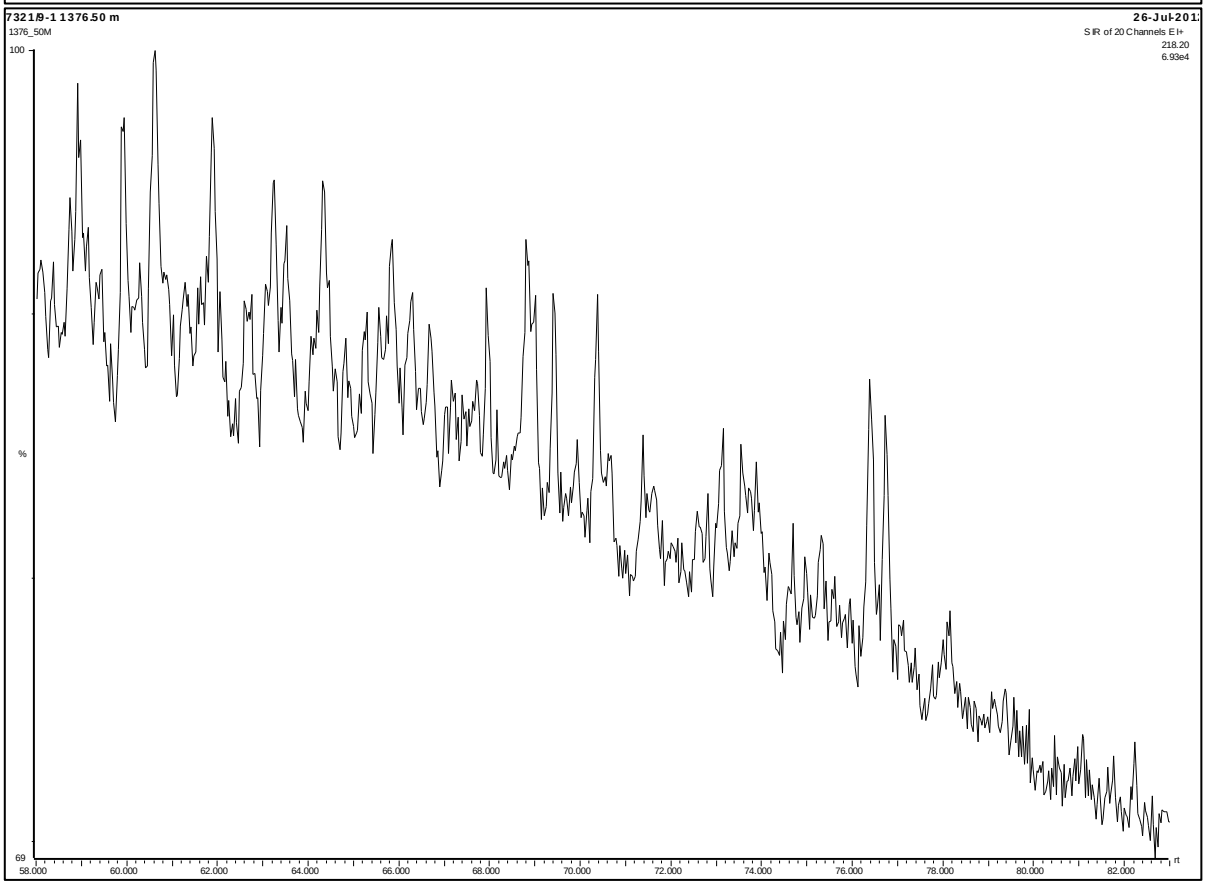
7321/9-1 1376.50 m
1376_50M
26-Jul-201
SIR of 20 Channels EI+
218.20
6.93e4
100
%
69
58.000
60.000
62.000
64.000
66.000
68.000
70.000
72.000
74.000
76.000
78.000
80.000
82.000
rt

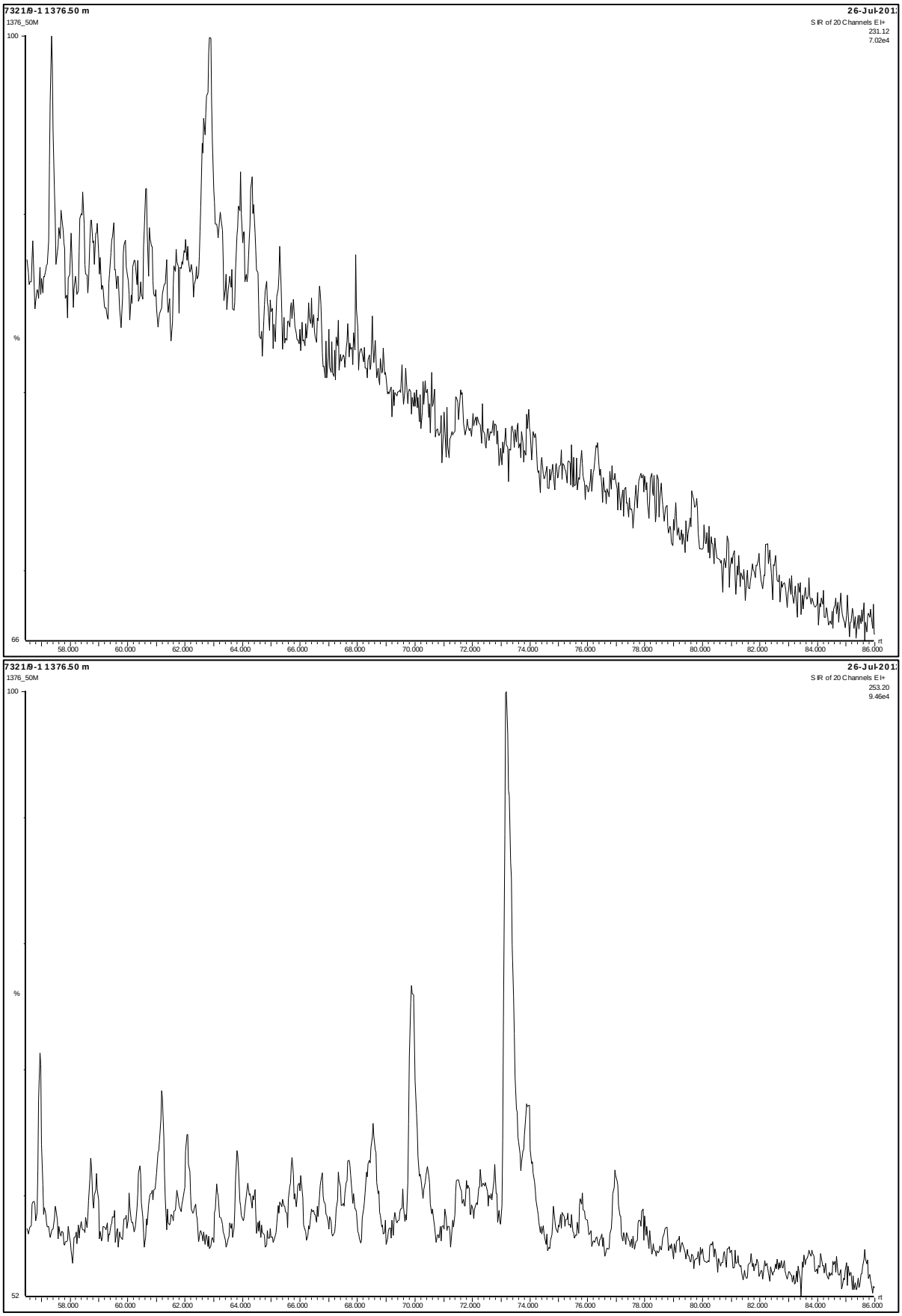
7321/9-1 1376.50 m
1376_50M
26-Jul-201
SIR of 20 Channels EI+
231.12
7.02e4
100
%
66
58.000
60.000
62.000
64.000
66.000
68.000
70.000
72.000
74.000
76.000
78.000
80.000
82.000
84.000
86.000
rt
7321/9-1 1376.50 m
1376_50M
26-Jul-201
SIR of 20 Channels EI+
253.20
9.46e4
100
%
52
58.000
60.000
62.000
64.000
66.000
68.000
70.000
72.000
74.000
76.000
78.000
80.000
82.000
84.000
86.000
rt

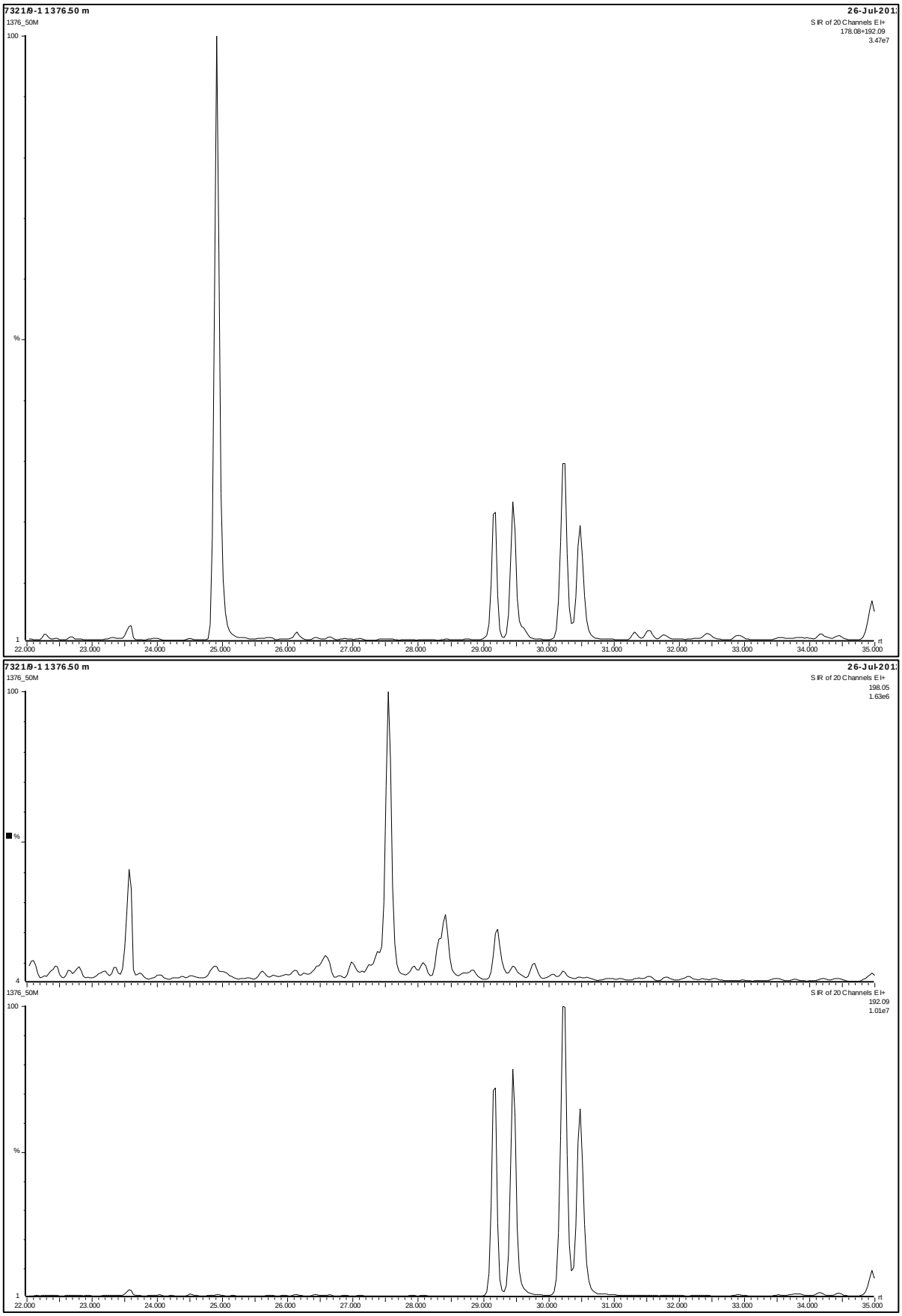
7321/9-1 1376.50 m
26-Jul-201
1376_50M
SIR of 20 Channels EI+
178.08+192.09
3.47e7
100
%
1
22.000
23.000
24.000
25.000
26.000
27.000
28.000
29.000
30.000
31.000
32.000
33.000
34.000
35.000
rt
7321/9-1 1376.50 m
26-Jul-201
1376_50M
SIR of 20 Channels EI+
198.05
1.63e6
100
%
4
1376_50M
SIR of 20 Channels EI+
192.09
1.01e7
100
%
1
22.000
23.000
24.000
25.000
26.000
27.000
28.000
29.000
30.000
31.000
32.000
33.000
34.000
35.000
rt

Appendix D (TLC-FID Results)

Sample Identifier: nso2

Data Processing Parameters

Injected on: 01.10.2012 Injected at: 15:48

Slice Width (ms): 500 Noise (µV/s): undefined

Threshold (mV): 0 Skim Ratio: 0

Parameter Files:

Data Handling File:Iatrosc1 Calculation-File:~atrosc10004

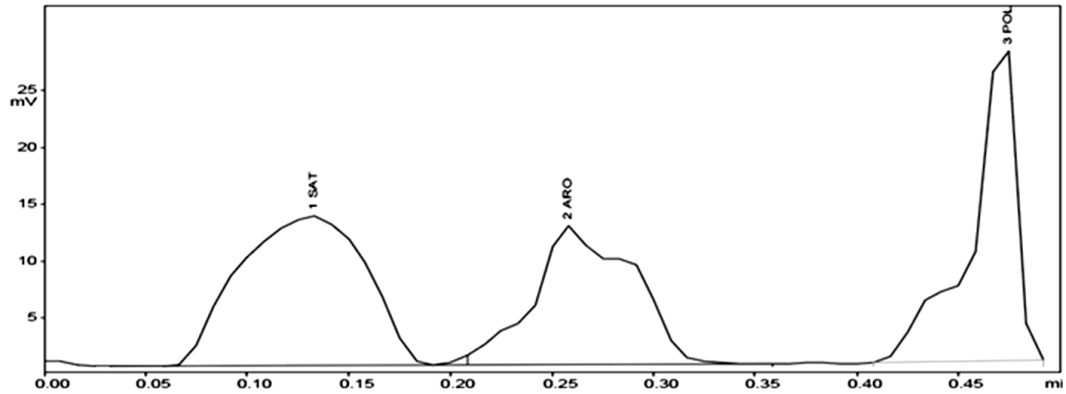

Calculation Method : Percent

Peak No	Win No.	Ret.Time (min)	Area	Resp.- Fact.	Area%	Name
1	1	0.133	30588	1.000	40.795	SAT
2	2	0.258	21668	1.000	28.898	ARO
3	3	0.475	22725	1.000	30.307	POL
			74981		100.000	

Sample Identifier: 2979

Data Processing Parameters

Injected on: 02.10.2012 Injected at: 14:11

Slice Width (ms): 500 Noise (µV/s): undefined

Threshold (mV): 0 Skim Ratio: 0

Parameter Files:

Data Handling File:Iatrosc1 Calculation-File:Iatrosc1

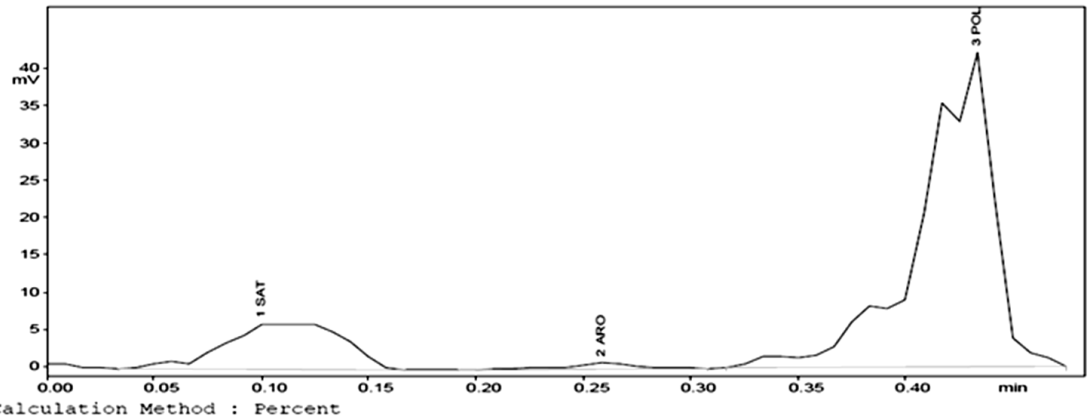

Calculation Method : Percent

Peak No	Win No.	Ret.Time (min)	Area	Resp.- Fact.	Area%	Name
1	1	0.100	12540	1.000	18.880	SAT
2	2	0.258	1156	1.000	1.741	ARO
3	3	0.433	52727	1.000	79.380	POL
			66423		100.000	

Sample Identifier: 2980

Data Processing Parameters

Injected on:	02.10.2012	Injected at:	14:12
Slice Width (ms):	500	Noise (µV/s):	undefined
Threshold (mV):	0	Skim Ratio:	0

Parameter Files:

Data Handling File: Iatrosc1 Calculation-File: Iatrosc1

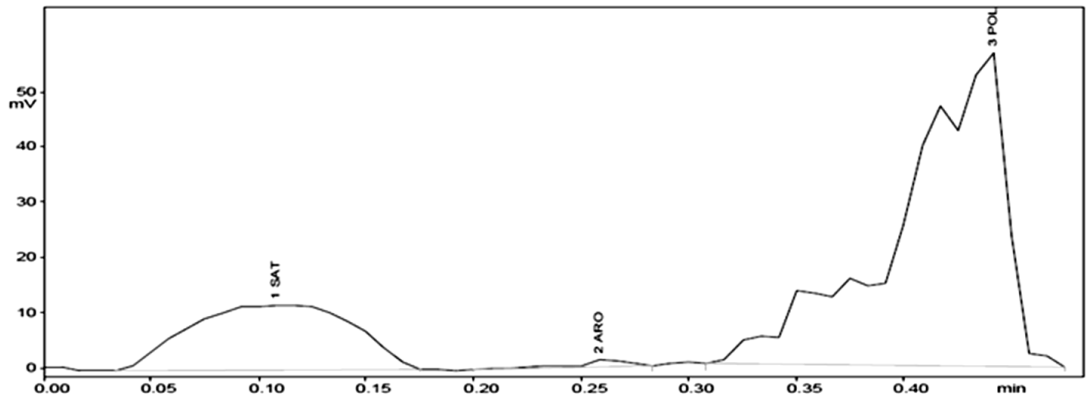

Calculation Method : Percent

Peak No	Win No.	Ret.Time (min)	Area	Resp.-Fact.	Area%	Name
1	1	0.108	32886	1.000	24.069	SAT
2	2	0.258	1256	1.000	0.919	ARO
3	3	0.442	102489	1.000	75.011	POL
			136631		100.000	

Sample Identifier: 4163

Data Processing Parameters

Injected on:	02.10.2012	Injected at:	14:13
Slice Width (ms):	500	Noise (µV/s):	undefined
Threshold (mV):	0	Skim Ratio:	0

Parameter Files:

Data Handling File: Iatrosc1 Calculation-File: Iatrosc1

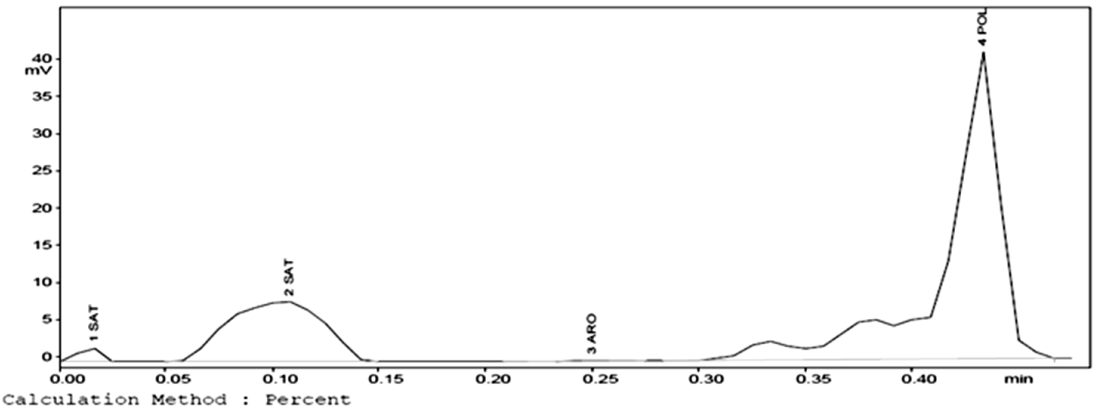

Calculation Method : Percent

Peak No	Win No.	Ret.Time (min)	Area	Resp.-Fact.	Area%	Name
1	1	0.017	769	1.000	1.474	SAT
2	1	0.108	13548	1.000	25.967	SAT
3	2	0.250	51	1.000	0.097	ARO
4	3	0.433	37807	1.000	72.463	POL
			52175		100.000	

Sample Identifier: 4163.8

Data Processing Parameters

Injected on: 02.10.2012 Injected at: 14:14

Slice Width (ms): 500 Noise (µV/s): undefined

Threshold (mV): 0 Skim Ratio: 0

Parameter Files:

Data Handling File: Iatrosc1 Calculation-File: Iatrosc1

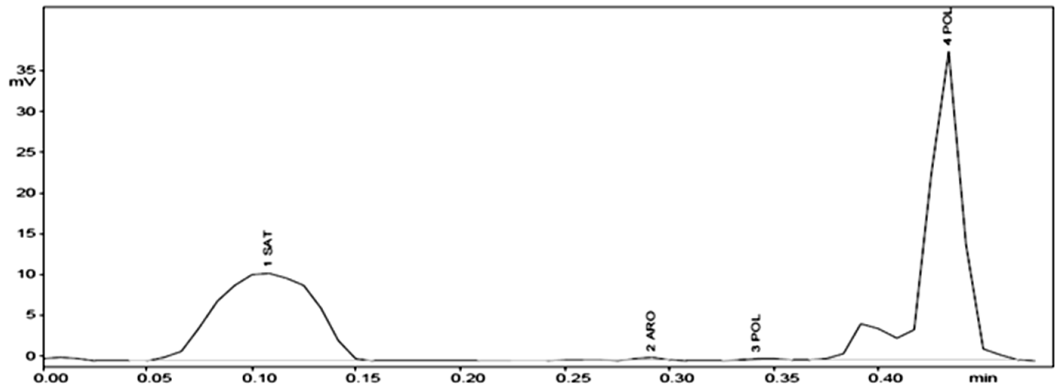

Calculation Method : Percent

Peak No	Win No.	Ret.Time (min)	Area	Resp.- Fact.	Area%	Name
1	1	0.108	19129	1.000	43.947	SAT
2	2	0.292	176	1.000	0.404	ARO
3	3	0.342	132	1.000	0.304	POL
4	3	0.433	24089	1.000	55.345	POL
			43526		100.000	

Sample Identifier: 4168

Data Processing Parameters

Injected on: 02.10.2012 Injected at: 14:15

Slice Width (ms): 500 Noise (µV/s): undefined

Threshold (mV): 0 Skim Ratio: 0

Parameter Files:

Data Handling File: Iatrosc1 Calculation-File: Iatrosc1

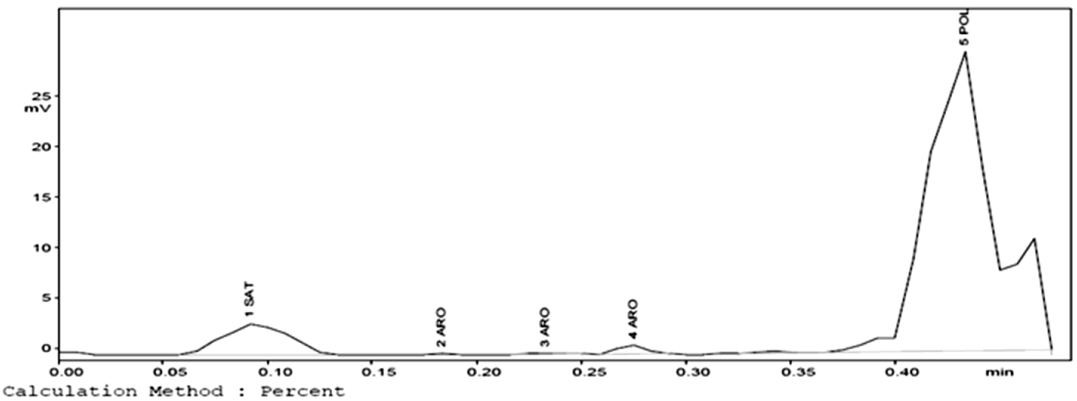

Calculation Method : Percent

Peak No	Win No.	Ret.Time (min)	Area	Resp.- Fact.	Area%	Name
1	1	0.092	3540	1.000	9.074	SAT
2	2	0.183	34	1.000	0.087	ARO
3	2	0.233	63	1.000	0.162	ARO
4	2	0.275	451	1.000	1.155	ARO
5	3	0.433	34922	1.000	89.522	POL
			39010		100.000	

Sample Identifier: 4170

Data Processing Parameters

Injected on:	02.10.2012	Injected at:	14:16
Slice Width (ms):	500	Noise (µV/s):	undefined
Threshold (mV):	0	Skim Ratio:	0

Parameter Files:

Data Handling File: Iatrosc1 Calculation-File: Iatrosc1

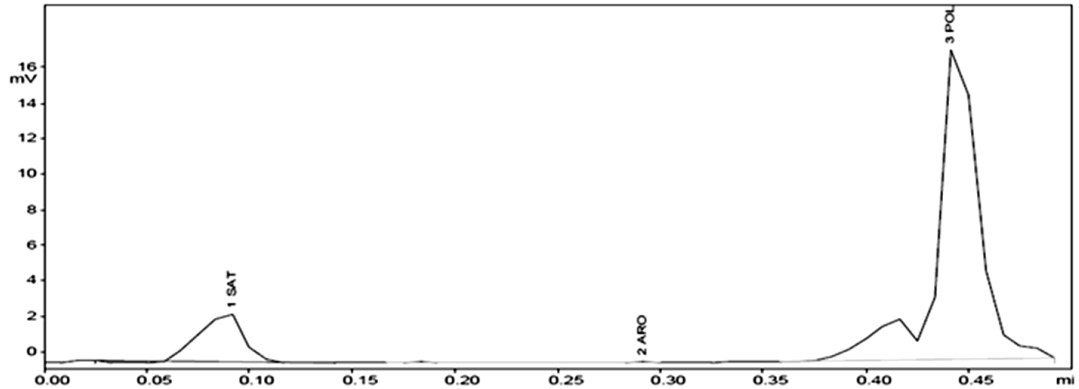

Calculation Method : Percent

Peak No	Win No.	Ret.Time (min)	Area	Resp.- Fact.	Area%	Name
1	1	0.092	1975	1.000	12.774	SAT
2	2	0.292	68	1.000	0.442	ARO
3	3	0.442	13419	1.000	86.784	POL
			15462		100.000	

Sample Identifier: 4171

Data Processing Parameters

Injected on:	02.10.2012	Injected at:	15:30
Slice Width (ms):	500	Noise (µV/s):	undefined
Threshold (mV):	0	Skim Ratio:	0

Parameter Files:

Data Handling File: Iatrosc1 Calculation-File: Iatrosc1

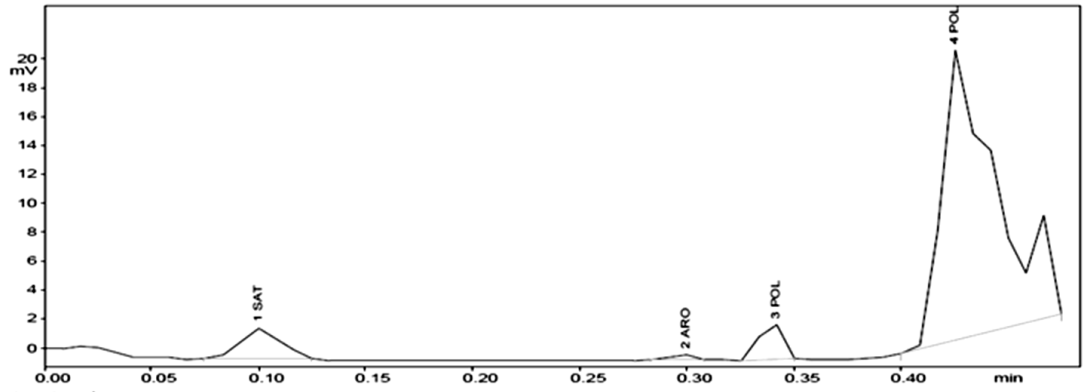

Calculation Method : Percent

Peak No	Win No.	Ret.Time (min)	Area	Resp.- Fact.	Area%	Name
1	1	0.100	1446	1.000	6.634	SAT
2	2	0.300	127	1.000	0.585	ARO
3	2	0.342	1060	1.000	4.864	POL
4	2	0.425	19160	1.000	87.918	POL
			21793		100.000	

Sample Identifier: 4183

Data Processing Parameters

Injected on:	02.10.2012	Injected at:	15:31
Slice Width (ms):	500	Noise (µV/s):	undefined
Threshold (mV):	0	Skim Ratio:	0

Parameter Files:

Data Handling File: Iatrosc1 Calculation-File: Iatrosc1

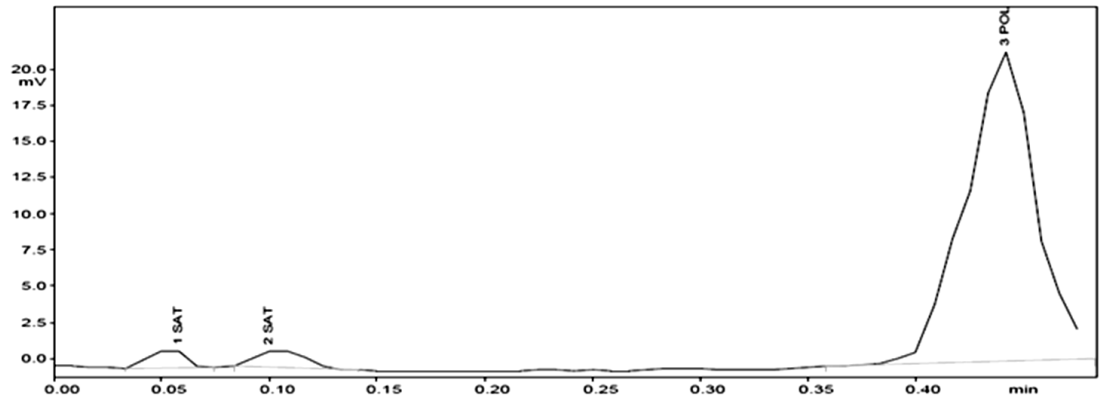

Calculation Method : Percent

Peak No	Win No.	Ret.Time (min)	Area	Resp.-Fact.	Area%	Name
1	1	0.058	801	1.000	2.917	SAT
2	1	0.100	964	1.000	3.509	SAT
3	2	0.442	25710	1.000	93.574	POL
			27476		100.000	

Sample Identifier: 4187

Data Processing Parameters

Injected on:	02.10.2012	Injected at:	15:32
Slice Width (ms):	500	Noise (µV/s):	undefined
Threshold (mV):	0	Skim Ratio:	0

Parameter Files:

Data Handling File: Iatrosc1 Calculation-File: Iatrosc1

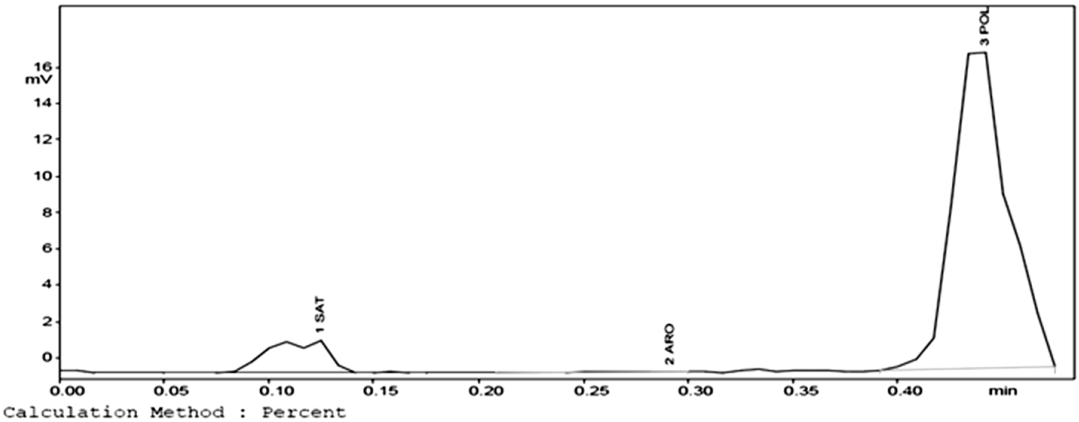

Calculation Method : Percent

Peak No	Win No.	Ret.Time (min)	Area	Resp.-Fact.	Area%	Name
1	1	0.125	1958	1.000	10.212	SAT
2	2	0.292	29	1.000	0.153	ARO
3	3	0.442	17184	1.000	89.635	POL
			19171		100.000	

Sample Identifier: 2224

Data Processing Parameters

Injected on:	02.10.2012	Injected at:	15:33
Slice Width (ms):	500	Noise (µV/s):	undefined
Threshold (mV):	0	Skim Ratio:	0

Parameter Files:

Data Handling File: Iatrosc1 Calculation-File: Iatrosc1

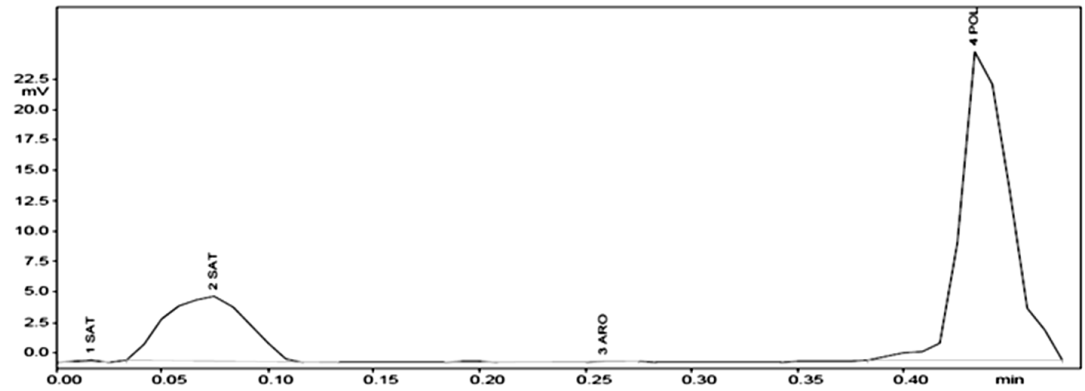

Calculation Method : Percent

Peak No	Win No.	Ret.Time (min)	Area	Resp.-Fact.	Area%	Name
1	1	0.017	105	1.000	0.363	SAT
2	1	0.075	7442	1.000	25.806	SAT
3	2	0.258	34	1.000	0.119	ARO
4	3	0.433	21258	1.000	73.712	POL
			28840		100.000	

Sample Identifier: 2225

Data Processing Parameters

Injected on:	02.10.2012	Injected at:	15:33
Slice Width (ms):	500	Noise (µV/s):	undefined
Threshold (mV):	0	Skim Ratio:	0

Parameter Files:

Data Handling File: Iatrosc1 Calculation-File: Iatrosc1

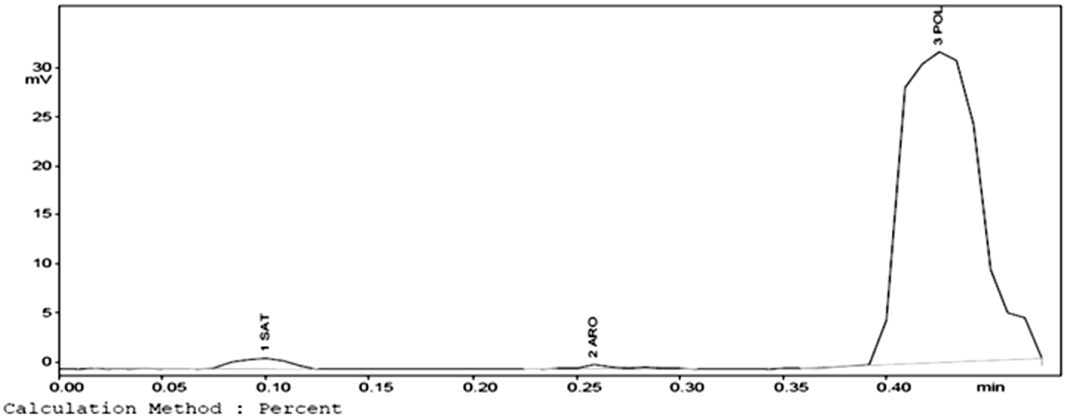

Calculation Method : Percent

Peak No	Win No.	Ret.Time (min)	Area	Resp.-Fact.	Area%	Name
1	1	0.100	874	1.000	1.930	SAT
2	2	0.258	336	1.000	0.743	ARO
3	3	0.425	44092	1.000	97.328	POL
			45302		100.000	

Sample Identifier: 2459a

Data Processing Parameters

Injected on: 02.10.2012 Injected at: 17:08

Slice Width (ms): 500 Noise (µV/s): undefined

Threshold (mV): 0 Skim Ratio: 0

Parameter Files:

Data Handling File: Iatrosc1 Calculation-File: Iatrosc1

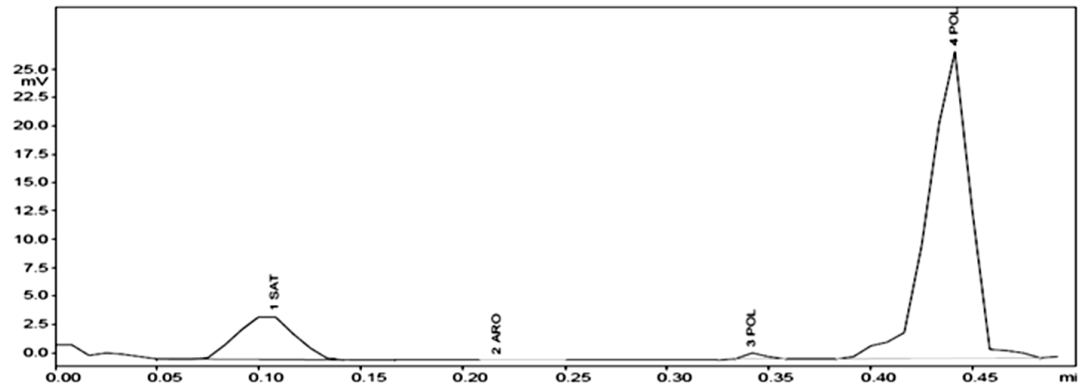

Calculation Method : Percent

Peak No	Win No.	Ret.Time (min)	Area	Resp.-Fact.	Area%	Name
1	1	0.108	3946	1.000	16.168	SAT
2	2	0.217	8	1.000	0.035	ARO
3	3	0.342	193	1.000	0.789	POL
4	3	0.442	20261	1.000	83.008	POL
			24409		100.000	

Sample Identifier: 2463

Data Processing Parameters

Injected on: 02.10.2012 Injected at: 17:10

Slice Width (ms): 500 Noise (µV/s): undefined

Threshold (mV): 0 Skim Ratio: 0

Parameter Files:

Data Handling File: Iatrosc1 Calculation-File: Iatrosc1

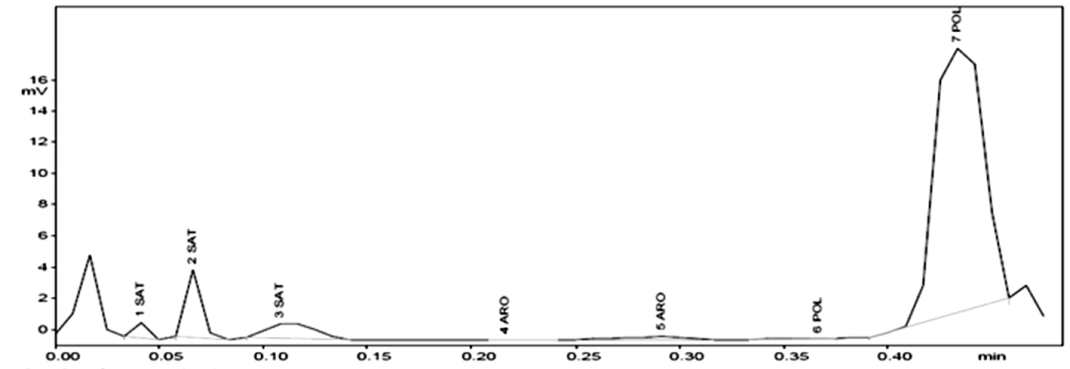

Calculation Method : Percent

Peak No	Win No.	Ret.Time (min)	Area	Resp.-Fact.	Area%	Name
1	1	0.042	225	1.000	1.291	SAT
2	1	0.067	1190	1.000	6.827	SAT
3	1	0.108	785	1.000	4.505	SAT
5	2	0.292	195	1.000	1.117	ARO
6	3	0.367	31	1.000	0.175	POL
7	3	0.433	15007	1.000	86.084	POL
			17433		100.000	

Sample Identifier: 2565

Data Processing Parameters

Injected on:	03.10.2012	Injected at:	15:18
Slice Width (ms):	500	Noise (µV/s):	undefined
Threshold (mV):	0	Skim Ratio:	0

Parameter Files:

Data Handling File: Iatrosc1 Calculation-File: Iatrosc1

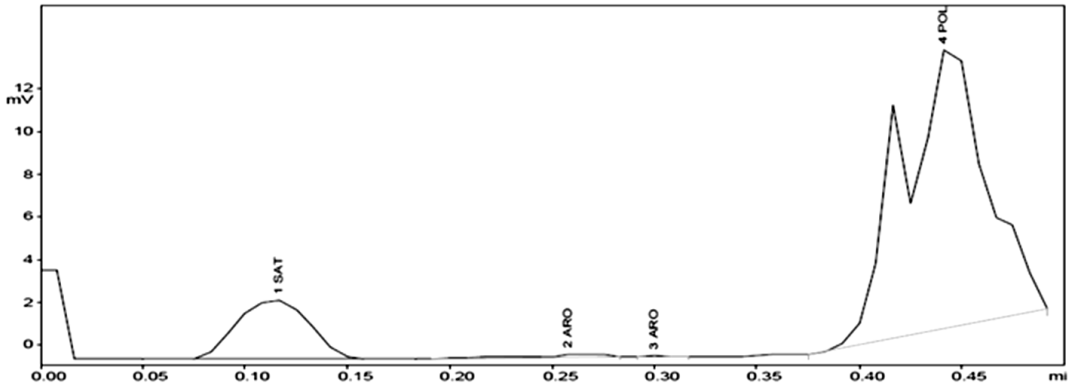

Calculation Method : Percent

Peak No	Win No.	Ret.Time (min)	Area	Resp.- Fact.	Area%	Name
1	1	0.117	3593	1.000	15.224	SAT
2	2	0.258	152	1.000	0.642	ARO
3	2	0.300	11	1.000	0.047	ARO
4	2	0.442	19846	1.000	84.087	POL
			23602		100.000	

Sample Identifier: 2003.9

Data Processing Parameters

Injected on:	03.10.2012	Injected at:	12:10
Slice Width (ms):	500	Noise (µV/s):	undefined
Threshold (mV):	0	Skim Ratio:	0

Parameter Files:

Data Handling File: Iatrosc1 Calculation-File: Iatrosc1

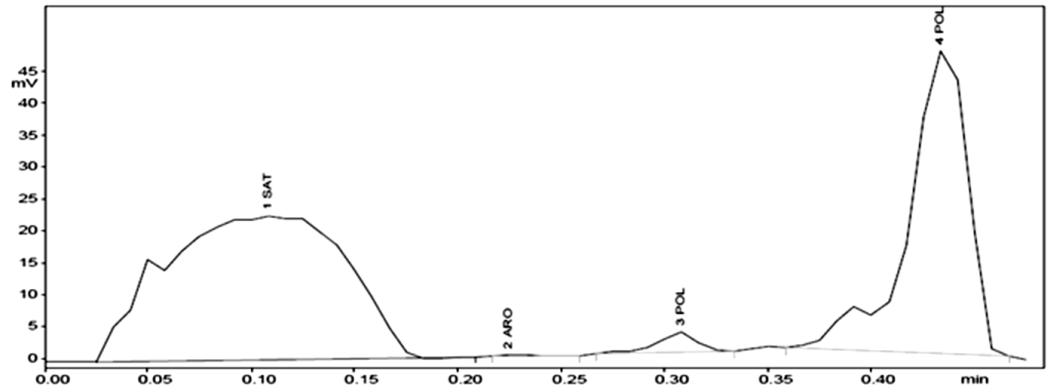

Calculation Method : Percent

Peak No	Win No.	Ret.Time (min)	Area	Resp.- Fact.	Area%	Name
1	1	0.108	73375	1.000	58.428	SAT
2	2	0.225	106	1.000	0.084	ARO
3	3	0.308	2122	1.000	1.690	POL
4	3	0.433	49979	1.000	39.798	POL
			125582		100.000	

Sample Identifier: 2005

Data Processing Parameters

Injected on: 03.10.2012 Injected at: 12:10

Slice Width (ms): 500 Noise (µV/s): undefined

Threshold (mV): 0 Skim Ratio: 0

Parameter Files:

Data Handling File: Iatrosc1 Calculation-File: Iatrosc1

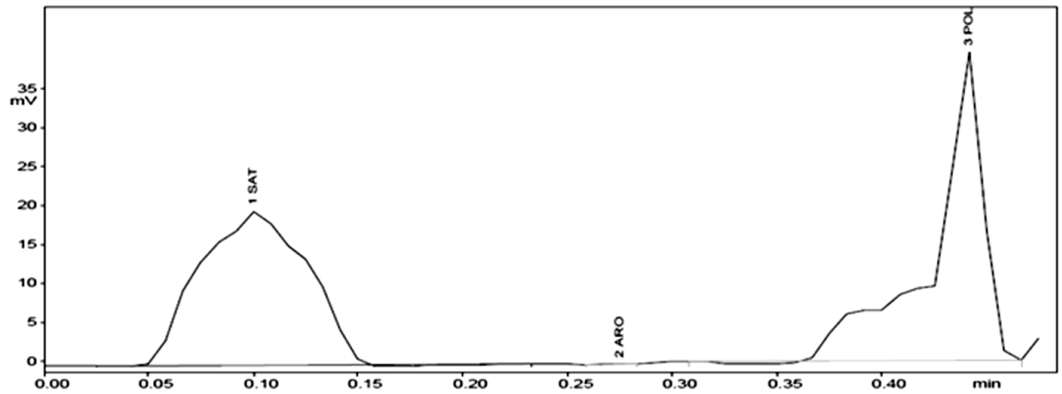

Calculation Method : Percent

Peak No	Win No.	Ret.Time (min)	Area	Resp.- Fact.	Area%	Name
1	1	0.100	37071	1.000	52.179	SAT
2	2	0.275	62	1.000	0.087	ARO
3	3	0.442	33912	1.000	47.734	POL
			71045		100.000	

Sample Identifier: 2006

Data Processing Parameters

Injected on: 03.10.2012 Injected at: 12:11

Slice Width (ms): 500 Noise (µV/s): undefined

Threshold (mV): 0 Skim Ratio: 0

Parameter Files:

Data Handling File: Iatrosc1 Calculation-File: Iatrosc1

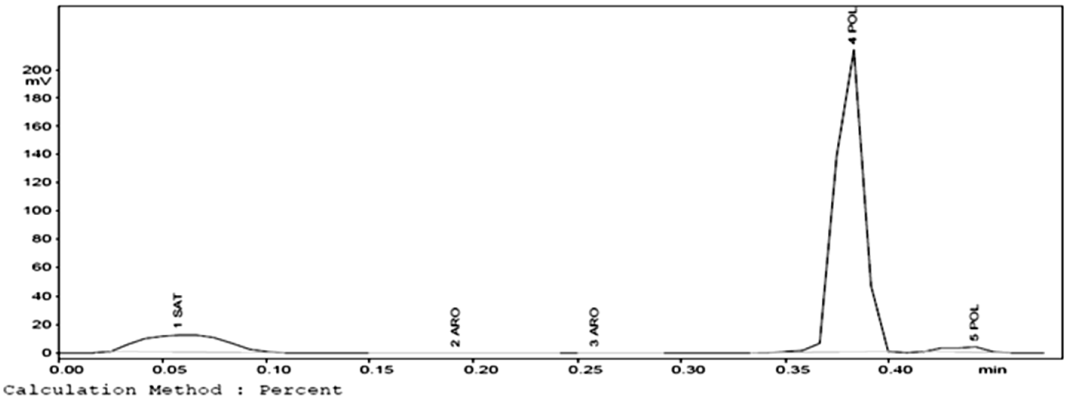

Calculation Method : Percent

Peak No	Win No.	Ret.Time (min)	Area	Resp.- Fact.	Area%	Name
1	1	0.058	18535	1.000	14.515	SAT
3	2	0.258	28	1.000	0.022	ARO
4	3	0.383	106621	1.000	83.495	POL
5	3	0.442	2512	1.000	1.967	POL
			127697		100.000	

Sample Identifier: 2006.6

Data Processing Parameters

Injected on: 03.10.2012 Injected at: 12:12

Slice Width (ms): 500 Noise (µV/s): undefined

Threshold (mV): 0 Skim Ratio: 0

Parameter Files:

Data Handling File: Iatrosc1 Calculation-File: Iatrosc1

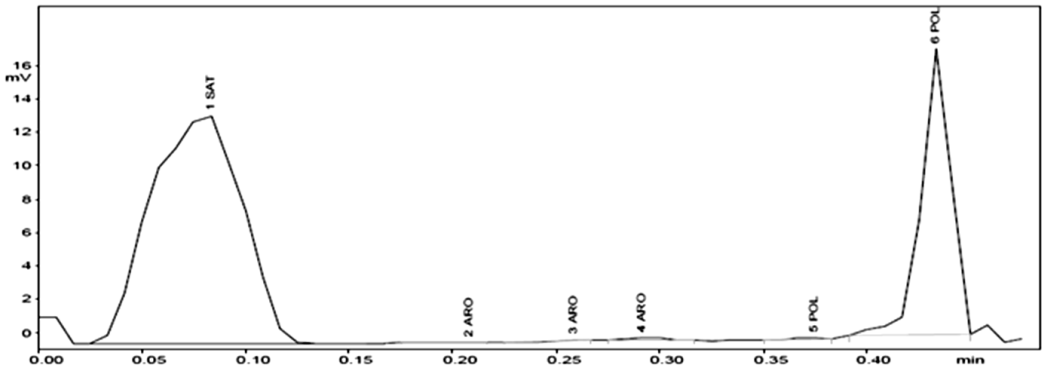

Calculation Method : Percent

Peak No	Win No.	Ret.Time (min)	Area	Resp.- Fact.	Area%	Name
1	1	0.083	21880	1.000	70.395	SAT
2	2	0.208	27	1.000	0.088	ARO
3	2	0.258	27	1.000	0.085	ARO
4	2	0.292	99	1.000	0.317	ARO
5	3	0.375	41	1.000	0.131	POL
6	3	0.433	9009	1.000	28.984	POL
			31082		100.000	

Sample Identifier: 2386

Data Processing Parameters

Injected on: 03.10.2012 Injected at: 12:13

Slice Width (ms): 500 Noise (µV/s): undefined

Threshold (mV): 0 Skim Ratio: 0

Parameter Files:

Data Handling File: Iatrosc1 Calculation-File: Iatrosc1

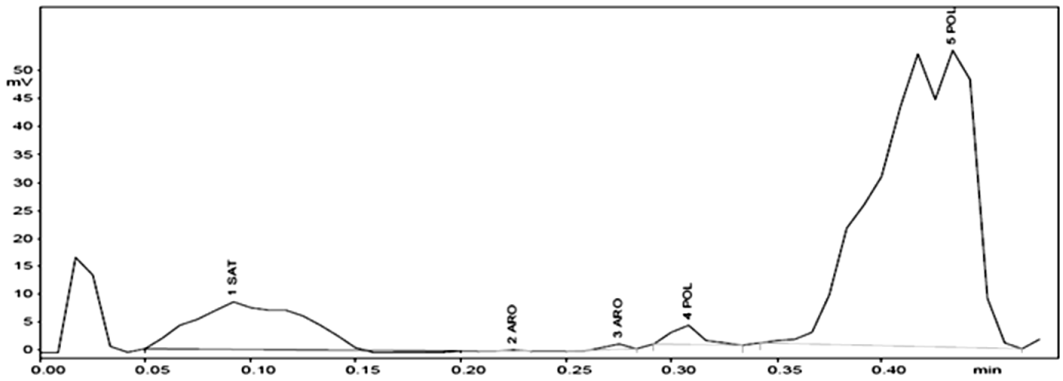

Calculation Method : Percent

Peak No	Win No.	Ret.Time (min)	Area	Resp.- Fact.	Area%	Name
1	1	0.092	16153	1.000	15.118	SAT
2	2	0.225	32	1.000	0.030	ARO
3	2	0.275	417	1.000	0.390	ARO
4	3	0.308	1774	1.000	1.660	POL
5	3	0.433	88472	1.000	82.802	POL
			106848		100.000	

Sample Identifier: 2391

Data Processing Parameters

Injected on: 03.10.2012 Injected at: 12:14

Slice Width (ms): 500 Noise (µV/s): undefined

Threshold (mV): 0 Skim Ratio: 0

Parameter Files:

Data Handling File: Iatrosc1 Calculation-File: Iatrosc1

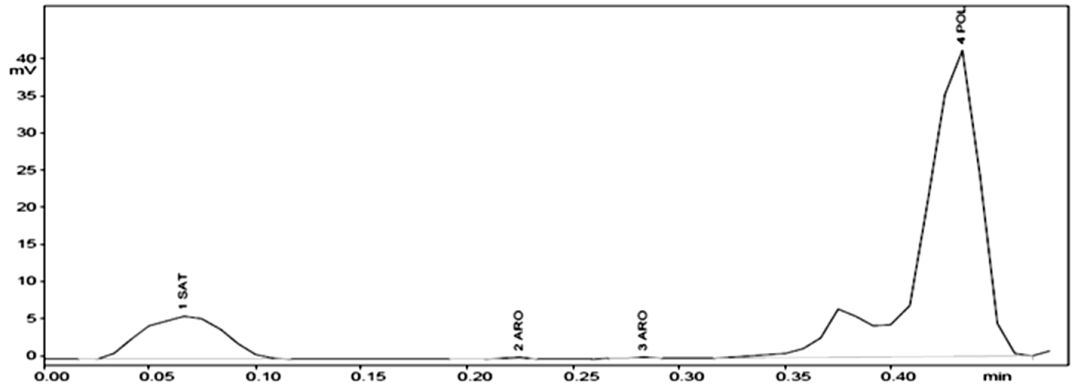

Calculation Method : Percent

Peak No	Win No.	Ret.Time (min)	Area	Resp.- Fact.	Area%	Name
1	1	0.067	8304	1.000	16.515	SAT
2	2	0.225	60	1.000	0.120	ARO
3	2	0.283	36	1.000	0.071	ARO
4	3	0.433	41881	1.000	83.293	POL
			50281		100.000	

Sample Identifier: 2393

Data Processing Parameters

Injected on: 03.10.2012 Injected at: 12:15

Slice Width (ms): 500 Noise (µV/s): undefined

Threshold (mV): 0 Skim Ratio: 0

Parameter Files:

Data Handling File: Iatrosc1 Calculation-File: Iatrosc1

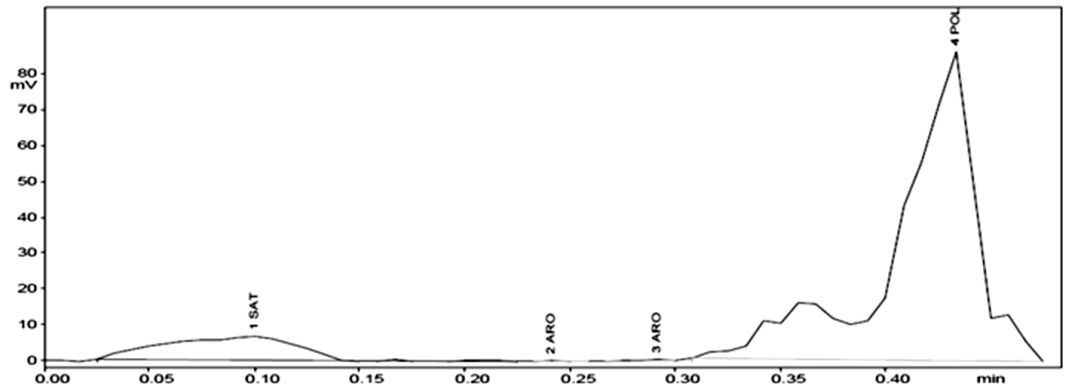

Calculation Method : Percent

Peak No	Win No.	Ret.Time (min)	Area	Resp.- Fact.	Area%	Name
1	1	0.100	14472	1.000	11.095	SAT
2	2	0.242	58	1.000	0.044	ARO
3	2	0.292	196	1.000	0.151	ARO
4	3	0.433	115715	1.000	88.710	POL
			130442		100.000	

Sample Identifier: 1482

Data Processing Parameters

Injected on:	03.10.2012	Injected at:	13:48
Slice Width (ms):	500	Noise (µV/s):	undefined
Threshold (mV):	0	Skim Ratio:	0

Parameter Files:

Data Handling File: Iatrosc1 Calculation-File: Iatrosc1

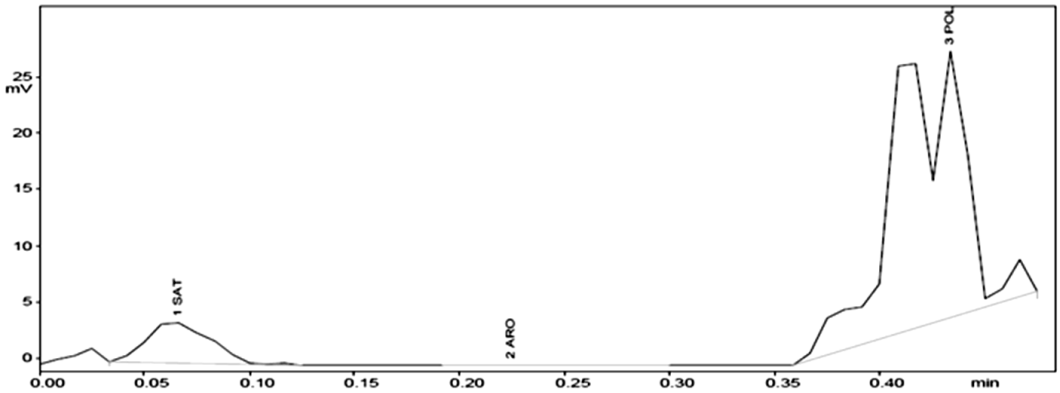

Calculation Method : Percent

Peak No	Win No.	Ret.Time (min)	Area	Resp.-Fact.	Area%	Name
1	1	0.067	4146	1.000	11.576	SAT
2	2	0.225	20	1.000	0.055	ARO
3	3	0.433	31655	1.000	88.369	POL
			35821		100.000	

Sample Identifier: 1490

Data Processing Parameters

Injected on:	03.10.2012	Injected at:	13:49
Slice Width (ms):	500	Noise (µV/s):	undefined
Threshold (mV):	0	Skim Ratio:	0

Parameter Files:

Data Handling File: Iatrosc1 Calculation-File: Iatrosc1

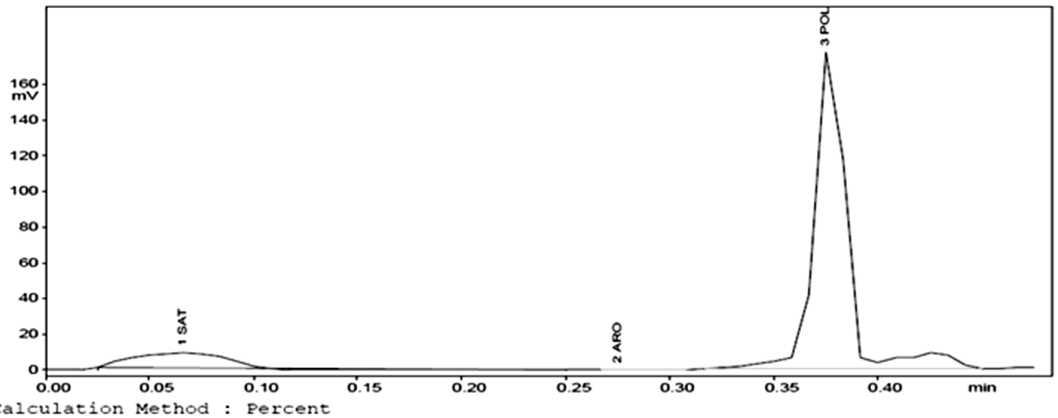

Calculation Method : Percent

Peak No	Win No.	Ret.Time (min)	Area	Resp.-Fact.	Area%	Name
1	1	0.067	11462	1.000	9.972	SAT
2	2	0.275	67	1.000	0.059	ARO
3	3	0.375	103403	1.000	89.969	POL
			114932		100.000	

Sample Identifier: 1497

Data Processing Parameters

Injected on:	03.10.2012	Injected at:	13:50
Slice Width (ms):	500	Noise (µV/s):	undefined
Threshold (mV):	0	Skim Ratio:	0

Parameter Files:

Data Handling File: Iatrosc1 Calculation-File: Iatrosc1

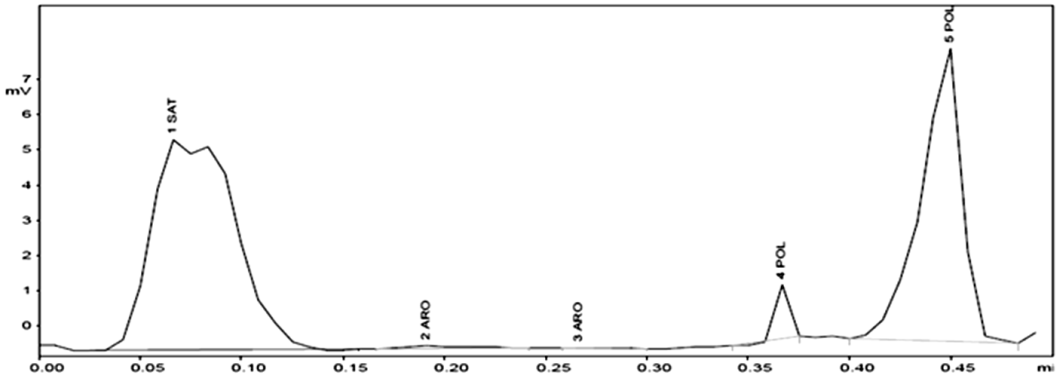

Calculation Method : Percent

Peak No	Win No.	Ret.Time (min)	Area	Resp.-Fact.	Area%	Name
1	1	0.067	9064	1.000	57.944	SAT
2	2	0.192	81	1.000	0.517	ARO
3	2	0.267	6	1.000	0.036	ARO
4	3	0.367	421	1.000	2.688	POL
5	3	0.450	6072	1.000	38.815	POL
			15643		100.000	

Sample Identifier: 1503

Data Processing Parameters

Injected on:	03.10.2012	Injected at:	13:52
Slice Width (ms):	500	Noise (µV/s):	undefined
Threshold (mV):	0	Skim Ratio:	0

Parameter Files:

Data Handling File: Iatrosc1 Calculation-File: Iatrosc1

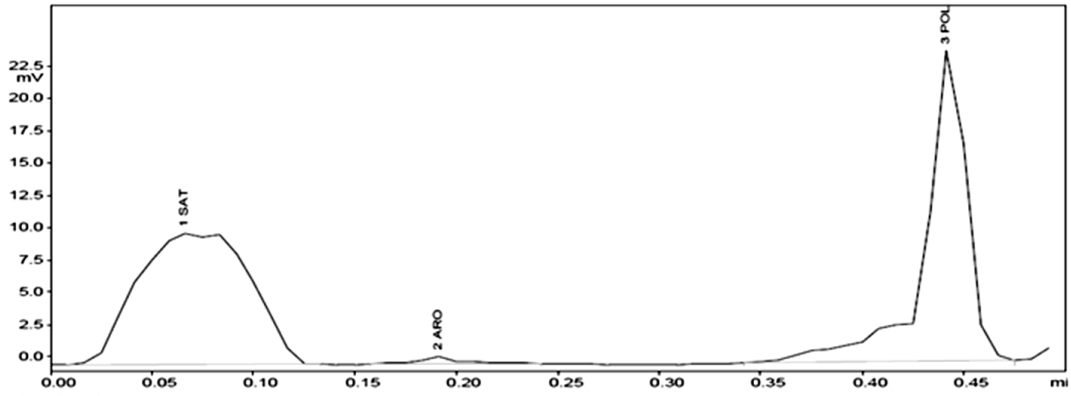

Calculation Method : Percent

Peak No	Win No.	Ret.Time (min)	Area	Resp.-Fact.	Area%	Name
1	1	0.067	20857	1.000	52.725	SAT
2	2	0.192	399	1.000	1.008	ARO
3	3	0.442	18302	1.000	46.266	POL
			39557		100.000	

Sample Identifier: 1505

Data Processing Parameters

Injected on: 03.10.2012 Injected at: 13:53

Slice Width (ms): 500 Noise (µV/s): undefined

Threshold (mV): 0 Skim Ratio: 0

Parameter Files:

Data Handling File: Iatrosc1 Calculation-File: Iatrosc1

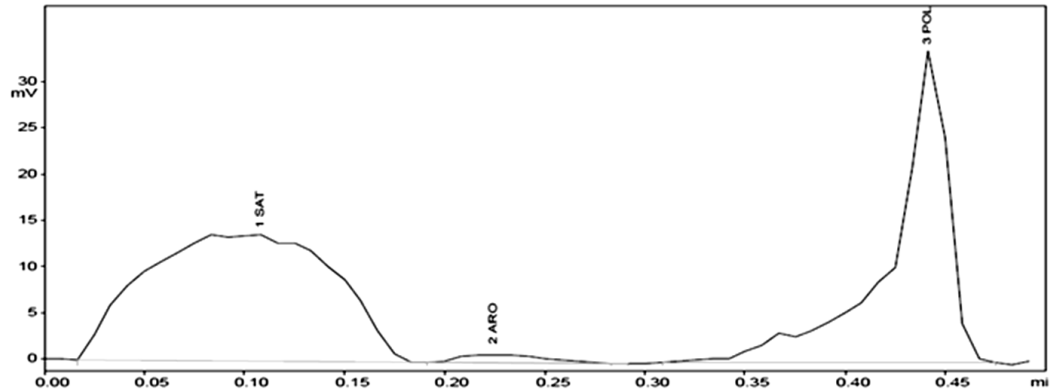

Calculation Method : Percent

Peak No	Win No.	Ret.Time (min)	Area	Resp.- Fact.	Area%	Name
1	1	0.108	48098	1.000	57.034	SAT
2	2	0.225	1353	1.000	1.604	ARO
3	3	0.442	34882	1.000	41.362	POL
			84332		100.000	

Sample Identifier: 1507

Data Processing Parameters

Injected on: 03.10.2012 Injected at: 15:18

Slice Width (ms): 500 Noise (µV/s): undefined

Threshold (mV): 0 Skim Ratio: 0

Parameter Files:

Data Handling File: Iatrosc1 Calculation-File: Iatrosc1

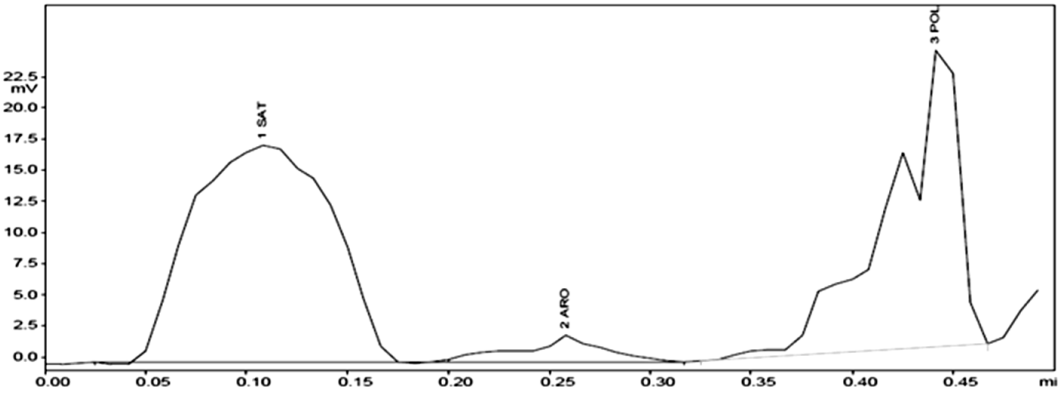

Calculation Method : Percent

Peak No	Win No.	Ret.Time (min)	Area	Resp.- Fact.	Area%	Name
1	1	0.108	44018	1.000	57.017	SAT
2	2	0.258	3020	1.000	3.912	ARO
3	3	0.442	30164	1.000	39.071	POL
			77203		100.000	

Sample Identifier: 1381

Data Processing Parameters

Injected on: 03.10.2012 Injected at: 15:20

Slice Width (ms): 500 Noise (µV/s): undefined

Threshold (mV): 0 Skim Ratio: 0

Parameter Files:

Data Handling File: Iatrosc1 Calculation-File: Iatrosc1

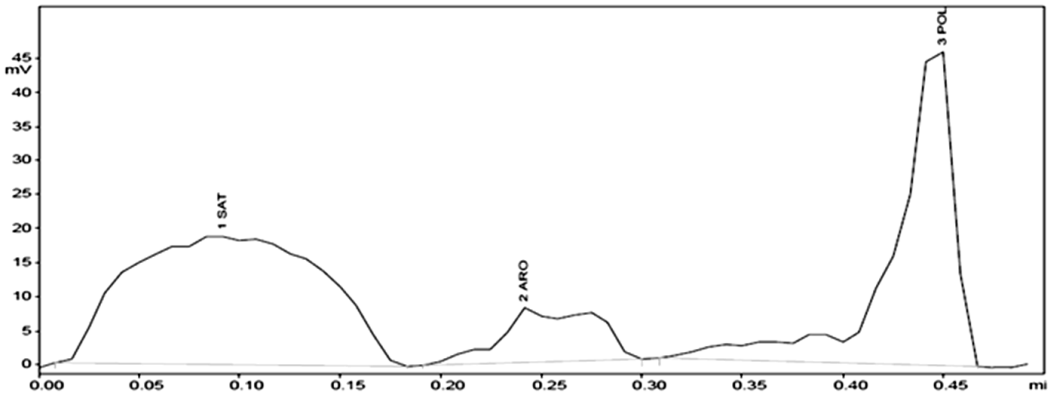

Calculation Method : Percent

Peak No	Win No.	Ret.Time (min)	Area	Resp.-Fact.	Area%	Name
1	1	0.092	68014	1.000	51.994	SAT
2	2	0.242	13714	1.000	10.484	ARO
3	3	0.450	49082	1.000	37.522	POL
			130810		100.000	

Sample Identifier: 1383

Data Processing Parameters

Injected on: 03.10.2012 Injected at: 15:21

Slice Width (ms): 500 Noise (µV/s): undefined

Threshold (mV): 0 Skim Ratio: 0

Parameter Files:

Data Handling File: Iatrosc1 Calculation-File: Iatrosc1

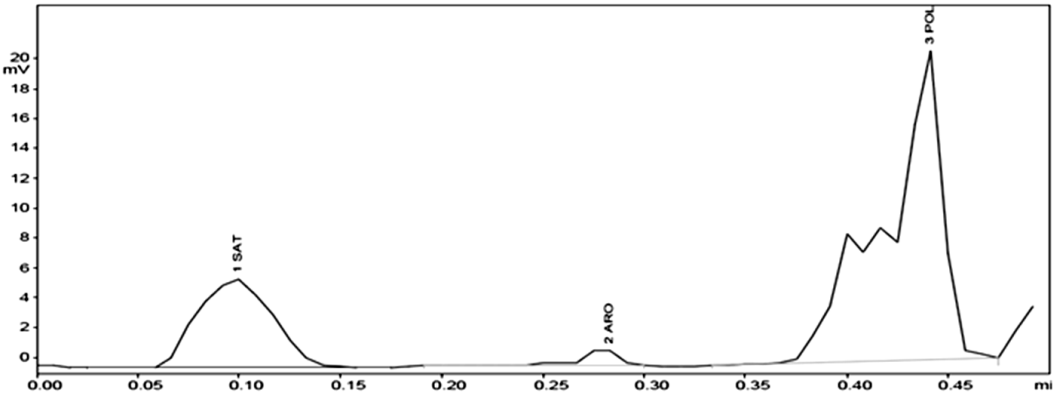

Calculation Method : Percent

Peak No	Win No.	Ret.Time (min)	Area	Resp.-Fact.	Area%	Name
1	1	0.100	7967	1.000	26.156	SAT
2	2	0.283	717	1.000	2.353	ARO
3	3	0.442	21776	1.000	71.491	POL
			30460		100.000	

Sample Identifier: 1390

Data Processing Parameters

Injected on: 03.10.2012 Injected at: 15:22

Slice Width (ms): 500 Noise (µV/s): undefined

Threshold (mV): 0 Skim Ratio: 0

Parameter Files:

Data Handling File: Iatrosc1 Calculation-File: Iatrosc1

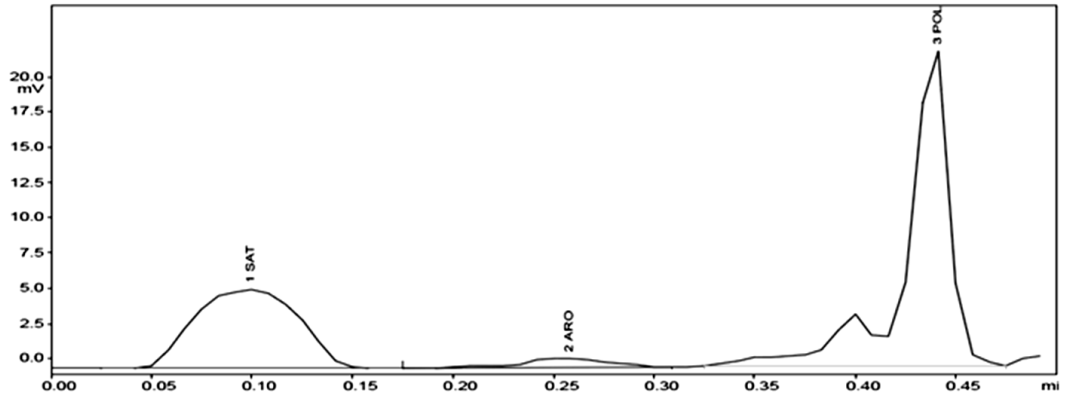

Calculation Method : Percent

Peak No	Win No.	Ret.Time (min)	Area	Resp.-Fact.	Area%	Name
1	1	0.100	10495	1.000	35.380	SAT
2	2	0.258	1141	1.000	3.845	ARO
3	3	0.442	18029	1.000	60.775	POL
			29665		100.000	

Sample Identifier: 1393

Data Processing Parameters

Injected on: 03.10.2012 Injected at: 15:22

Slice Width (ms): 500 Noise (µV/s): undefined

Threshold (mV): 0 Skim Ratio: 0

Parameter Files:

Data Handling File: Iatrosc1 Calculation-File: Iatrosc1

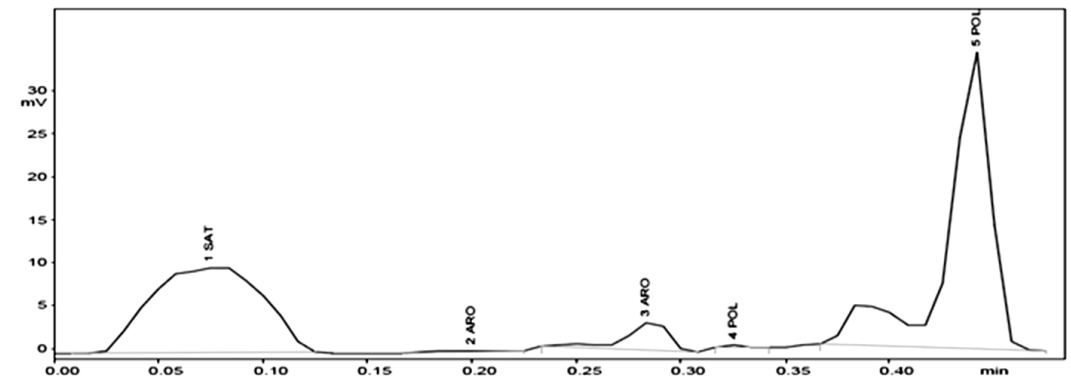

Calculation Method : Percent

Peak No	Win No.	Ret.Time (min)	Area	Resp.-Fact.	Area%	Name
1	1	0.075	19616	1.000	40.126	SAT
2	2	0.200	148	1.000	0.303	ARO
3	2	0.283	2398	1.000	4.905	ARO
4	3	0.325	112	1.000	0.229	POL
5	3	0.442	26613	1.000	54.437	POL
			48887		100.000	

Sample Identifier: 1589

Data Processing Parameters

Injected on:	03.10.2012	Injected at:	15:23
Slice Width (ms):	500	Noise (µV/s):	undefined
Threshold (mV):	0	Skim Ratio:	0

Parameter Files:

Data Handling File: Iatrosc1 Calculation-File: Iatrosc1

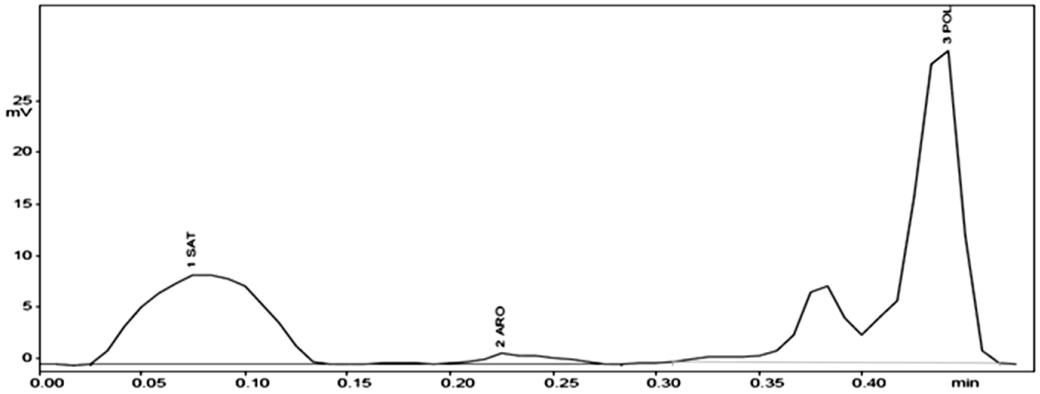

Calculation Method : Percent

Peak No	Win No.	Ret.Time (min)	Area	Resp.-Fact.	Area%	Name
1	1	0.075	18542	1.000	34.918	SAT
2	2	0.225	1314	1.000	2.475	ARO
3	3	0.442	33244	1.000	62.607	POL
			53100		100.000	

Appendix E (Light hydrocarbons Chromatograms)

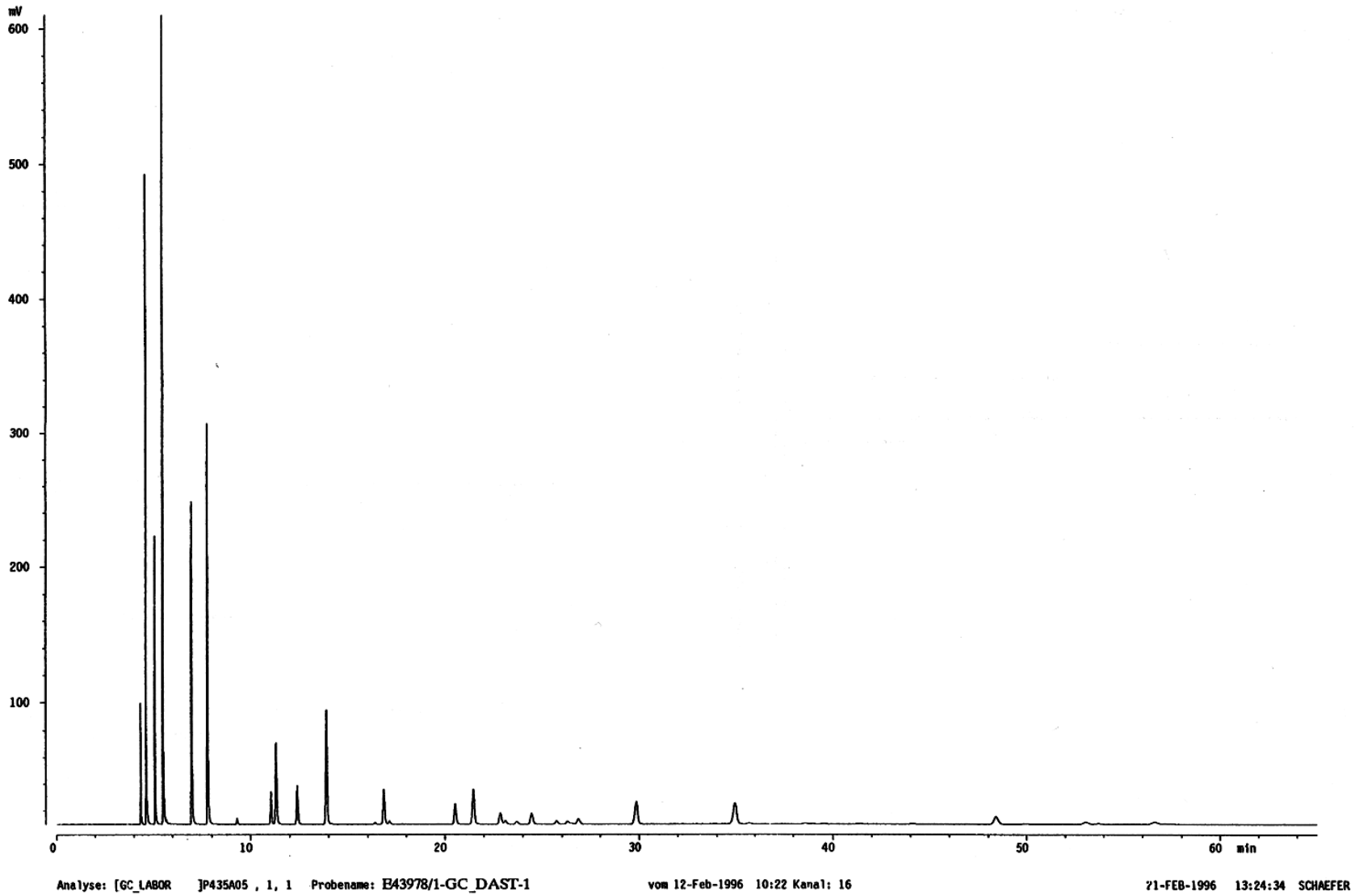
mV
600
500
400
300
200
100
0
10
20
30
40
50
60 min
Analyse: [GC_LABOR]P435A05 , 1, 1 Probename: B43978/1-GC_DAST-1
vom 12-Feb-1996 10:22 Kanal: 16
21-FEB-1996 13:24:34 SCHAEFER

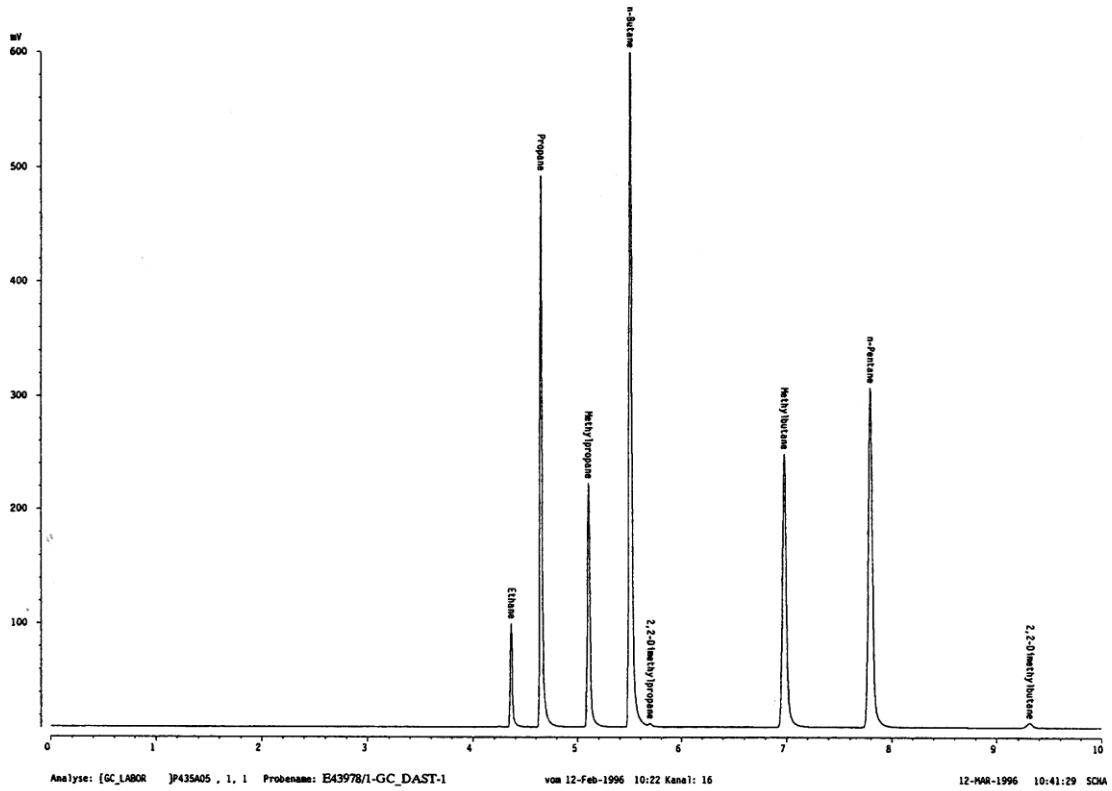
mV
600
500
400
300
200
100
Ethane
Propane
Methylpropane
n-Butane
2,2-Dimethylpropane
Methylbutane
n-Pentane
2,2-Dimethylbutane
0
1
2
3
4
5
6
7
8
9
10
Analyse: [GC_LABOR]P435A05 , 1, 1 Probename: E43978/1-GC_DAST-1
vom 12-Feb-1996 10:22 Kanal: 16
12-MAR-1996 10:41:29 SCHA

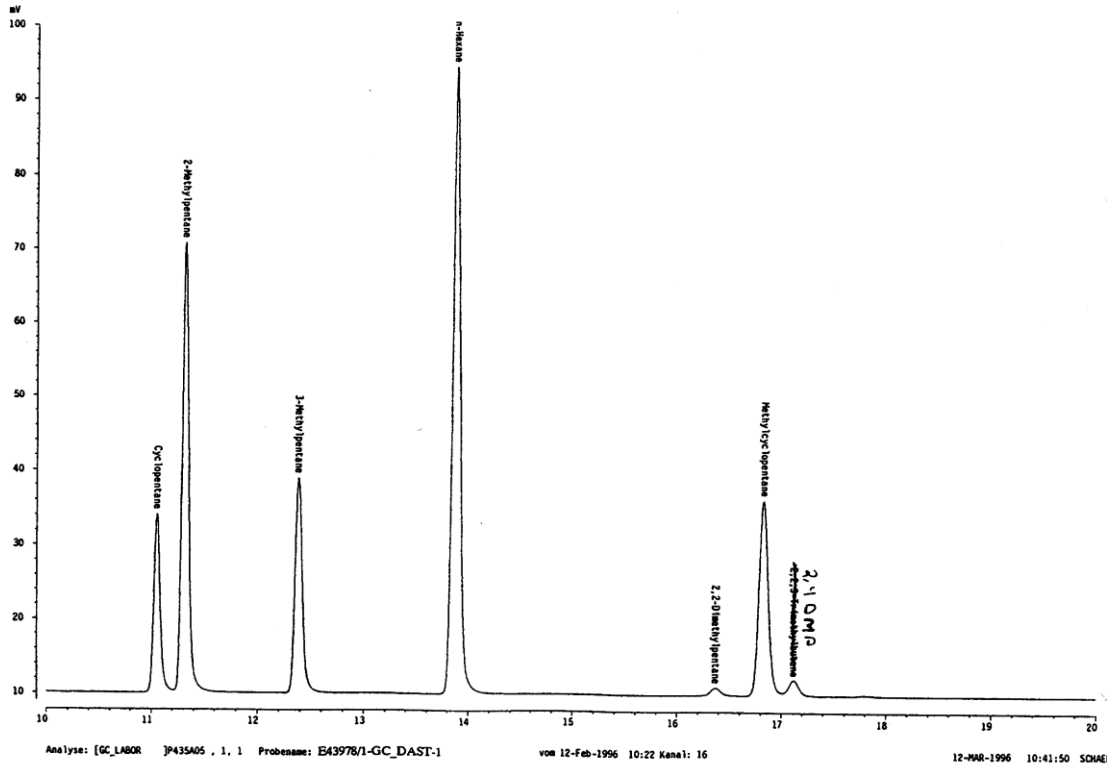
mV
100
90
80
70
60
50
40
30
20
10
Cyclopentane
2-Methylpentane
3-Methylpentane
n-Hexane
2,2-Dimethylpentane
Methylcyclopentane
2,4 DMP
10
11
12
13
14
15
16
17
18
19
20
Analyse: [GC_LABOR]P435A05 , 1, 1 Probename: E43978/1-GC_DAST-1
vom 12-Feb-1996 10:22 Kanal: 16
12-MAR-1996 10:41:50 SCHAE

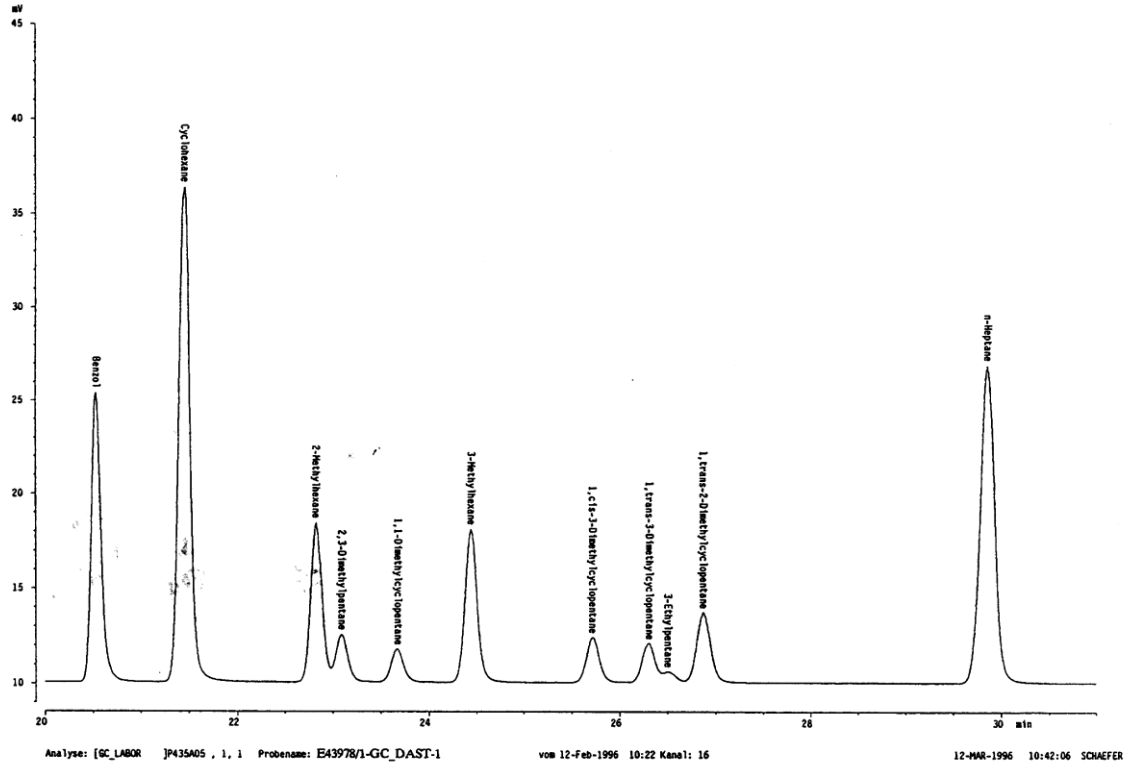
mV
45
40
35
30
25
20
15
10
Benzol
Cyclohexane
2-Methylhexane
2,3-Dimethylpentane
1,1-Dimethylcyclopentane
3-Methylhexane
1,cis-3-Dimethylcyclopentane
1,trans-3-Dimethylcyclopentane
3-Ethylpentane
1,trans-2-Dimethylcyclopentane
n-Heptane
20
22
24
26
28
30 min
Analyse: [GC_LABOR]P435A05 , 1, 1 Probename: E43978/1-GC_DAST-1
vom 12-Feb-1996 10:22 Kanal: 16
12-MAR-1996 10:42:06 SCHAEFER

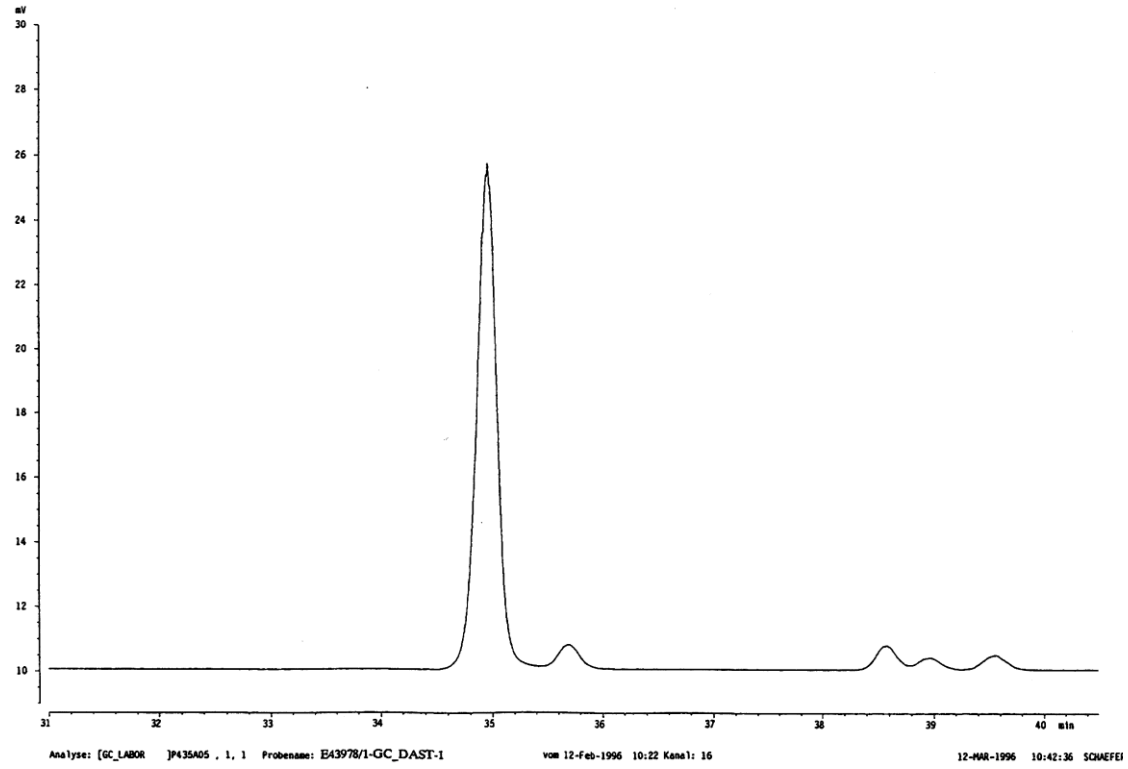
mV
30
28
26
24
22
20
18
16
14
12
10
31
32
33
34
35
36
37
38
39
40 min
Analyse: [GC_LABOR]P435A05 , 1, 1 Probename: E43978/1-GC_DAST-1
vom 12-Feb-1996 10:22 Kanal: 16
12-MAR-1996 10:42:36 SCHAEFE

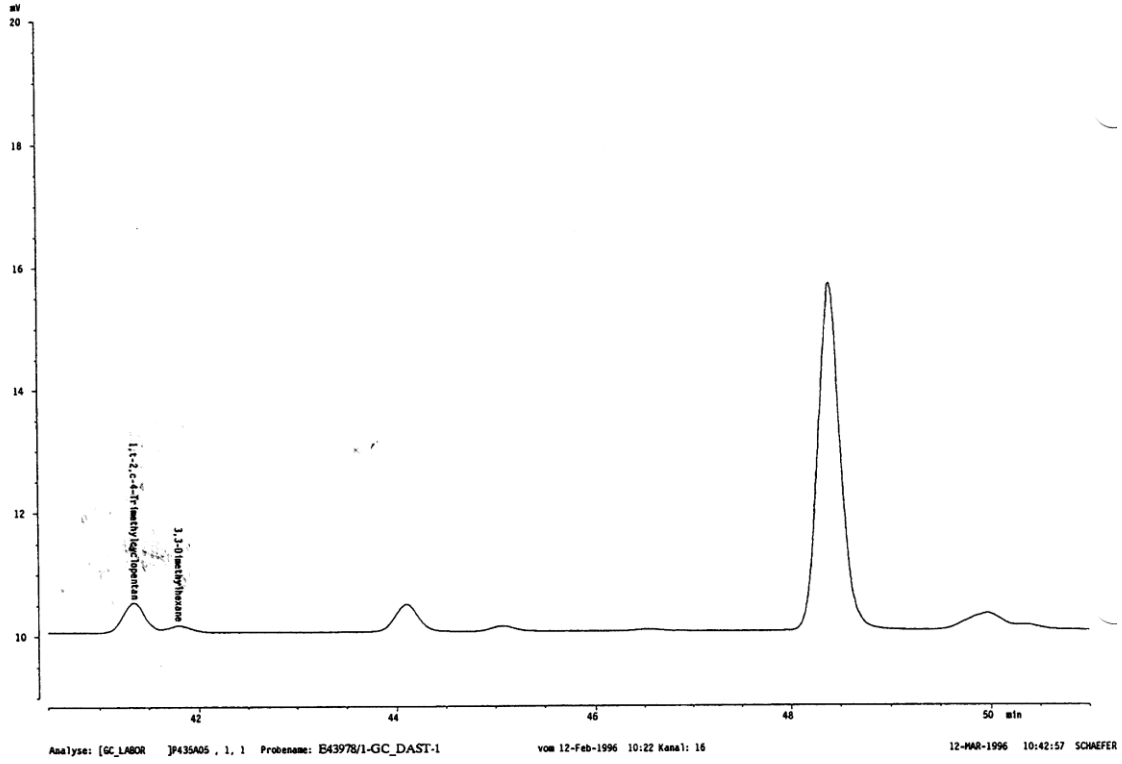
mV
20
18
16
14
12
10
1,t-2,c-4-Trimethylcyclopentan
3,3-Dimethylhexane
42
44
46
48
50 min
Analyse: [GC_LABOR]P435A05 , 1, 1 Probename: B43978/1-GC_DAST-1 vom 12-Feb-1996 10:22 Kanal: 16 12-MAR-1996 10:42:57 SCHAEFER

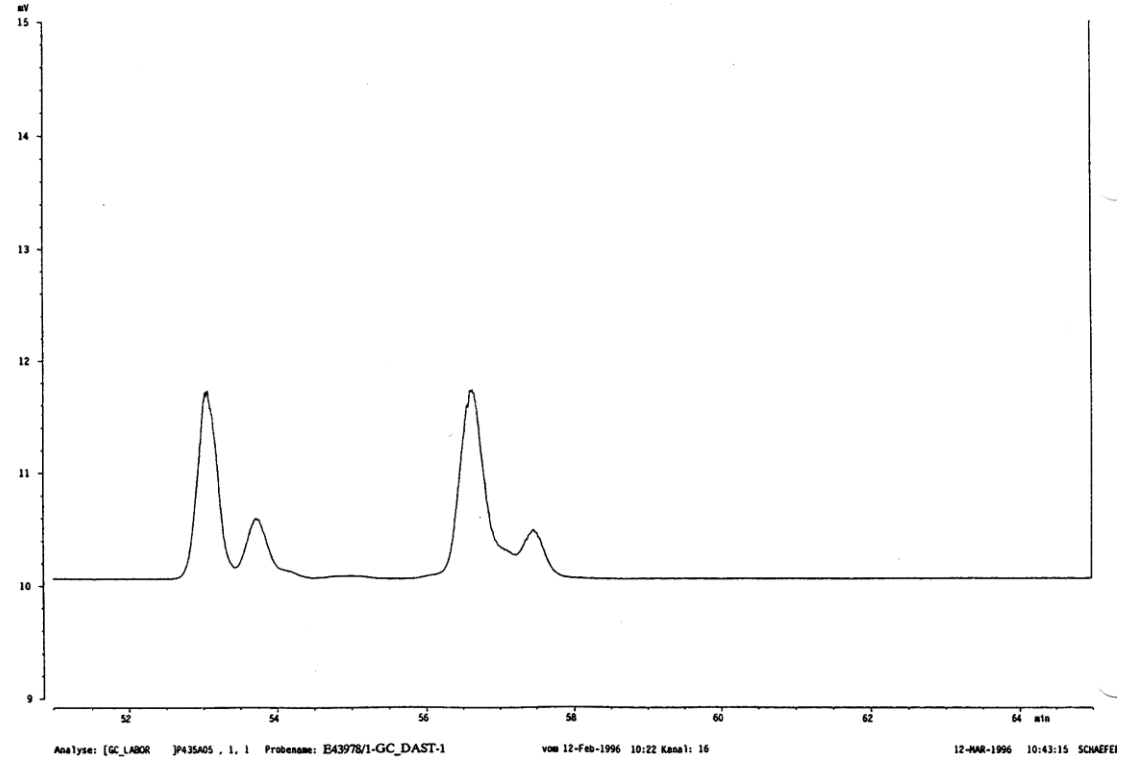
mV
15
14
13
12
11
10
9
52
54
56
58
60
62
64 min
Analyse: [GC_LABOR]P435A05 , 1, 1 Probename: B43978/1-GC_DAST-1 vom 12-Feb-1996 10:22 Kanal: 16 12-MAR-1996 10:43:15 SCHAEFEI

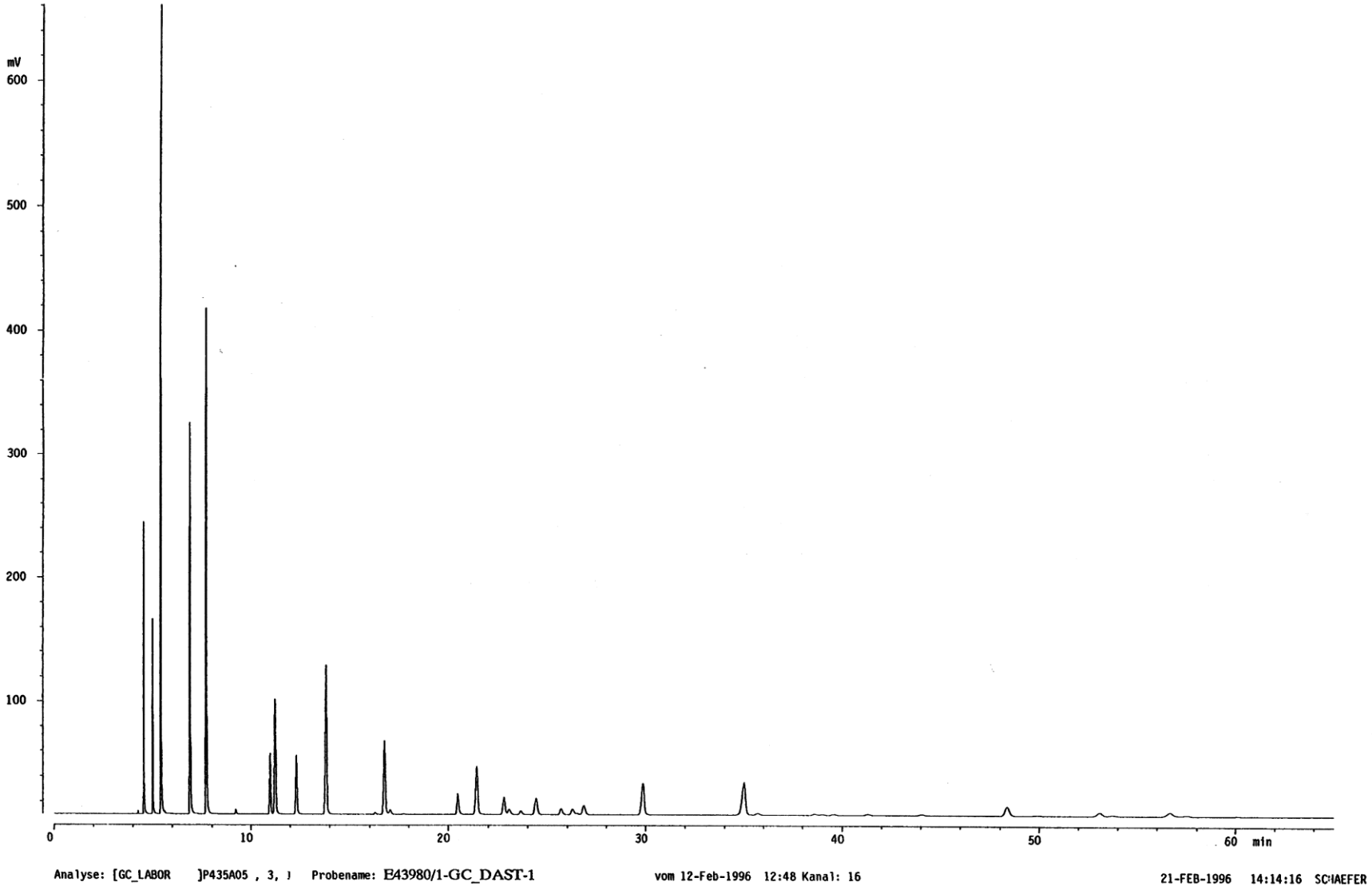
mV
600
500
400
300
200
100
0
10
20
30
40
50
60 min
Analyse: [GC_LABOR]P435A05 , 3,) Probename: E43980/1-GC_DAST-1
vom 12-Feb-1996 12:48 Kanal: 16
21-FEB-1996 14:14:16 SCHAEFER

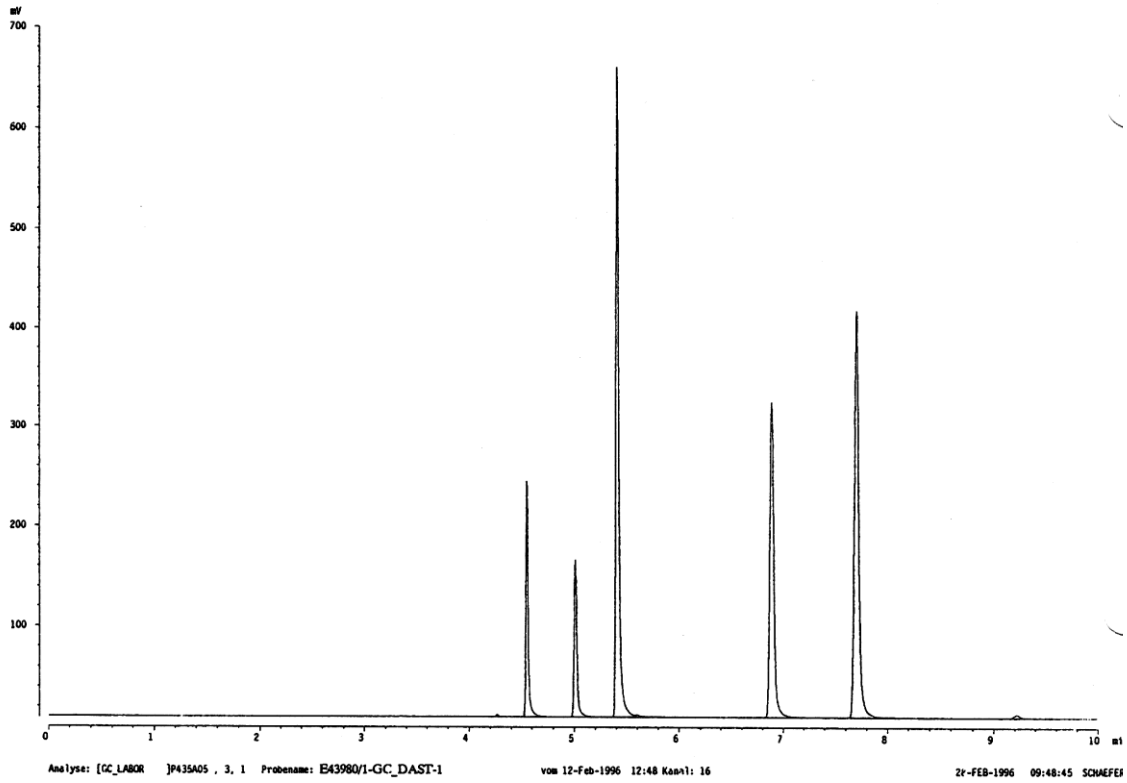
mV
700
600
500
400
300
200
100
0 1 2 3 4 5 6 7 8 9 10
Analyse: [GC_LABOR]P435A05 , 3, 1 Probename: E43980/1-GC_DAST-1
vom 12-Feb-1996 12:48 Kanal: 16
28-FEB-1996 09:48:45 SCHAEFER

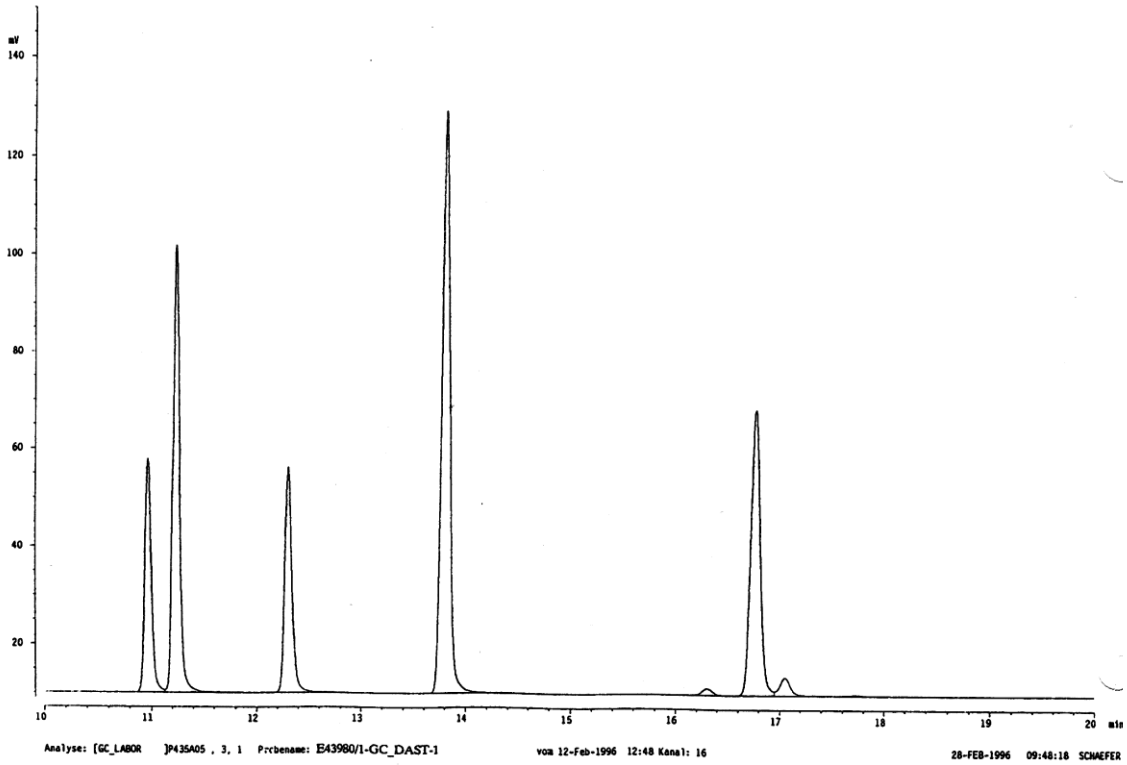
mV
140
120
100
80
60
40
20
10 11 12 13 14 15 16 17 18 19 20
Analyse: [GC_LABOR]P435A05 , 3, 1 Probename: E43980/1-GC_DAST-1
vom 12-Feb-1996 12:48 Kanal: 16
28-FEB-1996 09:48:18 SCHAEFER

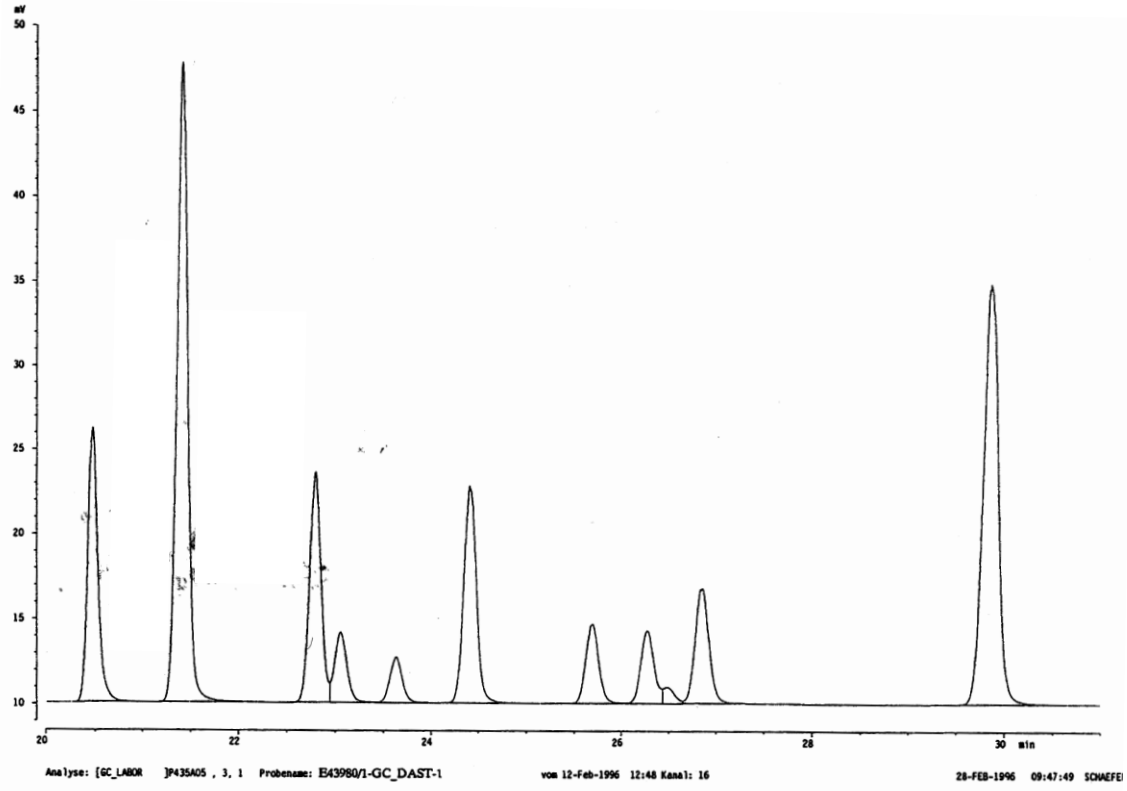
mV
50
45
40
35
30
25
20
15
10
20
22
24
26
28
30 min
Analyse: [GC_LABOR]P435A05 , 3, 1 Probename: E43980/1-GC_DAST-1
vom 12-Feb-1996 12:48 Kanal: 16
28-FEB-1996 09:47:49

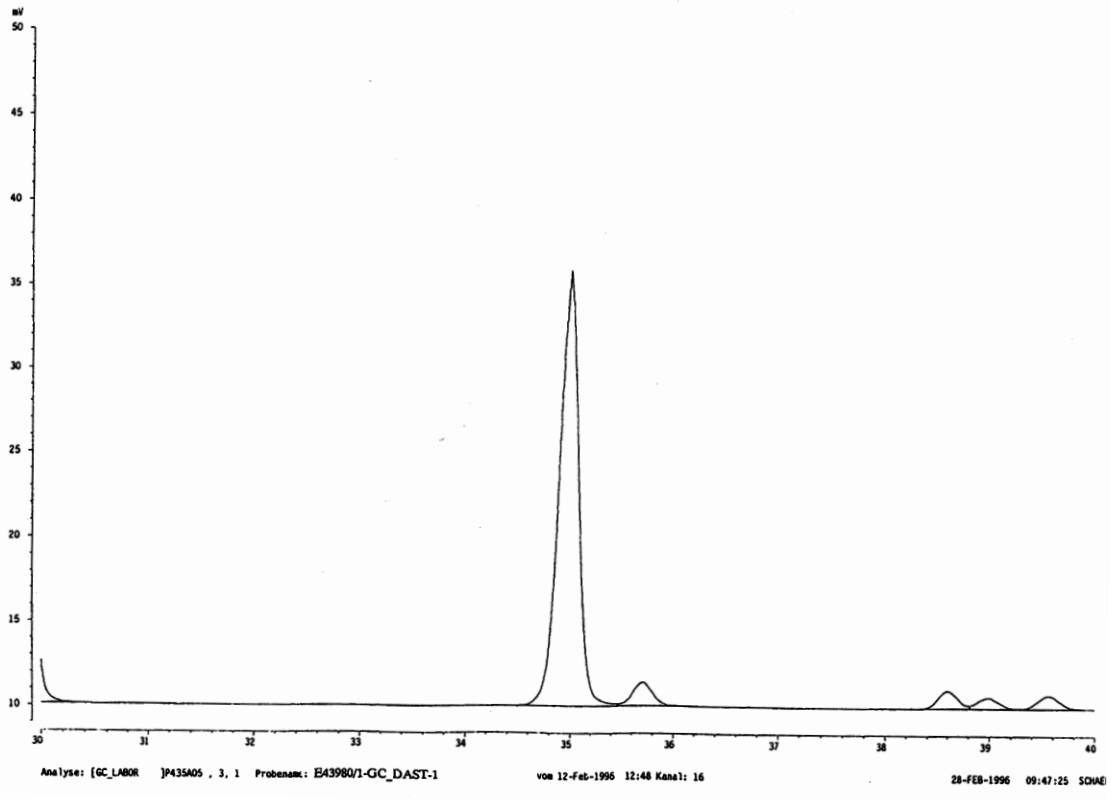
mV
50
45
40
35
30
25
20
15
10
30
31
32
33
34
35
36
37
38
39
40
Analyse: [GC_LABOR]P435A05 , 3, 1 Probename: E43980/1-GC_DAST-1
vom 12-Feb-1996 12:48 Kanal: 16
28-FEB-1996 09:47:25

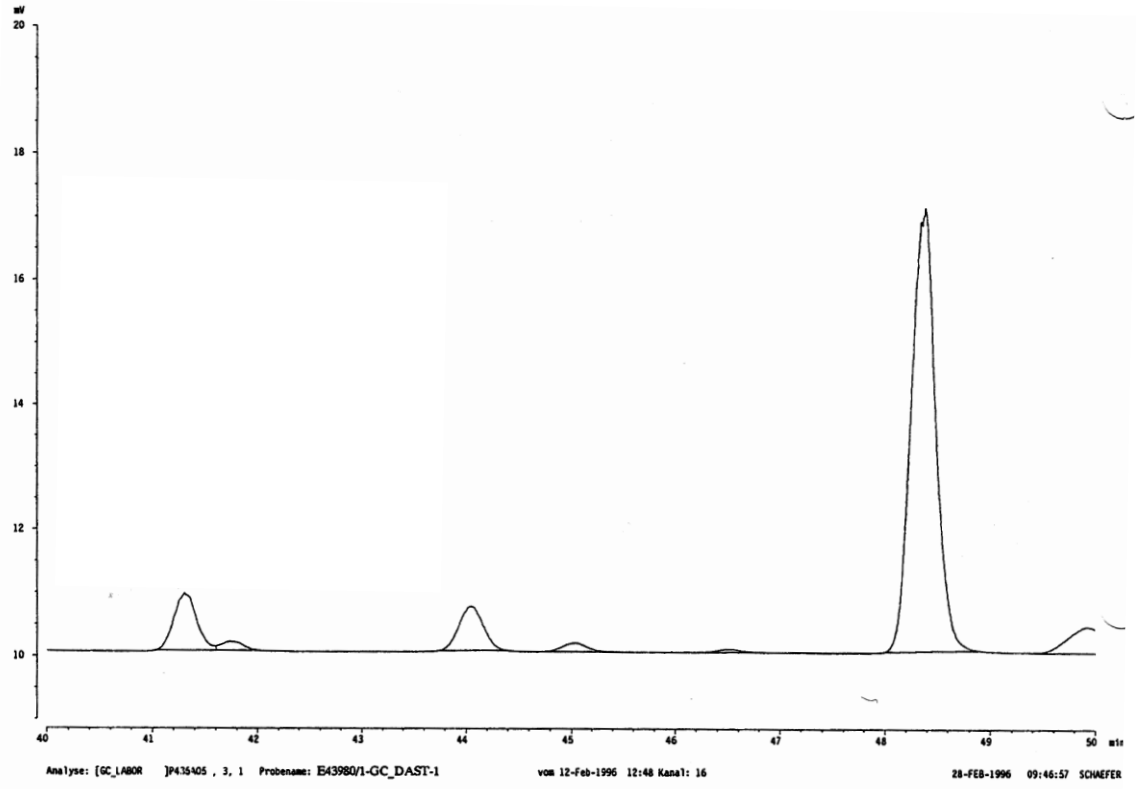
mV
20
18
16
14
12
10
40
41
42
43
44
45
46
47
48
49
50
Analyse: [GC_LABOR]P435A05 , 3, 1 Probename: E43980/1-GC_DAST-1 vom 12-Feb-1996 12:48 Kanal: 16 28-FEB-1996 09:46:57 SCHAEFER

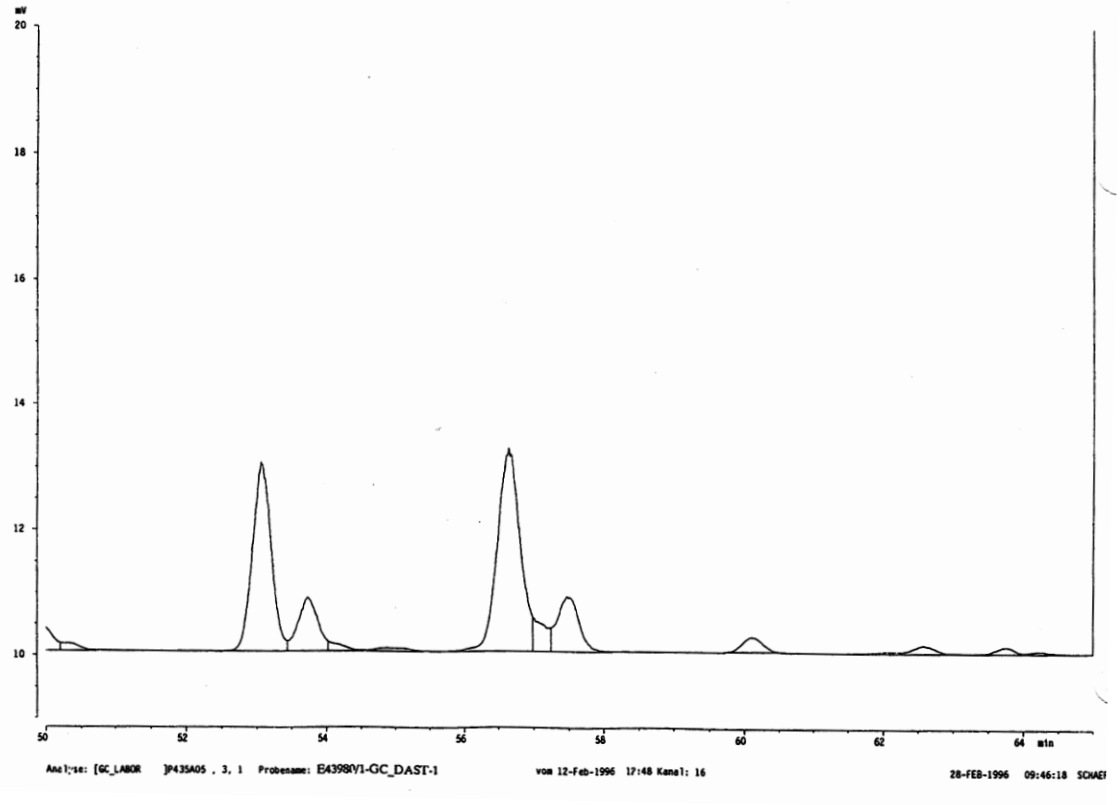
mV
20
18
16
14
12
10
50
52
54
56
58
60
62
64 min
Analyse: [GC_LABOR]P435A05 , 3, 1 Probename: E43980/1-GC_DAST-1 vom 12-Feb-1996 12:48 Kanal: 16 28-FEB-1996 09:46:18 SCHAEF

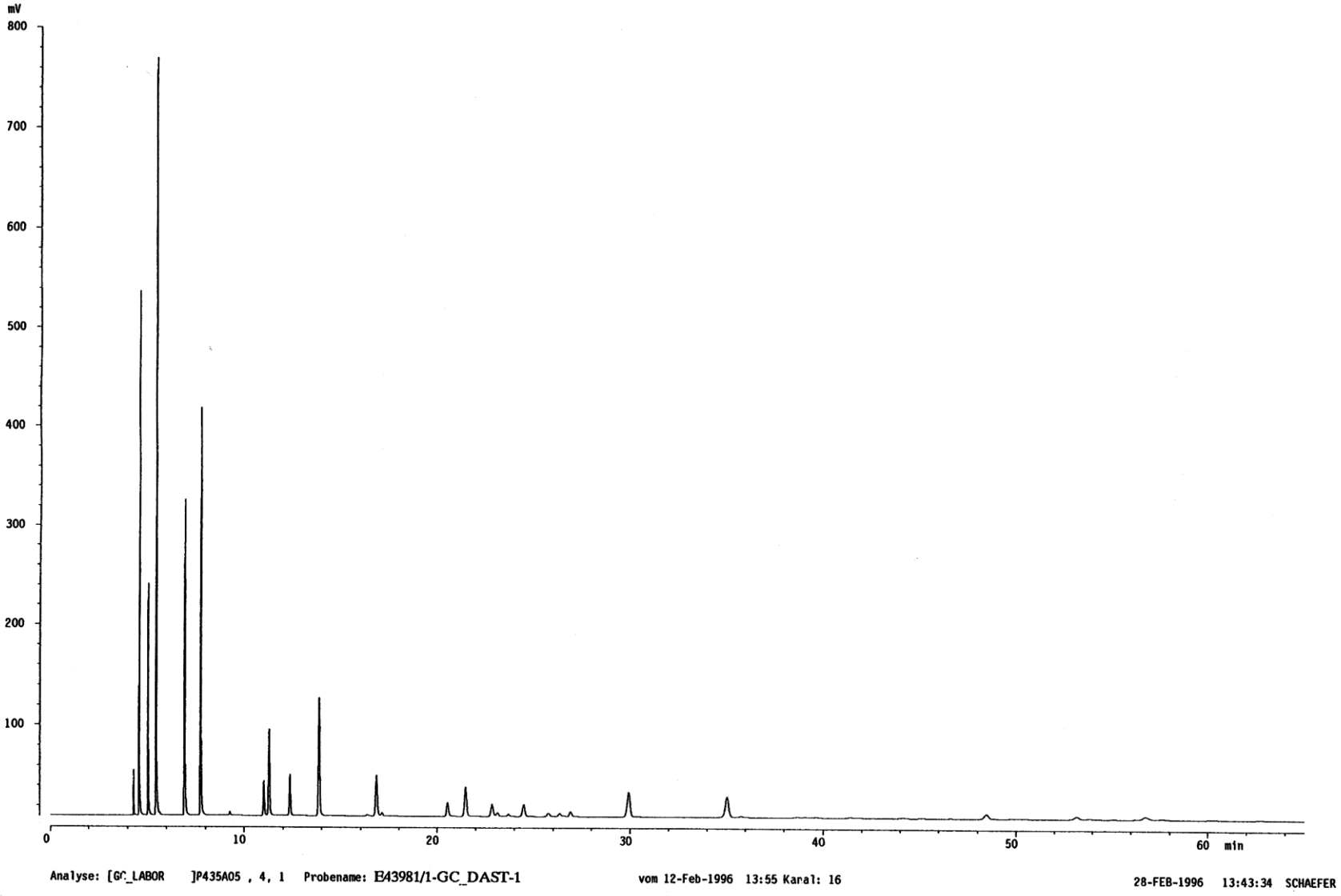
mV
800
700
600
500
400
300
200
100
0
10
20
30
40
50
60 min
Analyse: [GC_LABOR]P435A05 , 4, 1 Probename: B43981/1-GC_DAST-1
vom 12-Feb-1996 13:55 Kanal: 16
28-FEB-1996 13:43:34 SCHAEFER

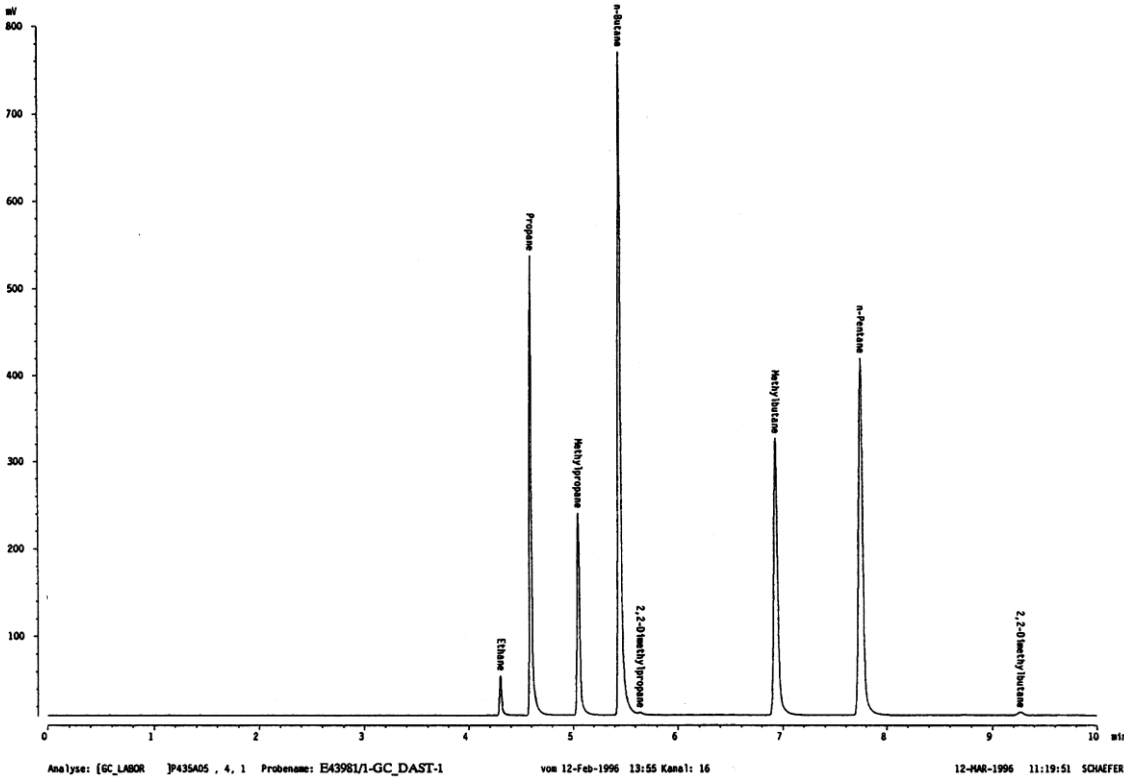
mV
800
700
600
500
400
300
200
100
Ethane
Propane
Methylpropane
n-Butane
2,2-Dimethylpropane
Methylbutane
n-Pentane
2,2-Dimethylbutane
0
1
2
3
4
5
6
7
8
9
10
Analyse: [GC_LABOR]P435A05 , 4, 1 Probename: E43981/1-GC_DAST-1 vom 12-Feb-1996 13:55 Kanal: 16 12-MAR-1996 11:19:51 SCHAEFER

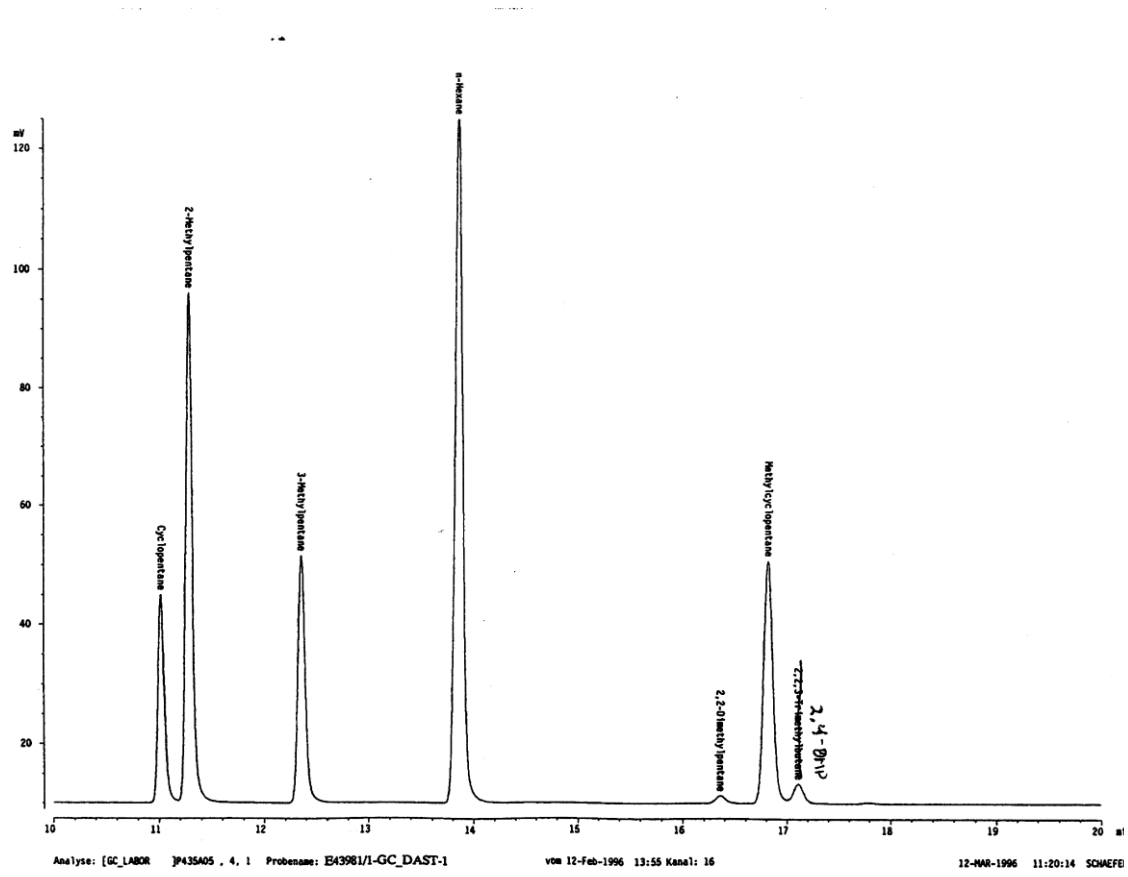
mV
120
100
80
60
40
20
Cyclopentane
2-Methylpentane
3-Methylpentane
n-Hexane
2,2-Dimethylpentane
Methylcyclopentane
2,4-Dmp
10
11
12
13
14
15
16
17
18
19
20
Analyse: [GC_LABOR]P435A05 , 4, 1 Probename: E43981/1-GC_DAST-1 vom 12-Feb-1996 13:55 Kanal: 16 12-MAR-1996 11:20:14 SCHAEFE

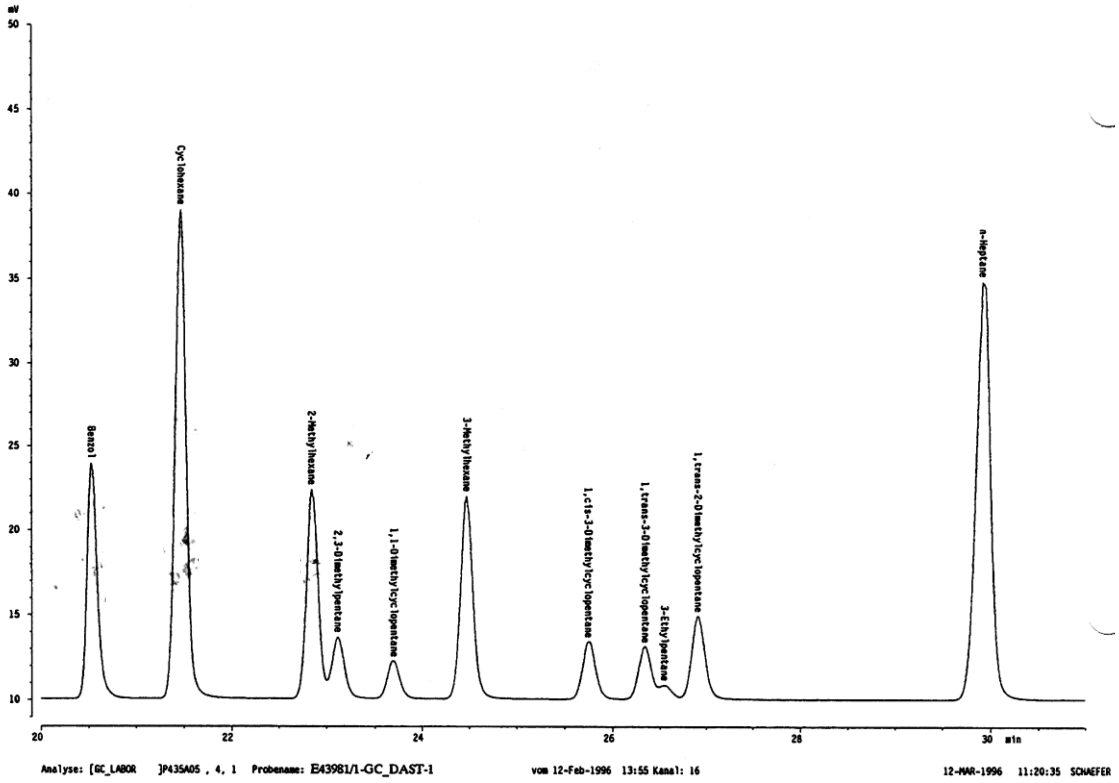
mV
Benzol
Cyclohexane
2-Methylhexane
2,3-Dimethylpentane
1,1-dimethylcyclopentane
3-Methylhexane
1,cis-3-Dimethylcyclopentane
1,trans-3-dimethylcyclopentane
3-Ethylpentane
1,trans-2-Dimethylcyclopentane
n-Heptane
min
Analyse: [GC_LABOR]P435A05 , 4, 1 Probename: E43981/1-GC_DAST-1 vom 12-Feb-1996 13:55 Kanal: 16 12-MAR-1996 11:20:35 SCHAEFER

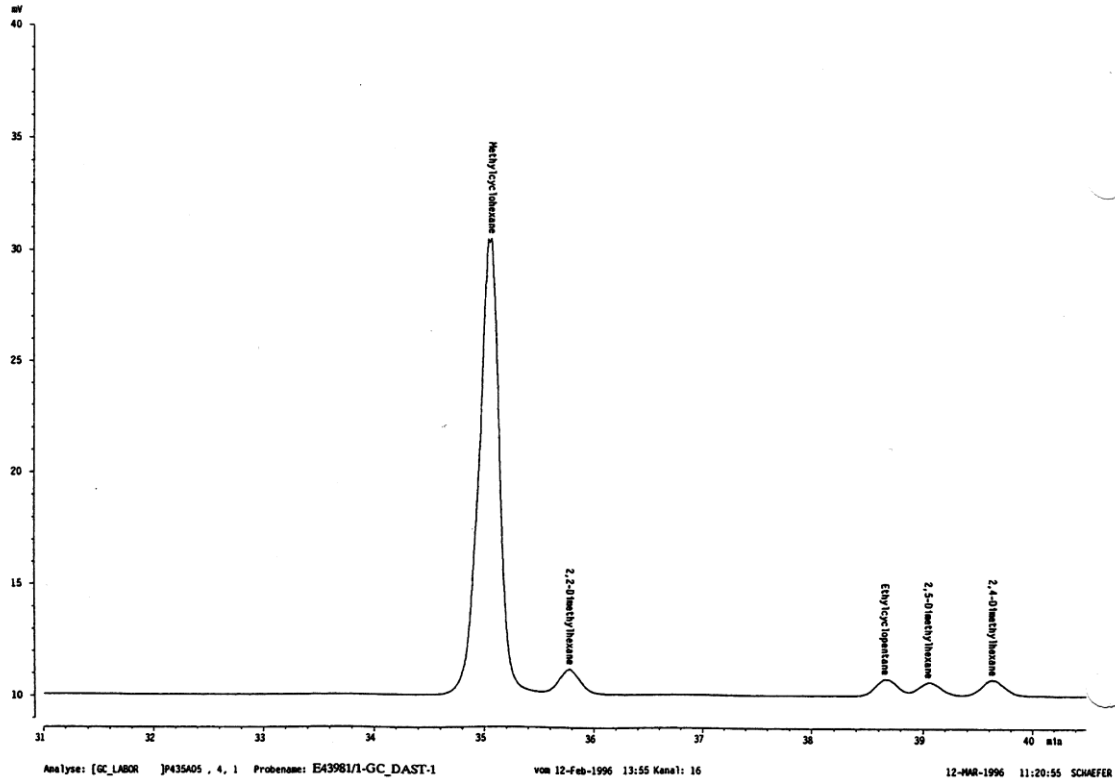
mV
Methylcyclohexane
2,2-Dimethylhexane
Ethylcyclopentane
2,5-Dimethylhexane
2,4-Dimethylhexane
min
Analyse: [GC_LABOR]P435A05 , 4, 1 Probename: E43981/1-GC_DAST-1 vom 12-Feb-1996 13:55 Kanal: 16 12-MAR-1996 11:20:55 SCHAEFER

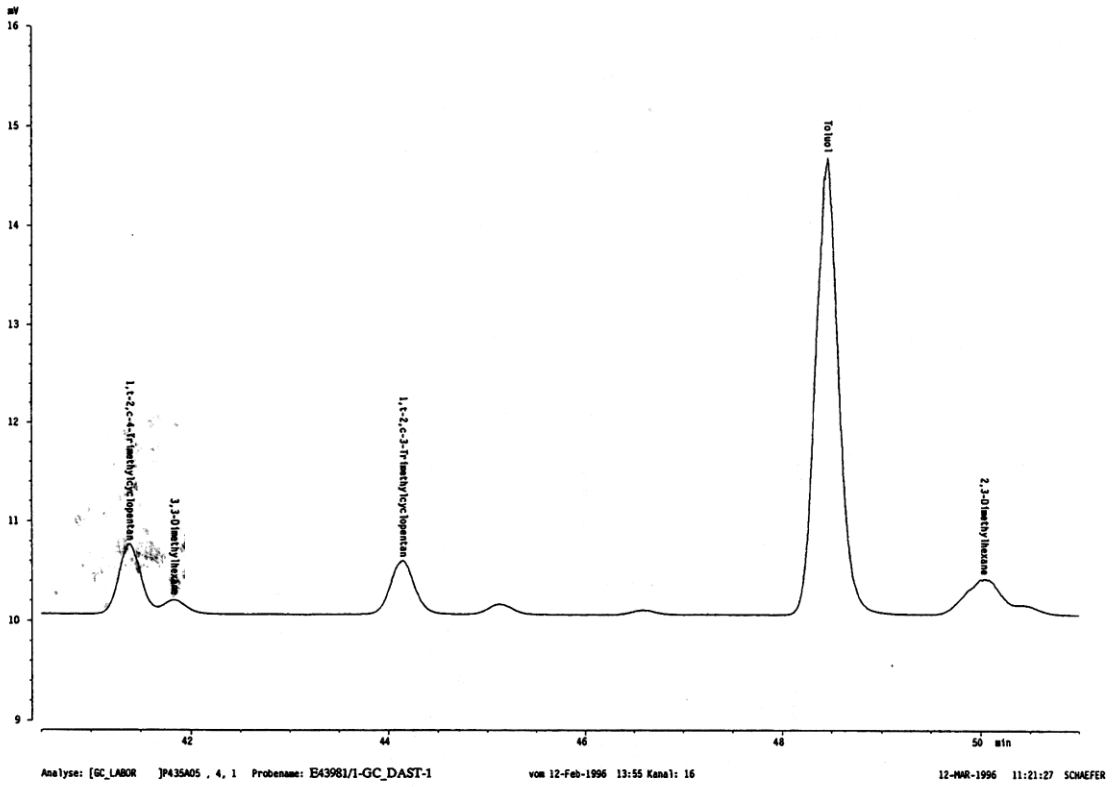
mV
16
15
14
13
12
11
10
9
1,t-2,c-4-Trimethylcyclopentan
3,3-Dimethylhexan
1,t-2,c-3-Trimethylcyclopentan
Toluol
2,3-Dimethylhexane
42
44
46
48
50 min
Analyse: [GC_LABOR]P435A05 , 4, 1 Probename: E43981/1-GC_DAST-1
vom 12-Feb-1996 13:55 Kanal: 16
12-MAR-1996 11:21:27 SCHAEFER

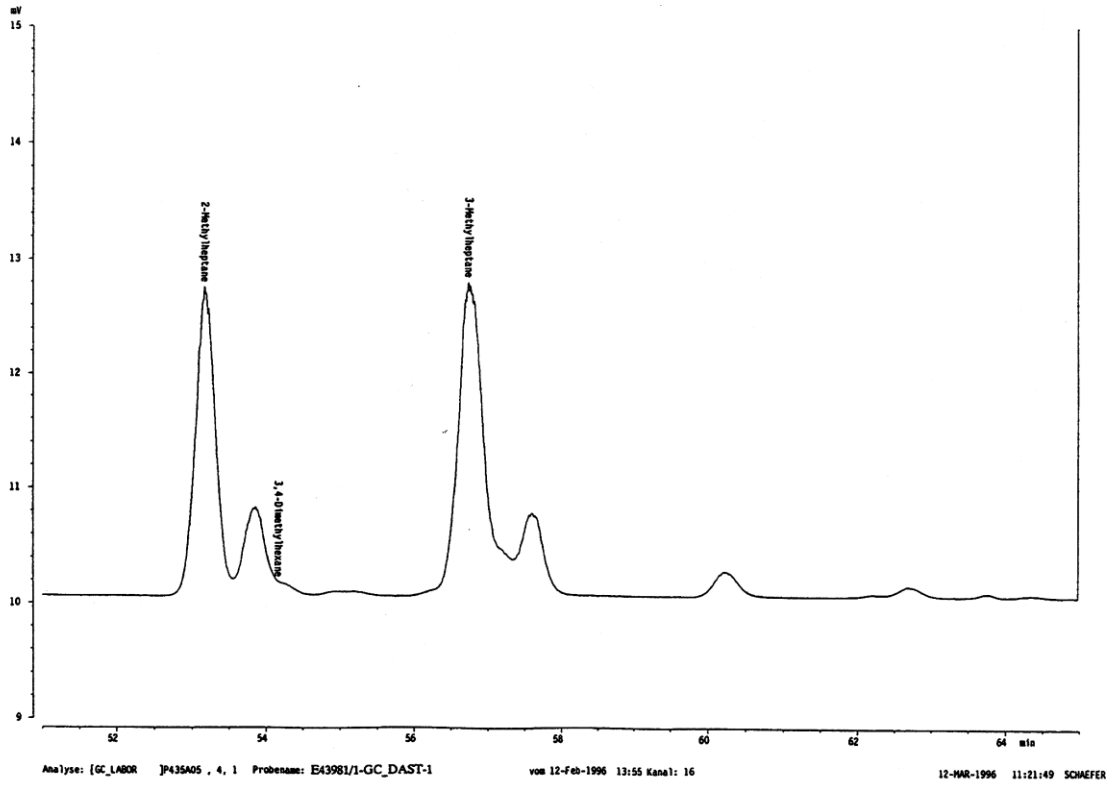
mV
15
14
13
12
11
10
9
2-Methylheptane
3,4-Dimethylhexane
3-Methylheptane
52
54
56
58
60
62
64 min
Analyse: [GC_LABOR]P435A05 , 4, 1 Probename: E43981/1-GC_DAST-1
vom 12-Feb-1996 13:55 Kanal: 16
12-MAR-1996 11:21:49 SCHAEFER

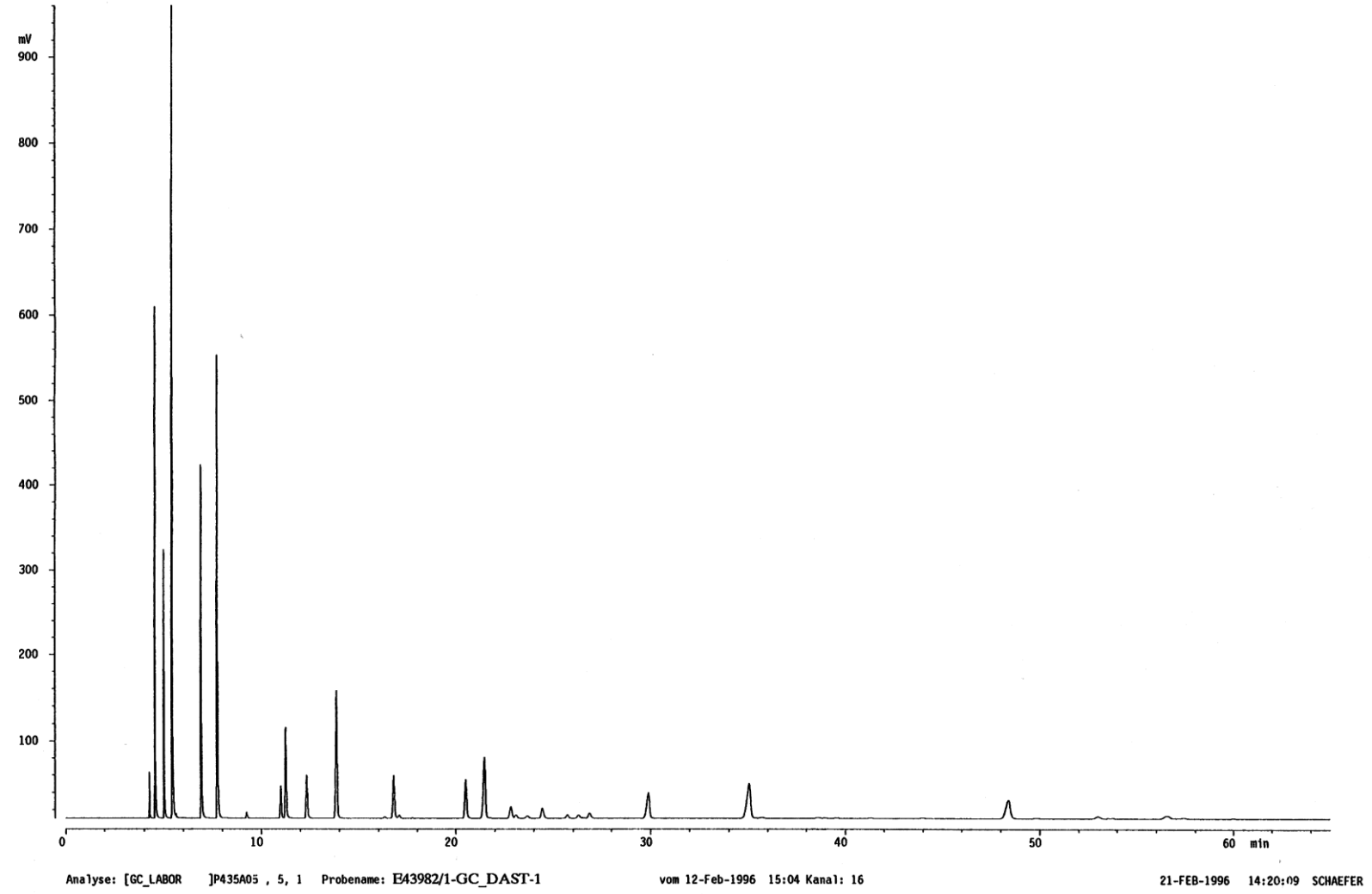
mV
900
800
700
600
500
400
300
200
100
0
10
20
30
40
50
60 min
Analyse: [GC_LABOR]P435A05 , 5, 1 Probename: E43982/1-GC_DAST-1
vom 12-Feb-1996 15:04 Kanal: 16
21-FEB-1996 14:20:09 SCHAEFER

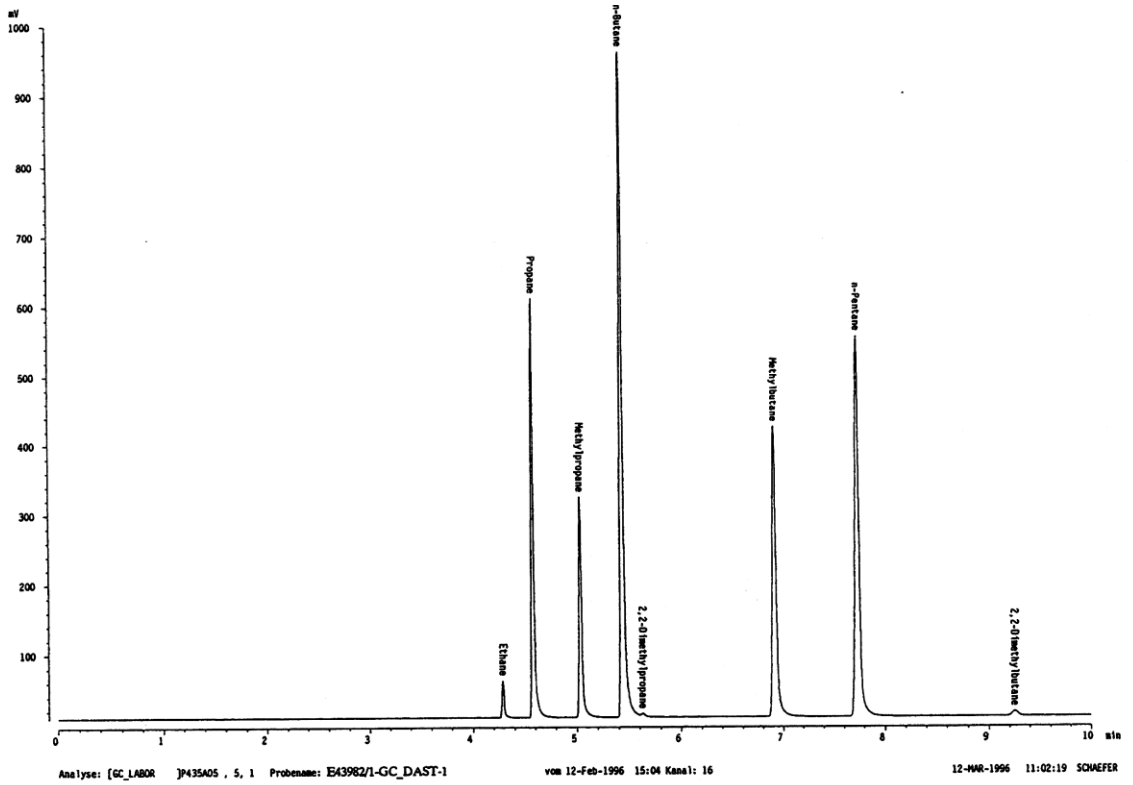
mV
1000
900
800
700
600
500
400
300
200
100
Ethane
Propane
Methylpropane
n-Butane
2,2-Dimethylpropane
Methylbutane
n-Pentane
2,2-Dimethylbutane
0
1
2
3
4
5
6
7
8
9
10 min
Analyse: [GC_LABOR]P435A05 , 5, 1 Probename: E43982/1-GC_DAST-1
vom 12-Feb-1996 15:04 Kanal: 16
12-MAR-1996 11:02:19 SCHAEFER

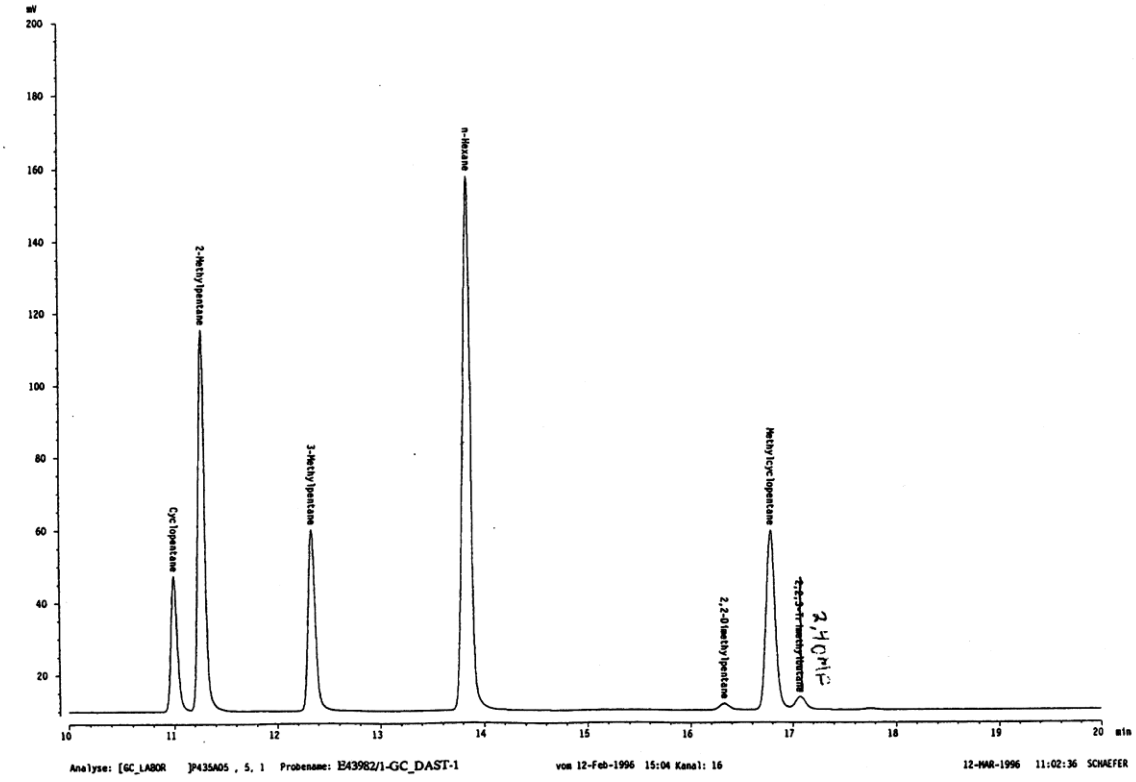
mV
200
180
160
140
120
100
80
60
40
20
Cyclopentane
2-Methylpentane
3-Methylpentane
n-Hexane
2,2-Dimethylpentane
Methylcyclopentane
2,4-Dimethylhexane
10
11
12
13
14
15
16
17
18
19
20 min
Analyse: [GC_LABOR]P435A05 , 5, 1 Probename: E43982/1-GC_DAST-1
vom 12-Feb-1996 15:04 Kanal: 16
12-MAR-1996 11:02:36 SCHAEFER

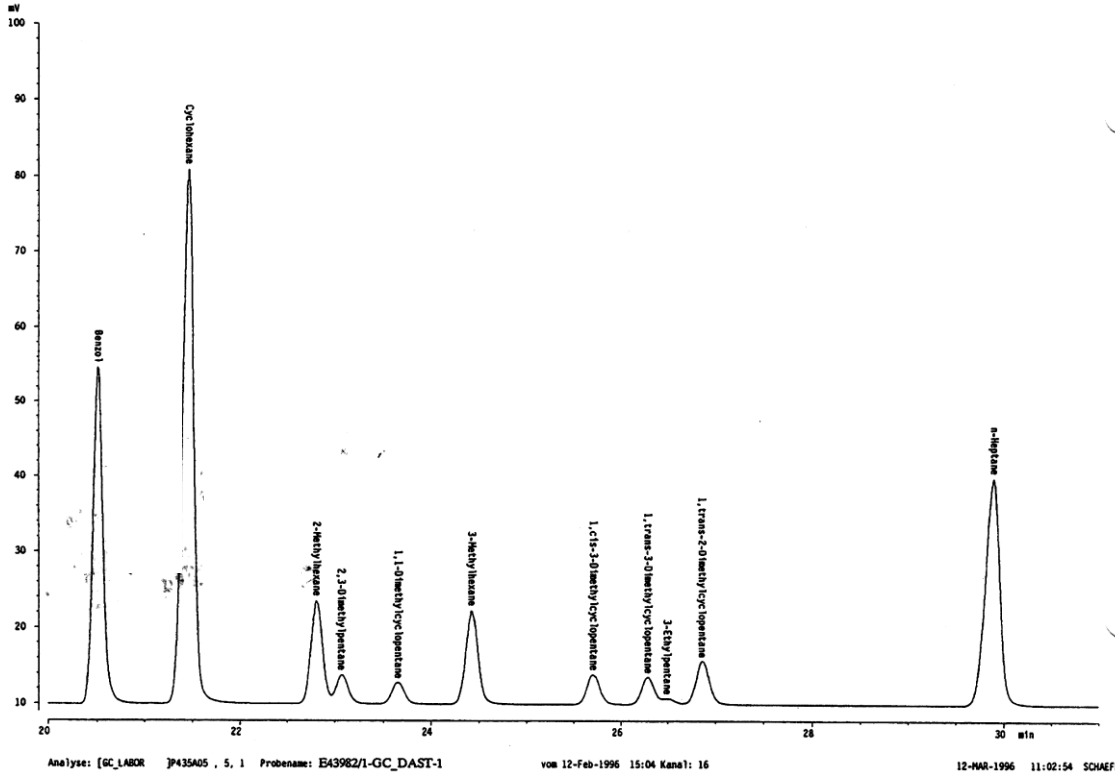
mV
Benzol
Cyclohexane
2-Methylhexane
2,3-Dimethylpentane
1,1-Dimethylcyclopentane
3-Methylhexane
1,cis-3-Dimethylcyclopentane
1,trans-3-Dimethylcyclopentane
3-Ethylpentane
1,trans-2-Dimethylcyclopentane
n-Heptane
min
Analyse: [GC_LABOR]P435A05 , 5, 1 Probename: E43982/1-GC_DAST-1 vom 12-Feb-1996 15:04 Kanal: 16 12-MAR-1996 11:02:54 SCHAEF

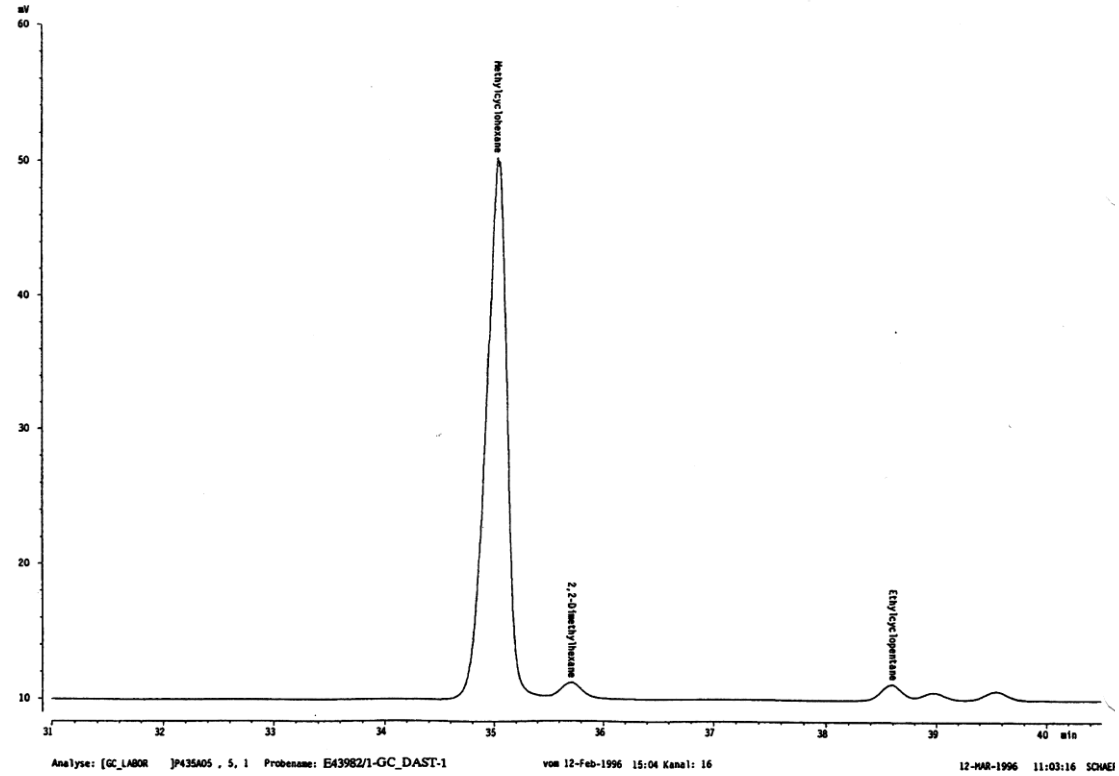
mV
Methylcyclohexane
2,2-Dimethylhexane
Ethylcyclopentane
min
Analyse: [GC_LABOR]P435A05 , 5, 1 Probename: E43982/1-GC_DAST-1 vom 12-Feb-1996 15:04 Kanal: 16 12-MAR-1996 11:03:16 SCHAEI

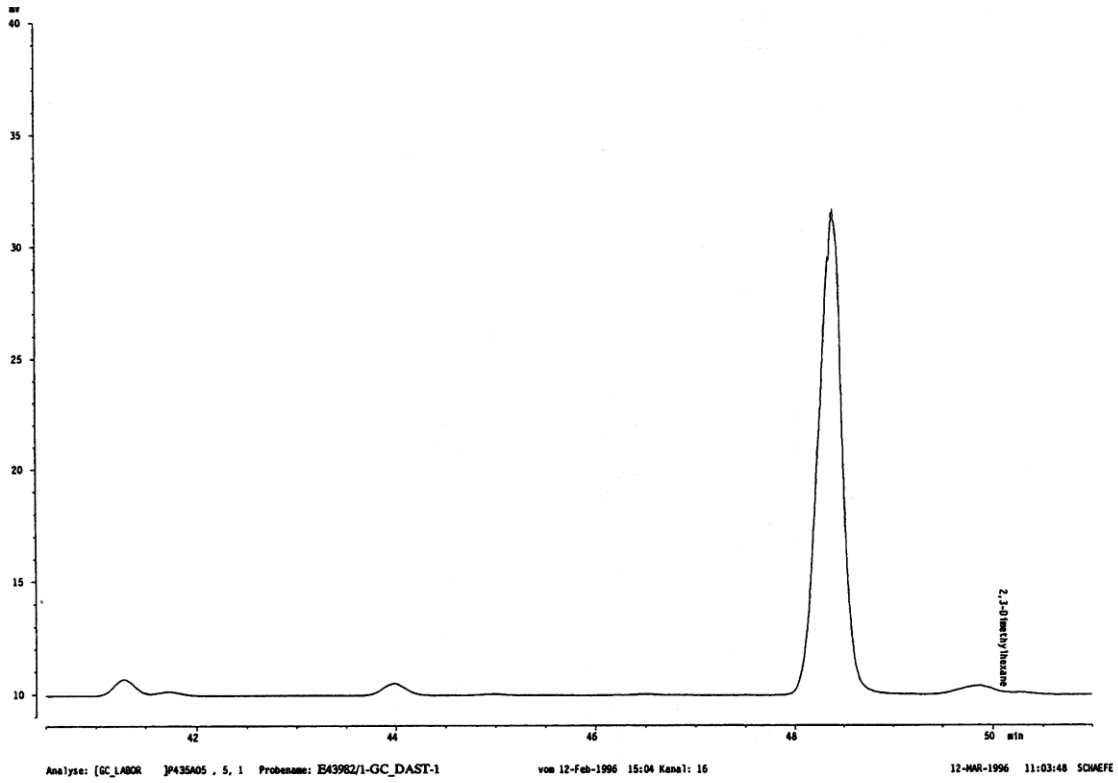
mV
40
35
30
25
20
15
10
2,3-Dimethylhexane
42
44
46
48
50 min
Analyse: [GC_LABOR]P435A05 , 5, 1 Probename: E43982/1-GC_DAST-1 vom 12-Feb-1996 15:04 Kanal: 16 12-MAR-1996 11:03:48 SCHAEFE

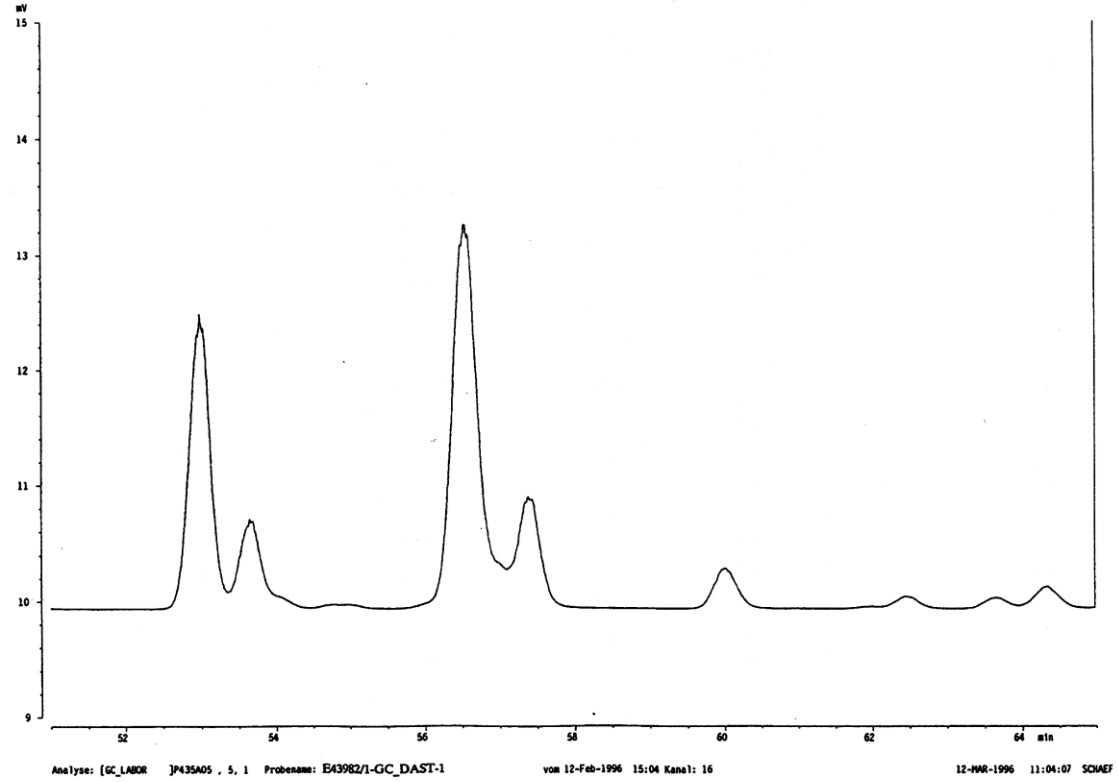
mV
15
14
13
12
11
10
9
52
54
56
58
60
62
64 min
Analyse: [GC_LABOR]P435A05 , 5, 1 Probename: E43982/1-GC_DAST-1 vom 12-Feb-1996 15:04 Kanal: 16 12-MAR-1996 11:04:07 SCHAEF

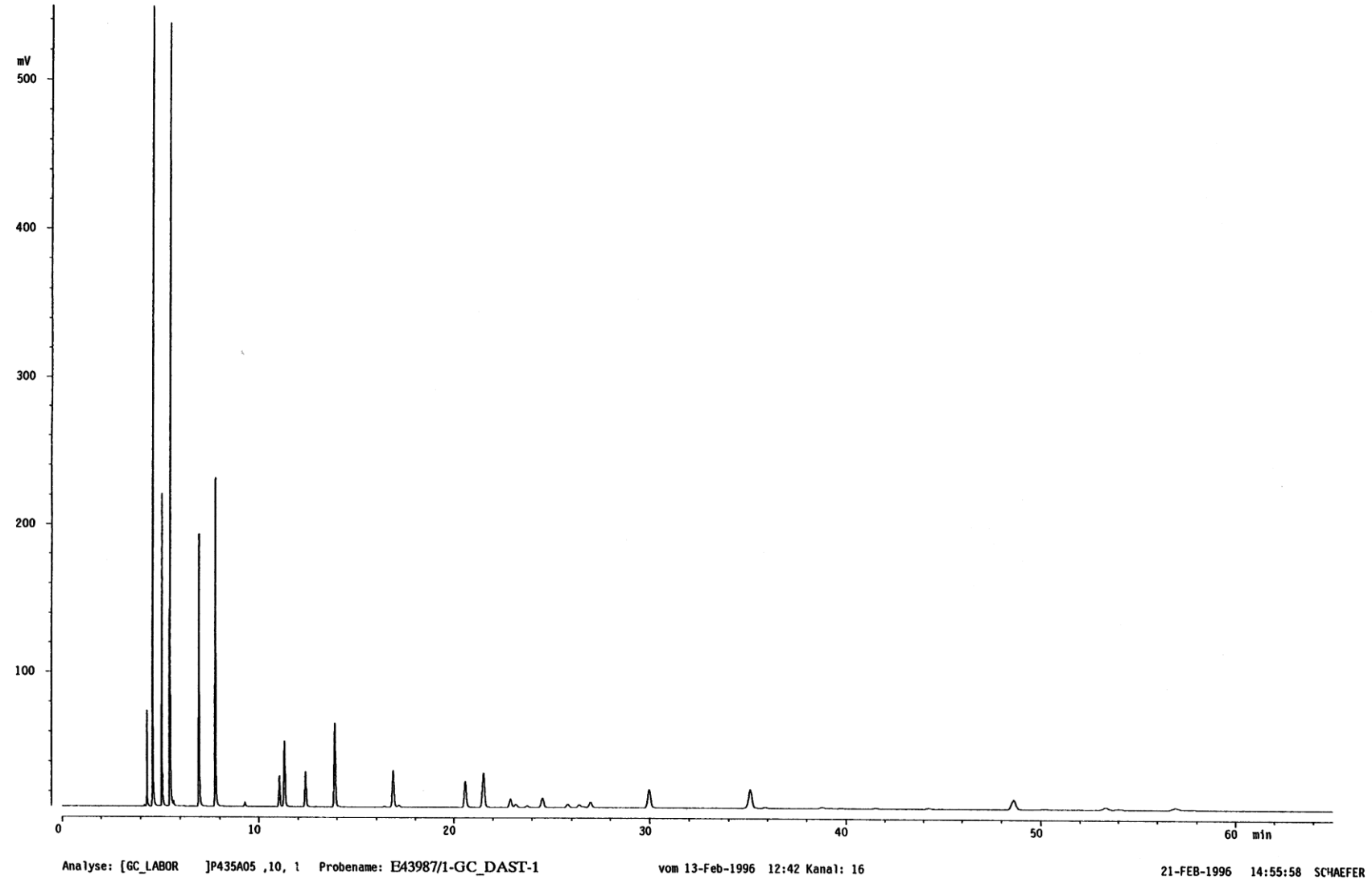
mV
500
400
300
200
100
0
10
20
30
40
50
60 min
Analyse: [GC_LABOR]P435A05 ,10, 1 Probename: B43987/1-GC_DAST-1
vom 13-Feb-1996 12:42 Kanal: 16
21-FEB-1996 14:55:58 SCHAEFER

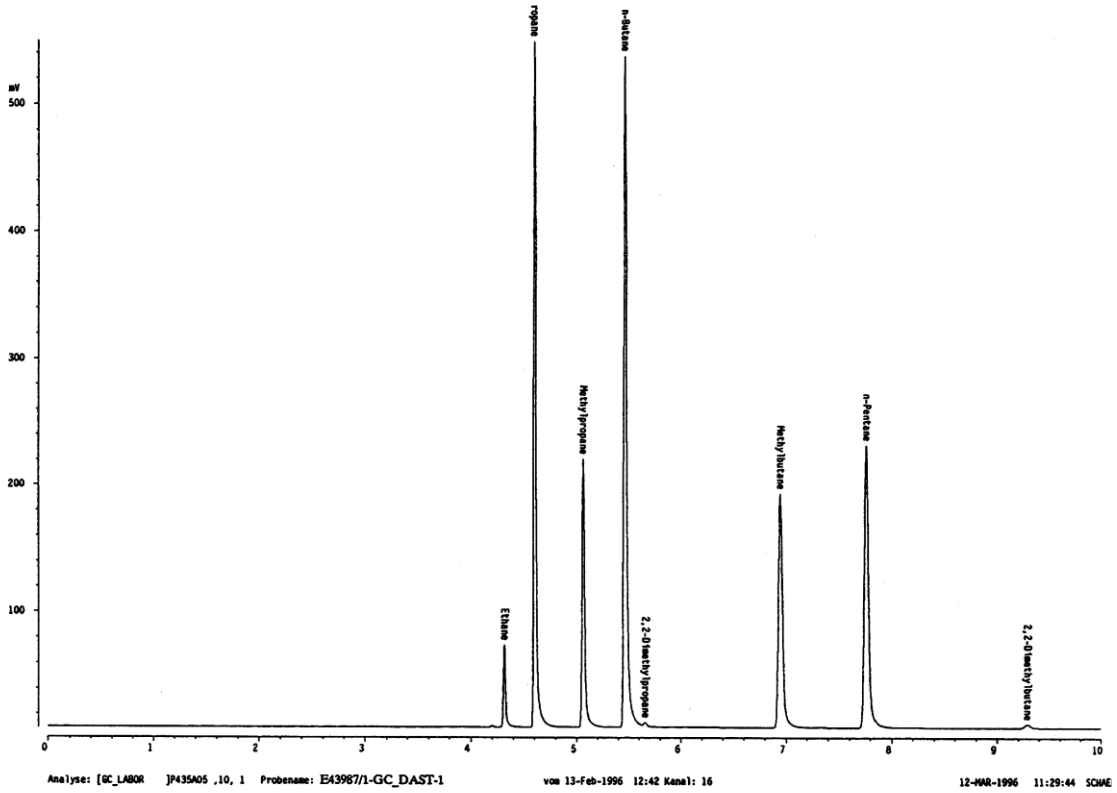
mV
500
400
300
200
100
ropane
n-Butane
Ethane
Methylpropane
2,2-Dimethylpropane
Methylbutane
n-Pentane
2,2-Dimethylbutane
0
1
2
3
4
5
6
7
8
9
10
Analyse: [GC_LABOR]P435A05 ,10, 1 Probename: E43987/1-GC_DAST-1
vom 13-Feb-1996 12:42 Kanal: 16
12-MAR-1996 11:29:44 SCHAE

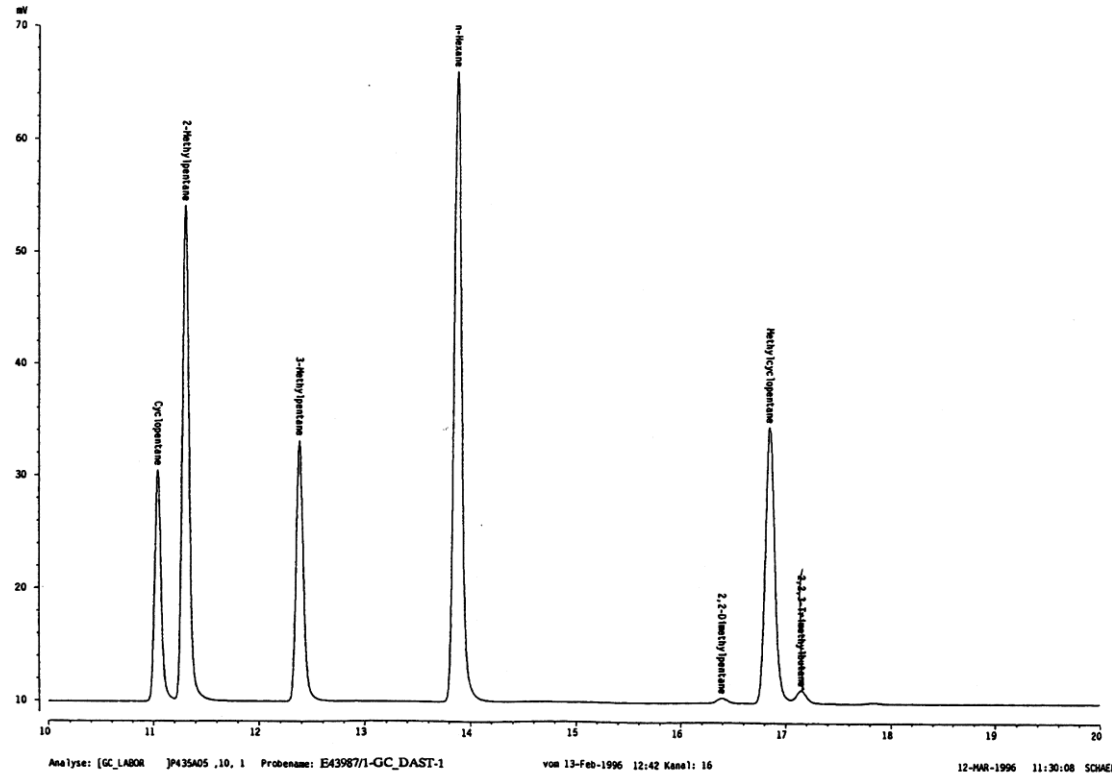
mV
70
60
50
40
30
20
10
n-Hexane
2-Methylpentane
Cyclopentane
3-Methylpentane
2,2-Dimethylpentane
Methylcyclopentane
2,2,3-Trimethylbutane
10
11
12
13
14
15
16
17
18
19
20
Analyse: [GC_LABOR]P435A05 ,10, 1 Probename: E43987/1-GC_DAST-1
vom 13-Feb-1996 12:42 Kanal: 16
12-MAR-1996 11:30:08 SCHAE

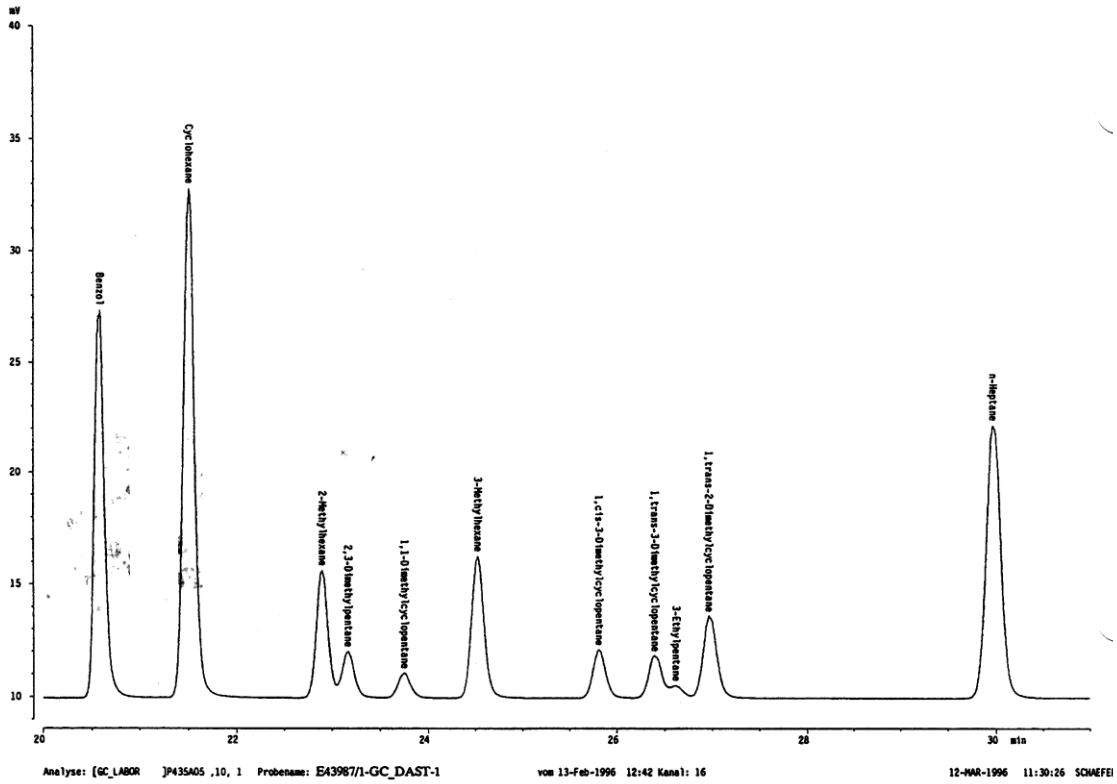
mV
40
35
30
25
20
15
10
Benzol
Cyclohexane
2-Methylhexane
2,3-Dimethylpentane
1,1-Dimethylcyclopentane
3-Methylhexane
1,cis-3-Dimethylcyclopentane
1,trans-3-Dimethylcyclopentane
3-Ethylpentane
1,trans-2-Dimethylcyclopentane
n-Heptane
20
22
24
26
28
30 min
Analyse: [GC_LABOR]P435A05 ,10, 1 Probename: E43987/1-GC_DAST-1 vom 13-Feb-1996 12:42 Kanal: 16 12-MAR-1996 11:30:26 SCHAEFE

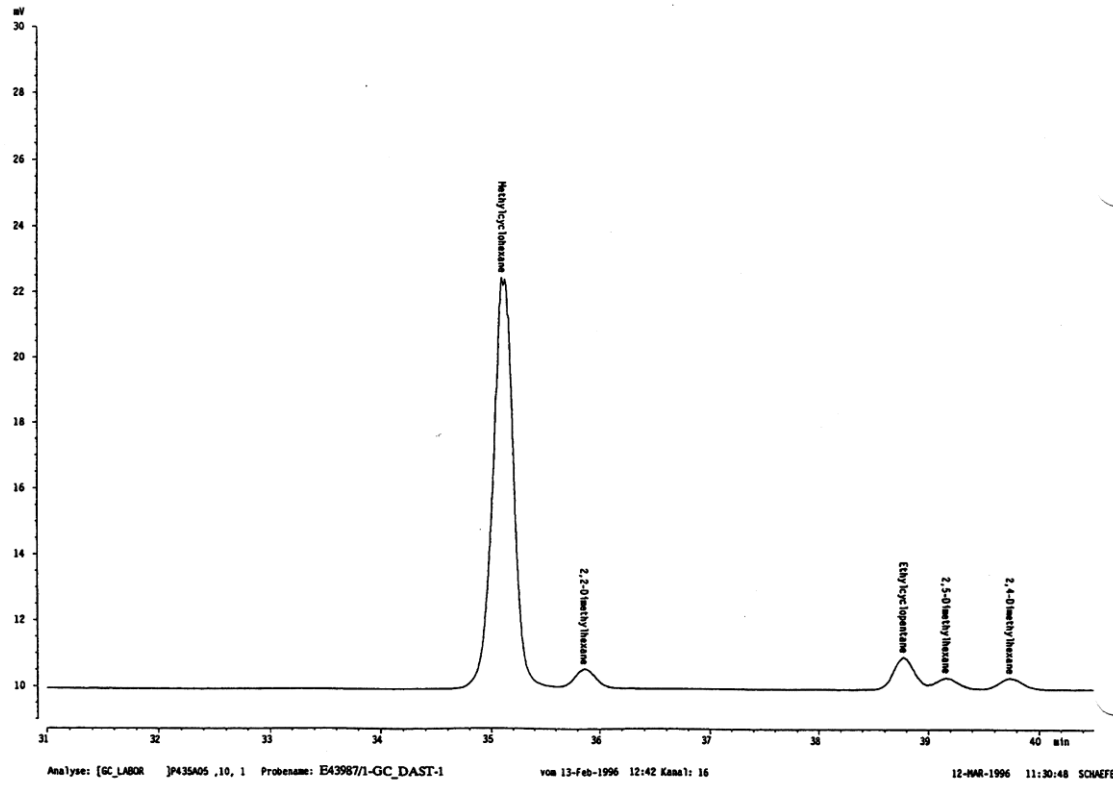
mV
30
28
26
24
22
20
18
16
14
12
10
Methylcyclohexane
2,2-Dimethylhexane
Ethylcyclopentane
2,5-Dimethylhexane
2,4-Dimethylhexane
31
32
33
34
35
36
37
38
39
40 min
Analyse: [GC_LABOR]P435A05 ,10, 1 Probename: E43987/1-GC_DAST-1 vom 13-Feb-1996 12:42 Kanal: 16 12-MAR-1996 11:30:48 SCHAEFE

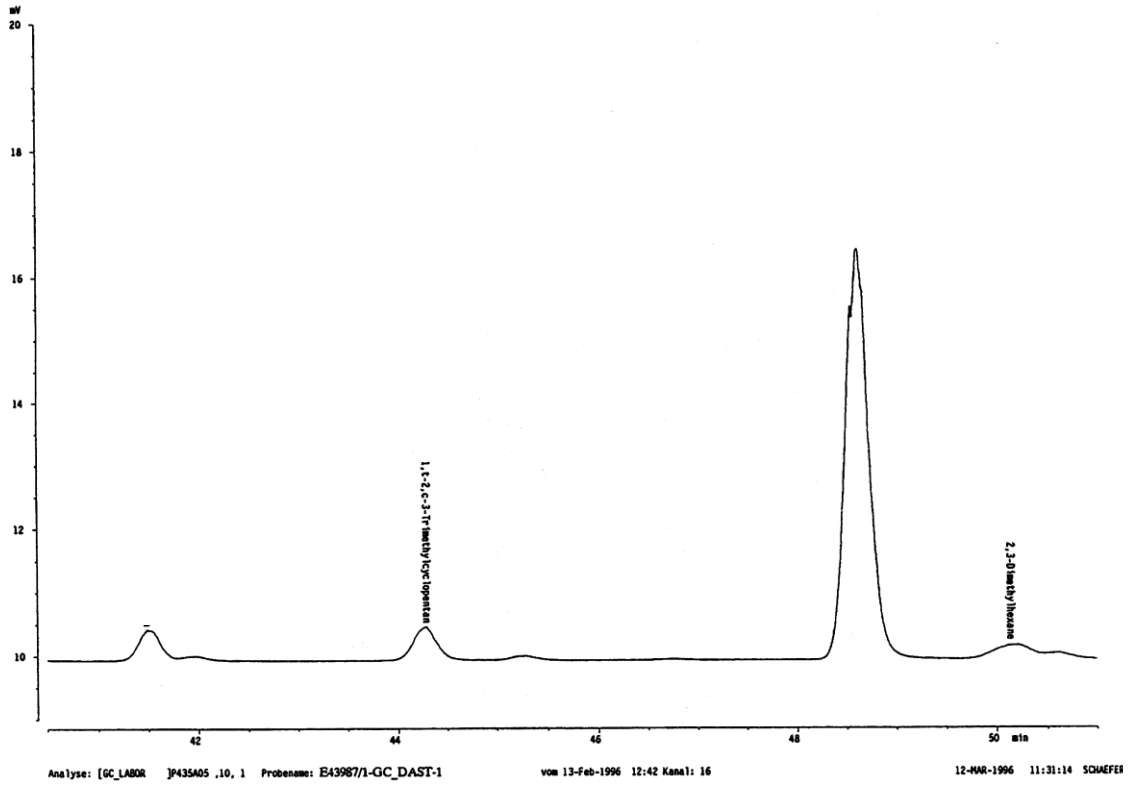
mV
20
18
16
14
12
10
1,t-2,c-3-Trimethylcyclopentan
2,3-Dimethylhexane
42
44
46
48
50 min
Analyse: [GC_LABOR]P435A05 ,10, 1 Probename: E43987/1-GC_DAST-1 vom 13-Feb-1996 12:42 Kanal: 16 12-MAR-1996 11:31:14 SCHAEFER

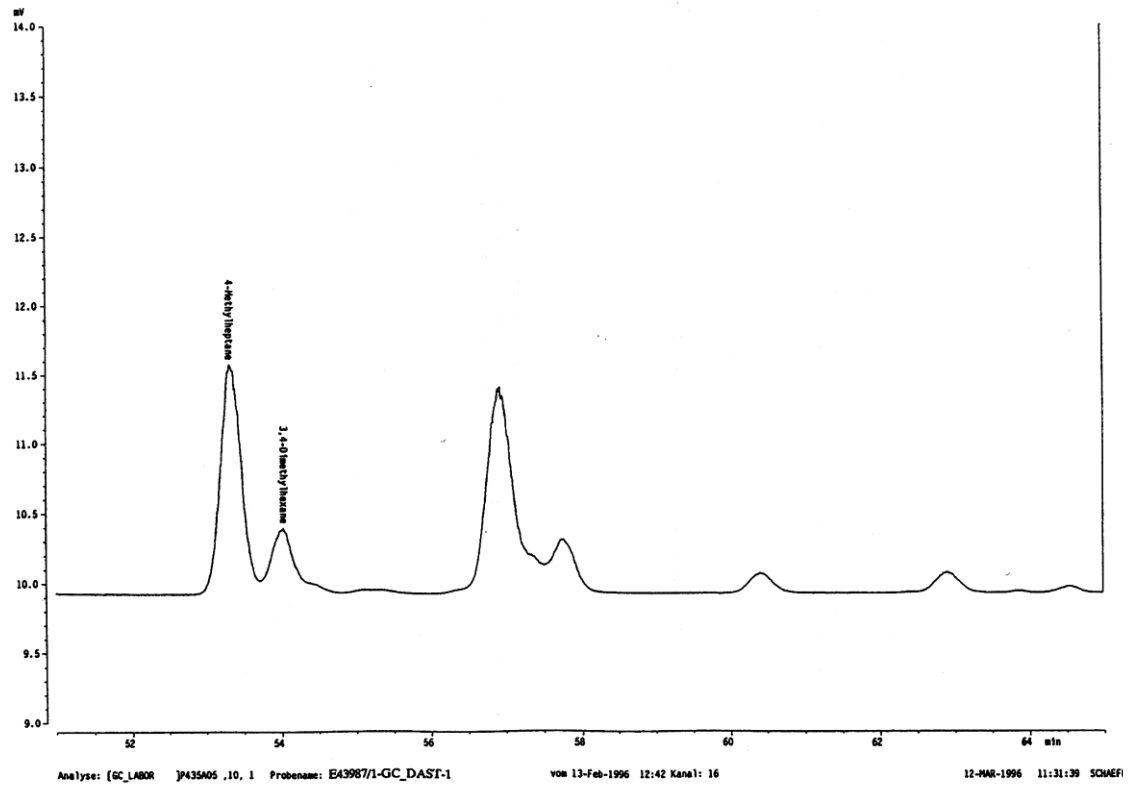
mV
14.0
13.5
13.0
12.5
12.0
11.5
11.0
10.5
10.0
9.5
9.0
4-Methylheptane
3,4-Dimethylhexane
52
54
56
58
60
62
64 min
Analyse: [GC_LABOR]P435A05 ,10, 1 Probename: E43987/1-GC_DAST-1 vom 13-Feb-1996 12:42 Kanal: 16 12-MAR-1996 11:31:39 SCHAEFE

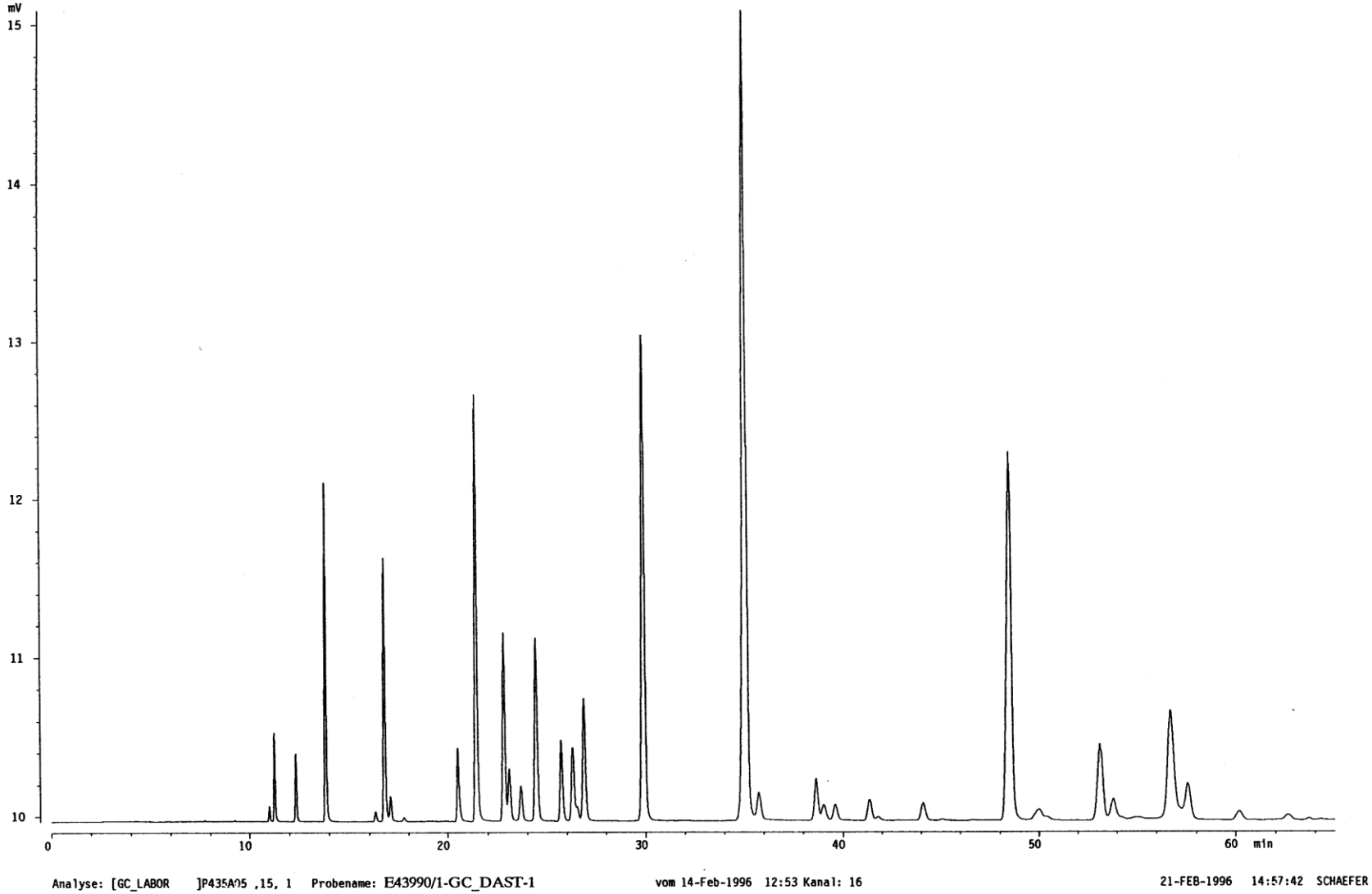
mV
15
14
13
12
11
10
0
10
20
30
40
50
60 min
Analyse: [GC_LABOR]P435A05 ,15, 1 Probename: E43990/1-GC_DAST-1
vom 14-Feb-1996 12:53 Kanal: 16
21-FEB-1996 14:57:42 SCHAEFER

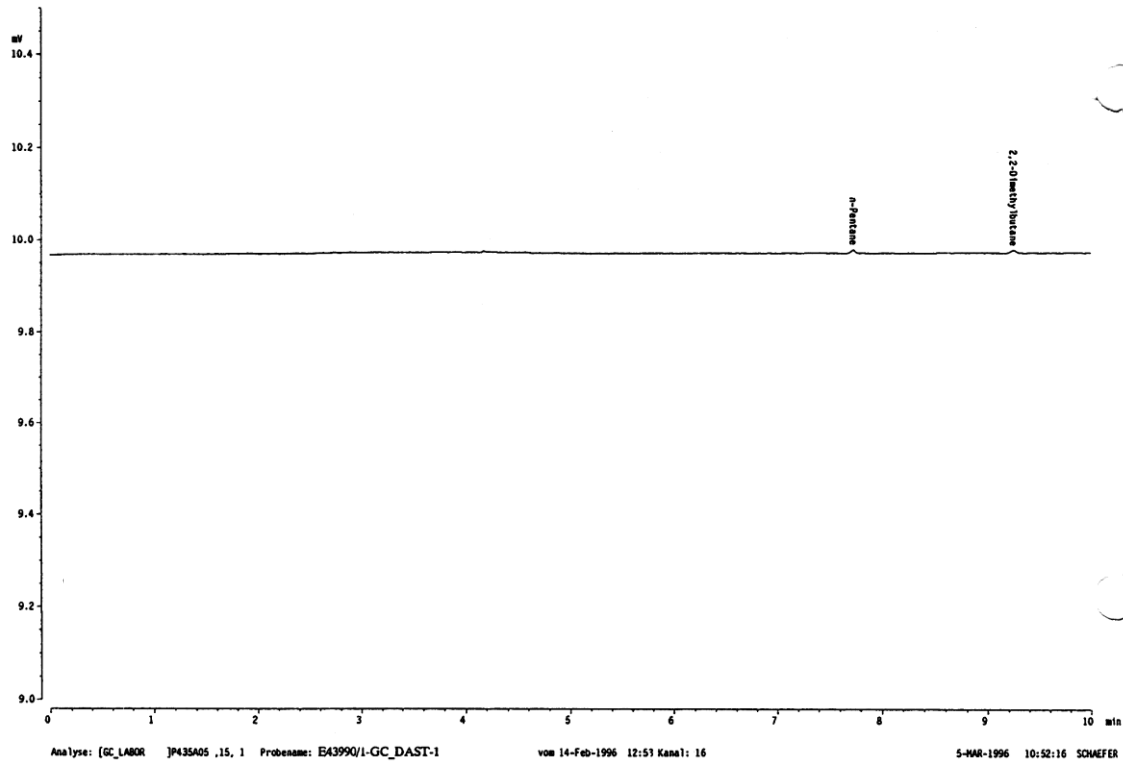
mV
10.4
10.2
10.0
9.8
9.6
9.4
9.2
9.0
n-Pentane
2,2-Dimethylbutane
0 1 2 3 4 5 6 7 8 9 10 min
Analyse: [GC_LABOR]P435A05 ,15, 1 Probename: E43990/1-GC_DAST-1 vom 14-Feb-1996 12:53 Kanal: 16 5-MAR-1996 10:52:16 SCHAEFER

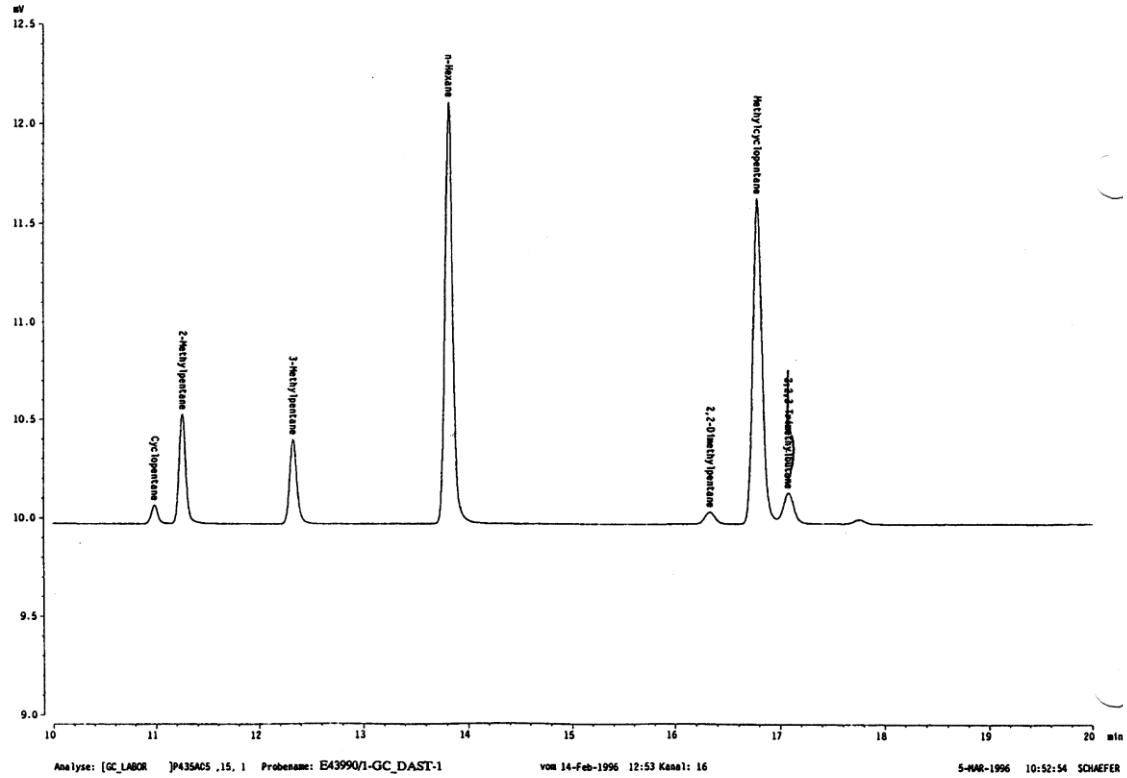
mV
12.5
12.0
11.5
11.0
10.5
10.0
9.5
9.0
Cyclopentane
2-Methylpentane
3-Methylpentane
n-Hexane
2,2-Dimethylpentane
Methylcyclopentane
10 11 12 13 14 15 16 17 18 19 20 min
Analyse: [GC_LABOR]P435A05 ,15, 1 Probename: E43990/1-GC_DAST-1 vom 14-Feb-1996 12:53 Kanal: 16 5-MAR-1996 10:52:54 SCHAEFER

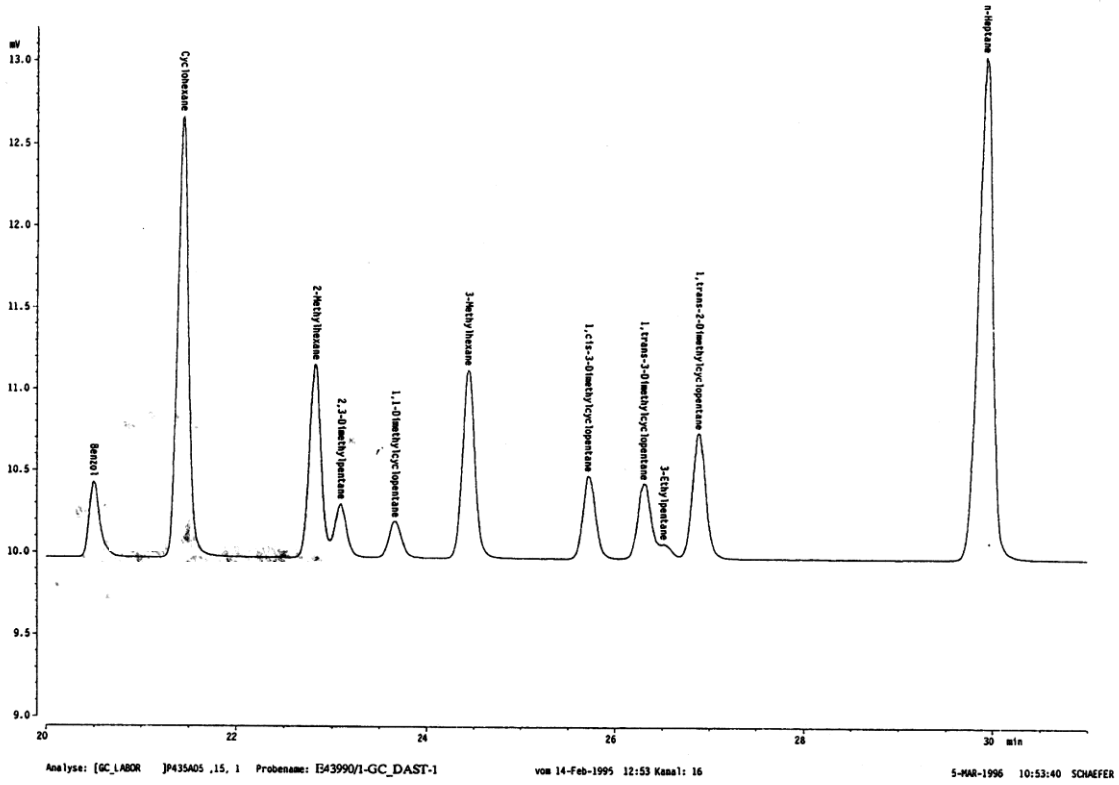
mV
13.0
12.5
12.0
11.5
11.0
10.5
10.0
9.5
9.0
Benzol
Cyclohexane
2-Methylhexane
2,3-Dimethylpentane
1,1-Dimethylcyclopentane
3-Methylhexane
1,cis-3-Dimethylcyclopentane
1,trans-3-Dimethylcyclopentane
3-Ethylpentane
1,trans-2-Dimethylcyclopentane
n-Heptane
20
22
24
26
28
30 min
Analyse: [GC_LABOR]P435A05 ,15, 1 Probename: E43990/1-GC_DAST-1 vom 14-Feb-1995 12:53 Kanal: 16 5-MAR-1996 10:53:40 SCHAEFER

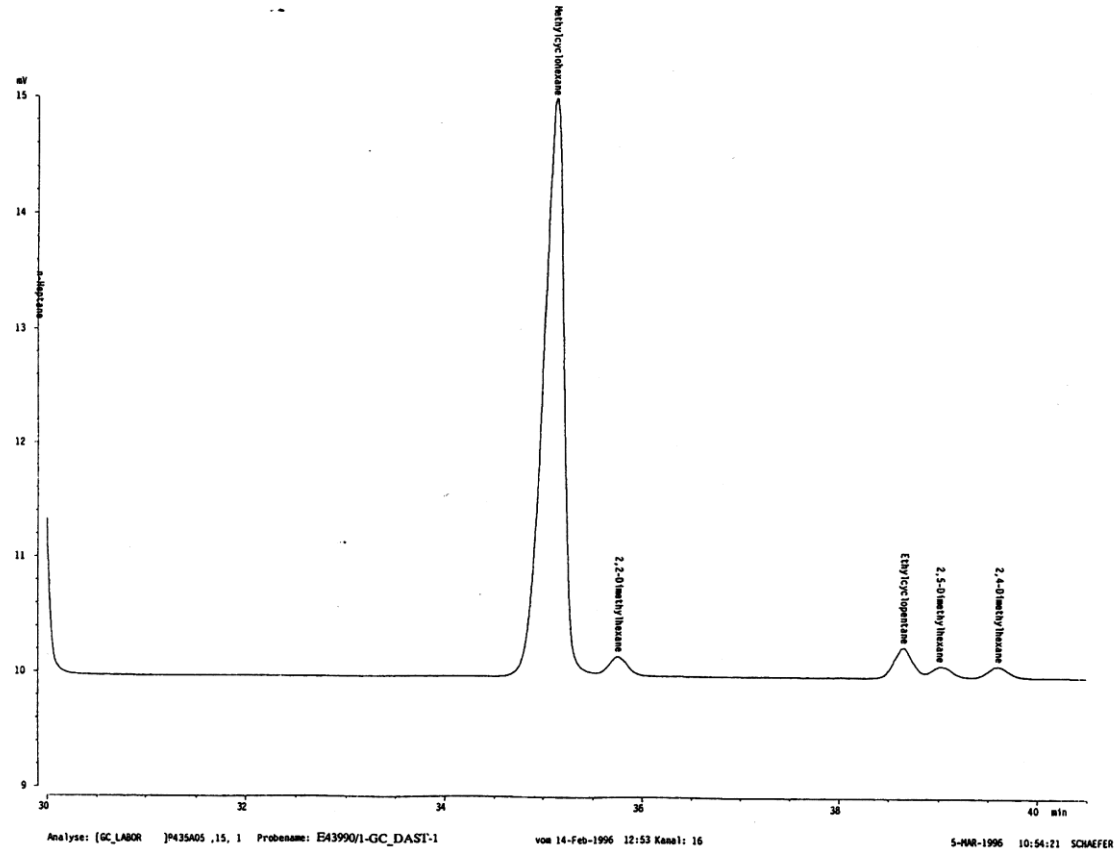
mV
15
14
13
12
11
10
9
n-Heptane
Methylcyclohexane
2,2-Dimethylhexane
Ethylcyclopentane
2,5-Dimethylhexane
2,4-Dimethylhexane
30
32
34
36
38
40 min
Analyse: [GC_LABOR]P435A05 ,15, 1 Probename: E43990/1-GC_DAST-1 vom 14-Feb-1996 12:53 Kanal: 16 5-MAR-1996 10:54:21 SCHAEFER

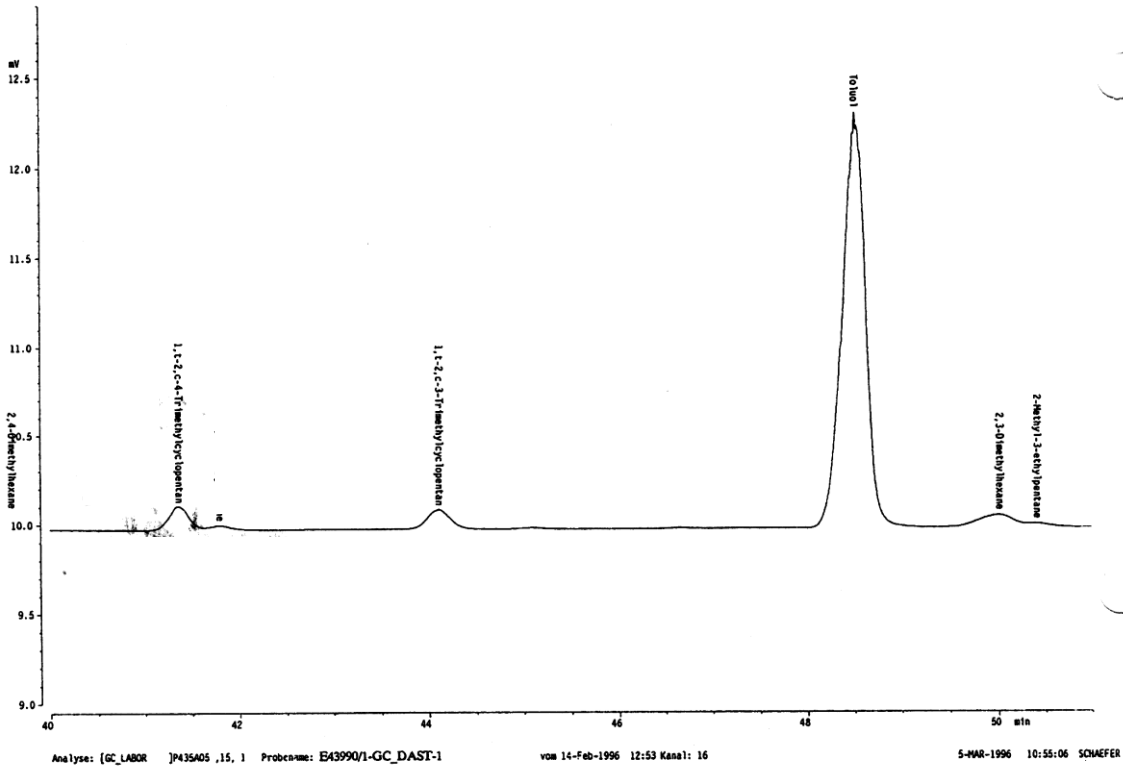
mV
12.5
12.0
11.5
11.0
10.5
10.0
9.5
9.0
2,4-Dimethylhexane
1,1,2-Trimethylcyclopentan
1,1,2-Trimethylcyclopentan
Toluol
2,3-Dimethylhexane
2-Methyl-3-ethylpentane
40
42
44
46
48
50 min
Analyse: [GC_LABOR]P435A05 ,15, 1 Probename: E43990/1-GC_DAST-1
vom 14-Feb-1996 12:53 Kanal: 16
5-MAR-1996 10:55:06 SCHAEFER

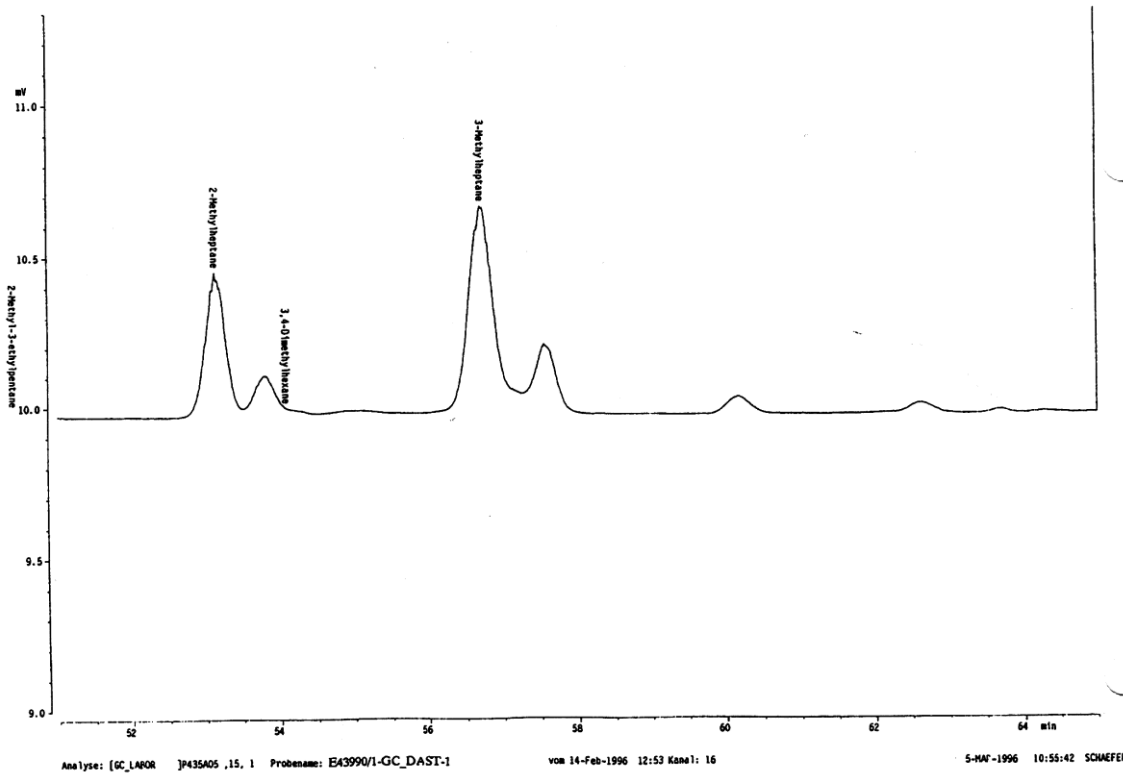
mV
11.0
10.5
10.0
9.5
9.0
2-Methyl-3-ethylpentane
2-Methylheptane
3,4-Dimethylhexane
3-Methylheptane
52
54
56
58
60
62
64 min
Analyse: [GC_LABOR]P435A05 ,15, 1 Probename: E43990/1-GC_DAST-1
vom 14-Feb-1996 12:53 Kanal: 16
5-MAR-1996 10:55:42 SCHAEFE

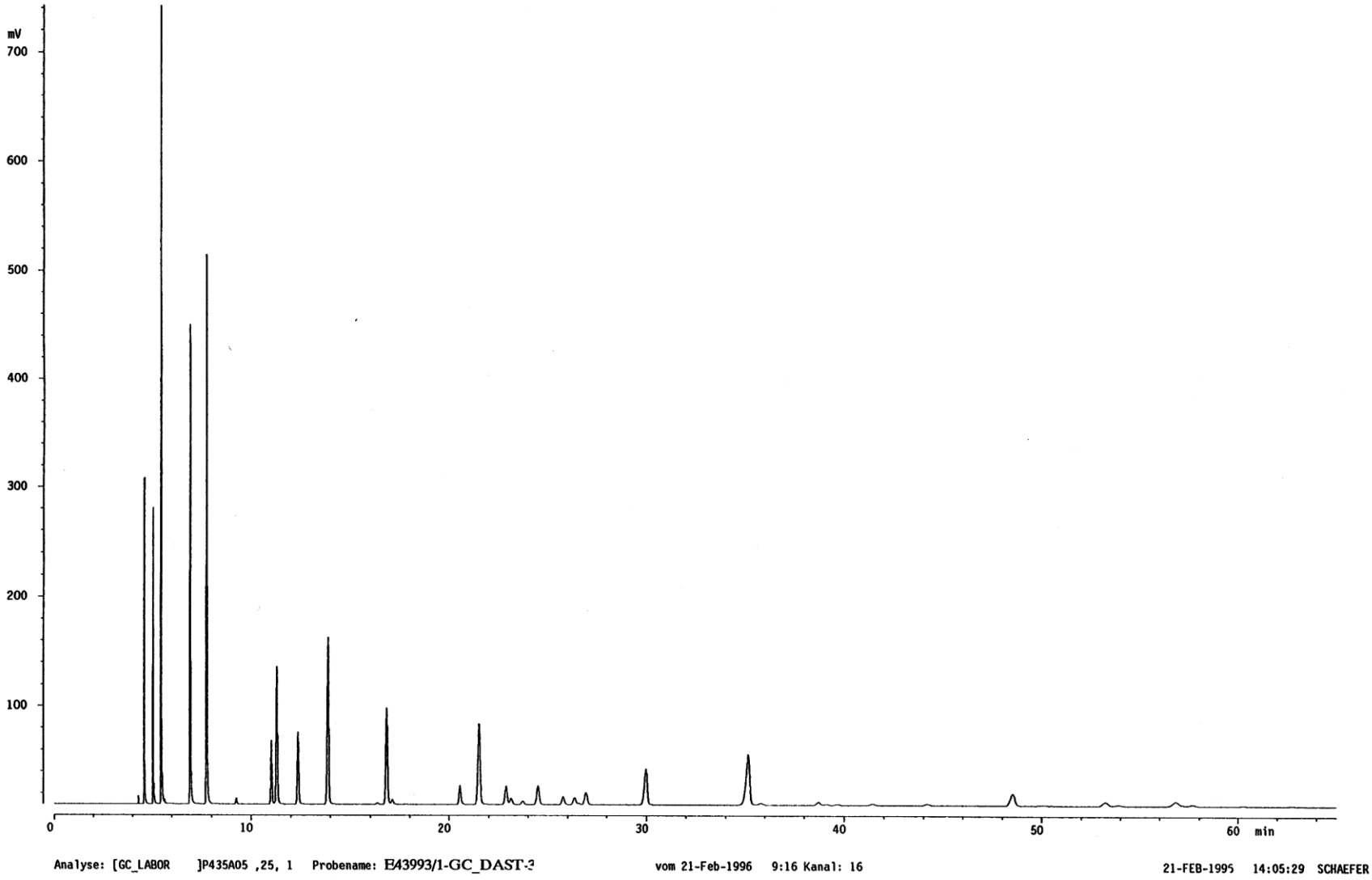
mV
700
600
500
400
300
200
100
0
10
20
30
40
50
60 min
Analyse: [GC_LABOR]P435A05 ,25, 1 Probename: E43993/1-GC_DAST-3
vom 21-Feb-1996 9:16 Kanal: 16
21-FEB-1995 14:05:29 SCHAEFER

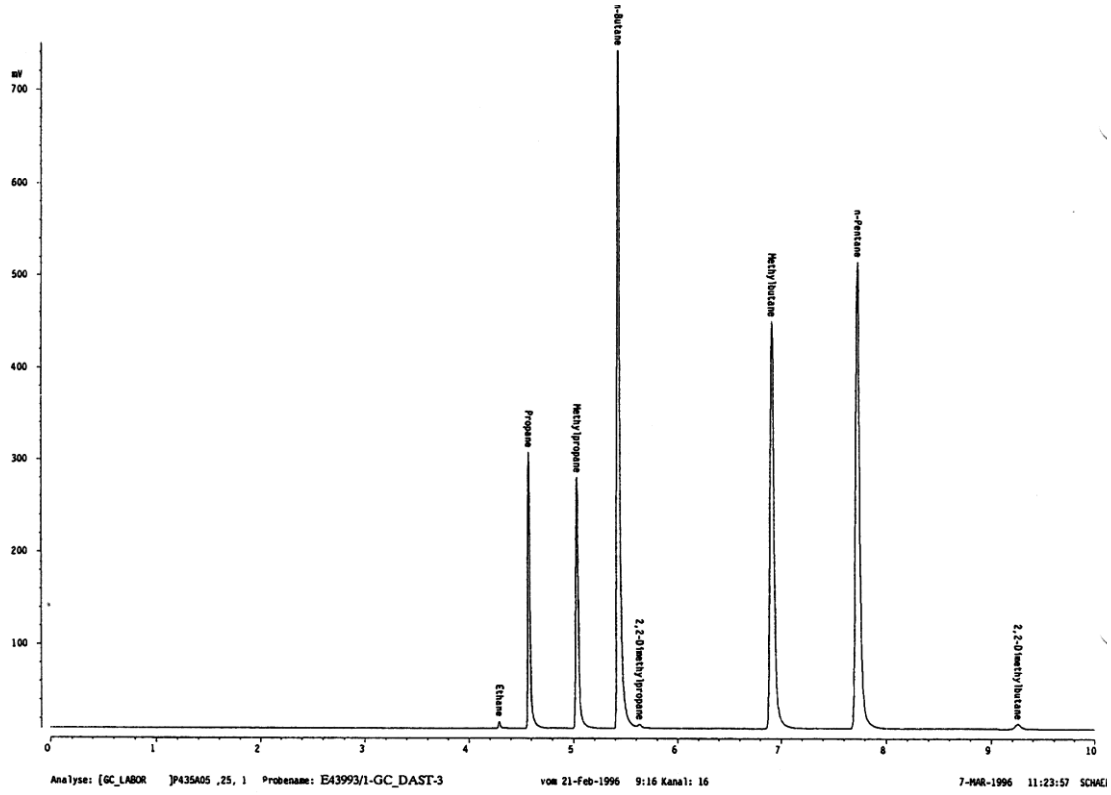
mV
700
600
500
400
300
200
100
Ethane
Propane
Methylpropane
n-Butane
2,2-Dimethylpropane
Methylbutane
n-Pentane
2,2-Dimethylbutane
0
1
2
3
4
5
6
7
8
9
10
Analyse: [GC_LABOR]P435A05 ,25, 1 Probename: E43993/1-GC_DAST-3 vom 21-Feb-1996 9:16 Kanal: 16 7-MAR-1996 11:23:57 SCHAE

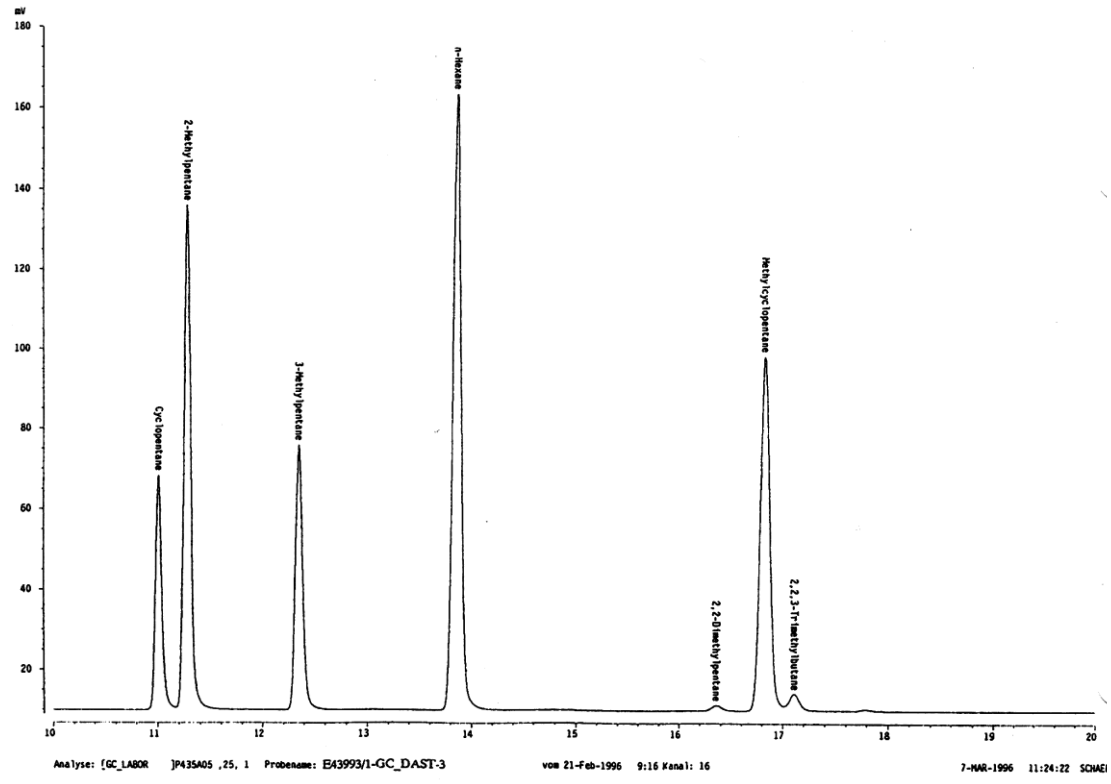
mV
180
160
140
120
100
80
60
40
20
Cyclopentane
2-Methylpentane
3-Methylpentane
n-Hexane
2,2-Dimethylpentane
Methylcyclopentane
2,2,3-Trimethylbutane
10
11
12
13
14
15
16
17
18
19
20
Analyse: [GC_LABOR]P435A05 ,25, 1 Probename: E43993/1-GC_DAST-3 vom 21-Feb-1996 9:16 Kanal: 16 7-MAR-1996 11:24:22 SCHAE

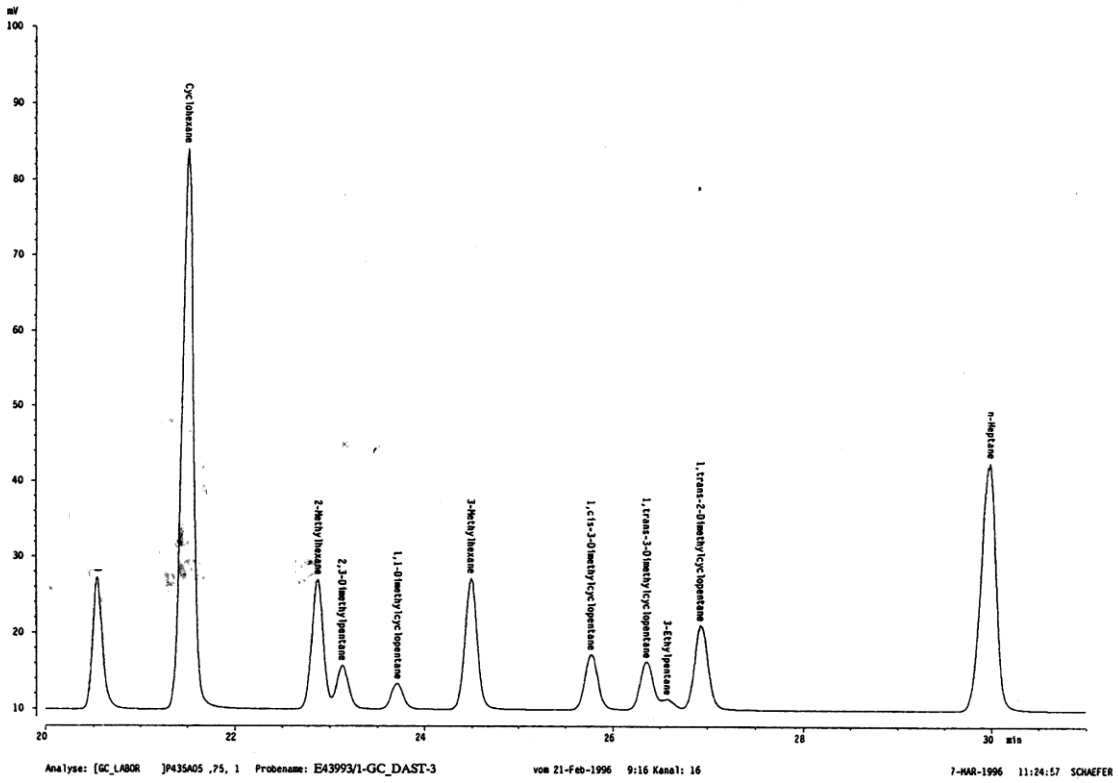
mV
Cyclohexane
2-Methylhexane
2,3-Dimethylpentane
1,1-Dimethylcyclopentane
3-Methylhexane
1,cis-3-Dimethylcyclopentane
1,trans-3-Dimethylcyclopentane
3-Ethylpentane
1,trans-2-Dimethylcyclopentane
n-Heptane
min
Analyse: [GC_LABOR]P435A05 ,75, 1 Probename: E43993/1-GC_DAST-3 vom 21-Feb-1996 9:16 Kanal: 16 7-MAR-1996 11:24:57 SCHAEFER

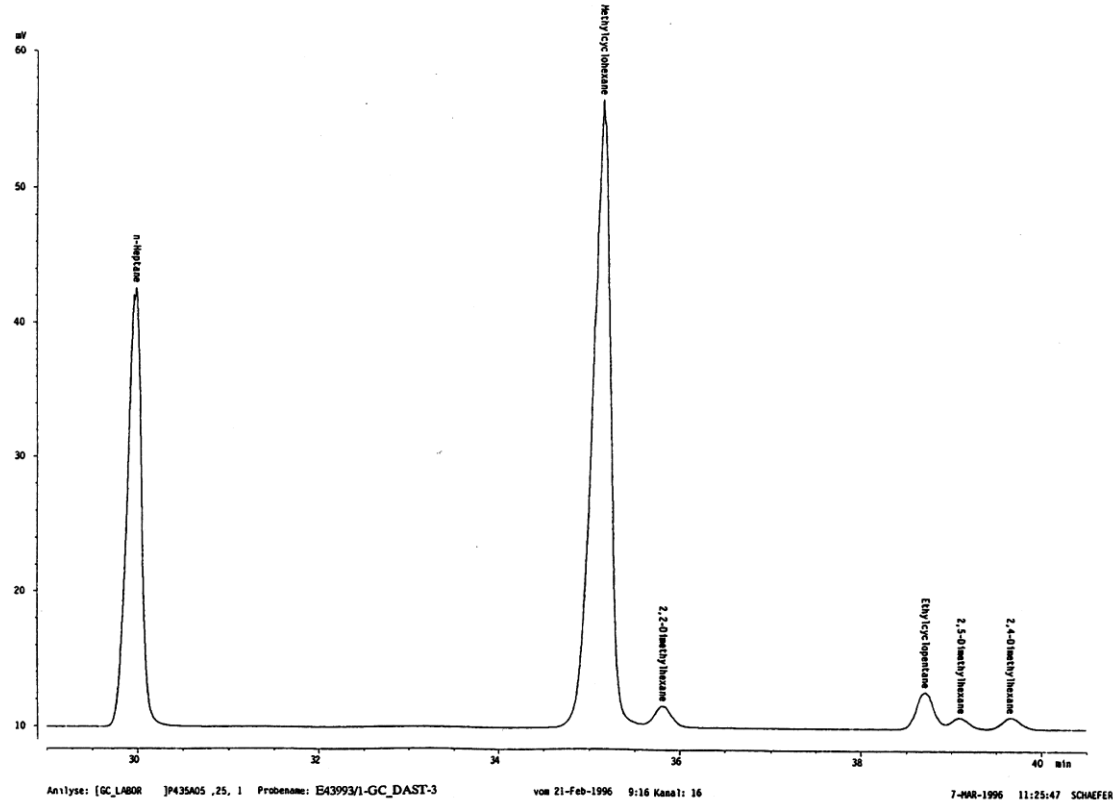
mV
n-Heptane
Methylcyclohexane
2,2-Dimethylhexane
Ethylcyclopentane
2,5-Dimethylhexane
2,4-Dimethylhexane
min
Analyse: [GC_LABOR]P435A05 ,25, 1 Probename: E43993/1-GC_DAST-3 vom 21-Feb-1996 9:16 Kanal: 16 7-MAR-1996 11:25:47 SCHAEFER

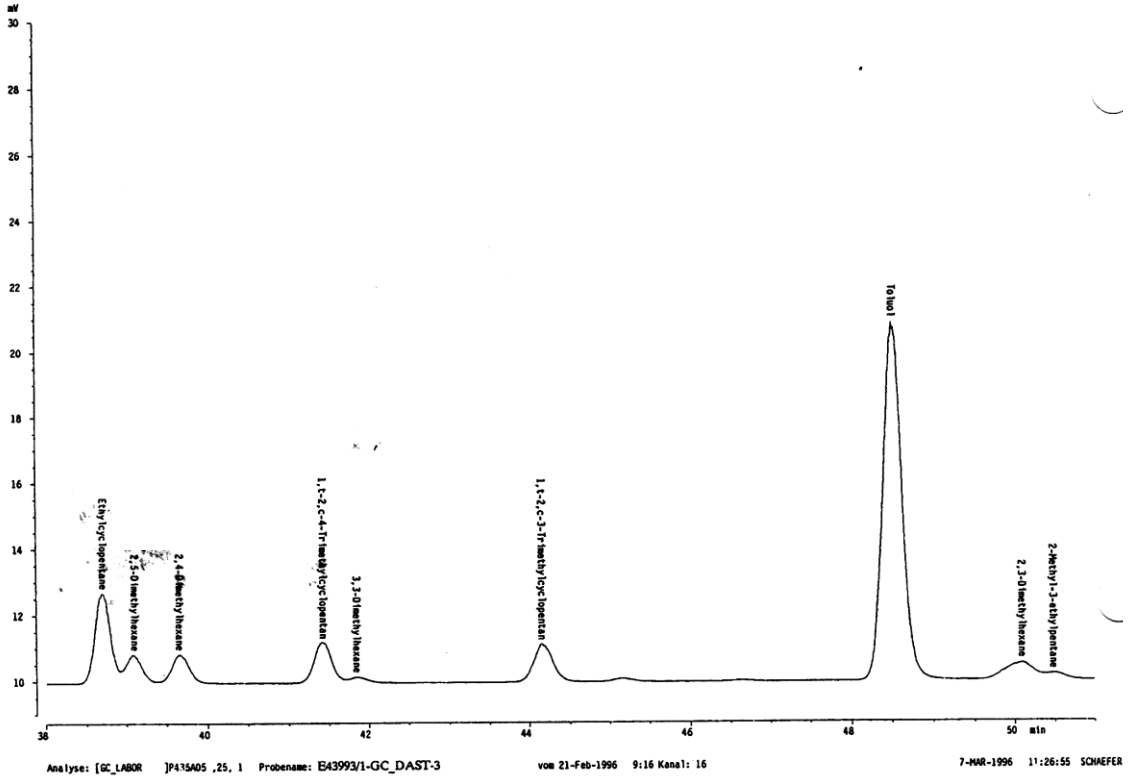
mV
Ethylcyclopentane
2,5-Dimethylhexane
2,4-Dimethylhexane
1,t-2-c-4-Trimethylcyclopentan
3,3-Dimethylhexane
1,t-2,c-3-Trimethylcyclopentan
Toluol
2,3-Dimethylhexane
2-Methyl-3-ethylpentane
min
Analyse: [GC_LABOR]P435A05 ,25, 1 Probename: E43993/1-GC_DAST-3 vom 21-Feb-1996 9:16 Kanal: 16
7-MAR-1996 11:26:55 SCHAEFER

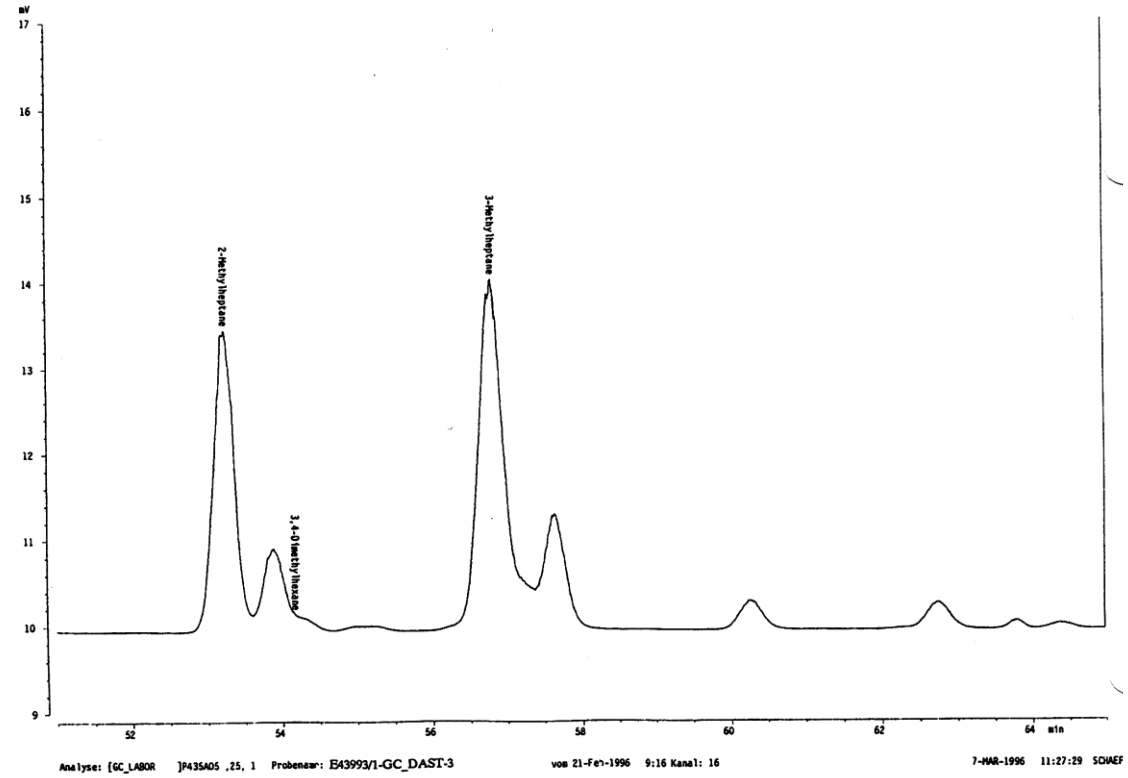
mV
2-Methylheptane
3,4-Dimethylhexane
3-Methylheptane
min
Analyse: [GC_LABOR]P435A05 ,25, 1 Probename: E43993/1-GC_DAST-3 vom 21-Feb-1996 9:16 Kanal: 16
7-MAR-1996 11:27:29 SCHAEF

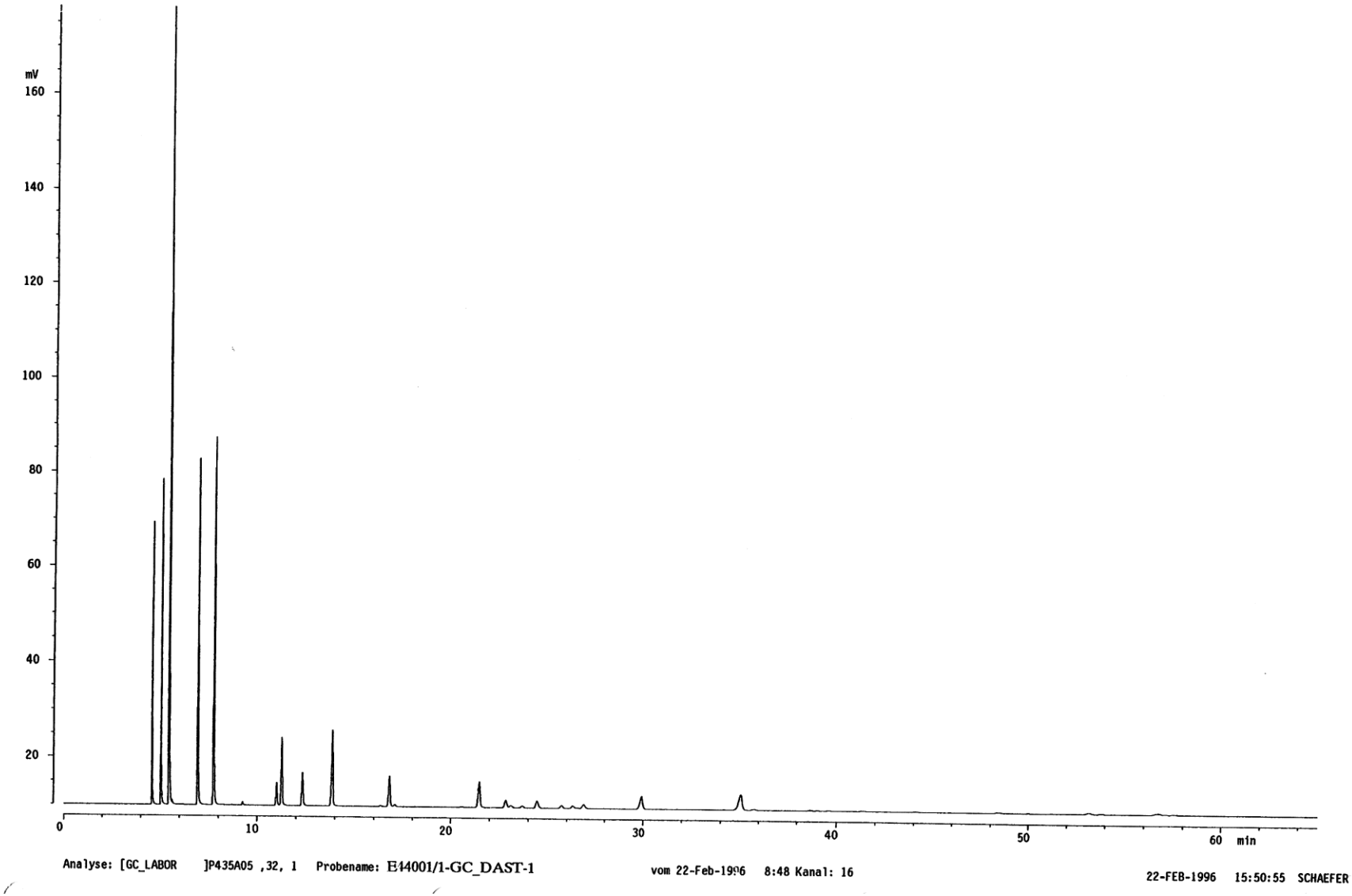
mV
160
140
120
100
80
60
40
20
0
10
20
30
40
50
60 min
Analyse: [GC_LABOR]P435A05 ,32, 1 Probename: B14001/1-GC_DAST-1
vom 22-Feb-1996 8:48 Kanal: 16
22-FEB-1996 15:50:55 SCHAEFER

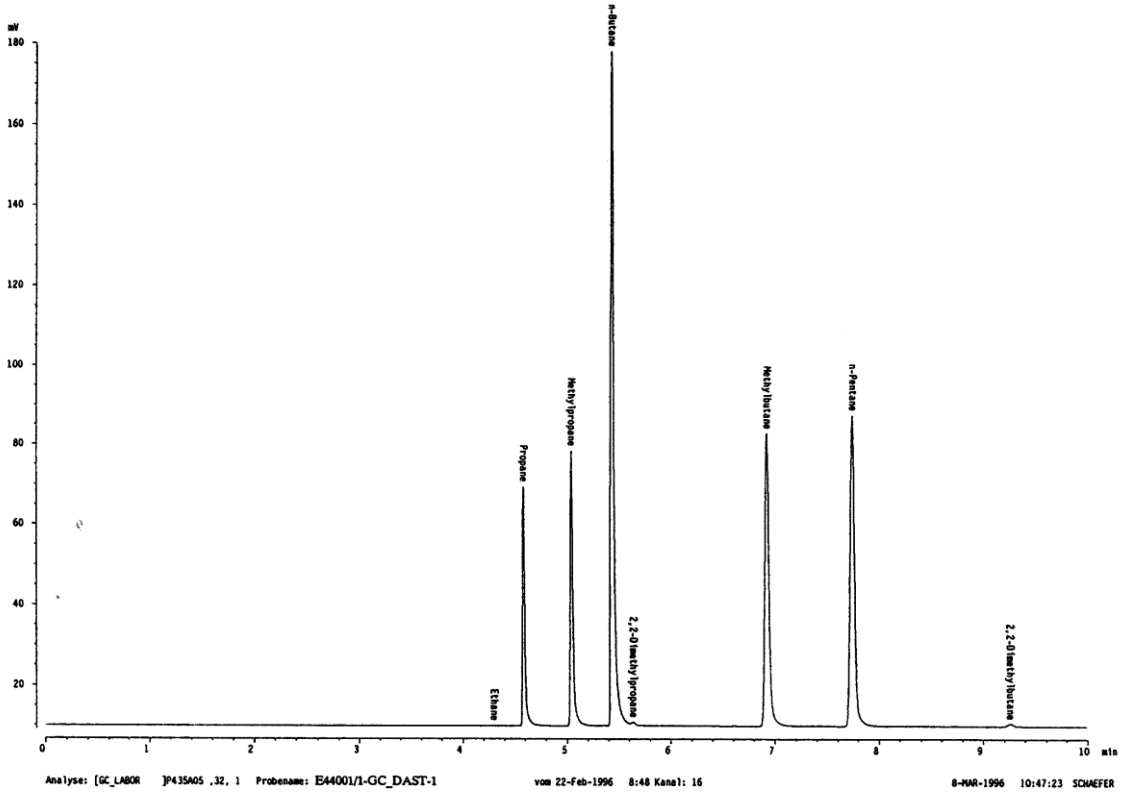
mV
Ethane
Propane
Methylpropane
n-Butane
2,2-Dimethylpropane
Methylbutane
n-Pentane
2,2-Dimethylbutane
min
Analyse: [GC_LABOR]P435A05 ,32, 1 Probename: E44001/1-GC_DAST-1 vom 22-Feb-1996 8:48 Kanal: 16 8-MAR-1996 10:47:23 SCHAEFER

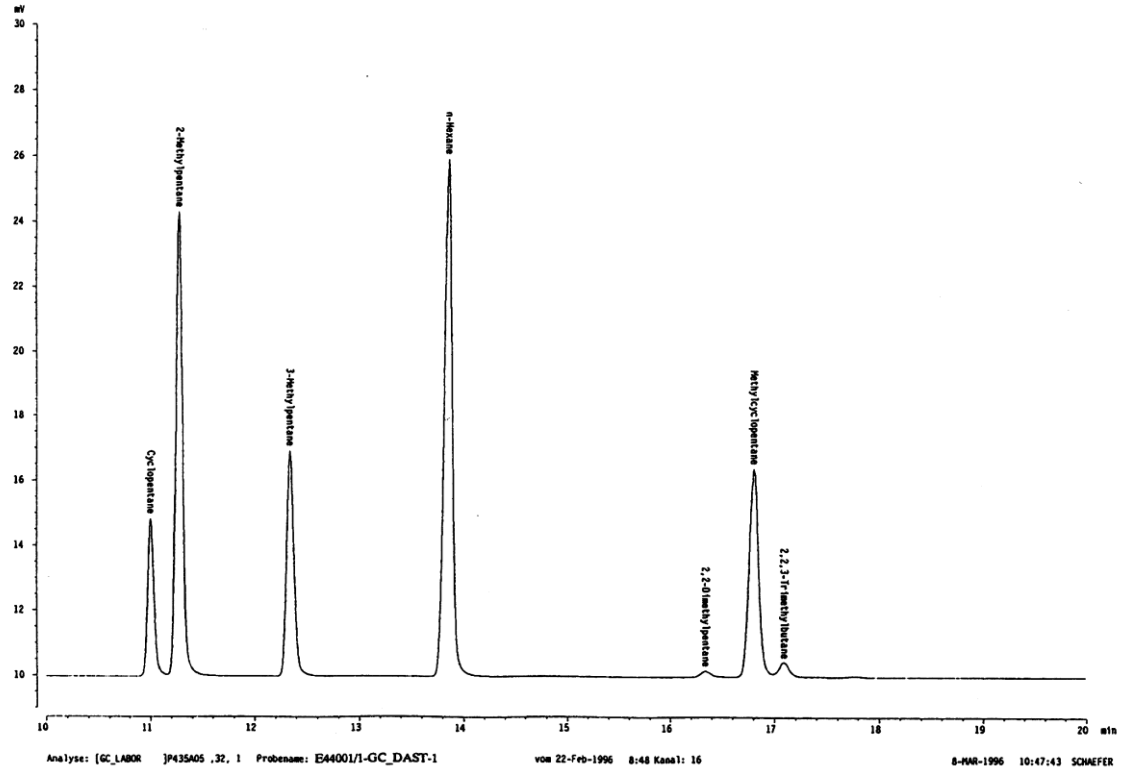
mV
Cyclopentane
2-Methylpentane
3-Methylpentane
n-Hexane
2,2-Dimethylpentane
Methylcyclopentane
2,2,3-Trimethylbutane
min
Analyse: [GC_LABOR]P435A05 ,32, 1 Probename: E44001/1-GC_DAST-1 vom 22-Feb-1996 8:48 Kanal: 16 8-MAR-1996 10:47:43 SCHAEFER

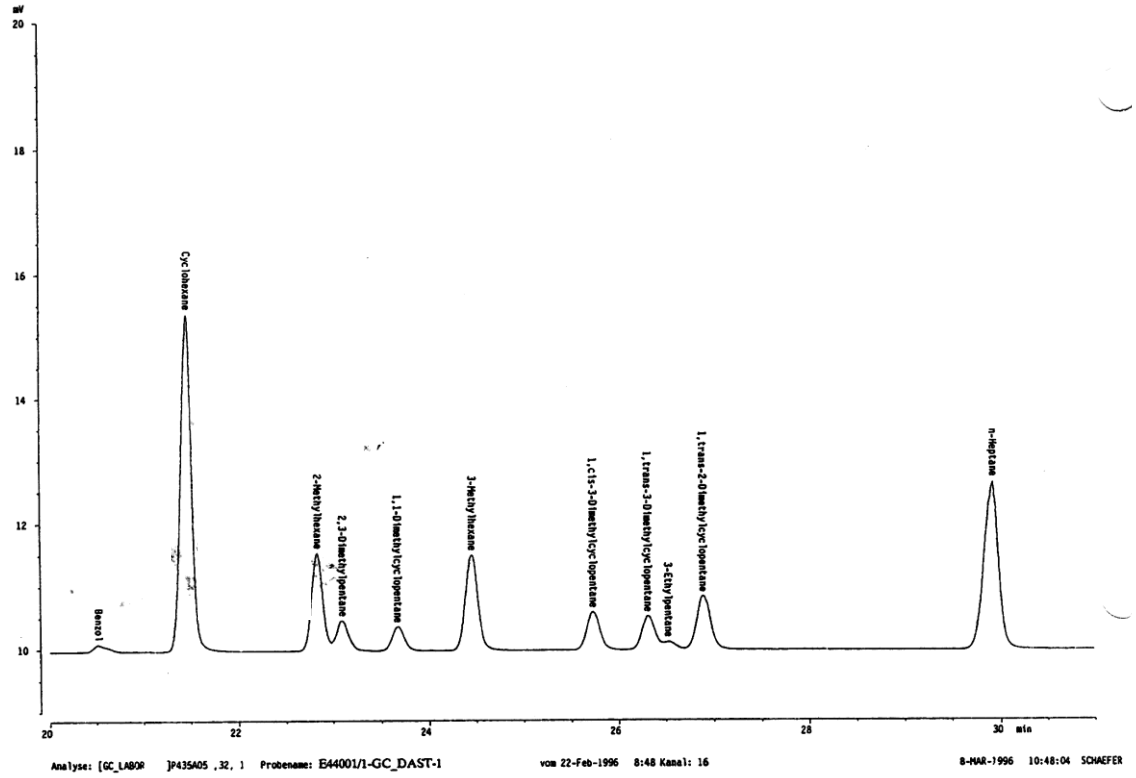
mV
20
18
16
14
12
10
Benzol
Cyclohexane
2-Methylhexane
2,3-Dimethylpentane
1,1-Dimethylcyclopentane
3-Methylhexane
1,cis-3-Dimethylcyclopentane
1,trans-3-Dimethylcyclopentane
3-Ethylpentane
1,trans-2-Dimethylcyclopentane
n-Heptane
20
22
24
26
28
30 min
Analyse: [GC_LABOR]P435A05 ,32, 1 Probename: E44001/1-GC_DAST-1
vom 22-Feb-1996 8:48 Kanal: 16
8-MAR-1996 10:48:04 SCHAEFER

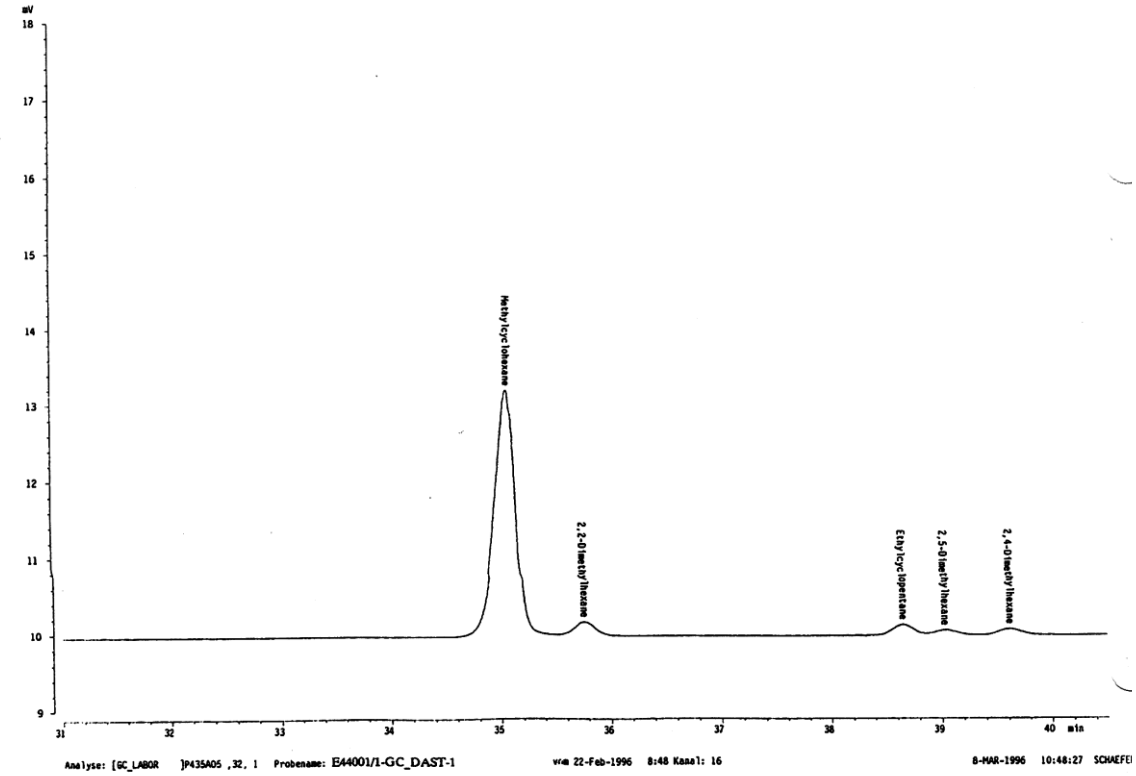
mV
18
17
16
15
14
13
12
11
10
9
Methylcyclohexane
2,2-Dimethylhexane
Ethylcyclopentane
2,5-Dimethylhexane
2,4-Dimethylhexane
31
32
33
34
35
36
37
38
39
40 min
Analyse: [GC_LABOR]P435A05 ,32, 1 Probename: E44001/1-GC_DAST-1
vom 22-Feb-1996 8:48 Kanal: 16
8-MAR-1996 10:48:27 SCHAEFE

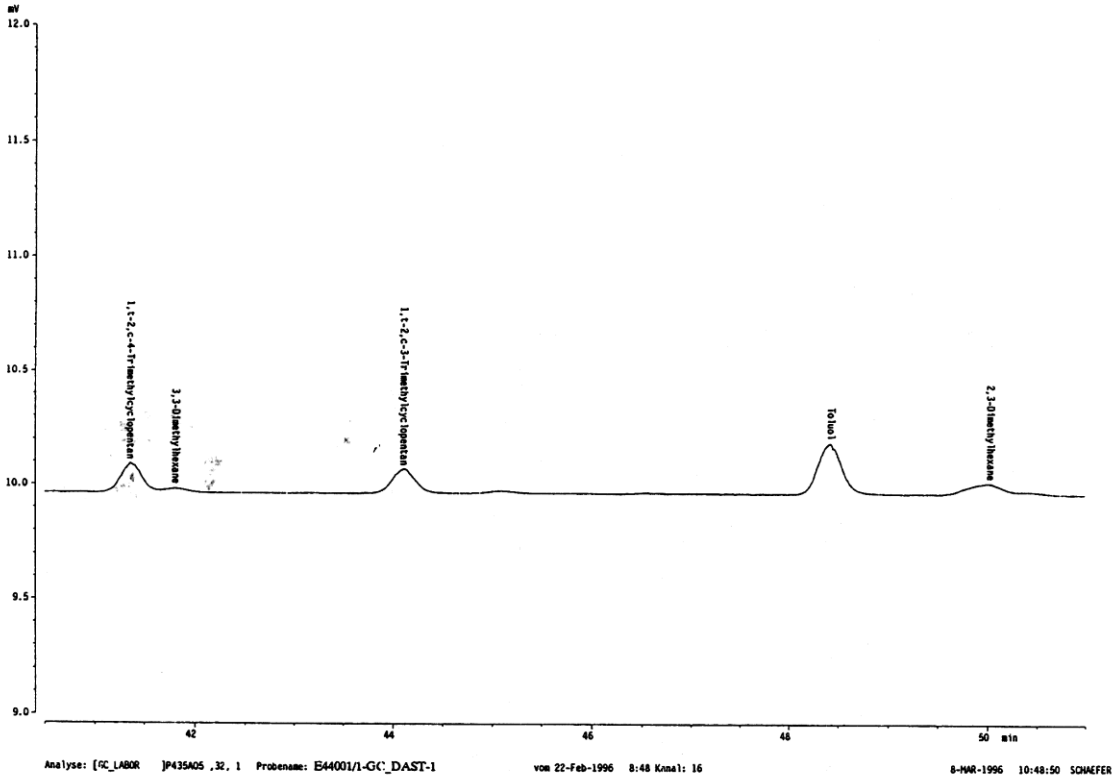
mV
12.0
11.5
11.0
10.5
10.0
9.5
9.0
1,t-2,c-4-Trimethylcyclopentan
3,3-Dimethylhexane
1,t-2,c-3-Trimethylcyclopentan
Toluol
2,3-Dimethylhexane
42
44
46
48
50 min
Analyse: [GC_LABOR]P435A05 ,32, 1 Probename: B44001/1-GC_DAST-1 vom 22-Feb-1996 8:48 Kanal: 16 8-MAR-1996 10:48:50 SCHAEFER

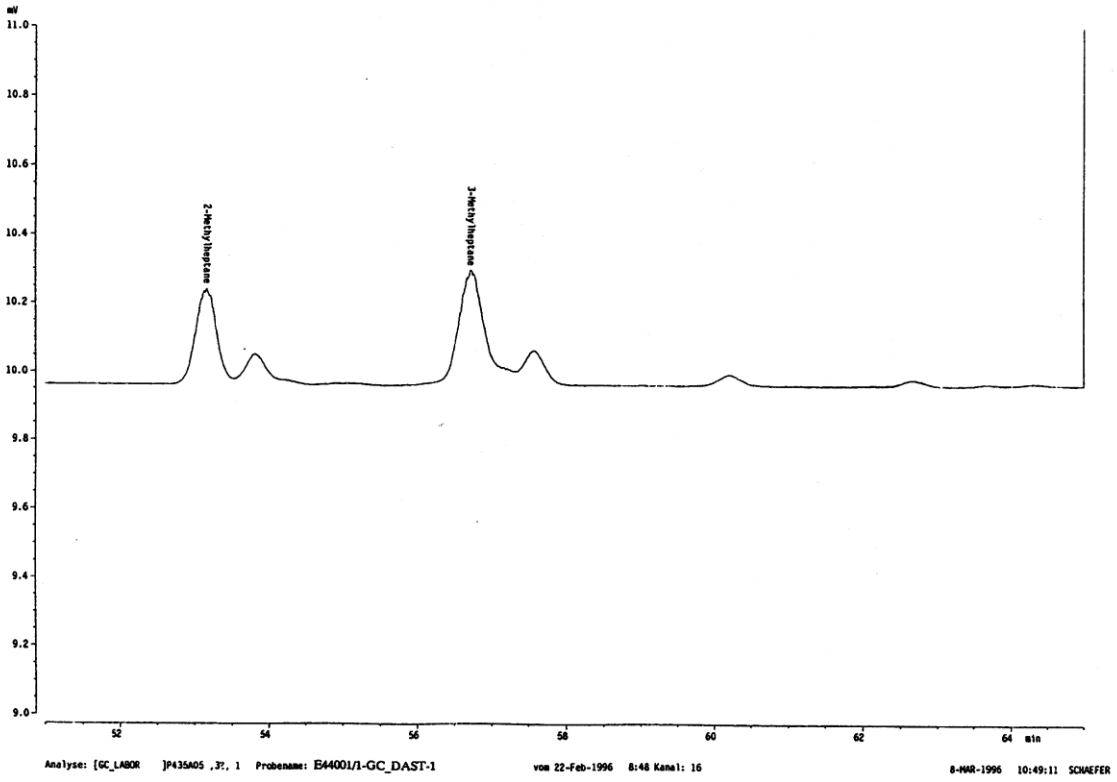
mV
11.0
10.8
10.6
10.4
10.2
10.0
9.8
9.6
9.4
9.2
9.0
2-Methylheptane
3-Methylheptane
52
54
56
58
60
62
64 min
Analyse: [GC_LABOR]P435A05 ,33, 1 Probename: B44001/1-GC_DAST-1 vom 22-Feb-1996 8:48 Kanal: 16 8-MAR-1996 10:49:11 SCHAEFER

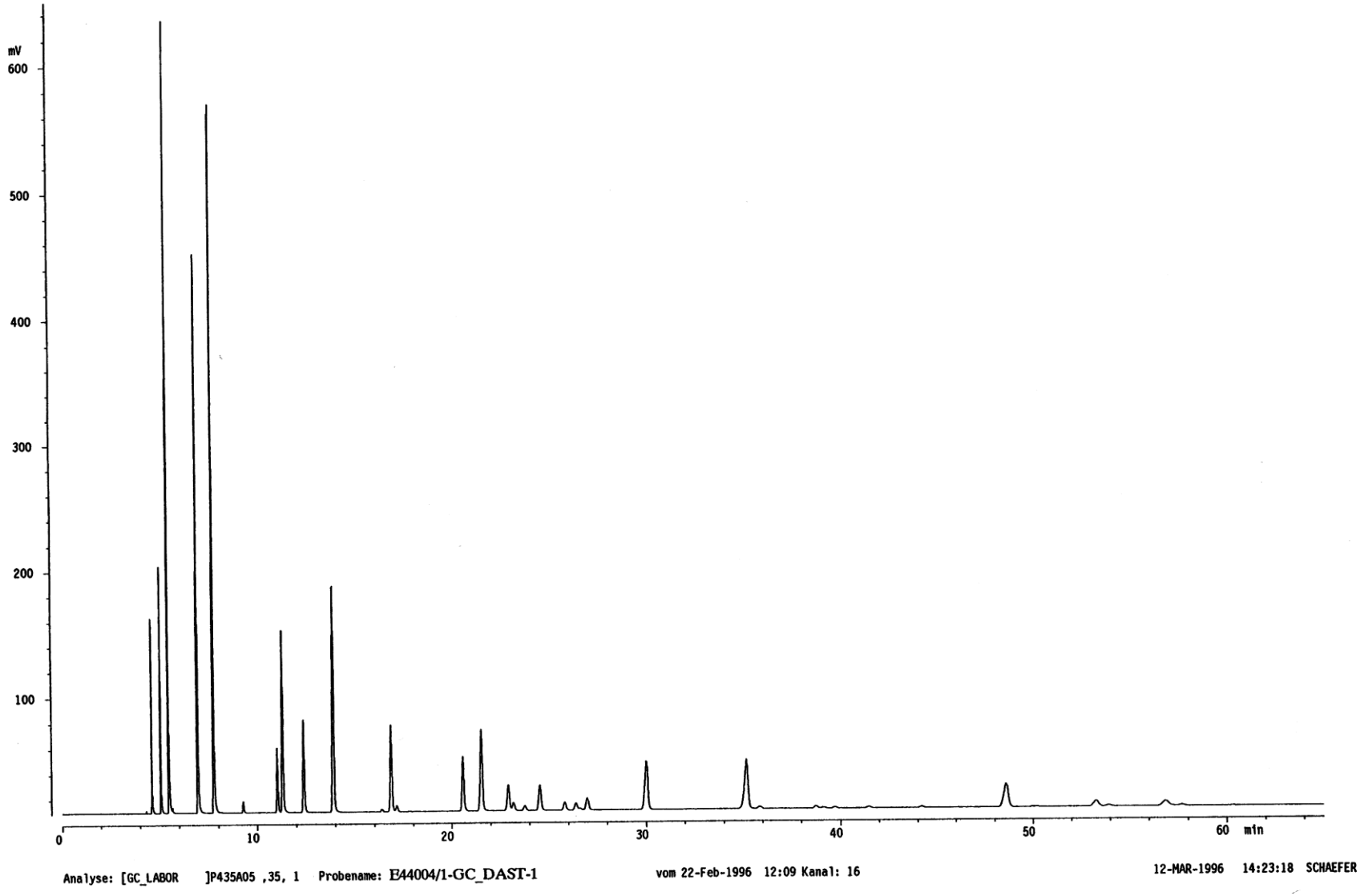
mV
600
500
400
300
200
100
0
10
20
30
40
50
60 min
Analyse: [GC_LABOR]P435A05 ,35, 1 Probename: B44004/1-GC_DAST-1
vom 22-Feb-1996 12:09 Kanal: 16
12-MAR-1996 14:23:18 SCHAEFER

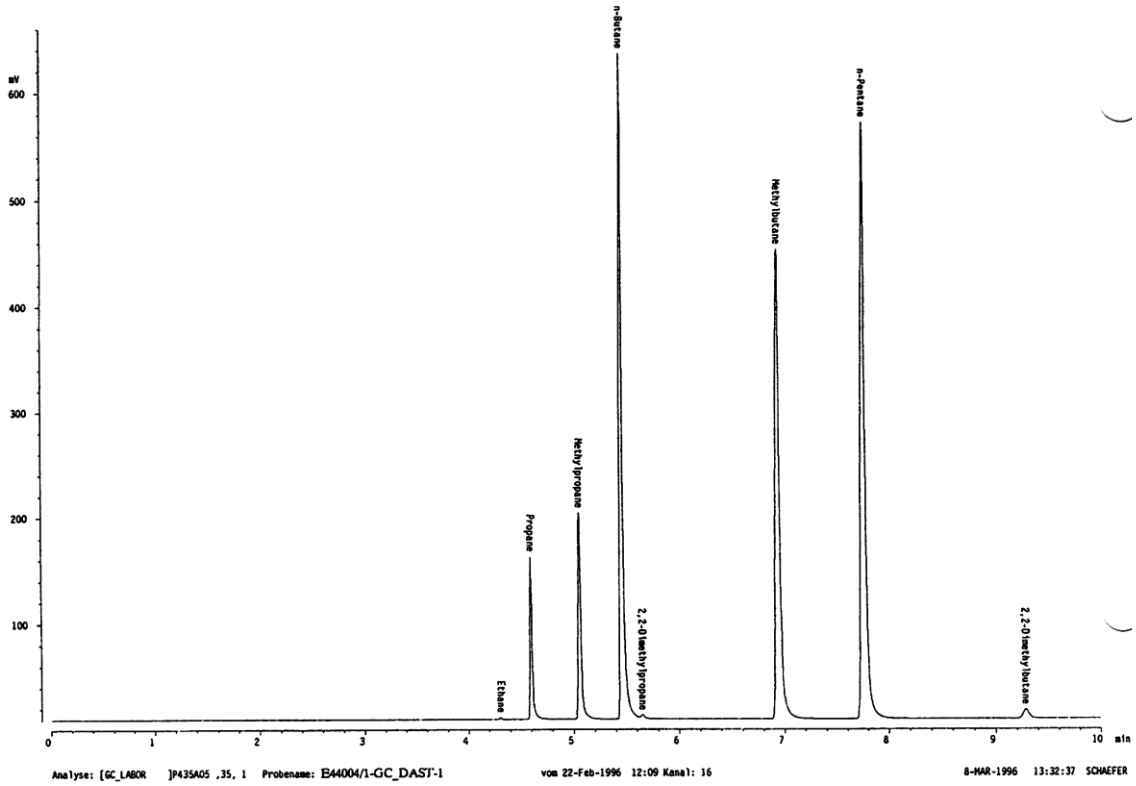
mV
600
500
400
300
200
100
Ethane
Propane
Methylpropane
n-Butane
2,2-Dimethylpropane
Methylbutane
n-Pentane
2,2-Dimethylbutane
0
1
2
3
4
5
6
7
8
9
10
min
Analyse: [GC_LABOR]P435A05 ,35, 1 Probename: B44004/1-GC_DAST-1 vom 22-Feb-1996 12:09 Kanal: 16 8-MAR-1996 13:32:37 SCHAEFER

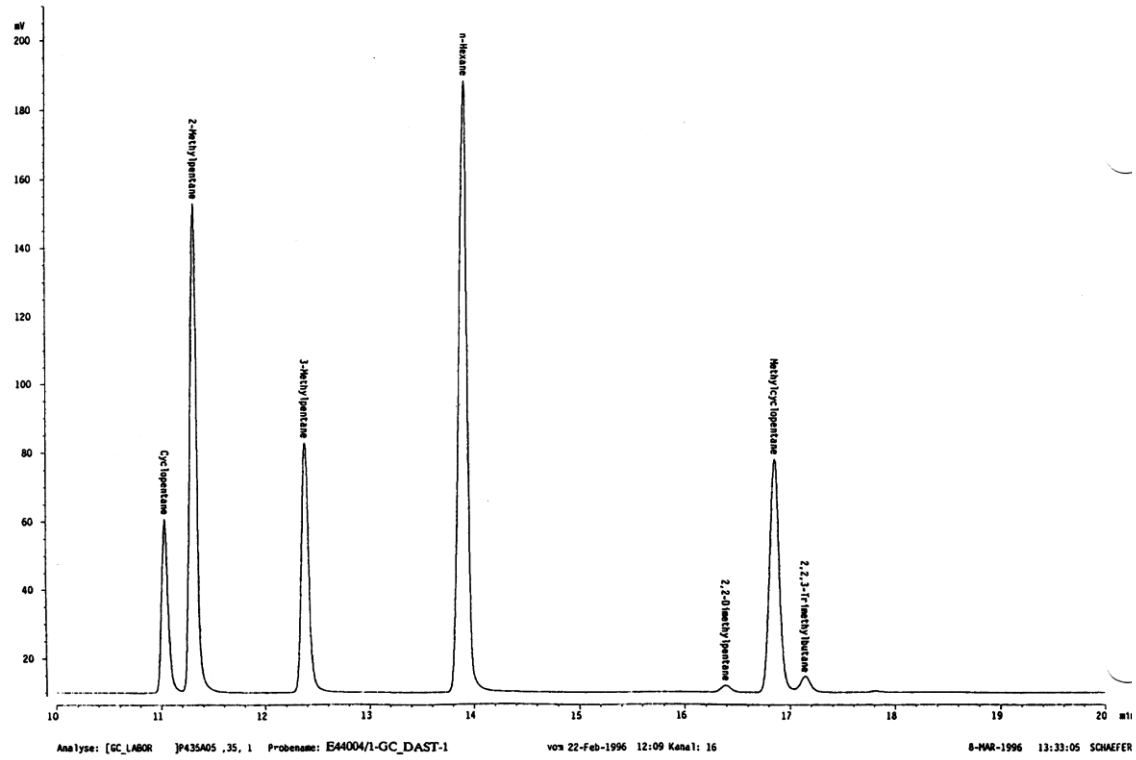
mV
200
180
160
140
120
100
80
60
40
20
Cyclopentane
2-Methylpentane
3-Methylpentane
n-Hexane
2,2-Dimethylpentane
Methylcyclopentane
2,2,3-Trimethylbutane
10
11
12
13
14
15
16
17
18
19
20
min
Analyse: [GC_LABOR]P435A05 ,35, 1 Probename: B44004/1-GC_DAST-1 vom 22-Feb-1996 12:09 Kanal: 16 8-MAR-1996 13:33:05 SCHAEFER

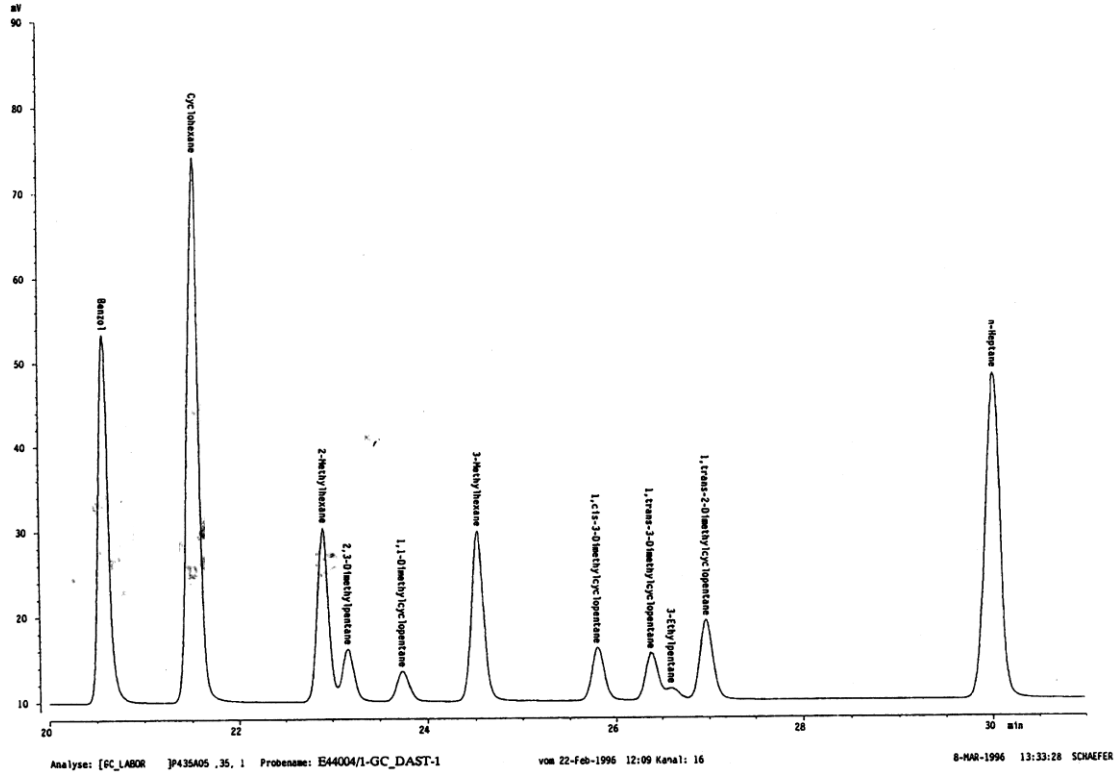
mV
Benzol
Cyclohexane
2-Methylhexane
2,3-Dimethylpentane
1,1-Dimethylcyclopentane
3-Methylhexane
1,cis-3-Dimethylcyclopentane
1,trans-3-Dimethylcyclopentane
3-Ethylpentane
1,trans-2-Dimethylcyclopentane
n-Heptane
min
Analyse: [GC_LABOR]P435A05 ,35, 1 Probename: E44004/1-GC_DAST-1
vom 22-Feb-1996 12:09 Kanal: 16
8-MAR-1996 13:33:28 SCHAEFER

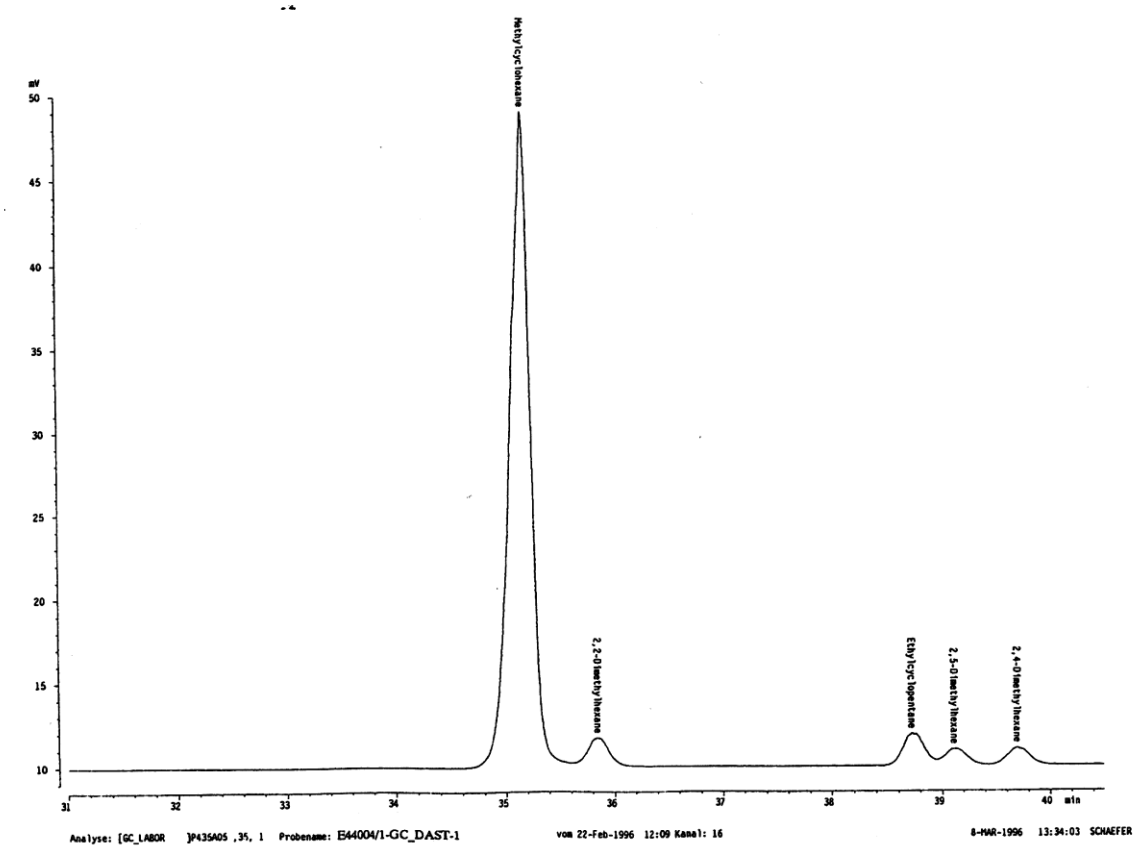
mV
Methylcyclohexane
2,2-Dimethylhexane
Ethylcyclopentane
2,5-Dimethylhexane
2,4-Dimethylhexane
min
Analyse: [GC_LABOR]P435A05 ,35, 1 Probename: E44004/1-GC_DAST-1
vom 22-Feb-1996 12:09 Kanal: 16
8-MAR-1996 13:34:03 SCHAEFER

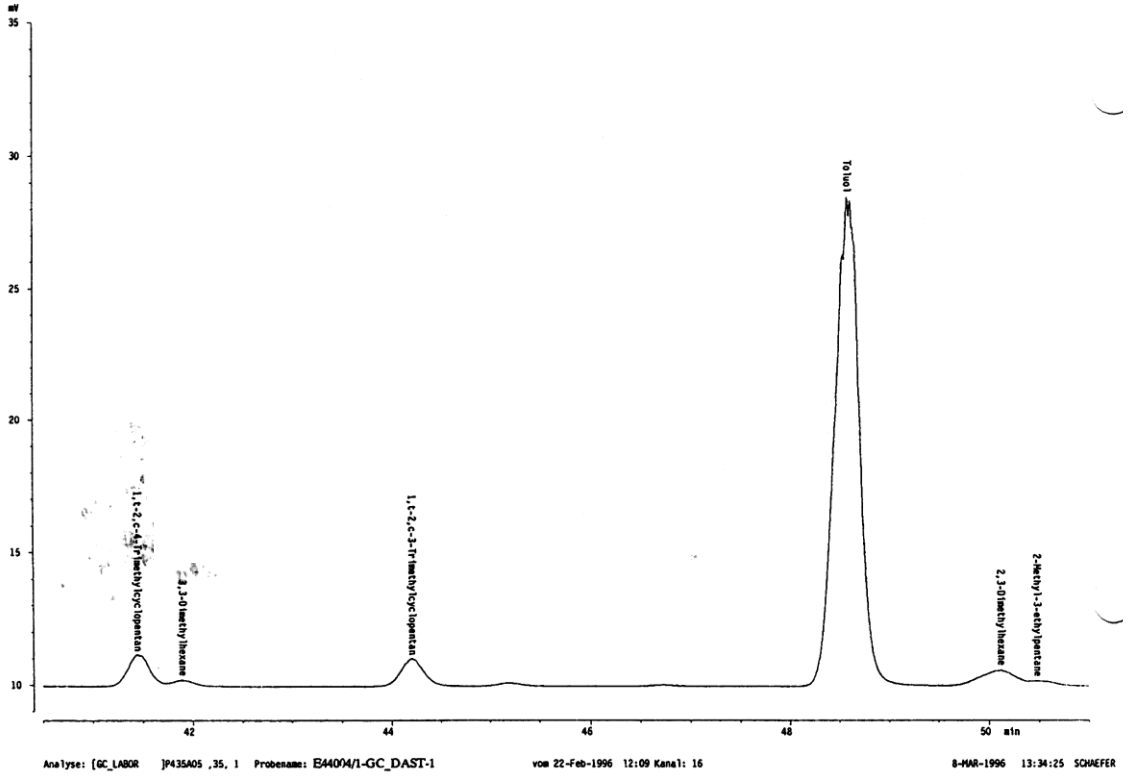
mV
35
30
25
20
15
10
1,t-2,c-4-Trimethylcyclopentan
2,3-Dimethylhexane
1,t-2,c-3-Trimethylcyclopentan
Toluol
2,3-Dimethylhexane
2-Methyl-3-ethylpentane
42
44
46
48
50 min
Analyse: [GC_LABOR]P435A05 ,35, 1 Probename: B44004/1-GC_DAST-1 vom 22-Feb-1996 12:09 Kanal: 16 8-MAR-1996 13:34:25 SCHAEFER

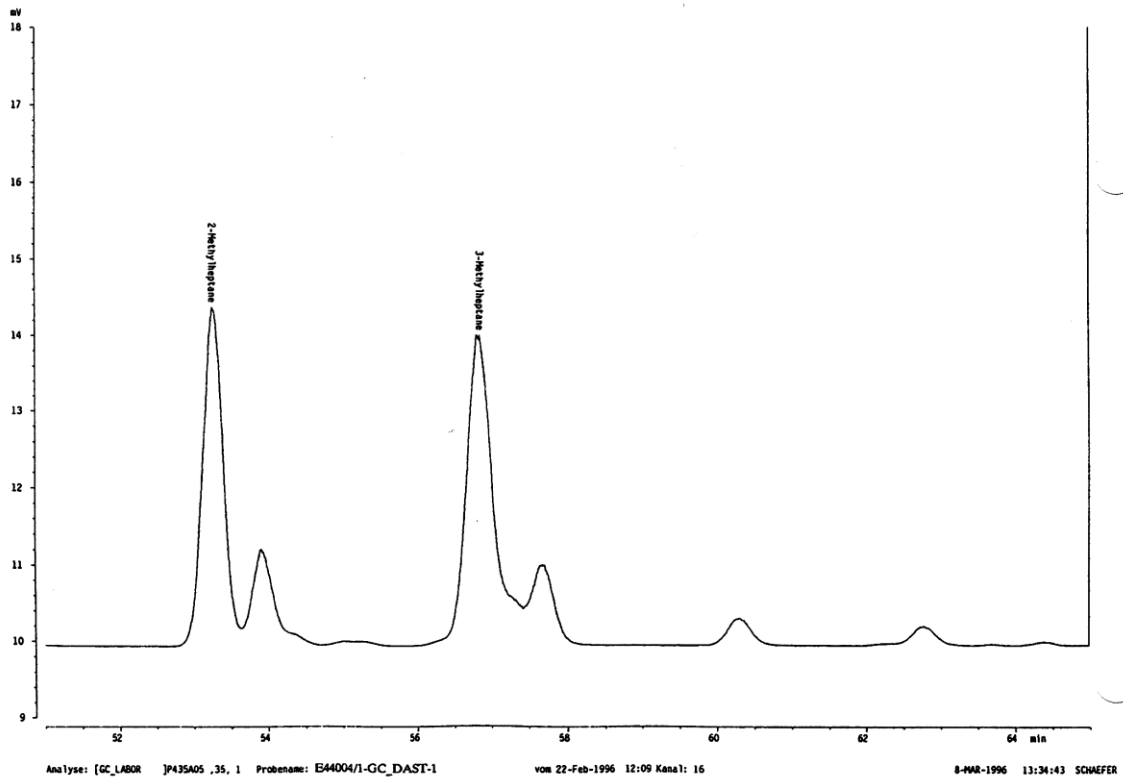
mV
18
17
16
15
14
13
12
11
10
9
2-Methylheptane
3-Methylheptane
52
54
56
58
60
62
64 min
Analyse: [GC_LABOR]P435A05 ,35, 1 Probename: B44004/1-GC_DAST-1 vom 22-Feb-1996 12:09 Kanal: 16 8-MAR-1996 13:34:43 SCHAEFER

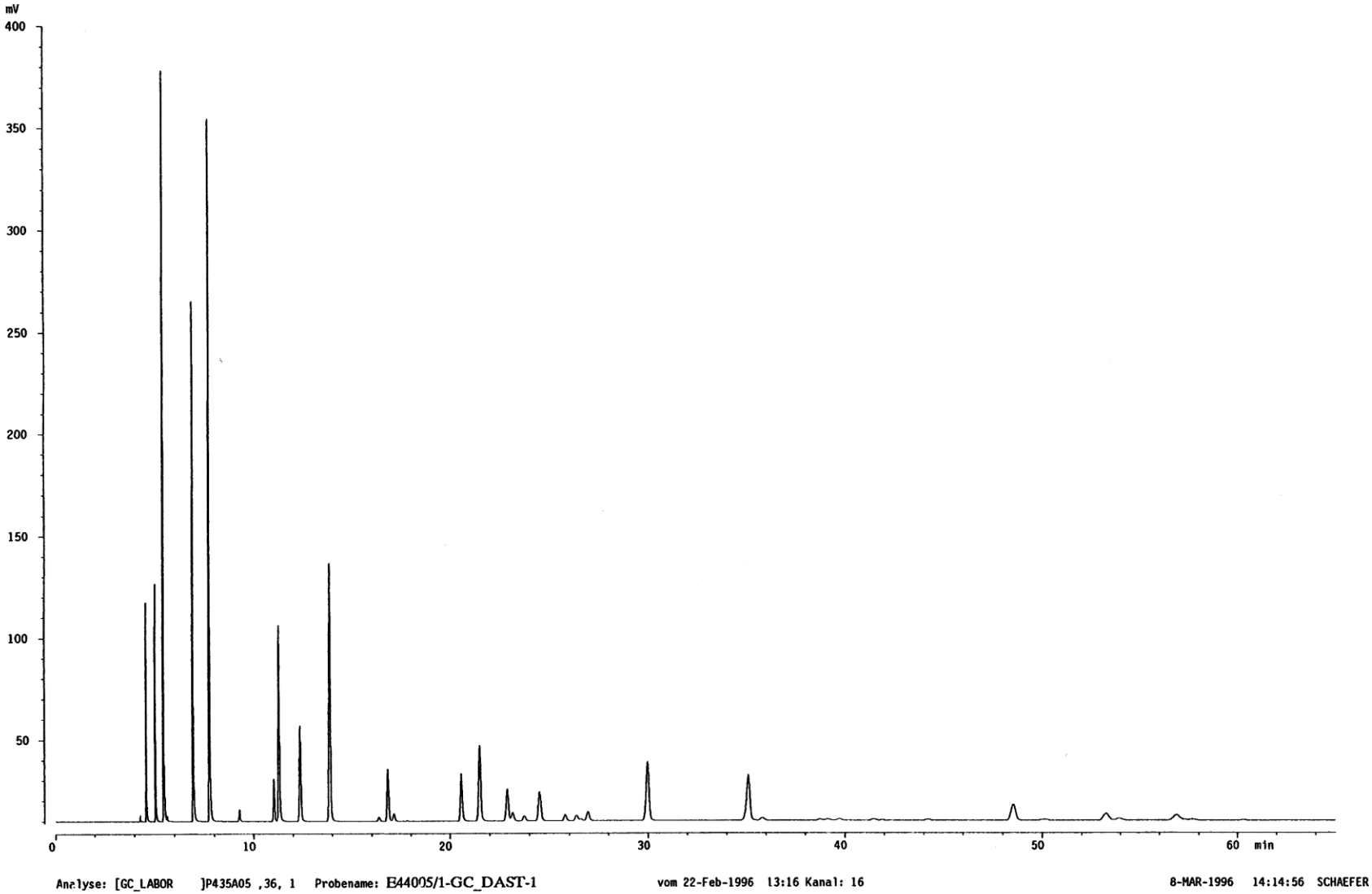
mV
400
350
300
250
200
150
100
50
0
10
20
30
40
50
60 min
Analyse: [GC_LABOR]P435A05 ,36, 1 Probename: B44005/1-GC_DAST-1
vom 22-Feb-1996 13:16 Kanal: 16
8-MAR-1996 14:14:56 SCHAEFER

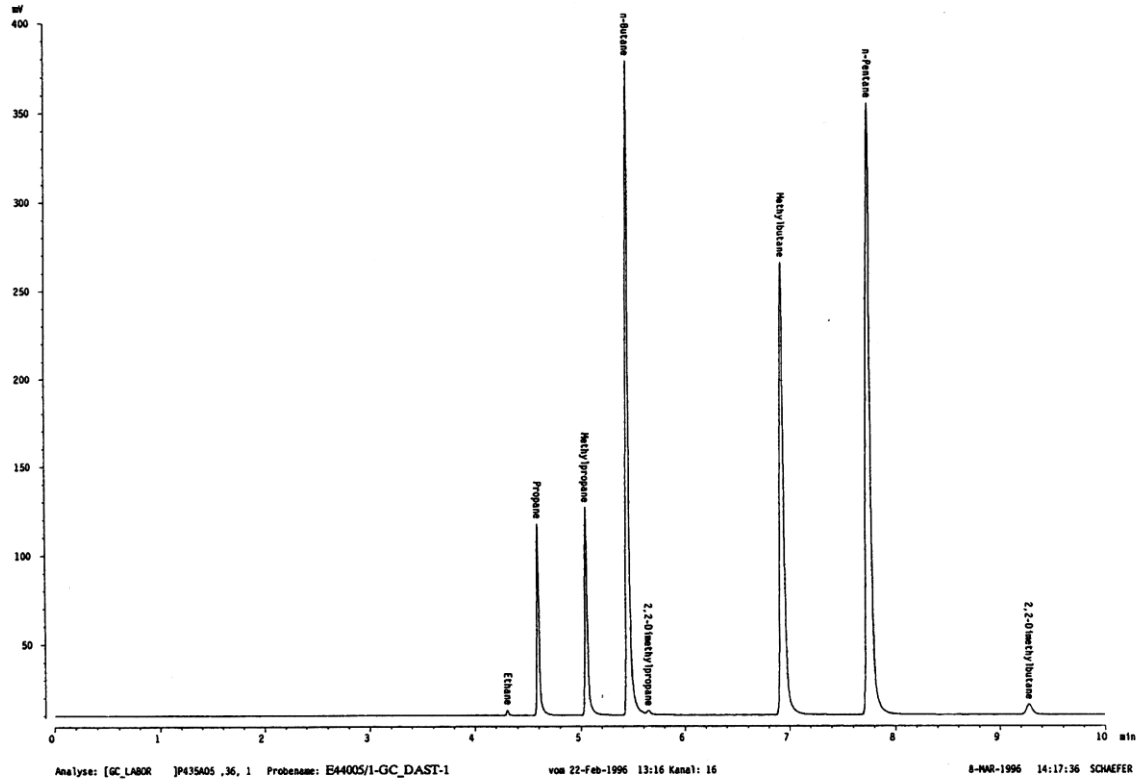
mV
400
350
300
250
200
150
100
50
Ethane
Propane
Methylpropane
n-Butane
2,2-Dimethylpropane
Methylbutane
n-Pentane
2,2-Dimethylbutane
0
1
2
3
4
5
6
7
8
9
10
min
Analyse: [GC_LABOR]P435A05 ,36, 1 Probename: E44005/1-GC_DAST-1
vom 22-Feb-1996 13:16 Kanal: 16
8-MAR-1996 14:17:36 SCHAEFER

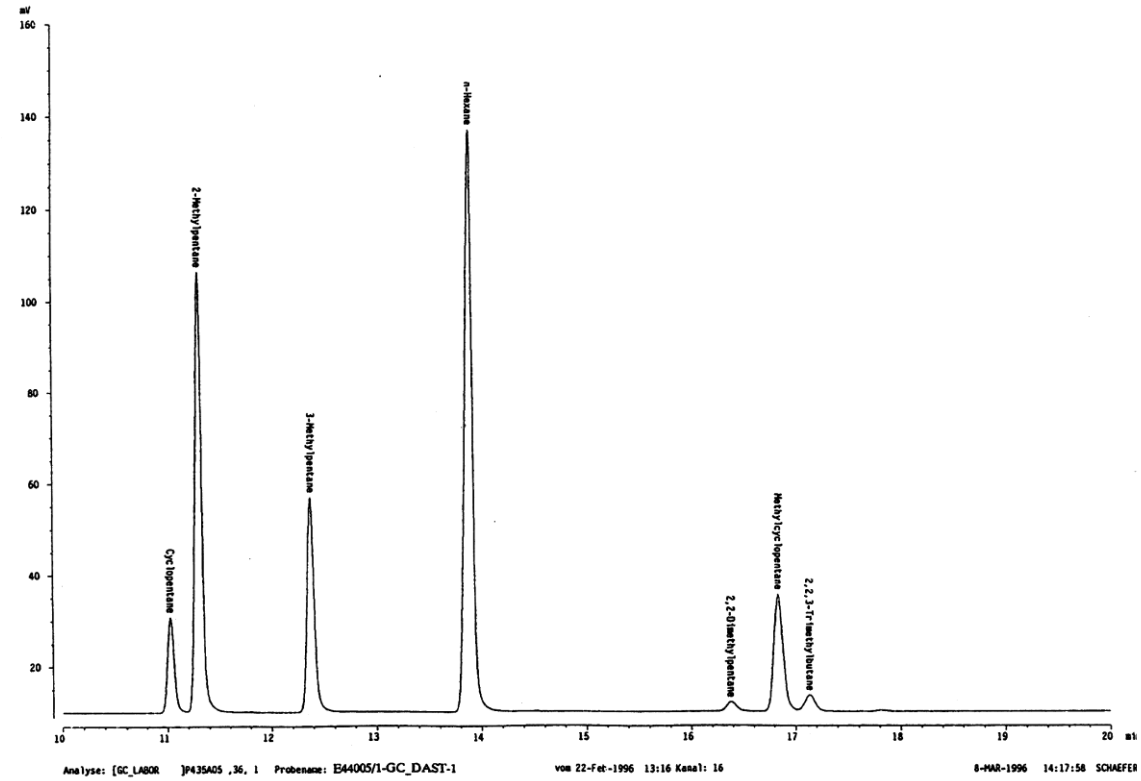
mV
160
140
120
100
80
60
40
20
Cyclopentane
2-Methylpentane
3-Methylpentane
n-Hexane
2,2-Dimethylpentane
Methylcyclopentane
2,2,3-Trimethylbutane
10
11
12
13
14
15
16
17
18
19
20
Analyse: [GC_LABOR]P435A05 ,36, 1 Probename: E44005/1-GC_DAST-1
vom 22-Feb-1996 13:16 Kanal: 16
8-MAR-1996 14:17:58 SCHAEFER

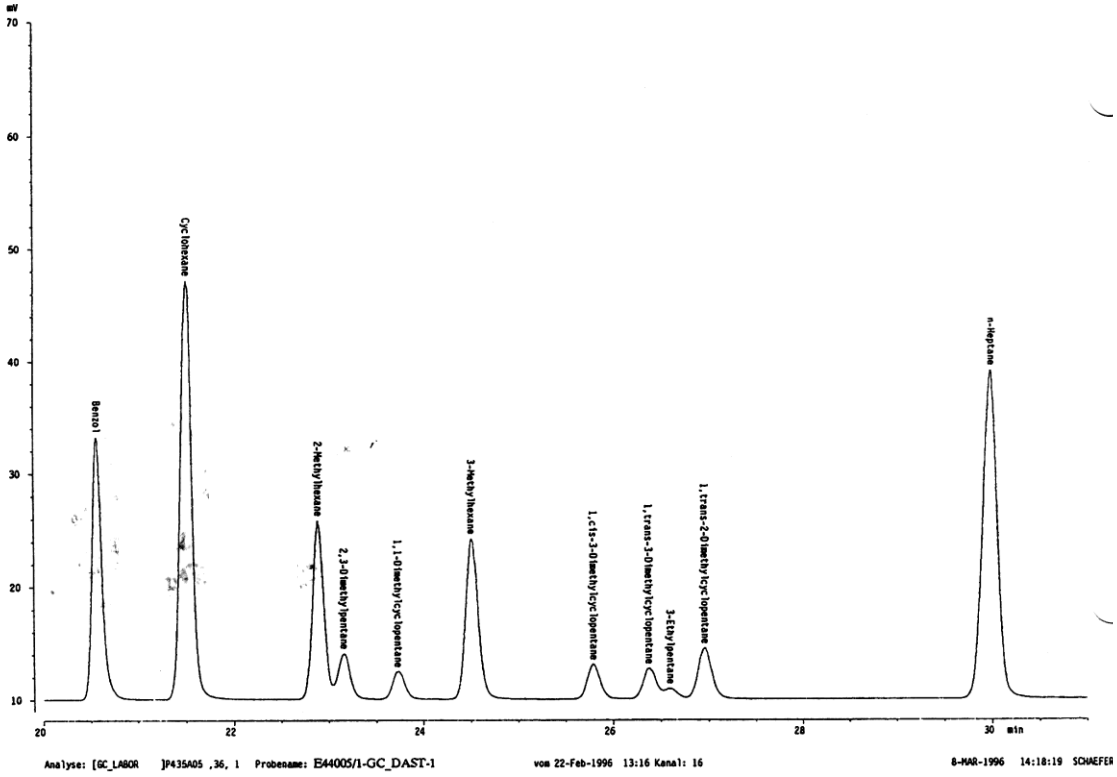
mV
70
60
50
40
30
20
10
Benzol
Cyclohexane
2-Methylhexane
2,3-Dimethylpentane
1,1-Dimethylcyclopentane
3-Methylhexane
1,cis-3-Dimethylcyclopentane
1,trans-3-Dimethylcyclopentane
3-Ethylpentane
1,trans-2-Dimethylcyclopentane
n-Heptane
20
22
24
26
28
30 min
Analyse: [GC_LABOR]P435A05 ,36, 1 Probename: E44005/1-GC_DAST-1
vom 22-Feb-1996 13:16 Kanal: 16
8-MAR-1996 14:18:19 SCHAEFER

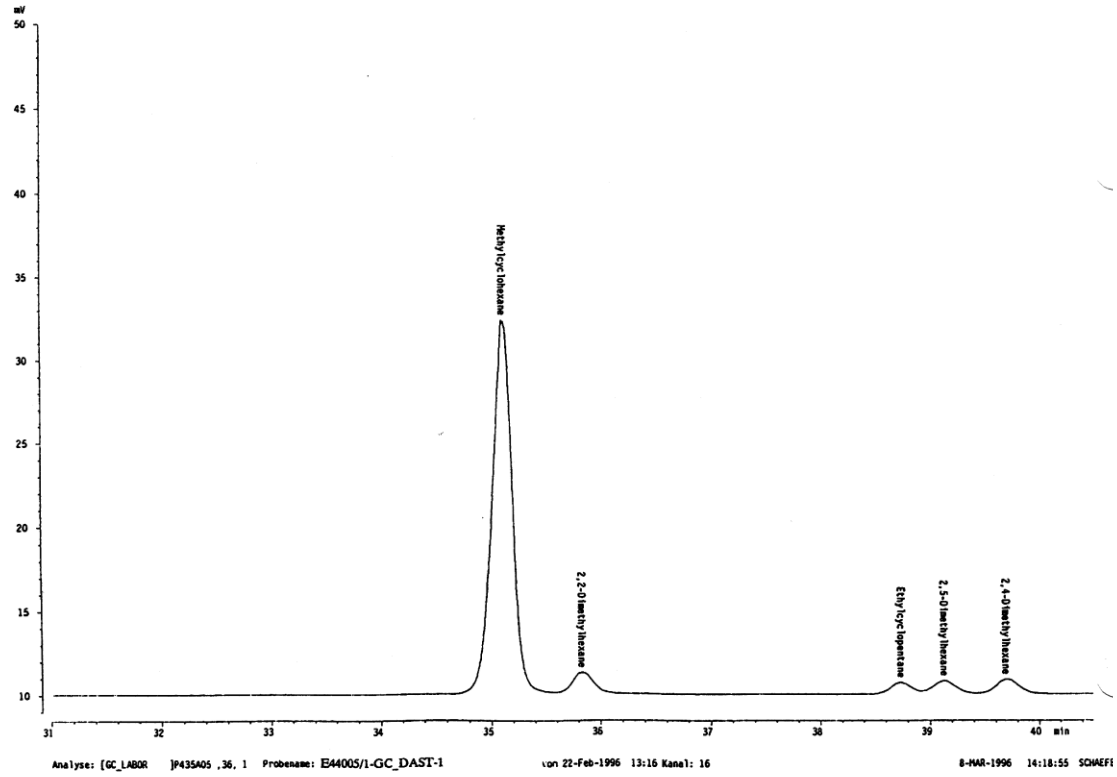
mV
50
45
40
35
30
25
20
15
10
Methylcyclohexane
2,2-Dimethylhexane
Ethylcyclopentane
2,5-Dimethylhexane
2,4-Dimethylhexane
31
32
33
34
35
36
37
38
39
40 min
Analyse: [GC_LABOR]P435A05 ,36, 1 Probename: E44005/1-GC_DAST-1
von 22-Feb-1996 13:16 Kanal: 16
8-MAR-1996 14:18:55 SCHAEFE

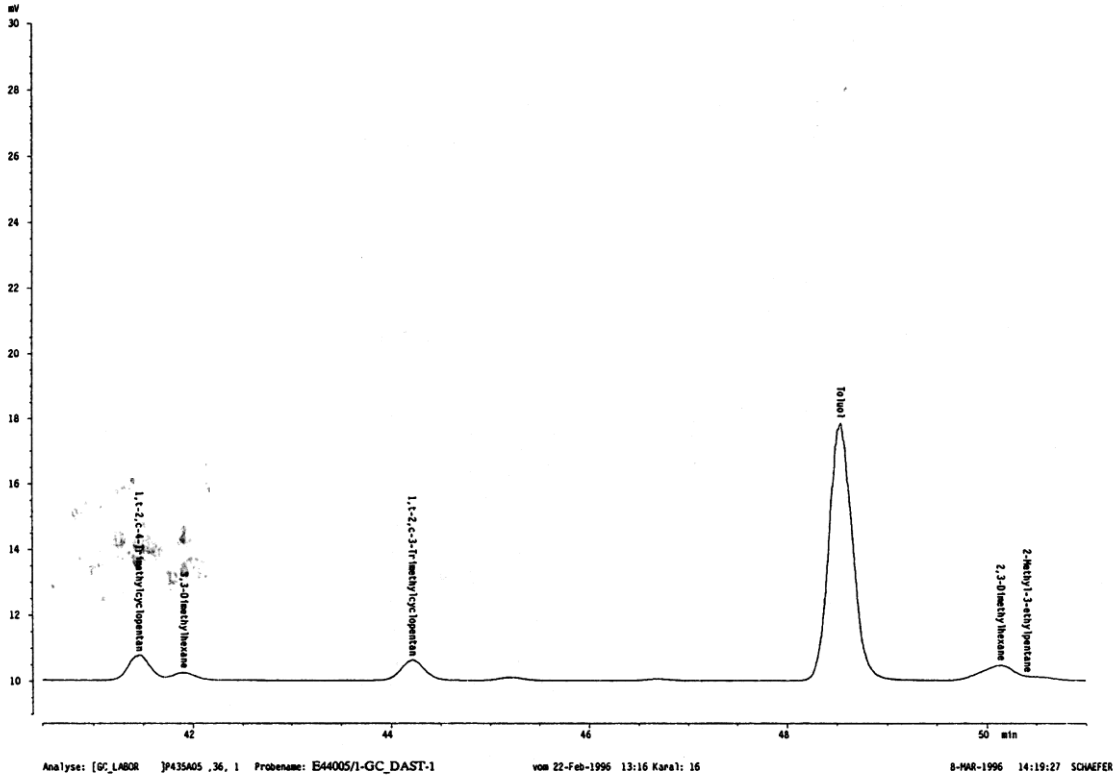
mV
30
28
26
24
22
20
18
16
14
12
10
1,t-2,c-4-Trimethylcyclopentan
2,3-Dimethylhexane
1,t-2,c-3-Trimethylcyclopentan
Toluol
2,3-Dimethylhexane
2-Methyl-3-ethylpentane
42
44
46
48
50 min
Analyse: [GC_LABOR]P435A05 ,36, 1 Probename: E44005/1-GC_DAST-1 vom 22-Feb-1996 13:16 Kanal: 16 8-MAR-1996 14:19:27 SCHAEFER

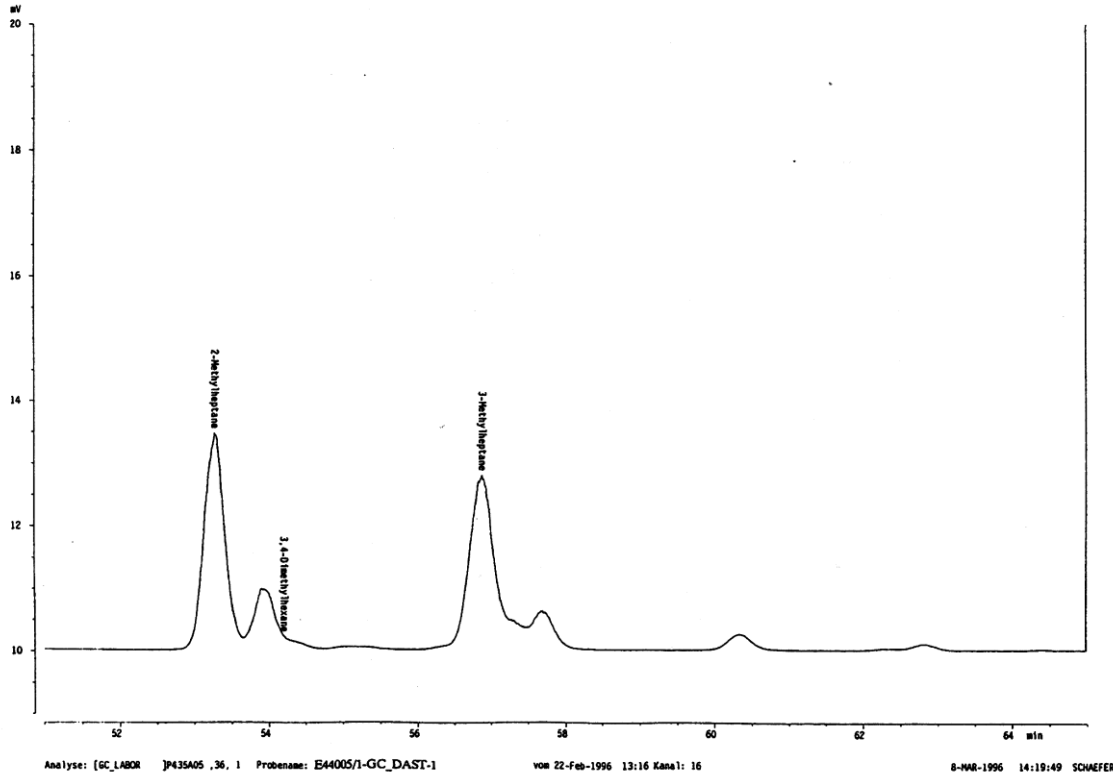
mV
20
18
16
14
12
10
2-Methylheptane
3,4-Dimethylhexane
3-Methylheptane
52
54
56
58
60
62
64 min
Analyse: [GC_LABOR]P435A05 ,36, 1 Probename: E44005/1-GC_DAST-1 vom 22-Feb-1996 13:16 Kanal: 16 8-MAR-1996 14:19:49 SCHAEFER